VOLUME 29 / NUMBER 2
JANUARY 23, 1991
ACC. NOS. N91-10839 TO N91-11665

STAR
AN ABSTRACT JOURNAL

Scientific and Technical Aerospace Reports

PRODUCED BY THE
SCIENTIFIC AND TECHNICAL
INFORMATION
DIVISION

NASA

NATIONAL AERONAUTICS AND SPACE ADMINISTRATION

***Scientific and Technical Aerospace Reports* (*STAR*)** is an abstract journal that provides comprehensive coverage of worldwide aerospace-related reports. It is a major product of the International Aerospace Database managed by the NASA Scientific and Technical Information (STI) Program. The coverage includes reports on aeronautics, space, and supporting disciplines. *STAR* lists current, publicly available reports entered into the NASA STI Database during the 2-week period preceding publication. An explanation of items that appear in each citation is given on the last page of each volume.

NASA sponsors a companion journal, *International Aerospace Abstracts* (*IAA*), that lists abstracts of the open literature on aerospace subjects available worldwide. *IAA* is available through the American Institute of Aeronautics and Astronautics.

Entries found in *STAR* and *IAA* are available through NASA's online service, RECON, as the International Aerospace Database and through DIALOG as the Aerospace Database.

Information on aerospace and related subjects is gathered by the NASA STI Program through national and international agreements and exchanges and is made available to the NASA community as well as to the public in many forms through various outlets. The section on NASA STI Program Products and Services contains additional information.

US ISSN 0036-8741

Volume 29 Number 2 / January 23, 1991

TABLE OF CONTENTS

AERONAUTICS For related information see also *Astronautics.*

01 AERONAUTICS (GENERAL) ..... **N.A.**

02 AERODYNAMICS **143**
Includes aerodynamics of bodies, combinations, wings, rotors, and control surfaces; and internal flow in ducts and turbomachinery. For related information see also *34 Fluid Mechanics and Heat Transfer.*

03 AIR TRANSPORTATION AND SAFETY **161**
Includes passenger and cargo air transport operations; and aircraft accidents. For related information see also *16 Space Transportation* and *85 Urban Technology and Transportation.*

04 AIRCRAFT COMMUNICATIONS AND NAVIGATION **167**
Includes digital and voice communication with aircraft; air navigation systems (satellite and ground based); and air traffic control. For related information see also *17 Space Communications, Spacecraft Communications, Command and Tracking* and *32 Communications and Radar.*

05 AIRCRAFT DESIGN, TESTING AND PERFORMANCE **172**
Includes aircraft simulation technology. For related information see also *18 Spacecraft Design, Testing and Performance* and *39 Structural Mechanics.* For land transportation vehicles see *85 Urban Technology and Transportation.*

06 AIRCRAFT INSTRUMENTATION ..... **N.A.**
Includes cockpit and cabin display devices; and flight instruments. For related information see also *19 Space craft Instrumentation* and *35 Instrumentation and Photography.*

07 AIRCRAFT PROPULSION AND POWER **181**
Includes prime propulsion systems and systems components, e.g., gas turbine engines and compressors; and onboard auxiliary power plants for aircraft. For related information see also *20 Spacecraft Propulsion and Power, 28 Propellants and Fuels,* and *44 Energy Production and Conversion.*

08 AIRCRAFT STABILITY AND CONTROL **182**
Includes aircraft handling qualities; piloting; flight controls; and autopilots. For related information see also *05 Aircraft Design, Testing and Performance.*

09 RESEARCH AND SUPPORT FACILITIES (AIR) **182**
Includes airports, hangars and runways; aircraft repair and overhaul facilities; wind tunnels; shock tubes; and aircraft engine test stands. For related information see also *14 Ground Support Systems and Facilities (Space).*

ASTRONAUTICS For related information see also *Aeronautics.*

12 ASTRONAUTICS (GENERAL) **183**
For extraterrestrial exploration see *91 Lunar and Planetary Exploration.*

13 ASTRODYNAMICS **183**
Includes powered and free-flight trajectories; and orbital and launching dynamics.

14 GROUND SUPPORT SYSTEMS AND FACILITIES (SPACE) **184**
Includes launch complexes, research and production facilities; ground support equipment, e.g., mobile transporters; and simulators. For related information see also *09 Research and Support Facilities (Air).*

15 LAUNCH VEHICLES AND SPACE VEHICLES ..... **N.A.**
Includes boosters; operating problems of launch/space vehicle systems; and reusable vehicles. For related information see also *20 Spacecraft Propulsion and Power.*

16 SPACE TRANSPORTATION **184**
Includes passenger and cargo space transportation, e.g., shuttle operations; and space rescue techniques. For related information see also *03 Air Transportation and Safety* and *18 Spacecraft Design, Testing and Performance.* For space suits see *54 Man/System Technology and Life Support.*

17 SPACE COMMUNICATIONS, SPACECRAFT COMMUNICATIONS, COMMAND AND TRACKING . **N.A.**
Includes telemetry; space communications networks; astronavigation and guidance; and radio blackout. For related information see also *04 Aircraft Communications and Navigation* and *32 Communications and Radar.*

N.A.—no abstracts were assigned to this category for this issue.

18 SPACECRAFT DESIGN, TESTING AND PERFORMANCE **185**
Includes satellites; space platforms; space stations; spacecraft systems and components such as thermal and environmental controls; and attitude controls. For life support systems see *54 Man/System Technology and Life Support.* For related information see also *05 Aircraft Design, Testing and Performance, 39 Structural Mechanics,* and *16 Space Transportation.*

19 SPACECRAFT INSTRUMENTATION **187**
For related information see also *06 Aircraft Instrumentation* and *35 Instrumentation and Photography.*

20 SPACECRAFT PROPULSION AND POWER **187**
Includes main propulsion systems and components, e.g., rocket engines; and spacecraft auxiliary power sources. For related information see also *07 Aircraft Propulsion and Power, 28 Propellants and Fuels, 44 Energy Production and Conversion,* and *15 Launch Vehicles and Space Vehicles.*

CHEMISTRY AND MATERIALS

23 CHEMISTRY AND MATERIALS (GENERAL) **190**

24 COMPOSITE MATERIALS **190**
Includes physical, chemical, and mechanical properties of laminates and other composite materials. For ceramic materials see *27 Nonmetallic Materials.*

25 INORGANIC AND PHYSICAL CHEMISTRY **192**
Includes chemical analysis, e.g., chromatography; combustion theory; electrochemistry; and photochemistry. For related information see also *77 Thermodynamics and Statistical Physics.*

26 METALLIC MATERIALS **195**
Includes physical, chemical, and mechanical properties of metals, e.g., corrosion; and metallurgy.

27 NONMETALLIC MATERIALS **200**
Includes physical, chemical, and mechanical properties of plastics, elastomers, lubricants, polymers, textiles, adhesives, and ceramic materials. For composite materials see *24 Composite Materials.*

28 PROPELLANTS AND FUELS **201**
Includes rocket propellants, igniters and oxidizers; their storage and handling procedures; and aircraft fuels. For related information see also *07 Aircraft Propulsion and Power, 20 Spacecraft Propulsion and Power,* and *44 Energy Production and Conversion.*

29 MATERIALS PROCESSING ..... **N.A.**
Includes space-based development of products and processes for commercial application. For biological materials see *55 Space Biology.*

ENGINEERING For related information see also *Physics.*

31 ENGINEERING (GENERAL) **202**
Includes vacuum technology; control engineering; display engineering; cryogenics; and fire prevention.

32 COMMUNICATIONS AND RADAR **203**
Includes radar; land and global communications; communications theory; and optical communications. For related information see also *04 Aircraft Communications and Navigation* and *17 Space Communications, Spacecraft Communications, Command and Tracking.* For search and rescue see *03 Air Transportation and Safety,* and *16 Space Transportation.*

33 ELECTRONICS AND ELECTRICAL ENGINEERING **204**
Includes test equipment and maintainability; components, e.g., tunnel diodes and transistors; microminiaturization; and integrated circuitry. For related information see also *60 Computer Operations and Hardware* and *76 Solid-State Physics.*

34 FLUID MECHANICS AND HEAT TRANSFER **208**
Includes boundary layers; hydrodynamics; fluidics; mass transfer and ablation cooling. For related information see also *02 Aerodynamics* and *77 Thermodynamics and Statistical Physics.*

35 INSTRUMENTATION AND PHOTOGRAPHY **215**
Includes remote sensors; measuring instruments and gauges; detectors; cameras and photographic supplies; and holography. For aerial photography see *43 Earth Resources and Remote Sensing.* For related information see also *06 Aircraft Instrumentation* and *19 Spacecraft Instrumentation.*

36 LASERS AND MASERS **216**
Includes parametric amplifiers. For related information see also *76 Solid-State Physics.*

37 MECHANICAL ENGINEERING **217**
Includes auxiliary systems (nonpower); machine elements and processes; and mechanical equipment.

38 QUALITY ASSURANCE AND RELIABILITY **220**
Includes product sampling procedures and techniques; and quality control.

39 STRUCTURAL MECHANICS **221**
Includes structural element design and weight analysis; fatigue; and thermal stress. For applications see *05 Aircraft Design, Testing and Performance* and *18 Spacecraft Design, Testing and Performance.*

GEOSCIENCES For related information see also *Space Sciences.*

42 GEOSCIENCES (GENERAL) ..... **N.A.**

43 EARTH RESOURCES AND REMOTE SENSING **227**
Includes remote sensing of earth resources by aircraft and spacecraft; photogrammetry; and aerial photography. For instrumentation see *35 Instrumentation and Photography.*

44 ENERGY PRODUCTION AND CONVERSION **229**
Includes specific energy conversion systems, e.g., fuel cells; global sources of energy; geophysical conversion; and windpower. For related information see also *07 Aircraft Propulsion and Power, 20 Spacecraft Propulsion and Power,* and *28 Propellants and Fuels.*

45 ENVIRONMENT POLLUTION **233**
Includes atmospheric, noise, thermal, and water pollution.

46 GEOPHYSICS **235**
Includes aeronomy; upper and lower atmosphere studies; ionospheric and magnetospheric physics; and geomagnetism. For space radiation see *93 Space Radiation.*

47 METEOROLOGY AND CLIMATOLOGY **239**
Includes weather forecasting and modification.

48 OCEANOGRAPHY **242**
Includes biological, dynamic, and physical oceanography; and marine resources. For related information see also *43 Earth Resources and Remote Sensing.*

LIFE SCIENCES

51 LIFE SCIENCES (GENERAL) **242**

52 AEROSPACE MEDICINE **243**
Includes physiological factors; biological effects of radiation; and effects of weightlessness on man and animals.

53 BEHAVIORAL SCIENCES **244**
Includes psychological factors; individual and group behavior; crew training and evaluation; and psychiatric research.

54 MAN/SYSTEM TECHNOLOGY AND LIFE SUPPORT **248**
Includes human engineering; biotechnology; and space suits and protective clothing. For related information see also *16 Space Transportation.*

55 SPACE BIOLOGY ..... **N.A.**
Includes exobiology; planetary biology; and extraterrestrial life.

MATHEMATICAL AND COMPUTER SCIENCES

59 MATHEMATICAL AND COMPUTER SCIENCES (GENERAL) **249**

60 COMPUTER OPERATIONS AND HARDWARE **250**
Includes hardware for computer graphics, firmware, and data processing. For components see *33 Electronics and Electrical Engineering.*

61 COMPUTER PROGRAMMING AND SOFTWARE **251**
Includes computer programs, routines, algorithms, and specific applications, e.g., CAD/CAM.

62 COMPUTER SYSTEMS **256**
Includes computer networks and special application computer systems.

63 CYBERNETICS **258**
Includes feedback and control theory, artificial intelligence, robotics and expert systems. For related information see also *54 Man/System Technology and Life Support.*

64 NUMERICAL ANALYSIS **258**
Includes iteration, difference equations, and numerical approximation.

65 STATISTICS AND PROBABILITY **263**
Includes data sampling and smoothing; Monte Carlo method; and stochastic processes.

66 SYSTEMS ANALYSIS **264**
Includes mathematical modeling; network analysis; and operations research.

67 THEORETICAL MATHEMATICS **265**
Includes topology and number theory.

PHYSICS For related information see also *Engineering.*

70 PHYSICS (GENERAL) **265**
For precision time and time interval (PTTI) see *35 Instrumentation and Photography;* for geophysics, astrophysics or solar physics see *46 Geophysics, 90 Astrophysics,* or *92 Solar Physics.*

71 ACOUSTICS **266**
Includes sound generation, transmission, and attenuation. For noise pollution see *45 Environment Pollution.*

72 ATOMIC AND MOLECULAR PHYSICS **267**
Includes atomic structure, electron properties, and molecular spectra.

73 NUCLEAR AND HIGH-ENERGY PHYSICS **269**
Includes elementary and nuclear particles; and reactor theory. For space radiation see *93 Space Radiation.*

74 OPTICS **270**
Includes light phenomena and optical devices. For lasers see *36 Lasers and Masers.*

75 PLASMA PHYSICS **271**
Includes magnetohydrodynamics and plasma fusion. For ionospheric plasmas see *46 Geophysics.* For space plasmas see *90 Astrophysics.*

76 SOLID-STATE PHYSICS **276**
Includes superconductivity. For related information see also *33 Electronics and Electrical Engineering* and *36 Lasers and Masers.*

77 THERMODYNAMICS AND STATISTICAL PHYSICS **282**
Includes quantum mechanics; theoretical physics; and Bose and Fermi statistics. For related information see also *25 Inorganic and Physical Chemistry* and *34 Fluid Mechanics and Heat Transfer.*

SOCIAL SCIENCES

80 SOCIAL SCIENCES (GENERAL) ..... **N.A.**
Includes educational matters.

81 ADMINISTRATION AND MANAGEMENT **283**
Includes management planning and research.

82 DOCUMENTATION AND INFORMATION SCIENCE **283**
Includes information management; information storage and retrieval technology; technical writing; graphic arts; and micrography. For computer documentation see *61 Computer Programming and Software.*

83 ECONOMICS AND COST ANALYSIS ..... **N.A.**
Includes cost effectiveness studies.

84 LAW, POLITICAL SCIENCE AND SPACE POLICY ..... **N.A.**
Includes NASA appropriation hearings; aviation law; space law and policy; international law; international cooperation; and patent policy.

85 URBAN TECHNOLOGY AND TRANSPORTATION ..... **N.A.**
Includes applications of space technology to urban problems; technology transfer; technology assessment; and surface and mass transportation. For related information see *03 Air Transportation and Safety, 16 Space Transportation,* and *44 Energy Production and Conversion.*

SPACE SCIENCES For related information see also *Geosciences.*

88 SPACE SCIENCES (GENERAL) ..... **N.A.**

89 ASTRONOMY **286**
Includes radio, gamma-ray, and infrared astronomy; and astrometry.

90 ASTROPHYSICS **288**
Includes cosmology; celestial mechanics; space plasmas; and interstellar and interplanetary gases and dust. For related information see also *75 Plasma Physics.*

91 LUNAR AND PLANETARY EXPLORATION **293**
Includes planetology; and manned and unmanned flights. For spacecraft design or space stations see *18 Spacecraft Design, Testing and Performance.*

92 SOLAR PHYSICS **294**
Includes solar activity, solar flares, solar radiation and sunspots. For related information see *93 Space Radiation.*

93 SPACE RADIATION **295**
Includes cosmic radiation; and inner and outer earth's radiation belts. For biological effects of radiation see *52 Aerospace Medicine.* For theory see *73 Nuclear and High-Energy Physics.*

GENERAL

Includes aeronautical, astronautical, and space science related histories, biographies, and pertinent reports too broad for categorization; histories or broad overviews of NASA programs.

99 GENERAL **297**

SUBJECT INDEX **I-1**

PERSONAL AUTHOR INDEX **I-53**

CORPORATE SOURCE INDEX **I-59**

CONTRACT NUMBER INDEX **I-69**

REPORT/ACCESSION NUMBER INDEX **I-71**

APPENDIX **A-1**

VOLUME 29 NUMBER 2 / JANUARY 23, 1991

Scientific and Technical Aerospace Reports

A Semimonthly Publication of the National Aeronautics and Space Administration

01 AERONAUTICS (GENERAL)

No abstracts in this category.

02 AERODYNAMICS

Includes aerodynamics of bodies, combinations, wings, rotors, and control surfaces; and internal flow in ducts and turbomachinery.

For related information see also *34 Fluid Mechanics and Heat Transfer.*

N91-10839*# National Aeronautics and Space Administration. Ames Research Center, Moffett Field, CA.
NASA COMPUTATIONAL FLUID DYNAMICS CONFERENCE. VOLUME 1: SESSIONS 1-6
Sep. 1989 475 p Conference held at Moffett Field, CA, 7-9 Mar. 1989 Original contains color illustrations
(NASA-CP-10038-Vol-1; A-89160-Vol-1; NAS 1.55:10038-Vol-1)
Avail: NTIS HC/MF A20; 25 functional color pages CSCL 01A

Presentations given at the NASA Computational Fluid Dynamics (CFD) Conference held at the NASA Ames Research Center, Moffett Field, California, March 7-9, 1989 are given. Topics covered include research facility overviews of CFD research and applications, validation programs, direct simulation of compressible turbulence, turbulence modeling, advances in Runge-Kutta schemes for solving 3-D Navier-Stokes equations, grid generation and invicid flow computation around aircraft geometries, numerical simulation of rotorcraft, and viscous drag prediction for rotor blades. For individual titles, see N91-10840 through N91-10867.

N91-10840*# National Aeronautics and Space Administration. Ames Research Center, Moffett Field, CA.
COMPUTATIONAL FLUID DYNAMICS PROGRAM AT NASA AMES RESEARCH CENTER
Terry L. Holst *In its* NASA Computational Fluid Dynamics Conference. Volume 1: Sessions 1-6 Sep. 1989 p 3-34 (For primary document see N91-10839 02-02)
Avail: NTIS HC/MF A20; 25 functional color pages CSCL 01A

The Computational Fluid Dynamics (CFD) Program at NASA Ames Research Center is reviewed and discussed. The technical elements of the CFD Program are listed and briefly discussed. These elements include algorithm research, research and pilot code development, scientific visualization, advanced surface representation, volume grid generation, and numerical optimization. Next, the discipline of CFD is briefly discussed and related to other areas of research at NASA Ames including experimental fluid dynamics, computer science research, computational chemistry, and numerical aerodynamic simulation. These areas combine with CFD to form a larger area of research, which might collectively be called computational technology. The ultimate goal of computational technology research at NASA Ames is to increase the physical understanding of the world in which we live, solve problems of national importance, and increase the technical capabilities of the aerospace community. Next, the major programs at NASA Ames that either use CFD technology or perform research in CFD are listed and discussed. Briefly, this list includes turbulent/transition physics and modeling, high-speed real gas flows, interdisciplinary research, turbomachinery demonstration computations, complete aircraft aerodynamics, rotorcraft applications, powered lift flows, high alpha flows, multiple body aerodynamics, and incompressible flow applications. Some of the individual problems actively being worked in each of these areas is listed to help define the breadth or extent of CFD involvement in each of these major programs. State-of-the-art examples of various CFD applications are presented to highlight most of these areas. The main emphasis of this portion of the presentation is on examples which will not otherwise be treated at this conference by the individual presentations. Finally, a list of principal current limitations and expected future directions is given. Author

N91-10841*# National Aeronautics and Space Administration. Langley Research Center, Hampton, VA.
COMPUTATIONAL FLUID DYNAMICS RESEARCH AND APPLICATIONS AT NASA LANGLEY RESEARCH CENTER
Jerry C. South, Jr. *In* NASA, Ames Research Center, NASA Computational Fluid Dynamics Conference. Volume 1: Sessions 1-6 Sep. 1989 p 35-47 (For primary document see N91-10839 02-02)
Avail: NTIS HC/MF A20; 25 functional color pages CSCL 01A

Information on computational fluid dynamics (CFD) research and applications carried out at the NASA Langley Research Center is given in viewgraph form. The Langley CFD strategy, the five-year plan in CFD and flow physics, 3-block grid topology, the effect of a patching algorithm, F-18 surface flow, entropy and vorticity effects that improve accuracy of unsteady transonic small disturbance theory, and the effects of reduced frequency on first harmonic components of unsteady pressures due to airfoil pitching are among the topics covered. Author

N91-10842*# National Aeronautics and Space Administration. Lewis Research Center, Cleveland, OH.
COMPUTATIONAL FLUID DYNAMICS AT THE LEWIS RESEARCH CENTER: AN OVERVIEW
Robert M. Stubbs *In* NASA, Ames Research Center, NASA Computational Fluid Dynamics Conference. Volume 1: Sessions 1-6 Sep. 1989 p 49-61 (For primary document see N91-10839 02-02)
Avail: NTIS HC/MF A20; 25 functional color pages CSCL 01A

Lewis is a multidisciplinary Center with strong research and development programs in aeronautical and space propulsion, power, space communications, space experiments and materials. Computational fluid dynamics (CFD) is playing an important and growing role in most of these areas. Described here is how CFD is integrated into these programs and highlights elements of the CFD activities. Examples are presented of codes developed to predict flow fields in advanced propulsion systems and several of the code validation experiments are described. The CFD effort at Lewis ranges from basic research on new and improved algorithms through code development to the application of these codes to specific engineering problems. Because of the substantial improvement in CFD's predictive capability, its use at Lewis is on a steep growth path, spreading rapidly into new areas which had not traditionally taken advantage of the techniques of numerical

simulation. Multidisciplinary codes and the future direction of CFD at Lewis are discussed. Author

N91-10843*# National Aeronautics and Space Administration. Marshall Space Flight Center, Huntsville, AL.
MARSHALL SPACE FLIGHT CENTER CFD OVERVIEW
Luke A. Schutzenhofer *In* NASA, Ames Research Center, NASA Computational Fluid Dynamics Conference. Volume 1: Sessions 1-6 Sep. 1989 p 65-94 (For primary document see N91-10839 02-02)
Avail: NTIS HC/MF A20; 25 functional color pages CSCL 01A

Computational Fluid Dynamics (CFD) activities at Marshall Space Flight Center (MSFC) have been focused on hardware specific and research applications with strong emphasis upon benchmark validation. The purpose here is to provide insight into the MSFC CFD related goals, objectives, current hardware related CFD activities, propulsion CFD research efforts and validation program, future near-term CFD hardware related programs, and CFD expectations. The current hardware programs where CFD has been successfully applied are the Space Shuttle Main Engines (SSME), Alternate Turbopump Development (ATD), and Aeroassist Flight Experiment (AFE). For the future near-term CFD hardware related activities, plans are being developed that address the implementation of CFD into the early design stages of the Space Transportation Main Engine (STME), Space Transportation Booster Engine (STBE), and the Environmental Control and Life Support System (ECLSS) for the Space Station. Finally, CFD expectations in the design environment will be delineated. Author

N91-10844*# National Aeronautics and Space Administration. Lyndon B. Johnson Space Center, Houston, TX.
JOHNSON SPACE CENTER CFD OVERVIEW
Chien P. Li *In* NASA, Ames Research Center, NASA Computational Fluid Dynamics Conference. Volume 1: Sessions 1-6 Sep. 1989 p 95-121 (For primary document see N91-10839 02-02)
Avail: NTIS HC/MF A20; 25 functional color pages CSCL 01A

Recent applications and development of CFD technology have focused on flow problems that are critically important to the operation and design of space flight vehicles. The main effort is spent on the Space Shuttle in order to provide an understanding of the cryogenic fluid in the duct connecting the External Tank and the Main Engines, the subsonic flow surrounding the Orbiter during crew egress maneuvers, the transonic aerodynamic forces on the Orbiter fuselage and wing, the high angle-of-attack abort flight, and the aerodynamic heating during entry. To provide in-depth analyses for such diverse problems within a timely schedule, matured panel codes and a state-of-the-art incompressible turbulent flow code were adapted. Collaboration with Ames Research Center has resulted in a Shuttle ascent aerodynamic code; and a viscous chemical nonequilibrium code is being developed for predicting Orbiter real-gas aerodynamics and finite-catalytic heating. The remaining activities are devoted to the prediction of the flow environment around the Aeroassist Flight Experiment vehicle at hypersonic speeds and high altitudes. A thermochemical nonequilibrium Navier-Stokes code has been developed on the basis of two- temperature and 11-species models for solving both the shock layer and near wake. After validating the code against wind-tunnel aerodynamic, pressure and heating data, the code is being used to supplement the ground test facilities in predicting a more realistic flight environment. CFD technology is being relied upon by other programs as well in the consideration of candidate configurations. Author

N91-10845*# National Aeronautics and Space Administration, Washington, DC.
NASA'S CFD VALIDATION PROGRAM
Dale R. Satran *In* NASA, Ames Research Center, NASA Computational Fluid Dynamics Conference. Volume 1: Sessions 1-6 Sep. 1989 p 123-134 (For primary document see N91-10839 02-02)
Avail: NTIS HC/MF A20; 25 functional color pages CSCL 01A

With computational fluid dynamics (CFD) becoming a productive research and design tool, the requirement to validate CFD codes has grown significantly. NASA had emphasized CFD validation activities since 1986 when a separate work element was formed to fund experimental activities related to validation. NASA's CFD and CFD validation programs are closely coordinated to ensure that experimental data bases are available as soon as possible for validating codes. In response to industry and academic requirements, four levels of experimental research have been defined as part of CFD validation with NASA's Aeronautics Advisory Committee (AAC) support although only the fourth level actually has the detailed information necessary for validating codes. Critical flow physics especially turbulence modeling are key to improved CFD codes. NASA has focused additional resources on transition and turbulence physics to meet these requirements. With improved turbulence models, CFD codes will be more accurate, robust, and efficient. However, with the level of detailed information available from CFD codes, highly accurate and detailed experiments are required to capture the critical information for validating codes. Advanced instrumentation especially non-intrusive instrumentation is required to acquire this information in validation experiments. The CFD validation program is being coordinated and managed to address these critical activities. A list of experiments which are currently being supported at least partially are included. Author

N91-10846*# National Aeronautics and Space Administration. Ames Research Center, Moffett Field, CA.
UNDERSTANDING TRANSITION AND TURBULENCE THROUGH DIRECT SIMULATIONS
P. R. Spalart and J. J. Kim *In its* NASA Computational Fluid Dynamics Conference. Volume 1: Sessions 1-6 Sep. 1989 p 137-149 (For primary document see N91-10839 02-02)
Avail: NTIS HC/MF A20; 25 functional color pages CSCL 01A

Direct simulations consist in solving the full Navier-Stokes equations, without any turbulence model, and describing all the detailed features of the flow. Usually the flows are three-dimensional and time-dependent and contain both coarse and fine structures, which makes the numerical task very challenging in terms of both the algorithm and the computational effort. Most of the work until now has involved spectral methods, which are highly accurate but not very flexible in terms of geometry or complex equations. For that reason, future work will also rely on high-order finite-difference or other methods. Direct simulations complement experimental work, and both contribute to the theory and the empirical knowledge of turbulence. Once such a simulation has been shown to be accurate, the flow field is completely known in three dimensions and time, including the pressure, the vorticity and any other quantity. On the other hand, most simulations to date solved the incompressible equations in rather simple geometries, and direct simulations will always be limited to moderate Reynolds numbers. Extensive simulations have been conducted in homogeneous turbulence, channel flows, boundary layers, and mixing layers. Much effort is devoted to addressing flows with compressibility and chemical reactions, and to new geometries such as a backward-facing step. Author

N91-10847*# National Aeronautics and Space Administration. Langley Research Center, Hampton, VA.
DIRECT SIMULATION OF COMPRESSIBLE TURBULENCE
T. A. Zang, Gordon Erlebacher, and M. Y. Hussaini (Institute for Computer Applications in Science and Engineering, Hampton, VA.) *In* NASA, Ames Research Center, NASA Computational Fluid Dynamics Conference. Volume 1: Sessions 1-6 Sep. 1989 p 151-165 (For primary document see N91-10839 02-02)
Avail: NTIS HC/MF A20; 25 functional color pages CSCL 01A

Several direct simulations of 3-D homogeneous, compressible turbulence are presented with emphasis on the differences with incompressible turbulent simulations. A fully spectral collocation algorithm, periodic in all directions coupled with a 3rd order Runge-Kutta time discretization scheme is sufficient to produce well-resolved flows at Taylor Reynolds numbers below 40 on grids of 128x128x128. A Helmholtz decomposition of velocity is useful to differentiate between the purely compressible effects and those effects solely due to vorticity production. In the context of

homogeneous flows, this decomposition in unique. Time-dependent energy and dissipation spectra of the compressible and solenoidal velocity components indicate the presence of localized small scale structures. These structures are strongly a function of the initial conditions. Researchers concentrate on a regime characterized by very small fluctuating Mach numbers Ma (on the order of 0.03) and density and temperature fluctuations much greater than sq Ma. This leads to a state in which more than 70 percent of the kinetic energy is contained in the so-called compressible component of the velocity. Furthermore, these conditions lead to the formation of curved weak shocks (or shocklets) which travel at approximately the sound speed across the physical domain. Various terms in the vorticity and divergence of velocity production equations are plotted versus time to gain some understanding of how small scales are actually formed. Possible links with Burger turbulence are examined. To visualize better the dynamics of the flow, new graphic visualization techniques have been developed. The 3-D structure of the shocks are visualized with the help of volume rendering algorithms developed in-house. A combination of stereographic projection and animation greatly increase the number of visual cues necessary to properly interpret the complex flow. Author

N91-10848*# National Aeronautics and Space Administration. Langley Research Center, Hampton, VA.
NON LINEAR EVOLUTION OF A SECOND MODE WAVE IN SUPERSONIC BOUNDARY LAYERS
Gordon Erlebacher and M. Y. Hussaini (Institute for Computer Applications in Science and Engineering, Hampton, VA.) *In* NASA, Ames Research Center, NASA Computational Fluid Dynamics Conference. Volume 1: Sessions 1-6 Sep. 1989 p 167-181 (For primary document see N91-10839 02-02)
Avail: NTIS HC/MF A20; 25 functional color pages CSCL 01A

Presented here are several direct simulations of one 2-D second mode perturbation wave, superimposed upon a prescribed mean flow. Periodicity is assumed in the streamwise direction (Fourier) and the variables are expanded in Chebyshev series in the direction normal to the flat plate. The code is fully explicit and is time advanced with a 3rd order Runge-Kutta scheme. The second mode wave (R delta prime = 8000), interacts with itself to generate higher streamwise harmonics. Physical parameters are chosen to maximize the linear growth rate at the prescribed Reynolds number. Initial results indicate that the nonlinear processes begin in the critical layer region and are the result of the cubic interactions in the momentum equations, rather than due to the higher streamwise harmonics. Analysis of the various terms in the momentum equations combined with numerical experiments in which various modes are artificially suppressed, lead to the conclusion that asymptotic methods will produce the saturated state in one or two order of magnitude less computer time than that required by the direct numerical simulations. Author

N91-10849*# National Aeronautics and Space Administration. Lewis Research Center, Cleveland, OH.
NUMERICAL SIMULATION OF NONLINEAR DEVELOPMENT OF INSTABILITY WAVES
Reda R. Mankbadi (Cairo Univ., Egypt) *In* NASA, Ames Research Center, NASA Computational Fluid Dynamics Conference. Volume 1: Sessions 1-6 Sep. 1989 p 183-191 (For primary document see N91-10839 02-02)
(E-4658) Avail: NTIS HC/MF A20; 25 functional color pages CSCL 01A

The nonlinear interactions of high amplitude instability waves in turbulent jets are described. In plane shear layers Riley and Metcalf (1980) and Monkewitz (1987) have shown that these interactions are dependent, among other parameters, on the phase-difference between the two instability waves. Therefore, here researchers consider the nonlinear development of both the amplitudes and the phase of the instability waves. The development of these waves are also coupled with the development of the mean flow and the background turbulence. In formulating this model it is assumed that each of the flow components can be characterized by conservation equations supplemented by closure models. Results for the interactions between the two instability waves under high-amplitude forcing at fundamental and subharmonic frequencies are presented here. Qualitative agreements are found between the present predictions and available experimental data. Author

N91-10850*# National Aeronautics and Space Administration. Ames Research Center, Moffett Field, CA.
MORE ACCURATE PREDICTIONS WITH TRANSONIC NAVIER-STOKES METHODS THROUGH IMPROVED TURBULENCE MODELING
Dennis A. Johnson *In its* NASA Computational Fluid Dynamics Conference. Volume 1: Sessions 1-6 Sep. 1989 p 193-204 (For primary document see N91-10839 02-02)
Avail: NTIS HC/MF A20; 25 functional color pages CSCL 01A

Significant improvements in predictive accuracies for off-design conditions are achievable through better turbulence modeling; and, without necessarily adding any significant complication to the numerics. One well established fact about turbulence is it is slow to respond to changes in the mean strain field. With the 'equilibrium' algebraic turbulence models no attempt is made to model this characteristic and as a consequence these turbulence models exaggerate the turbulent boundary layer's ability to produce turbulent Reynolds shear stresses in regions of adverse pressure gradient. As a consequence, too little momentum loss within the boundary layer is predicted in the region of the shock wave and along the aft part of the airfoil where the surface pressure undergoes further increases. Recently, a 'nonequilibrium' algebraic turbulence model was formulated which attempts to capture this important characteristic of turbulence. This 'nonequilibrium' algebraic model employs an ordinary differential equation to model the slow response of the turbulence to changes in local flow conditions. In its original form, there was some question as to whether this 'nonequilibrium' model performed as well as the 'equilibrium' models for weak interaction cases. However, this turbulence model has since been further improved wherein it now appears that this turbulence model performs at least as well as the 'equilibrium' models for weak interaction cases and for strong interaction cases represents a very significant improvement. The performance of this turbulence model relative to popular 'equilibrium' models is illustrated for three airfoil test cases of the 1987 AIAA Viscous Transonic Airfoil Workshop, Reno, Nevada. A form of this 'nonequilibrium' turbulence model is currently being applied to wing flows for which similar improvements in predictive accuracy are being realized. Author

N91-10851*# National Aeronautics and Space Administration. Langley Research Center, Hampton, VA.
RECENT ADVANCES IN RUNGE-KUTTA SCHEMES FOR SOLVING 3-D NAVIER-STOKES EQUATIONS
Veer N. Vatsa, Bruce W. Wedan, and Ridha Abid *In* NASA, Ames Research Center, NASA Computational Fluid Dynamics Conference. Volume 1: Sessions 1-6 Sep. 1989 p 207-221 Original contains color illustrations (For primary document see N91-10839 02-02)
Avail: NTIS HC/MF A20; 25 functional color pages CSCL 01A

A thin-layer Navier-Stokes has been developed for solving high Reynolds number, turbulent flows past aircraft components under transonic flow conditions. The computer code has been validated through data comparisons for flow past isolated wings, wing-body configurations, prolate spheroids and wings mounted inside wind-tunnels. The basic code employs an explicit Runge-Kutta time-stepping scheme to obtain steady state solution to the unsteady governing equations. Significant gain in the efficiency of the code has been obtained by implementing a multigrid acceleration technique to achieve steady-state solutions. The improved efficiency of the code has made it feasible to conduct grid-refinement and turbulence model studies in a reasonable amount of computer time. The non-equilibrium turbulence model of Johnson and King has been extended to three-dimensional flows and excellent agreement with pressure data has been obtained for transonic separated flow over a transport type of wing. Author

N91-10852*# National Aeronautics and Space Administration. Ames Research Center, Moffett Field, CA.
COMPUTATIONS OF THREE-DIMENSIONAL STEADY AND UNSTEADY VISCOUS INCOMPRESSIBLE FLOWS
Dochan Kwak, Stuart E. Rogers, Seokkwan Yoon, Moshe Rosenfeld, and Leon Chang *In its* NASA Computational Fluid Dynamics Conference. Volume 1: Sessions 1-6 Sep. 1989 p 223-237 (For primary document see N91-10839 02-02)
Avail: NTIS HC/MF A20; 25 functional color pages CSCL 01A

The INS3D family of computational fluid dynamics computer codes is presented. These codes are used to as tools in developing and assessing algorithms for solving the incompressible Navier-Stokes equations for steady-state and unsteady flow problems. This work involves applying the codes to real-world problems involving complex three-dimensional geometries. The algorithms utilized include the method of pseudocompressibility including both central and upwind differencing, several types of artificial dissipation schemes, approximate factorization, and an implicit line-relaxation scheme. These codes have been validated using a wide range of problems including flow over a backward-facing step, driven cavity flow, flow through various types of ducts, and steady and unsteady flow over a circular cylinder. Many diverse flow applications have been solved using these codes including parts of the Space Shuttle Main Engine, problems in naval hydrodynamics, low-speed aerodynamics, and biomedical fluid flows. The presentation details several of these, including the flow through a Space Shuttle Main Engine inducer, vortex shedding behind a circular cylinder, and flow through an artificial heart. Author

N91-10853*# National Aeronautics and Space Administration. Ames Research Center, Moffett Field, CA.
SAGE: A 2-D SELF-ADAPTIVE GRID EVOLUTION CODE AND ITS APPLICATION IN COMPUTATIONAL FLUID DYNAMICS
Carol B. Davies, Ethiraj Venkatapathy (Eloret Corp., Sunnyvale, CA.), and George S. Deiwert *In its* NASA Computational Fluid Dynamics Conference. Volume 1: Sessions 1-6 Sep. 1989 p 239-253 (For primary document see N91-10839 02-02)
Avail: NTIS HC/MF A20; 25 functional color pages CSCL 01A

SAGE is a user-friendly, highly efficient, two-dimensional self-adaptive grid code based on Nakahashi and Deiwert's variational principles method. Grid points are redistributed into regions of high flowfield gradients while maintaining smoothness and orthogonality of the grid. Efficiency is obtained by splitting the adaption into 2 directions and applying one-sided torsion control, thus producing a 1-D elliptic system that can be solved as a set of tridiagonal equations. Author

N91-10854*# National Aeronautics and Space Administration. Lewis Research Center, Cleveland, OH.
TIME DEPENDENT VISCOUS INCOMPRESSIBLE NAVIER-STOKES EQUATIONS
John W. Goodrich *In* NASA, Ames Research Center, NASA Computational Fluid Dynamics Conference. Volume 1: Sessions 1-6 Sep. 1989 p 255-270 (For primary document see N91-10839 02-02)
Avail: NTIS HC/MF A20; 25 functional color pages CSCL 01A

Information on time dependent incompressible Navier-Stokes equations is given in viewgraph form. Information is given on streamfunction equations for unsteady incompressible flow, the streamfunction algorithm for unsteady incompressible flow, and a multigrid solver for the laminar implicit equations. Author

N91-10855*# National Aeronautics and Space Administration. Ames Research Center, Moffett Field, CA.
CFD FOR APPLICATIONS TO AIRCRAFT AEROELASTICITY
Guru P. Guruswamy *In its* NASA Computational Fluid Dynamics Conference. Volume 1: Sessions 1-6 Sep. 1989 p 271-286 (For primary document see N91-10839 02-02)
Avail: NTIS HC/MF A20; 25 functional color pages CSCL 01A

Strong interactions of structures and fluids are common in many engineering environments. Such interactions can give rise to physically important phenomena such as those occurring for aircraft due to aeroelasticity. Aeroelasticity can significantly influence the safe performance of aircraft. At present exact methods are available for making aeroelastic computations when flows are in either the linear subsonic or supersonic range. However, for complex flows containing shock waves, vortices and flow separations, computational methods are still under development. Several phenomena that can be dangerous and limit the performance of an aircraft occur due to the interaction of these complex flows with flexible aircraft components such as wings. For example, aircraft with highly swept wings experience vortex induced aeroelastic oscillations. Correct understanding of these complex aeroelastic phenomena requires direct coupling of fluids and structural equations. Here, a summary is presented of the development of such coupled methods and applications to aeroelasticity since about 1978 to present. The successful use of the transonic small perturbation theory (TSP) coupled with structures is discussed. This served as a major stepping stone for the current stage of aeroelasticity using computational fluid dynamics. The need for the use of more exact Euler/Navier-Stokes (ENS) equations for aeroelastic problems is explained. The current development of unsteady aerodynamic and aeroelastic procedures based on the ENS equations are discussed. Aeroelastic results computed using both TSP and ENS equations are discussed. Author

N91-10856*# National Aeronautics and Space Administration. Langley Research Center, Hampton, VA.
APPLICATION OF UNSTRUCTURED GRID METHODS TO STEADY AND UNSTEADY AERODYNAMIC PROBLEMS
John T. Batina *In* NASA, Ames Research Center, NASA Computational Fluid Dynamics Conference. Volume 1: Sessions 1-6 Sep. 1989 p 287-308 Original contains color illustrations (For primary document see N91-10839 02-02)
Avail: NTIS HC/MF A20; 25 functional color pages CSCL 01A

The purpose is to describe the development of unstructured grid methods which have several advantages when compared to methods which make use of structured grids. Unstructured grids, for example, easily allow the treatment of complex geometries, allow for general mesh movement for realistic motions and structural deformations of complete aircraft configurations which is important for aeroelastic analysis, and enable adaptive mesh refinement to more accurately resolve the physics of the flow. Steady Euler calculations for a supersonic fighter configuration to demonstrate the complex geometry capability; unsteady Euler calculations for the supersonic fighter undergoing harmonic oscillations in a complete-vehicle bending mode to demonstrate the general mesh movement capability; and vortex-dominated conical-flow calculations for highly-swept delta wings to demonstrate the adaptive mesh refinement capability are discussed. The basic solution algorithm is a multi-stage Runge-Kutta time-stepping scheme with a finite-volume spatial discretization based on an unstructured grid of triangles in 2D or tetrahedra in 3D. The moving mesh capability is a general procedure which models each edge of each triangle (2D) or tetrahedra (3D) with a spring. The resulting static equilibrium equations which result from a summation of forces are then used to move the mesh to allow it to continuously conform to the instantaneous position or shape of the aircraft. The adaptive mesh refinement procedure enriches the unstructured mesh locally to more accurately resolve the vortical flow features. These capabilities are described in detail along with representative results which demonstrate several advantages of unstructured grid methods. The applicability of the unstructured grid methodology to steady and unsteady aerodynamic problems and directions for future work are discussed. Author

N91-10857*# National Aeronautics and Space Administration. Langley Research Center, Hampton, VA.
GRID GENERATION AND INVISCID FLOW COMPUTATION ABOUT AIRCRAFT GEOMETRIES
Robert E. Smith *In* NASA, Ames Research Center, NASA Computational Fluid Dynamics Conference. Volume 1: Sessions 1-6 Sep. 1989 p 311-326 Original contains color illustrations

(For primary document see N91-10839 02-02)
Avail: NTIS HC/MF A20; 25 functional color pages CSCL 01A

Grid generation and Euler flow about fighter aircraft are described. A fighter aircraft geometry is specified by an area ruled fuselage with an internal duct, cranked delta wing or strake/wing combinations, canard and/or horizontal tail surfaces, and vertical tail surfaces. The initial step before grid generation and flow computation is the determination of a suitable grid topology. The external grid topology that has been applied is called a dual-block topology which is a patched C (exp 1) continuous multiple-block system where inner blocks cover the highly-swept part of a cranked wing or strake, rearward inner-part of the wing, and tail components. Outer-blocks cover the remainder of the fuselage, outer-part of the wing, canards and extend to the far field boundaries. The grid generation is based on transfinite interpolation with Lagrangian blending functions. This procedure has been applied to the Langley experimental fighter configuration and a modified F-18 configuration. Supersonic flow between Mach 1.3 and 2.5 and angles of attack between 0 degrees and 10 degrees have been computed with associated Euler solvers based on the finite-volume approach. When coupling geometric details such as boundary layer diverter regions, duct regions with inlets and outlets, or slots with the general external grid, imposing C (exp 1) continuity can be extremely tedious. The approach taken here is to patch blocks together at common interfaces where there is no grid continuity, but enforce conservation in the finite-volume solution. The key to this technique is how to obtain the information required for a conservative interface. The Ramshaw technique which automates the computation of proportional areas of two overlapping grids on a planar surface and is suitable for coding was used. Researchers generated internal duct grids for the Langley experimental fighter configuration independent of the external grid topology, with a conservative interface at the inlet and outlet. Author

N91-10858*# National Aeronautics and Space Administration. Ames Research Center, Moffett Field, CA.
A ZONAL NAVIER-STOKES METHODOLOGY FOR FLOW SIMULATION ABOUT A COMPLETE AIRCRAFT
Jolen Flores *In its* NASA Computational Fluid Dynamics Conference. Volume 1: Sessions 1-6 Sep. 1989 p 327-343 Original contains color illustrations (For primary document see N91-10839 02-02)
Avail: NTIS HC/MF A20; 25 functional color pages CSCL 01A

The thin layer, Reynolds-averaged, Navier-Stokes equations are used to simulate the transonic viscous flow about the complete F-16A fighter aircraft. These computations demonstrate how computational fluid dynamics can be used to simulate turbulent viscous flow about realistic aircraft geometries. A zonal grid approach is used to provide adequate viscous grid clustering on all aircraft surfaces. Zonal grids extend inside the F-16A inlet and up to the compressor face while power on conditions are modeled by employing a zonal grid extending from the exhaust nozzle to the far field. Computations are compared with existing experimental data and are in fair agreement. Computations for the F-16A in side slip are also presented. Author

N91-10859*# National Aeronautics and Space Administration. Ames Research Center, Moffett Field, CA.
NUMERICAL SIMULATION OF F-18 FUSELAGE FOREBODY FLOWS AT HIGH ANGLES OF ATTACK
Lewis B. Schiff, Russell M. Cummings, Reese L. Sorenson, and Yehia M. Rizk (Sterling Software, Palo Alto, CA.) *In its* NASA Computational Fluid Dynamics Conference. Volume 1: Sessions 1-6 Sep. 1989 p 345-359 (For primary document see N91-10839 02-02)
Avail: NTIS HC/MF A20; 25 functional color pages CSCL 01A

Fine-grid Navier-Stokes solutions were obtained for flow over the fuselage forebody and wing leading edge extension of the F/A-18 High Alpha Research Vehicle at large incidence. The resulting flows are complex, and exhibit cross flow separation from the sides of the forebody and from the leading edge extension. A well-defined vortex pattern is observed in the leeward-side flow. Results obtained for laminar flow show good agreement with flow visualizations obtained in ground-based experiments. Further, turbulent flows computed at high Reynolds-number flight-test conditions show good agreement with surface and off-surface visualizations obtained in flight. Author

N91-10860*# National Aeronautics and Space Administration. Langley Research Center, Hampton, VA.
NAVIER-STOKES SOLUTIONS ABOUT THE F/A-18 FOREBODY-LEX CONFIGURATION
Farhad Ghaffari, James M. Luckring, James L. Thomas, and Brent L. Bates (Vigyan Research Associates, Inc., Hampton, VA.) *In* NASA, Ames Research Center, NASA Computational Fluid Dynamics Conference. Volume 1: Sessions 1-6 Sep. 1989 p 361-383 Original contains color illustrations (For primary document see N91-10839 02-02)
Avail: NTIS HC/MF A20; 25 functional color pages CSCL 01A

Three-dimensional viscous flow computations are presented for the F/A-18 forebody-LEX (Leading Edge EXtensions) geometry. Solutions are obtained from an algorithm for the compressible Navier-Stokes equations which incorporates an upwind-biased, flux-difference-splitting approach along with longitudinally-patched grids. Results are presented for both laminar and fully turbulent flow assumptions and include correlations with wind tunnel as well as flight-test results. A good quantitative agreement for the forebody surface pressure distribution is achieved between the turbulent computations and wind tunnel measurements at Mach number 0.6. The computed turbulent surface flow patterns on the forebody qualitatively agree well with in-flight surface flow patterns obtained on an F/A-18 aircraft at Mach number 0.34. Author

N91-10861*# National Aeronautics and Space Administration. Langley Research Center, Hampton, VA.
NAVIER-STOKES SOLUTIONS FOR FLOWS RELATED TO STORE SEPARATION
Oktay Baysal (Old Dominion Univ., Norfolk, VA.), Robert L. Stallings, Jr., and Elizabeth B. Plentovich *In* NASA, Ames Research Center, NASA Computational Fluid Dynamics Conference. Volume 1: Sessions 1-6 Sep. 1989 p 385-410 Original contains color illustrations (For primary document see N91-10839 02-02)
Avail: NTIS HC/MF A20; 25 functional color pages CSCL 01A

The objective is developing CFD capabilities to obtain solutions for viscous flows about generic configurations of internally and externally carried stores. The emphasis is placed on the supersonic flow regime with extensions being made to the transonic regime. The project is broken into four steps: (1) Cavity flows for internal carriage configurations; (2) High angle of attack flows, which may be experienced during the separation of the stores: (3) Flows about a body near a flat plate for external carriage configurations; and (4) Flows about a body inside or in the proximity of a cavity. Three-dimensional unsteady cavity flow solutions are obtained by an explicit, MacCormack algorithm, EMCAV3, for open, close, and transitional cavities. High angle of attack flows past cylinders are solved by an implicit, upwind algorithm. All the results compare favorably with the experimental data. For flows about multiple body configurations, the Chimera embedding scheme is modified for finite-volume and multigrid algorithms, MaGGiE. Then a finite volume, implicit, upwind, multigrid Navier-Stokes solver which uses on overlapped/embedded and zonal grids, VUMXZ3, is developed from the CFL3D code. Supersonic flows past a cylinder near a flat plate are computed using this code. The results are compared with the experimental data. Currently the VUMXZ3 code is being modified to accomplish step 4 of this project. Wind tunnel experiments are also being conducted for validation purposes. Author

N91-10862*# National Aeronautics and Space Administration. Ames Research Center, Moffett Field, CA.
TRANAIR: RECENT ADVANCES AND APPLICATIONS
Michael D. Madson *In its* NASA Computational Fluid Dynamics Conference. Volume 1: Sessions 1-6 Sep. 1989 p 411-427 (For primary document see N91-10839 02-02)
Avail: NTIS HC/MF A20; 25 functional color pages CSCL 01A

TranAir is a computer code which solves the full-potential

equation for transonic flow about very general and complex configurations. Piecewise flat surface panels are used to describe the surface geometry. This paneled definition is then embedded in an unstructured cartesian flow field grid. Finite elements are used in the discretization of the flow field grid in a manner which is fully conservative and second-order accurate. Since geometries may be defined with relative ease, and since the user is not involved in the generation of the flow field grid, computational results may be generated rather quickly for a wide range of geometries. For transonic cases in the cruise angle-of-attack range, TranAir has generated results which are in generally good agreement with both Euler results and wind tunnel data. A typical transonic case runs in 1 to 2 CPU hours on a Cray X-MP. For subcritical cases, the code runs in 15 to 30 CPU minutes, even for geometries in which several thousand surface panels are used in the definition. This ability to rapidly and accurately provide both subsonic and transonic predictions about very complex aircraft configurations gives TranAir the potential of being a very powerful and widely used design tool. Author

N91-10863*# National Aeronautics and Space Administration. Ames Research Center, Moffett Field, CA.
NUMERICAL SIMULATION OF ROTORCRAFT
William J. McCroskey (Army Aviation Systems Command, Moffett Field, CA.) *In its* NASA Computational Fluid Dynamics Conference. Volume 1: Sessions 1-6 Sep. 1989 p 431-446 Original contains color illustrations (For primary document see N91-10839 02-02)
Avail: NTIS HC/MF A20; 25 functional color pages CSCL 01A

The objective of the research is to develop and validate accurate, user-oriented viscous CFD codes (with inviscid options) for three-dimensional, unsteady aerodynamic flows about arbitrary rotorcraft configurations. Unsteady, three-dimensional Euler and Navier-Stokes codes are developed, adapted, and extended to rotor-body combinations. Flow solvers are coupled with zonal grid topologies, including rotating and nonrotating blocks. Special grid clustering and wave-fitting techniques were developed to capture low-level radiating acoustic waves. Significant progress was made in computing the propagation of acoustic waves due to the interaction of a concentrated vortex and a helicopter airfoil. The need for higher-order schemes was firmly established in relatively inexpensive two-dimensional calculations. In three dimensions, the number of grid points required to capture the low-level acoustic waves becomes very large, so that large supercomputer memory becomes essential. Good agreement was obtained between the numerical results obtained with a thin-layer Navier-Stokes code and experimental data from a model rotor. In addition, several nonrotating configurations that are sometimes proposed to simulate rotor blade tips in conventional wind tunnels were examined, and the complex flow around the radical tip shape of the world's fastest helicopter is under investigation. These studies demonstrate the flexibility and power of CFD to gain physical insight, study novel ideas, and examine various possibilities that might be difficult or impossible to set up in physical experiments. As a prelude to studies of rotor-body aerodynamic interactions, a preliminary grid topology and moving-interface strategy were developed. A new Euler/Navier-Stokes code using these techniques computes the vortical wake directly, rather than modeling it, as in most previous rotorcraft studies. Several hover cases were run for conventional and advanced-geometry blades. Numerical schemes using multi-zones and/or adaptive grids appear to be necessary to simulate the complex vortical flows in rotor wakes. Author

N91-10864*# Sterling Federal Systems, Inc., Moffett Field, CA.
CALCULATION OF THE ROTOR INDUCED DOWNLOAD ON AIRFOILS
C. S. Lee *In* NASA, Ames Research Center, NASA Computational Fluid Dynamics Conference. Volume 1: Sessions 1-6 Sep. 1989 p 447-458 (For primary document see N91-10839 02-02)
Avail: NTIS HC/MF A20; 25 functional color pages CSCL 01A

Interactions between the rotors and wing of a rotary wing aircraft in hover have a significant detrimental effect on its payload performance. The reduction of payload results from the wake of lifting rotors impinging on the wing, which is at 90 deg angle of attack in hover. This vertical drag, often referred as download, can be as large as 15 percent of the total rotor thrust in hover. The rotor wake is a three-dimensional, unsteady flow with concentrated tip vortices. With the rotor tip vortices impinging on the upper surface of the wing, the flow over the wing is not only three-dimensional and unsteady, but also separated from the leading and trailing edges. A simplified two-dimensional model was developed to demonstrate the stability of the methodology. The flow model combines a panel method to represent the rotor and the wing, and a vortex method to track the wing wake. A parametric study of the download on a 20 percent thick elliptical airfoil below a rotor disk of uniform inflow was performed. Comparisons with experimental data are made where the data are available. This approach is now being extended to three-dimensional flows. Preliminary results on a wing at 90 deg angle of attack in free stream is presented. Author

N91-10865*# National Aeronautics and Space Administration. Ames Research Center, Moffett Field, CA.
THREE-DIMENSIONAL VISCOUS DRAG PREDICTION FOR ROTOR BLADES
Ching S. Chen (National Academy of Sciences - National Research Council, Washington, DC.) *In its* NASA Computational Fluid Dynamics Conference. Volume 1: Sessions 1-6 Sep. 1989 p 459-472 (For primary document see N91-10839 02-02)
Avail: NTIS HC/MF A20; 25 functional color pages CSCL 01A

The state-of-the-art in rotor blade drag prediction involves the use of two-dimensional airfoil tables to calculate the drag force on the blade. One of the most serious problems with the current methods is that they cannot be used for airfoils that have yet to be tested. Most of the drag prediction methods also do not take the Reynolds number or the rotational effects of the blade into account, raising doubts about the accuracy of the results. These problems are addressed with the development of an analytical method which includes the shape of airfoil, the effects of Reynolds number, and the rotational motion of the blade. Author

N91-10866*# National Aeronautics and Space Administration. Lewis Research Center, Cleveland, OH.
PROGRESS TOWARD THE DEVELOPMENT OF AN AIRFOIL ICING ANALYSIS CAPABILITY
Mark G. Potapczuk, Colin S. Bidwell, and Brian M. Berkowitz (Sverdrup Technology, Inc., Mayfield, OH.) *In* NASA, Ames Research Center, NASA Computational Fluid Dynamics Conference. Volume 1: Sessions 1-6 Sep. 1989 p 473-487 (For primary document see N91-10839 02-02)
Avail: NTIS HC/MF A20; 25 functional color pages CSCL 01A

The NASA-Lewis aircraft icing analysis program is composed of three major sub-programs. These sub-programs are ice accretion simulation, performance degradation evaluation, and ice protection system evaluation. These topics cover all areas of concern related to the simulation of aircraft icing and its consequences. The motivation for these activities is twofold, reduction of time and effort required in experimental programs and the ability to provide reliable information for aircraft certification in icing, over the complete range of environmental conditions. In addition to the analytical activities associated with development of these codes, several experimental programs are underway to provide verification information for existing codes. These experimental programs are also used to investigate the physical processes associated with ice accretion and removal for improvement of present analytical models. The NASA-Lewis icing analysis program is thus striving to provide a full range of analytical tools necessary for evaluation of the consequences of icing and of ice protection systems. Author

N91-10867*# National Aeronautics and Space Administration. Lewis Research Center, Cleveland, OH.
THE BREAKUP OF TRAILING-LINE VORTICES
David Jacqmin *In* NASA, Ames Research Center, NASA Computational Fluid Dynamics Conference. Volume 1: Sessions

1-6 Sep. 1989 p 489-494 (For primary document see N91-10839 02-02)
Avail: NTIS HC/MF A20; 25 functional color pages CSCL 01A

It is now known that Batchelor's trailing-line vortex is extremely unstable to small amplitude disturbances for swirl numbers in the neighborhood of 0.83. The results of numerical calculations are presented that show the response of the vortex in this range of swirl numbers to finite amplitude, temporal, helical disturbances. Phenomena observed include: (1) ejection of axial vorticity and momentum from the core resulting in the creation of secondary, separate vortices; (2) a great intensification of core axial vorticity and a weakening of core momentum; and (3) the production of azimuthal vorticity in the form of a tightly wrapped spiral wave. The second phenomenon eventually stablizes the vortex, which then smooths and gradually returns to an axisymmetric state. The calculations are mixed spectral-finite-difference, fourth-order accurate, and have been carried out at Reynolds numbers of 1000 to 2000. Some linearized results are also discussed in an attempt to explain the process of vortex intensification. Author

N91-10868*# National Aeronautics and Space Administration. Ames Research Center, Moffett Field, CA.
NASA COMPUTATIONAL FLUID DYNAMICS CONFERENCE. VOLUME 2: SESSIONS 7-12
Sep. 1989 525 p Conference held at Moffett Field, CA, 7-9 Mar. 1989 Original contains color illustrations
(NASA-CP-10038-Vol-2; A-89160-Vol-2; NAS 1.55:10038-Vol-2)
Avail: NTIS HC/MF A22; 30 functional color pages CSCL 01A

The objectives of the conference were to disseminate CFD research results to industry and university CFD researchers, to promote synergy among NASA CFD researchers, and to permit feedback from researchers outside of NASA on issues pacing the discipline of CFD. The focus of the conference was on the application of CFD technology but also included fundamental activities. For individual titles, see N91-10869 through N91-10901.

N91-10869*# National Aeronautics and Space Administration. Langley Research Center, Hampton, VA.
A COMPARATIVE STUDY OF NAVIER-STOKES CODES FOR HIGH-SPEED FLOWS
David H. Rudy, James L. Thomas, Ajay Kumar, Peter A. Gnoffo, and Sukumar R. Chakravarthy (Rockwell International Science Center, Thousand Oaks, CA.) *In* NASA, Ames Research Center, NASA Computational Fluid Dynamics Conference. Volume 2: Sessions 7-12 Sep. 1989 p 3-18 (For primary document see N91-10868 02-02)
Avail: NTIS HC/MF A22; 30 functional color pages CSCL 01A

A comparative study was made with four different codes for solving the compressible Navier-Stokes equations using three different test problems. The first of these cases was hypersonic flow through the P8 inlet, which represents inlet configurations typical of a hypersonic airbreathing vehicle. The free-stream Mach number in this case was 7.4. This 2-D inlet was designed to provide an internal compression ratio of 8. Initial calculations were made using two state-of-the-art finite-volume upwind codes, CFL3D and USA-PG2, as well as NASCRIN, a code which uses the unsplit finite-difference technique of MacCormack. All of these codes used the same algebraic eddy-viscosity turbulence model. In the experiment, the cowl lip was slightly blunted; however, for the computations, a sharp cowl leading edge was used to simplify the construction of the grid. The second test problem was the supersonic (Mach 3.0) flow in a three-dimensional corner formed by the intersection of two wedges with equal wedge angles of 9.48 degrees. The flow in such a corner is representative of the flow in the corners of a scramjet inlet. Calculations were made for both laminar and turbulent flow and compared with experimental data. The three-dimensional versions of the three codes used for the inlet study (CFL3D, USA-PG3, and SCRAMIN, respectively) were used for this case. For the laminar corner flow, a fourth code, LAURA, which also uses recently-developed upwind technology, was also utilized. The final test case is the two-dimensional hypersonic flow over a compression ramp. The flow is laminar with a free-stream Mach number of 14.1. In the experiment, the ramp angle was varied to change the strength of the ramp shock and the extent of the viscous-inviscid interaction. Calculations were made for the 24-degree ramp configuration which produces a large separated-flow region that extends upstream of the corner. Author

N91-10870*# National Aeronautics and Space Administration. Langley Research Center, Hampton, VA.
MODELING OF HIGH SPEED CHEMICALLY REACTING FLOW-FIELDS
J. P. Drummond, Mark H. Carpenter, and H. Kamath (Analytical Services and Materials, Inc., Hampton, VA.) *In* NASA, Ames Research Center, NASA Computational Fluid Dynamics Conference. Volume 2: Sessions 7-12 Sep. 1989 p 19-41 (For primary document see N91-10868 02-02)
Avail: NTIS HC/MF A22; 30 functional color pages CSCL 01A

The SPARK3D and SPARK3D-PNS computer programs were developed to model 3-D supersonic, chemically reacting flow-fields. The SPARK3D code is a full Navier-Stokes solver, and is suitable for use in scramjet combustors and other regions where recirculation may be present. The SPARK3D-PNS is a parabolized Navier-Stokes solver and provides an efficient means of calculating steady-state combustor far-fields and nozzles. Each code has a generalized chemistry package, making modeling of any chemically reacting flow possible. Research activities by the Langley group range from addressing fundamental theoretical issues to simulating problems of practical importance. Algorithmic development includes work on higher order and upwind spatial difference schemes. Direct numerical simulations employ these algorithms to address the fundamental issues of flow stability and transition, and the chemical reaction of supersonic mixing layers and jets. It is believed that this work will lend greater insight into phenomenological model development for simulating supersonic chemically reacting flows in practical combustors. Currently, the SPARK3D and SPARK3D-PNS codes are used to study problems of engineering interest, including various injector designs and 3-D combustor-nozzle configurations. Examples, which demonstrate the capabilities of each code are presented. Author

N91-10871*# Sverdrup Technology, Inc., Cleveland, OH.
THREE-DIMENSIONAL CALCULATION OF SUPERSONIC REACTING FLOWS USING AN LU SCHEME
Sheng-Tao Yu, Y-L Peter Tsai, and Jian-Shun Shuen *In* NASA, Ames Research Center, NASA Computational Fluid Dynamics Conference. Volume 2: Sessions 7-12 Sep. 1989 p 43-57 (For primary document see N91-10868 02-02)
Avail: NTIS HC/MF A22; 30 functional color pages CSCL 01A

A new three-dimensional numerical program incorporated with comprehensive real gas property models was developed to simulate supersonic reacting flows. The code employs an implicit finite volume, Lower-Upper (LU) time-marching method to solve the complete Navier-Stokes and species equations in a fully-coupled and very efficient manner. A chemistry model with nine species and eighteen reaction steps are adopted in the program to represent the chemical reaction of H2 and air. To demonstrate the capability of the program, flow fields of underexpanded hydrogen jets transversely injected into supersonic air stream inside the combustors of scramjets are calculated. Results clearly depict the flow characteristics, including the shock structure, separated flow regions around the injector, and the distribution of the combustion products. Author

N91-10872*# National Aeronautics and Space Administration. Ames Research Center, Moffett Field, CA.
PROGRESS IN COMPUTING NOZZLE/PLUME FLOW FIELDS
Stephen M. Ruffin, Ethiraj Venkatapathy, William J. Feiereisen, and Seung-Ho Lee (Eloret Corp., Sunnyvale, CA.) *In its* NASA Computational Fluid Dynamics Conference. Volume 2: Sessions 7-12 Sep. 1989 p 59-74 Original contains color illustrations (For primary document see N91-10868 02-02)
Avail: NTIS HC/MF A22; 30 functional color pages CSCL 01A

The long-term goal is to develop the capability to predict chemically-reacting, multi-stream nozzle and plume flow fields. Two

basic Navier-Stokes solvers, including the widely used F-3D code, are upgraded to include several upwind difference schemes and portable chemistry packages. Current computational capabilities for solving equilibrium single-stream and multi-stream, frozen gas, and finite rate chemistry problems are described. A variety of complex nozzle and plume flows were computed. Solutions presented include axisymmetric plume flow for ideal and equilibrium air, 3-D NASP nozzle/afterbody flow, and an internal nozzle calculation comparing various finite-rate chemistry packages.
Author

N91-10873*# National Aeronautics and Space Administration. Langley Research Center, Hampton, VA.
APPLICATION OF CFD CODES FOR THE SIMULATION OF SCRAMJET COMBUSTOR FLOWFIELDS
Tawit Chitsomboom (Vigyan Research Associates, Inc., Hampton, VA.) and G. Burton Northam *In* NASA, Ames Research Center, NASA Computational Fluid Dynamics Conference. Volume 2: Sessions 7-12 Sep. 1989 p 75-89 (For primary document see N91-10868 02-02)
Avail: NTIS HC/MF A22; 30 functional color pages CSCL 01A

An overview of CFD activities in the Hypersonic Propulsion Branch is given. Elliptic and PNS codes that are being used for the simulation of hydrogen-air combusting flowfields for scramjet applications are discussed. Results of the computer codes are shown in comparison with those of the experiments where applicable. Two classes of experiments will be presented: parallel injection of hydrogen into vitiated supersonic air flow; and normal injection of hydrogen into supersonic crossflow of vitiated air.
Author

N91-10874*# National Aeronautics and Space Administration. Langley Research Center, Hampton, VA.
HYPERSONIC CFD APPLICATIONS AT NASA LANGLEY USING CFL3D AND CFL3DE
Pamela F. Richardson *In* NASA, Ames Research Center, NASA Computational Fluid Dynamics Conference. Volume 2: Sessions 7-12 Sep. 1989 p 91-113 Original contains color illustrations (For primary document see N91-10868 02-02)
Avail: NTIS HC/MF A22; 30 functional color pages CSCL 01A

The CFL3D/CFL3DE CFD codes and the industrial use status of the codes are outlined. Comparison of grid density, pressure, heat transfer, and aerodynamic coefficience are presented. Future plans related to the National Aerospace Plane Program are briefly outlined.
Author

N91-10875*# National Aeronautics and Space Administration. Lyndon B. Johnson Space Center, Houston, TX.
NUMERICAL AERODYNAMIC SIMULATION OF THE SPACE SHUTTLE ASCENT ENVIRONMENT
Jeff P. Slotnick, F. W. Martin, Jr., P. G. Buning, Ing-Tsau Chiu, R. L. Meakin, Shigeru Obayashi, Yehia M. Rizk, S. Ben-Shmuel, Joseph L. Steger, and M. Yarrow (National Aeronautics and Space Administration. Ames Research Center, Moffett Field, CA.) *In* NASA, Ames Research Center, NASA Computational Fluid Dynamics Conference. Volume 2: Sessions 7-12 Sep. 1989 p 117-131 (For primary document see N91-10868 02-02)
Avail: NTIS HC/MF A22; 30 functional color pages CSCL 01A

After the STS 51-L accident, an extensive review of the Space Shuttle Orbiter's ascent aerodynamic loads uncovered several questionable areas that required further analysis. The insight gained by comparing the Shuttle ascent CFD numerical simulations, obtained by the NASA Ames Space Shuttle Flow Simulation Group, to the current IVBC-3 aerodynamic loads database was instrumental in resolving uncertainties on the Orbiter payload bay doors and fuselage. Initial confidence in the numerical simulations was gained by comparing them with the limited flight data that had been obtained during the Orbiter Flight Test (OFT) program. Current CFD results exist for Mach numbers 0.6, 0.9, 1.05, 1.55, 2.0, and 2.5. Since the pre STS-1 wind tunnel test program (IA-105) often yields considerable differences when compared to STS-5 flight data, the M(sub infinity) = 1.05 transonic case is the most investigated. The IA308 mated-vehicle hot gas plume wind tunnel test, recently completed at AEDC 16T (transonic) and Lewis (hypersonic), is also used to compare with the computation where applicable.
Author

N91-10876*# Lockheed Engineering and Sciences Co., Houston, TX.
COMPUTATIONAL FLUID DYNAMICS ANALYSIS OF SPACE SHUTTLE MAIN PROPULSION FEED LINE 17-INCH DISCONNECT VALVES
Max Kandula and Daniel Pearce *In* NASA, Ames Research Center, NASA Computational Fluid Dynamics Conference. Volume 2: Sessions 7-12 Sep. 1989 p 133-148 (For primary document see N91-10868 02-02)
Avail: NTIS HC/MF A22; 30 functional color pages CSCL 01A

A steady incompressible three-dimensional (3-D) viscous flow analysis was conducted for the Space Shuttle Main Propulsion External Tank (ET)/Orbiter (ORB) propellant feed line quick separable 17-inch disconnect flapper valves for liquid oxygen (LO2) and liquid hydrogen (LH2). The main objectives of the analysis were to predict and correlate the hydrodynamic stability of the flappers and pressure drop with available water test data. Computational Fluid Dynamics (CFD) computer codes were procured at no cost from the public domain, and were modified and extended to carry out the disconnect flow analysis. The grid generator codes SVTGD3D and INGRID were obtained. NASA Ames Research Center supplied the flow solution code INS3D, and the color graphics code PLOT3D. A driver routine was developed to automate the grid generation process. Components such as pipes, elbows, and flappers can be generated with simple commands, and flapper angles can be varied easily. The flow solver INS3D code was modified to treat interior flappers, and other interfacing routines were developed, which include a turbulence model, a force/moment routine, a time-step routine, and initial and boundary conditions. In particular, an under-relaxation scheme was implemented to enhance the solution stability. Major physical assumptions and simplifications made in the analysis include the neglect of linkages, slightly reduced flapper diameter, and smooth solid surfaces. A grid size of 54 x 21 x 25 was employed for both the LO2 and LH2 units. Mixing length theory applied to turbulent shear flow in pipes formed the basis for the simple turbulence model. Results of the analysis are presented for LO2 and LH2 disconnects.
Author

N91-10877*# National Aeronautics and Space Administration. Marshall Space Flight Center, Huntsville, AL.
ANALYSIS OF THE SSME HPOTP BEARING INLET CAVITY
P. K. McConnaughey *In* NASA, Ames Research Center, NASA Computational Fluid Dynamics Conference. Volume 2: Sessions 7-12 Sep. 1989 p 149-160 (For primary document see N91-10868 02-02)
Avail: NTIS HC/MF A22; 30 functional color pages CSCL 01A

Analysis of the flow in the Space Shuttle Main Engine (SSME) high pressure oxygen turbopump (HPOTP) bearing no. 1 inlet cavity was completed in support of return-to-flight. With the incorporation of several design changes in the Phase 2 turbopump, rotordynamic stability of the pumps was enhanced, but the durability and life of the LOX-cooled bearings has decreased. During the post-Challenger SSME recertification, the causes of limited bearing durability were investigated. One topic addressed was the flow environment upstream of the pump-end bearing and the effect of seal exit swirl and a cavity anti-vortex rib on the bearing environment and life. The objective is to define the hydrodynamic environment upstream of the pump-end bearing and determine the effect of seal exit swirl and the anti-vortex rib on bearing inlet swirl. The problem was posed as an axisymmetric cavity flow with the computational domain extending from the seal exit to the bearing inlet. This domain was discretized with 22800 grid points. Boundary conditions were obtained from a 1-D model of the SSME coolant path. The inlet Mach number was 0.19 and the problem was solved with the CMINT code utilizing the Briley-McDonald/Beam-Warming algorithm with preconditioning to speed convergence at low Mach numbers. Three parametric cases with inlet swirl of 50 percent shaft speed (labyrinth seal), 20 percent

shaft speed (damping seal), and no inlet swirl were considered. Computational results indicate large vortical flow structures in the cavity, with the labyrinth, damping, and no-swirl cases yielding bearing inlet swirl rates of 14, 10, and 9 percent of shaft speed, respectively. When these results were used as input to the SHABRETH bearing model, limited durability could not be explained by these small differences in swirl. Also, based on these results, a proposed design change for the cavity anti-vortex rib was not implemented by the SSME chief engineer. Author

N91-10878*# National Aeronautics and Space Administration. Marshall Space Flight Center, Huntsville, AL.

A COMBINED EULERIAN-LAGRANGIAN TWO-PHASE ANALYSIS OF THE SSME HPOTP NOZZLE PLUG TRAJECTORIES

Robert Garcia, P. K. McConnaughey, F. J. deJong, J. S. Sabnis, and D. Pribik (Rockwell International Corp., Canoga Park, CA.) *In* NASA, Ames Research Center, NASA Computational Fluid Dynamics Conference. Volume 2: Sessions 7-12 Sep. 1989 p 161-177 Original contains color illustrations (For primary document see N91-10868 02-02)

Avail: NTIS HC/MF A22; 30 functional color pages CSCL 01A

As a result of high cycle fatigue, hydrogen embrittlement, and extended engine use, it was observed in testing that the trailing edge on the first stage nozzle plug in the High Pressure Oxygen Turbopump (HPOTP) could detach. The objective was to predict the trajectories followed by particles exiting the turbine. Experiments had shown that the heat exchanger soils, which lie downstream of the turbine, would be ruptured by particles traveling in the order of 360 ft/sec. An axisymmetric solution of the flow was obtained from the work of Lin et. al., who used INS3D to obtain the solution. The particle trajectories were obtained using the method of de Jong et. al., which employs Lagrangian tracking of the particle through the Eulerian flow field. The collision parameters were obtained from experiments conducted by Rocketdyne using problem specific alloys, speeds, and projectile geometries. A complete 3-D analysis using the most likely collision parameters shows maximum particle velocities of 200 ft/sec. in the heat exchanger region. Subsequent to this analysis, an engine level test was conducted in which seven particles passed through the turbine but no damage was observed on the heat exchanger coils. Author

N91-10879*# National Aeronautics and Space Administration. Marshall Space Flight Center, Huntsville, AL.

CONJUGATE (SOLID/FLUID) COMPUTATIONAL FLUID DYNAMICS ANALYSIS OF THE SPACE SHUTTLE SOLID ROCKET MOTOR NOZZLE/CASE AND CASE FIELD JOINTS

D. Doran, L. W. Keeton, P. J. Dionne, and A. K. Singhal (CFD Research Corp., Huntsville, ALa.) *In* NASA, Ames Research Center, NASA Computational Fluid Dynamics Conference. Volume 2: Sessions 7-12 Sep. 1989 p 179-191 (For primary document see N91-10868 02-02)

Avail: NTIS HC/MF A22; 30 functional color pages CSCL 01A

Three-dimensional, conjugate (solid/fluid) heat transfer analyses of new designs of the Solid Rocket Motor (SRM) nozzle/case and case field joints are described. The main focus was to predict the consequences of multiple rips (or debonds) in the ambient cure adhesive packed between the nozzle/case joint surfaces and the bond line between the mating field joint surfaces. The models calculate the transient temperature responses of the various materials neighboring postulated flow/leakpaths into, past, and out from the nozzle/case primary O-ring cavity and case field capture O-ring cavity. These results were used to assess if the design was failsafe (i.e., no potential O-ring erosion) and reusable (i.e., no excessive steel temperatures). The models are adaptions and extensions of the general purpose PHOENICS fluid dynamics code. A non-orthogonal coordinate system was employed and 11,592 control cells for the nozzle/case and 20,088 for the case field joints are used with non-uniform distribution. Physical properties of both fluid and solids are temperature dependent. A number of parametric studies were run for both joints with results showing temperature limits for reuse for the steel case on the nozzle joint being exceeded while the steel case temperatures for the field joint were not. O-ring temperatures for the nozzle joint predicted erosion while for the field joint they did not. Author

N91-10880*# National Aeronautics and Space Administration. Lewis Research Center, Cleveland, OH.

SIMULATION OF TURBOMACHINERY FLOWS

John J. Adamczyk *In* NASA, Ames Research Center, NASA Computational Fluid Dynamics Conference. Volume 2: Sessions 7-12 Sep. 1989 p 195-204 (For primary document see N91-10868 02-02)

Avail: NTIS HC/MF A22; 30 functional color pages CSCL 01A

Significant advancements have been made in the last five years in the ability to model turbomachinery flows of engineering interest. This advancement can be directly attributed to the second generation of supercomputers like the Cray XMP and Cray 2 and advanced instrumentation techniques. Early on, the National Aeronautics and Space Administration Lewis Research Center recognized the potential gains in turbomachinery performance and life that could be achieved by taking advantage of this technology and instituted a comprehensive research program in turbomachinery flow modeling. This activity combined the areas of fluid flow analysis, computational fluid dynamics, and experimental fluid mechanics. As a result of this activity, Lewis has become an internationally recognized leader in turbomachinery flow modeling. Many of the research activities conducted under this program are utilized by industry. The presentation gives an overview of this program and provides sample illustration of simulation performed to date. Author

N91-10881*# National Aeronautics and Space Administration. Ames Research Center, Moffett Field, CA.

PREDICTION OF TURBINE ROTOR-STATOR INTERACTION USING NAVIER-STOKES METHODS

Nateri K. Madavan, Man Mohan Rai, and Sharad Gavali (Amdahl Corp., Sunnyvale, CA.) *In its* NASA Computational Fluid Dynamics Conference. Volume 2: Sessions 7-12 Sep. 1989 p 205-216 (For primary document see N91-10868 02-02)

Avail: NTIS HC/MF A22; 30 functional color pages CSCL 01A

Flows in turbomachinery are generally complex and do not easily lend themselves to numerical computation. The flows are three-dimensional and inherently unsteady. Complicated blade geometries and flow phenomena such as separation and periodic transition from laminar to turbulent flow add to the numerical complexity. Nevertheless, the accurate numerical analysis of such flows is a problem of considerable interest and practical importance to the turbomachinery community. Much of the early work in turbomachinery flow prediction focussed on airfoil cascades. While such analyses of flows in isolated airfoil rows have helped improve understanding of the flow phenomena and have gained widespread acceptance in the industrial community as a design tool, they do not yield any information regarding the unsteady effects arising out of rotor-stator aerodynamic interaction. These interaction effects become increasingly important as the distance between successive stator and rotor rows is decreased. Thus, the need exists for analytical tools that treat the rotor and stator airfoils as a system and provide information regarding the magnitude and the impact of the unsteady effects. The focus a three-dimensional, time-accurate, thin-layer Navier-Stokes code that was recently developed to study rotor-stator interaction problems. A system of patched and overlaid grids that move relative to each other is used to discretize the flow field and the governing equations are integrated using a third-order upwind scheme set in an iterative, implicit framework. The code was used to simulate subsonic flow through an axial turbine configuration for which considerable experimental data exists. Grid refinement studies were also conducted as part of the code validation process. The current status of the research, along with planned future directions, are also discussed. Author

N91-10882*# National Aeronautics and Space Administration. Marshall Space Flight Center, Huntsville, AL.
TURBINE STAGE AERODYNAMICS AND HEAT TRANSFER PREDICTION
Lisa W. Griffin and H. V. McConnaughey *In* NASA, Ames Research Center, NASA Computational Fluid Dynamics Conference. Volume 2: Sessions 7-12 Sep. 1989 p 217-229 (For primary document see N91-10868 02-02)
Avail: NTIS HC/MF A22; 30 functional color pages CSCL 01A

A numerical study of the aerodynamic and thermal environment associated with axial turbine stages is presented. Computations were performed using a modification of the unsteady NASA Ames viscous code, ROTOR1, and an improved version of the NASA Lewis steady inviscid cascade system MERIDL-TSONIC coupled with boundary layer codes BLAYER and STAN5. Two different turbine stages were analyzed: the first stage of the United Technologies Research Center Large Scale Rotating Rig (LSRR) and the first stage of the Space Shuttle Main Engine (SSME) high pressure fuel turbopump turbine. The time-averaged airfoil midspan pressure and heat transfer profiles were predicted for numerous thermal boundary conditions including adiabatic wall, prescribed surface temperature, and prescribed heat flux. Computed solutions are compared with each other and with experimental data in the case of the LSRR calculations. Modified ROTOR1 predictions of unsteady pressure envelopes and instantaneous contour plots are also presented for the SSME geometry. Relative merits of the two computational approaches are discussed. Author

N91-10883*# National Aeronautics and Space Administration. Lewis Research Center, Cleveland, OH.
AUTOMATED DESIGN OF CONTROLLED DIFFUSION BLADES
Jose M. Sanz *In* NASA, Ames Research Center, NASA Computational Fluid Dynamics Conference. Volume 2: Sessions 7-12 Sep. 1989 p 231-244 Previously announced in IAA as A89-15967 (For primary document see N91-10868 02-02)
Avail: NTIS HC/MF A22; 30 functional color pages CSCL 01A

A numerical automation procedure was developed to be used in conjunction with an inverse hodograph method for the design of controlled diffusion blades. With this procedure a cascade of airfoils with a prescribed solidity, inlet Mach No., inlet air flow angle and air flow turning can be produced automatically. The trailing edge thickness of the airfoil, an important quantity in inverse methods, is also prescribed. The automation procedure consists of a multi-dimensional Newton iteration in which the objective design conditions are achieved by acting on the hodograph input parameters of the underlying inverse code. The method, although more general in scope, is applied to the design of axial flow turbomachinery blade sections, both compressors and turbines. A collaborative effort with U.S. Engine Companies to identify designs of interest to the industry will be described. Author

N91-10884*# National Aeronautics and Space Administration. Lewis Research Center, Cleveland, OH.
NUMERICAL ANALYSIS OF FLOW THROUGH OSCILLATING CASCADE SECTIONS
Dennis L. Huff *In* NASA, Ames Research Center, NASA Computational Fluid Dynamics Conference. Volume 2: Sessions 7-12 Sep. 1989 p 245-257 Previously announced in IAA as A89-28413 (For primary document see N91-10868 02-02)
Avail: NTIS HC/MF A22; 30 functional color pages CSCL 01A

The design of turbomachinery blades requires the prevention of flutter for all operating conditions. However, flow field predictions used for aeroelastic analysis are not well understood for all flow regimes. The present research focuses on numerical solutions of the Euler and Navier-Stokes equations using an ADI procedure to model two-dimensional, transonic flow through oscillating cascades. The model prescribes harmonic pitching motions for the blade sections for both zero and non-zero inter-blade phase angles. The code introduces the use of a deforming grid technique for convenient specification of the periodic boundary conditions. Approximate nonreflecting boundary conditions have been coded for the inlet and exit boundary conditions. Sample unsteady solutions have been performed for an oscillating cascade and compared to experimental data. Also, test cases were fun for a flat plate cascade to compare with an unsteady, small-perturbation, subsonic analysis. The predictions for oscillating cascades with non-zero inter-blade phase angles are in good agreement with experimental data and small-perturbation theory. The zero degree inter-blade phase angle cases, which were near a resonant condition, differ from the experiment and theory. Studies on reflecting versus non-reflecting inlet and exit boundary conditions show that the treatment of the boundary can have a significant effect on the first harmonic, unsteady pressure distributions for certain flow conditions. This code is expected to be used as a tool for reviewing simpler models that do not include the full nonlinear aerodynamics or as a final check for designs against flutter in turbomachinery. Author

N91-10885*# National Aeronautics and Space Administration. Lewis Research Center, Cleveland, OH.
ANALYSIS OF THREE-DIMENSIONAL VISCOUS FLOW IN A SUPERSONIC THROUGHFLOW FAN
Rodrick V. Chima *In* NASA, Ames Research Center, NASA Computational Fluid Dynamics Conference. Volume 2: Sessions 7-12 Sep. 1989 p 259-272 (For primary document see N91-10868 02-02)
Avail: NTIS HC/MF A22; 30 functional color pages CSCL 01A

A 3-D Navier-Stokes code was developed for analysis of turbomachinery blade rows and other internal flows. The Navier-Stokes equations are written in a Cartesian coordinate system rotating about the x-axis, and then mapped to a general body-fitted coordinate system. Streamwise viscous terms are neglected using the thin layer assumption, and turbulence effects are modelled using the Baldwin-Lomax turbulence model. The equations are discretized using finite differences on stacked C-type grids and are solved using a multistage Runge-Kutta algorithm with a spatially varying time step and implicit residual smoothing. Calculations were made of the flow around a supersonic throughflow fan blade. The fan was designed as a key component in a supersonic cruise engine. The 3-D calculations were done on a 129x29x33 grid and took 50 minutes of cpu time. Comparisons with the quasi-3-D results show minor differences in loading due to 3-D effects. Particle traces show nearly 2-D flows near the pressure surface, but large secondary flows within the suction surface boundary layer. The horseshoe vortex ahead of the leading edge is clearly seen. Author

N91-10886*# National Aeronautics and Space Administration. Ames Research Center, Moffett Field, CA.
SIMULATION OF POWERED-LIFT FLOWS
William R. VanDalsem, Kalpana Chawla, Karlin R. Roth, Merritt H. Smith, Kuditipudi V. Rao, and Thomas C. Blum (Boeing Co., Seattle, WA.) *In its* NASA Computational Fluid Dynamics Conference. Volume 2: Sessions 7-12 Sep. 1989 p 275-290 (For primary document see N91-10868 02-02)
Avail: NTIS HC/MF A22; 30 functional color pages CSCL 01A

The primary objective is to expose government, industry, and academic scientists to work underway at NASA-Ames towards the application of CFD to the powered lift area. One goal is to produce the technologies which will be required in the application of numerical techniques to, for example, the Supersonic STOVL program. The progress to date on the following specific projects is presented: Jet in ground effect with crossflow; Jet in a crossflow; Delta planform with multiple jets in ground effect; Integration of CFD with thermal and acoustic analyses; Improved flow visualization techniques for unsteady flows; YAV-8B Harrier simulation program; and E-7 simulation program. Author

N91-10887*# National Aeronautics and Space Administration. Lewis Research Center, Cleveland, OH.
A NUMERICAL STUDY OF THE HOT GAS ENVIRONMENT AROUND A STOVL AIRCRAFT IN GROUND PROXIMITY
Thomas J. VanOverbeke and James D. Holdeman *In* NASA, Ames Research Center, NASA Computational Fluid Dynamics Conference. Volume 2: Sessions 7-12 Sep. 1989 p 291-310

Previously announced in IAA as A88-48752 Original contains color illustrations (For primary document see N91-10868 02-02)
Avail: NTIS HC/MF A22; 30 functional color pages CSCL 01A

The development of Short Takeoff Vertical Landing (STOVL) aircraft has historically been an empirical- and experienced-based technology. A 3-D turbulent flow CFD code was used to calculate the hot gas environment around an STOVL aircraft operating in ground proximity. Preliminary calculations are reported for a typical STOVL aircraft configuration to identify key features of the flow field, and to demonstrate and assess the capability of current 3-D CFD codes to calculate the temperature of the gases ingested at the engine inlet as a function of flow and geometric conditions. Author

N91-10888*# National Aeronautics and Space Administration. Lewis Research Center, Cleveland, OH.
CFD ANALYSIS FOR HIGH SPEED INLETS
Tom Benson *In* NASA, Ames Research Center, NASA Computational Fluid Dynamics Conference. Volume 2: Sessions 7-12 Sep. 1989 p 311-319 (For primary document see N91-10868 02-02)
Avail: NTIS HC/MF A22; 30 functional color pages CSCL 01A

The increased national interest in high speed flight has increased research for high speed propulsion components. The highly 3-D flows present in supersonic/hypersonic inlets are currently being studied at NASA-Lewis both experimentally and computationally using a family of steady Parabolized Navier-Stokes (PNS) and Navier-Stokes (NS) solvers and unsteady NS solvers. Some of the results of these efforts are presented with an emphasis on the comparison of the computational and experimental results. The flow in high speed inlets typically involves the interaction of compression shock waves and boundary layers on the internal surfaces. The fundamentals of these interactions have been studied experimentally for many years, while more recently, computations have been used to study these complex 3-D flow fields. Attempts to control the flow through boundary layer bleed are being investigated computationally prior to wind tunnel experiments. The ultimate goal is the higher performing inlets required for high speed flight. Author

N91-10889*# National Aeronautics and Space Administration. Langley Research Center, Hampton, VA.
THE USE OF A NAVIER-STOKES CODE IN THE WING DESIGN PROCESS
S. Naomi McMillin *In* NASA, Ames Research Center, NASA Computational Fluid Dynamics Conference. Volume 2: Sessions 7-12 Sep. 1989 p 321-342 Original contains color illustrations (For primary document see N91-10868 02-02)
Avail: NTIS HC/MF A22; 30 functional color pages CSCL 01A

The feasibility was determined of incorporating the Navier-Stokes computational code, CFL3D, into the supersonic wing design process. The approach taken is of two steps. The first step was to calibrate CFL3D against existing experimental data sets obtained on thin sharp edged delta wings. The experimental data identified six flow types which are dependent on the similarity parameters of Mach number and angle of attack normal to the leading edge. The calibration showed CFL3D capable of simulating these various separated and attached flow conditions. The second step was to use CFL3D to study the initial formation of leading edge separation over delta wings at supersonic speeds. This consisted of examining solutions obtained on a 65 deg delta wing at Mach number of 1.6 with varying cross sectional shapes. Reynolds number was held constant at 1000000 and the Baldwin-Lomax turbulence model was used. The study showed that through the use of leading edge radius and/or camber, the onset of leading edge separation can be delayed to a higher angle of attack than observed on a flat sharp edged wing. Based on the geometries studied, three wind tunnel models are being designed to verify these results. Author

N91-10890*# National Aeronautics and Space Administration. Langley Research Center, Hampton, VA.
APPLICATIONS OF A TRANSONIC WING DESIGN METHOD
Richard L. Campbell and Leigh A. Smith *In* NASA, Ames Research Center, NASA Computational Fluid Dynamics Conference. Volume 2: Sessions 7-12 Sep. 1989 p 343-358 (For primary document see N91-10868 02-02)
Avail: NTIS HC/MF A22; 30 functional color pages CSCL 01A

A method for designing wings and airfoils at transonic speeds using a predictor/corrector approach was developed. The procedure iterates between an aerodynamic code, which predicts the flow about a given geometry, and the design module, which compares the calculated and target pressure distributions and modifies the geometry using an algorithm that relates differences in pressure to a change in surface curvature. The modular nature of the design method makes it relatively simple to couple it to any analysis method. The iterative approach allows the design process and aerodynamic analysis to converge in parallel, significantly reducing the time required to reach a final design. Viscous and static aeroelastic effects can also be accounted for during the design or as a post-design correction. Results from several pilot design codes indicated that the method accurately reproduced pressure distributions as well as the coordinates of a given airfoil or wing by modifying an initial contour. The codes were applied to supercritical as well as conventional airfoils, forward- and aft-swept transport wings, and moderate-to-highly swept fighter wings. The design method was found to be robust and efficient, even for cases having fairly strong shocks. Author

N91-10891*# National Aeronautics and Space Administration. Langley Research Center, Hampton, VA.
AN EMBEDDED GRID FORMULATION APPLIED TO DELTA WINGS
James L. Thomas and Sherrie L. Krist (Vigyan Research Associates, Inc., Hampton, VA.) *In* NASA, Ames Research Center, NASA Computational Fluid Dynamics Conference. Volume 2: Sessions 7-12 Sep. 1989 p 361-377 (For primary document see N91-10868 02-02)
Avail: NTIS HC/MF A22; 30 functional color pages CSCL 01A

An embedded grid algorithm for the Euler and/or Navier-Stokes equations is developed and applied to delta wings at high angles of attack in low speed flow. The Navier-Stokes code is an implicit, finite volume algorithm, using flux difference splitting for the convective and pressure terms and central differencing for the viscous and heat transfer terms. Calculations are compared with detailed experimental results over an angle of attack range up to and beyond the maximum lift coefficient, corresponding to vortex breakdown at the trailing edge, for a delta wing nominally of unit aspect ratio. The results indicate that the overall flowfield, including surface pressures, surface streamlines, and vortex trajectories, can be simulated accurately with the global grid version of the present algorithm. However, comparison of computed velocities and vorticity with experimentally measured off-body values at an angle of attack of 20.5 deg indicates the core region is substantially more diffuse in the computations than that measured with either a five-hole probe or a laser velocimeter. Embedded grids, used to improve the numerical discretization in the core region, are formulated within the framework of the implicit, upwind-biased multi-grid algorithm. Structured levels of local nested refinements are made. Three-dimensional results for both Euler and Navier-Stokes calculations are shown, with up to 3 levels of embedded refinement. The embedding procedure was effective in eliminating a crossflow secondary separation produced in the Euler solutions on coarse grids. Author

N91-10892*# National Aeronautics and Space Administration. Ames Research Center, Moffett Field, CA.
UNSTRUCTURED MESH SOLUTION OF THE EULER AND NAVIER-STOKES EQUATIONS
Timothy J. Barth *In its* NASA Computational Fluid Dynamics Conference. Volume 2: Sessions 7-12 Sep. 1989 p 379-393 (For primary document see N91-10868 02-02)
Avail: NTIS HC/MF A22; 30 functional color pages CSCL 01A

Mesh generation procedures as well as solution algorithms for solving the Euler and Navier-Stokes equations on unstructured meshes are presented. The solution algorithms discussed utilize

approximate Riemann solver, upwind differencing to achieve high spatial accuracy. Numerical results for Euler flow over single and multi-element airfoils are presented. Author

N91-10893*# National Aeronautics and Space Administration. Langley Research Center, Hampton, VA.
THREE DIMENSIONAL UNSTRUCTURED GRIDS FOR THE SOLUTION OF THE EULER EQUATIONS
Clyde Gumbert, P. Parikh, S. Pirzadeh, and R. Loehner (George Washington Univ., Hampton, VA.) *In* NASA, Ames Research Center, NASA Computational Fluid Dynamics Conference. Volume 2: Sessions 7-12 Sep. 1989 p 395-436 Original contains color illustrations (For primary document see N91-10868 02-02)
Avail: NTIS HC/MF A22; 30 functional color pages CSCL 01A

The advancing front technique is being used to develop a code to generate grids around complex 3-D configurations for use in computing the invisid flow solutions by the Euler equations. By the advancing front technique points are introduced concurrently with the connectivity information so that a separate library is not required. The generation of a 3-D grid is accomplished in several steps. First the boundaries of the domain to be gridded must be described by two-, three- or four-sided surface patches. Next, a background mesh is required to control the grid spacing and stretching throughout the domain. This coarse tetrahedral grid is not required to conform to any of the boundaries. Next, each of the patches is mapped to 2-D, triangulated by the advancing front technique and mapped back to 3-D. These triangles form the initial front for the generation of the final tetrahedral mesh.
Author

N91-10894*# National Aeronautics and Space Administration. Lewis Research Center, Cleveland, OH.
FLUX SPLITTING ALGORITHMS FOR TWO-DIMENSIONAL VISCOUS FLOWS WITH FINITE-RATE CHEMISTRY
Jian-Shun Shuen (Sverdrup Technology, Inc., Cleveland, OH.) and Meng-Sing Liou *In* NASA, Ames Research Center, NASA Computational Fluid Dynamics Conference. Volume 2: Sessions 7-12 Sep. 1989 p 437-450 Previously announced in IAA as A89-28409 (For primary document see N91-10868 02-02)
Avail: NTIS HC/MF A22; 30 functional color pages CSCL 01A

The Roe flux difference splitting method was extended to treat 2-D viscous flows with nonequilibrium chemistry. The derivations have avoided unnecessary assumptions or approximations. For spatial discretization, the second-order Roe upwind differencing is used for the convective terms and central differencing for the viscous terms. An upwind-based TVD scheme is applied to eliminate oscillations and obtain a sharp representation of discontinuities. A two-state Runge-Kutta method is used to time integrate the discretized Navier-Stokes and species transport equations for the asymptotic steady solutions. The present method is then applied to two types of flows: the shock wave/boundary layer interaction problems and the jet in cross flows. Author

N91-10895*# National Aeronautics and Space Administration. Ames Research Center, Moffett Field, CA.
VISUALIZATION OF FLUID DYNAMICS AT NASA AMES c34
Val Watson *In its* NASA Computational Fluid Dynamics Conference. Volume 2: Sessions 7-12 Sep. 1989 p 451-465 (For primary document see N91-10868 02-02)
Avail: NTIS HC/MF A22; 30 functional color pages CSCL 01A

The hardware and software currently used for visualization of fluid dynamics at NASA Ames is described. The software includes programs to create scenes (for example particle traces representing the flow over an aircraft), programs to interactively view the scenes, and programs to control the creation of video tapes and 16mm movies. The hardware includes high performance graphics workstations, a high speed network, digital video equipment, and film recorders. Author

N91-10896*# National Aeronautics and Space Administration. Ames Research Center, Moffett Field, CA.
COMPUTATIONAL FLUID DYNAMICS ON A MASSIVELY PARALLEL COMPUTER c34
Dennis C. Jespersen and Creon Levit *In its* NASA Computational Fluid Dynamics Conference. Volume 2: Sessions 7-12 Sep. 1989 p 467-481 (For primary document see N91-10868 02-02)
Avail: NTIS HC/MF A22; 30 functional color pages CSCL 01A

A finite difference code was implemented for the compressible Navier-Stokes equations on the Connection Machine, a massively parallel computer. The code is based on the ARC2D/ARC3D program and uses the implicit factored algorithm of Beam and Warming. The codes uses odd-even elimination to solve linear systems. Timings and computation rates are given for the code, and a comparison is made with a Cray XMP. Author

N91-10897*# National Aeronautics and Space Administration. Langley Research Center, Hampton, VA.
CONSERVATION EQUATIONS AND PHYSICAL MODELS FOR HYPERSONIC AIR FLOWS OVER THE AEROASSIST FLIGHT EXPERIMENT VEHICLE
Peter A. Gnoffo *In* NASA, Ames Research Center, NASA Computational Fluid Dynamics Conference. Volume 2: Sessions 7-12 Sep. 1989 p 485-500 (For primary document see N91-10868 02-02)
Avail: NTIS HC/MF A22; 30 functional color pages CSCL 01A

The code development and application program for the Langley Aerothermodynamic Upwind Relaxation Algorithm (LAURA), with emphasis directed toward support of the Aeroassist Flight Experiment (AFE) in the near term and Aeroassisted Space Transfer Vehicle (ASTV) design in the long term is reviewed. LAURA is an upwind-biased, point-implicit relaxation algorithm for obtaining the numerical solution to the governing equations for 3-D, viscous, hypersonic flows in chemical and thermal nonequilibrium. The algorithm is derived using a finite volume formulation in which the inviscid components of flux across cell walls are described with Roe's averaging and Harten's entropy fix with second-order corrections based on Yee's Symmetric Total Variation Diminishing scheme. Because of the point-implicit relaxation strategy, the algorithm remains stable at large Courant numbers without the necessity of solving large, block tri-diagonal systems. A single relaxation step depends only on information from nearest neighbors. Predictions for pressure distributions, surface heating, and aerodynamic coefficients compare well with experimental data for Mach 10 flow over an AFE wind tunnel model. Predictions for the hypersonic flow of air in chemical and thermal nonequilibrium over the full scale AFE configuration obtained on a multi-domain grid are discussed. Author

N91-10898*# National Aeronautics and Space Administration. Ames Research Center, Moffett Field, CA.
THE COMPUTATION OF THERMO-CHEMICAL NONEQUILIBRIUM HYPERSONIC FLOWS
Graham Candler *In its* NASA Computational Fluid Dynamics Conference. Volume 2: Sessions 7-12 Sep. 1989 p 501-513 (For primary document see N91-10868 02-02)
Avail: NTIS HC/MF A22; 30 functional color pages CSCL 01A

Several conceptual designs for vehicles that would fly in the atmosphere at hypersonic speeds have been developed recently. For the proposed flight conditions the air in the shock layer that envelops the body is at a sufficiently high temperature to cause chemical reaction, vibrational excitation, and ionization. However, these processes occur at finite rates which, when coupled with large convection speeds, cause the gas to be removed from thermo-chemical equilibrium. This non-ideal behavior affects the aerothermal loading on the vehicle and has ramifications in its design. A numerical method to solve the equations that describe these types of flows in 2-D was developed. The state of the gas is represented with seven chemical species, a separate vibrational temperature for each diatomic species, an electron translational temperature, and a mass-average translational-rotational temperature for the heavy particles. The equations for this gas model are solved numerically in a fully coupled fashion using an implicit finite volume time-marching technique. Gauss-Seidel line-relaxation is used to reduce the cost of the solution and flux-dependent differencing is employed to maintain stability. The

numerical method was tested against several experiments. The calculated bow shock wave detachment on a sphere and two cones was compared to those measured in ground testing facilities. The computed peak electron number density on a sphere-cone was compared to that measured in a flight test. In each case the results from the numerical method were in excellent agreement with experiment. The technique was used to predict the aerothermal loads on an Aeroassisted Orbital Transfer Vehicle including radiative heating. These results indicate that the current physical model of high temperature air is appropriate and that the numerical algorithm is capable of treating this class of flows. Author

N91-10899*# National Aeronautics and Space Administration. Lyndon B. Johnson Space Center, Houston, TX.

AERODYNAMIC STABILITY AND HEATING ANALYSES FOR THE AEROASSIST FLIGHT EXPERIMENT VEHICLE

J. McGary and Chien P. Li *In* NASA, Ames Research Center, NASA Computational Fluid Dynamics Conference. Volume 2: Sessions 7-12 Sep. 1989 p 515-528 Prepared in cooperation with Lockheed Engineering and Sciences Co., Houston, TX (For primary document see N91-10868 02-02)

Avail: NTIS HC/MF A22; 30 functional color pages CSCL 01A

Since ground based flow simulations are presently unable to model flight conditions expected for AOTVs (Aeroassist Orbital Transfer Vehicle) and other hypersonic space vehicles, computer codes are being developed to provide design parameters necessary for structure, guidance, and control aspects. Over the past four years, VRFLO (Viscous Reactive Flow) has been written to model finite-rate chemistry and viscous effects for a variety of aerobrake bodies. VRFLO includes a number of unique features that are summarized as follows: (1) Grid generation is an integral part of the code for several aerobrake configurations which includes the wake flow region; (2) The formulation is valid for three air chemical models; (3) An ADI central difference technique is used to solve the Navier-Stokes and species continuity equations in split groups; and (4) Grid density and numerical damping are minimized by shock-fitting and conformal mapping of body points. Author

N91-10900*# National Aeronautics and Space Administration. Marshall Space Flight Center, Huntsville, AL.

AEROASSIST FLIGHT EXPERIMENT AERODYNAMICS AND AEROTHERMODYNAMICS

Edwin B. Brewer *In* NASA, Ames Research Center, NASA Computational Fluid Dynamics Conference. Volume 2: Sessions 7-12 Sep. 1989 p 529-543 Original contains color illustrations (For primary document see N91-10868 02-02)

Avail: NTIS HC/MF A22; 30 functional color pages CSCL 01A

The problem is to determine the transitional flow aerodynamics and aerothermodynamics, including the base flow characteristics, of the Aeroassist Flight Experiment (AFE). The justification for the computational fluid dynamic (CFD) Application stems from MSFC's system integration responsibility for the AFE. To insure that the AFE objectives are met, MSFC must understand the limitations and uncertainties of the design data. Perhaps the only method capable of handling the complex physics of the rarefied high energy AFE trajectory is Bird's Direct Simulation Monte Carlo (DSMC) technique. The 3-D code used in this analysis is applicable only to the AFE geometry. It uses the Variable Hard Sphere (VHS) collision model and five specie chemistry model available from Langley Research Center. The code is benchmarked against the AFE flight data and used as an Aeroassisted Space Transfer Vehicle (ASTV) design tool. The code is being used to understand the AFE flow field and verify or modify existing design data. Continued application to lower altitudes is testing the capability of the Numerical Aerodynamic Simulation Facility (NASF) to handle 3-D DSMC and its practicality as an ASTV/AFE design tool. Author

N91-10901*# National Aeronautics and Space Administration. Langley Research Center, Hampton, VA.

DIRECT SIMULATION OF RAREFIED HYPERSONIC FLOWS

James N. Moss *In* NASA, Ames Research Center, NASA Computational Fluid Dynamics Conference. Volume 2: Sessions 7-12 Sep. 1989 p 545-558 (For primary document see N91-10868 02-02)

Avail: NTIS HC/MF A22; 30 functional color pages CSCL 01A

As the capability of the space transportation vehicles (STV's) expand to meet the requirements for future space exploration and utilization, the effects of rarefied hypersonic flows will play a more significant role in defining the aerodynamic and aerothermodynamic performance of STV's. This is particularly true of the low lift/drag aeroassisted STV's where aerobraking occurs at relatively high altitudes and high velocity. Because of the limitations of the continuum description as expressed by the Navier-Stokes equations and the difficulties of solving the Boltzmann equation, the particle of molecular approach has been developed over the last three decades for modeling rarefied gas effects. The direct simulation Monte Carlo (DSMC) method of Bird is the most used method today for simulating rarefied flows. The DSMC method provides a direct physical simulation as opposed to a numerical solution of a set of model equations. This is accomplished by developing phenomenological models of the relevant physical events. The DSMC method accounts for translational, thermal, chemical, and radiative nonequilibrium effects. The general features of the DSMC method, the numerical requirements for obtaining meaningful results, the modeling used to simulate high temperature gas effects, and applications of the method to calculate the flow about an aeroassist flight experiment vehicle (AFE) are reviewed. The AFE simulates a geosynchronous return while entering the Earth's upper atmosphere at approximately 10 km/s. Results obtained using a general 3-D code are presented for the more rarefied portion of the atmospheric encounter (altitudes of 200 to 100 km) emphasizing surface, flowfield, and aerodynamic characteristics of the AFE. Finally, results obtained using axisymmetric and 1-D versions of the code are presented for lower altitude conditions. Author

N91-10902*# National Aeronautics and Space Administration. Langley Research Center, Hampton, VA.

PREDICTION OF EFFECTS OF WING CONTOUR MODIFICATIONS ON LOW-SPEED MAXIMUM LIFT AND TRANSONIC PERFORMANCE FOR THE EA-6B AIRCRAFT

Dennis O. Allison and E. G. Waggoner Washington Nov. 1990 48 p

(NASA-TP-3046; L-16741; NAS 1.60:3046) Avail: NTIS HC/MF A03 CSCL 01A

Computational predictions of the effects of wing contour modifications on maximum lift and transonic performance were made and verified against low speed and transonic wind tunnel data. This effort was part of a program to improve the maneuvering capability of the EA-6B electronics countermeasures aircraft, which evolved from the A-6 attack aircraft. The predictions were based on results from three computer codes which all include viscous effects: MCARF, a 2-D subsonic panel code; TAWFIVE, a transonic full potential code; and WBPPW, a transonic small disturbance potential flow code. The modifications were previously designed with the aid of these and other codes. The wing modifications consists of contour changes to the leading edge slats and trailing edge flaps and were designed for increased maximum lift with minimum effect on transonic performance. The prediction of the effects of the modifications are presented, with emphasis on verification through comparisons with wind tunnel data from the National Transonic Facility. Attention is focused on increments in low speed maximum lift and increments in transonic lift, pitching moment, and drag resulting from the contour modifications. Author

N91-10903*# Old Dominion Univ., Norfolk, VA. Dept. of Mechanical Engineering and Mechanics.

ANALYSIS AND CONTROL OF SUPERSONIC VORTEX BREAKDOWN FLOWS Progress Report, 1 Jan. - 15 Aug. 1990

Osama A. Kandil Aug. 1990 47 p

(Grant NAG1-994)

(NASA-CR-186897; NAS 1.26:186897) Avail: NTIS HC/MF A03 CSCL 01A

Analysis and computation of steady, compressible, quasi-axisymmetric flow of an isolated, slender vortex are consid-

ered. The compressible, Navier-Stokes equations are reduced to a simpler set by using the slenderness and quasi-axisymmetry assumptions. The resulting set along with a compatibility equation are transformed from the diverging physical domain to a rectangular computational domain. Solving for a compatible set of initial profiles and specifying a compatible set of boundary conditions, the equations are solved using a type-differencing scheme. Vortex breakdown locations are detected by the failure of the scheme to converge. Computational examples include isolated vortex flows at different Mach numbers, external axial-pressure gradients and swirl ratios. Author

N91-10904*# National Aeronautics and Space Administration. Langley Research Center, Hampton, VA.
CONICAL EULER SIMULATION AND ACTIVE SUPPRESSION OF DELTA WING ROCKING MOTION
Elizabeth M. Lee and John T. Batina Oct. 1990 34 p
(NASA-TM-102683; NAS 1.15:102683) Avail: NTIS HC/MF A03 CSCL 01A

A conical Euler code was developed to study unsteady vortex-dominated flows about rolling highly-swept delta wings, undergoing either forced or free-to-roll motions including active roll suppression. The flow solver of the code involves a multistage Runge-Kutta time-stepping scheme which uses a finite volume spatial discretization of the Euler equations on an unstructured grid of triangles. The code allows for the additional analysis of the free-to-roll case, by including the rigid-body equation of motion for its simultaneous time integration with the governing flow equations. Results are presented for a 75 deg swept sharp leading edge delta wing at a freestream Mach number of 1.2 and at alpha equal to 10 and 30 deg angle of attack. A forced harmonic analysis indicates that the rolling moment coefficient provides: (1) a positive damping at the lower angle of attack equal to 10 deg, which is verified in a free-to-roll calculation; (2) a negative damping at the higher angle of attack equal to 30 deg at the small roll amplitudes. A free-to-roll calculation for the latter case produces an initially divergent response, but as the amplitude of motion grows with time, the response transitions to a wing-rock type of limit cycle oscillation. The wing rocking motion may be actively suppressed, however, through the use of a rate-feedback control law and antisymmetrically deflected leading edge flaps. The descriptions of the conical Euler flow solver and the free-to-roll analysis are presented. Results are also presented which give insight into the flow physics associated with unsteady vortical flows about forced and free-to-roll delta wings, including the active roll suppression of this wing-rock phenomenon. Author

N91-10905# Center for Mathematics and Computer Science, Amsterdam (Netherlands). Dept. of Numerical Analysis.
DAMPED, DIRECTION-DEPENDENT MULTIGRID FOR HYPERSONIC FLOW COMPUTATIONS
B. Koren and P. W. Hemker Nov. 1989 19 p Sponsored by ESA
(CWI-NM-R8922; ETN-90-97676) Copyright Avail: NTIS HC/MF A03

A nonlinear multigrid technique with improved robustness is developed for the solution of the steady Euler equations. The system of nonlinear equations is discretized by an upwind finite volume method. Collective symmetric point Gauss-Seidel relaxation is applied as the standard smoothing technique. In case of failure of the point relaxation, a switch is made to a local evolution technique. The novel robustness improvements to the nonlinear multigrid method are a local damping of the restricted defect, and a global upwind prolongation of the correction. The defect damping is derived from a two grid convergence analysis. The upwind prolongation makes efficient use of the P-variant of Osher's approximate Riemann solver. Satisfactory convergence results are shown for the computation of a hypersonic launch and reentry flow around a blunt forebody with canopy. For test cases considered, it appears that the improved multigrid method performs significantly better than a standard nonlinear multigrid method. ESA

N91-10906 Colorado Univ., Boulder.
COMPUTATION OF TRANSONIC FLOW OVER ELASTIC ROTOR BLADE Ph.D. Thesis
Lie-Mine Gea 1989 121 p
Avail: Univ. Microfilms Order No. DA9024828

The understanding of the aeroelastic behavior of transonic rotor blades is essential in the design of advanced vertical-takeoff and landing vehicles such as the tilt-rotor and x-wing aircraft. A computational tool is developed by coupling an aerodynamic code with a structural dynamic code, which can be used to predict the performance of an elastic rotor blade when operating at transonic speeds. The full-potential transonic rotor flow code TFAR2, based on the finite-difference approach, is used to compute the inviscid, isentropic, and irrotational flow field in a blade-fixed coordinate system. On the other hand, the finite-element approach based on beam theory is employed in the structural dynamic code. Flutter equations are solved in time domain instead of in frequency domain of using modal analysis, and a global-local transformation matrix is derived to improve the accuracy for large blade deflections. The computer natural frequencies of a modal blade in the first five modes (three flapping, one lagging, and one torsion) agree very well with experimental data. To demonstrate the capability of this computational tool, both hovering and forward flight cases for the model blade are examined. Numerical results are presented separately to show the differences between rigid and elastic blade calculations. The comparison reveals that the blade elasticity plays an important role in the transonic regime, especially when the rotor is in forward flight. Dissert. Abstr.

N91-10907 Colorado Univ., Boulder.
EXPERIMENTAL INVESTIGATION OF THE MECHANISMS UNDERLYING VORTEX KINEMATICS IN UNSTEADY SEPARATED FLOWS Ph.D. Thesis
Scott Jeffrey Schreck 1989 155 p
Avail: Univ. Microfilms Order No. DA9024868

Current research in the area of unsteady separated flows has been strongly motivated by potential enhancements to air vehicle performance. Dynamic motions of lifting surfaces give rise to the emergence and fleeting presence of energetic, large-scale vortical structures characteristic of unsteady separated flow fields. While present over the lifting surface, these vortices substantially augment lift and moment coefficients and exact only modest penalties in terms of elevated drag coefficients. However, the feasibility of utilizing unsteady separation relies upon thorough comprehension of the fluid dynamic mechanisms responsible for vortex presence and behavior. To date, these mechanisms remain relatively obscure. Unsteady separated flow fields in the vicinity of a flat plate oscillating sinusoidally in pitch about the quarterchord were investigated for a broad range of pitching parameters. Phase locked photograph of smoke flow visualization was employed in conjunction with hotwire anemometry to quantify vortex development as well as some of the primary boundary layer interactions contributing to the observed vortex kinematics. Leading edge vortex development was strongly influenced by both the freestream and boundary layer flows. These and other observations facilitated formulation of a conceptual model which accounts for many of these observations. Quantitative refinement of such a model is one methodology through which unsteady separation may eventually be understood, predicted, and controlled for employment in future air vehicles. Dissert. Abstr.

N91-10908 Princeton Univ., NJ.
NONOVERLAPPING COMPOSITE MESHES FOR MULTI-ELEMENT AIR-FOILS Ph.D. Thesis
Mark Eric Michael Stewart 1990 157 p
Avail: Univ. Microfilms Order No. DA9024542

Developing the ability to place grids for numerical calculations in geometrically complex regions is a problem of current interest in many engineering and scientific disciplines. Its importance arises because grid generation is a prominent limitation in computational problems involving complex geometries. One direction of grid generation research is the multiblock approach where the domain is decomposed into simple, non-overlapping sub-regions. Multiblock

grids for non-trivial, three-dimensional aircraft configurations with solutions have been generated in the past. Yet, the procedures used are not automatic, and require substantial human intervention to determine the overall block structure, and grid point distribution. Automation of this procedure is necessary before these methods can come into common usage. A novel algorithm was developed and investigated for substantially automating the decomposition of arbitrary two-dimensional domains into non-overlapping, topologically rectangular blocks. To demonstrate the technique, solutions to the Euler equations for several multi-element airfoil configurations are presented, including a four element landing configuration. Further, accuracy estimates for the grids are developed analytically, and approximated numerically to demonstrate the accuracy characteristics of the singularities which occur in the grids. Dissert. Abstr.

N91-10909 Louisiana State Univ., Baton Rouge.
FINE SCALE VELOCITY MEASUREMENTS IN A TURBULENT JET IN A CONFINED CROSSFLOW Ph.D. Thesis
Julie Ann Mathis 1989 158 p
Avail: Univ. Microfilms Order No. DA9025320

Measurements of the fine scale velocity field are made for a turbulent jet in a confined crossflow. With a crossflow velocity of 10.0 m/sec, jet-to-crossflow velocity ratios of 1, 2, and 4 are examined. Velocity measurements are obtained by laser velocimetry. The velocimetry system consists of a 15 mW laser with a fringe mode optics setup, operated in the backscatter mode. Signal processing is accomplished with a tracker processor. At each measuring location, 28,400 velocity readings are obtained at a sampling frequency of 38,460/sec. Calculations include construction of autocorrelation functions, Kolmogorov-normalized energy spectra and their moments, skewness and flatness of the velocity derivatives, an estimate of mu (the constant appearing in Kolmogorov's lognormal hypothesis), and of the fractal dimension of the dissipation structures. Turbulent Reynolds numbers are found to range from 22 to 800. The average value of mu is found to be 0.31; it is also found to be Reynolds number dependent. The fractal dimension is estimated as 2.45. Dissert. Abstr.

N91-10910 North Carolina State Univ., Raleigh.
AERODYNAMIC INTERACTION OF COUNTER ROTATING PROPELLERS Ph.D. Thesis
Yoonsang Lee 1989 81 p
Avail: Univ. Microfilms Order No. DA9017689

Axial and circumferential flow velocity components were measured at discrete points between rotors of a 28 cm diameter counter rotating propeller using both a single and a two-component hot-film anemometer. The tests were performed in an open-jet anechoic wind tunnel with a 0.61 m x 0.61 m square nozzle and a free-stream speed of 0.09 Mach number. Primary test variables were radial and axial positions of the hot-film sensor and rotor-to-rotor spacing of the CRP. Axial flow measurements from a single sensor agreed well with those of a two-component X-probe. Single sensor and X-probe measurements of circumferential flow did not agree as well. Axial mean flow data show significant upstream influence of the aft rotor. The circumferential mean flow between rotors appears relatively uninfluenced by the aft rotor. Turbulence intensity abruptly increased near the blade tip suggesting a possible tip vortex from the forward rotor. Turbulence intensity decreased between rotors as rotor-to-rotor spacing increased. The analysis was extended to determine the velocity fluctuations at the blade passing frequencies and the blade interaction frequency. Velocity fluctuation at each of these discrete frequencies were observed, including the forward-aft rotor interaction frequencies. Dissert. Abstr.

N91-10911 Pennsylvania State Univ., University Park.
A COMPUTATIONAL MODEL FOR THE PREDICTION OF HYPERSONIC, REACTING FLOWS Ph.D. Thesis
Gregory Alan Molvik 1989 124 p
Avail: Univ. Microfilms Order No. DA9018255

Two new algorithms are presented to predict the flow of viscous, hypersonic, chemically reacting gases over three-dimensional bodies. Both algorithms take advantage of the benefits of upwind differencing, Total Variation Diminishing (TVD) techniques, and of a finite-volume framework, but obtain their solution in two separate manners. The first algorithm is a time-marching scheme, and is generally used to obtain solutions in the subsonic portions of the flow field. The second algorithm is a much less expensive, space-marching scheme and can be used for the computation of the larger, supersonic portion of the flow field. Both codes compute their interface fluxes with a new temporal Riemann solver and the resulting schemes are made fully implicit including all chemistry effects. Capabilities for perfect, equilibrium, and nonequilibrium gases were developed and a strong coupling is used between the fluid dynamic and chemical equations. Results are included for the hypersonic laminar flow of reacting air over three different geometries. Comparison of the results with existing experimental and computational data shows good agreement. Dissert. Abstr.

N91-10912 Washington Univ., Seattle.
NUMERICAL SIMULATION OF SHOCK-INDUCED COMBUSTION FOR APPLICATION TO THE RAM ACCELERATOR CONCEPT Ph.D. Thesis
Shaye Yungster 1989 110 p
Avail: Univ. Microfilms Order No. DA9020986

A numerical scheme for calculating hypersonic flows involving shock-induced combustion is presented. The scheme is applied to a hyper-velocity mass launcher concept known as the ram accelerator. The analysis is carried out using a TVD numerical scheme that includes nonequilibrium chemistry, real gas effects, and a 7 species-8 reaction combustion model for hydrogen/oxygen mixtures. Inviscid flow is assumed. The flow, combustion phenomena, and performance characteristics of the ram accelerator are investigated for several projectile configurations in the superdetonative velocity range of 5.0 to 10.0 km/s. The distribution of various physical quantities along the ram accelerator, as well as temperature contours, are presented. Plots of ballistic efficiency and thrust pressure ratio are also included. Ballistic efficiencies of up to 28 percent and thrust pressure ratios as high as 17 percent were obtained. The effects of nose blunting on the flow and combustion processes in the ram accelerator are also investigated for a particular configuration. Several code validation tests are presented. In particular, the hypersonic, exothermic blunt body flow problem is examined in detail for mixtures of hydrogen/oxygen and hydrogen/air, and the numerical results are compared with experimental results. Dissert. Abstr.

N91-10913 George Washington Univ., Washington, DC.
EJECTOR THRUST AUGMENTORS: PULSE-STARTING APPROACH TO THE SECOND SOLUTION Ph.D. Thesis
Mohamed Ahmed Abdel-Wahab 1990 156 p
Avail: Univ. Microfilms Order No. DA9020742

While the steady flow supersonic solution to the ejector problem has been studied analytically, experimental validation has been elusive. Lack of validation may be explained by the possibility that localized processes may violate the second law of thermodynamics even though there is no overall violation. To detect the process mechanism, a pulse-starting simulation, analogous to the one used to analyze supersonic and hypersonic shock tunnels, was used to analyze the dynamics of the ejector. Compared to the steady flow CFD approach, this method greatly reduces the uncertainties associated with simulating mixing processes. The computation analysis used can reveal local violation of the second law of thermodynamics that cannot be detected by control volume analysis and that would rule out a second solution even when the associated overall entropy increment is positive. Analysis also reveals important details of the mechanism by which momentum and energy are exchanged in flow induction devices operating on the basis of wave processes. To illustrate the application of the proposed method, the method of analysis was applied to a specific set of boundary conditions that would, according to control volume analysis, lead to a second solution only marginally permitted by the second law. Analysis is performed until the front of the advancing flow is a substantially normal shock. The study validates

the analysis and its conclusions for one case by a double-flow shock tube experiment. Dissert. Abstr.

N91-10914 Ohio State Univ., Columbus.
STRUCTURE OF SUPERSONIC TURBULENT REATTACHING SHEAR LAYERS Ph.D. Thesis
Bassam Abdel-Karim A Abu-Hijleh 1990 149 p
Avail: Univ. Microfilms Order No. DA9022469

The structure of a turbulent reattaching shear layer was studied experimentally. Modifying the structure of the shear layer via acoustic excitation was also explored. The flow field was generated by the geometrical separation of a Mach 1.83 fully developed turbulent boundary layer over a backward facing step. In the last set of the experiments, base blowing was used to extend the constant pressure region of the flow. The flow field was investigated using Schlieren systems, static and dynamic pressure measurements, and a two-component coincident laser Doppler velocimeter. The results of the unexcited flow showed that large scale structures formed in the separated shear layer. These structures had limited spanwise extent and/or were tilted relative to the mean flow direction. Going through recompression and reattachment, the structures seemed to remain spatially intact but lost their coherency. This process was accompanied with rigorous mixing and dissipation and was referred to as a reorientation process. A few step heights downstream of reattachment, the structures regained their coherency, formed a 40 to 45 deg angle with the mean flow direction, and convected downstream with minimal mixing and dissipation. The effect of acoustic excitation was inconclusive. Dissert. Abstr.

N91-10915 Oxford Univ. (England).
THE AERODYNAMIC EFFECTS OF NOZZLE GUIDE VANE SHOCK WAVE AND WAKE PASSING ON A TRANSONIC TURBINE ROTOR Ph.D. Thesis
A. B. Johnson 1988 233 p
Avail: Univ. Microfilms Order No. BRD-89420

Flow perturbations are intrinsic in the operation of any turbine and are often associated with the periodic chopping of the wakes from an upstream blade row by the next row. The effect of these perturbations on the aerodynamic performance of the passage, the thermal loading of the blades and the blade profile losses needs to be understood. An experimental study of some of these effects was made using a nozzle guide vane wake and trailing edge shock wave simulator. Measurements of time resolved and time averaged surface pressures and heat transfer rates were made, together with schlieren photography flow visualization tests. This was supported by tests made in a 9x3 inch induced flow transonic tunnel to examine the characteristics of the wakes and shock waves being tested by the simulation. The results were used to study the propagation of the shock waves and wakes through the rotor passage. Shock wave passing was shown to nucleate a vortex and separation bubble at the leading edge of the blade and cause a novel shock wave pressure surface interaction. The interaction between the shock wave and blade boundary layer can cause large, rapid fluctuations in the surface heat transfer rate, and a negative heat transfer rate in some cases. A theoretical model was proposed to explain this phenomenon. The passing of the wake over the pressure surface was shown to cause both positive and negative fluctuations in the surface heat transfer rate. Two computational fluid dynamics codes were tested to predict the steady and unsteady flows. A sensitivity to the effects of surface discontinuities was identified in one code. The results were compared with those found in the equivalent experimental tests with very good agreement. Dissert. Abstr.

N91-10916 Illinois Univ. at Urbana-Champaign, Savoy.
NUMERICAL CALCULATIONS FOR FLOWS PAST AN UNCONVENTIONAL AIRFOIL Ph.D. Thesis
Ping-Ho Tsai 1990 122 p
Avail: Univ. Microfilms Order No. DA9021770

A computer program was developed for both 2-D compressible and incompressible turbulent flows around airfoils. Numerical solutions were obtained by solving the steady state Reynolds-averaged Navier-Stokes equations in primitive variable form. The standard k-epsilon turbulence model was employed and a compression turbulence model was also discussed. Based on a non-staggered arrangement on a body-fitted grid system, the discretized transport equations were solved either by a hybrid or a second-order upwind differencing scheme. A multiple pressure correction procedure with implicit density treatment was used. The solutions were obtained through an under-relaxed iterative process. Various cases of flow past NACA 0012 and 4412 airfoils were examined first. The results were good when compared with experimental data. Many cases of incompressible and compressible flows past an unconventional airfoil were then computed. The general behavior of the unconventional airfoil is presented. Dissert. Abstr.

N91-10917# Oak Ridge National Lab., TN. Energy Div.
STUDY OF ASYMMETRIC SUPERSONIC JET FLOW FOR EJECTORS
C. M. Ho, G. S. Knoke, E. W. Geller, H. T. Liu, and W. H. Jou (Flow Research, Inc., Kent, WA.) 1990 13 p Presented at the International Symposium on Gas-Liquid Two-Phase Flows in Conjunction With the Winter Annual Meeting of the ASME, Dallas, TX, 25-30 Nov. 1990 Submitted for publication
(Contract DE-AC05-84OR-21400)
(DE90-015598; CONF-901109-14) Avail: NTIS HC/MF A03

An asymmetric subsonic jet nozzle with a small aspect ratio can entrain a mass several times higher than a circular jet can entrain in a low subsonic flow. In this study, we extend the Mach number of the jet to 2.5. The advantage an asymmetric jet has over a circular jet in enhancing mass transfer still exists in the supersonic range. The main objective of this study is to explore the possibility of applying the asymmetric jet to a supersonic ejector with pressure build-up. The wall confinement was found to have a strong effect on the entrainment. DOE

N91-10918*# National Aeronautics and Space Administration. Langley Research Center, Hampton, VA.
IMPLICIT FLUX-SPLIT EULER SCHEMES FOR UNSTEADY AERODYNAMIC ANALYSIS INVOLVING UNSTRUCTURED DYNAMIC MESHES
John T. Batina Nov. 1990 11 p Presented at the 31st AIAA/ASME/ASCE/AHS/ASC Structures, Structural Dynamics, and Materials Conference, Long Beach, CA, 2-4 Apr. 1990 Previously announced in IAA as A90-29362
(NASA-TM-102732; NAS 1.15:102732; AIAA-90-0936) Avail: NTIS HC/MF A03 CSCL 01A

Improved algorithm for the solution of the time-dependent Euler equations are presented for unsteady aerodynamic analysis involving unstructured dynamic meshes. The improvements were developed recently to the spatial and temporal discretizations used by unstructured grid flow solvers. The spatial discretization involves a flux-split approach which is naturally dissipative and captures shock waves sharply with at most one grid point within the shock structure. The temporal discretization involves an implicit time-integration scheme using a Gauss-Seidel relaxation procedure which is computationally efficient for either steady or unsteady flow problems. For example, very large time steps may be used for rapid convergence to steady state, and the step size for unsteady cases may be selected for temporal accuracy rather than for numerical stability. Steady and unsteady flow results are presented for the NACA 0012 airfoil to demonstrate applications of the new Euler solvers. The unsteady results were obtained for the airfoil pitching harmonically about the quarter chord. The resulting instantaneous pressure distributions and lift and moment coefficients during a cycle of motion compare well with experimental data. A description of the Euler solvers is presented along with results and comparisons which assess the capability. Author

N91-10919*# National Aeronautics and Space Administration. Langley Research Center, Hampton, VA.
TEMPORAL-ADAPTIVE EULER/NAVIER-STOKES ALGORITHM FOR UNSTEADY AERODYNAMIC ANALYSIS OF AIRFOILS USING UNSTRUCTURED DYNAMIC MESHES

William L. Kleb, John T. Batina, and Marc H. Williams (Purdue Univ., West Lafayette, IN.) Nov. 1990 10 p Presented at the 21st AIAA Fluid Dynamics, Plasma Dynamics, and Lasers Conference, Seattle, WA, 18-20 Jun. 1990 Previously announced in IAA as A90-38778
(NASA-TM-102734; NAS 1.15:102734; AIAA-90-1650) Avail: NTIS HC/MF A02 CSCL 01A

A temporal adaptive algorithm for the time-integration of the two-dimensional Euler or Navier-Stokes equations is presented. The flow solver involves an upwind flux-split spatial discretization for the convective terms and central differencing for the shear-stress and heat flux terms on an unstructured mesh of triangles. The temporal adaptive algorithm is a time-accurate integration procedure which allows flows with high spatial and temporal gradients to be computed efficiently by advancing each grid cell near its maximum allowable time step. Results indicate that an appreciable computational savings can be achieved for both inviscid and viscous unsteady airfoil problems using unstructured meshes without degrading spatial or temporal accuracy. Author

N91-10920# Deutsche Forschungsanstalt fuer Luft- und Raumfahrt, Goettingen (Germany, F.R.). Inst. fuer Aeroelastik.
CONTRIBUTIONS IN THE FIELD OF AEROELASTICS ON THE OCCASION OF THE 60TH ANNIVERSARY OF PROFESSOR DR.-ING. HABIL. HANS WILHELM FOERSCHING [BEITRAEGE AUS DEM BEREICH DER AEROELASTIK ZUM 60. GEBURTSTAG VON PROFESSOR DR.-ING. HABIL. HANS WILHELM FOERSCHING]
Apr. 1990 287 p In ENGLISH and GERMAN
(ETN-90-97630) Avail: NTIS HC/MF A13

A numerical procedure for the calculation of unsteady transonic flow about oscillating airfoils is presented. The status of stuctural dynamics qualification of spacecraft is depicted. Aeroelastics and dynamics of wind turbines are treated. The structural analysis and optimization of a propfan blade were studied using the finite element method. The derivative balance for a transonic wind tunnel was designed. The pressure distribution on an oscillating airfoil in incompressible flow was calculated. Unsteady aerodynamic forces on engines were determined with a view to flutter investigations. Unsteady wind tunnel wall interferences in subsonic and transonic profile flows were studied theoretically. Adaptive digital real time filtering in strutural dynamics was investigated. The nonlinear vibration of large, imperfect space structures was studied. For individual titles, see N91-10921 through N91-10932.

N91-10921# Deutsche Forschungsanstalt fuer Luft- und Raumfahrt, Goettingen (Germany, F.R.). Inst. fuer Aeroelastik.
THE CALCULATION OF UNSTEADY COMPRESSIBLE FLOW ABOUT OSCILLATING AIRFOIL PROFILES USING THE EULER UPWIND METHOD [DIE BERECHNUNG VON INSTATIONAEREN KOMPRESSIBLEN STROEMUNGEN UM SCHWINGENDE PROFILE MIT HILFE EINES EULER-UPWIND-VERFAHRENS]
Volker Carstens *In its* Contributions in the Field of Aeroelastics on the Occasion of the 60th Anniversary of Professor Dr.-Ing. Habil. Hans Wilhelm Foersching Apr. 1990 p 13-3 In GERMAN; ENGLISH summary (For primary document see N91-10920 02-02)
Avail: NTIS HC/MF A13

A numerical procedure for the calculation of the unsteady transonic flow about oscillating airfoils, based on the Euler equations in conservative form is presented. The selected solution method, called flux vector splitting, is similar to a characteristic method, and is characterized by the use of spatially one sided differences (upwinding). This method has a good numerical stability and excellent shock capturing properties. The wall boundary conditions at the profile surface, and, in the case of unsteady flow, the nonreflecting boundary conditions at the outer grid boundary were implemented in a numerical algorithm. The close agreement between numerical results and experimental data is illustrated by an AGARD standard test case. Numerical results for reduced frequencies give an impression of the influence of the reduced frequency on unsteady pressure and lift. ESA

N91-10922# Deutsche Forschungsanstalt fuer Luft- und Raumfahrt, Goettingen (Germany, F.R.). Inst. fuer Aeroelastik.
STRUCTURAL DYNAMICS QUALIFICATION OF SPACECRAFT [STRUKTURDYNAMISCHE QUALIFIKATION VON RAUMFAHRZEUGEN]
H. Hueners *In its* Contributions in the Field of Aeroelastics on the Occasion of the 60th Anniversary of Professor Dr.-Ing. Habil. Hans Wilhelm Foersching Apr. 1990 p 39-5 In GERMAN; ENGLISH summary (For primary document see N91-10920 02-02)
Avail: NTIS HC/MF A13

The status of various feasibility studies on improved spacecraft dynamic qualification concepts using hydraulic multi-axial vibration simulators is presented. Dynamic mechanical loads in the low frequency range determine to a large extent the design of the primary and partially the secondary structures of most present day spacecraft. A dynamic qualification concept based on an experimental flight load simulation requires a multi-axis transient test approach, which cannot be offered current vibration test specifications. Vibration tests on single-axis electrodynamic shakers, flight load simulation on multi-axis hydraulic vibration simulators, and the further development of multi-axis hydraulic test stands are described. The possible prospects of the approach to dynamic structural verification are discussed. ESA

N91-10923# Deutsche Forschungsanstalt fuer Luft- und Raumfahrt, Goettingen (Germany, F.R.). Inst. fuer Aeroelastik.
AEROELASTICS AND DYNAMICS OF WIND TURBINES [ZUR AEROELASTIK UND DYNAMIK VON WINDTURBINEN]
Fritz Kiessling and Martin Rippl *In its* Contributions in the Field of Aeroelastics on the Occasion of the 60th Anniversary of Professor Dr.-Ing. Habil. Hans Wilhelm Foersching Apr. 1990 p 55-8 In GERMAN; ENGLISH summary (For primary document see N91-10920 02-02)
Avail: NTIS HC/MF A13

Computational and experimental procedures for investigating aeroelastic stability and dynamic response of wind turbines for electricity production are presented. The emphasis was on the wind turbine with horizontal axis and high speed rotor. It is shown that the known construction recommendations against aeroelastic problems are also valid for wind turbines. The aeroelastic and dynamic correlations in wind turbines are not always easy to assess, as illustrated by selected examples. ESA

N91-10924# Deutsche Forschungsanstalt fuer Luft- und Raumfahrt, Goettingen (Germany, F.R.). Inst. fuer Aeroelastik.
STRUCTURAL ANALYSIS AND OPTIMIZATION OF A PROPFAN-BLADE BY USE OF THE FINITE ELEMENT METHOD
Rolf Lammering *In its* Contributions in the Field of Aeroelastics on the Occasion of the 60th Anniversary of Professor Dr.-Ing. Habil. Hans Wilhelm Foersching Apr. 1990 p 85-104 Previously announced as N90-26006 (For primary document see N91-10920 02-02)
Avail: NTIS HC/MF A13

Algorithms applicable to the finite element method were used for the structural analysis of advanced propellers (propfans). The propfan blade was discretized as a shallow shell. The constitutive equations for isotropic and for layered material were implemented into the formulation of the finite elements. The quasistatic deformations resulting from centrifrugal forces as well as the eigenmodes and eigenfrequencies are presented. For a propfan blade of composite material the methods of mathematical optimization were used to minimize the displacement at the blade tip, using the fiber orientation as a design variable. In a second calculation, the twisting of the blade was minimized. It is shown that the deformation behavior can be greatly influenced by the fiber orientation. ESA

N91-10925# Deutsche Forschungsanstalt fuer Luft- und Raumfahrt, Goettingen (Germany, F.R.). Inst. fuer Aeroelastik.
DESIGN OF THE DERIVATIVE BALANCE FOR THE TRANSONIC WIND TUNNEL [KONSTRUKTIVE AUSLEGUNG DER TRANSKANAL-DERIVATIVAWAAGE (TRAD)] **c09**
Eberhard Schmidt and Joachim Wagener *In its* Contributions in the Field of Aeroelastics on the Occasion of the 60th Anniversary of Professor Dr.-Ing. Habil. Hans Wilhelm Foersching Apr. 1990 p 105-125 In GERMAN; ENGLISH summary (For primary document see N91-10920 02-02)
Avail: NTIS HC/MF A13

The design of a dynamic derivative balance for a transonic wind tunnel is presented. Several technical problems had to be overcome to obtain, despite the extremely high model loads (normal force of 2800 N at an angle of attack of 32 deg), oscillatory model motions with constant amplitudes, while limiting the rig diameter within the model to that of a conventional strain gauge force balance. The final construction of the five component balance, the spring element bearings for pitch and roll oscillations, and the forcing mechanisms for the sinusoidal motions using a stepping motor drive are described. These technical details may be useful for the design of other dynamic test installations or special industrial machinery. ESA

N91-10926# Deutsche Forschungsanstalt fuer Luft- und Raumfahrt, Goettingen (Germany, F.R.). Inst. fuer Aeroelastik.
CALCULATION OF THE PRESSURE DISTRIBUTION ON AN OSCILLATING AIRFOIL IN INCOMPRESSIBLE FLOW CONSIDERING NONLINEAR EFFECTS Ph.D. Thesis
Lorenz Tichy *In its* Contributions in the Field of Aeroelastics on the Occasion of the 60th Anniversary of Professor Dr.-Ing. Habil. Hans Wilhelm Foersching Apr. 1990 p 127-139 (For primary document see N91-10920 02-02)
Avail: NTIS HC/MF A13

Panel methods were used to calculate the pressure on a two dimensional airfoil which performs harmonic plunging and pitching oscillations in an incompressible potential flow. Two panel methods are described which allow the examination of the influence of profile and wake geometries on pressure distribution and aerodynamic coefficients. The first method operates in the frequency domain; it only takes into account the nonlinear influences resulting from the slope of the airfoil contour (i.e., from airfoil thickness and angle of attack). The second method is applicable in the time domain; it provides a more exact description of the wake geometry. Comparisons of the results from both methods with the linear flat plate solution demonstrate the significance of the above mentioned influences. ESA

N91-10927# Deutsche Forschungsanstalt fuer Luft- und Raumfahrt, Goettingen (Germany, F.R.). Inst. fuer Aeroelastik.
DETERMINATION OF UNSTEADY AERODYNAMIC FORCES ON ENGINES WITH A VIEW TO FLUTTER INVESTIGATIONS [BESTIMMUNG INSTATIONAERER TRIEBWERKSLUFTKRAEFTE FUER DIE ANWENDUNG BEI FLATTERUNTERSUCHUNGEN] **c07**
Hermann Triebstein, Guenter Schewe, and Hartmut Zingel (Messerschmitt-Boelkow-Blohm G.m.b.H., Bremen, Germany, F.R.) *In its* Contributions in the Field of Aeroelastics on the Occasion of the 60th Anniversary of Professor Dr.-Ing. Habil. Hans Wilhelm Foersching Apr. 1990 p 141-168 In GERMAN; ENGLISH summary (For primary document see N91-10920 02-02)
Avail: NTIS HC/MF A13

Experimental investigations of the steady and unsteady aerodynamic forces were performed on an ejector engine model and a wing/engine combination in the subsonic and transonic regimes. The aim was to find out how well the commonly used aerodynamic models for flutter calculations correspond to the actual conditions observed in engines. The comparison of experimental and theoretical results shows that the linear lifting surface theory provides quite accurate unsteady aerodynamic forces. The effects of Mach number and reduced frequency are correctly described. For the wing/engine combination the unsteady interference effect for engine oscillation on the lower side of the wing is strongly influenced by flow separation at the wing/pylon connection. In general, the unsteady aerodynamic forces on the wing are small and, at this order of magitude, can be correctly calculated with the linear lifting surface theory. The interference effect on the oscillating wing on the engine is much more significant. ESA

N91-10928# Deutsche Forschungsanstalt fuer Luft- und Raumfahrt, Goettingen (Germany, F.R.). Inst. fuer Aeroelastik.
UNSTEADY WIND TUNNEL WALL INTERFERENCES IN SUBSONIC AND TRANSONIC PROFILE FLOWS [INSTATIONAERE WINDKANALWAND-INTERFERENZEN BEI SUB- UND TRANSSONISCHER PROFILUMSTROEMUNG] **c09**
Ralph Voss *In its* Contributions in the Field of Aeroelastics on the Occasion of the 60th Anniversary of Professor Dr.-Ing. Habil. Hans Wilhelm Foersching Apr. 1990 p 169-185 In GERMAN; ENGLISH summary (For primary document see N91-10920 02-02)
Avail: NTIS HC/MF A13

Unsteady wind tunnel wall interference effects in subsonic and transonic flows about oscillating 2-D airfoils were theoretically investigated using a panel method and a finite difference time marching method. The results show strong effects on magnitude and phase of unsteady pressure and lift coefficients. Transonic interference effects are even stronger than the well known subsonic ones. Tunnel resonance appears in subsonic and transonic flows for the same flow parameters. Based on the subsonic panel method transonic measurements can be approximately corrected for unsteady interference effects, if pressure distributions at the walls are known. ESA

N91-10929# Deutsche Forschungsanstalt fuer Luft- und Raumfahrt, Goettingen (Germany, F.R.). Inst. fuer Aeroelastik.
ADAPTIVE DIGITAL REAL TIME FILTERING IN STRUCTURAL DYNAMICS: A CONTRIBUTION TO THE REALIZATION ON ACTIVELY REACTING ELASTIC STRUCTURES (ARES) [ADAPTIVE DIGITALE ECHTZEITFILTERUNG IN DER STRUKTURDYNAMIK: EIN BEITRAG ZUR REALISIERUNG AKTIV REAGIERENDER ELASTISCHER STRUKTUREN (ARES)] **c63**
Roger Wimmel and Joerg Melcher *In its* Contributions in the Field of Aeroelastics on the Occasion of the 60th Anniversary of Professor Dr.-Ing. Habil. Hans Wilhelm Foersching Apr. 1990 p 187-202 In GERMAN; ENGLISH summary (For primary document see N91-10920 02-02)
Avail: NTIS HC/MF A13

Adaptive digital real time filtering was investigated in the framework of the research program ARES for active shape control and active vibration suppression on technical systems. The efforts were focussed on active impedance control using adaptive digital controllers which are based on much more stringent specifications than ever before. The principles of capabilities of such controllers, which consist of digital real time filters, are described and analyzed taking the example of a systems identification circuit. The experimental investigations are based on a powerful signal processor system which significantly improve controller adjustment times by up to 0.5 seconds and fulfills the real time requirements up to 10 kHz. The essential adaptive algorithms are presented. ESA

N91-10930# Messerschmitt-Boelkow-Blohm/Entwicklungspring Nord, Bremen (Germany, F.R.).
NON-LINEAR VIBRATION OF LARGE, IMPERFECT SPACE STRUCTURES **c39**
E. Hornung and H. Oery (Technische Hochschule, Aachen, Germany, F.R.) *In* DLR, Contributions in the Field of Aeroelastics on the Occasion of the 60th Anniversary of Professor Dr.-Ing. Habil. Hans Wilhelm Foersching Apr. 1990 p 203-222 (For primary document see N91-10920 02-02)
Avail: NTIS HC/MF A13

The fundamental dynamic behavior of a large framework structure with imperfect struts was investigated under periodic excitations. It is shown that initial imperfections have an important influence on the effective stiffness of the struts and on their loading

capacity. At low excitation levels, the stiffness can be considered with the linearized values, even if the struts introduce important frequency shifts. At higher excitation levels the mathematical model becomes strongly nonlinear, leading to very high dynamic factors in transient load cases and chaotic responses at harmonic excitations in the critical frequency range. It is concluded that an active shape control, ensuring also the straightness of the struts, seems to be mandatory for large space structures. ESA

N91-10931# Deutsche Forschungsanstalt fuer Luft- und Raumfahrt, Goettingen (Germany, F.R.). Inst. fuer Aeroelastik.
A QUARTER OF A CENTURY OF AEROELASTIC COOPERATION BETWEEN RESEARCH AND INDUSTRY (A REVIEW). PART 1: FIGHTER AIRPLANES AND HELICOPTERS **c81**
O. Sensburg, J. Becker, H. Hoenlinger, and G. Strehlow *In its* Contributions in the Field of Aeroelastics on the Occasion of the 60th Anniversary of Professor Dr.-Ing. Habil. Hans Wilhelm Foersching Apr. 1990 p 223-270 (For primary document see N91-10920 02-02)
Avail: NTIS HC/MF A13

Tests and developments which enabled the German aircraft industry and the DLR Institute of Aeroelasticity to become competitive again with other leading nations are described. The first steps, the development of the first German vertical takeoff airplane VJ 101 are depicted. The Tornado fighter airplane aeroelastic investigations are reviewed. Developments and tests for the introduction of active control technology into aircraft design are described. The research work for the European fighter aircraft is outlined. Helicopter aeroelasticity investigations are presented. ESA

N91-10932# Deutsche Airbus G.m.b.H., Bremen (Germany, F.R.).
A QUARTER OF A CENTURY OF AEROELASTIC COOPERATION BETWEEN RESEARCH AND INDUSTRY (A REVIEW). PART 2: TRANSPORT AIRPLANES AND OTHER CIVIL APPLICATIONS **c05**
S. Vogel, H. Zimmermann, and K. Koenig *In* DLR, Contributions in the Field of Aeroelastics on the Occasion of the 60th Anniversary of Professor Dr.-Ing. Habil. Hans Wilhelm Foersching Apr. 1990 p 271-287 (For primary document see N91-10920 02-02)
Avail: NTIS HC/MF A13

Studies and developments in the field of civil aviation by the German aircraft industry and the DLR Institute of Aeroelasticity are described. The application of aerolasticity to wind turbine systems for energy supply is outlined. Aeroservoelasticity and active control technology are introduced. Methods for the calculation of unsteady aerodynamic forces in the transonic domain are presented. The measurement of unsteady aerodynamic loads is discussed. ESA

N91-10933*# National Aeronautics and Space Administration. Ames Research Center, Moffett Field, CA.
THE CALCULATION OF ROTOR/FUSELAGE INTERACTION FOR TWO-DIMENSIONAL BODIES
Paul M. Stremel Aug. 1990 35 p Presented at the 16th European Rotorcraft Forum, Glasgow, Scotland, 18-21 Sep. 1990 (NASA-TM-102855; A-90256; NAS 1.15:102855) Avail: NTIS HC/MF A03 CSCL 01A

Unsteady rotor wake interactions with the empennage, tail boom, and other aerodynamic surfaces have a significant influence on the aerodynamic performance of the helicopter, ride quality, and vibration. A Computational Fluid Dynamic (CFD) method for computing the aerodynamic interaction between an interacting vortex wake and the viscous flow about arbitrary 2-D bodies was developed to address this helicopter problem. The vorticity and flow field velocities are calculated on a body-fitted computational mesh using an uncoupled iterative solution. The interacting vortex wake is represented by an array of discrete vortices which, in turn, are represented by a finite core model. The evolution of the interacting vortex wake is calculated by Lagrangian techniques. The flow around circular and elliptic cylinders in the absence of an interacting vortex wake was calculated. These results compare very well with other numerical results and with results obtained from experiment and thereby demonstrate the accuracy of the viscous solution. The interaction of a simulated rotor wake with the flow about 2-D bodies, representing cross sections of fuselage components, was calculated to address the vortex interaction problem. The vortex interaction was calculated for the flow about a circular and an elliptic cylinder at 45 and 90 degrees incidence. The results demonstrate the significant variation in lift and drag on the 2-D bodies during the vortex interaction. Author

N91-10934*# Stanford Univ., CA. Dept. of Aeronautics and Astronautics.
A NUMERICAL STUDY OF THE EFFECTS OF WIND TUNNEL WALL PROXIMITY ON AN AIRFOIL MODEL
Mark Potsdam and Leonard Roberts Sep. 1990 72 p (Contract NCC2-055)
(NASA-CR-187322; NAS 1.26:187322; JIAA-TR-99) Avail: NTIS HC/MF A04 CSCL 01A

A procedure was developed for modeling wind tunnel flows using computational fluid dynamics. Using this method, a numerical study was undertaken to explore the effects of solid wind tunnel wall proximity and Reynolds number on a two-dimensional airfoil model at low speed. Wind tunnel walls are located at varying wind tunnel height to airfoil chord ratios and the results are compared with freestream flow in the absence of wind tunnel walls. Discrepancies between the constrained and unconstrained flows can be attributed to the presence of the walls. Results are for a Mach Number of 0.25 at angles of attack through stall. A typical wind tunnel Reynolds number of 1,200,000 and full-scale flight Reynolds number of 6,000,000 were investigated. At this low Mach number, wind tunnel wall corrections to Mach number and angle of attack are supported. Reynolds number effects are seen to be a consideration in wind tunnel testing and wall interference correction methods. An unstructured grid Navier-Stokes code is used with a Baldwin-Lomax turbulence model. The numerical method is described since unstructured flow solvers present several difficulties and fundamental differences from structured grid codes, especially in the area of turbulence modeling and grid generation. Author

N91-10935# Messerschmitt-Boelkow-Blohm G.m.b.H., Munich (Germany, F.R.). Hubschrauber und Flugzeuge.
CALCULATION OF VISCOUS HYPERSONIC FLOWS USING A COUPLED EULER/2ND ORDER BOUNDARY LAYER METHOD
C. Mundt, M. Pfitzner, and M. A. Schmatz 3 Oct. 1989 13 p Presented at 8th GAM Conference on Numerical Methods in Fluid Mechanics, Delft, Netherlands, 27-29 Sep. 1989
(MBB/FE122/S/PUB/387; ETN-90-97846) Copyright Avail: NTIS HC/MF A03

A method which allows the calculation of flows with weak viscous interaction by solving the second order boundary layer equations in the viscous and the Euler equations in the inviscid regions is presented. Both parts of the solution are coupled. Ideal and equilibrium real gas results for laminar flows are presented. A comparison with Navier-Stokes results shows good agreement. ESA

03 AIR TRANSPORTATION AND SAFETY

Includes passenger and cargo air transport operations; and aircraft accidents.

For related information see also *16 Space Transportation* and *85 Urban Technology and Transportation.*

N91-10936*# National Aeronautics and Space Administration. Langley Research Center, Hampton, VA.
AVIATION SAFETY/AUTOMATION PROGRAM CONFERENCE
Samuel A. Morello, comp. Washington Oct. 1990 270 p Conference held in Virginia Beach, VA, 11-12 Oct. 1989

(NASA-CP-3090; L-16840; NAS 1.55:3090) Avail: NTIS HC/MF A12 CSCL 01C

The Aviation Safety/Automation Program Conference - 1989 was sponsored by the NASA Langley Research Center on 11 to 12 October 1989. The conference, held at the Sheraton Beach Inn and Conference Center, Virginia Beach, Virginia, was chaired by Samuel A. Morello. The primary objective of the conference was to ensure effective communication and technology transfer by providing a forum for technical interchange of current operational problems and program results to date. The Aviation Safety/Automation Program has as its primary goal to improve the safety of the national airspace system through the development and integration of human-centered automation technologies for aircraft crews and air traffic controllers. For individual titles, see N91-10937 through N91-10962.

N91-10937*# Boeing Commercial Airplane Co., Seattle, WA.
BOEING FLIGHT DECK DESIGN PHILOSOPHY c05
Harty Stoll *In* NASA, Langley Research Center, Aviation Safety/Automation Program Conference Oct. 1990 p 17-25 (For primary document see N91-10936 02-03)
Avail: NTIS HC/MF A12 CSCL 01C

Information relative to Boeing flight deck design philosophy is given in viewgraph form. Flight deck design rules, design considerations, functions allocated to the crew, redundancy and automation concerns, and examples of accident data that were reviewed are listed. Author

N91-10938*# Honeywell, Inc., Minneapolis, MN.
COCKPIT AVIONICS INTEGRATION AND AUTOMATION c06
Keith M. Pischke *In* NASA, Langley Research Center, Aviation Safety/Automation Program Conference Oct. 1990 p 27-44 (For primary document see N91-10936 02-03)
Avail: NTIS HC/MF A12 CSCL 01C

Information on cockpit avionics integration and automation is given in viewgraph form, with a number of photographs. The benefits of cockpit integration are listed. The MD-11 flight guidance/flight deck system is illustrated. Author

N91-10939*# Douglas Aircraft Co., Inc., Long Beach, CA.
DOUGLAS FLIGHT DECK DESIGN PHILOSOPHY c05
Paul Oldale *In* NASA, Langley Research Center, Aviation Safety/Automation Program Conference Oct. 1990 p 45-53 (For primary document see N91-10936 02-03)
Avail: NTIS HC/MF A12 CSCL 01C

The systems experience gained from 17 years of DC-10 operation was used during the design of the MD-11 to automate system operation and reduce crew workload. All functions, from preflight to shutdown at the termination of flight, require little input from the crew. The MD-11 aircraft systems are monitored for proper operation by the Aircraft Systems Controllers (ASC). In most cases, system reconfiguration as a result of a malfunction is automated. Manual input is required for irreversible actions such as engine shutdown, fuel dump, fire agent discharge, or Integrated Drive Generator (IDG) disconnect. During normal operations, when the cockpit is configured for flight, all annunciators on the overhead panel will be extinguished. This Dark Cockpit immediately confirms to the crew that the panels are correctly configured and that no abnormalities are present. Primary systems annunciations are shown in text on the Alert Area of the Engine and Alert Display (EAD). This eliminates the need to scan the overhead. The MD-11 aircraft systems can be manually controlled from the overhead area of the cockpit. The center portion of the overhead panel is composed of the primary aircraft systems panels, which include FUEL, AIR, Electrical (ELEC) and Hydraulic (HYD) systems, which are easily accessible from both flight crew positions. Each Aircraft Systems Controller (ASC) has two automatic channels and a manual mode. All rectangular lights are annunciators. All square lights are combined switches and annunciators called switch/lights. Red switch/lights on the overhead (Level 3 alerts) are for conditions requiring immediate crew action. Amber (Level 2 or Level 1 alerts) indicates a fault or switch out of position requiring awareness or crew interaction. Overhead switches used in normal operating conditions will illuminate blue when in use (Level 0 alerts) such as WING ANTI-ICE - ON. An overhead switch/light with BLACK LETTERING on an amber or red background indicates a system failure and that crew interaction is required. A switch/light with blue or amber lettering and a BLACK BACKGROUND indicates a switch out of normal position and that crew action is necessary only if the system is in manual operation. Author

N91-10940*# Federal Aviation Administration, Washington, DC.
NATIONAL PLAN TO ENHANCE AVIATION SAFETY THROUGH HUMAN FACTORS IMPROVEMENTS
Clay Foushee *In* NASA, Langley Research Center, Aviation Safety/Automation Program Conference Oct. 1990 p 55-65 (For primary document see N91-10936 02-03)
Avail: NTIS HC/MF A12 CSCL 01C

The purpose of this section of the plan is to establish a development and implementation strategy plan for improving safety and efficiency in the Air Traffic Control (ATC) system. These improvements will be achieved through the proper applications of human factors considerations to the present and future systems. The program will have four basic goals: (1) prepare for the future system through proper hiring and training; (2) develop a controller work station team concept (managing human errors); (3) understand and address the human factors implications of negative system results; and (4) define the proper division of responsibilities and interactions between the human and the machine in ATC systems. This plan addresses six program elements which together address the overall purpose. The six program elements are: (1) determine principles of human-centered automation that will enhance aviation safety and the efficiency of the air trafic controller; (2) provide new and/or enhanced methods and techniques to measure, assess, and improve human performance in the ATC environment; (3) determine system needs and methods for information transfer between and within controller teams and between controller teams and the cockpit; (4) determine how new controller work station technology can optimally be applied and integrated to enhance safety and efficiency; (5) assess training needs and develop improved techniques and strategies for selection, training, and evaluation of controllers; and (6) develop standards, methods, and procedures for the certification and validation of human engineering in the design, testing, and implementation of any hardware or software system element which affects information flow to or from the human. Author

N91-10941*# National Aeronautics and Space Administration. Langley Research Center, Hampton, VA.
AVIATION SAFETY/AUTOMATION PROGRAM OVERVIEW
Samuel A. Morello *In its* Aviation Safety/Automation Program Conference Oct. 1990 p 67-73 (For primary document see N91-10936 02-03)
Avail: NTIS HC/MF A12 CSCL 01C

The goal is to provide a technology base leading to improved safety of the national airspace system through the development and integration of human-centered automation technologies for aircraft crews and air traffic controllers. Information on the problems, specific objectives, human-automation interaction, intelligent error-tolerant systems, and air traffic control/cockpit integration is given in viewgraph form. Author

N91-10942*# National Aeronautics and Space Administration. Ames Research Center, Moffett Field, CA.
SUMMARY OF THE INDUSTRY/NASA/FAA WORKSHOP ON PHILOSOPHY OF AUTOMATION: PROMISES AND REALITIES c06
Susan D. Norman *In* NASA, Langley Research Center, Aviation Safety/Automation Program Conference Oct. 1990 p 77-82 (For primary document see N91-10936 02-03)
Avail: NTIS HC/MF A12 CSCL 01C

Issues of flight deck automation are multi-faceted and complex. The rapid introduction of advanced computer based technology on to the flight deck of transport category aircraft has had considerable impact on both aircraft operations and the flight crew. As part of NASA's responsibility to facilitate an active exchange

of ideas and information between members of the aviation community, an Industry/NASA/FAA workshop was conducted in August 1988. One of the most important conclusions to emerge from the workshop was that the introduction of automation has clearly benefited aviation and has substantially improved the operational safety and efficiency of our air transport system. For example, one carrier stated that they have been flying the Boeing 767 (one of the first aircraft to employ substantial automation) since 1982, and they have never had an accident or incident resulting in damage to the aircraft. Notwithstanding its benefits, many issues associated with the design, certification, and operation of automated aircraft were identified. For example two key conceptual issues were the need for the crew to have a thorough understanding of the system and the importance of defining the pilot's role. With respect to certification, a fundamental issue is the lack of comprehensive human factors requirements in the current regulations. Operational considerations, which have been a factor in incidents involving automation, were also cited. Viewgraphs used in the presentation are given. Author

N91-10943*# Miami Univ., Coral Gables, FL.
HUMAN FACTORS OF THE HIGH TECHNOLOGY COCKPIT **c54**

Earl L. Wiener *In* NASA, Langley Research Center, Aviation Safety/Automation Program Conference Oct. 1990 p 83-90 (For primary document see N91-10936 02-03)
Avail: NTIS HC/MF A12 CSCL 05H

The rapid advance of cockpit automation in the last decade has outstripped the ability of the human factors profession to understand the changes in human functions required. High technology cockpits require less physical (observable) workload, but are highly demanding of cognitive functions such as planning, alternative selection, and monitoring. Furthermore, automation creates opportunity for new and more serious forms of human error, and many pilots are concerned about the possibility of complacency affecting their performance. On the positive side, the equipment works as advertized with high reliability, offering highly efficient, computer-based flight. These findings from the cockpit studies probably apply equally to other industries, such as nuclear power production, other modes of transportation, medicine, and manufacturing, all of which traditionally have looked to aviation for technological leadership. The challenge to the human factors profession is to aid designers, operators, and training departments in exploiting the positive side of automation, while seeking solutions to the negative side. Viewgraphs are given. Author

N91-10944*# National Aeronautics and Space Administration. Ames Research Center, Moffett Field, CA.
HUMAN-CENTERED AUTOMATION: DEVELOPMENT OF A PHILOSOPHY **c54**

Curtis Graeber and Charles E. Billings *In* NASA, Langley Research Center, Aviation Safety/Automation Program Conference Oct. 1990 p 91-104 (For primary document see N91-10936 02-03)
Avail: NTIS HC/MF A12 CSCL 05H

Information on human-centered automation philosophy is given in outline/viewgraph form. It is asserted that automation of aircraft control will continue in the future, but that automation should supplement, not supplant the human management and control function in civil air transport. Author

N91-10945*# National Aeronautics and Space Administration. Ames Research Center, Moffett Field, CA.
CREW WORKLOAD STRATEGIES IN ADVANCED COCKPITS **c54**

Sandra G. Hart *In* NASA, Langley Research Center, Aviation Safety/Automation Program Conference Oct. 1990 p 105-125 (For primary document see N91-10936 02-03)
Avail: NTIS HC/MF A12 CSCL 05H

Many methods of measuring and predicting operator workload have been developed that provide useful information in the design, evaluation, and operation of complex systems and which aid in developing models of human attention and performance. However, the relationships between such measures, imposed task demands, and measures of performance remain complex and even contradictory. It appears that we have ignored an important factor: people do not passively translate task demands into performance. Rather, they actively manage their time, resources, and effort to achieve an acceptable level of performance while maintaining a comfortable level of workload. While such adaptive, creative, and strategic behaviors are the primary reason that human operators remain an essential component of all advanced man-machine systems, they also result in individual differences in the way people respond to the same task demands and inconsistent relationships among measures. Finally, we are able to measure workload and performance, but interpreting such measures remains difficult; it is still not clear how much workload is too much or too little nor the consequences of suboptimal workload on system performance and the mental, physical, and emotional well-being of the human operators. The rationale and philosophy of a program of research developed to address these issues will be reviewed and contrasted to traditional methods of defining, measuring, and predicting human operator workload. Viewgraphs are given. Author

N91-10946*# National Aeronautics and Space Administration. Ames Research Center, Moffett Field, CA.
ASSESSING INFORMATION TRANSFER IN FULL MISSION FLIGHT SIMULATIONS

Alfred T. Lee *In* NASA, Langley Research Center, Aviation Safety/Automation Program Conference Oct. 1990 p 127-130 (For primary document see N91-10936 02-03)
Avail: NTIS HC/MF A12 CSCL 01C

Considerable attention must be given to the important topic of aircrew situation awareness in any discussion of aviation safety and flight deck design. Reliable means of assessing this important aspect of crew behavior without simultaneously interfering with the behavior are difficult to develop. Unobtrusive measurement of crew situation awareness is particularly important in the conduct of full mission simulations where considerable effort and cost is expended to achieve a high degree of operational fidelity. An unobtrusive method of assessing situational awareness is described here which employs a topical analysis of intra-crew communications. The communications were taken from videotapes of crew behavior prior to, during, and following an encounter with a microburst/windshear event. The simulation scenario re-created an actual encounter with an event during an approach into Denver Stapleton Airport. The analyses were conducted on twelve experienced airline crews with the objective of determining the effect on situation awareness of uplinking ground-based information of the crew during the approach. The topical analysis of crew communication was conducted on all references to weather or weather-related topics. The general weather topic was further divided into weather subtopical references such as surface winds, windshear, precipitation, etc., thereby allowing for an assessment of the relative frequency of subtopic reference during the scenario. Reliable differences were found between the relative frequency of subtopic references when comparing the communications of crews receiving a cockpit display of ground-based information to the communications of a control group. The findings support the utility of this method of assessing situation awareness and information value in full mission simulations. A limiting factor in the use of this measure is that crews vary in the amount of intra-crew communications that may take place due to individual differences and other factors associated with crew coordination. This factor must be taken into consideration when employing this measure. Viewgraphs are given. Author

N91-10947*# National Aeronautics and Space Administration. Ames Research Center, Moffett Field, CA.
TECHNOLOGICAL ADVANCES FOR STUDYING HUMAN BEHAVIOR **c53**

Renate J. Roske-Hofstrand *In* NASA, Langley Research Center, Aviation Safety/Automation Program Conference Oct. 1990 p 131-141 (For primary document see N91-10936 02-03)
Avail: NTIS HC/MF A12 CSCL 05I

Technological advances for studying human behavior are noted in viewgraph form. It is asserted that performance-aiding systems

are proliferating without a fundamental understanding of how they would interact with the humans who must control them. Two views of automation research, the hardware view and the human-centered view, are listed. Other viewgraphs give information on vital elements for human-centered research, a continuum of the research process, available technologies, new technologies for persistent problems, a sample research infrastructure, the need for metrics, and examples of data-link technology. Author

N91-10948*# Pacific Northwest Lab., Richland, WA.
ASSESSING THE FEASIBILITY, COST, AND UTILITY OF DEVELOPING MODELS OF HUMAN PERFORMANCE IN AVIATION c53
William Stillwell *In* NASA, Langley Research Center, Aviation Safety/Automation Program Conference Oct. 1990 p 143-149 (For primary document see N91-10936 02-03)
Avail: NTIS HC/MF A12 CSCL 05I

The purpose of the effort outlined in this briefing was to determine whether models exist or can be developed that can be used to address aviation automation issues. A multidisciplinary team has been assembled to undertake this effort, including experts in human performance, team/crew, and aviation system modeling, and aviation data used as input to such models. The project consists of two phases, a requirements assessment phase that is designed to determine the feasibility and utility of alternative modeling efforts, and a model development and evaluation phase that will seek to implement the plan (if a feasible cost effective development effort is found) that results from the first phase. Viewgraphs are given. Author

N91-10949*# National Aeronautics and Space Administration. Langley Research Center, Hampton, VA.
OVERVIEW OF ERROR-TOLERANT COCKPIT RESEARCH Abstract Only c05
Kathy Abbott *In its* Aviation Safety/Automation Program Conference Oct. 1990 p 153-156 (For primary document see N91-10936 02-03)
Avail: NTIS HC/MF A12 CSCL 01C

The objectives of research in intelligent cockpit aids and intelligent error-tolerant systems are stated. In intelligent cockpit aids research, the objective is to provide increased aid and support to the flight crew of civil transport aircraft through the use of artificial intelligence techniques combined with traditional automation. In intelligent error-tolerant systems, the objective is to develop and evaluate cockpit systems that provide flight crews with safe and effective ways and means to manage aircraft systems, plan and replan flights, and respond to contingencies. A subsystems fault management functional diagram is given. All information is in viewgraph form. Author

N91-10950*# National Aeronautics and Space Administration. Langley Research Center, Hampton, VA.
FAULT MONITORING c06
Paul Schutte *In its* Aviation Safety/Automation Program Conference Oct. 1990 p 157-163 (For primary document see N91-10936 02-03)
Avail: NTIS HC/MF A12 CSCL 01C

Information on fault monitoring of aircraft systems is given in viewgraph form. Information is given on monitor architecture and benefits, implementation characteristics, and an engine monitoring and control system. Author

N91-10951*# National Aeronautics and Space Administration. Langley Research Center, Hampton, VA.
FAULT DIAGNOSIS
Kathy Abbott *In its* Aviation Safety/Automation Program Conference Oct. 1990 p 165-174 (For primary document see N91-10936 02-03)
Avail: NTIS HC/MF A12 CSCL 01C

The objective of the research in this area of fault management is to develop and implement a decision aiding concept for diagnosing faults, especially faults which are difficult for pilots to identify, and to develop methods for presenting the diagnosis information to the flight crew in a timely and comprehensible manner. The requirements for the diagnosis concept were identified by interviewing pilots, analyzing actual incident and accident cases, and examining psychology literature on how humans perform diagnosis. The diagnosis decision aiding concept developed based on those requirements takes abnormal sensor readings as input, as identified by a fault monitor. Based on these abnormal sensor readings, the diagnosis concept identifies the cause or source of the fault and all components affected by the fault. This concept was implemented for diagnosis of aircraft propulsion and hydraulic subsystems in a computer program called Draphys (Diagnostic Reasoning About Physical Systems). Draphys is unique in two important ways. First, it uses models of both functional and physical relationships in the subsystems. Using both models enables the diagnostic reasoning to identify the fault propagation as the faulted system continues to operate, and to diagnose physical damage. Draphys also reasons about behavior of the faulted system over time, to eliminate possibilities as more information becomes available, and to update the system status as more components are affected by the fault. The crew interface research is examining display issues associated with presenting diagnosis information to the flight crew. One study examined issues for presenting system status information. One lesson learned from that study was that pilots found fault situations to be more complex if they involved multiple subsystems. Another was pilots could identify the faulted systems more quickly if the system status was presented in pictorial or text format. Another study is currently under way to examine pilot mental models of the aircraft subsystems and their use in diagnosis tasks. Future research plans include piloted simulation evaluation of the diagnosis decision aiding concepts and crew interface issues. Information is given in viewgraph form. Author

N91-10952*# BBN Systems and Technologies Corp., Cambridge, MA.
FAULT RECOVERY RECOMMENDATION
Eva Hudlicka and Kevin Corker *In* NASA, Langley Research Center, Aviation Safety/Automation Program Conference Oct. 1990 p 175-185 (For primary document see N91-10936 02-03)
Avail: NTIS HC/MF A12 CSCL 01C

Information on Recovery Recommendation System (RECORS) is given in viewgraph form. The system goal is to provide intelligent aiding for monitoring, diagnosis and response to aircraft system failures. Information is given on levels of abstraction, RECORS implementation, and architecture. Author

N91-10953*# National Aeronautics and Space Administration. Ames Research Center, Moffett Field, CA.
A FUNCTION-BASED APPROACH TO COCKPIT PROCEDURE AIDS
Anil V. Phatak, Parveen Jain (Expert-EASE Systems, Inc., Belmont, CA.), and Everett Palmer *In* NASA, Langley Research Center, Aviation Safety/Automation Program Conference Oct. 1990 p 187-197 (For primary document see N91-10936 02-03)
Avail: NTIS HC/MF A12 CSCL 01C

The objective of this research is to develop and test a cockpit procedural aid that can compose and present procedures that are appropriate for the given flight situation. The procedure would indicate the status of the aircraft engineering systems, and the environmental conditions. Prescribed procedures already exist for normal as well as for a number of non-normal and emergency situations, and can be presented to the crew using an interactive cockpit display. However, no procedures are prescribed or recommended for a host of plausible flight situations involving multiple malfunctions compounded by adverse environmental conditions. Under these circumstances, the cockpit procedural aid must review the prescribed procedures for the individual malfunction (when available), evaluate the alternatives or options, and present one or more composite procedures (prioritized or unprioritized) in response to the given situation. A top-down function-based conceptual approach towards composing and presenting cockpit procedures is being investigated. This approach is based upon the thought process that an operating crew must go through while

attempting to meet the flight objectives given the current flight situation. In order to accomplish the flight objectives, certain critical functions must be maintained during each phase of the flight, using the appropriate procedures or success paths. The viability of these procedures depends upon the availability of required resources. If resources available are not sufficient to meet the requirements, alternative procedures (success paths) using the available resources must be constructed to maintain the critical functions and the corresponding objectives. If no success path exists that can satisfy the critical functions/objectives, then the next level of critical functions/objectives must be selected and the process repeated. Information is given in viewgraph form.
Author

N91-10954*# National Aeronautics and Space Administration. Ames Research Center, Moffett Field, CA.
PROCEDURAL ERROR MONITORING AND SMART CHECKLISTS
Everett Palmer *In* NASA, Langley Research Center, Aviation Safety/Automation Program Conference Oct. 1990 p 199-208 (For primary document see N91-10936 02-03)
Avail: NTIS HC/MF A12 CSCL 01C

Human beings make and usually detect errors routinely. The same mental processes that allow humans to cope with novel problems can also lead to error. Bill Rouse has argued that errors are not inherently bad but their consequences may be. He proposes the development of error-tolerant systems that detect errors and take steps to prevent the consequences of the error from occurring. Research should be done on self and automatic detection of random and unanticipated errors. For self detection, displays should be developed that make the consequences of errors immediately apparent. For example, electronic map displays graphically show the consequences of horizontal flight plan entry errors. Vertical profile displays should be developed to make apparent vertical flight planning errors. Other concepts such as energy circles could also help the crew detect gross flight planning errors. For automatic detection, systems should be developed that can track pilot activity, infer pilot intent and inform the crew of potential errors before their consequences are realized. Systems that perform a reasonableness check on flight plan modifications by checking route length and magnitude of course changes are simple examples. Another example would be a system that checked the aircraft's planned altitude against a data base of world terrain elevations. Information is given in viewgraph form. Author

N91-10955*# National Aeronautics and Space Administration. Langley Research Center, Hampton, VA.
INFLIGHT REPLANNING FOR DIVERSIONS
Michael Palmer *In its* Aviation Safety/Automation Program Conference Oct. 1990 p 209-218 (For primary document see N91-10936 02-03)
Avail: NTIS HC/MF A12 CSCL 01C

Current procedures for handling flight plan diversions can require too much of the crew's resources. This increases workload and may compromise safety and cause delays in modifying the flight plan. The goal of NASA Langley Research Center's Diverter research program is to develop guidelines for a prototype pilot decision aid for diversions that will reduce cognitive workload, improve safety, increase capacity and traffic flow, and increase aircraft efficiency. The Diverter program has been partitioned into five phases, the first three of which were performed under contract by Lockheed Aeronautical Systems Company, Marietta, GA. In the first two phases, which have been completed, the system requirements and desired functions were defined and a prototype decision-making aid was implemented and demonstrated on a workstation. In phase three, which is currently under way, the pilot/vehicle interface is being defined and the capability of the prototype is being improved. In the last two phases, which will be performed at NASA Langley Research Center, the interface will be implemented, tied into the prototype aiding software, and installed in an advanced simulation facility for testing. In addition, significant implementation issues may be addressed through flight testing on NASA research aircraft. Information is given in viewgraph form.
Author

N91-10956*# Ohio State Univ., Columbus.
GRAPHICAL INTERFACES FOR COOPERATIVE PLANNING SYSTEMS
Philip J. Smith, Chuck Layton, and C. Elaine McCoy (San Jose State Univ., CA.) *In* NASA, Langley Research Center, Aviation Safety/Automation Program Conference Oct. 1990 p 219-228 (For primary document see N91-10936 02-03)
Avail: NTIS HC/MF A12 CSCL 01C

Based on a cognitive task analysis of 5 airline flight crews in a simulator study, researchers have designed a testbed for studying computer aids for en route flight path planning. This testbed runs on a Mac II controlling three color monitors, and is being used to study the design of aids for both dispatchers and flight crews. Specifically, the research focuses on design concepts for developing cooperative problem-solving systems. We use en route flight planning (selecting alternate routes or destinations due to unanticipated weather, traffic, malfunctions, etc.) as the context for studying the design of such systems. Researchers are currently exploring three questions in this test environment: (1) When interacting with a flight planning aid, how does the role of the pilot influence overall system performance; (2) Can the architecture for a cooperative planning system be built around Sacerdoti's (1983) concept of an abstraction hierarchy, where the pilot can interact with the system at many different levels of detail (but where the computer aid by default handles lower level details that the pilot has chosen not to deal with); and (3) Can graphical displays and direct manipulation of these displays provide perceptual enhancements (Larkin and Simon, 1987) of the pilot's problem-solving activities. Information is given in viewgraph form.
Author

N91-10957*# National Aeronautics and Space Administration. Ames Research Center, Moffett Field, CA.
ATC AUTOMATION CONCEPTS **c04**
Heinz Erzberger *In* NASA, Langley Research Center, Aviation Safety/Automation Program Conference Oct. 1990 p 231-247 (For primary document see N91-10936 02-03)
Avail: NTIS HC/MF A12 CSCL 01C

Information on the design of human-centered tools for terminal area air traffic control (ATC) is given in viewgraph form. Information is given on payoffs and products, guidelines, ATC as a team process, automation tools for ATF, and the traffic management advisor.
Author

N91-10958*# National Aeronautics and Space Administration. Ames Research Center, Moffett Field, CA.
TIME-BASED OPERATIONS IN AN ADVANCED ATC ENVIRONMENT **c04**
Steven M. Green *In* NASA, Langley Research Center, Aviation Safety/Automation Program Conference Oct. 1990 p 249-260 (For primary document see N91-10936 02-03)
Avail: NTIS HC/MF A12 CSCL 17G

Information on time-based operations in an advanced air traffic control (ATC) environment is given in viewgraph form. The objectives are to develop and evaluate procedures and clearances for 4D equipped aircraft, study the effect of dissimilar airborne and ground based speed strategies, and evaluate the effectiveness and acceptability of ATC automation tools. Information is given on ATC simulation, ATC automation tools, Denver arrival airspace, time-based ATC procedures, and future plans.
Author

N91-10959*# National Aeronautics and Space Administration. Langley Research Center, Hampton, VA.
TIME-BASED AIRCRAFT/ATC OPERATIONS STUDY **c04**
David H. Williams *In its* Aviation Safety/Automation Program Conference Oct. 1990 p 261-269 (For primary document see N91-10936 02-03)
Avail: NTIS HC/MF A12 CSCL 17G

Information on a time-based aircraft/air traffic control (ATC) operations study is given in viewgraph form. Study objectives are

to develop and evaluate procedures for incorporating 4D-equiped aircraft into a 4D ATC system, determine the impact on the system of dissimilar airborne and ground 4D speed strategies, and evaluate the effectiveness of airborne time guidance. Information is given on future plans, separation conflict induced by dissimilar speed schedules, and airborne 4D procedures. Author

N91-10960*# National Aeronautics and Space Administration. Ames Research Center, Moffett Field, CA.
TERMINAL WEATHER INFORMATION MANAGEMENT
Abstract Only **c47**
Alfred T. Lee *In* NASA, Langley Research Center, Aviation Safety/Automation Program Conference Oct. 1990 p 271-274 (For primary document see N91-10936 02-03)
Avail: NTIS HC/MF A12 CSCL 04B

Since the mid-1960's, microburst/windshear events have caused at least 30 aircraft accidents and incidents and have killed more than 600 people in the United States alone. This study evaluated alternative means of alerting an airline crew to the presence of microburst/windshear events in the terminal area. Of particular interest was the relative effectiveness of conventional and data link ground-to-air transmissions of ground-based radar and low-level windshear sensing information on microburst/windshear avoidance. The Advanced Concepts Flight Simulator located at Ames Research Center was employed in a line oriented simulation of a scheduled round-trip airline flight from Salt Lake City to Denver Stapleton Airport. Actual weather en route and in the terminal area was simulated using recorded data. The microburst/windshear incident of July 11, 1988 was re-created for the Denver area operations. Six experienced airline crews currently flying scheduled routes were employed as test subjects for each of three groups: (1) A baseline group which received alerts via conventional air traffic control (ATC) tower transmissions; (2) An experimental group which received alerts/events displayed visually and aurally in the cockpit six miles (approx. 2 min.) from the microburst event; and (3) An additional experimental group received displayed alerts/events 23 linear miles (approx. 7 min.) from the microburst event. Analyses of crew communications and decision times showed a marked improvement in both situation awareness and decision-making with visually displayed ground-based radar information. Substantial reductions in the variability of decision times among crews in the visual display groups were also found. These findings suggest that crew performance will be enhanced and individual differences among crews due to differences in training and prior experience are significantly reduced by providing real-time, graphic display of terminal weather hazards. Author

N91-10961*# National Aeronautics and Space Administration. Langley Research Center, Hampton, VA.
INFORMATION MANAGEMENT
Wendell Ricks and Kevin Corker (BBN Systems and Technologies Corp., Cambridge, MA.) *In its* Aviation Safety/Automation Program Conference Oct. 1990 p 275-288 (For primary document see N91-10936 02-03)
Avail: NTIS HC/MF A12 CSCL 01C

Primary Flight Display (PFD) information management and cockpit display of information management research is presented in viewgraph form. The information management problem in the cockpit, information management burdens, the key characteristics of an information manager, the interface management system handling the flow of information and the dialogs between the system and the pilot, and overall system architecture are covered. Author

N91-10962*# National Aeronautics and Space Administration. Langley Research Center, Hampton, VA.
A FLIGHT TEST FACILITY DESIGN FOR EXAMINING DIGITAL INFORMATION TRANSFER
Charles E. Knox *In its* Aviation Safety/Automation Program Conference Oct. 1990 p 289-296 (For primary document see N91-10936 02-03)
Avail: NTIS HC/MF A12 CSCL 01C

Information is given in viewgraph form on a flight test facility design for examining digital information transfer. Information is given on aircraft/ground exchange, data link research activities, data link display format, a data link flight test, and the flight test setup. Author

N91-10963# Allgemeiner Deutscher Automobil-Club-e.V., Munich (Germany, F.R.). Luftrettung.
AIR RESCUE IN THE FEDERAL REPUBLIC OF GERMANY [LUFFTRETTUNG IN DER BUNDESREPUBLIK DEUTSCHLAND]
Ingo Karger 1990 7 p In GERMAN
(ETN-90-97878) Avail: NTIS HC/MF A02

The air rescue system currently developed in the Federal Republic of Germany is such that any human being living there can be rescued within 8 to 15 minutes, using a rescue helicopter. The origin and operation of the rescue system are explained. The same rescue system is being developed in East Germany. ESA

N91-10964*# Atlantic Research Corp., Landover, MD. Professional Services Group.
CURRENT EMERGENCY LOCATOR TRANSMITTER (ELT) DEFICIENCIES AND POTENTIAL IMPROVEMENTS UTILIZING TSO-C91a ELTs Report, 1988-1990
Bernard J. Trudell and Ryland R. Dreibelbis Oct. 1990 108 p (Contracts NASw-4228; NASw-4518)
(NASA-CR-4330; NAS 1.26:4330) Avail: NTIS HC/MF A06 CSCL 01C

An analysis was conducted of current ELT problems and potential improvements that could be made by employing the TSO-C91a ELTs to replace the current TSO-C91 ELTs. The scope of the study included the following: (1) validate the problems; (2) determine specific failure causes; (3) determine false alarm causes; (4) estimate improvements from TSO-C91a; (5) estimate benefits from replacement of the current ELTs; and (6) determine need and benefits for improved ELT inspection and maintenance. A detailed comparison between the two requirements documents (TSO-C91 and -91a) was made to assess improved performance of the ELT in each category of failure cause and each cause of false alarms. The comparison and analysis resulted in projecting a success of operation rate approximately 3 times the current rate and a reduction in false alarms to 0.25 of those generated by TSO-C91 ELTs. These improvements led to a projection of benefits of approximately 25 additional lives to be saved each year with TSO-C91a ELTs and an improved inspection and maintenance program. Author

N91-10965# European Space Agency, Paris (France).
CONTRIBUTIONS TO THE IMPROVEMENT OF FLIGHT SAFETY IN WIND SHEAR
Reinhard Koenig (Deutsche Forschungs- und Versuchsanstalt fuer Luft- und Raumfahrt, Brunswick, Germany, F.R.) Aug. 1990 193 p Transl. into ENGLISH of Beitraege zur Erhoehung der Flugsicherheit in Windscherungen (Brunswick, Fed. Republic of Germany, DFVLR), Dec. 1988 186 p Original language document was announced as N89-25144
(ESA-TT-1141; DFVLR-FB-88-49; ETN-90-98003) Avail: NTIS HC/MF A09

The problem of wind shear in aviation was addressed. On the basis of a suitable safety criterion which relates the aircraft's energy deviation to a permitted energy deviation level, uncontrolled, controlled and manual landing approach are analyzed. The wind disturbances employed are simplified simulations of horizontal wind shears, vertical winds and thunderstorm conditions. From the description of the repercussions of wind shear on the aircraft's energy budget, theoretical solutions for open/closed loop control producing increased flight safety are derived. Suitable measurement and filtering methods are selected. Advantages over conventional flight directors are exhibited by the concrete facilities for decreasing wind shear effects. The use of energy and performance error signals from instruments modified in relation to conventional specification give improvement in manual flight. Experimental investigations using a cockpit simulator prove that wind shear hazard can be reduced by suitable instrumentation. ESA

04 AIRCRAFT COMMUNICATIONS AND NAVIGATION

Includes digital and voice communication with aircraft; air navigation systems (satellite and ground based); and air traffic control.

For related information see also *17 Space Communications, Spacecraft Communications, Command and Tracking* and *Communications and Radar.*

N91-10966# National Aerospace Lab., Tokyo (Japan). STOL Aircraft Project Team.

FLIGHT EVALUATION TEST OF THE PAPI (PRECISION APPROACH PATH INDICATOR) SYSTEM

Keiji Tanaka, Yuushi Terui, and Toshiharu Inagaki Jul. 1988 14 p In JAPANESE; ENGLISH summary

(NAL-TM-592; ISSN-0452-2982; JTN-90-80135) Avail: NTIS HC/MF A03

The National Aerospace Laboratory (NAL) quiet short takeoff and landing (QSTOL) experimental aircraft, ASUKA, is being tested at Gifu Airfield. Flight tests were conducted to evaluate the Precision Approach Path Indicator (PAPI) system, which Gifu Airfield recently installed. In order to support the ASUKA's flight test program, this PAPI has been designed to provide two reference approach path angles: three degrees (conventional takeoff and landing type) and six degrees (STOL type). The flight evaluation of the PAPI is evaluated here. The NAL experimental airplane, B65, in which a high-resolution type video tape recorder (VTR) camera was installed, was utilized to obtain images of PAPI lights. The tracing radar system on the ground recorded the traces of the B65 position. VTR images and radar data were then synchronized to confirm setting angles of PAPI lighting units, which can be estimated by the aircraft positions at the instant of color transition of each PAPI light. The results of the analysis as well as pilot comments, such as that PAPI has decreased pilot workload, proved the effectiveness and performance of the PAPI system. NASDA

N91-10967# Advisory Group for Aerospace Research and Development, Neuilly-Sur-Seine (France). Guidance and Control Panel.

AIRCRAFT TRAJECTORIES: COMPUTATION, PREDICTION, CONTROL, VOLUME 1. PART 1: FUNDAMENTALS. PART 2: FLIGHT IN CRITICAL ATMOSPHERIC CONDITIONS. PART 3: IMPACT OF NEW ON-BOARD TECHNOLOGIES ON AIRCRAFT OPERATION

Andre Benoit, ed. Mar. 1990 267 p In ENGLISH and FRENCH

(AGARD-AG-301-Vol-1-Pt-1-3; ISBN-92-835-0547-6) Copyright Avail: NTIS HC/MF A12; Non-NATO Nationals requests available only from AGARD/Scientific Publications Executive

This volume (part of a set of three) is composed of a preface and 11 papers covering respectively: fundamentals - general outline, optimal trajectories, and nonlinear models of aircraft; flight in critical atmospheric conditions - genesis of wind and influence on airplane trajectories, flight control in windshear, and flight simulation; and impact of new on-board technologies on aircraft operation - flight management in air transport, and crew/automation interface. For individual titles, see N91-10968 through N91-10977.

N91-10968*# Rice Univ., Houston, TX. Aero-Astronautics Group.

OPTIMAL TRAJECTORIES OF AIRCRAFT AND SPACECRAFT

A. Miele *In* AGARD, Aircraft Trajectories: Computation, Prediction, Control, Volume 1. Part 1: Fundamentals. Part 2: Flight in Critical Atmospheric Conditions. Part 3: Impact of New On-Board Technologies on Aircraft Operation Mar. 1990 56 p Sponsored in part by Boeing Commercial Airplane Co.; Air Line Pilots Association, International; United States Aviation Underwriters; and Boeing Military Airplane Development (For primary document see N91-10967 02-04)

(Contract NAG1-516; JPL-956415)

Copyright Avail: NTIS HC/MF A12; Non-NATO Nationals requests available only from AGARD/Scientific Publications Executive CSCL 17G

Work done on algorithms for the numerical solutions of optimal control problems and their application to the computation of optimal flight trajectories of aircraft and spacecraft is summarized. General considerations on calculus of variations, optimal control, numerical algorithms, and applications of these algorithms to real-world problems are presented. The sequential gradient-restoration algorithm (SGRA) is examined for the numerical solution of optimal control problems of the Bolza type. Both the primal formulation and the dual formulation are discussed. Aircraft trajectories, in particular, the application of the dual sequential gradient-restoration algorithm (DSGRA) to the determination of optimal flight trajectories in the presence of windshear are described. Both take-off trajectories and abort landing trajectories are discussed. Take-off trajectories are optimized by minimizing the peak deviation of the absolute path inclination from a reference value. Abort landing trajectories are optimized by minimizing the peak drop of altitude from a reference value. Abort landing trajectories are optimized by minimizing the peak drop of altitude from a reference value. The survival capability of an aircraft in a severe windshear is discussed, and the optimal trajectories are found to be superior to both constant pitch trajectories and maximum angle of attack trajectories. Spacecraft trajectories, in particular, the application of the primal sequential gradient-restoration algorithm (PSGRA) to the determination of optimal flight trajectories for aeroassisted orbital transfer are examined. Both the coplanar case and the noncoplanar case are discussed within the frame of three problems: minimization of the total characteristic velocity; minimization of the time integral of the square of the path inclination; and minimization of the peak heating rate. The solution of the second problem is called nearly-grazing solution, and its merits are pointed out as a useful engineering compromise between energy requirements and aerodynamics heating requirements. Author

N91-10969# Technische Univ., Brunswick (Germany, F.R.).

COMPARISON OF A MATHEMATICAL ONE-POINT MODEL AND A MULTI-POINT MODEL OF AIRCRAFT MOTION IN MOVING AIR **c05**

R. Brockhaus *In* AGARD, Aircraft Trajectories: Computation, Prediction, Control, Volume 1. Part 1: Fundamentals. Part 2: Flight in Critical Atmospheric Conditions. Part 3: Impact of New On-Board Technologies on Aircraft Operation Mar. 1990 17 p (For primary document see N91-10967 02-04)

Copyright Avail: NTIS HC/MF A12; Non-NATO Nationals requests available only from AGARD/Scientific Publications Executive

The steadily growing capacity of computers favors increasingly exact simulation of even complex processes. On the other hand, parameter identification and state estimation require much more precise models than are generally used for the design of feedback systems. A multi-point model of the aircraft motion is proposed in which the different coupling effects between the two sub-processes, aircraft and air flow, can be modeled with much higher accuracy than is obtained by using the ordinary one-point model, where all the force, moment, and velocity vectors are referred to the aircraft center of gravity. The modeling of the effects of aircraft rotation, wing down-wash, wind gradients, and other unstationary effects should be greatly improved by a multi-point approach, provided that the aerodynamic effects on the aircraft components can be described appropriately. The nonlinear equations of the total process are set up for the one-point and multi-point models and compiled into block diagrams, from which the physical background of the interrelations between air and aircraft motion can be seen very clearly. The possible improvement in model quality and the additional computer capacity needed are estimated by comparing the two approaches. Author

N91-10970# Office National d'Etudes et de Recherches Aerospatiales, Paris (France).

COMPUTATION OF SUB-OPTIMAL REAL-TIME GUIDANCE LAWS FOR COMBAT AIRCRAFT TRAJECTORIES

Huu Thanh Huynh *In* AGARD, Aircraft Trajectories: Computation,

Prediction, Control, Volume 1. Part 1: Fundamentals. Part 2: Flight in Critical Atmospheric Conditions. Part 3: Impact of New On-Board Technologies on Aircraft Operation Mar. 1990 29 p In FRENCH, ENGLISH summary (For primary document see N91-10967 02-04)
Copyright Avail: NTIS HC/MF A12; Non-NATO Nationals requests available only from AGARD/Scientific Publications Executive

An application of singular perturbation theory (SPT) for the computation of real-time control laws for Combat Aircraft trajectories is presented. The principle of SPT is first briefly reviewed for solving a multiple-time scale differential equations, then its application to optimization of nonlinear systems is presented. The main drawbacks and difficulties which were encountered in the computation of real-time control laws for Aircraft trajectories are described, then various techniques are also pointed out in order to overcome with these problems. Basing of this SPT, real-time guidance law, of closed-loop type, was developed for minimum time to climb in a vertical plane and three-dimensional interception for a combat Aircraft. The performances of these suboptimal guidance laws were then compared, in numerical simulation using a typical Aircraft model, with optimal control laws, of open-loop type, provided by an iterative numerical algorithm, using a generalized projected gradient technique. A better than 1 percent accuracy was obtained for the performance index (time-to-climb) for vertical climb trajectories. The real-time guidance laws are slightly less accurate for interception trajectories. The suboptimal guidance laws can fulfill final conditions on altitude or/and flight path angle and remain valid for a large flight envelope domain. Their computation times are very small and are compatible with real-time an board computer applications. Author

N91-10971# Toronto Univ. (Ontario). Inst. for Aerospace Studies.
CRITICAL ASPECTS OF TRAJECTORY PREDICTION: FLIGHT IN NON-UNIFORM WIND **c05**
Bernard Etkin and David Alexander Etkin (Canadian Climate Centre, Downsview, Ontario) *In* AGARD, Aircraft Trajectories: Computation, Prediction, Control, Volume 1. Part 1: Fundamentals. Part 2: Flight in Critical Atmospheric Conditions. Part 3: Impact of New On-Board Technologies on Aircraft Operation Mar. 1990 12 p (For primary document see N91-10967 02-04)
Copyright Avail: NTIS HC/MF A12; Non-NATO Nationals requests available only from AGARD/Scientific Publications Executive

The genesis of natural wind is described from a meteorological standpoint. Its influence on aircraft trajectories is discussed with reference to steady winds, turbulence, and wind shear. The main problems exist when flight is close to the ground, during landing, take-off, or terrain following. A model for analysis and simulation is presented consisting of four components - dynamics, kinematics and transformations, aerodynamics, and wind. The axis systems chosen are well suited to simulation of landing and take-off. Author

N91-10972# Technische Univ., Brunswick (Germany, F.R.). Inst. of Flight Guidance and Control.
EFFECT OF WIND AND WIND VARIATION ON AIRCRAFT FLIGHT-PATHS **c05**
K.-U. Hahn, T. Heintsch, B. Kaufmann, G. Schaenzer, and M. Swolinsky *In* AGARD, Aircraft Trajectories: Computation, Prediction, Control, Volume 1. Part 1: Fundamentals. Part 2: Flight in Critical Atmospheric Conditions. Part 3: Impact of New On-Board Technologies on Aircraft Operation Mar. 1990 27 p Sponsored by DFG (For primary document see N91-10967 02-04)
Copyright Avail: NTIS HC/MF A12; Non-NATO Nationals requests available only from AGARD/Scientific Publications Executive

Wind shear accidents during landing and approach could generally be avoided by using modern flight control systems. The problem is to inform the pilot by an adequate wind shear warning display, that he can understand the reaction of the control system. Wind shear is particularly dangerous if it occurs in a height of approximately 80 to 120 m, where the attention of the cockpit crew is affected by getting view contact to the ground. Wind shear during take-off and go-around is a pure flight performance problem. Pilots should avoid a take-off into a thunderstorm. In moderate downbursts a practicable escape maneuver is to maintain the flight level at a low height to pass the core of the downburst before starting the climb. This procedure can also be applied on the go-around. Author

N91-10973# Southampton Univ. (England).
AIRCRAFT FLIGHT IN WIND-SHEAR **c05**
D. McLean *In* AGARD, Aircraft Trajectories: Computation, Prediction, Control, Volume 1. Part 1: Fundamentals. Part 2: Flight in Critical Atmospheric Conditions. Part 3: Impact of New On-Board Technologies on Aircraft Operation Mar. 1990 10 p (For primary document see N91-10967 02-04)
Copyright Avail: NTIS HC/MF A12; Non-NATO Nationals requests available only from AGARD/Scientific Publications Executive

A brief account of wind-shear and some representations is given before discussing the effects of wind-shear on aircraft motion. A procedure for estimating the vertical and horizontal velocity components of a wind-shear microburst, based on observer theory is developed, and a brief discussion of flying in wind-shear concludes the paper. Author

N91-10974# Airbus Industrie, Blagnac (France).
HOW TO FLY WINDSHEAR **c05**
Paul Camus *In* Agard, Aircraft Trajectories: Computation, Prediction, Control, Volume 1. Part 1: Fundamentals. Part 2: Flight in Critical Atmospheric Conditions. Part 3: Impact of New On-Board Technologies on Aircraft Operation Mar. 1990 10 p (For primary document see N91-10967 02-04)
Copyright Avail: NTIS HC/MF A12; Non-NATO Nationals requests available only from AGARD/Scientific Publications Executive

Aviation safety history is a long fight against severe environmental constaint. Modern aircraft are able to face safely most of them but one still remains a potential killer, that is what is generally described as a windshear situation. What can be done, necessarily fall either in how to timely detect such a situation in order to avoid it or/and what tools could be given to the crew to better escape should they are trapped in. Latest state of build-in equipment, 3-D Navigation, electronic displays and flight control, provide now all necessary tools to develop an efficient in-board detection and protection system. Such a system will be described altogether with a review of some fundamental criteria to be considered when assessing their efficiency. Author

N91-10975# Technische Univ., Brunswick (Germany, F.R.). Inst. of Flight Guidance and Control.
WIND MODELS FOR FLIGHT SIMULATION **c09**
K.-U. Hahn, T. Heintsch, B. Kaufmann, G. Schaenzer, and M. Swolinsky *In* AGARD, Aircraft Trajectories: Computation, Prediction, Control, Volume 1. Part 1: Fundamentals. Part 2: Flight in Critical Atmospheric Conditions. Part 3: Impact of New On-Board Technologies on Aircraft Operation Mar. 1990 32 p Sponsored by DFG (For primary document see N91-10967 02-04)
Copyright Avail: NTIS HC/MF A12; Non-NATO Nationals requests available only from AGARD/Scientific Publications Executive

Wind shear, downdraft, and turbulence can endanger takeoff and landing approach. The effects of wind results in a modified dynamic response of the aircraft as well as in flight performance variation. In each case flight path deviation can occur, more or less controlled by the pilot. For the analysis of the aircraft behavior in a changing wind field, a mathematical model of the aircraft is used including the wind effects. It can be said, that gusts and turbulence will have more influence on the pilot workload and reaction to this short scale wind disturbances. Large scale wind variations can produce significant flight path safety problems. An important aspect for the flight safety is the energy situation of an aircraft affected by wind. Therefore this was chosen as a useful criterion for the determination of the influences of the wind and wind variation. Author

N91-10976# Smiths Industries, Inc., Grand Rapids, MI.
AIRCRAFT TRAJECTORY: PREDICTION AND CONTROL IN THE AIR TRANSPORT FLIGHT MANAGEMENT COMPUTER SYSTEMS **c05**
Peter J. Howells *In* AGARD, Aircraft Trajectories: Computation, Prediction, Control, Volume 1. Part 1: Fundamentals. Part 2: Flight in Critical Atmospheric Conditions. Part 3: Impact of New On-Board Technologies on Aircraft Operation Mar. 1990 13 p (For primary document see N91-10967 02-04)
Copyright Avail: NTIS HC/MF A12; Non-NATO Nationals requests available only from AGARD/Scientific Publications Executive

The declining cost of computing power and memory has enabled avionic manufacturers to develop sophisticated airborne computing systems. One of the most complex aircraft systems on modern air transport aircraft is the Flight Management Computer System (FMCS). The FMCS has reduced pilot workload by taking over the more mundane but complex functions, such as calculating the most economical speed, and, together with improvements in cockpit displays and monitoring systems, has allowed the transition from the three to two crew airline cockpit. The FMCS can compute the most economical path from one airport to another and then fly the aircraft along that path. To achieve this the computer must be able to select the most economical speed schedules for each phase of flight, then predict the complex vertical and horizontal profile that the aircraft would fly and, when connected to the aircraft's autopilot, control the aircraft along that three dimensional flight path. The forth dimension of time can also be selected as a control criteria, and the FMCS will compute the speed schedules and flight path based on a required time of a arrival at a selected point along the flight plan. In addition to reducing pilot workload, air traffic control efficiency is increased because the airborne navigation data base can be used to select and accurately fly published arrival and departure procedures without supervision from the ground controllers. The algorithms used for the Smiths Industries 737 FMCS prediction and control functions are described. The requirements for successful implementation and some of the difficulties that may be encountered are identified. Author

N91-10977# Airbus Industrie, Blagnac (France). Flight Div.
IMPACT OF NEW TECHNOLOGY ON OPERATIONAL INTERFACE: FROM DESIGN AIMS TO FLIGHT EVALUATION AND MEASUREMENT **c05**
J. J. Speyer, C. Monteil, R. D. Blomberg, and J. P. Fouillot (Paris V Univ., France) *In* AGARD, Aircraft Trajectories: Computation, Prediction, Control, Volume 1. Part 1: Fundamentals. Part 2: Flight in Critical Atmospheric Conditions. Part 3: Impact of New On-Board Technologies on Aircraft Operation Mar. 1990 37 p (For primary document see N91-10967 02-04)
Copyright Avail: NTIS HC/MF A12; Non-NATO Nationals requests available only from AGARD/Scientific Publications Executive

Since the early 1980s Airbus Industrie has conducted a progressive research program investigating the ergonomic, physiological, and psychological factors affecting flight crew in their working environment, and progressively refining the data acquisition and analysis techniques. This self-imposed commitment to a dedicated appreciation of man-machine aspects was met in two ways: informally, by stringent application of human engineering principles, although in short supply in as far as their explicit formulation is concerned; and formally, by continuous development of statistical methods and engineering experiments, concentrating on pilot questionnaires, performance evaluations and workload models. A statistical workload calculation model highlights the link that enables correlation of pilot performance parameters with estimates on the impact of new technology on the operational interface. The purpose is to review the space between initial design aims and subsequent flight evaluation and measurement. A practical review is presented of the operational objectives and technological modules that marked the outgrowth of the Airbus family of commercial aircraft. Author

N91-10978# Advisory Group for Aerospace Research and Development, Neuilly-Sur-Seine (France). Guidance and Control Panel.
AIRCRAFT TRAJECTORIES: COMPUTATION, PREDICTION, CONTROL, VOLUME 3. PART 9: BOOK OF ABSTRACTS. PART 10: BIBLIOGRAPHY. PART 11: LIST OF CONTRIBUTORS
Andre Benoit, ed. May 1990 155 p In ENGLISH and FRENCH
(AGARD-AG-301-Vol-3-Pt-9-11; ISBN-92-835-0563-8) Copyright Avail: NTIS HC/MF A08; Non-NATO Nationals requests available only from AGARD/Scientific Publications Executive

This volume (part of a set of three) is composed of a short introduction, a Book of Abstracts of 39 papers included in the overall work, an extensive Bibliography which incorporate, in particular, most of the references cited by the 56 authors and co-authors, and a List of Contributors ordered by countries alphabetically. Both the Bibliography and the List of Contributors are each completed by an adequate index. Author

N91-10979# National Academy of Sciences - National Research Council, Washington, DC. Committee for the Study of Long-Term Airport Capacity Needs.
AIRPORT SYSTEM CAPACITY STRATEGIC CHOICES
1990 145 p
(SR-226; ISBN-0-309-04956-3; ISSN-0360-859X; LC-90-34787)
Avail: NTIS HC/MF A07

The study reports on one element of overall future air transport systems needs: airport capacity. It was requested by the Federal Aviation Administration (FAA) to assist in a major undertaking by FAA and the U.S. Department of Transportation (DOT) that will lead to a national strategy for meeting long-term capacity needs. The Transportation Research Board (TRB) of the National Research Council assembled an expert committee to provide advice on alternative strategies that might be adopted to meet long-term airport capacity needs. The committee was charged with four tasks: (1) to examine long-term airport capacity needs and measures to meet these needs; (2) to formulate alternative strategies reflecting varying assumptions about the growth of air traffic and intercity travel demand, technological development, government roles, and institutional arrangements; (3) to identify the advantages and disadvantages of these strategies; and (4) to recommend strategies for further analysis and evaluation by FAA. The committee identified an array of actions or options that could be taken to meet demand. Seven strategies, made up of various combinations of these options, were devised and assessed under three growth scenarios. These scenarios, designated High Growth, Maturing Economy, and Economic Difficulty, embrace a range of plausible assumptions about the state of the economy, the cost of air travel, propensity for travel, and technological innovation in air and surface transportation. Each is described. The strategies are as follows: (1) continue on present course; (2) build more airports; (3) centralize system management; (4) build an expanded, centrally managed system; (5) let the market decide; (6) reconfigure the airport system; and (7) revolutionize the intercity transportation technology. The study evaluates the strategies suggested. Author

N91-10980 Drexel Univ., Philadelphia, PA.
A STOCHASTIC ANALYSIS OF STATE TRANSITIONS IN AN AIR SPACE MANAGEMENT SYSTEM Ph.D. Thesis
Emanuel Irwin Ringel 1990 187 p
Avail: Univ. Microfilms Order No. DA9021382

The application of stochastic process ideas to answer some fundamental questions about a state system which arises in the Mode Select Beacon System (MODE-S), an air space management system is explored. A series of successively more powerful models is developed, based on Markov chains, semi-Markov processes, population models, and Monte Carlo simulation. Computer programs in the APL programming language to implement the models and to process the resulting data are developed. The outputs of the models illuminate the behavior of the state system by providing predictions with confidence bounds about the movements of aircraft among the states over time. Appendices

develop a recursive method for calculating probabilities for the success runs distribution, give APL code listings, validate the APL random number generator, and explore a special case in discrete time queueing theory. Dissert. Abstr.

N91-10957*# National Aeronautics and Space Administration. Ames Research Center, Moffett Field, CA.
ATC AUTOMATION CONCEPTS
Heinz Erzberger *In* NASA, Langley Research Center, Aviation Safety/Automation Program Conference Oct. 1990 p 231-247 (For primary document see N91-10936 02-03)
Avail: NTIS HC/MF A12 CSCL 01C

N91-10958*# National Aeronautics and Space Administration. Ames Research Center, Moffett Field, CA.
TIME-BASED OPERATIONS IN AN ADVANCED ATC ENVIRONMENT
Steven M. Green *In* NASA, Langley Research Center, Aviation Safety/Automation Program Conference Oct. 1990 p 249-260 (For primary document see N91-10936 02-03)
Avail: NTIS HC/MF A12 CSCL 17G

N91-10959*# National Aeronautics and Space Administration. Langley Research Center, Hampton, VA.
TIME-BASED AIRCRAFT/ATC OPERATIONS STUDY
David H. Williams *In its* Aviation Safety/Automation Program Conference Oct. 1990 p 261-269 (For primary document see N91-10936 02-03)
Avail: NTIS HC/MF A12 CSCL 17G

N91-10982# European Organization for the Safety of Air Navigation, Brussells (Belgium). Engineering Directorate.
OPTIMUM ON-LINE HANDLING OF AIR TRAFFIC OVER WESTERN EUROPE
Andre Benoit and Sip Swierstra *In* AGARD, Aircraft Trajectories: Computation, Prediction, Control, Volume 2: Air Traffic Handling and Ground-Based Guidance of Aircraft. Part 4: Air Traffic Handling. Part 5: Guidance of Aircraft in a Time-Based Constrained Environment. Part 6: May 1990 Presented at the International Seminar ATC 2000, Luxembourg, 23-25 Feb. 1988 (For primary document see N91-10981 02-05)
Copyright Avail: NTIS HC/MF A20; Non-NATO Nationals requests available only from AGARD/Scientific Publications Executive

N91-10983# European Organization for the Safety of Air Navigation, Brussells (Belgium). Engineering Directorate.
THE EUROCONTROL FUTURE ATS SYSTEM CONCEPT AND THE PROGRAMME OF STUDIES, TESTS, AND TRIALS
V. Vachiery *In* AGARD, Aircraft Trajectories: Computation, Prediction, Control, Volume 2: Air Traffic Handling and Ground-Based Guidance of Aircraft. Part 4: Air Traffic Handling. Part 5: Guidance of Aircraft in a Time-Based Constrained Environment. Part 6: May 1990 (For primary document see N91-10981 02-05)
Copyright Avail: NTIS HC/MF A20; Non-NATO Nationals requests available only from AGARD/Scientific Publications Executive

N91-10988# Consiglio Nazionale delle Ricerche, Rome (Italy). Progetto Finalizzato Trasporti and Ist. di Analisi dei Sistemi ed Informatica.
OPTIMIZATION MODELS AND TECHNIQUES TO IMPROVE AIR TRAFFIC MANAGEMENT
Lucio Bianco *In* AGARD, Aircraft Trajectories: Computation, Prediction, Control, Volume 2: Air Traffic Handling and Ground-Based Guidance of Aircraft. Part 4: Air Traffic Handling. Part 5: Guidance of Aircraft in a Time-Based Constrained Environment. Part 6: May 1990 (For primary document see N91-10981 02-05)
Copyright Avail: NTIS HC/MF A20; Non-NATO Nationals requests available only from AGARD/Scientific Publications Executive

N91-10989# European Organization for the Safety of Air Navigation, Brussells (Belgium). Engineering Directorate.
THE HIGH-RESOLUTION GRAPHIC DISPLAY: A POSSIBLE MAN/MACHINE INTERFACE FOR A COMPUTER ASSISTED ATC MANAGEMENT SYSTEM
Carlos Garcia Avello *In* AGARD, Aircraft Trajectories: Computation, Prediction, Control, Volume 2: Air Traffic Handling and Ground-Based Guidance of Aircraft. Part 4: Air Traffic Handling. Part 5: Guidance of Aircraft in a Time-Based Constrained Environment. Part 6: May 1990 (For primary document see N91-10981 02-05)
Copyright Avail: NTIS HC/MF A20; Non-NATO Nationals requests available only from AGARD/Scientific Publications Executive

N91-10990# European Organization for the Safety of Air Navigation, Brussells (Belgium). Engineering Directorate.
THE 4-D CONTROL OF CURRENT AIR CARRIERS IN THE PRESENT ENVIRONMENT: OBJECTIVES, STATUS, AND PLANS
Andre Benoit *In* AGARD, Aircraft Trajectories: Computation, Prediction, Control, Volume 2: Air Traffic Handling and Ground-Based Guidance of Aircraft. Part 4: Air Traffic Handling. Part 5: Guidance of Aircraft in a Time-Based Constrained Environment. Part 6: May 1990 (For primary document see N91-10981 02-05)
Copyright Avail: NTIS HC/MF A20; Non-NATO Nationals requests available only from AGARD/Scientific Publications Executive

N91-10991# Centre d'Etudes et de Recherches, Toulouse (France).
FOUR DIMENSIONAL NAVIGATION IN AIR TRAFFIC WITH 4-D NAVIGATION AIRCRAFT [NAVIGATION 4-D EN CIRCULATION AERIENNE AIRCRAFT 4-D NAVIGATION]
Nicole Imbert and Marc J. Pelegrin *In* AGARD, Aircraft Trajectories: Computation, Prediction, Control, Volume 2: Air Traffic Handling and Ground-Based Guidance of Aircraft. Part 4: Air Traffic Handling. Part 5: Guidance of Aircraft in a Time-Based Constrained Environment. Part 6: May 1990 In FRENCH; ENGLISH summary (For primary document see N91-10981 02-05)
Copyright Avail: NTIS HC/MF A20; Non-NATO Nationals requests available only from AGARD/Scientific Publications Executive

N91-10992# European Organization for the Safety of Air Navigation, Brussells (Belgium). Engineering Directorate.
THE CONTROL OF INBOUND FLIGHTS
Andre Benoit and Sip Swierstra *In* AGARD, Aircraft Trajectories: Computation, Prediction, Control, Volume 2: Air Traffic Handling and Ground-Based Guidance of Aircraft. Part 4: Air Traffic Handling. Part 5: Guidance of Aircraft in a Time-Based Constrained Environment. Part 6: May 1990 (For primary document see N91-10981 02-05)
Copyright Avail: NTIS HC/MF A20; Non-NATO Nationals requests available only from AGARD/Scientific Publications Executive

N91-10993*# National Aeronautics and Space Administration. Langley Research Center, Hampton, VA.
GUIDANCE CONCEPTS FOR TIME-BASED FLIGHT OPERATIONS
Dan D. Vicroy *In* AGARD, Aircraft Trajectories: Computation, Prediction, Control, Volume 2: Air Traffic Handling and Ground-Based Guidance of Aircraft. Part 4: Air Traffic Handling. Part 5: Guidance of Aircraft in a Time-Based Constrained Environment. Part 6: May 1990 (For primary document see N91-10981 02-05)
Copyright Avail: NTIS HC/MF A20; Non-NATO Nationals requests available only from AGARD/Scientific Publications Executive CSCL 17G

N91-10994*# National Aeronautics and Space Administration. Langley Research Center, Hampton, VA.
THE 4-D DESCENT TRAJECTORY GENERATION TECHNIQUES UNDER REALISTIC OPERATING CONDITIONS
David H. Williams and Charles E. Knox *In* AGARD, Aircraft

Trajectories: Computation, Prediction, Control, Volume 2: Air Traffic Handling and Ground-Based Guidance of Aircraft. Part 4: Air Traffic Handling. Part 5: Guidance of Aircraft in a Time-Based Constrained Environment. Part 6: May 1990 (For primary document see N91-10981 02-05)
Copyright Avail: NTIS HC/MF A20; Non-NATO Nationals requests available only from AGARD/Scientific Publications Executive CSCL 17G

N91-10995# Massachusetts Inst. of Tech., Cambridge. Flight Transportation Lab.
EXPERT SYSTEMS FOR THE GENERATION OF THERMAL AREA ARRIVAL PATHS FOR CIVIL TRANSPORT
Robert W. Simpson *In* AGARD, Aircraft Trajectories: Computation, Prediction, Control, Volume 2: Air Traffic Handling and Ground-Based Guidance of Aircraft. Part 4: Air Traffic Handling. Part 5: Guidance of Aircraft in a Time-Based Constrained Environment. Part 6: May 1990 (For primary document see N91-10981 02-05)
Copyright Avail: NTIS HC/MF A20; Non-NATO Nationals requests available only from AGARD/Scientific Publications Executive

N91-10996*# National Aeronautics and Space Administration. Langley Research Center, Hampton, VA.
A DESCRIPTION AND EVALUATION OF TIMER: A TIME-BASED TERMINAL FLOW-CONTROL CONCEPT
Leonard Credeur and William R. Capron (PRC Kentron, Inc., Hampton, VA.) *In* AGARD, Aircraft Trajectories: Computation, Prediction, Control, Volume 2: Air Traffic Handling and Ground-Based Guidance of Aircraft. Part 4: Air Traffic Handling. Part 5: Guidance of Aircraft in a Time-Based Constrained Environment. Part 6: May 1990 (For primary document see N91-10981 02-05)
Copyright Avail: NTIS HC/MF A20; Non-NATO Nationals requests available only from AGARD/Scientific Publications Executive CSCL 17G

N91-10997# Boeing Commercial Airplane Co., Seattle, WA.
USE OF 4-D RNAV IN TIME-BASED EN ROUTE ARRIVAL METERING
R. L. Erwin and K. H. Izumi *In* AGARD, Aircraft Trajectories: Computation, Prediction, Control, Volume 2: Air Traffic Handling and Ground-Based Guidance of Aircraft. Part 4: Air Traffic Handling. Part 5: Guidance of Aircraft in a Time-Based Constrained Environment. Part 6: May 1990 (For primary document see N91-10981 02-05)
Copyright Avail: NTIS HC/MF A20; Non-NATO Nationals requests available only from AGARD/Scientific Publications Executive

N91-10998# European Organization for the Safety of Air Navigation, Brussells (Belgium). Enguneering Directorate.
AIR TRAFFIC MANAGEMENT AND AIRCRAFT GUIDANCE IN A ZONE OF CONVERGENCE
Andre Benoit and Sip Swierstra *In* AGARD, Aircraft Trajectories: Computation, Prediction, Control, Volume 2: Air Traffic Handling and Ground-Based Guidance of Aircraft. Part 4: Air Traffic Handling. Part 5: Guidance of Aircraft in a Time-Based Constrained Environment. Part 6: May 1990 (For primary document see N91-10981 02-05)
Copyright Avail: NTIS HC/MF A20; Non-NATO Nationals requests available only from AGARD/Scientific Publications Executive

N91-10999# European Organization for the Safety of Air Navigation, Brussells (Belgium). Engineering Directorate.
GROUND-BASED 4-D GUIDANCE OF FLIGHTS IN STRONG WIND
Andre Benoit and Sip Swierstra *In* AGARD, Aircraft Trajectories: Computation, Prediction, Control, Volume 2: Air Traffic Handling and Ground-Based Guidance of Aircraft. Part 4: Air Traffic Handling. Part 5: Guidance of Aircraft in a Time-Based Constrained Environment. Part 6: May 1990 (For primary document see N91-10981 02-05)
Copyright Avail: NTIS HC/MF A20; Non-NATO Nationals requests available only from AGARD/Scientific Publications Executive

N91-11000*# National Aeronautics and Space Administration. Ames Research Center, Moffett Field, CA.
A PILOTED SIMULATOR EVALUATION OF A GROUND-BASED 4-D DESCENT ADVISOR ALGORITHM
Thomas J. Davis, Steven M. Green, and Heinz Erzberger *In* AGARD, Aircraft Trajectories: Computation, Prediction, Control, Volume 2: Air Traffic Handling and Ground-Based Guidance of Aircraft. Part 4: Air Traffic Handling. Part 5: Guidance of Aircraft in a Time-Based Constrained Environment. Part 6: May 1990 Previously announced in IAA as A87-50525 (For primary document see N91-10981 02-05)
Copyright Avail: NTIS HC/MF A20; Non-NATO Nationals requests available only from AGARD/Scientific Publications Executive CSCL 17G

N91-11001# European Organization for the Safety of Air Navigation, Brussells (Belgium). Engineering Directorate.
THE AIR TRAFFIC CONTROLLER FACING AUTOMATION: CONFLICT OR COOPERATION
Andre Benoit, Sip Swierstra, and Rene DeWispelaere (Eurocontrol Agency, Brussels, Belgium) *In* AGARD, Aircraft Trajectories: Computation, Prediction, Control, Volume 2: Air Traffic Handling and Ground-Based Guidance of Aircraft. Part 4: Air Traffic Handling. Part 5: Guidance of Aircraft in a Time-Based Constrained Environment. Part 6: May 1990 Presented at the International Conference NAV 1987, London, England, 29 Sep. - 1 Oct. 1987 (For primary document see N91-10981 02-05)
Copyright Avail: NTIS HC/MF A20; Non-NATO Nationals requests available only from AGARD/Scientific Publications Executive

N91-11002# European Organization for the Safety of Air Navigation, Brussells (Belgium). Engineering Directorate.
AIRCRAFT TRAJECTORY RECONSTITUTION ON THE BASIS OF MULTI-RADAR PLOT INFORMATION
P. vanderKraan *In* AGARD, Aircraft Trajectories: Computation, Prediction, Control, Volume 2: Air Traffic Handling and Ground-Based Guidance of Aircraft. Part 4: Air Traffic Handling. Part 5: Guidance of Aircraft in a Time-Based Constrained Environment. Part 6: May 1990 (For primary document see N91-10981 02-05)
Copyright Avail: NTIS HC/MF A20; Non-NATO Nationals requests available only from AGARD/Scientific Publications Executive

N91-11003# National Aerospace Lab., Amsterdam (Netherlands).
BAYESIAN MULTI-SENSOR TRACKING FOR ADVANCED AIR TRAFFIC CONTROL SYSTEMS
H. A. P. Blom, R. A. Hogendoorn, and F. J. vanSchaik *In* AGARD, Aircraft Trajectories: Computation, Prediction, Control, Volume 2: Air Traffic Handling and Ground-Based Guidance of Aircraft. Part 4: Air Traffic Handling. Part 5: Guidance of Aircraft in a Time-Based Constrained Environment. Part 6: May 1990 Sponsored by Dutch Civil Aviation Board (For primary document see N91-10981 02-05)
Copyright Avail: NTIS HC/MF A20; Non-NATO Nationals requests available only from AGARD/Scientific Publications Executive

N91-11004# Technical Univ. of Crete, Athens (Greece).
THE USE OF DOWNLINKED MEASUREMENTS TO TRACK CIVIL AIRCRAFT
C. C. Lefas *In* AGARD, Aircraft Trajectories: Computation, Prediction, Control, Volume 2: Air Traffic Handling and Ground-Based Guidance of Aircraft. Part 4: Air Traffic Handling. Part 5: Guidance of Aircraft in a Time-Based Constrained Environment. Part 6: May 1990 (For primary document see N91-10981 02-05)
Copyright Avail: NTIS HC/MF A20; Non-NATO Nationals requests available only from AGARD/Scientific Publications Executive

N91-11005# Service Technique de la Navigation Aerienne, Paris (France). Dept. Radiocommunication et Radioguidage.
CONTRIBUTION OF THE SATELLITE TECHNIQUES TO THE SURVEILLANCE OF AIR TRAFFIC [L'APPORT DES TECHNIQUES SATELLITAIRES A LA SURVEILLANCE DE LA NAVIGATION AERIENNE]
Olivier Carel *In* AGARD, Aircraft Trajectories: Computation, Prediction, Control, Volume 2: Air Traffic Handling and Ground-Based Guidance of Aircraft. Part 4: Air Traffic Handling. Part 5: Guidance of Aircraft in a Time-Based Constrained Environment. Part 6: May 1990 In FRENCH; ENGLISH summary (For primary document see N91-10981 02-05)
Copyright Avail: NTIS HC/MF A20; Non-NATO Nationals requests available only from AGARD/Scientific Publications Executive

N91-11007# European Organization for the Safety of Air Navigation, Brussells (Belgium). Engineering Directorate.
INTEGRATION OF AIRCRAFT CAPABILITY IN AIR TRAFFIC HANDLING SIMULATIONS
Andre Benoit, Sip Swierstra, and Yves Delnatte (Belgian World Airlines, Brussels.) *In* AGARD, Aircraft Trajectories: Computation, Prediction, Control, Volume 2: Air Traffic Handling and Ground-Based Guidance of Aircraft. Part 4: Air Traffic Handling. Part 5: Guidance of Aircraft in a Time-Based Constrained Environment. Part 6: May 1990 (For primary document see N91-10981 02-05)
Copyright Avail: NTIS HC/MF A20; Non-NATO Nationals requests available only from AGARD/Scientific Publications Executive

N91-11008# Technische Univ., Brunswick (Germany, F.R.). Inst. of Aeronautics and Astronautics.
SIMULATION OF AUTOMATED APPROACH PROCEDURES CONSIDERING DYNAMIC FLIGHT OPERATIONS
Manfred Fricke and Andreas Hoermann *In* AGARD, Aircraft Trajectories: Computation, Prediction, Control, Volume 2: Air Traffic Handling and Ground-Based Guidance of Aircraft. Part 4: Air Traffic Handling. Part 5: Guidance of Aircraft in a Time-Based Constrained Environment. Part 6: May 1990 (For primary document see N91-10981 02-05)
Copyright Avail: NTIS HC/MF A20; Non-NATO Nationals requests available only from AGARD/Scientific Publications Executive

05 AIRCRAFT DESIGN, TESTING AND PERFORMANCE

Includes aircraft simulation technology.

For related information see also *18 Spacecraft Design, Testing and Performance* and *39 Structural Mechanics*.For land transportation vehicles see *85 Urban Technology and Transportation*.

N91-10981# Advisory Group for Aerospace Research and Development, Neuilly-Sur-Seine (France). Guidance and Control Panel.
AIRCRAFT TRAJECTORIES: COMPUTATION, PREDICTION, CONTROL, VOLUME 2: AIR TRAFFIC HANDLING AND GROUND-BASED GUIDANCE OF AIRCRAFT. PART 4: AIR TRAFFIC HANDLING. PART 5: GUIDANCE OF AIRCRAFT IN A TIME-BASED CONSTRAINED ENVIRONMENT. PART 6: SURVEILLANCE. PART 7: METEOROLOGICAL FORECASTS. PART 8: AIRCRAFT OPERATION IN AIR TRAFFIC HANDLING SIMULATION
Andre Benoit, ed. May 1990 453 p In ENGLISH and FRENCH
(AGARD-AG-301-Vol-2-Pt-4-8; ISBN-92-835-0562-X) Copyright Avail: NTIS HC/MF A20; Non-NATO Nationals requests available only from AGARD/Scientific Publications Executive

This volume (part of a set of three) is composed of a preface and 28 papers covering respectively, the following topics. (1) Air traffic handling: Integration of control phases; A future European ATC concept; On-line prediction of aircraft trajectories; and Air traffic management. (2) Guidance of aircraft in a time based constrained environment: Guidance and control principles and concepts; Conduct of Air Traffic Control in a Zone of Convergence; Ground-based 4-D guidance of aircraft in moving atmosphere; and The Computer/Controller/Pilot dialogs. (3) Surveillance: Radar tracking; and Satellite techniques. (4) Meteorological forecasts: Impact of forecasts quality on trajector prediction; and Flight operations within a terminal area. (5) Aircraft operation in air traffic handling simulation: Realistic operation and motion of aircraft; and Flight operations within a terminal area. For individual titles, see N91-10982 through N91-11008.

N91-10982# European Organization for the Safety of Air Navigation, Brussells (Belgium). Engineering Directorate.
OPTIMUM ON-LINE HANDLING OF AIR TRAFFIC OVER WESTERN EUROPE **c04**
Andre Benoit and Sip Swierstra *In* AGARD, Aircraft Trajectories: Computation, Prediction, Control, Volume 2: Air Traffic Handling and Ground-Based Guidance of Aircraft. Part 4: Air Traffic Handling. Part 5: Guidance of Aircraft in a Time-Based Constrained Environment. Part 6: May 1990 Presented at the International Seminar ATC 2000, Luxembourg, 23-25 Feb. 1988 (For primary document see N91-10981 02-05)
Copyright Avail: NTIS HC/MF A20; Non-NATO Nationals requests available only from AGARD/Scientific Publications Executive

For today's airlines, Western Europe is not very large and the flights they make within it do not last very long. Consequently it should be possible within such an area as Western Europe to arrange Air Traffic Control (ATC) clearances and instructions so that any flight will, from departure clearance to touch-down be conducted in accordance with airline policy and without the changes to route and profile due to short term planning which are so disruptive to air traffic. An approach is recommended for the on-line handling of air traffic over such an area, covering in particular the integration of control phases from departure to destination. This leads to a central on-line optimal definition of departure/arrival sequences and essential characteristics of all flights, and a series of regional units to implement the relevant proposals/directives. This should provide the optimum integration of adjacent Zones of Convergence in which the time and altitude at which aircraft enter and leave each Zone are precisely controlled and are affected by the traffic conditions in their corresponding space/time sphere of influence. As a prerequisite to the above, a system is proposed for the purpose of accurately predicting and controlling the 4-D trajectory of an aircraft over any part of a flight, and in particular that part which extends from entry into until exit from the airspace of a given control center. Author

N91-10983# European Organization for the Safety of Air Navigation, Brussells (Belgium). Engineering Directorate.
THE EUROCONTROL FUTURE ATS SYSTEM CONCEPT AND THE PROGRAMME OF STUDIES, TESTS, AND TRIALS **c04**
V. Vachiery *In* AGARD, Aircraft Trajectories: Computation, Prediction, Control, Volume 2: Air Traffic Handling and Ground-Based Guidance of Aircraft. Part 4: Air Traffic Handling. Part 5: Guidance of Aircraft in a Time-Based Constrained Environment. Part 6: May 1990 (For primary document see N91-10981 02-05)
Copyright Avail: NTIS HC/MF A20; Non-NATO Nationals requests available only from AGARD/Scientific Publications Executive

The era of parallel, uncoordinated development of ground systems and guidance, navigation and communications avionics is at an end. The pursuit of optimum economic operating conditions, coupled with the need to handle an increasing volume of traffic, demand that those responsible for Air Traffic Management apply solutions that easily combine available ground and air technologies. Cooperation between pilot and controller actions constitutes one of the keystones of the future systems. It is possible to increase the capacity and efficiency of air traffic management, while at the same time maintaining essential safety requirements, only by making more use of automation for control planning functions. It is considered that increased automation cannot provide real advantages, however, unless the accuracy of aircraft trajectory prediction is greatly improved. This was made clear in the

description of the Future ATS Concept drawn up by EUROCONTROL. The Concept is presented in broad outline. Its implementation will call for a number of studies and trials, and a rundown is given of EUROCONTROL's program. The program places great emphasis on analysis of the conditions that need to be met to enable ground systems in future to have available facilities for the acquisition and exploitation of aircraft state vector parameters. The key aspects of the program are: (1) Improvement of the surveillance system; (2) Improvement of Air/Ground communications (Automatic data link); (3) Increased automation; and (4) Improvement of evaluation methods by using a realistic representation of the airborne side. Author

N91-10984# Royal Radar Establishment, Malvern (England).
PREDICTION OF AIRCRAFT TRAJECTORIES
Stanley Ratcliffe *In* AGARD, Aircraft Trajectories: Computation, Prediction, Control, Volume 2: Air Traffic Handling and Ground-Based Guidance of Aircraft. Part 4: Air Traffic Handling. Part 5: Guidance of Aircraft in a Time-Based Constrained Environment. Part 6: May 1990 (For primary document see N91-10981 02-05)
Copyright Avail: NTIS HC/MF A20; Non-NATO Nationals requests available only from AGARD/Scientific Publications Executive

Air traffic management, in designing route structures, drawing up rules for flight in various types of airspace, and in framing the instructions for air traffic controllers, are concerned with predicting the behavior, often on worst case assumptions, of each class of traffic with which they may have to deal. The problems are examined of on-line trajectory prediction to a time-horizon perhaps a little longer than the estimated time of the flight or as short as a few tens of seconds, the object being to predict and avoid collision with terrain or with another aircraft, and to ensure that any in-flight delays due to traffic congestion along the route are absorbed as economically as possible. Military aircraft are concerned with the avoidance of anti-aircraft missiles and in intercepting airborne targets. This latter problem may, very loosely, be regarded as collision avoidance in reverse, and is briefly discussed, as is the problem of terrain-following by high performance low flying military aircraft. The conclusion draws attention to areas where further R and D would seen desirable. Author

N91-10985# Universite Catholique, Louvain (Belgium). Dept. de Mecanique.
AIRCRAFT DYNAMICS FOR AIR TRAFFIC CONTROL
P.-Y. Willems *In* AGARD, Aircraft Trajectories: Computation, Prediction, Control, Volume 2: Air Traffic Handling and Ground-Based Guidance of Aircraft. Part 4: Air Traffic Handling. Part 5: Guidance of Aircraft in a Time-Based Constrained Environment. Part 6: May 1990 (For primary document see N91-10981 02-05)
Copyright Avail: NTIS HC/MF A20; Non-NATO Nationals requests available only from AGARD/Scientific Publications Executive

The equations of motion of airplanes in the context of Air Traffic Control (ATC) are discussed. The basic laws of mechanics are examined together with a mathematical model of mechanical systems which is suitable for airborne systems; the generally accepted (but often implicit) assumptions of usual models are pointed out. A simplified description of the main dynamical effects (gravity and aerodynamical interactions) are given together with a complete kinematical description of the system. The coherence with ISO norms (ISO - 1985) are respected as far as possible; some dynamical short commings of these norms are mentioned. Author

N91-10986# National Aerospace Lab., Amsterdam (Netherlands).
THE APPLICATION OF TRAJECTORY PREDICTION ALGORITHMS FOR PLANNING PURPOSES IN THE NETHERLANDS ATC-SYSTEM **c61**
J. N. P. Beers, T. B. Dalm, J. M. tenHave, and H. Visscher (Department of Civil Aviation, An Hoofddorp, Netherlands) *In* AGARD, Aircraft Trajectories: Computation, Prediction, Control, Volume 2: Air Traffic Handling and Ground-Based Guidance of Aircraft. Part 4: Air Traffic Handling. Part 5: Guidance of Aircraft in a Time-Based Constrained Environment. Part 6: May 1990 Previously announced as N89-20115 (For primary document see N91-10981 02-05)
Copyright Avail: NTIS HC/MF A20; Non-NATO Nationals requests available only from AGARD/Scientific Publications Executive

The Netherlands ATC-environment, the basic set-up of the trajectory prediction module, improvements realized, and the performance figures are presented. Applications of the trajectory prediction results in the system are listed, including data distribution rules, presentation of estimated times of arrival, boundary estimates, and, in particular, long term detection of conflicts for overflying aircraft, planning of inbound traffic for Schiphol airport, and planning of departure times for an efficient engine start-up procedure. Author

N91-10987# European Organization for the Safety of Air Navigation, Brussells (Belgium). Engineering Directorate.
GENERATION OF AIRCRAFT TRAJECTORIES FOR ON-LINE OPERATION: METHODS, TECHNIQUES, AND TOOLS
Andre Benoit and Sip Swierstra *In* AGARD, Aircraft Trajectories: Computation, Prediction, Control, Volume 2: Air Traffic Handling and Ground-Based Guidance of Aircraft. Part 4: Air Traffic Habdling. Part 5: Guidance of Aircraft in a Time-Based Constrained Environment. Part 6: May 1990 (For primary document see N91-10981 02-05)
Copyright Avail: NTIS HC/MF A20; Non-NATO Nationals requests available only from AGARD/Scientific Publications Executive

An appreciable amount of work has been conducted at the EUROCONTROL Agency's Engineering Directorate in the division engaged in the Study of Long Term Air Traffic Control (ATC) System Requirements in order to generate accurate aircraft trajectory predictions for use in both ATC on-line operation and real time simulations in current and realistic conditions, human interfaces included. The basic approach developed for two distinct classes of application are outlined: (1) the on-line generation of predictions for use in actual operation and, accessorily, real time ATC simulations; and (2) the introduction of realistic aircraft response and motion into ATC simulations, with pilot/auto-pilot interfaces included. Author

N91-10988# Consiglio Nazionale delle Ricerche, Rome (Italy). Progetto Finalizzato Trasporti and Ist. di Analisi dei Sistemi ed Informatica.
OPTIMIZATION MODELS AND TECHNIQUES TO IMPROVE AIR TRAFFIC MANAGEMENT **c04**
Lucio Bianco *In* AGARD, Aircraft Trajectories: Computation, Prediction, Control, Volume 2: Air Traffic Handling and Ground-Based Guidance of Aircraft. Part 4: Air Traffic Handling. Part 5: Guidance of Aircraft in a Time-Based Constrained Environment. Part 6: May 1990 (For primary document see N91-10981 02-05)
Copyright Avail: NTIS HC/MF A20; Non-NATO Nationals requests available only from AGARD/Scientific Publications Executive

A survey of earlier works is given with particular emphasis on optimization models and solution techniques. First, a multilevel model of the different ATC functions is proposed. Then, attention is devoted to the on-line control functions (flow control, on-line strategic control of flights and aircraft sequencing in the terminal area); for each problem, an optimization model is established and a solution technique is illustrated. The numerical behavior is also discussed. Author

N91-10989# European Organization for the Safety of Air Navigation, Brussells (Belgium). Engineering Directorate.
THE HIGH-RESOLUTION GRAPHIC DISPLAY: A POSSIBLE MAN/MACHINE INTERFACE FOR A COMPUTER ASSISTED ATC MANAGEMENT SYSTEM **c04**
Carlos Garcia Avello *In* AGARD, Aircraft Trajectories: Computation, Prediction, Control, Volume 2: Air Traffic Handling and Ground-Based Guidance of Aircraft. Part 4: Air Traffic Handling. Part 5: Guidance of Aircraft in a Time-Based Constrained

Environment. Part 6: May 1990 (For primary document see N91-10981 02-05)
Copyright Avail: NTIS HC/MF A20; Non-NATO Nationals requests available only from AGARD/Scientific Publications Executive

An application is described of high resolution graphic display in the field of management and control of air traffic in an extended area including a major terminal, the radius of the area being liable to vary from 150 to 300 nm. Reference is made to air traffic management and 4-D guidance techniques for individual aircraft in a Zone of Convergence (ZOC) in the knowledge that the graphic display techniques are applicable virtually to all systems affording the controller assistance at the decision making level. For the purpose of presenting data to the controller, a graphic rectangular display is employed having a resolution of 1280 by 1024 points, capable of displaying 16 colors. A circular display similar to most existing radar scopes could of course be used if it had equivalent resolution and color characteristics. The management directives and orders for guidance are presented to the operator, area manager or controller of an individual sector as part of the set of data displayed on the radar surveillance and control scope without the use of additional special tabular displays. Author

N91-10990# European Organization for the Safety of Air Navigation, Brussells (Belgium). Engineering Directorate.
THE 4-D CONTROL OF CURRENT AIR CARRIERS IN THE PRESENT ENVIRONMENT: OBJECTIVES, STATUS, AND PLANS **c04**
Andre Benoit *In* AGARD, Aircraft Trajectories: Computation, Prediction, Control, Volume 2: Air Traffic Handling and Ground-Based Guidance of Aircraft. Part 4: Air Traffic Handling. Part 5: Guidance of Aircraft in a Time-Based Constrained Environment. Part 6: May 1990 (For primary document see N91-10981 02-05)
Copyright Avail: NTIS HC/MF A20; Non-NATO Nationals requests available only from AGARD/Scientific Publications Executive

The accurate control of the time of arrival of aircraft will play an essential role in the efficient conduct of air traffic in terms of both economy and capacity. A technique was developed to select efficiently and control accurately each aircraft trajectory inbound to medium to high density traffic airports. The selection is made in terms of the overall traffic on the basis of the airline or pilot-preferred criterion, either cost, consumption or time, and the subsequent control is made in a ground/air co-operative manner, using whenever applicable speed and/or track corrections. The 4-D control is studied along with individual trajectories as applicable to current air carriers in the present environment directly adaptable to future automated air/ground digital communications. The overall control loop was simulated in an environment representing in particular the Belgian airspace configuration, using various flight simulators in conjunction with airline pilots and air traffic controllers. The results obtained to date make it possible to envisage on-line tests in the near future, aiming at a 10-second accuracy at the runway threshold for current commercial aircraft. Author

N91-10991# Centre d'Etudes et de Recherches, Toulouse (France).
FOUR DIMENSIONAL NAVIGATION IN AIR TRAFFIC WITH 4-D NAVIGATION AIRCRAFT [NAVIGATION 4-D EN CIRCULATION AERIENNE AIRCRAFT 4-D NAVIGATION] **c04**
Nicole Imbert and Marc J. Pelegrin *In* AGARD, Aircraft Trajectories: Computation, Prediction, Control, Volume 2: Air Traffic Handling and Ground-Based Guidance of Aircraft. Part 4: Air Traffic Handling. Part 5: Guidance of Aircraft in a Time-Based Constrained Environment. Part 6: May 1990 In FRENCH; ENGLISH summary (For primary document see N91-10981 02-05)
Copyright Avail: NTIS HC/MF A20; Non-NATO Nationals requests available only from AGARD/Scientific Publications Executive

Bearing in mind that the waiting times before landing are always increasing while the maximum landing rates are not reached, the monitoring of one more parameter during the approach is suggested. This is, in fact, two speed corrections and one heading correction (Nav. 4D, 3 space dimension + time). The first problem to be solved is the choice of the mathematical model to be used to simulate a plane. A model as complete as possible (in fact of the 18th order) was the starting point and it was degraded until a criterion was no longer satisfied. This criterion was a measurement of the error between the complete model and the degraded model along a reference trajectory (Roissy approach) of 54 km extension. It was assumed that the error due to the use of a simpler model should not reach + or - 320 m at the ILS entry beacon. A 6th order model was declared acceptable. After a number of simulations it was shown that corrections must arise after the entrance in the zone of convergence (ZOC) during the flight at constant level (speed correction) in the middle of the descent flown at constant indicated speed, (speed correction) and during the last leg before the ILS capture (heading correction). By a management method using a mathematical model on a fast time basis, an optimal time of arrival at the ILS entrance beacon can be determined, corresponding to an easy to fly trajectory. A model of the atmosphere must be used and it was checked that the robustness of the method (3 corrections) with regard to this model is correct. It was also checked that the time when the final beacon is reached is not sensitive to the mass of the plane at the entrance point. Author

N91-10992# European Organization for the Safety of Air Navigation, Brussells (Belgium). Engineering Directorate.
THE CONTROL OF INBOUND FLIGHTS **c04**
Andre Benoit and Sip Swierstra *In* AGARD, Aircraft Trajectories: Computation, Prediction, Control, Volume 2: Air Traffic Handling and Ground-Based Guidance of Aircraft. Part 4: Air Traffic Handling. Part 5: Guidance of Aircraft in a Time-Based Constrained Environment. Part 6: May 1990 (For primary document see N91-10981 02-05)
Copyright Avail: NTIS HC/MF A20; Non-NATO Nationals requests available only from AGARD/Scientific Publications Executive

The basic principles are described of the method to guide aircraft accurately down to the runway in a time-of-arrival constrained environment. The method is designed to be used in a Zone of Convergence context or in any similar advanced Air Traffic Control (ATC) system characterized by the integration of control phases over an extended area on the one hand and true computer assistance to the air traffic controller on the other, i.e., assistance provided at the decision making level through the automatic generation of guidance advisories. The method includes two closely coupled basic components, namely, a predictor, which computes a trajectory once initial conditions and plans are known, and a profile manager, which adapts the plans to meet the time constraint and generates the guidance directives on the basis of present position, actual surveillance information, aircraft operation and route constraints. Author

N91-10993*# National Aeronautics and Space Administration. Langley Research Center, Hampton, VA.
GUIDANCE CONCEPTS FOR TIME-BASED FLIGHT OPERATIONS **c04**
Dan D. Vicroy *In* AGARD, Aircraft Trajectories: Computation, Prediction, Control, Volume 2: Air Traffic Handling and Ground-Based Guidance of Aircraft. Part 4: Air Traffic Handling. Part 5: Guidance of Aircraft in a Time-Based Constrained Environment. Part 6: May 1990 (For primary document see N91-10981 02-05)
Copyright Avail: NTIS HC/MF A20; Non-NATO Nationals requests available only from AGARD/Scientific Publications Executive CSCL 17G

Airport congestion and the associated delays are severe in today's airspace system and are expected to increase. NASA and the FAA is investigating various methods of alleviating this problem through new technology and operational procedures. One concept for improving airspace productivity is time-based control of aircraft. Research to date has focused primarily on the development of time-based flight management systems and Air Traffic Control operational procedures. Flight operations may, however, require special onboard guidance in order to satisfy the Air Traffic Control imposed time constraints. The results are presented of a simulation study aimed at evaluating several time-based guidance concepts

in terms of tracking performance, pilot workload, and subjective preference. The guidance concepts tested varied in complexity from simple digital time-error feedback to an advanced time-referenced-energy guidance scheme. Author

N91-10994*# National Aeronautics and Space Administration. Langley Research Center, Hampton, VA.
THE 4-D DESCENT TRAJECTORY GENERATION TECHNIQUES UNDER REALISTIC OPERATING CONDITIONS **c04**

David H. Williams and Charles E. Knox *In* AGARD, Aircraft Trajectories: Computation, Prediction, Control, Volume 2: Air Traffic Handling and Ground-Based Guidance of Aircraft. Part 4: Air Traffic Handling. Part 5: Guidance of Aircraft in a Time-Based Constrained Environment. Part 6: May 1990 (For primary document see N91-10981 02-05)

Copyright Avail: NTIS HC/MF A20; Non-NATO Nationals requests available only from AGARD/Scientific Publications Executive CSCL 17G

NASA-Langley has been conducting and sponsoring research in airborne energy management for a number of years. During the course of this research, two fundamental techniques for the generation of 4D (fixed time) descent trajectories have emerged as viable candidates for advanced flight management systems. The first technique utilizes speed schedules of constant Mach number transitioning to constant calibrated airspeed chosen empirically to produce minimum fuel usage. The second technique computes cost optimized speed schedules of variable airspeed developed through application of optimal control theory. Both techniques have been found to produce reasonable and flyable descent trajectories. The formulation of the algorithms for each technique is evaluated and their suitability for operations in realistic conditions is discussed. Operational factors considered include: airplace speed, thrust, and altitude rate constaints; wind, temperature, and pressure variations; Air Traffic Control altitude, speed, and time constaints; and pilot interface and guidance considerations. Time flexibility, fuel usage, and airborne computational requirements were the primary performance measures. Author

N91-10995# Massachusetts Inst. of Tech., Cambridge. Flight Transportation Lab.
EXPERT SYSTEMS FOR THE GENERATION OF THERMAL AREA ARRIVAL PATHS FOR CIVIL TRANSPORT **c04**

Robert W. Simpson *In* AGARD, Aircraft Trajectories: Computation, Prediction, Control, Volume 2: Air Traffic Handling and Ground-Based Guidance of Aircraft. Part 4: Air Traffic Handling. Part 5: Guidance of Aircraft in a Time-Based Constrained Environment. Part 6: May 1990 (For primary document see N91-10981 02-05)

Copyright Avail: NTIS HC/MF A20; Non-NATO Nationals requests available only from AGARD/Scientific Publications Executive

Efficiencies can be gained from dynamic scheduling of the takeoff and landing operations for the system of runways at a major civil airport. It is then necessary to be able to generate a conflict-free set of flight paths which implements this schedule, and which can be easily changed. For landing arrival aircraft, these flight paths start at a known time, point and speed in the descent towards the airport, and end at a reduced speed and time at the outer marker of the final approach to the assigned runway where desired in-trail separations must be achieved. To generate sets of conflict-free arrival paths, an expert systems computer program finds and selects a path feasible within the performance limits of each aircraft from a set of patterns which are easily understandable by the human controller. This technique is easily adaptable to the geometric characteristics of different terminal areas and runway configurations, and easily accepts rules and procedural limitations which can be specified and implemented by ATC controllers themselves, as desired. Author

N91-10996*# National Aeronautics and Space Administration. Langley Research Center, Hampton, VA.
A DESCRIPTION AND EVALUATION OF TIMER: A TIME-BASED TERMINAL FLOW-CONTROL CONCEPT **c04**

Leonard Credeur and William R. Capron (PRC Kentron, Inc., Hampton, VA.) *In* AGARD, Aircraft Trajectories: Computation, Prediction, Control, Volume 2: Air Traffic Handling and Ground-Based Guidance of Aircraft. Part 4: Air Traffic Handling. Part 5: Guidance of Aircraft in a Time-Based Constrained Environment. Part 6: May 1990 (For primary document see N91-10981 02-05)

Copyright Avail: NTIS HC/MF A20; Non-NATO Nationals requests available only from AGARD/Scientific Publications Executive CSCL 17G

A description of a time-based ATC concept called TIMER (Traffic Intelligence for the Management of Efficient Runway-scheduling) and the results of a fast time and real time computer evaluation are presented. The concept was designed to improve the efficiency of extended terminal area operations (en route approach, transition, and terminal flight to the runway). TIMER integrates en route metering, fuel efficient cruise and profile descents, terminal sequencing and spacing together with computer-generated controller aids, in order to fully use runway capacity and improve efficiency of delay absorption. The concept, by using simplified aircraft models, accommodates both 4-D and non 4-D equipped aircraft and is designed for integration into the manual, voice linked ATC system in an evolutionary manner and still be able to accommodate proposed system upgrade features such as data link and further ground automation. Fast time and real time computer simulation results identify and show the effects and interactions of such key variables as horizon of control, metering fix and final approach delivery time errors, aircraft separation requirements, delay discounting, wind, flight technical error, and knowledge of aircraft final approach speed. The current ATC system has a runway interarrival-error standard deviation of approx. 26 seconds. Simulation results indicate that, with computer aiding, the runway interarrival-error standard deviation for non 4-D equipped traffic can be reduced to the region of 8 to 12 seconds if expected final approach speed is known; however, the reduction is only in the region of 16 to 20 seconds if expected final approach speed is unknown. Another major finding is that en route metering fix delivery-error standard deviation should be kept to less than a number somewhere between 35 to 45 seconds to achieve full runway capacity. This requirement implies the need for either airborne automation or assistance to the controller since the current manual performance in today's en route metering environment is in the order of 1.5 minutes. Author

N91-10997# Boeing Commercial Airplane Co., Seattle, WA.
USE OF 4-D RNAV IN TIME-BASED EN ROUTE ARRIVAL METERING **c04**

R. L. Erwin and K. H. Izumi *In* AGARD, Aircraft Trajectories: Computation, Prediction, Control, Volume 2: Air Traffic Handling and Ground-Based Guidance of Aircraft. Part 4: Air Traffic Handling. Part 5: Guidance of Aircraft in a Time-Based Constrained Environment. Part 6: May 1990 (For primary document see N91-10981 02-05)

Copyright Avail: NTIS HC/MF A20; Non-NATO Nationals requests available only from AGARD/Scientific Publications Executive

Arrival metering in en route airspace can match the demand rate to the airport acceptance rate. Air traffic control (ATC) is evolving time-based control techniques to facilitate en route arrival metering. This allows fuel savings by using speed reduction to absorb delay. The logic for en route arrival metering: (1) estimates the undelayed landing time of each arrival; (2) assigns the earliest available landing time; and (3) controls each arrival to its terminal area arrival (feeder) fix according to the common schedule developed for all arrivals. The airplane flight management system (FMS), used along with the ATC computer as part of a distributed data processing system, can define a minimum fuel cruise and descent flight profile which is consistent with ATC constraints. A study of four-dimensional area navigation (4D RNAV) operational requirements for use in en route arrival metering has determined

the functions and time-guidance accuracies needed for ATC compatible operations. A 4D RNAV capability is most easily achieved by wrapping a time navigation capability around a 3D FMS. Concepts for controlling a mix of 4D RNAV equipped and unequipped aircraft in a time-based en route arrival metering system have been the subject of on-going analyses and simulations by NASA-Ames. The use of 4D RNAV in en route arrival metering operations can save the operator fuel, reduce both pilot and controller workload, and reduce terminal airspace congestion.
Author

N91-10998# European Organization for the Safety of Air Navigation, Brussells (Belgium). Enguneering Directorate.
AIR TRAFFIC MANAGEMENT AND AIRCRAFT GUIDANCE IN A ZONE OF CONVERGENCE **c04**
Andre Benoit and Sip Swierstra *In* AGARD, Aircraft Trajectories: Computation, Prediction, Control, Volume 2: Air Traffic Handling and Ground-Based Guidance of Aircraft. Part 4: Air Traffic Handling. Part 5: Guidance of Aircraft in a Time-Based Constrained Environment. Part 6: May 1990 (For primary document see N91-10981 02-05)
Copyright Avail: NTIS HC/MF A20; Non-NATO Nationals requests available only from AGARD/Scientific Publications Executive

The basic principles of air traffic management and guidance of individual aircraft in a Zone of Convergence (ZOC) have been presented in previous papers at successive stages in the development of the project. These principles are summarized as is their applicability to the actual operational environment, compatibility with present technology and direct adaptability to future developments, the quality of the interfaces involving the air traffic controller and the aircraft crew and the resultant benefits to the community in terms of economy, use of available capacity and safety.
Author

N91-10999# European Organization for the Safety of Air Navigation, Brussells (Belgium). Engineering Directorate.
GROUND-BASED 4-D GUIDANCE OF FLIGHTS IN STRONG WIND **c04**
Andre Benoit and Sip Swierstra *In* AGARD, Aircraft Trajectories: Computation, Prediction, Control, Volume 2: Air Traffic Handling and Ground-Based Guidance of Aircraft. Part 4: Air Traffic Handling. Part 5: Guidance of Aircraft in a Time-Based Constrained Environment. Part 6: May 1990 (For primary document see N91-10981 02-05)
Copyright Avail: NTIS HC/MF A20; Non-NATO Nationals requests available only from AGARD/Scientific Publications Executive

In strong wind, groundspeed may vary appreciably during a turn, just as for example in the case of a landing after a U-turn preceding the localizer intercept. Such conditions are critical for maximum use of the runway, and render human estimation of aircraft motion extremely difficult. The tests are summarized which were conducted using a ground-based 4D guidance program, developed to assist the air traffic controller in maintaining the predicted landing time sequence with an accuracy better than 10 seconds for each arrival.
Author

N91-11000*# National Aeronautics and Space Administration. Ames Research Center, Moffett Field, CA.
A PILOTED SIMULATOR EVALUATION OF A GROUND-BASED 4-D DESCENT ADVISOR ALGORITHM **c04**
Thomas J. Davis, Steven M. Green, and Heinz Erzberger *In* AGARD, Aircraft Trajectories: Computation, Prediction, Control, Volume 2: Air Traffic Handling and Ground-Based Guidance of Aircraft. Part 4: Air Traffic Handling. Part 5: Guidance of Aircraft in a Time-Based Constrained Environment. Part 6: May 1990 Previously announced in IAA as A87-50525 (For primary document see N91-10981 02-05)
Copyright Avail: NTIS HC/MF A20; Non-NATO Nationals requests available only from AGARD/Scientific Publications Executive CSCL 17G

A ground-based, four dimensional (4D) descent-advisor algorithm is under development at NASA-Ames. The algorithm combines detailed aerodynamic, propulsive, and atmospheric models with an efficient numerical integration scheme to generate 4D descent advisories. The ability is investigated of the 4D descent advisor algorithm to provide adequate control of arrival time for aircraft not equipped with on-board 4D guidance systems. A piloted simulation was conducted to determine the precision with which the descent advisor could predict the 4D trajectories of typical straight-in descents flown by airline pilots under different wind conditions. The effects of errors in the estimation of wind and initial aircraft weight were also studied. A description of the descent advisor as well as the result of the simulation studies are presented.
Author

N91-11001# European Organization for the Safety of Air Navigation, Brussells (Belgium). Engineering Directorate.
THE AIR TRAFFIC CONTROLLER FACING AUTOMATION: CONFLICT OR COOPERATION **c04**
Andre Benoit, Sip Swierstra, and Rene DeWispelaere (Eurocontrol Agency, Brussels, Belgium) *In* AGARD, Aircraft Trajectories: Computation, Prediction, Control, Volume 2: Air Traffic Handling and Ground-Based Guidance of Aircraft. Part 4: Air Traffic Handling. Part 5: Guidance of Aircraft in a Time-Based Constrained Environment. Part 6: May 1990 Presented at the International Conference NAV 1987, London, England, 29 Sep. - 1 Oct. 1987 (For primary document see N91-10981 02-05)
Copyright Avail: NTIS HC/MF A20; Non-NATO Nationals requests available only from AGARD/Scientific Publications Executive

Today, developments in ground-based and on-board computers, navigation and digital air/ground/air communications make it possible to envision, for tomorrow, extensive automation of the overall air traffic control process, always provided that reliability, safety and responsibilities can be absolutely covered in all possible eventualities, however remote. Accordingly, before tomorrow, an appreciable amount of traffic will cross our skies and be handled by air traffic controllers without the support of advanced automated tools. Nevertheless, at the same time, the potential of automation will continue to increase. This subject is discussed in the light of the experience gained during the development of an approach to the definition, assessment and testing in an operational environment of a procedure suitable for guiding aircraft along 4-D trajectories illustrative of the next system generation of ATC. The essential aspects are examined of the computer/controller/pilot/aircraft chain of dialogues, placing the emphasis on the interface between the computer and the controller, the intelligent interpretation of the surveillance information by the computer, the definition, generation, and relay of guidance directives to the pilot and finally, the use of navigation aids. The integration of the ground-based 4-D guidance and control system messages on a standard ATC radar display is shown, illustrating this for the guidance of flights conducted by SABENA crews operating B-737 and DC-10 aircraft.
Author

N91-11002# European Organization for the Safety of Air Navigation, Brussells (Belgium). Engineering Directorate.
AIRCRAFT TRAJECTORY RECONSTITUTION ON THE BASIS OF MULTI-RADAR PLOT INFORMATION **c04**
P. vanderKraan *In* AGARD, Aircraft Trajectories: Computation, Prediction, Control, Volume 2: Air Traffic Handling and Ground-Based Guidance of Aircraft. Part 4: Air Traffic Handling. Part 5: Guidance of Aircraft in a Time-Based Constrained Environment. Part 6: May 1990 (For primary document see N91-10981 02-05)
Copyright Avail: NTIS HC/MF A20; Non-NATO Nationals requests available only from AGARD/Scientific Publications Executive

A short description of the various techniques in use for the establishment of aircraft reference trajectories is presented. Then a description of the principles and operation of the EUROCONTROL program MURATREC (Multi-Radar Trajectory Reconstitution) follows, covering in particular: (1) estimation of systematic radar errors; (2) curve fitting by the use of B-splines and dynamically adaptable spline steps; (3) accuracy of the reconstructed positional information; and (4) reconstitution of altitude, accelerations and speed. Applications of the MURATREC program are outlined, including application for the analysis of radar plot and track

accuracy (examples) and possible applications for incident investigations, on-line alignment of multi-radar information and simulation of aircraft trajectories in a given radar environment.
Author

N91-11003# National Aerospace Lab., Amsterdam (Netherlands).
BAYESIAN MULTI-SENSOR TRACKING FOR ADVANCED AIR TRAFFIC CONTROL SYSTEMS **c04**
H. A. P. Blom, R. A. Hogendoorn, and F. J. vanSchaik *In* AGARD, Aircraft Trajectories: Computation, Prediction, Control, Volume 2: Air Traffic Handling and Ground-Based Guidance of Aircraft. Part 4: Air Traffic Handling. Part 5: Guidance of Aircraft in a Time-Based Constrained Environment. Part 6: May 1990 Sponsored by Dutch Civil Aviation Board (For primary document see N91-10981 02-05)
Copyright Avail: NTIS HC/MF A20; Non-NATO Nationals requests available only from AGARD/Scientific Publications Executive

An overview is given of a Bayesian tracking system for a multi-sensor environment. The main modules perform track initiation, track continuation and systematic error estimation, respectively. The track continuation module plays for Air Traffic Control the most important role. It consists of a combination of those approximate Bayesian methods that proved to be the most efficient for the main problems of track continuation: Extended-Kalman filtering for nonlinear dynamics, Probabilistic Data Association for unassociated measurements and Interacting-Multiple-Model filtering for sudden maneuvers. Comparison of this new tracking system with alpha-beta Kalman based and state-of-the-art tracking systems show its superiority for application to Air Traffic Control surveillance. It provides better track continuity, more accurate expectations of position and velocity and more complete additional information in the form of probabilities of modes of flight (turning, accelerating and straight modes) and consistent estimates of its own accuracy. With this track information, advanced Air Traffic Control systems may better cope with the many uncertainties that are inherent to air traffic.
Author

N91-11004# Technical Univ. of Crete, Athens (Greece).
THE USE OF DOWNLINKED MEASUREMENTS TO TRACK CIVIL AIRCRAFT **c04**
C. C. Lefas *In* AGARD, Aircraft Trajectories: Computation, Prediction, Control, Volume 2: Air Traffic Handling and Ground-Based Guidance of Aircraft. Part 4: Air Traffic Handling. Part 5: Guidance of Aircraft in a Time-Based Constrained Environment. Part 6: May 1990 (For primary document see N91-10981 02-05)
Copyright Avail: NTIS HC/MF A20; Non-NATO Nationals requests available only from AGARD/Scientific Publications Executive

The use is described of measurements made on board civil aircraft to improve tracking accuracy in air traffic control (ATC) systems. The measurements are transmitted to the ground station via the Secondary Surveillance Radar (SSR) mode S data link. First the widely used alpha-beta filter and the first order Kalman filter are reviewed. Next the problem of maneuver handling is described and it is established that significant improvements, in terms of tracking accuracy, are expected when tracking maneuvering aircraft. The shape of maneuvers is examined using recordings made on board civil aircraft during normal scheduled services. The on-board measurements considered are roll angle, heading, and true air speed (TAS). Roll angle and the rate of change of heading are theoretically equivalent, since they are related though aircraft velocity. Maneuver tracking filters using either roll angle or heading are described and compared. It is shown that the filter using heading provides a better performance in the event of missing replies, since changes of heading are eventually detected. Both filters cannot track longitudinally accelerating targets. Next the use of velocity measurements, derived from TAS and heading, is considered. A filter is described that is capable of estimating the wind speed in the vicinity of the aircraft. The same filter provides satisfactory tracking accuracy during maneuvers and can handle longitudinal accelerations. Under monoradar coverage, where the data rate and accuracy are fairly constant, the filters reduce to a particularly simple form, that may be regarded as an enhanced alpha-beta filter. The performance of the filters is evaluated using data recorded during normal scheduled services.
Author

N91-11005# Service Technique de la Navigation Aerienne, Paris (France). Dept. Radiocommunication et Radioguidage.
CONTRIBUTION OF THE SATELLITE TECHNIQUES TO THE SURVEILLANCE OF AIR TRAFFIC [L'APPORT DES TECHNIQUES SATELLITAIRES A LA SURVEILLANCE DE LA NAVIGATION AERIENNE] **c04**
Olivier Carel *In* AGARD, Aircraft Trajectories: Computation, Prediction, Control, Volume 2: Air Traffic Handling and Ground-Based Guidance of Aircraft. Part 4: Air Traffic Handling. Part 5: Guidance of Aircraft in a Time-Based Constrained Environment. Part 6: May 1990 In FRENCH; ENGLISH summary (For primary document see N91-10981 02-05)
Copyright Avail: NTIS HC/MF A20; Non-NATO Nationals requests available only from AGARD/Scientific Publications Executive

The International Civil Aviation Organization asked a special committee FANS (Future Air Navigation Systems) to study satellite system implementation for communication navigation and surveillance applications. This committee recently issued its final report. FANS work is presented and the consequences are analyzed of satellite system implementation in case of the surveillance of air traffic. The most important element will be Automatic Dependent Surveillance (ADS) which implies the automatic air to ground return transmission of various airborne measured parameters, i.e., mainly aircraft position as supplied by the aircraft navigation equipments. This concept allows a much more efficient air traffic control in every area lacking a ground infrastructure. In continents areas with heavy air traffic, satellites will not substitute the secondary surveillance radar. The new techniques however will allow a flexible design of the ground infrastructure.
Author

N91-11006# European Organization for the Safety of Air Navigation, Brussells (Belgium). Engineering Directorate.
DEVELOPMENTS TO ENHANCE METEOROLOGICAL FORECASTING FOR AIR TRAFFIC SERVICES **c47**
M. E. Cox and D. A. Forrester (Meteorological Office, Bracknell, England) *In* AGARD, Aircraft Trajectories: Computation, Prediction, Control, Volume 2: Air Traffic Handling and Ground-Based Guidance of Aircraft. Part 4: Air Traffic Handling. Part 5: Guidance of Aircraft in a Time-Based Constrained Environment. Part 6: May 1990 (For primary document see N91-10981 02-05)
Copyright Avail: NTIS HC/MF A20; Non-NATO Nationals requests available only from AGARD/Scientific Publications Executive

In the future, the quality of the meteorological data available for use both in ground-based systems and on aircraft will become even more important as ATC strives to handle increasing volumes of traffic in the most efficient manner. An indication of the effect of errors in meteorological data on the precision of predictions of aircraft trajectories is discussed and the variability of wind and temperature is examined, showing the influence of location, altitude and season, in the European area. An outline of present-day forecasting methods follows (the data used and accuracies achieved are included). Potential sources of improvements are then discussed with the emphasis being placed on the use of aircraft-derived data (details are given of the accuracy of such data, possible methods of recovery, and their application within the Meteorological Services). The impact is described of turbulence on both the safety of air traffic and the accuracy of flight profile predictions (possible methods of providing aircraft with the means for the automatic reporting of turbulence are included). Some experimental work either performed or being planned in the European area is also described, aimed at improving the quality of the meteorological data made available for ATS purposes as a result of using data recovered from aircraft through both satellite and ground-based (Mode S SSR) systems.
Author

N91-11007# European Organization for the Safety of Air Navigation, Brussells (Belgium). Engineering Directorate.
INTEGRATION OF AIRCRAFT CAPABILITY IN AIR TRAFFIC HANDLING SIMULATIONS **c04**
Andre Benoit, Sip Swierstra, and Yves Delnatte (Belgian World Airlines, Brussels.) *In* AGARD, Aircraft Trajectories: Computation, Prediction, Control, Volume 2: Air Traffic Handling and Ground-Based Guidance of Aircraft. Part 4: Air Traffic Handling. Part 5: Guidance of Aircraft in a Time-Based Constrained Environment. Part 6: May 1990 (For primary document see N91-10981 02-05)
Copyright Avail: NTIS HC/MF A20; Non-NATO Nationals requests available only from AGARD/Scientific Publications Executive

The incorporation of airline/aircrew/aircraft specific procedures and performances into simulations and air traffic handling operations is a prerequisite for the next generation of management and control techniques. This matter is analyzed in the light of the shortcomings inherent in the present situation, in order to meet operators' demands in terms of capacity and efficiency. A practical approach is then proposed which includes the operators (aircrew/aircraft/avionics) in the overall ground/air/ground control loop at development, assessment, validation, and real time simulation levels. As an illustration of the potential offered, this approach is used to assess a ground/air coordinated 4-D guidance technique, and the results are summarized. Author

N91-11008# Technische Univ., Brunswick (Germany, F.R.). Inst. of Aeronautics and Astronautics.
SIMULATION OF AUTOMATED APPROACH PROCEDURES CONSIDERING DYNAMIC FLIGHT OPERATIONS **c04**
Manfred Fricke and Andreas Hoermann *In* AGARD, Aircraft Trajectories: Computation, Prediction, Control, Volume 2: Air Traffic Handling and Ground-Based Guidance of Aircraft. Part 4: Air Traffic Handling. Part 5: Guidance of Aircraft in a Time-Based Constrained Environment. Part 6: May 1990 (For primary document see N91-10981 02-05)
Copyright Avail: NTIS HC/MF A20; Non-NATO Nationals requests available only from AGARD/Scientific Publications Executive

During peak hours almost all major commercial airports operate close to their capacity limits. Moreover, the traffic demand often exceeds the offered capacities leading to more or less stringent restrictions in slot allocation. The purpose of the fast-time air traffic simulations, was to analyze and assess the performance and the practicability of automated time-based approach concepts, currently developed to optimize the terminal area air traffic process with respect to safety, capacity and economy. The developed program system TASIMD (Terminal Area SIMulation considering the aircraft Dynamics) simulates flight operations of arriving aircraft within a terminal area during a specific time interval. TASIMD models all major elements of a TMA scenario related to the control and operations of automated approach procedures on the ground and in the air (e.g., surveillance, control procedures, aircraft dynamics, flight guidance). The aircraft fly along 4D-trajectories, described by a horizontal profile, an altitude profile and a speed profile to integrate the time element, considering influences on the path following accuracy in space and time. Sources of error impact are: entry fix time deviation, navigation, wind, airspeed error and profile management algorithm error. Errors are modeled in Monte-Carlo technique. Two types of automated approach procedures were developed and analyzed: a variable path speed control concept (VPSC) and a fixed path speed control concept (FPSC). Both concepts presume a shared air/ground responsibility for profile control. Author

N91-11009 Kansas Univ., Lawrence.
CALCULATION OF AERODYNAMIC CHARACTERISTICS OF AIRPLANE CONFIGURATIONS AT HIGH ANGLE OF ATTACK IN STEADY AND UNSTEADY FLOW Ph.D. Thesis
Homayoun Emdad 1989 117 p
Avail: Univ. Microfilms Order No. DA9024169

A computational method for steady and unsteady lateral directional aerodynamics of fighter configurations is developed. The leading-edge vortices are represented by free vortex filaments which are adjusted iteratively to satisfy the force-free condition. The forebody vortex separation, both symmetrical and asymmetrical, is calculated with slender body theory. The effect of the boundary layer separation on lifting surfaces is accounted for by using the effective sectional angles of attack. Results for several fighter configurations are employed for comparison with available data. It is shown that the present steady-flow method produces reasonable results in predicting slideslip derivatives, while roll- and yaw-rate derivatives do not compare very well with forced-oscillation test data at high angles of attack. To account for unsteady aerodynamics, a theoretical method is developed to determine the aerodynamic derivatives due to pitching, plunging, flapping, side movement, rolling, and yawing for a wing in a compressible flow. The present method is based on the frequency approach, instead of time-domain integration. The wing is represented by a series of oscillatory horseshoe vortices, and the leading-edge vortices are represented by oscillatory line vortices. Results for 60 and 80 deg delta wings are compared with experimental data. It is shown that the present method produces reasonable results for roll damping derivatives before occurrence of vortex breakdown. Other dynamic derivatives were not compared. Dissert. Abstr.

N91-11010 Purdue Univ., West Lafayette, IN.
DEVELOPMENT AND APPLICATION OF THE TIME DOMAIN PANEL METHOD Ph.D. Thesis
Maxwell Blair 1989 196 p
Avail: Univ. Microfilms Order No. DA9018788

The utility of the Time Domain Panel (TDP) algorithm for wing design and analysis is developed and demonstrated. This is a linear unsteady aerodynamic method for simulating loads on an oscillating wing in subsonic compressible flow. This time stepping simulation is based on Guderley's integral formulae. Other current work, which is similar in application, is either based on computationally expensive nonlinear finite difference schemes, or is based on inverse transforms of linear harmonic aerodynamic loads. The TDP method is a direct integral (panel) method which has the efficiency of linear aerodynamics but is in a suitable form for developing simulation models with nonlinear structural dynamics or nonlinear controls. This is a linear time stepping method which falls between linear harmonic aerodynamic methods and higher order nonlinear time stepping aerodynamic methods. The developmental details in numerically implementing Guderley's integral formula is given here. Several applications are presented in order to provide confidence that the TDP method is practical and numerically accurate. Dissert. Abstr.

N91-11011 Stanford Univ., CA.
CONTROLLED VORTICAL FLOW ON DELTA WINGS THROUGH UNSTEADY LEADING EDGE BLOWING Ph.D. Thesis
Kyung-Tae Lee 1990 147 p
Avail: Univ. Microfilms Order No. DA9024343

The vortical flow over a delta wing contributes an important part of the lift - the so called nonlinear lift. Controlling this vortical flow with its favorable influence would enhance aircraft maneuverability at high angle of attack. Several previous studies have shown that control of the vortical flow field is possible through the use of blowing jets. Vortical flow control is studied by applying a new blowing scheme to the rounded leading edge of a delta wing; this blowing scheme is called Tangential Leading Edge Blowing (TLEB). Vortical flow response both to steady blowing and to unsteady blowing is investigated. It is found that TLEB can redevelop stable, strong vortices even in the post-stall angle of attack regime. Analysis of the steady data shows that the effect of leading edge blowing can be interpreted as an effective change in angle of attack. The examination of the fundamental time scales for vortical flow re-organization after the application of blowing for differential initial states of the flow field is studied. Different time scales for flow re-organization are shown to depend upon the effective angle of attack. A faster response time can be achieved at angles of attack beyond stall by a suitable choice of the initial blowing momentum strength. Consequently, TLEB shows the

potential of controlling the vortical flow over a wide range of angles of attack; i.e., in both for pre-stall and post-stall conditions.
Dissert. Abstr.

N91-11012 Maryland Univ., College Park.
COUPLED ROTOR/AIRFRAME VIBRATION ANALYSIS Ph.D. Thesis
Shmuel Fledel 1989 171 p
Avail: Univ. Microfilms Order No. DA9021500

A consistent finite-element formulation developed for the prediction of vibration in rotor/body helicopter systems in forward flight, taking into account interactional rotor/body aerodynamic loads and dynamic coupling is presented. The rotor blades are assumed to be elastic beams undergoing flap and lag bending, torsion and axial deflections. The coupled analysis is formulated retaining nonlinear structural, inertial and aerodynamic terms in a consistent manner. Rotor excitation includes rotor/body interactional loads and fuselage dynamic coupling. Effects of several parameters on vibratory hub loads and body vibration are investigated, including blade stiffness, rotor/body clearance, hub location, fuselage stiffness and advance ratio. A significant influence of body upwash on the rotor disk in causing vibratory hub shear is shown, an effect which generally increases with smaller rotor/body clearance. Tuning of rotor and body natural modes substantially reduces vibration levels. Elastic deflections of the body have considerable influence on vibratory hub loads. Analyses assuming clamped body motion (wind tunnel condition) or rigid body motion yield inadequate vibration predictions for the rotor/body system. Dissert. Abstr.

N91-11013 Tennessee Univ., Knoxville.
AERODYNAMIC DESIGN OPTIMIZATION USING COMPUTATIONAL FLUID DYNAMICS Ph.D. Thesis
David Howard Huddleston 1989 122 p
Avail: Univ. Microfilms Order No. DA9021023

An aerodynamic design optimization technique is presented that couples direct optimization algorithms with the analysis capability provided by appropriate computational fluid dynamics (CFD) programs. This technique is intended to be an aid in designing the aerodynamic shapes and establishing test conditions required for the successful simulation of aircraft engine inlet conditions in a ground test environment. However, the method is also applicable to other aerodynamic design problems such as airfoil design, turbomachinery cascade design, and nozzle design. The approach involves minimization of a nonlinear least-squares objective function which may be defined in a region remote to the geometric surface being optimized. Finite-difference Euler and Navier-Stokes codes were applied to obtain the objective function evaluations, although the applied optimization method can be coupled with any appropriate CFD analysis technique. Using CFD to compute design space gradients within an optimization algorithm has received little prior attention in the literature. It is demonstrated, that CFD can be used in this manner by applying the developed design technique to a variety of aerodynamic design problems. Results are presented for several typical aerospace examples, including algebraic test functions, inviscid and viscous flow over airfoils, flows in convergent/divergent nozzles in both two and three dimensions, and supersonic flow about a planar forebody simulator. Dissert. Abstr.

N91-11014 California Inst. of Tech., Pasadena.
APPLICATION OF DYNAMICAL SYSTEMS THEORY TO NONLINEAR AIRCRAFT DYNAMICS Ph.D. Thesis
Craig Charles Jannke 1990 281 p
Avail: Univ. Microfilms Order No. DA9022286

A continuation method was used to determine the steady states of three nonlinear aircraft models: a general aviation aircraft with a canard configuration, a generic jet fighter, and the F-14. The continuation method calculated the steady states of the aircraft as functions of the control surface deflections. Bifurcations of these steady states were determined and shown to cause instabilities which resulted in qualitative changes in the state of the aircraft. A longitudinal instability which resulted in a deep stall was determined for the general aviation aircraft. Roll-coupling and high angle of attack instabilities were determined for the generic jet fighter, and wing rock, directional divergence and high angle of attack instabilities were determined for the F-14. Knowledge of the control surface deflections at which bifurcations occurred was used to either put limits on the control surface deflections or to program the control surface deflections at which bifurcations occur could not be attained. Simple control systems were included in the aircraft models to determine the effects of control systems on the instabilities of each aircraft. Steady spin modes were determined for each aircraft. A successful recovery technique was determined for the general aviation aircraft, but no successful recovery technique could be found for the F-14. Dissert. Abstr.

N91-11015# Federal Aviation Administration, Atlantic City, NJ.
GENERATION OF A BUOYANT PLUME OF ARTIFICIAL SMOKE FOR AIRPLANE TESTS Final Report
Thor I. Eklund Sep. 1990 28 p
(DOT/FAA/CT-90/9) Avail: NTIS HC/MF A03

A buoyant artificial smoke generator was developed for airplane test applications. In the device, theatrical smoke is mixed with a mixture of helium and air. The total gas flow, the helium to air ratio, and the theatrical smoke particulate generation rate can all be varied in the device. A gas mixture of 50 percent each of helium and air has the buoyancy properties of air, alone, heated to 475 F. The device was used in cabin smoke evacuation tests in a modified Boeing 757 aircraft. Generation of the buoyant smoke in an aircraft resulted in dramatically different behavior from that previously observed with nonbuoyant theatrical smoke. The buoyant smoke spread further through the aircraft in a manner that was not predicted by an analytical model on cabin smoke spread. Besides being used to assess airplane cabin smoke evacuation capability, the buoyant smoke generator has been used to evaluate smoke detector performance and optimal location in Air Force jet aircraft. Author

N91-11016# Messerschmitt-Boelkow-Blohm G.m.b.H., Munich (Germany, F.R.). Hurschrauber und Flugzeuge.
MARGINAL AIRCRAFT RELEASE DISTURBANCE ON ADVANCED MISSILES
Ronald Deslandes 20 Apr. 1988 26 p Presented at AGARD FMP Symposium on Stability and Control of Tactical Missile Systems, Ankara, Turkey, 9-12 May 1988
(MBB/FE121/S/PUB/329; ETN-90-97841) Copyright Avail: NTIS HC/MF A03

Marginal aircraft release effects are demonstrated and the determination of the leading parameters for the design specifications are indicated. Based on simulations performed with a powerful six degrees of freedom code, inconsistencies implicated by excessive roll or pitch-motion during different rail-launch situations are studied. The basic algorithms are described and computed results involving data from flight test movies as well as from telemetry are displayed by three dimensional video, in order to prove that the problem area is well handled. ESA

N91-10932# Deutsche Airbus G.m.b.H., Bremen (Germany, F.R.).
A QUARTER OF A CENTURY OF AEROELASTIC COOPERATION BETWEEN RESEARCH AND INDUSTRY (A REVIEW). PART 2: TRANSPORT AIRPLANES AND OTHER CIVIL APPLICATIONS
S. Vogel, H. Zimmermann, and K. Koenig *In* DLR, Contributions in the Field of Aeroelastics on the Occasion of the 60th Anniversary of Professor Dr.-Ing. Habil. Hans Wilhelm Foersching Apr. 1990 p 271-287 (For primary document see N91-10920 02-02)
Avail: NTIS HC/MF A13

N91-10937*# Boeing Commercial Airplane Co., Seattle, WA.
BOEING FLIGHT DECK DESIGN PHILOSOPHY
Harty Stoll *In* NASA, Langley Research Center, Aviation Safety/Automation Program Conference Oct. 1990 p 17-25 (For primary document see N91-10936 02-03)
Avail: NTIS HC/MF A12 CSCL 01C

N91-10939*# Douglas Aircraft Co., Inc., Long Beach, CA.
DOUGLAS FLIGHT DECK DESIGN PHILOSOPHY
Paul Oldale *In* NASA, Langley Research Center, Aviation Safety/Automation Program Conference Oct. 1990 p 45-53 (For primary document see N91-10936 02-03)
Avail: NTIS HC/MF A12 CSCL 01C

N91-10949*# National Aeronautics and Space Administration. Langley Research Center, Hampton, VA.
OVERVIEW OF ERROR-TOLERANT COCKPIT RESEARCH Abstract Only
Kathy Abbott *In its* Aviation Safety/Automation Program Conference Oct. 1990 p 153-156 (For primary document see N91-10936 02-03)
Avail: NTIS HC/MF A12 CSCL 01C

N91-10969# Technische Univ., Brunswick (Germany, F.R.).
COMPARISON OF A MATHEMATICAL ONE-POINT MODEL AND A MULTI-POINT MODEL OF AIRCRAFT MOTION IN MOVING AIR
R. Brockhaus *In* AGARD, Aircraft Trajectories: Computation, Prediction, Control, Volume 1. Part 1: Fundamentals. Part 2: Flight in Critical Atmospheric Conditions. Part 3: Impact of New On-Board Technologies on Aircraft Operation Mar. 1990 17 p (For primary document see N91-10967 02-04)
Copyright Avail: NTIS HC/MF A12; Non-NATO Nationals requests available only from AGARD/Scientific Publications Executive

N91-10971# Toronto Univ. (Ontario). Inst. for Aerospace Studies.
CRITICAL ASPECTS OF TRAJECTORY PREDICTION: FLIGHT IN NON-UNIFORM WIND
Bernard Etkin and David Alexander Etkin (Canadian Climate Centre, Downsview, Ontario) *In* AGARD, Aircraft Trajectories: Computation, Prediction, Control, Volume 1. Part 1: Fundamentals. Part 2: Flight in Critical Atmospheric Conditions. Part 3: Impact of New On-Board Technologies on Aircraft Operation Mar. 1990 12 p (For primary document see N91-10967 02-04)
Copyright Avail: NTIS HC/MF A12; Non-NATO Nationals requests available only from AGARD/Scientific Publications Executive

N91-10972# Technische Univ., Brunswick (Germany, F.R.). Inst. of Flight Guidance and Control.
EFFECT OF WIND AND WIND VARIATION ON AIRCRAFT FLIGHT-PATHS
K.-U. Hahn, T. Heintsch, B. Kaufmann, G. Schaenzer, and M. Swolinsky *In* AGARD, Aircraft Trajectories: Computation, Prediction, Control, Volume 1. Part 1: Fundamentals. Part 2: Flight in Critical Atmospheric Conditions. Part 3: Impact of New On-Board Technologies on Aircraft Operation Mar. 1990 27 p Sponsored by DFG (For primary document see N91-10967 02-04)
Copyright Avail: NTIS HC/MF A12; Non-NATO Nationals requests available only from AGARD/Scientific Publications Executive

N91-10973# Southampton Univ. (England).
AIRCRAFT FLIGHT IN WIND-SHEAR
D. McLean *In* AGARD, Aircraft Trajectories: Computation, Prediction, Control, Volume 1. Part 1: Fundamentals. Part 2: Flight in Critical Atmospheric Conditions. Part 3: Impact of New On-Board Technologies on Aircraft Operation Mar. 1990 10 p (For primary document see N91-10967 02-04)
Copyright Avail: NTIS HC/MF A12; Non-NATO Nationals requests available only from AGARD/Scientific Publications Executive

N91-10974# Airbus Industrie, Blagnac (France).
HOW TO FLY WINDSHEAR
Paul Camus *In* Agard, Aircraft Trajectories: Computation, Prediction, Control, Volume 1. Part 1: Fundamentals. Part 2: Flight in Critical Atmospheric Conditions. Part 3: Impact of New On-Board Technologies on Aircraft Operation Mar. 1990 10 p (For primary document see N91-10967 02-04)
Copyright Avail: NTIS HC/MF A12; Non-NATO Nationals requests available only from AGARD/Scientific Publications Executive

N91-10976# Smiths Industries, Inc., Grand Rapids, MI.
AIRCRAFT TRAJECTORY: PREDICTION AND CONTROL IN THE AIR TRANSPORT FLIGHT MANAGEMENT COMPUTER SYSTEMS
Peter J. Howells *In* AGARD, Aircraft Trajectories: Computation, Prediction, Control, Volume 1. Part 1: Fundamentals. Part 2: Flight in Critical Atmospheric Conditions. Part 3: Impact of New On-Board Technologies on Aircraft Operation Mar. 1990 13 p (For primary document see N91-10967 02-04)
Copyright Avail: NTIS HC/MF A12; Non-NATO Nationals requests available only from AGARD/Scientific Publications Executive

N91-10977# Airbus Industrie, Blagnac (France). Flight Div.
IMPACT OF NEW TECHNOLOGY ON OPERATIONAL INTERFACE: FROM DESIGN AIMS TO FLIGHT EVALUATION AND MEASUREMENT
J. J. Speyer, C. Monteil, R. D. Blomberg, and J. P. Fouillot (Paris V Univ., France) *In* AGARD, Aircraft Trajectories: Computation, Prediction, Control, Volume 1. Part 1: Fundamentals. Part 2: Flight in Critical Atmospheric Conditions. Part 3: Impact of New On-Board Technologies on Aircraft Operation Mar. 1990 37 p (For primary document see N91-10967 02-04)
Copyright Avail: NTIS HC/MF A12; Non-NATO Nationals requests available only from AGARD/Scientific Publications Executive

06 AIRCRAFT INSTRUMENTATION

Includes cockpit and cabin display devices; and flight instruments.

For related information see also *19 Spacecraft Instrumentation* and *35 Instrumentation and Photography.*

N91-10938*# Honeywell, Inc., Minneapolis, MN.
COCKPIT AVIONICS INTEGRATION AND AUTOMATION
Keith M. Pischke *In* NASA, Langley Research Center, Aviation Safety/Automation Program Conference Oct. 1990 p 27-44 (For primary document see N91-10936 02-03)
Avail: NTIS HC/MF A12 CSCL 01C

N91-10942*# National Aeronautics and Space Administration. Ames Research Center, Moffett Field, CA.
SUMMARY OF THE INDUSTRY/NASA/FAA WORKSHOP ON PHILOSOPHY OF AUTOMATION: PROMISES AND REALITIES
Susan D. Norman *In* NASA, Langley Research Center, Aviation Safety/Automation Program Conference Oct. 1990 p 77-82 (For primary document see N91-10936 02-03)
Avail: NTIS HC/MF A12 CSCL 01C

N91-10950*# National Aeronautics and Space Administration. Langley Research Center, Hampton, VA.
FAULT MONITORING
Paul Schutte *In its* Aviation Safety/Automation Program Conference Oct. 1990 p 157-163 (For primary document see N91-10936 02-03)
Avail: NTIS HC/MF A12 CSCL 01C

07 AIRCRAFT PROPULSION AND POWER

Includes prime propulsion systems and systems components, e.g., gas turbine engines and compressors; and onboard auxilliary power plants for aircraft.

For related information see also *20 Spacecraft Propulsion and Power, 28 Propellants and Fuels,* and *44 Energy Production and Conversion.*

N91-11017# Technische Hochschule, Aachen (Germany, F.R.). Fakultaet fuer Maschinenwesen.

A CONTRIBUTION TO THE OUTPUT ANALYSIS AND LAYOUT OF TRANSONIC AXIAL TURBINE STAGES Ph.D. Thesis [EIN BEITRAG ZUR LEISTUNGSANALYSE UND AUSLEGUNG TRANSSONISCHER AXIALTURBINENSTUFEN]

Peter Pretzsch 1989 141 p In GERMAN
(ETN-90-97862) Avail: NTIS HC/MF A07

The course of iteration in the turbine layout, using a transonic axial turbine stage, is described. This covers equally the process of fashioning the turbine, as well as the experimental and theoretical verification of volumes in the final layout. In this given field, the possibilities of efficiency analysis of turbine stages are demonstrated and set right for use in the direction of cost minimization for efficient layout of high output turbine stages. ESA

N91-11018# Stuttgart Univ. (Germany, F.R.). Inst. fuer Luftfahrtantriebe.

TEST LAUNCH FOR TURBOAIRCRAFT ENGINE. DESCRIPTION OF THE INSTALLATION [HOCHENPRUEFSTAND FUER TURBOFLUGTRIEBWERKE. BESCHREIBUNG DER ANLAGE]

1987 23 p In GERMAN
(ILA-87-A-02; ETN-90-97879) Avail: NTIS HC/MF A03

In the framework of aeronautical research, a test bench for aircraft engine was built. Using different economic principles, such as compact construction, it was possible to build a modern test installation at relatively low cost. The environmental noise problem was particularly studied and solved. ESA

N91-11019# Universitaet der Bundeswehr, Hamburg (Germany, F.R.). Fachbereich Maschinenbau.

INTEGRATION OF MODEL AND KNOWLEDGE BASED DIAGNOSIS, WITH THE EXAMPLE OF A TURBOJET ENGINE Ph.D. Thesis [INTEGRATION VON MODELLBEZOGENER UND WISSENSBASIERTER DIAGNOSE AM BEISPIEL EINES TURBOFLUGTRIEBWERKES]

Uwe Willan 1990 169 p In GERMAN Sponsored by Bundesministerium der Verteidigung
(ETN-90-97900) Avail: NTIS HC/MF A08

The early detection of failures in technical processes in general, and in aircraft engines in particular is of great importance. Besides the precise statement of place and size of a failure already apparent (diagnosis), it is also of interest to predict its occurrence (prediction). The aim of this investigation is to utilize for an actual project, various processes which are able to fulfill these tasks. The point is the possible utilization of a microcomputer. Two basic principles are carried out, the model based diagnosis and the knowledge based diagnosis. The two systems are presented with some criteria for the choice of the system more adapted for use in precise actual cases. A work developed in this connection for an aircraft engine has led to the production of largely automatized model which is valid for any gas turbine. The design of an expert system for the diagnosis of the part of an aircraft which cannot be modeled, is stated. Various processes suitable for connecting together both types of diagnosis are presented and discussed. The resulting integrated system unites the advantages of both methods, not taking into account their drawbacks. ESA

N91-11020# Rolls-Royce Ltd., Bristol (England).

CARBON DEPOSITION IN GAS TURBINE COMBUSTORS

H. C. Low and C. W. Wilson Derby, England 4 Oct. 1989 14 p Presented at CEGB Institute of Physics, 4 Oct. 1989
(PNR-90692; ETN-90-97933) Copyright Avail: NTIS HC/MF A03

Flame soot, a product of incomplete combustion, may be produced in fuel rich regions of gas turbine combustors. From this soot, carbon and a mixture of hydrogen, oxygen and other species can be accumulated on flame tube walls, heat shields and fuel injector surfaces. The ways the soot can be formed are proposed. Liquid phase fuel pyrolysis leading to carbon accretions are reported. Carbon deposition causes blade erosion as it passes through the turbine system. If deposition becomes excessive, the fuel distribution and fuel/air mixing processes may become modified. ESA

N91-11021# Rolls-Royce Ltd., Derby (England).

RECENT ADVANCES AND DEVELOPMENTS IN COATINGS

G. W. Meetham 22 Jul. 1989 17 p Presented at Seminar on Advances in Plating Coating Technology, India, 20-22 Jul. 1989
(PNR-90698; ETN-90-97934) Copyright Avail: NTIS HC/MF A03

The developments which took place in the coating technologies required by the gas turbine engine are summarized. The increasing sophistication found to be necessary is illustrated. Special attention is given to corrosion resistant, thermal barrier, wear resistant and abradable coats. Improvements in coating processes for future requirements are underlined. ESA

N91-11022# Advisory Group for Aerospace Research and Development, Neuilly-Sur-Seine (France). Propulsion and Energetics Panel.

TEST CASES FOR COMPUTATION OF INTERNAL FLOWS IN AERO ENGINE COMPONENTS

Leonhard Fottner, ed. (Universitaet der Bundeswehr Muenchen, Neubiberg, Germany, F.R.) Jul. 1990 393 p
(AGARD-AR-275; ISBN-92-835-0573-5) Copyright Avail: NTIS HC/MF A17; Non-NATO Nationals requests available only from AGARD/Scientific Publications Executive

An analytical and experimental data base intended as support in the development of new and the refinement of existing codes for computing internal flows in aero engine components, specifically in cascades, compressors, turbines and ducts ahead of and between them is presented. All the analytical test cases described are relevant to steady, 2-dimensional, inviscid flow calculations. The experimental test cases are relevant to steady 2-dimensional, quasi- or fully 3-dimensional flow calculations for viscous flows in axial turbomachinery components. These data are believed to represent the highest quality analytical and experimental test cases available today. However, in appraising the large amount of experimental data submitted, the Working Group necessarily had to consider what the requirements for a satisfactory test case are and what experimental precautions and problems have to be addressed and overcome. It also became apparent where gaps exist in the available test cases and what is required for the future. Author

N91-10927# Deutsche Forschungsanstalt fuer Luft- und Raumfahrt, Goettingen (Germany, F.R.). Inst. fuer Aeroelastik.

DETERMINATION OF UNSTEADY AERODYNAMIC FORCES ON ENGINES WITH A VIEW TO FLUTTER INVESTIGATIONS [BESTIMMUNG INSTATIONAERER TRIEBWERKSLUFTKRAEFTE FUER DIE ANWENDUNG BEI FLATTERUNTERSUCHUNGEN]

Hermann Triebstein, Guenter Schewe, and Hartmut Zingel (Messerschmitt-Boelkow-Blohm G.m.b.H., Bremen, Germany, F.R.) *In its* Contributions in the Field of Aeroelastics on the Occasion of the 60th Anniversary of Professor Dr.-Ing. Habil. Hans Wilhelm Foersching Apr. 1990 p 141-168 In GERMAN; ENGLISH summary (For primary document see N91-10920 02-02)
Avail: NTIS HC/MF A13

08 AIRCRAFT STABILITY AND CONTROL

Includes aircraft handling qualities; piloting; flight controls; and autopilots.

For related information see also *05 Aircraft Design, Testing and Performance.*

N91-11023 Oklahoma State Univ., Stillwater.
A NEW APPROACH TO THE FLIGHT CONTROL SYSTEM RECONFIGURATION FOLLOWING A BATTLE DAMAGE AND/OR GENERIC FAILURE ON A CONTROL SURFACE Ph.D. Thesis
Marcello Rosario Napolitano 1989 200 p
Avail: Univ. Microfilms Order No. DA9019502

Battle damages and/or generic failures are the cause of many accidents involving the loss of aircraft. Particular approaches for three tasks of the overall flight control system reconfiguration problem are considered. These tasks are: damaged model estimation, reconfiguration law design and feedback structure redesign. First, the estimated model of the damaged aircraft is obtained by using a multiple model Kalman filtering approach. Then, a particular algorithm is applied to the flight control reconfiguration. The determination of the desired control law, which can adapt in a very short period of time to a major damage on a main control surface, is obtained by making use of the recent control and response time histories. Furthermore, a particular approach is proposed in order to calculate a new set of feedback gains of the flight control system such that dynamic uncoupling and desirable handling qualities are retained even after the damage. The model estimation, the control algorithm, and the feedback gains updating process were codified in computer simulation programs for a 6 degrees of freedom aircraft model. The simulation results of the reconfiguration are presented. Dissert. Abstr.

N91-11024 Oxford Univ. (England).
H INFINITY-DESIGN AND THE IMPROVEMENT OF HELICOPTER HANDLING QUALITIES Ph.D. Thesis
Andrew Yue 1988 245 p
Avail: Univ. Microfilms Order No. BRD-89468

The results of a study into the use of H(infinity)-optimization for the design of feedback control laws for improving the handling qualities of a Lynx helicopter are presented. An important improvement to the H(infinity)-optimization procedure is the reduction in the number of iterative steps in the gamma iteration before convergence to the optimal gamma. Some new algorithms are derived which significantly reduce the computation time for the gamma iteration. Both 2-block and 4-block cases are considered. Control laws are designed for precise control of pitch and roll attitude, yaw rate and heave velocity. Analysis of the raw helicopter showed the need for a stability augmentation system as the dynamic characteristics of the unaugmented helicopter do not comply with military helicopter handling qualities requirements. Results from current research on helicopter handling qualities were used as guidelines in order to define the required dynamic characteristics. A six-degree of freedom nonlinear simulation was used to analyze the helicopter dynamic time histories. A possible solution to the problem of incorporating helicopter handling qualities in the design of robust controllers is to use a two-degree of freedom controller structure. This is illustrated using both H2 and H(infinity)-optimization. A piloted simulation study to assess the effectiveness of advanced control laws was initiated at the Royal Aerospace Establishment (RAE), Bedford. The trials were carried out in the single seat cockpit flight simulator, at the Flight Research Division and represent the first ever real-time piloted simulation using a H(infinity)-controller. Dissert. Abstr.

N91-11025# Messerschmitt-Boelkow-Blohm G.m.b.H., Munich (Germany, F.R.). Aircraft Div.
REVIEW OF ACTIVE STRUCTURAL CONTROL SYSTEMS AND FLIGHT TEST TECHNIQUES FOR DYNAMIC STABILITY INVESTIGATIONS
Otto Sensburg Apr. 1989 36 p Presented at Gabriel Coupry Memorial Lecture
(MBB/FYT256/S/PUB/361/A; ETN-90-97845) Copyright Avail: NTIS HC/MF A03

The influence of G. Coupry on aerolastics with focus on his studies of dynamic response to atmospheric turbulence with the introduction of a non cyclindrical gust, gust alleviation with an open loop flight control system, and vibration testing by transient excitation for application to flight flutter tests is reported. His work on dynamic response to atmospheric turbulence proved that for modern transport airplanes a non cyclindrical gust must be used to achieve a weight optional design. The methods he developed for identification of dynamic stability parameters finally led to the way to an integrated flight test procedure. ESA

09 RESEARCH AND SUPPORT FACILITIES (AIR)

Includes airports, hangars and runways; aircraft repair and overhaul facilities; wind tunnels; shock tubes; and aircraft engine test stands.

For related information see also *14 Ground Support Systems and Facilities (Space).*

N91-11026# National Aerospace Lab., Tokyo (Japan).
FLIGHT SIMULATOR EVALUATION TEST OF MULTI-FUNCTIONAL DISPLAY UNIT [TAKINO HYOJI SOCHI NO HIKO SHIMYURE-SHON HYOKASHIKEN]
Hiroyasu Kawahara, Akira Watanabe, Kaoru Wakairo, and Keiji Tanaka Oct. 1988 34 p In JAPANESE
(NAL-TM-596; ISSN-0452-2982; JTN-90-80122) Avail: NTIS HC/MF A03

As a part of the design of the new cockpit, in order to make clear the efficiency and the technical feasibility of the cathode ray tube-type display system, the simulation test for both the headdown display system and the digital map display system was made to evaluate results. The evaluation test was made using the multi-purpose flight simulator of the National Aerospace Laboratory in Japan. As a result, some items which need to be improved for the headdown display unit were suggested. They are as follows: (1) the improvement of the scale of the bank angle and the bank pointer, (2) the improvement of the display of digits on the magnified digital display, (3) the improvement of the magnified display of velocity, (4) the change of the shape of both the glide slope and the pointer localizer, (5) to keep the stability of a color tone on brightness regulation function, and (6) to study the edge-smoothing technique. For the digital map display system, the following items needed for improvement were suggested: (1) introduction of the scale-up and -down function, (2) moving down the symbol of an airplane itself from the center of a display, (3) to make colors of each displayed item recognizable, (4) to display the higher mountain and obstacles by using warning colors and to make one pay attention to them by using flickering light, (5) to use a three dimensional display technique, and (6) to improve the resolution of it by increasing scanning lines. NASDA

N91-11027*# Physical Sciences, Inc., Andover, MA.
PROPULSION SIMULATION FOR MAGNETICALLY SUSPENDED WIND TUNNEL MODELS Final Report, Jan.-Sep. 1988
Prakash B. Joshi, Henry P. Beerman, James Chen, Robert H. Krech, Andrew L. Lintz, and David I. Rosen Oct. 1990 73 p
(Contract NAS1-18616)
(NASA-CR-182093; NAS 1.26:182093; PSI-2055/TR-859) Avail: NTIS HC/MF A04 CSCL 14B

The feasibility of simulating propulsion-induced aerodynamic effects on scaled aircraft models in wind tunnels employing Magnetic Suspension and Balance Systems. The investigation concerned itself with techniques of generating exhaust jets of appropriate characteristics. The objectives were to: (1) define thrust and mass flow requirements of jets; (2) evaluate techniques for generating propulsive gas within volume limitations imposed by magnetically-suspended models; (3) conduct simple diagnostic

experiments for techniques involving new concepts; and (4) recommend experiments for demonstration of propulsion simulation techniques. Various techniques of generating exhaust jets of appropriate characteristics were evaluated on scaled aircraft models in wind tunnels with MSBS. Four concepts of remotely-operated propulsion simulators were examined. Three conceptual designs involving innovative adaptation of convenient technologies (compressed gas cylinders, liquid, and solid propellants) were developed. The fourth innovative concept, namely, the laser-assisted thruster, which can potentially simulate both inlet and exhaust flows, was found to require very high power levels for small thrust levels. Author

N91-10925# Deutsche Forschungsanstalt fuer Luft- und Raumfahrt, Goettingen (Germany, F.R.). Inst. fuer Aeroelastik.
DESIGN OF THE DERIVATIVE BALANCE FOR THE TRANSONIC WIND TUNNEL [KONSTRUKTIVE AUSLEGUNG DER TRANSKANAL-DERIVATIVAWAAGE (TRAD)]
Eberhard Schmidt and Joachim Wagener *In its* Contributions in the Field of Aeroelastics on the Occasion of the 60th Anniversary of Professor Dr.-Ing. Habil. Hans Wilhelm Foersching Apr. 1990 p 105-125 In GERMAN; ENGLISH summary (For primary document see N91-10920 02-02)
Avail: NTIS HC/MF A13

N91-10928# Deutsche Forschungsanstalt fuer Luft- und Raumfahrt, Goettingen (Germany, F.R.). Inst. fuer Aeroelastik.
UNSTEADY WIND TUNNEL WALL INTERFERENCES IN SUBSONIC AND TRANSONIC PROFILE FLOWS [INSTATIONAERE WINDKANALWAND-INTERFERENZEN BEI SUB- UND TRANSSONISCHER PROFILUMSTROEMUNG]
Ralph Voss *In its* Contributions in the Field of Aeroelastics on the Occasion of the 60th Anniversary of Professor Dr.-Ing. Habil. Hans Wilhelm Foersching Apr. 1990 p 169-185 In GERMAN; ENGLISH summary (For primary document see N91-10920 02-02)
Avail: NTIS HC/MF A13

N91-10975# Technische Univ., Brunswick (Germany, F.R.). Inst. of Flight Guidance and Control.
WIND MODELS FOR FLIGHT SIMULATION
K.-U. Hahn, T. Heintsch, B. Kaufmann, G. Schaenzer, and M. Swolinsky *In* AGARD, Aircraft Trajectories: Computation, Prediction, Control, Volume 1. Part 1: Fundamentals. Part 2: Flight in Critical Atmospheric Conditions. Part 3: Impact of New On-Board Technologies on Aircraft Operation Mar. 1990 32 p Sponsored by DFG (For primary document see N91-10967 02-04)
Copyright Avail: NTIS HC/MF A12; Non-NATO Nationals requests available only from AGARD/Scientific Publications Executive

12 ASTRONAUTICS (GENERAL)

For extraterrestrial exploration see *91 Lunar and Planetary Exploration.*

N91-11028*# National Aeronautics and Space Administration, Washington, DC.
CIVIL SPACE TECHNOLOGY INITIATIVE
Aug. 1990 24 p Original contains color illustrations
(NASA-TM-103017; NAS 1.15:103017) Avail: NTIS HC/MF A03; 19 functional color pages CSCL 22A

The Civil Space Technology Initiative (CSTI) is a major, focused, space technology program of the Office of Aeronautics, Exploration and Technology (OAET) of NASA. The program was initiated to advance technology beyond basic research in order to expand and enhance system and vehicle capabilities for near-term missions. CSTI takes critical technologies to the point at which a user can confidently incorporate the new or expanded capabilities into relatively near-term, high-priority NASA missions. In particular, the CSTI program emphasizes technologies necessary for reliable and efficient access to and operation in Earth orbit as well as for support of scientific missions from Earth orbit. Author

13 ASTRODYNAMICS

Includes powered and free-flight trajectories; and orbital and launching dynamics.

N91-11029 Texas Univ., Austin.
NOMINAL OCEAN TIDE MODELS FOR TOPEX PRECISE ORBIT DETERMINATION Ph.D. Thesis
Stefano Casotto 1989 235 p
Avail: Univ. Microfilms Order No. DA9016857

The increasing accuracy of satellite laser tracking systems and the stringent requirements on the radial error budget of the TOPEX/Poseidon mission put severe demands on the force model used for orbit determination. The ocean tide component of the force model is addressed in order to establish a nominal tide model that meets the requirement of 2 cm RMS perturbation amplitude in the radial direction. However, the methods developed can be applied to the case of any satellite. The determination of the tide model is carried out by first providing a method for interpolating or extrapolating the known spherical harmonic expansions of the major tidal constituents to a number of minor constituents in order to reduce aliasing effects. Using a suitable extension of Kaula's satellite theory to describe tidal perturbations in the radial, transverse, and normal directions, the perturbation spectrum and the associated time domain statistics of the perturbation magnitudes by constituent, degree, order, and coefficient, are computed. A nominal tide model is finally determined, based on the RMS amplitude of the perturbations generated by each tidal coefficient and taking into account the relation between the tidal perturbation frequencies and the length of the orbital arc selected for data reduction. Dissert. Abstr.

N91-11030 Stanford Univ., CA.
BOOSTING A TETHERED SATELLITES'S ORBIT AROUND AN OBLATE PLANET THROUGH RESONANT PUMPING Ph.D. Thesis
James Walter Gearhart 1990 119 p
Avail: Univ. Microfilms Order No. DA9024328

The center of mass of a satellite, which consists of two masses connected by a rigid, massless tether, moves in a circular non-equatorial orbit about an oblate planet. The satellite is made to tumble forward essentially in the orbital plane such that its average pitch rate relative to the local vertical equals the orbital rate. This tumbling motion is phased such that the tether axis is aligned with the local vertical 1/8th of an orbit prior to each crossing of the equatorial bulge and with the local horizontal 1/8th of an orbit alter each crossing. The angular momentum of the orbit is increased by this phasing of the force from the equatorial bulge with the variations in satellite orientation. Periodic modulation or pump of the tether length in resonance with the equatorial crossings is required to maintain this phasing, and the resulting transfer of energy from the pumping mechanism to the orbit increases the altitude of the mass center. The dynamics of this orbit-boosting effect are examined in detail through a second-order perturbation analysis. Elastic deflections of the tether and the effects of atmospheric drag are neglected. Equations of motion governing the orbital and attitude behavior of the satellite are presented, and a formula for the rate of orbit-boosting is obtained and shown to be maximized for a polar orbit. The correct schedule for varying the tether length is derived through consideration of the rate of work required by the tether-pumping mechanism. The analytical results for the polar orbit case are checked through a numerical simulation which includes a feedback control scheme for maintaining the optimum orbit/attitude phasing. Out-plane deviations from the nominally in-plane tumbling motion are analyzed for the non-polar orbit case and are shown to remain small. The effects of higher-order perturbations and some practical application issues are also discussed. Dissert. Abstr.

14 GROUND SUPPORT SYSTEMS AND FACILITIES (SPACE)

Includes launch complexes, research and production facilities; ground support equipment, e.g., mobile transporters; and simulators.

For related information see also *09 Research and Support Facilities (Air).*

N91-11031*# Fairchild Technical Support Center, Huntsville, AL.
AUTOMATED FLUID INTERFACE SYSTEM (AFIS) Final Report
Apr. 1990 49 p
(Contract NAS8-37457)
(NASA-CR-183969; NAS 1.26:183969) Avail: NTIS HC/MF A03 CSCL 14B

Automated remote fluid servicing will be necessary for future space missions, as future satellites will be designed for on-orbit consumable replenishment. In order to develop an on-orbit remote servicing capability, a standard interface between a tanker and the receiving satellite is needed. The objective of the Automated Fluid Interface System (AFIS) program is to design, fabricate, and functionally demonstrate compliance with all design requirements for an automated fluid interface system. A description and documentation of the Fairchild AFIS design is provided. Author

N91-11032# Lawrence Livermore National Lab., CA.
RAILGUN PERFORMANCE WITH A TWO-STAGE LIGHT-GAS GUN INJECTOR
R. S. Hawke, A. R. Susoeff, J. R. Asay, J. A. Ang, C. A. Hall, C. H. Konrad, G. W. Wellman, R. J. Hickman, W. A. Heath, and J. R. Martinez (Ktech Corp., Albuquerque, NM.) et al 1990 6 p Presented at the 5th IEEE Symposium on Electromagnetic Launch Technology, Destin, FL, 1-5 Apr. 1990 Prepared in cooperation with Edgerton, Germeshausen and Grier, Inc., Albuquerque, NM; and New Mexico Univ., Albuquerque
(Contracts W-7405-eng-48; DE-AC04-76DP-00789)
(DE90-016211; UCRL-101932-Rev-1; CONF-9004136-9-Rev-1)
Avail: NTIS HC/MF A02

The results are summarized which were obtained with the HELEOS railgun which uses a two stage light gas gun (2SLGG) as an injector. The high velocity 2SLGG injector pre-accelerates projectiles up to (approx)7 km/s. The high injection velocity reduces the exposure duration of the railgun barrel to the passing high temperature plasma armature, thereby reducing the ablation and subsequent armature growth. The 2SLGG also provides a column of cool, high pressure hydrogen gas to insulate the rails behind the projectile, thereby eliminating restrike. A means to form an armature behind the injected projectile was developed. In preliminary tests, the third stage railgun has successfully increased the projectile velocity by 1.35 km/s. Extensive diagnostics were used to determine the behavior of the armature and track the launcher's performance. In some cases, velocity increases in the railgun section were achieved, which are in close agreement with theoretical predictions, whereas in other experiments deviations from theoretical predictions have been observed. The reasons for and implications of these results are addressed. Recent tests are reported. DOE

N91-11033# Sandia National Labs., Albuquerque, NM. Experimental Mechanics Dept.
COMPUTER MODELING OF 12-INCH ACTUATOR SHOCK TEST PERFORMANCE
R. Glenn Bell and Thomas J. Baca 1990 11 p Presented at the 61st Shock and Vibration Symposium, Pasadena, CA, 16-18 Oct. 1990
(Contract DE-AC04-76DP-00789)
(DE90-017038; SAND-90-1323C; CONF-9010172-3) Avail: NTIS HC/MF A03

The 12-Inch Horizontal Actuator is a high velocity mechanical shock simulation testing device used for component development shock testing at Sandia National Laboratories. This machine is pneumatically driven and propels a ram sled along a track where a programmed shock pulse is generated during an impact with another sled containing the test item. Computer models have been developed which allow prediction of: (1) actuator performance in terms of pressure setting which produce the desired initial thrust of the ram sled; (2) sled brake performance which is needed to ensure stopping the sleds within length of the sled track; and (3) shock pulse amplitude and duration parameters associated with the desired shock test input. Experimental results are presented which verify the accuracy of the models. The modeling effort has significantly improved test efficiency by reducing the number of calibration tests required to develop required shock loading conditions. Successful development of these computer models demonstrates the great potential of computer applications in improving the quality of unique test capabilities such as the 12-Inch Actuator. DOE

15 LAUNCH VEHICLES AND SPACE VEHICLES

Includes boosters; operating problems of launch/space vehicle systems; and reusable vehicles.

For related information see also *20 Spacecraft Propulsion and Power.*

No abstracts in this category.

16 SPACE TRANSPORTATION

Includes passenger and cargo space transportation, e.g., shuttle operations; and space rescue techniques.

For related information see also *03 Air Transportation and Safety* and *18 Spacecraft Design, Testing and Performance.* For space suits see *54 Man/System Technology and Life Support.*

N91-11034*# Morton Thiokol, Brigham City, UT. Space Operations.
FIRST INCREMENTAL BUY FOR INCREMENT 2 OF THE SPACE TRANSPORTATION SYSTEM (STS) Final Report
Dec. 1989 268 p
(Contract NAS8-30490)
(NASA-CR-183855; NAS 1.26:183855; TWR-50181) Avail: NTIS HC/MF A12 CSCL 22B

Thiokol manufactured and delivered 9 flight motors to KSC on schedule. All test flights were successful. All spent SRMs were recovered. Design, development, manufacture, and delivery of required transportation, handling, and checkout equipment to MSFC and to KSC were completed on schedule. All items of data required by DPD 400 were prepared and delivered as directed. In the system requirements and analysis area, the point of departure from Buy 1 to the operational phase was developed in significant detail with a complete set of transition documentation available. The documentation prepared during the Buy 1 program was maintained and updated where required. The following flight support activities should be continued through other production programs: as-built materials usage tracking on all flight hardware; mass properties reporting for all flight hardware until sample size is large enough to verify that the weight limit requirements were met; ballistic predictions and postflight performance assessments for all production flights; and recovered SRM hardware inspection and anomaly identification. In the safety, reliability, and quality assurance area, activities accomplished were assurance oriented in nature and specifically formulated to prevent problems and hardware failures. The flight program to date has adequately demonstrated the success of this assurance approach. The attention focused on details of design, analysis, manufacture, and inspection to assure the production of high-quality hardware has resulted in the absence of flight failures. The few anomalies which

did occur were evaluated, design or manufacturing changes incorporated, and corrective actions taken to preclude recurrence. Author

N91-11035# National Aerospace Lab., Tokyo (Japan). Control Systems Div.
FLIGHT SIMULATION PROGRAMS FOR SPACE PLANE [UCHU OKANKI HIKO SHIMYURE-SHON PUROGURAMU]
Masaaki Yanagihara Aug. 1988 45 p In JAPANESE
(NAL-TM-594; ISSN-0452-2982; JTN-90-80120) Avail: NTIS HC/MF A03

A flight simulation program that could simulate the flight of an spaceplane from the ground surface to the orbit around the earth was developed. This program is the advanced version of the general purpose program for the flight simulation which has been developed in the National Aerospace Laboratory of Japan. Two programs are available to analyze the rigid body motion with six degrees of freedom or the mass point motion with three degrees of freedom. They are written in FORTRAN. The merits and limitations of the program are as follows: (1) it is composed of two package programs, that is, fuselage models and onboard calculations (these packages are replaceable and thus the program is widely usable); (2) the heating rates of the fuselage, load factors and dynamic pressures are calculated along the flight path and are used for the assessment of the path; (3) the earth is assumed to be a sphere and the revolution is neglected (the angular velocity of the rotation is assumed to be constant); (4) a U.S. 62 standard atmosphere table is used; (5) it contains the models of the westerly wind, the steady wind in the low altitude, the gusts and the wind shears. The contents of the program and the construction of the mathematical model are described and the good results of the evaluation are presented in which the three degrees of freedom flight simulation program was tested using the data of the space shuttle of U.S.A. NASDA

N91-11036# National Aerospace Lab., Tokyo (Japan). Aerodynamics Div.
WEIGHT EVALUATION AND SENSITIVITY ANALYSIS FOR SPACE PLANE: SSTO Report No. 1 [UCHU OKANKI NO JURYO HYOKA TO KANDO KAISEKI: SSTO]
Masao Shirouzu Jan. 1989 34 p In JAPANESE
(NAL-TM-598-1; ISSN-0452-2982; JTN-90-80141) Avail: NTIS HC/MF A03

The performance of the Single Stage To Orbit (SSTO) is analyzed for sensitivity and weight by using existing data. In the case of the real takeoff weight (350 ton), it is pointed out that the empty weight could be reduced by about 50 percent by using the present technology. Also the simulation is done by changing data of the flight path and the engine performance parametrically. The result shows the difficulty of the realization of the SSTO quantitatively and gives us a guide to the next development. If the engine performance and the aerodynamic characteristics are improved, and consequently the specific impulse of the engine can be increased by 1.5 times, and the aerodynamic drag can be reduced by 0.7 times, the above-mentioned weight reduction of 50 percent could be reduced to about 30 percent. A plan of a typical SSTO is shown here by using that data. Since that data is insufficient, the present weight analysis needs to be studied more precisely. NASDA

N91-11037*# Remtech, Inc., Huntsville, AL.
EXTERNAL TANK AEROTHERMAL DESIGN CRITERIA VERIFICATION, VOLUME 1 Final Report
William K. Crain, Cynthia Frost, and John Warmbrod May 1990 124 p
(Contract NAS8-36946)
(NASA-CR-183996; NAS 1.26:183996; RTR-174-01-Vol-1) Avail: NTIS HC/MF A06 CSCL 22B

The objective of this study was to produce an independent set of ascent environments which would serve as a check on the Rockwell IVBC-3 environments and provide an independent reevaluation of the thermal design criteria for the External Tank (ET). Design heating rates and loads were calculated at 367 acreage body point locations. Ascent flight regimes covered were lift-off, first stage ascent, Solid Rocket Booster (SRB) staging and second stage ascent through ET separation. The purpose here is to document these results, briefly describe the methodology used and present the environments along with a comparison with the Rockwell IVBC-3 counterpart. The methodology and environment summaries are given. Author

N91-11038*# Remtech, Inc., Huntsville, AL.
EXTERNAL TANK AEROTHERMAL DESIGN CRITERIA VERIFICATION, VOLUME 2
William K. Crain, Cynthia Frost, and John Warmbrod Jun. 1990 389 p
(Contract NAS8-36946)
(NASA-CR-183997; NAS 1.26:183997; RTR-174-01-Vol-2) Avail: NTIS HC/MF A17 CSCL 22B

The objective of the study was to produce an independent set of ascent environments which would serve as a check on the Rockwell International (RI) IVBC-3 environments and provide an independent reevaluation of the thermal design criteria for the External Tank (ET). Given here are the plotted timewise environments comparing REMTECH results to the RI IVBC results. Author

17 SPACE COMM., SPACECRAFT COMM., COMMAND & TRACKING

Includes telemetry; space communications networks; astronavigation and guidance; and radio blackout.

For related information see also *04 Aircraft Communications and Navigation* and *32 Communications and Radar.*

No abstracts in this category.

18 SPACECRAFT DESIGN, TESTING AND PERFORMANCE

Includes satellites; space platforms; space stations; spacecraft systems and components such as thermal and environmental controls; and attitude controls.

For life support systems see *54 Man/System Technology and Life Support.* For related information see also *05 Aircraft Design, Testing and Performance, 39 Structural Mechanics,* and *16 Space Transportation.*

N91-11039*# Naval Postgraduate School, Monterey, CA.
SPACECRAFT DESIGN PROJECT: HIGH LATITUDE COMMUNICATIONS SATELLITE Final Report
Carl Josefson, Jack Myers, Mike Cloutier, Steve Paluszek, Gerry Michael, Dan Hunter, Dan Sakoda, Wes Walters, Dennis Johnson, and Terry Bauer et al Dec. 1989 236 p
(Contract NASw-4435)
(NASA-CR-186689; NAS 1.26:186689) Avail: NTIS HC/MF A11 CSCL 22B

The spacecraft design project was part of AE-4871, Advanced Spacecraft Design. The project was intended to provide experience in the design of all major components of a satellite. Each member of the class was given primary responsibility for a subsystem or design support function. Support was requested from the Naval Research Laboratory to augment the Naval Postgraduate School faculty. Analysis and design of each subsystem was done to the extent possible within the constraints of an eleven week quarter and the design facilities (hardware and software) available. The project team chose to evaluate the design of a high latitude communications satellite as representative of the design issues and tradeoffs necessary for a wide range of satellites. The High-Latitude Communications Satellite (HILACS) will provide a continuous UHF communications link between stations located

north of the region covered by geosynchronous communications satellites, i.e., the area above approximately 60 N latitude. HILACS will also provide a communications link to stations below 60 N via a relay Net Control Station (NCS), which is located with access to both the HILACS and geosynchronous communications satellites. The communications payload will operate only for that portion of the orbit necessary to provide specified coverage. Author

N91-11040* National Aeronautics and Space Administration. Marshall Space Flight Center, Huntsville, AL.
COMBINED RELEASE AND RADIATION EFFECTS SATELLITE (CRRES): ATLAS 1 (ATLAS/CENTAUR-69) LAUNCH VEHICLE
Jul. 1990 26 p Prepared in cooperation with Air Force Space Div., Los Angeles, CA; and Ball Aerospace Systems Div.,Boulder, CO
(NASA-TM-103460; NAS 1.15:103460; P90-10094) Avail: Issuing Activity CSCL 22B

The objectives of the Combined Release and Radiation Effects Satellite (CRRES), to be launched aboard an Atlas 1 (Atlas/Centaur-69) launch vehicle are described along with major flight activities, prelaunch and launch operations, the trajectory sequence of events, and landing and post-landing operations. CRRES will carry 24 canisters containing various chemicals. For each experiment, one or two canisters will be ejected by the spacecraft. Approximately 25 minutes later, after the canister and spacecraft are far enough apart to prevent contamination, the canister will release its chemical vapors. The chemical vapors will be ionized, creating luminous clouds about 60 miles in diameter. By observing the motion of the cloud, measurements of electric fields in outer space can be made to see how these fields interact with charged particles to form waves and to better understand how the Earth extracts energy from the solar wind. B.G.

N91-11041*# National Aeronautics and Space Administration. Langley Research Center, Hampton, VA.
THERMAL-DISTORTION ANALYSIS OF A SPACECRAFT BOX TRUSS IN GEOSTATIONARY ORBIT
Patrick A. Cosgrove (Lockheed Engineering and Sciences Co., Hampton, VA.), Jeffery T. Farmer, and Lawrence F. Rowell Washington Nov. 1990 26 p
(NASA-TP-3054; L-16828; NAS 1.60:3054) Avail: NTIS HC/MF A03 CSCL 22B

The Mission to Planet Earth enlists the use of a geostationary platform to support Earth science monitoring instruments. The strongback for a proposed geostationary platform is a deployable box truss that supports two large diameter passive microwave radiometer (PMR) and several other science instruments. A study was performed to estimate the north-south and east-west pointing errors at the mounting locations of the two PMRs due to on-orbit thermal distortions of the main truss. The baseline configuration indicated that the east-west pointing error greatly exceeded the required limits. Primary origins of the pointing errors were identified, and methods for their reduction were discussed. Thermal performance enhancements to the truss structure were modeled and analyzed, including state-of-the-art surface coatings and insulation techniques. Comparisons of the thermal enhancements to the baseline were performed. Results demonstrated that using a thermal enclosure insulating technique reduced external heat fluxes, and distributed those heat fluxes more evenly throughout the structure, sufficiently reducing the pointing error to satisfy pointing accuracy requirements for the PMR's. Author

N91-11042*# Old Dominion Univ., Norfolk, VA. Dept. of Mechanical Engineering and Mechanics.
GRID GENERATION AND FLOW COMPUTATION ABOUT A MARTIAN ENTRY VEHICLE Progress Report, period ending 30 Jun. 1990
J. E. Stewart and S. N. Tiwari Oct. 1990 86 p
(Contract NCC1-68)
(NASA-CR-187032; NAS 1.26:187032) Avail: NTIS HC/MF A05 CSCL 22B

A number of vehicles are currently being proposed for a manned mission to Mars. One of these vehicles has a modified blunt-nosed cone configuration. Experimental results were obtained for this vehicle in 1968. They show lift-over-drag ratios comparable to those needed for Mars entry. Computations are performed to verify the earlier results and to further describe the flight characteristics of this vehicle. An analytical method is used to define the surface of this vehicle. A single-block volume grid is generated around the vehicle using the algebraic Two-Boundary Grid Generation algorithm (TBGG) and transfinite interpolation. Euler solutions are then obtained from a Langley Aerodynamic Upward Relaxation Algorithm (LAURA) at Mach 6.0 and angles of attack of 0, 6, and 12 deg. The lift coefficient determined from the LAURA code agree very well with the experimental results. The drag and pitching moment coefficients, however, are underestimated by the code since viscous effects are not considered. Contour plots of the flowfield show no evidence of separation for angles of attack up to 12 deg. Author

N91-11043 Cincinnati Univ., OH.
CONTROLLER METHODOLOGIES FOR INTEGRATED CONTROL/STRUCTURE DESIGN OPTIMIZATION OF LARGE FLEXIBLE STRUCTURES Ph.D. Thesis
Mark Duncan McLaren 1989 260 p
Avail: Univ. Microfilms Order No. DA9019854

The integrated control/structure design optimization problem is investigated for large flexible structures subject to stochastic disturbance forces. Various controllers are considered, including full-state feedback, direct output feedback, output filter feedback, and positive real filter feedback. The problem is formulated as a mathematical programming problem, and two solution techniques are presented. The first is a sequential nonlinear approximations technique coupled with a nonlinear programming code, and the second is a continuation method coupled with sequential linear programming. The solution algorithms are applied to the DRAPER I tetrahedral truss structure and the DRAPER II space telescope model, to obtain optimal designs for varying controller constraints. Dissert. Abstr.

N91-11044 South Carolina Univ., Columbia.
OPTIMAL CONTROL DESIGN BY VOLTERRA SERIES AND ITS APPLICATION TO SPACECRAFT MANEUVERS Ph.D. Thesis
Fu-Sung Chang 1989 97 p
Avail: Univ. Microfilms Order No. DA9017111

The Volterra series is actually the generalization of the Taylor series in terms of control u. Therefore the higher order optimal necessary condition from the Volterra approach gives a more accurate result than the traditional Pontryagin's Minimum Principle. The application of this necessary condition to the spacecraft maneuvers are divided into square and nonsquare cases. The Euler's equation of motion is optimized first to meet the performance criteria for the square case. Later nonsquare optimal control problems including time-invariant, time-variant, state-constraint, control-constraint, and finally attitude control are considered. The proposal of this future research leads to an important area of research to the nonlinear system..
Dissert. Abstr.

N91-11045 Stanford Univ., CA.
ATTITUDE CONTROL OF TETHERED SATELLITES Ph.D. Thesis
Xiaohua He 1990 164 p
Avail: Univ. Microfilms Order No. DA9024330

Methods of attitude control of tethered satellites are presented. The main effort is focused on the case of a tethered space observatory that requires high pointing accuracy. A tethered satellite is connected to a parent spacecraft by a long tether. The gravity gradient caused tension in the tether passively provides satellite attitude stability about two axes. However, active attitude control is necessary for high accuracy pointing and new control methods are required since conventional methods are not efficient due to the tether tension. With a movable tether attachment point on a tethered satellite, active control torques can be produced about two axes by varying the offset of tether tension vector from the satellite's center of mass. For the third axis, parallel to the tension

vector, the control torque can be provided by momentum devices. No mass ejection is needed. Tether dynamics especially damping properties have significant effects on the satellite's pointing accuracy, which are studied with a flexible continuum model. Dynamic equations are solved analytically with approximations. Various damping mechanisms are analyzed including viscous, structural, and linear friction damping. Ground test results are extrapolated to predict space behavior of tethers of much different sizes. Methods are developed to enhance damping. Numerical simulations of kinetic isolation tether experiment (KITE), an orbital flight experiment being designed to demonstrate the new attitude control methods, show the pointing accuracy of one arcsecond. Dissert. Abstr.

N91-11046 Stanford Univ., CA.
PRECISION TETHERED SATELLITE ATTITUDE CONTROL Ph.D. Thesis
Robert John Kline-Schoder 1990 144 p
Avail: Univ. Microfilms Order No. DA9024338

Tethered spacecraft possess unique dynamic characteristics which make them advantageous for certain classes of experiments. In practice, all satellites have some requirement on the attitude control of the spacecraft, and tethered satellites are no exception. It has previously been shown that conventional means of performing attitude control for tethered satellites are insufficient for any mission with pointing requirements more stringent than about 1 deg. Herein, theoretical development is examined of both a large angle slew and long term, precision pointing control algorithm for tethered satellites, and the simulation of the Kinetic Isolation Tether Experiment (KITE) mission in an Earth laboratory environment. To that end, a scaled, 1-D, air bearing supported laboratory simulator of the KITE satellite configuration was constructed and is described in detail. The system equations are derived and a suitable control law is described. The precision control algorithm consists of a Linear Quadratic Gaussian, full state feedback control law in conjunction with a multivariable Kalman filter. The control algorithm has been shown to regulate the vehicle orientation to within 0.60 arcsec RMS. In addition, a tether dynamics simulator was constructed in order to implement the natural dynamic behavior of a 2 km long tether in the earth laboratory environment. The tether simulator is used to test the ability of the control algorithm to regulate the air-bearing vehicle orientation in the presence of variations in the tether tension magnitude and direction. Dissert. Abstr.

N91-11047# Consiglio Nazionale delle Ricerche, Frascati (Italy). Ist. di Fisica dello Spazio Interplanetario.
DATA ANALYSIS OF HOLLOW CATHODE EXPERIMENT TO SUPPORT ELECTRODYNAMIC TETHER APPLICATIONS
G. Vannaroni, U. Guidoni, I. R. Durran, and F. DeVenuto Sep. 1989 50 p
(IFSI-89-16; ETN-90-97777) Avail: NTIS HC/MF A03

Data analysis was carried out on the interaction experiments between two hollow cathode plasma sources in a plasma chamber to simulate the electrodynamic phenomena occurring in power/motor generation experiments using the Tethered Satellite System (TSS) orbiting at ionospheric altitudes. The interaction region between the two plasmas was investigated by means of Langmuir probes. Plasma parameter maps were accomplished for different voltage polarizations of the hollow cathode plasma contactor with respect to the ambient plasma. The data analysis shows the presence of two regions, the first where a double layer is formed and the second where electron heating effect takes place. This latter phenomenon is probably due to the anomalous collisions related to the ion acoustic instability onset. ESA

19 SPACECRAFT INSTRUMENTATION

For related information see also *06 Aircraft Instrumentation* and *35 Instrumentation and Photography.*

N91-11048# Instituto de Pesquisas Espaciais, Sao Jose dos Campos (Brazil).
FUNCTIONAL DESCRIPTION AND ANALYSIS OF PROCESSOR PERFORMANCE FOR DATA COLLECTION [DESCRICAO FUNCIONAL E ANALISE DE DESEMPENHO DO PROCESSADOR DE COLETA DE DADOS]
Luiz Carlos PacolaSobrinho Feb. 1990 26 p In PORTUGUESE; ENGLISH summary
(INPE-5037-RPE/620) Avail: NTIS HC/MF A03

The characteristics of the signal processor for the data collecting system of the Brazilian Complete Space Mission first satellite are presented, as well as a theoretical analysis of its performance. The processor receives data collecting platform transmissions which are relayed by a low altitude satellite. These transmissions are random both in time and frequency. The processors main functions needed to receive and process these transmissions are described. The probability of a data collecting platform transmission processed correctly is calculated. Author

20 SPACECRAFT PROPULSION AND POWER

Includes main propulsion systems and components, e.g., rocket engines; and spacecraft auxilliary power sources.

For related information see also *07 Aircraft Propulsion and Power, 28 Propellants and Fuels, 44 Energy Production and Conversion,* and *15 Launch Vehicles and Space Vehicles.*

N91-11049*# Pratt and Whitney Aircraft, West Palm Beach, FL. Government Products Div.
RL10 IGNITION LIMITS TEST FOR SHUTTLE CENTAUR Final Report, Mar. - May 1986
May 1987 60 p
(Contract NAS3-22902)
(NASA-CR-183199; NAS 1.26:183199; FR-19556-1) Avail: NTIS HC/MF A04 CSCL 21H

During routine development testing of the RL10A-3-3B engine a potential no-ignition condition was encountered when operating at certain propellant inlet conditions within the Shuttle Centaur G operating region. The conditions, the resulting investigative program, and methods to correct the potential problem are discussed. The Shuttle Centaur program was cancelled prior to completion of this effort. Although the RL10 engine in the Atlas Centaur vehicle is required by specification to operate over a wide range of propellant inlet conditions. The vehicle actually operates over a narrow range of conditions. This factor, combined with configuration differences between Atlas Centaur (or Titan Centaur) and the Shuttle Centaur RL10 engines, indicates the ignition problem does not exist for these vehicles. As a precautionary measure the vehicle manufacturer was requested to coordinate with Pratt and Whitney any anticipated changes in propellant inlet conditions from the current narrow range. An engineering change will be proposed for future RL10 deliveries to provide more consistent propellant flow to the igniter. This will permit operation of the engine throughout the wide range specification inlet conditions if desired. Author

N91-11050*# California Polytechnic State Univ., San Luis Obispo. Dept. of Mechanical Engineering.
DESIGN AND EVALUATION OF THRUST VECTORED NOZZLES USING A MULTICOMPONENT THRUST STAND Final Progress Report, 1 Oct. 1988 - 31 Jan. 1990
Thomas W. Carpenter, Ernest W. Blattner, Robert E. Stagner, Juanita Contreras, Dennis Lencioni, and Greg McIntosh 1990 63 p Original contains color illustrations

(Grant NAG2-559)
(NASA-CR-180474; NAS 1.26:180474) Avail: NTIS HC/MF A04; 3 functional color pages CSCL 21H

Future aircraft with the capability of short takeoff and landing, and improved maneuverability especially in the post-stall flight regime will incorporate exhaust nozzles which can be thrust vectored. In order to conduct thrust vector research in the Mechanical Engineering Department at Cal Poly, a program was planned with two objectives; design and construct a multicomponent thrust stand for the specific purpose of measuring nozzle thrust vectors; and to provide quality low moisture air to the thrust stand for cold flow nozzle tests. The design and fabrication of the six-component thrust stand was completed. Detailed evaluation tests of the thrust stand will continue upon the receipt of one signal conditioning option (-702) for the Fluke Data Acquisition System. Preliminary design of thrust nozzles with air supply plenums were completed. The air supply was analyzed with regard to head loss. Initial flow visualization tests were conducted using dual water jets. Author

N91-11051# National Aerospace Lab., Tokyo (Japan).
EXPERIMENTAL MANUFACTURING OF DATA RECORDING SYSTEM FOR ROCKET COMBUSTION THERMAL FLUX DISTRIBUTION [ROKKETO NENSHOKI NO NETSURYUSOKU BUMPU DE-TA SHUROKUSOCHI NO SHISAKU]
Hiroshi Sakamoto Sep. 1988 132 p In JAPANESE
(DE90-702432; NAL-TM-595; ISSN-0452-2982; JTN-90-80121) Avail: NTIS HC/MF A07

As supporting research for the development of the liquid oxygen-liquid hydrogen engine for the H-2 Launch Vehicle, fundamental data were obtained using water-cooled combustors in the National Aerospace Laboratory (NAL) of Japan. The measuring system which was used in NAL had some defects: the measuring time for the flow rate of cooling water was too long because the difference pressure at orifice was measured with the mechanical scanner. Keeping watch on the flow rate of water in the combustion test was very difficult because it was monitored with an oscillograph, and troublesome work was needed to avoid freezing of the system in winter. The new data acquisition system which was installed as part of the real-time monitoring system of the flow rate, was developed to refine the efficiency of the measurement. In this system, the pressure data of orifices are acquired with the pressure transducer for each orifice, under the control of a personal computer and are processed in the computer. The data can be easily watched by an operator through a communication link in the real time. Here, the overall description of the system and the result of the performance test are reported, including the list of source programs. NASDA

N91-11052# National Aerospace Lab., Tokyo (Japan).
DIGITAL DATA PROCESSING SYSTEM FOR BIPROPELLANT APOGEE ENGINE [NIEKISHIKI APOJI ENJINYO DEJITARU DE-TA SHORI SHISUTEMU]
Katsuhito Kisara, Takayuki Sudo, Akira Chiba, and Ryuichi Nagashima Jan. 1989 27 p In JAPANESE
(NAL-TM-599; ISSN-0452-2928; JTN-90-80142) Avail: NTIS HC/MF A03

In 1972, the high altitude test stand for rocket engines was established in Kakuda Branch of the National Aerospace Laboratory. A digital measuring system based on a mini-computer was installed for a test stand. In view of the progress of the digital technology, this system was not efficient enough and its reliability was getting worse. Recently, this system was used in the development program of the Hydrazine/NTO (nitrogen tetraoxide) liquid apogee engine and the insufficiency of its accuracy for the measurement was pointed out. Hence, the digital measuring system was upgraded with a personal computer. The specifications of the new measuring system are as follows: (1) the whole process of the measurement, from the preparation to the output of graphs and tables, could be carried out consistently; (2) it demanded no skill on the part of the operator; (3) it was sufficiently accurate; and (4) its cost was not so high. Here, the hardware and the software of this system are described. The satisfactory present state of the system and some problems are also described. NASDA

N91-11053*# Virginia Polytechnic Inst. and State Univ., Blacksburg. Dept. of Electrical Engineering.
ANALYSIS AND DESIGN OF A HIGH POWER, DIGITALLY-CONTROLLED SPACECRAFT POWER SYSTEM Semiannual Report
F. C. Lee and B. H. Cho 16 May 1990 126 p
(Grant NAG5-1232)
(NASA-CR-186546; NAS 1.26:186546) Copyright Avail: NTIS HC/MF A07 CSCL 10B

The progress to date on the analysis and design of a high power, digitally controlled spacecraft power system is described. Several battery discharger topologies were compared for use in the space platform application. Updated information has been provided on the battery voltage specification. Initially it was thought to be in the 30 to 40 V range. It is now specified to be 53 V to 84 V. This eliminated the tapped-boost and the current-fed auto-transformer converters from consideration. After consultations with NASA, it was decided to trade-off the following topologies: (1) boost converter; (2) multi-module, multi-phase boost converter; and (3) voltage-fed push-pull with auto-transformer. A non-linear design optimization software tool was employed to facilitate an objective comparison. Non-linear design optimization insures that the best design of each topology is compared. The results indicate that a four-module, boost converter with each module operating 90 degrees out of phase is the optimum converter for the space platform. Large-signal and small-signal models were generated for the shunt, charger, discharger, battery, and the mode controller. The models were first tested individually according to the space platform power system specifications supplied by NASA. The effect of battery voltage imbalance on parallel dischargers was investigated with respect to dc and small-signal responses. Similarly, the effects of paralleling dischargers and chargers were also investigated. A solar array and shunt model was included in these simulations. A model for the bus mode controller (power control unit) was also developed to interface the Orbital replacement Unit (ORU) model to the platform power system. Small signal models were used to generate the bus impedance plots in the various operating modes. The large signal models were integrated into a system model, and time domain simulations were performed to verify bus regulation during mode transitions. Some changes have subsequently been incorporated into the models. The changes include the use of a four module boost discharger, and a new model for the mode controller, which includes the effects of saturation. The new simulations for the boost discharger show the improvement in bus ripple that can be achieved by phase-shifted operation of each of the boost modules. Author

N91-11054*# Aerojet Solid Propulsion Co., Sacramento, CA.
HYBRID PROPULSION TECHNOLOGY PROGRAM, PHASE 1. VOLUME 1: EXECUTIVE SUMMARY Final Report
23 Oct. 1989 24 p Prepared in cooperation with Aerojet TechSystems Co., Sacramento, CA and Martin Marietta Corp., Bethesda, MD
(Contract NAS8-37775)
(NASA-CR-183950; NAS 1.26:183950) Avail: NTIS HC/MF A03 CSCL 21H

The study program was contracted to evaluate concepts of hybrid propulsion, select the most optimum, and prepare a conceptual design package. Further, this study required preparation of a technology definition package to identify hybrid propulsion enabling technologies and planning to acquire that technology in Phase 2 and demonstrate that technology in Phase 3. Researchers evaluated two design philosophies for Hybrid Rocket Booster (HRB) selection. The first is an ASRM modified hybrid wherein as many components/designs as possible were used from the present Advanced Solid Rocket Motor (ASRM) design. The second was an entirely new hybrid optimized booster using ASRM criteria as a point of departure, i.e., diameter, thrust time curve, launch facilities, and external tank attach points. Researchers selected

the new design based on the logic of optimizing a hybrid booster to provide NASA with a next generation vehicle in lieu of an interim advancement over the ASRM. The enabling technologies for hybrid propulsion are applicable to either and vehicle design may be selected at a downstream point (Phase 3) at NASA's discretion. The completion of these studies resulted in ranking the various concepts of boosters from the RSRM to a turbopump fed (TF) hybrid. The scoring resulting from the Figure of Merit (FOM) scoring system clearly shows a natural growth path where the turbopump fed solid liquid staged combustion hybrid provides maximized payload and the highest safety, reliability, and low life cycle costing. Author

N91-11055*# Aerojet Solid Propulsion Co., Sacramento, CA.
HYBRID PROPULSION TECHNOLOGY PROGRAM, PHASE 1. VOLUME 2: TECHNICAL DISCUSSION Final Report
23 Oct. 1989 539 p Prepared in cooperation with Aerojet TechSystems Co., Sacramento, CA and Martin Marietta Corp., Bethesda, MD
(Contract NAS8-37775)
(NASA-CR-183951; NAS 1.26:183951) Avail: NTIS HC/MF A23 CSCL 21H

Information on hybrid propulsion system concepts is given largely in the form of outlines, charts and graphs. Included are the concept definition, trade study data generation, concept evaluation and selection, conceptual design definition, and technology definition. Author

N91-11056 Utah Univ., Salt Lake City.
A SIMULATION OF THE FLOW NEAR A BURNING PROPELLANT IN A SOLID PROPELLANT ROCKET MOTOR Ph.D. Thesis
Yiping Ma 1990 93 p
Avail: Univ. Microfilms Order No. DA9022355

An investigation was conducted related to the velocity coupling phenomenon reported in acoustically unstable solid propellant rocket motors. An innovative simulation facility was built using solid carbon dioxide as the simulated propellant. The use of dry ice allows direct focus on the fluid mechanical aspect of the problem. Mass flow rate and acoustic pressure measurements indicate the existence of a coupling mechanism, strongly dependent on velocity amplitude, between the acoustic disturbance and dry ice sublimation process. Flow visualization and hot film anemometry both indicate the occurrence of turbulence in the case of strong acoustic excitation. Transition near a velocity antinode appears to be associated with shear instability, while transition near a velocity node was also observed and appears to be influenced by the strong velocity gradient or any initial disturbances. Study of the velocity signal indicates that turbulence is probable to have occurred during only part of oscillation cycle as the flow always recovers to be laminar during the same cycle. Acoustically induced turbulent forced convection is believed to be responsible for the increase in the sublimation rate of the dry ice (simulated burning of the propellant). An empirical correlation was developed that showed the turbulent heat convection rate was dependent on the ratio of an acoustic Reynolds number to the 0.8 power. These experiments lead one to believe that turbulence is one of the principal mechanisms in the velocity coupling phenomenon.
Dissert. Abstr.

N91-11057# Sandia National Labs., Albuquerque, NM. Advanced Systems Div.
TETHERED ROCKET AS A VEHICLE FOR PENETRATION AND IMPACT TESTING: DEVELOPMENT REPORT
N. R. Hansen Jun. 1990 108 p
(Contract DE-AC04-76DP-00789)
(DE90-014865; SAND-90-1250) Avail: NTIS HC/MF A06

A new technique, called tethered rocket, has been developed for testing in the penetration and/or impact modes. The technique involves tethering a rocket-motor assembly to an earth-fixed pivot so that the resulting semicircular arc delivers a payload to a precise impact point. Discussions are presented which describe the analytical and experimental activities of the tethered rocket technique. A series of analytical models has been integral to the success of the tethered rocket development. The analytic results were verified by testing. The tests demonstrated the viability of the technique for penetration and/or impact testing. Also included is a discussion of potential applications of the method. DOE

N91-11058*# National Aeronautics and Space Administration. Lewis Research Center, Cleveland, OH.
PRELIMINARY RESULTS FROM THE ADVANCED PHOTOVOLTAIC EXPERIMENT FLIGHT TEST
David J. Brinker, Russell E. Hart, Jr., and John R. Hickey (Eppley Lab., Inc., Newport, RI.) May 1990 12 p Presented at the 21st Photovoltaic Specialists Conference, Kissimmee, FL, 21-25 May 1990; sponsored in part by IEEE
(NASA-TM-103269; E-5709; NAS 1.15:103269) Avail: NTIS HC/MF A03 CSCL 21H

The Advanced Photovoltaic Experiment is a space flight test designed to provide reference cell standards for photovoltaic measurement as well as to investigate the solar spectrum and the effect of the space environment on solar cells. After a flight of 69 months in low earth orbit as part of the Long Duration Exposure Facility set of experiments, it was retrieved in January, 1990. The electronic data acquisition system functioned as designed, measuring and recording cell performance data over the first 358 days of flight; limited by battery lifetime. Significant physical changes are also readily apparent, including erosion of front surface paint, micrometeoroid and debris catering and contamination. Author

N91-11059*# National Aeronautics and Space Administration. Lewis Research Center, Cleveland, OH.
A LIFE COMPARISON OF TUBE AND CHANNEL COOLING PASSAGES FOR THRUST CHAMBERS
R. S. Jankovsky and J. M. Kazaroff 1990 9 p Presented at the 1990 JANNAF Propulsion Meeting, Anaheim, CA, 3-5 Oct. 1990
(NASA-TM-103613; E-5724; NAS 1.15:103613) Avail: NTIS HC/MF A02 CSCL 21H

The life analysis used to compare copper tubes and milled copper channels for rocket engine cooling passages is described. Copper tubes were chosen as a possible replacement for the existing milled copper channel configuration because (1) they offer increased surface area for additional enthalpy extraction; (2) they have ideal pressure vessel characteristics; and (3) the shape of the tube is believed to allow free expansion, thus accommodating the strain resulting from thermal expansion. The analysis was a two-dimensional elastic-plastic comparison, using a finite element method, to illustrate that, under the same thermal and pressure loading, the compliant shape of the tube increases the life of the chamber. The analysis indicates that for a hot-gas-side-wall temperature of 100 F the critical strain decreases from 1.25 percent in the channel to 0.94 percent in the tube. Since the life of rocket thrust chambers is most often limited by cyclic strain or strain range, this decrease corresponds to an expected tube life which is nearly twice the channel life. Author

N91-11060*# National Aeronautics and Space Administration. Lewis Research Center, Cleveland, OH.
INVESTIGATION OF THE ARCJET PLUME NEAR FIELD USING ELECTROSTATIC PROBES
John M. Sankovic Nov. 1990 19 p Presented at the 1990 JANNAF Propulsion Meeting, Anaheim, CA, 2-4 Oct. 1990
(NASA-TM-103638; E-5817; NAS 1.15:103638) Avail: NTIS HC/MF A03 CSCL 21H

The near field plum of a 1 kW class arcjet thruster was investigated using electrostatic probes of various geometries. The electron number densities and temperatures were determined in a simulated hydrazine plume at axial distances between 3 cm (1.2 in) and 15 cm (5.9 in) and radial distances extending to 10 cm (3.9 in) off centerline. Values of electron number densities obtained using cylindrical and spherical probes of different geometries agreed very well. The electron density on centerline followed a source flow approximation for axial distances as near as 3 cm

(1.2 in) from the nozzle exit plane. The model agreed well with previously obtained data in the far field. The effects of propellant mass flow rate and input power level were also studied. Cylindrical probes were used to obtain ion streamlines by changing the probe orientation with respect to the flow. The effects of electrical configuration on the plasma characteristics of the plume were also investigated by using a segmented anode/nozzle thruster. The results showed that the electrical configuration in the nozzle affected the distribution of electrons in the plume. Author

N91-11061*# National Aeronautics and Space Administration. Lewis Research Center, Cleveland, OH.
PHOTOVOLTAIC OPTIONS FOR SOLAR ELECTRIC PROPULSION
Paul M. Stella (Jet Propulsion Lab., California Inst. of Tech., Pasadena.) and Dennis J. Flood Jul. 1990 16 p Presented at the 26th Joint Propulsion Conference, Orlando, FL, 16-18 Jul. 1990; sponsored in part by AIAA, ASME, SAE, and ASEE
(NASA-TM-103284; E-5739; NAS 1.15:103284) Avail: NTIS HC/MF A03 CSCL 21H

During the past decade, a number of advances have occurred in solar cell and array technology. These advances have lead to performance improvement for both conventional space arrays and for advanced technology arrays. Performance enhancements have occurred in power density, specific power, and environmental capability. Both state-of-the-art and advanced development cells and array technology are discussed. Present technology will include rigid, rollout, and foldout flexible substrate designs, with silicon and GaAs solar cells. The use of concentrator array systems is also discussed based on both DOD and NASA efforts. The benefits of advanced lightweight array technology, for both near term and far term utilization, and of advanced high efficiency, thin, radiation resistant cells is examined. This includes gallium arsenide on germaniun substrates, indium phosphide, and thin film devices such as copper indium diselenide. Author

23 CHEMISTRY AND MATERIALS (GENERAL)

N91-11062*# National Aeronautics and Space Administration. Lewis Research Center, Cleveland, OH.
GRAPHITE FLUORIDE FIBERS AND THEIR APPLICATIONS IN THE SPACE INDUSTRY
Ching-chen Hung, Martin Long, and Therese Dever (Cleveland State Univ., OH.) Aug. 1990 14 p Presented at the AIChE Summer National Meeting, San Diego, CA, 19-22 Aug. 1990
(NASA-TM-103265; E-5679; NAS 1.15:103265) Avail: NTIS HC/MF A03 CSCL 07A

Characterization and potential space applications of graphite fluoride fibers from commercially available graphitized carbon fibers are presented. Graphite fluoride fibers with fluorine to carbon ratios of 0.65 and 0.68 were found to have electrical resistivity values of 10(exp 4) and 10(exp 11) Ohms-cm, respectively, and thermal conductivity values of 24 and 5 W/m-K, respectively. At this fluorine content range, the fibers have tensile strength of 0.25 + or - 0.10 GPa (36 + or - 14 ksi), Young's modulus of 170 + or - 30 GPa (25 + or - 5 Msi). The coefficient of thermal expansion value of a sample with fluorine to carbon ratio of 0.61 was found to be 7 ppm/C. These properties change and approach the graphite value as the fluorine content approach 0. Electrically insulative graphite fluoride fiber is at least five times more thermally conductive than fiberglass. Therefore, it can be used as a heat sinking printed circuit board material for low temperature, long life power electronics in spacecraft. Also, partially fluorinated fiber with tailor-made physical properties to meet the requirements of certain engineering design can be produced. For example, a partially fluorinated fiber could have a predetermined CTE value in -1.5 to 7 ppm/C range and would be suitable for use in solar concentrators in solar dynamic power systems. It could also have a predetermined electrical resistivity value suitable for use as a low observable material. Experimental data indicate that slightly fluorinated graphite fibers are more durable in the atomic oxygen environment than pristine graphite. Therefore, fluorination of graphite used in the construction of spacecraft that would be exposed to the low Earth orbit atomic oxygen may protect defect sites in atomic oxygen protective coatings and therefore decrease the rate of degradation of graphite. Author

24 COMPOSITE MATERIALS

Includes physical, chemical, and mechanical properties of laminates and other composite materials.
For ceramic materials see *27 Nonmetallic Materials.*

N91-11063 Texas A&M Univ., College Station.
DEFORMATION AND DELAMINATION OF INELASTIC LAMINATES UNDER TENSILE AND TORSIONAL LOADING Ph.D. Thesis
Mark Jackson Lamborn 1989 267 p
Avail: Univ. Microfilms Order No. DA9015530

Mechanical work as a multivalued potential function which characterizes the deformation and fracture behavior of inelastic materials during damage growth processes is examined. Experimental data from fiber-reinforced plastic laminates subjected to axial and torsional deformation are analyzed for the existence of a work potential. A work potential-based method is employed to analyze data from proportional deformation tests and make predictions of load response. Good agreement is obtained between theory and experiment. Data from nonproportional deformation tests are then evaluated for displacement-path independence of work and load response. Domains of path independence are found from specimens strained well into the range of nonlinear inelastic behavior. Thus, the results of these experimental studies are consistent with the existence of a work potential. Work potential theory and experimental results are then used to determine critical energy release rates for mixed mode delamination of laminates subjected to axial and torsional deformations. Dissert. Abstr.

N91-11064# Department of Energy, Washington, DC.
COMPOSITE SLIP TABLE OF DISSIMILAR MATERIALS FOR DAMPING LONGITUDINAL MODES Patent Application
Danny L. Gregory, inventor (to DOE), Tommy G. Priddy, inventor (to DOE), David O. Smallwood, inventor (to DOE), and Tommy D. Woodall, inventor (to DOE) (AT and T Technologies, Inc., Albuquerque, NM.) 30 Jun. 1989 15 p
(Contract DE-AC04-76DP-00789)
(DE90-015128; US-Patent-Appl-SN-373416; Patents-US-A7373416) Avail: NTIS HC/MF A03

A vibration slip table for use in a vibration testing apparatus was designed. The table is comprised of at least three composite layers of materials; a first metal layer, a second damping layer, and a third layer having a relatively high acoustic velocity relative to the first layer. The different acoustic velocities between the first and third layers cause relative shear displacements between the layers with the second layer damping the displacements between the first and third layers to reduce the table longitudinal vibration modes. DOE

N91-11065# Institut National des Sciences Appliquees de Lyon, Villeurbanne (France).
RELATIONS BETWEEN MICROSTRUCTURE AND MECHANICAL BEHAVIOUR OF SiC/SiC COMPOSITES: INTERFACE EFFECTS ON MULTIPLE CRACKING IN MULTIFILAMENT MATERIALS Ph.D. Thesis
Veronique Arnault 1989 261 p In FRENCH; ENGLISH summary
(ISAL-89-0098; ETN-90-97824) Avail: NTIS HC/MF A12

In order to establish relations between the microstructure and the mechanical behavior of SiC/SiC composites, a micromechanical approach is investigated. A modelization of the interfacial shear strength is performed. It controls fiber-matrix sliding and load transfer between the components near a matrix crack. This model

describes friction conditions including Poisson's effect caused by the indentation load. In situ tensile tests under optical microscope are carried out. The kinetics of damage cumulation is described. The interpretation of the progressive cracking phenomena is based on a numerical simulation using concepts of fiber-matrix sliding by interfacial shear strength, and failure statistics. ESA

N91-11066# Messerschmitt-Boelkow-Blohm G.m.b.H., Munich (Germany, F.R.). Dienstleistungsbereich.
ULTRASONIC EXAMINATION OF FIBER COMPOSITE MATERIALS BY MEANS OF VIRTUAL C-SCAN TEST AND MODEL RECOGNITION [ULTRASCHALLPRUFUNG VON FASERVERBUNDWERKSTOFFEN MITTELS VIRTUELLEM C-SCAN UND MUSTERERKENNUNG]
R. Bilgram and A. Gessler 1989 11 p In GERMAN Presented at the Seminar Ultraschallpruefung Neuer Werkstoffe, Berlin, Fed. Republic of Germany, 6-7 Nov. 1989
(MBB-Z-0299-89-PUB; ETN-90-97857) Avail: NTIS HC/MF A03

Two experimental ultrasonic systems are presented which offer new possibilities for the examination of fiber composite materials. Fundamental examinations, practical uses, and possible developments are examined. A multidimensional feature-based decision process is indicated. ESA

N91-11067# Cologne Univ. (Germany, F.R.). Mathematisch-Naturwissenschaftlichen Fakultaet.
ELASTIC PROPERTIES OF CERAMIC COMPOSITE MATERIALS AT HIGH TEMPERATURES Ph.D. Thesis [ELASTISCHE EIGENSCHAFTEN VON KERAMISCHEN VERBUNDWERKSTOFFEN BEI HOHEN TEMPERATUREN]
Rolf Wagner 1989 104 p In GERMAN
(ETN-90-97897) Avail: NTIS HC/MF A06

An installation for measuring the elastic properties up to maximal temperatures of 2000C, under vacuum is described. A program is developed for the full automatic control of the installation with a personal computer. The elastic properties of Al2O3-SIC systems up to 1400C, and of Mullit-SIC systems up to 1200C are measured, as well as the bending resistance and rupture toughness, on the basis of Al2O3 and Mullit. A distinct rupture toughness increase was noted only in the case of whiskers reinforcement. ESA

N91-11068 Texas Univ., Austin.
RESIDUAL STRESS MEASUREMENTS AND MICROSTRUCTURAL CHARACTERIZATION OF GRAPHITE-ALUMINUM METAL MATRIX COMPOSITE Ph.D. Thesis
Hun Sub Park 1989 139 p
Avail: Univ. Microfilms Order No. DA9016948

The P 100 graphite fiber reinforced aluminum metal matrix composites used have residual stresses due to the difference in coefficients of thermal expansion of the components. The residual stresses which are dependent on the thermal history cannot be neglected in their magnitude. Residual stresses of the metal matrix with various thermal histories were measured by x ray diffraction (XRD) method and compared with the mathematical analysis. Before these measurements the XRD method was calibrated by measuring elastic properties of the monolithic 6061 aluminum plate with three-point bend fixture and comparing with those obtained by the tension test. To better understand thermal and mechanical behaviors of P 100 Gr/6061 Al composites, it is important to fully characterize the microstructures of the composites and the graphite fiber-aluminum matrix interface was observed by electron microscopy techniques. The microstructural features which play a key role in controlling the strength of the composites were analyzed using (Scanning) Transmission Electron Microscope, with its capability for energy dispersive spectroscopy (EDS) for elemental analysis of particles and phases. Differential scanning calorimetry (DSC) was also conducted to examine precipitation behavior of both the composite and the monolithic 6061 Al plate.
Dissert. Abstr.

N91-11069# Oak Ridge National Lab., TN. Applied Technology Div.
POTENTIAL FOR ADVANCED THERMOPLASTIC COMPOSITES IN SPACE SYSTEMS
R. E. Garvey 1990 15 p Presented at the 22nd International Technical Conference of the Society for the Advancement of Material and Process Engineering, Boston, MA, 6-8 Nov. 1990
(Contract DE-AC05-84OR-21400)
(DE90-014447; CONF-901104-1) Avail: NTIS HC/MF A03

This paper provides a rational for incorporating graphite/thermoplastic into future Strategic Defense Initiative space systems. Graphite/PEEK is compared with the best available graphite/epoxy materials, which today are graphite/1962 produced by Amoco and graphite/934 produced by Fiberite. A first-order comparison reveals similar performance between these classes of materials with respect to maximum stiffness, minimum gage, maximum damping and threat hardness. There are significant differences in the behavior of graphite/polyether ether ketone and graphite/epoxy with respect to the following characteristics: water absorption, condensible-volatile contents, space-environment effects, dimensional stability, weight-savings options, joining alternatives, and production costs. A comparison is also made between organic composites, such as graphite/PEEK, with other spacecraft structural materials, such as aluminum and beryllium (which are commonly used today). The differing requirements for each spacecraft component will determine which of these material options is best suited for the particular structural application.
DOE

N91-11070# Ames Lab., IA.
ANALYSIS OF DEFORMATION CHARACTERISTICS OF A HEAVILY DEFORMED Cu-20 PERCENT Nb COMPOSITE
S. B. Biner and W. A. Spitzig 1989 11 p Presented at the Metallurgical Society Fall Meeting: Materials Week, Indianapolis, IN, 1-5 Oct. 1989
(Contract W-7405-eng-82)
(DE90-018041; IS-M-646; CONF-891024-9) Avail: NTIS HC/MF A03

In this study, the deformation and strengthening behavior of a Cu-Nb composite is simulated by using an elastic-plastic finite element analysis. Results indicate that a whisker strengthening mechanism due to the Nb filaments behaving as whiskers is not sufficient to increase the strength level of the composite to the observed strength level. To predict the measured strength levels some portion of the Cu matrix should have a strength level as high as the theoretical strength of Cu, in agreement with predictions from an earlier analysis based on the Hall-Petch relation. DOE

N91-11071# Ames Lab., IA.
CHARACTERIZATION OF SHORT FATIGUE CRACKS AT NOTCHES IN SiC PARTICULATE ALUMINUM COMPOSITE
S. B. Biner 1989 13 p Presented at the Metallurgical Society Fall Meeting: Materials Week, Indianapolis, IN, 1-5 Oct. 1989
(Contract W-7405-eng-82)
(DE90-018043; IS-M-645; CONF-891024-8) Avail: NTIS HC/MF A03

The initiation and growth of cracks emanating from blunt notches in 6061-Al alloy reinforced with 25 percent particulate SiC metal matrix composite was investigated. To elucidate the role of the aging condition of the matrix on the fatigue behavior, the studies were carried out at T6 and overaged conditions. The results indicate that the initiation of fatigue cracks are insensitive to the notch severity and to the aging condition of the matrix. The overaging heat treatment resulted in slower fatigue crack growth rates. The failure of the SiC particles during the fatigue process is given as the reason for the observed initiation and crack growth characteristics. It is also shown that the growth rate of short cracks emanating from blunt notches can be accurately described by an effective stress intensity factor range (Delta)K(sub eff). This could provide an adequate engineering method for design against fatigue failure from various stress concentrations for this composite system. DOE

N91-11072*# National Aeronautics and Space Administration. Langley Research Center, Hampton, VA.
MATERIALS DIVISION RESEARCH AND TECHNOLOGY ACCOMPLISHMENTS FOR FY 89 AND PLANS FOR FY 90
Kay L. Brinkley Oct. 1990 133 p
(NASA-TM-102649; NAS 1.15:102649) Avail: NTIS HC/MF A07 CSCL 11D

The research program of the Materials Division is presented as FY-89 accomplishments and FY-90 plans. The accomplishments for each Branch are highlighted and plans are outlined. Publications of the Division are included by Branch. This material will be useful in program coordination with other government organizations, universities, and industries in areas of mutual interest. Author

N91-11073# Rolls-Royce Ltd., Derby (England).
HIGH TEMPERATURE MATERIALS: THE OVERALL VIEW
G. W. Meetham 24 Nov. 1989 12 p Presented at EUROMAT 1989, European Conference on Advanced Materials and Processes, Aachen, Fed. Republic of Germany, 22-24 Nov. 1989
(PNR-90699; ETN-90-97935) Copyright Avail: NTIS HC/MF A03

In the scope of the European conference on advanced materials and processes the need for high temperature materials is discussed. The temperature capabilities and typical operating temperatures of the materials is given. Some mechanical characteristics versus temperature of aluminum alloys and steels nickel alloys are given. The applications and advantages of coating high temperature alloys, of ceramics, of carbon and carbon-carbon composites are summarized. The thermal conductivities of several insulating materials are presented. Some materials used as heat sinks are reported. ESA

N91-11074*# National Aeronautics and Space Administration. Lewis Research Center, Cleveland, OH.
ELASTIC/PLASTIC ANALYSES OF ADVANCED COMPOSITES INVESTIGATING THE USE OF THE COMPLIANT LAYER CONCEPT IN REDUCING RESIDUAL STRESSES RESULTING FROM PROCESSING
Steven M. Arnold, Vinod K. Arya (Toledo Univ., OH.), and Matthew E. Melis Sep. 1990 51 p
(NASA-TM-103204; E-5661; NAS 1.15:103204) Avail: NTIS HC/MF A04 CSCL 11D

High residual stresses within intermetallic and metal matrix composite systems can develop upon cooling from the processing temperature to room temperature due to the coefficient of thermal expansion (CTE) mismatch between the fiber and matrix. As a result, within certain composite systems, radial, circumferential, and/or longitudinal cracks have been observed to form at the fiber-matrix interface. The compliant layer concept (insertion of a compensating interface material between the fiber and matrix) was proposed to reduce or eliminate the residual stress buildup during cooling and thus minimize cracking. The viability of the proposed compliant layer concept is investigated both elastically and elastoplastically. A detailed parametric study was conducted using a unit cell model consisting of three concentric cylinders to determine the required character (i.e., thickness and material properties) of the compliant layer as well as its applicability. The unknown compliant layer mechanical properties were expressed as ratios of the corresponding temperature dependent Ti-24Al-11Nb (a/o) matrix properties. The fiber properties taken were those corresponding to SCS-6 (SiC). Results indicate that the compliant layer can be used to reduce, if not eliminate, radial and circumferential residual stresses within the fiber and matrix and therefore also reduce or eliminate the radial cracking. However, with this decrease in in-plane stresses, one obtains an increase in longitudinal stress, thus potentially initiating longitudinal cracking. Guidelines are given for the selection of a specific compliant material, given a perfectly bonded system. Author

N91-11075# Office National d'Etudes et de Recherches Aerospatiales, Paris (France).
LOAD TRANSFER BETWEEN FIBER AND MATRIX IN CARBON FIBER REINFORCED PLASTIC COMPOSITES TENSILE BEHAVIOR OF AN EMBEDDED SINGLE FILAMENT SPECIMEN Ph.D. Thesis - Inst. National Polytechnique de Lorraine
Didier Jacques Sep. 1989 143 p In FRENCH; ENGLISH summary Report will also be announced as translation (ESA-TT-1230)
(ONERA-NT-1989-9; ISSN-0018-3781; ETN-90-98018) Avail: NTIS HC/MF A07

The load transfer between fiber and matrix in carbon fiber reinforced plastic composites was studied through the tensile behavior of an embedded single filament specimen. This fragmentation test was made suitable for brittle aeronautical matrices. It was shown to be a sensitive method for qualifying the effects of any system modification. A tensile device was designed for simultaneous observations during testing in order to assess the interfacial micromechanisms. These mechanisms were combined in a stochastic computer simulated model of the fiber fragmentation process. The influence of component characteristics was evaluated. An extension to composites is suggested. ESA

25 INORGANIC AND PHYSICAL CHEMISTRY

Includes chemical analysis, e.g., chromatography; combustion theory; electrochemistry; and photochemistry.

For related information see also *77 Thermodynamics and Statistical Physics.*.

N91-11076# Societe Bertin et Cie, Tarnos (France).
CHARACTERIZATION AND OPTIMIZATION OF A PNEUMATIC INJECTOR FOR A 60 BAR COMBUSTION CHAMBER
C. Belot, C. Leonard, H. Martin-Neuville, and J. C. Mulet 1990 7 p Presented at the 6th ILASS-Europe Annual Conference on Liquid Atomization and Spray Systems, Pisa, Italy, 4-6 Jul. 1990
(ETN-90-97580) Avail: NTIS HC/MF A02

A 60 bar combustion chamber was tuned up with a thermal power of 400 kW, running on methanol/oxygen, and cooled by recirculated combustion products at 25C. The following are presented: sizing of the pneumatic injector by which methanol is atomized in the combustion chamber; the atomization trials performed in a specific test bench (internal pressure up to 100 bar) and the comparison between experimental and calculated droplets trajectories; then the numerical optimization of the injector; the effect of the pressure upon the mean mass diameter of the droplets generated by the optimized injector. The combustion obtained with the injector was very stable and the combustion efficiency greater than 0.997. The main conclusion is that good atomization control allows good combustion control. ESA

N91-11077# Max-Planck-Inst. fuer Stroemungsforschung, Goettingen (Germany, F.R.).
THEORY OF HOMOGENEOUS NUCLEATION FROM THE VAPOR PHASE
Andreas Dillmann 1989 58 p In GERMAN; ENGLISH summary
(MPIS-Mitt-93; ISSN-0374-1257; ETN-90-97867) Avail: NTIS HC/MF A04

A theory of homogeneous nucleation from the vapor phase is presented. The classical Becker-Doering-Zeldovich theory is contained as a limiting case. The theory is based on a semi-phenomenological droplet model for the Gibbs free enthalpy of formation of the cluster. Since this droplet model also allows the construction of a thermal equation of state for real gases below the critical point, all free parameters of the model can be determined from macroscopic measurements. The new theory gives a much better prediction of observed nucleation rates than the classical theory. ESA

N91-11078# Acurex Corp., Research Triangle Park, NC.
RECOMMENDED OPERATING PROCEDURE NO. 45: ANALYSIS OF NITROUS OXIDE FROM COMBUSTION SOURCES Final Report, Sep. 1989 - May 1990
J. S. Ford Jun. 1990 33 p
(Contracts EPA-68-02-4701; EPA-68-02-4291)
(PB90-238502; EPA/600/8-90/053) Avail: NTIS HC/MF A03 CSCL 21B

The recommended operating procedure (ROP) has been prepared for use in research activities conducted by the Environmental Protection Agency's (EPA's) Air and Energy Engineering Research Laboratory (AEERL). The procedure applies to the measurement of nitrous oxide (N2O) in dry gas samples extracted from gas streams where N2O concentrations range from 0.5 to 200 ppm. N2O concentrations are interpreted by an electron capture detector (ECD). The ECD uses a 63Ni constant current cell. The upper limits of this procedure can be extended by changing the sample loop pressure to reduce the volume of sample in the look or by diluting the sample. ROPs describe non-routine or experimental research operations where some judgment in application may be warranted. ROPs may not be applicable to activities conducted by other research groups, and should not be used in place of standard operating procedures. Use of ROPs must be accompanied by an understanding of their purpose and scope. GRA

N91-11079# Pacific Northwest Lab., Richland, WA.
COMBINED CAPILLARY ELECTROPHORESIS AND ELECTROSPRAY IONIZATION MASS SPECTROMETRY
Richard D. Smith, Joseph A. Loo, Charles G. Edmonds, and Harold R. Udseth Jul. 1990 17 p Presented at the Spectroscopy Across the Spectra, Hertford, England, 9-12 Jul. 1990
(Contract DE-AC06-76RL-01830)
(DE90-016535; PNL-SA-18081; CONF-9007162-1) Avail: NTIS HC/MF A03

The development of new capillary electrophoresis (CE) methods provides a basis for the efficient manipulation and separation of subpicomole quantities of polypeptides and proteins. Recent advances in microscale methods, such as the demonstration of the tryptic digestion of low picomole quantities of proteins using the immobilized enzyme in small diameter packed reactor column, provide the basis for such further developments. The use of capillary (free solution) zone electrophoresis (CZE) for separation of proteins, and recent demonstrations of restriction mapping of large deoxyribonucleotides, has propelled potential CE applications into the realm of conventional electrophoresis, while adding the attributes of speed, relatively simple on-line detection, automation, and reduced sample requirements (10(exp -17) - 10 (exp -13) mole). A literal explosion of ancillary methods for sample manipulation, derivatization, and detection as well as new methods of obtaining separation selectivity are being reported. Additionally, other CE formats are attracting increased interest, with the aim of exploiting the unique features of capillary isotachophoresis (CITP), capillary isoelectric focusing (CIEF), capillary electrokinetic chromatograpgy (CEC), and most recently, capillary polyacrylamide gel electrophoresis (CGE). As a result, there are concomitant and increasing demands upon detector sensitivity and information density. DOE

N91-11080# Oak Ridge National Lab., TN. Chemical Physics Section.
RESONANCE IONIZATION SPECTROSCOPY OF MOLECULAR CLUSTERS USING PICOSECOND LASERS
John C. Miller and D. Barton Smith 1990 6 p Presented at the 5th International Symposium on Resonance Ionization Spectroscopy and its Applications, Varese, Italy, 16-21 Sep. 1990
(Contract DE-AC05-84OR-21400; NATO-0474/87)
(DE90-017334; CONF-9009174-1) Avail: NTIS HC/MF A02

High peak-power picosecond laser pulses were used for the first time to effect nonresonant or resonant multiphoton ionization (MPI) of clusters generated in a supersonic nozzle expansion. The resultant ions are subsequently detected and characterized by time-of-flight mass spectroscopy. Specifically, results are presented involving MPI of the cluster series Ar(n)NO, (NO)(n), and Ar(n)I(2). Previous MPI studies of the latter two species using nanosecond lasers were not successful in detecting the parent ion, presumably due to fast dissociation channels. It is proposed that the present technique is a new and rather general ionization source for cluster studies which is complementary to electron impact but in addition, may provide unique spectroscopic or dynamical information. DOE

N91-11081# Lawrence Livermore National Lab., CA. Nondestruction Evaluation Section.
MULTIPLE-ENERGY TECHNIQUES IN INDUSTRIAL COMPUTERIZED TOMOGRAPHY
Dan Schneberk, Harry Martz, and Steve Azevedo 1 Aug. 1990 8 p Presented at the Review of Progress in Quantitative NDE, La Jolla, CA, 15-20 Jul. 1990
(Contract W-7405-eng-48)
(DE90-017518; UCRL-JC-103762; CONF-900791-2) Avail: NTIS HC/MF A02

Considerable effort is being applied to develop multiple-energy industrial CT techniques for materials characterization. Multiple-energy CT can provide reliable estimates of effective Z (Z sub eff), weight fraction, and rigorous calculations of absolute density, all at the spatial resolution of the scanner. Currently, a wide variety of techniques exist for CT scanners, but each has certain problems and limitations. Ultimately, the best multi-energy CT technique would combine the qualities of accuracy, reliability, and wide range of application, and would require the smallest number of additional measurements. Techniques were developed for calculating material properties of industrial objects that differ somewhat from currently used methods. Methods are presented for calculating Z sub eff, weight fraction, and density. The simplest case start (methods for multiple-energy CT using isotopic sources) and proceed to multiple-energy work with x ray machine sources. The methods discussed are illustrated on CT scans of PBX-9502 high explosives, a lexan-aluminum phantom, and a cylinder of glass beads used in a preliminary study to determine if CT can resolve three phases: air, water, and a high-Z oil. In the CT project at LLNL, several CT scanners of varying scanning geometries were constructed using gamma and x ray sources. In the research, two of these scanners were used: pencil beam CAT for CT data using isotopic sources and video-CAT equipped with an IRT micro-focal x ray machine source. DOE

N91-11082# Lawrence Livermore National Lab., CA.
ALUMINUM METAL COMBUSTION IN WATER REVEALED BY HIGH SPEED MICROPHOTOGRAPHY
William C. Tao, Alan M. Frank, Rochelle E. Clements, and Joseph E. Shepherd Jul. 1990 13 p Presented at the SPIE's International Symposium on Optical and Optoelectronic Applied Science and Engineering Exhibit, San Diego, CA, 8-13 Jul. 1990
(Contract W-7405-eng-48)
(DE90-017525; UCRL-JC-104276; CONF-900756-40) Avail: NTIS HC/MF A03

In high explosives designed for air blast, cratering, fragmentation, and underwater applications, metallic additives chemically react with the oxidizer and are used to tailor the rate of energy delivery by the expansion medium. Although the specific mechanism for sustained metal combustion in the dense detonation medium remains in question, it is generally accepted that the fragmentation of the molten particle and disruption of its oxide layer are a necessity. High speed microphotography was used to examine the ignition of small 25 to 76 microns diameter and 23 mm long aluminum wires, rapidly heated by a capacitor discharge system, in water. Streak and framing photographs detailing the combustion phenomenon and the fragmentation of the molten aluminum were obtained over periods of 100 nsec to 100 microsecs with a spatial resolution of 2 microns. The wire temperature was determined as a function of time by integrating the circuit equation together with the energy equation for an adiabatic wire, and incorporating known aluminum electrical resistivity and temperature functions of energy density in the integration. In order for the aluminum to sustain a rapid chemical reaction with the water, it

was found that the wire temperature has to be raised above the melting temperature of aluminum oxide. The triggering mechanism for this rapid reaction appears to be the fragmentation of the molten aluminum from the collapse of a vapor blanket about the wire during its first oscillation. DOE

N91-11083# Iowa State Univ. of Science and Technology, Ames. Center for New Industrial Materials.
TRANSIENT INFRARED EMISSION SPECTROSCOPY
John F. McClelland and Roger W. Jones 1989 1 p Presented at the 6th International Topical Meeting on Photoacoustic and Photothermal Phenomena, Baltimore, MD, 31 Jul. - 3 Aug. 1989
(Contract W-7405-eng-82)
(DE90-017253; IS-M-636; CONF-890754-2) Avail: NTIS HC/MF A01

Conventional infrared emission spectroscopy has normally been applied only to optically thin samples because of the phenomenon of self-absorption. In an optically thick material, self-absorption severely alters the emission so that the resulting spectrum closely resembles a black-body emission spectrum. Spectral features characteristic of the material are very weak and grossly altered in appearance, making the spectrum analytically of little use. Transient infrared emission spectroscopy (TIRES) produces useful emission spectra from optically thick samples by greatly reducing self-absorption. In TIRES a laser beam is used to rapidly heat the sample surface creating a transient hot layer. A spectrometer collects the emission from this layer before it cools and thickens by thermal diffusion. The layer is optically thin at infrared wavelengths, and so self-absorption is reduced. If a pulsed laser is used, the desired thin layer will exist at the laser spot on the sample surface for a short time immediately after the laser pulse, so the emission collection must be synchronized with the laser firing. If a continuous-wave (CW) laser is used, the sample must move through the beam or the beam must move over the sample surface. The transient layer will then exist along the beam path on the sample surface immediately behind the beam position, and thus the emission observation must be spatially correlated with the laser beam, but no synchronization is needed. Results using both types of lasers will be discussed. DOE

N91-11084# Oak Ridge National Lab., TN. Analytical Chemistry Div.
APPLICATIONS OF DIODE LASERS TO RESONANCE IONIZATION MASS SPECTROMETRY
J. P. Young, R. W. Shaw, and D. H. Smith 1990 9 p Presented at the 5th International Symposium on Resonance Ionization Spectroscopy and Its Applications, Ispra, Italy, 16-21 Sep. 1990
(Contract DE-AC05-84OR-21400)
(DE90-017768; CONF-900964-2) Avail: NTIS HC/MF A02

Diode lasers have been utilized in resonance ionization mass spectrometry (RIMS). These devices have been used to excite the first transition of several 1 + 1 + 1 multiple photon processes for both lanthanum 138 and 139. Enhanced isotopic selectivity resulted. Very-high resolution spectra were also obtained with the diode laser step to yield new atomic hyperfine structure constants for several levels of lanthanum. An isotopically selective RIMS instrument can be envisioned that used only diode lasers for optical excitation followed by a non-optical ionization step. DOE

N91-11085# Los Alamos National Lab., NM.
AN APPARATUS FOR STUDIES OF HYDROGEN ISOTOPE EXCHANGE OVER METALS USING LASER-RAMAN SPECTROSCOPY
Dean H. W. Carstens Oct. 1990 6 p
(Contract W-7405-eng-36)
(DE90-018038; LA-11884-MS) Avail: NTIS HC/MF A02

An apparatus that uses laser-Raman spectroscopy measures the dynamic gas composition and pressure of mixed hydrogen isotopes as they exchange over hydride-forming metals or alloys. Data for the exchange of protium and deuterium over ZrCo alloy at 260 C indicate that this alloy begins exchanging at temperatures only slightly above room temperature and rapidly and completely exchanges at the higher temperature. The method is suitable for studies of bulk hydrogen/metal interactions. DOE

N91-11086# Fermi National Accelerator Lab., Batavia, IL.
AN INVESTIGATION OF THERMALLY DRIVEN ACOUSTICAL OSCILLATIONS IN HELIUM SYSTEMS
J. D. Fuerst Aug. 1990 6 p Presented at the Low Temperature Engineering and Cryogenics Conference, Southampton, England, 17-19 Jul. 1990
(Contract DE-AC02-76CH-03000)
(DE90-018049; FNAL-TM-1676; CONF-900708-1) Avail: NTIS HC/MF A02

The phenomenon of thermal-acoustic oscillation is seen to arise spontaneously in gas columns subjected to steep temperature gradients, particularly in tubes connecting liquid helium reservoirs with the ambient environment. This is often the arrangement for installed cryogenic instrumentation and is accompanied by undesirably large heat transfer rates to the cold region. Experimental data are collected and matched to theoretical predictions of oscillatory behavior; these results are in good agreement with the analytical model and with previously collected data. The present experiment places the open ends of oscillating tubes of the various lengths and cross sections in communication with flowing helium in the subcooled, 2-phase, or superheated state while the other ends are maintained at some controlled, elevated temperature. Assorted cold end conditions are achieved through adjustments to the Fermilab Tevatron satellite test refrigerator to which the test cryostat is connected. The warm, closed ends of the tubes are maintained by isothermal baths of liquid nitrogen, ice water, and boiling water. The method is contrasted to previous arrangements whereby tubes are run from room temperature into or adjacent to a stagnant pool of liquid helium. Additionally, the effect of pulsations in the flowing helium stream is explored through operation of the refrigerator's wet and dry expanders during data collection. These data confirm the theory to which they were compared and support its use in the design of cryogenic sensing lines for avoidance of thermoacoustic oscillation. DOE

N91-11087# New Energy Development Organization, Tokyo (Japan).
SURVEY ON SOLIDIFICATION AND UTILIZATION TECHNOLOGY OF CO2
Mar. 1990 173 p In JAPANESE; ENGLISH summary
(DE91-701465; NEDO-P-8919) Avail: NTIS (US Sales Only) HC/MF A08

A survey on solidification and utilization technology of CO2 was conducted, promising technologies were selected and their realization was forecasted. Then, the contribution to the CO2 issue and future development subjects were investigated. There are two main methods for solidification. One is biological, and the other is chemical solidification. It is necessary for chemical solidification to separate as large volumes of high-density CO2 as possible which is emitted, for example in a thermal power plant of large scale. Separation by membrane is competent for rough separation of CO2, and can be followed by absorption or adsorption in the secondary concentration. In biological solidification which is used for low-density CO2 in the atmosphere, a process of protein production from micro-algae is considered to be used in a large scale solidification. However for that, it is indispensable to come up with highly productive microalagae and make further development in production processes and systems. Meanwhile, there is on-going research for the catalytic hydrogenation of CO2, which is offering possibility for practical use in the near future. This technology is considered to be the most promising one, as it will see a big demand in the form of fuel for automobiles as a substitute for petroleum. DOE

N91-11088# Ecole Centrale de Lyon (France).
THEORETICAL AND NUMERICAL ASPECTS OF WAVE STABILITY IN COMBUSTION MODELS Ph.D. Thesis [ASPECTS THEORIQUES ET NUMERIQUES DE STABILITE

D'ONDES DANS DES MODELES DE COMBUSTION]
Samadollah NoorEbad 1989 113 p In FRENCH
(ECL-89-21; ETN-90-97816) Avail: NTIS HC/MF A06

Combustion and deflagration models are created. The mathematical tools required for studying stability are shown: spectral analysis, analytic half-groups, regularity of parabolic problems. The study of the nonlinear stability of a unilateral problem is carried out. Numerical algorithms for solving free boundary problems are developed. Numerical examples illustrate the theoretical results on stability. ESA

N91-11089# Sandia National Labs., Albuquerque, NM.
IN-SITU PORE STRUCTURE ANALYSIS DURING AGING AND DRYING OF GELS
Douglas M. Smith, Pamela J. Davis (New Mexico Univ., Albuquerque.), and C. Jeffrey Brinker 1990 13 p Presented at the Spring Meeting of the Materials Research Society, San Francisco, CA, 16-21 Apr. 1990
(Contract DE-AC04-76DP-00789)
(DE91-000044; SAND-90-2203C; CONF-900466-86) Avail: NTIS HC/MF A03

The use of nuclear magnetic resonance (NMR) relaxation measurements for the in-situ study of pore structure evolution during gel aging and drying is illustrated. The change in the pore size distribution and surface area of other wet and dried gels is examined as a function of aging conditions including temporal aging, thermal aging, changing pH, and changing pore fluid. The effect of pore fluid pH on dissolution/reprecipitation in ordered packings of monodisperse silica spheres is also examined as a model system for particulate gels. As expected, the pore size distribution narrows with increasing time of treatment in high pH pore fluids. Interpretation of high pH results for the wet state is complicated by a microporous layer which forms on colloidal silica resulting in significantly large wet surface area as compared to the final dried material. Narrowing of the pore size distribution, which is of interest for maximizing drying rates, is maximized in the least time by using either high pH or repeated ethanol washes for the base-catalyzed gel (B2) used. DOE

N91-11090# Office National d'Etudes et de Recherches Aerospatiales, Paris (France).
COMBUSTION TO MODELISATION TURBULENT COMBUSTION IN THE CASE OF STABILIZATION BY FLAME-LOCK Ph.D. Thesis - Paris VII Univ.
Pascale Gilbank Nov. 1989 145 p In FRENCH; ENGLISH summary Report will also be announced as translation (ESA-TT-1229) Original contains color illustrations
(ONERA-NT-1989-8; ISSN--0078-3781; ETN-90-98017) Avail: NTIS HC/MF A07

A new method for predicting turbulent reactive flows, capable of describing various combustion states and adapting to realistic reactive schemes is proposed. This method, called PEUL (Probabilities-Eulerian-Lagrangian) method, features the use of Eulerian balance equations to describe the variation of the variables characterizing the flow. The source term involved in the Eulerian balance equations for the mass fractions of the chemical species is determined by Lagrangian equations. The Lagrangian approach describes the flow from phenomenological standpoint. The PEUL model numerically predicts multireactive turbulent flows. It was applied to a turbulent air/methane premixing flame developing in a two-dimensional channel with a constant section or a channel with a step behind which a recirculation region is set up. ESA

26 METALLIC MATERIALS

Includes physical, chemical, and mechanical properties of metals, e.g., corrosion; and metallurgy.

N91-11091*# Alabama Univ., Huntsville.
HEAT TREATMENT STUDY 2 Final Report
Gary L. Workman 13 Apr. 1990 7 p
(NASA Order H-80579-B)
(NASA-CR-184009; NAS 1.26:184009) Avail: NTIS HC/MF A02 CSCL 11F

The microstructural variations in nickel-based superalloys that result from modifications in processing were examined. These superalloys include MAR-M246(HF) and PWA1480. Alternate heat treatments for equiaxed as-cast specimens were studied and a sample matrix of 42 variations in the heat treatments were processed, as well as different directional solidification parameters. Variation in temperature and times for both solution and aging were performed. Photomicrographs were made of the microstructure and volume fraction analysis of primary gamma-prime and aged gamma-prime precipitates were performed. The results of the heat treatment, cooling rate, and directional solidification experiments are discussed. M.G.

N91-11092# Oregon Graduate Inst. of Science and Technology, Beaverton.
DEFORMATION EFFECTS ON THE DEVELOPMENT OF GRAIN BOUNDARY CHRONIUM DEPLETION (SENSITIZATION) IN TYPE 316 AUSTENITIC STAINLESS STEELS
D. G. Atteridge, W. E. Wood, A. H. Advani, and S. M. Bruemmer (Pacific Northwest Lab., Richland, WA.) 1990 263 p
(Contract DE-AC06-86NE-37963)
(DE90-016130; DOE/NE-37963/12) Avail: NTIS HC/MF A13

Deformation induces an acceleration in the kinetics and reduction in the thermodynamic barrier to carbide precipitation and grain boundary chromium depletion (GBCD) development of a high carbon Type 316 stainless steel (SS). This was observed in a study on strain effects on GBCD (or sensitization) development in the range of 575 to 775 C. Grain boundary chromium depletion behavior of SS was examined using the indirect electrochemical potentiokinetic reactivation (EPR) test and supported by studies on carbide precipitation using transmission electron microscopy (TEM). DOE

N91-11093 Cornell Univ., Ithaca, NY.
THERMAL STRESS-INDUCED GRAIN BOUNDARY CAVITATION IN NARROW, ALUMINUM ALLOY METALLIZATIONS Ph.D. Thesis
Ronald Douglas Black 1990 385 p
Avail: Univ. Microfilms Order No. DA9027122

The nucleation and growth of thermal stress-induced cavities in aluminum alloy metallizations are investigated from a theoretical viewpoint. Based on published and newly presented experimental data it is proposed that cavity nucleation occurs by a grain boundary sliding mechanism. Growth is proposed to occur by stress-driven diffusion processes through the bulk, as well as along grain boundaries which intersect the cavity. A model for cavity growth, which describes the rate of change in cavity volume as a function of time, is presented. Actual use of the model requires an accurate knowledge of the evolution, as a function of temperature and time, of stresses in the metallization. To verify the model for growth, thermal stresses in metallizations are first extensively investigated. Using experimental data published in the literature, as well as newly presented data, deformation mechanisms for the metallizations are suggested. Based on these mechanisms, constitutive stress-inelastic strain rate relations are deduced. These relations are shown to accurately describe the temperature and time evolution of thermal stresses in metallizations. Combining the model for cavity growth and thermal stress calculations from the suggested constitutive equations, cavity growth simulations are performed and shown to accurately describe experimental data. Finally, the growth model is used to describe failure data of engineering interest. Dissert. Abstr.

N91-11094 University Coll., Cardiff (Wales).
THE ULTRASONIC EXAMINATION OF TITANIUM ALLOYS Ph.D. Thesis
K. Bassir 1989 229 p
Avail: Univ. Microfilms Order No. BRDX89151

The aim was to establish the causes of high level noise encountered during ultrasonic examination of titanium alloys and

to increase the possibility of the defect detection by increasing the signal to noise ratio. The project was divided into two sections: to determine the source of the noise of titanium (Ti-6Al-4V) alloy bars and; to find a method of increasing the amplitude of the signal from defects or reducing the noise level and hence increasing the detectability. The ultrasonic examination of the noise level was carried out on Ti-6Al-4V (Ti 318). A commercially pure titanium alloy (Ti 130) was also used. Emphasis on defect detectability was placed on the detection of elliptically shaped defects. A nickel alloy bar containing some elliptically shaped alumina seeds was used. The source of noise in titanium was traced to the bands of different elongated grain sizes and it was found that the greater the degree of working the fewer are the bands of different elongated grain sizes. A notable improvement in signal to noise ratio was achieved using the pitch-catch method in combination with a PVDF probe receiver. Dissert. Abstr.

N91-11095 North Carolina State Univ., Raleigh.
EFFECTS OF ELECTRIC CURRENT AND FIELD ON THE BEHAVIOR OF METALLIC MATERIALS Ph.D. Thesis
Wei-Di Cao 1989 270 p
Avail: Univ. Microfilms Order No. DA9017673

The effects of electric current and field on the behavior of metallic materials was studied in terms of the drop in flow stress caused by an electric current pulse and the changes in superplastic behavior and phase transformation kinetics resulting from applying an external electric field. The experimental procedures employed previously by Conrad et al to investigate the electroplastic effect was modified to facilitate the elimination of side effects from the observed drop in flow stress due to a current pulse, to determine the electron wind force on dislocations, and to establish the effect of electric current on each of the thermal activation parameters in the Arrhenius strain rate equation. The experimental values of the electron wind force were in general accord with those predicted by available theories for face centered cubic (FCC) metals, but a much higher value was obtained for body centered cubic (BCC) Nb. The measured electron wind force decreased with increasing stacking fault energy and in turn with decreasing width of extended dislocations in FCC metals. An external electric field reduced the flow stress and work hardening, significantly suppressed the cavitation and retarded strain-enhanced grain growth of 7475 Al during superplastic deformation. In addition, the application of an external electric field during the heat treatment of two steels accelerated austenization, increased hardenability and retarded the dissociation of quenched martensite during tempering. Possible mechanism for these effects are discussed. Dissert. Abstr.

N91-11096 Illinois Univ., Urbana-Champaign.
DEFORMATION MECHANISMS IN RAPIDLY SOLIDIFIED ALUMINUM ALLOYS Ph.D. Thesis
Daira Lagzdina 1989 143 p
Avail: Univ. Microfilms Order No. DA9010929

The deformation mechanisms of four rapidly solidified (RS) and hot extruded aluminum alloys were investigated. Al-8.8Fe-3.7Ce (all composition in wt percent) and Al-8.9Fe-6.9Ce alloys produced from RS powders and two Al-8Fe-2Mo alloys one produced from RS ribbons and the other from powders, respectively, were creep tested in the temperature range 250 to 350 C over a range of stresses from 15 to 250 MPa. The Al-8.8Fe-3.7Ce alloy exhibited a diffusional creep region at low stresses and a power law creep region as the stress increased beyond a given transition stress. To investigate the influence of the thermal degradation on the creep behavior of the Al-Fe-Ce alloys, both alloys were heat treated for 165 hours at 450, 500 and 550 C, respectively, and creep tested at 300 C. Both a diffusional and a power law region was observed for both alloys and all heat treatment temperatures. An increase in the diffusional creep rates was observed for the heat treated alloys instead of the expected decrease, confirming that the grain size of the material does not determine the creep rates in the diffusional creep region. Dissert. Abstr.

N91-11097# Oak Ridge National Lab., TN.
DEFECTS IN CLOSE-PACKED METALS AND ALLOYS
M. H. Yoo 30 Aug. 1990 17 p Presented at the Adriatic Research Conference on Defects in Hexagonal Close-Packed Metals, Trieste, Italy, 13-18 Aug. 1990
(Contract DE-AC05-84OR-21400)
(DE90-017502; ORNL/FTR-3721) Avail: NTIS HC/MF A03

The International Conference on Defects in Hexagonal Close-Packed Metals was held to assess our current understanding of the structures and properties of lattice defects in hexagonal close-packed (hcp) materials and to outline future directions of research in this field. Fourteen keynote overview lectures and 18 additional lectures covering more specific topics were presented by researchers from 13 countries. The traveler presented a keynote lecture on deformation twinning in hcp metals and alloys. While in Trieste, the traveler acquired the research highlights on lattice defects and mechanical properties of metals and alloys in Europe. DOE

N91-11098# Lawrence Livermore National Lab., CA.
HIGH-RESOLUTION ELECTRON MICROSCOPY OBSERVATIONS OF ATHERMAL OMEGA PHASE IN Ti-Mo ALLOYS
D. Schryvers (Antwerp Univ., Belgium) and L. E. Tanner 26 Jun. 1990 7 p Presented at the International Conference on Martensitic Phase Transformations (ICOMAT-89), Sydney, Australia, 3-7 Jul. 1989
(Contract W-7405-eng-48)
(DE90-017526; UCRL-JC-104721; CONF-8907114-4) Avail: NTIS HC/MF A02

The commensurate and incommensurate structural configurations underlying the diffuse scattering from athermal omega found in the as-quenched beta phase of Ti with 8 and 15 at. percent Mo were investigated by high resolution electron microscopy. Image interpretations were based on a simulation code developed via observed images of the commensurate omega phase formed by annealing Ti-8 at. percent Mo. Athermal omega is observed as linear structural arrays or strings of less than 1.5 nm length. When commensurate (in quenched Ti-8 at. percent Mo), the strings are confined group of zone axes 111 directions which are parallel to the longitudinal displacement wavevector associated with this phase transformation. However, when the athermal (omega) is incommensurate (in quenched Ti-15 at. percent Mo), the strings tend to deviate from this direction. Atomic models for 1-D and 2-D transition structures are proposed. DOE

N91-11099# Cornell Univ., Ithaca, NY.
SURFACE PHASES AND THEIR INFLUENCE ON METAL-OXIDE INTERFACES
Jack Blakely 1990 10 p
(Contract DE-FG02-87ER-45328)
(DE90-017608; DOE/ER-45328/4) Avail: NTIS HC/MF A02

A scanning tunneling microscope was set up. A UHV system equipped with LEED, electron spectroscopy, and a sulfur beam source was modified and rebuilt. A small portable vacuum system was also constructed for synchrotron x ray diffraction studies of surface structure. Some preliminary results were obtained on the projects detailed in the original proposal. The effects were studied of submonolayers of adsorbed S on the growth and stability of oxide layers. These studies are of central interest to the field of oxide adhesion and high temperature stability of protective oxide scales. Although the work is of a rather fundamental nature it is nevertheless closely connected to real high temperature corrosion situations. The breakdown of adhesion between oxide and metal substrate due to the presence of impurities such as S, ultimately depends on the nature and strength of the bonds between O-Metal, W-Metal and clusters of these elements. DOE

N91-11100# Argonne National Lab., IL. Chemistry Div.
CHEMICAL IDENTIFICATION OF ICOSAHEDRAL STRUCTURE FOR COBALT AND NICKEL CLUSTERS
B. J. Winter, T. D. Klots, E. K. Parks, and S. J. Riley 1990 10 p Presented at the 5th International Symposium on Small Particles and Inorganic Clusters, Konstanz, Fed. Republic of

Germany, 10-14 Sep. 1990 Submitted for publication
(Contract W-31-109-eng-38)
(DE90-017688; CONF-900975-1) Avail: NTIS HC/MF A02

Reactions of bare and hydrogenated cobalt and nickel clusters with ammonia and with water are used to determine cluster geometrical structure. Saturation measurements determine the total number of ammonia binding sites on cluster surfaces. A pattern of minima in the number of such sites is found to correlate with the sequence of closed shells and subshells expected for icosahedral packing in the 50 to 120 atom size range (50 to 200 atom range for hydrogenated clusters). In many cases there are 12 sites at the minima, the number that would be expected for preferred ammonia binding sites on closed subshells of icosahedral clusters. The equilibrium adsorption of a single water molecule provides a sensitive measure of changes in cluster-water binding energy. A pattern of binding energy maxima is found, once again correlating with icosahedral structure, but for clusters having one metal atom more than the closed subshells. In general, hydrogenation enhances the patterns of minima and maxima. These observations are explained in terms of the expected nature of ammonia and water binding to icosahedral clusters. DOE

N91-11101# Ames Lab., IA.
NUCLEAR MAGNETIC RESONANCE SURVEY OF HYDROGEN MOTION AND ELECTRONIC STRUCTURE IN (ALPHA)-PHASE (Nb-Mo)-H ALLOYS
Rodrigo Ibanez-Meier, D. R. Torgeson, and R. G. Barnes 1990 11 p Presented at the International Symposium on Metal-hydrogen Systems, Banff, Alberta, 2-7 Sep. 1990
(Contract W-7405-eng-82)
(DE90-018044; IS-M-639; CONF-9009141-4) Avail: NTIS HC/MF A03

The results of a proton nuclear magnetic resonance (NMR) survey of hydrogen motion and electronic structure in the solid solution alpha phase of niobium rich Nb(1-y)Mo(y)H(x) alloys are reported (y less than or = 0.2, x less than or = 0.2). Measurements of the temperature dependence of the proton spin-lattice relaxation time T sub 1 over the range 20 less than or = T less than or = 800 K were analyzed to yield values of the activation energy (E sub a) and jump attempt frequency nu sub 0 for hydrogen diffusive hopping and of the product T(sub 1e)T = C sub e indicative of the electronic density-of-states at the Fermi level, N(E(sub F)), where T(sub 1e) is that contribution to T(sub 1). The T(sub 1) vs T behavior shows features characteristic of hydrogen in random alloys, reflecting a distribution of E(sub a) and (nu)(sub 0) values. At high temperatures (approx. 500 K), T(sub 1) exhibits anomalous behavior, passing through a maximum and decreasing again at higher temperatures in the same manner found in the Nb--H and (Nb--V)-H systems. DOE

N91-11102# Argonne National Lab., IL.
LIQUID ALLOYS WITH STRONG INTERACTIONS
Marie-Louise Saboungi, D. L. Price, G. K. Johnson, and H. T. J. Reijers (Groningen Rijksuniv., Netherlands) 1990 8 p Presented at the Thermodynamics of Alloys Conference, Barccelona, Spain, 23-26 May 1990 Submitted for publication
(Contract W-31-109-eng-38)
(DE90-017661; CONF-9005270-1) Avail: NTIS HC/MF A02

Liquid alkali metals alloyed with either Pb or Sn show remarkable features in the electronic, thermodynamic, and structural properties at the octet composition and/or the equiatomic composition. A review of these properties will be presented, with special emphasis on the complementarity of information obtained from different experimental results. Recent molecular dynamics simulations of the structure and dynamics of the equiatomic alloys reveal interesting insights into the atomic structure and explain results obtained from inelastic neutron scattering. DOE

N91-11103# Oak Ridge National Lab., TN. Ceramics Div.
THE STABILITY OF IRRADIATION-INDUCED DEFECTS IN NiAl
J. A. Caro (Paul Scherrer Inst., Villigen, Switzerland) and D. F. Pedraza 1990 12 p Presented at the 7th International Conference on Ion Beam Modification of Materials, Knoxville, TN, 9-14 Sep. 1990
(Contracts DE-AC05-84OR-21400; FNSRS-2.866-0.88)
(DE90-017744; CONF-900936-6) Avail: NTIS HC/MF A03

Vacancies, interstitials and antisite defects are produced in intermetallic compounds by irradiation with energetic particles. The manner in which these defects evolve during irradiation may contribute to microstructural changes such as the generation of dislocations, dislocation loops, voids, phase transformations and amorphization. The embedded-atom potentials for nickel and aluminum developed by Foiles, Baskes and Daw were used to calculate the energy of formation of antisite defects, of vacancies, and of various possible interstitial configurations in the B2 NiAl compound. The crowdion in the group of zone axes (111) direction that incorporates an extra nickel atom is found to be the lowest energy interstitial configuration. Using the same potentials, the distance for spontaneous recombination of Frenkel pairs is found to be third nearest neighbor provided the chemical order is maintained. However, if the chemical order of the sites nearest to the interstitial is altered at a bcc cell adjacent to the cell occupied by the vacancy at the cell center, recombination is inhibited in several cases in which the Frenkel pair is found to be stable. The implications of these results for irradiation-induced amorphization are discussed. DOE

N91-11104# Argonne National Lab., IL. Materials Science Div.
MOLECULAR-DYNAMICS STUDY OF GRAIN-BOUNDARY MIGRATION IN METALS
J. M. Rickman, S. R. Phillpot, and D. Wolf May 1990 9 p Presented at the Spring Meeting of the Materials Research Society, San Francisco, CA, 16-17 Apr. 1990 Submitted for publication
(Contracts W-31-109-eng-38; N00014-88-F-0019)
(DE90-017856; CONF-900466-85) Avail: NTIS HC/MF A02

The migration of a (100) Theta = 43.6 degree Sigma 29 twist grain boundary is observed during the course of a molecular-dynamics (MD) simulation. The migration is investigated by calculating changes in the planar structure factor S sub p (k), the orientation of interparticle bonds in the migrating plane, and the motion of the center of mass planes near the grain boundary. It is found that migration is accompanied by sliding, and each migration step consists of a series of local bond rearrangements. It appears that, as a precursor to migration, Frenkel-like defects are produced at the grain boundary. DOE

N91-11105# Argonne National Lab., IL.
RELATIONSHIP OF MICROSTRUCTURE AND TENSILE PROPERTIES FOR NEUTRON-IRRADIATED VANADIUM ALLOYS
Ben A. Loomis and Dale L. Smith 1990 28 p Presented at the 15th Symposium on Effects of Radiation on Materials, Nashville, TN, 17-21 Jun. 1990
(Contract W-31-109-eng-38)
(DE90-017863; CONF-900623-19) Avail: NTIS HC/MF A03

The microstructures in V-15Cr-5Ti, V-10Cr-5RTi, V-3Ti-1Si, V-15Ti-7.5Cr, and V-20Ti alloys were examined by transmission electron microscopy after neutron irradiation at 600 C to 21 to 84 atom displacements per atom in the Materials Open Test Assembly of the Fast Flux Test Facility. The microstructures in these irradiated alloys were analyzed to determine the radiation-produced dislocation density, precipitate number density and size, and void number density and size. The results of these analyses were used to compute increases in yield stress and swelling of the irradiated alloys. The computed increase in yield stress was compared with the increase in yield stress determined from tensile tests on these irradiated alloys. This comparison made it possible to evaluate the influence of alloy composition on the evolution of radiation-damaged microstructures and the resulting tensile properties. DOE

N91-11106# Japan Atomic Energy Research Inst., Tokyo.
EFFECTS OF ENVIRONMENT AND AGING ON CREEP PROPERTIES OF ALLOY 800H
Katsutoshi Watanabe, Hirokazu Tsuji, Hajime Nakajima, Tatsuhiko Tanabe, Keijiro Hiraga, Yoshikazu Sakai, and Haruki Shiraishi

(National Research Inst. for Metals, Tokyo, Japan) Mar. 1990 38 p In JAPANESE; ENGLISH summary
(DE90-520207; JAERI-M-90-061) Avail: NTIS (US Sales Only) HC/MF A03

A series of creep tests were conducted at temperatures ranging from 750 to 900 C on a Fe-base heat-resistant alloy, Alloy 800H, which would be used for the cladding material of the neutron absorber rods of the High-Temperature Engineering Test Reactor. The maximum rupture life was 3552 h. In those tests the effects of environment and aging on its creep properties were studied. The obtained results are as follows: (1) No significant difference in creep rupture strength, creep ductility and creep deformation resistance was observed between in high temperature gas-cooled reactor (HTGR) helium and in air. The creep rupture strength in HTGR helium and in air had no difference from that obtained in pure argon with a remote controlled creep testing machine which would be used for the evaluation of irradiation effect. (2) There was no notable difference in creep rupture strength, creep ductility and creep deformation resistance among three different heat treated materials, i.e., solution annealed at 1120 C for 1 h, solution annealed at 1120 C for 1 h and then aged at 700 C for 530 h, and solution annealed at 1120 C for 1 h and then aged at 1050 C for 3 h. (3) The creep rupture strength obtained in the present work was situated within the scatter range of the available data in literature. DOE

N91-11107# Rolls-Royce Ltd., Derby (England).
INFLUENCE OF HEAT TREATMENT ON MICROSTRUCTURE AND PROPERTIES OF AN ADVANCED HIGH TEMPERATURE TITANIUM ALLOY
M. A. Daeubler (Motoren- und Turbinen-Union Muenchen G.m.b.H., Germany, F.R.), N. A. Walker, and M. T. Cope 22 Nov. 1989 6 p Presented at EUROMAT 1989, European Conference on Advanced Materials and Processes, Aachen, Fed. Republic of Germany, 22-24 Nov. 1989
(PNR-90689; ETN-90-97932) Copyright Avail: NTIS HC/MF A02

The influence of the quench rate, aging treatment and re-solution heat treatment on the tensile behavior at 20, 600, and 600 C creep behavior of IMI 834 disc material is described. IMI 834 is a near alpha alloy with applications in aircraft engines as a compressor disc and blade material. IMI 834 offers considerable benefits over previous coarse grained beta processed alloys IMI 685 and IMI 829 in terms of strength, low cycle fatigue and creep resistance. The alloy is designed to be processed within the alpha plus beta phase field, for optimizing the balance of mechanical properties through microstructural modifications. ESA

N91-11108# Brookhaven National Lab., Upton, NY.
DETERMINATION OF HYDROGEN (DEUTERIUM) DENSITY PROFILES IN THIN METAL FILMS AND MULTILAYERS BY NEUTRON REFLECTION
C. F. Majkrzak, S. Satija, D. A. Neumann, J. J. Rush, D. Lashmore, C. Johnson, J. Bradshaw, L. Passell (Optoline Associates, Andover, MA.), and R. DiNardo 1990 7 p Presented at the Fall Meeting of the Materials Research Society, Boston, MA, 26 Nov. - 1 Dec. 1990
(Contract DE-AC02-76CH-00016)
(DE90-007150; BNL-43758; CONF-901105-1) Avail: NTIS HC/MF A02

The density of hydrogen in thin films or multilayers of metal hydrides can be inferred from an expansion of the host lattice as measured by conventional x ray diffraction techniques. However, because hydrogen and deuterium have scattering lengths for neutrons that are comparable to those of most metal nuclei, unlike the corresponding case for x ray atomic scattering amplitudes, the hydrogen density profile normal to the surface of a flat, thin film can be determined directly from neutron reflectivity measurements. The hydrogen (deuterium) density modulation in an artificial superlattice along the growth direction can also be determined in this manner. The thin film or multilayer host metal material need not even be crystalline. Furthermore, because relatively large, flat single crystal substrates such as Si or quartz are nearly transparent to neutrons, the substrate can serve as the incident medium and the reflectivities of films or multilayers in contact with liquid solutions can be obtained. Thus, in situ studies employing active electrochemical cells, for example, can be performed. In addition to discussing the sensitivity of the method, the results of some neutron reflectivity experiments on metal multilayers and films, electrolytically loaded in situ with deuterium, are reported. DOE

N91-11109# Argonne National Lab., IL. Materials Science Div.
LASER RAMAN SPECTROSCOPY FOR IN-SITU ANALYSIS OF CORROSION FILMS ON METALS
Carlos A. Melendres Aug. 1990 34 p Presented at the 178th Meeting of the Electrochemical Society, Seattle, WA, 14-19 Oct. 1990
(Contract W-31-109-eng-38)
(DE90-017822; CONF-901073-7) Avail: NTIS HC/MF A03

The principles of laser Raman spectroscopy (LRS) are discussed, with particular reference to its applications to the study of corrosion and passivation phenomena in metals in aqueous solution environments. Results of studies on corrosion inhibition by organic compounds and passivity breakdown on iron are presented. The advantages and limitation of the LRS technique are pointed out. New directions toward corrosion studies in high temperature high pressure systems as well as the development of a technique for near monolayer detection sensitivity are discussed. DOE

N91-11110# Sandia National Labs., Albuquerque, NM.
SOLDERABILITY OF ENVIRONMENTALLY EXPOSED Sn-PLATED SURFACES
F. M. Hosking and N. R. Sorensen 1990 14 p Presented at the 3rd Electronic Materials and Processing Congress, San Francisco, CA, 20-24 Aug. 1990
(Contract DE-AC04-76DP-00789)
(DE91-000035; SAND-90-2108C; CONF-900854-1) Avail: NTIS HC/MF A03

Solderability of Class II environmentally exposed Ni-Sn plated Cu substrates was evaluated with 60Sn-40Pb solder. Tin thicknesses were 10, 50, and 150 (mu)in. The 10 (mu)in. plating gave the smallest solder meniscus rise. A general decrease in contact angle, or increase in wettability, was observed with increasing Sn plating. The environmental exposures retarded the wetting rate and increased the time to maximum wetting, particularly with only 10 (mu)in. of Sn. Although the solderability of the 50 and 150 (mu)in. surfaces were not significantly affected by the test conditions, an intermediate plating thickness of 100 (mu)in. is preferred for processing flexibility. DOE

N91-11111# Sandia National Labs., Albuquerque, NM.
MICROSTRUCTURES OF CUBIC Al2O3 PRECIPITATES IN OXYGEN-IMPLANTED ALUMINUM
D. M. Follstaedt, S. M. Myers, and R. J. Bourcier 1990 11 p Presented at the 7th International Conference on Ion Beam Modification of Materials, Knoxville, TN, 9-14 Sep. 1990
(Contract DE-AC04-76DP-00789)
(DE91-000038; SAND-90-0993C; CONF-900936-7) Avail: NTIS HC/MF A03

The microstructure of Al ion-implanted at room temperature with 17 at. percent 0 has been characterized with transition electron microscopy (TEM). The alloy has extremely small (1.5 to 3.5 nm) oxide precipitates whose crystal structure is interpreted to be a disordered version of (gamma)-Al2O3 having a fcc lattice of O(sup 2(minus)) ions with Al(sup 3+) ions in random interstitial sites. The small sizes can account for the exceptionally high strength of as-implanted alloys: 2500 to 3300 MPa. Larger precipitates are found when the alloy is annealed 1/2 hour at 550 C, which is consistent with its somewhat lower strength: 800 to 1600 MPa. DOE

N91-11112# Ames Lab., IA.
PHYSICAL METALLURGY AND MAGNETIC BEHAVIOR OF Cd STABILIZED bcc (BETA) Gd ALLOYS M.S. Thesis - Iowa State Univ.
Jinke Tang 21 Sep. 1990 53 p
(Contract W-7405-eng-82)
(DE91-000196; IS-T-1474) Avail: NTIS HC/MF A04

As a continuation of the research on bcc Gd-Mg alloy system by Herchenroeder and Gschneidner, the metastable bcc Gd-Cd alloys were studied with the emphasis on their metallurgical and magnetic properties. An essentially single phase alloy could be retained for Cd concentrations from 15 at. percent Cd to 19 at. percent Cd, which is in the vicinity of the eutectoid composition of (beta)Gd in the Gd-Cd system. The lattice constants obtained for these alloys were used to determine the lattice constant of pure bcc Gd by extrapolation to 0 at. percent Cd. Good agreement between this extrapolated value and that obtained from Gd-Mg alloys by using the same method suggested the validity of such an extrapolation method. Thermal stability of these metastable bcc Gd-Cd alloys was examined by using differential thermal analysis DOE

N91-11113# California Univ., Berkeley. Lawrence Berkeley Lab. Materials and Chemical Sciences Div.
A STUDY OF CHROMIUM CARBIDE PRECIPITATION AT INTERPHASE BOUNDARIES IN STAINLESS STEEL WELDS Ph.D. Thesis
Christopher Fowler Willis Apr. 1990 59 p
(Contracts DE-AC03-76SF-00098; W-7405-eng-48)
(DE91-000360; LBL-29311) Avail: NTIS HC/MF A04

Sensitization is a deleterious process which can occur in stainless steels. It is caused by grain boundary or phase boundary precipitation of chromium carbides and the resulting formation of a chromium depleted zone adjacent to these boundaries. The carbides in question actually have the composition (Cr,Fe)23C6 (usually written M23C6), and precipitate in the temperature range 450 to 900 C. Since a minimum chromium content is required to maintain the passive film necessary for resistance to electrochemical attack, the result of chromium depletion is that the steel becomes sensitized to possible intergranular corrosion. Sensitization often occurs as a result of welding operations. The material close to the fusion line reaches temperatures within the sensitization range. This region is called the heat affected zone (HAZ). Since many welds are multi-pass welds, the actual weld bead of one pass may lie in the heat affected zone of the next pass. The weld bead of the first pass might therefore be sensitized. Furthermore there are applications where welds will be exposed to sensitizing temperatures for very long periods of time, such as welded labels on retrievable nuclear waste containers. For these reasons the sensitization behavior of the actual weld-bead microstructures must be understood. It has been known for many years that duplex stainless steels (steels with both ferrite and austenite phases present at room temperature) have superior resistance to intergranular corrosion. A model is proposed to explain the sensitization behavior of these alloys. The validity is tested of aspects of this model using transmission electron microscopy and further understanding of the sensitization process in duplex stainless steel welds. DOE

N91-11114# Los Alamos National Lab., NM. Chemical and Laser Sciences Div.
THE REACTION OF VAPOR-DEPOSITED Al WITH Cu OXIDES
T. N. Taylor and J. A. Martin 1990 21 p Presented at the 37th National American Vacuum Society Symposium, Toronto, Ontario, 8-12 Oct. 1990
(Contract W-7405-eng-36)
(DE91-000367; LA-UR-90-3048; CONF-901035-1) Avail: NTIS HC/MF A03

Interfaces formed by controlled deposition of Al on Cu oxides at 300 K were characterized using Auger electron spectroscopy (AES) and x ray photoelectron spectroscopy (XPS). When Al is deposited onto a thin oxide grown on Cu(110) by atmospheric exposure, it completely scavenges the oxygen from the substrate material, increasing the O(1s) binding energy by 2.0 eV to give the value found for atmospheric oxidation of a thin Al film. Similar oxygen behavior is seen for Al deposition on sputter deposited CuO with an enriched oxygen surface region, where multilayers of Al erase the shakeup satellites in the Cu(2p) region of the XPS spectrum to give features like those exhibited by Cu2O or metallic Cu. Having calibrated the fluence of the Al source with Rutherford backscattering spectrometry, the attenuation of the Cu 2p sub 1/2 satellite after approximately one monolayer of Al deposition is associated with the removal of oxygen from the top 20A of the CuO. Approximately 7 to 8 equivalent monolayers of Al are converted to an oxide in the initial rapid reaction process. Further deposition leads to progressive development of the metallic Al signature in both the XPS and AES spectra. These measurements clearly demonstrate the dominant role played by Al, a strong oxide former, when it is placed in intimate contact with the distinctively weaker Cu oxide. DOE

N91-11115# Los Alamos National Lab., NM. Materials Science Div.
MICROWAVE SINTERING OF NANOCRYSTALLINE TiO2
J. A. Eastman, Y. X. Liao (Argonne National Lab., IL), K. E. Sickafus, J. D. Katz, S. G. Boeke, R. D. Blake, C. R. Evans, and R. B. Schwarz Apr. 1990 7 p Presented at the Spring Meeting of the Materials Research Society, San Francisco, CA, 16-21 Apr. 1990 Submitted for publication
(Contracts W-7405-eng-36; W-31-109-eng-38)
(DE91-000375; LA-UR-90-3160; CONF-900466-89) Avail: NTIS HC/MF A02

Nanocrystalline TiO2 compacts having initial approximate mean grain sizes of 14 nm and approximate green densities of 70 percent of theoretical were sintered by short time exposure in a 2.45 GHz microwave cavity to maximum temperatures of 800, 1000 or 1200 C. Sample densities were measured before and after exposure to microwaves using Archimede's method. Transmission electron microscopy and x ray diffraction were utilized to monitor grain growth and phase changes. Rutherford backscattering was used to monitor any changes in oxygen stoichiometry. The results indicate that enhanced densification behavior is obtained for microwave sintered samples relative to samples sintered using conventional pressureless sintering techniques. DOE

N91-11116# Universiteit Twente, Enschede (Netherlands).
PROJECTIVE SCALES AGAINST HIGH TEMPERATURE CORROSION Ph.D. Thesis
Erik Alexander Polman 1989 100 p
(ETN-90-97770) Avail: NTIS HC/MF A05

Corrosion mechanisms for mixed oxidizing/sulfidizing environments are summarized with particular reference to coal conversion systems. Application methods and general properties of a few protective coatings are described. Research on and results for the following are reported: the use of various coatings for the protection of high temperature stainless steels in sulphidizing environments; the high temperature corrosion and mechanical properties of protective scales on Incoloy 800H and the influence of preoxidation and ion implantation; grain boundary segregation and diffusion in chromia scales; calculations on grain boundary segregation and surface energies of chromia; oxidation kinetics of chromium and morphological phenomena; measurements on the electrochemical conductivity of oxide scales. ESA

N91-11117# Office National d'Etudes et de Recherches Aerospatiales, Paris (France).
DETERMINATION OF PAIR POTENTIALS BY ANALYSIS OF DIFFUSE SCATTERING OF THE LOCAL FIELD IN Pd3V AND Ni3V Ph.D. Thesis - Paris VII Univ.
Francine Solal Dec. 1989 97 p In FRENCH; ENGLISH summary Report will also be announced as translation (ESA-TT-1228)
(ONERA-NT-1989-7; ISSN-0078-3781; ETN-90-98016) Avail: NTIS HC/MF A05

Neutron and x ray diffuse scattering experiments on Pd3V were performed. A change is found in local order between the disordered

state characterized by diffuse intensity maxima at (100) points of the reciprocal space and the ordered phase DO22 built on (1 1/2 0) concentration waves on the fcc lattice. The Ni3V alloy is studied and no such change appears in the local order. The order energy of substitutional alloys on a fixed underlying lattice is described by an Ising Hamiltonian. At intermediate temperatures, approximate statistical models describe order properties. The Cluster Variation Method (CVM) reveals the existence of two regimes, corresponding to Pd3V and Ni3V. In order to account quantitatively for experimental data, a CVM approximation including pair interactions up to the fourth neighbor, in agreement with an electronic structure calculations, was used. A set of such interactions for both alloy is proposed. ESA

N91-11251# Royal Aircraft Establishment, Farnborough (England). Materials and Structures Dept.
TEXTURE ANALYSIS OF 2090-T8E41 ALUMINUM-LITHIUM ALLOY SHEET: ANNEX
A. W. Bowen *In* AGARD, Short-Crack Growth Behaviour in Various Aircraft Materials Aug. 1990 5 p (For primary document see N91-11240 02-39)
Copyright Avail: NTIS HC/MF A09; Non-NATO Nationals requests available only from AGARD/Scientific Publications Executive

27 NONMETALLIC MATERIALS

Includes physical, chemical, and mechanical properties of plastics, elastomers, lubricants, polymers, textiles, adhesives, and ceramic materials.

For composite materials see *24 Composite Materials.*

N91-11118*# National Aeronautics and Space Administration. Langley Research Center, Hampton, VA.
STUDIES OF MOLECULAR PROPERTIES OF POLYMERIC MATERIALS Final Report, period ending 31 Aug. 1990
W. L. Harries (Old Dominion Univ., Norfolk, VA.), Sheila Ann T. Long, and Edward R. Long, Jr. May 1990 169 p
(Contract NCC1-90)
(NASA-TM-101854; NAS 1.15:101854; PTR-90-3) Avail: NTIS HC/MF A08 CSCL 11B

Aerospace environment effects (high energy electrons, thermal cycling, atomic oxygen, and aircraft fluids) on polymeric and composite materials considered for structural use in spacecraft and advanced aircraft are examined. These materials include Mylar, Ultem, and Kapton. In addition to providing information on the behavior of the materials, attempts are made to relate the measurements to the molecular processes occurring in the material. A summary and overview of the technical aspects are given along with a list of the papers that resulted from the studies. The actual papers are included in the appendices and a glossary of technical terms and definitions is included in the front matter. M.G.

N91-11119 Illinois Univ., Chicago.
MICROMECHANICS OF SEMI-BRITTLE CERAMICS Ph.D. Thesis
Aleksandar L. Stojimirovic 1989 162 p
Avail: Univ. Microfilms Order No. DA9015767

The formulation of analytical damage mechanics models describing the overall behavior of ceramics materials is studied. The establishment of a micromechanically based analytical model for an MgO polycrystalline specimen subjected to quasi-static tension is described. The inelastic strain is attributed to the plastic slip within the shear bands in the crystal, and the crack opening displacement of Zener-Stroh cracks along the grain boundaries. A micromechanical model is addressed for the time-dependent deformation of polycrystalline alumina. The inelastic strain associated with the steady-state creep phase is attributed to the dominant micro mechanism of deformation, the grain boundary sliding and subsequent propagation of small initially existing cracks. The strategy employed in formulation of the analytical models consists of two steps: analytical description of the dominant mechanism of the irreversible change of the microstructure, and homogenization (averaging) of these micromechanical models into a relations mapping macro-stresses on macro strains.
Dissert. Abstr.

N91-11120# Japan Atomic Energy Research Inst., Tokyo. Dept. of Development.
STUDY ON RADIATION-INDUCED DETERIORATION OF GREASE AT HIGH TEMPERATURE. PART 1: TEST METHOD ON THERMAL AGING
Takao Soda, Hiroshi Nakanishi, Tamio Akada, Mitsuo Hirohama, Tetsuya Yagi (Matsumura Oil Research Corp., Japan), Kazuo Arakawa, Tsuneo Sasuga, Miyuki Hagiwara, and Tadao Seguchi Feb. 1990 28 p In JAPANESE; ENGLISH summary
(DE90-508070; JAERI-M-90-010) Avail: NTIS (US Sales Only) HC/MF A03

As a series of the studies on radiation-induced deterioration of grease at high temperature, a test method is persented of thermal aging of greases which can be applied to the test of greases under the gamma irradiation at elevated temperatures. The grease properties (penetration, free acid, oil separation) are affected by an amount of base oil evaporated from the grease at high temperature. The base oil evaporation depends on depth of a vessel and thickness of the greases in the vessel for test. As results of the investigation of the evaporation of oil in relation to the shape the vessel and the thickness of the grease, the amount of evaporated oil when 17 mm deep glass vessel and 6 mm thick grease was equivalent to that observed by a test conducted using a JIS K-2220, B method. It was found that the sample vessel need to be put on the lid when the several kinds of grease samples are heated in the same oven at same time. DOE

N91-11121*# National Aeronautics and Space Administration. John F. Kennedy Space Center, Cocoa Beach, FL.
EVALUATION OF THERMAL SPRAYED METALLIC COATINGS FOR USE ON THE STRUCTURES AT LAUNCH COMPLEX 39
Peter J. Welch Jan. 1990 13 p Original contains color illustrations
(NASA-TM-103807; MTB-1058-89; NAS 1.15:103807) Avail: NTIS HC/MF A03; 4 functional color pages CSCL 11C

The current status of the evaluation program is presented. The objective was to evaluate the applicability of Thermal Sprayed Coatings (TSC) to protect the structures in the high temperature acid environment produced by exhaust of the Solid Rocket Boosters during the launches of the Shuttle Transportation System. Only the relatively low cost aluminum TSC which provides some cathodic protection for steel appears to be a practical candidate for further investigation. Author

N91-11122# Oak Ridge National Lab., TN.
MECHANICAL BEHAVIOR OF CERAMICS AND COMPOSITES Foreign Trip Report
A. F. Rowcliffe Sep. 1990 6 p
(Contract DE-AC05-84OR-21400)
(DE90-017311; ORNL/FTR-3713) Avail: NTIS HC/MF A02

The ceramic programs in the Royal Institute of Technology represent a new initiative in the area of processing and mechanical behavior of ceramics and composite materials. This venture is still growing in terms of equipment and personnel and is currently funded at approx. $1.0 M/year. Several projects are related to a new investigation at ORNL to assess the radiation performance of composite materials and their possible application in fusion energy systems. Theoretical and experimental investigations of fiber toughening mechanisms were reviewed, including the application of nanoindentation techniques. The stability of Nicalon fibers was discussed, and sources of alternative SiC fibers from European manufacturers identified. DOE

N91-11123# Oak Ridge National Lab., TN.
ANALYSIS AND PREDICTION OF THERMAL PROPERTIES OF MESOPHASES AND CRYSTALS BY CALORIMETRY AND SUPERCOMPUTERS
Bernhard Wunderlich (Tennessee Univ., Knoxville.) 1990 27 p Presented at the Association for the Progress of New Chemistry

Conference, Tokyo, Japan, 6-9 Nov. 1990
(Contract DE-AC05-84OR-21400; NSF DMR-88-18412)
(DE90-015538; CONF-901177-1) Avail: NTIS HC/MF A03

Thermal analysis as developed in the ATHAS, the Advanced THermal Analysis System, has led in the last 10 years to the description of about 150 polymers. The discussion of the entropy and the detailed study of the heat capacities has resulted in understanding of disorder and motion in many polymers, and has led to the development of theory-backed and empirical prediction schemes of the thermodynamic functions. The conformationally disordered state (condis crystalline state) was identified and shown to be different from liquid or plastic crystals. Example polymers range from the flexible polyethylene, polybutadienes, PTFE and nylons to the more rigid polyparaxylylene and aromatic polyesters and polyamides. The conformational disorder could be shown to be introduced either gradually or at a sharp transition. To get more insight, molecular dynamics simulation on supercomputers was used. At present crystals with over 6000 chain atoms can be simulated for times up to 30 ps. The crystal is normally 100 chain atoms long (crystallographic c-axis) and data were predicted for a variety of temperatures for (1) single chains, (2) chains included in one rigid ring of nearest neighbors (7 chains), and a chain surrounded by (3) one, (4) two, and (5) three mobile rings of nearest neighbors, held at constant volume by an additional rigid ring (19, 37, and 61 chains, respectively), as well as (6) without a rigid ring of chains (37 mobile chains). The computed heat capacity effect agrees with the simulation. Rotational isomers are altered by the intermolecular forces. The lifetime of defects that were proposed based on molecular mechanics calculations were determined. DOE

N91-11124# Wisconsin Univ., Madison.
MORPHOLOGICAL ANALYSIS OF IONOMERS Progress Report, 1 Apr. 1989 - 31 Mar. 1990
1990 6 p
(Contract DE-FG02-88ER-45370)
(DE90-017611; DOE/ER-45370/3) Avail: NTIS HC/MF A02

Topics covered are: SANS of Telechelic Ionomers; SANS of Sulfonated Polyurethanes; Effect of Matrix Polarity and Ambient Aging on the Morphology of Sulfonated Polyurethane Ionomers; Adhesive Sphere Model for Analysis of SAXS Data from Ionomers; Comparison of Structure-Property Relationships in Carboxylated and Sulfonated Polyurethane Ionomers; Development of a Liquid-like Hard Sphere Model for Deformed Ionomer Samples; and Polymer Synthesis for Proposed Research. DOE

N91-11125# Oak Ridge National Lab., TN.
CHEMICALLY VAPOR DEPOSITED DIAMOND FILMS Foreign Trip Report
Robert E. Clausing and Lee Heatherly, Jr. 22 Sep. 1990 17 p
(Contract DE-AC05-84OR-21400)
(DE91-000384; ORNL/FTR-3751) Avail: NTIS HC/MF A03

The NATO-ASI on Diamond and Diamond-Like Films and Coatings was an opportunity for us to learn the latest research results from ongoing programs in the leading laboratories of the world and relate. Specific examples are given. The meeting format provided an ideal environment to meet and interact with our international counterparts. New opportunities for collaboration were identified. A panel discussion at the end of the meeting addressed the needs and opportunities in the synthesis of CVD diamond. The key scientific needs are those related to modeling the nucleation and growth processes and to elucidation of the critical roles of atomic hydrogen and the mechanisms of carbon addition to the growing surfaces. The development and more extensive use of in situ diagnostics for both surface and gas phases are important for solving these issues. The more immediate practical questions concern the identification of the growth rate limiting steps, the relation of growth parameters to the resulting film structure, and the dependence of properties on structure. DOE

28 PROPELLANTS AND FUELS

Includes rocket propellants, igniters, and oxidizers; their storage and handling procedures; and aircraft fuels.

For related information see also *07 Aircraft Propulsion and Power, 20 Spacecraft Propulsion and Power,* and *44 Energy Production and Conversion.*

N91-11126# Geo-Centers, Inc., Lake Hopatcong, NJ.
STABILITY OF LIQUID PROPELLANTS UNDER LONG-TERM STORAGE Technical Report, Jul. 1987 - Sep. 1988
Stanley P. Griff, Gerald Doyle, Edward Turngren, and William P. Seals Jun. 1990 45 p
(Contract DAAA21-86-C-0101)
(AD-A223934; ARAED-CR-90003) Avail: NTIS HC/MF A03
CSCL 19/1

The commitment of the army to replace solid propellants with liquid propellants in some applications requires extensive characterization of the propellant system. This study, as part of the program to establish fail-safe criteria, deals with the effect of temperature and transition metal impurities on the stability of Liquid Propellant 1846 (LP 1846). In order to determine these effects on the stability of LP 1846, analytical methods were developed to compare the propellant before and after exposure, and an apparatus was designed to monitor the pressure build-up as a function time. GRA

N91-11127# Department of Energy, Washington, DC.
ASSESSMENT OF COSTS AND BENEFITS OF FLEXIBLE AND ALTERNATIVE FUEL USE IN THE US TRANSPORTATION SECTOR: VEHICLE AND FUEL DISTRIBUTION REQUIREMENTS Technical Report No. 4
Aug. 1990 54 p
(DE90-014847; DOE/PE-0095P) Avail: NTIS HC/MF A04

Alternatives to conventional motor gasoline and diesel fuel are being researched for energy security and environmental reasons. The three fuels with the most potential to displace a significant portion (e.g., 1 million barrels per day) of conventional fuels over the next 10 to 15 years are methanol (either neat or blended with gasoline), compressed natural gas (CNG), and electricity. Each has vehicle fuel characteristics very different from gasoline or diesel fuel that require changes to existing vehicle designs and fuel distribution systems. For example, although methanol is a liquid like gasoline, it requires nearly twice the storage space in terminals, delivery trucks, refueling stations, and vehicles. It is also more corrosive than gasoline, which can create materials compatibility problems in current highway vehicles and petroleum product distribution equipment. CNG (a gas, not a liquid) must be distributed by natural gas pipelines rather than petroleum pipelines or trucks. Service stations will need equipment to compress the gas sufficiently in vehicle storage cylinders to make it a useful vehicle fuel. Even compressed, CNG requires approximately 6 times the storage volume of gasoline on an energy equivalent basis. A substantial storage battery pack is required to use electricity as a vehicle fuel. For example, a 4-passenger electric vehicle (EV) with nickel-iron batteries may contain a battery pack weighing 1100 lb (499 kg). Further, EV's must be plugged in to an electric outlet to be fueled. This report is a synthesis of these DOE-sponsored studies. It characterizes methanol, natural gas, and electric vehicles, discusses their costs and displacement potential, identified distribution system changes and costs for each fuel, and finally, compares and evaluates the three sets of infrastructure changes and costs. DOE

N91-11128# Idaho National Engineering Lab., Idaho Falls.
THREE-DIMENSIONAL FLUID FLOW IN JFTOT (JET FUEL THERMAL OXIDATION TESTER)
C. H. Oh, B. J. Merrill, and R. P. Wadkins 1990 23 p Presented at the International Symposium on Gas-Liquid Two-Phase Flows in Conjunction with the Winter Annual Meeting of the ASME, Dallas, TX, 25-30 Nov. 1990
(Contract DE-AC07-76ID-01570)
(DE90-010929; EGG-M-90041; CONF-901109-3) Avail: NTIS HC/MF A03

This paper describes flow and temperature distributions in the Jet Fuel Thermal Oxidation Tester (JFTOT), a standard qualification apparatus for examining thermal stability of jet fuels. A three-dimensional numerical analysis is presented in this paper performed with the KIVA code. This work represents a preliminary attempt to calibrate a Computational Fluid Dynamics/Chemistry (CFDC) model using existing data from a modified JFTOT. Due to the limited amount of data, the deposition model used in this study is a global type Arrhenius relationship. Upon the findings of future JFTOT experiments, the relevant parameters to mass transfer, heat transfer, and fluid dynamics can be combined to define the thermal stability of jet fuel with a higher degree of accuracy. DOE

N91-11129# New Energy Development Organization, Tokyo (Japan).
CO-RESEARCHES WITH RESEARCHERS OF ALTERNATIVE ENERGY OF PETROLEUM IN EC COUNTRIES
Mar. 1990 110 p In JAPANESE and ENGLISH
(DE91-701466; NEDO-P-8951) Avail: NTIS (US Sales Only) HC/MF A06

Here are the results of information exchanges and co-researches with researchers of alternative energy of petroleum in EC countries. In the research on gas turbine parts applying the explosion shock sintering process, a solid compound was synthesized from the mixed fine particles of Ti and B at 10 GPA. In coal liquefaction, solid and liquid were economically separated with a candle filter. In the coal liquefaction plant in Bergbau Forshung, it became possible to predict hydrobehaviors, and a pilot plant of 200 tons/day is being operated in Bottrop. Circumstances of 1 ton/day PSU of NEDOL liquefaction, universities and national laboratories are also explained. In the research on functional materials, high molecular and electrolyte thick aqueous solution of cellulose system formed nematic liquid crystals. Research results on the InGaAs type high electron mobility transistor are explained, too. In fused carbonate fuel cells, dissolution, diffusion and re-precipitation of the cathode material NiO cause problems; and as a measure against these problems, thermodynamic fundamental researches were carried out. DOE

N91-11130# New Energy Development Organization, Tokyo (Japan).
INTERCHANGE OF RESEARCHERS ON ALTERNATIVE ENERGY OF PETROLEUM IN EC COUNTRIES
Mar. 1990 26 p In JAPANESE and ENGLISH
(DE91-701468; NEDO-P-8953) Avail: NTIS (US Sales Only) HC/MF A03

Researchers on alternative energy of petroleum in EC countries were invited and informations were exchanged between the researchers and research organizations in Japan. Geothermal power generation in Japan is 250 MW. In the Hijiori high temperature rock project, the depth of the well is about 2 km, and the temperature at the bottom of the well is more than 250 C; and press fit and circulation experiments of water are being carried out. In this project development of a heat resisting packer is a subject to reform channels for the improvement of recovery percentage. In the Tohoku University's project in Higashi Hachimantai, design research on artificial cracks for heat extraction is being pushed forward. While geothermal resources in Japan is of high temperature (more than 200 C), those in Europe are deeper in the underground and of low temperature (less than 200 C), and mutual and close technical co-operations between Japan and European countries are hoped for. In the research on the amorphous semiconductors for photovoltaic power generation, importance is put on the efficiency and the development of crystallization method. Researches are also made on the solar cells of hetero structure with high capacity of light gathering, the SiC electron emission elements, and the large-area cells of high efficiency. The growth mechanism of multicrystal semiconductors was studied. Multilayer structures were deposited. And concerning the efficiency, factors which limit cell performances have been clarified. DOE

N91-11131# Sandia National Labs., Albuquerque, NM. Explosive Projects and Diagnostics Div.
ATTENUATION STUDIES OF BOOSTER-ROCKET PROPELLANTS AND THEIR SIMULANTS
Larry J. Weirick Aug. 1990 20 p
(Contract DE-AC04-76DP-00789)
(DE91-000098; SAND-89-2656) Avail: NTIS HC/MF A03

A series of impact experiments on a composite propellant, an energetic propellant, and their simulants was recently completed using a light-gas gun. Previous experiments were done to obtain Hugoniot data, to investigate the pressure threshold at which a reaction occurs, and to measure spall damage at various impact velocities. The present studies measured the attenuation of shock waves in these materials, completing the shock characterization needed for material modeling. An initial impulse of 2.0 GPa magnitude and approx. 0.6 microsec duration was imposed upon samples of various thicknesses. VISAR was used to measure the free surface velocity at the back of the samples; these data were used to generate a curve of shock wave attenuation versus sample thickness for each material. Results showed that all four materials attenuated the shock wave very similarly. Material thicknesses of 3.0, 7.62, 12.7, and 19.0 mm attenuated the shock wave approx. 16, 33, 50, and 66 percent respectively. DOE

29 MATERIALS PROCESSING

Includes space-based development of products and processes for commercial applications.
For biological materials see *55 Space Biology*.

No abstracts in this category.

31 ENGINEERING (GENERAL)

Includes vacuum technology; control engineering; display engineering; cryogenics; and fire prevention.

N91-11132# Federal Railroad Administration, Washington, DC. Office of Research and Development.
INDUSTRY PERSPECTIVE ON MAGLEV Final Report
Jun. 1990 27 p Prepared in cooperation with Little (Arthur D.), Inc., Cambridge, MA
(PB90-252305; DOT/FRA/ORD-90/07) Avail: NTIS HC/MF A03 CSCL 13H

Most of the recent discussion and proposed legislation concerning Maglev (magnetic levitation) assumes that U.S. industry has a strong interest in Maglev and will be willing to take a proactive, cost-sharing role in the development of Maglev systems. As part of the preliminary feasibility studies on Maglev, the Federal Railroad Administration obtained the perceptions of several major U.S. corporations and identified their interest in a Maglev program, their willingness to participate, and any potential barriers to their participation. The industry perspectives were obtained through an independent and unbiased external study that included in-depth interviews with senior executives from 22 major U.S. corporations. The study, conducted during April and May 1990, was primarily directed at the development and implementation of a next-generation leapfrog Maglev system in the United States. GRA

N91-11133# Office National d'Etudes et de Recherches Aerospatiales, Paris (France).
STUDY OF AN ELECTROTHERMAL DE-ICER: NUMERICAL SIMULATION AND MEASUREMENT OF THE SKIN TEMPERATURE BY INFRARED TECHNIQUE IN AN ICING WIND TUNNEL Ph.D. Thesis - Clermont-Ferrand Univ.
Robert Henry Dec. 1989 183 p In FRENCH; ENGLISH summary Report will also be announced as translation

(ESA-TT-1231)
(ONERA-NT-1989-10; ISSN-0078-3781; ETN-90-98019) Avail: NTIS HC/MF A09

As part of the research on aircraft icing protection, a numerical simulation of an electrothermal deicer for a helicopter was developed. For validation, it was necessary to measure the skin temperature of the blade, during the deicing process in real conditions. The infrared techniques was used. The measurements required calibration at low temperatures, the determination of the different emissivity factors and the calculation of the icing cloud transmission factor. Infrared pictures were recorded and digitized to obtain the time variation of the skin temperature during a dry air test and two tests under icing conditions. The results show that the numerical simulation must take the ice/water phase change into account. In new code, the grid follows a flat plate geometry and the deicer is supposed to be covered by an ice layer of constant thickness. The simulated results are in good agreement with the results obtained by similar codes and with those obtained by a finite element code. The measured temperatures are consistent with the results of the code. Numerical results depend on the material thermal properties of the deicer. ESA

32 COMMUNICATIONS AND RADAR

Includes radar; land and global communications; communications theory; and optical communications.

For related information see also *04 Aircraft Communications and Navigation* and *17 Space Communications, Spacecraft Communications, Command and Tracking.* For search and rescue see *03 Air Transportation and Safety,* and *16 Space Transportation.*

N91-11134*# Ford Aerospace Corp., Palo Alto, CA.
ADVANCED TECHNOLOGY SATELLITE DEMODULATOR DEVELOPMENT Final Report
Stephen A. Ames 29 Aug. 1989 268 p
(Contract NAS3-24678)
(NASA-CR-185127; NAS 1.26:185127) Avail: NTIS HC/MF A12 CSCL 17B

Ford Aerospace has developed a proof-of-concept satellite 8 phase shift keying (PSK) modulation and coding system operating in the Time Division Multiple Access (TDMA) mode at a data range of 200 Mbps using rate 5/6 forward error correction coding. The 80 Msps 8 PSK modem was developed in a mostly digital form and is amenable to an ASIC realization in the next phase of development. The codec was developed as a paper design only. The power efficiency goal was to be within 2 dB of theoretical at a bit error rate (BER) of 5x10(exp 7) while the measured implementation loss was 4.5 dB. The bandwidth efficiency goal was 2 bits/sec/Hz while the realized bandwidth efficiency was 1.8 bits/sec/Hz. The burst format used a preamble of only 40 8 PSK symbol times including 32 symbols of all zeros and an eight symbol unique word. The modem and associated special test equipment (STE) were fabricated mostly on a specially designed stitch-weld board although a few of the highest rate circuits were built on printed circuit cards. All the digital circuits were ECL to support the clock rates of from 80 MHz to 360 MHz. The transmitter and receiver matched filters were square-root Nyquist bandpass filters realized at the 3.37 GHz i.f. The modem operated as a coherent system although no analog phase locked (PLL) loop was employed. Within the budgetary constraints of the program, the approach to the demodulator has been proven and is eligible to proceed to the next phase of development of a satellite demodulator engineering model. This would entail the development of an ASIC version of the digital portion of the demodulator, and MMIC version of the quadrature detector, and SAW Nyquist filters to realize the bandwidth efficiency. Author

N91-11135# Quadrant Engineering, Inc., Amherst, MA.
AZIMUTHAL RESOLUTION DEGRADATION DUE TO OCEAN SURFACE MOTION IN FOCUSED ARRAYS AND SARS
18 Jun. 1990 9 p
(Contract N00014-90-C-0108)
(AD-A223315; QUADRANT-TN-90-1) Avail: NTIS HC/MF A02 CSCL 17/9

During the meeting at WHOI (5-18-90), a discussion arose of the ability of the focused array to simulate the R/v ratios typical of airborne and/or spaceborne SARs. In particular, the ability was questioned of the focused array to yield the same azimuthal resolution, rho, as the SAR. Although the focused array can be sampled to yield the same azimuthal resolution as the SAR, it is likely that the images generated by the focused array will not be identical to those produced by a SAR with the same azimuth resolution. For a true SAR, biases in the Doppler history of azimuthally traveling waves due to their along-track motion will cause shifts in their apparent position. This will cause waves which are physically at one location to shift over several pixel widths in the image. The limited swath width of the focused array will prevent if from observing scattered power from waves falling outside the swath, thus such waves will not affect the image formed within the swath, as would happen in the SAR. Thus, it is likely that the focused array will not yield the same image as a SAR having the same resolution. GRA

N91-11136# Centre National d'Etudes Spatiales, Toulouse (France).
APERTURE DIFFRACTION IN RAYLEIGH ZONE: CALCULATION OF THE FIELD IN THE QUIET ZONE OF COMPACT RANGES
P. Rochette 30 Aug. 1988 19 p In FRENCH; ENGLISH summary
(CNES-CT/DRT/TIT/AN-88/234; ETN-90-97814) Avail: NTIS HC/MF A03

Software for analysis of diffraction of a serrated aperture in the Rayleigh zone was developed. The goal was to estimate fluctuations inside the quiet zone of a compact range using a serrated reflector. Results are compared with those from other software. ESA

N91-11137# Universitaet der Bundeswehr Muenchen, Neubiberg (Germany, F.R.). Fachberech Elektrotechnik.
MODELING AND CODING IN AERONAUTICAL SATELLITE CHANNEL Ph.D. Thesis [MODULATION UND CODIERUNG IM AERONAUTISCHEN SATELLITENKANAL]
Andreas Neul 1989 127 p In GERMAN
(ETN-90-97899) Avail: NTIS HC/MF A07

Dependable means of communication between aircraft and flight security centers are indispensable for flight safety. A satellite aided communication system has been worked out. The aeronautical satellite channel belongs to the class of linear, time variable channels. The fundamentals of these channels are described. The modeling of the aeronautical satellite channel is derived from Rice fading channel. An analysis of the defect behavior in the aeronautical channel is mentioned. Theoretical results are compared to simulation results. On the grounds of the crucial criterion that soft-decision values are very simple and very useful in the decoding process, convolution codes are considered with Viterbi decoding. Considerations on the dimensioning of the necessary interleaver are given. ESA

N91-11138# Universitaet der Bundeswehr, Hamburg (Germany, F.R.). Fachbereich Elektrotechnik.
ALGORITHM AIDED EVALUATION OF DIRECTIONAL SIGNALS Ph.D. Thesis [WISSENSBASIERTE AUSWERTUNG VON PEILSIGNALEN]
Ansgar Rieks 1990 184 p In GERMAN
(ETN-90-97902) Avail: NTIS HC/MF A09

This report deals with the computerized evaluation of directional signals, in the field of high frequency direction finding (1 to 30 MHz). This frequency field presents the properties to transfer electromagnetic waves not only over short distances and in a direct way from transmitter to receiver, but also through reflections, above all, towards the ionosphere, to create interferences. The system works with a great number of possible algorithms, the classification of which allows an almost perfect evaluation. ESA

N91-11139 Syracuse Univ., NY.
SIDELOBE BLANKING SYSTEM PERFORMANCE: AN EXTENSION OF THE THEORY LEADING TO A NEW DETECTION LOGIC Ph.D. Thesis
Kim McKee Harrington 1990 235 p
Avail: Univ. Microfilms Order No. DA9024980

Radar systems employ sidelobe blanking in order to eliminate unwanted low duty cycle signals received through the antenna sidelobes. A comprehensive theory of radar sidelobe blanking is described. A unified analysis and discussion of various detection schemes, namely Maisel Logic, Dual Logic, and Triple Logic are contained. The effects of noncoherent integration of multiple radar pulses and of target fluctuations (Swerling 1, 2, 3, and 4) are considered. Extensive performance curves are presented. Square law detection is assumed throughout. A Maximum Likelihood Ratio approach is then used with some approximations to arrive at a nearly optimum detection logic which is referred to as the Modified Maisel technique. It is a function of the number of pulses integrated, mainlobe and sidelobe target gain margins, and the target class apriori probabilities. The performance of this detection method is investigated and compared to the other types of logic.
Dissert. Abstr.

N91-11140 Southampton Univ. (England).
VOICE COMMUNICATIONS IN THE COCKPIT NOISE ENVIRONMENT: THE ROLE OF ACTIVE NOISE REDUCTION Ph.D. Thesis
Peter David Wheeler 1986 259 p
Avail: Univ. Microfilms Order No. BRDX88858

The topic of voice communications in the cockpit noise environment of modern fast-jet aircraft and helicopters is addressed, and in particular, research undertaken in support of the development of a system for reducing the noise level at the operators' ear is described by acoustic cancellation within the ear defender, known as active noise reduction (ANR). The internal noise spectra of today's high performance fast-jet aircraft and military helicopters is described, and the complex interaction of acoustic noise transmission, speech, and microphone noise pick-up, which produces the total acoustic environment at the aircrews' ears, is discussed. Means of mathematically modelling the audio channel, quantifying the components identified above, and identifying areas of shortfall in performance are derived, leading to a procedure for the development of attenuation requirements, described as the communications audit. A model of the electroacoustic characteristics of the ANR ear defender assembly is presented and the sound field distribution within the ear defender/ear cavity, and its effect upon cancellation performance, is discussed. The extensive laboratory and flight testing of the ANR system that was undertaken is reviewed, paying particular attention to the measurement and analysis techniques employed in such testing. Finally, the performance characteristics of ANR are discussed and compared with the requirements previously established. Design limitations placed upon the system by the constraints of its area of application are described, and the scope for future improvements is considered. Dissert. Abstr.

N91-11141# Lawrence Livermore National Lab., CA.
COMPACT REPRESENTATION OF RADIATION PATTERNS USING SPHERICAL MODE EXPANSIONS
T. L. Simpson and Yinchao Chen (South Carolina Univ., Columbia.) 15 Jul. 1990 39 p
(Contract W-7405-eng-48)
(DE91-000019; UCRL-CR-104589) Avail: NTIS HC/MF A03

The results are presented for an investigation of SM (Spherical Mode) expansions as a compact and efficient alternative to the use of current distributions for generating radiation patterns. The study included three areas: SM expansion from the radiation pattern; SM expansion from the antenna current; and literature search. SM expansions were obtained from radiation patterns during the initial phase of this study. Although straightforward in principal, however, this technique was found to be awkward for the treatment on theoretical radiation patterns. It is included here for completeness and for possible use to summarize experimental results in a more meaningful way than with an exhaustive display of amplitude with azimuth and elevation angles. In essence, the work in this area served as as warm-up problem to develop our skills in computing and manipulating spherical modes as mathematical entities. DOE

N91-11142 British Broadcasting Corp., Kingswood (England). Engineering Div.
DIGITAL AUDIO EDITING: THE DEVELOPMENT OF A RANDOM ACCESS EDITOR
D. G. Kirby and A. B. Gentles 1990 13 p
(BBC-RD-1990/5) Copyright Avail: Issuing Activity

Digital audio techniques offer many advantages over their analogue counterparts, but the difficulty of editing digital recordings detracted from the widespread adoption of this technology in broadcasting. The BBC continued its research in this field with the development of a disc-based Digital Audio Editor to assess the capabilities of this type of equipment in a broadcast environment. This equipment was used for a wide variety of programs with differing requirements. Some of the editing techniques implemented are presented and the advantages and disadvantages of disc editing which became apparent under operational conditions are discussed. Author

N91-11143# Consiglio Nazionale delle Ricerche, Frascati (Italy). Ist. di Fisica dello Spazio Interplanetario.
INSTRUMENTING A ROOM TEMPERATURE GRAVITATIONAL RADIATION ANTENNA FOR SUB-KELVIN TEMPERATURES
Franco Bordoni, Munawar Karim, and Tang Mengxi (Zhongshan Univ., Guangzhou, China) Jun. 1990 21 p
(IFSI-90-20; ETN-90-97802) Avail: NTIS HC/MF A03

Design improvements on a tunneling probe used in the search for gravitational waves are described. The original design proposed by Weber is revived because new electromechanical tranducers based on the vacuum tunnel probe open new vistas to lower sensitivity. It is shown that a room temperature antenna can reach sub-Kelvin temperatures. The antenna of Guangzhou (China) is used as the model for the development of the design. The characteristics of Guangzhou antenna are listed. The duty cycle is predicted to be close to 100 percent. ESA

33 ELECTRONICS AND ELECTRICAL ENGINEERING

Includes test equipment and maintainability; components, e.g., tunnel diodes and transistors; microminiaturization; and integrated circuitry.

For related information see also *60 Computer Operations and Hardware* and *76 Solid-State Physics.*

N91-11144*# Virginia Univ., Charlottesville. Dept. of Electrical Engineering.
FABRICATION AND OPTIMIZATION OF A WHISKERLESS SCHOTTKY BARRIER DIODE FOR SUBMILLIMETER WAVE APPLICATIONS Final Progress Report, 15 Apr. - 31 Dec. 1989
W. Bishop and R. J. Mattauch Mar. 1990 14 p
(Grant NAG5-712)
(NASA-CR-186381; NAS 1.26:186381; UVA/528247/EE90/101)
Avail: NTIS HC/MF A03 CSCL 09A

The following accomplishments were made towards the goal of an optimized whiskerless diode chip for submillimeter wavelength applications. (1) Surface channel whiskerless diode structure was developed which offers excellent DC and RF characteristics, reduced shunt capacitance and simplified fabrication compared to mesa and proton isolated structures. (2) Reliable fabrication technology was developed for the surface channel structure. The new anode plating technology is a major improvement. (3) DC and RF characterization of the surface channel diode was compared with whisker contacted diodes. This data indicates electrical performance as good as the best reported for similar whisker contacted devices. (4) Additional batches of surface channel diodes were fabricated with excellent I-V and reduced

shunt capacitance. (5) Large scale capacitance modelinng was done for the planar diode structure. This work revealed the importance of removing the substrate gallium arsenide for absolute minimum pad capacitance. (6) A surface channel diode was developed on quartz substrate and this substrate was completely removed after diode mounting for minimum parasitic capacitance. This work continues with the goal of producing excellent quality submillimeter wavelength planar diodes which satisfy the requirements of easy handling and robustness. These devices will allow the routine implementation of Schottky receivers into space-based applications at frequencies as high as 1 THz, and, in the future, beyond. Author

N91-11145# National Inst. of Standards and Technology, Gaithersburg, MD. Center for Electronics and Electrical Engineering.

CENTER FOR ELECTRONICS AND ELECTRICAL ENGINEERING TECHNICAL PUBLICATION ANNOUNCEMENTS COVERING CENTER PROGRAMS, JULY - SEPTEMBER, 1989, WITH 1990 CEEE EVENTS CALENDAR

E. J. Walters Apr. 1990 25 p
(PB90-206491; NISTIR-90/4296) Avail: NTIS HC/MF A03 CSCL 09C

The article is the twenty-second issue of a quarterly publication providing information on the technical work of the National Institute of Standards and Technology (formerly the National Bureau of Standards) Center for Electronics and Electrical Engineering. The issue of the Center for Electronics and Electrical Engineering Technical Publication Announcements covers the third quarter of calendar year 1989. Abstracts are provided by technical area for papers published this quarter. GRA

N91-11146# Helsinki Univ. of Technology, Espoo (Finland).

ADVANCED SECONDARY BATTERIES: THEIR APPLICATIONS, TECHNOLOGICAL STATUS, MARKET AND OPPORTUNITY

M. Yao (Yao International, Inc., Clarendon Hills, Il.) Mar. 1989 138 p
(DE90-796146; NEMO-8) Avail: NTIS (US Sales Only) HC/MF A07

Program planning for advanced battery energy storage technology is supported within the NEMO Program. Specifically this study had focused on the review of advanced battery applications; the development and demonstration status of leading battery technologies; and potential marketing opportunity. Advanced secondary (or rechargeable) batteries have been under development for the past two decades in the U.S., Japan, and parts of Europe for potential applications in electric utilities and for electric vehicles. In the electric utility applications, the primary aim of a battery energy storage plant is to facilitate peak power load leveling and/or dynamic operations to minimize the overall power generation cost. In the application for peak power load leveling, the battery stores the off-peak base load energy and is discharged during the period of peak power demand. This allows a more efficient use of the base load generation capacity and reduces the need for conventional oil-fired or gas-fire peak power generation equipment. Batteries can facilitate dynamic operations because of their basic characteristics as an electrochemical device capable of instantaneous response to the changing load. Dynamic operating benefits results in cost savings of the overall power plant operation. Battery-powered electric vehicles facilitate conservation of petroleum fuel in the transportation sector, but more importantly, they reduce air pollution in the congested inner cities. DOE

N91-11147# Office of the Secretary of Defense, Washington, DC.

DEPARTMENT OF DEFENSE METHODOLOGY GUIDELINES FOR HIGH POWER MICROWAVE (HPM) SUSCEPTIBILITY ASSESSMENTS

Nancy C. Chesser, ed. (Directed Technologies, Inc., Arlington, VA.) Jan. 1990 100 p
(Contract W-7405-eng-48)
(DE90-015405; UCRL-CR-104314) Avail: NTIS HC/MF A05

It is the intention of the National High Power Microwave (HPM) Program to complete a series of tests over the next two years to validate the methodology described in these guidelines. When those tests are completed and results analyzed, this document will be revised to reflect lessons learned during the validation process. In addition, the Methodology Sub-Panel is compiling a second volume on specific measurement techniques. This volume (Volume 1) is intended to provide guidance to the Program Manager on the critical steps in a well-conceived test program. Volume 2 will provide detailed step-by-step information to the engineer who is responsible for performing the tests. The body of this volume is divided into seven sections. Sections 2 through 7 provide detailed descriptions of the activities within each of the modular steps which comprise the methodology schematically; Section 2: pre-test system analysis; Section 3: low power microwave tests -- coupling/subsystem component tests; Section 5: susceptibility assessment and test planning; Section 6: high power microwave tests; and Section 7: susceptibility assessment and test evaluation. The executive summary reviews the reasons for development of the methodology and provides brief descriptions of each module. Appendix B provides definitions of special terms and acronyms which are used throughout the document. DOE

N91-11148*# Westinghouse Electric Corp., Pittsburgh, PA. Science and Technology Center.

THREE-MAN SOLID ELECTROLYTE CARBON DIOXIDE ELECTROLYSIS BREADBOARD Final Report

Arnold O. Isenberg Jun. 1989 153 p
(Contract NAS9-17590)
(NASA-CR-185612; NAS 1.26:185612) Avail: NTIS HC/MF A08 CSCL 09C

The development of the Three-Man (2.2 lb CO2/man-day) Solid Electrolyte CO2 Electrolysis Breadboard consisted of a Phase 1 and 2 effort. The Phase 1 effort constituted fabrication of three electrolysis cell types and performing parametric testing, off-design testing, and cell life testing. The Phase 2 consisted of the preliminary design, incorporation of palladium (Pd) tubes for hydrogen separation from the electrolyzer cathode feed gases, design support testing, final design, fabrication, and performance testing of the breadboard system. The results of performance tests demonstrated that CO2 electrolysis in an oxygen reclamation system for long duration space-based habitats is feasible. Closure of the oxygen system loop, therefore, can be achieved by CO2 electrolysis. In a two step process the metabolic CO2 and H2O vapor are electrolyzed into O2, H2, and CO. The CO can subsequently be disproportionated into carbon and CO2 in a carbon deposition reactor and the CO2 in turn be recycled and electrolyzed for total O2 recovery. The development effort demonstrated electrolyzer system can be designed and built to operate safely and reliably and the incorporation of Pd tubes for hydrogen diffusion can be integrated safely with predictable performance. Author

N91-11149# Metal Air Technology Systems International, Inc., Lawrenceville, GA.

ZINC AIR BATTERY DEVELOPMENT FOR ELECTRIC VEHICLES Final Report

Ronald A. Putt May 1990 27 p Prepared for California Univ., Berkeley. Lawrence Berkeley Lab.
(Contracts DE-AC03-76SF-00098; LBL-455610)
(DE90-016639; LBL-29078) Avail: NTIS HC/MF A03

This document reports the progress and accomplishments of a 16 month program to develop a rechargeable zinc-air battery for electric vehicle propulsion, from October 1988 through January 1990. The program was the first stage in the transition of alkaline zinc electrode technology, invented at Lawrence Berkeley Laboratory, to private industry. The LBL invention teaches the use of a copper metal foam substrate for the zinc electrode, in combination with forced convection of electrolyte through the foam during battery operation. Research at LBL showed promise that this approach would avoid shape change (densification and dendrite growth), the primary failure mode of this electrode. The program comprised five tasks: (1) cell design, (2) capacity maximization, (3) cycle testing, (4) materials qualification, and (5) a cost/design

study. The cell design contemplates a plate and frame stack, with alternating zinc and oxygen electrode frame assemblies between rigid end plates. A 200 Ah cell, as may be required for the EV application, would comprise a stack of five zinc and six oxygen electrode frame/assemblies. DOE

N91-11150# Institut National Polytechnique, Grenoble (France). Lab. de Technique de l'Informatique, de la Microelectronique et de la Microscopie Quantitative.
APPLICATION OF SELF-TESTING INTEGRATED CIRCUITS TO THE SAFETY OF SYSTEMS OPERATION Ph.D. Thesis [APPLICATION DES CIRCUITS INTEGRES AUTOTESTABLES A LA SURETE DE FONCTIONNEMENT DES SYSTEMES]
Serge Noraz 1989 157 p In FRENCH; ENGLISH summary
(ETN-90-97828) Avail: NTIS HC/MF A08

The use of self-testing circuits, and specially self-checking circuits (able to detect instantaneously their own errors) to the high dependability integrated systems design, is investigated. The general fail-safe theory is discussed. An application involving a built-in-self testing interface able to transform the outputs of self-checking circuits into safe signals adequate to drive electromechanical actuators is presented. This interface allows the implementation in MOS technologies of strongly fail-safe VLSI (Very Large Scale Integration) circuits. All the practical considerations for the design of circuits are based on the analytical faults hypotheses bounded to the CMOS technology. ESA

N91-11151# Sandia National Labs., Albuquerque, NM. Storage Batteries Div.
TERRESTRIAL NICKEL/HYDROGEN BATTERY EVALUATION
Donald M. Bush Jul. 1990 12 p
(Contract DE-AC04-76DP-00789)
(DE90-014863; SAND-90-0390) Avail: NTIS HC/MF A03

The nickel/hydrogen battery was developed in the 1970s as an energy storage subsystem for commercial communication satellites. The advantages offered by nickel/hydrogen batteries, including long life, low maintenance and high reliability, make it very attractive for terrestrial applications such as stand-alone photovoltaic systems. The major drawback to the wider use of the nickel/hydrogen battery is its high initial cost. Sandia National Laboratories has directed cost-shared contracts at Comsat Laboratories and Johnson Controls, Inc. to reduce the cost, and a battery consisting of prismatic cells in a common pressure vessel has evolved. Contract deliverables include cells and batteries that are evaluated at Sandia. This report summarizes the results over the past two years of both cycle and solar testing. DOE

N91-11152# Wisconsin Univ., Madison. Dept. of Electrical and Computer Engineering.
HIGH-POWER MICROWAVE TRANSMISSION SYSTEMS FOR ELECTRON CYCLOTRON RESONANCE PLASMA HEATING, VOLUME 5 Progress Report, 1 Sep. 1989 - 31 Aug. 1990
Ronald J. Vernon Aug. 1990 38 p
(Contract DE-FG02-85ER-52122)
(DE90-017600; DOE/ER-52122/5-Vol-5) Avail: NTIS HC/MF A03

The design, development, and fabrication of ECRF transmission and mode conversion systems to transport microwave power from a gyrotron, or other high power source, to a magnetically confined plasma was studied. The development of new and improved components for such systems and underlying theory, where necessary, is the focus of this project. Devising and improving component testing and diagnostic techniques is also an important part of this effort. The development of possible designs for sections of gyrotrons themselves, such as tapers or Vlasov-type launchers, in support of the Varian gyrotron development program is also considered. DOE

N91-11153# Sandia National Labs., Albuquerque, NM.
DEVELOPMENT OF HERMETIC MICROMINIATURE CONNECTORS
M. K. Neilsen, L. A. Andrews, S. L. Monroe, and H. L. McCollister 1990 6 p Presented at the International Symposium on Gas-Liquid Two-Phase Flows in Conjunction with the Winter Annual Meeting of the American Society of Mechanical Engineers, Dallas, TX, 25-30 Nov. 1990
(Contract DE-AC04-76DP-00789)
(DE90-015562; SAND-90-0650C; CONF-901109-16) Avail: NTIS HC/MF A02

Miniaturization of hermetic packages has provided the incentive to develop a new family of hermetic microminiature connectors. Microminiature connectors, with a pin spacing of 1.27 mm, have previously been available only in the non-hermetic form. New microminiature connectors with compression seal materials, 304 Stainless Steel housings, Alloy 52 pins, and TM-9 Glass insulators, were examined because compression seals are currently used in larger hermetic connectors and are typically designed to create a residual compressive stress state in the insulator during manufacture. The new microminiature connectors with compression seals were evaluated analytically with 2-D and 3-D finite element models and experimentally by fabrication of prototype connectors. The finite element analyses predicted the development of undesirable tensile stress in the insulator during manufacture and identified the mechanism responsible for the generation of tensile stress in the glass. The experimental investigation confirmed the existence of desirable tensile stress in the glass with the observation of crack development during manufacture. Since the design requirements would not allow the geometric modifications needed to manufacture crack-free connectors with compression seals, insulator materials that generate a matched seal with 304 Stainless Steel housings were developed. Connectors with these matched seals were successfully manufactured. DOE

N91-11154# Sandia National Labs., Albuquerque, NM.
A RADIATION HARDENED SONOS/CMOS EEPROM FAMILY
V. F. Klein, G. M. Wood, J. F. Buller (Harris Corp., Melbourne, FL.), J. R. Murray, and J. L. Rodriquez 1990 3 p Presented at the Government Microcircuit Applications Conference: Technology Strategies for the 90's, Las Vegas, NV, 6-8 Nov. 1990
(Contract DE-AC04-76DP-00789)
(DE90-015993; SAND-90-2173C; CONF-901124-2) Avail: NTIS HC/MF A01

There has long been a need for fast read nonvolatile, rad hard memories for military and space applications. Recent advances in Electrically Erasably Programmable Read Only Memory (EEPROM) technology now allow this need to be met for many applications. Harris/Sandia have developed a 16k and a 256k rad hard EEPROM. The EEPROMs utilize a Silicon Oxide Nitride Oxide Silicon (SONOS) memory transistor integrated into a 2 microns rad hard two level metal CMOS process. Both the 16k and the 256k parts were designed to interface with the Intel 8085 or 80C51 and National 32000 series microprocessors and feature page and block clear modes. Both parts are functionally identical, and are produced by the same fabrication process. They are also pin for pin compatible with each other, except for the extra address and ground pins on the 256k. The characteristics of this EEPROM family are described. DOE

N91-11155# Sandia National Labs., Albuquerque, NM. Advanced Power Systems Div.
REFERENCE CONCEPTS FOR A SPACE-BASED HYDROGEN-OXYGEN COMBUSTION, TURBOALTERNATOR, BURST POWER SYSTEM
Michael W. Edenburn Jul. 1990 40 p
(Contract DE-AC04-76DP-00789)
(DE90-016692; SAND-89-0423) Avail: NTIS HC/MF A03

This report describes reference concepts for a hydrogen-oxygen combustion, turboalternator power system that supplies power during battle engagement to a space-based, ballistic missile defense platform. All of the concepts are open that is, they exhaust hydrogen or a mixture of hydrogen and water vapor into space. We considered the situation where hydrogen is presumed to be free to the power system because it is also needed to cool the platform's weapon and the situation where hydrogen is not free and its mass must be added to that of the

power system. We also considered the situation where water vapor is an acceptable exhaust and the situation where it is not. The combination of these two sets of situations required four different power generation systems, and this report describes each, suggests parameter values, and estimates masses for each of the four. These reference concepts are expected to serve as a baseline to which other types of power systems can be compared, and they are expected to help guide technology development efforts in that they suggest parameter value ranges that will lead to optimum system designs. DOE

N91-11156# Lawrence Livermore National Lab., CA.
A HYBRID PULSE FORMING TECHNIQUE
W. R. Cravey, W. M. Portnoy, and T. R. Burkes (Texas Technological Univ., Lubbock.) 1990 9 p Presented at the 19th Power Modulator Symposium, San Diego, CA, 26-28 Jun. 1990
(Contract W-7405-eng-48)
(DE90-016860; UCRL-JC-103328; CONF-9006176-15) Avail: NTIS HC/MF A02

Circuits for producing high power pulses with fast risetimes involve either charged transmission lines or pulse forming networks (PFN), depending on the width of the required pulse. In general, very fast risetimes can be obtained only with transmission lines, which are not practical for pulses wider than a few microseconds because of the excessive lengths of line required. Wider pulses can be obtained with a PFN, but a fast risetime mandates many stages, which may also be impractical. The work described here examined a pulse forming technique which incorporates the advantages of both the T-Line and the PFN: the combined or hybrid circuit. Both series and parallel arrangements were theoretically and experimentally investigated, and the qualities of and problems with each were identified. As expected, discontinuities were observed for each arrangement, but their effect could be reduced by insertion of appropriate additional elements at the junction of the T-Line and the PFN; this type of filtering was found to be more successful with a parallel hybrid. DOE

N91-11157# Edgerton, Germeshausen and Grier, Inc., Idaho Falls, ID.
A MICROPROCESSOR BASED CHARGE CONTROL SYSTEM FOR THE SIMULTANEOUS CHARGING OF SEVERAL BATTERIES WITH ONE CHARGE CONTROLLER
Dieter Nowak (Alabama Univ., Huntsville.) 16 May 1990 52 p
(Contract DE-AC07-76ID-01570)
(DE90-017089; DOE/ID-10287; JRC-90-02) Avail: NTIS HC/MF A04

The objective of this project as covered in this report, is the reduction of the cost of microprocessor controlled charging with complex algorithms, such as the UAH (University of Alabama in Huntsville) charge algorithm for sealed lead-acid batteries. The use of one charge controller for the simultaneous charging of several vehicles reduces the cost of hardware proportional to the number of vehicles that can be charged per controller. This cost savings is the order of several hundred dollars per vehicle (cost of the controller). However, more complex controller programming is required. Thus, there is a one-time investment in software development. DOE

N91-11158# Allied-Signal Aerospace Co., Kansas City, MO.
ION CHROMATOGRAPHY IN THE MANUFACTURE OF MULTILAYER CIRCUIT BOARDS
Robert E. Smith Sep. 1990 27 p Presented at the International Ion Chromatography Symposium, San Diego, CA, 30 Sep. - 3 Oct. 1990
(Contract DE-AC04-76DP-00613)
(DE90-017647; KCP-613-4404; CONF-9009247-1) Avail: NTIS HC/MF A03

Ion chromatography (IC) has proven useful in analyzing chemical solutions used in the manufacture of multilayer circuit boards. The manufacturing process is described briefly and previously published IC methods are reviewed. Then, methods are described for determining chlorate and chlorite in a brown oxide solution; salicylic acid in an epoxy cure agent; formate, sulfate, and tartrate in an electroless copper bath; anionic detergents in a tin-lead brightener and in a cleaning solution; and aqueous photoresist and nonionic brightener in a tin-lead bath. Anion exchange, reverse phase HPLC on a poly(styrene/divinylbenzene), PS/DVB, column and 2-D liquid chromatography also are described. Chemically suppressed conductivity and photometric detection are used. DOE

N91-11159# Argonne National Lab., IL.
DEVELOPMENT OF HIGH PERFORMANCE SODIUM/METAL CHLORIDE CELLS
D. R. Vissers, I. D. Bloom, M. C. Hash, L. Redey, C. L. Hammer, D. W. Dees, and P. A. Nelson 1990 31 p Presented at the 8th Beta Battery Workshop, Chester, England, 12-18 Jun. 1990
(Contract W-31-109-eng-38)
(DE90-017668; CONF-9006243-2) Avail: NTIS HC/MF A03

Sodium/metal chloride (MCl2) cells and batteries are being studied at Argonne National Laboratory (ANL) for stationary energy storage and transportation applications. The work is being directed toward (1) development of thin, high capacity density electrodes and inexpensive beta double prime alumina-glass composite electrolyte materials to replace beta double prime alumina, and (2) the development of models to project MCl2 system performances. In our NiCl2 electrode work, the effects of charge/discharge rates, temperature, electrode porosity, and sulfur content on electrode performance were determined using annular electrodes fabricated in the uncharged state. Of all electrode design parameters mentioned, electrode porosity, sulfur content, and charge rates have the greatest effect on utilization and on the area-specific impedance. The beta double prime alumina-glass composite electrolyte work has led to the development of a highly conductive (3.3 x 10(exp -2)S/cm at 250 C) composite material. Preliminary modeling studies indicate that the performance of the MCl2 electrodes can be fitted by a mathematic model very successfully and that cell electrolyte configurations of either multiple tubes joined at a header or compartmented flat structures of either beta double prime alumina or of the composite material would result in high performance batteries with power-to-energy ratios of about 5. DOE

N91-11160# Joint Inst. for Nuclear Research, Dubna (USSR). Lab. of Neutron Physics.
MICROPROCESSOR SYSTEM FOR TEMPERATURE REGULATION AND STABILIZATION
Nhi Dien Nguyen and K. G. Rodionov 1989 6 p In RUSSIAN; ENGLISH summary
(DE90-634244; JINR-R-10-89-454) Avail: NTIS (US Sales Only) HC/MF A02

Microprocessor based system for temperature regulation and stabilization of an operation external object is described. The system has the direct current amplifier working according to modulator-demodulator principle. The overal gain is 100, 1000, 2000. The maximum output signal is (plus minus)10 V. The power amplifier is a thyristor one and its line voltage is 220 V, 50 Hz. The output power is 0 to 2 kVA. The microcontroller has a remote display terminal. Data input is 8 and data output is one. Input and output voltage is + or - (0 to 10) V. The preselection time for stabilization is within 1 s - 18 h. The program algorithm is given. DOE

N91-11161# California Univ., Berkeley. Lawrence Berkeley Lab. Materials and Chemical Sciences Div.
CURRENT AND POTENTIAL DISTRIBUTIONS ON A CYLINDER ELECTRODE M.S. Thesis
Anthony Joseph Grabowski Jul. 1990 92 p Prepared in cooperation with California Univ., Berkeley
(Contract DE-AC03-76SF-00098)
(DE91-000170; LBL-29312) Avail: NTIS HC/MF A05

This work presents the numerical solution for the current and potential distributions of a cylindrical electrode. In particular, it investigates the primary current distribution, the secondary current distribution with linearized kinetics, and the potential distribution due to constant current density on the working electrode. DOE

N91-11162# Los Alamos National Lab., NM.
INCREASING OUTPUT POWER OF AN 850 MHz TETRODE WITH A FLOATING-DECK MODULATOR
Daniel Rees and Carl Friedrichs 1990 4 p Presented at the 1990 LINAC Conference, Albuquerque, NM, 10-14 Sep. 1990
(Contract W-7405-eng-36)
(DE91-000433; LA-UR-90-3046; CONF-9009200-17) Avail: NTIS HC/MF A01

Designers of high power amplifiers generally regard the region above 300 MHz as a domain dominated by velocity modulated (klystron/TWT) devices. However, as the power requirements diminish, there are attractive alternatives. The high power 850 MHz requirements of the ground test accelerator (GTA) program can be filled by 1 MW klystrons, but it would be more efficient to use a lower power device for a 50 kW requirement. To meet the 850 MHz medium power requirements, Los Alamos National Laboratory is developing an 850 MHz tetrode amplifier. These amplifiers will provide RF power to the momentum compactor and bunch rotator cavities of the GTA. Available tubes provide only a limited safety margin for a low risk design at the power levels and duty factor required for GTA cavities. At 850 MHz, the output power capability of available tubes is reduced because of transit time effects and limited anode voltage holdoff. Pulsing the anode of the output tetrode amplifier will allow higher output power with minimum design risk. A floating deck modulator acts as a high voltage/high current switch, so voltage is applied to the anode of the gridded tube only during the RF pulse. The anode voltage holdoff capability of the tube is substantially enhanced by operating in this mode. The design of the floating deck modulator and its impact on the design risk of the 850 MHz tetrode amplifier is described. DOE

34 FLUID MECHANICS AND HEAT TRANSFER

Includes boundary layers; hydrodynamics; fluidics; mass transfer; and ablation cooling.

For related information see also *02 Aerodynamics* and *77 Thermodynamics and Statistical Physics.*

N91-11163 Ohio State Univ., Columbus.
VORTEX-INDUCED NOISE AND VIBRATION IN FLOW PAST SEVERAL FLAT PLATES Ph.D. Thesis
Chan Mun Kim 1989 274 p
Avail: Univ. Microfilms Order No. DA9014441

A model formulation for the problem of vortex impingement on a pair of elastic tandem cylinders is presented. The parametric relations among a variety of fluid dynamic and structural dynamic properties are illustrated. The noise field essentially responds at the cylinder response frequency and the sound pressure level is generally increased by the vibration of the cylinders. The interaction of an array of vortices is also considered and the results indicate that four vortices are required for the possibility of the chaotic motion and the broadband noise. The vortex shedding off an inclined flat plane is modelled using the discrete vortex method along with the Lamb vortex model. The model tested for the rolling-up of a vortex sheet behind the elliptically loaded wing demonstrates that the smooth rollup is achieved inside the core region of the vortex sheet. The subsequent application of the model to the vortex shedding problem shows that the computed results such as the kinematics of the wake development, the fluid loading and the Strouhal number are in fair agreement with previous experimental measurements. The noise field exhibits a broadband character with the peak occurring at the vortex shedding frequency. A numerical conformal mapping technique is developed to transform multiple flat plates into the same number of circular cylinders. Employing the multiple body mapping method, the flow past a series of flat plates is investigated. The calculated results indicate that the presence of a downstream body in the wake of another body produces a feedback effect upstream which, in turn, has a significant effect on the upstream flow. In the case of vortex shedding, the presence of a downstream splitter plate in the center of the wake of an inclined plate appears to suppress the regular, periodic vortex shedding process. The addition of more inclined plates appears to reduce the Strouhal frequency which is the frequency at which the noise field responds. Dissert. Abstr.

N91-11164# Illinois Univ., Champaign. Dept. of Aeronautical and Astronautical Engineering.
THE STRUCTURE AND STABILITY OF THREE DIMENSIONAL DETONATION WAVES Final Report, 1 May 1989 - 30 Apr. 1990
John Buckmaster 30 Apr. 1990 12 p
(Grant AF-AFOSR-0143-86; AF Proj. 2304)
(AD-A224465; AFOSR-90-0768TR) Avail: NTIS HC/MF A03 CSCL 21/2

Detonation waves were the focal point of the research conducted during the contract period, described in Technical Report (TR) 8, TR11, TR17, TR19, and TR26. Microgravity combustion was a secondary focal point, described in TR14, TR15, TR22, TR24, TR28, and TR29. A total of 29 technical reports were generated. The titles and abstracts of these reports are given in the appendix. Author

N91-11165*# MCAT Inst., San Jose, CA.
DEVELOPMENT OF A TIME-DEPENDENT INCOMPRESSIBLE NAVIER-STOKES SOLVER BASED ON A FRACTIONAL-STEP METHOD Final Report, 1 Oct. 1988 - 15 Feb. 1990
Moshe Rosenfeld Sep. 1990 25 p
(Contract NCC2-562)
(NASA-CR-187254; NAS 1.26:187254) Avail: NTIS HC/MF A03 CSCL 20D

The development, validation and application of a fractional step solution method of the time-dependent incompressible Navier-Stokes equations in generalized coordinate systems are discussed. A solution method that combines a finite-volume discretization with a novel choice of the dependent variables and a fractional step splitting to obtain accurate solutions in arbitrary geometries was previously developed for fixed-grids. In the present research effort, this solution method is extended to include more general situations, including cases with moving grids. The numerical techniques are enhanced to gain efficiency and generality.
Author

N91-11166# Center for Mathematics and Computer Science, Amsterdam (Netherlands). Dept. of Operations Research, Statistics, and System Theory.
SYSTEM IDENTIFICATION OF LOSSLESS LAYERED MEDIA FROM INPUT-OUTPUT DATA
J. W. vanderWoude Nov. 1989 21 p
(CWI-BS-R8929; ETN-90-97663) Copyright Avail: NTIS HC/MF A03

The interior of the Earth is modeled as a lossless layered medium, and the reconstruction of the parameters of such a medium from the input and the output (input-output data) are studied. The study assumes that the input-output data is noise free, and derives a so-called layer stripping algorithm for the reconstruction of the parameters of the medium. The algorithm is just one of the many versions of layer stripping algorithms that are available in the literature. The study then assumes that both the input and the output are corrupted by noise, and derives two new methods for the estimation of the parameters of the medium using the noisy input-output data. The methods are based on the estimation of the parameters of an ARX-representation of a lossless layered medium. The distinction between the two methods is that in one method the ARX parameters are free, while in the other method the ARX parameters have to correspond to parameters of a lossless layered medium that are physically realistic. The methods are illustrated by means of a numerical experiment.
ESA

N91-11167# Center for Mathematics and Computer Science, Amsterdam (Netherlands). Dept. of Numerical Analysis.
STABILIZATION OF A TIME INTEGRATOR FOR THE 3D SHALLOW WATER EQUATIONS BY SMOOTHING TECHNIQUES
Erik D. deGoede Aug. 1989 16 p Submitted for publication Sponsored by Rijkwaterstaat
(CWI-NM-R8916; ETN-90-97671) Copyright Avail: NTIS HC/MF A03

A smoothing technique is applied to improve the stability of a semi-implicit time integrator for the three dimensional shallow water equations. In this method the vertical terms are treated implicitly. The stability condition on the time step only depends on the horizontal mesh sizes. Therefore, in horizontal direction an explicit smoothing operator is added. Due to the smoothing, the maximally stable time step increases considerably, while the accuracy is hardly affected. The explicit smoothing operator is efficient on any type of computer, in particular on vector and parallel computers. ESA

N91-11168# Stuttgart Univ. (Germany, F.R.). Inst. fuer Aerodynamik und Gasdynamik.
EXAMINATION OF A THREE DIMENSIONAL ASYMMETRICAL FLOW FIELD USING THE INTERFERENCE METHOD Ph.D. Thesis [UNTERSUCHUNG EINES DREIDIMENSIONALEN ASYSMMETRISCHEN DICHTEFELDS MIT HILFE DER INTERFERENZMETHODE]
Christoph Zeller 1989 118 p In GERMAN
(ETN-90-97859) Avail: NTIS HC/MF A06

In order to determine the multidimensional interpolation and compensation problems which are frequently occurring, new algorithms were developed on the basis of Bezier functions. The total evaluation process was developed and checked out through a spatial asymmetrical blunt bodies flow in the supersonic region. The resulting three-dimensional flow fields were experimentally examined for different angles of attack. In order to control, pressure distribution measurements were carried out on the surface of bodies. The greatest part of time consumption for the measurement of a spatial flow field with the interference method is due to the equipment used, principally the punctual image digitizing and the interactive error correction. The processing velocity can be increased, using high resolution electronic cameras, with computer aided image handling. ESA

N91-11169# Karlsruhe Univ. (Germany, F.R.). Fakultaet fuer Maschinenbau.
EXAMINATION OF NUMERICAL FORMULATIONS TO DESCRIBE COMPLEX GEOMETRY TURBULENT ELLIPTICAL FLOWS, USING CONTOUR MATCHED COORDINATES Ph.D. Thesis [UEBERPRUEFUNG NUMERISCHER ANSAETZE ZUR BESCHREIBUNG TURBULENTER ELLIPTISCHER STROEMUNGEN IN KOMPLEXEN GEOMETRIEN MIT HILFE KONTURANGEPASSTER KOORDINATEN]
Hans-Joerg Bauer 1989 156 p In GERMAN Sponsored by DFG
(ETN-90-97864) Avail: NTIS HC/MF A08

A numerical process for the calculation of turbulent, parabolic or elliptic flows in complex geometries is developed. In order to represent the computational field, contour matched curvilinear and generally nonorthogonal grids were used. Originally, in the framework of the special research field of high loaded combustion chambers stationary balanced pressure combustion for the calculation of flows in gas turbine combustion chambers with complex geometry, the finite volume process presented was considered so generally valid that it is capable of describing almost any stationary two dimensional flow, among which typical combustion chamber flows only represent a definite application case. For the description of turbulence the k,epsilon model was used. In order to avoid first order discretization errors, which occur for simple formulations such as upwind or hybrid scheme and are often the cause of a high loss of calculation accuracy, the so-called quick scheme had to be used in the developed program. Experimentally obtained turbulence flow data were used to check the numerical process. ESA

N91-11170# California Univ., Los Angeles. Dept. of Mechanical, Aerospace and Nuclear Engineering.
ENHANCEMENT OF FORCED CONVECTION HEAT TRANSFER IN TUBES USING STAGED TANGENTIAL FLOW INJECTION Final Report, Jun. 1987 - Dec. 1989
V. K. Dhir, F. Chang, and J. Yu Apr. 1990 88 p
(Contract GRI-5087-260-1535)
(PB90-247594; GRI-90/0134) Avail: NTIS HC/MF A05 CSCL 20D

Experiments using air as the test fluid were carried out to study enhancement in heat transfer in tangential injection induced swirl flow. In the experiments, 25.4 mm (1 in) and 50.8 mm (2 in) diameter tubes were employed. The tubes were heated electrically. The heated length of the tubes varied from 3.05 to 3.66 m. Three series of experiments were conducted. In the 1st series, fluid was tangentially injected in stages through two sets of 5.08 mm (0.2 in) diameter tubular injectors. In the 2nd series, injection was accomplished through a manifold. In the 3rd seried, a 50.8 mm (2 in) diameter tube instead of 25.4 mm (1 in) diameter tube used in series 1 and 2 was used, and fluid injected through a manifold having six 11.1 mm (0.44 in) diameter passages. In all tests, Reynolds numbers varied from 15,000 to 57,000. In comparison to single stage injection, fluid injection at several places along the direction of flow can improve net enhancement in heat transfer. With a manifold type of injection through a chamber, which simulates the application of the method in a multitube heat exchanger, net enhancement was greatly improved over that for tubular injectors. Author

N91-11171 Georgia Inst. of Tech., Atlanta.
HEAT TRANSFER IN VARIABLE DENSITY, LOW MACH NUMBER, STAGNATING TURBULENT FLOWS Ph.D. Thesis
Danny James Huval 1990 137 p
Avail: Univ. Microfilms Order No. DA9023816

Variable-density, low Mach number turbulent flows are investigated analytically with a two equation turbulence model and experimentally with a modified NASA Lewis research facility. In order to qualify the use of a two equation turbulence model, the experimental verification of anisotropy development and stress transport modeling was required to examine and determine the strength of the anisotropy along the stagnating streamline. Theoretical and experimental results are compared to measure the importance of turbulent length scale and intensity as free-stream variables. Past theories imply intensity alone is responsible with little emphasis given to the contribution of length scale. When comparing theoretical heat transfer results to existing experimental data, a new viscous-inviscid matching condition shows little improvement over past work. However, there was room for improvement in the existing experimental data which was used for comparison. Experimental evidence compiled at NASA-Lewis Research Center show good accord with theory. Additionally, these experiments considered different length scales, different model diameters, and systematic procedures. Theoretical results that are based on typical turbine environments show that free-stream temperature fluctuations can have a significant effect upon stagnation point heat transfer. Dissert. Abstr.

N91-11172 Michigan Univ., Ann Arbor.
A VISCOUS-INVISCID INTERACTIVE METHOD FOR UNSTEADY FLOWS Ph.D. Thesis
Hong-Ming Jang 1990 197 p
Avail: Univ. Microfilms Order No. DA9023574

A model for simulating the incompressible flow over a practical airfoil executing a pitching motion is constructed in terms of solutions of viscous and inviscid flow equations. The inviscid flow is computed by an unsteady panel method involving a blowing-velocity which accounts for viscous effects. The viscous flow is computed by a finite-difference boundary layer scheme which makes use of an interactive boundary condition that provides a coupling between the potential and viscous flows. A simplified

unsteady wake model is also devised to represent the effects of the wake on the airfoil-surface flow. The computational model was tested in relation to steady, quasi-steady (slow pitching airfoil), and unsteady (quick pitching airfoil) flows. The steady and quasi-steady models correctly simulate the stall phenomena and agree with the experimental data. The cases tested with the unsteady model demonstrate reasonable hysteresis and stall-delay phenomena and justify the use of the numerical model for simulating the flows over an airfoil executing harmonic oscillation with a reduced frequency less than 0.5 or a ramp-type motion with a constant pitch rate less than 0.02. However, the simulation of flows over an airfoil performing a higher degree of pitching and the flows with big reversal region requires improvement.

Dissert. Abstr.

N91-11173 Kansas Univ., Lawrence.
SOLUTIONS OF THIN-LAYER NAVIER-STOKES EQUATIONS FOR MISSILE CONFIGURATIONS Ph.D. Thesis
Seid Hossein Pourtakdoust 1989 256 p
Avail: Univ. Microfilms Order No. DA9024204

Solutions of the thin-layer Navier-Stokes equations were obtained for two typical missile bodies as well as two complete missile configurations. The finite-differenced three-dimensional equations are solved using a modified NASA Ames solver code on a body-fitted curvi-linear grid system developed in conjunction with the flowfield solver. The grid program is based on the method of algebraic interpolation and is capable of generating three-dimensional grid systems for missile bodies and finned-missiles having up to eight control surfaces. The numerical procedure is based on an implicit approximate factorization algorithm employing a multi-grid approach in the simulation of flow about complex finned-missile configurations. The present procedures are proven effective in dealing with complete missile configurations flying at high angles of attack. The predicted aerodynamic loading coefficients and pressure distributions match the available wind-tunnel data with good accuracy. Flow non-linearities such as shock, streamwise and cross-flow separations, and reverse flow were detected and verified with the available experimental reports. Leading-edge separation and classical patterns of vortical flow were also numerically obtained and studied for interaction effects. The Mach number and Reynolds number effects on the convergence of the numerical process are also discussed. Dissert. Abstr.

N91-11174 Colorado Univ., Boulder.
APPLICATION OF COMPUTATIONAL FLUID DYNAMICS TO THREE-DIMENSIONAL BODIES IN HYPERSONIC FLOW Ph.D. Thesis
James Stevenson Ryan 1989 85 p
Avail: Univ. Microfilms Order No. DA9024865

Hypersonic aircraft are now being designed. For that work to be completed, improved computational tools are required. The flow simulation capabilities which are needed are being sought. In order to accomplish this, features of several existing codes were combined and enhanced. The Compressible Navier-Stokes (CNS) computer code solves the thin-layer Navier-Stokes equations in three dimensions for arbitrary vehicle shapes. The solver can capture strong or weak shocks, and can model separated flow. Boundary-layer turbulence is accounted for empirically by use of the Baldwin-Lomax turbulence model. The code uses ideal gas assumptions or an equilibrium real gas model. Geometries are gridded in a zonal fashion, allowing for flexible convergence strategies and use of the best available equation set for each zone. The grid on which the computations are performed is critical to the efficient generation of accurate solutions. Some of the criteria for grid quality are discussed, and a simple method of adapting grids to supersonic flow fields is presented. The code was tested against analytical, experimental, and numerical results, and shows excellent agreement for critical quantities such as heat transfer and skin friction. The zonal approach of the code and its modular structure allow for future inclusion of internal flow options, more complex geometrical models, nonequilibrium air chemistry, combustion chemistry, and other improvements. Dissert. Abstr.

N91-11175 Old Dominion Univ., Norfolk, VA.
AN EXPERIMENTAL STUDY OF AN AXISYMMETRIC TURBULENT BOUNDARY LAYER DISTURBED BY A PERIODIC FREESTREAM Ph.D. Thesis
Chithrabhanu Koodalattupuram 1990 214 p
Avail: Univ. Microfilms Order No. DA9025214

Behavior of an axisymmetric equilibrium turbulent boundary layer disturbed by a propeller wake in the freestream was investigated experimentally. Tests were conducted in a low speed wind tunnel and measurements of turbulence quantities were made using an X wire probe and a constant temperature anemometer. The boundary layer flow on a cylindrical body was characterized by measuring its gross parameters and comparing them with classical values. Propeller speed was measured using an electronic circuit whose output signal was also used to trigger hot wire probes. Gross boundary characteristics of the disturbed boundary layer did not deviate appreciably from the classical two-dimensional turbulent boundary layer except immediately behind the propeller. From conditional sampling it was found that the near wall periodic Reynolds stress approached 30 percent of the conventional time averaged Reynolds stress. Turbulent kinetic energy, kinetic energy of the organized field, and various kinetic energy production terms responsible for exchange of turbulent kinetic energy between different flow fields were calculated from the experimental data. It was found that kinetic energy was being transferred from the organized flow field to the random turbulent flow field, as expected. The variation of both periodic and turbulent kinetic energy were governed by similar equations. A mechanism for the transport of turbulent kinetic energy was suggested. Dissert. Abstr.

N91-11176 Johns Hopkins Univ., Baltimore, MD.
THE CALCULATION OF CORRELATION FUNCTIONS IN THE STATISTICAL THEORY OF TURBULENT FLOWS Ph.D. Thesis
William Stanley Burgett 1990 177 p
Avail: Univ. Microfilms Order No. DA9018564

The field theory of turbulence is developed in a manner that eliminates inconsistencies found in earlier treatments, and leads to new insight into the nature of bounded shear flows. Formal results include the construction of a Ward identity that greatly simplifies analysis at the non-perturbative level, and the specific inclusion of a background field that is not a saddle-point of the Navier-Stokes equation of motion. Correlation functions are calculated that correspond to the bare propagator given by a path integral generating functional developed by Domokos, Kovesi-Domokos and Zoltani. The functions are computed numerically for Gaussian, exponential, and white-noise force-force correlations. From these results it appears that an exponential form most closely realizes the observed correlation functions. For the white-noise case, a simple, but very accurate, analytic form is derived for the xx and yy stresses, and frequency spectra are then obtained. The case of homogeneous isotropic turbulence using the DK-DZ formalism is considered, and Schwinger-Dyson equations are presented for the exact Green's functions through the third order. Dissert. Abstr.

N91-11177 Cincinnati Univ., OH.
A GLOBAL PRESSURE RELAXATION FOR HIGH SPEED LAMINAR AND TURBULENT FLOWS Ph.D. Thesis
Te Liang 1989 199 p
Avail: Univ. Microfilms Order No. DA9019851

The applicability of the Reduced Navier-Stokes (RNS) model is extended to high supersonic flows. The steady-state primitive variable formulation of the RNS equations is employed. The discretization used is a form of flux-difference splitting. The splitting of the streamwise pressure gradient term allows for upstream elliptic influence in subsonic regions through the forward-differenced portion of this term. The finite-difference equations are solved by a streamwise marching line-relaxation procedure developed in previous work. The pressure is the relaxed variable. For some of the flows considered, all shock waves are captured using the conservation form of the governing equations. For flows at higher Mach numbers, the outer bow shock is fitted with the aid of the Rankine-Hugoniot jump conditions. This allows the computational

domain to be limited to the region between the outer shock and the body. All embedded shocks in this region are captured. Flows over a number of geometries including cone, aircraft forebody, cone-cylinder-boattail, cone-cylinder-trough, cone-cylinder-cavity, cone-cylinder-flare, cone-cylinder-base, and base flow with and without a centered jet are investigated. The flow over these geometries at high Reynolds number involves strong viscous-inviscid interactions, embedded shocks and moderate to large separation regions. Laminar and turbulent flows are considered for these axisymmetric bodies. Both the Cebeci-Smith and Baldwin-Lomax turbulence models are employed for turbulent flow calculations. Supersonic and high supersonic flow solutions are obtained. Some comparisons with experimental results are made. Dissert. Abstr.

N91-11178 Oregon State Univ., Corvallis.
AN EXPERIMENTAL STUDY OF NATURAL CONVECTION HEAT TRANSFER FROM A HORIZONTAL CYLINDER ARRAY VERTICALLY ALIGNED TO AND CONFINED BY A SINGLE WALL AND TWO WALLS Ph.D. Thesis
Thamir Rauf Al-Alusi 1989 241 p
Avail: Univ. Microfilms Order No. DA9019151

Convection heat transfer was experimentally investigated for two different geometries. One case had three horizontal cylinders in a vertical plane placed between two vertical walls. The second case had three horizontal cylinders in a vertical plane with only one vertical wall. Several different cylinder center-to-center spacings were investigated. The wall spacings for the two wall and single wall cases were also varied. The cylinders were placed in a still air medium at atmospheric pressure and were maintained at a constant heat flux. The modified Rayleigh number, based on the diameter of the cylinders, ranged from 6.2 x 10(exp 4) to 1.2 x 10(exp 6). A scale analysis was performed to predict the relationship between the Nusselt number and the modified Rayleigh number. A standard finite-difference code was employed to show the temperature distribution and velocity vectors distribution around the cylinders. The results showed that there was a maximum heat transfer from each cylinder at a specific wall-array spacing and a specific center-to-center spacing. Comparisons of heat transfer results with a single free cylinder and a free array of horizontal cylinders were made and discussed. Empirical equations were proposed to predict the effects of the experimental parameters on the heat transfer as expressed by the average Nusselt number of each cylinder or the average Nusselt number of the whole array. Flow visualization was accomplished using laser sheets. The resulting studies showed that the presence of a single wall or the asymmetrical placement of the array between the two walls eliminated the presence of the vortices in the spaces between the cylinders and displaced the stagnation points. The asymmetrical placement of the array between two walls created a reversed current between the two walls. Dissert. Abstr.

N91-11179 California Univ., Los Angeles.
HEAT PIPE VAPOR DYNAMICS Ph.D. Thesis
Farrokh Issacci 1990 173 p
Avail: Univ. Microfilms Order No. DA9022008

The dynamic behavior of the vapor flow in heat pipes is investigated at startup and during operational transients. The vapor is modeled as two-dimensional, compressible viscous flow in an enclosure with inflow and outflow boundary conditions. For steady-state and operating transients, the SIMPLER method is used. In this method a control volume approach is employed on a staggered grid which makes the scheme very stable. It is shown that for relatively low input heat fluxes the compressibility of the vapor flow is low and the SIMPLER scheme is suitable for the study of transient vapor dynamics. It is shown that for a wide range of input heat fluxes, the standard methods, including the SIMPLER scheme, are not suitable. A nonlinear filtering technique, along with the centered difference scheme, are then used for shock capturing as well as solving the cell Reynolds number problem. For high heat flux, the startup transient phase involves multiple shock reflections in the evaporator region. The maximum and maximum-averaged pressure drops in different sections of the heat pipe oscillate periodically with time because of multiple shock reflections. The pressure drop converges to a constant value at steady state. However, it is significantly higher than its steady state value at the initiation of the startup transient. The time for the vapor core to reach steady-state condition depends on the input heat flux, the heat pipe geometry, the working fluid, and the condenser conditions. However, the vapor transient time, for an Na-filled heat pipe is on the order of seconds. Depending on the time constant for the overall system, the vapor transient time may be very short. Therefore, the vapor core may be assumed to be quasi-steady in the transient analysis of a heat pipe operation. Dissert. Abstr.

N91-11180 Drexel Univ., Philadelphia, PA.
HEAT TRANSFER AND FLOW STUDIES IN AN ABRUPT EXPANSION PIPE WITH NON-NEWTONIAN FLUIDS Ph.D. Thesis
Bockchoon Pak 1989 224 p
Avail: Univ. Microfilms Order No. DA9009701

The heat transfer and flow behaviors of non-Newtonian fluids through an abrupt expansion circular pipe were investigated. The current study consists of two parts: (1) experimental heat transfer and pressure distribution tests in turbulent flow for water and drag reducing viscoelastic fluids with expansion ratios (D/d) of 1.39 and 1.90; and (2) flow visualization experiments studying the separation and reattachment behavior of water and non-Newtonian fluids (i.e., purely viscous fluids and viscoelastic fluids), in both laminar and turbulent flows, using a dye injection technique with expansion ratios of 2.00 and 2.67 and numerical simulation for fluid flows. The hypothesis of the current investigation that the long thermal entrance length of a viscoelastic fluid could be used as a tool to enhance convective heat transfer through an abrupt expansion pipe was validated. In flow visualization studies the reattachment length for aqueous solutions of polyacrylamide in the laminar flow was found to be much shorter than that for water. Dissert. Abstr.

N91-11181 Stanford Univ., CA.
INSTABILITIES OF TWO-DIMENSIONAL INVISCID COMPRESSIBLE VORTICES Ph.D. Thesis
William Machado Chan 1990 186 p
Avail: Univ. Microfilms Order No. DA9024317

The linear stability and subsequent nonlinear evolution and acoustic radiation of a perturbed circular two-dimensional inviscid compressible vortex is examined. Initially, a normal-mode linear-stability analysis is performed for distributions more general than uniform vorticity and entropy. It is found that vortices with smoother vorticity profiles than an isolated uniform-vorticity (Rankine) are also unstable; however, only neutrally-stable waves are found for the Oseen (Gaussian) profile. The effects of entropy gradient are investigated through a model problem. For the particular entropy profile chosen, a positive average entropy-gradient in the vortex core is found to have a destabilizing effect while the opposite is true for a negative average entropy-gradient. The far-field acoustic flux computed from eigenfunctions for a homentropic case obeys the scaling relation of Lighthill at small Mach numbers and provides a correction for higher Mach numbers. Next, the linear initial-value problem is studied by finite-difference methods. It is found that these methods are capable of accurately computing the frequencies and weak growth rates of the normal modes. The sensitivity of the results to different numerical parameters is investigated. Finally, the nonlinear development of an elliptic-mode perturbation is studied by numerical solution of the Euler equations with finite differences. The initial linear phase is followed by elongation of the vortex core and steepening of compression regions. The elongation of the core continues until the vortex fissions into two co-rotating vortices. The individual vortices then gradually move away from each other while their rate of rotation about the mid-point between them slowly decreases. The acoustic flux reaches a maximum at the time of the fission and decreases as the vortices move apart. Dissert. Abstr.

N91-11182 Arizona Univ., Tucson.
BOUNDARY LAYER RECEPTIVITY MECHANISMS RELEVANT TO LAMINAR FLOW CONTROL Ph.D. Thesis
Meelan Choudhari 1990 183 p
Avail: Univ. Microfilms Order No. DA9022102

Receptivity processes by which free-stream acoustic waves generate instability waves in boundary layers are investigated. Concentration is placed on mechanisms associated with local regions of short scale variation in wall suction or admittance distribution. These mechanisms are relevant to laminar flow control technology, in which suction is utilized to control the growth of boundary layer instabilities. The receptivity process requires a transfer of energy from the long wavelength of the free-stream disturbance to the short wavelength of the instability wave. Time harmonic, 2-D and 3-D interactions are analyzed using the asymptotic, high Reynolds number, triple deck structure. The acoustic wave orientation and the geometry of the wall suction or admittance distribution are found to significantly influence the amplitude of the generated instability wave. Dissert. Abstr.

N91-11183 Mississippi State Univ., Starkville.
MEASUREMENT AND CALCULATION OF SURFACE ROUGHNESS EFFECTS ON TURBULENT FLOW AND HEAT TRANSFER Ph.D. Thesis
Mohammad Hosein Hosni 1989 255 p
Avail: Univ. Microfilms Order No. DA9020651

Fluid dynamics and heat transfer data for turbulent boundary layer flow of air over a smooth surface and three well-defined rough surfaces were taken in the Turbulent Heat Transfer Test Facility (THTTF) for x-Reynolds numbers ranging up to 10,000,000. The smooth wall data provided base line data for comparison with the data from rough surfaces. The three rough surfaces were composed of 1.27 mm diameter hemispheres spaced 2, 4, and 10 diameters apart, respectively, in staggered arrays on otherwise smooth flat plates. Skin friction coefficient distributions and boundary layer profiles of mean velocity and Reynolds stresses were obtained using hot-wire anemometry. The THTTF heat transfer data taken in aerodynamically smooth, transitionally rough, and fully rough flow regimes over the three well-defined rough surfaces for freestream velocities of 6, 12, 28, 43, 58, and 67 m/s were compared with the data sets taken at Stanford University using a single well-defined rough surface. It was observed that the Stanton numbers for a given surface collapse together in x-Reynolds number coordinates as the freestream velocity increases, with the Stanton number level being larger for rougher surfaces. The THTTF heat transfer data and the Stanford data were used to modify the roughness energy transport model in the discrete element prediction method. This method was used in calculation of the fluid dynamics and heat transfer for the THTTF and Stanford surfaces. The predictions were in excellent agreement with all data sets within the data uncertainty. Dissert. Abstr.

N91-11184 Tennessee Univ., Knoxville.
ACCURACY, CONVERGENCE AND STABILITY OF FINITE ELEMENT ALGORITHMS FOR INCOMPRESSIBLE FLUID FLOW Ph.D. Thesis
Wilbert Paul Noronha 1989 243 p
Avail: Univ. Microfilm Order No. DA9021040

Taylor weak statement finite element CFD algorithms were developed for the two-dimensional unsteady, incompressible Navier-Stokes equations in the form of vorticity-streamfunction, a penalty method, and a new harmonic constraint formulation. A multi-dimensional (tensorial) artificial dissipative mechanism is derived and verified for effective stability control. An asymptotic rate of convergence study is conducted and compared with model problem theoretical estimates. The harmonic constraint algorithm is developed in an efficient time-accurate algorithm and proposed as a viable candidate for extension to three dimensions. The linear algebra problem associated with an embedded elliptic equation is resolved by a newly developed robust and accurate consistent sparse factorization numerical linear algebra procedure.
Dissert. Abstr.

N91-11185# Oak Ridge National Lab., TN.
PERFORMANCES OF FOUR MAGNETIC HEAT-PUMP CYCLES
F. C. Chen, R. W. Murphy, V. C. Mei, and G. L. Chen 1990 14 p Presented at the International Symposium on Gas-Liquid Two-Phase Flows in Conjunction With the Winter Annual Meeting of the ASME, Dallas, TX, 25-30 Nov. 1990
(Contract DE-AC05-84OR-21400)
(DE90-015606; CONF-901109-18) Avail: NTIS HC/MF A03

Magnetic heat pumps (MHP) have been successfully used for refrigeration applications at near absolute-zero-degree temperatures. In these applications, a temperature lift of a few degrees in a cryogenic environment is sufficient and can be easily achieved by a simple magnetic heat-pump cycle. To extend magnetic heat pumping to other temperature ranges and other types of applications in which the temperature lift is more than just a few degrees requires more involved cycle processes. This paper investigates the characteristics of a few better-known thermomagnetic heat-pump cycles (Carnot, Ericsson, Stirling, and regenerative) in extended ranges of temperature lift. The regenerative cycle is the most efficient one. For gadolinium operating between 0 and 7 T (Tesla) in a heat pump cycle with a heat-rejection temperature of 320 K, our analysis predicted a 42 percent loss in coefficient of performance at 260 K cooling temperature, and a 15 percent loss in capacity at 232 K cooling temperature for the constant-field cycle as compared with the ideal regenerative cycle. Such substantial penalties indicate that the potential irreversibilities from this one source (the additional heat transfer that would be needed for the constant-field vs the ideal regenerative cycle) may adversely affect the viability of certain proposed MHP concepts if the relevant loss mechanisms are not adequately addressed. DOE

N91-11186# Oak Ridge National Lab., TN.
THERMAL PERFORMANCE ANALYSIS FOR HEAT EXCHANGERS USING NONAZEOTROPIC REFRIGERANT MIXTURES
E. Granryd (Royal Inst. of Tech., Stockholm, Sweden) and J. C. Conklin 1990 9 p Presented at the ASME Winter Annual Meeting, Dallas, TX, 25-30 Nov. 1990
(Contract DE-AC05-84OR-21400)
(DE90-016030; CONF-901194-1) Avail: NTIS HC/MF A02

Nonazeotropic refrigerant mixtures (NARMs) are under investigation to replace chlorofluorocarbon compounds. This analysis describes a general approach for analyzing the thermal performance of heat exchangers using NARMs. The thermal performance of a NARM evaporator or condenser is analyzed as a heat exchanger operating between two fluids, one of which has a varying specific heat with respect to enthalpy. For NARMs in the two-phase region, the saturation temperature is not only a function of pressure, but also of vapor quality or enthalpy. Many NARMs have nonlinear enthalpy and temperature relationships in the two-phase region that require corrections to the conventional heat exchanger thermal performance relationships. A pinch point may occur under certain conditions in the heat exchanger, with the resultant penalties. These pinch points may be avoided by selecting a NARM with a desirably shaped temperature-enthalpy curve so that a condenser or evaporator will have a desirable thermal performance. A criterion is presented to identify when such a desirable thermal performance occurs in heat exchangers. Heat exchanger effectiveness and number of transfer units (NTU) relationships are presented for fluids having an assumed linear and quadratic dependence of specific heat with respect to quality. The thermal performance method is general, such that NTU effectiveness relationships can be generated for fluids having a specific heat that is an arbitrary function of quality. DOE

N91-11187# Pennsylvania State Univ., University Park.
MAGNETOHYDRODYNAMIC MODIFICATION OF THE TEACH-T CODE AND THE PREDICTION OF THE MAXIMUM AZIMUTHAL VELOCITY IN A CONDUCTING FLUID M.S. Thesis
Michael Greene Willis Dec. 1989 80 p
(Contract DE-AC05-76OR-00033)
(DE90-017510; DOE/OR-00033/T444) Avail: NTIS HC/MF A05

An extension of the 2-D turbulent fluid dynamics code, TEACH, is developed. This extension incorporates a third (azimuthal) velocity component, with azimuthal symmetry assumed. Also included is the ability to solve for an electrostatic potential field with given boundary conditions. This electrostatic potential yields an electric field which, when coupled with the included constant magnetic field, produces Lorentz forces. These are accounted for as body forces in the appropriate components of the Navier-Stokes' momentum equation. The extensions in the code are compared with analytic results where possible and are found to be highly accurate. Finally, a semi-empirical correlation is developed to predict the magnitude and position of the maximum value of the added velocity component give the magnetic field strength and the value of the potential difference between an assumed central electrode and grounded outer shell. The correlation is seen to give excellent results for a wide range of electrostatic potential boundary conditions and magnetic field strengths acting on the working fluid sodium. DOE

N91-11188# Oak Ridge National Lab., TN. Instrumentation and Controls Div.

MEASUREMENT OF TWO-PHASE FLOW MOMENTUM WITH FORCE TRANSDUCERS

J. E. Hardy and J. E. Smith 1990 8 p Presented at the International Symposium on Gas-Liquid Two-Phase Flows in Conjunction with the Winter Annual Meeting of ASME, Dallas, TX, 25-30 Nov. 1990

(Contract DE-AC05-84OR-21400)

(DE90-008748; CONF-901109-1) Avail: NTIS HC/MF A02

Two strain-gage-based drag transducers were developed to measure two-phase flow in simulated pressurized water reactor (PWR) test facilities. One transducer, a drag body (DB), was designed to measure the bidirectional average momentum flux passing through an end box. The second drag sensor, a break through detector (BTD), was designed to sense liquid downflow from the upper plenum to the core region. After prototype sensors passed numerous acceptance tests, transducers were fabricated and installed in two experimental test facilities, one in Japan and one in West Germany. High-quality data were extracted from both the DBs and BTDs for a variety of loss-of-coolant accident (LOCA) scenarios. The information collected from these sensors has added to the understanding of the thermohydraulic phenomena that occur during the refill/reflood stage of a loss of coolant accident (LOCA) in a PWR. DOE

N91-11189# Idaho Nuclear Corp., Idaho Falls.

RESIDUAL STRESS AT FLUID INTERFACES

Paul E. Murray 1990 12 p Presented at the International Symposium on Gas-Liquid Two-Phase Flows in Conjunction with the Winter Annual Meeting of ASME, Dallas, TX, 25-30 Nov. 1990

(Contract DE-AC07-76ID-01570)

(DE90-012964; EGG-M-90064; CONF-901109-7) Avail: NTIS HC/MF A03

We extend the Navier-Stokes equations to allow for residual stress in Newtonian fluids. A fluid, which undergoes a constrained volume change, will have residual stress. Corresponding to every constrained volume change is an eigenstrain. We present a method to include in the equations of fluid motion the eigenstrain that is a result of the presence in a fluid of a soluble chemical species. This method is used to calculate the residual stress associated with a chemical transformation. DOE

N91-11190# Argonne National Lab., IL. Materials and Components Technology Div.

UNSTEADY FLUID FORCES AND FLUIDELASTIC VIBRATION OF A GROUP OF CIRCULAR CYLINDERS

S. S. Chen 1990 15 p Presented at the International Symposium on Gas-Liquid Two-Phase Flows in Conjunction with the Winter Annual Meeting of the ASME, Dallas, TX, 25-30 Nov. 1990

(Contract W-31-109-eng-38)

(DE90-013661; CONF-901109-8) Avail: NTIS HC/MF A03

When a single cylinder oscillates in a quiescent fluid, its natural frequencies and model damping values are affected by the surrounding fluid; these fluid effects can generally be accounted for by fluid added mass and fluid damping forces. In a flowing fluid, added mass and fluid damping are dependent of flow velocity, and other fluid force components, fluid-stiffness force and fluid excitation force, are also important. In contrast to an isolated cylinder, the motion of a particular cylinder in a group will excite the surrounding cylinders; this type of oscillation is generally called fluidelastic vibration. Fluidelastic vibrations of multiply cylinders are attributed to fluid inertia, fluid damping, and fluid stiffness forces as well as fluid excitation forces. Once the fluid excitation forces and motion-dependent fluid forces acting on cylinders are known, coupled fluidelastic oscillations of a group of cylinders can be analyzed. The objectives of this note are to summarize the recent development of the state-of-the-art of this subject, including quiescent fluid, axial flow, crossflow, and future research needs. DOE

N91-11191# Pacific Northwest Lab., Richland, WA.

JAPANESE POWER ELECTRONICS INVERTER TECHNOLOGY AND ITS IMPACT ON THE AMERICAN AIR CONDITIONING INDUSTRY

Kenji Ushimaru (Energy International, Inc., Bellevue, WA.) Aug. 1990 77 p

(Contract DE-AC06-76RL-01830)

(DE90-014843; PNL-7397) Avail: NTIS HC/MF A05

Since 1983, technological advances and market growth of inverter-driven variable-speed heat pumps in Japan have been dramatic. The high level of market penetration was promoted by a combination of political, economic, and trade policies in Japan. A unique environment was created in which the leading domestic industries, microprocessor manufacturing, compressors for air conditioning and refrigerators, and power electronic devices, were able to direct the development and market success of inverter-driven heat pumps. As a result, leading U.S. variable-speed heat pump manufacturers should expect a challenge from the Japanese producers of power devices and microprocessors. Because of the vertically-integrated production structure in Japan, in contrast to the out-sourcing culture of the United States, price competition at the component level (such as inverters, sensors, and controls) may impact the structure of the industry more severely than final product sales. DOE

N91-11192*# National Aeronautics and Space Administration. Lewis Research Center, Cleveland, OH.

NAVIER-STOKES ANALYSIS OF TRANSONIC CASCADE FLOW

A. Arnone (Florence Univ., Italy), M.-S. Liou, and L. Povinelli Oct. 1990 12 p

(NASA Order C-99066-G)

(NASA-TM-103624; E-5791; NAS 1.15:103624; ICOMP-90-23) Avail: NTIS HC/MF A03 CSCL 20D

A new kind of C-type grid is proposed, this grid is non-periodic on the wake and allows minimum skewness for cascades with high turning and large camber. Reynolds-averaged Navier-Stokes equations are solved on this type of grid using a finite volume discretization and a full multigrid method which uses Runge-Kutta stepping as the driving scheme. The Baldwin-Lomax eddy-viscosity model is used for turbulence closure. A detailed numerical study is proposed for a highly loaded transonic blade. A grid independence analysis is presented in terms of pressure distribution, exit flow angles, and loss coefficient. Comparison with experiments clearly demonstrates the capability of the proposed procedure. Author

N91-11193# Max-Planck-Inst. fuer Stroemungsforschung, Goettingen (Germany, F.R.).

THE GENERALIZED DIFFUSION THEORY OF SIMPLY DEFORMABLE PARTICLE-FLUID TWO-PHASE FLOWS

Nguyen VanDiep (National Center for Scientific Research of Vietnam, Hanoi.) Apr. 1990 38 p Sponsored by Deutsche Akademie Austauschdienst

(MPIS-7/1990; ISSN-0436-1199; ETN-90-97903) Avail: NTIS HC/MF A03

The generalized diffusion theory of deformable particle fluid two phase flows is constructed. A theory for fluids with microstructure, the extended theory of irrotational flow due to a moving deformable body and the generalized diffusion theory of heterogeneous mixtures are applied. By using the principle of form invariance of the energy change under superposed arbitrary rigid motions, the equations to determine the main parameters of the motion are obtained. On the basis of generalized irreversible thermodynamics the linear and nonlinear constitutive equations are obtained. The case of the fluid flow with deformable spherical particles is considered. The obtained equations are used to study bubble liquid two phase flows. The problems of kinematic wave and acoustic wave propagation, and of bubble migration in pipe flows are considered as examples to illustrate the theory. ESA

N91-11194# West Virginia Univ., Morgantown. Dept. of Civil Engineering.
THEORETICAL AND NUMERICAL STUDIES OF CONSTITUTIVE RELATIONS FOR FRICTIONAL GRANULAR FLOW Annual Report, Jan. - Dec. 1989
D. D. Gray and J. M. Stiles Apr. 1990 37 p
(Contract DE-FC21-87MC-24207)
(DE90-009662; DOE/MC-24207/2852) Avail: NTIS HC A03/MF A01

This report describes progress made during the period January 1 through December 31, 1989. Most of the effort in the first three quarters of this period was devoted to assigning numerical values to material constants used in the frictional granular constitutive relationship and implementing that constitutive relationship in the computer program MFIX. MFIX is a hydrodynamic code that models the fluidized flow of solid particles of various sizes and densities. However, because of the apparent lack of success in implementing the frictional constitutive relationship in the computer program MFIX, it was decided that future work should be directed toward writing problem-specific computer programs for several test problems. The computer program CHUTE is a three-dimensional semi-implicit finite difference hydrodynamic code designed to solve the truncated momentum equation along with the other governing equations for the frictional gravity flow of granular materials down an inclined open channel. The initial results generated by program CHUTE have indicated that fatal errors are present in the subroutine that adjusts the velocities. Work to rectify these errors is in progress. DOE

N91-11195# Lawrence Livermore National Lab., CA.
TOPAZ2D HEAT TRANSFER CODE USERS MANUAL AND THERMAL PROPERTY DATA BASE
A. B. Shapiro and A. L. Edwards May 1990 188 p
(Contract W-7405-eng-48)
(DE91-000075; UCRL-ID-104558) Avail: NTIS HC/MF A09

TOPAZ2D is a two dimensional implicit finite element computer code for heat transfer analysis. This user's manual provides information on the structure of a TOPAZ2D input file. Also included is a material thermal property data base. This manual is supplemented with The TOPAZ2D Theoretical Manual and the TOPAZ2D Verification Manual. TOPAZ2D has been implemented on the CRAY, SUN, and VAX computers. TOPAZ2D can be used to solve for the steady state or transient temperature field on two dimensional planar or axisymmetric geometries. Material properties may be temperature dependent and either isotropic or orthotropic. A variety of time and temperature dependent boundary conditions can be specified including temperature, flux, convection, and radiation. Time or temperature dependent internal heat generation can be defined locally be element or globally by material. TOPAZ2D can solve problems of diffuse and specular band radiation in an enclosure coupled with conduction in material surrounding the enclosure. Additional features include thermally controlled reactive chemical mixtures, thermal contact resistance across an interface, bulk fluid flow, phase change, and energy balances. Thermal stresses can be calculated using the solid mechanics code NIKE2D which reads the temperature state data calculated by TOPAZ2D. A three dimensional version of the code, TOPAZ3D is available. DOE

N91-11196# Universiteit Twente, Enschede (Netherlands).
GAS-LIQUID CONTACTING AT ELEVATED PRESSURES Ph.D. Thesis
Martin Herke Oyevaar 1989 159 p Sponsored by Netherlands Foundation for Chemical Research, and Netherlands Organization for the Advancement of Scientific Research
(ETN-90-97773) Avail: NTIS HC/MF A08

The influence of pressure on gas-liquid contacting was investigated in several gas-liquid reactors. Interfacial areas and gas hold-ups in mechanically agitated gas-liquid reactors and bubble columns were determined at elevated pressures up to 8.0 MPa. Results indicate that the operating pressure in these gas-liquid contactors has a considerable effect on the interfacial area and the gas hold-up. Correlations between them may therefore lead to miscalculations at higher pressure, and specific attention should be paid to the effect of pressure on the interfacial area and the gas hold-up. ESA

N91-11197# European Space Agency, Paris (France).
PARALLELIZATION ON A MULTI-PROCESSOR SYSTEM OF A SOLVING METHOD FOR THE UNSTEADY NAVIER-STOKES EQUATIONS AT HIGH REYNOLDS NUMBERS
Laure Mane Aug. 1990 144 p Transl. into ENGLISH of Parallelisation sur un Systeme Multiprocesseur d'une Methode de Resolution des Equations de Navier-Stokes Instationnaires a Grands Nombres de Reynolds (Paris, France, ONERA), 1987 111 p Original language document was announced as N88-26632
(ESA-TT-1116; ONERA-NT-1987-8; ETN-90-97999) Avail: NTIS HC/MF A07

A method for the simulation of viscous incompressible flows around an airfoil is presented which provides resolution of the two dimensional Navier-Stokes equations in stream function and vorticity function formulation. High precision finite difference schemes and Alternating Directions Implicit (ADI) techniques are combined. The algorithm was implemented on a multiprocessor to cope with the parallelism required by ADI methods. The parallelization of the algorithm and performance levels of the parallel code are set out. Pulsed-start numerical simulations on a NACA 0012 airfoil were performed for various airfoil incidence angles and for Reynolds number up to 10 to the 5th power. The phenomena obtained, the influence of the calculation parameters are discussed and comparison between numerical and experimentally visualized results validates the method. ESA

N91-11198# European Space Agency, Paris (France).
LARGE EDDY-SIMULATION OF CONVECTIVE BOUNDARY LAYERS
Helmut Schmidt (Deutsche Forschungs- und Versuchsanstalt fuer Luft- und Raumfahrt, Oberpfaffenhofen, Germany, F.R.) Aug. 1990 195 p Transl. into ENGLISH of Grobstruktur-Simulation Konvektiver Grenzschichten (Oberpfaffenhofen, Fed. Republic of Germany, DFVLR), Aug. 1988 146 p Original language document was announced as N89-19522
(ESA-TT-1138; DFVLR-FB-88-30; ETN-90-98002) Avail: NTIS HC/MF A09

A numerical method for calculating the large eddy structure (coarse structure) of three dimensional and non-stationary turbulent flows is presented. The calculation of free convection in the atmosphere using this method shows coherent spoke-like thermal structure in the lower boundary layer and isolated thermal plumes and thermal bubbles in the upper boundary layer. By comparison with the homogeneous case, large scale inhomogeneous heat fluxes at the surface cause an increase in horizontal velocity fluctuations in the entire boundary layer. By contrast with gradient relationships, the use of a turbulence model derived from the closure equations of second order yields substantially more exact results with little increase in computing costs. ESA

N91-11199# European Space Agency, Paris (France).
NUMERICAL SIMULATION OF TRANSITION FROM LAMINAR TO TURBULENT DUCT FLOW
Norbert Gilbert (Deutsche Forschungs- und Versuchsanstalt fuer Luft- und Raumfahrt, Goettingen, Germany, F.R.) Aug. 1990

191 p Transl. into ENGLISH of Numerische Simulation der Transition von der Laminaren in die Turbulente Kanalstroemung (Goettingen, Fed. Republic of Germany, DFVLR), Mar. 1988 148 p Original language document was announced as N89-25430 (ESA-TT-1144; DFVLR-FB-88-55; ETN-90-98004) Avail: NTIS HC/MF A09; original German version available from DFVLR, Wissenschaftliches Berichtwesen, Postfach 90 60 58, 5000 Cologne, Fed. Republic of Germany, 50.50 Deutsche marks

Laminar turbulent transition in a 2-D duct is simulated, starting from laminar Poiseuille flow with super-imposed Tollmien-Schlichting waves and continuing until the turbulent range is reached. The 3-D incompressible Navier-Stokes equations are solved directly by a spectral method, i.e., without a turbulence model. A model in which the flow develops in time and is periodic in space is used. The results of a simulation using a spatial resolution of up to 128 cubed grid points are presented and compared with available experimental data. Good agreement with experiment is found in both the transition range and the fully turbulent range. A transition function, for use when modeling laminar turbulent transitions by means of algebraic turbulence models, is derived from the simulation data. Modeling assumptions used in conventional turbulence models are examined and discussed using the numerical results obtained in the fully developed turbulence range. ESA

N91-10895*# National Aeronautics and Space Administration. Ames Research Center, Moffett Field, CA.
VISUALIZATION OF FLUID DYNAMICS AT NASA AMES
Val Watson *In its* NASA Computational Fluid Dynamics Conference. Volume 2: Sessions 7-12 Sep. 1989 p 451-465 (For primary document see N91-10868 02-02)
Avail: NTIS HC/MF A22; 30 functional color pages CSCL 01A

N91-10896*# National Aeronautics and Space Administration. Ames Research Center, Moffett Field, CA.
COMPUTATIONAL FLUID DYNAMICS ON A MASSIVELY PARALLEL COMPUTER
Dennis C. Jespersen and Creon Levit *In its* NASA Computational Fluid Dynamics Conference. Volume 2: Sessions 7-12 Sep. 1989 p 467-481 (For primary document see N91-10868 02-02)
Avail: NTIS HC/MF A22; 30 functional color pages CSCL 01A

35 INSTRUMENTATION AND PHOTOGRAPHY

Includes remote sensors; measuring instruments and gages; detectors; cameras and photographic supplies; and holography.

For aerial photography see *43 Earth Resources and Remote Sensing*. For related information see also *06 Aircraft Instrumentation*, and *19 Spacecraft Instrumentation*.

N91-11200# National Aerospace Lab., Tokyo (Japan).
EXPERIMENTAL MANUFACTURING OF PERFORMANCE EVALUATION SYSTEM FOR SOLID IMAGE SENSOR [KOTAI GAZO SENSA SEINO HYOUKA SHISUTEMU NO SHISAKUKENKYU]
Kozo Honma, Masao Naka, and Hajime Koshiishi Jul. 1988 34 p In JAPANESE
(NAL-TM-591; ISSN-0452-2982; JTN-90-80134) Avail: NTIS HC/MF A03

The main purpose of this research is to construct a basic performance evaluation system in order to grasp the characteristics of the charge coupled device (CCD) sensor. The CCD sensor is made by combining the solid charge coupled device and the image optical system. Therefore, to use remote sensing data derived from the CCD sensor effectively, it is necessary to grasp such characteristics of the image as the sensitivity, the interaction characteristics between pixels, the geometrical deformation of optical system, and the modulation transfer function sufficiently. This evaluation system involves initial performances and functions. Therefore it can be used for the performance evaluation of the modulation transfer function of the CCD image sensor. It could also be widely used for the evaluation of other types of sensors. Furthermore the automation of the measurement of modulation transfer function enables this system to extend the widely used one. The upgrading of the system is also possible. NASDA

N91-11201# Messerschmitt-Boelkow-Blohm G.m.b.H., Munich (Germany, F.R.). Dienstleistungsbereich.
BIOSENSORS: DEVELOPMENT STATUS [BIOSENSOREN: STAND DER ENTWICKLUNG]
R. Hilpert 1989 23 p In GERMAN
(MBB-Z-0305-90-PUB; ETN-90-97882) Avail: NTIS HC/MF A03

The progress achieved in the field of biosensors is described. Following a definition of the concept, the main function of biosensors is explained, using an example. Several measuring transformers and their functions are presented. The proper methods of connection between biological constituents and measuring transformers are indicated. Possible uses, biosensor markets, currently available commercial biosensors are mentioned. Main problems and their solutions in the framework of biosensor develoment are outlined. National and international centers of development are indicated. A project concerning biosensors for water supervision is described. ESA

N91-11202# Cologne Univ. (Germany, F.R.). Inst. fuer Geophysik und Meteorologie.
THE CONTROL SYSTEM OF AN AIRBORNE RADIOMETER: A PROCESS FOR A TWO DIMENSIONAL RECONSTRUCTION OF IRREGULAR SCANNED RADIOMETER DATA [DIE STEUERUNG EINES FLUGZEUGGETRAGENEN RADIOMETERS. EIN VERFAHREN ZUR ZWEIDIMENSIONALEN REKONSTRUKTION VON UNREGELMAESSIG ABGETASTETEN RADIOMETERDATEN]
Peter Armbruester 1990 111 p In GERMAN
(Mitt-70; ISSN-0069-5887; ETN-90-97894) Avail: NTIS HC/MF A06

The instrumental control and data processing software of an airborne radiometer, the AVCSR (Airborne Version of the Conical Scan Radiometer) is investigated. The scientific aims and the instrument itself are described and the programs for the control of the instrument and the data processing are given. The program for static and dynamic simulation of the instrument and its scanning properties are presented. Another program performs a data report after flight that gives a more detailed insight into the instrument parameters and the measurements taken during flight. A two dimensional reconstruction algorithm for the irregularly spaced measurement points of the AVCSR is described. This new algorithm is compared to standard methods (bilinear interpolation and bicubic spline interpolation) for a one dimensional test scene. It is found to be superior to linear interpolation, but not to bicubic spline interpolation. ESA

N91-11203# Universitaet der Bundeswehr, Hamburg (Germany, F.R.). Fachbereich Maschinenbau.
EVALUATION PROCESS FOR THE EXAMINATION OF CURVED SURFACE WORKPIECES USING COORDINATE MEASURING INSTRUMENTS Ph.D. Thesis [AUSWERTEVERFAHREN FUER DIE PRUEFUNG VON WERKSTUECKEN MIT GEKRUEMMTEN OBERFLAECHEN MIT KOORDINATENMESSGERAETEN]
Bernd Gawande 1989 103 p In GERMAN
(ETN-90-97901) Avail: NTIS HC/MF A06

Formulations for implicit surface description and for description through standard formal elements are presented. On the basis of these descriptions adjusting algorithms were developed, allowing the Gauss as well as the Tschebyscheff adjusting criterion. The suitability of the surface description and the operativeness of the adjusting algorithms were demonstrated, using test data records and real measuring values. ESA

N91-11204# Oak Ridge Y-12 Plant, TN.
AN AUTOMATED LINEARITY TEST FOR DIRECT VOLTAGE CALIBRATORS
Ross Endsley 12 Apr. 1990 9 p Presented at the 1990 National Conference of Standards Laboratories (NCSL) Symposium and Workshop, Washington, DC, 19-23 Aug. 1990
(Contract DE-AC05-84OS-21400)
(DE90-016927; Y/IB-20; CONF-9008134-3) Avail: NTIS HC/MF A02

The complete calibration of direct voltage calibrators should include a linearity calibration. The method described uses a string of thermally lagged resistors in series across a stable voltage source to provide fixed reference points for the calibration. A high-resolution digital multimeter is used to compare voltage increments in the output of the calibrator. The calibrator and the instruments in the linearity test system are controlled by computer via the IEEE-488 bus. The measured linearity is the result of standard ration techniques. The test is suggested not only as a general purpose technique, but also as a source of assistance in dealing with traceability questions arising over instruments employing international calibration routines. DOE

N91-11205*# National Aeronautics and Space Administration. Lewis Research Center, Cleveland, OH.
HEAT FLUX MEASUREMENT IN SSME TURBINE BLADE TESTER
Curt H. Liebert Nov. 1990 20 p Presented at the 2nd Annual Conference on Health Monitoring for Space Propulsion Systems, Cincinnati, OH, 14-15 Nov. 1990; sponsored in part by Cincinnati Univ.
(NASA-TM-103274; E-5719; NAS 1.15:103274) Avail: NTIS HC/MF A03 CSCL 14B

Surface heat flux values were measured in the turbine blade thermal cycling tester located at NASA-Marshall. This is the first time heat flux has been measured in a space shuttle main engine turbopump environment. Plots of transient and quasi-steady state heat flux data over a range of about 0 to 15 MW/sq m are presented. Data were obtained with a miniature heat flux gage device developed at NASA-Lewis. The results from these tests are being incorporated into turbine design models. Also, these gages are being considered for airfoil surface heat flux measurement on turbine vanes mounted in SSME turbopump test bed engine nozzles at Marshall. Heat flux effects that might be observed on degraded vanes are discussed. Author

36 LASERS AND MASERS

Includes parametric amplifiers.
For related information see also *76 Solid-State Physics.*

N91-11206# Naval Research Lab., Washington, DC.
REVIEW OF FREE ELECTRON LASERS
C. W. Roberson and P. Sprangle 1990 151 p
(PB90-255480) Avail: NTIS HC/MF A08 CSCL 20E

Free electron laser (FEL) theory and experiments are reviewed. The physical mechanism responsible for the generation of coherent radiation in the FEL is described and the fundamental role of the beam is emphasized. The relationship of the FEL interaction to the beam plasma interaction is pointed out. Various FEL operating regimes are discussed; these include the high gain Compton and Raman regimes, both with and without an axial guiding magnetic field. The linear and nonlinear regimes are examined in detail, with particular emphasis on techniques for achieving efficiency enhancement. The quality of the electron beam used to drive FELs is a critical factor in determining the gain and efficiency. The subject of electron beam quality, for different accelerators, is discussed. Key proof-of-principle experiments for FELs in an axial guiding magnetic field, as well as those driven by induction linacs, RF linacs, electrostatic accelerators, and storage rings are reviewed. Finally, the requirements on wiggler and resonators are discussed. Author

N91-11207# National Inst. of Standards and Technology, Boulder, CO. Electromagnetic Technology Div.
SCANNING SYSTEM FOR MEASURING UNIFORMITY OF LASER DETECTOR RESPONSE AND LASER BEAM DIMENSIONS
A. L. Rasmussen, W. E. Case, and A. A. Sanders Apr. 1990 101 p
(PB90-257619; NISTIR-90/3937) Avail: NTIS HC/MF A06 CSCL 20E

The reliability of detector calibration depends upon the uniformity of detector response and the dimensions of the interacting laser beam. The report describes a computer-controlled scanning system for measuring these parameters. Appendixes A through J present many important details needed to understand and use the system. Appendix J describes the linear detector (ROSY 7-1) that monitors the detector under calibration in the scanning system. The device to be measured is scanned in a plane perpendicular to the axis of a stationary laser beam. Software using output and position data give surface graphics and information, and beam radius and shape. To determine linearity, measurements are made at two or more power densities. The user may determine experimentally the effect of changing beam size on uniformity measurements. Uniformity scans in the report fluctuated more for smaller beams than larger ones. They were smoothed and rounded for beams larger than coordinate steps. The remainder of the report describes system layout and interfacing parts, software, measurement procedures, examples, applications, and conclusions. GRA

N91-11208 Dartmouth Coll., Hanover, NH.
PLANAR OROTRON: A TUNABLE, GRATING-BASED FREE ELECTRON LASER Ph.D. Thesis
Purabi Mukhopadhyay Phillips 1987 130 p
Avail: Univ. Microfilms Order No. DA9018548

A compact, coherent, and tunable source of mm wavelength radiation was developed. In the device a periodic, rectangular, metallic grating is used as a slow wave structure, in an electron beam driven open resonator. Methods of optimizing grating and electron beam parameters, in order to achieve high frequency, a broad tuning range, high gain and maximum output power are discussed. Experiments performed with several gratings produced radiation from 28 to 100 GHz. Beam voltages were less than 20 kV. The highest output power achieved is 5 kW and the highest efficiency recorded is 7 percent. Based on the general theory developed and its agreement with the experimental observations in the mm wavelength range, the possibility of producing coherent radiation from microwave to visible wavelengths with structures of this type are considered. Dissert. Abstr.

N91-11209# Oak Ridge National Lab., TN. Chemical Physics Section.
LASER APPLICATIONS FOR HIGH-T(SUB c) SUPERCONDUCTORS
C. H. Chen, R. C. Phillips, and M. P. McCann 1990 6 p Presented at the 5th International Symposium on Resonance Ionization Spectroscopy and Its Applications, Varese, Italy, 16-21 Sep. 1990
(Contract DE-AC05-84OR-21400)
(DE90-017743; CONF-9009174-2) Avail: NTIS HC/MF A02

Laser ablation and resonance ionization were used to monitor superconductive film preparation. From the desorption spectra, trapped O2 in high (Tc) superconductors was found to play an important role in superconductivity. DOE

N91-11210# Universiteit Twente, Enschede (Netherlands).
PULSE EVOLUTION IN MULTI-ATMOSPHERE CO2 LASERS Ph.D. Thesis
Ronald Johannes Mari Bonnie 1989 97 p Sponsored by Netherlands Organization for the Advancement of Pure Research
(ETN-90-97765) Copyright Avail: NTIS HC/MF A05

Research carried out to gain insight into the fundamental processes occurring in (mode locked) high pressure CO2 lasers is described. Pulse formation and line broadening in an amplitude modulation mode locked transverse excited atmospheric CO2 laser

are investigated. Calculation and measurement of initial electron densities in x ray pre-ionized avalanche discharge lasers was carried out. High pressure x ray pre-ionized transverse excited multi-atmospheric pressure (TEMA) CO2 laser and subnanosecond pulse measurements of 10.6 micron radiation with tellurium are reported. ESA

N91-11211# Office National d'Etudes et de Recherches Aerospatiales, Paris (France).
THEORITICAL AND EXPERIMENTAL STUDY OF KINETICS MECHANISMS IN THE CHEMICAL OXYGEN-IODINE LASER (COIL) Ph.D. Thesis - Paris-Sud Univ.
Veronique Joly Jan. 1990 306 p In FRENCH; ENGLISH summary Report will also be announced as translation (ESA-TT-1227)
(ONERA-P-1990-1; ISSN-0078-379X; ETN-90-98015) Avail: NTIS HC/MF A14

The chemical oxygen-iodine laser gives high power and is the only chemical laser with an electronic transition. The energy source of the laser is excited metastable oxygen obtained by chemical generator. The first step of the reaction corresponds to the dissociation of molecular iodine following a not entirely understood mechanism. A kinetic model is proposed. The intermediate excited unknown species of the atomic iodine are investigated. The rate of the vibrational coefficients are determined. The results of this model are in agreement with the experiment of Heidner. High resolution excitation spectra of vibrational levels of fundamental iodine in an iodine metastable oxygen mixture are presented. By inversion of the spectra and using an appropriate fitting code, the distribution of population as a function of the vibrational state is deduced. ESA

37 MECHANICAL ENGINEERING

Includes auxiliary systems (nonpower); machine elements and processes; and mechanical equipment.

N91-11212# Argonne National Lab., IL.
WEAR REDUCTION IN CUTTING TOOLS: TRIBOLOGICAL PROPERTIES OF HARD COATINGS
B. P. Bandyopadhyay, E. Fabiszak (Micro-Surface Corp., Morris, IL.), G. R. Fenske, and F. A. Nichols 1990 6 p Presented at the Japan International Tribology Conference, Nagoya, Japan, 29 Oct. - 1 Nov. 1990
(Contract W-31-109-eng-38)
(DE90-009705; CONF-901009-2) Avail: NTIS HC/MF A02

The cutting tool industry has become the pioneer in the use of hard coatings on different types of tools. Hard coatings, which improve the performance and lifetime of cutting tools, have been used for more than 20 years. Herein, performance evaluations were made of high speed steel and carbide tool inserts that were coated with tungsten disulfide (WS2), titanium nitride (TiN), and with TiN and then with WS2; uncoated inserts were also evaluated. The aim was to determine whether the WS2 coating improved tool life and reduced cutting-force requirements. The WS2-coated inserts demonstrated significantly lower flank wear than the uncoated inserts. Use of WS2 also reduced flank and notch wear of uncoated and TiN-coated inserts. The greatest wear reductions were observed for inserts coated with both TiN and WS2. DOE

N91-11213# EG and G Rocky Flats, Inc., Golden, CO.
PENETRATION IN GTA WELDING
C. R. Heiple and P. Burgardt 1990 17 p Presented at the Fall Meeting of the Minerals, Metals and Materials Society on Physical Metallurgy and Materials in Conjunction With Materials Week and the Material Applications and Services Exposition, Detroit, MI, 7-11 Oct. 1990
(Contract DE-AC04-76DP-0353)
(DE90-008971; RFP-4390; CONF-901008-1) Avail: NTIS HC/MF A03

The size and shape of the weld bead produced in GTA welding depends on the magnitude and distribution of the energy incident on the workpiece surfaces as well as the dissipation of that energy in the workpiece. The input energy is largely controllable through the welding parameters selected, however the dissipation of that energy in the workpiece is less subject to control. Changes in energy dissipation can produce large changes in weld shape or penetration. Heat transport away from the weld pool is almost entirely by conduction, but heat transport in the weld pool is more complicated. Heat conduction through the liquid is an important component, but heat transport by convection (mass transport) is often the dominant mechanism. Convective heat transport is directional and changes the weld pool shape from that produced by conduction alone. Surface tension gradients are often the dominant forces driving fluid flow in GTA weld pools. These gradients are sensitive functions of weld pool chemistry and the energy input distribution to the weld. Experimental and theoretical work conducted primarily in the past decade has greatly enhanced our understanding of weld pool fluid flow, the forces which drive it, and its effects on weld pool shape. This work is reviewed here. While less common, changes in energy dissipation through the unmelted portion of the workpiece can also affect fusion zone shape or penetration. These effects are also described. DOE

N91-11214# Lawrence Livermore National Lab., CA.
THE MEASUREMENT AND FINITE ELEMENT ANALYSIS OF THE DYNAMIC STIFFNESS OF NON-UNIFORM CLEARANCE, GAS, THRUST BEARINGS
P. Holster, J. Jacobs (Philips Gloeilampenfabrieken N.V., Eindhoven, Netherlands), and J. Roblee Jun. 1990 29 p Presented at the Joint STLE-ASME Tribology Conference, Toronto, Ontario, 7-10 Oct. 1990
(Contract W-7405-eng-48)
(DE90-015120; UCRL-JC-104362; CONF-901071-6) Avail: NTIS HC/MF A03

An overview is presented of a finite element method (FEM) approach for the calculation of the dynamic stiffness of circular, externally pressurized, gas, thrust bearings with a non-uniform clearance. Some observations are made about the characteristic behavior of gas bearings subject to dynamic loading. The primary emphasis, however, is the development and qualification of a test apparatus and the necessary test techniques for measuring dynamic stiffness up to 250 N/micron at frequencies up to 2000 Hz. A complete, experimental verification of the FEM model will be presented in a later paper. DOE

N91-11215# Laboratoire d'Automatique et d'Analyse des Systemes, Toulouse (France).
GEOMETRIC METHOD AND SYNTHESIS AF ASSEMBLY STRATEGIES IN ROBOTIC SYSTEMS Ph.D. Thesis - Toulouse Univ. [RAISONNEMENT GEOMETRIQUE ET SYNTHESE DES STRATEGIES D'ASSEMBLAGE EN ROBOTIQUE]
Daniel Sidobre 1990 120 p In FRENCH; ENGLISH summary
(LAAS-90041; ETN-90-97815) Avail: NTIS HC/MF A06

The problem of automatic programming for robotic systems is presented. The study concerns the synthesis of assembly strategies for two objects described by their polyhedral models in their assembled position. A theoretical study of the linear model associated with the contact links and a method for the computation of assembly strategies are presented. The notions of generalized coordinates and of contact constraints are introduced. The relative motion between both objects is obtained. It is shown that an assembly strategy can be represented by a path in a graph. The nodes correspond to contacts with zero degrees of freedom and the arcs are associated with contacts with one degree of freedom. A method is proposed for an incremental construction of this graph based on the generation of contact constraint quintuplets which lead to motions consistent with the polyhedral models of the objects. ESA

N91-11216*# Georgia Inst. of Tech., Atlanta. School of Mechanical Engineering.
DYNAMIC ANALYSIS AND CONTROL OF LIGHTWEIGHT MANIPULATORS WITH FLEXIBLE PARALLEL LINK MECHANISMS Ph.D. Thesis

Jeh Won Lee Jun. 1990 228 p
(Grant NAG1-623)
(NASA-CR-187347; NAS 1.26:187347) Avail: NTIS HC/MF A11 CSCL 13I

The objective is the theoretical analysis and the experimental verification of dynamics and control of a two link flexible manipulator with a flexible parallel link mechanism. Nonlinear equations of motion of the lightweight manipulator are derived by the Lagrangian method in symbolic form to better understand the structure of the dynamic model. The resulting equation of motion have a structure which is useful to reduce the number of terms calculated, to check correctness, or to extend the model to higher order. A manipulator with a flexible parallel link mechanism is a constrained dynamic system whose equations are sensitive to numerical integration error. This constrained system is solved using singular value decomposition of the constraint Jacobian matrix. Elastic motion is expressed by the assumed mode method. Mode shape functions of each link are chosen using the load interfaced component mode synthesis. The discrepancies between the analytical model and the experiment are explained using a simplified and a detailed finite element model. Author

N91-11217 California Univ., Davis.
ROBOT TRAJECTORY CONTROL WITH A MODEL REFERENCE ADAPTIVE CONTROL SYSTEM USING TAP DELAY FILTERS Ph.D. Thesis
Farhad Bolourchi 1989 147 p
Avail: Univ. Microfilms Order No. DA9017733

The problem of trajectory control of a robot manipulator is studied using a model reference adaptive control (MRAC) technique realized with tap delay (TD) filters. A simple two-link, planar robot with revolute joints serves throughout as a model of the manipulator for analysis and simulation. The adaptive logic is based upon Lyapunov stability with the Lyapunov function consisting of a quadratic sum of trajectory errors and TD filter weights. The TD filter allows a straightforward implementation of an inverse control scheme which can be used in the initiation of robot motion, before the MRAC system can effectively compensate. The resulting trajectory control system is, computationally, very simple and requires adaptation of as few as five weights per each joint and measurement of only angular orientation and rate of the links. Robustness properties are examined analytically and the control scheme is evaluated in simulation. The effects of disturbance torques (up to 30 percent of steady state) and large variations in payload (a factor of plus or minus 3 about nominal) are examined and it is demonstrated that the proposed control system yields excellent performance (to within a couple of degrees) in a series of large amplitude step response tasks. The proposed MRAC-TD filter control scheme appears to have considerable potential for application to a variety of nonlinear control problems.
Dissert. Abstr.

N91-11218 Illinois Univ., Chicago.
INSTANTANEOUS KINEMATICS, MOTION PLANNING AND MECHANICAL EFFICIENCY OF A QUADRUPEDAL WALKING MACHINE Ph.D. Thesis
Jong-Kil Lee 1990 325 p
Avail: Univ. Microfilms Order No. DA9023221

It has been well recognized that legged locomotion is superior to wheeled locomotion and tracked locomotion on rough terrain. The development of a practical walking machine, however, is hindered by many technological obstacles. Some technological problems in walking machine kinematics, motion planning, and mechanical efficiency areas are being resolved. The walking machine under study is a quadruped with pantograph type legs. Since the kinematics of one individual leg is the same as a manipulator, the kinematics of a six-degree-of-freedom, pantograph type manipulator is studied first. The kinematics of the quadruped, which consists of four three-degree-of-freedom, pantograph type legs, are then studied. In order to accurately derive the lengthy kinematic equations, a symbolic computer package is applied. The motion planning is to enable a walking machine body to precisely follow a three-dimensional curve, which is designed based on Beizer curve and obstacle avoidance considerations. Due to the arbitrary motion direction during walking, special strategies of gaits are developed to ensure positive stability. The gait strategies are based on wave and wave-crab gaits. The mechanical efficiency of different walking machine legs are studied using a redefined geometric work concept. The mechanical efficiency of both insect type and mammal type walking posture of three types of legs are also studied. Dissert. Abstr.

N91-11219 Stanford Univ., CA.
MINIMUM TIME FEEDBACK CONTROL OF ARTICULATED ROBOTIC MANIPULATORS Ph.D. Thesis
Hon Yuen Tam 1990 87 p
Avail: Univ. Microfilms Order No. DA9024366

Algorithms for minimum-time feedback control of articulated robotic manipulators are developed. Two types of robot motion are considered. They are the minimum time point-to-point motion and the minimum time tracking of a specified path. The corresponding closed-loop control strategies are developed using perturbation control methods. All feedback schemes are verified by simulations. The point-to-point minimum time control is usually bang-bang. Feedback involves time varying gains which determines how the switching times of the bang-bang control strategy should be perturbed due to deviation from the nominal trajectory during execution. In real time, table lookup of the off-line computed gains is mechanized by a time-to-go scheme. The feedback is also extended to perturbing the switching times due to small changes in the tip-mass. An on-line parameter identification scheme is adopted to determine this change. When a manipulator is commanded to track a specified path, the open-loop minimum time control strategy usually requires one control to be saturated and the rest to remain unsaturated. This nature is retained in a feedback control scheme similar to the above. However, the scheme considers not only switching time perturbations, but also changes of the control level of the unsaturated controls. The feedback gains depend on the penalty weights associated with deviation from the tracked path. The transient of the regulating response is adjusted by tuning these weights. It is known that singular arcs can appear in the minimum time path of point-to-point motion. This is characterized by having an unsaturated control in part of the minimum time control history. Feedback control adjusts the level of the unsaturated control depending on the deviation from the nominal path, and can also require short changes in control direction in the beginning and/or toward the end of the singular arc. Dissert. Abstr.

N91-11220 Illinois Univ., Chicago.
DYNAMIC MODEL ERROR ANALYSIS OF ROBOT MANIPULATORS Ph.D. Thesis
Salem Mohamed Samak 1990 212 p
Avail: Univ. Microfilms Order No. DA9023227

The mechanical manipulator model-based controllers required knowledge of the full dynamic model and accurate physical parameter values. However, this requirement can be difficult to meet in practice. Some of these parameters may not be considered significant by the designer and others are too complex to model. Accordingly, the behavior of the dynamic model errors of robot manipulators was studied and analyzed. All of the formulations, techniques and discussions presented are devoted to general manipulators. They do not depend upon a specific manipulator configuration or dimensions. The kinematic relationships between the links are described by using the zero-reference-position method. The velocity Jacobian matrix is constructed to formulate a governing kinematic equation in terms of the joint variable rates. These equations are integrated by using a predictor-corrector scheme. The generalized speeds are used to take advantage of special features of a given physical system. Both the inverse dynamics and the direct dynamics problems are developed by employing Kane's dynamical equations as an analytical tool. Three different models are introduced based upon the nature of the relationship between the rates of the generalized coordinates and the generalized speeds. The dynamic behavior of robots with realistic complexity is examined with a view to investigate the effect of

system model errors on the precision of trajectory execution for the case when a good knowledge of robot physical parameters, such as its link dimensions, masses and inertias, may not be available. Dissert. Abstr.

N91-11221# Sandia National Labs., Albuquerque, NM.
AN EXPERT SYSTEM FOR AUTOMATED ROBOTIC GRASPING
S. A. Stansfield 10 May 1990 3 p Presented at the American Nuclear Society Winter Meeting, Washington, DC, 11-15 Nov. 1990
(Contract DE-AC04-76DP-00789)
(DE90-010820; SAND-90-1200-C-Extd-Abst; CONF-901101-1)
Avail: NTIS HC/MF A01

Many DOE sites and facilities will be environmentally remediated during the next several decades. A number of the restoration activities (decontamination and decommissioning of inactive nuclear facilities is an example) can only be carried out by remote means and will be manipulation-intensive tasks. Experience has shown that manipulation tasks are especially slow and fatiguing for the human operator of a remote manipulator. A rule-based expert system is presented for automated, dextrous robotic grasping. This system reasons about the features of an object to generate hand shaping and wrist orientation for a robot hand and arm. The system can be used in several different ways to lessen the demands on the human operator of a remote manipulation system --- either as a fully autonomous grasping system or one which generates grasping options for a human operator and which then automatically carries out the one selected. These systems are examined. DOE

N91-11222# Sandia National Labs., Albuquerque, NM.
IMPROVED TRACKING FOR BILATERAL TELEOPERATORS WITH TIME DELAY
Robert J. Anderson 5 Jul. 1990 14 p Presented at the International Symposium on Gas-Liquid Two-Phase Flows in Conjunction With the Winter Annual Meeting of the ASME, Dallas, TX, 25-30 Nov. 1990
(Contract DE-AC04-76DP-00789)
(DE90-015392; SAND-90-2053C; CONF-901109-13) Avail: NTIS HC/MF A03

A bilateral teleoperation system consists of a local master manipulator and a remotely located slave manipulator. Generalized velocity commands are sent forward from the master to the slave, and generalized force/torque information is reflected back from the slave to the master. Often there is a transmission delay incurred when communicating between the two subsystems which causes instability in the bilateral teleoperator. Recently, a solution for this instability problem was found, based on mimicking the behavior of a lossless transmission line. Although this solution provides steady-state force and velocity tracking, it does not provide steady-state force and position tracking, as is desired for bilateral teleoperation. In this paper a modification is given to the basic control law which overcomes this difficulty. DOE

N91-11223# Clarkson Univ., Potsdam, NY.
EXPERIMENTAL AND THEORETICAL STUDIES OF FRICTION AND HEAT TRANSFER IN ROUGH PASSAGES Progress Report
N. T. Obot, E. B. Esen, and K. H. Snell Aug. 1990 9 p
(Contract DE-FG02-89CE-90029)
(DE90-016302; DOE/CE-90029/3) Avail: NTIS HC/MF A02

Experimental and theoretical studies of friction and heat transfer in rough passages were conducted. Efforts were directed to the experimental studies. Measurements of isothermal pressure drop in smooth and spirally-fluted tubes that were intended to establish the reliability of the flowmeter and pressure transducer calibrations as well as the instrumentation were completed. DOE

N91-11224# Oak Ridge National Lab., TN. Metals and Ceramics Div.
INDENTATION TESTING OF THIN FILMS AND HARD MATERIALS
Carl J. McHargue 1990 13 p Presented at the NATO Advisory Study Inst. on Diamond and Diamond-Like Films, Castelvecchio Pascoli, Italy, 22 Jul. - 2 Aug. 1990
(Contract DE-AC05-84OR-21400)
(DE90-017758; CONF-900731-2) Avail: NTIS HC/MF A03

Indentation testing techniques can provide important information about the near-surface mechanical and deformation properties of solids. Properly executed and interpreted, such techniques can provide information regarding hardness, elastic modulus, compressive yield strength (for metals), fracture toughness (in ceramics) and residual stresses (in ceramics). However, the apparent simplicity of the test procedures often belies the difficulties of obtaining quantitative information of specific properties of interest. Indentation test techniques for the testing of thin films or coatings are discussed. DOE

N91-11225# Michigan Univ., Ann Arbor. Dept. of Mechanical Engineering and Applied Mechanics.
INJECTOR AND VALVE TRAIN FRICTION STUDIES: CUMMINS L-10 ENGINE Progress Report, 1 Oct. 1988 - 31 Dec. 1989
Russell R. Mitchell and Donald J. Patterson 15 Feb. 1990 78 p
(Contract DE-FG02-88CE-90025)
(DE90-017288; DOE/CE-90025/2) Avail: NTIS HC/MF A05

This report discusses measurement techniques developed and experimental results obtained for a valve and injector train friction study supported by the U.S. Department of Energy. The incentives for this research are the higher injector train forces and potential friction problems associated with advanced technology diesel engines. As a convenient way to begin the program, the instrumentation was developed around the exhaust valve of cylinder number 1. Results are presented for that valve in a motored Cummins L-10 engine. The instantaneous cam/roller friction force was determined from the instantaneous roller speed and the pin friction torque. Measured as well were the pushrod force and displacement. Friction work loss was determined for both the cam and roller interface as well as the upper valve train. Future efforts will address the injector train and a fired engine with advanced technology components. DOE

N91-11226# Oak Ridge National Lab., TN.
MOBILE ROBOTS AND INTELLIGENT MOTION CONTROL
Francois G. Pin Sep. 1990 7 p Presented at the IEEE International Workshop, Istanbul, Turkey, 20-24 Aug. 1990
(Contract DE-AC05-84OR-21400)
(DE90-017312; ORNL/FTR-3731) Avail: NTIS HC/MF A02

The traveler attended the IEEE International Workshop on Intelligent Motion Control, presented a paper entitled, Autonomous Trajectory Generation for Mobile Robots with Non-Holonomic and Steering Angel Constraints, and chaired the session on mobile robots. Sessions of particular interest included Mobile Robots 1, 2, and 3, Motion Planning 1 and 2, Flexible Robots, Knowledge-Based Robotics Systems, Multi-Robot Systems, Redundant Robots, and Learning and Fuzzy Control 1 and 2. The traveler also visited the robotics laboratory of Bogazici University and held several discussions on design of redundant, compliant, reconfigurable, and dynamically balanced manipulators. DOE

N91-11227# Japan Atomic Energy Research Inst., Tokyo. Dept. of Reactor Engineering.
A METHOD OF USING THE INVERSE MATRIX FOR MANIPULATOR KINEMATICS
Shinobu Sasaki Mar. 1990 33 p In JAPANESE; ENGLISH summary
(DE90-520210; JAERI-M-90-064) Avail: NTIS (US Sales Only) HC/MF A03

Up to now, some approaches have been proposed and used for the inverse problems of manipulators. As for a six-link manipulator, the kinematic relationships can be simplified into an equation system with four variables by the introduction of a virtual manipulator, which seems novel as an alternative way of looking at the entity of the inverse problem. In place of such an auxiliary method, the inversion of the homogeneous transformation matrix in this process was found to lead to the same results. In this

paper, this derivation is shown laying an emphasis on the usefulness of the inverse matrix having the possibility of facilitating the calculation of the link chain. DOE

N91-11228# Technische Univ., Eindhoven (Netherlands).
ON THE CALCULATION OF LEAKAGE AND FRICTION OF RECIPROCATING ELASTOMERIC SEALS Ph.D. Thesis
Arnoldus Franciscus Kanters 1990 169 p Sponsored by Netherlands Foundation for Technical Research
(ETN-90-97751) Avail: NTIS HC/MF A08

Research on reciprocating elastomeric seals is reviewed. The aim is to contribute to the development of adequate theoretical models for leakage and friction as tools for design, and involves the modeling of the tribological process in the seal contact as well as proper experimental verification of theoretical predictions of leakage and friction. Attention is confined to axisymmetric, stationary and isothermal situation. Results are presented for a simple shaped polyurethane rod seal. Calculation by finite element method is studied. An approach to solve the elastohydrodynamic lubrication problem is developed and incorporated into a computer program PROGRES. Viscous shear stresses and the influence of seal roughness on the lubrication are investigated. ESA

N91-11229# Ecole Centrale de Lyon (France). Lab. de Materiaux-Mecanique Physique.
STUDY OF THE WEAR BEHAVIOR INDUCED BY FRETTING IN ALUMINUM AND TITANIUM ALLOYS Ph.D. Thesis [ETUDE DU COMPORTEMNT EN USURE INDUITE SOUS PETITS DEBATTEMENTS D'ALLIAGE D'ALUMINIUM ET DE TITANE]
Vincent Pellerin 1990 128 p In FRENCH
(ECL-90-01; ETN-90-97817) Avail: NTIS HC/MF A07

A synthesis of several approaches and studies concerning the fretting fatigue is presented. The influence of the parameters relating to the structure and the mechanical properties of the materials is considered. Special attention is given to the tribology of interfaces. The results of wear experiments obtained on titanium and aluminum are summarized. The investigation shows that the fretting wear depends on the balance of several fretting accommodation mechanisms. A new method for studying fretting phenomena is proposed. ESA

N91-11230# Lawrence Livermore National Lab., CA.
A MOLECULAR DYNAMICS MODEL OF THE ORTHOGONAL CUTTING PROCESS
James F. Belak and Irving F. Stowers 16 Jul. 1990 4 p Presented at the 1990 American Society of Photoptical Engineers Annual Conference, Rochester, NY, 23-28 Sep. 1990 Submitted for publication
(Contract W-7405-eng-48)
(DE90-015911; UCRL-102697; CONF-9009241-1) Avail: NTIS HC/MF A01

Material removal, as found in the cutting and grinding processes, is important in many areas of fabrication technology. Examples include high speed machining by single point turning, surface milling and drilling. An idealized model that contains the essential physics of these processes is the 2-D orthogonal cutting geometry. Following the work of Shaw, an attempt is made to obtain a fundamental understanding of the commonly observed phenomena in the chip forming process: the atomistic mechanisms of plastic deformation within the primary shear zone and the observed shear angle (phi); the resultant energy flow from the tool doing work; the stress, strain and material flow fields; the morphology of the chip (smooth, segmented, crystalline or amorphous); the role of different depths of cut (t), rake angles (alpha), and clearance angles (theta); and the role of the tool tip radius, roughness (friction), and wear. The molecular dynamics computer simulation method is an ideal tool for the study of the atomistic mechanisms of these deformation processes. Simulations are performed for a model of copper at room temperature using 10(exp 3) to 10(exp 6) atoms, depths of cut in the range 1 to 50nm. and cutting speeds of 1 to 2500 meters per second (m/s). These simulations are strictly 2-D (plane strain). Here, focus is on the chip forming process, the atomistic mechanisms of plastic deformation, the flow of energy into the chip and workpiece, and the material flow and stress fields for the orthogonal geometry (alpha = 0), sharp tools, and shallow depths of cut (t approx = 5 nm). DOE

N91-11231# Sandia National Labs., Albuquerque, NM.
ARCHIMEDES: A SYSTEM THAT PLANS AND EXECUTES MECHANICAL ASSEMBLIES
David Strip 1990 6 p Presented at the IEEE International Conference on Robotics and Automation, Sacramento, CA, 7-12 Apr. 1990
(Contract DE-AC04-76DP-00789)
(DE91-000036; SAND-90-2400C; CONF-9004243-1) Avail: NTIS HC/MF A02

Archimedes is a prototype mechanical assembly system which generates and executes robot assembly programs from a computer aided design (CAD) model input. The system addresses the unrealized potential for flexibility in robotic mechanical assembly applications by automating the programming task. Input is a solid model of the finished assembly. Parts relationships and geometric constraints are deduced from the solid model. A rule-based planner generates a generic assembly plan that satisfies the geometric constraints, as well as other constraints embodied in the rules. A retargetable plan compiler converts the generic plan into code specific to an application environment. Execution of the compiled plan in a workcell containing an Adept Two robot, a vision system, and other parts handling equipment will be shown on videotape. DOE

N91-11232 Virginia Polytechnic Inst. and State Univ., Blacksburg.
STATISTICAL SYSTEM IDENTIFICATION OF STRUCTURES WITH FLEXIBLE JOINTS Ph.D. Thesis
Sathya Narayan Gangadharan 1990 174 p
Avail: Univ. Microfilms Order No. DA9028037

The flexibility of welded joints is an important issue in design of car bodies. Two generic, 3-D, design-oriented models (simple and complex) are developed to represent the compliant behavior of multibranch flexibile joints. The simple model consists of torsional springs restraining the relative rotation of the joint branches in the three planes, while all branches are assumed to be rigidly connected in translation. Coupling between motions in different planes is neglected. The complex model accounts for such coupling. A statistical system identification method is proposed for inferring the model parameters from the static response of the structure. The method is demonstrated by applying it to a simple cube frame structure and a car body. Finally, the two models are compared in terms of their ability to predict static response. Dissert. Abstr.

38 QUALITY ASSURANCE AND RELIABILITY

Includes product sampling procedures and techniques; and quality control.

N91-11233*# Rockwell International Corp., Canoga Park, CA. Rocketdyne Div.
REAL-TIME FAILURE CONTROL (SAFD) Final Report
Hagop V. Panossian, Victoria R. Kemp, and Sherry J. Eckerling Jul. 1990 195 p
(Contract NAS8-40000)
(NASA-CR-184025; NAS 1.26:184025; RSS-8826-12) Avail: NTIS HC/MF A09 CSCL 14D

The Real Time Failure Control program involves development of a failure detection algorithm, referred as System for Failure and Anomaly Detection (SAFD), for the Space Shuttle Main Engine (SSME). This failure detection approach is signal-based and it entails monitoring SSME measurement signals based on predetermined and computed mean values and standard deviations. Twenty four engine measurements are included in the algorithm and provisions are made to add more parameters if needed. Six

major sections of research are presented: (1) SAFD algorithm development; (2) SAFD simulations; (3) Digital Transient Model failure simulation; (4) closed-loop simulation; (5) SAFD current limitations; and (6) enhancements planned for. Author

N91-11234# Ames Lab., IA.
DEDUCING MECHANICAL PROPERTIES DUE TO INTERFACES FROM THEIR ACOUSTICAL RESPONSE
O. Buck, R. B. Thompson, D. K. Rehbein, L. J. H. Brasche, and D. D. Palmer 1989 10 p Presented at the 7th International Conference on Fracture (ICF-7), Houston, TX, 20-24 Mar. 1989
(Contract W-7405-eng-82)
(DE90-016704; IS-M-623; CONF-890310-7) Avail: NTIS HC/MF A02

The ultrasonic interrogation of a partially contacting interface provides details on the contact topology. This information is used to deduce important mechanical properties of structures containing fatigue cracks and diffusion bonds as specific examples of such interfaces. The information is sufficient to determine the residual stress distribution in the wake of the crack. These residual stresses produce a stress intensity factor which, in part, shields the crack from the externally applied stress intensity range and thus affects the fatigue crack propagation rate. For diffusion bonds in materials of low ductility, the information appears to be sufficient to determine the bond strength in uniaxial tension, using LEFM concepts. DOE

N91-11235# Sandia National Labs., Albuquerque, NM.
IMPLEMENTATION OF A QML (QUALIFIED MANUFACTURER'S LIST) METHODOLOGY FOR DISCRETE SEMICONDUCTORS
L. L. Halbleib, P. S. Wormington, S. W. Lumpe, and J. P. Dwyer (Alliance Electronics, Albuquerque, NM.) 1990 3 p Presented at the Government Microcircuit Applications Conference: Technology Strategies for the 90's, Las Vegas, NV, 6-8 Nov. 1990
(Contract DE-AC04-76DP-00789)
(DE90-015715; SAND-90-2153C; CONF-901124-1) Avail: NTIS HC/MF A01

Agencies that are prime contractors to DOE have developed and are currently instituting a quality initiative which applies a QML-like methodology to a complete discrete semiconductor process. The goal is to demonstrate that improving the quality of this process is a more efficient method than screening to improve the quality of the semiconductor. The QML methodology, MIL-I-38535, is used to achieve this goal for integrated circuits. The methods, for discrete semiconductor, applies many of the principles found in this specification to provide structured continuous improvement. Improvement in product performance reduces incoming inspection requirements, resulting in reduced cost and product lead time. The methodology for this initiative is described; it consists of a certification, qualification, and monitoring (CQM) program for the complete semiconductor process. This process includes all technical and administrative activities that effect the quality of a device, beginning with circuit design and ending with the installation of the manufactured device into the electronic component assembly. For the initial application, the CQM program is being implemented on a small signal transistor. DOE

N91-11236# Pacific Northwest Lab., Richland, WA.
CLASSIFICATION OF ACOUSTIC EMISSION WAVEFORMS FOR NONDESTRUCTIVE EVALUATION USING NEURAL NETWORKS
Roger S. Barga, Ronald B. Melton, and Mark A. Friesel Apr. 1990 13 p Presented at the Society of Photo-Optical Institution Engineering (SPIE) Applications of Neural Networks, Orlando, FL, 16-19 Mar. 1990
(Contract DE-AC06-76RL-01830)
(DE90-017239; PNL-SA-18095; CONF-9003200-1) Avail: NTIS HC/MF A03

Neural networks were applied to the classification of two types of acoustic emission (AE) events, crack growth and fretting, from a simulated airframe joint specimen. Signals were obtained from four sensors at different locations on the test specimen. Multilayered neural networks were trained to classify the signals using the error backpropagation learning algorithm, enabling AE events arising from crack growth to be distinguished from those caused by fretting. In this paper we evaluate the neural network classification performance for sensor location dependent and sensor location independent training and testing sets. Further, we present a new training strategy which significantly reduces the time required to learn large training sets using the error backpropagation learning algorithm, and improves the generalization performance of the network. DOE

39 STRUCTURAL MECHANICS

Includes structural element design and weight analysis; fatigue; and thermal stress.

For applications see *05 Aircraft Design, Testing and Performance* and *18 Spacecraft Design, Testing and Performance*.

N91-11237 Ohio State Univ., Columbus.
FORCED VIBRATION ANALYSIS OF PLATES AND SHALLOW SHELLS Ph.D. Thesis
Yi-Tzong Chern 1989 221 p
Avail: Univ. Microfilms Order No. DA9014407

The forced vibrations of plates (simply supported rectangular plate and circular plates with simply supported and clamped boundaries) and shallow shells (planform with shear diaphragm boundary) with viscous or structural damping excited sinusoidally with uniform pressure are studied. The approaches used are eigenfunction, closed-form, and an energy method. From the results, it is seen that: dynamic displacement responses for plates are inversely proportional to the viscous damping coefficient (or the loss factor for a structural damping) for small damping; closed-form method provided a very good way to obtain exact solutions and a different viewpoint to explain the dynamic response curve; and negative static or dynamic displacement at the center of a cylindrical shell panel may happen. Dissert. Abstr.

N91-11238 Georgia Inst. of Tech., Atlanta.
ALTERNATING METHOD APPLIED TO 3-D PART-THROUGH CRACK PROBLEMS, WITH APPLICATION TO THE WEIGHT FUNCTION METHOD Ph.D. Thesis
Cheng-Young Liao 1989 190 p
Avail: Univ. Microfilms Order No. DA9014867

The Schwarz-Neumann alternating method is applied to three dimensional circular crack problems, as part of an effort to develop an efficient method for analyzing the frequently encountered part-through surface and corner flaw problems. The analytical solution of a penny-shaped flaw embedded in an infinite body is completely derived, and its numerical evaluation is done by a part analytical and part numerical method. Numerical properties of the alternating finite element method are carefully examined and summarized, with the aid of a special variation of the alternating method that incorporates minimum numerical approximations. Also presented is a weight function technique for computing fracture parameters of three dimensional circular and elliptical crack problems. In the frame work of the alternating method, the weight function for a cracked finite elastic solid is decomposed into infinite-domain and boundary-correction problems. The former is evaluated using analytical expressions for the first order variation of the crack opening displacements due to crack geometry changes. On the other hand, the latter may be derived by a regular alternating procedure. Numerical examples show that the alternating method is the most efficient technique in computing stress intensity factors. Dissert. Abstr.

N91-11239 Michigan Univ., Ann Arbor.
CONTACT AND IMPACT PROBLEMS USING ADAPTIVE FINITE ELEMENT METHODS Ph.D. Thesis
Toshikazu Torigaki 1989 286 p
Avail: Univ. Microfilms Order No. DA9014029

Finite element analyses of friction contact problems in linear elasticity and large deformation impact problems are presented. Error analysis and adaptive methods for linear elastic problems are discussed and extended to be applicable to the contact and impact problems. Kinematical contact condition is derived with the Coulomb friction law in order to formulate contact problems of linearly elastic solids using a variational principle. The penalty and the regularity methods are introduced in the finite element formulation to approximate the friction contact condition. Although these problems are limited in small deformation, all geometric relations of friction contact conditions are considered in current (deformed) configuration in numerical procedures. A finite element formulation of large deformation impact problems is derived using Lagrangian description and explicit time integration. Elastic-plastic constitutive model is assumed with combination of isotropic and kinematic hardening rules. A new incremental friction law and its numerical procedures are presented. Very efficient programming techniques for vector parallel computers are also presented by using a symbolic manipulation software. Three types of the calculable error measures are presented for linear elastic problems, and all of them are well verified by comparing them with the true error measure obtained for a problem whose analytical solution is known. Two of these error measures are computed using interpolation error which is explicitly derived for QUAD4 and HEXA8 finite elements. Several error measures for contact and impact problems are also derived and compared. R- and h-adaptive methods are presented. Dissert. Abstr.

N91-11240# Advisory Group for Aerospace Research and Development, Neuilly-Sur-Seine (France). Structures and Materials Panel.

SHORT-CRACK GROWTH BEHAVIOUR IN VARIOUS AIRCRAFT MATERIALS

P. R. Edwards, comp. and James C. Newman, Jr., comp. (National Aeronautics and Space Administration. Langley Research Center, Hampton, VA.) Aug. 1990 198 p

(AGARD-R-767; ISBN-92-835-0577-8) Copyright Avail: NTIS HC/MF A09; Non-NATO Nationals requests available only fron AGARD/Scientific Publications Executive

The results of the first phase of an AGARD Cooperative Test Program on the behavior and growth of short fatigue cracks are reviewed. The establishment of a common test method, means of data collection/analysis and crack growth modeling in an aircraft alloy AA 2024-T3 are described. The second phase allowed testing of various materials and loading conditions. The results of this second phase are described. All materials exhibited a short-crack effect to some extent. The effect was much less evident in 4340 steel than in the other materials. For the aluminum, aluminum-lithium, and titanium alloys, short cracks grew at stress-intensity factor ranges lower, in some cases much lower, than the thresholds obtained from long crack tests. Several laboratories used the same crack growth model to analyze the growth of short cracks. Reasonable agreement was found between measured and predicted short-crack growth rates and fatigue lives. For individual titles, see N91-11241 through N91-11251.

N91-11241*# National Aeronautics and Space Administration. Langley Research Center, Hampton, VA.

AN AGARD SUPPLEMENTAL TEST PROGRAMME ON THE BEHAVIOUR OF SHORT CRACKS UNDER CONSTANT AMPLITUDE AND AIRCRAFT SPECTRUM LOADING

P. R. Edwards (P. P. Data Ltd., Fleet, England) and James C. Newman, Jr. *In* AGARD, Short-Crack Growth Behaviour in Various Aircraft Materials Aug. 1990 43 p (For primary document see N91-11240 02-39)

Copyright Avail: NTIS HC/MF A09; Non-NATO Nationals requests available only from AGARD/Scientific Publications Executive CSCL 20K

An AGARD Supplemental Test Program on the growth of short fatigue cracks was conducted to allow testing of various materials and loading conditions that were of interest. Twenty-two participants from ten laboratories in eight countries contributed to the supplemental test program. The objective is to review the supplemental test program and to summarize the results obtained from all laboratories. The materials tested in the supplemental program were: 2024-T3 and 7075-T6 aluminum alloys, 2090-T8E41 aluminum-lithium alloy, Ti6Al4V titanium alloy, and 4340 steel. Tests on single-edge-notch-tension specimens were conducted under several constant-amplitude loading conditions and spectrum loading conditions (FALSTAFF, Inverted FALSTAFF, GAUSSIAN, TWIST, Felix, and the Fokker 100 spectra). The plastic-replica method was used to measure the growth of short cracks at the notch root. The results from the supplemental test program show good agreement among the several laboratories who measured short-crack growth rates on the aluminum-lithium alloy. Author

N91-11242# Air Force Wright Aeronautical Labs., Wright-Patterson AFB, OH. Structural Integrity.

DETERMINATION OF THE SHORT CRACK EFFECT IN 2090-T8E41 ALUMINUM LITHIUM

Christopher J. Mazur and James L. Rudd *In* AGARD, Short-Crack Growth Behaviour in Various Aircraft Materials Aug. 1990 11 p (For primary document see N91-11240 02-39)

Copyright Avail: NTIS HC/MF A09; Non-NATO Nationals requests available only from AGARD/Scientific Publications Executive

The United States Air Force developed two primary sets of design requirements to ensure the structural integrity of aircraft: damage tolerance and durability. The purposes of these design requirements are to ensure structural safety and preclude the occurrence of expensive maintenance and repair costs, respectively. These requirements are generally satisfied through the use of linear elastic fracture mechanics and crack growth rate data experimentally generated for long cracks. Recently, various investigators have indicated that short cracks may grow significantly faster than long cracks for the same crack-driving force. The end result may be unconservative life predictions when situations arise where short crack lengths are included in the analysis. To accurately predict the growth of these short cracks, the short crack phenomenon must be understood. The objective is to describe the work of the Flight Dynamics Laboratory as a participating agency in the AGARD Supplement Test Program on Short Cracks. The manufacturing and testing of 2090-T8E41 aluminum-lithium short and long crack specimens were performed under this effort. Constant amplitude and spectrum fatigue tests were conducted at various stress ratios and stress levels. The short and long crack results were compared to verify the existence of any short crack effect. As a result of the unusual fracture patterns in the aluminum-lithium short crack tests, an analytical approach considering combined Mode 1 and Mode 2 type fracture was considered and compared to the standard Mode 1 analysis used in the previous AGARD Core Test Program. Author

N91-11243# Laboratorio Nacional de Engenharia e Tecnologia Industrial, Lisbon (Portugal).

SHORT CRACK BEHAVIOUR IN Al-Li ALLOY 2090

M. Helena Carvalho and M. deFreitas (Lisbon Univ., Portugal) *In* AGARD, Short-Crack Growth Behaviour in Various Aircraft Materials Aug. 1990 17 p (For primary document see N91-11240 02-39)

Copyright Avail: NTIS HC/MF A09; Non-NATO Nationals requests available only from AGARD/Scientific Publications Executive

Within the AGARD Cooperative Test Program on the behavior of short cracks, a common airframe aluminium alloy (2024-T3) was investigated and the significance of the short crack effect analyzed from tests conducted on a single edge notched fatigue specimens of sheet material. The follow up Supplemental Test Program dealt with other alloys such a Ti6Al4V, steel 4340, Al 7075 and Al-Li 2090, all of them of interest Al-Li alloy at LNETI/CEMUL are described. Author

N91-11244# Deutsche Forschungsanstalt fuer Luft- und Raumfahrt, Cologne (Germany, F.R.). Inst. for Materials Research.

CRACK BEHAVIOUR OF 2024-T3, 2090-T8E41 AND 7075-T6 UNDER CONSTANT AMPLITUDE AND DIFFERENT TYPES OF VARIABLE AMPLITUDE LOADING, ESPECIALLY GAUSSIAN LOADING

H. Nowack, K. H. Trautmann, and J. Strunck *In* AGARD, Short-Crack Growth Behaviour in Various Aircraft Materials Aug. 1990 14 p (For primary document see N91-11240 02-39)

Copyright Avail: NTIS HC/MF A09; Non-NATO Nationals requests available only from AGARD/Scientific Publications Executive

The contribution of the DFVLR (DLR) to the AGARD cooperative test program on short and long cracks is described. Within the core program tests on 2024-T3 single edge notch (SENT) specimens were performed with constant amplitude, FALSTAFF, and Gaussian loading. Within the supplemental program short and long crack tests on the aluminum-lithium alloy 2090-T8E41 were carried out with Gaussian loading and some further exploratory long crack tests with the conventional high strength aluminum alloy 7075-T6 were added. The long crack tests were performed on center crack (CCT-) specimens. From the investigations it came out that 2024-T3 and 2090-T8E41 showed the so-called short crack effect. This effect is mainly attributed to the influence of crack closure. The microscopical behavior of 2024-T3 and 2090-T8E41 was different. At 2024-T3 several cracks initiated, normally as center cracks, whereas at 2090-T8E41 corner cracks were the predominant cracks. In the long crack stage 2090-T8E41 turned out to be not such damage tolerant as expected. Author

N91-11245# Royal Aircraft Establishment, Farnborough (England).

THE GROWTH OF SHORT FATIGUE CRACKS IN 2024 AND 2090 ALUMINIUM ALLOYS UNDER VARIABLE AMPLITUDE LOADING

R. Cook *In* AGARD, Short-Crack Growth Behaviour in Various Aircraft Materials Aug. 1990 11 p (For primary document see N91-11240 02-39)

Copyright Avail: NTIS HC/MF A09; Non-NATO Nationals requests available only from AGARD/Scientific Publications Executive

Fatigue crack growth measurements were made on 2024-T3 and 2090-T8E41 aluminum alloys subjected to FALSTAFF, Inverted FALSTAFF, and FELIX standard loading sequences. Crack growth rates at short crack lengths under FALSTAFF and Inverted FALSTAFF in 2024-T3 were found to be similar at each of three applied stress levels. This result is explained in terms of crack opening stress levels and is qualitatively predicted by a closure based crack growth model. Short fatigue cracks were shown to grow at stress intensity factors well below the long crack growth threshold in 2090-T8E41 alloy under FELIX loading. The short cracks, however grew initially perpendicular to the applied loading direction and then abruptly changed direction and grew at 60 deg to the initial crack direction. Short crack growth rates in 2024-T3 and 2090-T8E41 were compared and found to be similar if the length of the short cracks in the 2090 alloy were taken to be the length of the crack projected onto the axis perpendicular to the loading direction. This work represents the United Kingdom contribution to the supplemental program of the AGARD coordinated short fatigue crack growth investigation. Author

N91-11246# Aeronautical Research Inst. of Sweden, Bromma. Dept. of Structures.

SHORT CRACK GROWTH UNDER REALISTIC FLIGHT LOADING: MODEL PREDICTIONS AND EXPERIMENTAL RESULTS FOR Al 2024 AND Al-Li 2090

A. F. Blom *In* AGARD, Short-Crack Growth Behaviour in Various Aircraft Materials Aug. 1990 15 p Sponsored by Defense Materials Administration (For primary document see N91-11240 02-39)

Copyright Avail: NTIS HC/MF A09; Non-NATO Nationals requests available only from AGARD/Scientific Publications Executive

The swedish contribution to the AGARD effort on short fatigue crack growth includes various experimental investigations on the aluminum alloys Al 2024-T3 and Al-Li 2090-T8E41. These two materials were subjected both to constant amplitude loading, at stress ratios R = -2, -1, 0, and 0.5 and also to spectrum loading with the standardized load sequences FALSTAFF and TWIST, representative for the lower wing surface of fighter and civil aircraft, respectively. The TWIST sequence was also used to generate long crack growth data for the two alloys. The experimental results are summarized and numerical predictions by means of a modified Dugdale-Barenblatt model originally proposed by Newman are also included. Numerical results correspond well to the observed experimental behavior for most of the performed tests. Author

N91-11247*# National Aeronautics and Space Administration. Langley Research Center, Hampton, VA.

THE GROWTH OF SHORT CRACKS IN 4340 STEEL AND ALUMINUM-LITHIUM 2090

M. H. Swain, R. A. Everett (Army Aviation Systems Command, Hampton, VA.), James C. Newman, Jr., and E. P. Phillips *In* AGARD, Short-Crack Growth Behaviour in Various Aircraft Materials Aug. 1990 30 p Sponsored by NASA (For primary document see N91-11240 02-39)

Copyright Avail: NTIS HC/MF A09; Non-NATO Nationals requests available only from AGARD/Scientific Publications Executive CSCL 20K

The objectives were to investigate crack initiation characteristics and short crack growth behavior for Al-Li 2090 and for 4340 steel and to evaluate the ability of a closure-based crack-growth model to predict fatigue crack growth rates and total fatigue lives for the steel. Single-edge-notched tension specimens of each alloy were used to obtain the short crack growth rate information via an acetate replica technique. In addition to constant amplitude loading, tests on the steel were conducted using the Felix/28 variable amplitude spectrum (a shortened form of a standard loading sequence for fixed or semi-rigid helicopter rotors). The short crack growth rates were compared to those for long cracks grown under similar loading conditions. Metallurgical features associated with crack initiation are discussed. For Al-Li 2090 under R = -1 loading, the short cracks grew well below the long crack threshold and grew at acute angles to the loading axis. For 4340 steel under constant amplitude loading at R = 0.5 and 0 and for the Felix/28 spectrum loading, short-crack growth rates agreed well with long-crack growth rates, even near the long-crack threshold. A slight short-crack effect, growth below the long-crack threshold, was observed at R = -1. Fatigue lives were found to depend on the size and type of initiation site, especially for the Felix/28 loading sequence. A semi-empirical crack-growth model incorporating crack-closure effects was used to predict crack growth rates and total fatigue lives of notched 4340 steel specimens. An initial defect size and shape typical of those identified in this steel was assumed for the life predictions. For all loading conditions, reasonable agreement was found between measured and predicted values for both crack growth rates and fatigue lives. Author

N91-11248# National Aerospace Lab., Amsterdam (Netherlands).

SHORT AND LONG FATIGUE CRACK GROWTH IN 2024-T3 UNDER FOKKER 100 SPECTRUM LOADING

R. J. H. Wanhill and L. Schra *In* AGARD, Short-Crack Growth Behaviour in Various Aircraft Materials Aug. 1990 26 p Sponsored by Netherlands Agency for Aerospace Programs (For primary document see N91-11240 02-39)

Copyright Avail: NTIS HC/MF A09; Non-NATO Nationals requests available only from AGARD/Scientific Publications Executive

The behavior of short and long fatigue cracks in the widely used damage tolerant aluminum alloy 2024-T3 was compared using flight simulation loading representatives for the Fokker 100 wing/fuselage structure. The results showed that the apparently anomalous behavior of short cracks is not significant for durability analysis of the current wing/fuselage structure. Also the data provide a reference for evaluating new, candidate materials for durable wing/fuselage structures in transport aircraft. Author

N91-11249# Middle East Technical Univ., Ankara (Turkey). Dept. of Metallurgical Engineering.
GROWTH OF SHORT FATIGUE CRACKS IN 7075-T6 ALUMINUM ALLOY
Cevdet Kaynak and Alpay Ankara *In* AGARD, Short-Crack Growth Behaviour in Various Aircraft Materials Aug. 1990 8 p (For primary document see N91-11240 02-39)
Copyright Avail: NTIS HC/MF A09; Non-NATO Nationals requests available only from AGARD/Scientific Publications Executive

The growth of short fatigue cracks was monitored using a plastic replica method for cracks propagating on the specimen notch from the initial length of 40 to 50 microns up to the specimen thickness of 2.3 mm. Single-edge-notched tension (SENT) Al 7075-T6 specimens were tested under R-ratios of 0.5, 0, and -1 and at two different stress levels of each R-ratio. The general conclusion is that the growth rates of short cracks seem to be faster than the growth rates of long cracks for an R-ratio of -1. No significant differences were observed for R = 0, and the short cracks actually grew more slowly at R = 0.5. Author

N91-11250# Pisa Univ. (Italy). Dept. of Aerospace Engineering.
SHORT CRACK OBSERVATIONS IN Ti-6Al-4V UNDER CONSTANT AMPLITUDE LOADING
A. Lanciotti and R. Galatolo *In* AGARD, Short-Crack Growth Behaviour in Various Aircraft Materials Aug. 1990 7 p (For primary document see N91-11240 02-39)
Copyright Avail: NTIS HC/MF A09; Non-NATO Nationals requests available only from AGARD/Scientific Publications Executive

The Italian contribution to the AGARD supplementary test program on the growth of short fatigue cracks is described. Constant amplitude loading fatigue tests (zero-to-tension and fully reversed loading) were carried out on annealed Ti6Al4V titanium alloy, to establish the behavior of short and long cracks in this material. The results indicate that short cracks grow faster than long cracks at the same stress intensity factor range and they can also grow below the long crack threshold stress intensity factor range. Author

N91-11251# Royal Aircraft Establishment, Farnborough (England). Materials and Structures Dept.
TEXTURE ANALYSIS OF 2090-T8E41 ALUMINUM-LITHIUM ALLOY SHEET: ANNEX **c26**
A. W. Bowen *In* AGARD, Short-Crack Growth Behaviour in Various Aircraft Materials Aug. 1990 5 p (For primary document see N91-11240 02-39)
Copyright Avail: NTIS HC/MF A09; Non-NATO Nationals requests available only from AGARD/Scientific Publications Executive

This annex describes the texture analysis that was made on the 2090-T8E41 aluminum-lithium alloy sheet used in the AGARD Supplemental Test Program. The information obtained in this analysis was supplied to all participants who tested the aluminum-lithium alloy. Author

N91-11252*# National Aeronautics and Space Administration. Langley Research Center, Hampton, VA.
HIGH-PERFORMANCE EQUATION SOLVERS AND THEIR IMPACT ON FINITE ELEMENT ANALYSIS
Eugene L. Poole, Norman F. Knight, Jr., and D. Dale Davis, Jr. (Army Aviation Systems Command, Hampton, VA.) Sep. 1990 17 p Presented at the 6th World Conference on Finite Element Methods, Banff, Alberta, 1-5 Oct. 1990 Submitted for publication (NASA-TM-102735; AVSCOM-TM-90-B-017; NAS 1.15:102735)
Avail: NTIS HC/MF A03 CSCL 20K

The role of equation solvers in modern structural analysis software is described. Direct and iterative equation solvers which exploit vectorization on modern high-performance computer systems are described and compared. The direct solvers are two Cholesky factorization methods. The first method utilizes a novel variable-band data storage format to achieve very high computation rates and the second method uses a sparse data storage format designed to reduce the number of operations. The iterative solvers are preconditioned conjugate gradient methods. Two different preconditioners are included; the first uses a diagonal matrix storage scheme to achieve high computation rates and the second requires a sparse data storage scheme and converges to the solution in fewer iterations that the first. The impact of using all of the equation solvers in a common structural analysis software system is demonstrated by solving several representative structural analysis problems. Author

N91-11253# Technische Hochschule, Aachen (Germany, F.R.). Lehrstuhl fuer Mechanik und Baukonstruktionen.
UTION OF THE EQUIVALENT SPACE WITH BESSEL INTEGRAL EQUATION FOR THE FRACTURED ORTHOTROPIC DISK UTION OF THE 'EQUIVALENT SPACE' WITH BESSEL INTEGRAL EQUATION FOR THE FRACTURED ORTHOTROPIC DISK [(1): ZUR BERECHNUNG DER ORTHOTROPEN SCHEIBE MIT RISS MIT HILFE DER RANDELEMENT-METHODE. (2): LOESUNG DES EQUIVALENT SPACE MIT BESSEL-INTEGRALGLEICHUNG FUER DIE ORTHOTROPE SCHEIBE MIT RISS]
Zongrou Tian 1990 88 p In GERMAN
(ISSN-0932-8599; ETN-90-97898) Avail: NTIS HC/MF A05

The theme of this study is the theoretical approach of stress and dislocation fields of the fractured orthotropic disk, as well as its examination through a coal fiber material disk trial. The problem is resolved with the indirect integral process of the boundary element method. The stress field and the dislocation field of the fractured orthotropic disk are determined in equivalent space in two different ways. The mathematical model for the fractured orthotropic disk is presented and resolved. ESA

N91-11254 Clemson Univ., SC.
ALTERNATE EQUILIBRIUM CONFIGURATIONS OF FLEXIBLE CANTILEVER BEAMS Ph.D. Thesis
Shahnam Navaee 1989 248 p
Avail: Univ. Microfilms Order No. DA9017797

Alternate equilibrium configurations of cantilever beams subjected to end loads with constant angles of inclination and cantilever beams subjected to uniform distributed loads are investigated. The beams studied in this work are considered to be initially straight and prismatic in addition to being homogeneous, elastic, and isotropic. The formulation of this problem is based on the Bernoulli-Euler theorem for beams which states that the curvature is proportional to the bending moment. Apart from the assumptions inherent in the use of the Bernoulli-Euler equation, it is also assumed the beams are inextensible. It is shown that for certain combinations of beam parameters and loads, it is possible to have alternate equilibrium configurations for a cantilever beam. The ranges of these possible combinations, along with examples of the deflected shapes of the beam are also provided.
Dissert. Abstr.

N91-11255 Ohio State Univ., Columbus.
BUCKLING AND VIBRATIONS OF PLATES SUBJECTED TO CONCENTRATED FORCES Ph.D. Thesis
Essam Fathi Ayoub 1989 182 p
Avail: Univ. Microfilms Order No. DA9014391

The stability and the free vibration is studied of simply supported rectangular and circular plates subjected to a pair of concentrated forces, each acting oppositely on the boundary. The forces may be either tensile or compressive. Initial, inplane stresses within the plate are first determined. For rectangular plates, the initial stresses are obtained by two methods, both using finite elements. For circular plates, the closed form, exact solution of the plane elasticity problem is used to provide the inplane stress distribution for the buckling and vibration problem. The Ritz method is then utilized for the vibration and buckling analysis for both rectangular and circular plates. Buckling loads and vibration frequencies are found for various aspect ratios and load locations for rectangular plates. Numerical results are given for the buckling and the vibration frequencies of the simply supported circular plate, which separate into four symmetry classes of mode shapes. Comparisons of buckling loads with previously published, less accurate results are made, where possible. Tracking the frequency versus loading data

with increasing tensile forces shows that buckling due to tensile force can also occur, and the critical value of the force is found for both rectangular and circular plates. Dissert. Abstr.

N91-11256 Boston Univ., MA.
ATTENUATION OF ELASTIC WAVES DUE TO SCATTERING FROM SPHERICAL CAVITIES AND ELASTIC INCLUSIONS Ph.D. Thesis
Mark Karl Hinders 1990 182 p
Avail: Univ. Microfilms Order No. DA9022977

The attenuation of elastic waves due to scattering from a spherical inclusion of arbitrary size in an infinitely extended medium is investigated. The spherical scatterer and the exterior medium are isotropic, homogeneous, and linearly elastic, but of arbitrarily differing material parameters, with compressional and shear waves supported in both media. Exact expressions for scattered and transmitted fields caused by an incident plane compressional or shear wave of unit amplitude are calculated analytically and general expressions for extinction and scattering cross-sections are derived for both lossy and lossless scattering. Application to ultrasonic determination of porosity in cast aluminum is investigated.
Dissert. Abstr.

N91-11257 Maryland Univ., College Park.
ANALYSIS OF DUCTILE CRACK EXTENSION IN PLASTIC FRACTURE Ph.D. Thesis
Jun Ming Hu 1989 232 p
Avail: Univ. Microfilms Order No. DA9021513

For highly ductile fracture the deformation field is affected by the geometry of the specimen far from the crack tip, and the fracture mode of the cracked body may be dominated by plastic collapse at limit load. To investigate the behavior of metal specimen under plastic fracture, the limit load solution reported in the literature for SE(N) and C(T) specimens are reviewed, modified as needed. It is revealed that after a certain amount of crack extension, the load carrying capacities of most small size fracture specimen used to measure J-R curve are actually fall on or very close to limit load solution derived from Green-type slip-line field. Because of large plastic deformation and unloading due to large crack extension the basic assumptions of J-integral in nonlinear elastic or elastic-plastic fracture mechanics are violated and the employment of J-R curve in that portion is questionable. To provide a criterion to judge the boundary between elastic-plastic fracture and fully plastic fracture, a ductility factor in fracture for SE(B) and C(T) specimens is proposed. This factor describes the state of plastic deformation in fracture and is a function of specimen geometry. Based on slip-line field solution, a plastic rotation factor for C(T) specimen is derived and it was used in determining plastic CTOD-R for the specimen with large ductility factor. From limit load solution and plastic CTOD-R curve, the load versus load line displacement curves are predicted. In the appendix, the different physical meaning between J-integral and global energy dissipation rate and the limitations of both methods are discussed.
Dissert. Abstr.

N91-11258 Florida Atlantic Univ., Boca Raton.
EFFECTS OF AN INTERNAL FLOW ON THE VIBRATION OF THIN CYLINDRICAL SHELLS Ph.D. Thesis
Gilles F. Leyrat 1990 243 p
Avail: Univ. Microfilms Order No. DA9022368

The response and the dynamic stability of thin cylindrical shells excited by a point force with an internal heavy medium (water) moving with a constant mean flow velocity are investigated. Two sets of analysis are discussed, one for infinitely long shells and one for shells of finite length. The infinite condition applies to shells which are sufficiently long to be considered infinite. In this case, the solution is obtained by means of a spatial Fourier transform in the axial direction and a modal decomposition in the circumferential direction. Using this solution, input and transfer accelerances are determined. The results of this part of this analysis show that input accelerances are globally preserved as the mean flow velocity changes. For the transfer accelerances, broadband peaks appear which are caused by the phase matching between propagating waves of different mode numbers. These broadband peaks are shifted and modified by the mean flow velocity. For shells of finite length, simply supported boundary conditions are assumed. In this case, the response is obtained by using a normal mode expansion of the in vacuo shell and the Kirchhof-Helmholtz equation derived for a fluid moving at constant flow velocity and bounded by a perfectly rigid cylinder. For finite shells, the main effect of the flow on the response is to decrease the natural frequencies of the shell. The extent of the change in frequency depends on the circumferential and axial mode numbers. Experimental results are also presented for a pipe shell of radius 0.025 m and wall thickness 1.5 mm. Dissert. Abstr.

N91-11259 Columbia Univ., New York, NY.
BOUNDARY INTEGRAL EQUATIONS FOR DYNAMIC FRACTURE PROBLEMS Ph.D. Thesis
Yuan Jie Lua 1989 128 p
Avail: Univ. Microfilms Order No. DA9020569

The time domain traction boundary integral equation was formulated for a finite 2-D crack embedded in an elastoplastic solid under a prescribed transient load. The formulation is based on the integral representation of displacement gradients in the cracked body. In contrast to the corresponding elastodynamic case, additional terms arising from the plastic deformation and differentiation of a singular integral are presented in the integral representation of the displacement gradients. The validity of these terms is verified by considering the stress induced by the sudden creation of a circular plastic inclusion. The final system of boundary integral equations, which are hypersingular, relates the unknown crack opening displacement and plastic deformation to the prescribed crack face traction components. In order to concentrate the attention on the hypersingular integrals, a special application of the developed traction boundary integral equation to an elastodynamic crack problem is considered. The hypersingular integrals presented in the resulting boundary integral equation are confronted directly by interpreting them in terms of finite part integrals. By introducing constant and quadratic interpolation (in space and time) of the unknown crack opening displacement, the double integral equation is transformed into an algebraic system of equations. The time-stepping scheme, in which the crack opening displacement at a time t is being calculated by taking account of its history up to and including the time t, is applied to obtain time domain solutions. Dissert. Abstr.

N91-11260 Nebraska Univ., Lincoln.
PERFORMANCE OF FINITE DYNAMIC ELEMENTS FOR COMPOSITE MATERIALS IN PLANE STRESS Ph.D. Thesis
Shun-Fat Lung 1989 128 p
Avail: Univ. Microfilms Order No. DA9022995

Development of finite dynamic elements can result in significant reduction of computing time and cost for calculation of natural frequencies and mode shapes, which is an essential part of flutter prediction. Analysis with and without the dynamic terms is an alternative to constructing a new finite element mesh, to determine whether the mesh is sufficiently refined. Finite dynamic elements show spectacular improvement in convergence of higher modes with mesh refinement, but the improvement for lower modes is not so great. The element described is an extension of the conventional 3-node triangular plane stress element. The test problem used to study efficiency of the dynamic element formulations was a square cantilever plate. Calculations were done for an isotropic material and for an orthotropic material. The reduced time and cost is a result of achieving adequate accuracy with a courser mesh, smaller bandwidth and fewer total degrees-of-freedom. Costs are compared for computing the first 6 modes of a plate, with no mode having an error greater than a specified level. Cost reduction ratios of 16 were observed for some modes. A cost reduction ratio of about 3 was achieved for the first 6 modes of three isotropic and orthotropic plates. Dissert. Abstr.

N91-11261 Harvard Univ., Cambridge, MA.
CRACK-GROWTH RESISTANCE IN REINFORCED CERAMIC COMPOSITES Ph.D. Thesis
David Michael Stump 1990 158 p
Avail: Univ. Microfilms Order No. DA9021813

Crack growth resistances in brittle ceramic materials reinforced by small phase transforming zirconia particles and/or ductile crack-bridging particles were studied. The zirconia particles are assumed to undergo a purely dilatant transformation, while the bridging particles are taken to be either very ductile (i.e., rigid ideally-plastic) or to soften as the crack faces are drawn apart. The reinforcing mechanisms are examined individually and in combination. The increased toughnesses and tensile-fracture strengths due to the presence of dilatantly transforming particles are studied by modeling the wake regions of transformed material left behind the advancing tips of growing precut (i.e., prexisting) semi-infinite and finite cracks. Surprisingly, maximum toughnesses and tensile-fracture strengths occur for finite amounts of growth from the initial tip positions. Similarly, tensile strengthening in ceramics reinforced with rigid ideally-plastic particles is examined by modeling the formation of bridging strips behind the advancing tips of growing finite cracks. The peak tensile-fracture strengths of this material also occur for finite amounts of crack growth. Next, the toughnesses and tensile-fracture strengths in ceramics reinforced with both dilatantly transforming and very-ductile crack-bridging particles are examined by combining the models to study the growth of precut semi-infinite and finite cracks.
Dissert. Abstr.

N91-11262 Maryland Univ., College Park.
A THREE-DIMENSIONAL SOLID ELEMENT MODEL FOR FINITE ROTATION OF COMPOSITE SHELLS Ph.D. Thesis
Yong Hyup Kim 1989 147 p
Avail: Univ. Microfilms Order No. DA9021527

An eighteen-node solid element was developed to model the behavior of isotropic as well as laminated composite shell structures undergoing finite rotation under static loading. The present three-dimensional solid element formulation is simpler than the degenerate solid shell element formulation. The element formulation utilizes independently assumed strain in addition to assumed displacement. Four sets of assumed strain fields are introduced to stabilize the finite element model while alleviating locking. A modified stress-strain relation is introduced to incorporate thin shell behavior by decoupling normal strain from other strain components. The strain and the determinant of Jacobian matrix are assumed to be linear in the thickness direction. This linear assumption allows analytic integration in the thickness direction regardless of ply layups in laminated composite shell structures. Numerical results demonstrate the validity and the accuracy of the present formulation. The present solid element model allows large incremental rotation in the Newton-Raphson iteration because it does not include trigonometric functions in the formulation. Therefore, it is more advantageous than other existing finite element models for the analysis of buckling and postbuckling problem. Even though numerical tests are concentrated on thin shell structures, the present finite element model can handle thick shell structures.
Dissert. Abstr.

N91-11263# Sandia National Labs., Albuquerque, NM.
THERMAL STRESSES IN LAYERED ELECTRICAL ASSEMBLIES BONDED WITH SOLDER
H. S. Morgan 1990 6 p Presented at the International Symposium on Gas-Liquid Two-Phase Flows in Conjunction With the Winter Annual Meeting of the ASME, Dallas, TX, 25-30 Nov. 1990 Submitted for publication
(Contract DE-AC04-76DP-00780)
(DE90-015563; SAND-90-0688C; CONF-901109-17) Avail: NTIS HC/MF A02

Thermal stresses in a layered electrical assembly joined with solder are computed with plane strain, generalized plane strain, and three-dimensional (3D) finite element models to assess the accuracy of the two-dimensional (2D) modeling assumptions. Cases in which the solder is treated as an elastic and as a creeping material are considered. Comparison of the various solutions shows that away from the corners, the generalized plane strain model produces residual stresses that are identical to those computed with the 3D model. Although the generalized plane strain model cannot capture corner stresses, the maximum stresses computed with this 2D model are, for the mesh discretization used, within 12 percent of the corner stresses computed with the 3D model when the solder is modeled elastically and within 5 percent when the solder is modeled as a creeping material. Plane strain is not a valid assumption for predicting thermal stresses, especially when creep of the solder is modeled. The effect of cooling rate on the residual stresses computed with creep models is illustrated.
DOE

N91-11264# Ames Lab., IA.
FATIGUE CRACK CHARACTERIZATION BY ULTRASONIC INSPECTION
O. Buck, R. B. Thompson, and D. K. Rehbein 1989 2 p Presented at the ASTM Symposium on Quantitative Methods in Assessment of Standard Defects, Kansas City, KS, 25-26 May 1989
(Contract W-7405-eng-82)
(DE90-017252; IS-M-627; CONF-8905344-1) Avail: NTIS HC/MF A01

Ultrasonic inspection of fatigue crack characterization was studied in detail.
DOE

N91-11265# Lawrence Livermore National Lab., CA. Dept. of Earth Sciences.
A CONTINUUM TENSILE FAILURE MODEL WITH FRICTION
M. B. Rubin (Technion - Israel Inst. of Tech., Haifa.) and A. V. Attia Aug. 1990 52 p
(Contract W-7405-eng-48)
(DE90-018006; UCRL-ID-104759) Avail: NTIS HC/MF A04

The objective of this report is to document improvements in the tensile failure model that has been implemented as Model 23 in the DYNA-2D computer code. In the following sections we document the equations used for Model 23 and describe various example problems that were used to help verify the implementation of equations in the DYNA-2D computer code.
DOE

N91-11266# Rolls-Royce Ltd., Bristol (England).
EXPERIENCES IN THE USE OF ABAQUS FOR CREEP ANALYSIS
E. O. A. Prempeh Derby, England 7 Sep. 1989 12 p Presented at ABAQUS Users Meeting, Harwell, England, 7 Sep. 1989
(PNR-90705; ETN-90-97937) Copyright Avail: NTIS HC/MF A03

Some of the experiences gained in the use of ABAQUS program for creep analysis are reported. The ABAQUS program was used to determine the creep behavior of aircraft engine components subject to elevated temperatures and stress. Considerable difficulty was experienced in obtaining any creep solution in the initial stages. Once the causes of the difficulties were identified and resolved, the creep law subroutine became properly synchronized with the ABAQUS program. Comparisons of the results with solutions of creep analyses using other programs were found to be satisfactory. A suggestion for improving the ABAQUS user manual is presented.
ESA

N91-11267# Ames Lab., IA.
A THEORETICAL INVESTIGATION ON STRUCTURAL, VIBRATIONAL, AND ELECTRONIC PROPERTIES OF AMORPHOUS SILICON
C. M. Soukoulis and R. Biswas 1989 21 p Presented at the 2nd International Workshop of Non-Crystalline Solids, San Sebastian, Spain, 11-15 Jul. 1989
(Contract W-7405-eng-82)
(DE90-018040; IS-M-638; CONF-8907216-1) Avail: NTIS HC/MF A03

Amorphous silicon (a-Si) structures were generated by quenching liquid silicon configurations using molecular-dynamics simulations. Localized vibrational modes were identified in these

amorphous silicon models. The densities of states and dynamic structure factors for localized, resonant, and extended modes are discussed and compared with neutron scattering data. Voids of various sizes were introduced into a-Si models. The voids lead to a rapidly increasing structure factor below 1/A, similar to the intense small wave vector Guinier scattering observed in experiment. The presence of voids decreases the local strain in the a-Si network and substantially reduces the number of 5-coordinated sites from the a-Si model without voids. Finally, the electronic structure of these realistic a-Si models were calculated with empirical tight binding parameters. An a-Si model that has only 4-coordinated atoms displays an electronic density of states (DOS) in good agreement with experiment, including an energy gap similar to that of the crystal. For models containing 3- and 5-coordinated defect sites, structural relaxation of the a-Si model using molecular dynamics was important in producing a gap. The electronic DOS of a-Si models that contain 3- and 5-coordinated defect sites will be presented. DOE

N91-10930# Messerschmitt-Boelkow-Blohm/Entwicklungspring Nord, Bremen (Germany, F.R.).
NON-LINEAR VIBRATION OF LARGE, IMPERFECT SPACE STRUCTURES
E. Hornung and H. Oery (Technische Hochschule, Aachen, Germany, F.R.) *In* DLR, Contributions in the Field of Aeroelastics on the Occasion of the 60th Anniversary of Professor Dr.-Ing. Habil. Hans Wilhelm Foersching Apr. 1990 p 203-222 (For primary document see N91-10920 02-02)
Avail: NTIS HC/MF A13

42 GEOSCIENCES (GENERAL)

No abstracts in this category.

43 EARTH RESOURCES AND REMOTE SENSING

Includes remote sensing of earth resources by aircraft and spacecraft; photogrammetry; and aerial photography.

For instrumentation see *35 Instrumentation and Photography.*

N91-11268# Princeton Scientific Instruments, Monmouth Junction, NJ.
REMOTE SENSING IN THE ULTRAVIOLET Final Report, 29 Jan. 1988 - 30 Apr. 1990
John L. Lowrance 1 May 1990 29 p
(Contract F19628-88-C-0018; AF Proj. 4643)
(AD-A224254; GL-TR-90-0066) Avail: NTIS HC/MF A03
CSCL 17/5

This research program on remote sensing in the ultraviolet emphasized the development of imaging spectrophotometers sensitive in the ultraviolet and suitable for satellite borne applications. In addition, a significant amount of effort was devoted to supporting ground based UV measurements of rocket exhaust signatures and in redesigning and configuring one of GL's existing ground based UV imaging systems for wide field of view observations of the aurora in the near ultraviolet. A micro channel plate (MCP) image intensifier tube employing magnetic focus between the photocathode and the MCP was developed and demonstrated to be a feasible way of electronically correcting for satellite yaw. GRA

N91-11269# Beleidscommissie Remote Sensing, Delft (Netherlands).
FOREST CLASSIFICATION WITH HIGH RESOLUTION SATELLITE IMAGES. RESEARCH INTO THE USE OF SPATIAL INFORMATION TO IMPROVE THE MULTI-SPECTRAL CLASSIFICATION WITH SPOT IMAGES
Apr. 1990 30 p Prepared in cooperation with EUROCONSULT B.V., Arnhem, Netherlands
(BCRS-89-32; ETN-90-97683) Avail: NTIS HC/MF A03

Computerized classification of remote sensing imagery is addressed. Texture information is used by the human interpreter to distinguish different classes while a spectral classification program may not be able to recognize the difference. To overcome this problem, an approach incorporating texture information into the computerized classification process was tested over the north west coast of Tunisia and the Noordoost Polder in the Netherlands. No significant improvement was found in the forest classification test in Tunisia, possibly due to local circumstances, or by restrictions under which the research was carried out. The classification test of the Noordoost Polder showed substantially improved results. ESA

N91-11270# International Bank for Reconstruction and Development, Washington, DC.
SATELLITE REMOTE SENSING FOR AGRICULTURAL PROJECTS
J. P. Gastellu-Etchegorry 1990 236 p
(PB90-257916; World-Bank-TP-126; ISBN-0-8213-1625-7; LC-90-12783) Copyright Avail: NTIS MF A02; paper copy available from World Bank Publications, P.O. Box 7247-8619, Philadelphia, PA 19170-8619 CSCL 08B

The Bank's experiences to date with remote sensing are reviewed (specifically satellite remote sensing) and the context in which remote sensing is used in the Bank's operations is discussed. The steps the Bank has taken in response to the challenge of incorporating this technology into its lending operations are considered and a number of operational constraints that hinder successful application of this technology are reviewed. Some topics examined are: Remote sensing activities in the World Bank; Satellite remote sensing; Land use mapping in the Phillipines using SPOT satellite imagery; Mapping from space; Inventory of small and medium sized irrigation schemes in Algeria using SPOT numerical data; The role of remote sensing in irrigation management; Remote sensing applied to hydrogeology through case studies; Satellite hydrogeology; Monitoring of natural renewable resources and crop forecasting in sahelian countries; Famine in Africa; and Remote sensing and agricultural information for crop forecasting. Author

N91-11271 Maine Univ., Orono.
GULF OF MAINE SEA SURFACE TOPOGRAPHY FROM GEOSAT ALTIMETRY Ph.D. Thesis
Steven R. Lambert 1989 217 p
Avail: Univ. Microfilms Order No. DA9023859

A series of computer programs suitable for implementation on a personal computer were developed for the processing of GEOSAT altimetry data. The first twenty four repeats of the GEOSAT altimeter mission over the Gulf of Maine were processed. Estimates for the sea surface topography along five ascending tracks were computed. Three local tide models have compared as possible replacements to the Schwiderski global ocean tide model contained in the GEOSAT data records in order to provide more representative tidal corrections to the observed sea heights. Finally, sea surface height time series for two locations along an ascending arc are compared to data from two nearby moorings established by Brown and Irish in Jordan Basin and Georges Basin in order to verify the results of the GEOSAT derived features in the Gulf of Maine. For the data comparisons, the same tide mode is used to remove the tidal signal from both the GEOSAT data and the bottom pressure gauge/thermistor data. Dissert. Abstr.

N91-11272 Columbia Univ., New York, NY.
SATELLITE ELEVATION MAGNETIC ANOMALIES AND THEIR

USE IN TECTONIC STUDIES Ph.D. Thesis
Carol Anne Raymond 1989 165 p
Avail: Univ. Microfilms Order No. DA9020595

The Magsat mission was the first satellite magnetic survey directed toward the resolution of the lithospheric anomaly field at intermediate wavelengths. Magsat anomalies are studied over the ocean basins. The approach was first to assess the validity of the Magsat field in a region, then to apply the information to attack various tectonic problems. Magsat anomalies in the North Atlantic are shown to arise from the remanent magnetization of the seafloor created during the Cretaceous Long Normal polarity interval. Skewness observations were explained, along with observations of amplitude variations in sea surface magnetic anomaly profiles, and natural remanent magnetization (NRM) of crust drilled by the Deep Sea Drilling Project, in a model which describes the effects of alteration, by low-temperature oxidation, of the magnetic source layer. In the model, alteration results in a chemical remanent magnetization (CRM), which is controlled in amplitude and phase by the polarity bias of the field following emplacement of a given piece of crust. Comparison of the Magsat field over West Antarctica and the Weddell Sea with aeromagnetic data has enabled the identification of crustal sources for Magsat anomalies over the Bransfield Strait and Antarctic Peninsula. Geological sampling and depth-to-basement from low-level aeromagnetic measurements indicate the calc-alkaline Andean Intrusive Suite gives rise to the satellite anomaly which extends from the base of the Antarctic Peninsula to Thurston Island. Dissert. Abstr.

N91-11273# Beleidscommissie Remote Sensing, Delft (Netherlands).
REMOTE SENSING FOR MARINE ACTIVITIES
F. Drenth, G. J. Wensink, and S. Boer (Delft Hydraulics Lab., Netherlands) Feb. 1990 252 p
(BCRS-89-41; ETN-90-97646) Avail: NTIS HC/MF A12

Information requirements in the marine domain are defined and the potential of remote sensing products to fullfil these requirements are assessed. A list of potential applications of remote sensing is given. A survey of useful satellites (geostationnary and polar orbiting satellites), sensors (active microwave sensors and passive optical sensors) and numerical models (meteorology and oceanography numerical models) is presented. A questionnaire has been sent to organizations representing marine activities, to get insight into existing or dormant information needs in the marine domain. Based on results obtained, recommendations are given. ESA

N91-11274# Beleidscommissie Remote Sensing, Delft (Netherlands).
REMOTE SENSING FOR MARINE ACTIVITIES: APPENDICES
F. Drenth, G. J. Wensink, and S. Boer (Delft Hydraulics Lab., Netherlands) Feb. 1990 117 p
(BCRS-89-41-App; ETN-90-97989) Avail: NTIS HC/MF A06

Appendices for the definition study of remote sensing for marine operations are presented. They include a detailed description of the sensors and costs. Data sources are listed. A description of marine activities covering shipping, offshore, fishery and harbor/coast sectors is given. A questionnaire and mailing list are included. ESA

N91-11275# Instituto de Pesquisas Espaciais, Sao Jose dos Campos (Brazil).
SAMPLING AND INTERPOLATIONS IN DIGITAL TERRAIN MODELS M.S. Thesis - 19 Dec. 1989 [AMOSTRAGEN E INTERPOLACOES EM MODE-LOS DIGITAIS DE TERRENO]
Walker Gomes Mar. 1990 107 p In PORTUGUESE; ENGLISH summary
(INPE-5041-TDL/404) Avail: NTIS HC/MF A06

The aim of this work is to improve the precision of the digital elevation models with the topographic maps as the data source. The regularization of the grid was considered a critical point for improving the model. The errors generated in this phase were studied. The geographic information system developed by INPE was used and a new methodology for regularizing the grid is shown considering that linear interpolation presents good results, provided that good samples are obtained. It was observed that the quality of the models is strongly associated to the sampling process, an algorithm was performed to select representative sample. Models with high precision were obtained. Author

N91-11276*# National Aeronautics and Space Administration. Earth Resources Lab., Bay Saint Louis, MS.
UTILITY OF REMOTELY SENSED DATA FOR IDENTIFICATION OF SOIL CONSERVATION PRACTICES
R. E. Pelletier and R. H. Griffin Jun. 1986 76 p Original contains color illustrations
(NASA-CR-176874; NASA/NSTL/ERL-234; NAS 1.26:176874; DC-Y5-00400) Avail: NTIS HC/MF A05; 3 functional color pages CSCL 08B

Discussed are a variety of remotely sensed data sources that may have utility in the identification of conservation practices and related linear features. Test sites were evaluated in Alabama, Kansas, Mississippi, and Oklahoma using one or more of a variety of remotely sensed data sources, including color infrared photography (CIR), LANDSAT Thematic Mapper (TM) data, and aircraft-acquired Thermal Infrared Multispectral Scanner (TIMS) data. Both visual examination and computer-implemented enhancement procedures were used to identify conservation practices and other linear features. For the Kansas, Mississippi, and Oklahoma test sites, photo interpretations of CIR identified up to 24 of the 109 conservation practices from a matrix derived from the SCS National Handbook of Conservation Practices. The conservation practice matrix was modified to predict the possibility of identifying the 109 practices at various photographic scales based on the observed results as well as photo interpreter experience. Some practices were successfully identified in TM data through visual identification, but a number of existing practices were of such size and shape that the resolution of the TM could not detect them accurately. A series of computer-automated decorrelation and filtering procedures served to enhance the conservation practices in TM data with only fair success. However, features such as field boundaries, roads, water bodies, and the Urban/Ag interface were easily differentiated. Similar enhancement techniques applied to 5 and 10 meter TIMS data proved much more useful in delineating terraces, grass waterways, and drainage ditches as well as the features mentioned above, due partly to improved resolution and partly to thermally influenced moisture conditions. Spatially oriented data such as those derived from remotely sensed data offer some promise in the inventory and monitoring of conservation practices as well as in supplying parameter data for a variety of computer-implemented agricultural models. Author

N91-11277# Instituto de Pesquisas Espaciais, Sao Jose dos Campos (Brazil).
METHODOLOGY OF REMOTE SENSING FOR MONITORING MODIFICATIONS IN THE FLUVIAL CHANNEL AND UPDATING NAUTICAL CHARTS M.S. Thesis [METODOLOGIA DE SENSORIAMENTO REMOTO NO MONITORAMENTO DE MODIFICACOES NO CANAL FLUVIAL E ATUALIZACAO DE CARTAS NAUTICAS]
Wagner SantosdeAlmeida Aug. 1989 195 p In PORTUGUESE; ENGLISH summary
(INPE-4863-TDL/374) Avail: NTIS HC/MF A09

A methodology of remote sensing is proposed for monitoring the fluvial morphology of a section of the Solimoes River (Brazil), as support for cartographic updating of nautical charts. In developing of the methodology, the following material was used; LANDSAT MSS and TM images, aerial photographs, cartographic documents (bathymetric and topographic maps), image processing techniques, and data base technologies for mapping applications in a geographical information system. Among the results obtained it should be emphasized that deposition and erosion of sediments were detected which have caused changes at the section of the section of the river channel under study. Due to these changes, a cartographic restitution was made, using a TM-LANDSAT image registered with an UTM cartographic grid. The control points were obtained during the field work. This restitution allowed the updating

of the contour-line of part of the nautical chart. The cartographic precision obtained is compatible with planimetric charts, in terms of Cartographic Accuracy Standard (PEC) class A, scale 1:100,000. Author

N91-11278# Instituto de Pesquisas Espaciais, Sao Jose dos Campos (Brazil).
INTEGRATION OF MULTISPECTRAL AND PANCROMATIC CHANNELS OF HRV (SPOT) SENSOR FOR OBTAINING COLOR COMPOSITIONS WITH A SPATIAL RESOLUTION OF APPROXIMATELY 10 m M.S. Thesis [INTEGRACAO DOS CANAIS MULTIESPECTRAIS E PANCROMATICOS DO SENSOR HRV (SPOT) PARA OBTENCAO DE COMPOSICOES COLORIDAS COM RESOLUCAO ESPACIAL PROXIMA A 10 M]
Eneas RodriguesBrum Nov. 1989 110 p In PORTUGUESE; ENGLISH summary
(INPE-5035-TDL/403) Avail: NTIS HC/MF A06

The methodological procedures and the results obtained through digital merging of multispectral and panchromatic image data collected by HRV-SPOT sensor are presented. The techniques described provided improvements in spatial and spectral resolutions through an algorithm based on a linear model. The computation parameters were based on data obtained from spectral responsivity curves and spatial relationship among pixels in each channel. Some other techniques are described. The IHS transformation and product square root methods are performed. A new algorithm for combining SPOT satellite images with two different resolutions is presented. A software to perform these operations was developed. Author

N91-11279# Instituto de Pesquisas Espaciais, Sao Jose dos Campos (Brazil).
IDENTIFICATION OF AREAS SUBJECT TO FLOODING THROUGH TM/LANDSAT IMAGES IN THE BASIN OF THE RIVERS PINDARE, MEARIM, JAGUARIBE, APODI, PIRANHAS, AND SAN FRANCISCO [IDENTIFICACAO DE AREAS SUBMETIDAS A INUNDACAO ATRAVES DE IMAGENS TM/LANDSAT NAS BACIAS DOS RIOS PINDARE, MEARIM, JAGUARIBE, APODI, PIRANHAS E SAO FRANCISCO]
Teresa GallottiFlorenzano, Mario ValerioFilho, and Ricardo Leonardo ViannaRodrigues Feb. 1990 33 p Presented at the 2nd phase of the Project Application of TM/LANDSAT Data for Mapping Areas Subject to Flooding, INPE/SUDENE
(INPE-5034-RPE/619) Avail: NTIS HC/MF A03

Analog LANDSAT-TM images for both normal and flood discharge were used to map those areas subject to inundation along the floodplain of rivers Pindare, Mearim, Jaguaribe, Apodi, Piranhas and San Francisco (NE of Brazil). Analog images (b/w) at bands TM-3 and TM-4, at the scale 1:100,000, as well as positive color transparencies at 1:100,000, band 3 (blue), 5 green), 4 (red), were 1:100,000 using the PROCOM-2 system. Multispectral, multitemporal and multitemporal-multispectral color composites were obtained from digital TM data. The digital processing was carried out at test sites in a selected section in the Jaguaribe river floodplain. The result of this study is a set (collection) of 25 thematic maps at 1:100,000, showing flooded areas during the flood of 1985. Author

44 ENERGY PRODUCTION AND CONVERSION

Includes specific energy conversion systems, e.g., fuel cells; global sources of energy; geophysical conversion; and windpower.

For related information see also *07 Aircraft Propulsion and Power, 20 Spacecraft Propulsion and Power,* and *28 Propellants and Fuels.*

N91-11280# Midwest Research Inst., Golden, CO. Solar Energy Research Inst.
HIGH EFFICIENCY CuInSe2 AND CuInGaSe2 CELLS AND MATERIALS RESEARCH
R. B. Gillette, W. E. Devaney, W. S. Chen, and J. M. Stewart (Boeing Electronics High Technology Center, Seattle, WA.) Jul. 1990 60 p
(Contract DE-AC02-83CH-10093)
(DE90-000362; SERI/TP-211-3909) Avail: NTIS HC/MF A04

The results of a two year research program are presented. A 1-sq cm ZnO/CdZnS/CuInGaSe2 solar cell with a total area efficiency of 12.5 percent (12.9 percent active area) as measured at SERI (AM1.5, 100 mW/sq cm) was fabricated. The quantum efficiency of this device at 400 nm is over 0.7 due to the improved transmission of the ZnO/thin CdZnS window layers. The fabrication and characteristics of each of the three layers and of the complete devices are discussed. An extensive optical analysis of this cell was done. This analysis is presented and the implications for cell performance discussed. A 4 sq cm cell with this same structure was fabricated with an efficiency of 11.1 percent (11.9 percent active area), again as measured at SERI. The I-V and Quantum Efficiency characteristics of this cell are presented and the reasons for the decreased conversion efficiency relative to the 1-sq cm cells are discussed. DOE

N91-11281# Stuttgart Univ. (Germany, F.R.). Inst. fuer Aerodynamik und Gasdynamik.
PROBLEMS OF STATIC DIVERGENCE CONCERNING THE RPM REGULATION OF WIND TURBINES USING CENTRIFUGAL FORCE CONTROLLING MEANS AND ROTATING SLAT Ph.D. Thesis [PROBLEME STATISCHER DIVERGENZ BEI DER DREHZAHLREGELUNG VON WINDTURBINEN MITTELS FLIEHKRAFTREGLER UND DREHBAREM VORFLUEGEL]
Siegfried Mickeler 1988 95 p In GERMAN
(ETN-90-97858) Avail: NTIS HC/MF A05

The verification of the static divergence of the aerodynamic pitch moment of the slat through combination of calculated and experimental means was addressed. Experiments were carried out to study the compensation of this aerodynamical divergence of the slat, using the statics of centrifugal force controlling means, as well as experiments with a view to the reduction or neutralization of the divergence through aerodynamical means. ESA

N91-11282# Midwest Research Inst., Golden, CO. Solar Energy Research Inst.
CONCEPTUAL DESIGN OF AN OPEN-CYCLE OCEAN THERMAL ENERGY CONVERSION NET POWER-PRODUCING EXPERIMENT (OC-OTEC NPPE)
D. Bharathan, H. J. Green, H. F. Link, B. K. Parsons, J. M. Parsons, and F. Zangrando Jul. 1990 154 p
(Contract DE-AC02-83CH-10093)
(DE90-000304; SERI/TP-253-3616) Avail: NTIS HC/MF A08

This report describes the conceptual design of an experiment to investigate heat and mass transfer and to assess the viability of open-cycle ocean thermal energy conversion (OC-OTEC). The experiment will be developed in two stages, the Heat- and Mass-Transfer Experimental Apparatus (HMTEA) and the Net Power-Producing Experiment (NPPE). The goal for the HMTEA is to test heat exchangers. The goal for the NPPE is to experimentally verify OC-OTEC's feasibility by installing a turbine and testing the power-generating system. The design effort met the goals of both the HMTEA and the NPPE, and duplication of hardware was minimal. The choices made for the design resource water flow rates are consistent with the availability of cold and warm seawater as a result of the seawater systems upgrade carried out by the U.S. Department of Energy (DOE), the state of Hawaii, and the Pacific International Center for High Technology Research. The choices regarding configuration of the system were made based on projected performance, degree of technical risk, schedule, and cost. The cost for the future phase of the design and the development of the HMTEA/NPPE is consistent with the projected future program funding levels. The HMTEA and NPPE were designed cooperatively by PICHTR, Argonne National Laboratory, and Solar Energy Research Institute under the guidance of DOE. The experiment will be located at the DOE's Seacoast Test Facility

at the Natural Energy Laboratory of Hawaii, Kailua-Kona, Hawaii. DOE

N91-11283# Midwest Research Inst., Golden, CO. Solar Energy Research Inst.
ASSESSMENT OF MUNICIPAL SOLID WASTE FOR ENERGY PRODUCTION IN THE WESTERN UNITED STATES
B. J. Goodman and R. H. Texeira Aug. 1990 95 p
(Contract DE-AC02-83CH-10093)
(DE90-000361; SERI/TP-231-3622) Avail: NTIS HC/MF A06

Municipal solid waste (MSW) represents both a significant problem and an abundant resource for the production of energy. The residential, institutional, and industrial sectors of this country generate about 250 million tons of MSW each year. Data were compiled on the status of MSW in the 13-state western region, including economic and environmental issues. The report is designed to assist the members of the Western Regional Biomass Energy Program Ad Hoc Resource Committee in determining the potential for using MSW to produce energy in the region. DOE

N91-11284# Midwest Research Inst., Golden, CO. Solar Energy Research Inst.
EVALUATION OF A HIGH-TEMPERATURE BURNER-DUCT-RECUPERATOR SYSTEM
Jul. 1990 13 p Prepared in cooperation with Energetics, Inc., Columbia, MD
(Contracts DE-AC02-83CH-10093; DE-AC01-87CE-40762)
(DE90-000366; DOE/CH-10093/78) Avail: NTIS HC/MF A03

The U.S. Department of Energy's (DOE) Office of Industrial Technologies (OIT) sponsors research and development (R and D) to improve the energy efficiency of American industry and to provide for fuel flexibility. OIT has funded a multiyear R and D project by the Babcock and Wilcox Company (B and W) to design, fabricate, field test, and evaluate a high-temperature burner-duct-recuperator (HTBDR) system. This ceramic-based recuperator system recovers waste heat from the corrosive, high-temperature (2170 F) flue gas stream of a steel soaking pit to preheat combustion air to as high as 1700 F. The preheated air is supplied to a high-temperature burner. The B and W R and D program, which is now complete, involved several activities, including selecting and evaluating ceramic materials, designing the system, and developing and evaluating the prototype. In addition, a full-scale unit was tested at a B and W steel soaking pit. The full-scale system consisted of a modular single-stage ceramic recuperator, a conventional two-pass metallic recuperator, a high-temperature burner, fans, insulated ducting, and associated controls and instrumentation. The metallic recuperator preheated combustion air to about 750 F before it passed to the ceramic module. This technical case study describes the DOE/B and W recuperator project and highlights the field tests of the full-scale recuperator system. The document makes results of field tests and data analysis available to other researchers and private industry. It discusses project status, summarizes field tests, and reviews the potential effects the technology will have on energy use and system economics. DOE

N91-11285# Solarex Corp., Newtown, PA. Thin Film Div.
RESEARCH ON HIGH-EFFICIENCY, LARGE AREA AMORPHOUS SILICON BASED SOLAR CELLS Final Report, 1 Feb. 1989 - 28 Feb. 1990
R. R. Arya, M. Bennett, B. Fieselmann, J. Morris, J. Newton, R. Podlesny, E. Twesme, S. Wiedeman, L. Yang, and A. Rothwarf (Drexel Univ., Philadelphia, PA.) et al Sep. 1990 75 p Prepared for Midwest Research Inst., Golden, CO
(Contracts DE-AC02-83CH-10093; ZB-7-06003-2)
(DE90-000356; SERI/TP-211-3906) Avail: NTIS HC/MF A04

This document presents the results of studies in three areas: materials research, non-semiconductor materials research, and submodule research. In materials research, hydrogen dilution of a SiGe:H alloys improved alloys homogeneity and reduced light-induced degradation. Performance improvements were made in both microcrystalline and amorphous doped films, and a method was demonstrated that appears to overcome nucleation and film growth problems by recrystallizing the amorphous n-layer. In non-semiconductor materials research, ITO/Ag production was scaled up to successfully coat 1000-cm(sup 2) submodules. Work on atmospheric chemical vapor deposition of zinc oxide produced 2-micron thick films with 50 to 80 (Omega)/sq. sheet resistance. In submodule research, all processes were scaled up and single-junction submodules were prepared with 9.9 percent aperture-area conversion efficiencies. Triple-junction submodules were produced with 8.98 percent aperture-area efficiencies, and laser scribing was improved to allow only a 2 percent loss in area. Modeling was used to optimize module performance by predicting parasitic losses given the material constraints of a given device design. Modules were laser patterned to define an array of small-area devices, and topographic maps were produced to alloy visualization of both isolated defects and performance gradients. DOE

N91-11286# Midwest Research Inst., Golden, CO.
PERFORMANCE AND COST PROJECTIONS FOR ADVANCED WIND TURBINES
Susan M. Hock, Robert W. Thresher, and Joseph M. Cohen (Science Applications, Inc., Golden, CO.) Aug. 1990 7 p Presented at the International Symposium on Gas-Liquid Two-Phase Flows in Conjunction With the Winter Annual Meeting of the ASME, Dallas, TX, 25-30 Nov. 1990
(Contract DE-AC02-83CH-10093)
(DE90-000370; SERI/TP-257-3795; CONF-901109-11) Avail: NTIS HC/MF A02

This paper identifies two possible wind turbine system architectures that represent the next generation of horizontal-axis designs, targeted for the mid-1990's. Estimates of the effects of projected design refinements on energy capture and cost are used to calculate cost-of-energy (COE) estimates. Two basic design philosophies are presented: the first represents a system using power electronics to allow variable speed operation and the second represents an optimized stall-controlled rotor. Both concepts take advantage of recent technological innovations including advanced airfoils; innovative control strategies; drive-train improvements; and site-dependent system optimization strategies, such as tall towers for sites with strong vertical wind shears. Our investigation indicates that these design improvements will increase energy capture about 40 to 50 percent with a corresponding negligible impact on cost, when compared with current state-of-the-art wind systems. These performance improvements result in COE estimates ranging between $0.03 and $0.06/kWh for the mid-1990's for sites with annual average hub-height wind speeds from 8.5 mps to 6.8 mps. DOE

N91-11287# Midwest Research Inst., Golden, CO.
ATMOSPHERIC PERFORMANCE OF THE SPECIAL-PURPOSE SOLAR ENERGY RESEARCH INSTITUTE (SERI) THIN-AIRFOIL FAMILY: FINAL RESULTS
J. Tangler, B. Smith, D. Jager, and T. Olsen Sep. 1990 5 p Presented at the European Community Wind Energy Conference and Exhibition, Madrid, Spain, 10-14 Sep. 1990
(Contract DE-AC02-83CH-10093)
(DE90-000373; SERI/TP-257-3939; CONF-900989-1) Avail: NTIS HC/MF A01

The Solar Energy Research Institute (SERI), in cooperation with SeaWest Energy Group, has completed extensive atmospheric testing of the special-purpose SERI thin-airfoil family during the 1990 wind season. The purpose of this test program was to experimentally verify the predicted performance characteristics of the thin-airfoil family on a geometrically optimized blade, and to compare it to original-equipment blades under atmospheric wind conditions. The tests were run on two identical Micon 65/13 horizontal-axis wind turbines installed side-by-side in a wind farm. The thin-airfoil family 7.96 m blades were installed on one turbine, and AeroStar 7.41 m blades were installed on the other. This paper presents final performance results of the side-by-side comparative field test for both clean and dirty blade conditions. DOE

N91-11288# Morgantown Technology Center, WV. Office of Fossil Energy.
PROCEEDINGS OF THE SECOND ANNUAL FUEL CELLS CONTRACTORS REVIEW MEETING
W. J. Huber, ed. May 1990 263 p Meeting held in Morgantown, WV, 2-3 May 1990
(DE90-000490; DOE/METC-90-6112; CONF-900591) Avail: NTIS HC/MF A12

The Second Annual Fuel Cells Contractors Review Meeting was held May 2 to 3, 1990, at the Lakeview Resort in Morgantown, West Virginia. This meeting was sponsored and hosted by the Morgantown Energy Technology Center of the U.S. Department of Energy. The purpose of this meeting was to bring together the research and development (R and D) participants in the DOE/Fossil Energy-sponsored Fuel Cells Program to present key results of their research. Major emphasis was on phosphoric acid, molten carbonate, and solid oxide technology efforts. Research results of the coal gasification and gas stream cleanup R and D activities pertinent to the Fuel Cells Program were also highlighted. One hundred forty-nine attendees from industry, academia, and government participated in this 2-day meeting. Twenty-eight papers were given. Individual papers are processed separately for the data bases. DOE

N91-11289# Sandia National Labs., Albuquerque, NM.
BENCH-SCALE TESTING OF A HEAT-PIPE RECEIVER FOR SOLAR THERMAL ELECTRIC APPLICATIONS
Douglas R. Adkins and Vernon Dudley (Edgerton, Germeshausen and Grier, Inc., Albuquerque, NM.) 1990 25 p Presented at the International Symposium on Gas-Liquid Two-Phase Flows in Conjunction with the Winter Annual Meeting of ASME, Dallas, TX, 25-30 Nov. 1990
(Contract DE-AC04-76DP-00789)
(DE90-009834; SAND-90-0097C; CONF-901109-2) Avail: NTIS HC/MF A03

Electric power generating systems that couple parabolic-dish solar-concentrators with Stirling engines and generators are currently being developed under the Department of Energy's solar thermal electric program. These systems will use liquid metal heat pipes to transfer energy from the focal point of a solar concentrator to the heater tubes of a Stirling engine. The heat-pipe solar-receivers are required to operate in adverse orientations and accept flux levels on the order of 100 W/sq. cm. To explore the operating limits of heat-pipe solar-receivers, a series of bench-scale heat pipe receivers are being designed and tested. Results from the bench-scale tests and their implications on a full-scale heat-pipe solar receiver are presented in this paper. DOE

N91-11290# Sandia National Labs., Albuquerque, NM.
GENERIC QUALITY ASSURANCE/QUALITY CONTROL GUIDE FOR PHOTOVOLTAIC CONCENTRATOR DESIGN, DEVELOPMENT AND SYSTEM INSTALLATION
V. S. Murty and J. L. Chamberlin 1990 5 p Presented at the National Conference on Energy Research Enhancement and Technology Transfer for Industry and Higher Education, Kingsville, TX, 16-18 Sep. 1990
(Contract DE-AC04-76DP-00789)
(DE90-017040; SAND-90-2272C; CONF-9009238-1) Avail: NTIS HC/MF A01

The U.S. Department of Energy National Photovoltaics Program considers the photovoltaic (PV) concentrator technology as a viable entity, likely to penetrate the utility market in the foreseeable future. To achieve this, it has launched the National Photovoltaic Concentrator Initiative under the management of Sandia National Laboratories. The objective of this program is to encourage PV concentrator system design and manufacture, with a view to bringing the energy cost to $0.12/kWh in the next four years and to $0.06/kWh by the year 2000. To achieve these goals, the systems have to perform reliably for 20 to 30 years. This necessitates a stringent quality assurance/quality control (QA/QC) program in all phases of PV concentrator design, production, and installation. In order to assist the PV industry in this effort a project was initiated to provide a generic QA/QC guide, capable of being adapted by any PV concentrator industry to prepare its individual QA/QC plan. The draft plan of the guide was prepared and circulated to various government laboratories and industries involved in PV concentrator work. Their input is now being incorporated into a final document, which will serve as an industry standard. DOE

N91-11291# Colorado State Univ., Fort Collins. Solar Energy Applications Lab.
COLORADO STATE UNIVERSITY PROGRAM FOR DEVELOPING, TESTING, EVALUATING AND OPTIMIZING SOLAR HEATING AND COOLING SYSTEMS Progress Report, 1 Jul. - 31 Aug. 1990
Sep. 1990 22 p
(Contract DE-FG03-86SF-16306)
(DE90-017273; DOE/SF-16306/23) Avail: NTIS HC/MF A03

This paper is a progress report for the period of July 1, 1990 to 31 August 1990 on activities at Colorado State University in a program for developing, testing, evaluating and optimizing solar heating and cooling systems. Topics covered are: solar heating with isothermal collectors; solid cooling with solid desiccant; liquid desiccant cooling systems; solar heating systems; solar water heaters; fields tests; and program management. DOE

N91-11292# Central Research Inst. of Electric Power Industry, Tokyo (Japan).
TECHNICAL ASSESSMENT AND ECONOMIC STUDY OF COMPRESSED AIR ENERGY STORAGE IN JAPAN
Y. Uchiyama and M. Kadoyu May 1990 38 p In JAPANESE; ENGLISH summary
(DE91-701405; CRIE-Y-90002) Avail: NTIS (US Sales Only) HC/MF A03

In order to clarify the technological feasibility of compressed air energy storage systems (CAES) in Japan, economical analyses and technical investigations of the storage systems were conducted. The definition of efficiency of CAES was made clear and CAES was compared with other energy storage technologies, then followings were elucidated: the efficiency of CAES was inferior to that of the superconducting magnetic energy so far, but was superior to that of the pumped hydro; and may be improved up to that of the superconducting magnetic energy by technological progress in future. Storage facility of compressed air can be constructed by the existed technique on hard rock caverns. As to soft rock caverns and seabed storage tanks, there are subjects to be developed. Hard rock CAES systems can compete on generating cost with the conventional pumped hydro and LNG combined cycle if the site conditions are acceptable, however in other systems, the technical developments to improve the economy are required. Since the increasing ratio of the construction cost of CAES is lower in comparison with the pumped hydro which the construction cost increases with the site conditions, CAES is an expectative system as substitute for the pumped hydro. DOE

N91-11293# New Energy Development Organization, Tokyo (Japan).
STUDY ON FEASIBLE APPLICATIONS OF STIRLING CYCLE MACHINE
Mar. 1990 494 p In JAPANESE; ENGLISH summary
(DE91-701463; NEDO-P-8927) Avail: NTIS (US Sales Only) HC/MF A21

The feasibily study of a stirling cycle machine was made on its application to air conditioners and refrigerating machines as well as on the utilization of various heat sources such as LNG cryogenic heat, solar energy, and that of incinerator waste heat. Its application to the air conditioners was technically verified already by the development research which has been made by New Energy and Industrial Technology Development Organization. Its application research on the field of the refrigerating machines is promoted, but it is considered that the machines will also play an important role in promoting the latest leading techniques such as superconductivity. LNG cryogenic power generation is the new field which has been technically developed first in Japan in the world in which country a large quantity of LNG is consumed, and

the high efficiency utilization of the stirling cycle machines in this field is expected to be realized in future. It is a important problem to establish the technical basis of a solar energy stirling cycle machine, and they are promoting to develop this machine for practical use not only in Japan but also in many countries in the world. Further, the technical development of the stirling cycle machines utilizing heat sources such as waste heat, geothermal heat, and woody fuel, is also laid on an important situation.
DOE

N91-11294# Technische Univ., Delft (Netherlands). Lab. for Measurement and Control.
DUWECS REFERENCE GUIDE V1.0: DELFT UNIVERSITY WIND ENERGY CONVERTER SIMULATION PROGRAM
Peter M. M. Bongers 1990 79 p
(Grants ENW3-0044-NL; NOVEM-41/33-020/10)
(MEMT-5; ISBN-90-370-0036-3; ETN-90-97754) Copyright Avail: NTIS HC/MF A05

The reference guide describes the wind turbine simulation program DUWECS (Delft University Energy Converter Simulation Package). DUWECS is suited for simulation and analysis of flexible wind turbines. The program is divided into a program shell and a user defined wind turbine model. The wind turbine model consists of an interconnection of different modules. The modules are mutually interacting via user specified interaction variables. The user can modify each module and use it in the wind turbine model. The DUWECS program is written in FORTRAN 77 with minor MS-FORTRAN extensions and can run on MS-DOS computer systems. The DUWECS version for other computer systems can be made available. The input of DUWECS can be given interactively or by files. The results of a DUWECS run are one or more files.
ESA

N91-11295# Midwest Research Inst., Golden, CO. Solar Energy Research Inst.
ELECTRONIC PROCESSES IN THIN FILM PV MATERIALS Final Report, 1 Sep. 1986 - 31 May 1989
P. C. Taylor, G. A. Williams, and W. D. Ohlsen (Utah Univ., Salt Lake City.) Aug. 1990 35 p
(Contract DE-AC02-83CH-10093)
(DE90-000359; SERI/TP-211-3905) Avail: NTIS HC A03/MF A01

This report describes research to study the effects of defects, impurities, and interfaces on the performance of photovoltaic (PV) devices, particularly hydrogenated amorphous silicon (a-Si:H) and related alloys. The studies of a-Si:H and related alloys involve understanding the metastabilities using various analysis techniques, characterizing the defects lying deep within the gap (such as Si dangling bonds) and the general density of electronic states throughout the gap, and understanding interfacial effects, especially as they relate to interfaces important to PV devices. Accomplishments include understanding the kinetics of light-induced defects in films, identifying trapped molecular hydrogen and discovering molecular hydrogen diffusion along the microvoids in a-Si:H, investigating the behavior of the defect photoluminescence band in Si-Ge alloys, discovering an E (prime) defect at some a-Si:H/SiO2 interfaces, initially characterizing some paramagnetic defects induced by rapid thermal quenching, developing a new technique to measure low levels of absorption in films and discovering a peak in the below-gap absorption spectrum that may be interface related, using subgap excitation of electron spin resonance and photoluminescence to probe deep defects, and developing a bistable optical switch based on thermal modulation of the index of refraction in films.
DOE

N91-11296# Midwest Research Inst., Golden, CO. Solar Energy Research Inst.
RESEARCH ON HIGH-EFFICIENCY, MULTIPLE-GAP, MULTI-JUNCTION AMORPHOUS SILICON-BASED ALLOY THIN-FILM SOLAR CELLS Final Report, 1 Mar. 1987 - 28 Feb. 1990
S. Guha (Energy Conversion Devices, Inc., Troy, MI.), A. Bannerjee, J. Burdick, E. Chen, T. Glatfelter, G. Hammond, M. Hopson, T. Laarman, M. Lycette, and R. Mohr et al Aug. 1990 146 p
(Contract DE-AC02-83CH-10093)
(DE90-000364; SERI/TP-211-3918) Avail: NTIS HC/MF A08

This report documents the results of material development, single-junction solar cell research, and high-efficiency multijunction cell development. High-quality a-Si:Ge:H:F alloys were made with optical band gaps as low as 1.3 eV; high-conductivity microcrystalline p(sup +) and n(sup +) doped alloys were developed with optical band gaps greater than 2 eV. A double-layer antireflection coating was developed, and the cell's quantum efficiency at 400 nm improved from 60 to 77 percent. A novel solar cell structure was developed using band gap profiling in the intrinsic layer to obtain high efficiency. Single-junction solar cells with a-SiGe:H alloys in the intrinsic layer were fabricated with active-area efficiencies of 9.7 percent. Dual-gap tandem cells were fabricated with active-area efficiencies of 13 percent, and triple-junction cells were fabricated with active-area efficiencies of 13.7 percent, the highest reported to date for any thin-film amorphous solar cell. Degradation rates of 12 to 17 percent after 300 hours illumination were measured in triple-junction cells, a significant increase over the degradation of single-junction cells with comparable efficiencies. A triple-junction module with a subaperture area of 818 cm(sup 2) was measured at SERI with a conversion efficiency of 8.4 percent.
DOE

N91-11297# Midwest Research Inst., Golden, CO.
ANALYSIS OF LOSS MECHANISMS IN POLYCRYSTALLINE THIN FILM SOLAR CELLS
J. R. Sites (Colorado State Univ., Fort Collins.) Aug. 1990 34 p
(Contract DE-AC02-83CH-10093)
(DE90-000372; SERI/TP-211-3950) Avail: NTIS HC/MF A03

Our goal for thin-film polycrystalline solar cell analysis was to increase the useful information extracted from relatively straightforward electrical measurements. The strategy was to (1) systematize measurements and reporting, (2) organize results in terms of quantitative values for individual sources of current and voltage loss, and (3) evaluate possible analytical techniques to enhance precision and avoid pitfalls, and (4) insist on a viable physical explanation of each loss mechanism. Current-voltage, quantum efficiency, and capacitance measurements on CuInSe2 and CdTe solar cells from a variety of sources have been analyzed. In many cases losses were identified that may be lessened relatively easily. However, the operating voltage loss due to excessive forward recombination current throughout the depletion region remains the primary obstacle to efficiencies competitive with single crystal cells.
DOE

N91-11298# International Fuel Cells Corp., South Windsor, CT.
MOLTEN CARBONATE FUEL CELL POWER PLANT SYSTEMS STUDIES
W. H. Johnson Jun. 1990 73 p
(Contract DE-AC21-87MC-23270)
(DE90-009697; DOE/MC-23270/2876) Avail: NTIS HC/MF A04

The goal of the DOE and IFC Molten Carbonate Fuel Cell (MCFC) Program is to develop a MCFC technology base capable of providing clean electrical energy at competitive cost when integrated with coal gasification (CG) systems. To be successful, a coal-fueled MCFC system must provide cost of electricity (COE) which is lower than that of current electric generation technologies and which is competitive with other long range electric generating systems. The strategy for the study was to initially evaluate the status of non-fuel cell systems to establish the basis for a competitive CG/MCFC power plant and the corresponding MCFC subsystem goals. Secondly, an iterative and comparative analysis of potential CG/MCFC systems was conducted. This analysis included a detailed examination of MCFC integration with gasifier technology in which the technical basis for MCFC compatibility with a broad range of gasifiers was established. Lastly, a detailed conceptual design was prepared for the most desirable CG/MCFC system. The design established the potential of the CG/MCFC power plant to meet the goals and provide a competitive cost of electricity at very high efficiency and significantly reduced

emissions. The design also provided focus for the technical issues still outstanding and required for commercialization of the CG/MCFC technology. DOE

N91-11299# Argonne National Lab., IL.
OCEAN THERMAL ENERGY CONVERSION: PERSPECTIVE AND STATUS
Anthony Thomas and David L. Hillis 1990 7 p Presented at the MTS 1990, Washington, DC, 26-28 Sep. 1990
(Contract W-31-109-eng-38)
(DE90-017665; CONF-9009249-1) Avail: NTIS HC/MF A02

The use of the thermal gradient between the warm surface waters and the deep cold waters of tropical oceans was first proposed by J. A. d'Arsonval in 1881 and tried unsuccessfully by George Claude in 1930. Interest in Ocean Thermal Energy Conversion (OTEC) and other renewable energy sources revived in the 1970s as a result of oil embargoes. At that time, the emphasis was on large floating plants miles from shore producing 250 to 400 MW for maintained grids. When the problems of such plants became better understood and the price of oil reversed its upward trend, the emphasis shifted to smaller (10 MW) shore based plants on tropical islands. Such plants would be especially attractive if they produce fresh water as a by-product. During the past 15 years, major progress has been made in converting OTEC unknowns into knowns. Mini-OTEC proved the closed cycle concept. Cost effective heat exchanger concepts were identified. An effective biofouling control technique was discovered. Aluminum was determined to be promising for OTEC heat exchangers. Heat transfer augmentation techniques were identified, which promised a reduction on heat exchanger size and cost. Fresh water was produced by an OTEC open cycle flash evaporator, using the heat energy in the seawater itself. The current R and D emphasis is on the design and construction of a test facility to demonstrate the technical feasibility of the open cycle process. The 10 MW shore-based, closed cycle plant can be built with today's technology; with the incorporation of a flash evaporator, it will produce fresh water as well as electrical power; both valuable commodities on many tropical islands. The open cycle process has unknowns that require solution before the technical feasibility can be demonstrated. The economic viability of either cycle depends on reducing the capital costs of OTEC plants and on future trends in the costs of conventional energy sources. DOE

N91-11300# Argonne National Lab., IL.
ENERGY MODELS AND NATIONAL ENERGY POLICY
Cary N. Bloyd, David G. Streets, and Ronald E. Fisher 1990 6 p Presented at the 25th Intersociety Energy Conversion Engineering Conference, Reno, NV, 12-17 Aug. 1990
(Contract W-31-109-eng-38)
(DE90-017682; CONF-900801-30) Avail: NTIS HC/MF A02

As work begins on the development of a new National Energy Strategy (NES), the role of energy models is becoming increasingly important. Such models are needed to determine and assess both the short and long term effects of new policy initiatives on U.S. energy supply and demand. A central purpose of the model is to translate overall energy strategy goals into policy options while identifying potential costs and environmental benefits. Three models currently being utilized in the NES process are described, followed by a detailed listing of the publicly identified NES goals. These goals are then viewed in light of the basic modeling scenarios that were proposed as part of the NES development process. DOE

N91-11301# Pacific Northwest Lab., Richland, WA.
RESULTS FROM A WORKSHOP ON RESEARCH NEEDS FOR MODELING AQUIFER THERMAL ENERGY STORAGE SYSTEMS
M. K. Drost Aug. 1990 13 p Presented at the Workshop on Aquifer Thermal Energy Storage Modeling System, Seattle, WA, 30 Nov. - 1 Dec. 1989
(Contract DE-AC06-76RL-01830)
(DE90-018007; PNL-7441; CONF-8911224-1) Avail: NTIS HC/MF A03

A workshop an aquifer thermal energy storage (ATES) system modeling was conducted by Pacific Northwest Laboratory (PNL). The goal of the workshop was to develop a list of high priority research activities that would facilitate the commercial success of ATES. During the workshop, participants reviewed currently available modeling tools for ATES systems and produced a list of significant issues related to modeling ATES systems. Participants assigned a priority to each issue on the list by voting and developed a list of research needs for each of four high-priority research areas; the need for a feasibility study model, the need for engineering design models, the need for aquifer characterization, and the need for an economic model. The workshop participants concluded that ATES commercialization can be accelerated by aggressive development of ATES modeling tools and made specific recommendations for that development. DOE

45 ENVIRONMENT POLLUTION

Includes atmospheric, noise, thermal, and water pollution.

N91-11302# National Oceanic and Atmospheric Administration, Boulder, CO. Climate Monitoring and Diagnostics Lab.
ECC OZONESONDE OBSERVATIONS AT SOUTH POLE, ANTARCTICA DURING 1989
W. D. Komhyr, E. A. Crozer, J. A. Lathrop, and M. A. Winey Jun. 1990 252 p
(PB90-258914; NOAA-DR-ERL-CMDL-5) Avail: NTIS HC/MF A12 CSCL 13B

Atmospheric ozone vertical distributions, air temperatures, and wind speed and wind direction data are presented for 60 balloon electrochemical concentration cell (ECC) ozonesonde soundings made at South Pole, Antarctica, in 1989. GRA

N91-11303# Michigan Univ., Ann Arbor. Dept. of Atmospheric, Oceanic and Space Sciences.
ESTIMATION OF SEASONAL AND ANNUAL ACIDIC DEPOSITION THROUGH AGGREGATION OF THREE-DAY EPISODIC PERIODS Report, Feb. 1989 - Feb. 1991
P. J. Samson, J. R. Brook, and S. Sillman Aug. 1990 248 p Sponsored by Environmental Protection Agency, Research Triangle Park, NC
(PB90-252628; EPA/600/3-90/059) Avail: NTIS HC/MF A11 CSCL 13B

A method for aggregating episodic deposition estimates has been developed and used to identify which meteorological situations merit simulation by regional acid deposition model (RADM) based on their likelihood of producing sulfate (SO4(-2)) wet deposition at multiple locations across eastern North America, their frequency of occurrence, and their seasonality. The aggregation technique was performed using four years (1982 to 1985) of precipitation chemistry data from the Utility Acid Precipitation Sampling Program (UAPSP). The method developed during the project improves upon random selection. It is based on the stratification of three-day periods into categories of similar 850 mb wind flow across eastern North America. The aggregation project has provided the RADM project with a list of simulation periods which represent the range of meteorological patterns over eastern North America. The selection of storm types was based on their likelihood of producing SO4(-2) wet deposition at multiple locations across eastern North America, their frequency of occurrence, and their seasonality. The project has also provided the RADM project with scaling factors for use in weighing episodic simulation results to seasonal and annual deposition. GRA

N91-11304# California Univ., Riverside. Air Pollution Research Center.
LIFETIMES AND FATES OF TOXIC AIR CONTAMINANTS IN CALIFORNIA'S ATMOSPHERE Final Report
R. Atkinson Mar. 1990 290 p Sponsored by California State Air Resources Board, Sacramento

(Contract CA-ARB-A732-107)
(PB90-253204; ARB-R-90/441) Avail: NTIS HC/MF A13 CSCL 13B

A literature review of the atmospheric chemistry of eight potentially toxic air contaminants was carried out: chloroform, 1,3-butadiene, benzo(a)pyrene (BaP; a polycyclic aromatic hydrocarbon or PAH), formaldehyde, acetaldehyde, ethylene oxide, styrene, and diesel exhaust particles (including gas- and particle-phase PAH'sand derivatives). Experimental studies were carried out on styrene (reaction with nitrate radical and ozone), 1,4-dioxane (reaction with ozone), nitrobenzene (reaction with ozone), and p-dichlorobenzene (reaction with nitrate radical and ozone). These data were obtained by the California Air Resources Board for incorporation into reports on exposure assessments for these compounds, which is required as part of the process of identifying and controlling toxic air contaminants. Also investigated were ring-retaining products formed from the hydroxyl radical reactions (in the presence of nitrogen oxides) with benzene, toluene, and the three xylene isomers. The resulting data showed that new chemical mechanisms for the atmospheric chemistry of the aromatic hydrocarbons are needed. GRA

N91-11305# Dayton Univ., OH.
MINIMIZATION AND CONTROL OF HAZARDOUS COMBUSTION BYPRODUCTS
B. Dellinger, P. H. Taylor, and D. A. Tirey Aug. 1990 399 p Sponsored by Environment Protection Agency, Cincinnati, OH
(PB90-259854; EPA/600/S2-90/039) Avail: NTIS HC/MF A17 CSCL 13B

The report describes the results of a research effort in which all relevant information regarding the minimization and control of hazardous combustion byproducts (products of incomplete combustion, PIC's) that result from operations in which hazardous waste is thermally destroyed (e.g., in incinerators, boilers and kilns) is summarized, analyzed and thoroughly described. The research was conducted cooperatively by the University of Dayton Research Institute (UDRI) and the EPA Risk Reduction Engineering Laboratory (RREL). The report covers a period from February 1989 to February 1990. GRA

N91-11306# Southwest Research Inst., San Antonio, TX.
MEASUREMENTS OF TOXIC EXHAUST EMISSIONS FROM GASOLINE-POWERED LIGHT-DUTY VEHICLES Final Report
M. A. Warner-Selph Nov. 1989 192 p
(Contract CA-ARB-A6-198-32)
(PB90-259649; ARB-R-90/445) Avail: NTIS HC/MF A09 CSCL 13B

Exhaust emission rates of selected toxic substances were determined for two gasoline-powered passenger cars. These substances, which have appeared on California Air Resources Board's Toxic Air Contaminant list or have been candidates for the lists, include volatile and semi-volatile halogenated hydrocarbons, 1,3-butadiene, acrolein, phenols, nitrobenzene, dialkylnitrosamines, and a number of other unregulated emissions. Regulated gaseous emissions and fuel economy were also measured. A literature search was performed to determine if any of these compounds had previously been measured in the exhaust of gasoline-powered vehicles and if appropriate analytical procedures were available. When unavailable, procedures were developed for sampling and analyzing the unregulated toxic emissions compounds. The two vehicles were then tested to determine the emission rates of the targeted compounds. In the tests, a 1987 Ford Taurus equipped with a 3-way plus oxidation catalyst and a 1986 Toyota Camry equipped with a 3-way catalyst only were operated over the Federal Test Procedure, the Highway Fuel Economy Test, and the New York City Cycle. The test fuel was a regular unleaded gasoline without ethanol or methanol, and was obtained from California. GRA

N91-11307# Rolls-Royce Ltd., Derby (England).
COMMERCIAL AIRCRAFT AND THE ENVIRONMENT
Anthony B. Wassel 15 Mar. 1990 15 p Presented at Aeropropulsion 1990, Paris, France, Mar. 1990
(PNR-90687; ETN-90-97931) Copyright Avail: NTIS HC/MF A03

The impact of both noise and emission control on engine design is considered. New technology developed to meet the regulatory objectives are underlined. The reduction of noise in turbofan engines is discussed. Conflicting requirements and considerations of safety are stressed. Subsonic and supersonic noise generation and regulations proposed are reviewed. The reduction in CO2 and other emissions from aircraft propulsion systems are investigated. ESA

N91-11308# Oak Ridge National Lab., TN. Energy Div.
DEMOCRATIC THEORY, SCIENCE, AND DECISION MAKING IN GLOBAL CLIMATE CHANGE: CULPABILITY, UNCERTAINTY, AND FAIRNESS
David Lewis Feldman 1990 13 p Presented at the Political Science Association Annual Meeting on Global Climate Problems and Public Policy, San Francisco, CA, 29 Aug. - 2 Sep. 1990
(Contract DE-AC05-84OR-21400)
(DE90-017316; CONF-9008153-1) Avail: NTIS HC/MF A03

Uncertainty over the causes and consequences of global climate change poses three challenges to policy makers: (1) countries may become divided into winners and losers as a result of the distribution of positive and negative impacts from global warming: (2) climate change beneficiaries may be jeopardized by covetous losers; and (3) the costs of climate change will be borne by future generations. It is contended that durable responses to climate change will be difficult to formulate because any policy can be criticized as empirically deficient, and thus, a hasty response which is likely to hurt economic growth. Three paths for ethically appropriate policies are suggested: (1) policy makers should develop rules for allocating benefits and costs of climate related activities which are not dependent on preserving existing economic and political structures. These structures mask inequities between developed and developing countries; (2) science has a limited capacity for establishing consensus over the impacts of, or solutions to, climate change. Thus, novel means of incorporating public preferences in the search for durable policy are required; and (3) the impacts of climate change are unclear. Thus, any response is likely to be fallible and should be designed to be adjustable and negotiable. This reasonable fallibility approach emphasizes limited confidence in the ability to effect positive or negative changes to nature. DOE

N91-11309# Argonne National Lab., IL. Environmental Assessment and Information Sciences Div.
EVALUATING THE ENVIRONMENTAL IMPACTS OF THE ENERGY SYSTEM: THE ENPEP (ENERGY AND POWER EVALUATION PROGRAM) APPROACH
B. P. Hamilton, P. F. Sapinski, R. R. Cirillo, and W. A. Buehring 1990 11 p Presented at the IAEA Advisory Group Meeting on Experience with Using The Agency's Model WASP for Energy and Nuclear Power Planning in Developing Countries, Vienna, Austria, 21-25 May 1990
(Contract W-31-109-eng-38)
(DE90-017862; CONF-9005272-1) Avail: NTIS HC/MF A03

Argonne National Laboratory (ANL) has developed the ENergy and Power Evaluation Program (ENPEP), a PC-based energy planning package intended for energy/environmental analysis in developing countries. The IMPACTS module of ENPEP examines environmental implications of overall energy and electricity supply strategies that can be developed with other ENPEP modules, including ELECTRIC, the International Atomic Energy Agency's Wien Automatic System Planning Package (WASP-III). The status and characteristics of a new IMPACTS module that is now under development at ANL is presented. DOE

46 GEOPHYSICS

Includes aeronomy; upper and lower atmosphere studies; ionospheric and magnetospheric physics; and geomagnetism.

For space radiation see *93 Space Radiation.*

N91-11310*# Flight Mechanics and Control, Inc., Hampton, VA.
FINAL SHUTTLE-DERIVED ATMOSPHERIC DATABASE: DEVELOPMENT AND RESULTS FROM THIRTY-TWO FLIGHTS Final Report
John T. Findlay and Rachel A. Jasinski Jul. 1990 86 p
(Contract NAS9-17394)
(NASA-CR-185636; NAS 1.26:185636) Avail: NTIS HC/MF A05 CSCL 04A

The final Shuttle-derived atmospheric data base is presented. The relational data base is comprised of data from 32 Space Transportation System (STS) descent flights, to include available meteorology data taken in support of each flight. For the most part, the available data are restricted to the middle atmosphere. In situ accelerations, sensed by the tri-redundant Inertial Measurement Unit (IMU) to an accuracy better than 1 mg, are combined with post-flight Best Estimate Trajectory (BET) information and predicted, flight-substantiated Orbiter aerodynamics to provide determinations up to altitudes of 95 km. In some instances, alternate accelerometry data with micro-g resolution were utilized to extend the data base well into the thermosphere. Though somewhat limited, the ensemble of flights permit a reasonable sampling of monthly, seasonal, and latitudinal variations which can be utilized for atmospheric science investigations and model evaluations and upgrades as appropriate. More significantly, the unparallel vertical resolution in the Shuttle-derived results indicate density shears normally associated with internal gravity waves or local atmospheric instabilities. Consequently, these atmospheres can also be used as stress-atmospheres for Guidance, Navigation and Control (GN and C) system development and analysis as part of any advanced space vehicle design activities. Author

N91-11311*# Massachusetts Inst. of Tech., Cambridge.
LARGE-SCALE DYNAMICS AND TRANSPORT IN THE STRATOSPHERE Semiannual Report, 1 Mar. - 1 Sep. 1990
R. A. Plumb Sep. 1990 28 p
(Grant NAGw-1727)
(NASA-CR-187327; NAS 1.26:187327) Avail: NTIS HC/MF A03 CSCL 04A

Stationary planetary waves in the southern stratosphere display a characteristic seasonal cycle. Previous research based on a one-dimensional model suggests that this behavior is mainly determined by seasonally varying transmission properties of the atmosphere with respect to wave propagation. The issue is investigated with the help of a hemispheric, linear, quasigeostrophic model. It reproduces well some of the observed qualitative features and is internally consistent in the sense that its seasonal wave cycle can be explained in terms of varying wave transmission properties of the mean circulation. On the other hand, the model does not yield the observed seasonal cycle. Despite considerable sensitivity to modifications in the basic state wind and dissipation parametrization, the model could not be reasonably fit to reproduce the observed seasonal cycle. Author

N91-11312# Royal Inst. of Tech., Stockholm (Sweden). Dept. of Plasma Physics.
ELECTRIC FIELDS IN MAGNETOSPHERE
Carl-Gunne Faelthammar 16 Aug. 1990 42 p Presented at the International Conference on Plasma Physics, Delhi, India, 22-28 Nov. 1989
(TRITA-EPP-89-06; ISSN-0348-7539; ETN-90-97981) Avail: NTIS HC/MF A03

The large scale ionospheric electric field were determined from measurements on the ground and in low satellite orbit. For must of the magnetosphere, concepts of the electric field were mostly based on theoretical considerations and extrapolations of the ionospheric electric field. Direct in situ electric field measurements in the outer parts of the magnetosphere were made only relatively recently. A few satellite missions, most recently the Viking mission, extended the direct empirical knowledge so as to include major parts of the magnetosphere. These measurements revealed a number of unexpected features. The actual electric field was found to have unexpectedly strong space and time variations, which reflect the dynamic nature of the system. Examples are given of measured electric fields in the plasmasphere, the plasmasheet, the neutral sheet, the magnetotail, the flanks of the magnetosphere, the dayside magnetopause and the auroral acceleration region. ESA

N91-11313# National Center for Atmospheric Research, Boulder, CO.
COMPARISON OF CLEAR AIR ATMOSPHERIC RADAR TECHNIQUES FOR THE STUDY OF ATMOSPHERIC DYNAMICS IN THE TROPOSPHERE AND THE STRATOSPHERE Ph.D. Thesis
Joel Stephan Henry M VanBaelen 1990 207 p Prepared in cooperation with Colorado Univ., Boulder Sponsored by NSF
(PB90-256314; NCAR/CT-128) Avail: NTIS HC/MF A10 CSCL 04A

Using the Middle and Upper Atmospheric (MU) radar, an experiment was designed to perform a comparison between wind measurements obtained by 3 different techniques at VHF in the troposphere and lower stratosphere: Doppler Beam Swinging (DBS), Spaced Antenna (SA) with the Full Correlation Analysis (FCA), and Radar Interferometry (RI). The great versatility of the MU radar enables fast switching from one mode of operation to the other (DBS and SA). The DBS technique cyclically swings its beam in one of five beam directions every interpulse period. The FCA and RI techniques share the same SA data using four subgroups of antenna elements as separate receivers. It is believed that it is the first time that a 3-D radar interferometry technique has been implemented for continuous wind profiling. The horizontal wind profiles obtained with the different techniques generally agree well. Author

N91-11314# National Center for Atmospheric Research, Boulder, CO.
[ADVANTAGES OF THE COMMUNITY CLIMATE MODEL (CCM) CONCEPT] Progress Report, Jul. 1990
David L. William Jul. 1990 112 p Sponsored by NSF
(PB90-256348; NCAR/TN-351+PPR) Avail: NTIS HC/MF A06 CSCL 04A

The advantages of the Community Climate Model (CCM) concept in which many scientist use the same basic model for a variety of scientific studies, were demonstrated in the CCM workshop. At these workshops, many diverse experiments were seen to relate to each other when performed with the same model, and much constructive dialogue took place between experts in different disciplines. The 3rd workshop on CCM was held in July 1990. To augment these workshops and to foster interchange between all users of the NCAR CCM, the CCM Advisory Committee recommended that a CCM progress report be prepared periodically for all users and potential users. Author

N91-11315# Lamont-Doherty Geological Observatory, Palisades, NY.
NCEER STRONG-MOTION DATA BASE: A USER MANUAL FOR THE GEOBASE RELEASE (VERSION 1.0 FOR THE SUN3)
P. Friberg and K. Jacob Mar. 1990 64 p Sponsored in part by National Center for Earthquake Engineering Research, Buffao, NY
(Grant NSF ECE-86-07591)
(PB90-258062; NCEER-90-0005) Avail: NTIS HC/MF A04 CSCL 08K

The purpose of the report is to describe the initial implementation of a strong-motion data base developed by Lamont-Doherty Geological Observatory (Lamont) under the auspices of the National Center for Earthquake Engineering Research (NCEER). The report details how to install Lamont's data base access tool, GeoBase, and how to obtain strong-motion

data. NCEER's strong-motion data base combines features never before available for a single strong-motion database. These are: (1) both parametric and time-series data are accessible over a computer network; (2) the parametric data are maintained in a relational format; (3) the time-series data are stored on-line; and (4) the time-series are stored in a consistent format. GRA

N91-11316 Georgia Inst. of Tech., Atlanta.
A SIMPLE ZONAL AVERAGE ENERGY BUDGET MODEL OF THE EARTH-ATMOSPHERE SYSTEM Ph.D. Thesis
Omar Bello-Torres 1990 204 p
Avail: Univ. Microfilms Order No. DA9023832

A zonal average energy budget of the earth-atmosphere system resolving land and ocean areas is developed. The globe is divided into ten-degree-wide latitudinal belts characterized by longitudinally-average meteorological and geographical properties. Satellite-derived total cloud cover data are used to construct cloud optical depth and cloud-top height climatologies so that the model reproduces satellite measured values of planetary albedo and outgoing longwave radiation at the top of the atmosphere. A heat budget analysis is carried out for each latitude zone identifying all relevant heat sources and sinks. The physical processes that drive the energetics of the earth-atmosphere system are modeled or parameterized to obtain estimates of the components of the energy budget at the Earth's surface and in the atmosphere for the months of January, April, July and October. These months are assumed to be representative of each of the seasons. The model attains two-dimensional global coverage by combining adjacent latitude belts. Zonally-averaged meridional heat fluxes by the global ocean and by the atmosphere are computed by differencing the energy imbalances between continuous latitude belts. The results obtained indicate that it is the atmosphere rather than the ocean which accomplishes most of the poleward flux of heat required to maintain the global energy balance. An evaluation of the albedo and greenhouse effects of clouds is performed as well as an analysis of the effects of the diurnal variation of solar zenith angle in the estimation of planetary albedo. Dissert. Abstr.

N91-11317 State Univ. of New York, Albany.
PLANETARY BOUNDARY LAYER DYNAMICS OVER THE AMAZON RAIN FOREST Ph.D. Thesis
Amauri PereiradeOliveira 1990 312 p
Avail: Univ. Microfilms Order No. DA9025884

Observations of the diurnal evolution of the planetary boundary layer (PBL) over the Amazon rain forest, in the area of the Amazon boundary layer experiment (ABLE) 2A and 2B experiments showed the existence of a low level circulation with low level nocturnal maxima winds. These circulations are shown to be induced by the thermal contrast between the river and the forest. A linear model was applied to identify the horizontal extent of these circulations and an associated perturbation pressure gradient consistent with the observations. A second order closure model was used to simulate changes in the PBL caused by the thermal circulation. Good agreement with the observations was obtained when the forcing was a horizontal pressure gradient equal to 0.5 mb/100km of limited vertical extent. The dynamics of the equatorial PBL was shown to be plausibly explained using a hypothesis of a river breeze circulation. Dissert. Abstr.

N91-11318 University of Northern Colorado, Greeley.
NORTHWEST AFRICAN DEPRESSIONS AND THEIR RELATIONSHIP TO JET STREAMS Ph.D. Thesis
Abdulgader M. Ahmad 1989 238 p
Avail: Univ. Microfilms Order No. DA9016595

The two-fold purpose was to examine the intensity, movement, and duration of northwest African depressions and to determine if there was any relationship between the jet stream and the depressions. Northwest African lows are generally weak though they may intensify. The lows are found as open troughs or closed circulations at the 850 millibar level, but rarely higher. Cyclogenesis over northwest Africa takes place when a trough or a weak disturbance occurs in the presence of a jet stream. Upper level divergence associated with the jet stream creates favorable conditions for cyclogenesis. Further development may take place in the presence of either the polar or the subtropical jet. The depressions move in an east-northeast direction in association with an upper level trough and the jet stream. Depressions that move in a northeasterly track have the longest duration and travel the longest distance. The weakness of the relationship between the intensity of the lows and the strength of the jet probably is a result of the dominance of the subtropical jet. The impact of this jet on depressions development is less pronounced than that of the polar jet. Dissert. Abstr.

N91-11319 Colorado State Univ., Fort Collins.
THE EVOLUTION OF VORTICAL PATTERNS AND VORTICES IN MESOSCALE CONVECTIVE COMPLEXES Ph.D. Thesis
Michael Allan Fortune 1989 195 p
Avail: Univ. Microfilms Order No. DA9017412

The evolution and flow structure of four mesoscale convective complexes (MCCs) that manifested some form of vortical pattern of convective rainfall were investigated with datasets from the PRE-STORM field program. Intersecting convective bands that resembles an extratropical, frontal-wave cyclone evolved in the growth stage of three cases. A spiral pattern also emerged in one case, while the fourth developed a comma-shaped occlusion. A strong divergent wind response to the mesoscale heat source was observed in all systems, but only a weak rotational wind developed in the frontal wave systems. The frontal wave pattern resulted from the intersection of a mesoscale cold front advancing into the most unstable air with an existing stationary front. The convectively active core of the MCC's propagated with the intersection. When upper level directional shear spread a stratiform cloud in more than one direction around the core, and when intense convection developed well south of the core and the front, the eventual spin-up of a vortex was fostered. In other cases, advection of the stratiform cloud north of the core may have hindered spin-up because a dry mind-level inflow beneath the cloud developed counter to the direction of rotation. A conceptual model of the mesoscale frontal-wave cyclone employs the conveyor belt model of the extratropical cyclone. The conceptual models presented here for a weakly rotating (frontal wave) MCC and a strongly rotating MCC are compared with conceptual models of larger-scale extratropical cyclones and smaller-scale supercell thunderstorms. Dissert. Abstr.

N91-11320 Alaska Univ., Fairbanks.
A SIMULATION STUDY OF MAGNETIC RECONNECTION PROCESSES AT THE DAYSIDE MAGNETOPAUSE Ph.D. Thesis
Yong Shi 1989 283 p
Avail: Univ. Microfilms Order No. DA9017186

The dayside reconnection processes are studied by using computer simulations. First, the global magnetic reconnection patterns at the dayside magnetopause are studied based on a two-dimensional incompressible magnetohydrodynamic (MHD) code. It is found that multiple X line reconnection may prevail at the dayside magnetopause when the magnetic Reynolds number is large. The formation and subsequent poleward convection of magnetic islands are observed in the simulation. The Alfven Mach number of the solar wind, M(sub Asw), can also change the reconnection patterns. For a large M(sub Asw), reconnection tends to occur at the higher latitude region. Secondly, the structure of the dayside reconnection layer is studied by a two-dimensional compressible MHD simulation. In a highly asymmetric configuration typical of the dayside magnetopause, the pair of slow shocks bounding the reconnection layer in Petschek's symmetric model is found to be replaced by an intermediate shock on the magnetosheath side and a weak slow shock on the magnetospheric side. In addition, a mechanism for the enhancement of B(sub y), which is observed in the magnetopause current layer and magnetic flux tubes, is proposed. Dissert. Abstr.

N91-11321 California Univ., Los Angeles.
WAVE-MEAN FLOW INTERACTION IN THE STORM-TIME THERMOSPHERE USING A TWO-DIMENSIONAL MODEL Ph.D. Thesis
Douglas George Brinkman 1990 121 p
Avail: Univ. Microfilms Order No. DA9024990

A 2-D pole-to-pole numerical model with background solstitial winds was used to study the global dynamical response of the thermosphere to high latitude energy inputs associated with a model geomagnetic storm. This model storm, consisting of a series of substorms, has four distinct pulses of heat input over a 12-hr period. The storm generated six groups of wave disturbances in the form of internal gravity waves. Characteristics of these disturbance such as their vertical structure, phase propagation speeds, and influences of dispersion and dissipation are illustrated. The disturbances in the velocity field and in the temperature field are shown, along with their mutual phase relationship with regard to the meridional and vertical transport of heat and momentum. The main purpose is to investigate the interaction between the disturbances and the mean flow associated with the storm. It is shown that this interaction can be represented in terms of an induced circulation. This induced circulation is forced by the time dependent nature of the eddy flux convergences (divergences) of heat and momentum. The influence of this induced circulation is detectable most noticeably in the heat sources and sinks set up by the Eulerian mean circulation. At altitudes above 150 km, in the equatorial region, the equivalent temperature changes due to such sources and sinks resulting from the induced circulation are 1/3 to 1/4 of the changes due to the Eulerian mean circulation. Dissert. Abstr.

N91-11322 Utah Univ., Salt Lake City.
THE EVOLUTION AND TIME SCALES OF THE ATMOSPHERIC RESPONSE TO TROPICAL DIABATIC HEATING EVENTS Ph.D. Thesis
Lawrence Edward Buja 1990 198 p
Avail: Univ. Microfilms Order No. DA9021120

Simulations of tropical-midlatitude interactions have shown tropical heating anomalies to provoke significant responses in the midlatitude circulation on time scales shorter than those of current operational forecasts. In order to determine the impact of these tropical forcings, a series of 36 day real data global forecasts are used to examine the evolution and time scales of the geopotential height and zonal wind response to both realistic and theoretical configurations of imposed tropical diabatic heating. The principal goals are to determine: (1) the time scale at which the transient response of real data integrations with a general circulation model begins to resemble the perpetual season response found in the same model for long term climate integrations; (2) the sensitivity of extended range forecasts to the presence or absence of time oscillations in the tropical heating; and (3) the ways in which the responses forced in real data forecasts vary with the geographic location of the tropical heating anomaly. Remote responses to anomalous heating placed in the eastern Pacific are first evident between days 5 to 10. The transition from a local, short term type of response, to a large scale response pattern similar to that seen in perpetual climate runs occurs after approx. 3 to 15 days into the integration. Dissert. Abstr.

N91-11323 Illinois Univ. at Urbana-Champaign, Savoy.
FLUCTUATING CONCENTRATIONS IN ATMOSPHERIC DISPERSION Ph.D. Thesis
George Ellis DeVaull, III 1990 498 p
Avail: Univ. Microfilms Order No. DA9021670

Theoretical models and experimental results are presented of average and instantaneous concentration measurements from a series of atmospheric dispersion experiments conducted under both unstable and stable meteorological conditions. The experiments were undertaken at two different sites, over both flat and gently rolling terrain. Two types of surface-level point aerosol sources were used. One is a fog-oil smoke and the other is a hexachloroethane chemical smoke. Measurements of concentration at points along crosswind transects were taken over time periods of an hour at distances to several kilometers from the source. These measurements included both aerosol photometer records of the instantaneous concentration taken at a 1 Hz sampling rate and aspirated filters for mean concentration measurements. Meteorological measurements were used in determining the atmospheric boundary layer scaling parameters in the unstable tests and in characterizing the complex wind field for the stable tests. The data compare favorably with developed models for both the mean and variance in concentration. Point concentration histograms are shown to agree with the exponential distribution for concentrations greater than zero. Dissert. Abstr.

N91-11324 Oxford Univ. (England).
RADIOMETRIC OBSERVATION OF THE ATMOSPHERIC BOUNDARY LAYER (THE ROSSA PROJECT) Ph.D. Thesis
C. L. Hepplewhite 1989 243 p
Avail: Univ. Microfilms Order No. BRD-89417

Radiometric measurements of the ocean skin temperature together with bulk water temperatures, simultaneous radiosonde ascents, and satellite infrared radiances are used to investigate the oceanic skin effect, the sea surface emissivity, and the atmospheric transmission of infrared radiation, in the window region of 8 to 12 microns. A radiometer sensitive to infrared radiation in the spectral range 6.5 to 14 microns, was designed, built, and used to obtain sea surface skin temperatures to an accuracy of between 0.20 K and 0.25 K with a resolution of between 0.03 K and 0.05 K. Satellite radiances were provided by the advanced very high resolution radiometer (AVHRR)/2 instrument on NOAA-9, and atmospheric temperature and humidity profiles from Vaisala radiosondes launched from the ship. Investigations of the oceanic skin effect were made by comparing the measurements of skin sea surface temperature obtained using the radiometer with bulk temperatures. In terms of the overall average of the complete Atlantic Ocean data set, the skin of the sea was found to be 0.30 K cooler than the bulk, about 10 cm below the surface. The variability of the skin effect was found to be smaller in the tropics and greater at higher latitudes. The sea surface emissivity was found to vary very little with sea state at viewing angles less than about 45 deg. However, at these viewing angles and under calm, clear conditions, the surface brightness temperature was observed to fall when viewed at the vertical. Studies of the transmission of radiation in the atmospheric window region show that the effect on the atmospheric temperature deficit of different water vapor continuum models can not be distinguished from the effects of aerosols. When there are aerosols present, the retrieval of the sea surface temperature (SST) from space using the split window algorithms is subject to large errors. The dual angle technique is shown to be capable of retrieving SST to a higher degree of accuracy than the multi-channel technique, particularly in the presence of aerosol. Dissert. Abstr.

N91-11325 Tennessee Univ., Knoxville.
THE INFLUENCE OF ENVIRONMENTAL FACTORS ON THE TEMPERATURE OF THE RADIOSONDE THERMISTOR Ph.D. Thesis
James K. Luers 1989 186 p
Avail: Univ. Microfilms Order No. DA9021036

A technique was developed to calculate the radiosonde temperature error as a function of altitude under different environmental conditions. The environmental conditions analyzed include the surface (or cloud) temperature, the atmospheric gaseous constinuents, the aerosol and thermodynamic structure of the atmosphere, the solar elevation angle, the solar albedo, the rise rate of the balloon, and the atmospheric density. The heat balance equations for the thermistor and lead wires were derived and a sensitivity analysis performed to establish the significance of each heating term. The Air Force LOWTRAN 6 code was used to model the solar and infrared irradiation of the thermistor in terms of the environmental parameters. LOWTRAN 6 output was then used to generate the radiation input to the heat balance equations of the thermistor and lead wires. The temperature error of the radiosonde was derived by solving these heat balance equations. This technique for calculating the

radiosonde temperature error was validated by comparing with data from flights of experimental radiosondes containing the Standard NWS radiosonde thermistor and three other thermistors with different radiative coatings. Results suggest that the radiosonde temperature error is likely to differ at different latitudes and solar elevation angles because of differing radiative fluxes to the thermistor and because of differing atmospheric temperature profiles. Dissert. Abstr.

N91-11326 Oxford Univ. (England).
ATMOSPHERIC CHEMISTRY: LABORATORY STUDIES OF KINETICS OF IMPORTANT REACTIONS Ph.D. Thesis
S. J. Smith 1989 269 p
Avail: Univ. Microfilms Order No. BRD-89463

Experiments to measure the rate constants for some reactions of the atmospherically important nitrate radical (NO3) are described using the discharge-flow technique. The nitrate radical was monitored by optical absorption at lambda = 662 nm. The reactions of NO3 with some stable organic and inorganic substrates are reported. The temperature dependences of some of the rate constants were also determined (298 less than T less than 523 K). In most cases, computer simulation was used to extract the rate constant for the primary process because the time-dependent behavior of (NO3) was affected by secondary reactions of NO3 with products of the primary interaction. The Arrhenius parameter for the reactions of NO3 with CH3CH3, CH2CH2, CH3OH, CHCl3, and HCl were determined. The activation energies for the reactions studied between NO3 and some alkynes are presented along with the corresponding pre-exponential factors. Some reactions were studied at room temperature (298 plus or minus 2 K) only and the rate constants found (in units of cubic cm/molecule sec) are: buta-1,3-diene (1.8 x 10 (exp -13), isobutene (2.8 x 10 (exp -13), HBr (1.3 x 10 (exp -15) and hex-2-yne (3.0 x 10 (exp -14). Non-Arrhenius behavior was found in the reactions of NO3 with n-butane, isobutane and propene. The empirical variation of these rate constants with temperature is presented. The curvature of the Arrhenius plots is discussed in terms of (1) a temperature-dependent pre-exponential factor, and (2) the possibility that two competing channels, possessing differing activation energies, exist for each reaction. The atmospheric implications of these reactions are discussed with reference to the nighttime production of nitric acid and the importance of the these reactions as loss processes for NO3. Dissert. Abstr.

N91-11327 Oxford Univ. (England).
MODELLING OF LARGE-SCALE UNSTABLE WAVES IN THE MIDDLE ATMOSPHERE Ph.D. Thesis
John Thuburn 1988 175 p
Avail: Univ. Microfilms Order No. BRD-89459

Observations of the zonal mean state of the middle atmosphere suggest that it may be unstable, in certain regions and certain seasons, to large-scale wave-like disturbances of appropriate zonal wavenumbers and phase speeds. Possible candidates for such waves have also been observed, including a 4-day wave in the winter stratosphere and a 2-day wave in the summer mesosphere. An attempt was made to model the observed waves, extending the linear calculations of earlier authors to look at the nonlinear evolution. Some of the mechanisms which may limit the growth of unstable waves are elucidated. The effect of the unstable waves on the zonal mean circulation was investigated. The competition between this wave feedback and thermal and frictional forcing of the mean circulation was also investigated. In order to address these questions some analytical models are developed, including a weakly nonlinear model, and also a numerical model which uses a fully three-dimensional spectral representation of the stream function to integrate the quasigeostrophic potential vorticity equation in spherical geometry. A systematic derivation of the quasigeostrophic potential vorticity equation in spherical geometry is given, along with several results which are extensions of earlier theorems in the field of hydrodynamic stability or analogues of results in primitive equation theory or quasigeostrophic beta-plane theory. The numerical model reproduces the wavenumbers and phase speeds of the 4-day wave and the 2-day wave, but not all of the details of the wave structures agree with the observations. In the case of the 4-day wave, it is suggested that the observed warm pool may, in fact, have an origin other than instability of the type modelled here. Dissert. Abstr.

N91-11328 California Univ., Irvine.
SEASONAL VARIATIONS IN THE LATITUDINAL DISTRIBUTION OF TROPOSPHERIC CARBON MONOXIDE, 1986 TO 1988 Ph.D. Thesis
Dale Frederick Hurst 1990 285 p
Avail: Univ. Microfilms Order No. DA9022313

Carbon monoxide (CO) largely controls the oxidizing capacity of the Earth's atmosphere and indirectly influences the concentrations of many atmospheric trace gases. Previous studies have indicated that the abundance of CO in the lower troposphere depends primarily on latitude and season. A few researchers have reported that the atmospheric abundance of CO is increasing globally. Elevated levels of CO in the atmosphere may enhance global warming, stratospheric ozone depletion and photochemical smog production in urban areas. CO was measured in remote tropospheric air samples collected quarterly in the Pacific region during 1986 to 1988. Each season, sets of samples were collected over a wide latitude range during a two-week period, then were returned to the home laboratory for analysis by gas chromatography. The CO mixing ratio data were analyzed using a 1-dimensional, 16-latitude-band model of the atmosphere. During 1986 to 1988, carbon monoxide mixing ratios in the Northern Hemisphere were consistently greater than those in the Southern Hemisphere. The north-south ratio of hemisphere-averaged CO mixing ratios varied seasonally from about 1.4 in September to about 2.6 in March, and averaged 1.9 during 1986 to 1988. Dissert. Abstr.

N91-11329 Columbia Univ., New York, NY.
ASPECTS OF THE EARTHQUAKE GEOLOGY AND SEISMOTECTONICS OF THE SOUTHERN SAN ANDREAS AND RELATED FAULTS Ph.D. Thesis
Patrick Lee Williams 1989 305 p
Avail: Univ. Microfilms Order No. DA9020629

Aspects of the mechanics and movement history of the southernmost San Andreas or related faults are addressed. The seismotectonic context of the southernmost San Andreas fault is investigated. Microstratigraphic and geomorphological investigations of the fault's segmentation, slip potential and latest seismogenic slip history are presented. Measurements of geological deposits, man-made structures, alignment arrays and creepmeters offset across the southernmost San Andreas fault are presented. These measure the fault's aseismic slip rate during the past three hundred years. Observations of triggered aseismic slippage along the southernmost 100 km of the San Andreas fault soon after the North Palm Springs earthquake are described. Dextral surficial slip ranging from less than or equal to 9 mm and occurred on three sections of the San Andreas fault that lie between 44 and 86 km from the epicenter near North Palm Springs. Data complied and interpretations gleaned from repeated measurements of surface slip at dozens of site along the Superstition Hills fault during the period of two hours to one year after the Superstition Hills earthquake are presented. The common result of these five investigations is increased understanding of phenomena associated with fault motion along the highly active border between the Pacific and North American plates. Dissert. Abstr.

N91-11330# Los Alamos National Lab., NM. Earth and Environmental Sciences Div.
NUMERICAL MODELS OF 2-D AND 3-D GEOPHYSICAL CONVECTION
Bryan J. Travis 1990 7 p Presented at the International Symposium on Gas-Liquid Two-Phase Flows in Conjunction With the Winter Annual Meeting of the ASME, Dallas, TX, 25-30 Nov. 1990
(Contract W-7405-eng-36)
(DE90-014979; LA-UR-90-2571; CONF-901109-10) Avail: NTIS HC/MF A02

A suite of computational models has been developed which simulate thermal/chemical convection over a wide range of Rayleigh numbers both in 2-D annular and 3-D Cartesian geometries, for small Reynolds number flow, and a variety of boundary conditions. These simulators are revealing the patterns of convection that may occur in the earth, from mantle scale down to more localized regions such as mid-ocean spreading centers, on down to the scale of magma chambers. Features such as surface plates, variable viscosity and chemical buoyancy can have a dramatic impact on convective patterns compared to those seen in simple, constant property, free or fixed surface systems. In most cases, the nonlinear dynamics of these systems derive from thermal and chemical forces, rather than inertial. These models can be used to study general features and dynamics of convecting viscous fluids, and can also be used to constrain possible explanations for geophysical observations such as heat flow, gravity, topography, plate speeds, and isotopic distributions. Computational resources have reached a level at which numerical solutions of complex processes are feasible. DOE

N91-11331# Hiroshima Univ., Takehara (Japan). Research Inst. for Theoretical Physics.
GRAVITATIONAL FIELD OF STATIC AND THICK DOMAIN WALLS
Kenji Tomita Feb. 1990 7 p
(DE90-513706; RRK-90-2) Avail: NTIS (US Sales Only) HC/MF A02

The behavior of static and thick domain walls with a scalar field is studied. If in both sides of a domain wall there are asymptotically vacuum regions, their regions can be expressed by the static Kasner solutions and the relation between the Kasner parameters in both sides is the same as that in the case of thin domain Walls. An analytic solution is shown as the example. DOE

N91-11332# Instituto de Pesquisas Espaciais, Sao Jose dos Campos (Brazil).
SPECTRAL LITHOSTRATIGRAPHIC CORRELATION OF BOREHOLES M.S. Thesis [CORRELACIONAMENTO LITOSTRATIGRAFICO ESPECTRAL DE POCOS DE PERFURACAO]
Lenio SoaresGalvao Dec. 1989 73 p In PORTUGUESE; ENGLISH summary
(INPE-5022-TDL/402) Avail: NTIS HC/MF A04

The use of spectral radiometry (from 400 to 1000 nm) for lithostratigraphic correlation of rock samples from Parnaiba Basin (Piaui and Maranhao States) boreholes were studied from a quantitative and qualitative standpoint. The former involves the application of the following statistical techniques: cluster analysis, factor analysis, linear discriminant functions and cross-correlations. The effects of chemical composition and of weathering upon the spectral response from stratigraphic units were also investigated. The results indicate the following conclusions: (1) lithostratigraphic correlation between boreholes was successfully done with the use of Mahalanobis' Distance Tests, based on discriminant functions as a measure of similarity among lithological samples; (2) the spectral discrimination of Parnaiba Basin lithologics units was greatly affected by minor rock components, mainly iron and organic matter; and (3) the weathering processes reduce the reflectance values of rock samples, even though it is not known if they significantly affect the spectral separation of rock groups in comparison with the separation of fresh rock material. Author

N91-11333# Consiglio Nazionale delle Ricerche, Frascati (Italy). Ist. di Fisica dello Spazio Interplanetario.
THE ROTATION OF LAGEOS
B. Bertotti (Pavia Univ., Italy) and L. Iess Apr. 1990 24 p
(IFSI-90-10; ETN-90-97793) Avail: NTIS HC/MF A03

In view of the need of an accurate modeling of non gravitational forces on laser tracked satellites, it is important to understand their rotational dynamics, which determines the temperature anisotropy and the ensuing radiation recoil effects. A model of the torques acting on Lageos due to eddy currents and gravity gradient is proposed. The electromotive forces induced in the spacecraft by its rotation in the magnetic field of the Earth dissipate angular momentum and produce a precession of the spin axis; the oblate spacecraft will precess in the gravitational field of the Earth at a rate proportional to the rotation period. Therefore the gravitational torques become more and more important with time and eventually may produce chaotic dynamics. The predicted evolution of the spin period agrees very well with the few experimental data available and corresponds to an approximately exponential growth rate of about three years. ESA

47 METEOROLOGY AND CLIMATOLOGY

Includes weather forecasting and modification.

N91-11334# Centre National d'Etudes Spatiales, Toulouse (France).
WIND LIDAR FOR TROPICAL CLIMATOLOGY
G. Chalon 17 May 1988 45 p In FRENCH; ENGLISH summary
(CNES-CT/DRT/TIT/IO-88/126; ETN-90-97813) Avail: NTIS HC/MF A03

In the scope of a study for a space mission named BEST (Tropical System Energy Budget) a wind Doppler lidar is investigated. A conical scan and a four fixed telescopes lidar concepts are presented. The four fixed telescopes configuration alleviates the dynamical lag angle and minimizes the instrument power requirement given an appropriate operation cycle. ESA

N91-11335# Cologne Univ. (Germany, F.R.). Inst. fuer Geophysik und Meteorologie.
ENERGETICS OF 60 DAYS PREDICTIONS WITH THE EZMW-T21 MODEL IN ITS MEAN TEMPORARY DEVELOPMENT AND ITS RELATIONSHIP TO FORECAST SKILL [DIE ENERGETIK VON 60-TAGE-VORHERSAGEN MIT DEM EZMW-T21-MODELL IN IHRER MITTLEREN ZEITLICHEN ENTWICKLUNG UND IHER BEZIERHUNG ZUR VORHERSAGEGUETE]
Wilfried Jacobs 1990 133 p In GERMAN Sponsored by BMFT
(Mitt-71; ISSN-0069-5882; ETN-90-97895) Avail: NTIS HC/MF A07

A theory of homogeneous nucleation from the vapor phase is presented. The classical Becker-Doering-Zeldovich theory is contained as a limiting case. The theory is based on a semi-phenomenological droplet model for the Gibbs free enthalpy of formation of the cluster. Since this droplet model also allows the construction of a thermal equation of state for real gases below the critical point, all free parameters of the model can be determined from macroscopic measurements. The new theory gives a much better prediction of observed nucleation rates than the classical theory. ESA

N91-11336# National Center for Atmospheric Research, Boulder, CO. Mesoscale and Microscale Meteorology Div.
TAIWAN AREA MESOSCALE EXPERIMENT: A GUIDE TO PRECIPITATION PATTERNS DURING THE 1987 FIELD PHASE
Stanley B. Trier May 1990 339 p Sponsored by NSF
(PB90-256355; NCAR/TN-350+STR) Avail: NTIS HC/MF A15 CSCL 04B

The Taiwan Area Mesoscale Experiment (TAMEX) is a cooperative research program between scientists from the Rep. of China (ROC) and the U.S. The primary goals of TAMEX are to examine: (1) the mesoscale circulations of the Mei-Yu front; (2) the mesoscale convective systems that form in the vicinity of the front; and (3) the interactions of topography with frontal and convective circulations. The field phase of TAMEX occurred during the period from 1 May to 29 June 1987. During the period, three ground based C band Doppler radars were deployed along the northwest coast of Taiwan. Other ground based remote sensing facilities for TAMEX included a wind profiler, and an array of conventional radar situated on both the east and west sides of

the island. Radar reflectivity patterns are summarized in the Doppler radar coverage area during the field phase of the experiment. A condensed sample data set is provided for scientists to aid in the selection of Doppler radar data to be used for scientific analysis, and investigators who are not necessarily interested in using Doppler radar data are provided with a general summary of precipitation patterns during the experiment. Author

N91-11337 Colorado Univ., Boulder.
A NUMERICAL MODEL OF POLAR MESOSPHERIC CLOUD FORMATION AND EVOLUTION Ph.D. Thesis
Eric Jon Jensen 1989 183 p
Avail: Univ. Microfilms Order No. DA9024834

A time-dependent numerical model of polar mesospheric cloud (PMC) formation is used to study the physics of ice particle formation at the mesopause. These clouds occur during the summer months at polar latitudes where the mesopause temperatures are known to fall below 140 K. All physical processes believed to be important are simulated, including ice particle nucleation, growth by deposition of water vapor, sublimation, diffusion, and advection. Ice particles, meteoric dust particles and water vapor are treated as fully interactive elements in the model. Comparisons between simulated cloud properties and Solar Mesosphere Explorer measurements of PMC ultraviolet brightness indicate that the nominal model predicts relatively weak PMC. The simulated cloud brightness is found to be particularly sensitive to water vapor concentration and vertical wind speed, but not very sensitive to the mesopause temperature. The temperature variations predicted by atmospheric tidal models are shown to induce a factor of 4 to 8 diurnal variation in UV brightness and a 2 km variation in cloud height with maximum brightness and minimum height occurring a few hours before local midnight. The comparisons between different measurement of PMC albedo provide consistent results when small-particle size distributions are used to scale the measurements, but discrepancies arise when larger particle sizes are assumed. The linear polarization calculated with the optical model is shown to be in reasonable agreement with ground-based and rocket measurements. Dissert. Abstr.

N91-11338 North Carolina State Univ., Raleigh.
TROPICAL CYCLONE SIMULATIONS WITH THE BETTS CONVECTIVE ADJUSTMENT SCHEME Ph.D. Thesis
Jong-Jin Baik 1989 165 p
Avail: Univ. Microfilms Order No. DA9017667

A new convective adjustment scheme (Betts, 1986) is incorporated into a tropical cyclone model. The scheme adjusts local temperature and moisture structures towards the observed quasi-equilibrium thermodynamic state and includes non-precipitating shallow convection as well as deep convection. The numerical model is an axisymmetric, primitive equation, hydrostatic, finite difference model with 15 vertical levels and 20 km horizontal resolution. The model domain covers 1000 km and the spectral radiation boundary condition is implemented. It is shown that the convective scheme can simulate the developing, rapidly intensifying and mature stages of a tropical cyclone from a weak vortex. Sensitivity of the model storm evolution to the convective parameters is investigated. The storm develops earlier as the adjustment time scale becomes small and as the stability weight on the moist adiabat is increased. The storm evolution is very sensitive to variations in the saturation pressure departure and the mature storm is more intense as the magnitude of the saturation pressure departure is increased. Sensitivity of the model to variations in the sea surface temperature, latitude, initial vortex amplitude, initial moisture distribution and radiation is studied. The simulation with both deep and shallow convection results in earlier storm development than that without shallow convection, but the final intensities are similar. Dissert. Abstr.

N91-11339 Illinois Univ. at Urbana-Champaign, Savoy.
BASIC DYNAMICS OF LOW FREQUENCY VARIABILITY AND THE STORM TRACKS Ph.D. Thesis
Ming Cai 1990 197 p
Avail: Univ. Microfilms Order No. DA9021657

A study was made of the dynamics of storm tracks from the perspective of local instability of a class of zonally inhomogeneous basic jet streams. An unstable local mode consists of a group of dominant waves which jointly give rise to a maximum local energy downstream of the jet core. Its growth rate diminishes very rapidly as the constant part of the basic zonal wind is increased, but is not sensitive to the zonally averaged part of the shear flow. The non-modal analysis shows the excitation of a local mode within a few days from an initially isolated disturbance depends strongly on the initial position relative to the jet core but less strongly on the initial configuration of the isolated disturbance. A complete set of local energy equations was formulated to reveal the nature of the various physical mechanisms of the instability of a zonally inhomogeneous basic flow. The problem was examined of the mutual dependence of planetary and synoptic scale waves in the context of a high resolution, zonally forced, dissipative, two-layer quasi-geostrophic channel model. Specifically, the dynamical properties of the equilibrated flow in a 6000-day numerical experiment with a realistic forcing parameter was considered. The wave field in the equilibrated state is dominated by the planetary scale wave with wavenumber (m,n) = (2,2) and the synoptic scale waves (m,n) = (4,1) and (5,1). The modified zonal flow together with the internally forced planetary scale wave may be viewed as a zonally inhomogeneous background flow upon which the synoptic scale eddies grow preferentially downstream of the planetary scale jet streams. Dissert. Abstr.

N91-11340 Washington Univ., Seattle.
METEOROLOGICAL CHARACTERISTICS OF THE EL NINO/SOUTHERN OSCILLATION PHENOMENON Ph.D. Thesis
Clara Deser 1989 210 p
Avail: Univ. Microfilms Order No. DA9020910

Variations in the tropical Pacific atmospheric circulation and surface energy balance associated with the El Nino/Southern Oscillation phenomenon are described, using marine surface observations from ships-of-opportunity, satellite measurements of tropical convection, and 850 mb wind analyses. The results are based on linear regression analyses between the meteorological parameters and an index of sea surface temperature (SST) in the equatorial Pacific. Warm episodes along the Peru coast (i.e., El Nino events) and basin-wide warmings associated with the Southern Oscillation are examined separately. Charts of the total fields as well as anomalies are presented. During warm episodes, the intertropical convection zone (ITCZ) expands southward toward the equator and the Indonesian convection zone shifts eastward into the western Pacific, following the warmest SSTs. Sea level pressure anomalies over the equatorial eastern Pacific during warm episodes appear to be induced in part by temperature anomalies in the planetary boundary layer. Static stability in the atmospheric surface layer appears to play an important role in determining the surface wind, humidity and cloudiness characteristics over the equatorial eastern Pacific. It is argued that the warming of the equatorial cold tongue during warm episodes destabilizes the surface layer, leading to an increase in surface wind speed and decrease in relative humidity through enhanced vertical mixing. Dissert. Abstr.

N91-11341 Florida State Univ., Tallahassee.
GENERALIZED DYNAMIC NORMAL MODE INITIALIZATION Ph.D. Thesis
Arun Kumar 1990 227 p
Avail: Univ. Microfilms Order No. DA9024098

During the early phase of the numerical weather forecast, the initial analysis of the divergence plays an important role. However, using the conventional data analysis schemes, a successful initial analysis of the divergent circulation is difficult to achieve. It is proposed that over the convective regions, incorporating known convective heating information during the initialization can lead to an improved initial specification of the divergent circulation. Success of the proposed methodology depends on the efficiency of the initialization scheme. For the dynamical normal mode initialization (DNMI) method used in the present study to perform the initialization, it is shown that this method does not succeed in

initializing higher vertical modes. Since the assimilation of the convective heating into the initialized divergence crucially depends on the ability to initialize the correct vertical modes, use of DNMI would not be very appropriate. An improved initialization procedure where the DNMI is performed in the vertical mode space was then formulated. A comparison of initialization experiments performed with the conventional DNMI and the new scheme demonstrated that with the new initialization method, the initialization of the higher vertical modes could be better achieved. The effects of including the convective heating during the initialization on the final initialized state were next explored. It is demonstrated that the dominant effect of the convective heating would be on the initialized divergence field. Further, it was illustrated that to some extent, the initialization with the specific convective heating can recover the corresponding divergent circulation in the initialized state. Dissert. Abstr.

N91-11342*# Massachusetts Univ., Amherst.
DEVELOPMENT OF A VALIDATION MODEL FOR THE DEFENSE METEOROLOGICAL SATELLITE PROGRAM'S SPECIAL SENSOR MICROWAVE IMAGER
C. T. Swift, M. A. Goodberlet, and J. C. Wilkerson (National Oceanic and Atmospheric Administration, Suitland, MD.) 18 Nov. 1990 44 p
(Grant NAGw-0908)
(NASA-CR-187369; NAS 1.26:187369) Avail: NTIS HC/MF A03 CSCL 04B

The Defence Meteorological Space Program's (DMSP) Special Sensor Microwave/Imager (SSM/I), an operational wind speed algorithm was developed. The algorithm is based on the D-matrix approach which seeks a linear relationship between measured SSM/I brightness temperatures and environmental parameters. D-matrix performance was validated by comparing algorithm derived wind speeds with near-simultaneous and co-located measurements made by off-shore ocean buoys. Other topics include error budget modeling, alternate wind speed algorithms, and D-matrix performance with one or more inoperative SSM/I channels. Author

N91-11343# Instituto de Pesquisas Espaciais, Sao Jose dos Campos (Brazil).
NUMERICAL EXPERIMENTS WITH CLIMATIC ZONALLY-AVERAGED MODELS Ph.D. Thesis [EXPERIMENTOS NUMERICOS COM MODELOS CLIMATICOS MEDIA ZONAL]
Sergio Henrique Franchito Nov. 1989 192 p In PORTUGUESE; ENGLISH summary
(INPE-5083-TDL/417) Avail: NTIS HC/MF A09

Two statistical-dynamical models, a quasi-geostrophic and a primitive equations model are developed. These are used to conduct numerical experiments about the zonally-averaged atmosphere, with emphasis on the Southern Hemisphere climatic processes. The experiments consider the climatic effects caused by the sea-surface temperature (SST) anomalies and by land surface alterations. The experiments regarding the SST anomalies consider the situations of El Nino, La Nina, and the dipole involving centers of positive and negative anomalies. The results show that in the El Nino situation the sub-tropical jet stream and the Hadley circulation are intensified and the surface temperature increases in the perturbed region. The opposite situation occurs in the case of La Nina. The dipole experiment there is an intensification of the Hadley cell in the Northern Hemisphere (region of positive anomalies) and a weakening in the ascending branch in the Southern Hemisphere (region of negative anomalies). In the experiment of the surface state modification the interaction between the geobotanic state and the climate is considered. The interaction constitutes a biofeedback mechanism. Experiments are done for the deforestation, desertification, and irrigation situations. The results show that the change in the evapotranspiration rather than the change in the surface albedo is the predominant effect in regulating the changes in the surface temperature. A notable aspect in these biofeedback experiments is that all the variations are smaller in the Southern Hemisphere. Author

N91-11344# Argonne National Lab., IL. Environmental Research Div.
PARAMETERIZATIONS OF MICROPHYSICAL PROCESSES IN CLOUDS
In Young Lee Sep. 1990 118 p
(Contract W-31-109-eng-38)
(DE90-017820; ANL/ER-2) Avail: NTIS HC/MF A06

Cloud physics parameterizations are reviewed comprehensively in order to examine their theoretical bases and to evaluate their applicability to mesoscale modeling. It was found that the constant distribution function of hydrometeors assumed in previous work are unrealistic. To circumvent this problem, new parameterizations were made by multiple regression on mixing ratios of water vapor, cloud water, rainwater, cloud ice, graupel, and snowflakes. Solution field derived from simulations were used with a cloud model that incorporates sophisticated treatments of microphysics and dynamics. In the detailed simulations from which they were derived, the regression parameterizations generally give better results than do the existing parameterizations tested. In a Lagrangian air parcel model under variable atmospheric conditions, the new parameterizations give consistent results and are computationally more efficient than previously available parameterizations. DOE

N91-11345# Office National d'Etudes et de Recherches Aerospatiales, Paris (France).
STUDY OF THE RETURN-STROKE PHASE OF THE GLIDING SPARK IN AMBIENT AIR Ph.D. Thesis - Paris-Sud Univ.
Frank Boulanger Apr. 1990 164 p In FRENCH; ENGLISH summary Report will also be announced as translation (ESA-TT-1232)
(ONERA-NT-1990-1; ISSN-0078-3781; ETN-90-98020) Avail: NTIS HC/MF A08

The return-stroke phase immediately follows the contact between the lightning leader and the ground. A current wave of velocity c/3 to c/10 climbs up to the storm cloud. This phenomena is studied in the laboratory with a 10 nF to 100 kV charged capacitor gliding spark. Capacity probes are used to measure the development of the voltage along the spark channel. The hydrodynamic expansion is recorded by an holographic device. A Navier-Stokes numerical model is applied. ESA

N91-10960*# National Aeronautics and Space Administration. Ames Research Center, Moffett Field, CA.
TERMINAL WEATHER INFORMATION MANAGEMENT Abstract Only
Alfred T. Lee *In* NASA, Langley Research Center, Aviation Safety/Automation Program Conference Oct. 1990 p 271-274
(For primary document see N91-10936 02-03)
Avail: NTIS HC/MF A12 CSCL 04B

N91-11006# European Organization for the Safety of Air Navigation, Brussells (Belgium). Engineering Directorate.
DEVELOPMENTS TO ENHANCE METEOROLOGICAL FORECASTING FOR AIR TRAFFIC SERVICES
M. E. Cox and D. A. Forrester (Meteorological Office, Bracknell, England) *In* AGARD, Aircraft Trajectories: Computation, Prediction, Control, Volume 2: Air Traffic Handling and Ground-Based Guidance of Aircraft. Part 4: Air Traffic Handling. Part 5: Guidance of Aircraft in a Time-Based Constrained Environment. Part 6: May 1990 (For primary document see N91-10981 02-05)
Copyright Avail: NTIS HC/MF A20; Non-NATO Nationals requests available only from AGARD/Scientific Publications Executive

48 OCEANOGRAPHY

Includes biological, dynamic, and physical oceanography; and marine resources.

For related information see also *43 Earth Resources and Remote Sensing.*

N91-11346# Naval Oceanographic and Atmospheric Research Lab., Bay Saint Louis, MS. Numerical Modeling Div.
A COMPENDIUM OF ENVIRONMENTAL DATA COLLECTED DURING THE ICESHELF-88 EXERCISE
P. J. Bucca May 1990 58 p Sponsored by Office of Naval Technology
(AD-A223518; NOARL-TN-32) Avail: NTIS HC/MF A04 CSCL 08/3

From 4 through 28 April 1988, the first in a series of Arctic Ocean acoustic exercises, Iceshelf-88 was conducted in the Lincoln Sea to the north of Ellesmere Island. Ice Camp Jerry was established at a nominal position of 83 deg 39 min N, 58 deg 40 min W to support this effort. During the exercise, a large quantity of environmental measurements were made to aid in the interpretation of the acoustic data. These measurements include both time series and vertical current meter casts, Conductivity Salinity Temperature-Depth (CSTD) casts, expendable sound velocimeter data, and ice floe navigation. In addition, meteorological data such as wind speed and direction, air temperature, barometric pressure, and solar radiation were automatically logged over the duration of the acoustic measurement period. These measurements are documented by providing a brief description of how the data was collected and processed and provides plots and abbreviated tabulations of each data set in the appendices. GRA

N91-11347# Naval Oceanographic and Atmospheric Research Lab., Bay Saint Louis, MS. Ocean Sensing and Prediction Div.
NOTES ON THE NOARL NOWCAST FOR THE 1989 TO 1990 EL NINO FORCED BY FNOC WINDS
H. E. Hurlburt, J. C. Kindle, E. J. Metzger, and A. J. Wallcraft (JAYCOR, Bay Saint Louis, MS.) May 1990 19 p Sponsored by ONR, Arlington, VA
(AD-A223520; NOARL-TN-29) Avail: NTIS HC/MF A03 CSCL 08/3

The Naval Oceanographic and Atmospheric Research Laboratory (NOARL) one active layer reduced gravity global ocean model is running in real time at the Fleet Numerical Oceanography Center forced by the Navy Operational Global Atmospheric Prediction System (NOGAPS) wind fields. The model has a resolution of .5 deg x .7 deg (lat., long.) and depicts a few eddies but it is basically non eddy-resolving; it does depict most of the major current systems and large-scale fronts. In addition, the model clearly shows evidence of an El Nino-like event in the equatorial Pacific Ocean during 1989 to 1990. GRA

N91-11348# Beleidscommissie Remote Sensing, Delft (Netherlands).
WAVE DATA ASSIMILATION IN A 3RD GENERATION. WAVE PREDICTION MODEL FOR THE NORTH SEA: AN OPTIMAL CONTROL APPROACH
C. F. DeValk and C. J. Calkoen Feb. 1990 125 p Sponsored in part by EEC Prepared in cooperation with Delft Hydraulics Lab., DeVoorst, Netherlands; Royal Netherlands Meteorological Inst., The Hague; and Rijkswaterstaat, Delft, Netherlands
(BCRS-89-22; ETN-90-97682) Avail: NTIS HC/MF A06

An algorithm was developed for assimilation of wave and wind data in the numerical Wave Prediction Model (WAM) with the purpose of effectively using data from ERS-1 and other satellites. Based on given requirements, wave data assimilation was formulated as an optimal control problem: wind fields are adjusted in order to minimize a cost function, which penalizes differences between the simulation and observations as well as deviations from the predicted wind fields. A nonlinear approximation of the wave model is used in the optimization. The adjoint model is used to compute the gradient of the cost function. These ideas were implemented in a data assimilation scheme for a regional WAM model for the North Sea. Results of the first tests show that the approach works; even large errors in the driving wind fields can be corrected, and computational requirements are modest. ESA

N91-11349# National Marine Fisheries Service, Woods Hole, MA. Northeast Fisheries Center.
SURFACE AND BOTTOM TEMPERATURE DISTRIBUTION FOR THE NORTHEAST CONTINENTAL SHELF
D. G. Mountain and T. J. Holzwarth Dec. 1989 39 p
(PB90-252172; NOAA-TM-NMFS-F/NEC-73) Avail: NTIS HC/MF A03 CSCL 08C

Horizontal distributions of expected or mean surface and bottom temperatures on the Northeast Continental Shelf from Cape Hatteras to the Gulf of Maine are presented for the beginning and middle of each month. Data used to generate these distributions are from the period 1977 to 1987. The distributions, therefore, represent an 11 year mean annual temperature cycle. Horizontal distributions of the interannual variability in temperature within the 11 year period are also presented. Author

N91-11350# National Ocean Service, Anchorage, AK. Ocean Assessments Div.
OUTER CONTINENTAL SHELF ENVIRONMENTAL ASSESSMENT PROGRAM: COMPREHENSIVE BIBLIOGRAPHY, JUNE 1990
Jun. 1990 648 p Sponsored in part by Minerals Management Service, Anchorage, AK
(PB90-258609; OCS/MMS-90/0043) Avail: NTIS HC/MF A99 CSCL 08C

The objectives of the Outer Continental Shelf Environmental Assessment Program (OCSEAP) are as follows: To provide information about the OCS environment that will enable the Department of the Interior (DOI) to make sound management decisions regarding the development of mineral resources on the OCS; To acquire information that will enable DOI to identify those aspects of the environment that might be affected by oil and gas exploration and development; To establish a basis for predicting the effects of OCS oil and gas activities on the environment; and To acquire impact data that may result in modification of leasing stipulations, operating regulations, and OCS operating orders in order to permit more efficient resource recovery with adequate environmental protection. The bibliography is a compilation of publications and reports that have resulted from research funded by OCSEAP since its inception in 1975 and is an updated version of the Comprehensive Bibliography published in January 1988. Certain other publications that have appeared in other government documents, books, or referred literature relating to environmental problems associated with oil and gas development are included in the bibliography. GRA

51 LIFE SCIENCES (GENERAL)

N91-11351# Los Alamos National Lab., NM. Complex Systems Group.
OSCILLATION ONSET IN NEURAL DELAYED FEEDBACK
Andre Longtin Nov. 1990 7 p Presented at the IEEE Conference on Neural Information Processing: Natural and Synthetic, Denver, CO, 26-29 Nov. 1990
(Contract DE-W-7405-eng-36)
(DE90-015057; LA-UR-90-2562; CONF-901150-2) Avail: NTIS HC/MF A02

This paper studies dynamical aspects of neural systems with delayed negative feedback modelled by nonlinear delay-differential equations. These systems undergo a Hopf bifurcation from a stable fixed point to a limit cycle oscillation as certain parameters are varied. We show that their frequency of oscillation is robust to parameter variations and noisy fluctuations, a property that makes these systems good candidates for pacemakers. The onset of oscillation is postponed by both additive and parametric noise in

the sense that the state variable spends more time near the fixed point. Finally, we show that a distributed delay (rather than a fixed delay) also stabilizes the fixed point solution. DOE

N91-11352# Argonne National Lab., IL. Biological and Medical Research Div.
PROTECTION BY WR-2721 AND WR-151327 AGAINST LATE EFFECTS OF GAMMA RAYS AND NEUTRONS
D. J. Grdina, B. A. Carnes, and B. Nagy 1990 7 p Presented at the 28th COSPAR Plenary Conference, The Hague, Netherlands, 25 Jun. - 6 Jul. 1990
(Contract W-31-109-eng-38)
(DE90-017792; CONF-9006220-4) Avail: NTIS HC A02/MF A01

Two thiophosphoroate compounds WR-2721 and WR-151327 were assessed for their ability to modify the deleterious effects (life shortening and carcinogenesis) of fission-spectrum neutrons or gamma rays on B6CF1 hybrid mice. Male and female mice were irradiated individually at 110 days of age. Radioprotectors were administered intraperitoneally 30 min prior to irradiation. Animals were housed five to a cage; cage locations in the holding rooms were randomized by computer. Animals were checked daily and all deceased animals were necropsied. WR-2721 afforded protection against both neutron- and gamma-ray-induced carcinogenesis and subsequent life shortening. Cumulative survival curves for unirradiated mice of either sex were unaffected by protectors. DOE

N91-11353# Argonne National Lab., IL.
THE STRUCTURE AND FUNCTION OF MEMBRANE PROTEIN PHOTOSYNTHETIC REACTION CENTER
Chong-Hwan Chang, D. Tiede, J. Norris, and M. Schiffer 1990 5 p Presented at the 11th International Science and Technology Symposium, Seoul, Republic of Korea, 25-29 Jun. 1990
(Contract W-31-109-eng-38)
(DE90-017795; CONF-9006194-2) Avail: NTIS HC/MF A01

The three dimensional structure of the photosynthetic reaction center from Rhodobacter (Rb.) sphaeroides has been determined using x ray diffraction technique. It has 11 membrane spanning helixes, five each from the L and M subunit and one from the H subunit. There is a pseudo-twofold symmetry between the L and M subunits and their amino acid sequences have some similarity. The pigment components, which are located at the hydrophobic core of the reaction center also have this symmetry. We confirmed that two bacteriochlorophylls have a predicted conformation called a special pair. The nonheme iron is liganded with four histidines and one glutamic acid. DOE

52 AEROSPACE MEDICINE

Includes physiological factors; biological effects of radiation; and effects of weightlessness on man and animals.

N91-11354# Joint Publications Research Service, Arlington, VA.
JPRS REPORT: SCIENCE AND TECHNOLOGY. USSR: LIFE SCIENCES
10 Feb. 1989 57 p Transl. into ENGLISH from various Russian articles
(JPRS-ULS-89-003) Avail: NTIS HC/MF A04

Abstracts of U.S.S.R. research in the life sciences are given. Topics covered include aerospace medicine, biochemistry, biophysics, biotechnology, immunology, laser bioeffects, microbiology, military medicine, molecular biology, toxicology, physiology, public health, psychology, and virology. For individual titles, see N91-11355 through N91-11355.

N91-11355# Joint Publications Research Service, Arlington, VA.
ENHANCEMENT OF HUMAN TOLERANCE OF ACUTE HYPOXIA BY ADAPTATION AND INTENSE TRAINING AT HIGH ALTITUDES Abstract Only
A. Yu. Katkov *In its* JPRS Report: Science and Technology. USSR: Life Sciences 10 Feb. 1989 p 1 Transl. into ENGLISH from Fiziologiya Cheloveka (Moscow, USSR), v. 14, no. 3, May - Jun. 1988 p 441-445 (For primary document see N91-11354 02-52)
Avail: NTIS HC/MF A04

A comparative analysis was conducted on tolerance of acute hypoxia by mountain climbers (74 males) and non-climbers (48 males), the latter subjected to adaptation and/or 3 days of intensive training under pressure chamber conditions (5000 to 9000 m). Pressure chamber studies showed that the mountain climbers residing in subalpine areas tolerated an altitude of 9700 plus or minus 170 m for 56 plus or minus 2.2 min before mental clouding 5 to 6 months after the last climb. The corresponding parameters for mountain climbers residing in lowland areas were, respectively, 9200 plus or minus 150 m and 50 plus or minus 1.2 min. Maximum tolerance of the non-climber controls reached 8300 plus or minus 100 m, with a tolerance time of 41 plus or minus 1.0 min at that altitude. A day after the 3-day adaptation/training regimen, the figures improved to 9300 plus or minus 90 m and 50 plus or minus min. A 7- to 56-day excursion to elevations of 5621 to 8848 m by the lowland mountain climber raised their tolerance of hypoxia persisted for some 20 days. Analysis of cardio-vascular function tests and respiratory studies demonstrated that after adaptation to high altitudes in a pressure chamber set at 9000 m the coefficient of oxygen utilization in the climbers was higher than in the nonclimbers subjected to the 3-day regimen. Author

N91-11356*# National Aeronautics and Space Administration. Lyndon B. Johnson Space Center, Houston, TX.
RADIOLOGICAL HEALTH RISKS TO ASTRONAUTS FROM SPACE ACTIVITIES AND MEDICAL PROCEDURES
Leif E. Paterson (Kelsey Seybold Clinic, P.A., Houston, TX.) and D. Stuart Nachtwey Aug. 1990 23 p
(NASA-TM-102164; S-610; NAS 1.15:102164) Avail: NTIS HC/MF A03 CSCL 06S

Radiation protection standards for space activities differ substantially from those applied to terrestrial working situations. The levels of radiation and subsequent hazards to which space workers are exposed are quite unlike anything found on Earth. The new more highly refined system of risk management involves assessing the risk to each space worker from all sources of radiation (occupational and non-occupational) at the organ level. The risk coefficients were applied to previous space and medical exposures (diagnostic x ray and nuclear medicine procedures) in order to estimate the radiation-induced lifetime cancer incidence and mortality risk. At present, the risk from medical procedures when compared to space activities is 14 times higher for cancer incidence and 13 times higher for cancer mortality; however, this will change as the per capita dose during Space Station Freedom and interplanetary missions increases and more is known about the risks from exposure to high-LET radiation. Author

N91-11357# New Mexico Univ., Albuquerque. School of Medicine.
NITROGEN DIOXIDE AND RESPIRATORY INFECTION: PILOT INVESTIGATIONS Research Report, Jan. 1984 - Sep. 1987
Jonathan M. Samet and John D. Spengler Sep. 1989 48 p Prepared in cooperation with Harvard School of Public Health, Boston, MA Sponsored by Health Effects Inst., Cambridge, MA
(PB90-247339; HEI/RR-89/28) Avail: NTIS HC/MF A03 CSCL 06P

A longitudinal study was designed with infants to determine if NO2 exposure from cooking stoves increase the incidence or severity of respiratory infections during the first 18 months of life. Results of pilot investigations for the longitudinal study are reported. In the one study, 147 families of infants were recruited at two Albuquerque hospitals, and their homes were monitored for NO2 using a passive sampling tube. Higher levels of NO2 were found in homes with gas stoves than in homes with electric stoves. A sample of the homes showed that personal exposures of the infants could be estimated by room concentrations and mothers would complete a daily calender-diary on respiratory symptoms and provide information every two weeks on illnesses occurring. In the other pilot study, 75 infants were recruited and followed for

four months. The illness surveillance system was compared with the clinical assessments by the nurse practitioners and the subjects' physicians, and with viral cultures. Author

N91-11370# Royal Air Force Inst. of Aviation Medicine, Farnborough (England).
THE APPLICATION OF USAF FEMALE ANTHROPOMETRIC DATA TO IDENTIFY PROBLEMS WITH THE INTRODUCTION OF FEMALE AIRCREW INTO THE ROYAL AIR FORCE
G. M. Turner *In* AGARD, Recruiting, Selection, Training and Military Operations of Female Aircrew Aug. 1990 3 p (For primary document see N91-11358 02-53)
Copyright Avail: NTIS HC/MF A08; Non-NATO Nationals requests available only from AGARD/Scientific Publications Executive

N91-11376# Institute of Aviation Medicine, Oslo (Norway).
PREGNANCY: A CAUSE FOR GROUNDING OF FEMALE AIR CREW
Harald T. Andersen and Ottar Lunde *In* AGARD, Recruiting, Selection, Training and Military Operations of Female Aircrew Aug. 1990 3 p Prepared in cooperation with University Hospital, Oslo, Norway (For primary document see N91-11358 02-53)
Copyright Avail: NTIS HC/MF A08; Non-NATO Nationals requests available only from AGARD/Scientific Publications Executive

N91-11377# School of Aerospace Medicine, Brooks AFB, TX. Clinical Sciences Div.
EKG FINDINGS IN FEMALE AVIATORS IN THE US AIR FORCE
Robert A. Munson *In* AGARD, Recruiting, Selection, Training and Military Operations of Female Aircrew Aug. 1990 5 p (For primary document see N91-11358 02-53)
Copyright Avail: NTIS HC/MF A08; Non-NATO Nationals requests available only from AGARD/Scientific Publications Executive

N91-11378# Aerospace Medical Research Labs., Wright-Patterson AFB, OH. Human Systems Div.
IMPACT ON WOMEN: A RETROSPECTIVE LOOK AT IMPACT ACCELERATION TESTING AT THE HARRY G. ARMSTRONG AEROSPACE MEDICAL RESEARCH LABORATORY
Cynthia N. Randall and James W. Brinkley *In* AGARD, Recruiting, Selection, Training and Military Operations of Female Aircrew Aug. 1990 6 p (For primary document see N91-11358 02-53)
Copyright Avail: NTIS HC/MF A08; Non-NATO Nationals requests available only from AGARD/Scientific Publications Executive

N91-11379# School of Aerospace Medicine, Brooks AFB, TX.
RELATIONSHIP OF MENSTRUAL HISTORY TO ALTITUDE CHAMBER DECOMPRESSION SICKNESS
Frederick W. Rudge *In* AGARD, Recruiting, Selection, Training and Military Operations of Female Aircrew Aug. 1990 4 p Submitted for publication (For primary document see N91-11358 02-53)
Copyright Avail: NTIS HC/MF A08; Non-NATO Nationals requests available only from AGARD/Scientific Publications Executive

53 BEHAVIORAL SCIENCES

Includes psychological factors; individual and group behavior; crew training and evaluation; and psychiatric research.

N91-11358# Advisory Group for Aerospace Research and Development, Neuilly-Sur-Seine (France). Aerospace Medical Panel.
RECRUITING, SELECTION, TRAINING AND MILITARY OPERATIONS OF FEMALE AIRCREW
Aug. 1990 173 p In ENGLISH and FRENCH Symposium held in Tours, France, 4-5 Apr. 1990
(AGARD-CP-491; ISBN-92-835-0576-X) Copyright Avail: NTIS HC/MF A08; Non-NATO Nationals requests available only from AGARD/Scientific Publications Executive

There are now approximately one thousand female military aviators flying within the NATO nations. The experience of each nation with recruiting, selection, training, and military operations of female aircrew was reviewed. In addition, a section was devoted to the discussion of the physiological differences between male and female aviators, pregnancy, and flying. Once selected, there appear to be no basic differences in flight capabilities between men and women. There is a requirement to develop smaller helmets, oxygen masks and NBC respirators for females, and data were presented which showed that females are more susceptible to decompression sickness. For individual titles, see N91-11359 through N91-11379.

N91-11359# Naval Air Station, Norfolk, VA. Fleet Logistics Support Squadron.
THE INTEGRATION OF WOMEN INTO US NAVY AIRCREW TRAINING AND SQUADRON ASSIGNMENTS
Linda Vaught Hutton *In* AGARD, Recruiting, Selection, Training and Military Operations of Female Aircrew Aug. 1990 5 p (For primary document see N91-11358 02-53)
Copyright Avail: NTIS HC/MF A08; Non-NATO Nationals requests available only from AGARD/Scientific Publications Executive

Aviation and military service are non-traditional career choices for women. Though obvious, the fact remains crucial to the success of integration programs. Much is written and said about the average woman: size, weight, strength, mental acuity, leadership, competitiveness, and drive to excel. But discussions on the average woman are erroneous; the average woman does not seek non-traditional career paths. The woman who seeks a non-traditional military career will be an intelligent, outspoken student of above-average ability; confident, gregarious, and competitive by nature; active and athletically inclined; and routinely found in leadership positions. This dynamic over-achiever personality does not fit statistical norms for a population wide average woman. However, these attributes do fit military aviator candidate profiles; the reason for successful integration. Cultural attitudes and biases are displaced by time. However with forethought and planning, the integration of women into naval aircrew training and squadron assignments can progress smoothly. A planning outline which covers employment intentions, development of an accession model, flight training attrition, aviation retention, and addresses integration concerns and lessons learned is provided. Author

N91-11360# Canadian Forces Base Cold Lake, Medley (Alberta).
A CANADIAN FEMALE CF-18 PILOT'S EXPERIENCE
Deanna Marie Brasseur *In* AGARD, Recruiting, Selection, Training and Military Operations of Female Aircrew Aug. 1990 5 p (For primary document see N91-11358 02-53)
Copyright Avail: NTIS HC/MF A08; Non-NATO Nationals requests available only from AGARD/Scientific Publications Executive

Educational experiences, early military career, flight training, advanced jet aircraft training, experience as a flight instructor, fighter aircraft training, and operational fighter squadron experience of a Canadian female CF-18 pilot are summarized. Author

N91-11361# Royal Netherlands Air Force, Soesterberg.
THE SELECTION, TRAINING, AND OPERATIONAL WORK OF FEMALE HELICOPTER PILOTS IN THE ROYAL NETHERLANDS AIR FORCE
Marielle Winnubst *In* AGARD, Recruiting, Selection, Training and Military Operations of Female Aircrew Aug. 1990 5 p (For primary document see N91-11358 02-53)
Copyright Avail: NTIS HC/MF A08; Non-NATO Nationals requests available only from AGARD/Scientific Publications Executive

In 1976 it was decided in the Netherlands to allow women into almost all functions within the armed forces, which included flying. Being one of the few female helicopter pilots of the 298 squadron for two years now, some of the practical problems female helicopter pilots in the R.N.L.A.F. were (and still are) faced with, are highlighted. Presently there are only 9 female helicopter pilots in the Netherlands Air Force; one female transport aircraft pilot; and one female jet aircraft pilot. Being unfamiliar with the last two

categories, the experiences of myself, 8 female colleagues and the few predecessors are the focus of interest. Because of the low numbers, this is a highly personal account. Author

N91-11362# Air Force Human Resources Lab., Brooks AFB, TX.
COMPARISON OF MALE AND FEMALE USAF PILOT CANDIDATES
Frederick M. Siem and Linda L. Sawin *In* AGARD, Recruiting, Selection, Training and Military Operations of Female Aircrew Aug. 1990 7 p (For primary document see N91-11358 02-53)
Copyright Avail: NTIS HC/MF A08; Non-NATO Nationals requests available only from AGARD/Scientific Publications Executive

Female Air Force pilot candidates were compared to male candidates in terms of factors related to pilot training performance. The factors examined included selection test scores, background measures such as college academic performance and major, and ratings from a college military training program. Successful candidates of both sexes, compared to less successful candidates, had higher ratings and test scores, and also a higher percentage of technical majors and licensed private pilots. The data were analyzed for predictive equity or whether the utility of the factors for prediction of flying training outcomes differed for females and males. The results of regression analyses indicated that the factors examined were equally useful for candidates of both sexes. Author

N91-11363# Naval Aerospace Medical Research Lab., Pensacola, FL.
NAVAL AVIATION SELECTION TEST SCORES AND FEMALE AVIATOR PERFORMANCE
David J. Blower, Daniel L. Dolgin, and Ronald N. Shull *In* AGARD, Recruiting, Selection, Training and Military Operations of Female Aircrew Aug. 1990 5 p (For primary document see N91-11358 02-53)
Copyright Avail: NTIS HC/MF A08; Non-NATO Nationals requests available only from AGARD/Scientific Publications Executive

The majority of U.S. Navy pilots are white males. Of the 12,477 Navy pilots, only 225 (1.8 percent) are women. Navy women are prohibited from permanent assignment on ships or aircraft designated for potential combat missions. Data comparing female and male performance on aviation selection tests over the past five years is present. Female and male student naval aviator performance in primary flight training and on a cognitive/psychomotor test battery are compared. The data examined uncovered some differences in aviation selection test scores as well as differences in cognitive/psychomotor performance, but corresponding effect of these variables on success in primary flight training was discovered. Author

N91-11364# Deutsche Forschungsanstalt fuer Luft- und Raumfahrt, Hamburg (Germany, F.R.). Dept. of Aviation and Space Psychology.
SEX DIFFERENCES CONCERNING PERFORMANCE AND PERSONALITY TRAITS OF APPLICANTS FOR HIGHLY QUALIFIED OPERATOR FUNCTIONS IN AVIATION
Klaus-Martin Goeters and Hinnerk Eissfeldt *In* AGARD, Recruiting, Selection, Training and Military Operations of Female Aircrew Aug. 1990 6 p (For primary document see N91-11358 02-53)
Copyright Avail: NTIS HC/MF A08; Non-NATO Nationals requests available only from AGARD/Scientific Publications Executive

Today, in the West German civil aviation females apply for training as pilots as well as air traffic controllers. Female pilot applicants are still a minority of less than 10 percent. Representative data only exists in the area of air traffic control (ATC) where about 30 to 40 percent of all applicants are female. In the psychological selection of applicants for ATC training the rate of acceptance is significantly smaller for females than for males. Therefore sex differences were investigated in cognitive aptitudes as well as in aspects of personality. The results revealed clear deficiencies for the majority of female applicants in two basic operational aptitudes: spatial orientation and technical comprehension. A lower performance of females was also revealed with regard to mathematical reasoning. Advantages of the female group with respect to other aptitudes (English and perceptual speed) were found to be relatively small. Sex differences in personality were observed for aspects of emotionality, activity, and interpersonal behavior. Females scored higher in scales of emotional instability, empathy, and achievement motivation, but lower in scales of vitality and dominance. Author

N91-11365# Institute of Aviation Medicine, Oslo (Norway).
PSYCHOLOGICAL AND SOCIOLOGICAL ASPECTS OF THE ENTRANCE OF FEMALE AIRCREW TO THE NORWEGIAN AIRFORCE
G. Myhre, B. Ovesen, and M. Martinussen (Norwegian Defence Psychological and Educational Center, Oslo.) *In* AGARD, Recruiting, Selection, Training and Military Operations of Female Aircrew Aug. 1990 5 p (For primary document see N91-11358 02-53)
Copyright Avail: NTIS HC/MF A08; Non-NATO Nationals requests available only from AGARD/Scientific Publications Executive

The total number of applicants for pilot screening and officer school in the Royal Norwegian Air Force (RNoAF) from 1982 to 1989 were studied in order to reveal the fate of female applicants during these years and establish if the females accepted represented a fairly constant percentage of the total number of applicants. The results from the psychological tests for 17 female applicants admitted to pilot screening and officer school were compared with those of the 173 accepted male applicants. A survey was performed in the RNoAF, in order to map the attitudes of squadron commanders and flight commanders (34 males) about their professional experience with the present female air crew in the RNoAF. In addition the females (5) answered questions regarding how they experience their situation seen from a female point of view. The results are briefly summarized. Author

N91-11366# Centro de Instruccion de Medicina Aeroespatial, Madrid (Spain).
EVALUATION OF FEMALE AND MALE AIRCREW APPLICANTS USING A COGNITIVE AND PSYCHOMOTOR TEST
Marquez delaPlata *In* AGARD, Recruiting, Selection, Training and Military Operations of Female Aircrew Aug. 1990 3 p (For primary document see N91-11358 02-53)
Copyright Avail: NTIS HC/MF A08; Non-NATO Nationals requests available only from AGARD/Scientific Publications Executive

The Spanish Institute of Aviation Medicine (CIMA) has developed a system and the equipment for the assessment of performance of complex tasks, which will be used for the evaluation of candidates cognitive and psychomotor abilities in order to become a pilot. This system also permits the investigator to evaluate the learning capability of an individual in those tasks. The equipment consists of the following: modules for the programming and emission of visual and auditory stimuli; desks with devices for transmission of stimuli (visor and headsets) and responses (two buttons and two pedals); and modules for the recording, counting, and timing of responses. The procedure requires that the subject has to give a response to the programmed stimuli according to a previous criterion established after the significant physical features of each stimulus, which were previously divided into four categories. This test was administered to a sample of 135 subjects, 115 males and 20 females; they were applicants for a commercial pilot license. The age ranged from 17 to 25 years, and nobody had any previous piloting experience. The goal of the experiment was focused on testing whether there were significant differences between men and women in the cognitive-psychomotor task assigned. In other words if the factor sex influences on the performance (R) and on the average time of response (T), considering as a null hypothesis that there are no significant statistical differences between the group of males and the group of females. The statistical analysis of the results obtained from each subject in both trials was oriented to verify the null hypothesis. The statistical analysis shows that the results obtained in the pilot applicants in the cognitive-psychomotor test

proposed were not significantly different in men compared to women. Author

N91-11367# Defence and Civil Inst. of Environmental Medicine, North York (Ontario). Central Medical Board.
FEMALE AIRCREW: THE CANADIAN FORCES EXPERIENCE
R. J. Hicks *In* AGARD, Recruiting, Selection, Training and Military Operations of Female Aircrew Aug. 1990 6 p (For primary document see N91-11358 02-53)
Copyright Avail: NTIS HC/MF A08; Non-NATO Nationals requests available only from AGARD/Scientific Publications Executive

Data collected since females first started aircrew training in Canada in 1979 is reviewed. Females are less successful than males in selective competition for training, but once into the training scheme there is no significant sex difference in achieving wings standard. Although numbers are still relatively small, female aircrew are now participating equally with their male peers in all aspects of military flying including tactical fighter operations. Author

N91-11368# Belgian Air Force, Brussels.
REVIEW OF FEMALE APPLICANT AIRCREW IN THE BELGIAN FORCES
C. Vancutsem and P. Vandenbosch *In* AGARD, Recruiting, Selection, Training and Military Operations of Female Aircrew Aug. 1990 5 p In FINNISH; ENGLISH summary (For primary document see N91-11358 02-53)
Copyright Avail: NTIS HC/MF A08; Non-NATO Nationals requests available only from AGARD/Scientific Publications Executive

The female applicant pilots in the Belgian Armed Forces were evaluated. In the period from January 1983 to July 1989, seventy-three female applicants were examined in the Centre of Aerospace Medicine. Only five of them were declared physically fit as a pilot, but no one could start the instruction. The physical reasons of rejection are studied according to the frequency in the total population, and ranked in accordance with the different criteria and the category of recruitment. A comparison is made between male and female applicants. The most frequent causes of rejection are: insufficient psychomotoric score, myopia, and too short legs. Author

N91-11369# Defence and Civil Inst. of Environmental Medicine, North York (Ontario).
AIRCREW/COCKPIT COMPATIBILITY: A MULTIVARIATE PROBLEM SEEKING A MULTIVARIATE SOLUTION **c54**
Keith C. Hendy *In* AGARD, Recruiting, Selection, Training and Military Operations of Female Aircrew Aug. 1990 8 p (For primary document see N91-11358 02-53)
Copyright Avail: NTIS HC/MF A08; Non-NATO Nationals requests available only from AGARD/Scientific Publications Executive

Aircrew/cockpit compatibility depends on an interaction between the anthropometry of individual aircrew members and the geometry of the cockpit. Selection criteria in the past have attempted to deal with this interaction, but the model was too simple. This is a multi-variate problem which requires a multi-variate solution. Essentially the problem is one of charging the region of intersection between the anthropometric data domain and a set of rules or criteria which define operability. The nature of this problem was demonstrated through computer simulated fitting trials of subjects in a number of cockpit-like geometries. The simulations clearly demonstrate that membership in a particular category of fit depends on interactions between workspace and anthropometry which are geometry specific. Further, the simulations show that the establishment of analytical expressions to define class membership is complex and appears to require a nonlinear approach. The consequences of these results are discussed in terms of establishing selection standards and determining design criteria for cockpits which are compatible with these standards. It is argued that cockpit design must be based on an extensive sampling of human characteristics in order that the full range of interactions, between various anthropometric dimensions and the workspace, is represented. Author

N91-11370# Royal Air Force Inst. of Aviation Medicine, Farnborough (England).
THE APPLICATION OF USAF FEMALE ANTHROPOMETRIC DATA TO IDENTIFY PROBLEMS WITH THE INTRODUCTION OF FEMALE AIRCREW INTO THE ROYAL AIR FORCE **c52**
G. M. Turner *In* AGARD, Recruiting, Selection, Training and Military Operations of Female Aircrew Aug. 1990 3 p (For primary document see N91-11358 02-53)
Copyright Avail: NTIS HC/MF A08; Non-NATO Nationals requests available only from AGARD/Scientific Publications Executive

The Royal Air Force (RAF) decided in 1989 to recruit female pilots and navigators. Since there is little statistical data on the distribution of the critical body dimensions for the UK female population the USAF female anthropometric data was employed to predict the effects of imposing the present RAF minimum selection limits on the female population. These predictions are discussed and the effects for individual aircraft types considered. Certain questions are raised concerning limb strength related to aircraft controls and to the possible requirement for a minimum weight for ejection seat occupants. The USAF female data so far employed was only from the published percentile tables. Further studies will be conducted using the raw data transferred from the US AMRL Data Bank Library to the Institute of Aviation Medicine computer. Author

N91-11371# Defence and Civil Inst. of Environmental Medicine, North York (Ontario).
ANTHROPOMETRIC ACCOMMODATION OF FEMALES IN CANADIAN FORCES AIRCRAFT CREW STATIONS **c54**
P. L. Rothwell and R. A. Pigeau *In* AGARD, Recruiting, Selection, Training and Military Operations of Female Aircrew Aug. 1990 13 p (For primary document see N91-11358 02-53)
Copyright Avail: NTIS HC/MF A08; Non-NATO Nationals requests available only from AGARD/Scientific Publications Executive

To ensure physical accommodation of humans in aircraft crew stations, aircrew traditionally were selected on the basis of specific standards. To be effective, these standards must be based on anthropometric limitations imposed by actual crew stations. Evidence suggests this generally is not the case. Instead, selection standards have frequently evolved from (1) aircraft design recommendations, which often bear little relationship to the finished product, or (2) anthropometry of existing aircrew, which ignores the issue. Recognizing this problem, the Canadian Forces (CF) has undertaken a large-scale study known as ACCE (Aircrew/Cockpit Compatibility Evaluation). A computer-based modelling strategy was developed to determine anthropometric limitations, on a crew station by crew station basis, and their subsequent effect on accommodation of pilot and navigator populations. The approach is attractive because it encompasses possible multivariate relationships between anthropometry and crew station geometries, and it is sub-population independent; it assumes a human anthropometry but is blind to gender, nationality, and race-specific differences. The flexibility of this strategy has allowed assessments of fit for both female and male populations in two CF aircraft - the CT133 utility jet and the CH136 light observation helicopter. Results show that current CF selection standards do not represent the range of anthropometry these aircraft can accommodate. This leads to biases in selection against females and small males. Author

N91-11372# Laboratoire de Medecine Aerospatiale, Bretigny-sur-Orge (France).
PROBLEMS POSED BY THE ADAPTATION OF PHYSIOLOGICAL PROTECTIVE EQUIPMENT FOR FEMALE COMBAT PILOTS [PROBLEMES POSES PAR L'ADAPTATION DES EQUIPEMENTS DE PROTECTION PHYSIOLOGIQUE AUX PILOTES FEMININS D'AVIONS DE COMBAT] **c54**
D. Lejeune, J. C. Amichaud, A. Turillon (Aerazur C.A., Issy-les-Moulineaux, France), J. M. Clere, and H. Marotte *In* AGARD, Recruiting, Selection, Training and Military Operations of Female Aircrew Aug. 1990 4 p In FRENCH; ENGLISH summary (For primary document see N91-11358 02-53)

Copyright Avail: NTIS HC/MF A08; Non-NATO Nationals requests available only from AGARD/Scientific Publications Executive

Female pilots would have to pilot fighter in the future. The problem of adaptation for flight equipment is induced by this new population of pilots. The specific female equipment functioning is studied from theoretical basis and from the literature. Operational solutions are presented for high G protection, thermal stress induced by C.W. flight equipment. Some questions are, today, without response and require further laboratory experiments.
Author

N91-11373# Royal Air Force Inst. of Aviation Medicine, Farnborough (England).
SOME EQUIPMENT PROBLEMS ASSOCIATED WITH THE INTRODUCTION OF FEMALE AIRCREW INTO THE ROYAL AIR FORCE **c54**
G. M. Turner *In* AGARD, Recruiting, Selection, Training and Military Operations of Female Aircrew Aug. 1990 3 p (For primary document see N91-11358 02-53)
Copyright Avail: NTIS HC/MF A08; Non-NATO Nationals requests available only from AGARD/Scientific Publications Executive

Female aircrew have been employed for several years as Air Loadmasters operating on VC10 transport aircraft. When it was required that all transport aircrew be issued with nuclear, biological and chemical (NBC) protective equipment an anthropometry and sizing exercise was conducted with 21 randomly selected female loadmasters. The problems experienced are described and related to the anthropometry data. Mention is also made of the anticipated problems with the Royal Air Force's recent decision (1989) to train female pilots and navigators. Author

N91-11374# Laboratoire de Medecine Aerospatiale, Bretigny-sur-Orge (France).
MORPHOLOGICAL AND FUNCTIONAL ADAPTATION OF PERSONAL EQUIPMENT DESIGNED FOR FEMALE PERSONNEL [ADAPTATION MORPHOLOGIQUE ET FONCTIONNELLE DES EQUIPEMENTS DE VOL DESTINES AUX PERSONNELS FEMININS] **c54**
H. Marotte, D. Lejeune, G. Gutman, R. Beaussant, P. Pelloux-Gervais, and R. Zapata (L'Air Liquide, Sassenage, France) *In* AGARD, Recruiting, Selection, Training and Military Operations of Female Aircrew Aug. 1990 3 p In FRENCH; ENGLISH summary (For primary document see N91-11358 02-53)
Copyright Avail: NTIS HC/MF A08; Non-NATO Nationals requests available only from AGARD/Scientific Publications Executive

Personal equipment is dedicated to protecting aircrews against adverse effects during flight. The equipment operates either in close loop or in open loop. In close loop situations, there is a control of the protective device in relation to the user's demand so that such equipment creates only a few problems. It is not so with open loop equipment. In this case, there is only a statistical relationship between functional characteristics of the equipment and the user's needs. It is especially difficult to adapt the equipment to females. As far as respiratory protection equipment is concerned, such problems were noticed in open loop equipment for technical aircrews and in closed circuit smoke-hoods for cabin attendants.
Author

N91-11375# Naval Air Development Center, Warminster, PA. Dept. of Air Vehicle and Crew Systems Technology.
ACCOMMODATION OF FEMALE AIRCREW IN USN PROTECTIVE FLIGHT CLOTHING AND EQUIPMENT **c54**
S. M. Reeps, H. T. Pheeny, and J. A. Brady (Naval Aerospace Medical Research Lab., Pensacola, FL.) *In* AGARD, Recruiting, Selection, Training and Military Operations of Female Aircrew Aug. 1990 7 p (For primary document see N91-11358 02-53)
Copyright Avail: NTIS HC/MF A08; Non-NATO Nationals requests available only from AGARD/Scientific Publications Executive

The number of United States Navy aviation designated female personnel has increased substantially over the past two decades. Along with this increase has come the ever pressing requirement to provide these aircrew members with safe and effective protective clothing and life support equipment. A variety of problems which have arisen in attempting to accommodate the female aircrew in a clothing and equipment system which was designed for a male population are discussed. Although no overall integrated approach was employed in this effort, a review of the various methods and solutions which were successfully employed to address both the particular needs of individuals and the specific items of clothing and equipment are discussed. Based on a review of problem reports and personal contacts with currently designated female aircrew personnel, many problem areas remain. These areas are discussed as they will provide the basis for future work in this continuing effort.
Author

N91-11376# Institute of Aviation Medicine, Oslo (Norway).
PREGNANCY: A CAUSE FOR GROUNDING OF FEMALE AIR CREW **c52**
Harald T. Andersen and Ottar Lunde *In* AGARD, Recruiting, Selection, Training and Military Operations of Female Aircrew Aug. 1990 3 p Prepared in cooperation with University Hospital, Oslo, Norway (For primary document see N91-11358 02-53)
Copyright Avail: NTIS HC/MF A08; Non-NATO Nationals requests available only from AGARD/Scientific Publications Executive

Military aviation is a rather demanding profession. The medical priorities pertinent to pregnant aviators are considered. Complications to pregnancy which are capable of causing events which interfere with flying duties are examined. The three trimesters of pregnancy are explained along with the problems each presents. The medical consequences of the operational requirements are considered as well as the complications outlined, since adequate treatment depends upon skilled intervention in well equipped institutions.
Author

N91-11377# School of Aerospace Medicine, Brooks AFB, TX. Clinical Sciences Div.
EKG FINDINGS IN FEMALE AVIATORS IN THE US AIR FORCE **c52**
Robert A. Munson *In* AGARD, Recruiting, Selection, Training and Military Operations of Female Aircrew Aug. 1990 5 p (For primary document see N91-11358 02-53)
Copyright Avail: NTIS HC/MF A08; Non-NATO Nationals requests available only from AGARD/Scientific Publications Executive

The initial EKGs from 309 female aviators and 309 age-matched male aviators were read to compare the prevalence of findings. Abnormal readings were unusual, as would be expected in this selected group. About 1.3 percent of the males and none of the females had abnormal readings, a difference which is not significant ($p = .0455$). The abnormal readings were two cases of left anterior hemiblock and two of Wolff-Parkinson-White. Possibly abnormal findings, which required a second order workup to rule out the presence of cardiac disease, occurred at a similar rate between the groups (22.7 percent of females vs 16.2 percent of males, $p = .0634$). The preponderance of possibly abnormal findings in women were due to nonspecific ST and T-wave abnormalities. Normal variant tracings were more common in men (60.2 percent female vs 74.1 percent male, $p = .0004$) while women were more likely to have an EKG without significant finding (17.1 percent females vs 8.4 percent male, $p = .0018$). These findings support the concept that EKG criteria that were developed for men can be used aeromedically for women.
Author

N91-11378# Aerospace Medical Research Labs., Wright-Patterson AFB, OH. Human Systems Div.
IMPACT ON WOMEN: A RETROSPECTIVE LOOK AT IMPACT ACCELERATION TESTING AT THE HARRY G. ARMSTRONG AEROSPACE MEDICAL RESEARCH LABORATORY **c52**
Cynthia N. Randall and James W. Brinkley *In* AGARD, Recruiting, Selection, Training and Military Operations of Female Aircrew Aug. 1990 6 p (For primary document see N91-11358 02-53)
Copyright Avail: NTIS HC/MF A08; Non-NATO Nationals requests available only from AGARD/Scientific Publications Executive

In today's society, women are occupying an increasing number of previously male dominated jobs. This is especially true in the United States Armed Forces. Women have served as pilots in the

military since the early 1970's (1973 for Army and Navy; 1976 for Air Force) but cannot be assigned to high performance, ejection seat aircraft unless they are an instructor or test pilot. Consequently, research was directed at the 5th to 95th percentile male crewmember, and little information is available with respect to performance, limitations, and potential dangers that might be encountered with female aircrew. In the Biomechanical Protection Branch of the Harry G. Armstrong Aerospace Medical Research Laboratory (AAMRL), women are routinely used as subjects in impact experiments since 1976. Seven women of 132 total subjects (5.3 percent) have taken part in 110 of 2108 (5.2 percent) of the impact testing. Although the numbers are small, a retrospective review of the data obtained from these female subjects at AAMRL is provided and compared to the male subject data to determine if there are any trends. Author

N91-11379# School of Aerospace Medicine, Brooks AFB, TX.
RELATIONSHIP OF MENSTRUAL HISTORY TO ALTITUDE CHAMBER DECOMPRESSION SICKNESS **c52**
Frederick W. Rudge *In* AGARD, Recruiting, Selection, Training and Military Operations of Female Aircrew Aug. 1990 4 p Submitted for publication (For primary document see N91-11358 02-53)
Copyright Avail: NTIS HC/MF A08; Non-NATO Nationals requests available only from AGARD/Scientific Publications Executive

Records at the United States Air Force School of Aerospace Medicine, Division of Hyperbaric Medicine, were reviewed to determine the relationship between the incidence of altitude chamber decompression sickness (DCS) in females and menstrual history. The study period spans 11 years, from January 1978 to December 1988. Eighty-one records were suitable for study. A significant inverse linear relationship was noted between the number of days since the start of last menstrual period and the incidence of DCS. This relationship was noted with both Type 1 and Type 2 DCS. Lack of information on the population at risk precluded an analysis of the effects of birth control pills on this phenomenon. The underlying mechanism for the correlation between menstrual cycle and susceptibility to development of DCS is unknown. The conclusion is that women are at higher risk of developing altitude-related decompression sickness during menses, with the risk decreasing linearly as the time since last menstrual period increases. Author

N91-11380*# Georgia Inst. of Tech., Atlanta. Center for Human-Machine Systems Research.
OPERATOR FUNCTION MODELING: COGNITIVE TASK ANALYSIS, MODELING AND INTELLIGENT AIDING IN SUPERVISORY CONTROL SYSTEMS Final Report
Christine M. Mitchell Sep. 1990 67 p
(Grant NAG2-413)
(NASA-CR-187331; NAS 1.26:187331) Avail: NTIS HC/MF A04 CSCL 05I

The design, implementation, and empirical evaluation of task-analytic models and intelligent aids for operators in the control of complex dynamic systems, specifically aerospace systems, are studied. Three related activities are included: (1) the models of operator decision making in complex and predominantly automated space systems were used and developed; (2) the Operator Function Model (OFM) was used to represent operator activities; and (3) Operator Function Model Expert System (OFMspert), a stand-alone knowledge-based system was developed, that interacts with a human operator in a manner similar to a human assistant in the control of aerospace systems. OFMspert is an architecture for an operator's assistant that uses the OFM as its system and operator knowledge base and a blackboard paradigm of problem solving to dynamically generate expectations about upcoming operator activities and interpreting actual operator actions. An experiment validated the OFMspert's intent inferencing capability and showed that it inferred the intentions of operators in ways comparable to both a human expert and operators themselves. OFMspert was also augmented with control capabilities. An interface allowed the operator to interact with OFMspert, delegating as much or as little control responsibility as the operator chose. With its design based on the OFM, OFMspert's control capabilities were available at multiple levels of abstraction and allowed the operator a great deal of discretion over the amount and level of delegated control. An experiment showed that overall system performance was comparable for teams consisting of two human operators versus a human operator and OFMspert team. Author

N91-11381# European Space Agency, Paris (France).
DETERMINANTS OF DUAL-TASK INTERFERENCE AND RESOURCE THEORIES IN COGNITIVE PSYCHOLOGY
Dietrich Manzey Aug. 1990 238 p Transl. into ENGLISH of Determinanten der Aufgabeninterferenz bei Doppeltaetigkeiten und Ressourcentheoretische Modellvorstellungen in der Kognitiven Psychologie (Hamburg, Fed. Republic of Germany, DFVLR), Feb. 1988 234 p Original language document was announced as N88-27748
(ESA-TT-1127; DFVLR-FB-88-14; ETN-90-98000) Avail: NTIS HC/MF A11

As a rule, an attempt to perform two tasks simultaneously will lead to performance loss in at least one of the two. In two experiments (22 subjects), the determinants of these interference effects were investigated by analyzing Performance Operating Characteristic (POC) curves for various task combinations. It was shown that the level of task interference in dual-task is primarily influenced by the similarity between the two tasks with regard to their perceptive-cognitive and response-related demands and that the degree of task difficulty is of subordinate importance. The results are interpreted as proof of the prognostic value of the theory of multiple resources. ESA

N91-10947*# National Aeronautics and Space Administration. Ames Research Center, Moffett Field, CA.
TECHNOLOGICAL ADVANCES FOR STUDYING HUMAN BEHAVIOR
Renate J. Roske-Hofstrand *In* NASA, Langley Research Center, Aviation Safety/Automation Program Conference Oct. 1990 p 131-141 (For primary document see N91-10936 02-03)
Avail: NTIS HC/MF A12 CSCL 05I

N91-10948*# Pacific Northwest Lab., Richland, WA.
ASSESSING THE FEASIBILITY, COST, AND UTILITY OF DEVELOPING MODELS OF HUMAN PERFORMANCE IN AVIATION
William Stillwell *In* NASA, Langley Research Center, Aviation Safety/Automation Program Conference Oct. 1990 p 143-149 (For primary document see N91-10936 02-03)
Avail: NTIS HC/MF A12 CSCL 05I

54 MAN/SYSTEM TECHNOLOGY AND LIFE SUPPORT

Includes human engineering; biotechnology; and space suits and protective clothing.

For related information see also *16 Space Transportation.*

N91-11382# Lawrence Livermore National Lab., CA.
CHLORINE DIOXIDE AND HEMODIALYSIS
Roger P. Smith (Dartmouth Coll., Hanover, NH.) 1 May 1989 35 p
(Contract W-7405-eng-48)
(DE90-015912; UCRL-CR-103401) Avail: NTIS HC/MF A03

Because it has little or no tendency to generate carcinogenic trihalomethanes such as chloroform, chlorine dioxide is an attractive alternative to chlorine for drinking water disinfection. There are, however, concerns about its acute toxicity, and the toxic effects of its by-products, chlorite and chlorate. The human experience with chlorine dioxide in both controlled, prospective studies and in actual use situations in community water supplies have as yet failed to reveal adverse health effects. Among groups who may be at special risk from oxychlorines in drinking water are patients who must undergo chronic extracorporeal hemodialysis. Although

even units for home hemodialysis are supposed to be equipped with devices which effectively remove oxychlorines, there is always a possibility of operator error or equipment failure. A hemodialysis and the effects of oxychlorine are discussed. DOE

N91-11383# Messerschmitt-Boelkow-Blohm G.m.b.H., Munich (Germany, F.R.). Helicopter Div.
REQUIREMENTS OF AN HMS/D FOR A NIGHT-FLYING HELICOPTER
H.-D. Boehm and R. Schranner Apr. 1990 17 p Presented at SPIE'S Technical Symposium on Engineering and Photonics in Aerospace Sensing Conf. 1290 Helmet-Mounted Displays 2, Orlando, FL, 16-20 Apr. 1990
(MBB-UD-0570-90-PUB; ETN-90-97840) Avail: NTIS HC/MF A03

Requirements of a Helmet Mounted Sight (HMS/D) are studied. The development goal for the near future should be an integrated, lightweight helmet with a binocular display on the visor providing two or three sensor images. Operational requirements, human engineering aspects and the requirements of an integrated lightweight helmet with two Night Vision Goggle (NVG) tubes and two cathode ray tubes to display superimposed NVG and thermal imaging images with flight symbologies are described. ESA

N91-10943*# Miami Univ., Coral Gables, FL.
HUMAN FACTORS OF THE HIGH TECHNOLOGY COCKPIT
Earl L. Wiener *In* NASA, Langley Research Center, Aviation Safety/Automation Program Conference Oct. 1990 p 83-90 (For primary document see N91-10936 02-03)
Avail: NTIS HC/MF A12 CSCL 05H

N91-10944*# National Aeronautics and Space Administration. Ames Research Center, Moffett Field, CA.
HUMAN-CENTERED AUTOMATION: DEVELOPMENT OF A PHILOSOPHY
Curtis Graeber and Charles E. Billings *In* NASA, Langley Research Center, Aviation Safety/Automation Program Conference Oct. 1990 p 91-104 (For primary document see N91-10936 02-03)
Avail: NTIS HC/MF A12 CSCL 05H

N91-10945*# National Aeronautics and Space Administration. Ames Research Center, Moffett Field, CA.
CREW WORKLOAD STRATEGIES IN ADVANCED COCKPITS
Sandra G. Hart *In* NASA, Langley Research Center, Aviation Safety/Automation Program Conference Oct. 1990 p 105-125 (For primary document see N91-10936 02-03)
Avail: NTIS HC/MF A12 CSCL 05H

N91-11369# Defence and Civil Inst. of Environmental Medicine, North York (Ontario).
AIRCREW/COCKPIT COMPATIBILITY: A MULTIVARIATE PROBLEM SEEKING A MULTIVARIATE SOLUTION
Keith C. Hendy *In* AGARD, Recruiting, Selection, Training and Military Operations of Female Aircrew Aug. 1990 8 p (For primary document see N91-11358 02-53)
Copyright Avail: NTIS HC/MF A08; Non-NATO Nationals requests available only from AGARD/Scientific Publications Executive

N91-11371# Defence and Civil Inst. of Environmental Medicine, North York (Ontario).
ANTHROPOMETRIC ACCOMMODATION OF FEMALES IN CANADIAN FORCES AIRCRAFT CREW STATIONS
P. L. Rothwell and R. A. Pigeau *In* AGARD, Recruiting, Selection, Training and Military Operations of Female Aircrew Aug. 1990 13 p (For primary document see N91-11358 02-53)
Copyright Avail: NTIS HC/MF A08; Non-NATO Nationals requests available only from AGARD/Scientific Publications Executive

N91-11372# Laboratoire de Medecine Aerospatiale, Bretigny-sur-Orge (France).
PROBLEMS POSED BY THE ADAPTATION OF PHYSIOLOGICAL PROTECTIVE EQUIPMENT FOR FEMALE COMBAT PILOTS [PROBLEMES POSES PAR L'ADAPTATION DES EQUIPEMENTS DE PROTECTION PHYSIOLOGIQUE AUX PILOTES FEMININS D'AVIONS DE COMBAT]
D. Lejeune, J. C. Amichaud, A. Turillon (Aerazur C.A., Issy-les-Moulineaux, France), J. M. Clere, and H. Marotte *In* AGARD, Recruiting, Selection, Training and Military Operations of Female Aircrew Aug. 1990 4 p In FRENCH; ENGLISH summary (For primary document see N91-11358 02-53)
Copyright Avail: NTIS HC/MF A08; Non-NATO Nationals requests available only from AGARD/Scientific Publications Executive

N91-11373# Royal Air Force Inst. of Aviation Medicine, Farnborough (England).
SOME EQUIPMENT PROBLEMS ASSOCIATED WITH THE INTRODUCTION OF FEMALE AIRCREW INTO THE ROYAL AIR FORCE
G. M. Turner *In* AGARD, Recruiting, Selection, Training and Military Operations of Female Aircrew Aug. 1990 3 p (For primary document see N91-11358 02-53)
Copyright Avail: NTIS HC/MF A08; Non-NATO Nationals requests available only from AGARD/Scientific Publications Executive

N91-11374# Laboratoire de Medecine Aerospatiale, Bretigny-sur-Orge (France).
MORPHOLOGICAL AND FUNCTIONAL ADAPTATION OF PERSONAL EQUIPMENT DESIGNED FOR FEMALE PERSONNEL [ADAPTATION MORPHOLOGIQUE ET FONCTIONNELLE DES EQUIPEMENTS DE VOL DESTINES AUX PERSONNELS FEMININS]
H. Marotte, D. Lejeune, G. Gutman, R. Beaussant, P. Pelloux-Gervais, and R. Zapata (L'Air Liquide, Sassenage, France) *In* AGARD, Recruiting, Selection, Training and Military Operations of Female Aircrew Aug.1990 3 p In FRENCH; ENGLISH summary (For primary document see N91-11358 02-53)
Copyright Avail: NTIS HC/MF A08; Non-NATO Nationals requests available only from AGARD/Scientific Publications Executive

N91-11375# Naval Air Development Center, Warminster, PA. Dept. of Air Vehicle and Crew Systems Technology.
ACCOMMODATION OF FEMALE AIRCREW IN USN PROTECTIVE FLIGHT CLOTHING AND EQUIPMENT
S. M. Reeps, H. T. Pheeny, and J. A. Brady (Naval Aerospace Medical Research Lab., Pensacola, FL.) *In* AGARD, Recruiting, Selection, Training and Military Operations of Female Aircrew Aug. 1990 7 p (For primary document see N91-11358 02-53)
Copyright Avail: NTIS HC/MF A08; Non-NATO Nationals requests available only from AGARD/Scientific Publications Executive

55 SPACE BIOLOGY

Includes exobiology; planetary biology; and extraterrestrial life.

No abstracts in this category.

59 MATHEMATICAL AND COMPUTER SCIENCES (GENERAL)

N91-11384*# National Aeronautics and Space Administration. Ames Research Center, Moffett Field, CA.
PERFORMANCE OF A PARALLEL CODE FOR THE EULER EQUATIONS ON HYPERCUBE COMPUTERS

Eric Barszcz, Tony F. Chan, Dennis C. Jesperson, and Raymond S. Tuminaro (Stanford Univ., CA.) Apr. 1990 41 p Prepared in cooperation with Research Inst. for Advanced Computer Science, Moffett Field, CA
(NASA-TM-102260; A-90020; NAS 1.15:102260) Avail: NTIS HC/MF A03 CSCL 12A

The performance of hypercubes were evaluated on a computational fluid dynamics problem and the parallel environment issues were considered that must be addressed, such as algorithm changes, implementation choices, programming effort, and programming environment. The evaluation focuses on a widely used fluid dynamics code, FLO52, which solves the two dimensional steady Euler equations describing flow around the airfoil. The code development experience is described, including interacting with the operating system, utilizing the message-passing communication system, and code modifications necessary to increase parallel efficiency. Results from two hypercube parallel computers (a 16-node iPSC/2, and a 512-node NCUBE/ten) are discussed and compared. In addition, a mathematical model of the execution time was developed as a function of several machine and algorithm parameters. This model accurately predicts the actual run times obtained and is used to explore the performance of the code in interesting but yet physically realizable regions of the parameter space. Based on this model, predictions about future hypercubes are made. Author

60 COMPUTER OPERATIONS AND HARDWARE

Includes hardware for computer graphics, firmware, and data processing.

For components see *33 Electronics and Electrical Engineering.*

N91-11385# Navy Personnel Research and Development Center, San Diego, CA.
THE MS-DOS DEVICE HANDLER INTERFACE Interim Report, Sep. 1988 - Feb. 1990
Brian VandeWetering and Brian Thomason (Systems Engineering Associates, San Diego, CA.) Apr. 1990 117 p
(Contract N66001-88-D-0054)
(AD-A223856; NPRDC-TN-90-16) Avail: NTIS HC/MF A06 CSCL 12/5

Many vendors produce high performance, low cost training hardware, but bundle their products with proprietary software interfaces. Because these interfaces are proprietary, courseware and authoring systems written to operate on one set of hardware will not run on a competitor's hardware. Expensive reprogramming is needed to adapt to new hardware. These reprogramming costs can be eliminated by adopting standard software interfaces. The objectives of this effort were to describe and develop a standard software interface that will allow training systems to be assembled from separate plug-and-play components in the same way that stereo systems can be assembled from separate speakers, amplifiers, and other components. The Portable Courseware (PORTCO) architecture consists of two interfaces, the Device Services Interface and the Device Handler Interface. It also contains three layers: application, routing and configuration, and device handler. This architecture should allow applications software to run on any compliant set of hardware components. The series of reports describing the PORTCO architecture should direct development of portable MS-DOS applications and standard peripheral device handlers. The Device Handler Interface is described and should be of primary interest to device manufactures and system vendors who must develop device handler software. GRA

N91-11386# Systems Engineering Associates, San Diego, CA.
THE MS-DOS DEVICE SERVICES INTERFACE Interim Report, Sep. 1988 - Feb. 1990
Brian Thomason and Brian VandeWetering Apr. 1990 109 p
(Contract N66001-88-D-0054)
(AD-A223902; NPRDC-TN-90-15) Avail: NTIS HC/MF A06 CSCL 12/5

Many vendors produce high performance, low cost training hardware, but bundle their products with proprietary software interfaces. Because these interfaces are proprietary, courseware and authoring systems written to operate on one set of hardware will not run on a competitor's hardware. Expensive reprogramming is needed to adapt to new hardware. These reprogramming costs can be eliminated by adopting standard software interfaces. The objectives of this effort were to describe and develop a standard software interface that will allow training systems to be assembled from separate plug-and-play components in the same way that stereo systems can be assembled from separate speakers, amplifiers, and other components. The Portable Courseware (PORTCO) architecture consists of two interfaces, the Device Services Interface and the Device Handler Interface. It also contains three layers: application, routing and configuration, and the device handler. This architecture should allow applications software to run on any compliant set of hardware components. The series of reports describing the PORTCO architecture should direct development of portable MS-DOS applications and standard peripheral device handlers. The MS-DOS Device Services Interface is described and is intended primarily for programmers who want to develop portable application software. GRA

N91-11387*# North Carolina State Univ., Raleigh. Mars Mission Research Center.
DISTRIBUTED DIGITAL SIGNAL PROCESSORS FOR MULTI-BODY STRUCTURES Interim Report
Gordon K. Lee 1990 16 p
(Grant NAG1-1136)
(NASA-CR-187375; NAS 1.26:187375) Avail: NTIS HC/MF A03 CSCL 09B

Several digital filter designs were investigated which may be used to process sensor data from large space structures and to design digital hardware to implement the distributed signal processing architecture. Several experimental tests articles are available at NASA Langley Research Center to evaluate these designs. A summary of some of the digital filter designs is presented, an evaluation of their characteristics relative to control design is discussed, and candidate hardware microcontroller/microcomputer components are given. Future activities include software evaluation of the digital filter designs and actual hardware inplementation of some of the signal processor algorithms on an experimental testbed at NASA Langley. Author

N91-11388# Instituto de Pesquisas Espaciais, Sao Jose dos Campos (Brazil).
FUNDAMENTAL CONCEPTS FOR UTILIZATION OF THE FPS-5410 ARRAY PROCESSOR [NOCOES FUNDAMENTAIS PARA UTILIZACAO DO PROCESSADOR MATRICIAL FPS-5410]
Joao BeneditoDiehl and Juan SunePerez Jan. 1990 78 p In PORTUGUESE; ENGLISH summary
(INPE-5091-RPE/624) Avail: NTIS HC/MF A05

Fundamental concepts for the utilization of the FPS-5410 array processor from the Department of Mechanics are presented. The main characteristics of the FPS-5410, the hardware, and the software of the system are initially presented, followed by utilization examples. Author

61 COMPUTER PROGRAMMING AND SOFTWARE

Includes computer programs, routines, alogorithms, and specific applications, e.g., CAD/CAM.

N91-11389*# National Aeronautics and Space Administration. Goddard Space Flight Center, Greenbelt, MD.
PROCEEDINGS OF THE FIRST NASA Ada USERS' SYMPOSIUM
Dec. 1988 227 p Symposium held in Greenbelt, MD, 1 Dec. 1988
(NASA-TM-102941; SEL-88-005; NAS 1.15:102941) Avail: NTIS HC/MF A11 CSCL 09B

Ada has the potential to be a part of the most significant change in software engineering technology within NASA in the last twenty years. Thus, it is particularly important that all NASA centers be aware of Ada experience and plans at other centers. Ada activity across NASA are covered, with presenters representing five of the nine major NASA centers and the Space Station Freedom Program Office. Projects discussed included - Space Station Freedom Program Office: the implications of Ada on training, reuse, management and the software support environment; Johnson Space Center (JSC): early experience with the use of Ada, software engineering and Ada training and the evaluation of Ada compilers; Marshall Space Flight Center (MSFC): university research with Ada and the application of Ada to Space Station Freedom, the Orbital Maneuvering Vehicle, the Aero-Assist Flight Experiment and the Secure Shuttle Data System; Lewis Research Center (LeRC): the evolution of Ada software to support the Space Station Power Management and Distribution System; Jet Propulsion Laboratory (JPL): the creation of a centralized Ada development laboratory and current applications of Ada including the Real-time Weather Processor for the FAA; and Goddard Space Flight Center (GSFC): experiences with Ada in the Flight Dynamics Division and the Extreme Ultraviolet Explorer (EUVE) project and the implications of GSFC experience for Ada use in NASA. Despite the diversity of the presentations, several common themes emerged from the program: Methodology - NASA experience in general indicates that the effective use of Ada requires modern software engineering methodologies; Training - It is the software engineering principles and methods that surround Ada, rather than Ada itself, which requires the major training effort; Reuse - Due to training and transition costs, the use of Ada may initially actually decrease productivity, as was clearly found at GSFC; and real-time work at LeRC, JPL and GSFC shows that it is possible to use Ada for real-time applications. Author

N91-11390*# National Aeronautics and Space Administration. Goddard Space Flight Center, Greenbelt, MD.
Ada AND SOFTWARE MANAGEMENT IN NASA: SYMPOSIUM/FORUM
Jun. 1989 182 p Symposium held in Greenbelt, MD, 31 May - 1 Jun. 1989
(NASA-TM-103297; NAS 1.15:103297) Avail: NTIS HC/MF A09 CSCL 09B

The promises of Ada to improve software productivity and quality, and the claims that a transition to Ada would require significant changes in NASA's training programs and ways of doing business were investigated. The study assesses the agency's ongoing and planned Ada activities. A series of industry representatives (Computer Sciences Corporation, General Electric Aerospace, McDonnell Douglas Space Systems Company, TRW, Lockheed, and Boeing) reviewed the recommendations and assessed their impact from the Company's perspective. The potential effects on NASA programs were then discussed. B.G.

N91-11391*# National Aeronautics and Space Administration. Langley Research Center, Hampton, VA.
DATA BASE ARCHITECTURE FOR INSTRUMENT CHARACTERISTICS CRITICAL TO SPACECRAFT CONCEPTUAL DESIGN
Lawrence F. Rowell and Cheryl L. Allen Washington Nov. 1990 32 p
(NASA-TM-4213; L-16748; NAS 1.15:4213) Avail: NTIS HC/MF A03 CSCL 09B

Spacecraft designs are driven by the payloads and mission requirements that they support. Many of the payload characteristics, such as mass, power requirements, communication requirements, moving parts, and so forth directly affect the choices for the spacecraft structural configuration and its subsystem design and component selection. The conceptual design process, which translates mission requirements into early spacecraft concepts, must be tolerant of frequent changes in the payload complement and resource requirements. A computer data base was designed and implemented for the purposes of containing the payload characteristics pertinent for spacecraft conceptual design, tracking the evolution of these payloads over time, and enabling the integration of the payload data with engineering analysis programs for improving the efficiency in producing spacecraft designs. In-house tools were used for constructing the data base and for performing the actual integration with an existing program for optimizing payload mass locations on the spacecraft. Author

N91-11392*# Southwest Research Inst., San Antonio, TX.
RESEARCH INTO LANGUAGE CONCEPTS FOR THE MISSION CONTROL CENTER Final Report
Steven W. Dellenback, Timothy J. Barton, and Jeremiah M. Ratner 12 Jun. 1990 573 p
(Grant NAG9-339; SwRI Proj. 05-2768)
(NASA-CR-185928; NAS 1.26:185928) Avail: NTIS HC/MF A24 CSCL 09B

A final report is given on research into language concepts for the Mission Control Center (MCC). The Specification Driven Language research is described. The state of the image processing field and how image processing techniques could be applied toward automating the generation of the language known as COmputation Development Environment (CODE or Comp Builder) are discussed. Also described is the development of a flight certified compiler for Comps. Author

N91-11393*# Alabama Univ., Huntsville.
INTELLIGENT DATA REDUCTION (IDARE) Final Report, 1 Jun. 1988 - 31 May 1989
D. Michael Brady and Donnie R. Ford 19 Mar. 1990 32 p
(Grant NAG8-642)
(NASA-CR-186322; NAS 1.26:186322; UAH-90-30) Avail: NTIS HC/MF A03 CSCL 09B

A description of the Intelligent Data Reduction (IDARE) expert system and an IDARE user's manual are given. IDARE is a data reduction system with the addition of a user profile infrastructure. The system was tested on a nickel-cadmium battery testbed. Information is given on installing, loading, maintaining the IDARE system. Author

N91-11394# Navy Personnel Research and Development Center, San Diego, CA.
THE MS-DOS ROUTING AND CONFIGURATION PROGRAM DESIGN Interim Report, Sep. 1988 - Feb. 1990
Brian VandeWetering and Brian Thomason (Systems Engineering Associates, San Diego, CA.) Apr. 1990 33 p
(Contract N66001-88-D-0054)
(AD-A223858; NPRDC-TN-90-17) Avail: NTIS HC/MF A03 CSCL 12/5

Many vendors produce high performance, low cost training hardware, but bundle their products with proprietary software interfaces. Because these interfaces are proprietary, courseware and authoring systems written to operate on one set of hardware will not run on a competitor's hardware. Expensive reprogramming is needed to adapt to new hardware. These reprogramming costs can be eliminated by adopting standard software interfaces. The objectives of this effort were to describe and develop a standard software interface that will allow training systems to be assembled from separate plug-and-play components in the same way that stereo systems can be assembled from separate speakers,

amplifiers, and other components. The Portable Courseware (PORTCO) architecture consists of two interfaces, the Device Services Interface and the Device Handler Interface. It also contains three layers application, routing and configuration, and device handler layer. This architecture should allow applications software to run on any compliant set of hardware components. The series of reports describing the PORTCO architecture should direct development of portable MS-DOS applications and standard peripheral device handlers. Intended for system vendors, and the design of the first PORTCO routing and configuration program is described. GRA

N91-11395# Army Engineer Waterways Experiment Station, Vicksburg, MS. Information Technology Lab.
COMPUTER-AIDED STRUCTURAL ENGINEERING (CASE) PROJECT: INVESTIGATION AND DESIGN OF U-FRAME STRUCTURES USING PROGRAM CUFRBC. VOLUME C: USER'S GUIDE FOR CHANNELS Final Report
Clifford O. Hays, Jr. and Clifford Ford May 1990 236 p
(AD-A224388; WES/TR/ITL-90-3-Vol-C) Avail: NTIS HC/MF A11 CSCL 12/5

Instructions are given for routine use of the program CUFRBC for channel structures. CUFRBC is a program for interactive investigation and design of U-frame basin and channel structures. A short description of how to access the program on each of the systems, when the program is available, is provided. B.G.

N91-11396*# Environmental Research Inst. of Michigan, Ann Arbor. Space Automation and Robotics Center.
ON THREE DIMENSIONAL OBJECT RECOGNITION AND POSE-DETERMINATION: AN ABSTRACTION BASED APPROACH Ph.D. Thesis - Michigan Univ. Final Report
Kok How Francis Quek Jun. 1990 248 p
(Grant NAGw-1198)
(NASA-CR-186894; NAS 1.26:186894; ERIM-205400-8-F) Avail: NTIS HC/MF A11 CSCL 09B

A method of computing reliable Gaussian and mean curvature sign-map descriptors from the polynomial approximation of surfaces was demonstrated. Such descriptors which are invariant under perspective variation are suitable for hypothesis generation. A means for determining the pose of constructed geometric forms whose algebraic surface descriptors are nonlinear in terms of their orienting parameters was developed. This was done by means of linear functions which are capable of approximating nonlinear forms and determining their parameters. It was shown that biquadratic surfaces are suitable companion linear forms for cylindrical approximation and parameter estimation. The estimates provided the initial parametric approximations necessary for a nonlinear regression stage to fine tune the estimates by fitting the actual nonlinear form to the data. A hypothesis-based split-merge algorithm for extraction and pose determination of cylinders and planes which merge smoothly into other surfaces was developed. It was shown that all split-merge algorithms are hypothesis-based. A finite-state algorithm for the extraction of the boundaries of run-length regions was developed. The computation takes advantage of the run list topology and boundary direction constraints implicit in the run-length encoding. Author

N91-11397*# Institute for Computer Applications in Science and Engineering, Hampton, VA.
INFLATED SPEEDUPS IN PARALLEL SIMULATIONS VIA MALLOC() Final Report
David M. Nicol (College of William and Mary, Williamsburg, VA.) Sep. 1990 18 p Submitted for publication
(Contract NAS1-18605; NAG1-1060; NSF ASC-88-19373)
(NASA-CR-182104; ICASE-90-63; NAS 1.26:182104) Avail: NTIS HC/MF A03 CSCL 09B

Discrete-event simulation programs make heavy use of dynamic memory allocation in order to support simulation's very dynamic space requirements. When programming in C one is likely to use the malloc() routine. However, a parallel simulation which uses the standard Unix System V malloc() implementation may achieve an overly optimistic speedup, possibly superlinear. An alternate implementation provided on some (but not all systems) can avoid the speedup anomaly, but at the price of significantly reduced available free space. This is especially severe on most parallel architectures, which tend not to support virtual memory. It is shown how a simply implemented user-constructed interface to malloc() can both avoid artificially inflated speedups, and make efficient use of the dynamic memory space. The interface simply catches blocks on the basis of their size. The problem is demonstrated empirically, and the effectiveness of the solution is shown both empirically and analytically. Author

N91-11398# Center for Mathematics and Computer Science, Amsterdam (Netherlands). Dept. of Operations Research, Statistics, and System Theory.
MINIMIZING MAXIMUM EARLINESS AND MAXIMUM LATENESS ON A SINGLE MACHINE
J. A. Hoogeveen Feb. 1990 16 p
(CWI-BS-R9001; ETN-90-97668) Copyright Avail: NTIS HC/MF A03

A set of n jobs has to be scheduled on a single machine which can handle only one job at a time. Each job requires a given positive uninterrupted processing time and has a given due date. The problem is to find a schedule that minimizes a function of maximum earliness and maximum lateness that is nondecreasing in both arguments. O(n squared log n) algorithms are presented for the variant in which idle time is not allowed and for the special case in which the objective function is linear. The problem is proved np-hard if neither of these restrictions is imposed. ESA

N91-11399# Center for Mathematics and Computer Science, Amsterdam (Netherlands). Dept. of Numerical Analysis.
NUMVEC FORTRAN LIBRARY MANUAL. CHAPTER: PARTIAL DIFFERENTIAL EQUATIONS. ROUTINE: OEHPC
Erik D. deGoede and J. H. M. tenThijeBoonkkamp Aug. 1989 14 p
(CWI-NM-R8915; ETN-90-97670) Copyright Avail: NTIS HC/MF A03

The NUMVEC FORTRAN library routine OEHPC (Odd-Even Hopscotch Pressure Correction) which solves the two dimensional, time-dependent, incompressible Navier-Stokes equations on a rectangular domain, is described. For the time-integration the odd-even hopscotch method is combined with an efficient Poisson-solver. ESA

N91-11400# Technische Univ., Delft (Netherlands). Faculty of Technical Mathematics and Informatics.
WHAT IS A DEFAULT
Nico Roos 1990 13 p
(Rept-90-12; ISSN-0922-5641; ETN-90-97707) Copyright Avail: NTIS HC/MF A03

Four different kinds of defaults are distinguished. This distinction is made because in the opinion of the author, a number of problems which can be found in literature about non-monotonic logics and inheritance networks are based on the fact that all defaults are treated the same. The division in categories described is a personal view of the author and is intended to induce a discussion about the meaning of a default. To model default reasoning, the meaning of a default should be clear. ESA

N91-11401# Technische Univ., Delft (Netherlands). Faculty of Technical Mathematics and Informatics.
A LOGICAL BACKGROUND OF A METHOD FOR THE HANDLING OF INCOMPATIBLE PIECES OF KNOWLEDGE
Jaroslav Chudacek 1990 120 p
(Rept-90-13; ISSN-0922-5641; ETN-90-97708) Copyright Avail: NTIS HC/MF A06

Techniques for the study of semantics of inconsistent theories, while keeping the syntax, logical axioms and inference rules of first order predicate logic are presented. Partial models, nth partial models and a semantic measure of consistency are defined. In the main theorem it is proved that partial models are suitable approximations of classical models. This theorem is a new version of Herbrand's theorem, a basic theorem in automated theorem

proving. (Generalized) semantic trees ordered according to substitution depth are defined and used to give an equivalent condition for the existence of an nth partial model of a set of clauses. A method for using the semantical method in a decision support system which helps the user to handle incompatible pieces of knowledge is outlined. ESA

N91-11402# Technische Univ., Delft (Netherlands). Faculty of Technical Mathematics and Informatics.
A POTENTIAL REDUCTION VARIANT OF RENEGAR'S SHORT-STEP PATH-FOLLOWING METHOD FOR LINEAR PROGRAMMING
D. denHertog, C. Roos, and T. Terlaky 31 Jan. 1990 24 p
(Rept-90-14; ISSN-0922-5641; ETN-90-97709) Copyright Avail: NTIS HC/MF A03

A new polynomial potential reduction method for linear programming, which can also be seen as a large-step path-following method, is proposed. The method uses an (approximate) linesearch along the Newton direction with respect to Renegar's strictly convex potential function if the iterate is far away from the central trajectory. If the iterate lies close to the trajectory, the lower bound is updated for the optimal value. Dependent of the updating scheme the iteration bound can be proved to be O(square root of n(L)) or O(nL). The method differs from the recently published potential reduction methods in the choice of the potential function and the search direction. ESA

N91-11403# Technische Univ., Delft (Netherlands). Faculty of Technical Mathematics and Informatics.
A FORMAL SEMANTICS FOR THE PREFERRED SUBTHEORIES
Nico Roos 1990 11 p
(Rept-90-20; ISSN-0922-5641; ETN-90-97713) Copyright Avail: NTIS HC/MF A03

A formal semantics for the preferred subtheories of G. Brewka is specified. This semantics is based on the ideas of Y. Shoham. The semantics described defines a preference relation on the set of semantical structures of the logical language. The models of the preferred subtheories are those structures which satisfy more premisses (hypotheses) with a higher preference than some other structure. ESA

N91-11404# Institut National Polytechnique, Grenoble (France). Lab. de Technique de l'Informatique, de la Microelectronique et de la Microscopie Quantitative.
SILICON COMPILATION AND THE SYCO SILICON COMPILER Ph.D. Thesis
Ahmed Amine Jerraya 1989 215 p In FRENCH; ENGLISH summary
(ETN-90-97827) Avail: NTIS HC/MF A10

Silicon compilers which perform the automatic synthesis of integrated circuits are considered. Silicon compilation, several silicon compilation schemes, and compilation levels are presented. Behavioral silicon compilation techniques are analyzed. The SYCO silicon compiler is detailed. The translation scheme used by SYCO (from behavior to layout) is easy to understand thanks to the correspondence between the target architecture and the behavioral description. ESA

N91-11405# National Inst. of Standards and Technology, Boulder, CO.
TIME DOMAIN FREQUENCY STABILITY CALCULATED FROM THE FREQUENCY DOMAIN DESCRIPTION: USE OF THE SIGINT SOFTWARE PACKAGE TO CALCULATE TIME DOMAIN FREQUENCY STABILITY FROM THE FREQUENCY DOMAIN
F. L. Walls, J. Gary, A. OGallagher, R. Sweet, and L. Sweet 1989 35 p
(PB90-257684; NISTIR-89/3916) Avail: NTIS HC/MF A03 CSCL 09B

The use of SIGINT, a new interactive software package, is described. This package facilitates the calculation of time domain frequency stability in terms of the Allan variance as a function of measuring time from frequency domain data. Except for the graphic output, the code is written in standard FORTRAN 77 and runs on AT compatible computers that have a math co-processor. It also runs on many other systems; however, calls to an available graphics library will need to be substituted for those that are included in this version. The program uses either a user defined function for the input noise or default functions that describe the noise types commonly found in oscillators, amplifiers, frequency multipliers, frequency dividers, and general signal processing equipment. These default functions make it simple to analyze the time domain frequency stability as a function of measuring bandwidth using realistic first-, second-, or third-order low-pass filters or the simplified infinitely sharp cutoff parameter. The default functions are also set up to examine the effect of various servo parameters on the performance of a frequency source locked to a frequency reference. GRA

N91-11406 Florida Univ., Gainesville.
BOUNDARY ELEMENT METHODS IN STRUCTURAL SHAPE SYNTHESIS Ph.D. Thesis
Junhaur Jih 1989 148 p
Avail: Univ. Microfilms Order No. DA9021865

The purpose is to present an efficient implementation for optimal structural shape synthesis which is based on a combination of the boundary element method (BEM) with nonlinear programming (NLP) optimization algorithms. Shape optimization involving 2-D elastic, torsional shaft problems, and small strain elastostatics problems, is introduced. An approach for grid refinement and grid adaptation for the BEM is developed for application in plane elasticity problems. To prevent distortion of the original domain, master nodes are introduced to control the geometry of the structure. Two strategies for the solution of the adaptive schemes are investigated, one based on a variational approach and another employing nonlinear programming methods. The use of nonlinear programming methods in grid distribution allows greater flexibility in selecting the form and relative importance of criteria employed for grid adaptation and refinement. By utilizing the characteristics of both the BEM and the LU-decomposition methods, an efficient use of a semi-analytical sensitivity analysis for optimum design is obtained. The use of BEM in optimal shape synthesis from the standpoint of an integrated formulation is also examined. A set of linear equations obtained from the boundary element analysis is treated as equality constraints in the mathematical programming optimization problem. Several numerical examples are presented for illustrating the effectiveness and convenience of using BEM with these techniques. Dissert. Abstr.

N91-11407*# Old Dominion Univ., Norfolk, VA.
SURROGATE ORACLES, GENERALIZED DEPENDENCY AND SIMPLER MODELS
Larry Wilson 1990 22 p
(Grant NAG1-750)
(NASA-CR-187360; NAS 1.26:187360) Avail: NTIS HC/MF A03 CSCL 09B

Software reliability models require the sequence of interfailure times from the debugging process as input. It was previously illustrated that using data from replicated debugging could greatly improve reliability predictions. However, inexpensive replication of the debugging process requires the existence of a cheap, fast error detector. Laboratory experiments can be designed around a gold version which is used as an oracle or around an n-version error detector. Unfortunately, software developers can not be expected to have an oracle or to bear the expense of n-versions. A generic technique is being investigated for approximating replicated data by using the partially debugged software as a difference detector. It is believed that the failure rate of each fault has significant dependence on the presence or absence of other faults. Thus, in order to discuss a failure rate for a known fault, the presence or absence of each of the other known faults needs to be specified. Also, in simpler models which use shorter input sequences without sacrificing accuracy are of interest. In fact, a possible gain in performance is conjectured. To investigate these propositions, NASA computers running LIC (RTI) versions

are used to generate data. This data will be used to label the debugging graph associated with each version. These labeled graphs will be used to test the utility of a surrogate oracle, to analyze the dependent nature of fault failure rates and to explore the feasibility of reliability models which use the data of only the most recent failures. Author.

N91-11408# Oak Ridge National Lab., TN.
PARALLEL PERFORMANCE MODELS FOR THE NODAL TRANSPORT METHOD ON THE HYPERCUBE
Y. Y. Azmy 1990 8 p Presented at the American Nuclear Society Winter Meeting, Washington, DC, 11-15 Nov. 1990
(Contract DE-AC05-84OR-21400)
(DE90-015162; CONF-901101-24) Avail: NTIS HC/MF A02

In this paper, we derive and validate a parallel performance model for a previously derived parallel algorithm used in solving the nodal transport method equations with zero- and first-order spatial approximations. DOE

N91-11409# Lawrence Livermore National Lab., CA. Weapons Engineering Div.
IGES EFFICIENCY EVALUATION
M. Christensen, J. Farrell, and S. Green 12 Jun. 1990 28 p Presented at the CUBE: Computer Use By Engineers Symposium, Santa Fe, NM, 27-30 Nov. 1990
(Contract W-7405-eng-48)
(DE90-015192; UCRL-JC-104493; CONF-901179-1) Avail: NTIS HC/MF A03

This report describes the Initial Graphics Exchange Specifications (IGES) Efficiency Study, a joint effort of Weapons Engineering Division (WED) and Materials Fabrication Division (MFD). The goal of the study was to quantify the impact of accurate geometry in design, manufacturing and inspection of mechanical parts. Two parts were designed, manufactured and inspected; a hemispherical and non-hemispherical part. Each part was designed in WED using computer aided design (CAD). Three sources of numerical control (NC) tool paths and inspection probe paths were received in MFD: (1) an unchecked CAD/IGES database, (2) a guaranteed CAD/IGES database, and (3) an electronic Hewlett-Packard Graphics Language (HPGL) file presenting the CAD drawing. DOE

N91-11410# Sandia National Labs., Albuquerque, NM.
AN ADAPTIVE FINITE ELEMENT TECHNIQUE USING ELEMENT EQUILIBRIUM AND PAVING
Ted D. Blacker, Joseph Jung, and Walter R. Witkowski 1990 30 p Presented at the International Symposium on Gas-Liquid Two-Phase Flows in Conjunction With the Winter Annual Meeting of the ASME, Dallas, TX, 25-30 Nov. 1990
(Contract DE-AC04-76DP-00789)
(DE90-015829; SAND-90-2034C; CONF-901109-10) Avail: NTIS HC/MF A03

This paper presents an adaptive finite element technique to automatically control analysis errors. This scheme uses a new error measure and the paving meshing algorithm. With this technique, a 2-D finite element problem can be adaptively meshed to produce an answer within a desired error tolerance. In this paper we describe the new error measure as well as the paving mesh generation technique. We then describe the process of controlling the mesh generation with the error measure and present several examples that demonstrate the capacity of this adaptive technique. DOE

N91-11411# Washington Univ., Seattle.
TWO AND THREE DIMENSIONAL MAGNETOTELLURIC INVERSION Annual Progress Report
1990 15 p
(Contract DE-FG06-89ER-14064)
(DE90-016187; DOE/ER-14064/1) Avail: NTIS HC/MF A03

This paper is an annual progress report. In prior reporting periods, a numerically efficient algorithm to invert large magnetotelluric (MT) data sets for conductive structures has been developed. The method is iterative and approximates lateral derivatives of the electric and magnetic fields inside the model by their values from the previous iteration. The model is made unique by minimizing a function which measures the complexity of the model. The purpose is to find the model with the least structure for a given level of misfit to the data. The method is called the Rapid Relaxation Inverse (RRI). During the past year, effort has been split between improving the two-dimensional (2D) version of the code and developing a three-dimensional (3D) version. The 2D work has involved a thorough study of synthetic data generated from known models with random noise added. This study resulted in the implementation of three stabilization schemes. One which operates in model space and damps efforts by the algorithm to make the model rough. The second operates in data space and down-weights data with large residuals at each iteration. This means that data that is easy to fit will be fit first. DOE

N91-11412# Florida State Univ., Tallahassee. High Energy Physics Lab.
CAD TOOLS FOR DETECTOR DESIGN
John Womersley, Nicholas DiGiacomo, and Kendrick Killian (Martin Marietta Aerospace, Denver, CO.) Apr. 1990 11 p Presented at the International Industrial Symposium on the Supercollider, Miami Beach, FL, 14-16 Mar. 1990
(Contract DE-FG05-87ER-40319)
(DE90-017337; FSU-HEP-041090; CONF-9003202-1) Avail: NTIS HC/MF A03

Detailed detector design has traditionally been divided between engineering optimization for structural integrity and subsequent physicist evaluation. The availability of CAD systems for engineering design enables the tasks to be integrated by providing tools for particle simulation within the CAD system. It is believed this will speed up detector design and avoid problems due to the late discovery of shortcomings in the detector. This could occur because of the slowness of traditional verification techniques (such as detailed simulation with GEANT). One such new particle simulation tool is described. It is being used with the I-DEAS CAD package for SSC detector design at Martin-Marietta Astronautics and is to be released through the SSC Laboratory. DOE

N91-11413# Argonne National Lab., IL. Mathematics and Computer Science Div.
SYMBOLIC MANIPULATION SOFTWARE AND THE STUDY OF DIFFERENTIAL EQUATIONS
Marc Garbey (Lyon-1 Univ., Villeurbanne, France), Hans G. Kaper, and Man Kam Kwong 25 Jul. 1990 25 p Presented at the Workshop on Asymptotic Analysis and Numerical Solution of Partial Differential Equations, Argonne, IL, 26-28 Feb. 1990
(Contract W-31-109-eng-38)
(DE90-017674; CONF-9002131-3) Avail: NTIS HC/MF A03

Some of the experiences with symbolic manipulation software for the analysis of differential equations are described. Several examples are given from the work on semilinear diffusion equations and from a bifurcation analysis of a nonlinear problem in combustion. DOE

N91-11414# Lawrence Livermore National Lab., CA. Computing Research Group.
SISAL VERSUS FORTRAN: A COMPARISON USING THE LIVERMORE LOOPS
David Cann and John Feo Apr. 1990 16 p Presented at the Association for Computing Machinery/IEEE Supercomputing Conference, New York, NY, 12-16 Nov. 1990 Revised
(Contract W-7405-eng-48)
(DE90-010872; UCRL-102263-Rev-2; CONF-901121-1) Avail: NTIS HC/MF A03

The acquisition of parallel processors in the scientific community is increasing, but the difficulties of programming parallel machines persist. Two approaches have emerged: automatic parallelizing compilers for extant languages, and new languages that provide an easier-to-use and cleaner parallel programming model. Unfortunately most new languages have acquired a reputation for inefficiency because of their semantics. This paper compares the performance of SISAL, an applicative language for parallel

numerical computations, and FORTRAN using the Livermore Loops. Our intent is to show that applicative programs when compiled using a set of powerful yet simple optimization techniques can achieve sequential execution speeds comparable to FORTRAN, and automatically exploit conventional shared memory multiprocessors. DOE

N91-11415# Instituto de Pesquisas Espaciais, Sao Jose dos Campos (Brazil).
BETA SPLINES INTERPOLATION FOR DEM'S
Carlos Eduardo Nery and Luiz Alberto VieiraDias Mar. 1990 13 p Presented at the International Society of Photogrammetry and Remote Sensing, Tsukuba, Japan, 15-18 May 1990 Submitted for publication
(INPE-5039-PRE/1572) Avail: NTIS HC/MF A03

The interpolators used for the densification of Digital Elevation Models normally do not take into account additional information known to the operator, like rivers, lakes (flat areas), or mountain ridges. They interpolate based on the control points only. The Beta-splines curves, on the other hand, have properties that enable the operator to modify the bias and the tension for each cell by assigning values to the parameters beta 1 and beta 2. Thus, it is possible to force the resulting three dimensional surface to acquire a desirable shape. The disadvantage is the relatively large amount of extra calculations, but with the now available faster, and cheaper microcomputers, this disadvantage can be overcome. This work tests the use of Beta-splines interpolators for DEM's running on an IBM-PC-like environment. Author

N91-11416# Rolls-Royce Ltd., Derby (England).
THE ROLE OF PROCESS MODELLING IN MANUFACTURE AND DESIGN
G. J. S. Higginbotham 9 Sep. 1989 20 p Presented at the 9th ISABE Symposium, Athens, Greece, 4-9 Sep. 1989
(PNR-90702; ETN-90-97936) Copyright Avail: NTIS HC/MF A03

The relationship between the design and manufacturing functions in the development of aircraft engine components is examined. The design manufacturing interface is addressed from a total engineering process point of view. It identifies how the introduction of computer modeling of manufacturing processes can lead to reduced lead times and speedier introduction of new components, processes or alloys into applications for aircraft engine power plants, and compares this approach with the traditional iterative development process. The target for computer modeling are to simultaneously achieve a right first time design while establishing clear process manufacturing rules. It is shown that in this way, both risk and cost can be reduced. ESA

N91-11417# Instituto de Pesquisas Espaciais, Sao Jose dos Campos (Brazil).
RECEPTION AND DISPLAY OF WEFAX IMAGES: 4 BITS WITH MICRO LINE IBM-PC, USERS MANUAL [RECEPCAO E VISUALIZACAO DE IMAGENS WEFAX - 4 BITS COM MICROS LINHA IBM-PC - MANUAL DO USARIO]
Sofia Sundfeld Nov. 1989 25 p In PORTUGUESE; ENGLISH summary
(INPE-5086-NTE/294) Avail: NTIS HC/MF A03

How to receive meteorological satellite images using microcomputers, regular phone lines, and Embratel's STM-400 database network is described. The images have low resolution (WEFAX) and are regularly processed and distributed by INPE, remaining available for 48 hs. Users need an IBM-PC compatible microcomputer with at least one disk-drive, video display, dot matrix printer, communications modem, and a phone line. The images have eight gray levels, obtained from four bits resolution, and are printed with seven. Routine procedures to access the images are presented. Author

N91-11418# Instituto de Pesquisas Espaciais, Sao Jose dos Campos (Brazil).
A TOOL FOR HELP IN SOFTWARE REUTILIZATION M.S. Thesis - 12 Sep. 1989 [UMA FERRAMENTA PARA AUXILIO NA REUTILIZACAO DE SOFTWARE]
Mario Marcio RamosTeixeira Jan. 1990 121 p In PORTUGUESE; ENGLISH summary
(INPE-5077-TDL/341) Avail: NTIS HC/MF A06

The applicability of reuse as a way of achieving reduction on software production costs is discussed. The various existing methods of reuse are presented and a hierarchical multi-face methodology is proposed, based on Prieto Diaz-Freeman's method. Aspects and details of the proposed methodology and corresponding tool, with examples, are also presented. Finally, remaining difficulties and possible solutions are considered. Author

N91-11419# Instituto de Pesquisas Espaciais, Sao Jose dos Campos (Brazil).
COMBINATION OF HATLEY AND WARD/MELLOR METHODS FOR REAL TIME SYSTEMS M.S. Thesis [COMBINACAO DOS METODOS HATLEY E WARD/MELLOR PARA SISTEMAS TEMPO-REAL]
Andre Luiz Rosa Mayoral May 1990 174 p In PORTUGUESE; ENGLISH summary
(INPE-5078-TDL/412) Avail: NTIS HC/MF A08

The increasing use of structured analysis techniques for business applications yielded to its use for engineering applications. In so doing, the use of structured analysis for real-time systems development showed the need to extend the method to represent aspects specific to those systems. Two such extensions were made, one by Hatley and the other by Ward and Mellor. A combination of these two real-time structured analysis methods is described. The hybrid method uses the event-driven approach (from Ward and Mellor) in the Hatley's requirements model structure. JSD structure diagrams where added to the model structure to describe external entities. Author

N91-11420# Allied-Signal Aerospace Co., Kansas City, MO.
SOFTWARE QUALITY ASSURANCE HANDBOOK
Sep. 1990 79 p
(Contract DE-AC04-76DP-00613)
(DE91-000060; KCP-613-4118) Avail: NTIS HC/MF A05

There are two important reasons for Software Quality Assurance (SQA) at Allied-Signal Inc., Kansas City Division (KCD): First, the benefits from SQA make good business sense. Second, the Department of Energy has requested SQA. This handbook is one of the first steps in a plant-wide implementation of Software Quality Assurance at KCD. The handbook has two main purposes. The first is to provide information that you will need to perform software quality assurance activities. The second is to provide a common thread to unify the approach to SQA at KCD. DOE

N91-11421# Instituto de Pesquisas Espaciais, Sao Jose dos Campos (Brazil).
CLASSIFICATION OF TEXTURES USING THE ARMA MODELS AND DISTANCES OVER THE AUTOCORRELATION FUNCTION Ph.D. Thesis - 14 Dec. 1989 [CLASSIFICACAO DE TEXTURAS USANDO MODELOS ARMA E DISTANCIAS DA FUNCAO DE AUTOCORRELACAO]
Luciano VieiraDutra Apr. 1990 153 p In PORTUGUESE; ENGLISH summary
(INPE-5067-TDL/406) Avail: NTIS HC/MF A08

As the spatial resolution of remote sensing imagery increases, texture information becomes an important feature to help in the process of detection and measurement of objects present in these images. Several methods for describing texture were proposed in the literature, although, up to the oresent time, no formal definition of texture was stated. A method for the description and classification of textures using two-dimensional autoregressive moving average (ARMA) models is proposed. These models are derived from uni-dimensional models estimated over uni-dimensional series obtained through the concatenation of rows

or columns of the image. The image is filtered by inverse filters derived from the models, generating as many channels (residuals) as the number of textures classes. The joint distribution of the filters outputs is considered for each class. The image is classified on a pixel by pixel basis using a maximum likelihood classifier or on a sample basis (set of connected pixels) using the JM-distance, sample maximum likelihood or majority criteria. A new sample classifier, based on distances defined over two-dimensional autocorrelation functions, is also proposed. The methods were tested using synthetic aperture radar (SAR), Brodatz' book and SPOT panchromatic images. The obtained models for the defined classes were presented and discussed, relating them to the characteristics of the textures and the formation process of the image. The classification results showed substantial improvement of the average performance (an estimation of the correct classification probability) mainly for the cases in which the differences of classes means were negligible. Good performance was also verified using the sample classifier based on distances between two-dimensional autocorrelation functions. Author

N91-11422# Instituto de Pesquisas Espaciais, Sao Jose dos Campos (Brazil).
PERFORMANCE COMPARISON OF EDGE DEFECTION MORPHOLOGIES M.S. Thesis [COMPARACAO DO DESEMPENHO DE DETETORES DE BORDA MORFOLOGICOS]
Erivaldo Antonio daSilva Dec. 1989 96 p In PORTUGUESE; ENGLISH summary
(INPE-5012-TDL/400) Avail: NTIS HC/MF A05

The problem of edge detections is of fundamental importance in digital image processing. The performance of edge detectors derived from mathematical morphology is studied. In particular, the performance of six different types of morphological detectors is evaluated. The detectors are known as erosion residue (Ge), dilation residue (Gd), maximum combined (Gmax), minimum combined (Gmin), sum combined (Gsum) and blue and minimum operator (Gblur). These detectors are visually evaluated through simulated image and real satellite images. Quantitative evaluation of these detectors, with respect to edge shift, both horizontal and diagonal, and edge orientation is also presented. Author

N91-11423# Instituto de Pesquisas Espaciais, Sao Jose dos Campos (Brazil).
GEOMETRIC CORRECTION OF SPOT IMAGERY WITH THE USE OF A DIGITAL ELEVATION MODEL M.S. Thesis - Nov. 1989 [CORRECAO GEOMETRICA DE IMAGENS SPOT COM USO DE UM MODELO DIGITAL DE ELEVACAO]
Oswaldo CaldasBarbosa Feb. 1990 115 p In PORTUGUESE; ENGLISH summary
(INPE-5014-TDL/401) Avail: NTIS HC/MF A06

A theoretical and practical methodology is described for geometric correction of satellite imagery including effects of relief. The methodology presented is applicable over the unfavorable situations, such as images obtained in lateral view with large inclination angle and pronounced height differences. The images already corrected must be superposed to a topographic map at the scale of 1:50,000 or smaller. The SPOT sensor was chosen in face of the possibility of lateral views, which emphasized the relief displacement. The correction process uses ephemeris and attitude data, ground control points, collinearity equations, and a digital elevation model. The implementation is done in a microcomputer environment and uses some functions of the Image Processing System (SITM) and the Geographic Information System (GIS) developed at the Brazilian Space Research Institute.
Author

N91-11424# Messerschmitt-Boelkow-Blohm G.m.b.H., Munich (Germany, F.R.). Hubschrauber und Flugzeuge.
USE OF THE VP-200 COMPUTER FOR AEROTHERMODYNAMIC PROBLEMS
Luciano Fornasier 8 Dec. 1989 11 p Presented at International Workshop on Supercomputing Tools for Science and Engineering, Pisa, Italy, 4-7 Dec. 1989
(MBB/FE122/S/PUB/388; ETN-90-97848) Copyright Avail: NTIS HC/MF A03

The implementation and application of four aerodynamic flow solvers on the Siemens VP-200 vector processor is presented. The experience from all cases demonstrates the benefits of vector processing for aerodynamic codes characterized by very large computational effort. The high autovectorization level obtainable by the VP-200 allows optimal performance to be achieved with speedup factors between 20 to 30 while requiring very marginal code modifications. ESA

N91-10986# National Aerospace Lab., Amsterdam (Netherlands).
THE APPLICATION OF TRAJECTORY PREDICTION ALGORITHMS FOR PLANNING PURPOSES IN THE NETHERLANDS ATC-SYSTEM
J. N. P. Beers, T. B. Dalm, J. M. tenHave, and H. Visscher (Department of Civil Aviation, An Hoofddorp, Netherlands) *In* AGARD, Aircraft Trajectories: Computation, Prediction, Control, Volume 2: Air Traffic Handling and Ground-Based Guidance of Aircraft. Part 4: Air Traffic Handling. Part 5: Guidance of Aircraft in a Time-Based Constrained Environment. Part 6: May 1990 Previously announced as N89-20115 (For primary document see N91-10981 02-05)
Copyright Avail: NTIS HC/MF A20; Non-NATO Nationals requests available only from AGARD/Scientific Publications Executive

62 COMPUTER SYSTEMS

Includes computer networks and special application computer systems.

N91-11425*# Sterling Federal Systems, Inc., Palo Alto, CA.
OSI IN THE NASA SCIENCE INTERNET: AN ANALYSIS
Rebecca Nitzan Jun. 1990 58 p
(Contract NAS2-11555)
(NASA-CR-177561; A-90240; NAS 1.26:177561) Avail: NTIS HC/MF A04 CSCL 09B

The Open Systems Interconnection (OSI) protocol suite is a result of a world-wide effort to develop international standards for networking. OSI is formalized through the International Organization for Standardization (ISO) and the International Electrotechnical Commission (IEC). The goal of OSI is to provide interoperability between network products without relying on one particular vendor, and to do so on a multinational basis. The National Institute for Standards and Technology (NIST) has developed a Government OSI Profile (GOSIP) that specified a subset of the OSI protocols as a Federal Information Processing Standard (FIPS 146). GOSIP compatibility has been adopted as the direction for all U.S. government networks. OSI is extremely diverse, and therefore adherence to a profile will facilitate interoperability within OSI networks. All major computer vendors have indicated current or future support of GOSIP-compliant OSI protocols in their products. The NASA Science Internet (NSI) is an operational network, serving user requirements under NASA's Office of Space Science and Applications. NSI consists of the Space Physics Analysis Network (SPAN) that uses the DECnet protocols and the NASA Science Network (NSN) that uses TCP/IP protocols. The NSI Project Office is currently working on an OSI integration analysis and strategy. A long-term goal is to integrate SPAN and NSN into one unified network service, using a full OSI protocol suite, which will support the OSSA user community. Author

N91-11426# Center for Mathematics and Computer Science, Amsterdam (Netherlands). Dept. of Operations Research, Statistics, and System Theory.
PERFORMANCE ANALYSIS OF TRANSACTION DRIVEN COMPUTER SYSTEMS VIA QUEUEING ANALYSIS OF POLLING MODELS
Wim P. Groenendijk and Hanoch Levy (Tel-Aviv Univ., Israel) Dec. 1989 21 p Submitted for publication

(CWI-BS-R8931; ETN-90-97664) Copyright Avail: NTIS HC/MF A03

The modeling and analysis of a class of computer systems whose primary task is the massive processing of batch transactions and are called Transaction Driven Computer Systems (TDCS's) are addressed. A generic queueing model for TDCS's is presented and the mean sojourn time experienced by the different transactions is calculated. The approach is to model a TDCS by a cyclic polling system with bulk arrivals, deterministic service times, limited-1 service and zero switch-over periods. Since the performance analysis of this polling model has not been provided before, the study concentrates on deriving mean delay approximations for it. The analysis is carried out for models with general switch-over periods, and a special case of it (zero switch-over periods) is suitable for analyzing a TDCS. ESA

N91-11427# Center for Mathematics and Computer Science, Amsterdam (Netherlands). Dept. of Numerical Analysis.

A-STABLE PARALLEL BLOCK METHODS

B. P. Sommeijer, W. Couzy, and P. J. vanderHouwen Aug. 1989 12 p

(CWI-NM-R8918; ETN-90-97673) Copyright Avail: NTIS HC/MF A03

The stability of a class of block methods which are suitable for use on parallel computers is studied. A-stable methods of orders 3 and 4 and A(alpha)-stable methods with alpha greater than 89.9 degrees of order 5 are constructed. On multiprocessor computers these methods are of the same computational complexity as implicit linear multistep methods on one-processor computers. ESA

N91-11428# Center for Mathematics and Computer Science, Amsterdam (Netherlands). Dept. of Numerical Analysis.

ITERATED RUNGE-KUTTA METHODS ON PARALLEL COMPUTERS

P. J. vanderHouwen and B. P. Sommeijer Jan. 1990 29 p

(CWI-NM-R9001; ETN-90-97679) Copyright Avail: NTIS HC/MF A03

Diagonally implicit iteration methods for solving implicit Runge-Kutta methods with high stage order on parallel computers are studied. These iteration methods are such that after a finite number of m iterations, the iterated Runge-Kutta method belongs to the class of Diagonally Implicit Runge-Kutta methods (DIRK methods) using mk implicit stages where k is the number of stages of the generating implicit Runge-Kutta method (corrector method). However, a large number of the stages of this DIRK method can be computed in parallel, so that the number of stages that have to be computed sequentially is only m. The iteration parameters of the method are tuned in such a way as to get fast convergence to the stability characteristics of the corrector method. By means of numerical experiments it is shown that the solution produced by the resulting iteration method converges rapidly to the corrector solution so that both stability and accuracy characteristics are comparable with those of the corrector. This implies that the reduced accuracy often shown when integrating stiff problems by means of DIRK methods already available in the literature (which is caused by a low stage order), is not shown by the DIRK methods developed provided that the corrector method has a sufficiently high stage order. Moreover, by iterating e.g., Radau correctors, methods of any order can be constructed, whereas the order of accuracy of the conventionally constructed DIRK methods is limited to four. ESA

N91-11429# Technische Univ., Delft (Netherlands). Faculty of Technical Mathematics and Informatics.

A FAST PARALLEL RECOGNIZER

J. P. M. deVreught and H. J. Honig 1990 46 p

(Rept-90-16; ISSN-0922-5641; ETN-90-97711) Copyright Avail: NTIS HC/MF A03

Algorithms that can recognize a language described by a context free grammar are studied. The Gibbons and Rytter algorithm, which relies heavily on a pebble game theorem is given. A previous de Vreught and Honig time algorithm is recalled, and a fast parallel version is described by rephrasing the Gibbons and Rytter algorithm. When the grammar is acyclic it is possible to parse the language within O(log n) time and with Theta (n to the 6th power) processors. ESA

N91-11430*# Institute for Computer Applications in Science and Engineering, Hampton, VA.

PARALLELIZED RELIABILITY ESTIMATION OF RECONFIGURABLE COMPUTER NETWORKS Final Report

David M. Nicol, Subhendu Das (College of William and Mary, Williamsburg, VA.), and Dan Palumbo Sep. 1990 25 p Submitted for publication

(Contract NAS1-18605; NAG1-787; NAG1-1132; NSF ASC-88-19373)

(NASA-CR-182101; ICASE-90-60; NAS 1.26:182101) Avail: NTIS HC/MF A03 CSCL 09B

A parallelized system, ASSURE, for computing the reliability of embedded avionics flight control systems which are able to reconfigure themselves in the event of failure is described. ASSURE accepts a grammar that describes a reliability semi-Markov state-space. From this it creates a parallel program that simultaneously generates and analyzes the state-space, placing upper and lower bounds on the probability of system failure. ASSURE is implemented on a 32-node Intel iPSC/860, and has achieved high processor efficiencies on real problems. Through a combination of improved algorithms, exploitation of parallelism, and use of an advanced microprocessor architecture, ASSURE has reduced the execution time on substantial problems by a factor of one thousand over previous workstation implementations. Furthermore, ASSURE's parallel execution rate on the iPSC/860 is an order of magnitude faster than its serial execution rate on a Cray-2 supercomputer. While dynamic load balancing is necessary for ASSURE's good performance, it is needed only infrequently; the particular method of load balancing used does not substantially affect performance. Author

N91-11431# Oak Ridge National Lab., TN. Engineering Physics and Mathematics Div.

ON THE ADEQUACY OF MESSAGE-PASSING PARALLEL SUPERCOMPUTERS FOR SOLVING NEUTRON TRANSPORT PROBLEMS

Y. Y. Azmy 1990 8 p Presented at the Association for Computing Machinery/IEEE Supercomputing Conference, New York, NY, 12-16 Nov. 1990 Submitted for publication

(Contract DE-AC05-84OR-21400)

(DE90-016041; CONF-901121-6) Avail: NTIS HC/MF A02

A coarse-grained, static-scheduling parallelization of the standard iterative scheme used for solving the discrete-ordinates approximation of the neutron transport equation is described. The parallel algorithm is based on a decomposition of the angular domain along the discrete ordinates, thus naturally producing a set of completely uncoupled systems of equations in each iteration. Implementation of the parallel code on Intel's iPSC/2 hypercube, and solutions to test problems are presented as evidence of the high speedup and efficiency of the parallel code. The performance of the parallel code on the iPSC/2 is analyzed, and a model for the CPU time as a function of the problem size (order of angular quadrature) and the number of participating processors is developed and validated against measured CPU times. The performance model is used to speculate on the potential of massively parallel computers for significantly speeding up real-life transport calculations at acceptable efficiencies. We conclude that parallel computers with a few hundred processors are capable of producing large speedups at very high efficiencies in very large three-dimensional problems. DOE

63 CYBERNETICS

Includes feedback and control theory, artificial intelligence, robotics and expert systems.

For related information see also *54 Man/System Technology and Life Support.*

N91-11432*# Martin Marietta Corp., Denver, CO. Astronautics Group.
INTELLIGENT ROBOTIC SYSTEMS STUDY (IRSS), PHASE 2 Final Report
May 1990 44 p
(Contract NAS8-36431)
(NASA-CR-183963; NAS 1.26:183963; MCR-89-559) Avail: NTIS HC/MF A03 CSCL 09B

Under the Intelligent Robotics System Study (IRSS) contract, a generalized robotic control architecture was developed for use with the ProtoFlight Manipulator Arm (PFMA). The controller built for the PFMA provides localized position based force control, teleoperation and advanced path recording and playback capabilities. Various hand controllers can be used with the system in conjunction with a synthetic time delay capability to provide a realistic test bed for typical satellite servicing tasks. The configuration of the IRSS system is illustrated and discussed. The PFMA has six computer controllable degrees of freedom (DOF) plus a seventh manually indexable DOF, making the manipulator a pseudo 7 DOF mechanism. Because the PFMA was not developed to operate in a gravity field, but rather in space, it is counter balanced at the shoulder, elbow and wrist and a spring counterbalance has been added near the wrist to provide additional support. Built with long slender intra-joint linkages, the PFMA has a workspace nearly 2 meters deep and possesses sufficient dexterity to perform numerous satellite servicing tasks. The manipulator is arranged in a shoulder-yaw, pitch, elbow-pitch, and wrist-pitch, yaw, roll configuration, with an indexable shoulder roll joint. Digital control of the PFMA is implemented using a variety of single board computers developed by Heurikon Corporation and other manufacturers. The IRSS controller is designed to be a multi-rate, multi-tasking system. Independent joint servos run at a 134 Hz rate and position based impedance control functions at 67 Hz. Autonomous path generation and hand controller inputs are processed at a 33 Hz. Author

N91-11433 California Univ., Los Angeles.
CONSTRAINED OPTIMIZATION APPROACH TO FEEDBACK CONTROL OF STATE-AUGMENTED SYSTEMS Ph.D. Thesis
Won-Zon Chen 1990 124 p
Avail: Univ. Microfilms Order No. DA9022003

The Linear/Quadratic (LQ) optimal control theory, introduced by Kalman, has attracted much attention due to the guaranteed control optimality with respect to a quadratic performance measure, and its inherent capability to handle Multiple-Input-Multiple Output (MIMO) systems. The LQ design process can be automated through an array of analytical procedures, greatly easing the design efforts. However, unsatisfactory performance and lack of robustness were experienced with the LQ design method. Numerous methods have been proposed in the past attempting to solve either the performance and/or the robustness problems of LQ optimal control theory. A method that combines the merits of time-domain and frequency-domain techniques for designing feedback control systems is studied. The approach involves the use of state augmentation to introduce dynamic compensators for performance enhancement first and, then, optimize a quadratic cost functional with the constraint of minimum multivariable stability margins. This robustness constrained optimization of quadratic performance measure approach is direct and matches well with the formulation and design objectives of real-life design problems. Multivariable examples of designing aircraft flight control laws with state feedback and output feedback are included to illustrate and demonstrate the effectiveness of the approach. The subject of how to augment the state of a dynamic system for performance enhancement is also examined from the standpoint of controllability, feedback equivalence, and minimum order. Dissert. Abstr.

N91-11434# Oak Ridge National Lab., TN. Engineering Physics and Mathematics Div.
A UNIFIED FRAMEWORK FOR CREDIT ASSIGNMENT
Gunar E. Liepins and Richard S. Sutton (GTE Labs., Inc., Waltham, MA.) 1990 6 p Presented at the IEEE Conference on Neural Information Processing: Natural and Synthetic, Denver, CO, 26-29 Nov. 1990
(Contract DE-AC05-84OR-21400)
(DE90-011636; CONF-901150-1) Avail: NTIS HC/MF A02

Credit assignment is a central issue in a variety of connectionist paradigms including artificial neural networks and genetic classifier systems. For neural networks, credit assignment is implicit in the training algorithms used to update connection weights. In classifier systems, it is used to estimate rule strengths. This paper introduces a unifying framework that covers and helps explain the differences and similarities between a large number of approaches to credit assignment, including Q-learning, policy iteration, bucket brigade and profit sharing. Each of these can be formulated as a version of the Adaptive Heuristic Critic (AHC). DOE

N91-10929# Deutsche Forschungsanstalt fuer Luft- und Raumfahrt, Goettingen (Germany, F.R.). Inst. fuer Aeroelastik.
ADAPTIVE DIGITAL REAL TIME FILTERING IN STRUCTURAL DYNAMICS: A CONTRIBUTION TO THE REALIZATION ON ACTIVELY REACTING ELASTIC STRUCTURES (ARES) [ADAPTIVE DIGITALE ECHTZEITFILTERUNG IN DER STRUKTURDYNAMIK: EIN BEITRAG ZUR REALISIERUNG AKTIV REAGIERENDER ELASTISCHER STRUKTUREN (ARES)]
Roger Wimmel and Joerg Melcher *In its* Contributions in the Field of Aeroelastics on the Occasion of the 60th Anniversary of Professor Dr.-Ing. Habil. Hans Wilhelm Foersching Apr. 1990 p 187-202 In GERMAN; ENGLISH summary (For primary document see N91-10920 02-02)
Avail: NTIS HC/MF A13

64 NUMERICAL ANALYSIS

Includes iteration, difference equations, and numerical approximation.

N91-11435# National Inst. of Standards and Technology, Gaithersburg, MD. Applied and Computational Mathematics Div.
EXPECTED COMPLEXITY OF THE 3-DIMENSIONAL VORONOI DIAGRAM
J. Bernal May 1990 21 p
(PB90-221862; NISTIR-4321) Avail: NTIS HC/MF A03 CSCL 12A

Let S be a set of n sites chosen independently from a uniform distribution in a cube in 3-D Euclidean space. Work by Bently, Weide, and Yao is extended to show that the Voronoi diagram for S has an expected O(n) number of faces. A consequence of the proof of this result is that the Voronoi diagram for S can be constructed in expected (9n) time. Author

N91-11436# National Inst. of Standards and Technology, Gaithersburg, MD. Applied and Computational Mathematics Div.
EXPECTED LINEAR 3-DIMENSIONAL VORONOI DIAGRAM ALGORITHM
J. Bernal Jun. 1990 17 p
(PB90-227984; NISTIR-4340) Avail: NTIS HC/MF A03 CSCL 12A

Let S be a set of n sites chosen independently from a uniform distribution in a cube in 3-D Euclidean space. An expected O(n) algorithm for constructing the Voronoi diagram for S together with numerical results obtained from an implementation of the algorithm are presented. Author

N91-11437# National Inst. of Standards and Technology, Gaithersburg, MD. Center for Radiation Research.
EVALUATION OF THE INTEGRAL

L. C. Maximon Jun. 1990 30 p
(PB90-235011; NISTIR-4355) Avail: NTIS HC/MF A03 CSCL 12A

The integral I (sub l,l')(k,K') = integral from 0 to infinity (j sub l)(kr)(j sub l')(k'r) squared dr, in which the spherical Bessel functions (j sub l)(kr) are the radial eigenfunctions of the 3-D wave equation in spherical coordinates, is evaluated in terms of distribution, in particular step functions and delta functions. It is shown that the behavior of I (sub l,l') is very different in the cases l-l' even (0, + or -2, + or -4,...) and l-l' odd (+ or -1, + or -3,...). For l-l' even, it is expressed in terms of the delta function, step function, and Legendre polynomials. For l-l' odd, it is expressed in terms of Legendre functions of the second kind and step functions; no delta functions appear. Author

N91-11438# Center for Mathematics and Computer Science, Amsterdam (Netherlands). Dept. of Analysis, Algebra, and Geometry.

APPROXIMATION OF THE SOLUTION TO THE MOMENT PROBLEM IN A HILBERT SPACE

M. Zwaan Dec. 1989 13 p
(CWI-AM-R8923; ETN-90-97653) Copyright Avail: NTIS HC/MF A03

A construction of the solution to a moment problem was obtained. The results are used to derive a truncation error for sinc-interpolation, which generalizes the error bounds in the literature to the case of nonuniform sampling. The space of bandlimited functions, those functions whose Fourier transforms have compact support, is introduced. ESA

N91-11439# Center for Mathematics and Computer Science, Amsterdam (Netherlands). Dept. of Analysis, Algebra, and Geometry.

MATHEMATICAL MORPHOLOGY ON HOMOGENEOUS SPACES. PART 1: THE SIMPLY TRANSITIVE CASE

J. B. T. M. Roerdink Dec. 1989 25 p
(CWI-AM-R8924-Pt-1; ETN-90-97654) Copyright Avail: NTIS HC/MF A03

A generalization of mathematical morphology by dropping the assumption that the invariance group is commutative is studied. To this end an arbitrary homogeneous space, a set on which a transitive but not necessarily commutative group of invertible transformations is defined, and considered. As the object space, the Boolean algebra of all subsets of this homogeneous space is taken. The case that the transformation group is simply transitive, or equivalently, that the basic set is itself a group, is considered. For clarity of exposition as well to emphasize the connection with classical Euclidean morphology, the study was restricted to the case of Boolean lattices, which is appropriate for binary image transformations. ESA

N91-11440# Center for Mathematics and Computer Science, Amsterdam (Netherlands). Dept. of Analysis, Algebra, and Geometry.

UNIFORM ASYMPTOTIC APPROXIMATION OF FERMI-DIRAC INTEGRALS

N. M. Temme and A. B. Olde Daalhuis Jan. 1990 9 p
(CWI-AM-R9001; ETN-90-97655) Copyright Avail: NTIS HC/MF A02

A given Fermi-Dirac integral is considered for large positive values of x and q. The results are obtained from a contour integral in the complex plane. The approximation contains a finite sum of simple terms, an incomplete gamma function, and an infinite asymptotic series. As follows from earlier results, the incomplete gamma function can be approximated in terms of an error function. ESA

N91-11441# Center for Mathematics and Computer Science, Amsterdam (Netherlands). Dept. of Analysis, Algebra, and Geometry.

DYNAMIC MRI RECONSTRUCTION AS A MOMENT PROBLEM. PART 3: AN ERROR ANALYSIS OF RECONSTRUCTION BY SINC AND SPLINE INTERPOLATION IN A HILBERT SPACE SETTING

M. Zwaan Jan. 1990 22 p
(CWI-AM-R9002-Pt-3; ETN-90-97656) Copyright Avail: NTIS HC/MF A03

A solution and an error analysis of a reconstruction problem that appears in Magnetic Resonance Imaging (MRI), which is a diagnostic technique to measure and display cross sections of human organs is given. The reconstruction problem is solved in the setting of L squared-spaces of vector valued functions. After obtaining the solution, error estimates are proved and the solution is shown to be stable for perturbation of the data and of the time markers. ESA

N91-11442# Center for Mathematics and Computer Science, Amsterdam (Netherlands). Dept. of Analysis, Algebra, and Geometry.

GREY-LEVEL MORPHOLOGY

H. J. A. M. Heijmans Jan. 1990 31 p
(CWI-AM-R9003; ETN-90-97657) Copyright Avail: NTIS HC/MF A03

A detailed study of morphological operators on the space of grey-level functions is presented. It is shown how classical morphological operators for binary images can be extended to the space of grey-level images. Particular attention is given to the class of so-called flat operators, i.e., operators which commute with thresholding. It is also shown how to define dilations and erosions with non-flat structuring elements if the grey-level set is finite. ESA

N91-11443# Center for Mathematics and Computer Science, Amsterdam (Netherlands). Dept. of Operations Research, Statistics, and System Theory.

ON THE UNIQUENESS OF KERNELS

A. Schrijver Oct. 1989 17 p
(CWI-BS-R8924; ETN-90-97658) Copyright Avail: NTIS HC/MF A03

The case where S is a compact orientable surface is studied. For any graph G embedded on S and any closed curve D on S, (mu sub G)(D) is defined as the minimum number of intersections of G and D', where D' ranges over all closed curves freely homotopic to D. G is called a kernel if (mu sub G') does not equal (mu sub G) for each proper minor G' of G. It is proved that if G and G' are kernels with (mu sub G) equal to (mu sub G'), then G' can be obtained from G by a series of the following operations: homotopic shifts over S; taking the surface dual graph; replacing a vertex v of degree 3 by a triangle connecting the three vertices adjacent to v, or conversely. ESA

N91-11444# Center for Mathematics and Computer Science, Amsterdam (Netherlands). Dept. of Operations Research, Statistics, and System Theory.

CONES OF MATRICES AND SETFUNCTIONS, AND 0-1 OPTIMIZATION

L. Lovasz (Eoetvoes Lorand Univ., Budapest, Hungary) and A. Schrijver Oct. 1989 38 p
(CWI-BS-R8925; ETN-90-97659) Copyright Avail: NTIS HC/MF A03

It has been recognized that to represent a polyhedron as the projection of a higher dimensional, but simpler, polyhedron, is a powerful tool in polyhedral combinatorics. A general method to construct higher dimensional polyhedra (or, in some cases convex sets) whose the projection approximates the convex hull of 0-1 valued solutions of a system of linear inequalities is developed. An important feature of these approximations is that any linear objective function can be optimized over them in polynomial time. In the special case of the vertex packing polytope, a sequence of systems of inequalities, such that already the first system includes

clique, odd hole, odd antihole, wheel, and orthogonality constraints is obtained. In particular, for perfect (and many other) graphs, this first system gives the vertex packing polytope. For various classes of graphs, including t-perfect graphs, it follows that the stable set polytope is the projection of a polytope with a polynomial number of facets. An extension of the method, which establishes a connection with certain submodular functions and the Moebius function of a lattice, is discussed. ESA

N91-11445# Center for Mathematics and Computer Science, Amsterdam (Netherlands). Dept. of Operations Research, Statistics, and System Theory.
ON SLLN FOR MARTINGALES WITH DETERMINISTIC QUADRATIC VARIATION
Kacha O. Dzhaparidze and Peter J. C. Spreij (Vrije Univ., Amsterdam, Netherlands) Dec. 1989 15 p
(CWI-BS-R8933; ETN-90-97666) Copyright Avail: NTIS HC/MF A03

The Strong Law of Large Numbers (SLLN) is proved for multivariate martingales with deterministic quadratic variation, along the same lines as in Lai, Wei and Robbins (1979), though the setting here is more general. The problem still has a relatively simple solution under the restriction that the quadratic variation process of the multivariate martingale in question is deterministic. ESA

N91-11446# Center for Mathematics and Computer Science, Amsterdam (Netherlands). Dept. of Operations Research, Statistics, and System Theory.
MINIMALITY OF DESCRIPTOR REPRESENTATIONS UNDER EXTERNAL EQUIVALENCE
M. Kuijper and J. M. Schumacher (Tilburg Univ., Netherlands) Feb. 1990 18 p Submitted for publication
(CWI-BS-R9002; ETN-90-97669) Copyright Avail: NTIS HC/MF A03

Necessary and sufficient conditions are derived for the minimality of descriptor representations under external equivalence. These conditions are stated completely in terms of the matrices E, A, B, C, and D. Use is made of the close connection between the descriptor representation and the so-called pencil representation. This connection is further exploited to derive the transformation group for minimal descriptor representations. The transformations are shown to coincide with the operations of strong equivalence as introduced by Verghese et al. ESA

N91-11447# Center for Mathematics and Computer Science, Amsterdam (Netherlands). Dept. of Numerical Analysis.
A NEW LOWER BOUND FOR THE DE BRUIJN-NEWMAN CONSTANT
H. J. J. teRiele Sep. 1989 11 p Submitted for publication
(CWI-NM-R8920; ETN-90-97674) Copyright Avail: NTIS HC/MF A03

A new lower bound, minus 5, is presented for the so-called de Bruijn-Newman constant. This constant is related to the Riemann hypothesis. The new bound is established by the high precision computation (with an accuracy of 250 decimal digits) of the coefficients of a so-called Jensen polynomial of degree 406, and the so-called Sturm sequence of this polynomial which shows that it has two complex zeros. These complex zeros are given explicitly. ESA

N91-11448# Center for Mathematics and Computer Science, Amsterdam (Netherlands). Dept. of Numerical Analysis.
IMPROVED TECHNIQUES FOR LOWER BOUNDS FOR ODD PERFECT NUMBERS
R. P. Brent, G. Cohen (Sydney Univ., Australia), and H. J. J. teRiele Oct. 1989 16 p Submitted for publication
(CWI-NM-R8921; ETN-90-97675) Copyright Avail: NTIS HC/MF A03

If N is an odd perfect number and q to the power K parallel verticle lines N, q prime, k even, then it is almost immediate that N is greater than q to the power (2k). Subject to certain conditions verifiable in polynomial time, it is proved that in fact N is greater than q to the power (5k/2). Using this and related results, the computations are extended to earlier work to show that N is greater than 10 to 300th power. ESA

N91-11449# Center for Mathematics and Computer Science, Amsterdam (Netherlands). Dept. of Numerical Analysis.
A STATIC-REGRIDDING METHOD FOR TWO-DIMENSIONAL PARABOLIC PARTIAL DIFFERENTIAL EQUATIONS
R. A. Trompert and J. G. Verwer Dec. 1989 30 p Submitted for publication
(CWI-NM-R8923; ETN-90-97677) Copyright Avail: NTIS HC/MF A03

The field of numerical solution of time dependent partial differential equations is addressed. Attention is focussed on parabolic problems in two space dimensions the solutions of which possess sharp moving transitions in space and time, such as steep moving fronts and emerging and disappearing layers. For such problems, a space grid held fixed throughout the entire calculation can be computationally inefficient, since, to afford an accurate approximation, such a grid would easily have to contain a very large number of nodes. A static-regridding method that adapts the space grid using nested, locally uniform grids, is considered. Several aspects occurring in such a static-regridding algorithm, such as the data structure, the regridding strategy and the determination of initial and boundary conditions at coarse-fine grid interfaces are discussed. Two numerical examples to demonstrate the performance of the method are presented: a hypothetical example to illustrate the convergence behavior of the method and an example originating from practice which describes a model combustion process. ESA

N91-11450# Center for Mathematics and Computer Science, Amsterdam (Netherlands). Dept. of Numerical Analysis.
CONVERGENCE OF LINEAR MULTISTEP AND ONE-LEG METHODS FOR STIFF NONLINEAR INITIAL VALUE PROBLEMS
W. H. Hundsdorfer and B. I. Steininger (Gehrenbergstrasse, Markdorf, Germany, F.R.) Dec. 1989 20 p
(CWI-NM-R8924; CWI-NM-R8911; ETN-90-97678) Copyright Avail: NTIS HC/MF A03

To prove convergence of numerical methods for stiff initial value problems, stability is needed but also estimates for the local errors which are not affected by stiffness. Global error bounds are derived for one-leg and linear multistep methods applied to classes of arbitrarily stiff, nonlinear initial value problems. It is shown that under suitable stability assumptions the multistep methods are convergent for stiff problems with the same order of convergence as for nonstiff problems, provided that the stepsize variation is sufficiently regular. ESA

N91-11451# Center for Mathematics and Computer Science, Amsterdam (Netherlands). Dept. of Numerical Analysis.
THE LINEARLY IMPLICIT EULER METHOD FOR QUASI-LINEAR PARABOLIC DIFFERENTIAL EQUATIONS
K. Strehmel, W. H. Hundsdorfer, R. Weiner, and A. Arnold (Martin Luther-Univ., Halle-Wittenberg, German D.R.) Feb. 1990 24 p Submitted for publication
(CWI-NM-R9002; ETN-90-97680) Copyright Avail: NTIS HC/MF A03

Following the method of lines approach, parabolic problems discretized in space by any usual method are discretized in time by the linearly implicit Euler method. To avoid order reduction occurring for problems with time dependent boundary conditions, a modification of the method is proposed. This modified method is proved to be of uniform (independently of the space discretization) order 1 of convergence for wide classes of semilinear and quasilinear problems. ESA

N91-11452# Technische Univ., Delft (Netherlands). Faculty of Technical Mathematics and Informatics.
CONNECTED COMPONENTS IN SUPERCRITICAL MANDELBROT PERCOLATION

Ronald W. J. Meester 1990 26 p
(Rept-90-15; ISSN-0922-5641; ETN-90-97710) Copyright Avail: NTIS HC/MF A03

The limiting set of the supercritical Mandelbrot percolation process is investigated. It is shown that the number of components which intersect the left and the right side of the unit square is finite a.s. Other components in the limiting set are studied. An alternative definition of percolation which involves arc-wise connectedness rather than connectedness is introduced. It is shown that this new concept of percolation is equivalent to the classical one. ESA

N91-11453# Technische Univ., Delft (Netherlands). Faculty of Technical Mathematics and Informatics.
A POLYNOMIAL METHOD OF WEIGHTED CENTERS FOR CONVEX QUADRATIC PROGRAMMING
D. denHertog, C. Roos, and T. Terlaky 1990 23 p
(Rept-90-17; ISSN-0922-5641; ETN-90-97712) Copyright Avail: NTIS HC/MF A03

A generalization of the weighted central path following method for convex quadratic programming is presented. This is done by uniting and modifying the main ideas of the weighted central path following method for linear programming and the interior point methods for convex quadratic programming. By means of linear approximation of the weighted logarithmic barrier function and weighted inscribed ellipsoids, 'weighted' trajectories are defined. Each strictly feasible primal dual point pair define such a weighted trajectory. The algorithm can start in any strictly feasible point that defines a weighted trajectory which is followed through the algorithm. This algorithm has the nice feature, that is not necessary to start the algorithm close to the central path and so additional transformations are not needed. Polynomiality is proved under the usual mild conditions. ESA

N91-11454# Technische Univ., Delft (Netherlands). Faculty of Technical Mathematics and Informatics.
A COMPARISON OF SOME GMRES-LIKE METHODS
C. Vuik 1990 35 p
(Rept-90-22; ISSN-0922-5641; ETN-90-97715) Copyright Avail: NTIS HC/MF A03

GMRES and CGS are well known iterative methods for the solution of certain sparse linear systems with a nonsymmetric matrix. These methods were compared experimentally in many studies and specific observations on the convergence behavior of GMRES was reported. An iterative method to solve a nonsymmetric system which was previously proposed is investigated and compared with GMRES. Problems for which this method is more efficient than GMRES are seen. But the method has as drawbacks in that it is not scaling invariant and in that it may suffer from numerical instability. A method proposed by Broyden seems to be somehow related to the new method and is therefore included in the comparison. ESA

N91-11455# Technische Univ., Delft (Netherlands). Faculty of Technical Mathematics and Informatics.
QUADRATIC SYSTEMS EQUIVALENT TO CLASS 3 SUB A NOT EQUAL TO 0
Andre Zegeling 1990 34 p
(Rept-90-38; ISSN-0922-5641; ETN-90-97719) Copyright Avail: NTIS HC/MF A03

The intersections of the three classes of quadratic systems developed by Chinese mathematicians are considered. Especially the intersection of other classes with class 3 sub(a not equal to 0) is discussed. The latter being the most promising class for finding the maximum number of limit cycles in quadratic systems, as asked for in Hilbert's sixteenth problem. The method is based on a transformation of straight line isoclines onto the coordinate axes. As a natural consequence the number, character and relative position of finite critical points are found. Bifurcation curves for critical points at infinity and the construction of rotated vector fields are described to illuminate the advantages of the method. ESA

N91-11456# Groningen Rijksuniv. (Netherlands). Dept. of Mathematics.
A SYNTHESIS OF TIME AND FREQUENCY DOMAIN METHODS FOR THE CONTROL OF INFINITE-DIMENSIONAL SYSTEMS: A SYSTEM THEORETIC APPROACH Final Report, Sep. 1989
Ruth F. Curtain 1989 78 p Submitted for publication Sponsored in part by Netherlands Foundation for Technical Research
(Contract ST2J-0066-3-NL(CD))
(W-8912; ETN-90-97721) Avail: NTIS HC/MF A05

An attempt to show how a system theoretic approach can lead to an integrated time and frequency domain treatment of control problems for infinite dimensional linear systems is made. The Callier-Desoer class of transfer matrices and the Pritchard-Salamon class of state-space systems are considered. The synthesis approach is used to solve two different robustness problems. ESA

N91-11457# Groningen Rijksuniv. (Netherlands). Dept. of Mathematics.
THE RELATION BETWEEN KNOWLEDGE AND HEURISTIC METHODS
A. vanStreun 1990 28 p
(W-9001; ETN-90-97722) Avail: NTIS HC/MF A03

Research on the first year students attempt to solve problems in the first stages of training in calculus is focused chiefly on the relation between knowledge and heuristic methods. The questions of whether an inadequate command of the concepts and characteristics of the specific subject is the main cause of failure to solve new problems and whether the approach to problem solving is so inadequate that success in coping with new problems is impossible are asked. The role of heuristics in the procedures unsuccessful novices, successful novices and experts follow in solving problems is considered. ESA

N91-11458# Groningen Rijksuniv. (Netherlands). Dept. of Mathematics.
ASYMPTOTIC BEHAVIOR OF LAGUERRE POLYNOMIALS WITH Re z LESS THAN 0 DERIVED BY THE CENTRAL LIMIT THEOREM
A. J. Stam 1990 19 p
(W-9004; ETN-90-97723) Avail: NTIS HC/MF A03

The asymptotic behavior of Laguerre polynomials is derived. The central limit theorem is applied for sums of independant integer valued random variable without a probability interpretation. ESA

N91-11459# Groningen Rijksuniv. (Netherlands). Dept. of Mathematics.
QUASI-PERIODIC BIFURCATIONS, APPLICATIONS
H. W. Broer 1989 22 p
(TW-8911; ETN-90-97724) Avail: NTIS HC/MF A03

Dissipative family of vector fields (ordinary differential equations) are considered, having quasi-periodic invariant tori in a way that is persistent for small perturbations. When the normal hyperbolicity vanishes bifurcations may occur, more or less similar to what happens in the periodic case. Examples are given in the context of oscillators with quasi-periodic forcing. ESA

N91-11460# Groningen Rijksuniv. (Netherlands). Dept. of Mathematics.
ON INDUCED CONGRUENCES
Roland Backhouse and Grant Malcom 1990 11 p
(CS-9001; ETN-90-97725) Avail: NTIS HC/MF A03

A proof of a theorem to be found in Ehrig and Mahr is given. The theorem states that a relation constructed from a given function is a congruence relation if that function is a homomorphisms; this result is generalized to relational homomorphisms previously studied. Specifically, a congruence relation is proved to be constructable from a relational homomorphism. The construction generalizes that of Ehrig and Mahr. The significance of the study lies both in the economy of the calculations and in the novel use made of weakest pre-specifications. ESA

N91-11461# Groningen Rijksuniv. (Netherlands). Dept. of Computer Science.
HIGH-ORDER IMPLICIT BLENDING SURFACES OF LOW DEGREE
Menno Kosters 1990 26 p
(CS-9005; ETN-90-97726) Avail: NTIS HC/MF A03

The applicability of the so-called potential method for blending implicitly defined surfaces is extended. The extended method is able to produce blendings which are C to the power k-continuous, where k may be chosen arbitrarily large. The blendings consist of piecewise algebraic surfaces of low degree. Specifically, the degree is k+1 for so-called convex corners, and 2k for an important class of non-convex corners. The method is illustrated by a concrete example, where a C squared blending surface of degree 4 is constructed for a certain non-convex corner. ESA

N91-11462# Grenoble Univ. (France). Lab. de Technique de l'Informatique, de la Microelectronique et de la Microscopie Quantitative.
MATHEMATICAL MODELS OF MIXTURE PROPERTIES: B-SPLINES AND OPTIMIZATION WITH FORM CONDITIONS Ph.D. Thesis [MODELISATION MATHEMATIQUE DES PROPRIETES DE MELANGE: B-SPLINES ET OPTIMISATION AVEC CONDITIONS DE FORME]
Nabih Odeh 1990 171 p In FRENCH; ENGLISH summary
(ETN-90-97829) Avail: NTIS HC/MF A08

A contribution to the numerical resolution of some problems arising in the study of oil separation is presented. Complex mixtures and simple mixtures are investigated. The performed study, of different problems of mixing management, led to implement an interactive and visual software and many experimental programs. ESA

N91-11463# Technische Univ., Berlin (Germany, F.R.). Fachbereich fuer Verkehrswesen.
METHODS FOR THE CONSTRUCTION OF CONSTANT CURVE FREE FORM SURFACES Ph.D. Thesis [METHODEN ZUR KONSTRUKTION KRUEMMUNGSSTETIGER FREIFORMFLAECHEN]
Joerg Weber 1990 141 p In GERMAN
(ETN-90-97861) Avail: NTIS HC/MF A07

A method for the optimization of the curve parametrization, based on the definition of geometric parameter continuity is described. For this method, it is shown how the unknown values are determined through placing the variation of function in a scalar and vectorial portion, by which a global linear equation system for the vectorial unknown values and a local nonlinear one for the scalar unknown values is developed. Similar to the curves, three different concepts are presented for surface continuity. It is also demonstrated how second order surfaces can be built, using the sweeping process. ESA

N91-11464# National Inst. of Standards and Technology, Gaithersburg, MD. Statistical Engineering Div.
MATHEMATICAL TREATMENT OF THE SPHERICAL STEREOLOGY
C. Hagwood Jul. 1990 22 p
(PB90-257593; NISTIR-4370) Avail: NTIS HC/MF A03 CSCL 12A

Stereology is the study of 3-dimensional particles based on their two dimensional cross-sections. The particles studied are assumed to be spheres with a random radii distribution. The mathematical aspects of this type of stereology are considered. GRA

N91-11465# Los Alamos National Lab., NM.
RANDOM NUMBER STRIDE IN MONTE CARLO CALCULATIONS
John S. Hendricks 1990 7 p Presented at the American Nuclear Society Winter Meeting, Washington, DC, 11-15 Nov. 1990 Submitted for publication
(Contract W-7405-eng-36)
(DE90-012000; LA-UR-90-1845; CONF-901101-4) Avail: NTIS HC/MF A02

Monte Carlo radiation transport codes use a sequence of pseudorandom numbers to sample from probability distributions. A common practice is to start each source particle a predetermined number of random numbers up the pseudorandom number sequence. This number of random numbers skipped between each source particles the random number stride, S. Consequently, the jth source particle always starts with the j x Sth random number providing correlated sampling between similar calculations. A new machine-portable random number generator was written for the Monte Carlo radiation transport code MCNP providing user's control of the random number stride. First the new MCNP random number generator algorithm is described and then the effects of varying the stride are presented. DOE

N91-11466# Los Alamos National Lab., NM. Computing and Communications Div.
A MONTE CARLO BOUNDARY PROPAGATION METHOD FOR THE SOLUTION OF POISSON'S EQUATION
Robert Hiromoto and Ralph G. Brickner 1990 6 p Presented at the American Nuclear Society Winter Meeting, Washington, DC, 11-15 Nov. 1990
(Contract W-7405-eng-36)
(DE90-015060; LA-UR-90-2577; CONF-901101-22) Avail: NTIS HC/MF A02

Too often the parallelism of a computational algorithm is used (or advertised) as a desirable measure of its performance. That is, the higher the computational parallelism the better the expected performance. With the current interest and emphasis on massively parallel computer systems, the notion of highly parallel algorithms is the subject of many conferences and funding proposals. Unfortunately, the revolution that this vision promises has served to further complicate the measure of parallel performance by the introduction of such notions as scaled speedup and scalable systems. As a counter example to the merits of highly parallel algorithms whose parallelism scales linearly with increasing problem size, a slight modification to a highly parallel Monte Carlo technique that is used to estimate the solution of Poisson's equation is introduced. This simple modification is shown to yield a much better estimate to the solution by incorporating a more efficient use of boundary data (Dirichlet boundary conditions). A by product of this new algorithm is a much more efficient sequential algorithm but at the expense of sacrificing parallelism. DOE

N91-11467# Oak Ridge National Lab., TN. Mathematical Sciences Section.
MODELING HISTOGRAM DATA WITH PIECEWISE POLYNOMIALS
Patrick H. Worley Aug. 1990 37 p
(Contract DE-AC05-84OR-21400)
(DE90-018037; ORNL/TM-11637) Avail: NTIS HC/MF A03

As part of a research project on the performance characterization of parallel programs, piecewise polynomials are used to model histogram data that represents the processor utilization curve. In this paper an algorithm is described that generates a discontinuous piecewise polynomial model in time proportional to the amount of data. DOE

N91-11468# Universiteit Twente, Enschede (Netherlands). Faculty of Applied Mathematics.
DECOMPOSITION OF THE n-CUBE INTO PATHS
Hans-Joachim Walther (Technische Hochschule, Ilmenau, German D.R.) May 1990 12 p
(MEMO-855; ISSN-0169-2690; ETN-90-97741) Avail: NTIS HC/MF A03

Minimum path decompositions of the edges of the n-cube (Q sub n) are studied. A conjecture of the Strassburger is answered. ESA

N91-11469# Universiteit Twente, Enschede (Netherlands). Faculty of Applied Mathematics.
INTERPOLATION OF SCATTERED DATA BY A BIVARIATE CONVEX FUNCTION. PART 1: PIECEWISE LINEAR C SUP 0-INTERPOLATION
Bernd Mulansky (Technische Univ., Dresden, German D.R.) May 1990 31 p
(MEMO-858-Pt-1; ISSN-0169-2690; ETN-90-97744) Avail: NTIS HC/MF A03

The problem of interpolation of scattered data by a bivariate continuous convex function is considered. The existence of such an interpolant is equivalent to the existence of a suitable triangulation of the data sites, where the corresponding piecewise linear interpolant is convex. In addition, the problem of convex interpolation with prescribed subgradients is studied and compatible subgradients are characterized. Two algorithms for the generation of a suitable (convex) triangulation are presented and justified. It is shown how the results fit into the recent considerations of data dependent triangulations. Some numerical experiments concerning convex triangulations are reported. ESA

N91-11470# Universiteit Twente, Enschede (Netherlands). Faculty of Applied Mathematics.
ON DOMINATING AND SPANNING CIRCUITS IN GRAPHS
H. J. Veldman May 1990 16 p
(MEMO-859; ISSN-0169-2690; ETN-90-97745) Avail: NTIS HC/MF A03

Gatlin's reduction technique to obtain a result which contains several known and new sufficient conditions for a graph to have a spanning or dominating circuit in terms of degree sums of adjacent vertices is refined. In particular, the result implies the truth of the following conjecture of Benhocine et al.: if G is a connected simple graph in order n such that every cut edge of G is incident with a vertex of degree 1 and d(u) + d(v) is greater than 2(n/5 - 1) for every edge uv of G, then, for n sufficiently large, L(G) is Hamiltonian. ESA

N91-11471# Joint Inst. for Nuclear Research, Dubna (USSR). Lab. of Computing Techniques and Automation.
ASYMPTOTIC ESTIMATES OF APPROXIMATION ERRORS BY THE GALERKIN METHOD FOR ONE CLASS OF QUASIPOTENTIAL EQUATIONS
E. P. Zhidkov, B. N. Khoromskij, and Eh. G. Nikonov (Academy of Pedagogical Sciences of the USSR, Moscow.) 1989 14 p In RUSSIAN; ENGLISH summary
(DE90-631600; JINR-R-11-89-191) Avail: NTIS (US Sales Only) HC/MF A03

In eigenvalue problem for one class of quasipotential integral equations the approximation error estimates by Galerkin's method were obtained. For completely continuous integral operators the conditions were obtained when numerical solution error of eigenvalue problem is presented as a series over parameter r(sup -1), where r is the length of discretization interval for operator determined on a semiaxis. DOE

N91-11472# Joint Inst. for Nuclear Research, Dubna (USSR). Lab. of Computing Techniques and Automation.
SEARCHING SPECTRUM POINTS OF DIFFERENCE INITIAL-BOUNDARY VALUE PROBLEMS WITH USING CAS
N. E. Mazepa 1989 12 p In RUSSIAN; ENGLISH summary
(DE90-634382; JINR-R-11-89-382) Avail: NTIS (US Sales Only) HC/MF A03

A new algorithm for searching spectrum points is proposed. The difference schemes which approximate systems of linear differential equations of hyperbolic type with constant coefficients and in one space dimension are considered. For important class of practicias problems this algorithm reduces the hard spectrum calculation problem to the polynomial equation solution. For complicated analytic manipulations connected with realization of this algorithm the computation algebraic system REDUCE is used. DOE

N91-11473# European Space Agency, Paris (France).
SOLUTION OF THE TWO-DIMENSIONAL EULER EQUATIONS BY A FINITE VOLUME DISCRETIZATION ON UNSTRUCTURED TRIANGULAR MESHES
Arno Ronzheimer Aug. 1990 97 p Transl. into ENGLISH of Loesung der Zweidimensionalen Euler-Gleichungen Durch Eine Finite-Volumen-Diskretisierung auf Unstrukturierten Netzen (Brunswick, Fed. Republic of Germany, DFVLR), Jul. 1988 82 p Original language document was announced as N89-15672
(ESA-TT-1135; DFVLR-FB-88-34; ETN-90-98001) Avail: NTIS HC/MF A05; original German version available from DFVLR, Wissenschaftliches Berichtwesen, Postfach 90 60 58, 5000 Cologne, Fed. Republic of Germany, 28 Deutsches marks

The main reason for using unstructured grids is the possibility of simulating flows around complicated geometries, for which the generation of structured grids fitted to the body is substantially more expensive. The starting point of the study is a solution method based on a two dimensional cell corner scheme for structured grids. The various components of the solution procedure were adapted to the special requirements of unstructured triangular grids. The solution method described is checked by calculating subsonic and transonic flows around aerofoils. The effects of artificial dissipation are investigated and the influence of several acceleration techniques is discussed. ESA

65 STATISTICS AND PROBABILITY

Includes data sampling and smoothing; Monte Carlo method; and stochastic processes.

N91-11474*# Rockwell International Corp., Canoga Park, CA.
LOWER BOUND ON RELIABILITY FOR WEIBULL DISTRIBUTION WHEN SHAPE PARAMETER IS NOT ESTIMATED ACCURATELY
Zhaofeng Huang and Albert A. Porter 1990 16 p
(Contract NAS8-40000)
(NASA-CR-180681; NAS 1.26:180681) Avail: NTIS HC/MF A03 CSCL 12A

The mathematical relationships between the shape parameter Beta and estimates of reliability and a life limit lower bound for the two parameter Weibull distribution are investigated. It is shown that under rather general conditions, both the reliability lower bound and the allowable life limit lower bound (often called a tolerance limit) have unique global minimums over a range of Beta. Hence lower bound solutions can be obtained without assuming or estimating Beta. The existence and uniqueness of these lower bounds are proven. Some real data examples are given to show how these lower bounds can be easily established and to demonstrate their practicality. The method developed here has proven to be extremely useful when using the Weibull distribution in analysis of no-failure or few-failures data. The results are applicable not only in the aerospace industry but anywhere that system reliabilities are high. Author

N91-11475# Center for Mathematics and Computer Science, Amsterdam (Netherlands). Dept. of Operations Research, Statistics, and System Theory.
STOCHASTIC APPROXIMATION OF THE MLE FOR A SPATIAL POINT PATTERN
R. A. Moyeed and A. J. Baddeley Oct. 1989 16 p Submitted for publication
(CWI-BS-R8926; ETN-90-97660) Copyright Avail: NTIS HC/MF A03

An iterative stochastic approximation to the Maximum Likelihood Estimate (MLE) has developed the Strauss point process. Existing theorems are modified to show that the approximation is consistent and asymptotically normal. It performs well in numerical tests. ESA

N91-11476# Center for Mathematics and Computer Science, Amsterdam (Netherlands). Dept. of Operations Research, Statistics, and System Theory.
OPTIMAL CHOICE OF SAMPLE FRACTION IN EXTREME-VALUE ESTIMATION
L. deHaan (Erasmus Univ., Rotterdam, Netherlands) and A. L. M. Dekkers Nov. 1989 15 p
(CWI-BS-R8927; ETN-90-97661) Copyright Avail: NTIS HC/MF A03

Estimators of the extreme-value index are typically functions of the K largest order statistics. Here K = K(n) to infinity and K(n)/n to 0 (n to infinity). The problem of choosing the number K in an (asymptotic) optimal way is considered. ESA

N91-11477# Center for Mathematics and Computer Science, Amsterdam (Netherlands). Dept. of Operations Research, Statistics, and System Theory.
ON DENSITY ESTIMATION IN THE VIEW OF KOLMOGOROV'S IDEAS IN APPROXIMATION THEORY
Rafael Hasminskii and Iidar Ibragimov (Steklov Mathematical Inst., Moscow, USSR) Nov. 1989 13 p
(CWI-BS-R8928; ETN-90-97662) Copyright Avail: NTIS HC/MF A03

Upper and lower bounds for the quality of (probability) density estimation are studied. Connections are established between these problems and the theory of approximation of functions. Particularly, it is demonstrated how some of Kolmogorov's concepts work. ESA

N91-11478# Technische Univ., Delft (Netherlands). Faculty of Technical Mathematics and Informatics.
CONVERGENCE OF SOLUTIONS OF ONE-DIMENSIONAL STOCHASTIC HEAT EQUATIONS
Ello Weits 1990 16 p Sponsored in part by Netherlands Foundation for Technical Research
(Rept-90-40; ISSN-0922-5641; ETN-90-97720) Copyright Avail: NTIS HC/MF A03

Given one dimensional stochastic heat equations are considered. Weak convergence of solutions in the situation that sigma is a particular fixed projection operator (depending only on m) is shown. The limit process is not a solution of some stochastic evolution equation on the set of real numbers. If the initial values are suitably chosen, the solutions are stationary Gaussian processes. With some minor modifications the stationary Gaussian limit process can serve as model of stationary freeway traffic flow. ESA

N91-11479# Argonne National Lab., IL.
COMPUTATION OF STANDARD DEVIATIONS IN EIGENVALUE CALCULATIONS
E. M. Gelbard and R. Prael (Los Alamos National Lab., NM.) 1990 10 p Presented at the International Conference on Monte Carlo Methods in Neutron and Photon Transport, Budapest, Hungary, 25-28 Sep. 1990
(Contract W-31-109-eng-38)
(DE90-017809; CONF-900970-3) Avail: NTIS HC/MF A02

Brissenden proposes a modified Monte Carlo method for eigenvalue calculations, designed to decrease biases in the flux and eigenvalue estimates, and in corresponding estimates of standard deviations. The proposed method is based on the generation of superhistories, chains of histories run in sequence without intervening renormalization of the fission source. This method appears to have some disadvantages, discussed in another paper of this conference, e.g., first, the new method requires substantial changes in existing codes and second, it may increase variances in computations where long superhistory chains are needed. In PWR's, for example, dominance ratios approx. greater than 0.95 are not unusual, and it seems likely that chains of length 10 will, in such cases, still be strongly correlated. Earlier numerical experiments suggest that biases in fluxes and eigenvalues are negligibly small, even for very small numbers of histories per generation. Now more recent experiments, run on the CRAY-XMP, tend to confirm these earlier conclusions. The new experiments discussed involve the solution of one-group 1D diffusion theory eigenvalue problems, in difference form, via Monte Carlo. Experiments covered a range of dominance ratios from (approx) 0.75 to (approx) 0.985. In all cases flux and eigenvalue biases were substantially smaller than one standard deviation. DOE

66 SYSTEMS ANALYSIS

Includes mathematical modeling; network analysis; and operations research.

N91-11480# INTEL Corp., Beaverton, OR. Intel Scientific Computers.
TOUCHSTONE PROJECT: MILESTONE EVENT Q4 Quarterly Technical Report No. 4
Sig Lillevik 28 Dec. 1989 21 p
(Contract MDA972-89-C-0034; ARPA Order 6402)
(AD-A224034; INTEL/311849-001) Avail: NTIS HC/MF A03
CSCL 12/6

The focus of this quarter's technical activities was demonstrating the DELTA numeric node and porting Mach to the IOTA I/O node. In addition, the MRC strategy was determined for the DELTA prototype, completed development of the GAMMA prototype, and finalized the DELTA system architecture. Based on the i860 microprocessor, the DELTA numeric node offers preliminary 40 MHz performance of 8.76 double precision MFLOP's on the 100 x 100 LINPACK test. The Mach port was successful but requires future work in the network message server and in improving message passing performance. For the DELTA prototype, the Caltec MRC will be used in the standard MOSIS package but limit its channel bandwidth to 40 MB/s. The GAMMA prototype proved highly successful and features up to 128 compute nodes and peak performance of 7.6 double precision GFLOP's. Finally, the expectations for the DELTA prototype are equally impressive as it will scale to 512 nodes in a mesh interconnection network and provide 30.7 peak double precision GFLOP's, up to 32 GBytes of distributed memory, and over 150 GBytes of off-line disk storage. GRA

N91-11481# INTEL Corp., Beaverton, OR. Intel Scientific Computers.
TOUCHSTONE PROJECT MACH PORT: MILESTONE EVENT Q4
Don Cameron and Joel Clark 28 Dec. 1989 23 p
(Contract MDA972-89-C-0034; ARPA Order 6402)
(AD-A224057; INTEL/311848-001) Avail: NTIS HC/MF A03
CSCL 12/5

The porting of the Mach operating system to the Touchstone IOTA prototype is described. The major activities are described which are associated with the port and the kernel design issues that they brought to our attention. Mach was ported to a small cube of integrated I/O nodes. Drivers for the SCSI disk drive, serial line, and the Direct-Connect hypercube routing hardware were written. Serial communication to the nodes was multiplexed through a terminal connected to an Intel SYP-301 host platform. It was found that to extend the Mach thread model onto a multicomputer architecture such as Touchstone, a compatible form of shared virtual memory must be provided. Alternately, supporting the multicomputing model of high speed inter-node message passing will require better support from the Mach kernel. For both of these usage models, the speed of inter-node message passing is critical. Further research is required into how to best provide this in the Mach environment. GRA

N91-11482# INTEL Corp., Beaverton, OR. Intel Scientific Computers.
TOUCHSTONE PROJECT DELTA NUMERIC NODE: MILESTONE EVENT Q4
Paul Close and Anthony Zilka 28 Dec. 1989 119 p

(Contract MDA972-89-C-0034; ARPA Order 6402)
(AD-A224060; INTEL/311847-001) Avail: NTIS HC/MF A06
CSCL 12/6

The aggregate performance of any parallel computer system is directly related to the performance of the system's individual processors. The DELTA numeric node prototype addresses this issue by utilizing the latest in high performance off the shelf microprocessor technology. The DELTA numeric code, named RX-1, is based on the Intel 80860 microprocessor. This single component provides an unprecedented amount of hardware integration which in turn allows a very high performance processing node to be packaged on a single printed circuit board. The RX-1 node design had two simple goals: Provide an i860 node for the DELTA prototype. The DELTA prototype is a 2D mesh-organized multicomputer also being developed under the DARPA sponsored Touchstone program; and Through the process of designing both hardware and software for the i860 node, gain valuable experience which could then be applied to a second generation effort. The RX-1 node was designed, built and tested. The major features are: 40MHz system clock; On board 8 M-byte DRAM array expandable to 32 M-bytes with 4 M-bit DRAM technology; A general purpose expansion connector for attaching additional DRAM, second level cache, frame buffer or any other imagined appendage; A FIFO based interface to the internal system network; A modular approach for attaching the internal system message passing circuitry; A low speed high reliability serial channel for system boot and diagnostics; I/O support for performance analysis instrumentation; and a 56-bit counter with 100 ns granularity for system timing. GRA

N91-11483# Center for Mathematics and Computer Science, Amsterdam (Netherlands). Dept. of Operations Research, Statistics, and System Theory.
INTERCONNECTED NETWORKS OF QUEUES WITH RANDOMIZED ARRIVAL AND DEPARTURE BLOCKING
Peter R. deWaal and Nico vanDijk (Vrije Univ., Amsterdam, Netherlands) Dec. 1989 19 p
(CWI-BS-R8934; ETN-90-97667) Copyright Avail: NTIS HC/MF A03

Two interconnected multiclass non-exponential queueing networks are studied. Jobs can jump from one cluster to another, but subject to randomized blocking depending on the class occupancies. Such systems naturally arise in communication networks, such as metropolitan area networks. Sufficient conditions for the existence of a product form equilibrium distribution under both the recirculate and the stop blocking protocol are presented. A number of examples are given. ESA

67 THEORETICAL MATHEMATICS

Includes topology and number theory.

N91-11484# Hiroshima Univ., Takehara (Japan). Research Inst. for Theoretical Physics.
ON A SIMPLE EVALUATION OF ANOMALIES FROM THE PATH INTEGRAL MEASURE
Takeshi Inagaki Feb. 1990 14 p
(DE90-513707; RRK-90-3) Avail: NTIS (US Sales Only) HC/MF A03

Anomalies can be evaluated as the non-trivial Jacobian factors of the path integral measure. Several comments are made on this calculation by taking 2-D gravity theories as examples. A new calculational method which makes practical calculations much simpler is presented. DOE

70 PHYSICS (GENERAL)

For precision time and time interval (PTTI) see *35 Instrumentation and Photography;* for geophysics, astrophysics or solar physics see *46 Geophysics, 90 Astrophysics,* or *92 Solar Physics.*

N91-11485# Los Alamos National Lab., NM.
ACCURATE REPRESENTATIONS OF GENERAL TEXTURES BY A SET OF WEIGHTED GRAINS
U. F. Kocks, J. S. Kallend, and A. C. Biondo (Illinois Inst. of Tech., Chicago.) 1990 7 p Presented at the 9th International Conference on Textures of Materials, Avignon, France, 17-21 Sep. 1990
(Contract W-7405-eng-36)
(DE90-016487; LA-UR-90-2828; CONF-9009236-1) Avail: NTIS HC/MF A02

The most compact way of describing general texture information is by way of a file of weighted discrete grains. When the textures are strong, this results in a great saving of necessary parameters. The most efficient way is a random file from which grains with low weights get discarded. This method is routine and independent of any preknowledge of the texture or even the symmetries. Typically, the order of 100 grains are sufficient for strong textures or fiber textures. Furthermore, these grain files are directly in the kind of format that is useful for computer simulation of current anisotropic properties or future texture development. For textures that are not very sharp, but nevertheless are not properly represented as random (which would imply isotropic properties), one may also use weighted-grains files, but here the number of grains needed may be large for an accurate representation. We have found that on the order of 1000 weighted grains are sufficient for most cases. When the symmetries are known, grains that are regularly (rather than randomly) arranged in orientation space are useful -- again better when they are weighted. DOE

N91-11486# Ames Lab., IA. Applied Mathematical Sciences.
ELEMENTARY INVERSION, ENERGY VELOCITY, AND A GENERALIZED SOMMERFELD THEOREM
Thomas M. Roberts and Mike Hobart 1990 10 p Presented at the SPIE's International Symposium on Optical and Optoelectronic Applied Science and Engineering Exhibit, San Diego, CA, 8-13 Jul. 1990
(Contracts W-7405-eng-82; N00014-83-K-0038)
(DE90-018046; IS-M-643; CONF-900756-41) Avail: NTIS HC/MF A02

It is shown how to infer elementarily from time-domain precursors some frequency-domain information. Observations are made on energy velocity that may be surprising. Sommerfeld's theory about the speed of light is generalized. DOE

N91-11487# Argonne National Lab., IL. Materials and Components Technology Div.
PHENOMENOLOGY OF FORCES ACTING BETWEEN MAGNETS AND SUPERCONDUCTORS
J. R. Hull, T. M. Mulcahy, L. Lynds, B. R. Weinberger, F. C. Moon, and P. Z. Chang (Cornell Univ., Ithaca, NY.) 1990 7 p Presented at the 25th Intersociety Energy Conversion Engineering Conference, Reno, NV, 12-17 Aug. 1990 Submitted for publication
(Contract W-31-109-eng-38)
(DE90-017864; CONF-900801-31) Avail: NTIS HC/MF A02

The forces acting between magnets and superconductors give rise to a rich diversity of phenomena that are understood physically only at a rudimentary level. Experimental results are presented for the levitational force, magnetic stiffness, drag, and damping of magnets interacting with high temperature superconductors. Empirical correlations and theoretical understanding of these phenomena are summarized. The use of high temperature superconductors in prototype experimental bearing devices is described. DOE

71 ACOUSTICS

Includes sound generation, transmission and attenuation. For noise pollution see *45 Environmental Pollution.*

N91-11488*# Duke Univ., Durham, NC. Dept. of Mechanical Engineering and Materials Science.
AIRCRAFT INTERIOR NOISE REDUCTION BY ALTERNATE RESONANCE TUNING Progress Report, period ending June 1990
Donald B. Bliss, James A. Gottwald, Ramakrishna Srinivasan, and Mark B. Gustaveson Aug. 1990 41 p
(Grant NAG1-722)
(NASA-CR-186879; NAS 1.26:186879) Avail: NTIS HC/MF A03 CSCL 20A

Existing interior noise reduction techniques for aircraft fuselages perform reasonably well at higher frequencies, but are inadequate at lower frequencies, particularly with respect to the low blade passage harmonics with high forcing levels found in propeller aircraft. A method is being studied which considers aircraft fuselage lined with panels alternately tuned to frequencies above and below the frequency that must be attenuated. Adjacent panels would oscillate at equal amplitude, to give equal source strength, but with opposite phase. Provided these adjacent panels are acoustically compact, the resulting cancellation causes the interior acoustic modes to become cutoff, and therefore be non-propagating and evanescent. This interior noise reduction method, called Alternate Resonance Tuning (ART), is currently being investigated both theoretically and experimentally. This new concept has potential application to reducing interior noise due to the propellers in advanced turboprop aircraft as well as for existing aircraft configurations. Author

N91-11489# Sonoquest/Advanced Ultrasonics Research, Wellesley Hills, MA.
ARCTIC ACOUSTICS ULTRASONIC MODELING STUDIES Final Report, Mar. 1987 - Feb. 1990
Jacques R. Chamuel Mar. 1990 136 p
(Contract N00014-86-C-0206)
(AD-A224165; JRC-10-90) Avail: NTIS HC/MF A07 CSCL 20/1

A unique collection of laboratory ultrasonic modeling results are presented revealing and characterizing hidden pulsed seismoacoustic wave phenomena from 3-D range dependent liquid/solid boundaries. The research succeeded in isolating and identifying low frequency (10 to 500 Hz) transmission loss mechanisms and provided physical insight into Arctic acoustic problems generally beyond the state-of-the-art of theoretical and numerical analysis. The ultrasonic modeling studies dealt with controversial issues and existing discrepancies on seismo-acoustic waves at water/ice interface, sea ice thickness determination, low frequency transmission loss, and bottom leaky Rayleigh waves. The areas investigated include leaky Rayleigh waves at water/ice interface, leaky flexural waves in floating ice plates, effects of dry/wet cracks in sea ice on plate waves and near grazing acoustic waves, edge waves in floating plates, low frequency backscatter from ice keel width resonances, conversion of underwater acoustic waves into plate waves by keels, nondispersive flexural wave along apex of small angle solid wedge, Scholte and leaky Rayleigh waves along apex of immersed 90 ice wedge, backscatter from trailing edge of floes, floating plate resonances associated with near-grazing underwater acoustic waves, acoustic coupling between adjacent floes, and multiple bottom leaky Rayleigh wave components in water layer over solid bottom. GRA

N91-11490# Universita Cattolica, Brescia (Italy). Fachbereich Maschinenbau.
CONTRIBUTIONS TO THE SOUND LOCATION IN THE ATMOSPHERE Ph.D. Thesis [BEITRAEGE ZUR SCHALLORTUNG IN DER ATMOSPHAERE]
Kai Harder 1990 124 p In GERMAN
(ETN-90-97863) Avail: NTIS HC/MF A06

The atmosphere in an inhomogeneous, anisotropic medium for sound diffusion is studied. The sound velocity depends on temperature, relative humidity, and air pressure, which are a function of location. The sound diffusion appears more complicated than, for instance, light diffusion. This investigation deals with special aspects of acoustics in the atmosphere. An important application, the possibility to localize sound sources, is described. A method is given to use a well known process of runaway recognition also in two dimensional cases. The radial distribution is described through a logarithmic normal distribution. ESA

N91-11491# Max-Planck-Inst. fuer Stroemungsforschung, Goettingen (Germany, F.R.).
A MODEL FOR THE SOUND GENERATION DUE TO COMPRESSIBLE VORTEX-BODY INTERACTION
Hans-Martin Lent 1990 74 p In GERMAN; ENGLISH summary
(MPIS-Mitt-96; ISSN-0374-1257; ETN-90-97869) Avail: NTIS HC/MF A04

During the interaction of a vortex with a rigid body, sound will be emitted. While this sound generation is well known for the low Mach number flow, this investigation deals with the influence of compressibility on the sound generation mechanism. Experiments for the vortex body interaction were performed in a shock tube. At high subsonic Mach numbers the region of the sound sources is shown to be no longer compact, and to behave like a noncompact piston source. Based on this knowledge, a model is constructed which is used to calculate the strength of the impulsive sound wave, as a function of the flow quantities. The results are compared with experimental data. For measuring the flow quantities and the strength of the sound wave, holographic interferometry and pressure measurements at the duct's wall were used. ESA

N91-11492 Mississippi Univ., University.
SOUND FIELD FLUCTUATIONS DUE TO LARGE SCALE WIND-DRIVEN TURBULENCE Ph.D. Thesis
John Michael Noble 1989 135 p
Avail: Univ. Microfilms Order No. DA9019277

A large scale wind driven turbulence model is put forth to account for long term (1 to 5 minutes) phase variations observed in outdoor sound propagation experiments. The long term variations experimentally observed can not be explained with small scale turbulence models. Fourier analysis of phase variations show outer scales of 200 meters and greater, which corresponds to turbulence in the energy-containing subrange. Turbulence in this region corresponds to turbule sizes as large as the planetary boundary layer. The large scale turbulence in the boundary layer is assumed to be elongated longitudinal vortex pairs roughly aligned with the mean wind. Large scale turbulence is a range-dependent problem. The best acoustical algorithm to handle range-dependency is the parabolic equation. The parabolic equation is a solution to the one-wave wave equation which is applicable to sound propagation where backscattered energy is negligible. The algorithm is set to compute the pressure and phase at a receiver as the vortex pair traverses the propagation path with the mean wind speed. The model provides good results with the same trends and variations in the magnitudes of the phase observed experimentally.
Dissert. Abstr.

N91-11493*# National Aeronautics and Space Administration. Lewis Research Center, Cleveland, OH.
NOISE MEASUREMENTS FROM AN EJECTOR SUPPRESSOR NOZZLE IN THE NASA LEWIS 9- BY 15-FOOT LOW SPEED WIND TUNNEL
Eugene A. Krejsa, Beth A. Cooper, David G. Hall, and Abbas Khavaran (Sverdrup Technology, Inc., Brook Park, OH.) Oct. 1990 62 p Presented at the 13th Aeroacoustics Conference, Tallahassee, FL, 22-24 Oct. 1990; sponsored in part by AIAA
(NASA-TM-103628; E-5717; NAS 1.15:103628; AIAA-90-3983)
Avail: NTIS HC/MF A04 CSCL 20A

Acoustic results are presented of a cooperative nozzle test program between NASA and Pratt and Whitney, conducted in the NASA-Lewis 9 x 15 ft Anechoic Wind Tunnel. The nozzle tested was the P and W Hypermix Nozzle concept, a 2-D lobed mixer nozzle followed by a short ejector section made to promote rapid

mixing of the induced ejector nozzle flow. Acoustic and aerodynamic measurements were made to determine the amount of ejector pumping, degree of mixing, and noise reduction achieved. A series of tests were run to verify the acoustic quality of this tunnel. The results indicated that the tunnel test section is reasonably anechoic but that background noise can limit the amount of suppression observed from suppressor nozzles. Also, a possible internal noise was observed in the air supply system. The P and W ejector suppressor nozzle demonstrated the potential of this concept to significantly reduce jet noise. Significant reduction in low frequency noise was achieved by increasing the peak jet noise frequency. This was accomplished by breaking the jet into segments with smaller dimensions than those of the baseline nozzle. Variations in ejector parameters had little effect on the noise for the geometries and the range of temperatures and pressure ratios tested. Author

N91-11494*# National Aeronautics and Space Administration. Lewis Research Center, Cleveland, OH.

THE EFFECT OF SWIRL RECOVERY VANES ON THE CRUISE NOISE OF AN ADVANCED PROPELLER

James H. Dittmar and David G. Hall (Sverdrup Technology, Inc., Brook Park, OH.) 1990 18 p Presented at the 13th Aeroacoustics Conference, Tallahassee, FL, 22-24 Oct. 1990; sponsored by AIAA

(NASA-TM-103625; E-5731; NAS 1.15:103625; AIAA-90-3932) Avail: NTIS HC/MF A03 CSCL 20A

The SR-7A propeller was acoustically tested with and without downstream swirl recovery vanes to determine if any extra noise was caused by the interaction of the propeller wakes and vortices with these vanes. No additional noise was observed at the cruise condition over the angular range tested. The presence of the swirl recovery vanes did unload the propeller and some small peak noise reductions were observed from lower propeller loading noise. The propeller was also tested alone to investigate the behavior of the peak propeller noise with helical tip Mach number. As observed before on other propellers, the peak noise first rose with helical tip Mach number and then leveled off or decreased at higher helical tip Mach numbers. Detailed pressure-time histories indicate that a portion of the primary pressure pulse is progressively cancelled by a secondary pulse as the helical tip Mach number is increased. This cancellation appears to be responsible for the peak noise behavior at high helical tip Mach numbers. Author

N91-11495*# National Aeronautics and Space Administration. Lewis Research Center, Cleveland, OH.

PREDICTION OF THE NOISE FROM A PROPELLER AT ANGLE OF ATTACK

Eugene A. Krejsa Oct. 1990 22 p Presented at the 13th Aeroacoustics Conference, Tallahassee, FL, 22-24 Oct. 1990; sponsored in part by AIAA

(NASA-TM-103627; E-5795; NAS 1.15:103627; AIAA-90-3954) Avail: NTIS HC/MF A03 CSCL 20A

An analysis is presented to predict the noise of a propeller at angle of attack. The analysis is an extension of that reported by Mani which predicted the change in noise due to angle of attack to both unsteady loading and to azimuthal variation of the radiation efficiency of steady noise sources. Mani's analysis, however, was limited to small angles of attack. The analysis reported herein removes this small angle limitation. Results from the analysis are compared with the data of Woodward for a single rotation propeller and a counter rotating propeller. The comparison shows that including the effect of angle of attack on the steady noise sources significantly improves the agreement with data. Including higher order effects of angle of attack, while changing the predicted noise at far forward and aft angles, has little effect near the propeller plane. Author

72 ATOMIC AND MOLECULAR PHYSICS

Includes atomic structure, electron properties, and molecular spectra.

N91-11496# Royal Inst. of Tech., Stockholm (Sweden). Dept. of Plasma Physics and Fusion Research.

COMPLEMENTARY ASPECTS ON MATTER-ANTIMATTER BOUNDARY LAYERS

B. Lehnert May 1990 32 p

(TRITA-EPP-90-04; ISSN-0348-7539; ETN-90-97986) Avail: NTIS HC/MF A03

Some complementary aspects on the problems of the matter-antimatter metagalaxy model and its cellular structure, as being proposed by Klein and Alfven are presented. A previously outlined one dimensional model of a magnetized matter-antimatter boundary layer is updated and extended, by introducing amended nuclear annihilation data, and by making improved approximations of the layer structure and its dependence on relevant parameters. The critical beta value obtained from this model leads to critical plasma densities which are not high enough to become reconcilable with a cellular matter-antimatter structure within the volume of a galaxy. ESA

N91-11497# Syracuse Univ., NY.

RESEARCH PROGRAM IN ELEMENTARY PARTICLE THEORY Progress Report, period ending 31 Dec. 1990

A. P. Balachandran, Carl Rosenzweig, and Joseph Schechter 1990 78 p

(Contract DE-FG02-85ER-40231)

(DE90-017284; DOE/ER-40231/T8) Avail: NTIS HC/MF A05

Topics discussed include: Topology in Physics; Skyrme Model; High Temperature Superconductivity; Fractional statistics, and generalized spin statistics theorem; QCD as a dual chromomagnetic superconductor; Confinement and string picture in QCD; Quark gluon plasmas; Cosmic strings; Effective Lagrangians for QCD; Proton spin, strange content and related topics; Physical basis of the Skyrme model; Gauge theories and weak interactions; Grand unification; Universal see saw mechanism; and Abelian and non-abelian interactions of a test string. DOE

N91-11498# North Carolina Univ., Chapel Hill.

MEASUREMENT OF RADIAL IONIZATION PROBABILITY IN MICROSCOPIC VOLUMES FOR 2.90 AND 3.79 MeV ALPHA PARTICLES Ph.D. Thesis

David M. Hamby 1989 217 p

(Contract DE-AC05-76OR-00033)

(DE90-017509; DOE/OR-00033/T443) Avail: NTIS HC/MF A11

Material subjected to a uniform field of radiation receives a uniform absorbed dose on a macroscopic scale, but it is quite possible to have large variations in energy density when individual small volumes of that medium are examined. These fluctuations are of importance in microscopic sites since it is likely that some volumes will absorb large quantities of energy. Cellular mutations or transformations take place if the energy density within subcellular target volumes exceeds some threshold. Gas-filled proportional counters are routinely used to experimentally measure energy deposition in such small volumes. However, in microscopic sites less than a few hundred nanometers in diameter (approaching the size of sensitive biological targets) the proportional counter is no longer useful for measurements of energy deposition. In order to determine energy deposition in nanometer size volumes, Monte Carlo computer programs have been written to generate (through the use of interaction cross-section data) three dimensional charged particle track structures which can be analyzed by additional computer codes to obtain distributions of energy deposition events on a microscopic scale. A parallel-plate avalanche counter capable of simulating microscopic volumes has been constructed and housed in a way that permits detection of ionizations at any given distance from the path of a charged particle. Measurements have been performed to determine the function of ionization probability versus distance from an alpha particle track. Data have been collected for 2.90 and 3.79 MeV alpha particles passing simulated spherical volumes of 44 nm radius at impact parameters from

zero to about 100 nanometers. The ionization probability functions can be compared to functions with identical parameters obtained from Monte Carlo computer calculations in an attempt to strengthen the validity of the computer codes. DOE

N91-11499# Lawrence Livermore National Lab., CA.
ATOMIC PHYSICS OF HIGHLY CHARGED IONS IN AN ELECTRON BEAM ION TRAP
R. E. Marrs Jul. 1990 15 p Presented at the 12th International Conference on Atomic Physics, Ann Arbor, MI, 30 Jul. - 3 Aug. 1990
(Contract W-7405-eng-48)
(DE90-017528; UCRL-JC-104665; CONF-900716-1) Avail: NTIS HC/MF A03

Two electron beam ion traps are in use at LLNL for the purpose of studying the properties of very highly charged ions and their interactions with electrons. The operation of the traps is reviewed and recent experiments in three areas are discussed: precision transition energy measurements in the limit of very high ion charge, dielectronic recombination measurements for the He-like isoelectronic sequence, and measurements of x ray polarization. DOE

N91-11500# Brookhaven National Lab., Upton, NY.
EMPIRICAL PROTON-NEUTRON INTERACTION ENERGIES AND NUCLEAR STRUCTURE
D. S. Brenner, W.-T. Chou, R. F. Casten, J.-Y. Zhang, C. Wesselborg, and D. D. Warner (Science Research Council, Daresbury, England) 1990 7 p Presented at the 8th International Conference on Atomic Masses and Fundamental Constants, Jerusalem, Israel, 9-14 Sep. 1990
(Contracts DE-AC02-76CH-00016; DE-FG02-88ER-40417)
(DE90-017632; BNL-45011; CONF-900912-2) Avail: NTIS HC/MF A02

Empirical proton-neutron (p-n) interaction energies are extracted for all even-even nuclei with well known binding energies using a simple double difference equation. Three features are disclosed: a systematic decrease of p-n interaction strengths (excepting N=Z nuclei) with increasing A, large interaction strengths for N=Z nuclei, and microstructure in doubly magic and deformed regions. Shell model calculations are used to explain the behavior of N=Z and other nuclei in the sd shell. Arguments based on orbit occupancy are introduced to explain microstructure effects in heavier nuclei and are given quantitative support by simple microscopic Nilsson and Shell Model calculations. The analysis sheds light on the relative roles of monopole and quadrupole components of the p-n interaction in determining nuclear structure. DOE

N91-11501# Toledo Univ., OH. Dept. of Physics and Astronomy.
SEMIEMPIRICAL STUDIES OF ATOMIC STRUCTURE Progress Report, 1 Jul. 1988 - 30 Jun. 1991
L. J. Curtis 1 Sep. 1990 30 p
(Contract DE-FG05-88ER-13958)
(DE90-017653; DOE/ER-13958/16) Avail: NTIS HC/MF A03

The following topics were studied: Review of Highly Ionized Atoms; Parametrized Systematizations of Spectroscopic Data; Transition Probability Computations; and Beam-foil Measurements. DOE

N91-11502# Los Alamos National Lab., NM.
SECONDARY-ELECTRON YIELD MEASUREMENTS FROM METALS IMPACTED BY HIGH-VELOCITY IONS, ELECTRONS, AND MOLECULES
David M. Suszcynsky, Joseph E. Borovsky, and Bruce L. Barraclough Sep. 1990 14 p
(Contract W-7405-eng-36)
(DE90-018023; LA-11915-MS) Avail: NTIS HC/MF A03

In support of several recent experiments, the Space Plasma Physics Group at Los Alamos National Laboratory has measured the secondary electron yields from metals impacted by high speed projectiles. Secondary electron yields from gold, tantalum, and oxidized aluminum surfaces were measured using H(+1), H2(+1), H3(+1),(3)He(+1), (3)He(+2), (4)He(+2), (9)Be(+4), (10)B(+5), (12)C(+6), and (16)O(+8) in projectiles in the 1 to 11 MeV/amu energy range. Measurements of secondary electron yields from titanium, copper, molybdenum, silver, tantalum, gold, lead, uranium, oxidized aluminum, brass, stainless steel, and aquadag surfaces were made with 0.8 to 40 keV electrons provided by scanning electron microscopes at Los Alamos and at the University of Iowa. These measured yields are presented in tabular form. DOE

N91-11503# Ames Lab., IA.
NOVEL MEASUREMENTS OF NUCLEAR SPIN CROSS-RELAXATION IN METAL HYDRIDES
David B. Baker, Mark S. Conradi (Washington Univ., Saint Louis, MO.), R. E. Norberg, D. R. Torgeson, and R. G. Barnes 1990 19 p Presented at the International Symposium on Metal-Hydrogen Systems, Banff, British Columbia, 2-7 Sep. 1990 Sponsored in part by Nishi Luthra Fund
(Contract W-7405-eng-82; NSF DMR-88-01260; NSF DMR-87-02847)
(DE90-018042; IS-M-640; CONF-9009141-5) Avail: NTIS HC/MF A03

Recent NMR measurements of proton relaxation have shown an unexpected frequency dependence in several metal-hydrogen systems at low temperatures. An explanation proposed by the Ames group involves cross relaxation of protons to quadrupolar metal nuclei. This hypothesis is tested with relaxation experiments involving large amplitude field modulation. The field modulation sweeps the proton resonance through the distribution of metal frequencies. Thus, the protons come into contact with more metal nuclei, increasing the proton relaxation rate. Relaxation measurements were performed on several samples and the proton resonance frequency, the modulation frequency, and the modulation amplitude were varied. Also reported are T sub 1 measurements on slowly spinning samples; the rotation produces periodic variations of metal quadrupolar frequencies. DOE

N91-11504# Northwestern Univ., Chicago, IL.
INTRAMOLECULAR ELECTRON TRANSFER RATES
Joseph T. Hupp 1990 15 p
(Contract DE-FG02-87ER-13808)
(DE90-017447; DOE/ER-13808/T1) Avail: NTIS HC/MF A03

The initial goals of this project were: (1) to construct pulsed-accelerated-flow and pulsed-laser (transient absorbance) instruments for intramolecular electron-transfer rate measurements, (2) to design and synthesize appropriate molecules and perform such measurements, (3) to develop further an electrochemical method for gauging site-to-site electronic coupling, and (4) to apply time-dependent Raman scattering theory to the problem of inner-shell reorganization in charge-transfer reactions. Although all four goals were met, we also found it necessary to pursue studies in some unforeseen directions. For example, early on we discovered that medium effects (aggregation and ion pairing) could play a very large, and previously unrecognized, role in some optical intervalence reactions. Given the importance of the effects to the areas above, we chose to map them in a fairly complete fashion. Also, in anticipation of possible renewal we initiated studies in a new area: bimolecular photoredox kinetics in supercritical media. Finally, in a small project carried out largely by undergraduates we examined solvent tuning effects upon lifetimes of photo-excited ruthenium am(m)ine bipyridine complexes. The key new findings and other highlights of these studies are outlined. DOE

N91-11505# British Columbia Univ., Vancouver. TRIUMF Facility.
CAPTURE AND TRANSFER OF PIONS IN HYDROGENOUS MATERIALS
D. S. Armstrong (Virginia Polytechnic Inst. and State Univ., Blacksburg.) May 1990 19 p Presented at the International Workshop on Exotic Atoms in Condensed Matter, Erice, Italy, 19-25 May 1990
(DE90-017756; TRI-PP-90-22; CONF-9005273-1) Avail: NTIS (US Sales Only) HC/MF A03

Pionic hydrogen is a short-lived exotic hydrogen isotope in

which a negative pion replaces the atomic electron. The formation and subsequent interactions of pionic hydrogen are discussed, with emphasis on the process of pion transfer. Recent results using the pion charge-exchange reaction (pi(-), pi(0)) obtained at TRIUMF are reviewed. DOE

N91-11506# Ames Lab., IA.
MUON SR STUDIES ON Sr2CuO2Cl2, La2CuO4, AND Nd2CuO4: 2-D MAGNETISM, LOCAL FIELDS AND MUON SITES
L. P. Le, G. M. Luke, B. J. Sternlieb, Y. J. Uemura, J. H. Brewer, T. M. Riseman (British Columbia Univ., Vancouver.), D. C. Johnston, and L. L. Miller 1990 7 p Presented at the 5th International Conference on Muon Spin Rotation, Relaxation and Resonance, Oxford, England, 2-12 Apr. 1990 Prepared in cooperation with Nippon Inst. of Tech., Japan Submitted for publication
(Contract W-7405-eng-82)
(DE90-018014; IS-M-642; CONF-900489-3) Avail: NTIS HC/MF A02

The temperature dependence of the zero-field muon spin precession frequency observed in Sr2CuO2Cl2 and La2CuO4 below the Neel temperature with a 2-D Heisenberg model with an additional small anisotropy. Good agreement of the observed results with this model reflects the highly 2-D magnetic properties of these cuprates. The measured local fields are compared with a simple calculation of dipolar fields in the crystal to search for muon site locations. The results provide evidence that the muon sites are to the oxygen atoms in these compounds. DOE

N91-11507# Australian Nuclear Science and Technology Organization, Lucas Heights.
ANSTO: AUSTRALIAN NUCLEAR SCIENCE AND TECHNOLOGY ORGANIZATION
1989 20 p
(DE90-637389; INIS-mf-12679) Avail: NTIS (US Sales Only) HC/MF A03

The Australian Nuclear Science and Technology Organization conducts or is engaged in collaborative research and development in the application of nuclear science and associated technology. Through its Australian radio-isotopes unit, it markets radioisotopes, their products and other services for the nuclear medicine industry and research. It also operates national nuclear facilities (HIFAR and Moata research reactors), promotes training, provides advice and disseminates information on nuclear science and technology. The booklet briefly outlines these activities. DOE

N91-11508# Consiglio Nazionale delle Ricerche, Frascati (Italy). Ist. di Fisica dello Spazio Interplanetario.
GENERALIZED BACK-ACTION EVASION SCHEMES FOR THE DETECTION OF WEAK CLASSICAL FORCES
F. Bordoni and R. Onofrio Jun. 1990 34 p
(IFSI-90-19; ETN-90-97801) Avail: NTIS HC/MF A03

The analysis techniques available for back-action evasion schemes are presented. A perturbative approach is introduced and applied to a simple case. As a generalization of the back-action evasion schemes, the concept of optimal pumping spectrum is introduced. It works for a unified treatment of stroboscopy and continuous quantum nondemolition strategies. Generalized back-action evasion strategies are introduced and studied in simple applications. They open the possibility for development of high sensitivity schemes for the measurement of small forces. Estimates of the noise figure for generalized back-action evasion transducers are discussed in detail. ESA

N91-11509# Oak Ridge National Lab., TN.
NEWLY APPRECIATED ROLES FOR ELECTRONS IN ION-ATOM COLLISIONS
Ivan A. Sellin 1990 17 p Presented at the Workshop on Fast Ion Collisions, Debrecen, Hungary, 17-19 Sep. 1990 Sponsored in part by NSF Prepared in cooperation with Tennessee Univ., Knoxville
(Contract DE-AC05-84OR-21400)
(DE91-000555; CONF-9009261-1) Avail: NTIS HC/MF A03

Since the previous Debrecen workshop on High Energy Ion-Atom Collisions there have been numerous experiments and substantial theoretical developments in the fields of fast ion-atom and ion-solid collisions concerned with explicating the previously largely underappreciated role of electrons as ionizing and exciting agents in such collisions. Examples discussed include the double electron ionization problem in He; transfer ionization by protons in He; double excitation in He; backward scattering of electrons in He; the role of electron-electron interaction in determining beta parameters for ELC; projectile K ionization by target electrons; electron spin exchange in transfer excitation; electron impact ionization in crystal channels; resonant coherent excitation in crystal channels; excitation and dielectronic recombination in crystal channels; resonant transfer and excitation; the similarity of recoil ion spectra observed in coincidence with electron capture vs. electron loss; and new research on ion-atom collisions at relativistic energies. DOE

73 NUCLEAR AND HIGH-ENERGY PHYSICS

Includes elementary and nuclear particles; and reactor theory.

For space radiation see *93 Space Radiation.*

N91-11510# Instituto de Pesquisas Espaciais, Sao Jose dos Campos (Brazil).
MULTIPLE APPLICATION INTENSE PARTICLE BEAM PROJECT [FEIXE INTENSO DE PARTICULAS DE APLICACOES MULTIPLAS]
M. Ueda and M. Machida (Universidade Estadual de Campinas, Brazil) Jun. 1988 39 p In PORTUGUESE; ENGLISH summary
(INPE-4576-RPE/568) Avail: NTIS HC/MF A03

The Multiple Application Intense Particle Beam project is an experiment in which an injector of high energy neutral or ionized particles will be used to diagnose high density and high temperature plasmas. The acceleration of the particles will be carried out feeding a diode with a high voltage pulse produced by a Marx generator. Other applications of intense particle beam generated by this injector that could be explored in the future include: heating and stabilization of compact toroids, treatment of metallic surfaces, and ion implantation. Author

N91-11511# Fermi National Accelerator Lab., Batavia, IL.
NUMERICAL MODELING OF TIME DOMAIN 3-D PROBLEMS IN ACCELERATOR PHYSICS
F. A. Harfoush and T. G. Jurgens Jun. 1990 6 p Presented at the 2nd European Particle Accelerator Conference, Nice, France, 12-16 Jun. 1990
(Contract DE-AC02-76CH-03000)
(DE90-015625; FNAL/C-90/140; CONF-900603-32) Avail: NTIS HC/MF A02

Time domain analysis is relevant in particle accelerators to study the electromagnetic field interaction of a moving source particle on a lagging test particle as the particles pass an accelerating cavity or some other structure. These fields are called wake fields. The travelling beam inside a beam pipe may undergo more complicated interactions with its environment due to the presence of other irregularities like wires, thin slots, joints and other types of obstacles. Analytical solutions of such problems is impossible and one has to resort to a numerical method. In this paper we present results of our first attempt to model these problems in 3-D using our finite difference time domain (FDTD) code. DOE

N91-11512# Florida State Univ., Tallahassee. Particle Physics Group.
TASK A: HIGH ENERGY PHYSICS PROGRAM EXPERIMENT AND THEORY. TASK B: HIGH ENERGY PHYSICS PROGRAM NUMERICAL SIMULATION Progress Report, 1 Aug. 1989 - 31 Jul. 1990

1990 77 p
(Contract DE-FG05-87ER-40319)
(DE90-017336; DOE/ER-40319/3) Avail: NTIS HC/MF A05

This report discusses progress in experimental and theoretical High Energy Physics at Florida State University. Fixed target experiments, collider experiments, computing, networking,. VAX upgrade, SSC preparation, detector development, and particle theory are some of the areas covered. DOE

N91-11513# Department of Energy, Washington, DC. Office of Superconducting Super Collider.
REPORT OF THE DEPARTMENT OF ENERGY (DOE) OFFICE OF ENERGY RESEARCH REVIEW COMMITTEE ON THE SITE-SPECIFIC CONCEPTUAL DESIGN OF THE SUPERCONDUCTING SUPER COLLIDER
Sep. 1990 320 p
(DE90-018021; DOE/ER-0463P) Avail: NTIS HC/MF A14

After it was established in early 1989, the Superconducting Super Collider Laboratory (SSCL) began to prepare a detailed site-specific SSC conceptual design, including cost and schedule estimates. As detailed in the SSC Site-Specific Conceptual Design Report (SCDR), this design builds upon the design in the March 1986 SSC Conceptual Design Report (CDR) and takes into account characteristics of the SSC site, results of continuing magnet R and D, and advances in accelerator design. DOE

N91-11514# Lawrence Livermore National Lab., CA.
MONT3E: A MONTE CARLO ELECTRON HEAT TRANSFER CODE
J. D. Maltby and B. T. Kornblum Apr. 1990 29 p Presented at the Association for Computing Machinery/IEEE Supercomputing Conference, New York, NY, 12-16 Nov. 1990 Submitted for publication
(Contract W-7405-eng-48)
(DE90-012091; UCRL-JC-103948; CONF-901121-3) Avail: NTIS HC/MF A03

A Monte Carlo code, MONT3E, was written to analyze heat transfer due to electron backscattering. The availability of supercomputers has made large-scale applications of this analysis technique possible. Statistically valid solutions of complicated engineering problems can now be performed. In this paper, the physical theory of electron trajectories is described and related to the implementation of an electron tracing algorithm. The analysis requires three types of information: a geometric description of the enclosed volume under analysis, magnetic field definition, and a model of electron-surface interaction. The implementation of these three components in MONT3E is presented. Suitability of the formulation to various computer architectures is discussed. An electron backscatter experiment was modeled using the code. The MONT3E predictions compared favorably to the experimental data, lending confidence to code predictions. Additional information available in the simulations provided new physical insights into the electron experiment. Comparison with the analytic solution to a related problem is also presented. DOE

N91-11515# Lawrence Livermore National Lab., CA. High Temperature Physics Div.
DESIGN AND OPERATION OF THE ELECTRON BEAM ION TRAP
David Vogel 30 May 1990 18 p
(Contract W-7405-eng-48)
(DE91-000074; UCRL-ID-104990) Avail: NTIS HC/MF A03

This report describes the basic features and operating principles of the Electron Beam Ion Trap (EBIT). The differences between EBIT and other sources of highly charged ions are outlined. Its features and operating parameters are discussed. The report also explains why certain design choices were necessary and the constraints involved in building an electron beam ion trap. EBIT's evaporation cooling system is described in detail. DOE

74 OPTICS

Includes light phenomena; and optical devices.
For lasers see *36 Lasers and Masers.*

N91-11516# Sandia National Labs., Albuquerque, NM.
THE DESIGN, TESTING AND FABRICATION OF AN EXTRUDED, LINEAR FOCUS FRESNEL LENS
Neil Kaminar and Don Curchod (Solar Engineering Applications Corp., San Jose, CA.) Aug. 1990 19 p
(Contracts DE-AC04-76DP-00789; SNL-63-8573)
(DE90-014852; SAND-90-7032) Avail: NTIS HC/MF A03

The objective of this program is to design and fabricate an extruded, curved, linear-focus Fresnel lens for use in a photovoltaic module operating at 10X concentration. The extrusion process is the least expensive lens manufacturing process, producing a lens at approx. $10/sq m. A goal to achieve 70 percent optical transmission was set. When used in a module, the housing sides are planned to be co-molded with the lens. This provides the least expensive module design available today. A 7-inch wide lens was designed, and tooling was fabricated. Several trial extrusions were made, with the best to date giving a 73 percent transmission. A post forming tool was designed and fabricated that improves the molded tooth profile to within 0.001 inch of the design. The achievement of over 70 percent transmission shows that a photovoltaic system with an installed ac buss-bar electricity cost of under $0.06/kWh can be produced. Solar Engineering Applications Corporation (SEA) is working on a second generation extruded lens with the goal to achieve 80 percent transmission and incorporation into a module. DOE

N91-11517 Deutsche Bundespost, Darmstadt (Germany, F.R.).
OPTICAL FAR-FIELD MEASUREMENTS OF EXTREMELY HIGH DYNAMIC TO INVESTIGATE THE ROUGHNESS OF FRONT FACES OF SINGLE-MODE FIBER CONNECTORS
Harmut Gruhl, Hartwig Richter, and York Rogotzki Nov. 1989 23 p In GERMAN; ENGLISH summary Original contains color illustrations
(FI-452-TB-67; ETN-90-97877) Avail: Fachinformationszentrum Karlsruhe, 7514 Egeenstein-Leopoldshafen 2, Fed. Republic of Germany

The investigation deals with the influence of surface preparation techniques applied to single mode fiber connectors on the coupling quality. The far-field intensity distribution of the light emittted from the plug is chosen as quality criterion. ESA

N91-11518 Sheffield Univ. (England).
INTEGRATED OPTICAL COMPONENTS PRODUCED IN GaAs AND InP EPITAXIAL LAYERS USING THE PHOTO-ELASTIC EFFECT Ph.D. Thesis
Trevor Mark Benson 1982 210 p
Avail: Univ. Microfilms Order No. BRDX88896

Studies were made of optical waveguides produced in GaAs and InP epitaxial layers. Of the possible waveguiding mechanisms present in these devices the contribution from the photoelastic effect dominates. Stresses in evaporated metal films and their control were investigated. Strain-induced waveguides were used to produce a novel directional-coupler structure with a short coupling length. In GaAs bias was applied to control the amount of light at the output of each of the two waveguides forming these couplers and it was possible to isolate the light in either the excited or the coupled waveguide. A new theoretical model, based on finite difference techniques, was developed and used to analyze strain-induced, slab, and rib waveguide structures. Results obtained were compared with those from other methods. Theoretical predictions of guiding properties in GaAs strain-induced waveguides give good agreement with experimental results in all cases. Dissert. Abstr.

N91-11519 Glasgow Univ. (Scotland).
INTEGRATED OPTICAL COMPONENTS FOR OPTICAL FIBRE SENSORS Ph.D. Thesis
Julian Paul Gregory Bristow 1985 267 p
Avail: Univ. Microfilms Order No. BRDX89070

The signal processing requirements of optical fiber sensors were examined and a range of integrated optical processing systems on lithium niobate substrates considered. Requirements on the constituent components of the system were analyzed. It was found that mode filters with extinction ratios of 60dB were required for Mach-Zender interferometers and for short-term gyroscopes, with the figure increasing to 90dB for inertial single-pass systems. Couplers were required to be stable and have as low an insertion loss as possible. A need for a new processing scheme for single fiber polarimetric sensors was identified. The phenomenon of surface plasma wave transverse magnetic (TM) attenuation resonance and the properties of the various surface waves were examined. These considerations were used to design metal clad stripe waveguide polarizers using silicon monoxide/aluminum claddings. Extinction ratios of up to 80 plus or minus 13dB with excess losses of 2 plus or minus 3dB were measured for an individual device, and methods for the measurement of such high ratios examined. Attempts at excitation of the short-range surface plasmon using waveguide geometries have been unsuccessful to date, but are shown to offer greatly enhanced extinction ratios or shorter devices. Other applications of a variety of surface plasma waves were considered. The design of waveguide polarizers using proton exchanged sections was considered and a geometry proposed. A device to enable efficient coupling between single-mode optical fibers and integrated stripe guides was designed and developed. The device used ion-milled grooves in lithium niobate to locate the fibers. A loss of 2.6dB was determined for the device with a projected loss of 1.8dB for the same device using index matching fluid. Dissert. Abstr.

N91-11520# Oak Ridge National Lab., TN. Metals and Ceramics Div.
X RAY MICROPROBE-MICROSCOPY
C. J. Sparks and G. E. Ice 1990 18 p Presented at the 15th International Conference on X Ray and Inner-Shell Processes, Knoxville, TN, 9-13 Jul. 1990
(Contract DE-AC05-84OR-21400)
(DE90-017327; CONF-900757-5) Avail: NTIS HC/MF A03

X rays have a unique interaction with matter that offers many advantages over electrons and other charged particles for the microcharacterization of materials. X rays are more efficient in photoejecting inner shell electrons resulting in characteristic x ray fluorescence. X rays also result in less Bremsstrahlung to produce higher fluorescent signal-to-background ratios than obtained with electrons. Detectable limits for x ray produced fluorescence could be a few parts per billion which are 10(exp -3) to 10(exp -5) lower than for electron excitation. Energy deposition in the sample from x rays is 10(exp -3) to 10(exp -4) less than for electrons for the same detectable limit. High-brightness storage rings, such as the planned Advanced Photon Source in the 7 GeV class with undulators, will have sources as brilliant as the most advanced electron probes. The highly collimated x ray beams from undulators simplify the x ray optics required to produce submicron-sized x ray probes having fluxes comparable electron sources. Such x ray microprobes will also produce unprecedentedly low levels of detection in diffraction, EXAFS, Auger, and photoelectron spectroscopies for structural and chemical characterization and elemental identification. An x ray microprobe will improve the microcharacterization capabilities and will have major applications in materials and environmental sciences and in physics, chemistry, geochemistry, biology, and medicine. Some current applications are shown. DOE

N91-11521# Centre National d'Etudes Spatiales, Toulouse (France).
FOURTEEN X FOURTEEN CCD ARRAY FOR OPTICAL INTERSATELLITE LINK TRACKING
J. C. Boutemy, G. Boucharlat, and P. Dautriche (Thomson-CSF, Sainte Egreve, France) 1 Jun. 1988 18 p In FRENCH; ENGLISH summary Presented at the 8th Journees Europeennes d'Optoelectronique, Paris, France, 17-19 May 1988
(CNES-CT/DRT/TIT/OE-88/144; ETN-90-97809) Avail: NTIS HC/MF A03

Optical intersatellite links and the SILEX program are generalized. The main constraints of the acquisition and tracking system are described. The specifications of a charge coupled device array devoted to the tracking, with the capability of high images rates (up to 20,000 im/s) are reviewed. It is shown that a low resolution and high image rate array allow the performances of the intersatellite laser acquisition system to be improved. ESA

N91-11522# Los Alamos National Lab., NM.
PRODUCTION OF UNIFORM AND WELL-CONFINED BEAMS BY NONLINEAR OPTICS
Barbara Blind 1990 5 p Presented at the 11th International Conference on the Applications of Accelerators in Research and Industry, Denton, TX, 5-8 Nov. 1990
(Contract W-7405-eng-36)
(DE91-000210; LA-UR-90-3293; CONF-901116-5) Avail: NTIS HC/MF A01

Particle beams with uniform and well-confined intensity distributions are desirable for medical treatments, food irradiation and ion implantation. Moreover, such beams are essential in the development of high-intensity accelerators to prevent target damage and optimize target efficiency. One accepted method for beam redistribution employs nonlinear beamline elements, in particular octupoles and to a lesser degree magnets of even higher odd multipolarity. The method is not limited to the production of uniform beam distributions. The development of this field is reviewed. Beam redistribution is explained and the degree of uniformity and confinement achievable under various conditions is discussed. A method for tuning the size of the irradiation area is presented. A possible alternative to the use of combined-function multipoles is given. The effect of beam jitter on the distribution is considered. Applications of the method are given as examples throughout. DOE

N91-11523# Oak Ridge National Lab., TN.
ADVANCED INFRARED OPTICALLY BLACK BAFFLE MATERIALS
Roland D. Seals, C. M. Egert, and David D. Allred (Brigham Young Univ., Provo, UT.) 1990 14 p Presented at the SPIE's International Symposium on Optical and Optoelectronic Applied Science and Engineering Exhibit, San Diego, CA, 8-13 Jul. 1990
(Contract DE-AC05-84OR-21400)
(DE91-000561; CONF-900756-44) Avail: NTIS HC/MF A03

Infrared optically black baffle surfaces are an essential component of many advanced optical systems. All internal surfaces in advanced infrared optical sensors that require stray light management to achieve resolution are of primary concern in baffle design. Current industrial materials need improvements to meet advanced optical sensor systems requirements for optical, survivability, and endurability. Baffles are required to survive and operate in potentially severe environments. Robust diffuse-absorptive black surfaces, which are (1) thermally and mechanically stable to threats of x ray, launch, and in-flight maneuver conditions, with specific densities to allow an acceptable weight load, (2) handleable during assembly, (3) cleanable, and (4) adaptive to affordable manufacturing, are required as optical baffle materials. An overview of recently developed advanced infrared optical baffle materials, requirements, manufacturing strategies, and the Optics MODIL (Manufacturing Operations Development and Integration Laboratory) Advanced Baffle Program is discussed. DOE

75 PLASMA PHYSICS

Includes magnetohydrodynamics and plasma fusion.
For ionospheric plasmas see *46 Geophysics*. For space plasmas see *90 Astrophysics*.

N91-11524# Sao Paulo Univ. (Brazil). Inst. de Fisica.
COMPUTER AND ENGINEERING CALCULATIONS OF BRAZILIAN TOKAMAK-2
S. Wang, Y. Chen, R. O. Pauletti (PROMON Engenharia S.A., Rio

de Janeiro, Brazil), W. P. DeSa, I. C. Nascimento, A. G. Tuszel, R. M. O. Galvao, and M. Machida 1990 17 p
(DE90-628758; INIS-BR-2121) Avail: NTIS (US Sales Only) HC/MF A03

Analytical and computer calculations carried out by researches of Physics Institute - University of Sao Paulo (IFUSP), for defining the engineering project and constructing the TBR-II tokamak are presented. Parameters were determined for magnetic confinement of the plasma. The computer code was developed using magnetohydrodynamics (MHD) equations which involve plasma interactions, magnetic field and electrical current circulating in more than 20 coils distributed around toroidal vase of the plasma. The electromagnetic, thermal and mechanical couplings are also presented. The TBR-II will be feed by two turbo-generators with 15 MW each one. DOE

N91-11525# Wisconsin Univ., Madison.
THE EVOLUTION OF RESISTIVE BALLOONING MODES IN THE BANANA-PLATEAU COLLISIONALITY REGIME
A. K. Sundaram (Institute for Plasma Research, Gandhingar, India) and J. D. Callen Aug. 1990 31 p Sponsored in part by Dept. of Science and Technology, Government of India
(Contract DE-FG02-86ER-53218)
(DE90-016672; UW-CPTC-90-6) Avail: NTIS HC/MF A03

The theory of resistive ballooning modes relevant to the banana-plateau collisionality regime is studied using the recently developed neoclassical MHD equations. Employing the ballooning mode formulation and a multiple length scale analysis, a generalized set of poloidal flux surface averaged equations coupling the parallel ion flow velocity, the vector potential, and the electrostatic potential are derived. A particularly simple case in which the parallel sound wave coupling reduces the order of the differential equation in the frequency range the absolute value of omega is much greater than omega(sub s), where omega(sub s) = sc(sub s)/qR(sub 0), s is the shear parameter, c(sub s) the sound speed and qR(sub 0) the connection length, is dealt with. The calculations show that a new class of localized pressure-gradient-driven ballooning modes with growth rates varying as (upsilon sub e + mu sub e)(sup 1/2) is possible, where upsilon(sub e) is the electron collision frequency and mu(sub e) is the electron neoclassical poloidal flow viscous damping frequency. It is shown that the resistive ballooning modes are sensitive to variations of a parameter eta (= the absolute value of dlnP(sub 0/dlnq) within the tokamak plasma. The enhanced ion polarization and pinch type currents are found to cause stabilization of resistive modes. Further, the model highlights a smooth transition from the Pfirsch-Schlueter to the (neoclassical) banana-plateau collisionality regimes. The relevance of these results to ISX-B experiments is briefly pointed out. DOE

N91-11526# Department of Energy, Washington, DC. Office of Health Physics and Industrial Hygiene.
IMPLICATIONS OF THE BIOLOGICAL EFFECTS OF IONIZING RADIATION (BEIR) 5 REPORT TO THE DEPARTMENT OF ENERGY Final Report
Anthony A. Weadock Aug. 1990 56 p
(DE90-016673; DOE/EH-0158T) Avail: NTIS HC/MF A04

The methodology and status of the DOE Biological Effects of Ionizing Radiation (BEIR) 5 review efforts are described. The results of the survey questionnaire that was distributed to the DOE contraction facilities which was designed to quantify potential impacts of the BEIR 5 report, are provided. The conclusions and recommendations are contained. DOE

N91-11527# Technische Univ., Delft (Netherlands). Faculty of Technical Mathematics and Informatics.
COMPENSABILITY OF UNCERTAIN SYSTEMS
W. L. deKoning 1990 18 p
(Rept-90-10; ISSN-0922-5641; ETN-90-97706) Copyright Avail: NTIS HC/MF A03

The uncertainty of linear discrete time systems with white stochastic parameters is considered in relation with the properties of mean square stability and compensability. A measure for the uncertainty in the system matrices is introduced. This measure is also a measure for the uncertainty in the system in the sense that stability and compensability decreases if this system uncertainty increases. It is indicated how to calculate numerically the mean square stability and compensability. The results are illustrated with examples. ESA

N91-11528# Royal Inst. of Tech., Stockholm (Sweden). Dept. of Plasma Physics.
DYNAMIC TRAPPING OF ELECTRONS IN SPACE PLASMAS
N. Brenning, M. Bohm, and Carl-Gunne Faelthammar Dec. 1989 37 p Sponsored by Swedish Natural Science Research Council and Swedish National Space Board
(TRITA-EPP-89-07; ISSN-0348-7539; ETN-90-97982) Avail: NTIS HC/MF A03

The neutralization of positive space charge is studied in a case where heavy positive ions are added to a limited region of length in a collisionfree magnetized plasma. It is found that electrons which become accelerated towards the positive space charge can only achieve a partial neutralization: they overshoot, and the positive region becomes surrounded by negative space charges which screen the electric field from the surroundings. The process is studied both analytically and by computer simulations with consistent results: large positive potentials can be built up with respect to the surrounding plasma. In the process in growth, the potential maximum traps electrons in transit so that quasineutrality is maintained. The potential is proportional to the ambient electron temperature and the square of the plasma density increase, but independent of both the ion injection rate and the length. The process explains several features of the Porcupine xenon beam injection experiment. It could also have importance for the electrodynamic coupling between plasmas of different densities, e.g., the injection of neutral clouds in the ionosphere of species that becomes rapidly photoionized, or penetration of dense plasma clouds from the solar wind into the magnetosphere. ESA

N91-11529# Royal Inst. of Tech., Stockholm (Sweden). Dept. of Plasma Physics.
THE PLASMA UNIVERSE
Carl-Gunne Faelthammar Dec. 1989 39 p Presented at the IAU Symposium on Basic Plasma Processes on the Sun, Bangalore, India, 1-5 Dec. 1989
(TRITA-EPP-89-08; ISSN-0348-7539; ETN-90-97983) Avail: NTIS HC/MF A03

The term plasma universe emphasizes the fact that plasma phenomena discovered in the laboratory and in accessible region of space, must be important also in the rest of the universe, which consists almost entirely of matter in the plasma state. Relevant aspects of this concept are discussed. They include the response of the plasma to electric currents, the support of magnetic field aligned electric fields, violation of the frozen field condition, rapid release of magnetically stored energy acceleration of charged particles, chemical separation, and filamentary and cellular structures. ESA

N91-11530# Royal Inst. of Tech., Stockholm (Sweden). Dept. of Plasma Physics.
LABORATORY EXPERIMENTS ON THE MAGNETIC FIELD AND NEUTRAL DENSITY LIMITS ON CIV INTERACTION
I. Axnaes and N. Brenning Mar. 1990 42 p
(TRITA-EPP-90-01; ISSN-0348-7539; ETN-90-97984) Avail: NTIS HC/MF A03

Laboratory experiments are reported which determine the magnetic field and neutral density limits for Critical Ionization Velocity (CIV) interaction in the impact configuration. A combination of microwave interferometry and spectroscopy was used to measure how the electron energy distribution varies with the neutral density and the magnetic field strength. The efficiency of the CIV process is evaluated in terms of the efficiency factor of energy transfer to the electrons. This efficiency is studied as function of the ratio VA/VO between the Alfven velocity and the plasma stream velocity and the ratio V/W between the ionization frequency and the ion gyro frequency. With other parameters kept constant, VA/VO is proportional to the square root of the magnetic field,

while V/W is proportional to the neutral density. These two dimensionless parameters are found to be coupled in such a fashion that a stronger magnetic field can compensate for a lower neutral density. For the strongest magnetic field, VA/VO = 4, CIV interaction is found to occur for a comparatively low value V/W is approximately equal to 0.1 for VA/VO = 1, a clear absence of CIV interaction even for V/W approaching unity is found. ESA

N91-11531# Royal Inst. of Tech., Stockholm (Sweden). Dept. of Plasma Physics.
POTENTIAL DROPS SUPPORTED BY ION DENSITY CAVITIES IN THE DYNAMIC RESPONSE OF PLASMA DIODE TO AN APPLIED FIELD
M. Bohm and S. Torven Jun. 1990 17 p Sponsored by Swedish Natural Science Research Council
(TRITA-EPP-90-03; ISSN-0348-7539; ETN-90-97985) Avail: NTIS HC/MF A03

Experiments showed that an applied voltage drop may either be supported by a cathode sheath or by a quasi-linear variation over the plasma lasting for several electron transit times. In the latter case an ion density cavity existed initially. An analytical model and numerical simulations are used to show that a cavity gives rise to a quasi-linear potential variation for applied voltage drops below a certain critical value. For larger values the drop concentrates to a cathode sheath. The quasi-linear profile steepens to a double layer for large cavity depths. ESA

N91-11532# National Inst. for Fusion Science, Nagoya (Japan).
A DESIGN METHOD OF DIVERTOR IN TOKAMAK REACTORS
N. Ueda, S.-I. Itoh, M. Tanaka, and K. Itoh Aug. 1990 38 p
(NIFS-36; ISSN-0915-633X) Avail: NTIS HC/MF A03

Computational method to design the efficient divertor configuration in tokamak reactor is presented. The two dimensional code was developed to analyze the distributions of the plasma and neutral particles for realistic configurations. Using this code, a method to design the efficient divertor configuration is developed. An example of new divertor, which consists of the baffle and fin plates, is analyzed. Author

N91-11533# Yale Univ., New Haven, CT.
THEORETICAL AND NUMERICAL STUDIES IN MAGNETIC MIRROR FUSION
1990 23 p
(Contract DE-FG02-86ER-53240)
(DE90-017605; DOE/ER-53240/3) Avail: NTIS HC/MF A03

The investigation is proposed of the dependence of neo-classical transport on aspect ratio and on the structure of the magnetic surfaces for general collisionality by use of relaxation models for collisions for a general mixture of electrons and ions. An optimum relaxation frequency is determined for each transport coefficient by fitting those limiting results available. Simple models of turbulent transport is added. A general purpose code is developed, including the resulting transport equations, and made accessible to the fusion community. The results of this code is compared with known results. The solutions using the simple relaxation model is compared with the counterpart results to be obtained by using a Lorentz model for collisions. DOE

N91-11534# Illinois Univ., Urbana. Fusion Studies Lab.
CTR PLASMA ENGINEERING STUDIES Annual Progress Report, 1 Dec. 1989 - 30 Nov. 1990
George H. Miley 1990 26 p
(Contract DE-FG02-86ER-52127)
(DE90-017774; DOE/ER-52127/72) Avail: NTIS HC/MF A03

The main focus of the work by the Fusion Plasma Engineering Group at the University during the prior contract year involved a study of fusion ash (helium) effects on burn efficiency and on potential ways to control ash buildup. This work has wide application to a variety of fusion reactor concepts, but the immediate application for the present work is in the ARIES tokamak reactor design study now being undertaken by a national design team headed by the UCLA. The examples presented here largely deal with the ARIES-I design which is a D-T device operating in the first instability regime. DOE

N91-11535# Wisconsin Univ., Madison. Plasma Physics Research.
CONFINEMENT AND FLUCTUATIONS IN THE MST (MADISON SYMMETRIC TORUS) REVERSED FIELD PINCH
J. C. Sprott, A. F. Almagri, S. Assadi, J. A. Beckstead, G. Chartas, N. Dexter, D. J. DenHartog, S. A. Hokin, D. J. Holly, and S. C. Prager et al Sep. 1990 11 p Presented at the 13th International Conference on Plasma Physics and Controlled Nuclear Fusion Research, Washington, DC, 1-6 Oct. 1990
(Contract DE-FG02-85ER-53198)
(DE90-018019; DOE/ER-53198/160; CONF-901025-7; IAEA-CN-53/C-2-2-(2)) Avail: NTIS HC/MF A03

MST is a large (R sub 0/a = 1.5/0.52 m) RFP which to date has obtained 80 ms discharges at a peak plasma current of 0.6 MA. Low loop voltages (15 volts) and modest temperatures (T sub e/T sub i) (approx) 350/250 eV) are routinely obtained giving estimated unoptimized energy confinement times of about 1 ms. Loop voltage and ion temperature are anomalous. Magnetic fluctuations are typically 0.5 percent with most of the power at frequencies below 30 kHz and mode numbers in agreement with MHD prediction for tearing modes. Electrostatic fluctuations are typically 10 to 20 percent with a spectrum that decreases with frequency. DOE

N91-11536# International Atomic Energy Agency, Vienna (Austria).
FLUCTUATIONS AND STABILITY IN THE ADVANCED TOROIDAL FACILITY (ATF) TORSATRON
J. H. Harris, L. A. Charlton, J. D. Bell, T. S. Bigelow, B. A. Carreras, R. J. Colchin, E. C. Crume, N. Dominguez, J. L. Dunlap, and G. R. Dyer et al 1990 12 p Presented at the 13th International Conference on Plasma Physics and Controlled Nuclear Fusion Research, Washington, DC, 1-6 Oct. 1990 Prepared in cooperation with Auburn Univ., AL; European Atomic Energy Community, Madrid, Spain; Wisconsin Univ., Madison; Georgia Inst. of Technology, Atlanta; and Texas Univ., Austin
(Contract DE-AC05-84OR-21400)
(DE90-017734; IAEA-CN-53/C-4-7; CONF-901025-8) Avail: NTIS HC/MF A03

We present the results of experimental and theoretical studies of fluctuations and instabilities in the Advanced Toroidal Facility (ATF) torsatron, a type of stellarator. Measurements of globally coherent magnetic fluctuations in high-(beta) plasmas with narrow pressure profiles produced by a field error show evidence of self-stabilization (second stability); the trends are compatible with theoretical analysis of self-stabilization of resistive curvature-driven instabilities, but there are discrepancies between the absolute experimental and theoretical fluctuation amplitudes. Fluctuation measurements in plasma with broad pressure profiles reveal new phenomena--specifically, toroidally localized magnetic fluctuations, whose amplitudes increase with plasma pressure, and coherent density fluctuations with significant radial width. DOE

N91-11537# Argonne National Lab., IL.
THREE-DIMENSIONAL COMPUTER SIMULATION OF NON-REACTING JET-GAS FLOW MIXING IN AN MHD SECOND STAGE COMBUSTOR
S. L. Chang, S. A. Lottes, and G. F. Berry 1990 9 p Presented at the 28th Symposium on Engineering Aspects of Magnetohydrodynamics, Chicago, IL, 26-28 Jun. 1990
(Contract W-31-109-eng-38)
(DE90-017831; CONF-9006105-12) Avail: NTIS HC/MF A02

Argonne National Laboratory is investigating the non-reacting jet-gas mixing patterns in a magnetohydrodynamics (MHD) second stage combustor by using a three-dimensional single-phase hydrodynamics computer program. The computer simulation is intended to enhance the understanding of flow and mixing patterns in the combustor, which in turn may improve downstream MHD channel performance. The code is used to examine the three-dimensional effects of the side walls and the distributed jet

flows on the non-reacting jet-gas mixing patterns. The code solves the conservation equations of mass, momentum, and energy, and a transport equation of a turbulence parameter and allows permeable surfaces to be specified for any computational cell. DOE

N91-11538# Argonne National Lab., IL. Energy Systems Div.
EFFECTS OF JET PORT ARRANGEMENT ON THREE-DIMENSIONAL NON-REACTING JET-GAS MIXING IN AN MHD SECOND STAGE COMBUSTOR
S. A. Lottes, S. L. Chang, and G. F. Berry 1990 6 p Presented at the 25th Intersociety Energy Conversion Engineering Conference, Reno, NV, 12-17 Aug. 1990 Submitted for publication
(Contract W-31-109-eng-38)
(DE90-017858; CONF-900801-33) Avail: NTIS HC/MF A02

A three-dimensional hydrodynamics computer code was used to investigate the flow mixing processes in a magneto-hydrodynamics (MHD) second stage combustor. The code solves the conservation equations of mass, momentum, energy, and a transport equation of turbulence kinetic energy. The flow mixing patterns of four different jet port arrangements, including a 12-jet, an 8-center-jet, an 8-side-jet, and an 8-mixed-jet (4 side and 4 center jets), were computed and compared. Jet and gas seems to mix in two stages: an early and more effective convective stage and a later diffusive stage. For the same bulk jet concentration, the 12-jet arrangement has better jet-gas mixing than the other three 8-jet arrangements. DOE

N91-11539# Montana State Univ., Bozeman. Dept. of Mechanical Engineering.
CORROSION AND ARC EROSION IN MHD CHANNELS
Quarterly Progress Report, Jan. - Mar. 1990
Richard J. Rosa and Richard J. Pollina 27 Apr. 1990 3 p
(Contract DE-AC22-84PC-70507)
(DE90-017889; DOE/PC-70507/T3) Avail: NTIS HC/MF A02

The objective of this task is to study the corrosion and arc erosion of magnetohydrodynamic (MHD) materials in a cooperative effort with, and to support, the MHD topping cycle program. Materials tested in the Avco Research Laboratory/Textron facility, or materials which have significant MHD importance, will be analyzed to document their physical deterioration. Conclusions shall be drawn about their wear mechanisms and lifetime in the MHD environment with respect to the following issues: sulfur corrosion, electrochemical corrosion, and arc erosion. The impact of any materials or slag conditions on the level of power output and on the level of leakage current in the MHD channel will also be noted, where appropriate. The detailed correlation and analysis of data obtained from nearly all of the tests performed since 1986 has shown that the apparent leakage current flowing through the slag on the channel walls depends upon channel operating parameters in an unexpected way. A comprehensive report of the results obtained to date and a first attempt at their interpretation has been prepared and a copy is attached. The second activity has concerned the examination of electrodes (platinum anodes/tungsten cathodes) by scanning electron microscopy and energy dispersive x ray spectroscopy of the surface degradation. Results of these examinations are reported. DOE

N91-11540# Texas Univ., Austin. Inst. for Fusion Studies.
NATURAL CURRENT PROFILES IN A TOKAMAK
J. B. Taylor Aug. 1990 12 p
(Contract DE-FG05-80ET-53088)
(DE91-000128; DOE/ET-53088/447; IFSR-447) Avail: NTIS HC/MF A03

How one may arrive at a universal, or natural, family of Tokamak profiles using only accepted physical principles is shown. These particular profiles are similar to ones proposed previously on the basis of ad hoc variational principles and the point of the present paper is to provide a justification for them. However in addition, an interesting view of Tokamak fluctuations is provided which leads to a new result -- a relationship between the inward particle pinch velocity, the diffusion coefficient and the current profile. The basic Tokamak model is described. Then an analogy is developed between Tokamak profiles and the equilibrium of a realizable dynamical system. Then the equations governing the natural Tokamak profiles are derived by applying standard statistical mechanics to this analog. The profiles themselves are calculated and some other results of the theory are described. DOE

N91-11541# Swedish Inst. of Space Physics, Umea.
A COMBINED WAVE DISTRIBUTION FUNCTION AND STABILITY ANALYSIS OF VIKING PARTICLE AND LOW-FREQUENCY WAVE DATA
Tord E. Oscarsson and Kjell G. Roennmark Apr. 1990 39 p Submitted for publication
(IRF-Preprint-115; ETN-90-97987) Avail: NTIS HC/MF A03

The low frequency waves observed on auroral field lines below the acceleration region by the Swedish satellite Viking are investigated. The measured frequency spectra are peaked at half the local proton gyrofrequency. The waves are observed in close connection with precipitating electrons. In order to obtain information about the distribution of wave energy in wavevector space, the Wave Distribution Function (WDF) is constructed from observed spectral densities. The scheme allows the simultaneous reconstruction of WDF over a broad frequency band. Available particle observations and Doppler shifts are taken into account. The distribution of energy in wavevector space suggested by the reconstructed WDF is found to be consistent with what is expected from a plasma instability driven by the observed precipitating electrons. It is demonstrated that the wave propagation directions indicated by the reconstructed WDFs are consistent with a simple model of the presumed wave source in the electron precipitation region. ESA

N91-11542# TRW, Inc., Redondo Beach, CA. Applied Technology Div.
MHD TECHNOLOGY TRANSFER, INTEGRATION, AND REVIEW COMMITTEE
May 1990 253 p
(Contract DE-AC22-87PC-90274)
(DE90-017886; DOE/PC-90274/T8; MHD-ITC-90-133) Avail: NTIS HC/MF A12

As part of Task 8 of the magnetohydrodynamic (MHD) Integrated Topping Cycle (ITC) project, TRW was given the responsibility to organize, charter and co-chair, with the Department of Energy (DOE), an MHD Technology Transfer, Integration and Review Committee (TTIRC). The TTIRC consists of an Executive Committee (EC) which acts as the governing body, and a General Committee (GC), also referred to as the main or full committee, consisting of representatives from the various POC contractors, participating universities and national laboratories, utilities, equipment suppliers, and other potential MHD users or investors. The purpose of the TTIRC is to: (1) review all Proof-of-Concept (POC) projects and schedules in the national MHD program; to assess their compatibility with each other and the first commercial MHD retrofit plant; (2) establish and implement technology transfer formats for users of this technology; (3) identify interfaces, issues, and funding structures directly impacting the success of the commercial retrofit; (4) investigate and identify the manner in which, and by whom, the above should be resolved; and (5) investigate and assess other participation (foreign and domestic) in the U.S. MHD Program. There are seven sections: introduction; Executive Committee and General Committee activity; Committee activities related to technology transfer; ongoing POC integration activities being performed under the auspices of the Executive Committee; recommendations passed on to the DOE by the Executive Committee; Planned activities for the next six months. DOE

N91-11543# Nagoya Univ. (Japan). Plasma Science Center.
ON HYDRODYNAMICS OF COLLISIONLESS RELATIVISTIC PLASMA IN A STRONG MAGNETIC FIELD
J. G. Lominadze, J. I. Javakhishvili, and E. G. Tsikarishvili (Abastumani Astrophysical Observatory, Georgia, USSR) Nov. 1989 14 p Presented at the Plasma Astrophysics Workshop, Nagoya, Japan, 11-18 Oct. 1989 Sponsored in part by Daiko

Foundation
(DE90-513926; PSC-2) Avail: NTIS (US Sales Only) HC/MF A03

A closed set of hydrodynamical equations based on a relativistic kinetic equation is presented. This set of equations describes relativistic strongly magnetized plasma with an anisotropic pressure tensor. Such a model was suggested previously by Chew, Goldberger, and Low for nonrelativistic plasma. Here, the main macroscopic parameters in the relativistic theory are determined based on a relativistic kinetic equation. Then, a closed system of hydrodynamic equations for relativistic collisionless plasma is derived. Thus, it is shown that a closed set of hydrodynamical equations for collisionless relativistic plasma in a strong magnetic field can be formulated. Such a strong magnetic field leads to anisotropy of macroscopic parameters of the plasma. The equations obtained are rather complicated, though analogous to those derived from the nonrelativistic theory. The difference is that the relativistic theory requires a larger number of parameters to describe the plasma: instead of the six unknown quantities in the nonrelativistic case, nine quantities are necessary in the relativistic case. DOE

N91-11544# China Nuclear Information Centre, Beijing.
INVESTIGATION ON THE PROJECTION BY A Z-PINCH DISCHARGE
Zhaoxing Ren, Shuqing Zhang, Chaosong Huang, Yahong Li, Deying Tao, and Weidong Xie Sep. 1988 10 p In ENGLISH and CHINESE Prepared in cooperation with Academia Sinica, Hefei (China)
(DE90-637548; CNIC-00234; ASIPP-0005) Avail: NTIS (US Sales Only) HC/MF A02

A projectile in a barrel can be propelled by thermal pressure and electromagnetic force produced in a Z-pinch discharge plasma. Comparing experimental results with the theoretical model find that the propelling force from the thermal pressure is higher than that from the electromagnetic force, when the muzzle velocity of the projectile is at the order of 100 m/s. DOE

N91-11545# Los Alamos National Lab., NM.
COMPLETE FLUID EQUATIONS FOR LOW-n SINGULAR MODES IN AXISYMMETRIC TORODIAL PLASMAS
Alan H. Glasser 1990 11 p Presented at the Joint Varenna-Lausanne International Workshop on Theory of Fusion Plasmas, Varenna, Italy, 27-31 Aug. 1990
(Contract W-7405-eng-36)
(DE91-000176; LA-UR-90-3345; CONF-900807-1) Avail: NTIS HC/MF A03

The goal was to develop a complete linear theory of the singular region, including all important dynamical effects. The present phase of the work treats the more collision fluid regime. A later phase will treat the less collisional gyrokinetic regime. The derivation and form of the fluid equations for the singular region of low-n modes. Later work will treat high-n ballooning modes is examined. In addition, the ordering in the present work must be amended before it is applicable to the neighborhood of the field reversal surface of the RFP. DOE

N91-11546# Los Alamos National Lab., NM. Theoretical Div.
CONCEPTS IN STRONG LANGMUIR TURBULENCE THEORY
D. F. DuBois and Harvey A. Rose 1990 32 p Presented at the 1990 Summer Workshop on Nonlinear and Chaotic Phenomena in Plasmas, Solids, and Fluids, Edmonton, Alberta, 16-27 Jul. 1990
(Contract W-7405-eng-36)
(DE91-000208; LA-UR-90-3311; CONF-9007136-4) Avail: NTIS HC/MF A03

Some of the basic concepts of strong Langmuir turbulence (SLT) theory are reviewed. In SLT system, a major fraction of the turbulent energy is carried by local, time-dependent, nonlinear excitations called cavitons. Modulational instability, localization of Langmuir fields by density fluctuations, caviton nucleation, collapse, and burnout and caviton correlations are reviewed. Recent experimental evidence will be presented for SLT phenomena in the interaction of powerful high-frequency (HF) waves with the ionosphere and in laser-plasma interaction experiments. DOE

N91-11547# Lawrence Livermore National Lab., CA.
ECH BY FEL AND GYROTRON SOURCES ON THE MICROWAVE TOKAMAK EXPERIMENT (MTX) TOKAMAK
B. W. Stallard, W. C. Turner, S. L. Allen, J. A. Byers, B. Felker, M. E. Fenstermacher, S. W. Ferguson, E. G. Hooper, K. I. Thomassen, and A. L. Throop et al 9 Aug. 1990 12 p Presented at the 16th Symposium on Fusion Technology, London, England, 3-7 Sep. 1990 Submitted for publication
(Contract W-7405-eng-48)
(DE91-000286; UCRL-JC-104573; CONF-900918-6) Avail: NTIS HC/MF A03

The Microwave Tokamak Experiment (MTX) at LLNL is studying the physics of intense pulse ECH is a high-density tokamak plasma using a microwave FEL. Related technology development includes the FEL, a windowless quasi-optical transmission system, and other microwave components. Initial plasma experiments have been carried out at 140 GHz with single RF pulses generated using the ETA-2 accelerator and the ELF wiggler. Peak power levels up to 0.2 GW and pulse durations up to 10 ns were achieved for injection into the plasma using as untapered wiggler. FEL pulses were transmitted over 33 m from the FEL to MTX using six mirrors mounted in a 50 cm diam evacuated pipe. Measurements of the microwave beam and transmission through the plasma were carried out. For future rapid pulse experiments at high average power (4 GW peak power, 5 kHz pulse rate, and bar P is greater than 0.5 MW) using the IMP wiggler with tapered magnetic field, a gyrotron (140 GHz, 400 kW CW or up to 1 MW short pulse) is being installed to drive the FEL input or to directly heat the tokamak plasma at full gyrotron power. Quasi-optic techniques will be used to couple the gyrotron power. For direct plasma heating, the gyrotron will couple into the existing mirror transport system. Using both sources of RF generation, experiments are planned to investigate intense pulse absorption and tokamak physics, such as the ECH of a pellet-fueled plasma and plasma control using localized heating. DOE

N91-11548# Texas Univ., Austin. Inst. for Fusion Studies.
NONLINEAR SATURATION OF IDEAL INTERCHANGE MODES IN A SHEARED MAGNETIC FIELD
A. D. Beklemishev (Kurchatov, I. V. Inst. of Atomic Energy, Moscow, USSR) Sep. 1990 45 p
(Contract DE-FG05-80ET-53088)
(DE91-000575; DOE/ET-53088/455; IFSR-455) Avail: NTIS HC/MF A03

Pressure-driven ideal modes cannot completely interchange flux tubes of a sheared magnetic field; instead, they saturate, forming new helical equilibria. These equilibria are studied both analytically and numerically with reduced MHD equations in a flux conserving Lagrangian representation. For unstable localized modes, the structure of the nonlinear layer generated around the resonant flux surface depends on the value of Mercier parameter D sub M. Its width is found to be proportional to the position of the inflection point on the linear eigenfunction. Perturbed surfaces in equilibrium always have folds, i.e., areas where the direction of the original reduced magnetic field is reserved. But only far from the instability threshold does the internal structure of the nonlinear layer resemble bubble formation. The appearance of sheet currents and island-like structures along the resonant flux surface may be of interest for the description of forced reconnection in models with finite resistivity. Analytic results are found to be in agreement with 2-D numerical simulations. The case of ballooning instability is included by representing nonlocal driving terms through the matching parameter (Delta prime), which defines the outer boundary conditions for the interchange layer. DOE

N91-11549# Missouri Univ., Rolla. Dept. of Physics.
COLLISIONAL PROCESSES OF INTEREST IN MFE PLASMA RESEARCH Annual Report, 1 Jun. 1989 - 31 May 1990
R. E. Olson 24 May 1990 14 p

(Contract DE-FG02-84ER-53175)
(DE91-000598; DOE/ER-53175/5) Avail: NTIS HC/MF A03

The calculation is studied of heavy particle collision cross sections needed for diagnostic studies of magnetic fusion plasmas. The development and testing of new theoretical methods is required along with the implementation of benchmarked techniques to collisions pertinent to fusion reactors. Within the last context, charge exchange recombination cross sections are provided for specific n,1-levels for diagnostic studies on TFTR and for a major compilation for IAEA. A cross section study was completed related to the planned neutral beam current drive for ITER. In addition, calculations were completed to assess the use of He neutral atom angular scattering measurements for JT-60. Also, new theoretical methods were developed to more accurately calculate cross sections involving either He or H2 targets and partially stripped multiply charged ions. DOE

N91-11550# Consiglio Nazionale delle Ricerche, Frascati (Italy). Ist. di Fisica dello Spazio Interplanetario.
ION DYNAMICS IN THE PLASMA MANTLE
J. Akinrimisi, S. Orsini, M. Candidi, and H. Balsiger (Bern Univ., Switzerland) Nov. 1989 33 p Original contains color illustrations
(IFSI-89-20; ETN-90-97781) Avail: NTIS HC/MF A03

A comprehensive statistical analysis was performed on plasma mantle data from the positive ion experiment on the International Sun Earth Explorer-2 (ISEE-2) and the ion composition experiment on ISEE-1 during the first six months of 1978 and 1979 in the Earth's magnetotail between 8 and 22 Re. Particular emphasis was given to plasma mantle-plasma sheet crossings so as to elucidate the role of mantle plasma in the refilling of the plasma sheet. It is shown that mantle plasma contiguous to the plasma sheet is convected primarily away from the magnetopause towards the center of the tail equatorial region. Subsequently it undergoes thermalization and isotropization and merges with the plasma sheet. ESA

N91-11551# Consiglio Nazionale delle Ricerche, Frascati (Italy). Ist. di Fisica dello Spazio Interplanetario.
THE SIM.PL.EX. PLASMA CHAMBER (SIMULATORI DI PLASMA EXTRATERRESTRE) Progress Report, Dec. 1988
P. Baldetti, P. Capizzi, C. B. Cosmovici, F. DeVenuto, Gianfranco Ferri, U. Guidoni, M. Leonetti, M. Maggi, A. Morbidini, and S. Ugazio et al Mar. 1990 45 p
(IFSI-90-8; ETN-90-97791) Avail: NTIS HC/MF A03

The use of the SIMPLEX nine cubic meter plasma chamber to simulate as far as possible the Tethered Satellite System (TSS) electrodynamic phenomena at ionospheric altitudes is described. The vacuum system, pressure gages, quadrupole mass spectrometer, spectrograph, additional vacuum chamber, hollow cathode source, magnetic field system and plasma diagnostic system are included in the technical description. TSS power generation and plasma characteristics are addressed. ESA

76 SOLID-STATE PHYSICS

Includes superconductivity.

For related information, see also *33 Electronics and Electrical Engineering* and *36 Lasers and Masers.*

N91-11552# Universal Sensors, Inc., Metairie, LA.
A PROTEIN COATED PIEZOELECTRIC CRYSTAL DETECTOR Final Report, Mar. 1987 - Aug. 1989
Ahmad Suleiman, Marie Pender, Jerome Ngeh-Ngwainbi, Glenn Lubrano, and George Guilbault May 1990 93 p
(Contract DAAA15-87-C-0004)
(AD-A223848; CRDEC-CR-075) Avail: NTIS HC/MF A05 CSCL 20/13

The purpose of this project was to develop a protein coated, portable piezoelectric crystal detector for organophosphorus compounds. The performance of acetylcholinesterase, GD-1 anti-soman, anti-DMMP antibody, and bovine serum albumin (BSA) coatings was evaluated. Different immobilization methods were also tested. The responses obtained with the protein coatings immobilized via cross-linking with glutaraldehyde were acceptable, provided that the reference crystal was coated with dextran. The proposed coatings showed good stability and reasonable lifetimes that ranged from approximately three weeks in the case of the antibody coatings to several months in the case of BSA. Although moisture, gasoline, and sulfur are potential interferents, their effects on the sensor were eliminated by using a sodium sulfate scrubber which did not affect the performance of the detector towards organophosphates. A small, battery operated portable instrument capable of real time measurements with alarm function was produced. The instrument can be used in a wide range of applications, depending on the coatings applied to the crystals. GRA

N91-11553# Center for Mathematics and Computer Science, Amsterdam (Netherlands). Dept. of Numerical Analysis.
NON-LINEAR MULTIGRID IN 2-D SEMICONDUCTOR DEVICE SIMULATION: THE ZERO CURRENT CASE
J. Molenaar Nov. 1989 18 p
(CWI-NM-R8917; ETN-90-97672) Copyright Avail: NTIS HC/MF A03

The nonlinear Poisson equation, encountered in semiconductor device simulation, is discretized by the mixed finite element method. Two nonlinear relaxation methods are presented to solve the discretized equations; both minimize appropriate functionals. One of them, a five-point Vanka-type relaxation is used in a multigrid algorithm. Numerical results are given for simple diode problems. ESA

N91-11554# Center for Mathematics and Computer Science, Amsterdam (Netherlands). Dept. of Numerical Analysis.
A MULTIGRID APPROACH FOR THE SOLUTION OF THE 2D SEMICONDUCTOR EQUATIONS
J. Molenaar and P. W. Hemker Feb. 1990 21 p
(CWI-NM-R9003; ETN-90-97681) Copyright Avail: NTIS HC/MF A03

A multigrid method for the solution of the steady semiconductor equations is presented. The discretization is made of an adaptive grid, by means of a mixed finite element method on rectangles, with the trapezoidal quadrature rule. In one dimension the resulting scheme reduces to the well known Scharfetter-Gummel discretization. The grid transfer operators are selected in accordance with the discretization. The multigrid solution method is based on a collective, symmetric 5-point Vanka relaxation, and in order to admit very coarse grids a local damping of the coarse grid is applied. It is shown that the convergence rate is independent of the grid size. Since nested iteration is combined with the multigrid iteration, the resulting solution method has optimal efficiency. ESA

N91-11555*# National Aeronautics and Space Administration. Lewis Research Center, Cleveland, OH.
MIS CAPACITOR STUDIES ON SILICON CARBIDE SINGLE CRYSTALS Final Report, 8 May - 8 Nov. 1989
J. J. Kopanski (National Inst. of Standards and Technology, Gaithersburg, MD.) Sep. 1990 43 p
(NASA Order C-30018-M; NASA Order C-30007-K)
(NASA-CR-187350; NAS 1.26:187350; PB90-257718; NISTIR-4352) Avail: NTIS HC/MF A03 CSCL 20L

Cubic SiC metal-insulator-semiconductor (MIS) capacitors with thermally grown or chemical-vapor-deposited (CVD) insulators were characterized by capacitance-voltage (C-V), conductance-voltage (G-V), and current-voltage (I-V) measurements. The purpose of these measurements was to determine the four charge densities commonly present in an MIS capacitor (oxide fixed charge, N(f); interface trap level density, D(it); oxide trapped charge, N(ot); and mobile ionic charge, N(m)) and to determine the stability of the device properties with electric-field stress and temperature. The section headings in the report include the following: Capacitance-voltage and conductance-voltage measurements;

Current-voltage measurements; Deep-level transient spectroscopy; and Conclusions (Electrical characteristics of SiC MIS capacitors). GRA

N91-11556 Oxford Univ. (England).
ION DYNAMICS IN SEMICONDUCTORS WITH SELF-CONSISTENT ELECTRONIC DENSITIES Ph.D. Thesis
Dahlia Karin Remler 1989 171 p
Avail: Univ. Microfilms Order No. BRD-89446

The recently introduced Car-Parrinello (CP) method combines molecular dynamics and electronic structure calculations to allow for the simulation of dynamics in materials not previously amenable to study. The use of the CP method to simulate the dynamics of core ions and the accompanying adiabatic dynamics of valence electrons in semi-conductors and metals is examined. All the equations and algorithms necessary to implement the CP method are derived and discussed. The choice of basis sets and in particular the appropriateness of Brillouin zone sampling schemes for CP simulations of dynamics in disordered systems is analyzed. It is suggested that the most important characteristic of the CP method is that it permits stable simulations of the ionic motion to be undertaken efficiently. Model simulations are performed with similar schemes which do not permit stable and efficient dynamics. The sources of stability in the CP method are analyzed. CP simulations of crystalline germanium undergoing thermal motion and various phonon motions were performed. The physical processes which contribute to the forbidden (2,2,2) x ray reflection in germanium were analyzed. The contributions from the core and valence electrons were separated. The effects of the ionic motion on those contributions was studied through simulation and analytic calculation. The effects on the (2,2,2) scattering of the finite size and imperfect equilibration of simulations were examined analytically. Dissert. Abstr.

N91-11557# Midwest Research Inst., Golden, CO. Solar Energy Research Inst.
STRUCTURE OF AMORPHOUS-SILICON AND GERMANIUM ALLOY FILMS
R. E. Norberg and P. A. Fedders (Washington Univ., Saint Louis, MO.) Aug. 1990 32 p
(Contract DE-AC02-83CH-10093)
(DE90-000355; SERI/TP-211-3908) Avail: NTIS HC/MF A03

The principal objective of this research program was to improve the understanding at the microscopic level of amorphous silicon-germanium alloy films deposited under various conditions to assist researchers to produce higher quality films. The method has been a joint theoretical and experimental approach to the correlation of NMR, ESR, and other characterizations, especially relating to rearrangements of hydrogen. Deuteron magnetic resonance reveals the presence of (and changes in) tightly bonded hydrogen (deuterium), weakly bonded hydrogen, molecular hydrogen, rotating silyl and hydrogen molecules trapped on nanovoid surfaces. Theoretical calculations show that there are serious errors in many computer simulations of amorphous solid Si and liquid Si. DOE

N91-11558# Oak Ridge National Lab., TN. Metals and Ceramics Div.
MECHANICAL PROPERTIES, FRACTURE BEHAVIOR, AND GRAIN-BOUNDARY CHEMISTRY OF B-DOPED NiAl
E. P. George, C. T. Liu, and J. J. Liao (Auburn Univ., AL.) 1990 6 p Presented at the Fall Meeting of the Materials Research Society, Boston, MA, 26 Nov. - 1 Dec. 1990
(Contract DE-AC05-84OR-21400)
(DE90-015153; CONF-901105-3) Avail: NTIS HC/MF A02

This paper summarizes the results of our work aimed at overcoming the intrinsic grain-boundary weakness of NiAl by microalloying with boron. In previous work we have shown that 300 wppm boron is very effective in suppressing intergranular fracture in NiAl. It does this by segregating strongly to the grain boundaries and strengthening them. Despite this dramatic effect on the fracture mode, however, boron is unable to improve ductility because it is a potent solid solution strengthener, more than doubling the yield strength relative to that of undoped NiAl. The present work attempts to decrease this deleterious hardening effect by lowering the bulk concentration of boron in NiAl. Our results show that if the boron concentration in the bulk is lowered to 30 wppm, the yield strength of boron-doped NiAl is only about 30 percent higher than that of undoped NiAl. In addition, there is enough boron at the grain boundaries of this alloy to suppress intergranular fracture. Under these conditions, boron-doped NiAl has a tensile ductility of 2 percent, which is essentially identical to that of undoped NiAl. This result, namely that the strengthening of grain boundaries might well be the weakest links in NiAl, cleavage planes are not much stronger. In other words, even though boron additions serve to strengthen the grain boundaries and suppress intergranular fracture, ductility is not improved, because the next brittle fracture mode, namely transgranular cleavage, takes over before significant plastic deformation can occur. DOE

N91-11559# Sandia National Labs., Albuquerque, NM.
ELECTRIC-FIELD DEPENDENT ELECTROREFLECTANCE AND PHOTOCURRENT SPECTROSCOPY IN InGaAs/InAlAs STRAINED-LAYER SUPERLATTICES
I. J. Fritz, J. F. Klem, T. M. Brennan, J. R. Wendt, and T. E. Zipperian 1990 4 p Presented at the Fall Meeting of the Materials Research Society, Boston, MA, 26 Nov. - 1 Dec. 1990
(Contract DE-AC04-76DP-00789)
(DE90-015698; SAND-90-1718C; CONF-901105-4) Avail: NTIS HC/MF A01

Strained-layer epitaxy provides unique flexibility in tailoring the physical properties of compound semiconductor quantum-well structures. For example, without constraints on lattice matching it is possible to vary bandgap by varying alloy composition in many material systems. Currently, InGaAs alloys are receiving much attention because their bandgaps span the near-infrared wavelength range of interest for optical communication. Sanders and Chang and Hong, et. al., have shown that superimposed HH and LH bandgaps lead to enhanced optical absorption at the bandgap due to: (1) the addition of the two oscillator strengths, and (2) an increase in the density of states due to the modified valence-band dispersion. These effects may enhance the performance of optoelectronic devices. In the following we consider the design of InGaAs/InAlAs strained quantum-well structures with wells in biaxial tension and bandgap energies near 0.80 eV (1.55 micron wavelength). We present first some model calculations and then data on two-strained layer superlattice (SLS) structures, including results with applied electric field. DOE

N91-11560# Sandia National Labs., Albuquerque, NM. Dept. of Compound Semiconductor and Device Research.
NONPARABOLIC CONDUCTION BANDS AND MASSES IN STRAINED-SINGLE-QUANTUM WELLS
E. D. Jones, J. F. Klem, K. Lyo, S. Y. Lin, and D. C. Tsui (Princeton Univ., NJ.) 1990 5 p Presented at the Fall Meeting of the Materials Research Society, Boston, MA, 26 Nov. - 1 Dec. 1990
(Contract DE-AC04-76DP-00789; AF-AFOSR-0248-88)
(DE90-017028; SAND-90-1755C; CONF-901105-8) Avail: NTIS HC/MF A01

Experimental measurements of the conduction band dispersion curves in bulk GaAs and GaAs/AlGaAs (and InGaAs/GaAs) quantum well structures generally have been restricted to cyclotron resonance measurements. To obtain an accurate conduction band E vs. k dispersion curve using cyclotron resonance measurements, many different samples with differing carrier concentrations are required. The various parameters to the band structure then have been obtained by fitting a k-p calculation to the data. The breaking of the usual selection rules for magneto-luminescence transitions by coulomb scattering of the carriers by the dopant ions has been discussed. Theory and experiment show that higher order transitions dominate the recombination process at low temperatures, while the direct transitions dominate at higher temperatures. The temperature dependences permit a simultaneous determination both the conduction and valence-band dispersion curves and has been reported for In(x)Ga(1-x)As/GaAs strained single quantum well (SSQW) structures. The results are presented

of the measurements the conduction band energy dispersion curve (and nonparabolic conduction band mass) obtained from magneto-luminescence measurement on a single In(0.25)Ga-(0.75)As/GaAs 80A n-type SSQW structure. Also presented are the results of the measurement, on the same sample, of the conduction band mass using far infrared cyclotron resonance techniques. DOE

N91-11561# Sandia National Labs., Albuquerque, NM. Dept. of Compound Semiconductor and Device Research.
PHOTOLUMINESCENCE STUDIES OF In(x)Ga(1-x)As/Al(y) Ga(1-y)As STRAINED-LAYER STRUCTURES
E. D. Jones, L. R. Dawson, J. F. Klem, D. R. Myers, J. R. Wendt, and T. E. Zipperian 1990 5 p Presented at the Fall Meeting of the Materials Research Society, Boston, MA, 26 Nov. - 1 Dec. 1990
(Contract DE-AC04-76DP-00789)
(DE90-017031; SAND-90-1756C; CONF-901105-9) Avail: NTIS HC/MF A01

Photoluminescence measurement techniques are a valuable tool in determining the purity of semiconductor materials. Low temperature photoluminescence measurements are presented to demonstrate the effects due to rapid thermal anneals (RTA) on three different In(x)Ga(1-x)As Al(y)Ga(1-y)As strained single quantum well (SSQW) structures. Two of the structures are unintentionally doped and the other is a beryllium doped, p-type structure. One of the unintentionally doped structures provides an example of strain metastability and the effects of annealing. The remaining structures provide examples of where the RTA had little effect, but other changes in the luminescence spectra are noted. DOE

N91-11562# Sandia National Labs., Albuquerque, NM.
STRESS ACCOMMODATION IN LARGE-MISMATCH SYSTEMS
Brian W. Dodson 1990 23 p Presented at the 6th International Conference on Molecular Beam Epitaxy, La Jolla, CA, 27-31 Aug. 1990
(Contract DE-AC04-76DP-00789)
(DE90-017032; SAND-90-2282C; CONF-900856-1) Avail: NTIS HC/MF A03

Accommodation of lattice mismatch is investigated for the case of large (epsilon greater than 0.02) mismatch. The conventional Matthews-Blakeslee mechanism for creation of misfit dislocations is found to be inadequate for the case of large lattice relaxation owing to interactions amongst the misfit dislocations at the interface. In particular, the regime where the separation D between misfit dislocations is much less than the strained layer thickness h is considered. The energetics of insertion of dense misfit dislocation networks is examined. According to St Venant's Principle, the existence of a new length scale, D, serves as a cutoff for the stress fields of the dislocation network. This observation has several consequences, including the prevention of relaxation by repulsive interaction amongst threading dislocation segments and the melting of moderately relaxed heterointerfaces at conventional semiconductor growth temperatures. A number of experimental observations may be explained via these models. DOE

N91-11563# Sandia National Labs., Albuquerque, NM.
OPTICAL CHARACTERIZATION OF CdZnTe/CdTe STRAINED QUANTUM WELLS
J. L. Reno and E. D. Jones 1990 5 p Presented at the Fall Meeting of the Materials Research Society, Boston, MA, 26 Nov. - 1 Dec. 1990
(Contract DE-AC04-76DP-00789)
(DE90-017036; SAND-90-2191C; CONF-901105-7) Avail: NTIS HC/MF A01

Strained layer structures have received a great deal of attention due both to their possible application in electronic devices and their intrinsic interest. The study of strained layer quantum wells grown using lattice mismatched materials has been widely developed for III-V semiconductors. Strained layer quantum wells grown using II-VI materials have not been studied nearly so much as those from III-V, but they are a rapidly growing field of semiconductor research. The wide gap II-VI materials are of interest because they are generally direct gap materials. This makes them attractive for optoelectronic devices. The majority of the work on strained layer structures in the wide gap tellurium based materials has focused in two areas. The first is the inclusion of Mn to produce dilute magnetic semiconductors (DMS) strained layers and superlattices. The other area is CdTe/ZnTe quantum wells and superlattices. Some related work has been done with CdZnTe/ZnTe structures. For the CdZnTe/CdTe very little work has been done and the majority of that used very small amounts of Zn. The growth and optical characterization of Cd(1-x)Zn(x)Te/CdTe strained single quantum wells (SSQW) where the Zn concentration ranges from about 10 to 50 percent is examined. DOE

N91-11564# Ames Lab., IA.
PROCESSING OF YBA2Cu3O7 TAPES FROM A MOLTEN SALT PRECURSOR M.S. Thesis
Richard P. Millis 10 Sep. 1990 89 p
(Contract W-7405-eng-82)
(DE90-017656; IS-T-1489) Avail: NTIS HC/MF A05

A novel process for forming a viscous nitrate precursor of the superconducting YBa2Cu3O(7-x) material, without the use of binders or plasticizers, is described. The precursor material is formed at 90 C from low melting salts such as Ba(OH)2 - 8H2O, Cu(NO3)2 - 3H2O and an aqueous nitrate solution of yttrium. The viscous precursor behaves as a concentrated suspension, being composed of particles of Ba(NO3)2 and Cu2(OH)3NO3 which are bound together by a gelatinous yttrium nitrate phase. This material has shown desirable properties for the formation of thin tapes through the doctor blade tape casting process. A technique is described for forming thin sheets of superconducting YBa2Cu3O(7-x) by tape casting a viscous molten salt precursor which shows desirable rheological properties without the addition of binders or plasticizers. The drying of these tapes has shown the formation of a yttrium nitrate binder phase to be important in reducing cracking. The firing of these tapes has shown that the metal nitrates in the dried material decompose individually when heated in an oxygen atmosphere and react to form the superconducting phase above 750 C. The decomposition of the nitrates has resulted in extensive porosity in the fired tapes. The superconducting phase was formed in a single heat treatment and oxygen anneal. Magnetometer measurements have shown a transition temperature of (Tc) = 88 K at 10 percent of 50 Oe field cooled saturation value. DOE

N91-11565# Argonne National Lab., IL. Materials Science Div.
EXCESS OXYGEN DEFECTS IN LAYERED CUPRATES
P. Lightfoot, S.-Y. Pei, J. D. Jorgensen, A. Manthiram, X. X. Tang, and J. B. Goodenough (Texas Univ., Austin.) Sep. 1990 8 p Presented at the International Conference on the Chemistry of Electronic Ceramic Materials, Grand Teton National Park, WY, 16-21 Aug. 1990 Submitted for publication Sponsored in part by R. A. Welch Foundation, Houston, TX
(Contract W-31-109-eng-38; NSF STC-88-09854)
(DE90-017669; CONF-900813-1) Avail: NTIS HC/MF A02

Neutron powder diffraction was used to study the oxygen defect chemistry of two non-superconducting layered cuprates, La(1.25)Dy(0.75)Cu(3.75)F(0.5), and La(1.85)Sr(1.15)Cu2O(6.25), having a structure related to that of the newly discovered double layer superconductor La(2-x)Sr(x)CaCu2O6. The role played by oxygen defects in determining the superconducting properties of layered cuprates is discussed. DOE

N91-11566# Argonne National Lab., IL.
STRUCTURE OF MOLTEN SALTS
Marie-Louise Saboungi, M. A. Howe, and D. L. Price 1990 11 p Presented at the Spring Meeting of the Electrochemical Society, Montreal, Quebec, 6-11 May 1990
(Contract W-31-109-eng-38)
(DE90-017704; CONF-900562-8) Avail: NTIS HC/MF A03

A brief review of the structure of molten salts is given with special emphasis on structural features in reciprocal space.

Selected diffraction results on halide salts containing monovalent and divalent cations are presented, along with recent results on salts containing trivalent cations. Different models and computational techniques, such as random packing of structural units, the reference interaction site model, and reverse Monte Carlo are used to derive structural information at the partial level. DOE

N91-11567# Oak Ridge National Lab., TN. Solid State Div.
SURFACE ANHARMONICITY: TEMPERATURE DEPENDENCE OF PHONON ENERGIES ON Cu(110)
A. P. Baddorf and E. W. Plummer (Pennsylvania Univ., Philadelphia.) 1990 16 p Presented at the Vibrations at Surfaces 6th Conference, Shelter Island, NY, 10-14 Sep. 1990 Submitted for publication
(Contract DE-AC05-84OR-21400)
(DE90-017735; CONF-900914-1) Avail: NTIS HC/MF A03

The temperature dependence of surface phonons on Cu(110) was determined with high resolution electron energy loss spectroscopy between 21 and 766 K. Phonons at Gamma and at Y, both with atomic motion perpendicular to the surface, were examined to assess the importance of anharmonicity at the surface. As the temperature is increased the observed phonon energies decrease and the linewidths increase. The same percentage decrease is observed at Gamma and Y. A simple model using an anharmonic potential can reproduce the magnitude and shape of the temperature dependence of the phonon at Gamma. Direct comparison with bulk phonon studies shows that the anharmonicity at the surface is 4.1 to 4.8 times greater. DOE

N91-11568# Oak Ridge National Lab., TN. Metals and Ceramics Div.
HIGH ENERGY IRON ION IMPLANTATION INTO SAPPHIRE
W. R. Allen and D. F. Pedraza 1990 16 p Presented at the 7th International Conference on Ion Beam Modification of Materials, Knoxville, TN, 9-14 Sep. 1990 Sponsored in part by Tennessee Univ., Knoxville
(Contract DE-AC05-84OR-21400)
(DE90-017736; CONF-900936-4) Avail: NTIS HC/MF A03

Sapphire specimens of c-axis orientation were implanted at room temperature with iron ions at energies of 1.2 and of 2 MeV to various fluences up to 8 x 10(exp 16)/sq cm. The damage induced by the implantations was assessed by Rutherford backscattering spectroscopy in random and channeling geometries. Dechanneling in both sublattices was observed to saturate for all implantation conditions. Disorder in the aluminum sublattice was found to increase with depth at a significantly slower rate than in the oxygen sublattice. In the oxygen sublattice, a relative yield, chi, of 0.80 (+ or -) 0.11 was attained at a depth of 0.1 micron and remained constant up to the measured depth of 0.45 micron. In the aluminum sublattice, the disorder increased with depth and the dechanneling asymptotically approached sub chi = 0.70 (+ or -) 0.04 at 0.45 micron. These results are discussed and compared with those for shallower Fe implantations obtained by other researchers. DOE

N91-11569# Oak Ridge National Lab., TN. Solid State Div.
ION MIXING OF SEMICONDUCTOR SUPERLATTICES
W. Xia, S. N. Hsu, C. C. Han, S. A. Pappert, B. Zhu, C. Cozzolino, P. K. L. Yu, S. S. Lau (California Univ., San Diego, La Jolla.), D. B. Poker, and C. W. White et al 1990 21 p Presented at the 7th International Conference on Ion Beam Modification of Materials, Knoxville, TN, 9-14 Sep. 1990
(Contracts DE-AC05-84OR-21400; DE-FG03-84ER-45156)
(DE90-017769; CONF-900936-5) Avail: NTIS HC/MF A03

Compositional disordering of III-V compound superlattice structures has received considerable attention recently due to its potential application for photonic devices. The conventional method in induce compositional disorder is to implant a moderate dose of impurity ions (approx. 10 (exp 15)/sq cm) into the structure at room temperature, followed by a high temperature annealing step (this process is referred to as IA here). Ion irradiation at room temperature alone does not cause any significant intermixing of layers. The subsequent high temperature annealing step tends to restrict device processing flexibility. Ion mixing (IM) is capable of enhancing compositional disordering of layers at a rate which increases exponentially with the ion irradiation temperature. As a processing technique to planarize devices, ion mixing appears to be an attractive technology. Compositional disordering was studied disordering in the AlGaAs/GaAs and the InGaAs/InP systems using ion mixing. It was found that the ion mixing behavior of these two systems shows a thermally activated regime as well as an athermal regime, similar to that observed for metal-metal and metal-semiconductor systems. Ion mixing is observed to induce compositional disordering at significantly lower temperatures than that for the IA process. The two processes were compared in terms of five parameters (1) irradiation temperature, (2) dose dependence (3) annealing, and (4) electrically active ions. It was found that the IM process is more efficient in utilizing the defects generated by ion irradiation to cause disordering. Both the physical mechanism of ion mixing and possible device implications will be discussed. DOE

N91-11570# Argonne National Lab., IL. Materials Science Div.
MAGNETIC PROPERTIES OF ULTRATHIN EPITAXIAL FILMS OF IRON
C. Liu and S. D. Bader 1990 22 p Presented at the Symposium on Surface Processing and Laser Assisted Chemistry in Conjunction with the Spring Meeting of the European Materials Research Society, Strasbourg, France, 29 May - 1 Jun. 1990 Submitted for publication
(Contract W-31-109-eng-38)
(DE90-017861; CONF-900577-2; Rept-58918-00-105) Avail: NTIS HC/MF A03

Ultrathin Fe films epitaxially grown on Cu(100), Au(100), Pd(100), and Ru(0001) substrates are used to study monolayers magnetism, surface magnetic anisotropy and 2-D critical behavior, by means of in-situ surface magneto-optical Kerr effect measurements. Epitaxial structures and growth modes are characterized by auxiliary low energy electron diffraction and Auger electron studies. The magnetic properties of the films depend on the growth temperature. For 100 K growth, all films exhibit a universal behavior of perpendicular spin orientations in the monolayer regime, while for 300 K growth, Fe/Pd(100) and Fe/Au(100) have in-plane easy-axis of magnetization for all thicknesses. Fe/Ru(0001) lacks a ferromagnetic response for thickness less than two monolayers (ML). Fe/Pd(100) has remarkable thermal stability in the monolayer and submonolayer range. Reversible magnetization data are obtained for 0.6 to 3.0 ML thick films, which show second-order phase transitions at thickness-dependent Curie temperatures (Tc). An effective magnetization exponent beta sub eff of 0.127 + or - 0.004 is obtained for a 1.2 ML Fe/Pd(100) film, agreement with the theoretical value of beta sub c = 0.125 for an ideal 2-D Ising model. The (Tc) trend with film thickness for Fe/Pd(100) is also in agreement with Monte Carlo calculations for Ising films. DOE

N91-11571# Ames Lab., IA.
MICROFILAMENTARY Bi2Sr2Ca1Cu2O8 FIBERS
T. A. Miller, S. C. Sanders, D. K. Finnemore, S. E. LeBeau, and J. Righi (Babcock and Wilcox Co., Alliance, OH.) 1990 9 p Presented at the International Conference on Superconductivity, Bangalore, India, 10-14 Jan. 1990 Prepared in cooperation with Iowa State Univ. of Science and Technology, Ames
(Contract W-7405-eng-82)
(DE90-018013; IS-M-641; CONF-900133-3) Avail: NTIS HC/MF A02

Techniques have been developed for the fabrication of superconducting microfilaments of Bi2 Sr2 Ca1 CU2 O8 as part of a larger project to produce microfilamentary composites. The process is based on a gas jet fiberization of a viscous liquid melt to form long slender amorphous fibers. A subsequent anneal then converts the fibers to the superconducting crystalline phase. Fiber diameters range from 1 to 6 microns and length to diameter ratios range between 10 to the 3rd power and 10 to the 4th power so the dimensions are favorable for composite formation. The details

of grain growth are reviewed with special emphasis on the role of the filament diameter on the morphology of the grain growth. DOE

N91-11572# Midwest Research Inst., Golden, CO.
SERI WORKSHOP ON THE ROLE OF POINT DEFECTS/DEFECT COMPLEXES IN SILICON DEVICE FABRICATION
1990 35 p Workshop held in Keystone, CO, 30-31 Aug. 1990
(Contract DE-AC02-83CH-10093)
(DE90-000377; SERI/CP-211-3976; CONF-9008149-Absts)
Avail: NTIS HC/MF A03

This document is composed of abstracts from papers presented at a workshop on the role of point defects and defect complexes in silicon device fabrication. Among the topics covered are: defects in silicon; defect/impurity control in material growth and gettering impurities and defects in silicon solar cells impurity-defect interactions; defect passivation/process interactions and annealing gettering/defect passivation for silicon solar cells. DOE

N91-11573# Sandia National Labs., Albuquerque, NM.
LIGHT-HEAVY-HOLE-MIXING-INDUCED SELECTION RULES FOR MAGNETO-LUMINESCENCE AND VALENCE-BAND ENERGY DISPERSION IN SEMICONDUCTOR QUANTUM WELLS
S. K. Lyo and E. D. Jones 1990 5 p Presented at the Fall Meeting of the Materials Research Society, Boston, MA, 26 Nov. - 1 Dec. 1990
(Contract DE-AC04-76DP-00789)
(DE90-015989; SAND-90-1676C; CONF-901105-6) Avail: NTIS HC/MF A01

The validity of the semiclassical approximation for the valence band structure of a QW (quantum well) was studied in a perpendicular magnetic field. The relative oscillator strengths of the main and forbidden transitions for magneto-luminescence were calculated for n-type quantum wells. DOE

N91-11574# Louisiana State Univ., Baton Rouge. Dept. of Physics and Astronomy.
COLOR FLUX DISTRIBUTION IN PURE SU(2) LATTICE GAUGE THEORY
Richard W. Haymaker, Yingcai Peng, Vandana Singh, and Jacek Wosiek (Jagellonian Univ., Cracow, Poland) 1990 3 p Presented at the DPF Summer Study on High Energy Physics, Snowmass, 25 Jun. - 13 Jul. 1990
(Contracts DE-AS05-77ER-05490; CPCB-01.09; CPCB-01.03; RRI-14)
(DE90-017403; DOE/ER-05490/112; CONF-9006267-3) Avail: NTIS HC/MF A01

The color field distribution around a static q(bar q) pair is studied in detail for pure SU(2) Lattice Gauge Theory in four dimensions. As a result of large cancellations between electric and magnetic components, the action density dominates the energy density typically by an order of magnitude, at points far from the quarks. DOE

N91-11575# Argonne National Lab., IL. Materials Science Div.
THE TRANSURANIUM ELEMENTS: MEMBERS OF THE 5f SERIES
Dieter M. Gruen 1990 21 p Presented at the 200th American Chemical Society National Meeting, Washington, DC, 27-29 Aug. 1990
(Contract W-31-109-eng-38)
(DE90-017680; CONF-900802-7) Avail: NTIS HC/MF A03

During the last 40 years, the electronic structure of the actinide elements has been investigated in great detail primarily by means of spectroscopic studies of gaseous atoms and ions, as well as of solutions and compounds, and by magnetic susceptibility and electron spin resonance studies of metals, alloys, and compounds. Both experimental and theoretical studies have resulted in accurate values for spin orbit coupling and crystal field parameters for 5f electrons, for example, which can be compared with values characteristic of 4f electrons. The somewhat greater spatial extent of 5f versus 4f wavefunctions gives rise to 5f orbital participation in the bonding of actinide element organometallic compounds and leads to an extensive and intricate organometallic chemistry for this group of elements. This report reviews the history of the development of ideas concerning the electronic structure of the new elements which, by determining their chemistry, would fix their position in the Periodic Table. DOE

N91-11576# Oak Ridge National Lab., TN. Solid State Div.
COMPOSITIONAL IMAGING OF SEMICONDUCTOR INTERFACES BY Z-CONTRAST SCANNING TRANSMISSION ELECTRON MICROSCOPE (STEM)
S. J. Pennycook, D. E. Jesson, and M. F. Chisholm Sep. 1990 5 p Presented at the Fall Meeting of the Materials Research Society, Boston, MA, 26 Nov. - 1 Dec. 1990 Submitted for publication
(Contract DE-AC05-84OR-21400)
(DE90-017763; CONF-901105-11) Avail: NTIS HC/MF A01

Conventional high resolution electron microscopy is a coherent imaging technique best thought of as an attempt to reconstruct an image of the object by recombining the diffracted beams emerging from the sample. The image represents a coherent interference pattern and the contrast depends on the relative phases of the various diffracted beams. This pattern can take many forms since the relative phases of the beams are very sensitive to objective lens defocus and sample thickness. In certain crystal structures phase contrast images can be quite sensitive to composition, provided that the other variables are carefully controlled. The technique requires structure factor difference reflections (such as the (200) beams in the zinc blends structures) to contribute strongly to the image, and even a first order interpretation requires extensive image simulation and comparison with experiment. DOE

N91-11577# Argonne National Lab., IL.
COMPUTER-CONTROLLED ION BEAM DEPOSITION SYSTEMS FOR HIGH T(SUB c) SUPERCONDUCTOR AND OTHER MULTI-COMPONENT OXIDE THIN FILMS AND LAYERED STRUCTURES
A. R. Krauss, Dieter M. Gruen, O. Auciello, A. I. Kingon, M. S. Ameen, T. M. Graettinger, C. S. Rou, and C. S. Soble (North Carolina Univ., Chapel Hill.) 1990 13 p Presented at the Symposium on Surface Processing and Laser Assisted Chemistry in Conjunction With the Spring Meeting of the European Materials Research Society, Strasbourg, France, 29 May - 1 Jun. 1990 Prepared in cooperation with Wisconsin Univ., Milwaukee
(Contract W-31-109-eng-38)
(DE90-017798; CONF-900577-3) Avail: NTIS HC/MF A03

A single beam, multiple target (SBMT) deposition system which features a rotating target holder with either elemental or simple compound targets has been developed for the production of layered thin film structures and multicomponent oxide, silicide or other compound thin films. We are employing the SBMT ion beam sputtering system for the deposition of high temperature superconducting films and electro-optical multilayer structures. The beam-target-substrate geometry and ion beam characteristics are designed to minimize beam implantation and secondary sputtering effects, while maintaining high deposition rates. Consequently, the amount of energy which is deposited into the film may be controlled providing enough energy to promote activated processes, such as the in-situ formation of oriented crystal structures of high temperature superconducting materials, while minimizing amorphization and gas incorporation. All parameters necessary to control the film properties are under computer control. A deposition cycle, defined as a number of sequential steps may be easily modified or added to previously existing deposition cycles, thereby permitting the creation of complicated deposition procedures suitable for the production of films with highly reproducible properties for research purposes, and the in-situ fabrication of complex devices for technological applications. Examples are given of the capabilities of the technique as they apply to the production of high T(sub c) superconducting devices. DOE

N91-11578# Argonne National Lab., IL. Materials Science Div.
EPITAXIAL TIO2 AND VO2 FILMS PREPARED BY MOCVD (METAL-ORGANIC CHEMICAL VAPOR DEPOSITION)
H. L. M. Chang, H. You, J. Guo, and D. J. Lam Aug. 1990 14 p Presented at the 5th International Conference on Solid Films and Surfaces, Providence, RI, 13-17 Aug. 1990 Submitted for publication
(Contract W-31-109-eng-38)
(DE90-017806; CONF-900830-2) Avail: NTIS HC/MF A03

Titanium and vanadium oxide systems were selected to study the growth of thin epitaxial film in a metal-organic chemical vapor deposition (MOCVD) process. Epitaxial TiO2 and VO2 films were obtained on sapphire but not on Si(111). Eight distinct substrate film epitaxial relationships were determined by x ray diffraction studies using a four circle diffractometer. It was found that none of the eight epitaxial systems had a good lattice match between substrate and film. But further investigation revealed that substantial similarity existed in the local atomic patterns of the substrate and the film for all these systems. Nevertheless, it should be emphasized that mismatches of the local atomic patterns for these systems are, in general, substantially larger than those observed in the epitaxial systems containing semiconductor materials such as silicon and GaAs. DOE

N91-11579# Argonne National Lab., IL.
DESIGN AND TESTING OF A HIGH TEMPERATURE SUPERCONDUCTING CURRENT LEAD
J. L. Wu, J. T. Dederer, P. W. Eckels, S. K. Singh (Westinghouse Electric Corp., Pittsburgh, PA.), J. R. Hull, R. B. Poeppel, C. A. Youngdahl, J. P. Singh, M. T. Lanagan, and U. Balachandran 1990 20 p Presented at the Applied Superconductivity Conference, Aspen, CO, 24-28 Sep. 1990 Submitted for publication
(Contract W-31-109-eng-38)
(DE90-017812; CONF-900944-2) Avail: NTIS HC A03

High critical temperature and low thermal conductivity of the ceramic superconductor Y-Ba-Cu-O were utilized to reduce the Joule heating and the heat leak in a vapor cooled current lead design of nominally 1 kA capacity. The lead consists of a lower superconducting part and an upper normal metal (copper) part. The superconducting part is an assembly of twenty rectangular bars fabricated from a composite of Y-Ba-Cu-O and Ag (15 percent vol). This part is designed to operate below the critical temperature of the ceramic superconductor. The copper part, consisting of twenty copper wires, extends outside of the cryostat and interfaces to the room temperature power supply. The lead was successfully tested for currents of up to 2 kA. At the optimum operating currents of 1.7 to 1.8 kA, the helium boil-off measurements show a heat leak reduction of approximately 40 percent from the conventional designs. Details of the design, fabrication issues and the testing are presented. DOE

N91-11580# Argonne National Lab., IL.
SUPERCONDUCTING AND STRUCTURAL PROPERTIES OF THE (Ba(0.6)K(0.4)) (Bi(1-y)Sb(y))O3 SYSTEM
B. Dabrowski, S. Pei, D. R. Richards, Y. Zheng, J. D. Jorgensen, D. G. Hinks, A. W. Mitchell, and C. W. Kimball (University of Northern Illinois, De Kalb.) 1989 5 p Presented at the Materials Research Society Fall Meeting, Boston, MA, 27 Nov. - 1 Dec. 1989
(Contract W-31-109-eng-38; NSF STC-88-09854; NSF DMR-87-19738)
(DE90-017836; CONF-891119-140) Avail: NTIS HC/MF A01

Single phase samples of (Ba(1-x)K(x) (Bi(1-y)Sb(y))O3 were synthesized over a limited compositional range using a two step procedure: high temperature firing in a low oxygen partial pressure followed by low temperature oxygen annealing. For y=0 and 0.37 less than x less than 0.50, samples have a simple cubic structure and are bulk superconductors with (Tc) gradually decreasing from 30 to 22 K as x increases to 0.50. For fixed x and y greater than 0 samples are superconducting again with a simple cubic structure and with (Tc) gradually decreasing as y increases. DOE

N91-11581# Japan Atomic Energy Research Inst., Tokyo.
THE TRANSVERSE STRESS EFFECT ON THE CRITICAL CURRENT OF JELLY-ROLL MULTIFILAMENTARY Nb3Al WIRES
D. Zeritis (Massachusetts Inst. of Tech., Cambridge.) Feb. 1990 60 p
(DE90-513710; JAERI-M-90-014) Avail: NTIS (US Sales Only) HC/MF A04

Experiments were conducted to determine the transverse stress sensitivity of the critical current of jelly-roll multifilamentary Nb3Al wires, primarily at 12T but also at other magnetic fields. For comparison, similar experiments were conducted on bronze-process Ti-alloyed multifilamentary Nb3Sn wires. In total four samples were experimented upon, two jelly-roll Nb3Al samples of 0.8 mm and 1.03mm diameter, respectively, one bronze-process Nb3Sn sample of 1.0 mm diameter, and one internally-stabilized bronze-process Nb3Sn sample of 1.09 mm diameter. As was expected, the Nb3Al samples proved vastly superior to the Nb3Sn samples with regard to transverse compressive stress, exhibiting significant I(sub c)-degradation for transverse stresses above 100MPa. At 12T and at 150MPa of transverse compression (conditions expected in fusion magnets) the 0.8 mm diameter sample exhibited an I(sub c)-degradation of (approx) 20 percent, whereas the 1.03 mm diameter sample of (approx) 28 percent. Under the same conditions, the 1.0 mm diameter Nb3Sn sample exhibited an I(sub c)-degradation of (approx) 65 percent, whereas at 12T and 120MPa the 1.09 mm diameter Nb3Sn sample exhibited an I(sub c)-degradation also of (approx) 65 percent. However, the measured non-copper critical current densities at high magnetic fields of the Nb3Al samples were lower than those of the Nb3Sn samples. Further development is needed to improve this aspect of their performance, nevertheless there is optimism that Nb3Al will eventually become a useful superconductor for large scale, high field applications. DOE

N91-11582# Argonne National Lab., IL. Chemistry and Materials Science Div.
STRUCTURE-PROPERTY RELATIONSHIPS FOR (BETA)- AND (KAPPA)-PHASE BEDT-TTF SALTS AND THEIR USE IN THE SYNTHESIS OF (KAPPA)-(BEDT-TTF)2Cu(N(CN)2)Br. A SALT HAVING THE HIGHEST T(SUB c) (INDUCTIVE ONSET = 11.6 K, RESISTIVE, ONSET = 12.5 K) YET OBSERVED IN AN ORGANIC SUPERCONDUCTOR
Jack M. Williams, Aravinda M Kini, Urs Geiser, Hau H. Wang, K. Douglas Carlson, W. K. Kwok, K. G. Vandervoort, James E. Thompson, D. L. Stupka, and D. Jung (North Carolina State Univ., Raleigh.) et al 1990 12 p Presented at the International Conference on Organic Superconductors, Lake Tahoe, CA, 20-24 May 1990
(Contract W-31-109-eng-38)
(DE90-017804; CONF-900528-3) Avail: NTIS HC A03/MF A01

A new ambient pressure organic superconductor, kappa-(BEDT-TTF)2Cu(N(CN)2)Br, was discovered with an inductive onset (Tc) = 11.6 + or - 0.1 K (resistive onset = 12.5 + or - 0.1 K). The anion in the new salt consists of a polymeric mixed halide-pseudohalide cuprate(I) species. Because of the large number of metal/halide/pseudohalide substitutions that can be made in this anionic species, it opens up an entirely new conceptual approach to the design of additional conducting and superconducting (with even higher (Tc)'s) cation-radical salts by use of planar polymeric anions. Studies along these lines are currently under way in the lab. It is also becoming increasingly clear that in terms of structure (both are layered superconductors) and the physics (both are type II-superconductors with anisotropic coherence lengths, anisotropic H(sub c2), and in which superconductivity is competing with magnetic ground states, etc.), the organic superconductors are more similar to the high (Tc) oxide superconductors than to other classes of superconductors. Thus, the prospects for discovering high (Tc) in organic systems appear very bright. DOE

N91-11583# Argonne National Lab., IL. Materials Science Div.
BRAGG INTENSITIES AND DIFFUSE SCATTERING IN Ag2Se: MOLECULAR DYNAMICS STUDY
Jose Pedro Rino (Universidade Federal de Sao Carlos, Brazil), Priya Vashishta, and Rajiv K. Kalia Aug. 1990 18 p Presented at the 14th Workshop on Condensed Matter Theories, Elba. Italy, 18-23 Jun. 1990
(Contract W-31-109-eng-38)
(DE90-017811; CONF-9006273-1) Avail: NTIS HC/MF A03

Superionic conductor Ag2Se is studied with the molecular dynamics technique using effective two-body interaction pair potentials. These interaction potentials include steric, charge transfer, and charge-dipole interactions. The superionic phase is characterized by a stable bcc sublattice of Se(sup --) ions in which Ag(sup +) ions exhibit liquid-like diffusion. The temperature dependence of the structural and dynamical correlations are studied. The results for structural correlations include the pair distribution functions, coordination numbers, bond angle distributions, and wave vector dependence of the Bragg intensities. A detailed comparison with neutron and x ray scattering results is made wherever possible. The anomalous diffuse neutron and x ray scattering in the vicinity of q(sub 0)=(1.6,1,0) is calculated. DOE

N91-11584# Sandia National Labs., Albuquerque, NM.
FORMATION AND STABILITY OF As-H BONDS IN H-IMPLANTED GaAs
H. J. Stein 1990 13 p Presented at the 7th International Conference on Ion Beam Modification of Materials, Knoxville, TN, 9-14 Sep. 1990
(Contract DE-AC04-76DP-00789)
(DE91-000043; SAND-90-2302C; CONF-900936-8) Avail: NTIS HC/MF A03

The chemical bonding and isochronal annealing of H implanted into GaAs at 80 K has been investigated by infrared absorption measurements. Based upon the frequency shift when deuterium is substituted for H, and an equivalent band formation in InAs, assignment of a new band at 2029 cm(sup minus 1) is made to As-H centers. Bonding of H at interstitial As of and As-vacancy pair which anneals between 150 and 250K is suggested as the structure for the defect. A previously-reported absorption band at 1834 cm(sup minus 1) assigned to Ga-H centers in H-implanted GaAS increase in intensity when H is released from As-H centers. DOE

N91-11585# California Univ., Berkeley. Lawrence Berkeley Lab. Materials and Chemical Sciences Div.
A STUDY OF THE CHEMICAL, MECHANICAL, AND SURFACE PROPERTIES OF THIN FILMS OF HYDROGENATED AMORPHOUS CARBON Ph.D. Thesis
Gilroy John Vandentop Jul. 1990 145 p Prepared in cooperation with California Univ., Berkeley
(Contract DE-AC03-76SF-00098)
(DE91-000357; LBL-29258) Avail: NTIS HC/MF A07

Amorphous hydrogenated carbon (a-C:H) films were studied with the objective of elucidating the nucleation and growth mechanisms, and the origin of their unique physical properties. The films were deposited onto Si(100) substrates both on the powered (negatively self-biased) and on the grounded electrodes from methane in an RF plasma (13.56 MHz) at 65 mTorr and 300 to 370 K. The films produced at the powered electrode exhibited superior mechanical properties, such as high hardness. A mass spectrometer was used to identify neutral species and positive ions incident on the electrodes from the plasma, and also to measure ion energies. The effect of varying ion energy flux on the properties of a-C:H films was investigated using a novel pulsed biasing technique. It was demonstrated that ions were not the dominant deposition species as the total ion flux measured was insufficient to account for the observed deposition rate. The interface between thin films of a-C:H and silicon substrates was investigated using angle resolved x ray photoelectron spectroscopy. A silicon carbide layer was detected at the interface of a hard a-C:H film formed at the powered electrode. At the grounded electrode, where the kinetic energy is low, no interfacial carbide layer was observed. Scanning tunneling microscopy and high energy electron energy loss spectroscopy was used to investigate the initial stages of growth of a-C:H films. On graphite substrates, films formed at the powered electrode were observed to nucleate in clusters approximately 50 (Angstrom) in diameter, while at the grounded electrode no cluster formation was observed. DOE

N91-11586# Technische Univ., Eindhoven (Netherlands).
THE INFLUENCE OF IONIZED IMPURITIES ON THE TRANSPORT PROPERTIES OF A TWO-DIMENSIONAL ELECTRON GAS Ph.D. Thesis
Paulus Maria Koenraad 1990 129 p
(ETN-90-97752) Avail: NTIS HC/MF A07

Experiments on 2-Dimensional Electron Gases (2DEG) in GaAs/Al(x)Ga(1-x)As heterostructures and Si delta doped GaAs structures are studied. Focus is on the influence of ionized impurities on the transport properties of a 2DEG. In the first heterostructures the changing of the interaction between the electrons and the charged impurities by illumination and by the application of a backgate voltage are studied. In the GaAs structures the influence of the charged impurities on the electrons in the various populated sub-bands are studied. The influence of the ionized donors on the integer and fractional Quantum Hall Effect (QHE) are studied. The integer and fractional QHE are shown to have a different physical origin. ESA

N91-11587# Office National d'Etudes et de Recherches Aerospatiales, Paris (France).
LONG PERIOD SUPERSTRUCTURES IN Pt3V AND Cu3Pd: TOWARDS A QUANTITATIVE DESCRIPTION Ph.D. Thesis - Paris VI Univ.
Jerome Planes Jun. 1990 195 p In FRENCH; ENGLISH summary Report will also be announced as translation (ESA-TT-1233)
(ONERA-NT-1990-2; ISSN-0078-3781; ETN-90-98021) Avail: NTIS HC/MF A09

One dimensional long period ordered superstructures in Pt3V and Cu3Pd alloys are studied, in order to reach a quantitative description of the periodic antiphase boundaries modulation and to understand the nature of the transitions betweeen phases. A digital analysis of high resolution electron microscopy images is presented. The profile of an antiphase boundary is presented. The reciprocal space complementary approach is realized through in situ x ray diffraction experiments. The intensity ratio of small order harmonics give the value of the boundary width: it increases with temperature. The results are discussed in relationship with statistical mechanics models. ESA

77 THERMODYNAMICS AND STATISTICAL PHYSICS

Includes quantum mechanics; theoretical physics; and Bose and Fermi statistics.

For related information see also *25 Inorganic and Physical Chemistry* and *34 Fluid Mechanics and Heat Transfer.*

N91-11588# Max-Planck-Inst. fuer Stroemungsforschung, Goettingen (Germany, F.R.).
COMPLETE ADIABATIC EVAPORATION OF HIGHLY SUPERHEATED LIQUID JETS
Thomas Kurschat 1990 115 p In GERMAN; ENGLISH summary
(MPIS-Mitt-95; ISSN-0374-1257; ETN-90-97868) Avail: NTIS HC/MF A06

A nozzle expansion into a vacuum chamber was used to investigate the evaporation of highly superheated liquid jets. The large molar heat of the fluid, in this case C6F14 was found to be an important parameter for the phase transition and the subsequent two phase flow. A cubic equation of state was used to describe the thermodynamic properties of the fluid. The evaporation was modeled as a sonic deflagration followed by a cylindrical supersonic

expansion. In analogy to the supersonic free jet, the final state is reached by a normal shock. For sufficiently high temperatures and expansion ratios a complete adiabatic evaporation was found. At even higher temperatures the fluid evaporates completely in a shock discontinuity. The predictions of the model are in good agreement with the experimental results. ESA

N91-11589# Joint Inst. for Nuclear Research, Dubna (USSR). Lab. of Theoretical Physics.
AN INVERSE PROBLEM FOR CLASSICAL RELATIVISTIC MECHANICS
H. Funke (Zentralinstitut fuer Kernforschung, Rossendorf bei Dresden, German D.R.) and Yu. L. Ratis 1989 6 p
(DE90-631599; JINR-E-4-89-275) Avail: NTIS (US Sales Only) HC/MF A02

The inverse problem is solved for a relativistic classical point particle trapped in a confining potential. The integral equation for the period T(E) is inverted by a Laplace-transformation technique, and finally the explicit formula is solved for the potential without any approximations. DOE

N91-11590# Los Alamos National Lab., NM.
ANTIMATTER GRAVITY EXPERIMENT
Ronald E. Brown, Jordan B. Camp, and Timothy W. Darling 1990 10 p Presented at the 11th International Conference on the Application of Accelerators in Research and Industry, Denton, OH, 5-8 Nov. 1990
(Contract W-7405-eng-36)
(DE91-000177; LA-UR-90-3344; CONF-901116-4) Avail: NTIS HC/MF A02

An experiment is being developed to measure the acceleration of the antiproton in the gravitational field of the earth. Antiprotons of a few MeV from the Low Energy Antiproton Ring (LEAR) facility at CERN will be slowed, captured, cooled to a temperature of about 10 K, and subsequently launched a few at a time into a drift tube where the effect of gravity on their motion will be determined by a time-of-flight method. Development of the experiment is proceeding at Los Alamos using normal matter. The fabrication of a drift tube that will produce a region of space in which gravity is the dominant force on moving ions is a major difficulty. This involves a study of methods of minimizing the electric fields produced by spatially varying work functions on conducting surfaces. Progress in a number of areas is described, with stress on the drift-tube development. DOE

80 SOCIAL SCIENCES (GENERAL)

Includes educational matters.

No abstracts in this category.

81 ADMINISTRATION AND MANAGEMENT

Includes management planning and research.

N91-11591*# National Aeronautics and Space Administration. John F. Kennedy Space Center, Cocoa Beach, FL.
TWENTY-SECOND ANNUAL NASA SUPPLY AND EQUIPMENT MANAGEMENT CONFERENCE
1989 384 p Conference held in Cocoa Beach, FL, 5-7 Dec. 1989
(NASA-CP-10042; NAS 1.55:10042) Avail: NTIS HC/MF A17 CSCL 05A

The status of actions from the 1988 conference is reviewed. Environmental safety issues, definitions, and regulations; contract transition, payload logistics transition, and safety and support equipment; supply products and services, bar code technology, and inventory accuracy; equipment management workshop topics; and contract property workshop topics are outlined. Author

N91-11592# Technische Univ., Delft (Netherlands). Faculty of Technical Mathematics and Informatics.
THE FRENCH AND THE AMERICAN SCHOOL IN MULTI-CRITERIA DECISION ANALYSIS
F. A. Lootsma 1990 22 p
(Rept-90-21; ISSN-0922-5641; ETN-90-97714) Copyright Avail: NTIS HC/MF A03

A crucial problem in multi-criteria analysis, the transition from the objective evaluation of the decision alternatives to the subjective weighing, is addressed. The French and American schools incorporate subjective human judgement in different ways. A thoroughly revised analytic hierarchy process is presented to demonstrate that the American school did not go far enough. Using the persistent pattern of human comparative judgement in many unrelated areas such as history, planning, and psychophysics, a natural scale to quantify verbal preferential statements of increasing intensity is shown to exist. The assumptions underlying the logarithmic-regression procedure to compute the impact scores and the criterion weights are analyzed. Violations of these assumptions imply that decision support is not merely supplied in order to identify the pre-existing consensus in a group of decision makers. The decision process is reformed by accelerating the deliberations in the direction of a compromise solution. Sensitivity analysis based on a variety of geometric scales shows that the results of the French and the American school of thinking are unexpectedly close to each other. ESA

N91-11593# Office of Technology Assessment, Washington, DC.
PROPOSAL PRESSURE IN THE 1980S: AN INDICATOR OF STRESS ON THE FEDERAL RESEARCH SYSTEM
J. Andelin and N. Carson Apr. 1990 26 p
(PB90-253147) Avail: NTIS HC/MF A03 CSCL 05A

The growing competition for research monies is discussed during a decade where R and D budgets increased in real terms. The significance of the competition for the allocation of Federal research funds in the 1990s is also discussed. GRA

N91-10931# Deutsche Forschungsanstalt fuer Luft- und Raumfahrt, Goettingen (Germany, F.R.). Inst. fuer Aeroelastik.
A QUARTER OF A CENTURY OF AEROELASTIC COOPERATION BETWEEN RESEARCH AND INDUSTRY (A REVIEW). PART 1: FIGHTER AIRPLANES AND HELICOPTERS
O. Sensburg, J. Becker, H. Hoenlinger, and G. Strehlow *In its* Contributions in the Field of Aeroelastics on the Occasion of the 60th Anniversary of Professor Dr.-Ing. Habil. Hans Wilhelm Foersching Apr. 1990 p 223-270 (For primary document see N91-10920 02-02)
Avail: NTIS HC/MF A13

82 DOCUMENTATION AND INFORMATION SCIENCE

Includes information management; information storage and retrieval technology; technical writing; graphic arts; and micrography.

For computer documentation see *61 Computer Programming and Software.*

N91-11594# Environmental Protection Agency, Washington, DC. Office of Information Resources Management.
TECHNOLOGY TRANSFER: HOTLINES
Feb. 1990 34 p
(PB90-237140; EPA/IMSD-90/003) Avail: NTIS HC/MF A03 CSCL 05B

The bibliography is part of the Technology Transfer Series which serves to improve awareness of major technology transfer issues and projects. The following are part of this series: Technology

Transfer (An Overview); Technology Transfer (Clearinghouse); and Technology Transfer (Hotlines). The bibliography is part of the Environmental Protection Agency Headquarters Library's continuing effort to provide information and foster communication about hotlines within the Agency. The citations and abstracts cover a period between 1980 to 1989 and were selected from books, reports, and nontechnical magazine articles. The bibliography categorizes the selected citations for an overview on hotlines, including case studies, evaluation, and technology. A list of databases used is also included. Author

N91-11595# Environmental Protection Agency, Washington, DC. Office of Information Resources Management.
GUIDE TO EPA LIBRARIES AND INFORMATION SERVICES
Sep. 1989 105 p
(PB90-237108; EPA/IMSD-89/008) Avail: NTIS HC/MF A06 CSCL 05B

The guide to Libraries and Information Services is a yearly publication of the Office of Information Resource Management of the Environmental Protection Agency and lists the 28 libraries in the regional network and three specialized information services. A full description for each entry is given including address, phone, staff, information services, publications, subject specialities, and database search services. There are separate indexes which provide cross references to the following: Subject holdings, databases, statistics on library collections, staff names and phone numbers, regions, and cities in which the libraries are located. GRA

N91-11596# Defense Logistics Agency, Alexandria, VA.
DEFENSE LOGISTICS AGENCY INFORMATION RESOURCES MANAGEMENT (IRM) NEAR-TERM PLANNING DOCUMENT FY 1990-1992
May 1990 226 p
(PB90-238494) Avail: NTIS HC/MF A11 CSCL 05B

The document was prepared to provide Information Resources Management (IRM) program direction and to serve as a baseline for development of the Defense Logistics Agency (DLA) IRM Five Year Plan. It is a decision document which reflects the objectives and strategies of the IRM program and is the cornerstone on which all other IRM planning, resourcing and acquisition documents are based. The document is organized into chapters dealing with the major segments of DLA IRM activities such as automated information systems (AISs) and technology. Taken together they represent both the IRM program vision of the future and near-term projects that are the building blocks that will make that future vision a reality. GRA

N91-11597# Office of Technology Assessment, Washington, DC.
HOLDING THE EDGE: MAINTAINING THE DEFENSE TECHNOLOGY BASE. VOLUME 2: APPENDIXES
Jan. 1990 190 p
(PB90-253345; OTA-ISC-422) Avail: NTIS HC/MF A09 CSCL 05B

Appendixes to the report Holding the Edge: Maintaining the Defense Technology Base are presented. Extensive analyses are provided on: DoD acquisition process; industry case studies on fiber optics, advanced composites, and software; and European and Japanese defense technology research, development, and management. GRA

N91-11598 Columbia Univ., New York, NY.
ONLINE SEARCHING IN PUBLIC LIBRARIES: A COMPARATIVE STUDY OF PERFORMANCE Ph.D. Thesis
Janice Helen McCue 1987 369 p
Avail: Univ. Microfilms Order No. DA9020571

The 1980s brought great emphasis on providing information resources to meet society's growing and changing needs. A major part of this movement was the growth of online database searching. The purpose of this exploratory study was to compare and analyze the quality of results of forty-two online database searches conducted in twenty-one public libraries located in sixteen states across the continental United States. Unobtrusive measurement was applied in the data collection process to obtain a true picture of the search service routinely offered at these twenty-one libraries from June 25, 1984, to October 24, 1984. An outside team of database search experts from leading United States financial institutions evaluated search results using a point system of scoring. The focus of the evaluation was the skill of the twenty-one online searchers in retrieving citations that would provide information for a single multifaceted research question and using two different databases. There are many issues within the sphere of quality online searching in public libraries that need answering. This study shows that the quality of the online search results in public libraries needs to be evaluated and measured with respect to the complete process such as the impact of the nature of the topic, the input with respect to the requestor, the level of skill of the searcher, and the input of the administrative practices. Dissert. Abstr.

N91-11599 Sheffield Univ. (England).
THE DERIVATION OF A BEHAVIOURAL MODEL FOR INFORMATION RETRIEVAL SYSTEM DESIGN Ph.D. Thesis
David Ellis 1987 340 p
Avail: Univ. Microfilms Order No. BRDX89202

The derivation of a behavioral model intended to underpin thinking on questions concerning the design of information retrieval systems for academic social scientists is studied. The historical background of information retrieval research is reviewed and the behavioral assumptions made in that research, characterized as the information retrieval model, are examined. Developments in the research tradition following from the early empirical tests on information retrieval systems are discussed, and problems experienced in the attempt to develop a coherent and practically useful research program around the notion of relevance as a quantitative concept are analyzed. A major alternative to work employing the information retrieval model has been the cognitive approach to information retrieval system design. In research so far undertaken in this approach, the system has had to construct a cognitive model of the searcher's requirements in order for retrieval to take place. It is argued that the characteristics of social science information present particular difficulties for building such a model, and that the step of the system building a cognitive model of the searcher's requirements as a pre-requisite for retrieval is unnecessary. The features of an exploratory retrieval system for social scientists based on the characteristics of their information seeking patterns are outlined, the extent to which such features are available in existing systems, and the requirements for implementing the model on an operational system are considered. The argument of the study is that the behavioral approach, and the analysis of information seeking patterns into their characteristics, represents a coherent and practically useful basis for the design of exploratory information retrieval systems for academic social scientists. Dissert. Abstr.

N91-11600# Pacific Northwest Lab., Richland, WA.
THE PRACTICAL CHALLENGES OF CONVERTING END-USE DATA INTO INFORMATION
Craig Connor, John Stoops, and Mark Halverson Jul. 1990 10 p Presented at the End-Use Load and Its Role in DSM, Irvine, CA, 11-12 Jul. 1990
(Contract DE-AC06-76RL-01830)
(DE90-016538; PNL-SA-18436; CONF-9007159-1) Avail: NTIS HC/MF A03

This paper focuses on issues faced by large-scale end-use data collection projects after the project design and meter installation. End-use data load data analysis presents unique problems, often centered on data management. The sheer size of the data collected, the frequency of change in the metered buildings, the need for integration of metered data and building characteristic data, and the need for information rather than just raw data are all problems that each new project must face. DOE

N91-11601# Los Alamos National Lab., NM.
INTERNATIONAL ENGLISH

Mable Amador and Ileana Buican 1990 26 p Presented at the IEEE International Professional Communication Conference, London, England, 12-14 Sep. 1990
(Contract W-7405-eng-36)
(DE90-016719; LA-UR-90-2637; CONF-9009154-2) Avail: NTIS HC/MF A03

This paper is a presentation to the International Professional Communication Conference on International English. Presidence is taken from the Royal Society of London in 1667 to purify and simplify the English language. Because English has become the most spoken language in the world, the case is made to make it plainer and more easily learned. Technical communications is stressed. DOE

N91-11602# New Energy Development Organization, Tokyo (Japan).
REPORT ON THE PREPARATORY INVESTIGATION OF THE PACIFIC ENERGY INFORMATION NETWORK SYSTEM
Mar. 1990 327 p In JAPANESE; ENGLISH summary
(DE91-701469; NEDO-P-2950) Avail: NTIS (US Sales Only) HC/MF A15

In order to collect and analyze promptly and precisely energy information in the nations in the Pacific region, the preparatory investigation was conducted. Countries visited were Korea and five Asian countries. High needs for energy information are shown in all countries, and systems for collecting domestic energy data are being established. Need is not limited to information on the domestic situation but spreads over to the areas of energy demand and supply of close trading partner countries. It is an urgent task to establish an international information exchange system. The National Energy Policy Office in Thailand and the Office of Energy Affairs in the Philippines have started to collect and maintain systematically energy related information in each country. In other countries, collection and maintenance of energy data and information are conducted steadily, if not systematically. In Korea monthly data are available with about a one month time lag. Great interest is shown by all countries to the Pacific Energy Information Nework System, which will cover a wide range of energy data. But some countries are not provided with systems to cope with an on-line-network immediately. Consequently, an efficient system for information exchange, if not on-line-system, seems necessary in this region. To establish the basis of the information system, large expectations for Japan are expressed. DOE

N91-11603# Oak Ridge National Lab., TN. Engineering Technology Div.
DEVELOPMENT OF THE STRUCTURAL MATERIALS INFORMATION CENTER
C. B. Oland and D. J. Naus 1990 36 p Presented at the 18th Water Reactor Safety Information Meeting, Gaithersburg, MD, 22 Oct. 1990
(Contract DE-AC05-84OR-21400)
(DE90-016521; CONF-9010185-1) Avail: NTIS HC/MF A03

The U.S. Nuclear Regulatory Commission has initiated a Structural Aging Program at the Oak Ridge National Laboratory to identify potential structural safety issues related to continued service of nuclear power plants and to establish criteria for evaluating and resolving these issues. One of the tasks in this program focuses on the establishment of a Structural Materials Information Center where data and information on the time variation of concrete and other structural material properties under the influence of pertinent environmental stressors and aging factors are being collected and assembled into a data base. This data base will be used to assist in the prediction of potential long term deterioration of critical structural components in nuclear power plants and to establish limits on hostile environmental exposure for these structures and materials. Two complementary data base formats were developed. The Structural Materials Handbook is an expandable, hard copy reference document that contains complete sets of data and information for selected portland cement concrete, metallic reinforcement, prestressing tendon, and structural steel materials. Baseline data, reference properties and environmental information are presented in the handbook as tables, notes and graphs. The handbook, which will be published in four volumes, serves as the information source for the electronic data base. The Structural Materials Electronic Data Base is accessible by an IBM-compatible personal computer and provides an efficient means for searching the various data base files to locate materials with similar properties. Properties will be reported in the International System of Units (SI) and in customary units whenever possible. DOE

N91-11604# Federal Information Exchange, Inc., Germantown, MD.
DESIGN, DEVELOP, TEST, AND IMPLEMENT AN ON-LINE RESEARCH AND EDUCATION INFORMATION SERVICE Technical Report, 30 Sep. 1989 - 30 Sep. 1990
1990 9 p
(Contract DE-FG05-89ER-75527)
(DE90-017654; DOE/ER-75527/2) Avail: NTIS HC/MF A02

On September 30, 1989, Federal Information Exchange, Inc. received a grant from DOE to operate the DOEINFO system, convert it to the FEDIX system, enlarge its scope to include programs at Argonne, Brookhaven, Lawrence Berkeley, Oak Ridge and Pacific Northwest Laboratories and add NASA and the Office of Naval Research (ONR) to the system. FEDIX was developed to give DOE, ONR, and NASA maximum editorial control over the content of the information provided on-line. Procedures were developed to ensure maximum consultation between Agency staff and Federal Information Exchange, Inc. The key features that make FEDIX attractive to the user community include: ease of use, no service charge, quality information, search by keywords, download capacity comprehensive information, and participation of several agencies. The objective and milestones outlined in the FEDIX proposal are on schedule and work requirements have been met. DOE

83 ECONOMICS AND COST ANALYSIS

Includes cost effectiveness studies.

No abstracts in this category.

84 LAW, POLITICAL SCIENCE AND SPACE POLICY

Includes NASA appropriation hearings; aviation law; space law and policy; international law; international cooperation; and patent policy.

No abstracts in this category.

85 URBAN TECHNOLOGY AND TRANSPORTATION

Includes applications of space technology to urban problems; technology transfer; technology assessment; and surface and mass transportation.

For related information see also *03 Air Transportation and Safety, 16 Space Transportation,* and *44 Energy Production and Conversion.*

No abstracts in this category.

88 SPACE SCIENCES (GENERAL)

No abstracts in this category.

89 ASTRONOMY

Includes radio, gamma-ray, and infrared astronomy, and astrometry.

N91-11605*# Space Telescope Science Inst., Baltimore, MD.
NOVAE AS DISTANCE INDICATORS
Holland C. Ford and Robin Ciardullo (Kitt Peak National Observatory, Tucson, AZ.) Aug. 1988 18 p Previously announced in IAA as A90-14144 Submitted for publication
(Contract NAS5-29293; NAGw-421)
(NASA-CR-186278; Preprint-Series-300; NAS 1.26:186278)
Avail: NTIS HC/MF A03 CSCL 03A

Nova shells are characteristically prolate with equatorial bands and polar caps. Failure to account for the geometry can lead to large errors in expansion parallaxes for individual novae. When simple prescriptions are used for deriving expansion parallaxes from an ensemble of randomly oriented prolate spheroids, the average distance will be too small by factors of 10 to 15 percent. The absolute magnitudes of the novae will be underestimated and the resulting distance scale will be too small by the same factors. If observations of partially resolved nova shells select for large inclinations, the systematic error in the resulting distance scale could easily be 20 to 30 percent. Extinction by dust in the bulge of M31 may broaden and shift the intrinsic distribution of maximum nova magnitudes versus decay rates. We investigated this possibility by projecting Arp's and Rosino's novae onto a composite B - 6200A color map of M31's bulge. Thirty two of the 86 novae projected onto a smooth background with no underlying structure due to the presence of a dust cloud along the line of sight. The distribution of maximum magnitudes versus fade rates for these unreddened novae is indistinguishable from the distribution for the entire set of novae. It is concluded that novae suffer very little extinction from the filamentary and patchy distribution of dust seen in the bulge of M31. Time average B and H alpha nova luminosity functions are potentially powerful new ways to use novae as standard candles. Modern CCD observations and the photographic light curves of M31 novae found during the last 60 years were analyzed to show that these functions are power laws. Consequently, unless the eruption times for novae are known, the data cannot be used to obtain distances. Author

N91-11606*# Wyoming Univ., Laramie. Dept. of Physics and Astronomy.
IMAGE RECONSTRUCTION OF IRAS SURVEY SCANS Final Report, 1 Sep. 1989 - 31 Oct. 1990
Tj. Romke Bontekoe 31 Oct. 1990 10 p
(Grant NAG5-1246)
(NASA-CR-187328; NAS 1.26:187328) Avail: NTIS HC/MF A02 CSCL 03A

The IRAS survey data can be used successfully to produce images of extended objects. The major difficulties, viz. non-uniform sampling, different response functions for each detector, and varying signal-to-noise levels for each detector for each scan, were resolved. The results of three different image construction techniques are compared: co-addition, constrained least squares, and maximum entropy. The maximum entropy result is superior. An image of the galaxy M51 with an average spatial resolution of 45 arc seconds is presented, using 60 micron survey data. This exceeds the telescope diffraction limit of 1 minute of arc, at this wavelength. Data fusion is a proposed method for combining data from different instruments, with different spacial resolutions, at different wavelengths. Data estimates of the physical parameters, temperature, density and composition, can be made from the data without prior image (re-)construction. An increase in the accuracy of these parameters is expected as the result of this more systematic approach. Author

N91-11607# National Geodetic Survey, Rockville, MD.
APPARENT PLACE OF POLARIS AND APPARENT SIDEREAL TIME AT 0 HOUR UT 1990-1994
Jul. 1990 64 p
(PB90-259169) Avail: NTIS HC/MF A04 CSCL 03A

The apparent right ascension and declination of Polaris and the Greenwich Sidereal Time at 0 hour Universal Time for each day is given. Tabulated apparent place coordinates are generated from the Fifth Fundamental Catalogue (FK5). Note that values for 1990 were previously published using the Fourth Fundamental Catalogue (FK4). Although values for apparent right ascension and declination of Polaris and Greenwich Sidereal Time differ between FK4 and FK5, the resulting differences in computed azimuth are small. The publication is prepared for the convenience of the surveyor who observes Polaris for azimuth control to orient a field survey project. The right ascension and declination values can be linearly interpolated directly from the tables using as an argument the decimal part (Universal Time converted to the decimal part of the day) of the Greenwich Civil Day (GCD). Author

N91-11608 Johns Hopkins Univ., Baltimore, MD.
POPULATION STUDIES IN GROUPS AND CLUSTERS OF GALAXIES, VOLUMES 1 AND 2 Ph.D. Thesis
Henry Closson Ferguson 1990 331 p
Avail: Univ. Microfilms Order No. DA9018578

Studies of galaxies and clusters of galaxies provide some of the best observational constraints on theories for the origin and evolution of the universe. However, most studies carried out to date have been biased toward galaxies with high luminosities, which are rare compared to low luminosity, low surface brightness dwarf galaxies. To begin to redress this bias, a deep optical survey was made of six nearby groups of galaxies using 40 large scale plates taken with the du Pont 2.5-m reflector, and have combined the catalogs with data from a similar study of the Virgo Cluster by Binggeli et al. (1985). By virtue of their low surface brightness, dwarf galaxies in nearby groups can be readily distinguished from background galaxies. The well defined relation between surface brightness and luminosity was confirmed for the dwarf galaxies in the sample, and show that this relation does not result from selection effects. The dwarf-to-giant ratio varies significantly from group to group in the sample. The variation is most pronounced for the early type galaxies; the Virgo Cluster contains five times as many early type dwarfs per early type giant as the poorest groups of galaxies in our survey. The dwarf to giant ratio shows a positive correlation with the richness of the groups.
Dissert. Abstr.

N91-11609 Wyoming Univ., Laramie.
A STUDY OF THE TEN AND TWENTY MICRON SILICATE FEATURES IN CELESTIAL INFRARED SOURCES Ph.D. Thesis
Thomas L. Hayward 1989 161 p
Avail: Univ. Microfilms Order No. DA9016660

Using two low spectral resolution infrared spectrometers and the 2.3-meter telescope of the Wyoming Infrared Observatory, photometry and imaging data were gathered on a number of compact HII regions and protostellar sources at wavelengths from 8 to 24 microns. Models using three components of dust, using a standard emissivity law for silicate grains, in which two of the dust components are warm enough to emit significantly at these wavelengths and the third component is cold but is seen through its extinction effect, successfully fit the observed spectra of many sources. These models are refinements to two-component models often used to fit the observed 8 to 13 microns spectra of these sources. The warmer dust component is typically hotter, and the cool component is typically cooler, than dust temperatures derived from two-component fits. The exact configuration of these three dust components varies among the different sources studied. Pixel-by-pixel fits to sources for which the best data were obtained

result in maps of dust optical depths and temperatures for each component. Dissert. Abstr.

N91-11610 Brandeis Univ., Waltham, MA.
MAXIMUM ENTROPY IMAGING OF RADIO ASTROPHYSICAL DATA Ph.D. Thesis
Mark Allan Holdaway 1990 247 p
Avail: Univ. Microfilms Order No. DA9017962

Imaging and deconvolution of linear polarization P in radio synthesis has generally been accomplished through the same means as imaging total intensity I, namely, by Fourier inversion followed by application of the CLEAN algorithm (Hoegbom, 1974). In very long baseline interferometry (VLBI) and the sources which can be investigated by VLBI, poor (u,v) coverage, lower SNR in the polarization data, high intrinsic degrees of polarization in the observed sources, and knotty source structure can result in nonphysical I and P images in which features are imaged to be more than 100 percent polarized. The maximum entropy method (MEM) is flexible enough to permit simultaneous image of I and P to ensure the image is everywhere less than 100 percent polarized. Here, the algorithm of Cornwell and Evans (1985) is applied to imaging I and P on milliarcsecond scales. The success of MEM in imaging VLBI data is gauged by simulations on test data. The first I and P radio images deconvolved simultaneously by MEM and generated from real data are presented. Applications of MEM to the problems of rotation measure imaging, imaging directly from closure and amplitudes, and length distribution deprojection are discussed. Dissert. Abstr.

N91-11611 California Univ., Santa Cruz.
OBSERVATIONS AND INTERPRETATION OF THE INFRARED EMISSION FROM SUPERNOVA SN1987A Ph.D. Thesis
Diane Holland Wooden 1989 183 p
Avail: Univ. Microfilms Order No. DA9021416

Infrared spectrophotometric observations of SN1987A from the Kuiper Airborne Observatory are presented for the wavelength range 1.5 to 12.5 microns for five epochs at about 60, 260, 415, 615, and 777 days after the explosion. These data are combined with the ultraviolet, optical, infrared (UVOIR) measurements from ESO/CTIO and SAAO in order to characterize the continuum by three components: a photospheric contribution, free-free radiation, and the infrared emission from dust characterized by greybody radiation. Line flux measurements from the continuum substracted spectra are given, including the Brackett, Pfund, and Humphreys series of hydrogen and neutral and singly-ionized nickel and argon from the core ejecta. Carbon monoxide and silicon monoxide vibration bands are identified in the spectra. A simple analysis of the hydrogen line and free-free emission is presented. Dust radiative equilibrium calculations are performed. At 415 days, excess infrared emission, not accountable by circumstellar dust, was observed. At 615 and 777 days, this new component dominated the infrared continuum and is evidence for dust condensation in the ejecta of SN1987A. The shape of the infrared emission from newly formed dust is well characterized by the Planck curve, i.e., by a greybody, and therefore the grains which formed in the ejecta are either large or their emission arises from optically thick clumps. The radiative equilibrium temperature of the observed greybody emission indicates that the dust is in the metal-rich volume of the ejected core. Dissert. Abstr.

N91-11612 Florida Univ., Gainesville.
LONG-TERM OBSERVATIONS OF THREE MASSIVE X RAY BINARY TRANSIENTS: 4U0115+63, V0332+53, AND GX301-2 Ph.D. Thesis
Laura Alice Whitlock 1989 100 p
Avail: Univ. Microfilms Order No. DA9021262

The known massive x ray binaries, 4U0115+63, V0332+53, and GX301-2, which are considered to be transients or highly variable, are looked at with the Vela 5B x ray data. In order to exploit the full richness of the data, a reorganization of the data base was necessary with two main objectives: convert from time to celestial coordinate order, and transfer the data base to reside and run on a VAX. Upon completion of this effort, access to each 1-second observation for a given x ray source for the 10 years spanned by the data could be accomplished quickly and easily, allowing a detailed study of the long term time histories as well as short term variations. The known periodicities in the sources are monitored for changes either in period or pulse shape. Also, new periods are searched for in the context of recent theoretical predictions. Combining the results obtained from these analyses, better models and perhaps a deeper understanding of the overall behavior of these systems can be achieved. The sources chosen here are all B or Be/neutron star binaries. However, it is seen that they exhibit diverse temporal and spectral behaviors. Four previously unknown recurrences for 4U0115+63 are reported. Also now available to analysis are the pulse periods of the sources and a well resolved monitor of the 41.5 day orbital period light curve for GX301-2. Dissert. Abstr.

N91-11613 Stanford Univ., CA.
THE EGRET GAMMA RAY TELESCOPE AND ITS ENERGY CALIBRATION Ph.D. Thesis
Arthur H. Walker 1990 244 p
Avail: Univ. Microfilms Order No. DA9024372

A current review is presented of the state of high energy gamma ray astronomy. Thereafter, the operating principles of the Energetic Gamma Ray Experiment Telescope (EGRET) gamma ray telescope are stated, together with the performance originally expected. The mechanical design and assembly of the large total absorption, or TASC, detector for EGRET is then described, followed by a review of the measurements made and actions taken to assure the integrity of the TASC detector in the five-year period between assembly and launch. A description of the electronic system associated with TASC is then provided, together with its operation in coordination with the rest of the EGRET telescope. The results of an initial exploration and calibration of the TASC detector alone in a positron beam at SLAC are then discussed. Thereafter, the design of an experiment to calibrate the fully assembled EGRET detector in a calibration gamma ray beam at SLAC is described. The results of this calibration relating particularly to the performance of the TASC detector are than outlined. Finally, a recalibration experiment conducted two years later at the MIT Bates Accelerator Center is discussed. Dissert. Abstr.

N91-11614 Florida Univ., Gainesville.
OBSERVATIONS OF PULSARS AT LOW RADIO FREQUENCIES Ph.D. Thesis
Francisco Jose Reyes 1989 264 p
Avail: Univ. Microfilms Order No. DA9021246

The emission of pulsars at low radio frequencies (less than 50 MHz) presents several unique characteristics which are related to the configuration and physical conditions of the magnetosphere at large distances from the neutron star. However, the existing data at low radio frequencies is scarce, due to the lack of adequate instruments and to intrinsic difficulties in carrying out the observations. Several intense, low-dispersion, long-period pulsars were observed, using the University of Chile 45 MHz radiotelescope and the University of Florida 26.3 MHz radiotelescope. A total of eleven pulsars were observed at 45 and 26.3 MHz. All pulsars were observed with one- or two-channel receivers and narrow bandwidths. Long term integration was used in order to improve the signal-to-noise ratio of the pulses. The data were digitized at sampling rates between 32 and 100 Hz. The basic parameters measured for the detected pulsars are given. The dispersion measure was computed using the delay of arrival times of the integrated pulse profiles. A collection of integrated pulse profiles for each of the detected pulsars is included. The measurements obtained at 45 and 26.3 MHz were compared with already published low frequency data. The results obtained were discussed in the context of current models of the pulsar magnetosphere. The results of the observations are consistent, within the context of the polar cap model, with emission originating in the distorted magnetic field at a distance comparable to the radius of the velocity-of-light cylinder. Dissert. Abstr.

N91-11615 Pennsylvania State Univ., University Park.
ASTRONOMICAL APPLICATIONS OF SURVIVAL ANALYSIS Ph.D. Thesis
Takashi Isobe 1989 236 p
Avail: Univ. Microfilms Order No. DA9018229

Astronomers often observe a sample of objects in search of statistical results such as luminosity functions and correlations. Statistical techniques are discussed which are applicable to a sample in which a portion of the variables are not detected, e.g., when upper limits are present in the variables. An extensive field of statistics called survival analysis addresses this problem. Several survival analysis techniques most useful to astronomical data analysis are presented. Using Monte Carlo simulations, the performance and accuracy of survival analysis in astronomical situations is tested. The simulations show that survival analysis is reliable in the search for correlations between luminosities at different bands. As an application of univariate survival analysis, a study is presented of continuum radiation from active galactic nuclei (AGNs). Several previous studies with correct statistical methods and large databases are confirmed: Radio selected quasars have two different emission mechanisms in the x ray band: BL Lac objects appear to be special cases of the radio selected quasars; some compact radio sources show the possibility of Synchritron-Self-Conpton in the optical band. Dissert. Abstr.

N91-11616 Oregon Univ., Eugene.
OBSERVATION AND ANALYSIS OF VARIABLE LINEAR POLARIZATION IN THE YELLOW SUPERGIANT STAR EPSILON AURIGAE Ph.D. Thesis
Gary Dewayne Henson 1989 136 p
Avail: Univ. Microfilms Order No. DA9010122

Epsilon Aurigae is an extremely long period eclipsing binary system whose primary component is a yellow supergiant star. The nature of the secondary component is uncertain, but it is believed to be a disk of cool dust and gas, possibly surrounding an unseen young hot star or binary star. The yellow supergiant is known to be an irregular long period variable star and the variability is considered to be the result of pulsations, the characteristics of which are unknown. Linear polarization measurements in U, B, and V filters were obtained over a four year period to investigate the possibility of a relationship between the variable polarization and pulsation modes in the star. A comparison with contemporaneous photometric observations was made to look for correlations between the light and polarization changes. A period analysis revealed no strict periodicities in the data although variations with a time scale on the order of 100 days were observed. The behavior of the polarization variations during cycles of maxima and minima in the light curve closely fit model predictions for nonradial pulsation. Changes in the direction of the major axis of the polarization variations strongly suggests the presence of at least two modes in the star at different times and perhaps even simultaneously. Although a definite mode or modes could not be identified, the variations were best interpreted as due to modes with $l = 2$ or $l = 3$. Also, rectilinear patterns of the polarization variations on the Q, U plane indicate that the inclination of the star's rotation axis is large, near 90 deg. Dissert. Abstr.

N91-11617 Harvard Univ., Cambridge, MA.
SPECKLE IMAGING OF COMPLICATED OBJECTS Ph.D. Thesis
James William Beletic 1989 161 p
Avail: Univ. Microfilms Order No. DA9013196

Speckle imaging theory and techniques are reviewed with emphasis on practical implementation. The extended Knox-Thompson and bispectrum phase recovery algorithms were developed and tested. It was determined that the bispectrum coupled with constrained amplitude recovery is the best procedure for image reconstruction. A numerical program that simulates atmospheric distortions, telescope aberrations, photon noise and sensor characteristics was developed. This computer simulation was verified by laboratory experiment and telescope data. The computer simulation was used to explore the quality of image reconstruction as a function of the target object, atmospheric seeing and detected light level. The information obtained from a reconstructed speckle image was shown to depend on the object which is being imaged and the questions which are being asked about the object. Thus, no universal rules can be made about the information content of images reconstructed from speckle data; each imaging scenario must be individually analyzed. Reconstructed images are shown to be very similar to those produced by two simple models. The first model, the white noise model, demonstrates that speckle image reconstruction can be mimicked by adding white noise to an atmospherically attenuated spectrum of the distortion-free object. The second model, the photon poor model, equates the reconstructed speckle image to an image of the distortion-free object produced from a limited number of photons. The white noise and photon poor models can be used to predict reconstructed image quality for any speckle imaging scenario. An assessment of the capabilities of speckle imaging for solar system research is presented, and the reconstructed image quality that can be obtained is demonstrated.
Dissert. Abstr.

90 ASTROPHYSICS

Includes cosmology; celestial mechanics; space plasmas; and interstellar and interplanetary gases and dust.
For related information see also *75 Plasma Physics*.

N91-11618 Arizona Univ., Tucson.
THE RELATIONSHIP OF GALAXY MORPHOLOGY TO NUCLEAR STAR FORMATION IN NON-INTERACTING SPIRAL GALAXIES Ph.D. Thesis
Stephen Mark Pompea 1989 140 p
Avail: Univ. Microfilms Order No. DA9013154

Three specific questions concerning the relationship between galactic morphology and infrared properties were addressed for noninteracting galaxies: (1) the scarcity of high infrared luminosity Sa galaxies compared to Sb and Sc; (2) the relationship between the bulge to total luminosity and the infrared properties of early type spirals; and (3) nuclear star formation processes in noninteracting galaxies. These questions were answered using IRAS data, CO (1 to 0) measurements, 2 micron, 10 micron, and visible CCD observations. Only four percent of Sa's in the Revised Shapley-Ames Catalog (RSAC) with B(gamma) is less than 12 have infrared luminosities 1/6th of the ratio for Sb's and Sc's. Less than three Sa's of 166 in the RSAC have nuclear starbursts not associated with interactions or active nuclei. A comparison of neutral hydrogen fluxes and CO fluxes with infrared fluxes implies that molecular cloud formation is inhibited in Sa's, leading to the lack of infrared activity. An investigation of the role of bulges in suppressing star formation in Sa through Sb spirals relied on the photometric observations of Kent, Kodaira, and Cornell and on IRAS infrared observatories. The results indicate that disk star formation is relatively unaffected by bulge size. The hypothesis that high far-infrared luminosities in noninteracting galaxies are dependent on material fed into the nuclei by bars was tested by near infrared imaging of a sample of 15 optically unbarred galaxies in a search for hidden bars. At least 8 of these galaxies do not appear to have bars. Strong bars therefore are not an absolute requirement for high infrared luminosity. Dissert. Abstr.

N91-11619*# Pennsylvania Univ., Philadelphia. Dept. of Astronomy and Astrophysics.
REEXAMINATION OF DATA FROM THE ASTEROID/METEOROID DETECTOR Final Report
Robert K. Soberman and Maurice Dubin (National Aeronautics and Space Administration. Goddard Space Flight Center, Greenbelt, MD.) 1 Nov. 1990 33 p
(Grant NAGw-1782)
(NASA-CR-185875; NAS 1.26:185875) Avail: NTIS HC/MF A03 CSCL 03B

A reexamination of the results of the Pioneer 10 and 11 Asteroid Meteoroid Detector, or Sisyphus, was carried out in the light of a recently derived theory characterizing interplanetary matter

and the Zodiacal Light (ZL). Sisyphus measured individual meteoroids from reflected sunlight and ZL between meteoroid events. The results were questioned because meteoroid orbits could not be calculated as intended and the ZL as computed from individual meteoroids did not agree with values determined from the ZL mode and from the other ZL sensor on the spacecraft. It is first shown that, independent of any explanation, the measurements are, with high probability, valid and strongly correlated with the ZL. The model which explains the strange behavior of the Sisyphus instrument also resolves the enigma why the three dust experiments on the Pioneer 10 and 11 spacecraft produced extreme disparate results for the distribution and orbits of meteoric particles and the ZL. The theory based primarily on these measurements requires a population in the inner solar system of cold meteoroid material composed mainly of volatile molecules. These meteoroids in orbits of high eccentricity are called cosmoids. They are impulsively disrupted from solar heating, resulting in order of magnitude increases in optical cross section. The dispersed particles, predominantly micron sized, scatter most of the ZL and supply the polarization. The sublimation time in sunlight for micron sized particles of volatile composition opposes the gravitational flux increase expected in approaching the sun. The other two Pioneer 10/11 dust experiments were: the Imaging Photopolarimeter for the ZL, and the Meteoroid Detection Experiment that measured penetration of 25 micron (Pioneer 10) and 50 micron (Pioneer 11) thick walls of pressurized gas cells. Author

N91-11620# Max-Planck-Inst. fuer Physik und Astrophysik, Garching (Germany, F.R.). Inst. fuer Extraterrestrische Physik.
[ACTIVITIES REPORT OF THE INSTITUTE FOR EXTRATERRESTRIAL PHYSICS] Annual Report, 1989 [INSTITUT FUER EXTRATERRESTRISCHE PHYSIK, TAETIGKEITSBERICHT 1989]
Jan. 1990 157 p In GERMAN
(MPE-217; ETN-90-97834) Copyright Avail: NTIS HC/MF A08

The fields of activity are divided into four parts: in situ space measurements; astrophysical measurements; laboratory measurements; and theory. The Institute's denomination originates for the main subject of research, space research, and from the research method. Articles dealing with near Earth space and solar system, infrared and submillimeter astronomy, x ray astronomy, gamma astronomy and laboratory astrophysics are covered.
ESA

N91-11621# Cologne Univ. (Germany, F.R.). Inst. fuer Geophysik und Meteorologie.
A TWO DIMENSIONAL MULTISONIC MODEL OF PLASMA INTERACTION FOR COMETARY ATMOSPHERE WITH SOLAR WIND [EIN ZWEIDIMENSIONALES, ANISOTROPES MULTIIONENMODELL DER PLASMAWECHSELWIRKUNG EINER KOMETENATMOSPHAERE MIT DEM SONNEWIND]
Joachim Raeder 1990 138 p In GERMAN
(Mitt-69; ISSN-0069-5882; ETN-90-97893) Avail: NTIS HC/MF A07

The first in situ measures of cometary plasmas and of their interaction with the solar wind have shown that the interaction is much more complex than it has been previously considered. It is demonstrated that the presence of various sorts of ions and the anisotropic distribution functions play an essential part in the interaction. A new numerical process is developed for the solution of equations relating to plasma properties. The comparison of different orientation models, and the magnetic fields in relation to the solar wind show that the angle between the solar wind speed and the IMF plays a decisive part for the interaction. Besides the numerical improvement, a better description of the interaction between the different sorts of ions seems necessary. The examinations should concentrate on the principal aspects of wave stimulation and structure interaction of solar winds with the atmosphere of a comet. Little is known of these processes and practically no simulation calculation has ever been carried out.
ESA

N91-11622 Minnesota Univ., Minneapolis.
FROM RED GIANTS TO PLANETARY NEBULAE: ASYMMETRIES, DUST, AND POLARIZATION Ph.D. Thesis
Joni Jayne Johnson 1990 107 p
Avail: Univ. Microfilms Order No. DA9024275

In order to investigate the development of aspherical planetary nebulae, polarimetry was obtained for a group of planetary nebulae and for objects that will evolve into planetary nebulae, i.e., red giants, late asymptotic giant branch (AGB) objects, proto-planetary nebulae, and young planetary nebulae. To study the dust around the objects in our sample, we also used data from the Infrared Astronomy Satellite (IRAS) mission. The youngest objects in our survey, red giants, had the hottest dust temperatures while planetary nebulae had the coolest. Most of the objects were intrinsically polarized, including the red giants. This indicated that the circumstellar dust shells of these objects were aspherical. Both carbon- and oxygen-rich objects could be intrinsically polarized. The intrinsic polarizations of a sample of our objects were modeled using an ellipsoidal circumstellar dust shell. The findings of this study suggest that the asphericities that lead to an aspherical planetary nebula originate when a red giant begins to undergo mass loss. The polarization and thus the asphericity as the star evolves, with both reaching a maximum during the proto-planetary nebula stage. The circumstellar dust shell will dissipate after the proto-planetary nebulae stage since no new material is being added. The polarization of planetary nebulae will thus be low. In the most evolved planetary nebulae, the dust has either been destroyed or dissipated into the interstellar medium. In these objects no polarization was observed. Dissert. Abstr.

N91-11623 Texas Univ., Austin.
MAGNETIC FIELD GENERATION IN ASTROPHYSICS Ph.D. Thesis
Gary Steven Bust 1989 150 p
Avail: Univ. Microfilms Order No. DA9016854

A study of the generation and maintenance of magnetic fields due to hydrodynamic motions was carried out. The physical system studied was a hydrodynamic shock wave. Under certain conditions the shock front is subject to a rippling instability. This instability can drive the generation of a magnetic field if the fluid is partially ionized. The generation of a magnetic field by such an instability was analyzed. Solutions were found for the evolution of the field, and for its spatial structure. For a spherical shock, the field was found to be a sum of spherical harmonics. It was found that the dominate scale for the magnetic field was the same as for the shock. Analysis by Vishniac and Ryu show that the fastest growing scale is approximately twice the minimal unstable scale, and that the minimal unstable scale is roughly the thickness of the shell. The maximum amplitude of the field B(sub max) was found to be approximately 10(exp -15) gauss. This however, is only the amplitude up to the time of fragmentation. The properties of a fragmenting shock were then analyzed in the weak nonlinear limit. The results were applied to the maintenance and/or amplification of the magnetic field found in the linear analysis. The induction equation for the magnetic field was analyzed. The nonlinear analysis of the shock was carried out by averaging over the thin shell of the shock. While necessary to make the problem tractable, the resulting velocities do not drive a magnetic dynamo.
Dissert. Abstr.

N91-11624 Texas Univ., Austin.
NITROGEN AND SULFUR IN IRREGULAR GALAXIES Ph.D. Thesis
Donald Roy Garnett 1989 140 p
Avail: Univ. Microfilms Order No. DA9016886

A study of nitrogen and sulfur in giant H II regions located within low abundance irregular galaxies is presented. Both observations and theoretical models are used in combination to examine variations in the abundances of nitrogen and sulfur relative to oxygen in these galaxies. A CCD spectrometer was used to observe the 9069 A and 9532 A emission lines of (S III). These observations yield greatly improved measurements of the abundance of S(+2) and, consequently, the total sulfur abundance.

Numerical models of the ionization structure of H II regions indicate that S(+3) can be important in the high ionization nebulae seen in irregular galaxies, but also indicate that the fraction of sulfur in the form of S(+3) can be estimated straightforwardly if one knows the O(+) fraction. Contrary to earlier claims, it is found that S/O does not increase as O/H decreases. The difference is attributed primarily to inadequate observations and the use of incorrect ionization correction schemes used in the earlier studies. It is concluded, after reanalysis of the earlier observations, that there is no evidence at present that S/O varies systematically as a function of the oxygen abundance. Dissert. Abstr.

N91-11625 Utah Univ., Salt Lake City.
NUMERICAL STUDIES OF ELECTRON SCATTERING IN ASTROPHYSICS Ph.D. Thesis
August L. Schultz 1990 140 p
Avail: Univ. Microfilms Order No. DA9019146

The application is described of numerical methods to astrophysical situations in which a detailed treatment of the scattering of radiation by electrons is required. A Monte Carlo computer code that simulates the scattering of photons on relativistic electrons is used. Electron-positron pair production in the spherical accretion flow onto a massive black hole is examined. A Monte Carlo code was used to check analytical expressions which describe the transfer of radiation through the atmosphere above the surface of a neutron star. Spherical accretion onto a massive black hole was studied, incorporating a detailed treatment of the scattering of photons between relativistically curved photon orbits. Dissert. Abstr.

N91-11626 Iowa Univ., Iowa City.
A SEARCH FOR SMALL COMETS IN CONSECUTIVE IMAGES ACQUIRED WITH A GROUND-BASED TELESCOPE Ph.D. Thesis
John B. Sigwarth 1989 130 p
Avail: Univ. Microfilms Order No. DA9019978

The Spacewatch Camera was calibrated in order to accurately determine the apparent V magnitudes of the observed objects and subsequently to estimate the corresponding masses. The Spacewatch Camera was cross-calibrated with The University of Iowa's 0.61-m Cassegrain at the Riverside Astronomical Observatory and with the observations by Sandage (1970) and by Sandage and Katem (1982). The three calibrations of the Spacewatch Camera agreed to within 0.1 mag. Twenty-four small body trails were identified in 48 pairs of consecutive images. To within statistical uncertainty, each pair of trails had equal brightness and length, was collinear and had the correct separation. An additional pair of trails was observed that satisfied the collinearity, length and separation criteria; however, the trail brightness could not be confirmed because the second small body trail crosses a star trail. The integral number densities as a function of apparent V magnitude and as a function of mass were determined for the small body trails observed by Yeates (1989) and the small body trails observed by the present observations. The observed small body trails have the orbital parameters, brightness, and spatial density inferred for the small comets proposed by Frank et al. (1986; 1987). Dissert. Abstr.

N91-11627 Massachusetts Univ., Amherst.
RECENT STARBIRTH AND STARBURST ACTIVITY IN NEARBY GALAXIES Ph.D. Thesis
William Howard Waller 1990 348 p
Avail: Univ. Microfilms Order No. DA9022755

The ionizing starbirth activity in M101, M82, and NGC 1569 was investigated via CCD imagery at H-Alpha, R, I, and (SIII) bands. The three galaxies are compared with one another and with M51, M83, and the Milky Way in terms of their starbirth intensities, starbirth efficiencies, and possible starbirth histories. The globally averaged starbirth intensities that are inferred from the extinction-corrected H-Alpha surface brightnesses vary by approx. 3 orders of magnitude, with M101 and the Milky Way defining the low end and with M82 defining the high intensity regime. The annular averaged starbirth intensities correlate strongly with the H2 surface densities and with the total gas surface densities, where near-linear relationships are obtained. Unusually high starbirth efficiencies and eruptive gaseous morphologies are evident in M82, NGC 1569, and NGC 5461, one of the supergiant HII region complexes in M101. Crude indices of the galaxies' starbirth histories indicate temporally declining starbirth intensities in M101 and the Milky Way but currently bursting starbirth intensities in M82 and NGC 1569. In M101, annular averaged photometry of the H-Alpha emission yields a much flatter galactocentric profile of surface brightness than that of the red-continuum starlight. The galactocentric variation in H-Alpha equivalent widths appears more closely related to the galaxy's radial profile of differential rotation than to its monotonic gradient in O/H abundances. The ionizing stellar populations in early type, late type, and starburst galaxies are discussed in terms of these results. Dissert. Abstr.

N91-11628 State Univ. of New York, Stony Brook.
ANALYTIC STUDIES IN NUCLEAR ASTROPHYSICS Ph.D. Thesis
Pierre Pizzochero 1989 206 p
Avail: Univ. Microfilms Order No. DA9021074

Five studies are presented in nuclear astrophysics, which deal with different stages of stellar evolution and which use analytic techniques as opposed to numerical ones. Two problems are described in neutrino astrophysics: the solar-neutrino puzzle is analyzed in the framework of the MSW mechanism for the enhancement of neutrino oscillations in matter; and the cooling of neutron stars is studied by calculating the neutrino emissivity from strangeness condensation. Radiative transfer is then examined as applied to SN1987A: its early spectrum and bolometric corrections are calculated by developing an analytic model which can describe both the extended nature of the envelope and the non-LTE state of the radiation field in the scattering-dominated early atmosphere; and a model-independent relation is derived between mass and kinetic energy for the hydrogen envelope of SN1987A, using only direct observations of its luminosity and photospheric velocity. Finally, an analytic approach is presented to relate the softness of the EOS of dense nuclear matter in the core of a supernova, the hydrostatic structure of such core and the initial strength of the shock wave. Dissert. Abstr.

N91-11629 Illinois Univ. at Urbana-Champaign, Savoy.
THE TRANSFER OF POLARIZED RADIATION IN ASTROPHYSICAL MASERS IN THE PRESENCE OF MAGNETIC FIELDS Ph.D. Thesis
Gerald Ernst Nedoluha 1990 130 p
Avail: Univ. Microfilms Order No. DA9021734

Polarized emission from astrophysical masers can provide important information about physical conditions in both star forming and circumstellar environments. Calculations are performed which give the spectra of the emergent maser radiation for different magnetic fields, radiative intensities, decay rates, and pumping rates thought to be appropriate in astrophysical masing regions. Results are obtained which for the first time make it possible to study the linear polarization of radiatively saturated masers when the stimulated emission rate and the Zeeman frequency are comparable, a regime which is of importance for nonparamagnetic masing molecules (i.e., H2O, SiO, CH3OH, H2CO) in astrophysics. The change in both the amount of linear polarization and its position angle as a function of the stimulated emission rate is followed through this regime. A striking feature of maser emission from OH molecules is the tendency for one of the circular polarizations to dominate the emission spectrum. The two mechanisms which may explain these observations both involve a masing gas in a velocity gradient. These mechanisms are studied by calculating the emergent spectra of the radiation without making the large velocity gradient approximation which has always been made in previous calculations of masing in a velocity gradient. Eliminating this approximation leads to previously unsuspected narrow line profiles even in regions where large velocity gradient are present, as well as to polarized spectra that resemble those of the observations. Dissert. Abstr.

N91-11630 Temple Univ., Philadelphia, PA.
AN INVESTIGATION OF THE NEWMAN-PENROSE CONSTANTS FOR MASSLESS FREE FIELDS OF ARBITRARY SPIN Ph.D. Thesis
David Michael Kerrick 1990 105 p
Avail: Univ. Microfilms Order No. DA9022917

The origin and significance of the Newman-Penrose absolutely conserved quantities for a spin s massless free fields including, and in particular, the gravitational field in general relativity is investigated. It is found that the NP conservation law for these fields can be generated by suitable (asymptotic) integration of a covariant wave equation satisfied by the fields at null infinity in an asymptotically flat spacetime resulting in a set of 2s + 1 complex constants of the motion, identified as the NP constants. The key to this derivation of the Newman-Penrose constants is the reduction of the above-mentioned wave equation to an intrinsic divergence on the null hypersurface, representing infinity in Penrose's treatment of asymptotic flat spacetimes. This result is refined and elaborated by considering the NP constants at a quasi-local level. In particular, a quasi-local NP conservation law for (linear) massless fields, valid on both Minkowski and Schwarzschild spacetime, is presented, corresponding to an integral formulation of the decoupled wave equations for a type D background given by Teukolsky in 1973. For a Minkowski background one obtains an exact quasi-local conservation law formally identical to the original, asymptotic version. In a Schwarzschild background, however, an exact conservation law is not possible due to the presence of the single non-vanishing component of the Weyl curvature characteristic of type D spacetimes. Invoking a recent theorem of Carminati and McLenaghan, it is argued that the non-exact nature of the quasi-local law on a Schwarzschild background is due to the non-Huygens character of (linear) massless fields propagating on a type D background. Conversely, it is conjectured that an exact quasi-local NP conservation law is possible only in those regions of spacetime in which the field propagates free of dispersion. The possible implications of this for the gravitational field in general relativity are discussed. Dissert. Abstr.

N91-11631 Georgia State Univ., Atlanta.
M51: THE WHIRLPOOL GALAXY, ANALYSIS AND SIMULATION Ph.D. Thesis
Sethanne Howard 1989 249 p
Avail: Univ. Microfilms Order No. DA9016644

The grand design spiral galaxy M51 (NGC 5194) was modeled as an interacting system and a three component self-gravitating N-body code was used to simulate the gravitational interaction. The problem reduces to choosing a finite set of orbits (for NGC 5195) that can model the observed features of M51. A simple gas cloud collision algorithm was included that permits features in the gas particles to strengthen. The code is stable and well tested. An analytic method was developed to set limits to some of the orbit parameters. This method is suitable for nearly face-on grand design galaxies with companions. The outer arms of M51 behave like material arms inward to approx. = 140 secs. The transition between the directly excited outer tidal arms and the indirectly excited inner arms explains the symmetrically placed bends in the outer arms of M51. The inner structure is consistent with resonantly excited m = 2 Lindblad dispersion orbits. Three regions of spiral structure in M51 are proposed: (1) the extended tidal arm created by the previous passage of NGC 5195; (2) the strong tidal arms seen in the optical and created by the most recent passage 70 to 84 million years ago; and (3) the inner density wave excited by these tidal arms. Dissert. Abstr.

N91-11632 Indiana Univ., Bloomington.
VIOLET AND VISUAL FLUX PROBLEMS IN RED GIANT STARS Ph.D. Thesis
Danny Reed Faulkner 1989 135 p
Avail: Univ. Microfilms Order No. DA9020712

Red giant stars are sites of many astrophysically interesting processes and are important links to late stages of stellar evolution and the chemical history of the galaxy. Much of what is known about stars comes from their spectra, which are formed in the outer layers (atmospheres). Unfortunately the low temperatures in red giant atmospheres promote the formation of many molecules, and the resultant complexity of the spectra has slowed progress in obtaining good models of these objects and leaves many unanswered questions. Several of these problems are investigated. Spectra of red giants provide a natural classification according to composition: M stars are oxygen rich, C stars are carbon rich, while S stars are intermediate. One long standing problem with C stars has been the explanation of the severe lack of energy flux in the violet and near ultraviolet part of their spectrum, generally attributed to an unusual opacity. Results show that one source, SiC, is untenable, while the case for the other, C3, is severely weakened. Synthetic spectra from atmospheric models are compared to spectra of TX Psc, a C star, to show that the contribution of thousands of atomic lines are probably responsible for the violet and ultraviolet flux deficiency. The agreement between the synthetic spectra and observations is very good. K and M type stars also have a violet flux deficiency, though it is less severe than with carbon stars. Dissert. Abstr.

N91-11633*# National Aeronautics and Space Administration. Goddard Space Flight Center, Greenbelt, MD.
LATE STAGES IN THE EVOLUTION OF CLASSICAL NOVAE
S. Starrfield, J. Krautter, G. Sonneborn, S. N. Shore, R. M. Wagner, S. Austin, P. Saizar, G. Ferland, R. Wade, and R. D. Gehrz (Minnesota Univ., Minneapolis.) et al 1990 26 p Presented at the Evolution in Astrophysics: IUE Astronomy in the Era of New Space Missions, Toulouse, France, 29 May - 1 Jun. 1990 Submitted for publication Prepared in cooperation with Los Alamos National Lab., NM
(Contract W-7405-eng-36)
(NASA-TM-102969; NAS 1.15:102969; DE90-014911; LA-UR-90-2389; CONF-9005248-2) Avail: NTIS HC/MF A03 CSCL 03B

We have begun a study of the long term evolution of novae in outburst in order to determine the means by which they return in quiescence when nuclear burning has ended. This project involves both IUE and optical observations and theoretical predictions. Recently, in the initial observational part of this project, we have obtained IUE Short Wavelength Prime (SWP) spectra of GQ Mus 1983 and QU Vul 1984. Each spectrum was a 16 hour exposure using a combined US1 plus Vilspa shift. No novae have been studied in the UV for as long as QU Vul and GQ Mus and observations of their spectral evolution are providing unique data on the turn-off time scale. We have also obtained the spectra of old novae from the IUE archives in order to compare and contrast the existing spectra with those of GQ Mus and Qu Vul. The theoretical prediction is that a nova should be very hot just before turnoff but x ray observations from EXOSAT do not confirm this prediction. DOE

N91-11634# Texas Univ., Austin. Dept. of Physics.
ON THE ORIGIN OF COSMOLOGICAL MAGNETIC FIELDS
T. Tajima, S. Cable, K. Shibata, and R. M. Kulsrud (Institute for Advanced Study, Princeton, NJ.) Aug. 1990 41 p Sponsored in part by NSF
(Contract DE-FG05-80ET-53088)
(DE90-017617; DOE/ET-53088/452; IFSR-452) Avail: NTIS HC/MF A03

It is shown that a plasma with temperature T sustains fluctuations of electromagnetic fields and particle density even if it is assumed to be in a thermal equilibrium. The level of fluctuations in the plasma for a given wavelength and frequency of electromagnetic fields is rigorously computed by the fluctuation-dissipation theorem. A large zero frequency peak of electromagnetic fluctuations is discovered. It is shown that the energy contained in this peak is complementary to the energy lost by the plasma cutoff effect. The level of the zero frequency magnetic fields is computed. The theoretical minimum magnetic field strength is also computed, as no turbulence is assumed. The size of the fluctuations is shown. These results are not in contradiction with the conventional black body radiation spectra but its extension, and as such, do not contradict the observed

lack of structure in the cosmic microwave background. The level of these is computed. The computer particle simulation shows the support of the theory and in fact exhibits a peaking of the magnetic energy spectrum at zero frequency. The level of magnetic fields is significant at the early radiation epoch of the Universe. Implications of these magnetic fields in the early Universe are discussed. DOE

N91-11635# Lawrence Livermore National Lab., CA.
A NEW SITE FOR THE ASTROPHYSICAL GAMMA-PROCESS
W. Michael Howard, Bradley S. Meyer, and Stanford E. Woosley (California Univ., Santa Cruz.) May 1990 6 p Presented at the International Symposium on Nuclear Astrophysics: Nuclei in the Cosmos, Vienna, Austria, 18-22 Jun. 1990
(Contract W-7405-eng-48)
(DE90-017519; UCRL-JC-104223-Rev-1; CONF-9006212-3-Rev-1) Avail: NTIS HC/MF A02

It is proposed that the requisite thermodynamic conditions may occur in Type Ia supernovae, when carbon-oxygen white dwarfs explode by deflagration. The cores of such stars have undergone extensive s-processing during helium flashes to provide sufficient s-process seeds for the light p-isotopes. When these stars undergo a deflagration disruption, these s-process isotopes can be transmuted into p-isotopes in the mass region of the core where the deflagration flame is extinguished and the temperatures approach the range 2.4 (approx less than) T(exp 9) (approx less than) 3.2. At these temperatures the enhanced s-process seeds are efficiently transmuted into p-isotopes on a timescale of less than 1 sec. To examine this astrophysical site, the nucleosynthesis is calculated that takes place when such mass zones are heated by the deflagration wave and then expand and compare the results with the solar-system distribution of the p-isotopes. DOE

N91-11636# Hirosaki Univ. (Japan). Research Inst. for Theoretical Physics.
THE ROLE OF SHEAR IN THE COSMOLOGICAL DISTANCE
Kazuya Watanabe and Misao Sasaki Mar. 1990 10 p
(DE90-513788; RRK-90-8) Avail: NTIS (US Sales Only) HC/MF A02

The effect of shear along light rays on the distance-redshift relation in an inhomogeneous universe is investigated on the basis of relativistic optical equations. With some reasonable assumptions, an analytic formula for the shear in a simplified cosmological model is derived. The derived formula is compared with numerical calculations and the validity and limitation of the formula is discussed. Then the role of shear in the distance-redshift relation is discussed in detail. DOE

N91-11637# Hiroshima Univ., Takehara (Japan). Research Inst. for Theoretical Physics. ia035223
APPLICATION OF THE EWALD METHOD TO COSMOLOGICAL N-BODY SIMULATIONS
Lars Hernquist, Yasushi Suto, and Francois R. Bouchet (Institut d'Astrophysique, Paris, France) Mar. 1990 21 p
(DE90-513789; RRK-90-07) Avail: NTIS (US Sales Only) HC/MF A03

Fully periodic boundary conditions are incorporated into a gridless cosmological N-body code using the Ewald method. It is shown that the linear evolution of density fluctuations agrees well with analytic calculations, contrary to the case of quasi-periodic boundary conditions where the fundamental mode grows too rapidly. The implementation of fully periodic boundaries is of particular importance to relative comparisons of methods based on hierarchical tree algorithms and more traditional schemes using Fourier techniques such as PM and P sup 3 M codes. DOE

N91-11638# Hiroshima Univ., Takehara (Japan). Research Inst. for Theoretical Physics.
COSMOLOGICAL N-BODY SIMULATIONS WITH A TREECODE
Tatsushi Suginohara and Yasushi Suto (Ibaraki Univ., Hitachi, Japan) Mar. 1990 34 p Sponored in part by Aid for Science Research Fund of the Ministry of Education, Science and Culture
(DE90-513790; RRK-90-06) Avail: NTIS (US Sales Only) HC/MF A03

Evolution of gravitationally interacting N-body systems in the universe is numerically studied. The N-body method is based on the hierarchical tree algorithm and the fully periodic boundary condition is implemented by applying the Ewald method. All of 262,144 particles were used in total, which are initially distributed to represent scale-free power spectra of density fluctuations P(k)proportional to k sup n, with n = -2, -1, 0 and 1. The subsequent evolution is followed in both flat and open universes. With this large number of particles, the discretized system can represent the initial linear phase, in good agreement with analytic theory. Dynamics in the strongly nonlinear regime depends on both the spectral index n and the density parameter Omega. In Omega = 1 universes, evolution of two-point correlation functions (xi) for (xi) greater than or approx. 100 agrees with the similarity solutions. In the weakly nonlinear regimes, the growth rate of density fluctuations sensitively depends on n. DOE

N91-11639# Hiroshima Univ., Takehara (Japan). Research Inst. for Theoretical Physics.
MICROWAVE BACKGROUND ANISOTROPIES AND THE PRIMORDIAL SPECTRUM OF COSMOLOGICAL DENSITY FLUCTUATIONS
Yasushi Suto, Naoteru Gouda, and Naoshi Sugiyama (Kyoto Univ., Japan) Mar. 1990 20 p
(DE90-513791; RRK-90-05) Avail: NTIS (US Sales Only) HC/MF A03

Microwave background anisotropies in various cosmological scenarios are studied. In particular, the extent to which non-scale invariant spectra of the primordial density fluctuations are consistent with the observational upper limits is examined. The resultant constraints are summarized as contours on (n, Omega) plane, where n is the power law index of the primordial spectrum of density fluctuations, and Omega is the cosmological density parameter. They are compared also with the constraints from the cosmic Mach number test, recently proposed by Ostriker and Suto. The parameter regions which pass both tests are not consistent with the theoretical prejudice inspired by the inflationary model. DOE

N91-11640# National Lab. for High Energy Physics, Ibaraki (Japan).
STATUS REPORTS OF SUPERCOMPUTING ASTROPHYSICS IN JAPAN
Takashi Nakamura, ed. and Mikio Nagasawa, ed. 1990 412 p Presented at the Workshop on Supercomputing Astrophysics, Tsukuba, Japan, 31 Aug. - 2 Sep. 1989
(DE90-513793; KEK-PR-89-2; CONF-8908246) Avail: NTIS (US Sales Only) HC/MF A18

More than 40 workshop participants of physicists, astronomers were attendant and discussed many topics in the informal atmosphere. The main purpose was focused on the theoretical activities in computational astrophysics in Japan. It was also aimed to promote effective collaboration between the numerical experimentists working on supercomputing technique. The various subjects of the presented papers of hydrodynamics, plasma physics, gravitating systems, radiative transfer, and general relativity are all stimulating. In fact, these numerical calculations become possible now in Japan owing to the power of Japanese supercomputer such as HITAC S820, Fujitsu VP400E and NEC SX-2. DOE

91 LUNAR AND PLANETARY EXPLORATION

Includes planetology; and manned and unmanned flights. For spacecraft design or space stations see *18 Spacecraft Design, Testing and Performance.*

N91-11641*# California Univ., Los Angeles. Dept. of Mechanical, Aerospace, and Nuclear Engineering.
DESIGN OF A SCIENTIFIC PROBE FOR OBTAINING MARS SURFACE MATERIAL Final Report
Miles Baker, Eric Deyerl, Tim Gibson, Bob Langberg, and Terrance Yee, ed. 5 Jun. 1990 154 p
(Contract NASw-4435)
(NASA-CR-186672; NAS 1.26:186672) Avail: NTIS HC/MF A08 CSCL 03B

The objective is to return a 1 Kg Martian soil sample from the surface of Mars to a mothership in a 60 km Mars orbit. Given here is information on the mission profile, the structural design and component placement, thermal control and guidance, propulsion systems, orbital mechanics, and specialized structures. Author

N91-11642*# Iowa Univ., Iowa City. Dept. of Physics and Astronomy.
WHISTLERS IN NEPTUNE'S MAGNETOSPHERE: EVIDENCE OF ATMOSPHERIC LIGHTNING
D. A. Gurnett, W. S. Kurth, I. H. Cairns, and L. J. Granroth Jun. 1990 42 p
(Contract JPL-957723)
(NASA-CR-187324; NAS 1.26:187324; U-of-Iowa-90-19) Avail: NTIS HC/MF A03 CSCL 03B

During the Voyager 2 flyby of Neptune, a series of 16 whistler-like events were detected by the plasma wave instrument near closest approach. These events were observed at radial distances from 1.30 to 1.99 R sub N and magnetic latitudes from -7 to 33 deg. The frequencies ranged from 6.1 to 12.0 kHz, and the dispersions fit the Eckersley law for lightning-generated whistlers. Lightning in the atmosphere of Neptune is the only known source of such signals. The frequency range of the whistlers (up to 12 kHz) indicates that the local electron densities are substantially higher (N sub e greater than 30 t0 100 per cu cm) than indicated by the in situ plasma measurements. The dispersion of the whistlers is very large, typically 26,000 sec Hz(exp 0.5). Based on existing plasma density models and measurements, the dispersions are too large to be accounted for by a single direct path from the lightning source to the spacecraft. Therefore, multiple bounces from one hemisphere to the other are required. The most likely propagation path probably involves a lightning source on the dayside of the planet, with repeated bounces through the dense dayside ionosphere at low L-values. Author

N91-11643 California Univ., Santa Cruz.
NUMERICAL CALCULATIONS OF THE FORMATION AND EVOLUTION OF GIANT PLANETS WITH ROTATION Ph.D. Thesis
Donald George Korycansky 1990 189 p
Avail: Univ. Microfilms Order No. DA9024733

Calculations relating to the formation and evolution of the giant-planet systems are presented. In particular, the effects of angular momentum and its transport are included. First, two-dimensional axisymmetric numerical calculations of the growth and non-linear development of an instability that may be present in radiative zones of the protoplanets are described. It is found that the amplitude of the instability correlates well with the length scale and linear growth rate of the instability. It is thus possible to model the angular momentum transport produced by the instability using linear perturbation-theory parameters. Second, these results are applied to quasi-spherical, quasi-hydrostatic evolutionary calculations of the formation of massive gaseous protoplanets. Of particular interest is the transport and distribution of angular momentum. It is found that a strong segregation or partition of angular momentum results, with the bulk of the total angular momentum residing in the outer few percent of the mass of the planetary envelope, at the end of the calculation. This is due to the presence of an outer convective region in the models. This distribution of angular momentum is similar to the distribution of angular momentum in the current giant-planet systems, suggesting that the processes described here might account for the formation of the satellite systems of the giant planets. Dissert. Abstr.

N91-11644*# Arkansas Coll., Batesville. Dept. of Chemistry.
AVAILABILITY OF HYDROGEN FOR LUNAR BASE ACTIVITIES
Roberta Bustin 1990 27 p
(Grant NAG9-474)
(NASA-CR-187367; NAS 1.26:187367) Avail: NTIS HC/MF A03 CSCL 03B

Hydrogen will be needed on a lunar base to make water for consumables, to provide fuel, and to serve as reducing agent in the extraction of oxygen from lunar minerals. The abundance and distribution of solar wind implanted hydrogen were studied. Hydrogen was found in all samples studied with concentrations varying widely depending on soil maturity, grain size, and mineral composition. Seven cores returned from the moon were studied. Although hydrogen was implanted in the upper surface layer of the regolith, it was found throughout the cores due to micrometeorite reworking of the soil. Author

N91-11645*# Stanford Univ., CA. STAR Lab.
TESTING FOR LIGHTNING AS A SOURCE OF RADIO BURSTS OBSERVED ON THE NIGHTSIDE OF VENUS
Vikas S. Sonwalkar, D. L. Carpenter, and R. J. Strangeway (California Univ., Los Angeles.) 6 Nov. 1990 42 p
(Grant NAG2-520)
(NASA-CR-187364; NAS 1.26:187364) Avail: NTIS HC/MF A03 CSCL 03B

In certain previous studies of radio burst events recorded by the Pioneer Venus Orbiting Electric Field Detector (OEFD), data were sorted for statistical purposes according to occurrence at filter band frequencies smaller than or greater than typical values of the ambient electron gyrofrequency. The expectation in making this distinction was that the lowest frequency signals, at 100 Hz, were candidates for propagation through the ionosphere to the spacecraft in the whistler mode, and that the higher frequency signals, if of subionospheric origin, would require some different ionospheric penetration mechanism. On the basis of certain assumptions about the homogeneity and horizontal stratification of the Venusian nightside ionosphere, methods were developed for case-by-case testing of the hypothesis that any particular burst event originated in subionospheric lightning. The tests, which are capable of refinement, allow prediction of the resonance cone angle, refractive index, wave dispersion, and wave polarization. The tests have been applied to data from 11 periods along 7 orbits, and are believed to represent an improved way of categorizing OEFD burst data for purposes of investigating source/propagation mechanisms. Four of the five burst events that were not found consistent with the lightning hypothesis involved receptions at multiple OEFD filter band frequencies. Author

N91-11646# Los Alamos National Lab., NM.
DISCUSSION PAPER ON ENVIRONMENTAL HAZARDS ON THE MOON, IN LOW EARTH ORBIT, AND IN LOW MARS ORBIT
Grant Heiken, comp. Sep. 1990 9 p
(Contract W-7405-eng-36)
(DE90-017854; LA-11882-MS; UC-900) Avail: NTIS HC/MF A02

In a lunar base era, potential problems with dust will be serious. Lunar soils, which make up most of the regolith that covers the Moon's surface, are similar to silty sands on Earth, with mean grain sizes of 45 to 100 microns. Lunar dust has very low electrical conductivity and dielectric losses, permitting accumulation of electric charge under ultraviolet irradiation. Dust coatings cover thermally-sensitive surfaces, windows and visors, clog moving parts,

and create continual abrasion hazards. Reduced gravity on the Moon favors the stability of aerosolized lunar soil and thereby will prolong its availability for inhalation if it is not removed from habitat atmosphere by filtration systems. Some other hazards must be considered. On the lunar surface it is difficult to judge topographic details and distances. New materials are needed to protect astronauts and equipment at a lunar base from micrometeoroid impacts. Spacecraft in low orbits around Earth and Mars experience strong chemical interactions where O2 and CO2 are photodissociated by sunlight. A ground-based facility at Los Alamos can be used to test these chemical interactions with materials proposed for use in spacecraft and satellites. Another component of the space exploration initiative is the environmental effects posed by man on the tenuous lunar and Martian atmospheres. Before significant development occurs on these planets, these atmospheres must be measured. Orbiting sensors designed to measure these atmospheres can also be used to search for water. DOE

N91-11647 Arizona Univ., Tucson.
TECTONICS OF ONE-PLATE PLANETS Ph.D. Thesis
Daniel Mark Janes 1990 151 p
Avail: Univ. Microfilms Order No. DA9028160

A general planetary shell model in spherical coordinates is developed that is capable of treating shells of arbitrary thickness and driving forces of arbitrary breadth. A methodology is then presented for finding the forces exerted on the shell from two processes. A treatment is developed for mantle convection driven by a density anomaly within a viscous mantle. This model is applied to the small moon of Uranus, Miranda, to study the three large coronae which dominate its surface and for which several competing hypotheses were offered, two of which invoked mantle convection driven by density anomalies of opposite sign. A general model is then developed for loading of the lithosphere and the effects of a range of loads breadths and lithosphere thicknesses are examined. The combinations of these two variables are mapped out where classical approximations such as the flat-plate and thin-shell models are applicable as well as the nature and extent of the transition between these two regimes are determined. Finite element modeling is employed to investigate the coronae on Venus, showing that morphological aspects of these features reported in the literature can be produced by flexure of the lithosphere beneath a volcanic load and gravitational sliding of a cooled crust off these volcanic mounds. Independent characteristic topographic profiles are produced for three of the more regular coronae which question how typical the reported morphologies are in the coronae in general. Dissert. Abstr.

92 SOLAR PHYSICS

Includes solar activity, solar flares, solar radiation and sunspots.

For related information see *93 Space Radiation.*

N91-11648# Tuebingen Univ. (Germany, F.R.). Astronomisches Inst.
TYPE 2 SOLAR RADIO BURSTS RECORDED AT WEISSENAU, 1966-1987
H. W. Urbarz Feb. 1990 87 p
(PB90-198334; UAG-98) Avail: NTIS HC/MF A05 CSCL 03B

The type 2 solar radio bursts are an improved list of the Weissenau Observatory Bulletin data. The list was obtained by carefully reinspecting the film records. A list of solar cycle 20 type 2 bursts was by Krivsky and Lukac (1980). A list containing the events of solar cycle 21 was published by Robinson et. al. (1983). The shock velocities were derived from the frequency drift assuming a proper density law. Included are the list of type 2 radio bursts and associated bursts and a list of supplementary type 2 bursts. B.G.

N91-11649*# National Center for Atmospheric Research, Boulder, CO.
WHIE LIGHT SOLAR CORONA: AN ATLAS OF 1988 K-CORONAMETER SYNOPTIC CHARTS, DECEMBER 1987 TO JANUARY 1989
D. G. Sime, C. Garcia, E. Yasukawa, and E. Lundin Mar. 1990 87 p Sponsored in part by NSF
(NASA Order W-15766)
(NASA-CR-184955; NAS 1.26:184955; PB90-256330; NCAR/TN-346+STR) Avail: NTIS HC/MF A05 CSCL 03B

The synoptic observing project of the High Altitude Observatory's Coronal Dynamics Program began on 30 July 1980. The data obtained for it are gathered by the Mark-III K-coronameter located at the Mauna Loa Solar Observatory, Hawaii, and are published yearly in volumes of The White Light Solar Corona: An Atlas of K-Coronameter Synoptic Charts (Table 1). The data, in the form of synoptic charts, are extended at both the beginning and the end of each year to provide some overlap with the preceding and succeeding volumes. This is also necessary to provide a complete set of the data organized into Carrington rotations covering a specific time period since the rotations do not coincide with the yearly calendar. Further observations are made at the limb, and west limb passage occurs 14 days after east limb passage. Thus, an entire rotation's data requires more than 28 days to collect. Together with the synoptic maps and polar synoptic maps, two additional sections designed to aid the user are included in the volume. As in previous Atlases, the Activity Report Summary for the year is given and the Mauna Loa Solar Observatory Calendar for 1988 (Table III) is also included. This is a list of days on which no coronal observations were achieved. These synoptic data should be regarded as a preliminary presentation in which corrections have not fully been made for the day-to-day variations and scattering of polarized light by the earth's atmosphere. Data from the east and west limbs are presented separately in the synoptic charts, as transient and evolutionary changes in the white light corona can substantially modify the distribution of coronal material over the 14 days between sequential limb passages. GRA

N91-11650 Georgia Inst. of Tech., Atlanta.
THE DELTA-SOBOLEV APPROACH FOR MODELING SOLAR SPECTRAL IRRADIANCE AND RADIANCE Ph.D. Thesis
Xuwu Xiang 1990 196 p
Avail: Univ. Microfilms Order No. DA9023836

The development and evaluation of a solar radiation model is reported, which gives irradiance and radiance results at the bottom and top of an atmosphere of specified optical depth for each of 145 spectral intervals from 0.29 to 4.05 microns. Absorption by water vapor, aerosols, ozone, and uniformly mixed gases; scattering by molecules and aerosols; and non-Lambertian surface reflectance are included in the model. For solving the radiative transfer equation, an innovative delta-Sobolev method is developed. It applies a delta-function modification to the conventional Sobolev solutions in a way analogous to the delta-Eddington method. The irradiance solution by the delta-Sobolev method turns out to be mathematically identical to the delta-Eddington approximation. The radiance solution by the delta-Sobolov method provides a convenient way to obtain the directional distribution pattern of the radiation transfer field, a feature unable to be obtained by most commonly used approximation methods. Such radiance solutions are also especially useful in models for satellite remote sensing. The model is tested against the rigorous Dave model, which solves the radiation transfer problem by the spherical harmonic method, an accurate but very time consuming process. Good agreement between the current model results and those of Dave's model are observed. The advantages of the delta-Sobolev model are simplicity, reasonable accuracy and capability for implementation on a minicomputer or microcomputer. Dissert. Abstr.

N91-11651# Texas Univ., Austin. Inst. for Fusion Studies.
NUMERICAL STUDY OF COMPRESSIBLE MAGNETOCONVECTION WITH AN OPEN TRANSITIONAL BOUNDARY

H. Hanami and T. Tajima Aug. 1990 43 p
(Contract DE-FG05-80ET-53088; NSF ATM-88-11128)
(DE91-000148; DOE/ET-53088/450; IFSR-450) Avail: NTIS HC/MF A03

Nonlinear evolution of magnetoconvection is studied by computerized simulation in a system with a dynamical open boundary between the convection region and corona of the sun. A model was studied in which the fluid is subject to the vertical gravitation, magnetohydrodynamics (MHD), and high stratification, through an MHD code with the MacCormack-Donner cell hybrid scheme in order to well represent convective phenomena. Initially the vertical fluid flux penetrates from the convectively unstable zone at the bottom into the upper diffuse atmosphere. As the instability develops, the magnetic fields are twisted by the convection motion and the folding magnetic fields is observed. When the magnetic pressure is comparable to the thermal pressure in the upper layer of convective zone, strong flux expulsion from the convective cell interior toward the cell boundary appears. Under appropriate conditions the simulation exhibits no shock formation incurred by the fluid convected to the photosphere, in contrast to earlier works with box boundaries. The magnetic field patterns observed are those of concentrated magnetic flux tubes, accumulation of dynamo flux near the bottom boundary, pinched flux near the downdraft region, and the surface movement of magnetic flux toward the downdraft region. Many of these computationally observed features are reminiscent of solar observations of the fluid and magnetic structures of their motions. DOE

N91-11652# Instituto de Pesquisas Espaciais, Sao Jose dos Campos (Brazil).
EXPLORATION OF DECREASED SOLAR ACTIVITY STATE (SMALL INTENSITY ACTIVITY) IN THE CORONA AND CHROMOSPHERE M.S. Thesis - 5 Jun. 1989 [EXPLORACAO DA ATIVIDADE SOLAR DE BAIXO NIVEL (ATIVIDADE DE PEQUENA INTENSIDADE) NA COROA E CROMOSFERA]
Cleiton Joni BenettiLattari Apr. 1990 101 p In PORTUGUESE; ENGLISH summary
(INPE-5059-TDL/405) Avail: NTIS HC/MF A06

In all previous attempts to show one-to-one correlation between type 3 bursts and x ray spikes, there have always been ambiguities as to which of several x ray spikes are correlated with any given type 3 burst. Observations are presented that show clear associations of x ray bursts with RS type 3 bursts between 16:46 UT and 16:52 UT on 1985, July 9. The hard x ray observations were made at energies above 25 keV with HXRBS on SMM and the radio observations were made at 1.63 GHz using the 13.7 m diameter in Itapetinga antenna in R and L polarization with a time resolution of 3 ms. Detailed comparison between the hard x ray and radio observations shows: (1) That in at least 12 cases the associated hard x ray and decimetric RS bursts can be identified; and (2) on the average, the x ray peaks were delayed from the peak of the RS bursts at 1.6 GHz by approximately 400 ms although a delay as long as 1 sec was observed in one case. One possible explanation of the long delays between the RS bursts and the associated x ray bursts is that the RS burst is produced at the leading edge of the electron beam whereas the x ray burst peaks at the time of arrival of the bulk of the electrons at the high density region mostly at the lower corona and upper chromosphere. Thus, comparison must be made between the time the peak of the radio pulse and the start of the x ray burst. In that case the delays are consistent with an electron travel time of approximately 0.3 c from the 800 MHz plasma level to the lower corona assuming that the radio emission is at the second harmonic. Author

N91-11653# Consiglio Nazionale delle Ricerche, Rome (Italy). Ist. di Fisica dello Spazio Interplanetario.
PLOTS OF THE 5-MINUTE NEUTRON MONITOR INTENSITY AND MULTIPLICITIES RECORDED BY THE ROME 17-NM64, JANUARY 1990
G. Villoresi, F. Re, F. Signoretti, N. L. Zangrilli, and N. Iucci (Rome Univ., Italy) Frascati, Italy Mar. 1990 69 p
(IFSI-90-5; ETN-90-97788) Avail: NTIS HC/MF A04

Data considered useful for study of solar activity maximun is presented. The data should be considered as preliminary. Attenuation coefficients used in the atmospheric pressure change correction are given. The five minute data of the total neutron intensity and of the intensities of multiplicities 1 to greater than or equal to 8 recorded during January 1990 by the Rome 17-NM64 are given in the form of daily plots. ESA

N91-11654# Consiglio Nazionale delle Ricerche, Rome (Italy). Ist. di Fisica dello Spazio Interplanetario.
PLOTS OF THE 5-MINUTE NEUTRON MONITOR INTENSITY AND MULTIPLICITIES RECORDED BY THE ROME 17-NM64, FEBRUARY 1990
G. Villoresi, F. Re, F. Signoretti, N. L. Zangrilli, and N. Iucci (Rome Univ., Italy) Frascati, Italy Mar. 1990 61 p
(IFSI-90-6; ETN-90-97789) Avail: NTIS HC/MF A04

Data considered useful for study of the solar activity maximun is presented. The data should be considered as preliminary. Attenuation coefficients used in the atmospheric pressure change correction are given. The five minute data of the total neutron intensity and of the intensities of multiplicities 1 to greater than or equal to 8 recorded during February 1990 by the Rome 17-NM64 are given in the form of daily plots. ESA

93 SPACE RADIATION

Includes cosmic radiation; and inner and outer earth's radiation belts.

For biological effects of radiation see *52 Aerospace Medicine*. For theory see *73 Nuclear and High-Energy Physics*.

N91-11655 Durham Univ. (England).
VERY HIGH ENERGY GAMMA RAYS FROM ISOLATED PULSARS AND NON-PULSATING OBJECTS Ph.D. Thesis
Stephen Mark Rayner 1989 163 p
Avail: Univ. Microfilms Order No. BRD-88659

The detection of very high energy gamma rays from isolated pulsars and objects that are not known to emit pulsed radiation, using the atmospheric Cerenkov technique is addressed. The first chapter summarizes the processes by which celestial gamma rays can be generated and absorbed. A discussion of the criteria for selecting objects for study is given. The second chapter describes the atmospheric Cerenkov technique and gives a brief outline of its historical development. Details of the design and operation of the current Durham University Very High Energy (VHE) gamma ray telescopes are given. The third chapter describes the standard analysis techniques used to search for pulsed and unpulsed emission. The fourth chapter presents results of new observations of four isolated pulsars. Upper limits to the VHE gamma ray flux are derived for each pulsar. A summary of the results is given and conclusions drawn regarding the consequences of the observations for the most popular pulsar model. The fifth chapter deals with new analysis techniques that have been developed to test data for the presence of a signal which is not necessarily periodic. A number of different approaches is described. The results of these techniques when applied to simulated data are presented and conclusions are drawn regarding the relative effectiveness of the tests. The sixth chapter applies the most successful test to data from three objects. Upper limits to the flux from Centaurus A and Supernova 1987a are derived from observations. Evidence for VHE gamma ray emission from Scorpius X-1 is presented, together with evidence that this emission is modulated with the period of the binary orbit of this system. Dissert. Abstr.

N91-11656# Tokyo Univ., Tanashi (Japan). Inst. for Nuclear Study.
ATMOSPHERIC NEUTRINO FLUXES
M. Honda, K. Kasahara, K. Hidaka (Tokyo Gakugei Univ., Koganei, Japan), and S. Midorikawa Feb. 1990 15 p
(DE90-508023; INS-807) Avail: NTIS (US Sales Only) HC/MF A03

A detailed Monte Carlo simulation of neutrino fluxes of atmospheric origin is made taking into account the muon polarization effect on neutrinos from muon decay. The flux was calculated with energies above 3 MeV for future experiments. There still remains a significant discrepancy between the calculated (nu sub e +anti nu sub e/(nu sub mu) +anti nu sub mu) ratio and that observed by the Kamiokande group. However, the ratio evaluated at the Frejus site shows a good agreement with the data. DOE

N91-11657 California Univ., Riverside.
IDENTIFICATION AND ANALYSIS OF COSMIC GAMMA RAY BURSTS FROM PIONEER VENUS ORBITER Ph.D. Thesis
Kuan-Wen Chuang 1990 211 p
Avail: Univ. Microfilms Order No. DA9023956

A search of the Pioneer Venus Orbiter (PVO) Gamma Burst Detector real time data was carried out to identify and study the characteristics of celestial gamma ray bursts. Each of the 5 channels of the detector were analyzed to determine the time width, rise time, and hardness ratio of the bursts. Solar flares and cosmic gamma ray bursts located by similar criteria are separated by hardness ratio and equivalent time width. Three new bursts GB861023, GB861123, and GB870127 seen on the PVO real time data tapes from 1978 to 1988 may be members of a possible new repeating gamma ray burst 6-13-79. Distances to and spatial distributions of gamma ray burst sources are studied with log N(is greater than P sub c)-log P(sub c), log N(is greater than P)-log P, and log N(is greater than S)-log S. Two hundred seventeen new cosmic gamma ray bursts and 126 solar flares not detected by the PVO gamma ray burst detector in the trigger mode were found. Dissert. Abstr.

N91-11658 Wisconsin Univ., Madison.
A SEARCH FOR VERY HIGH ENERGY GAMMA-RAYS FROM CYGNUS X-3 Ph.D. Thesis
John R. Jennings 1990 250 p
Avail: Univ. Microfilms Order No. DA9024062

Using the air shower Cerenkov telescope on Mt. Haleakala in Hawaii, Cygnus X-3 was monitored for over 100 hours in 1986. Searches were performed for continuous, burst, and pulsed emission, as well as for a candidate fast pulsar with a rotation period of 12.59 ms. No significant emission was observed on any of the time scales searched. An upper limit for the integral flux of Phi(E is greater than or equal to 500 GeV) = 1.5 x 10(exp -10) gamma prime s/sq cm/sec for continuous emission is established for this period of observation. An upper limit for an integral flux of Phi(E is greater than or equal to 500 GeV) = 3 x 10(esp -10) gamma prime s/sq cm/sec is obtained for gamma-ray emission modulated at the orbital period (4.79 hr) with 10 percent duty cycle. The candidate pulsar emission could not be confirmed. Dissert. Abstr.

N91-11659 California Univ., San Diego.
STABILITY OF EMISSION LINE CLOUDS IN ACTIVE GALACTIC NUCLEI Ph.D. Thesis
Irwin Scott Krinsky 1989 152 p
Avail: Univ. Microfilms Order No. DA9013672

A numerical model was developed for a Quasar Stellar Object (QSO) broad emission line cloud (ELC) imbedded within a confining hot intercloud medium (HIM) for the purpose of studying its stability to perturbations in its temperature and density. A self-consistent model in radiative, pressure and thermal equilibrium is presented. The effect of trapped line radiation pressure is also included with the total pressure (particle plus radiation) held constant. The equilibrium model is found to have regions with radiation pressure exceeding gas pressure. Energy transport includes the effects of an external broken power law continuum and thermal conduction of heat from the HIM. Conduction is found to be unimportant to the total energy budget of the cloud, but is important to the dynamics of the ELC/HIM interface. Independent of the ELC/HIM model, an extension of second order probabilistic radiative transfer that treats the diffuse radiation field as composed of two oppositely directed streams is presented. The high ionization zone of the ELC is found to be unstable to radiatively driven sound waves. Both the external radiation field and the force of trapped line radiation are potential sources for driving the growth of sound waves. The final picture that emerges is that the ELC must be in a constant state of flux. Dissert. Abstr.

N91-11660 Georgia State Univ., Atlanta.
NUMERICAL SIMULATIONS OF SUSPERSONIC EXTRAGALACTIC RADIO JETS Ph.D. Thesis
Richard Alexander Rosen 1989 218 p
Avail: Univ. Microfilms Order No. DA9016655

A boundary following code was used to simulate jets emanating from active galactic nuclei as they propagate through a bimodal external medium that first consists of an isothermal galactic halo with density falling roughly as a power law with radius, and later of a hotter, less dense, uniform intergalactic medium (IGM). By varying the beam power, the radius of the galactic halo/IGM interface, the redshift, the steepness of the power law fall-off of pressure within the halo, and the temperature ratio of the IGM to the halo, models of a wide range of radio galaxies were considered. The maximum linear sizes of the beams were found as functions of the beam and halo parameters using two different criteria, the nuclear activity time, and the point at which the advance of the beam goes subsonic. Good agreement was obtained with regard to the relationship between the observed linear size of such radio sources and both the cosmological redshift (at fixed power) and the total radio power (at fixed redshift). These results are also confirmed by a sample of fully hydrodynamical (2-D) simulations. Monte Carlo simulations which span the parameter space were employed to find the median distances for plausible distributions of the parameters for a number of constant values of density and temperature of the IGM. A statistical analysis comparing the distributions of radio galaxies in power-size-redshift bins with observational results supports the existence of a cosmologically significant IGM. The fashions in which this picture might be modified if the difference between radio galaxies, quasars, and blazars are due to orientation effects were also discussed. Dissert. Abstr.

N91-11661 Pennsylvania State Univ., University Park.
RADIO AND INFRARED EMISSION FROM STARBURST GALAXIES Ph.D. Thesis
Peter Culley Stine 1989 293 p
Avail: Univ. Microfilms Order No. DA9018286

Radio emission was compared to infrared emission for a sample of 58 starburst Markarian galaxies. New radio observations were from the very large array (VLA) at 6 and 20 cm in the B and A configurations. Infrared astronomy satellite (IRAS) data were reanalyzed using ADDSCAN for 25 of the starbursts that were undetected at either 25 or 100 mu in the IRS Point Source Catalog. The IR spectral indices are steeper for alpha (sup 25)(sub 12) and flatter for alpha (sup 60)(sub 25) and alpha (sup 100)(sub 60) when compared to normal galaxies. The IR spectral indices alpha (sup 25)(sub 12) and alpha (sup 100)(sub 60) are anticorrelated, indicating more than one population of dust grains in starbursts. The starbursts have a stronger warm component than normal galaxies. A significant portion of the warm component of the infrared emission is emitted at wavelengths shorter then 60 mu. A very tight correlation between radio and infrared luminosity exists over a factor of 10,000 in 60 mu luminosity density. The bulk of the radio emission is nonthermal. The radio spectral index does not appear to be correlated with the infrared emission. The sizes of the radio emitting regions appear to be larger than the starburst, and the radio spectral indices steepen away from the center. This indicates that the material generating the nonthermal emission leaks out of the starburst region. A three-component model describing the radio emission is discussed. The starburst region contains thermal radio emission from H II regions around hot stars, nonthermal radio emission from discrete supernova remnants, and nonthermal emission from cosmic rays generated by the supernovae. The outer region contains only the nonthermal emission from cosmic rays that have traveled away from the starburst region. Dissert. Abstr.

N91-11662 Louisiana State Univ., Baton Rouge.
POLARIZED RADIATION FROM INHOMOGENEOUS SHOCKS Ph.D. Thesis
Kin-wah Wu 1989 161 p
Avail: Univ. Microfilms Order No. DA9017309

Strongly polarized radiation from AM Herculis binaries is believed to be due to cyclotron emission from hot magnetized plasmas. The flat optically thin spectra and strong IR polarization observed in these binaries cannot be explained by models assuming a homogeneous emission region with a simple geometry. Therefore, the cyclotron emission from infinite plasma cylinders with uniform magnetic fields and temperatures was studied, but with a variety of axially symmetric electron density profiles and it was shown that such inhomogeneous plasmas are able to produce relatively flat spectra which cannot be produced by the homogeneous models. The polarization at low frequencies is shown to be stronger than that due to the homogeneous plasmas and the polarization at high frequencies is weaker. The steady state hydrodynamics was also studied of bremsstrahlung dominated shocks and the cyclotron emission was calculated from them. Three types of accretion rate profiles (uniform, axisymmetric and asymmetric) were considered. The shock-structure is planar for the uniform accretion rate case. The shock due to an axisymmetric accretion rate is a curved surface. For asymmetric accretion, the post-shock region is asymmetric and hence produces asymmetric light curves. All these inhomogeneous shocks produce flat optical/IR spectra and strong IR polarization. Dissert. Abstr.

N91-11663 Wisconsin Univ., Madison.
OBSERVATIONS OF THE SOFT X RAY BACKGROUND Ph.D. Thesis
Bradley Carl Edwards 1990 191 p
Avail: Univ. Microfilms Order No. DA9020439

The results from a recent sounding rocket experiment that observed the soft x ray background are presented. The observations include x ray spectra taken in the Be (77 to 111 eV) and B' (105 to 188 eV) bands at eight points on the sky. Observations of the soft x ray background have been made for over 20 years. The low energy Be band was used to search for absorption in the diffuse x ray background. The Be band is more sensitive to less absorbing material due to the energy dependence of the absorption. One target that was observed in the direction of an H I features was found to exhibit signs of absorption. If the observed change in the relative intensities of the different energy bands is assumed to be due to absorption, the H I feature would be in front of more than half of the soft x ray emission. This would constitute the first case of absorption of the diffuse x ray background by an H I feature that has been observed. The spectral analysis of the pulse height distribution from the Be counter was used to examine the soft x ray background's spectrum and to compare the observed spectrum to the thermal emission expected from a hot plasma. The spectral analysis was completed with the use of calibration lines obtained from a synchrotron source with a high resolution monochrometer. The monoenergetic x ray lines produced pulse height distributions in the detector which were fit with a semi-emperical model. This fitting procedure allowed us to obtain better values for the parameters which describe the model pulse height distribution. Dissert. Abstr.

99 GENERAL

N91-11664*# National Aeronautics and Space Administration. John F. Kennedy Space Center, Cocoa Beach, FL.
RESEARCH AND TECHNOLOGY AT KENNEDY SPACE CENTER Annual Report, 1989
Dec. 1989 135 p
(NASA-TM-102150; NAS 1.15:102150) Avail: NTIS HC/MF A07 CSCL 05D

As the NASA Center responsible for assembly, checkout, servicing, launch, recovery, and operational support of Space Transportation System elements and payloads, Kennedy Space Center is placing increasing emphasis on the Center's research and technology program. In addition to strengthening those areas of engineering and operations technology that contribute to safer, more efficient, and more economical execution of current mission, the technical tools are developed needed to execute Center's mission relative to future programs. The Engineering Development Directorate encompasses most of the laboratories and other Center resources that are key elements of research and technology program implementation and is responsible for implementation of the majority of the projects in this Kennedy Space Center 1989 Annual Report. Author

N91-11665# Technical Research Centre of Finland, Espoo.
[ACTIVITIES REPORT OF THE TECHNICAL RESEARCH CENTRE OF FINLAND] Annual Report, 1989
1990 34 p
(ISBN-951-38-3647; ISSN-0786-4558; ETN-90-97979) Avail: NTIS HC/MF A03

The scientific and technical activities are reported. The research programs were developed in the following fields: provision of energy, microelectronic and optoelectronic design work and manufacture, computers, information processing, communication systems, mechatronics, automation, processes for biotechnical, chemical and food industries, building technology and community development, and manufacturing technology. The organization, the economy, and the information systems of the center are presented. ESA

Typical Subject Index Listing

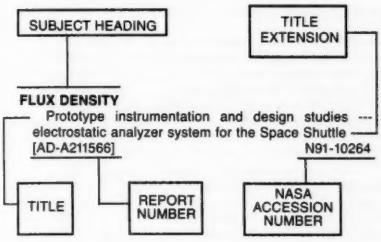

The subject heading is a key to the subject content of the document. Titles, report numbers, and accession numbers of pertinent documents are provided under each subject heading. When the title is insufficiently descriptive of the document content, a title extension has been added, separated from the title by three hyphens. The report number helps to indicate the type of document cited (e.g., NASA report, NASA translation, NASA contractor report). The NASA accession number is the number by which the document abstracts are arranged in this journal and by which the document is sold or requested. The titles, with title extensions if present, are arranged under each subject heading in ascending accession number order. The subject headings have been selected from the latest revision of the *NASA Thesaurus* (NASA SP-7064).

A

A STARS
Observation and analysis of variable linear polarization in the yellow supergiant star Epsilon Aurigae N91-11616

ABORT TRAJECTORIES
Optimal trajectories of aircraft and spacecraft N91-10968

ABSORPTION SPECTRA
Formation and stability of As-H bonds in H-implanted GaAs
[DE91-000043] N91-11584

ABSTRACTS
Aircraft trajectories: Computation, prediction, control, Volume 3. Part 9: Book of abstracts. Part 10: Bibliography. Part 11: List of contributors
[AGARD-AG-301-VOL-3-PT-9-11] N91-10978
Center for electronics and electrical engineering technical publication announcements covering Center programs, July - September, 1989, with 1990 CEEE events calendar
[PB90-206491] N91-11145
The structure and stability of three dimensional detonation waves
[AD-A224465] N91-11164

ABUNDANCE
Nitrogen and sulfur in irregular galaxies N91-11624

AC GENERATORS
Reference concepts for a space-based hydrogen-oxygen combustion, turboalternator, burst power system
[DE90-016692] N91-11155

ACCELERATION (PHYSICS)
Tethered rocket as a vehicle for penetration and impact testing: Development report
[DE90-014865] N91-11057
Injector and valve train friction studies: Cummins L-10 engine
[DE90-017288] N91-11225
Antimatter gravity experiment
[DE91-000177] N91-11590

ACCIDENT PREVENTION
Current Emergency Locator Transmitter (ELT) deficiencies and potential improvements utilizing TSO-C91a ELTs
[NASA-CR-4330] N91-10964

ACID RAIN
Estimation of seasonal and annual acidic deposition through aggregation of three-day episodic periods
[PB90-252628] N91-11303

ACOUSTIC ATTENUATION
Voice communications in the cockpit noise environment: The role of active noise reduction N91-11140

ACOUSTIC EMISSION
Classification of acoustic emission waveforms for nondestructive evaluation using neural networks
[DE90-017239] N91-11236

ACOUSTIC EXCITATION
Structure of supersonic turbulent reattaching shear layers N91-10914

ACOUSTIC MEASUREMENT
A compendium of environmental data collected during the Iceshelf-88 exercise
[AD-A223518] N91-11346

ACOUSTIC PROPERTIES
Aircraft interior noise reduction by alternate resonance tuning
[NASA-CR-186879] N91-11488

ACOUSTIC VELOCITY
Composite slip table of dissimilar materials for damping longitudinal modes
[DE90-015126] N91-11064
Prediction of the noise from a propeller at angle of attack
[NASA-TM-103627] N91-11495

ACOUSTICS
Contributions to the sound location in the atmosphere
[ETN-90-97863] N91-11490

ACTIVATION ENERGY
Atmospheric chemistry: Laboratory studies of kinetics of important reactions N91-11326

ACTIVE CONTROL
A quarter of a century of aeroelastic cooperation between research and industry (a review). Part 1: Fighter airplanes and helicopters N91-10931
A quarter of a century of aeroelastic cooperation between research and industry (a review). Part 2: Transport airplanes and other civil applications N91-10932
Attitude control of tethered satellites N91-11045
Voice communications in the cockpit noise environment: The role of active noise reduction N91-11140

ACTIVE GALACTIC NUCLEI
Astronomical applications of survival analysis N91-11615
Stability of emission line clouds in active galactic nuclei N91-11659
Numerical simulations of suspersonic extragalactic radio jets N91-11660

ACTUATORS
Computer modeling of 12-inch actuator shock test performance
[DE90-017038] N91-11033

ADA (PROGRAMMING LANGUAGE)
Proceedings of the First NASA Ada Users' Symposium
[NASA-TM-102941] N91-11389
Ada and software management in NASA: Symposium/forum
[NASA-TM-103297] N91-11390

ADAPTIVE CONTROL
Temporal-adaptive Euler/Navier-Stokes algorithm for unsteady aerodynamic analysis of airfoils using unstructured dynamic meshes
[NASA-TM-102734] N91-10919
Adaptive digital real time filtering in structural dynamics: A contribution to the realization on Actively Reacting Elastic Structures (ARES) N91-10929

ADHESION
Surface phases and their influence on metal-oxide interfaces
[DE90-017608] N91-11099

ADIABATIC CONDITIONS
Complete adiabatic evaporation of highly superheated liquid jets
[MPIS-MITT-95] N91-11588

ADVANCED VERY HIGH RESOLUTION RADIOMETER
Radiometric observation of the atmospheric boundary layer (the ROSSA Project) N91-11324

AEROASSIST
Conservation equations and physical models for hypersonic air flows over the aeroassist flight experiment vehicle N91-10897
The computation of thermo-chemical nonequilibrium hypersonic flows N91-10898
Aerodynamic stability and heating analyses for the aeroassist flight experiment vehicle N91-10899
Aeroassist flight experiment aerodynamics and aerothermodynamics N91-10900
Direct simulation of rarefied hypersonic flows N91-10901

AERODYNAMIC BALANCE
Design of the derivative balance for the transonic wind tunnel N91-10925

AERODYNAMIC CHARACTERISTICS
Aeroelastics and dynamics of wind turbines N91-10923
Calculation of aerodynamic characteristics of airplane configurations at high angle of attack in steady and unsteady flow N91-11009
Aerodynamic design optimization using computational fluid dynamics N91-11013
Application of dynamical systems theory to nonlinear aircraft dynamics N91-11014

AERODYNAMIC COEFFICIENTS
Grid generation and flow computation about a Martian entry vehicle
[NASA-CR-187032] N91-11042

AERODYNAMIC CONFIGURATIONS
A comparative study of Navier-Stokes codes for high-speed flows N91-10869
Calculation of aerodynamic characteristics of airplane configurations at high angle of attack in steady and unsteady flow N91-11009

AERODYNAMIC FORCES
Determination of unsteady aerodynamic forces on engines with a view to flutter investigations N91-10927

AERODYNAMIC HEAT TRANSFER
The aerodynamic effects of nozzle guide vane shock wave and wake passing on a transonic turbine rotor N91-10915

AERODYNAMIC HEATING
Johnson Space Center CFD overview N91-10844
Aerodynamic stability and heating analyses for the aeroassist flight experiment vehicle N91-10899
Optimal trajectories of aircraft and spacecraft N91-10968
External tank aerothermal design criteria verification, volume 1
[NASA-CR-183996] N91-11037
External tank aerothermal design criteria verification, volume 2
[NASA-CR-183997] N91-11038

AERODYNAMIC INTERFERENCE
Unsteady wind tunnel wall interferences in subsonic and transonic profile flows N91-10928
A numerical study of the effects of wind tunnel wall proximity on an airfoil model
[NASA-CR-187322] N91-10934

AERODYNAMIC LOADS
Numerical aerodynamic simulation of the space shuttle ascent environment N91-10875
The computation of thermo-chemical nonequilibrium hypersonic flows N91-10898
Short crack growth under realistic flight loading: Model predictions and experimental results for Al 2024 and Al-Li 2090 N91-11246
Short and long fatigue crack growth in 2024-T3 under Fokker 100 spectrum loading N91-11248

AERODYNAMIC STABILITY
Aerodynamic stability and heating analyses for the aeroassist flight experiment vehicle N91-10899

AERODYNAMIC STALLING
A viscous-inviscid interactive method for unsteady flows N91-11172
AERODYNAMICS
Turbine stage aerodynamics and heat transfer prediction N91-10882
Comparison of a mathematical one-point model and a multi-point model of aircraft motion in moving air N91-10969
Aerodynamic design optimization using computational fluid dynamics N91-11013
Tethered rocket as a vehicle for penetration and impact testing: Development report
[DE90-014865] N91-11057
AEROELASTICITY
CFD for applications to aircraft aeroelasticity N91-10855
Application of unstructured grid methods to steady and unsteady aerodynamic problems N91-10856
Computation of transonic flow over elastic rotor blade N91-10906
Contributions in the field of aeroelastics on the occasion of the 60th anniversary of Professor Dr.-Ing. Habil. Hans Wilhelm Foersching
[ETN-90-97630] N91-10920
Aeroelastics and dynamics of wind turbines N91-10923
A quarter of a century of aeroelastic cooperation between research and industry (a review). Part 1: Fighter airplanes and helicopters N91-10931
A quarter of a century of aeroelastic cooperation between research and industry (a review). Part 2: Transport airplanes and other civil applications N91-10932
AERONAUTICAL ENGINEERING
Test launch for turboaircraft engine. Description of the installation
[ILA-87-A-02] N91-11018
Civil space technology initiative
[NASA-TM-103017] N91-11028
AEROSOLS
Fluctuating concentrations in atmospheric dispersion N91-11323
AEROSPACE ENVIRONMENTS
Numerical aerodynamic simulation of the space shuttle ascent environment N91-10875
Preliminary results from the advanced photovoltaic experiment flight test
[NASA-TM-103269] N91-11058
Studies of molecular properties of polymeric materials
[NASA-TM-101854] N91-11118
AEROSPACE INDUSTRY
Computational Fluid Dynamics Program at NASA Ames Research Center N91-10840
AEROSPACE MEDICINE
JPRS report: Science and technology. USSR: Life sciences
[JPRS-ULS-89-003] N91-11354
Evaluation of female and male aircrew applicants using a cognitive and psychomotor test N91-11366
Review of female applicant aircrew in the Belgian forces N91-11368
The application of USAF female anthropometric data to identify problems with the introduction of female aircrew into the Royal Air Force N91-11370
EKG findings in female aviators in the US Air Force N91-11377
Impact on women: A retrospective look at impact acceleration testing at the Harry G. Armstrong Aerospace Medical Research Laboratory N91-11378
Relationship of menstrual history to altitude chamber decompression sickness N91-11379
AEROSPACE PLANES
Progress in computing nozzle/plume flow fields N91-10872
Weight evaluation and sensitivity analysis for space plane: SSTO
[NAL-TM-598-1] N91-11036
AEROSPACE SYSTEMS
Potential for advanced thermoplastic composites in space systems
[DE90-014447] N91-11069
Ada and software management in NASA: Symposium/forum
[NASA-TM-103297] N91-11390
AEROSPACE VEHICLES
Flight simulation programs for space plane
[NAL-TM-594] N91-11035
AEROTHERMODYNAMICS
Flux splitting algorithms for two-dimensional viscous flows with finite-rate chemistry N91-10894
The computation of thermo-chemical nonequilibrium hypersonic flows N91-10898
Aeroassist flight experiment aerodynamics and aerothermodynamics N91-10900
Direct simulation of rarefied hypersonic flows N91-10901
External tank aerothermal design criteria verification, volume 1
[NASA-CR-183996] N91-11037
Use of the VP-200 computer for aerothermodynamic problems
[MBB/FE122/S/PUB/388] N91-11424
AFRICA
Northwest African depressions and their relationship to jet streams N91-11318
AGING (MATERIALS)
Characterization of short fatigue cracks at notches in SiC particulate aluminum composite
[DE90-018043] N91-11071
In-situ pore structure analysis during aging and drying of gels
[DE91-000044] N91-11089
Effects of environment and aging on creep properties of Alloy 800H
[DE90-520207] N91-11106
Development of the structural materials information center
[DE90-016521] N91-11603
AGING (METALLURGY)
Influence of heat treatment on microstructure and properties of an advanced high temperature titanium alloy
[PNR-90689] N91-11107
AGRICULTURE
Satellite remote sensing for agricultural projects
[PB90-257916] N91-11270
AIR CONDITIONING
Japanese power electronics inverter technology and its impact on the American air conditioning industry
[DE90-014843] N91-11191
Colorado State University program for developing, testing, evaluating and optimizing solar heating and cooling systems
[DE90-017273] N91-11291
AIR CONDITIONING EQUIPMENT
Colorado State University program for developing, testing, evaluating and optimizing solar heating and cooling systems
[DE90-017273] N91-11291
AIR FLOW
Conservation equations and physical models for hypersonic air flows over the aeroassist flight experiment vehicle N91-10897
Enhancement of forced convection heat transfer in tubes using staged tangential flow injection
[PB90-247594] N91-11170
Evaluation of a high-temperature burner-duct-recuperator system
[DE90-000366] N91-11284
AIR NAVIGATION
Four dimensional navigation in air traffic with 4-D navigation aircraft N91-10991
Contribution of the satellite techniques to the surveillance of air traffic N91-11005
AIR POLLUTION
Recommended operating procedure No. 45: Analysis of nitrous oxide from combustion sources
[PB90-238502] N91-11078
Estimation of seasonal and annual acidic deposition through aggregation of three-day episodic periods
[PB90-252628] N91-11303
Lifetimes and fates of toxic air contaminants in California's atmosphere
[PB90-253204] N91-11304
Minimization and control of hazardous combustion byproducts
[PB90-259854] N91-11305
Measurements of toxic exhaust emissions from gasoline-powered light-duty vehicles
[PB90-259649] N91-11306
Commercial aircraft and the environment
[PNR-90687] N91-11307
AIR TRAFFIC
Inflight replanning for diversions N91-10955
Graphical interfaces for cooperative planning systems N91-10956
Airport system capacity strategic choices
[SR-226] N91-10979
AIR TRAFFIC CONTROL
Aviation Safety/Automation Program Conference
[NASA-CP-3090] N91-10936
National plan to enhance aviation safety through human factors improvements N91-10940
ATC automation concepts N91-10957
Time-based operations in an advanced ATC environment N91-10958
Time-based aircraft/ATC operations study N91-10959
Terminal weather information management N91-10960
A flight test facility design for examining digital information transfer N91-10962
Aircraft trajectories: Computation, prediction, control, Volume 3. Part 9: Book of abstracts. Part 10: Bibliography. Part 11: List of contributors
[AGARD-AG-301-VOL-3-PT-9-11] N91-10978
Airport system capacity strategic choices
[SR-226] N91-10979
Aircraft trajectories: Computation, prediction, control, volume 2: Air traffic handling and ground-based guidance of aircraft. Part 4: Air traffic handling. Part 5: Guidance of aircraft in a time-based constrained environment. Part 6: Surveillance. Part 7: Meteorological forecasts. Part 8: Aircraft operation in air traffic handling simulation
[AGARD-AG-301-VOL-2-PT-4-8] N91-10981
Optimum on-line handling of air traffic over Western Europe N91-10982
The EUROCONTROL future ATS system concept and the programme of studies, tests, and trials N91-10983
Prediction of aircraft trajectories N91-10984
Aircraft dynamics for air traffic control N91-10985
The application of trajectory prediction algorithms for planning purposes in the Netherlands ATC-system N91-10986
Generation of aircraft trajectories for on-line operation: Methods, techniques, and tools N91-10987
Optimization models and techniques to improve air traffic management N91-10988
The high-resolution graphic display: A possible man/machine interface for a computer assisted ATC management system N91-10989
The 4-D control of current air carriers in the present environment: Objectives, status, and plans N91-10990
Four dimensional navigation in air traffic with 4-D navigation aircraft N91-10991
The control of inbound flights N91-10992
Guidance concepts for time-based flight operations N91-10993
The 4-D descent trajectory generation techniques under realistic operating conditions N91-10994
Expert systems for the generation of thermal area arrival paths for civil transport N91-10995
A description and evaluation of TIMER: A time-based terminal flow-control concept N91-10996
Use of 4-D RNAV in time-based en route arrival metering N91-10997
Air traffic management and aircraft guidance in a zone of convergence N91-10998
Ground-based 4-D guidance of flights in strong wind N91-10999
A piloted simulator evaluation of a ground-based 4-D descent advisor algorithm N91-11000
The air traffic controller facing automation: Conflict or cooperation N91-11001
Aircraft trajectory reconstitution on the basis of multi-radar plot information N91-11002
Bayesian multi-sensor tracking for advanced air traffic control systems N91-11003
The use of downlinked measurements to track civil aircraft N91-11004
Contribution of the satellite techniques to the surveillance of air traffic N91-11005
Developments to enhance meteorological forecasting for air traffic services N91-11006
Integration of aircraft capability in air traffic handling simulations N91-11007
Simulation of automated approach procedures considering dynamic flight operations N91-11008
AIR TRAFFIC CONTROLLERS (PERSONNEL)
National plan to enhance aviation safety through human factors improvements N91-10940
Aviation safety/automation program overview N91-10941
ATC automation concepts N91-10957
The air traffic controller facing automation: Conflict or cooperation N91-11001
AIR TRANSPORTATION
Airport system capacity strategic choices
[SR-226] N91-10979
AIR WATER INTERACTIONS
A simple zonal average energy budget model of the earth-atmosphere system N91-11316
Meteorological characteristics of the El Nino/Southern Oscillation phenomenon N91-11340
AIRBORNE EQUIPMENT
The control system of an airborne radiometer: A process for a two dimensional reconstruction of irregular scanned radiometer data
[MITT-70] N91-11202
AIRCRAFT ACCIDENTS
Terminal weather information management N91-10960
Effect of wind and wind variation on aircraft flight-paths N91-10972
AIRCRAFT APPROACH SPACING
Optimization models and techniques to improve air traffic management N91-10988

The 4-D control of current air carriers in the present environment: Objectives, status, and plans N91-10990
The control of inbound flights N91-10992
Expert systems for the generation of thermal area arrival paths for civil transport N91-10995
Simulation of automated approach procedures considering dynamic flight operations N91-11008

AIRCRAFT COMPARTMENTS
Generation of a buoyant plume of artificial smoke for airplane tests
[DOT/FAA/CT-90/9] N91-11015
Voice communications in the cockpit noise environment: The role of active noise reduction N91-11140
Aircraft interior noise reduction by alternate resonance tuning
[NASA-CR-186879] N91-11488

AIRCRAFT CONFIGURATIONS
Application of unstructured grid methods to steady and unsteady aerodynamic problems N91-10856
A zonal Navier-Stokes methodology for flow simulation about a complete aircraft N91-10858
Navier-Stokes solutions about the F/A-18 forebody-LEX configuration N91-10860
TranAir: Recent advances and applications N91-10862
Nonoverlapping composite meshes for multi-element air-foils N91-10908
Aircraft interior noise reduction by alternate resonance tuning
[NASA-CR-186879] N91-11488

AIRCRAFT CONTROL
Human-centered automation: Development of a philosophy N91-10944
Assessing the feasibility, cost, and utility of developing models of human performance in aviation N91-10948
Contributions to the improvement of flight safety in wind shear
[ESA-TT-1141] N91-10965
Guidance concepts for time-based flight operations N91-10993
Ground-based 4-D guidance of flights in strong wind N91-10999
Developments to enhance meteorological forecasting for air traffic services N91-11006
A new approach to the flight control system reconfiguration following a battle damage and/or generic failure on a control surface N91-11023

AIRCRAFT DESIGN
Contributions in the field of aeroelastics on the occasion of the 60th anniversary of Professor Dr.-Ing. Habil. Hans Wilhelm Foersching
[ETN-90-97630] N91-10920
A quarter of a century of aeroelastic cooperation between research and industry (a review). Part 1: Fighter airplanes and helicopters N91-10931
A quarter of a century of aeroelastic cooperation between research and industry (a review). Part 2: Transport airplanes and other civil applications N91-10932
Boeing flight deck design philosophy N91-10937
Development and application of the time domain panel method N91-11010
Application of dynamical systems theory to nonlinear aircraft dynamics N91-11014
Some equipment problems associated with the introduction of female aircrew into the Royal Air Force N91-11373

AIRCRAFT ENGINES
Fault monitoring N91-10950
Fault diagnosis N91-10951
Test launch for turboaircraft engine. Description of the installation
[ILA-87-A-02] N91-11018
Test cases for computation of internal flows in aero engine components
[AGARD-AR-275] N91-11022
The role of process modelling in manufacture and design
[PNR-90702] N91-11416

AIRCRAFT GUIDANCE
Time-based aircraft/ATC operations study N91-10959
The 4-D control of current air carriers in the present environment: Objectives, status, and plans N91-10990
The control of inbound flights N91-10992
Guidance concepts for time-based flight operations N91-10993
Air traffic management and aircraft guidance in a zone of convergence N91-10998
Ground-based 4-D guidance of flights in strong wind N91-10999
A piloted simulator evaluation of a ground-based 4-D descent advisor algorithm N91-11000
The air traffic controller facing automation: Conflict or cooperation N91-11001

AIRCRAFT INSTRUMENTS
Boeing flight deck design philosophy N91-10937
Flight simulator evaluation test of multi-functional display unit
[NAL-TM-596] N91-11026
Morphological and functional adaptation of personal equipment designed for female personnel N91-11374

AIRCRAFT LANDING
Four dimensional navigation in air traffic with 4-D navigation aircraft N91-10991
The control of inbound flights N91-10992
Expert systems for the generation of thermal area arrival paths for civil transport N91-10995
Ground-based 4-D guidance of flights in strong wind N91-10999

AIRCRAFT MANEUVERS
Comparison of a mathematical one-point model and a multi-point model of aircraft motion in moving air N91-10969
Aircraft flight in wind-shear N91-10973

AIRCRAFT MODELS
A new approach to the flight control system reconfiguration following a battle damage and/or generic failure on a control surface N91-11023

AIRCRAFT NOISE
Aircraft interior noise reduction by alternate resonance tuning
[NASA-CR-186879] N91-11488

AIRCRAFT PARTS
Fault recovery recommendation N91-10952

AIRCRAFT PERFORMANCE
Integration of aircraft capability in air traffic handling simulations N91-11007

AIRCRAFT PILOTS
Recruiting, Selection, Training and Military Operations of Female Aircrew
[AGARD-CP-491] N91-11358
The integration of women into US Navy aircrew training and squadron assignments N91-11359
The selection, training, and operational work of female helicopter pilots in the Royal Netherlands Air Force N91-11361
Naval aviation selection test scores and female aviator performance N91-11363
Sex differences concerning performance and personality traits of applicants for highly qualified operator functions in aviation N91-11364
Female aircrew: The Canadian forces experience N91-11367
Problems posed by the adaptation of physiological protective equipment for female combat pilots N91-11372
Pregnancy: A cause for grounding of female air crew N91-11376
EKG findings in female aviators in the US Air Force N91-11377

AIRCRAFT SAFETY
Aviation Safety/Automation Program Conference
[NASA-CP-3090] N91-10936
Boeing flight deck design philosophy N91-10937
National plan to enhance aviation safety through human factors improvements N91-10940
Aviation safety/automation program overview N91-10941
Summary of the industry/NASA/FAA workshop on philosophy of automation: Promises and realities N91-10942
Technological advances for studying human behavior N91-10947
Terminal weather information management N91-10960
Current Emergency Locator Transmitter (ELT) deficiencies and potential improvements utilizing TSO-C91a ELTs
[NASA-CR-4330] N91-10964
How to fly windshear N91-10974

AIRCRAFT STRUCTURES
Fault diagnosis N91-10951

AIRFOIL OSCILLATIONS
Calculation of the pressure distribution on an oscillating airfoil in incompressible flow considering nonlinear effects N91-10926

AIRFOIL PROFILES
Numerical calculations for flows past an unconventional airfoil N91-10916
Temporal-adaptive Euler/Navier-Stokes algorithm for unsteady aerodynamic analysis of airfoils using unstructured dynamic meshes
[NASA-TM-102734] N91-10919
The calculation of unsteady compressible flow about oscillating airfoil profiles using the Euler upwind method N91-10921

AIRFOILS
Calculation of the rotor induced download on airfoils N91-10864
Progress toward the development of an airfoil icing analysis capability N91-10866
Prediction of turbine rotor-stator interaction using Navier-Stokes methods N91-10881
Turbine stage aerodynamics and heat transfer prediction N91-10882
Nonoverlapping composite meshes for multi-element air-foils N91-10908
A numerical study of the effects of wind tunnel wall proximity on an airfoil model
[NASA-CR-187322] N91-10934
Aerodynamic design optimization using computational fluid dynamics N91-11013
Development of a time-dependent incompressible Navier-Stokes solver based on a fractional-step method
[NASA-CR-187254] N91-11165
A viscous-inviscid interactive method for unsteady flows N91-11172
Parallelization on a multi-processor system of a solving method for the unsteady Navier-Stokes equations at high Reynolds numbers
[ESA-TT-1116] N91-11197
Atmospheric performance of the special-purpose Solar Energy Research Institute (SERI) thin-airfoil family: Final results
[DE90-000373] N91-11287

AIRFRAMES
Coupled rotor/airframe vibration analysis N91-11012

AIRLINE OPERATIONS
Aircraft trajectory: Prediction and control in the air transport flight management computer systems N91-10976
Optimum on-line handling of air traffic over Western Europe N91-10982

AIRPORT PLANNING
Airport system capacity strategic choices
[SR-226] N91-10979

AIRSPACE
A stochastic analysis of state transitions in an air space management system N91-10980

ALASKA
Outer continental shelf environmental assessment program: Comprehensive bibliography, June 1990
[PB90-258609] N91-11350

ALGAE
Survey on solidification and utilization technology of CO2
[DE91-701465] N91-11087

ALGEBRA
High-order implicit blending surfaces of low degree
[CS-9005] N91-11451

ALGORITHMS
Navier-Stokes solutions for flows related to store separation N91-10861
NASA Computational Fluid Dynamics Conference. Volume 2: Sessions 7-12
[NASA-CP-10038-VOL-2] N91-10868
Analysis of the SSME HPOTP bearing inlet cavity N91-10877
An embedded grid formulation applied to delta wings N91-10891
Unstructured mesh solution of the Euler and Navier-Stokes equations N91-10892
Flux splitting algorithms for two-dimensional viscous flows with finite-rate chemistry N91-10894
Conservation equations and physical models for hypersonic air flows over the aeroassist flight experiment vehicle N91-10897
The computation of thermo-chemical nonequilibrium hypersonic flows N91-10898
Nonoverlapping composite meshes for multi-element air-foils N91-10908
A computational model for the prediction of hypersonic, reacting flows N91-10911
Optimal trajectories of aircraft and spacecraft N91-10968
The application of trajectory prediction algorithms for planning purposes in the Netherlands ATC-system N91-10986
The 4-D descent trajectory generation techniques under realistic operating conditions N91-10994
A piloted simulator evaluation of a ground-based 4-D descent advisor algorithm N91-11000
Development and application of the time domain panel method N91-11010
A new approach to the flight control system reconfiguration following a battle damage and/or generic failure on a control surface N91-11023
H infinity-design and the improvement of helicopter handling qualities N91-11024
Controller methodologies for integrated control/structure design optimization of large flexible structures N91-11043
Precision tethered satellite attitude control N91-11046
Algorithm aided evaluation of directional signals
[ETN-90-97902] N91-11138

Examination of a three dimensional asymmetrical flow field using the interference method
[ETN-90-97859] N91-11168
Accuracy, convergence and stability of finite element algorithms for incompressible fluid flow N91-11184
The control system of an airborne radiometer: A process for a two dimensional reconstruction of irregular scanned radiometer data
[MITT-70] N91-11202
Minimum time feedback control of articulated robotic manipulators N91-11219
Real-time failure control (SAFD)
[NASA-CR-184025] N91-11233
Sampling and interpolations in digital terrain models
[INPE-5041-TDL/404] N91-11275
Integration of multispectral and pancromatic channels of HRV (SPOT) sensor for obtaining color compositions with a spatial resolution of approximately 10 m
[INPE-5035-TDL/403] N91-11278
Wave data assimilation in a 3rd generation. Wave prediction model for the North Sea: An optimal control approach
[BCRS-89-22] N91-11348
Boundary element methods in structural shape synthesis N91-11406
Two and three dimensional magnetotelluric inversion
[DE90-016187] N91-11411
Expected complexity of the 3-dimensional voronoi diagram
[PB90-221862] N91-11435
Expected linear 3-dimensional Voronoi diagram algorithm
[PB90-227984] N91-11436
A static-regridding method for two-dimensional parabolic partial differential equations
[CWI-NM-R8923] N91-11449
A polynomial method of weighted centers for convex quadratic programming
[REPT-90-17] N91-11453
A comparison of some GMRES-like methods
[REPT-90-22] N91-11454
Random number stride in Monte Carlo calculations
[DE90-012000] N91-11465
A Monte Carlo boundary propagation method for the solution of Poisson's equation
[DE90-015060] N91-11466
Modeling histogram data with piecewise polynomials
[DE90-018037] N91-11467
Contributions to the sound location in the atmosphere
[ETN-90-97863] N91-11490
Ion dynamics in semiconductors with self-consistent electronic densities N91-11556
Maximum entropy imaging of radio astrophysical data N91-11610
Speckle imaging of complicated objects N91-11617

ALLOYS
Defects in close-packed metals and alloys
[DE90-017502] N91-11097
Molecular-dynamics study of grain-boundary migration in metals
[DE90-017856] N91-11104

ALPHA PARTICLES
Measurement of radial ionization probability in microscopic volumes for 2.90 and 3.79 MeV alpha particles
[DE90-017509] N91-11498
CTR plasma engineering studies
[DE90-017774] N91-11534

ALTERNATING DIRECTION IMPLICIT METHODS
Parallelization on a multi-processor system of a solving method for the unsteady Navier-Stokes equations at high Reynolds numbers
[ESA-TT-1116] N91-11197

ALTITUDE
Enhancement of human tolerance of acute hypoxia by adaptation and intense training at high altitudes N91-11355

ALTITUDE ACCLIMATIZATION
Enhancement of human tolerance of acute hypoxia by adaptation and intense training at high altitudes N91-11355

ALTITUDE SIMULATION
Relationship of menstrual history to altitude chamber decompression sickness N91-11379

ALUMINUM
Aluminum metal combustion in water revealed by high speed microphotography
[DE90-017525] N91-11082
Microstructures of cubic Al2O3 precipitates in oxygen-implanted aluminum
[DE91-000038] N91-11111
The reaction of vapor-deposited Al with Cu oxides
[DE91-000367] N91-11114
Evaluation of thermal sprayed metallic coatings for use on the structures at Launch Complex 39
[NASA-TM-103807] N91-11121

ALUMINUM ALLOYS
Thermal stress-induced grain boundary cavitation in narrow, aluminum alloy metallizations N91-11093
The ultrasonic examination of titanium alloys N91-11094
Deformation mechanisms in rapidly solidified aluminum alloys N91-11096
The stability of irradiation-induced defects in NiAl
[DE90-017744] N91-11103
Study of the wear behavior induced by fretting in aluminum and titanium alloys
[ECL-90-01] N91-11229
Determination of the short crack effect in 2090-T8E41 aluminum lithium N91-11242
Short crack behaviour in Al-Li alloy 2090 N91-11243
The growth of short fatigue cracks in 2024 and 2090 aluminium alloys under variable amplitude loading N91-11245
Short crack growth under realistic flight loading: Model predictions and experimental results for Al 2024 and Al-Li 2090 N91-11246
The growth of short cracks in 4340 steel and aluminum-lithium 2090 N91-11247
Growth of short fatigue cracks in 7075-T6 aluminum alloy N91-11249
Short crack observations in Ti-6Al-4V under constant amplitude loading N91-11250
Texture analysis of 2090-T8E41 aluminum-lithium alloy sheet: Annex N91-11251
Mechanical properties, fracture behavior, and grain-boundary chemistry of B-doped NiAl
[DE90-015153] N91-11558
The transverse stress effect on the critical current of jelly-roll multifilamentary Nb3Al wires
[DE90-513710] N91-11581

ALUMINUM GALLIUM ARSENIDES
Nonparabolic conduction bands and masses in strained-single-quantum wells
[DE90-017028] N91-11560
Photoluminescence studies of In(x)Ga(1-x)As/Al(y)Ga(1-y)As strained-layer structures
[DE90-017031] N91-11561

ALUMINUM GRAPHITE COMPOSITES
Residual stress measurements and microstructural characterization of graphite-aluminum metal matrix composite N91-11068

AMAZON REGION (SOUTH AMERICA)
Planetary boundary layer dynamics over the Amazon rain forest N91-11317

AMBIENT TEMPERATURE
The influence of environmental factors on the temperature of the radiosonde thermistor N91-11325

AMORPHOUS MATERIALS
Structure of amorphous-silicon and germanium alloy films
[DE90-000355] N91-11557
A study of the chemical, mechanical, and surface properties of thin films of hydrogenated amorphous carbon
[DE91-000357] N91-11585

AMORPHOUS SILICON
A theoretical investigation on structural, vibrational, and electronic properties of amorphous silicon
[DE90-018040] N91-11267
Research on high-efficiency, large area amorphous silicon based solar cells
[DE90-000356] N91-11285

ANALYTIC GEOMETRY
High-order implicit blending surfaces of low degree
[CS-9005] N91-11461

ANALYZERS
Experimental manufacturing of performance evaluation system for solid image sensor
[NAL-TM-591] N91-11200

ANGLE OF ATTACK
Calculation of aerodynamic characteristics of airplane configurations at high angle of attack in steady and unsteady flow N91-11009
Prediction of the noise from a propeller at angle of attack
[NASA-TM-103627] N91-11495

ANGLES (GEOMETRY)
High-order implicit blending surfaces of low degree
[CS-9005] N91-11461

ANGULAR MOMENTUM
Numerical calculations of the formation and evolution of giant planets with rotation N91-11643

ANGULAR RESOLUTION
Azimuthal resolution degradation due to ocean surface motion in focused arrays and SARS
[AD-A223315] N91-11135

ANISOTROPY
Magnetic properties of ultrathin epitaxial films of iron
[DE90-017861] N91-11570
Microwave background anisotropies and the primordial spectrum of cosmological density fluctuations
[DE90-513791] N91-11639

ANNEALING
Effects of environment and aging on creep properties of Alloy 800H
[DE90-520207] N91-11106
Microstructures of cubic Al2O3 precipitates in oxygen-implanted aluminum
[DE91-000038] N91-11111
Photoluminescence studies of In(x)Ga(1-x)As/Al(y)Ga(1-y)As strained-layer structures
[DE90-017031] N91-11561
SERI Workshop on the Role of Point Defects/Defect Complexes in Silicon Device Fabrication
[DE90-000377] N91-11572

ANNIHILATION REACTIONS
Complementary aspects on matter-antimatter boundary layers
[TRITA-EPP-90-04] N91-11496

ANNUAL VARIATIONS
Seasonal variations in the latitudinal distribution of tropospheric carbon monoxide, 1986 to 1988 N91-11328

ANODES
Corrosion and arc erosion in MHD channels
[DE90-017889] N91-11539

ANOMALIES
Real-time failure control (SAFD)
[NASA-CR-184025] N91-11233
Numerical experiments with climatic zonally-averaged models
[INPE-5083-TDL/417] N91-11343
On a simple evaluation of anomalies from the path integral measure
[DE90-513707] N91-11484

ANTARCTIC REGIONS
ECC ozonesonde observations at South Pole, Antarctica during 1989
[PB90-258914] N91-11302

ANTENNA ARRAYS
Azimuthal resolution degradation due to ocean surface motion in focused arrays and SARS
[AD-A223315] N91-11135

ANTENNA DESIGN
Instrumenting a room temperature gravitational radiation antenna for sub-Kelvin temperatures
[IFSI-90-20] N91-11143

ANTENNA RADIATION PATTERNS
Aperture diffraction in Rayleigh zone: Calculation of the field in the quiet zone of compact ranges
[CNES-CT/DRT/TIT/AN-88/234] N91-11136
Compact representation of radiation patterns using spherical mode expansions
[DE91-000019] N91-11141

ANTHROPOMETRY
Aircrew/cockpit compatibility: A multivariate problem seeking a multivariate solution N91-11369
The application of USAF female anthropometric data to identify problems with the introduction of female aircrew into the Royal Air Force N91-11370
Anthropometric accommodation of females in Canadian forces aircraft crew stations N91-11371
Some equipment problems associated with the introduction of female aircrew into the Royal Air Force N91-11373

ANTIBODIES
A protein coated piezoelectric crystal detector
[AD-A223848] N91-11552

ANTIMATTER
Complementary aspects on matter-antimatter boundary layers
[TRITA-EPP-90-04] N91-11496
Antimatter gravity experiment
[DE91-000177] N91-11590

ANTIMONY COMPOUNDS
Superconducting and structural properties of the (Ba(0.6)K(0.4)) (Bi(1-y)Sb(y))O3 system
[DE90-017836] N91-11580

ANTIPROTONS
Antimatter gravity experiment
[DE91-000177] N91-11590

APERTURES
Aperture diffraction in Rayleigh zone: Calculation of the field in the quiet zone of compact ranges
[CNES-CT/DRT/TIT/AN-88/234] N91-11136

APEXES
Cones of matrices and setfunctions, and 0-1 optimization
[CWI-BS-R8925] N91-11444

APOGEE BOOST MOTORS
Digital data processing system for bipropellant apogee engine
[NAL-TM-599] N91-11052

APPLICATIONS PROGRAMS (COMPUTERS)
Conservation equations and physical models for hypersonic air flows over the aeroassist flight experiment vehicle N91-10897
Flight simulation programs for space plane [NAL-TM-594] N91-11035
Experimental manufacturing of data recording system for rocket combustion thermal flux distribution [DE90-702432] N91-11051
Digital data processing system for bipropellant apogee engine [NAL-TM-599] N91-11052
NCEER strong-motion data base: A user manual for the geobase release (version 1.0 for the SUN3) [PB90-258062] N91-11315
The MS-DOS device handler interface [AD-A223856] N91-11385
The MS-DOS device services interface [AD-A223902] N91-11386
The MS-DOS routing and configuration program design [AD-A223858] N91-11394
Time domain frequency stability calculated from the frequency domain description: Use of the SIGINT software package to calculate time domain frequency stability from the frequency domain [PB90-257684] N91-11405
APPROACH INDICATORS
Flight evaluation test of the PAPI (Precision Approach Path Indicator) System [NAL-TM-592] N91-10966
Flight simulator evaluation test of multi-functional display unit [NAL-TM-596] N91-11026
APPROXIMATION
The rotation of Lageos [IFSI-90-10] N91-11333
On three dimensional object recognition and pose-determination: An abstraction based approach [NASA-CR-186894] N91-11396
Approximation of the solution to the moment problem in a Hilbert space [CWI-AM-R8923] N91-11438
Uniform asymptotic approximation of Fermi-Dirac integrals [CWI-AM-R9001] N91-11440
Convergence of linear multistep and one-leg methods for stiff nonlinear initial value problems [CWI-NM-R8924] N91-11450
Asymptotic estimates of approximation errors by the Galerkin method for one class of quasipotential equations [DE90-631600] N91-11471
On density estimation in the view of Kolmogorov's ideas in approximation theory [CWI-BS-R8928] N91-11477
The delta-Sobolev approach for modeling solar spectral irradiance and radiance N91-11650
APTITUDE
Sex differences concerning performance and personality traits of applicants for highly qualified operator functions in aviation N91-11364
AQUIFERS
Results from a workshop on research needs for modeling aquifer thermal energy storage systems [DE90-018007] N91-11301
ARC JET ENGINES
Investigation of the arcjet plume near field using electrostatic probes [NASA-TM-103638] N91-11060
ARCHITECTURE (COMPUTERS)
Operator function modeling: Cognitive task analysis, modeling and intelligent aiding in supervisory control systems [NASA-CR-187331] N91-11380
The MS-DOS device handler interface [AD-A223856] N91-11385
The MS-DOS device services interface [AD-A223902] N91-11386
Distributed digital signal processors for multi-body structures [NASA-CR-187375] N91-11387
The MS-DOS routing and configuration program design [AD-A223858] N91-11394
Inflated speedups in parallel simulations via malloc() [NASA-CR-182104] N91-11397
Software quality assurance handbook [DE91-000060] N91-11420
A unified framework for credit assignment [DE90-011636] N91-11434
Touchstone project: Milestone event Q4 [AD-A224034] N91-11480
Touchstone project Mach port: Milestone event Q4 [AD-A224057] N91-11481
Touchstone project DELTA numeric node: Milestone event Q4 [AD-A224060] N91-11482
ARCTIC REGIONS
Arctic acoustics ultrasonic modeling studies [AD-A224165] N91-11489
AREA NAVIGATION
Use of 4-D RNAV in time-based en route arrival metering N91-10997
ARMED FORCES
The selection, training, and operational work of female helicopter pilots in the Royal Netherlands Air Force N91-11361
Review of female applicant aircrew in the Belgian forces N91-11368
ARTIFICIAL INTELLIGENCE
Overview of error-tolerant cockpit research N91-10949
Mobile robots and intelligent motion control [DE90-017312] N91-11226
A unified framework for credit assignment [DE90-011636] N91-11434
ASCENT
Numerical aerodynamic simulation of the space shuttle ascent environment N91-10875
ASHES
CTR plasma engineering studies [DE90-017774] N91-11534
ASPECT RATIO
Theoretical and numerical studies in magnetic mirror fusion [DE90-017605] N91-11533
ASPHERICITY
From red giants to planetary nebulae: Asymmetries, dust, and polarization N91-11622
ASSEMBLING
Geometric method and synthesis af assembly strategies in robotic systems [LAAS-90041] N91-11215
Archimedes: A system that plans and executes mechanical assemblies [DE91-000036] N91-11231
ASTEROIDS
Reexamination of data from the asteroid/meteoroid detector [NASA-CR-185875] N91-11619
ASTRONOMICAL CATALOGS
Apparent place of Polaris and apparent Sidereal Time at 0 hour UT 1990-1994 [PB90-259169] N91-11607
ASTROPHYSICS
Maximum entropy imaging of radio astrophysical data N91-11610
Activities report of the Institute for Extraterrestrial Physics [MPE-217] N91-11620
Magnetic field generation in astrophysics N91-11623
Numerical studies of electron scattering in astrophysics N91-11625
Analytic studies in nuclear astrophysics N91-11628
The transfer of polarized radiation in astrophysical masers in the presence of magnetic fields N91-11629
A new site for the astrophysical gamma-process [DE90-017519] N91-11635
Status reports of supercomputing astrophysics in Japan [DE90-513793] N91-11640
ASYMMETRY
Study of asymmetric supersonic jet flow for ejectors [DE90-015598] N91-10917
A simulation study of magnetic reconnection processes at the dayside magnetopause N91-11320
ASYMPTOTIC METHODS
Asymptotic estimates of approximation errors by the Galerkin method for one class of quasipotential equations [DE90-631600] N91-11471
An investigation of the Newman-Penrose constants for massless free fields of arbitrary spin N91-11630
ASYMPTOTIC PROPERTIES
Asymptotic behavior of Laguerre polynomials with Re z less than 0 derived by the central limit theorem [W-9004] N91-11458
ASYMPTOTIC SERIES
Uniform asymptotic approximation of Fermi-Dirac integrals [CWI-AM-R9001] N91-11440
ATLAS CENTAUR LAUNCH VEHICLE
RL10 ignition limits test for Shuttle Centaur [NASA-CR-183199] N91-11049
ATMOSPHERIC BOUNDARY LAYER
Large eddy-simulation of convective boundary layers [ESA-TT-1138] N91-11198
Radiometric observation of the atmospheric boundary layer (the ROSSA Project) N91-11324
Tropical cyclone simulations with the Betts convective adjustment scheme N91-11338
ATMOSPHERIC CHEMISTRY
Lifetimes and fates of toxic air contaminants in California's atmosphere [PB90-253204] N91-11304
Atmospheric Chemistry: Laboratory studies of kinetics of important reactions N91-11326
Seasonal variations in the latitudinal distribution of tropospheric carbon monoxide, 1986 to 1988 N91-11328
Parameterizations of microphysical processes in clouds [DE90-017820] N91-11344
ATMOSPHERIC CIRCULATION
A simple zonal average energy budget model of the earth-atmosphere system N91-11316
Planetary boundary layer dynamics over the Amazon rain forest N91-11317
Northwest African depressions and their relationship to jet streams N91-11318
The evolution of vortical patterns and vortices in mesoscale convective complexes N91-11319
Fluctuating concentrations in atmospheric dispersion N91-11323
Taiwan area mesoscale experiment: A guide to precipitation patterns during the 1987 field phase [PB90-256355] N91-11336
Meteorological characteristics of the El Nino/Southern Oscillation phenomenon N91-11340
ATMOSPHERIC COMPOSITION
ECC ozonesonde observations at South Pole, Antarctica during 1989 [PB90-258914] N91-11302
Fluctuating concentrations in atmospheric dispersion N91-11323
Atmospheric chemistry: Laboratory studies of kinetics of important reactions N91-11326
Seasonal variations in the latitudinal distribution of tropospheric carbon monoxide, 1986 to 1988 N91-11328
ATMOSPHERIC EFFECTS
Critical aspects of trajectory prediction: Flight in non-uniform wind N91-10971
ATMOSPHERIC GENERAL CIRCULATION MODELS
The evolution and time scales of the atmospheric response to tropical diabatic heating events N91-11322
ATMOSPHERIC HEAT BUDGET
A simple zonal average energy budget model of the earth-atmosphere system N91-11316
ATMOSPHERIC HEATING
The evolution and time scales of the atmospheric response to tropical diabatic heating events N91-11322
ATMOSPHERIC MODELS
Estimation of seasonal and annual acidic deposition through aggregation of three-day episodic periods [PB90-252628] N91-11303
Advantages of the Community Climate Model (CCM) concept [PB90-256348] N91-11314
A simple zonal average energy budget model of the earth-atmosphere system N91-11316
The evolution of vortical patterns and vortices in mesoscale convective complexes N91-11319
Modelling of large-scale unstable waves in the middle atmosphere N91-11327
Energetics of 60 days predictions with the EZMW-T21 model in its mean temporary development and its relationship to forecast skill [MITT-71] N91-11335
ATMOSPHERIC PHYSICS
Comparison of clear air atmospheric radar techniques for the study of atmospheric dynamics in the troposphere and the stratosphere [PB90-256314] N91-11313
Planetary boundary layer dynamics over the Amazon rain forest N91-11317
ATMOSPHERIC PRESSURE
Tropical cyclone simulations with the Betts convective adjustment scheme N91-11338
ATMOSPHERIC RADIATION
Atmospheric neutrino fluxes [DE90-508023] N91-11656
ATMOSPHERIC TEMPERATURE
ECC ozonesonde observations at South Pole, Antarctica during 1989 [PB90-258914] N91-11302
Meteorological characteristics of the El Nino/Southern Oscillation phenomenon N91-11340
ATOMIC COLLISIONS
Newly appreciated roles for electrons in ion-atom collisions [DE91-000555] N91-11509
Theoretical and numerical studies in magnetic mirror fusion [DE90-017605] N91-11533

ATOMIC PHYSICS
Atomic physics of highly charged ions in an electron beam ion trap
[DE90-017528] N91-11499
Task A: High energy physics program experiment and theory. Task B: High energy physics program numerical simulation
[DE90-017336] N91-11512
ATOMIC STRUCTURE
Nuclear magnetic resonance survey of hydrogen motion and electronic structure in (alpha)-phase (Nb-Mo)-H alloys
[DE90-018044] N91-11101
Liquid alloys with strong interactions
[DE90-017661] N91-11102
A theoretical investigation on structural, vibrational, and electronic properties of amorphous silicon
[DE90-018040] N91-11267
Semiempirical studies of atomic structure
[DE90-017653] N91-11501
The transuranium elements: Members of the 5f series
[DE90-017680] N91-11575
ATOMIZING
Characterization and optimization of a pneumatic injector for a 60 bar combustion chamber
[ETN-90-97580] N91-11076
ATTITUDE INDICATORS
Flight simulator evaluation test of multi-functional display unit
[NAL-TM-596] N91-11026
AUDIO EQUIPMENT
Digital audio editing: The development of a random access editor
[BBC-RD-1990/5] N91-11142
AUGMENTATION
Constrained optimization approach to feedback control of state-augmented systems N91-11433
AUSTENITIC STAINLESS STEELS
Deformation effects on the development of grain boundary chronium depletion (sensitization) in type 316 austenitic stainless steels
[DE90-016130] N91-11092
AUTOCORRELATION
Classification of textures using the ARMA models and distances over the autocorrelation function
[INPE-5067-TDL/406] N91-11421
AUTOMATED EN ROUTE ATC
A description and evaluation of TIMER: A time-based terminal flow-control concept N91-10996
Use of 4-D RNAV in time-based en route arrival metering N91-10997
AUTOMATED PILOT ADVISORY SYSTEM
A piloted simulator evaluation of a ground-based 4-D descent advisor algorithm N91-11000
AUTOMATIC CONTROL
Automated design of controlled diffusion blades N91-10883
Cockpit avionics integration and automation N91-10938
Aviation safety/automation program overview N91-10941
Summary of the industry/NASA/FAA workshop on philosophy of automation: Promises and realities N91-10942
Human-centered automation: Development of a philosophy N91-10944
Assessing the feasibility, cost, and utility of developing models of human performance in aviation N91-10948
ATC automation concepts N91-10957
Time-based operations in an advanced ATC environment N91-10958
The air traffic controller facing automation: Conflict or cooperation N91-11001
Automated Fluid Interface System (AFIS)
[NASA-CR-183969] N91-11031
An adaptive finite element technique using element equilibrium and paving
[DE90-015829] N91-11410
AUTOMATIC TEST EQUIPMENT
Application of self-testing integrated circuits to the safety of systems operation
[ETN-90-97828] N91-11150
AUTOMOBILES
Measurements of toxic exhaust emissions from gasoline-powered light-duty vehicles
[PB90-259649] N91-11306
AVIONICS
Aviation Safety/Automation Program Conference
[NASA-CP-3090] N91-10936
Cockpit avionics integration and automation N91-10938
Human-centered automation: Development of a philosophy N91-10944
Technological advances for studying human behavior N91-10947
Overview of error-tolerant cockpit research N91-10949
Fault monitoring N91-10950
Aircraft trajectory: Prediction and control in the air transport flight management computer systems N91-10976
AXIAL FLOW TURBINES
Turbine stage aerodynamics and heat transfer prediction N91-10882
AXIAL STRESS
The transverse stress effect on the critical current of jelly-roll multifilamentary Nb3Al wires
[DE90-513710] N91-11581
AXISYMMETRIC FLOW
Progress in computing nozzle/plume flow fields N91-10872
AZIMUTH
Azimuthal resolution degradation due to ocean surface motion in focused arrays and SARS
[AD-A223315] N91-11135
Magnetohydrodynamic modification of the TEACH-T code and the prediction of the maximum azimuthal velocity in a conducting fluid
[DE90-017510] N91-11187

B

BACKGROUND RADIATION
Microwave background anisotropies and the primordial spectrum of cosmological density fluctuations
[DE90-513791] N91-11639
Observations of the soft x ray background N91-11663
BACKSCATTERING
MONT3E: A Monte Carlo electron heat transfer code
[DE90-012091] N91-11514
BACTERIA
The structure and function of membrane protein photosynthetic reaction center
[DE90-017795] N91-11353
BAFFLES
Advanced infrared optically black baffle materials
[DE91-000561] N91-11523
BALLOON SOUNDING
ECC ozonesonde observations at South Pole, Antarctica during 1989
[PB90-258914] N91-11302
BALLOONING MODES
The evolution of resistive ballooning modes in the banana-plateau collisionality regime
[DE90-016672] N91-11525
BAND STRUCTURE OF SOLIDS
Nonparabolic conduction bands and masses in strained-single-quantum wells
[DE90-017028] N91-11560
BANDWIDTH
Pulse evolution in multi-atmosphere CO2 lasers
[ETN-90-97765] N91-11210
BARIUM OXIDES
Design and testing of a high temperature superconducting current lead
[DE90-017812] N91-11579
BATTERY CHARGERS
A microprocessor based charge control system for the simultaneous charging of several batteries with one charge controller
[DE90-017089] N91-11157
Development of high performance sodium/metal chloride cells
[DE90-017668] N91-11159
BAYES THEOREM
Bayesian multi-sensor tracking for advanced air traffic control systems N91-11003
BEAM INJECTION
Fluctuations and stability in the Advanced Toroidal Facility (ATF) torsatron
[DE90-017734] N91-11536
BEARING (DIRECTION)
Four dimensional navigation in air traffic with 4-D navigation aircraft N91-10991
BELGIUM
Review of female applicant aircrew in the Belgian forces N91-11368
BESSEL FUNCTIONS
Evaluation of the integral
[PB90-235011] N91-11437
BIAS
Beta splines interpolation for DEM's
[INPE-5039-PRE/1572] N91-11415
BIBLIOGRAPHIES
Aircraft trajectories: Computation, prediction, control, Volume 3. Part 9: Book of abstracts. Part 10: Bibliography. Part 11: List of contributors
[AGARD-AG-301-VOL-3-PT-9-11] N91-10978
Center for electronics and electrical engineering technical publication announcements covering Center programs, July - September, 1989, with 1990 CEEE events calendar
[PB90-206491] N91-11145
Outer continental shelf environmental assessment program: Comprehensive bibliography, June 1990
[PB90-258609] N91-11350
Technology transfer: Hotlines
[PB90-237140] N91-11594
BIG BANG COSMOLOGY
On the origin of cosmological magnetic fields
[DE90-017617] N91-11634
BINARY STARS
Polarized radiation from inhomogeneous shocks N91-11662
BINOCULAR VISION
Requirements of an HMS/D for a night-flying helicopter
[MBB-UD-0570-90-PUB] N91-11383
BIOCHEMISTRY
JPRS report: Science and technology. USSR: Life sciences
[JPRS-ULS-89-003] N91-11354
BIODYNAMICS
Impact on women: A retrospective look at impact acceleration testing at the Harry G. Armstrong Aerospace Medical Research Laboratory N91-11378
BIOINSTRUMENTATION
Biosensors: Development status
[MBB-Z-0305-90-PUB] N91-11201
A protein coated piezoelectric crystal detector
[AD-A223848] N91-11552
BIOLOGICAL EFFECTS
Chlorine dioxide and hemodialysis
[DE90-015912] N91-11382
Implications of the Biological Effects of Ionizing Radiation (BEIR) 5 report to the Department of Energy
[DE90-016673] N91-11526
BIOPHYSICS
JPRS report: Science and technology. USSR: Life sciences
[JPRS-ULS-89-003] N91-11354
BIOTECHNOLOGY
JPRS report: Science and technology. USSR: Life sciences
[JPRS-ULS-89-003] N91-11354
BIVARIATE ANALYSIS
Interpolation of scattered data by a bivariate convex function. Part 1: Piecewise linear C sup 0-interpolation
[MEMO-858-PT-1] N91-11469
BLADE-VORTEX INTERACTION
The aerodynamic effects of nozzle guide vane shock wave and wake passing on a transonic turbine rotor N91-10915
The calculation of rotor/fuselage interaction for two-dimensional bodies
[NASA-TM-102855] N91-10933
BLOCKS
A-stable parallel block methods
[CWI-NM-R8918] N91-11427
BLOWING
Controlled vortical flow on delta wings through unsteady leading edge blowing N91-11011
BODY-WING CONFIGURATIONS
Recent advances in Runge-Kutta schemes for solving 3-D Navier-Stokes equations N91-10851
BOEING 757 AIRCRAFT
Generation of a buoyant plume of artificial smoke for airplane tests
[DOT/FAA/CT-90/9] N91-11015
BOLZA PROBLEMS
Optimal trajectories of aircraft and spacecraft N91-10968
BONDING
Conjugate (solid/fluid) computational fluid dynamics analysis of the space shuttle solid rocket motor nozzle/case and case field joints N91-10879
Thermal stresses in layered electrical assemblies bonded with solder
[DE90-015563] N91-11263
Formation and stability of As-H bonds in H-implanted GaAs
[DE91-000043] N91-11584
BOOLEAN ALGEBRA
Mathematical morphology on homogeneous spaces. Part 1: The simply transitive case
[CWI-AM-R8924-PT-1] N91-11439
BOREHOLES
Spectral lithostratigraphic correlation of boreholes
[INPE-5022-TDL/402] N91-11332
BORON
Mechanical properties, fracture behavior, and grain-boundary chemistry of B-doped NiAl
[DE90-015153] N91-11558

BOUNDARIES
A new lower bound for the de Bruijn-Newman constant
[CWI-NM-R8920] N91-11447
Improved techniques for lower bounds for odd perfect numbers
[CWI-NM-R8921] N91-11448
BOUNDARY CONDITIONS
Turbine stage aerodynamics and heat transfer prediction N91-10882
Numerical analysis of flow through oscillating cascade sections N91-10884
Grid generation and flow computation about a Martian entry vehicle
[NASA-CR-187032] N91-11042
Two and three dimensional magnetotelluric inversion
[DE90-016187] N91-11411
BOUNDARY ELEMENT METHOD
ution of the equivalent space with Bessel integral equation for the fractured orthotropic disk ution of the 'equivalent space' with Bessel integral equation for the fractured orthotropic disk
[ISSN-0932-8599] N91-11253
Boundary element methods in structural shape synthesis N91-11406
BOUNDARY INTEGRAL METHOD
Boundary integral equations for dynamic fracture problems N91-11259
BOUNDARY LAYER CONTROL
Boundary layer receptivity mechanisms relevant to laminar flow control N91-11182
BOUNDARY LAYER FLOW
Experimental investigation of the mechanisms underlying vortex kinematics in unsteady separated flows N91-10907
Calculation of viscous hypersonic flows using a coupled Euler/2nd order boundary layer method
[MBB/FE122/S/PUB/387] N91-10935
An experimental study of an axisymmetric turbulent boundary layer disturbed by a periodic freestream N91-11175
Boundary layer receptivity mechanisms relevant to laminar flow control N91-11182
Measurement and calculation of surface roughness effects on turbulent flow and heat transfer N91-11183
BOUNDARY LAYER PLASMAS
Complementary aspects on matter-antimatter boundary layers
[TRITA-EPP-90-04] N91-11496
BOUNDARY LAYER SEPARATION
CFD for applications to aircraft aeroelasticity N91-10855
BOUNDARY LAYER STABILITY
Boundary layer receptivity mechanisms relevant to laminar flow control N91-11182
BOUNDARY LAYER TRANSITION
Numerical simulation of transition from laminar to turbulent duct flow
[ESA-TT-1144] N91-11199
BOUNDARY VALUE PROBLEMS
Theoretical and numerical aspects of wave stability in combustion models
[ECL-89-21] N91-11088
Generalized dynamic normal mode initialization N91-11341
Convergence of linear multistep and one-leg methods for stiff nonlinear initial value problems
[CWI-NM-R8924] N91-11450
Searching spectrum points of difference initial-boundary value problems with using CAS
[DE90-634382] N91-11472
BRAGG ANGLE
Bragg intensities and diffuse scattering in Ag2Se: Molecular dynamics study
[DE90-017811] N91-11583
BRANCHING (MATHEMATICS)
Quasi-periodic bifurcations, applications
[TW-8911] N91-11459
BRAZIL
Methodology of remote sensing for monitoring modifications in the fluvial channel and updating nautical charts
[INPE-4863-TDL/374] N91-11277
Identification of areas subject to flooding through TM/LANDSAT images in the basin of the rivers Pindare, Mearim, Jaguaribe, Apodi, Piranhas, and San Francisco
[INPE-5034-RPE/619] N91-11279
Geometric correction of SPOT imagery with the use of a digital elevation model
[INPE-5014-TDL/401] N91-11423
BRAZILIAN SPACE PROGRAM
Functional description and analysis of processor performance for data collection
[INPE-5037-RPE/620] N91-11048
BREADBOARD MODELS
Three-Man Solid Electrolyte Carbon Dioxide Electrolysis Breadboard
[NASA-CR-185612] N91-11148
BRIGHTNESS
Type 2 solar radio bursts recorded at Weissenau, 1966-1987
[PB90-198334] N91-11648
BRITTLENESS
Mechanical properties, fracture behavior, and grain-boundary chemistry of B-doped NiAl
[DE90-015153] N91-11558
BUCKLING
Buckling and vibrations of plates subjected to concentrated forces N91-11255
BUDGETING
Proposal pressure in the 1980s: An indicator of stress on the Federal Research System
[PB90-253147] N91-11593
BUILDINGS
The practical challenges of converting end-use data into information
[DE90-016538] N91-11600
BULGING
The relationship of galaxy morphology to nuclear star formation in non-interacting spiral galaxies N91-11618
BUOYANCY
Generation of a buoyant plume of artificial smoke for airplane tests
[DOT/FAA/CT-90/9] N91-11015
BURNERS
Evaluation of a high-temperature burner-duct-recuperator system
[DE90-000366] N91-11284

C

CADMIUM ALLOYS
Physical metallurgy and magnetic behavior of Cd stabilized bcc (beta) Gd alloys
[DE91-000196] N91-11112
CADMIUM TELLURIDES
Optical characterization of CdZnTe/CdTe strained quantum wells
[DE90-017036] N91-11563
CALIBRATING
An automated linearity test for direct voltage calibrators
[DE90-016927] N91-11204
Scanning system for measuring uniformity of laser detector response and laser beam dimensions
[PB90-257619] N91-11207
Experimental and theoretical studies of friction and heat transfer in rough passages
[DE90-016302] N91-11223
The EGRET gamma ray telescope and its energy calibration N91-11613
CANADA
A Canadian female CF-18 pilot's experience N91-11360
Female aircrew: The Canadian forces experience N91-11367
Anthropometric accommodation of females in Canadian forces aircraft crew stations N91-11371
CANARD CONFIGURATIONS
Grid generation and inviscid flow computation about aircraft geometries N91-10857
Application of dynamical systems theory to nonlinear aircraft dynamics N91-11014
CANCER
Protection by WR-2721 and WR-151327 against late effects of gamma rays and neutrons
[DE90-017792] N91-11352
Implications of the Biological Effects of Ionizing Radiation (BEIR) 5 report to the Department of Energy
[DE90-016673] N91-11526
CANTILEVER BEAMS
Alternate equilibrium configurations of flexible cantilever beams N91-11254
CANTILEVER PLATES
Performance of finite dynamic elements for composite materials in plane stress N91-11260
CAPACITORS
MIS capacitor studies on silicon carbide single crystals
[NASA-CR-187350] N91-11555
CAPTURE EFFECT
Capture and transfer of pions in hydrogenous materials
[DE90-017756] N91-11505
CARBIDES
Wear reduction in cutting tools: Tribological properties of hard coatings
[DE90-009705] N91-11212
CARBON
Carbon deposition in gas turbine combustors
[PNR-90692] N91-11020
CARBON COMPOUNDS
A study of the chemical, mechanical, and surface properties of thin films of hydrogenated amorphous carbon
[DE91-000357] N91-11585
CARBON DIOXIDE
Survey on solidification and utilization technology of CO2
[DE91-701465] N91-11087
Three-Man Solid Electrolyte Carbon Dioxide Electrolysis Breadboard
[NASA-CR-185612] N91-11148
CARBON DIOXIDE LASERS
Pulse evolution in multi-atmosphere CO2 lasers
[ETN-90-97765] N91-11210
CARBON FIBER REINFORCED PLASTICS
Load transfer between fiber and matrix in carbon fiber reinforced plastic composites tensile behavior of an embedded single filament specimen
[ONERA-NT-1989-9] N91-11075
CARBON FIBERS
Graphite fluoride fibers and their applications in the space industry
[NASA-TM-103265] N91-11062
CARBON MONOXIDE
Seasonal variations in the latitudinal distribution of tropospheric carbon monoxide, 1986 to 1988 N91-11328
CARBONATES
Molten carbonate fuel cell power plant systems studies
[DE90-009697] N91-11298
CASCADE FLOW
Numerical analysis of flow through oscillating cascade sections N91-10884
Navier-Stokes analysis of transonic cascade flow
[NASA-TM-103624] N91-11192
CASSEGRAIN OPTICS
A search for small comets in consecutive images acquired with a ground-based telescope N91-11626
CATALYSTS
Survey on solidification and utilization technology of CO2
[DE91-701465] N91-11087
Measurements of toxic exhaust emissions from gasoline-powered light-duty vehicles
[PB90-259649] N91-11306
CATHODE RAY TUBES
Requirements of an HMS/D for a night-flying helicopter
[MBB-UD-0570-90-PUB] N91-11383
CATHODES
Corrosion and arc erosion in MHD channels
[DE90-017889] N91-11539
CATHODIC COATINGS
Evaluation of thermal sprayed metallic coatings for use on the structures at Launch Complex 39
[NASA-TM-103807] N91-11121
CAVITATION FLOW
Thermal stress-induced grain boundary cavitation in narrow, aluminum alloy metallizations N91-11093
CAVITIES
Analysis of the SSME HPOTP bearing inlet cavity N91-10877
Attenuation of elastic waves due to scattering from spherical cavities and elastic inclusions N91-11256
CENTRIFUGAL FORCE
Problems of static divergence concerning the rpm regulation of wind turbines using centrifugal force controlling means and rotating slat
[ETN-90-97858] N91-11281
CERAMICS
Elastic properties of ceramic composite materials at high temperatures
[ETN-90-97897] N91-11067
Micromechanics of semi-brittle ceramics N91-11119
Mechanical behavior of ceramics and composites
[DE90-017311] N91-11122
Crack-growth resistance in reinforced ceramic composites N91-11261
CERENKOV COUNTERS
A search for very high energy gamma-rays from Cygnus X-3 N91-11658
CERENKOV RADIATION
A search for very high energy gamma-rays from Cygnus X-3 N91-11658
CHANNELS (DATA TRANSMISSION)
Modeling and coding in aeronautical satellite channel
[ETN-90-97899] N91-11137
CHARACTERIZATION
X ray microprobe-microscopy
[DE90-017327] N91-11520

CHARGE COUPLED DEVICES
Experimental manufacturing of performance evaluation system for solid image sensor
[NAL-TM-591] N91-11200
Fourteen x fourteen CCD array for optical intersatellite link tracking
[CNES-CT/DRT/TIT/OE-88/144] N91-11521
CHARGE DISTRIBUTION
MIS capacitor studies on silicon carbide single crystals
[NASA-CR-187350] N91-11555
CHARGE EXCHANGE
Capture and transfer of pions in hydrogenous materials
[DE90-017756] N91-11505
CHARGE TRANSFER
Bragg intensities and diffuse scattering in Ag2Se: Molecular dynamics study
[DE90-017811] N91-11583
CHECKOUT
Procedural error monitoring and smart checklists
N91-10954
CHEMICAL ANALYSIS
Recommended operating procedure No. 45: Analysis of nitrous oxide from combustion sources
[PB90-238502] N91-11078
Physical metallurgy and magnetic behavior of Cd stabilized bcc (beta) Gd alloys
[DE91-000196] N91-11112
Morphological analysis of ionomers
[DE90-017611] N91-11124
CHEMICAL BONDS
Chemical identification of icosahedral structure for cobalt and nickel clusters
[DE90-017688] N91-11100
Molecular-dynamics study of grain-boundary migration in metals
[DE90-017856] N91-11104
Formation and stability of As-H bonds in H-implanted GaAs
[DE91-000043] N91-11584
CHEMICAL COMPOSITION
Chemical identification of icosahedral structure for cobalt and nickel clusters
[DE90-017688] N91-11100
Spectral lithostratigraphic correlation of boreholes
[INPE-5022-TDL/402] N91-11332
CHEMICAL PROPERTIES
A study of the chemical, mechanical, and surface properties of thin films of hydrogenated amorphous carbon
[DE91-000357] N91-11585
CHEMICAL REACTIONS
Modeling of high speed chemically reacting flow-fields
N91-10870
Three-dimensional calculation of supersonic reacting flows using an LU scheme N91-10871
Flux splitting algorithms for two-dimensional viscous flows with finite-rate chemistry N91-10894
Intramolecular electron transfer rates
[DE90-017447] N91-11504
CHILDREN
Nitrogen dioxide and respiratory infection: Pilot investigations
[PB90-247339] N91-11357
CHLORATES
Ion chromatography in the manufacture of multilayer circuit boards
[DE90-017647] N91-11158
CHLORIDES
Development of high performance sodium/metal chloride cells
[DE90-017668] N91-11159
CHLORINATION
Chlorine dioxide and hemodialysis
[DE90-015912] N91-11382
CHLORINE
Chlorine dioxide and hemodialysis
[DE90-015912] N91-11382
CHOLESKY FACTORIZATION
High-performance equation solvers and their impact on finite element analysis
[NASA-TM-102735] N91-11252
CHROMIUM
Deformation effects on the development of grain boundary chronium depletion (sensitization) in type 316 austenitic stainless steels
[DE90-016130] N91-11092
CHROMIUM CARBIDES
A study of chromium carbide precipitation at interphase boundaries in stainless steel welds
[DE91-000360] N91-11113
CHROMOSPHERE
Exploration of decreased solar activity state (small intensity activity) in the corona and chromosphere
[INPE-5059-TDL/405] N91-11652
CHUTES
Theoretical and numerical studies of constitutive relations for frictional granular flow
[DE90-009662] N91-11194
CIRCUIT BOARDS
Ion chromatography in the manufacture of multilayer circuit boards
[DE90-017647] N91-11158
Touchstone ^roject DELTA numeric node: Milestone event Q4
[AD-A224060] N91-11482
CIRCUITS
On dominating and spanning circuits in graphs
[MEMO-859] N91-11470
CIRCULAR CYLINDERS
Vortex-induced noise and vibration in flow past several flat plates N91-11163
Unsteady fluid forces and fluidelastic vibration of a group of circular cylinders
[DE90-013661] N91-11190
CIRCULAR PLATES
Forced vibration analysis of plates and shallow shells
N91-11237
Buckling and vibrations of plates subjected to concentrated forces N91-11255
CIRCULAR POLARIZATION
The transfer of polarized radiation in astrophysical masers in the presence of magnetic fields N91-11629
CIRCULAR TUBES
An experimental study of natural convection heat transfer from a horizontal cylinder array vertically aligned to and confined by a single wall and two walls
N91-11178
CIVIL AVIATION
A quarter of a century of aeroelastic cooperation between research and industry (a review). Part 2: Transport airplanes and other civil applications N91-10932
Human-centered automation: Development of a philosophy N91-10944
The use of downlinked measurements to track civil aircraft N91-11004
Sex differences concerning performance and personality traits of applicants for highly qualified operator functions in aviation N91-11364
CLASSICAL MECHANICS
An inverse problem for classical relativistic mechanics
[DE90-631599] N91-11589
CLASSIFICATIONS
Classification of acoustic emission waveforms for nondestructive evaluation using neural networks
[DE90-017239] N91-11236
Classification of textures using the ARMA models and distances over the autocorrelation function
[INPE-5067-TDL/406] N91-11421
A unified framework for credit assignment
[DE90-011636] N91-11434
CLASSIFIERS
Classification of textures using the ARMA models and distances over the autocorrelation function
[INPE-5067-TDL/406] N91-11421
CLEARANCES
The measurement and finite element analysis of the dynamic stiffness of non-uniform clearance, gas, thrust bearings
[DE90-015120] N91-11214
CLIMATE
Advantages of the Community Climate Model (CCM) concept
[PB90-256348] N91-11314
Numerical experiments with climatic zonally-averaged models
[INPE-5083-TDL/417] N91-11343
CLIMATE CHANGE
Democratic theory, science, and decision making in global climate change: Culpability, uncertainty, and fairness
[DE90-017316] N91-11308
CLIMATOLOGY
Wind lidar for tropical climatology
[CNES-CT/DRT/TIT/IO-88/126] N91-11334
Numerical experiments with climatic zonally-averaged models
[INPE-5083-TDL/417] N91-11343
CLOSE PACKED LATTICES
Defects in close-packed metals and alloys
[DE90-017502] N91-11097
CLOSED ECOLOGICAL SYSTEMS
Three-Man Solid Electrolyte Carbon Dioxide Electrolysis Breadboard
[NASA-CR-185612] N91-11148
CLOUD PHYSICS
A numerical model of polar mesospheric cloud formation and evolution N91-11337
Parameterizations of microphysical processes in clouds
[DE90-017820] N91-11344
CLUSTER ANALYSIS
Spectral lithostratigraphic correlation of boreholes
[INPE-5022-TDL/402] N91-11332
CMOS
A radiation hardened SONOS/CMOS EEPROM family
[DE90-015993] N91-11154
COAL
Theoretical and numerical studies of constitutive relations for frictional granular flow
[DE90-009662] N91-11194
COAL GASIFICATION
Projective scales against high temperature corrosion
[ETN-90-97770] N91-11116
Molten carbonate fuel cell power plant systems studies
[DE90-009697] N91-11298
COAL LIQUEFACTION
Projective scales against high temperature corrosion
[ETN-90-97770] N91-11116
Co-researches with researchers of alternative energy of petroleum in EC countries
[DE91-701466] N91-11129
COATING
Recent advances and developments in coatings
[PNR-90698] N91-11021
COATINGS
Wear reduction in cutting tools: Tribological properties of hard coatings
[DE90-009705] N91-11212
A protein coated piezoelectric crystal detector
[AD-A223848] N91-11552
COBALT
Chemical identification of icosahedral structure for cobalt and nickel clusters
[DE90-017688] N91-11100
COCKPIT SIMULATORS
Flight simulator evaluation test of multi-functional display unit
[NAL-TM-596] N91-11026
COCKPITS
Aviation Safety/Automation Program Conference
[NASA-CP-3090] N91-10936
Cockpit avionics integration and automation
N91-10938
Douglas flight deck design philosophy N91-10939
Human factors of the high technology cockpit
N91-10943
Crew workload strategies in advanced cockpits
N91-10945
Assessing information transfer in full mission flight simulations N91-10946
Overview of error-tolerant cockpit research
N91-10949
A function-based approach to cockpit procedure aids
N91-10953
Terminal weather information management
N91-10960
Information management N91-10961
Voice communications in the cockpit noise environment: The role of active noise reduction N91-11140
Aircrew/cockpit compatibility: A multivariate problem seeking a multivariate solution N91-11369
Some equipment problems associated with the introduction of female aircrew into the Royal Air Force
N91-11373
Morphological and functional adaptation of personal equipment designed for female personnel N91-11374
CODING
Modeling and coding in aeronautical satellite channel
[ETN-90-97899] N91-11137
COGNITION
Graphical interfaces for cooperative planning systems
N91-10956
Determinants of dual-task interference and resource theories in cognitive psychology
[ESA-TT-1127] N91-11381
COGNITIVE PSYCHOLOGY
Determinants of dual-task interference and resource theories in cognitive psychology
[ESA-TT-1127] N91-11381
COHERENT RADIATION
Review of free electron lasers
[PB90-255480] N91-11206
Planar orotron: A tunable, grating-based free electron laser N91-11208
COLD FLOW TESTS
Design and evaluation of thrust vectored nozzles using a multicomponent thrust stand
[NASA-CR-180474] N91-11050
COLD WORKING
Analysis of deformation characteristics of a heavily deformed Cu-20 percent Nb composite
[DE90-018041] N91-11070

COLLINEARITY
Geometric correction of SPOT imagery with the use of a digital elevation model
[INPE-5014-TDL/401] N91-11423
COLLISIONAL PLASMAS
Collisional processes of interest in MFE plasma research
[DE91-000598] N91-11549
COLLISIONLESS PLASMAS
On hydrodynamics of collisionless relativistic plasma in a strong magnetic field
[DE90-513926] N91-11543
COLOR
Integration of multispectral and pancromatic channels of HRV (SPOT) sensor for obtaining color compositions with a spatial resolution of approximately 10 m
[INPE-5035-TDL/403] N91-11278
Color flux distribution in pure SU(2) Lattice Gauge Theory
[DE90-017403] N91-11574
COMBAT
Computation of sub-optimal real-time guidance laws for combat aircraft trajectories N91-10970
Problems posed by the adaptation of physiological protective equipment for female combat pilots N91-11372
COMBUSTION
Hybrid Propulsion Technology Program, phase 1. Volume 1: Executive summary
[NASA-CR-183950] N91-11054
Symbolic manipulation software and the study of differential equations
[DE90-017674] N91-11413
COMBUSTION CHAMBERS
Experimental manufacturing of data recording system for rocket combustion thermal flux distribution
[DE90-702432] N91-11051
Characterization and optimization of a pneumatic injector for a 60 bar combustion chamber
[ETN-90-97580] N91-11076
Three-dimensional computer simulation of non-reacting jet-gas flow mixing in an MHD second stage combustor
[DE90-017831] N91-11537
Effects of jet port arrangement on three-dimensional non-reacting jet-gas mixing in an MHD second stage combustor
[DE90-017858] N91-11538
COMBUSTION CHEMISTRY
Minimization and control of hazardous combustion byproducts
[PB90-259854] N91-11305
COMBUSTION CONTROL
Minimization and control of hazardous combustion byproducts
[PB90-259854] N91-11305
COMBUSTION PHYSICS
Numerical simulation of shock-induced combustion for application to the ram accelerator concept N91-10912
COMBUSTION PRODUCTS
Carbon deposition in gas turbine combustors
[PNR-90692] N91-11020
Recommended operating procedure No. 45: Analysis of nitrous oxide from combustion sources
[PB90-236502] N91-11078
Reference concepts for a space-based hydrogen-oxygen combustion, turboalternator, burst power system
[DE90-016692] N91-11155
Lifetimes and fates of toxic air contaminants in California's atmosphere
[PB90-253204] N91-11304
Minimization and control of hazardous combustion byproducts
[PB90-259854] N91-11305
Measurements of toxic exhaust emissions from gasoline-powered light-duty vehicles
[PB90-259649] N91-11306
COMBUSTION STABILITY
Theoretical and numerical aspects of wave stability in combustion models
[ECL-89-21] N91-11088
COMETARY ATMOSPHERES
A two dimensional multisonic model of plasma interaction for cometary atmosphere with solar wind
[MITT-89] N91-11621
A search for small comets in consecutive images acquired with a ground-based telescope N91-11626
COMMERCE
Combination of Hatley and Ward/Mellor methods for real time systems
[INPE-5078-TDL/412] N91-11419
COMMERCIAL AIRCRAFT
Commercial aircraft and the environment
[PNR-90687] N91-11307
COMMERCIAL ENERGY
Results from a workshop on research needs for modeling aquifer thermal energy storage systems
[DE90-018007] N91-11301
COMMUNICATION NETWORKS
Spacecraft design project: High latitude communications satellite
[NASA-CR-186689] N91-11039
COMMUNICATION SATELLITES
Spacecraft design project: High latitude communications satellite
[NASA-CR-186689] N91-11039
Modeling and coding in aeronautical satellite channel
[ETN-90-97899] N91-11137
COMPARISON
A comparison of some GMRES-like methods
[REPT-90-22] N91-11454
COMPATIBILITY
Aircrew/cockpit compatibility: A multivariate problem seeking a multivariate solution N91-11369
COMPETITION
Japanese power electronics inverter technology and its impact on the American air conditioning industry
[DE90-014843] N91-11191
COMPILERS
Research into language concepts for the mission control center
[NASA-CR-185926] N91-11392
Silicon compilation and the SYCO silicon compiler
[ETN-90-97827] N91-11404
COMPOSITE MATERIALS
Ultrasonic examination of fiber composite materials by means of virtual C-scan test and modal recognition
[MBB-Z-0299-89-PUB] N91-11066
Elastic properties of ceramic composite materials at high temperatures
[ETN-90-97897] N91-11067
Analysis of deformation characteristics of a heavily deformed Cu-20 percent Nb composite
[DE90-018041] N91-11070
Studies of molecular properties of polymeric materials
[NASA-TM-101854] N91-11118
Mechanical behavior of ceramics and composites
[DE90-017311] N91-11122
COMPOSITE PROPELLANTS
Attenuation studies of booster-rocket propellants and their simulants
[DE91-000098] N91-11131
COMPOSITE STRUCTURES
Composite slip table of dissimilar materials for damping longitudinal modes
[DE90-015128] N91-11064
Potential for advanced thermoplastic composites in space systems
[DE90-014447] N91-11069
Materials Division research and technology accomplishments for FY 89 and plans for FY 90
[NASA-TM-102649] N91-11072
A three-dimensional solid element model for finite rotation of composite shells N91-11262
COMPRESSED AIR
Technical assessment and economic study of compressed air energy storage in Japan
[DE91-701405] N91-11292
COMPRESSIBILITY EFFECTS
A model for the sound generation due to compressible vortex-body interaction
[MPIS-MITT-96] N91-11491
COMPRESSIBLE FLOW
Analysis and control of supersonic vortex breakdown flows
[NASA-CR-186897] N91-10903
Numerical calculations for flows past an unconventional airfoil N91-10916
The calculation of unsteady compressible flow about oscillating airfoil profiles using the Euler upwind method N91-10923
Heat pipe vapor dynamics N91-11179
Instabilities of two-dimensional inviscid compressible vortices N91-11181
COMPRESSION LOADS
Buckling and vibrations of plates subjected to concentrated forces N91-11255
COMPRESSOR BLADES
Automated design of controlled diffusion blades N91-10883
COMPUTATION
Aircraft trajectories: Computation, prediction, control, volume 1. Part 1: Fundamentals. Part 2: Flight in critical atmospheric conditions. Part 3: Impact of new on-board technologies on aircraft operation
[AGARD-AG-301-VOL-1-PT-1-3] N91-10967
Computation of sub-optimal real-time guidance laws for combat aircraft trajectories N91-10970
High-performance equation solvers and their impact on finite element analysis
[NASA-TM-102735] N91-11252
Research into language concepts for the mission control center
[NASA-CR-185926] N91-11392
A new lower bound for the de Bruijn-Newman constant
[CWI-NM-R8920] N91-11447
COMPUTATIONAL CHEMISTRY
Computational Fluid Dynamics Program at NASA Ames Research Center N91-10840
COMPUTATIONAL FLUID DYNAMICS
NASA Computational Fluid Dynamics Conference. Volume 1: Sessions 1-6
[NASA-CP-10038-VOL-1] N91-10839
Computational Fluid Dynamics Program at NASA Ames Research Center N91-10840
Computational fluid dynamics research and applications at NASA Langley Research Center N91-10841
Computational fluid dynamics at the Lewis Research Center: An overview N91-10842
Marshall Space Flight Center CFD overview N91-10843
Johnson Space Center CFD overview N91-10844
NASA's CFD Validation Program N91-10845
Computations of three-dimensional steady and unsteady viscous incompressible flows N91-10852
SAGE: A 2-D self-adaptive grid evolution code and its application in computational fluid dynamics N91-10853
CFD for applications to aircraft aeroelasticity N91-10855
Grid generation and inviscid flow computation about aircraft geometries N91-10857
A zonal Navier-Stokes methodology for flow simulation about a complete aircraft N91-10858
Numerical simulation of F-18 fuselage forebody flows at high angles of attack N91-10859
Navier-Stokes solutions about the F/A-18 forebody-LEX configuration N91-10860
Navier-Stokes solutions for flows related to store separation N91-10861
TranAir: Recent advances and applications N91-10862
Numerical simulation of rotorcraft N91-10863
Three-dimensional viscous drag prediction for rotor blades N91-10865
Progress toward the development of an airfoil icing analysis capability N91-10866
The breakup of trailing-line vortices N91-10867
NASA Computational Fluid Dynamics Conference. Volume 2: Sessions 7-12
[NASA-CP-10038-VOL-2] N91-10868
Modeling of high speed chemically reacting flow-fields N91-10870
Three-dimensional calculation of supersonic reacting flows using an LU scheme N91-10871
Progress in computing nozzle/plume flow fields N91-10872
Application of CFD codes for the simulation of scramjet combustor flowfields N91-10873
Hypersonic CFD applications at NASA Langley using CFL3D and CFL3DE N91-10874
Numerical aerodynamic simulation of the space shuttle ascent environment N91-10875
Computational fluid dynamics analysis of space shuttle main propulsion feed line 17-inch disconnect valves N91-10876
Conjugate (solid/fluid) computational fluid dynamics analysis of the space shuttle solid rocket motor nozzle/case and case field joints N91-10879
Simulation of turbomachinery flows N91-10880
Prediction of turbine rotor-stator interaction using Navier-Stokes methods N91-10881
Turbine stage aerodynamics and heat transfer prediction N91-10882
Numerical analysis of flow through oscillating cascade sections N91-10884
CFD analysis for high speed inlets N91-10888
The use of a Navier-Stokes code in the wing design process N91-10889
An embedded grid formulation applied to delta wings N91-10891
Computational fluid dynamics on a massively parallel computer N91-10896
Conical Euler simulation and active suppression of delta wing rocking motion
[NASA-TM-102683] N91-10904
Nonoverlapping composite meshes for multi-element air-foils N91-10908
Implicit flux-split Euler schemes for unsteady aerodynamic analysis involving unstructured dynamic meshes
[NASA-TM-102732] N91-10918

The calculation of unsteady compressible flow about oscillating airfoil profiles using the Euler upwind method N91-10921
A numerical study of the effects of wind tunnel wall proximity on an airfoil model [NASA-CR-187322] N91-10934
Aerodynamic design optimization using computational fluid dynamics N91-11013
Grid generation and flow computation about a Martian entry vehicle [NASA-CR-187032] N91-11042
Solutions of thin-layer Navier-Stokes equations for missile configurations N91-11173
Application of computational fluid dynamics to three-dimensional bodies in hypersonic flow N91-11174
Accuracy, convergence and stability of finite element algorithms for incompressible fluid flow N91-11184
Navier-Stokes analysis of transonic cascade flow [NASA-TM-103624] N91-11192
Performance of a parallel code for the Euler equations on hypercube computers [NASA-TM-102260] N91-11384

COMPUTATIONAL GEOMETRY
Expected complexity of the 3-dimensional voronoi diagram [PB90-221862] N91-11435
Expected linear 3-dimensional Voronoi diagram algorithm [PB90-227984] N91-11436

COMPUTATIONAL GRIDS
NASA Computational Fluid Dynamics Conference. Volume 1: Sessions 1-6 [NASA-CP-10038-VOL-1] N91-10839
Computational fluid dynamics research and applications at NASA Langley Research Center N91-10841
SAGE: A 2-D self-adaptive grid evolution code and its application in computational fluid dynamics N91-10853
Application of unstructured grid methods to steady and unsteady aerodynamic problems N91-10856
Grid generation and inviscid flow computation about aircraft geometries N91-10857
Numerical simulation of F-18 fuselage forebody flows at high angles of attack N91-10859
Navier-Stokes solutions about the F/A-18 forebody-LEX configuration N91-10860
Navier-Stokes solutions for flows related to store separation N91-10861
TranAir: Recent advances and applications N91-10862
Numerical simulation of rotorcraft N91-10863
Calculation of the rotor induced download on airfoils N91-10864
Analysis of the SSME HPOTP bearing inlet cavity N91-10877
Prediction of turbine rotor-stator interaction using Navier-Stokes methods N91-10881
Simulation of powered-lift flows N91-10886
An embedded grid formulation applied to delta wings N91-10891
Unstructured mesh solution of the Euler and Navier-Stokes equations N91-10892
Three dimensional unstructured grids for the solution of the Euler equations N91-10893
Implicit flux-split Euler schemes for unsteady aerodynamic analysis involving unstructured dynamic meshes [NASA-TM-102732] N91-10918
Grid generation and flow computation about a Martian entry vehicle [NASA-CR-187032] N91-11042
Development of a time-dependent incompressible Navier-Stokes solver based on a fractional-step method [NASA-CR-187254] N91-11165
Navier-Stokes analysis of transonic cascade flow [NASA-TM-103624] N91-11192
Performance of finite dynamic elements for composite materials in plane stress N91-11260
An adaptive finite element technique using element equilibrium and paving [DE90-015829] N91-11410
Expected complexity of the 3-dimensional voronoi diagram [PB90-221862] N91-11435
Expected linear 3-dimensional Voronoi diagram algorithm [PB90-227984] N91-11436
Solution of the two-dimensional Euler equations by a finite volume discretization on unstructured triangular meshes [ESA-TT-1135] N91-11473

COMPUTER AIDED DESIGN
Archimedes: A system that plans and executes mechanical assemblies [DE91-000036] N91-11231
Computer-Aided Structural Engineering (CASE) project: Investigation and design of U-frame structures using program CUFRBC. Volume C: User's guide for channels [AD-A224388] N91-11395
IGES efficiency evaluation [DE90-015192] N91-11409
CAD tools for detector design [DE90-017337] N91-11412
The role of process modelling in manufacture and design [PNR-90702] N91-11416
A design method of divertor in tokamak reactors [NIFS-36] N91-11532

COMPUTER AIDED MANUFACTURING
Geometric method and synthesis af assembly strategies in robotic systems [LAAS-90041] N91-11215
Archimedes: A system that plans and executes mechanical assemblies [DE91-000036] N91-11231
The role of process modelling in manufacture and design [PNR-90702] N91-11416

COMPUTER AIDED TOMOGRAPHY
Multiple-energy techniques in industrial computerized tomography [DE90-017518] N91-11081

COMPUTER GRAPHICS
Computational fluid dynamics analysis of space shuttle main propulsion feed line 17-inch disconnect valves N91-10876
Visualization of fluid dynamics at NASA Ames N91-10895
Graphical interfaces for cooperative planning systems N91-10956
The high-resolution graphic display: A possible man/machine interface for a computer assisted ATC management system N91-10989
Intelligent Data Reduction (IDARE) [NASA-CR-186322] N91-11393
IGES efficiency evaluation [DE90-015192] N91-11409
Two and three dimensional magnetotelluric inversion [DE90-016187] N91-11411

COMPUTER NETWORKS
The application of trajectory prediction algorithms for planning purposes in the Netherlands ATC-system N91-10986
OSI in the NASA science internet: An analysis [NASA-CR-177561] N91-11425
Parallelized reliability estimation of reconfigurable computer networks [NASA-CR-182101] N91-11430
Touchstone project: Milestone event Q4 [AD-A224034] N91-11480
Touchstone project Mach port: Milestone event Q4 [AD-A224057] N91-11481
Touchstone project DELTA numeric node: Milestone event Q4 [AD-A224060] N91-11482

COMPUTER PROGRAMMING
Proceedings of the First NASA Ada Users' Symposium [NASA-TM-102941] N91-11389
Minimizing maximum earliness and maximum lateness on a single machine [CWI-BS-R9001] N91-11398
Performance analysis of transaction driven computer systems via queueing analysis of polling models [CWI-BS-R8931] N91-11426

COMPUTER PROGRAMS
Recent advances in Runge-Kutta schemes for solving 3-D Navier-Stokes equations N91-10851
Computations of three-dimensional steady and unsteady viscous incompressible flows N91-10852
TranAir: Recent advances and applications N91-10862
Progress toward the development of an airfoil icing analysis capability N91-10866
Modeling of high speed chemically reacting flow-fields N91-10870
Application of CFD codes for the simulation of scramjet combustor flowfields N91-10873
Hypersonic CFD applications at NASA Langley using CFL3D and CFL3DE N91-10874
Computational fluid dynamics analysis of space shuttle main propulsion feed line 17-inch disconnect valves N91-10876
Analysis of three-dimensional viscous flow in a supersonic throughflow fan N91-10885
The use of a Navier-Stokes code in the wing design process N91-10889
An embedded grid formulation applied to delta wings N91-10891
Three dimensional unstructured grids for the solution of the Euler equations N91-10893
Visualization of fluid dynamics at NASA Ames N91-10895
Computational fluid dynamics on a massively parallel computer N91-10896
Aerodynamic stability and heating analyses for the aeroassist flight experiment vehicle N91-10899
Prediction of effects of wing contour modifications on low-speed maximum lift and transonic performance for the EA-6B aircraft [NASA-TP-3046] N91-10902
Numerical calculations for flows past an unconventional airfoil N91-10916
A stochastic analysis of state transitions in an air space management system N91-10980
Test cases for computation of internal flows in aero engine components [AGARD-AR-275] N91-11022
Aperture diffraction in Rayleigh zone: Calculation of the field in the quiet zone of compact ranges [CNES-CT/DRT/TIT/AN-88/234] N91-11136
Magnetohydrodynamic modification of the TEACH-T code and the prediction of the maximum azimuthal velocity in a conducting fluid [DE90-017510] N91-11187
Gulf of Maine sea surface topography from GEOSAT altimetry N91-11271
Evaluating the environmental impacts of the energy system: The ENPEP (Energy and Power Evaluation Program) approach [DE90-017862] N91-11309
Notes on the NOARL nowcast for the 1989 to 1990 El Nino forced by FNOC winds [AD-A223520] N91-11347
Fundamental concepts for utilization of the FPS-5410 array processor [INPE-5091-RPE/624] N91-11388
Ada and software management in NASA: Symposium/forum [NASA-TM-103297] N91-11390
On three dimensional object recognition and pose-determination: An abstraction based approach [NASA-CR-186894] N91-11396
Surrogate oracles, generalized dependency and simpler models [NASA-CR-187360] N91-11407
Symbolic manipulation software and the study of differential equations [DE90-017674] N91-11413
Software quality assurance handbook [DE91-000060] N91-11420
Random number stride in Monte Carlo calculations [DE90-012000] N91-11465
Computer and engineering calculations of Brazilian Tokamak-2 [DE90-628758] N91-11524
M51: The Whirlpool Galaxy, analysis and simulation N91-11631

COMPUTER SYSTEMS DESIGN
The MS-DOS device handler interface [AD-A223856] N91-11385
The MS-DOS device services interface [AD-A223902] N91-11386
The MS-DOS routing and configuration program design [AD-A223858] N91-11394
Touchstone project: Milestone event Q4 [AD-A224034] N91-11480

COMPUTER SYSTEMS PERFORMANCE
High-performance equation solvers and their impact on finite element analysis [NASA-TM-102735] N91-11252
The MS-DOS device handler interface [AD-A223856] N91-11385
The MS-DOS device services interface [AD-A223902] N91-11386
The MS-DOS routing and configuration program design [AD-A223858] N91-11394
Performance analysis of transaction driven computer systems via queueing analysis of polling models [CWI-BS-R8931] N91-11426
Parallelized reliability estimation of reconfigurable computer networks [NASA-CR-182101] N91-11430
Touchstone project: Milestone event Q4 [AD-A224034] N91-11480
Touchstone project DELTA numeric node: Milestone event Q4 [AD-A224060] N91-11482

COMPUTER SYSTEMS PROGRAMS
Simulation of automated approach procedures considering dynamic flight operations N91-11008
Experiences in the use of ABAQUS for creep analysis [PNR-90705] N91-11266

DUWECS reference guide V1.0: Delft University wind energy converter simulation program
[MEMT-5] N91-11294
Performance analysis of transaction driven computer systems via queueing analysis of polling models
[CWI-BS-R8931] N91-11426

COMPUTER TECHNIQUES
Forest classification with high resolution satellite images. Research into the use of spatial information to improve the multi-spectral classification with SPOT images
[BCRS-89-32] N91-11269

COMPUTERIZED SIMULATION
Computational Fluid Dynamics Program at NASA Ames Research Center N91-10840
A zonal Navier-Stokes methodology for flow simulation about a complete aircraft N91-10858
Numerical simulation of F-18 fuselage forebody flows at high angles of attack N91-10859
Numerical simulation of rotorcraft N91-10863
The breakup of trailing-line vortices N91-10867
Modeling of high speed chemically reacting flow-fields N91-10870
Application of CFD codes for the simulation of scramjet combustor flowfields N91-10873
Numerical aerodynamic simulation of the space shuttle ascent environment N91-10875
Simulation of turbomachinery flows N91-10880
Aeroassist flight experiment aerodynamics and aerothermodynamics N91-10900
Direct simulation of rarefied hypersonic flows N91-10901
Guidance concepts for time-based flight operations N91-10993
Integration of aircraft capability in air traffic handling simulations N91-11007
Simulation of automated approach procedures considering dynamic flight operations N91-11008
Aerodynamic design optimization using computational fluid dynamics N91-11013
Marginal aircraft release disturbance on advanced missiles
[MBB/FE121/S/PUB/329] N91-11016
Computer modeling of 12-inch actuator shock test performance
[DE90-017038] N91-11033
Flight simulation programs for space plane
[NAL-TM-594] N91-11035
Weight evaluation and sensitivity analysis for space plane: SSTO
[NAL-TM-598-1] N91-11036
Molecular-dynamics study of grain-boundary migration in metals
[DE90-017856] N91-11104
Analysis and prediction of thermal properties of mesophases and crystals by calorimetry and supercomputers
[DE90-015538] N91-11123
Compact representation of radiation patterns using spherical mode expansions
[DE91-000019] N91-11141
Application of computational fluid dynamics to three-dimensional bodies in hypersonic flow N91-11174
A molecular dynamics model of the orthogonal cutting process
[DE90-015911] N91-11230
Estimation of seasonal and annual acidic deposition through aggregation of three-day episodic periods
[PB90-252628] N91-11303
A simulation study of magnetic reconnection processes at the dayside magnetopause N91-11320
Numerical models of 2-D and 3-D geophysical convection
[DE90-014979] N91-11330
CAD tools for detector design
[DE90-017337] N91-11412
The role of process modelling in manufacture and design
[PNR-90702] N91-11416
Accurate representations of general textures by a set of weighted grains
[DE90-016487] N91-11485
MONT3E: A Monte Carlo electron heat transfer code
[DE90-012091] N91-11514
A design method of divertor in tokamak reactors
[NIFS-36] N91-11532
Three-dimensional computer simulation of non-reacting jet-gas flow mixing in an MHD second stage combustor
[DE90-017831] N91-11537
Structure of amorphous-silicon and germanium alloy films
[DE90-000355] N91-11557
Image reconstruction of IRAS survey scans
[NASA-CR-187328] N91-11606
Speckle imaging of complicated objects N91-11617
Application of the Ewald method to cosmological N-body simulations
[DE90-513789] N91-11637
Cosmological N-body simulations with a treecode
[DE90-513790] N91-11638
Status reports of supercomputing astrophysics in Japan
[DE90-513793] N91-11640
Numerical study of compressible magnetoconvection with an open transitional boundary
[DE91-000148] N91-11651
Numerical simulations of suspersonic extragalactic radio jets N91-11660

COMPUTERS
Fundamental concepts for utilization of the FPS-5410 array processor
[INPE-5091-RPE/624] N91-11388

CONCENTRATORS
Generic quality assurance/quality control guide for photovoltaic concentrator design, development and system installation
[DE90-017040] N91-11290

CONDENSERS (LIQUEFIERS)
Conceptual design of an Open-Cycle Ocean Thermal Energy Conversion Net Power-Producing Experiment (OC-OTEC NPPE)
[DE90-000304] N91-11282

CONDUCTING FLUIDS
Magnetohydrodynamic modification of the TEACH-T code and the prediction of the maximum azimuthal velocity in a conducting fluid
[DE90-017510] N91-11187

CONDUCTION BANDS
Nonparabolic conduction bands and masses in strained-single-quantum wells
[DE90-017028] N91-11560

CONES
Cones of matrices and setfunctions, and 0-1 optimization
[CWI-BS-R8925] N91-11444

CONFERENCES
NASA Computational Fluid Dynamics Conference. Volume 1: Sessions 1-6
[NASA-CP-10038-VOL-1] N91-10839
NASA Computational Fluid Dynamics Conference. Volume 2: Sessions 7-12
[NASA-CP-10038-VOL-2] N91-10868
Aviation Safety/Automation Program Conference
[NASA-CP-3090] N91-10936
Mobile robots and intelligent motion control
[DE90-017312] N91-11226
Proceedings of the Second Annual Fuel Cells Contractors Review Meeting
[DE90-000490] N91-11288
Advantages of the Community Climate Model (CCM) concept
[PB90-256348] N91-11314
Proceedings of the First NASA Ada Users' Symposium
[NASA-TM-102941] N91-11389
Twenty-Second Annual NASA Supply and Equipment Management Conference
[NASA-CP-10042] N91-11591

CONFINEMENT
Fine scale velocity measurements in a turbulent jet in a confined crossflow N91-10909

CONGRUENCES
On induced congruences
[CS-9001] N91-11460

CONICAL FLOW
Conical Euler simulation and active suppression of delta wing rocking motion
[NASA-TM-102683] N91-10904

CONJUGATES
Conjugate (solid/fluid) computational fluid dynamics analysis of the space shuttle solid rocket motor nozzle/case and case field joints N91-10879

CONNECTORS
Optical far-field measurements of extremely high dynamic to investigate the roughness of front faces of single-mode fiber connectors
[FI-452-TB-67] N91-11517

CONSERVATION
Utility of remotely sensed data for identification of soil conservation practices
[NASA-CR-176874] N91-11276

CONSERVATION EQUATIONS
Conservation equations and physical models for hypersonic air flows over the aeroassist flight experiment vehicle N91-10897

CONSERVATION LAWS
An investigation of the Newman-Penrose constants for massless free fields of arbitrary spin N91-11630

CONSTANTS
A new lower bound for the de Bruijn-Newman constant
[CWI-NM-R8920] N91-11447

CONSTRUCTION
Methods for the construction of constant curve free form surfaces
[ETN-90-97861] N91-11463

CONTACTORS
Gas-liquid contacting at elevated pressures
[ETN-90-97773] N91-11196

CONTAMINANTS
Measurements of toxic exhaust emissions from gasoline-powered light-duty vehicles
[PB90-259649] N91-11306

CONTINENTAL SHELVES
Surface and bottom temperature distribution for the Northeast continental shelf
[PB90-252172] N91-11349
Outer continental shelf environmental assessment program: Comprehensive bibliography, June 1990
[PB90-258609] N91-11350

CONTINUOUS SPECTRA
Astronomical applications of survival analysis N91-11615

CONTINUUM MODELING
A continuum tensile failure model with friction
[DE90-018006] N91-11265

CONTOURS
Prediction of effects of wing contour modifications on low-speed maximum lift and transonic performance for the EA-6B aircraft
[NASA-TP-3046] N91-10902
Examination of numerical formulations to describe complex geometry turbulent elliptical flows, using contour matched coordinates
[ETN-90-97864] N91-11169

CONTRAROTATING PROPELLERS
Aerodynamic interaction of counter rotating propellers N91-10910

CONTROL
Problems of static divergence concerning the rpm regulation of wind turbines using centrifugal force controlling means and rotating slat
[ETN-90-97858] N91-11261

CONTROL SIMULATION
A new approach to the flight control system reconfiguration following a battle damage and/or generic failure on a control surface N91-11023

CONTROL STABILITY
H infinity-design and the improvement of helicopter handling qualities N91-11024

CONTROL SURFACES
Application of dynamical systems theory to nonlinear aircraft dynamics N91-11014

CONTROL SYSTEMS DESIGN
Contributions to the improvement of flight safety in wind shear
[ESA-TT-1141] N91-10965
A description and evaluation of TIMER: A time-based terminal flow-control concept N91-10996
H infinity-design and the improvement of helicopter handling qualities N91-11024
Controller methodologies for integrated control/structure design optimization of large flexible structures N91-11043
Real-time failure control (SAFD)
[NASA-CR-184025] N91-11233
Operator function modeling: Cognitive task analysis, modeling and intelligent aiding in supervisory control systems
[NASA-CR-187331] N91-11380
Distributed digital signal processors for multi-body structures
[NASA-CR-187375] N91-11387

CONTROL THEORY
Computation of sub-optimal real-time guidance laws for combat aircraft trajectories N91-10970
Mobile robots and intelligent motion control
[DE90-017312] N91-11226
Constrained optimization approach to feedback control of state-augmented systems N91-11433

CONTROLLABILITY
Integration of aircraft capability in air traffic handling simulations N91-11007
H infinity-design and the improvement of helicopter handling qualities N91-11024

CONTROLLERS
Douglas flight deck design philosophy N91-10939
Fault monitoring N91-10950
Controller methodologies for integrated control/structure design optimization of large flexible structures N91-11043
A microprocessor based charge control system for the simultaneous charging of several batteries with one charge controller
[DE90-017069] N91-11157
An automated linearity test for direct voltage calibrators
[DE90-016927] N91-11204

Research into language concepts for the mission control center
[NASA-CR-185928] N91-11392
Intelligent Robotic Systems Study (IRSS), phase 2
[NASA-CR-183963] N91-11432

CONVECTION
Numerical models of 2-D and 3-D geophysical convection
[DE90-014979] N91-11330
Numerical study of compressible magnetoconvection with an open transitional boundary
[DE91-000148] N91-11651

CONVECTION CURRENTS
The evolution of vortical patterns and vortices in mesoscale convective complexes N91-11319
Tropical cyclone simulations with the Betts convective adjustment scheme N91-11338
Generalized dynamic normal mode initialization N91-11341

CONVECTIVE FLOW
Ion dynamics in the plasma mantle
[IFSI-89-20] N91-11550

CONVECTIVE HEAT TRANSFER
A simulation of the flow near a burning propellant in a solid propellant rocket motor N91-11056
Enhancement of forced convection heat transfer in tubes using staged tangential flow injection
[PB90-247594] N91-11170
An experimental study of natural convection heat transfer from a horizontal cylinder array vertically aligned to and confined by a single wall and two walls N91-11178
Heat transfer and flow studies in an abrupt expansion pipe with non-Newtonian fluids N91-11180
Penetration in GTA welding
[DE90-008971] N91-11213
Generalized dynamic normal mode initialization N91-11341

CONVERGENCE
Accuracy, convergence and stability of finite element algorithms for incompressible fluid flow N91-11184
A static-regridding method for two-dimensional parabolic partial differential equations
[CWI-NM-R8923] N91-11449
Convergence of linear multistep and one-leg methods for stiff nonlinear initial value problems
[CWI-NM-R8924] N91-11450

CONVEXITY
A polynomial method of weighted centers for convex quadratic programming
[REPT-90-17] N91-11453
Interpolation of scattered data by a bivariate convex function. Part 1: Piecewise linear C sup 0-interpolation
[MEMO-858-PT-1] N91-11469

COOLING
A life comparison of tube and channel cooling passages for thrust chambers
[NASA-TM-103613] N91-11059

COOLING SYSTEMS
Reference concepts for a space-based hydrogen-oxygen combustion, turboalternator, burst power system
[DE90-016692] N91-11155
Colorado State University program for developing, testing, evaluating and optimizing solar heating and cooling systems
[DE90-017273] N91-11291

COORDINATES
Development of a time-dependent incompressible Navier-Stokes solver based on a fractional-step method
[NASA-CR-187254] N91-11165
Examination of numerical formulations to describe complex geometry turbulent elliptical flows, using contour matched coordinates
[ETN-90-97864] N91-11169
Evaluation process for the examination of curved surface workpieces using coordinate measuring instruments
[ETN-90-97901] N91-11203

COPPER
Analysis of deformation characteristics of a heavily deformed Cu-20 percent Nb composite
[DE90-018041] N91-11070
Design and testing of a high temperature superconducting current lead
[DE90-017812] N91-11579

COPPER ALLOYS
Long period superstructures in Pt3V and Cu3Pd: Towards a quantitative description
[ONERA-NT-1990-2] N91-11587

COPPER OXIDES
The reaction of vapor-deposited Al with Cu oxides
[DE91-000367] N91-11114
Muon SR studies on Sr2CuO2Cl2, La2CuO4, and Nd2CuO4: 2-D magnetism, local fields and muon sites
[DE90-018014] N91-11506
Processing of YBA2Cu3O7 tapes from a molten salt precursor
[DE90-017656] N91-11564
Excess oxygen defects in layered cuprates
[DE90-017669] N91-11565

COPPER SELENIDES
High efficiency CuInSe2 and CuInGaSe2 cells and materials research
[DE90-000362] N91-11280

CORNERS
High-order implicit blending surfaces of low degree
[CS-9005] N91-11461

CORONAGRAPHS
Whie light solar corona: An atlas of 1988 K-coronameter synoptic charts, December 1987 to January 1989
[NASA-CR-184955] N91-11649

CORONAS
Tectonics of one-plate planets N91-11647
Exploration of decreased solar activity state (small intensity activity) in the corona and chromosphere
[INPE-5059-TDL/405] N91-11652

CORROSION
Laser Raman spectroscopy for in-situ analysis of corrosion films on metals
[DE90-017822] N91-11109
Evaluation of a high-temperature burner-duct-recuperator system
[DE90-000366] N91-11284
Corrosion and arc erosion in MHD channels
[DE90-017889] N91-11539

CORROSION PREVENTION
Surface phases and their influence on metal-oxide interfaces
[DE90-017608] N91-11099
Laser Raman spectroscopy for in-situ analysis of corrosion films on metals
[DE90-017822] N91-11109

COSMIC PLASMA
The SIM.PL.EX. plasma chamber (Simulatori di Plasma Extraterrestre)
[IFSI-90-8] N91-11551

COSMOLOGY
The role of shear in the cosmological distance
[DE90-513788] N91-11636
Application of the Ewald method to cosmological N-body simulations
[DE90-513789] N91-11637
Cosmological N-body simulations with a treecode
[DE90-513790] N91-11638
Microwave background anisotropies and the primordial spectrum of cosmological density fluctuations
[DE90-513791] N91-11639

COST ANALYSIS
Remote sensing for marine activities
[BCRS-89-41] N91-11273

COST EFFECTIVENESS
Molten carbonate fuel cell power plant systems studies
[DE90-009697] N91-11298

COST ESTIMATES
Report of the Department of Energy (DOE) Office of Energy research review committee on the site-specific conceptual design of the superconducting super collider
[DE90-018021] N91-11513

COST REDUCTION
Advanced secondary batteries: Their applications, technological status, market and opportunity
[DE90-796146] N91-11146
Terrestrial nickel/hydrogen battery evaluation
[DE90-014863] N91-11151

COSTS
Assessment of costs and benefits of flexible and alternative fuel use in the US transportation sector: Vehicle and fuel distribution requirements
[DE90-014847] N91-11127
Remote sensing for marine activities: Appendices
[BCRS-89-41-APP] N91-11274
Performance and cost projections for advanced wind turbines
[DE90-000370] N91-11286

CRACK CLOSURE
Crack behaviour of 2024-T3, 2090-T8E41 and 7075-T6 under constant amplitude and different types of variable amplitude loading, especially Gaussian loading N91-11244

CRACK GEOMETRY
Alternating method applied to 3-D part-through crack problems, with application to the weight function method N91-11238

CRACK OPENING DISPLACEMENT
Micromechanics of semi-brittle ceramics N91-11119
Alternating method applied to 3-D part-through crack problems, with application to the weight function method N91-11238
Boundary integral equations for dynamic fracture problems N91-11259

CRACK PROPAGATION
Characterization of short fatigue cracks at notches in SiC particulate aluminum composite
[DE90-018043] N91-11071
Deducing mechanical properties due to interfaces from their acoustical response
[DE90-016704] N91-11234
Classification of acoustic emission waveforms for nondestructive evaluation using neural networks
[DE90-017239] N91-11236
Short-crack growth behaviour in various aircraft materials
[AGARD-R-767] N91-11240
An AGARD supplemental test programme on the behaviour of short cracks under constant amplitude and aircraft spectrum loading N91-11241
Determination of the short crack effect in 2090-T8E41 aluminum lithium N91-11242
Short crack behaviour in Al-Li alloy 2090 N91-11243
Crack behaviour of 2024-T3, 2090-T8E41 and 7075-T6 under constant amplitude and different types of variable amplitude loading, especially Gaussian loading N91-11244
The growth of short fatigue cracks in 2024 and 2090 aluminium alloys under variable amplitude loading N91-11245
Short crack growth under realistic flight loading: Model predictions and experimental results for Al 2024 and Al-Li 2090 N91-11246
The growth of short cracks in 4340 steel and aluminum-lithium 2090 N91-11247
Short and long fatigue crack growth in 2024-T3 under Fokker 100 spectrum loading N91-11248
Growth of short fatigue cracks in 7075-T6 aluminum alloy N91-11249
Short crack observations in Ti-6Al-4V under constant amplitude loading N91-11250
Analysis of ductile crack extension in plastic fracture N91-11257
Crack-growth resistance in reinforced ceramic composites N91-11261
Fatigue crack characterization by ultrasonic inspection
[DE90-017252] N91-11264

CRACKING (FRACTURING)
Elastic/plastic analyses of advanced composites investigating the use of the compliant layer concept in reducing residual stresses resulting from processing
[NASA-TM-103204] N91-11074

CRACKS
Relations between microstructure and mechanical behaviour of SiC/SiC composites: Interface effects on multiple cracking in multifilament materials
[ISAL-89-0098] N91-11065
Micromechanics of semi-brittle ceramics N91-11119
Alternating method applied to 3-D part-through crack problems, with application to the weight function method N91-11238

CREEP PROPERTIES
Deformation mechanisms in rapidly solidified aluminum alloys N91-11096
Effects of environment and aging on creep properties of Alloy 800H
[DE90-520207] N91-11106
Mechanical behavior of ceramics and composites
[DE90-017311] N91-11122

CREEP RUPTURE STRENGTH
Experiences in the use of ABAQUS for creep analysis
[PNR-90705] N91-11266

CREEP STRENGTH
Influence of heat treatment on microstructure and properties of an advanced high temperature titanium alloy
[PNR-90689] N91-11107
Experiences in the use of ABAQUS for creep analysis
[PNR-90705] N91-11266

CREEP TESTS
Effects of environment and aging on creep properties of Alloy 800H
[DE90-520207] N91-11106

CREWS
Crew workload strategies in advanced cockpits N91-10945

CRITERIA
Evaluation of female and male aircrew applicants using a cognitive and psychomotor test N91-11366

CRITICAL VELOCITY
The plasma universe
[TRITA-EPP-89-08] N91-11529
Laboratory experiments on the magnetic field and neutral density limits on CIV interaction
[TRITA-EPP-90-01] N91-11530

CROSS FLOW
Fine scale velocity measurements in a turbulent jet in a confined crossflow N91-10909

CRUDE OIL
Co-researches with researchers of alternative energy of petroleum in EC countries
[DE91-701466] N91-11129
Interchange of researchers on alternative energy of petroleum in EC countries
[DE91-701468] N91-11130
CRYOGENIC EQUIPMENT
Instrumenting a room temperature gravitational radiation antenna for sub-Kelvin temperatures
[IFSI-90-20] N91-11143
CRYOGENIC FLUIDS
Johnson Space Center CFD overview N91-10844
CRYOGENICS
Performances of four magnetic heat-pump cycles
[DE90-015606] N91-11185
Design and testing of a high temperature superconducting current lead
[DE90-017812] N91-11579
CRYSTAL DEFECTS
Defects in close-packed metals and alloys
[DE90-017502] N91-11097
Excess oxygen defects in layered cuprates
[DE90-017669] N91-11565
CRYSTAL DISLOCATIONS
The stability of irradiation-induced defects in NiAl
[DE90-017744] N91-11103
CRYSTAL GROWTH
Chemically vapor deposited diamond films
[DE91-000384] N91-11125
Microfilamentary Bi2Sr2Ca1Cu2O8 fibers
[DE90-018013] N91-11571
SERI Workshop on the Role of Point Defects/Defect Complexes in Silicon Device Fabrication
[DE90-000377] N91-11572
CRYSTAL LATTICES
Stress accommodation in large-mismatch systems
[DE90-017032] N91-11562
CRYSTAL STRUCTURE
Defects in close-packed metals and alloys
[DE90-017502] N91-11097
Microstructures of cubic Al2O3 precipitates in oxygen-implanted aluminum
[DE91-000038] N91-11111
A theoretical investigation on structural, vibrational, and electronic properties of amorphous silicon
[DE90-018040] N91-11267
Accurate representations of general textures by a set of weighted grains
[DE90-016487] N91-11485
Muon SR studies on Sr2CuO2Cl2, La2CuO4, and Nd2CuO4: 2-D magnetism, local fields and muon sites
[DE90-018014] N91-11506
Stress accommodation in large-mismatch systems
[DE90-017032] N91-11562
Excess oxygen defects in layered cuprates
[DE90-017669] N91-11565
Structure of molten salts
[DE90-017704] N91-11566
Compositional imaging of semiconductor interfaces by Z-contrast Scanning Transmission Electron Microscope (STEM)
[DE90-017763] N91-11576
Superconducting and structural properties of the (Ba(0.6)K(0.4)) (Bi(1-y)Sb(y))O3 system
[DE90-017836] N91-11580
Long period superstructures in Pt3V and Cu3Pd: Towards a quantitative description
[ONERA-NT-1990-2] N91-11587
CRYSTAL SURFACES
Surface anharmonicity: Temperature dependence of phonon energies on Cu(110)
[DE90-017735] N91-11567
CRYSTALLINITY
Ion dynamics in semiconductors with self-consistent electronic densities N91-11556
CRYSTALLIZATION
Microfilamentary Bi2Sr2Ca1Cu2O8 fibers
[DE90-018013] N91-11571
CRYSTALLOGRAPHY
Long period superstructures in Pt3V and Cu3Pd: Towards a quantitative description
[ONERA-NT-1990-2] N91-11587
CRYSTALS
Analysis and prediction of thermal properties of mesophases and crystals by calorimetry and supercomputers
[DE90-015538] N91-11123
A protein coated piezoelectric crystal detector
[AD-A223848] N91-11552
CUBES (MATHEMATICS)
Decomposition of the n-cube into paths
[MEMO-855] N91-11468
CUBIC LATTICES
Superconducting and structural properties of the (Ba(0.6)K(0.4)) (Bi(1-y)Sb(y))O3 system
[DE90-017836] N91-11580
CURRENT DENSITY
Natural current profiles in a tokamak
[DE91-000128] N91-11540
CURRENT DISTRIBUTION
Current and potential distributions on a cylinder electrode
[DE91-000170] N91-11161
CURVES (GEOMETRY)
On the uniqueness of kernels
[CWI-BS-R8924] N91-11443
Methods for the construction of constant curve free form surfaces
[ETN-90-97861] N91-11463
CUTTING
A molecular dynamics model of the orthogonal cutting process
[DE90-015911] N91-11230
CYANIDES
Structure-property relationships for (beta)- and (kappa)-phase BEDT-TTF salts and their use in the synthesis of (kappa)-(BEDT-TTF)2Cu(N(CN)2)Br. A salt having the highest T(sub c) (inductive onset = 11.6 K, resistive, onset = 12.5 K) yet observed in an organic superconductor
[DE90-017804] N91-11582
CYCLES
Quadratic systems equivalent to class 3 sub A not equal to 0
[REPT-90-38] N91-11455
CYCLOGENESIS
Northwest African depressions and their relationship to jet streams N91-11318
Tropical cyclone simulations with the Betts convective adjustment scheme N91-11336
CYCLONES
The evolution of vortical patterns and vortices in mesoscale convective complexes N91-11319
Tropical cyclone simulations with the Betts convective adjustment scheme N91-11338
CYCLOTRON RADIATION
Polarized radiation from inhomogeneous shocks N91-11662
CYCLOTRON RESONANCE
High-power microwave transmission systems for electron cyclotron resonance plasma heating, volume 5
[DE90-017600] N91-11152
CYCLOTRON RESONANCE DEVICES
ECH by FEL and gyrotron sources on the Microwave Tokamak Experiment (MTX) tokamak
[DE91-000286] N91-11547
CYLINDRICAL BODIES
An experimental study of an axisymmetric turbulent boundary layer disturbed by a periodic freestream N91-11175
On three dimensional object recognition and pose-determination: An abstraction based approach
[NASA-CR-186894] N91-11396
CYLINDRICAL SHELLS
Forced vibration analysis of plates and shallow shells N91-11237
Effects of an internal flow on the vibration of thin cylindrical shells N91-11258

D

DAMAGE
Determination of the short crack effect in 2090-T8E41 aluminum lithium N91-11242
DAMAGE ASSESSMENT
A new approach to the flight control system reconfiguration following a battle damage and/or generic failure on a control surface N91-11023
DAMPING
Unsteady fluid forces and fluidelastic vibration of a group of circular cylinders
[DE90-013661] N91-11190
DATA ACQUISITION
Functional description and analysis of processor performance for data collection
[INPE-5037-RPE/620] N91-11048
Experimental manufacturing of data recording system for rocket combustion thermal flux distribution
[DE90-702432] N91-11051
Digital data processing system for bipropellant apogee engine
[NAL-TM-599] N91-11052
NCEER strong-motion data base: A user manual for the geobase release (version 1.0 for the SUN3)
[PB90-258062] N91-11315
Intelligent Data Reduction (IDARE)
[NASA-CR-186322] N91-11393
Online searching in public libraries: A comparative study of performance N91-11598
The practical challenges of converting end-use data into information
[DE90-016538] N91-11600
Report on the preparatory investigation of the Pacific energy information network system
[DE91-701469] N91-11602
Identification and analysis of cosmic gamma ray bursts from Pioneer Venus Orbiter N91-11657
DATA BASE MANAGEMENT SYSTEMS
Design, develop, test, and implement an on-line research and education information service
[DE90-017654] N91-11604
DATA BASES
NASA's CFD Validation Program N91-10845
TOPAZ2D heat transfer code users manual and thermal property data base
[DE91-000075] N91-11195
Final shuttle-derived atmospheric database: Development and results from thirty-two flights
[NASA-CR-185636] N91-11310
NCEER strong-motion data base: A user manual for the geobase release (version 1.0 for the SUN3)
[PB90-258062] N91-11315
A compendium of environmental data collected during the iceshelf-88 exercise
[AD-A223518] N91-11346
The application of USAF female anthropometric data to identify problems with the introduction of female aircrew into the Royal Air Force N91-11370
Data base architecture for instrument characteristics critical to spacecraft conceptual design
[NASA-TM-4213] N91-11391
Intelligent Data Reduction (IDARE)
[NASA-CR-186322] N91-11393
Reception and display of WEFAX images: 4 bits with micro line IBM-PC, users manual
[INPE-5086-NTE/294] N91-11417
Technology transfer: Hotlines
[PB90-237140] N91-11594
Development of the structural materials information center
[DE90-016521] N91-11603
Long-term observations of three massive x ray binary transients: 4U0115+63, V0332+53, and GX301-2 N91-11612
DATA LINKS
Terminal weather information management N91-10960
A flight test facility design for examining digital information transfer N91-10962
The EUROCONTROL future ATS system concept and the programme of studies, tests, and trials N91-10963
The use of downlinked measurements to track civil aircraft N91-11004
DATA MANAGEMENT
The practical challenges of converting end-use data into information
[DE90-016538] N91-11600
DATA PROCESSING
Data analysis of hollow cathode experiment to support electrodynamic tether applications
[IFSI-89-16] N91-11047
System identification of lossless layered media from input-output data
[CWI-BS-R8929] N91-11166
Experiences in the use of ABAQUS for creep analysis
[PNR-90705] N91-11266
Distributed digital signal processors for multi-body structures
[NASA-CR-187375] N91-11387
Minimizing maximum earliness and maximum lateness on a single machine
[CWI-BS-R9001] N91-11398
Interpolation of scattered data by a bivariate convex function. Part 1: Piecewise linear C sup 0-interpolation
[MEMO-858-PT-1] N91-11469
A combined wave distribution function and stability analysis of Viking particle and low-frequency wave data
[IRF-PREPRINT-115] N91-11541
Plots of the 5-minute neutron monitor intensity and multiplicities recorded by the Rome 17-NM64, January 1990
[IFSI-90-5] N91-11653
Plots of the 5-minute neutron monitor intensity and multiplicities recorded by the Rome 17-NM64, February 1990
[IFSI-90-6] N91-11654
DATA PROCESSING EQUIPMENT
Digital data processing system for bipropellant apogee engine
[NAL-TM-599] N91-11052
Experimental manufacturing of performance evaluation system for solid image sensor
[NAL-TM-591] N91-11200

DATA RECORDERS
Experimental manufacturing of data recording system for rocket combustion thermal flux distribution
[DE90-702432] N91-11051
DATA REDUCTION
Nominal ocean tide models for TOPEX precise orbit determination N91-11029
Intelligent Data Reduction (IDARE)
[NASA-CR-186322] N91-11393
DATA SMOOTHING
Stabilization of a time integrator for the 3D shallow water equations by smoothing techniques
[CWI-NM-R8916] N91-11167
DATA SYSTEMS
Proceedings of the First NASA Ada Users' Symposium
[NASA-TM-102941] N91-11389
DATA TRANSMISSION
Improved tracking for bilateral teleoperators with time delay
[DE90-015392] N91-11222
OSI in the NASA science internet: An analysis
[NASA-CR-177561] N91-11425
DECISION MAKING
Human-centered automation: Development of a philosophy N91-10944
Fault diagnosis N91-10951
Inflight replanning for diversions N91-10955
Graphical interfaces for cooperative planning systems N91-10956
Terminal weather information management N91-10960
Democratic theory, science, and decision making in global climate change: Culpability, uncertainty, and fairness
[DE90-017316] N91-11308
Operator function modeling: Cognitive task analysis, modeling and intelligent aiding in supervisory control systems
[NASA-CR-187331] N91-11380
Implications of the Biological Effects of Ionizing Radiation (BEIR) 5 report to the Department of Energy
[DE90-016673] N91-11526
The French and the American school in multi-criteria decision analysis
[REPT-90-21] N91-11592
DECISION THEORY
The French and the American school in multi-criteria decision analysis
[REPT-90-21] N91-11592
DECOMPOSITION
Decomposition of the n-cube into paths
[MEMO-855] N91-11468
DECOMPRESSION SICKNESS
Relationship of menstrual history to altitude chamber decompression sickness N91-11379
DECONTAMINATION
An expert system for automated robotic grasping
[DE90-010820] N91-11221
DEFECTS
Fault monitoring N91-10950
Fault recovery recommendation N91-10952
The ultrasonic examination of titanium alloys N91-11094
Electronic processes in thin film PV materials
[DE90-000359] N91-11295
DEFENSE INDUSTRY
Holding the edge: Maintaining the defense technology base. Volume 2: Appendixes
[PB90-253345] N91-11597
DEFENSE PROGRAM
Department of Defense methodology guidelines for High Power Microwave (HPM) susceptibility assessments
[DE90-015405] N91-11147
Defense logistics agency Information Resources Management (IRM) near-term planning document FY 1990-1992
[PB90-238494] N91-11596
DEFLAGRATION
Theoretical and numerical aspects of wave stability in combustion models
[ECL-89-21] N91-11088
DEFORMATION
Deformation and delamination of inelastic laminates under tensile and torsional loading N91-11063
Deformation effects on the development of grain boundary chronium depletion (sensitization) in type 316 austenitic stainless steels
[DE90-016130] N91-11092
Deformation mechanisms in rapidly solidified aluminum alloys N91-11096
Micromechanics of semi-brittle ceramics N91-11119
Contact and impact problems using adaptive finite element methods N91-11239
DEGREES OF FREEDOM
Marginal aircraft release disturbance on advanced missiles
[MBB/FE121/S/PUB/329] N91-11016
DEICING
Progress toward the development of an airfoil icing analysis capability N91-10866
Study of an electrothermal de-icer: Numerical simulation and measurement of the skin temperature by infrared technique in an icing wind tunnel
[ONERA-NT-1989-10] N91-11133
DELAMINATING
Deformation and delamination of inelastic laminates under tensile and torsional loading N91-11063
DELTA FUNCTION
Evaluation of the integral
[PB90-235011] N91-11437
The delta-Sobolev approach for modeling solar spectral irradiance and radiance N91-11650
DELTA WINGS
Grid generation and inviscid flow computation about aircraft geometries N91-10857
The use of a Navier-Stokes code in the wing design process N91-10889
An embedded grid formulation applied to delta wings N91-10891
Conical Euler simulation and active suppression of delta wing rocking motion
[NASA-TM-102683] N91-10904
Calculation of aerodynamic characteristics of airplane configurations at high angle of attack in steady and unsteady flow N91-11009
Controlled vortical flow on delta wings through unsteady leading edge blowing N91-11011
DEMODULATORS
Advanced technology satellite demodulator development
[NASA-CR-185127] N91-11134
DENSIFICATION
Microwave sintering of nanocrystalline TiO2
[DE91-000375] N91-11115
DEPOSITION
Carbon deposition in gas turbine combustors
[PNR-90692] N91-11020
Microfilamentary Bi2Sr2Ca1Cu2O8 fibers
[DE90-018013] N91-11571
Computer-controlled ion beam deposition systems for high T(sub c) superconductor and other multi-component oxide thin films and layered structures
[DE90-017798] N91-11577
DESCENT
Final shuttle-derived atmospheric database: Development and results from thirty-two flights
[NASA-CR-185636] N91-11310
DESCENT TRAJECTORIES
The 4-D descent trajectory generation techniques under realistic operating conditions N91-10994
A piloted simulator evaluation of a ground-based 4-D descent advisor algorithm N91-11000
DESIGN ANALYSIS
Boeing flight deck design philosophy N91-10937
Douglas flight deck design philosophy N91-10939
Aerodynamic design optimization using computational fluid dynamics N91-11013
First incremental buy for Increment 2 of the Space Transportation System (STS)
[NASA-CR-183855] N91-11034
Controller methodologies for integrated control/structure design optimization of large flexible structures N91-11043
Instrumenting a room temperature gravitational radiation antenna for sub-Kelvin temperatures
[IFSI-90-20] N91-11143
Generic quality assurance/quality control guide for photovoltaic concentrator design, development and system installation
[DE90-017040] N91-11290
Aircrew/cockpit compatibility: A multivariate problem seeking a multivariate solution N91-11369
Constrained optimization approach to feedback control of state-augmented systems N91-11433
DETECTION
Procedural error monitoring and smart checklists N91-10954
Terminal weather information management N91-10960
Real-time failure control (SAFD)
[NASA-CR-184025] N91-11233
Measurement of radial ionization probability in microscopic volumes for 2.90 and 3.79 MeV alpha particles
[DE90-017509] N91-11498
DETECTORS
Scanning system for measuring uniformity of laser detector response and laser beam dimensions
[PB90-257619] N91-11207
DETONATION WAVES
The structure and stability of three dimensional detonation waves
[AD-A224465] N91-11164
DEUTERIUM
An apparatus for studies of hydrogen isotope exchange over metals using laser-Raman spectroscopy
[DE90-018038] N91-11085
Determination of hydrogen (deuterium) density profiles in thin metal films and multilayers by neutron reflection
[DE90-007150] N91-11108
DIAGNOSIS
Integration of model and knowledge based diagnosis, with the example of a turbojet engine
[ETN-90-97900] N91-11019
DIALYSIS
Chlorine dioxide and hemodialysis
[DE90-015912] N91-11382
DIAMONDS
Chemically vapor deposited diamond films
[DE91-000384] N91-11125
DIELECTRICS
Elementary inversion, energy velocity, and a generalized Sommerfeld theorem
[DE90-018046] N91-11486
DIESEL ENGINES
Injector and valve train friction studies: Cummins L-10 engine
[DE90-017288] N91-11225
DIESEL FUELS
Assessment of costs and benefits of flexible and alternative fuel use in the US transportation sector: Vehicle and fuel distribution requirements
[DE90-014847] N91-11127
DIFFERENTIAL EQUATIONS
More accurate predictions with transonic Navier-Stokes methods through improved turbulence modeling N91-10850
Symbolic manipulation software and the study of differential equations
[DE90-017674] N91-11413
Quasi-periodic bifurcations, applications
[TW-8911] N91-11459
Searching spectrum points of difference initial-boundary value problems with using CAS
[DE90-634382] N91-11472
The evolution of resistive ballooning modes in the banana-plateau collisionality regime
[DE90-016672] N91-11525
DIFFUSION
Automated design of controlled diffusion blades N91-10883
Bragg intensities and diffuse scattering in Ag2Se: Molecular dynamics study
[DE90-017811] N91-11583
DIFFUSION THEORY
The generalized diffusion theory of simply deformable particle-fluid two-phase flows
[MPIS-7/1990] N91-11193
DIFFUSIVITY
CTR plasma engineering studies
[DE90-017774] N91-11534
DIGITAL DATA
Digital data processing system for bipropellant apogee engine
[NAL-TM-599] N91-11052
Sampling and interpolations in digital terrain models
[INPE-5041-TDL/404] N91-11275
Identification of areas subject to flooding through TM/LANDSAT images in the basin of the rivers Pindare, Mearim, Jaguaribe, Apodi, Piranhas, and San Francisco
[INPE-5034-RPE/619] N91-11279
Performance comparison of edge defection morphologies
[INPE-5012-TDL/400] N91-11422
DIGITAL FILTERS
Adaptive digital real time filtering in structural dynamics: A contribution to the realization on Actively Reacting Elastic Structures (ARES) N91-10929
Distributed digital signal processors for multi-body structures
[NASA-CR-187375] N91-11387
DIGITAL SYSTEMS
A flight test facility design for examining digital information transfer N91-10962
Analysis and design of a high power, digitally-controlled spacecraft power system
[NASA-CR-186546] N91-11053
Digital audio editing: The development of a random access editor
[BBC-RD-1990/5] N91-11142
DIGITAL TECHNIQUES
Digital audio editing: The development of a random access editor
[BBC-RD-1990/5] N91-11142

DIMENSIONAL MEASUREMENT
Scanning system for measuring uniformity of laser detector response and laser beam dimensions
[PB90-257619] N91-11207
DIOXIDES
Chlorine dioxide and hemodialysis
[DE90-015912] N91-11382
DIRECTION FINDING
Algorithm aided evaluation of directional signals
[ETN-90-97902] N91-11138
DIRECTIONAL SOLIDIFICATION (CRYSTALS)
Heat treatment study 2
[NASA-CR-184009] N91-11091
DIRECTORIES
Guide to EPA libraries and information services
[PB90-237108] N91-11595
DIRICHLET PROBLEM
A Monte Carlo boundary propagation method for the solution of Poisson's equation
[DE90-015060] N91-11466
DISCHARGERS
Analysis and design of a high power, digitally-controlled spacecraft power system
[NASA-CR-186546] N91-11053
DISCRETE FUNCTIONS
Computer-Aided Structural Engineering (CASE) project: Investigation and design of U-frame structures using program CUFRBC. Volume C: User's guide for channels
[AD-A224388] N91-11395
DISK OPERATING SYSTEM (DOS)
The MS-DOS device handler interface
[AD-A223856] N91-11385
The MS-DOS device services interface
[AD-A223902] N91-11386
The MS-DOS routing and configuration program design
[AD-A223858] N91-11394
DISKS (SHAPES)
ution of the equivalent space with Bessel integral equation for the fractured orthotropic disk ution of the 'equivalent space' with Bessel integral equation for the fractured orthotropic disk
[ISSN-0932-8599] N91-11253
DISPLAY DEVICES
Procedural error monitoring and smart checklists N91-10954
Graphical interfaces for cooperative planning systems N91-10956
Terminal weather information management N91-10960
Information management N91-10961
How to fly windshear N91-10974
Aircraft trajectory: Prediction and control in the air transport flight management computer systems N91-10976
Flight simulator evaluation test of multi-functional display unit
[NAL-TM-596] N91-11026
DISTANCE
Classification of textures using the ARMA models and distances over the autocorrelation function
[INPE-5067-TDL/406] N91-11421
Novae as distance indicators
[NASA-CR-186278] N91-11605
DISTANCE MEASURING EQUIPMENT
Novae as distance indicators
[NASA-CR-186278] N91-11605
DISTORTION
Thermal-distortion analysis of a spacecraft box truss in geostationary orbit
[NASA-TP-3054] N91-11041
DISTRIBUTED PROCESSING
Use of 4-D RNAV in time-based en route arrival metering N91-10997
Touchstone project: Milestone event Q4
[AD-A224034] N91-11480
DISTRIBUTION FUNCTIONS
Optimal choice of sample fraction in extreme-value estimation
[CWI-BS-R8927] N91-11476
A combined wave distribution function and stability analysis of Viking particle and low-frequency wave data
[IRF-PREPRINT-115] N91-11541
DIURNAL VARIATIONS
Planetary boundary layer dynamics over the Amazon rain forest N91-11317
DIVERGENCE
Problems of static divergence concerning the rpm regulation of wind turbines using centrifugal force controlling means and rotating slat
[ETN-90-97858] N91-11281
Generalized dynamic normal mode initialization N91-11341
DIVERTERS
A design method of divertor in tokamak reactors
[NIFS-36] N91-11532
DMSP SATELLITES
Development of a validation model for the defense meteorological satellite program's special sensor microwave imager
[NASA-CR-187369] N91-11342
DOMAIN WALL
Gravitational field of static and thick domain walls
[DE90-513706] N91-11331
DOMAINS
A synthesis of time and frequency domain methods for the control of infinite-dimensional systems: A system theoretic approach
[W-8912] N91-11456
DOPPLER RADAR
Wind lidar for tropical climatology
[CNES-CT/DRT/TIT/IO-88/126] N91-11334
DOWNLINKING
The use of downlinked measurements to track civil aircraft N91-11004
DRAG
Calculation of the rotor induced download on airfoils N91-10864
DRAINAGE
Computer-Aided Structural Engineering (CASE) project: Investigation and design of U-frame structures using program CUFRBC. Volume C: User's guide for channels
[AD-A224388] N91-11395
DRYING
In-situ pore structure analysis during aging and drying of gels
[DE91-000044] N91-11089
DUCTED FLOW
Numerical simulation of transition from laminar to turbulent duct flow
[ESA-TT-1144] N91-11199
DUCTILITY
Effects of environment and aging on creep properties of Alloy 800H
[DE90-520207] N91-11106
Analysis of ductile crack extension in plastic fracture N91-11257
Mechanical properties, fracture behavior, and grain-boundary chemistry of B-doped NiAl
[DE90-015153] N91-11558
DURABILITY
Crack behaviour of 2024-T3, 2090-T8E41 and 7075-T6 under constant amplitude and different types of variable amplitude loading, especially Gaussian loading N91-11244
DWARF STARS
Type 2 solar radio bursts recorded at Weissenau, 1966-1987
[PB90-198334] N91-11648
DYNAMIC CONTROL
Dynamic analysis and control of lightweight manipulators with flexible parallel link mechanisms
[NASA-CR-187347] N91-11216
DYNAMIC MODELS
Geometric method and synthesis af assembly strategies in robotic systems
[LAAS-90041] N91-11215
Dynamic analysis and control of lightweight manipulators with flexible parallel link mechanisms
[NASA-CR-187347] N91-11216
Dynamic model error analysis of robot manipulators N91-11220
DYNAMIC RESPONSE
Wind models for flight simulation N91-10975
Development and application of the time domain panel method N91-11010
DYNAMIC STABILITY
Review of active structural control systems and flight test techniques for dynamic stability investigations
[MBB/FYT256/S/PUB/361/A] N91-11025
Buckling and vibrations of plates subjected to concentrated forces N91-11255
Effects of an internal flow on the vibration of thin cylindrical shells N91-11258
DYNAMIC STRUCTURAL ANALYSIS
Contributions in the field of aeroelastics on the occasion of the 60th anniversary of Professor Dr.-Ing. Habil. Hans Wilhelm Foersching
[ETN-90-97630] N91-10920
Structural dynamics qualification of spacecraft N91-10922
Non-linear vibration of large, imperfect space structures N91-10930
Development and application of the time domain panel method N91-11010
Coupled rotor/airframe vibration analysis N91-11012
Forced vibration analysis of plates and shallow shells N91-11237
DYNAMICAL SYSTEMS
Application of dynamical systems theory to nonlinear aircraft dynamics N91-11014

E

EAR PROTECTORS
Voice communications in the cockpit noise environment: The role of active noise reduction N91-11140
EARTH (PLANET)
Numerical models of 2-D and 3-D geophysical convection
[DE90-014979] N91-11330
EARTH ATMOSPHERE
Seasonal variations in the latitudinal distribution of tropospheric carbon monoxide, 1986 to 1988 N91-11328
EARTH MAGNETOSPHERE
Electric fields in magnetosphere
[TRITA-EPP-89-06] N91-11312
EARTH SURFACE
Numerical experiments with climatic zonally-averaged models
[INPE-5063-TDL/417] N91-11343
EARTHQUAKES
NCEER strong-motion data base: A user manual for the geobase release (version 1.0 for the SUN3)
[PB90-258062] N91-11315
Aspects of the earthquake geology and seismotectonics of the southern San Andreas and related faults N91-11329
ECLIPSING BINARY STARS
Observation and analysis of variable linear polarization in the yellow supergiant star Epsilon Aurigae N91-11616
ECONOMIC ANALYSIS
Assessment of costs and benefits of flexible and alternative fuel use in the US transportation sector: Vehicle and fuel distribution requirements
[DE90-014847] N91-11127
Japanese power electronics inverter technology and its impact on the American air conditioning industry
[DE90-014843] N91-11191
Satellite remote sensing for agricultural projects
[PB90-257916] N91-11270
Conceptual design of an Open-Cycle Ocean Thermal Energy Conversion Net Power-Producing Experiment (OC-OTEC NPPE)
[DE90-000304] N91-11282
Assessment of municipal solid waste for energy production in the Western United States
[DE90-000361] N91-11283
Evaluation of a high-temperature burner-duct-recuperator system
[DE90-000366] N91-11284
Molten carbonate fuel cell power plant systems studies
[DE90-009697] N91-11298
Ocean thermal energy conversion: Perspective and status
[DE90-017665] N91-11299
Energy models and national energy policy
[DE90-017682] N91-11300
Results from a workshop on research needs for modeling aquifer thermal energy storage systems
[DE90-018007] N91-11301
ECONOMIC FACTORS
Democratic theory, science, and decision making in global climate change: Culpability, uncertainty, and fairness
[DE90-017316] N91-11308
ECONOMICS
Technical assessment and economic study of compressed air energy storage in Japan
[DE91-701405] N91-11292
EDDY VISCOSITY
Navier-Stokes analysis of transonic cascade flow
[NASA-TM-103624] N91-11192
EDGE DETECTION
Performance comparison of edge defection morphologies
[INPE-5012-TDL/400] N91-11422
EDITING
Digital audio editing: The development of a random access editor
[BBC-RD-1990/5] N91-11142
EDUCATION
Spacecraft design project: High latitude communications satellite
[NASA-CR-186689] N91-11039
Recruiting, Selection, Training and Military Operations of Female Aircrew
[AGARD-CP-491] N91-11358
The integration of women into US Navy aircrew training and squadron assignments N91-11359
The selection, training, and operational work of female helicopter pilots in the Royal Netherlands Air Force N91-11361

ANSTO: Australian Nuclear Science and Technology Organization
[DE90-637389] N91-11507
EFFICIENCY
A contribution to the output analysis and layout of transonic axial turbine stages
[ETN-90-97862] N91-11017
EIGENVALUES
Computation of standard deviations in Eigenvalue calculations
[DE90-017809] N91-11479
EJECTION SEATS
Impact on women: A retrospective look at impact acceleration testing at the Harry G. Armstrong Aerospace Medical Research Laboratory N91-11378
EJECTORS
Ejector thrust augmentors: Pulse-starting approach to the second solution N91-10913
Study of asymmetric supersonic jet flow for ejectors
[DE90-015598] N91-10917
Noise measurements from an ejector suppressor nozzle in the NASA Lewis 9- by 15-foot low speed wind tunnel
[NASA-TM-103628] N91-11493
EL NINO
Meteorological characteristics of the El Nino/Southern Oscillation phenomenon N91-11340
Numerical experiments with climatic zonally-averaged models
[INPE-5083-TDL/417] N91-11343
Notes on the NOARL nowcast for the 1989 to 1990 El Nino forced by FNOC winds
[AD-A223520] N91-11347
ELASTIC BODIES
Alternate equilibrium configurations of flexible cantilever beams N91-11254
ELASTIC CYLINDERS
Vortex-induced noise and vibration in flow past several flat plates N91-11163
ELASTIC PROPERTIES
Computation of transonic flow over elastic rotor blade N91-10906
A life comparison of tube and channel cooling passages for thrust chambers
[NASA-TM-103613] N91-11059
Elastic properties of ceramic composite materials at high temperatures
[ETN-90-97897] N91-11067
Contact and impact problems using adaptive finite element methods N91-11239
ELASTIC WAVES
Attenuation of elastic waves due to scattering from spherical cavities and elastic inclusions N91-11256
ELASTOMERS
On the calculation of leakage and friction of reciprocating elastomeric seals
[ETN-90-97751] N91-11228
ELASTOPLASTICITY
Elastic/plastic analyses of advanced composites investigating the use of the compliant layer concept in reducing residual stresses resulting from processing
[NASA-TM-103204] N91-11074
ELASTOSTATICS
Boundary element methods in structural shape synthesis N91-11406
ELECTRIC ARCS
Corrosion and arc erosion in MHD channels
[DE90-017889] N91-11539
ELECTRIC BATTERIES
Analysis and design of a high power, digitally-controlled spacecraft power system
[NASA-CR-186546] N91-11053
Assessment of costs and benefits of flexible and alternative fuel use in the US transportation sector: Vehicle and fuel distribution requirements
[DE90-014847] N91-11127
Advanced secondary batteries: Their applications, technological status, market and opportunity
[DE90-796146] N91-11146
A microprocessor based charge control system for the simultaneous charging of several batteries with one charge controller
[DE90-017089] N91-11157
Development of high performance sodium/metal chloride cells
[DE90-017668] N91-11159
ELECTRIC CONDUCTORS
Bragg intensities and diffuse scattering in Ag2Se: Molecular dynamics study
[DE90-017811] N91-11583
ELECTRIC CONNECTORS
Development of hermetic microminiature connectors
[DE90-015562] N91-11153
ELECTRIC CONTACTS
Development of hermetic microminiature connectors
[DE90-015562] N91-11153
Design and testing of a high temperature superconducting current lead
[DE90-017812] N91-11579
ELECTRIC CURRENT
Effects of electric current and field on the behavior of metallic materials N91-11095
Electric-field dependent electroreflectance and photocurrent spectroscopy in InGaAs/InAlAs strained-layer superlattices
[DE90-015698] N91-11559
ELECTRIC DIPOLES
Bragg intensities and diffuse scattering in Ag2Se: Molecular dynamics study
[DE90-017811] N91-11583
ELECTRIC EQUIPMENT
Thermal stresses in layered electrical assemblies bonded with solder
[DE90-015563] N91-11263
ELECTRIC FIELD STRENGTH
MIS capacitor studies on silicon carbide single crystals
[NASA-CR-187350] N91-11555
ELECTRIC FIELDS
Effects of electric current and field on the behavior of metallic materials N91-11095
Electric fields in magnetosphere
[TRITA-EPP-89-06] N91-11312
Dynamic trapping of electrons in space plasmas
[TRITA-EPP-89-07] N91-11528
Concepts in strong Langmuir turbulence theory
[DE91-000208] N91-11546
Electric-field dependent electroreflectance and photocurrent spectroscopy in InGaAs/InAlAs strained-layer superlattices
[DE90-015698] N91-11559
Testing for lightning as a source of radio bursts observed on the nightside of Venus
[NASA-CR-187364] N91-11645
ELECTRIC GENERATORS
A hybrid pulse forming technique
[DE90-016860] N91-11156
ELECTRIC MOTOR VEHICLES
Zinc air battery development for electric vehicles
[DE90-016639] N91-11149
ELECTRIC MOTORS
Japanese power electronics inverter technology and its impact on the American air conditioning industry
[DE90-014843] N91-11191
ELECTRIC NETWORKS
A hybrid pulse forming technique
[DE90-016860] N91-11156
ELECTRIC POTENTIAL
Analysis and design of a high power, digitally-controlled spacecraft power system
[NASA-CR-186546] N91-11053
An automated linearity test for direct voltage calibrators
[DE90-016927] N91-11204
Potential drops supported by ion density cavities in the dynamic response of plasma diode to an applied field
[TRITA-EPP-90-03] N91-11531
ELECTRIC POWER PLANTS
Survey on solidification and utilization technology of CO2
[DE91-701465] N91-11087
ELECTRICAL ENGINEERING
Center for electronics and electrical engineering technical publication announcements covering Center programs, July - September, 1989, with 1990 CEEE events calendar
[PB90-206491] N91-11145
ELECTRICAL MEASUREMENT
An automated linearity test for direct voltage calibrators
[DE90-016927] N91-11204
ELECTRICAL PROPERTIES
Fabrication and optimization of a whiskerless Schottky barrier diode for submillimeter wave applications
[NASA-CR-186381] N91-11144
Current and potential distributions on a cylinder electrode
[DE91-000170] N91-11161
Experimental manufacturing of performance evaluation system for solid image sensor
[NAL-TM-591] N91-11200
Electronic processes in thin film PV materials
[DE90-000359] N91-11295
Structure of amorphous-silicon and germanium alloy films
[DE90-000355] N91-11557
SERI Workshop on the Role of Point Defects/Defect Complexes in Silicon Device Fabrication
[DE90-000377] N91-11572
ELECTRICITY
Assessment of municipal solid waste for energy production in the Western United States
[DE90-000361] N91-11283
Evaluating the environmental impacts of the energy system: The ENPEP (Energy and Power Evaluation Program) approach
[DE90-017862] N91-11309
ELECTRO-OPTICS
Elementary inversion, energy velocity, and a generalized Sommerfeld theorem
[DE90-018046] N91-11486
ELECTROCARDIOGRAPHY
EKG findings in female aviators in the US Air Force N91-11377
ELECTROCATALYSTS
Proceedings of the Second Annual Fuel Cells Contractors Review Meeting
[DE90-000490] N91-11288
ELECTROCHEMICAL CORROSION
Zinc air battery development for electric vehicles
[DE90-016639] N91-11149
ELECTROCHEMISTRY
Terrestrial nickel/hydrogen battery evaluation
[DE90-014863] N91-11151
Current and potential distributions on a cylinder electrode
[DE91-000170] N91-11161
Intramolecular electron transfer rates
[DE90-017447] N91-11504
ELECTRODES
Current and potential distributions on a cylinder electrode
[DE91-000170] N91-11161
ELECTRODYNAMICS
Data analysis of hollow cathode experiment to support electrodynamic tether applications
[IFSI-89-16] N91-11047
The SIM.PL.EX. plasma chamber (Simulatori di Plasma Extraterrestre)
[IFSI-90-8] N91-11551
ELECTROLYSIS
Three-Man Solid Electrolyte Carbon Dioxide Electrolysis Breadboard
[NASA-CR-185612] N91-11148
ELECTROLYTES
Development of high performance sodium/metal chloride cells
[DE90-017668] N91-11159
Proceedings of the Second Annual Fuel Cells Contractors Review Meeting
[DE90-000490] N91-11288
ELECTROMAGNETIC ACCELERATION
Investigation on the projection by a Z-pinch discharge
[DE90-637548] N91-11544
ELECTROMAGNETIC FIELDS
Railgun performance with a two-stage light-gas gun injector
[DE90-016211] N91-11032
Department of Defense methodology guidelines for High Power Microwave (HPM) susceptibility assessments
[DE90-015405] N91-11147
Numerical modeling of time domain 3-D problems in accelerator physics
[DE90-015625] N91-11511
On the origin of cosmological magnetic fields
[DE90-017617] N91-11634
ELECTROMAGNETIC INTERACTIONS
Numerical modeling of time domain 3-D problems in accelerator physics
[DE90-015625] N91-11511
ELECTRON BEAMS
Atomic physics of highly charged ions in an electron beam ion trap
[DE90-017528] N91-11499
MONT3E: A Monte Carlo electron heat transfer code
[DE90-012091] N91-11514
Design and operation of the electron beam ion trap
[DE91-000074] N91-11515
ELECTRON BUNCHING
Review of free electron lasers
[PB90-255480] N91-11206
ELECTRON CYCLOTRON HEATING
High-power microwave transmission systems for electron cyclotron resonance plasma heating, volume 5
[DE90-017600] N91-11152
Fluctuations and stability in the Advanced Toroidal Facility (ATF) torsatron
[DE90-017734] N91-11536
ELECTRON DENSITY (CONCENTRATION)
Investigation of the arcjet plume near field using electrostatic probes
[NASA-TM-103638] N91-11060
Ion dynamics in semiconductors with self-consistent electronic densities N91-11556
ELECTRON GAS
The influence of ionized impurities on the transport properties of a two-dimensional electron gas
[ETN-90-97752] N91-11586

ELECTRON GUNS
Design and operation of the electron beam ion trap
[DE91-000074] N91-11515
ELECTRON MICROSCOPY
High-resolution electron microscopy observations of athermal omega phase in Ti-Mo alloys
[DE90-017526] N91-11098
Relationship of microstructure and tensile properties for neutron-irradiated vanadium alloys
[DE90-017863] N91-11105
Compositional imaging of semiconductor interfaces by Z-contrast Scanning Transmission Electron Microscope (STEM)
[DE90-017763] N91-11576
ELECTRON SCATTERING
Atomic physics of highly charged ions in an electron beam ion trap
[DE90-017528] N91-11499
Newly appreciated roles for electrons in ion-atom collisions
[DE91-000555] N91-11509
Numerical studies of electron scattering in astrophysics N91-11625
ELECTRON SPIN
The transuranium elements: Members of the 5f series
[DE90-017680] N91-11575
ELECTRON TRANSFER
Intramolecular electron transfer rates
[DE90-017447] N91-11504
ELECTRON TRANSITIONS
Theoritical and experimental study of kinetics mechanisms in the Chemical Oxygen-Iodine Laser (COIL)
[ONERA-P-1990-1] N91-11211
Semiempirical studies of atomic structure
[DE90-017653] N91-11501
ELECTRON-POSITRON PAIRS
Numerical studies of electron scattering in astrophysics N91-11625
ELECTRONIC PACKAGING
Development of hermetic microminiature connectors
[DE90-015562] N91-11153
ELECTRONICS
Center for electronics and electrical engineering technical publication announcements covering Center programs, July - September, 1989, with 1990 CEEE events calendar
[PB90-206491] N91-11145
ELECTRONS
Intramolecular electron transfer rates
[DE90-017447] N91-11504
The transuranium elements: Members of the 5f series
[DE90-017680] N91-11575
ELECTROPHORESIS
Combined capillary electrophoresis and electrospray ionization mass spectrometry
[DE90-016535] N91-11079
ELECTROSTATIC PROBES
Investigation of the arcjet plume near field using electrostatic probes
[NASA-TM-103638] N91-11060
ELEMENTARY PARTICLES
Research program in elementary particle theory
[DE90-017284] N91-11497
ELEVATION
Satellite elevation magnetic anomalies and their use in tectonic studies N91-11272
Beta splines interpolation for DEM's
[INPE-5039-PRE/1572] N91-11415
Geometric correction of SPOT imagery with the use of a digital elevation model
[INPE-5014-TDL/401] N91-11423
EMERGENCIES
Fault recovery recommendation N91-10952
A function-based approach to cockpit procedure aids N91-10953
EMERGENCY LOCATOR TRANSMITTERS
Current Emergency Locator Transmitter (ELT) deficiencies and potential improvements utilizing TSO-C91a ELTs
[NASA-CR-4330] N91-10964
EMISSION SPECTRA
Transient infrared emission spectroscopy
[DE90-017253] N91-11083
Observations of pulsars at low radio frequencies N91-11614
Nitrogen and sulfur in irregular galaxies N91-11624
Stability of emission line clouds in active galactic nuclei N91-11659
EMOTIONAL FACTORS
Crew workload strategies in advanced cockpits N91-10945
Sex differences concerning performance and personality traits of applicants for highly qualified operator functions in aviation N91-11364
ENERGETIC PARTICLES
Electric fields in magnetosphere
[TRITA-EPP-89-06] N91-11312
ENERGY BANDS
Light-heavy-hole-mixing-induced selection rules for magneto-luminescence and valence-band energy dispersion in semiconductor quantum wells
[DE90-015989] N91-11573
ENERGY CONSERVATION
Interchange of researchers on alternative energy of petroleum in EC countries
[DE91-701468] N91-11130
Study on feasible applications of stirling cycle machine
[DE91-701463] N91-11293
Energy models and national energy policy
[DE90-017682] N91-11300
ENERGY CONSUMPTION
The practical challenges of converting end-use data into information
[DE90-016538] N91-11600
Report on the preparatory investigation of the Pacific energy information network system
[DE91-701469] N91-11602
ENERGY CONVERSION
Assessment of municipal solid waste for energy production in the Western United States
[DE90-000361] N91-11283
ENERGY CONVERSION EFFICIENCY
Interchange of researchers on alternative energy of petroleum in EC countries
[DE91-701468] N91-11130
High efficiency CuInSe2 and CuInGaSe2 cells and materials research
[DE90-000362] N91-11280
Research on high-efficiency, large area amorphous silicon based solar cells
[DE90-000356] N91-11285
Research on high-efficiency, multiple-gap, multi-junction amorphous silicon-based alloy thin-film solar cells
[DE90-000364] N91-11296
Analysis of loss mechanisms in polycrystalline thin film solar cells
[DE90-000372] N91-11297
ENERGY DISSIPATION
Penetration in GTA welding
[DE90-008971] N91-11213
Analysis of ductile crack extension in plastic fracture N91-11257
ENERGY OF FORMATION
The stability of irradiation-induced defects in NiAl
[DE90-017744] N91-11103
ENERGY POLICY
Aeroelastics and dynamics of wind turbines N91-10923
Energy models and national energy policy
[DE90-017682] N91-11300
Evaluating the environmental impacts of the energy system: The ENPEP (Energy and Power Evaluation Program) approach
[DE90-017862] N91-11309
ENERGY REQUIREMENTS
Optimal trajectories of aircraft and spacecraft N91-10968
Evaluating the environmental impacts of the energy system: The ENPEP (Energy and Power Evaluation Program) approach
[DE90-017862] N91-11309
ENERGY SPECTRA
High energy iron ion implantation into sapphire
[DE90-017736] N91-11568
The EGRET gamma ray telescope and its energy calibration N91-11613
Microwave background anisotropies and the primordial spectrum of cosmological density fluctuations
[DE90-513791] N91-11639
ENERGY STORAGE
Advanced secondary batteries: Their applications, technological status, market and opportunity
[DE90-796146] N91-11146
Technical assessment and economic study of compressed air energy storage in Japan
[DE91-701405] N91-11292
Results from a workshop on research needs for modeling aquifer thermal energy storage systems
[DE90-018007] N91-11301
ENERGY TECHNOLOGY
Co-researches with researchers of alternative energy of petroleum in EC countries
[DE91-701466] N91-11129
Ocean thermal energy conversion: Perspective and status
[DE90-017665] N91-11299
Energy models and national energy policy
[DE90-017682] N91-11300
Report on the preparatory investigation of the Pacific energy information network system
[DE91-701469] N91-11602
Activities report of the Technical Research Centre of Finland
[ISBN-951-38-3647] N91-11665
ENERGY TRANSFER
Measurement and calculation of surface roughness effects on turbulent flow and heat transfer N91-11183
Bench-scale testing of a heat-pipe receiver for solar thermal electric applications
[DE90-009834] N91-11289
ENGINE CONTROL
Fault monitoring N91-10950
ENGINE DESIGN
Automated design of controlled diffusion blades N91-10883
Commercial aircraft and the environment
[PNR-90687] N91-11307
ENGINE FAILURE
Real-time failure control (SAFD)
[NASA-CR-184025] N91-11233
ENGINE INLETS
A comparative study of Navier-Stokes codes for high-speed flows N91-10869
A numerical study of the hot gas environment around a STOVL aircraft in ground proximity N91-10887
CFD analysis for high speed inlets N91-10888
ENGINE PARTS
The role of process modelling in manufacture and design
[PNR-90702] N91-11416
ENGINE TESTING LABORATORIES
Digital data processing system for bipropellant apogee engine
[NAL-TM-599] N91-11052
ENGINE TESTS
A combined Eulerian-Lagrangian two-phase analysis of the SSME HPOTP nozzle plug trajectories N91-10878
Test cases for computation of internal flows in aero engine components
[AGARD-AR-275] N91-11022
RL10 ignition limits test for Shuttle Centaur
[NASA-CR-183199] N91-11049
ENGINEERING
Research and technology at Kennedy Space Center
[NASA-TM-102150] N91-11664
ENGINEERING DRAWINGS
IGES efficiency evaluation
[DE90-015192] N91-11409
ENGLISH LANGUAGE
International English
[DE90-016719] N91-11601
ENTHALPY
A life comparison of tube and channel cooling passages for thrust chambers
[NASA-TM-103613] N91-11059
Thermal performance analysis for heat exchangers using nonazeotropic refrigerant mixtures
[DE90-016030] N91-11186
ENVIRONMENT EFFECTS
Outer continental shelf environmental assessment program: Comprehensive bibliography, June 1990
[PB90-258609] N91-11350
ENVIRONMENT MANAGEMENT
Utility of remotely sensed data for identification of soil conservation practices
[NASA-CR-176874] N91-11276
ENVIRONMENT MODELS
Estimation of seasonal and annual acidic deposition through aggregation of three-day episodic periods
[PB90-252628] N91-11303
ENVIRONMENT POLLUTION
Commercial aircraft and the environment
[PNR-90687] N91-11307
ENVIRONMENT PROTECTION
Minimization and control of hazardous combustion byproducts
[PB90-259854] N91-11305
Guide to EPA libraries and information services
[PB90-237108] N91-11595
ENVIRONMENTAL LABORATORIES
The SIM.PL.EX. plasma chamber (Simulatori di Plasma Extraterrestre)
[IFSI-90-8] N91-11551
ENVIRONMENTAL QUALITY
Biosensors: Development status
[MBB-Z-0305-90-PUB] N91-11201
ENVIRONMENTAL TESTS
Preliminary results from the advanced photovoltaic experiment flight test
[NASA-TM-103269] N91-11058
Effects of environment and aging on creep properties of Alloy 800H
[DE90-520207] N91-11106

Studies of molecular properties of polymeric materials [NASA-TM-101854] N91-11118
Evaluation of thermal sprayed metallic coatings for use on the structures at Launch Complex 39 [NASA-TM-103807] N91-11121

EPIDEMIOLOGY
Nitrogen dioxide and respiratory infection: Pilot investigations [PB90-247339] N91-11357

EPITAXY
Electric-field dependent electroreflectance and photocurrent spectroscopy in InGaAs/InAlAs strained-layer superlattices [DE90-015698] N91-11559
Magnetic properties of ultrathin epitaxial films of iron [DE90-017861] N91-11570
Epitaxial TiO2 and VO2 films prepared by MOCVD (Metal-Organic Chemical Vapor Deposition) [DE90-017806] N91-11578

EQUATIONS OF MOTION
Aircraft dynamics for air traffic control N91-10985
Boosting a tethered satellites's orbit around an oblate planet through resonant pumping N91-11030
Dynamic analysis and control of lightweight manipulators with flexible parallel link mechanisms [NASA-CR-187347] N91-11216

EQUATORIAL REGIONS
Notes on the NOARL nowcast for the 1989 to 1990 El Nino forced by FNOC winds [AD-A223520] N91-11347

EQUILIBRIUM FLOW
Calculation of viscous hypersonic flows using a coupled Euler/2nd order boundary layer method [MBB/FE122/S/PUB/387] N91-10935

EQUIVALENCE
Minimality of descriptor representations under external equivalence [CWI-BS-R9002] N91-11446

EROSION
Preliminary results from the advanced photovoltaic experiment flight test [NASA-TM-103269] N91-11058

ERROR ANALYSIS
Fault diagnosis N91-10951
Bayesian multi-sensor tracking for advanced air traffic control systems N91-11003
Advanced technology satellite demodulator development [NASA-CR-185127] N91-11134
Dynamic model error analysis of robot manipulators N91-11220
Contact and impact problems using adaptive finite element methods N91-11239

ERROR FUNCTIONS
The influence of environmental factors on the temperature of the radiosonde thermistor N91-11325

ERRORS
Compact representation of radiation patterns using spherical mode expansions [DE91-000019] N91-11141
Contact and impact problems using adaptive finite element methods N91-11239
An adaptive finite element technique using element equilibrium and paving [DE90-015829] N91-11410

ESTIMATES
Asymptotic estimates of approximation errors by the Galerkin method for one class of quasipotential equations [DE90-631600] N91-11471
Lower bound on reliability for Weibull distribution when shape parameter is not estimated accurately [NASA-CR-180681] N91-11474

ESTIMATING
On SLLN for martingales with deterministic quadratic variation [CWI-BS-R8933] N91-11445
Lower bound on reliability for Weibull distribution when shape parameter is not estimated accurately [NASA-CR-180681] N91-11474
Optimal choice of sample fraction in extreme-value estimation [CWI-BS-R8927] N91-11476
On density estimation in the view of Kolmogorov's ideas in approximation theory [CWI-BS-R8928] N91-11477

ETCHING
Research on high-efficiency, large area amorphous silicon based solar cells [DE90-000356] N91-11285

ETHYL ALCOHOL
Assessment of costs and benefits of flexible and alternative fuel use in the US transportation sector: Vehicle and fuel distribution requirements [DE90-014847] N91-11127

EUCLIDEAN GEOMETRY
Expected complexity of the 3-dimensional voronoi diagram [PB90-221862] N91-11435
Expected linear 3-dimensional Voronoi diagram algorithm [PB90-227984] N91-11436

EULER BUCKLING
Alternate equilibrium configurations of flexible cantilever beams N91-11254

EULER EQUATIONS OF MOTION
Numerical analysis of flow through oscillating cascade sections N91-10684
Unstructured mesh solution of the Euler and Navier-Stokes equations N91-10892
Three dimensional unstructured grids for the solution of the Euler equations N91-10893
Conical Euler simulation and active suppression of delta wing rocking motion [NASA-TM-102683] N91-10904
Damped, direction-dependent multigrid for hypersonic flow computations [CWI-NM-R8922] N91-10905
Implicit flux-split Euler schemes for unsteady aerodynamic analysis involving unstructured dynamic meshes [NASA-TM-102732] N91-10918
Temporal-adaptive Euler/Navier-Stokes algorithm for unsteady aerodynamic analysis of airfoils using unstructured dynamic meshes [NASA-TM-102734] N91-10919
The calculation of unsteady compressible flow about oscillating airfoil profiles using the Euler upwind method N91-10921
Calculation of viscous hypersonic flows using a coupled Euler/2nd order boundary layer method [MBB/FE122/S/PUB/387] N91-10935
Optimal control design by Volterra Series and its application to spacecraft maneuvers N91-11044
Performance of a parallel code for the Euler equations on hypercube computers [NASA-TM-102260] N91-11384
The linearly implicit Euler method for quasi-linear parabolic differential equations [CWI-NM-R9002] N91-11451
Solution of the two-dimensional Euler equations by a finite volume discretization on unstructured triangular meshes [ESA-TT-1135] N91-11473

EULER-LAGRANGE EQUATION
Combustion to modelisation turbulent combustion in the case of stabilization by flame-lock [ONERA-NT-1989-8] N91-11090

EVALUATION
Evaluation process for the examination of curved surface workpieces using coordinate measuring instruments [ETN-90-97901] N91-11203

EVAPORATION
Complete adiabatic evaporation of highly superheated liquid jets [MPIS-MITT-95] N91-11588

EVAPORATIVE COOLING
Design and operation of the electron beam ion trap [DE91-000074] N91-11515

EVEN-EVEN NUCLEI
Empirical proton-neutron interaction energies and nuclear structure [DE90-017632] N91-11500

EVOLUTION (DEVELOPMENT)
Non linear evolution of a second mode wave in supersonic boundary layers N91-10848

EXCHANGING
An apparatus for studies of hydrogen isotope exchange over metals using laser-Raman spectroscopy [DE90-018038] N91-11085

EXHAUST EMISSION
Lifetimes and fates of toxic air contaminants in California's atmosphere [PB90-253204] N91-11304
Measurements of toxic exhaust emissions from gasoline-powered light-duty vehicles [PB90-259649] N91-11306
Commercial aircraft and the environment [PNR-90687] N91-11307

EXHAUST NOZZLES
Design and evaluation of thrust vectored nozzles using a multicomponent thrust stand [NASA-CR-180474] N91-11050
Noise measurements from an ejector suppressor nozzle in the NASA Lewis 9- by 15-foot low speed wind tunnel [NASA-TM-103628] N91-11493

EXOTHERMIC REACTIONS
Numerical simulation of shock-induced combustion for application to the ram accelerator concept N91-10912

EXPERIMENT DESIGN
Combined Release and Radiation Effects Satellite (CRRES): Atlas 1 (Atlas/Centaur-69) launch vehicle [NASA-TM-103460] N91-11040
Conceptual design of an Open-Cycle Ocean Thermal Energy Conversion Net Power-Producing Experiment (OC-OTEC NPPE) [DE90-000304] N91-11282

EXPERT SYSTEMS
Fault recovery recommendation N91-10952
Information management N91-10961
Expert systems for the generation of thermal area arrival paths for civil transport N91-10995
Integration of model and knowledge based diagnosis, with the example of a turbojet engine [ETN-90-97900] N91-11019
An expert system for automated robotic grasping [DE90-010820] N91-11221
Operator function modeling: Cognitive task analysis, modeling and intelligent aiding in supervisory control systems [NASA-CR-187331] N91-11380
Intelligent Data Reduction (IDARE) [NASA-CR-186322] N91-11393

EXPLOSIVE FORMING
Co-researches with researchers of alternative energy of petroleum in EC countries [DE91-701466] N91-11129

EXTERNAL TANKS
Johnson Space Center CFD overview N91-10844
Computational fluid dynamics analysis of space shuttle main propulsion feed line 17-inch disconnect valves N91-10676
External tank aerothermal design criteria verification, volume 1 [NASA-CR-183996] N91-11037
External tank aerothermal design criteria verification, volume 2 [NASA-CR-183997] N91-11038

EXTINCTION
Attenuation of elastic waves due to scattering from spherical cavities and elastic inclusions N91-11256

EXTRATERRESTRIAL MATTER
Reexamination of data from the asteroid/meteoroid detector [NASA-CR-185875] N91-11619

EXTRATERRESTRIAL RADIATION
Radiological health risks to astronauts from space activities and medical procedures [NASA-TM-102164] N91-11356

EXTREMUM VALUES
Optimal choice of sample fraction in extreme-value estimation [CWI-BS-R8927] N91-11476

EXTRUDING
The design, testing and fabrication of an extruded, linear focus Fresnel lens [DE90-014852] N91-11516

F

F-16 AIRCRAFT
A zonal Navier-Stokes methodology for flow simulation about a complete aircraft N91-10858

F-18 AIRCRAFT
Numerical simulation of F-18 fuselage forebody flows at high angles of attack N91-10859
Navier-Stokes solutions about the F/A-18 forebody-LEX configuration N91-10860

FABRICATION
Automated Fluid Interface System (AFIS) [NASA-CR-183969] N91-11031
Fabrication and optimization of a whiskerless Schottky barrier diode for submillimeter wave applications [NASA-CR-186381] N91-11144
Experimental and theoretical studies of friction and heat transfer in rough passages [DE90-016302] N91-11223
Research on high-efficiency, multiple-gap, multi-junction amorphous silicon-based alloy thin-film solar cells [DE90-000364] N91-11296
Microfilamentary Bi2Sr2Ca1Cu2O8 fibers [DE90-018013] N91-11571
SERI Workshop on the Role of Point Defects/Defect Complexes in Silicon Device Fabrication [DE90-000377] N91-11572

FACE CENTERED CUBIC LATTICES
Determination of pair potentials by analysis of diffuse scattering of the local field in Pd3V and Ni3V [ONERA-NT-1989-7] N91-11117

FACTOR ANALYSIS
Spectral lithostratigraphic correlation of boreholes [INPE-5022-TDL/402] N91-11332

FAIL-SAFE SYSTEMS
Application of self-testing integrated circuits to the safety of systems operation
[ETN-90-97828] N91-11150
FAILURE
Current Emergency Locator Transmitter (ELT) deficiencies and potential improvements utilizing TSO-C91a ELTs
[NASA-CR-4330] N91-10964
Integration of model and knowledge based diagnosis, with the example of a turbojet engine
[ETN-90-97900] N91-11019
A continuum tensile failure model with friction
[DE90-018006] N91-11265
FAILURE ANALYSIS
First incremental buy for Increment 2 of the Space Transportation System (STS)
[NASA-CR-183855] N91-11034
Thermal stress-induced grain boundary cavitation in narrow, aluminum alloy metallizations N91-11093
Surrogate oracles, generalized dependency and simpler models
[NASA-CR-187360] N91-11407
FALSE ALARMS
Current Emergency Locator Transmitter (ELT) deficiencies and potential improvements utilizing TSO-C91a ELTs
[NASA-CR-4330] N91-10964
FAN BLADES
Analysis of three-dimensional viscous flow in a supersonic throughflow fan N91-10885
FAR FIELDS
Investigation of the arcjet plume near field using electrostatic probes
[NASA-TM-103638] N91-11060
Optical far-field measurements of extremely high dynamic to investigate the roughness of front faces of single-mode fiber connectors
[FI-452-TB-67] N91-11517
FATIGUE (MATERIALS)
Study of the wear behavior induced by fretting in aluminum and titanium alloys
[ECL-90-01] N91-11229
Deducing mechanical properties due to interfaces from their acoustical response
[DE90-016704] N91-11234
Fatigue crack characterization by ultrasonic inspection
[DE90-017252] N91-11264
FATIGUE LIFE
Short-crack growth behaviour in various aircraft materials
[AGARD-R-767] N91-11240
FATIGUE TESTS
Determination of the short crack effect in 2090-T8E41 aluminum lithium N91-11242
FAULT TOLERANCE
Overview of error-tolerant cockpit research N91-10949
Procedural error monitoring and smart checklists N91-10954
FEASIBILITY ANALYSIS
Weight evaluation and sensitivity analysis for space plane: SSTO
[NAL-TM-598-1] N91-11036
Conceptual design of an Open-Cycle Ocean Thermal Energy Conversion Net Power-Producing Experiment (OC-OTEC NPPE)
[DE90-000304] N91-11282
Assessment of municipal solid waste for energy production in the Western United States
[DE90-000361] N91-11283
Technical assessment and economic study of compressed air energy storage in Japan
[DE91-701405] N91-11292
Study on feasible applications of stirling cycle machine
[DE91-701463] N91-11293
Ocean thermal energy conversion: Perspective and status
[DE90-017665] N91-11299
Report of the Department of Energy (DOE) Office of Energy research review committee on the site-specific conceptual design of the superconducting super collider
[DE90-018021] N91-11513
Report on the preparatory investigation of the Pacific energy information network system
[DE91-701469] N91-11602
FEDERAL BUDGETS
Proposal pressure in the 1980s: An indicator of stress on the Federal Research System
[PB90-253147] N91-11593
FEEDBACK
Comparison of a mathematical one-point model and a multi-point model of aircraft motion in moving air N91-10969
Oscillation onset in neural delayed feedback
[DE90-015057] N91-11351
FEEDBACK CONTROL
Computation of sub-optimal real-time guidance laws for combat aircraft trajectories N91-10970
A new approach to the flight control system reconfiguration following a battle damage and/or generic failure on a control surface N91-11023
H infinity-design and the improvement of helicopter handling qualities N91-11024
Minimum time feedback control of articulated robotic manipulators N91-11219
Constrained optimization approach to feedback control of state-augmented systems N91-11433
FEMALES
Recruiting, Selection, Training and Military Operations of Female Aircrew
[AGARD-CP-491] N91-11358
The integration of women into US Navy aircrew training and squadron assignments N91-11359
A Canadian female CF-18 pilot's experience N91-11360
The selection, training, and operational work of female helicopter pilots in the Royal Netherlands Air Force N91-11361
Comparison of male and female USAF pilot candidates N91-11362
Naval aviation selection test scores and female aviator performance N91-11363
Sex differences concerning performance and personality traits of applicants for highly qualified operator functions in aviation N91-11364
Psychological and sociological aspects of the entrance of female aircrew to the Norwegian airforce N91-11365
Evaluation of female and male aircrew applicants using a cognitive and psychomotor test N91-11366
Female aircrew: The Canadian forces experience N91-11367
Review of female applicant aircrew in the Belgian forces N91-11368
The application of USAF female anthropometric data to identify problems with the introduction of female aircrew into the Royal Air Force N91-11370
Anthropometric accommodation of females in Canadian forces aircraft crew stations N91-11371
Problems posed by the adaptation of physiological protective equipment for female combat pilots N91-11372
Some equipment problems associated with the introduction of female aircrew into the Royal Air Force N91-11373
Morphological and functional adaptation of personal equipment designed for female personnel N91-11374
Accommodation of female aircrew in USN protective flight clothing and equipment N91-11375
Pregnancy: A cause for grounding of female air crew N91-11376
EKG findings in female aviators in the US Air Force N91-11377
Impact on women: A retrospective look at impact acceleration testing at the Harry G. Armstrong Aerospace Medical Research Laboratory N91-11378
Relationship of menstrual history to altitude chamber decompression sickness N91-11379
FERMI-DIRAC STATISTICS
Uniform asymptotic approximation of Fermi-Dirac integrals
[CWI-AM-R9001] N91-11440
FEYNMAN DIAGRAMS
On a simple evaluation of anomalies from the path integral measure
[DE90-513707] N91-11484
FIBER COMPOSITES
Deformation and delamination of inelastic laminates under tensile and torsional loading N91-11063
Ultrasonic examination of fiber composite materials by means of virtual C-scan test and model recognition
[MBB-Z-0299-89-PUB] N91-11066
FIBER OPTICS
Integrated optical components for optical fibre sensors N91-11519
FIBER STRENGTH
Load transfer between fiber and matrix in carbon fiber reinforced plastic composites tensile behavior of an embedded single filament specimen
[ONERA-NT-1989-9] N91-11075
FIBERS
Microfilamentary Bi2Sr2Ca1Cu2O8 fibers
[DE90-018013] N91-11571
FIELD ALIGNED CURRENTS
Dynamic trapping of electrons in space plasmas
[TRITA-EPP-89-07] N91-11528
Potential drops supported by ion density cavities in the dynamic response of plasma diode to an applied field
[TRITA-EPP-90-03] N91-11531
FIGHTER AIRCRAFT
Application of unstructured grid methods to steady and unsteady aerodynamic problems N91-10856
Grid generation and inviscid flow computation about aircraft geometries N91-10857
FINITE DIFFERENCE THEORY
A comparative study of Navier-Stokes codes for high-speed flows N91-10869
Computational fluid dynamics on a massively parallel computer N91-10896
Computation of transonic flow over elastic rotor blade N91-10906
A computational model for the prediction of hypersonic, reacting flows N91-10911
Development and application of the time domain panel method N91-11010
A viscous-inviscid interactive method for unsteady flows N91-11172
A global pressure relaxation for high speed laminar and turbulent flows N91-11177
An experimental study of natural convection heat transfer from a horizontal cylinder array vertically aligned to and confined by a single wall and two walls N91-11178
Instabilities of two-dimensional inviscid compressible vortices N91-11181
Theoretical and numerical studies of constitutive relations for frictional granular flow
[DE90-009662] N91-11194
Parallelization on a multi-processor system of a solving method for the unsteady Navier-Stokes equations at high Reynolds numbers
[ESA-TT-1116] N91-11197
Large eddy-simulation of convective boundary layers
[ESA-TT-1138] N91-11198
Searching spectrum points of difference initial-boundary value problems with using CAS
[DE90-634382] N91-11472
Numerical modeling of time domain 3-D problems in accelerator physics
[DE90-015625] N91-11511
Integrated optical components produced in GaAs and InP epitaxial layers using the photo-elastic effect N91-11518
FINITE ELEMENT METHOD
Computation of transonic flow over elastic rotor blade N91-10906
Structural analysis and optimization of a propfan-blade by use of the finite element method N91-10924
Coupled rotor/airframe vibration analysis N91-11012
A life comparison of tube and channel cooling passages for thrust chambers
[NASA-TM-103613] N91-11059
Analysis of deformation characteristics of a heavily deformed Cu-20 percent Nb composite
[DE90-018041] N91-11070
Accuracy, convergence and stability of finite element algorithms for incompressible fluid flow N91-11184
The measurement and finite element analysis of the dynamic stiffness of non-uniform clearance, gas, thrust bearings
[DE90-015120] N91-11214
On the calculation of leakage and friction of reciprocating elastomeric seals
[ETN-90-97751] N91-11228
Alternating method applied to 3-D part-through crack problems, with application to the weight function method N91-11238
Contact and impact problems using adaptive finite element methods N91-11239
High-performance equation solvers and their impact on finite element analysis
[NASA-TM-102735] N91-11252
Performance of finite dynamic elements for composite materials in plane stress N91-11260
A three-dimensional solid element model for finite rotation of composite shells N91-11262
An adaptive finite element technique using element equilibrium and paving
[DE90-015829] N91-11410
Non-linear multigrid in 2-D semiconductor device simulation: The zero current case
[CWI-NM-R8917] N91-11553
A multigrid approach for the solution of the 2D semiconductor equations
[CWI-NM-R9003] N91-11554
FINITE VOLUME METHOD
Solution of the two-dimensional Euler equations by a finite volume discretization on unstructured triangular meshes
[ESA-TT-1135] N91-11473
FINLAND
Activities report of the Technical Research Centre of Finland
[ISBN-951-38-3647] N91-11665
FLAME PROPAGATION
Combustion to modelisation turbulent combustion in the case of stabilization by flame-lock
[ONERA-NT-1989-8] N91-11090

FLAME STABILITY
Theoretical and numerical aspects of wave stability in combustion models
[ECL-89-21] N91-11088
FLAT PLATES
Vortex-induced noise and vibration in flow past several flat plates N91-11163
FLAT SURFACES
TranAir: Recent advances and applications N91-10862
FLEXIBILITY
Statistical system identification of structures with flexible joints N91-11232
FLIGHT CHARACTERISTICS
Effect of wind and wind variation on aircraft flight-paths N91-10972
Wind models for flight simulation N91-10975
Application of dynamical systems theory to nonlinear aircraft dynamics N91-11014
Recruiting, Selection, Training and Military Operations of Female Aircrew
[AGARD-CP-491] N91-11358
FLIGHT CLOTHING
Accommodation of female aircrew in USN protective flight clothing and equipment N91-11375
FLIGHT CONTROL
Aircraft trajectories: Computation, prediction, control, volume 1. Part 1: Fundamentals. Part 2: Flight in critical atmospheric conditions. Part 3: Impact of new on-board technologies on aircraft operation
[AGARD-AG-301-VOL-1-PT-1-3] N91-10967
Effect of wind and wind variation on aircraft flight-paths N91-10972
Aircraft flight in wind-shear N91-10973
How to fly windshear N91-10974
Aircraft trajectories: Computation, prediction, control, Volume 3. Part 9: Book of abstracts. Part 10: Bibliography. Part 11: List of contributors
[AGARD-AG-301-VOL-3-PT-9-11] N91-10978
The 4-D control of current air carriers in the present environment: Objectives, status, and plans N91-10990
A new approach to the flight control system reconfiguration following a battle damage and/or generic failure on a control surface N91-11023
Review of active structural control systems and flight test techniques for dynamic stability investigations
[MBB/FYT256/S/PUB/361/A] N91-11025
Research into language concepts for the mission control center
[NASA-CR-185928] N91-11392
Constrained optimization approach to feedback control of state-augmented systems N91-11433
FLIGHT CREWS
Douglas flight deck design philosophy N91-10939
Aviation safety/automation program overview N91-10941
Assessing information transfer in full mission flight simulations N91-10946
Assessing the feasibility, cost, and utility of developing models of human performance in aviation N91-10948
Overview of error-tolerant cockpit research N91-10949
Fault diagnosis N91-10951
Graphical interfaces for cooperative planning systems N91-10956
Recruiting, Selection, Training and Military Operations of Female Aircrew
[AGARD-CP-491] N91-11358
The integration of women into US Navy aircrew training and squadron assignments N91-11359
Psychological and sociological aspects of the entrance of female aircrew to the Norwegian airforce N91-11365
Evaluation of female and male aircrew applicants using a cognitive and psychomotor test N91-11366
Female aircrew: The Canadian forces experience N91-11367
Review of female applicant aircrew in the Belgian forces N91-11368
Aircrew/cockpit compatibility: A multivariate problem seeking a multivariate solution N91-11369
The application of USAF female anthropometric data to identify problems with the introduction of female aircrew into the Royal Air Force N91-11370
Anthropometric accommodation of females in Canadian forces aircraft crew stations N91-11371
Some equipment problems associated with the introduction of female aircrew into the Royal Air Force N91-11373
Accommodation of female aircrew in USN protective flight clothing and equipment N91-11375
FLIGHT INSTRUMENTS
A function-based approach to cockpit procedure aids N91-10953
FLIGHT MANAGEMENT SYSTEMS
Aircraft trajectories: Computation, prediction, control, volume 1. Part 1: Fundamentals. Part 2: Flight in critical atmospheric conditions. Part 3: Impact of new on-board technologies on aircraft operation
[AGARD-AG-301-VOL-1-PT-1-3] N91-10967
Aircraft trajectory: Prediction and control in the air transport flight management computer systems N91-10976
Aircraft trajectories: Computation, prediction, control, volume 2: Air traffic handling and ground-based guidance of aircraft. Part 4: Air traffic handling. Part 5: Guidance of aircraft in a time-based constrained environment. Part 6: Surveillance. Part 7: Meteorological forecasts. Part 8: Aircraft operation in air traffic handling simulation
[AGARD-AG-301-VOL-2-PT-4-8] N91-10981
The EUROCONTROL future ATS system concept and the programme of studies, tests, and trials N91-10983
Optimization models and techniques to improve air traffic management N91-10988
The 4-D descent trajectory generation techniques under realistic operating conditions N91-10994
A description and evaluation of TIMER: A time-based terminal flow-control concept N91-10996
Use of 4-D RNAV in time-based en route arrival metering N91-10997
FLIGHT MECHANICS
Aircraft dynamics for air traffic control N91-10985
FLIGHT OPERATIONS
Summary of the industry/NASA/FAA workshop on philosophy of automation: Promises and realities N91-10942
Aircraft trajectories: Computation, prediction, control, volume 1. Part 1: Fundamentals. Part 2: Flight in critical atmospheric conditions. Part 3: Impact of new on-board technologies on aircraft operation
[AGARD-AG-301-VOL-1-PT-1-3] N91-10967
Guidance concepts for time-based flight operations N91-10993
Air traffic management and aircraft guidance in a zone of convergence N91-10998
Simulation of automated approach procedures considering dynamic flight operations N91-11008
FLIGHT OPTIMIZATION
Optimum on-line handling of air traffic over Western Europe N91-10982
The EUROCONTROL future ATS system concept and the programme of studies, tests, and trials N91-10983
FLIGHT PATHS
Graphical interfaces for cooperative planning systems N91-10956
Aircraft trajectories: Computation, prediction, control, volume 1. Part 1: Fundamentals. Part 2: Flight in critical atmospheric conditions. Part 3: Impact of new on-board technologies on aircraft operation
[AGARD-AG-301-VOL-1-PT-1-3] N91-10967
Optimal trajectories of aircraft and spacecraft N91-10968
Computation of sub-optimal real-time guidance laws for combat aircraft trajectories N91-10970
Critical aspects of trajectory prediction: Flight in non-uniform wind N91-10971
Effect of wind and wind variation on aircraft flight-paths N91-10972
Aircraft flight in wind-shear N91-10973
Wind models for flight simulation N91-10975
Aircraft trajectory: Prediction and control in the air transport flight management computer systems N91-10976
Aircraft trajectories: Computation, prediction, control, Volume 3. Part 9: Book of abstracts. Part 10: Bibliography. Part 11: List of contributors
[AGARD-AG-301-VOL-3-PT-9-11] N91-10978
Optimum on-line handling of air traffic over Western Europe N91-10982
The EUROCONTROL future ATS system concept and the programme of studies, tests, and trials N91-10983
Prediction of aircraft trajectories N91-10984
The application of trajectory prediction algorithms for planning purposes in the Netherlands ATC-system N91-10986
Generation of aircraft trajectories for on-line operation: Methods, techniques, and tools N91-10987
Optimization models and techniques to improve air traffic management N91-10988
The 4-D control of current air carriers in the present environment: Objectives, status, and plans N91-10990
Expert systems for the generation of thermal area arrival paths for civil transport N91-10995
FLIGHT PLANS
Inflight replanning for diversions N91-10955
Graphical interfaces for cooperative planning systems N91-10956
FLIGHT SAFETY
Contributions to the improvement of flight safety in wind shear
[ESA-TT-1141] N91-10965
FLIGHT SIMULATION
Assessing information transfer in full mission flight simulations N91-10946
Aircraft trajectories: Computation, prediction, control, volume 1. Part 1: Fundamentals. Part 2: Flight in critical atmospheric conditions. Part 3: Impact of new on-board technologies on aircraft operation
[AGARD-AG-301-VOL-1-PT-1-3] N91-10967
Critical aspects of trajectory prediction: Flight in non-uniform wind N91-10971
Wind models for flight simulation N91-10975
Flight simulator evaluation test of multi-functional display unit
[NAL-TM-596] N91-11026
Flight simulation programs for space plane
[NAL-TM-594] N91-11035
Weight evaluation and sensitivity analysis for space plane: SSTO
[NAL-TM-598-1] N91-11036
FLIGHT STABILITY TESTS
Review of active structural control systems and flight test techniques for dynamic stability investigations
[MBB/FYT256/S/PUB/361/A] N91-11025
FLIGHT TESTS
The computation of thermo-chemical nonequilibrium hypersonic flows N91-10898
A flight test facility design for examining digital information transfer N91-10962
Flight evaluation test of the PAPI (Precision Approach Path Indicator) System
[NAL-TM-592] N91-10966
Impact of new technology on operational interface: From design aims to flight evaluation and measurement N91-10977
First incremental buy for Increment 2 of the Space Transportation System (STS)
[NASA-CR-183855] N91-11034
FLIGHT TRAINING
The integration of women into US Navy aircrew training and squadron assignments N91-11359
A Canadian female CF-18 pilot's experience N91-11360
The selection, training, and operational work of female helicopter pilots in the Royal Netherlands Air Force N91-11361
Comparison of male and female USAF pilot candidates N91-11362
Female aircrew: The Canadian forces experience N91-11367
FLIR DETECTORS
Requirements of an HMS/D for a night-flying helicopter
[MBB-UD-0570-90-PUB] N91-11383
FLOOD PLAINS
Identification of areas subject to flooding through TM/LANDSAT images in the basin of the rivers Pindare, Mearim, Jaguaribe, Apodi, Piranhas, and San Francisco
[INPE-5034-RPE/619] N91-11279
FLOODS
Identification of areas subject to flooding through TM/LANDSAT images in the basin of the rivers Pindare, Mearim, Jaguaribe, Apodi, Piranhas, and San Francisco
[INPE-5034-RPE/619] N91-11279
FLOW CHARACTERISTICS
Three-dimensional calculation of supersonic reacting flows using an LU scheme N91-10871
A numerical study of the effects of wind tunnel wall proximity on an airfoil model
[NASA-CR-187322] N91-10934
FLOW DISTRIBUTION
Computational fluid dynamics at the Lewis Research Center: An overview N91-10842
Understanding transition and turbulence through direct simulations N91-10846
SAGE: A 2-D self-adaptive grid evolution code and its application in computational fluid dynamics N91-10853
Modeling of high speed chemically reacting flow-fields N91-10870
Three-dimensional calculation of supersonic reacting flows using an LU scheme N91-10871
Progress in computing nozzle/plume flow fields N91-10872
Application of CFD codes for the simulation of scramjet combustor flowfields N91-10873
A combined Eulerian-Lagrangian two-phase analysis of the SSME HPOTP nozzle plug trajectories N91-10878
Prediction of turbine rotor-stator interaction using Navier-Stokes methods N91-10881
A numerical study of the hot gas environment around a STOVL aircraft in ground proximity N91-10887
CFD analysis for high speed inlets N91-10888

The use of a Navier-Stokes code in the wing design process N91-10889
Applications of a transonic wing design method N91-10890
An embedded grid formulation applied to delta wings N91-10891
Unstructured mesh solution of the Euler and Navier-Stokes equations N91-10892
Three dimensional unstructured grids for the solution of the Euler equations N91-10893
Visualization of fluid dynamics at NASA Ames N91-10895
Aeroassist flight experiment aerodynamics and aerothermodynamics N91-10900
Direct simulation of rarefied hypersonic flows N91-10901
Damped, direction-dependent multigrid for hypersonic flow computations [CWI-NM-R8922] N91-10905
Experimental investigation of the mechanisms underlying vortex kinematics in unsteady separated flows N91-10907
Ejector thrust augmentors: Pulse-starting approach to the second solution N91-10913
Structure of supersonic turbulent reattaching shear layers N91-10914
Numerical calculations for flows past an unconventional airfoil N91-10916
Unsteady wind tunnel wall interferences in subsonic and transonic profile flows N91-10928
Calculation of viscous hypersonic flows using a coupled Euler/2nd order boundary layer method [MBB/FE122/S/PUB/387] N91-10935
Controlled vortical flow on delta wings through unsteady leading edge blowing N91-11011
Solutions of thin-layer Navier-Stokes equations for missile configurations N91-11173
Heat transfer and flow studies in an abrupt expansion pipe with non-Newtonian fluids N91-11180
Instabilities of two-dimensional inviscid compressible vortices N91-11181
Boundary layer receptivity mechanisms relevant to laminar flow control N91-11182
Numerical simulation of transition from laminar to turbulent duct flow [ESA-TT-1144] N91-11199
Use of the VP-200 computer for aerothermodynamic problems [MBB/FE122/S/PUB/388] N91-11424

FLOW EQUATIONS
The generalized diffusion theory of simply deformable particle-fluid two-phase flows [MPIS-7/1990] N91-11193

FLOW GEOMETRY
Examination of numerical formulations to describe complex geometry turbulent elliptical flows, using contour matched coordinates [ETN-90-97864] N91-11169

FLOW MEASUREMENT
Measurement of two-phase flow momentum with force transducers [DE90-008748] N91-11188

FLOW STABILITY
Modeling of high speed chemically reacting flow-fields N91-10870
Computational fluid dynamics analysis of space shuttle main propulsion feed line 17-inch disconnect valves N91-10876
Analysis of the SSME HPOTP bearing inlet cavity N91-10877
The structure and stability of three dimensional detonation waves [AD-A224465] N91-11164
Instabilities of two-dimensional inviscid compressible vortices N91-11181
Modelling of large-scale unstable waves in the middle atmosphere N91-11327

FLOW VELOCITY
Aerodynamic interaction of counter rotating propellers N91-10910
Experimental manufacturing of data recording system for rocket combustion thermal flux distribution [DE90-702432] N91-11051
Measurement of two-phase flow momentum with force transducers [DE90-008748] N91-11188
Effects of an internal flow on the vibration of thin cylindrical shells N91-11258

FLOW VISUALIZATION
Direct simulation of compressible turbulence N91-10847
Simulation of powered-lift flows N91-10886
Visualization of fluid dynamics at NASA Ames N91-10895
Design and evaluation of thrust vectored nozzles using a multicomponent thrust stand [NASA-CR-180474] N91-11050
A simulation of the flow near a burning propellant in a solid propellant rocket motor N91-11056
Heat transfer and flow studies in an abrupt expansion pipe with non-Newtonian fluids N91-11180

FLUE GASES
Minimization and control of hazardous combustion byproducts [PB90-259854] N91-11305

FLUID DYNAMICS
Direct simulation of compressible turbulence N91-10847
Non linear evolution of a second mode wave in supersonic boundary layers N91-10848
Numerical simulation of nonlinear development of instability waves [E-4658] N91-10849
More accurate predictions with transonic Navier-Stokes methods through improved turbulence modeling N91-10850
Recent advances in Runge-Kutta schemes for solving 3-D Navier-Stokes equations N91-10851
Analysis and control of supersonic vortex breakdown flows [NASA-CR-186897] N91-10903
Development of a time-dependent incompressible Navier-Stokes solver based on a fractional-step method [NASA-CR-187254] N91-11165

FLUID FLOW
Accuracy, convergence and stability of finite element algorithms for incompressible fluid flow N91-11184
Measurement of two-phase flow momentum with force transducers [DE90-008748] N91-11188
Unsteady fluid forces and fluidelastic vibration of a group of circular cylinders [DE90-013661] N91-11190
Theoretical and numerical studies of constitutive relations for frictional granular flow [DE90-009662] N91-11194
Bench-scale testing of a heat-pipe receiver for solar thermal electric applications [DE90-009834] N91-11289
Numerical models of 2-D and 3-D geophysical convection [DE90-014979] N91-11330

FLUID INJECTION
Enhancement of forced convection heat transfer in tubes using staged tangential flow injection [PB90-247594] N91-11170

FLUID JETS
Effects of jet port arrangement on three-dimensional non-reacting jet-gas mixing in an MHD second stage combustor [DE90-017858] N91-11538

FLUID MECHANICS
Simulation of turbomachinery flows N91-10880
Experimental and theoretical studies of friction and heat transfer in rough passages [DE90-016302] N91-11223

FLUID-SOLID INTERACTIONS
The generalized diffusion theory of simply deformable particle-fluid two-phase flows [MPIS-7/1990] N91-11193

FLUORIDES
Graphite fluoride fibers and their applications in the space industry [NASA-TM-103265] N91-11062

FLUORINATION
Graphite fluoride fibers and their applications in the space industry [NASA-TM-103265] N91-11062

FLUTTER ANALYSIS
Performance of finite dynamic elements for composite materials in plane stress N91-11260

FLUX VECTOR SPLITTING
Flux splitting algorithms for two-dimensional viscous flows with finite-rate chemistry N91-10894
Implicit flux-split Euler schemes for unsteady aerodynamic analysis involving unstructured dynamic meshes [NASA-TM-102732] N91-10918

FOCUSING
Compact representation of radiation patterns using spherical mode expansions [DE91-000019] N91-11141

FOKKER-PLANCK EQUATION
Natural current profiles in a tokamak [DE91-000128] N91-11540

FOOD PROCESSING
Activities report of the Technical Research Centre of Finland [ISBN-951-38-3647] N91-11665

FORCED CONVECTION
Enhancement of forced convection heat transfer in tubes using staged tangential flow injection [PB90-247594] N91-11170

FORCED VIBRATION
Forced vibration analysis of plates and shallow shells N91-11237

FOREBODIES
Numerical simulation of F-18 fuselage forebody flows at high angles of attack N91-10859
Navier-Stokes solutions about the F/A-18 forebody-LEX configuration N91-10860
A global pressure relaxation for high speed laminar and turbulent flows N91-11177

FORECASTING
Energetics of 60 days predictions with the EZMW-T21 model in its mean temporary development and its relationship to forecast skill [MITT-71] N91-11335

FORMULATIONS
Numerical simulation of nonlinear development of instability waves [E-4658] N91-10849
Evaluation process for the examination of curved surface workpieces using coordinate measuring instruments [ETN-90-97901] N91-11203

FORTRAN
NUMVEC FORTRAN library manual. Chapter: Partial differential equations. Routine: OEHPC [CWI-NM-R8915] N91-11399
SISAL versus FORTRAN: A comparison using the Livermore loops [DE90-010872] N91-11414

FOURIER ANALYSIS
Sound field fluctuations due to large scale wind-driven turbulence N91-11492

FOURIER TRANSFORMATION
Application of the Ewald method to cosmological N-body simulations [DE90-513789] N91-11637

FRACTURE MECHANICS
Deformation and delamination of inelastic laminates under tensile and torsional loading N91-11063
Determination of the short crack effect in 2090-T8E41 aluminum lithium N91-11242
Short crack observations in Ti-6Al-4V under constant amplitude loading N91-11250
Analysis of ductile crack extension in plastic fracture N91-11257
Mechanical properties, fracture behavior, and grain-boundary chemistry of B-doped NiAl [DE90-015153] N91-11558

FRACTURE STRENGTH
Indentation testing of thin films and hard materials [DE90-017758] N91-11224
Crack-growth resistance in reinforced ceramic composites N91-11261

FRACTURES (MATERIALS)
ution of the equivalent space with Bessel integral equation for the fractured orthotropic disk ution of the 'equivalent space' with Bessel integral equation for the fractured orthotropic disk [ISSN-0932-8599] N91-11253

FRACTURING
Analysis of ductile crack extension in plastic fracture N91-11257
Boundary integral equations for dynamic fracture problems N91-11259

FREE CONVECTION
An experimental study of natural convection heat transfer from a horizontal cylinder array vertically aligned to and confined by a single wall and two walls N91-11178
Large eddy-simulation of convective boundary layers [ESA-TT-1138] N91-11198

FREE ELECTRON LASERS
Review of free electron lasers [PB90-255480] N91-11206
Planar orotron: A tunable, grating-based free electron laser N91-11208
ECH by FEL and gyrotron sources on the Microwave Tokamak Experiment (MTX) tokamak [DE91-000286] N91-11547

FREE FLOW
Heat transfer in variable density, low Mach number, stagnating turbulent flows N91-11171
An experimental study of an axisymmetric turbulent boundary la, ar disturbed by a periodic freestream N91-11175

FREE VIBRATION
Buckling and vibrations of plates subjected to concentrated forces N91-11255

FRENKEL DEFECTS
The stability of irradiation-induced defects in NiAl [DE90-017744] N91-11103

FREQUENCIES
Vortex-induced noise and vibration in flow past several flat plates N91-11163
A synthesis of time and frequency domain methods for the control of infinite-dimensional systems: A system theoretic approach
[W-8912] N91-11456
FREQUENCY CONTROL
Time domain frequency stability calculated from the frequency domain description: Use of the SIGINT software package to calculate time domain frequency stability from the frequency domain
[PB90-257684] N91-11405
FREQUENCY RANGES
Time domain frequency stability calculated from the frequency domain description: Use of the SIGINT software package to calculate time domain frequency stability from the frequency domain
[PB90-257684] N91-11405
FREQUENCY STABILITY
Time domain frequency stability calculated from the frequency domain description: Use of the SIGINT software package to calculate time domain frequency stability from the frequency domain
[PB90-257684] N91-11405
FRESH WATER
Ocean thermal energy conversion: Perspective and status
[DE90-017665] N91-11299
FRESNEL LENSES
The design, testing and fabrication of an extruded, linear focus Fresnel lens
[DE90-014852] N91-11516
FRETTING
Study of the wear behavior induced by fretting in aluminum and titanium alloys
[ECL-90-01] N91-11229
FRICTION
Injector and valve train friction studies: Cummins L-10 engine
[DE90-017288] N91-11225
On the calculation of leakage and friction of reciprocating elastomeric seals
[ETN-90-97751] N91-11228
Contact and impact problems using adaptive finite element methods N91-11239
FRICTION FACTOR
Theoretical and numerical studies of constitutive relations for frictional granular flow
[DE90-009662] N91-11194
FRONTS (METEOROLOGY)
Taiwan area mesoscale experiment: A guide to precipitation patterns during the 1987 field phase
[PB90-256355] N91-11336
FUEL CELLS
Proceedings of the Second Annual Fuel Cells Contractors Review Meeting
[DE90-000490] N91-11288
Molten carbonate fuel cell power plant systems studies
[DE90-009697] N91-11298
FUEL COMBUSTION
Numerical simulation of shock-induced combustion for application to the ram accelerator concept N91-10912
Reference concepts for a space-based hydrogen-oxygen combustion, turboalternator, burst power system
[DE90-016692] N91-11155
FUEL CONSUMPTION
The 4-D descent trajectory generation techniques under realistic operating conditions N91-10904
FUEL TESTS
Measurements of toxic exhaust emissions from gasoline-powered light-duty vehicles
[PB90-259649] N91-11306
FUNCTIONAL ANALYSIS
Functional description and analysis of processor performance for data collection
[INPE-5037-RPE/620] N91-11048
FUNCTIONAL DESIGN SPECIFICATIONS
CAD tools for detector design
[DE90-017337] N91-11412
FUNCTIONS (MATHEMATICS)
Cones of matrices and setfunctions, and 0-1 optimization
[CWI-BS-R8925] N91-11444
FUSELAGES
Grid generation and inviscid flow computation about aircraft geometries N91-10857
Numerical simulation of F-18 fuselage forebody flows at high angles of attack N91-10859

G

GADOLINIUM
Physical metallurgy and magnetic behavior of Cd stabilized bcc (beta) Gd alloys
[DE91-000196] N91-11112
GALACTIC CLUSTERS
Population studies in groups and clusters of galaxies, volumes 1 and 2 N91-11608
GALACTIC EVOLUTION
Population studies in groups and clusters of galaxies, volumes 1 and 2 N91-11608
Violet and visual flux problems in red giant stars N91-11632
On the origin of cosmological magnetic fields
[DE90-017617] N91-11634
GALACTIC RADIATION
Radio and infrared emission from starburst galaxies N91-11661
GALAXIES
Image reconstruction of IRAS survey scans
[NASA-CR-187326] N91-11606
The relationship of galaxy morphology to nuclear star formation in non-interacting spiral galaxies N91-11618
GALERKIN METHOD
Asymptotic estimates of approximation errors by the Galerkin method for one class of quasipotential equations
[DE90-631600] N91-11471
GALLIUM ARSENIDES
Integrated optical components produced in GaAs and InP epitaxial layers using the photo-elastic effect N91-11518
Electric-field dependent electroreflectance and photocurrent spectroscopy in InGaAs/InAlAs strained-layer superlattices
[DE90-015698] N91-11559
GAMMA RAY ASTRONOMY
The EGRET gamma ray telescope and its energy calibration N91-11613
Very high energy gamma rays from isolated pulsars and non-pulsating objects N91-11655
GAMMA RAY BURSTS
Identification and analysis of cosmic gamma ray bursts from Pioneer Venus Orbiter N91-11657
GAMMA RAY OBSERVATORY
The EGRET gamma ray telescope and its energy calibration N91-11613
GAMMA RAY TELESCOPES
The EGRET gamma ray telescope and its energy calibration N91-11613
Very high energy gamma rays from isolated pulsars and non-pulsating objects N91-11655
GAMMA RAYS
Study on radiation-induced deterioration of grease at high temperature. Part 1: Test method on thermal aging
[DE90-508070] N91-11120
Protection by WR-2721 and WR-151327 against late effects of gamma rays and neutrons
[DE90-017792] N91-11352
Very high energy gamma rays from isolated pulsars and non-pulsating objects N91-11655
A search for very high energy gamma-rays from Cygnus X-3 N91-11658
GAS BEARINGS
The measurement and finite element analysis of the dynamic stiffness of non-uniform clearance, gas, thrust bearings
[DE90-015120] N91-11214
GAS DENSITY
Determination of hydrogen (deuterium) density profiles in thin metal films and multilayers by neutron reflection
[DE90-007150] N91-11108
GAS FLOW
Heat pipe vapor dynamics N91-11179
GAS GIANT PLANETS
Numerical calculations of the formation and evolution of giant planets with rotation N91-11643
GAS TRANSPORT
Gas-liquid contacting at elevated pressures
[ETN-90-97773] N91-11196
GAS TUNGSTEN ARC WELDING
Penetration in GTA welding
[DE90-008971] N91-11213
GAS TURBINES
Carbon deposition in gas turbine combustors
[PNR-90692] N91-11020
Recent advances and developments in coatings
[PNR-90698] N91-11021
GAS-LIQUID INTERACTIONS
Gas-liquid contacting at elevated pressures
[ETN-90-97773] N91-11196
GASOLINE
Measurements of toxic exhaust emissions from gasoline-powered light-duty vehicles
[PB90-259649] N91-11306
GAUGE THEORY
Color flux distribution in pure SU(2) Lattice Gauge Theory
[DE90-017403] N91-11574
GAUSS EQUATION
Convergence of solutions of one-dimensional stochastic heat equations
[REPT-90-40] N91-11478
GELS
In-situ pore structure analysis during aging and drying of gels
[DE91-000044] N91-11089
GEOGRAPHIC INFORMATION SYSTEMS
Sampling and interpolations in digital terrain models
[INPE-5041-TDL/404] N91-11275
Geometric correction of SPOT imagery with the use of a digital elevation model
[INPE-5014-TDL/401] N91-11423
GEOLOGY
Aspects of the earthquake geology and seismotectonics of the southern San Andreas and related faults N91-11329
GEOMAGNETIC TAIL
Ion dynamics in the plasma mantle
[IFSI-89-20] N91-11550
GEOMORPHOLOGY
Aspects of the earthquake geology and seismotectonics of the southern San Andreas and related faults N91-11329
GEOPHYSICS
Numerical models of 2-D and 3-D geophysical convection
[DE90-014979] N91-11330
GEOSTROPHIC WIND
Modelling of large-scale unstable waves in the middle atmosphere N91-11327
GEOSYNCHRONOUS ORBITS
Thermal-distortion analysis of a spacecraft box truss in geostationary orbit
[NASA-TP-3054] N91-11041
GEOTHERMAL TECHNOLOGY
Interchange of researchers on alternative energy of petroleum in EC countries
[DE91-701468] N91-11130
GERMANIUM ALLOYS
Structure of amorphous-silicon and germanium alloy films
[DE90-000355] N91-11557
GLOBAL POSITIONING SYSTEM
Contribution of the satellite techniques to the surveillance of air traffic N91-11005
GOALS
Materials Division research and technology accomplishments for FY 89 and plans for FY 90
[NASA-TM-102649] N91-11072
GOVERNMENT/INDUSTRY RELATIONS
Industry perspective on Maglev
[PB90-252305] N91-11132
GRAIN BOUNDARIES
Deformation effects on the development of grain boundary chronium depletion (sensitization) in type 316 austenitic stainless steels
[DE90-016130] N91-11092
Thermal stress-induced grain boundary cavitation in narrow, aluminum alloy metallizations N91-11093
Molecular-dynamics study of grain-boundary migration in metals
[DE90-017856] N91-11104
A study of chromium carbide precipitation at interphase boundaries in stainless steel welds
[DE91-000360] N91-11113
Mechanical properties, fracture behavior, and grain-boundary chemistry of B-doped NiAl
[DE90-015153] N91-11558
GRAIN SIZE
Microwave sintering of nanocrystalline TiO2
[DE91-000375] N91-11115
GRAND UNIFIED THEORY
Research program in elementary particle theory
[DE90-017284] N91-11497
GRANTS
Proposal pressure in the 1980s: An indicator of stress on the Federal Research System
[PB90-253147] N91-11593
GRANULAR MATERIALS
Theoretical and numerical studies of constitutive relations for frictional granular flow
[DE90-009662] N91-11194
GRAPH THEORY
On dominating and spanning circuits in graphs
[MEMO-859] N91-11470

GRAPHIC ARTS
Computer-Aided Structural Engineering (CASE) project: Investigation and design of U-frame structures using program CUFRBC. Volume C: User's guide for channels [AD-A224388] N91-11395
GRAPHITE
Graphite fluoride fibers and their applications in the space industry [NASA-TM-103265] N91-11062
GRAPHS (CHARTS)
Cones of matrices and setfunctions, and 0-1 optimization [CWI-BS-R8925] N91-11444
GRAVITATION
Antimatter gravity experiment [DE91-000177] N91-11590
GRAVITATIONAL EFFECTS
M51: The Whirlpool Galaxy, analysis and simulation N91-11631
Numerical study of compressible magnetoconvection with an open transitional boundary [DE91-000148] N91-11651
GRAVITATIONAL FIELDS
Gravitational field of static and thick domain walls [DE90-513706] N91-11331
The rotation of Lageos [IFSI-90-10] N91-11333
Antimatter gravity experiment [DE91-000177] N91-11590
An investigation of the Newman-Penrose constants for massless free fields of arbitrary spin N91-11630
Cosmological N-body simulations with a treecode [DE90-513790] N91-11638
GRAVITATIONAL WAVE ANTENNAS
Instrumenting a room temperature gravitational radiation antenna for sub-Kelvin temperatures [IFSI-90-20] N91-11143
GRAVITY WAVES
Wave-mean flow interaction in the storm-time thermosphere using a two-dimensional model N91-11321
GRAY SCALE
Reception and display of WEFAX images: 4 bits with micro line IBM-PC, users manual [INPE-5086-NTE/294] N91-11417
Grey-level morphology [CWI-AM-R9003] N91-11442
GREASES
Study on radiation-induced deterioration of grease at high temperature. Part 1: Test method on thermal aging [DE90-508070] N91-11120
GRID GENERATION (MATHEMATICS)
NASA Computational Fluid Dynamics Conference. Volume 1: Sessions 1-6 [NASA-CP-10038-VOL-1] N91-10839
Computational Fluid Dynamics Program at NASA Ames Research Center N91-10840
Application of unstructured grid methods to steady and unsteady aerodynamic problems N91-10856
Grid generation and inviscid flow computation about aircraft geometries N91-10857
Computational fluid dynamics analysis of space shuttle main propulsion feed line 17-inch disconnect valves N91-10876
Unstructured mesh solution of the Euler and Navier-Stokes equations N91-10892
Three dimensional unstructured grids for the solution of the Euler equations N91-10893
Nonoverlapping composite meshes for multi-element air-foils N91-10908
Implicit flux-split Euler schemes for unsteady aerodynamic analysis involving unstructured dynamic meshes [NASA-TM-102732] N91-10918
Temporal-adaptive Euler/Navier-Stokes algorithm for unsteady aerodynamic analysis of airfoils using unstructured dynamic meshes [NASA-TM-102734] N91-10919
Grid generation and flow computation about a Martian entry vehicle [NASA-CR-187032] N91-11042
A static-regridding method for two-dimensional parabolic partial differential equations [CWI-NM-R8923] N91-11449
Solution of the two-dimensional Euler equations by a finite volume discretization on unstructured triangular meshes [ESA-TT-1135] N91-11473
GRINDING (MATERIAL REMOVAL)
A molecular dynamics model of the orthogonal cutting process [DE90-015911] N91-11230
GROUND EFFECT (AERODYNAMICS)
Simulation of powered-lift flows N91-10886
A numerical study of the hot gas environment around a STOVL aircraft in ground proximity N91-10887
GROUND SPEED
Ground-based 4-D guidance of flights in strong wind N91-10999
GROUND-AIR-GROUND COMMUNICATION
Contribution of the satellite techniques to the surveillance of air traffic N91-11005
GULFS
Gulf of Maine sea surface topography from GEOSAT altimetry N91-11271
GYROFREQUENCY
Testing for lightning as a source of radio bursts observed on the nightside of Venus [NASA-CR-187364] N91-11645

H

H I REGIONS
Observations of the soft x ray background N91-11663
H II REGIONS
A study of the ten and twenty micron silicate features in celestial infrared sources N91-11609
Nitrogen and sulfur in irregular galaxies N91-11624
Recent starbirth and starburst activity in nearby galaxies N91-11627
HABITATS
Three-Man Solid Electrolyte Carbon Dioxide Electrolysis Breadboard [NASA-CR-185612] N91-11148
HALIDES
Structure of molten salts [DE90-017704] N91-11566
HALL EFFECT
The influence of ionized impurities on the transport properties of a two-dimensional electron gas [ETN-90-97752] N91-11586
HALOS
Numerical simulations of suspersonic extragalactic radio jets N91-11660
HAMILTONIAN FUNCTIONS
On dominating and spanning circuits in graphs [MEMO-859] N91-11470
HARDNESS TESTS
Indentation testing of thin films and hard materials [DE90-017758] N91-11224
HARMONIC OSCILLATION
Application of unstructured grid methods to steady and unsteady aerodynamic problems N91-10856
HARMONICS
Aircraft interior noise reduction by alternate resonance tuning [NASA-CR-186879] N91-11488
HAZARDS
Terminal weather information management N91-10960
Impact on women: A retrospective look at impact acceleration testing at the Harry G. Armstrong Aerospace Medical Research Laboratory N91-11378
Discussion paper on environmental hazards on the Moon, in low Earth orbit, and in low Mars orbit [DE90-017854] N91-11646
HEALTH
Radiological health risks to astronauts from space activities and medical procedures [NASA-TM-102164] N91-11356
HEART DISEASES
EKG findings in female aviators in the US Air Force N91-11377
HEAT AFFECTED ZONE
A study of chromium carbide precipitation at interphase boundaries in stainless steel welds [DE91-000360] N91-11119
HEAT EXCHANGERS
Thermal performance analysis for heat exchangers using nonazeotropic refrigerant mixtures [DE90-016030] N91-11186
Conceptual design of an Open-Cycle Ocean Thermal Energy Conversion Net Power-Producing Experiment (OC-OTEC NPPE) [DE90-000304] N91-11282
Colorado State University program for developing, testing, evaluating and optimizing solar heating and cooling systems [DE90-017273] N91-11291
HEAT FLUX
Thermal-distortion analysis of a spacecraft box truss in geostationary orbit [NASA-TP-3054] N91-11041
Experimental manufacturing of data recording system for rocket combustion thermal flux distribution [DE90-702432] N91-11051
Heat pipe vapor dynamics N91-11179
Large eddy-simulation of convective boundary layers [ESA-TT-1138] N91-11198
Heat flux measurement in SSME turbine blade tester [NASA-TM-103274] N91-11205
A simple zonal average energy budget model of the earth-atmosphere system N91-11316
HEAT MEASUREMENT
Analysis and prediction of thermal properties of mesophases and crystals by calorimetry and supercomputers [DE90-015538] N91-11123
HEAT PIPES
Heat pipe vapor dynamics N91-11179
Bench-scale testing of a heat-pipe receiver for solar thermal electric applications [DE90-009834] N91-11289
HEAT PUMPS
Performances of four magnetic heat-pump cycles [DE90-015606] N91-11185
Japanese power electronics inverter technology and its impact on the American air conditioning industry [DE90-014843] N91-11191
HEAT RESISTANT ALLOYS
High temperature materials: The overall view [PNR-90699] N91-11073
Heat treatment study 2 [NASA-CR-184009] N91-11091
HEAT SHIELDING
High temperature materials: The overall view [PNR-90699] N91-11073
HEAT SINKS
High temperature materials: The overall view [PNR-90699] N91-11073
HEAT STORAGE
Results from a workshop on research needs for modeling aquifer thermal energy storage systems [DE90-018007] N91-11301
HEAT TRANSFER
Hypersonic CFD applications at NASA Langley using CFL3D and CFL3DE N91-10874
Conjugate (solid/fluid) computational fluid dynamics analysis of the space shuttle solid rocket motor nozzle/case and case field joints N91-10879
Turbine stage aerodynamics and heat transfer prediction N91-10882
An investigation of thermally driven acoustical oscillations in helium systems [DE90-018049] N91-11086
Three-dimensional fluid flow in JFTOT (Jet Fuel Thermal Oxidation Tester) [DE90-010929] N91-11128
Performances of four magnetic heat-pump cycles [DE90-015606] N91-11185
Thermal performance analysis for heat exchangers using nonazeotropic refrigerant mixtures [DE90-016030] N91-11186
TOPAZ2D heat transfer code users manual and thermal property data base [DE91-000075] N91-11195
Conceptual design of an Open-Cycle Ocean Thermal Energy Conversion Net Power-Producing Experiment (OC-OTEC NPPE) [DE90-000304] N91-11282
Evaluation of a high-temperature burner-duct-recuperator system [DE90-000366] N91-11284
Bench-scale testing of a heat-pipe receiver for solar thermal electric applications [DE90-009834] N91-11289
Colorado State University program for developing, testing, evaluating and optimizing solar heating and cooling systems [DE90-017273] N91-11291
Numerical models of 2-D and 3-D geophysical convection [DE90-014979] N91-11330
MONT3E: A Monte Carlo electron heat transfer code [DE90-012091] N91-11514
HEAT TREATMENT
Heat treatment study 2 [NASA-CR-184009] N91-11091
HEATING EQUIPMENT
Colorado State University program for developing, testing, evaluating and optimizing solar heating and cooling systems [DE90-017273] N91-11291
HELICOPTER CONTROL
H infinity-design and the improvement of helicopter handling qualities N91-11024
HELICOPTER DESIGN
A quarter of a century of aeroelastic cooperation between research and industry (a review). Part 1: Fighter airplanes and helicopters N91-10931
HELICOPTER PERFORMANCE
The calculation of rotor/fuselage interaction for two-dimensional bodies [NASA-TM-102855] N91-10933

HELICOPTERS
Numerical simulation of rotorcraft N91-10863
Air rescue in the Federal Republic of Germany [ETN-90-97878] N91-10963
H infinity-design and the improvement of helicopter handling qualities N91-11024
Requirements of an HMS/D for a night-flying helicopter [MBB-UD-0570-90-PUB] N91-11383

HELIUM
Design and testing of a high temperature superconducting current lead [DE90-017812] N91-11579

HELMET MOUNTED DISPLAYS
Requirements of an HMS/D for a night-flying helicopter [MBB-UD-0570-90-PUB] N91-11383

HERMETIC SEALS
Development of hermetic microminiature connectors [DE90-015562] N91-11153

HEURISTIC METHODS
The relation between knowledge and heuristic methods [W-9001] N91-11457

HEXAGONAL CELLS
Defects in close-packed metals and alloys [DE90-017502] N91-11097

HIERARCHIES
Graphical interfaces for cooperative planning systems N91-10956
The French and the American school in multi-criteria decision analysis [REPT-90-21] N91-11592

HIGH ALTITUDE ENVIRONMENTS
Enhancement of human tolerance of acute hypoxia by adaptation and intense training at high altitudes N91-11355

HIGH ENERGY INTERACTIONS
Task A: High energy physics program experiment and theory. Task B: High energy physics program numerical simulation [DE90-017336] N91-11512

HIGH ENERGY PROPELLANTS
Attenuation studies of booster-rocket propellants and their simulants [DE91-000098] N91-11131

HIGH PRESSURE
Gas-liquid contacting at elevated pressures [ETN-90-97773] N91-11196

HIGH PRESSURE OXYGEN
Analysis of the SSME HPOTP bearing inlet cavity N91-10877
A combined Eulerian-Lagrangian two-phase analysis of the SSME HPOTP nozzle plug trajectories N91-10878

HIGH RESOLUTION
High-resolution electron microscopy observations of athermal omega phase in Ti-Mo alloys [DE90-017526] N91-11098
Forest classification with high resolution satellite images. Research into the use of spatial information to improve the multi-spectral classification with SPOT images [BCRS-89-32] N91-11269

HIGH SPEED
Modeling of high speed chemically reacting flow-fields N91-10870
A global pressure relaxation for high speed laminar and turbulent flows N91-11177

HIGH TEMPERATURE
Elastic properties of ceramic composite materials at high temperatures [ETN-90-97897] N91-11067
Projective scales against high temperature corrosion [ETN-90-97770] N91-11116
Study on radiation-induced deterioration of grease at high temperature. Part 1: Test method on thermal aging [DE90-508070] N91-11120
Evaluation of a high-temperature burner-duct-recuperator system [DE90-000366] N91-11284
Design and testing of a high temperature superconducting current lead [DE90-017812] N91-11579

HIGH TEMPERATURE ENVIRONMENTS
Evaluation of thermal sprayed metallic coatings for use on the structures at Launch Complex 39 [NASA-TM-103807] N91-11121
Heat flux measurement in SSME turbine blade tester [NASA-TM-103274] N91-11205

HIGH TEMPERATURE SUPERCONDUCTORS
Laser applications for high-T(sub c) superconductors [DE90-017743] N91-11209
Phenomenology of forces acting between magnets and superconductors [DE90-017864] N91-11487
Muon SR studies on Sr2CuO2Cl2, La2CuO4, and Nd2CuO4: 2-D magnetism, local fields and muon sites [DE90-018014] N91-11506
Processing of YBA2Cu3O7 tapes from a molten salt precursor [DE90-017656] N91-11564
Excess oxygen defects in layered cuprates [DE90-017669] N91-11565
Structure-property relationships for (beta)- and (kappa)-phase BEDT-TTF salts and their use in the synthesis of (kappa)-(BEDT-TTF)2Cu(N(CN)2)Br. A salt having the highest T(sub c) (inductive onset = 11.6 K, resistive, onset = 12.5 K) yet observed in an organic superconductor [DE90-017804] N91-11582

HIGH VOLTAGES
A hybrid pulse forming technique [DE90-016860] N91-11156

HILBERT SPACE
Approximation of the solution to the moment problem in a Hilbert space [CWI-AM-R8923] N91-11438
Dynamic MRI reconstruction as a moment problem. Part 3: An error analysis of reconstruction by sinc and spline interpolation in a Hilbert space setting [CWI-AM-R9002-PT-3] N91-11441

HILBERT TRANSFORMATION
Quadratic systems equivalent to class 3 sub A not equal to 0 [REPT-90-38] N91-11455

HISTOGRAMS
Modeling histogram data with piecewise polynomials [DE90-018037] N91-11467

HISTORIES
A quarter of a century of aeroelastic cooperation between research and industry (a review). Part 2: Transport airplanes and other civil applications N91-10932

HOLE DISTRIBUTION (ELECTRONICS)
Light-heavy-hole-mixing-induced selection rules for magneto-luminescence and valence-band energy dispersion in semiconductor quantum wells [DE90-015989] N91-11573

HOLLOW CATHODES
Data analysis of hollow cathode experiment to support electrodynamic tether applications [IFSI-89-16] N91-11047

HOMOGENEITY
Mathematical morphology on homogeneous spaces. Part 1: The simply transitive case [CWI-AM-R8924-PT-1] N91-11439

HOMOGENEOUS TURBULENCE
Direct simulation of compressible turbulence N91-10847

HOMOMORPHISMS
On induced congruences [CS-9001] N91-11460

HOMOTROPY
On the uniqueness of kernels [CWI-BS-R8924] N91-11443

HORIZONTAL TAIL SURFACES
Grid generation and inviscid flow computation about aircraft geometries N91-10857

HOT CORROSION
Surface phases and their influence on metal-oxide interfaces [DE90-017608] N91-11099

HOVERCRAFT GROUND EFFECT MACHINES
Calculation of the rotor induced download on airfoils N91-10864

HOVERING
Computation of transonic flow over elastic rotor blade N91-10906

HUMAN BEHAVIOR
Technological advances for studying human behavior N91-10947

HUMAN FACTORS ENGINEERING
Aviation Safety/Automation Program Conference [NASA-CP-3090] N91-10936
Douglas flight deck design philosophy N91-10939
National plan to enhance aviation safety through human factors improvements N91-10940
Aviation safety/automation program overview N91-10941
Summary of the industry/NASA/FAA workshop on philosophy of automation: Promises and realities N91-10942
Human factors of the high technology cockpit N91-10943
Human-centered automation: Development of a philosophy N91-10944
Technological advances for studying human behavior N91-10947
Impact of new technology on operational interface: From design aims to flight evaluation and measurement N91-10977
An expert system for automated robotic grasping [DE90-010820] N91-11221
Anthropometric accommodation of females in Canadian forces aircraft crew stations N91-11371
Some equipment problems associated with the introduction of female aircrew into the Royal Air Force N91-11373
Morphological and functional adaptation of personal equipment designed for female personnel N91-11374
Accommodation of female aircrew in USN protective flight clothing and equipment N91-11375
The derivation of a behavioural model for information retrieval system design N91-11599

HUMAN PERFORMANCE
National plan to enhance aviation safety through human factors improvements N91-10940
Human-centered automation: Development of a philosophy N91-10944
Crew workload strategies in advanced cockpits N91-10945
Assessing the feasibility, cost, and utility of developing models of human performance in aviation N91-10948
Determinants of dual-task interference and resource theories in cognitive psychology [ESA-TT-1127] N91-11381

HUMAN TOLERANCES
Enhancement of human tolerance of acute hypoxia by adaptation and intense training at high altitudes N91-11355

HYBRID PROPELLANTS
Hybrid Propulsion Technology Program, phase 1. Volume 2: Technical discussion [NASA-CR-183951] N91-11055

HYBRID PROPULSION
Hybrid Propulsion Technology Program, phase 1. Volume 1: Executive summary [NASA-CR-183950] N91-11054
Hybrid Propulsion Technology Program, phase 1. Volume 2: Technical discussion [NASA-CR-183951] N91-11055

HYDRAULIC JETS
Design and evaluation of thrust vectored nozzles using a multicomponent thrust stand [NASA-CR-180474] N91-11050

HYDRIDES
A study of the chemical, mechanical, and surface properties of thin films of hydrogenated amorphous carbon [DE91-000357] N91-11585

HYDRODYNAMIC EQUATIONS
Theoretical and numerical studies of constitutive relations for frictional granular flow [DE90-009662] N91-11194

HYDRODYNAMICS
Computations of three-dimensional steady and unsteady viscous incompressible flows N91-10852
Analysis of the SSME HPOTP bearing inlet cavity N91-10877
Theoretical and numerical studies of constitutive relations for frictional granular flow [DE90-009662] N91-11194
On hydrodynamics of collisionless relativistic plasma in a strong magnetic field [DE90-513926] N91-11543

HYDROGEN
An apparatus for studies of hydrogen isotope exchange over metals using laser-Raman spectroscopy [DE90-018038] N91-11085
Nuclear magnetic resonance survey of hydrogen motion and electronic structure in (alpha)-phase (Nb-Mo)-H alloys [DE90-018044] N91-11101
Determination of hydrogen (deuterium) density profiles in thin metal films and multilayers by neutron reflection [DE90-007150] N91-11108
Formation and stability of As-H bonds in H-implanted GaAs [DE91-000043] N91-11584
Availability of hydrogen for lunar base activities [NASA-CR-187367] N91-11644

HYDROGEN EMBRITTLEMENT
A combined Eulerian-Lagrangian two-phase analysis of the SSME HPOTP nozzle plug trajectories N91-10878

HYDROGEN ISOTOPES
An apparatus for studies of hydrogen isotope exchange over metals using laser-Raman spectroscopy [DE90-018038] N91-11085
Capture and transfer of pions in hydrogenous materials [DE90-017756] N91-11505

HYDROGENATION
A study of the chemical, mechanical, and surface properties of thin films of hydrogenated amorphous carbon [DE91-000357] N91-11585

HYDROSTATICS
Analytic studies in nuclear astrophysics N91-11628
HYDROTHERMAL SYSTEMS
Results from a workshop on research needs for modeling aquifer thermal energy storage systems
[DE90-018007] N91-11301
HYPERBOLAS
Quasi-periodic bifurcations, applications
[TW-8911] N91-11459
HYPERBOLIC DIFFERENTIAL EQUATIONS
Searching spectrum points of difference initial-boundary value problems with using CAS
[DE90-634382] N91-11472
HYPERCUBE MULTIPROCESSORS
Performance of a parallel code for the Euler equations on hypercube computers
[NASA-TM-102260] N91-11384
Parallel performance models for the nodal transport method on the hypercube
[DE90-015162] N91-11408
Parallelized reliability estimation of reconfigurable computer networks
[NASA-CR-182101] N91-11430
On the adequacy of message-passing parallel supercomputers for solving neutron transport problems
[DE90-016041] N91-11431
Touchstone project Mach port: Milestone event Q4
[AD-A224057] N91-11481
HYPERSONIC AIRCRAFT
Application of computational fluid dynamics to three-dimensional bodies in hypersonic flow
N91-11174
HYPERSONIC FLOW
A comparative study of Navier-Stokes codes for high-speed flows N91-10869
Conservation equations and physical models for hypersonic air flows over the aeroassist flight experiment vehicle N91-10897
The computation of thermo-chemical nonequilibrium hypersonic flows N91-10898
Direct simulation of rarefied hypersonic flows
N91-10901
Damped, direction-dependent multigrid for hypersonic flow computations
[CWI-NM-R8922] N91-10905
A computational model for the prediction of hypersonic, reacting flows N91-10911
Numerical simulation of shock-induced combustion for application to the ram accelerator concept N91-10912
Calculation of viscous hypersonic flows using a coupled Euler/2nd order boundary layer method
[MBB/FE122/S/PUB/387] N91-10935
Application of computational fluid dynamics to three-dimensional bodies in hypersonic flow
N91-11174
HYPERSONIC INLETS
CFD analysis for high speed inlets N91-10888
HYPERSONIC VEHICLES
A comparative study of Navier-Stokes codes for high-speed flows N91-10869
Aerodynamic stability and heating analyses for the aeroassist flight experiment vehicle N91-10899
HYPERSONIC WIND TUNNELS
Ejector thrust augmentors: Pulse-starting approach to the second solution N91-10913
HYPERSONICS
NASA Computational Fluid Dynamics Conference. Volume 2: Sessions 7-12
[NASA-CP-10038-VOL-2] N91-10868
Hypersonic CFD applications at NASA Langley using CFL3D and CFL3DE N91-10874
A computational model for the prediction of hypersonic, reacting flows N91-10911
Numerical simulation of shock-induced combustion for application to the ram accelerator concept N91-10912
HYPOXIA
JPRS report: Science and technology. USSR: Life sciences
[JPRS-ULS-89-003] N91-11354
Enhancement of human tolerance of acute hypoxia by adaptation and intense training at high altitudes
N91-11355

I

ICE
A numerical model of polar mesospheric cloud formation and evolution N91-11337
ICE FORMATION
Progress toward the development of an airfoil icing analysis capability N91-10866
A numerical model of polar mesospheric cloud formation and evolution N91-11337
ICE PREVENTION
Progress toward the development of an airfoil icing analysis capability N91-10866
Study of an electrothermal de-icer: Numerical simulation and measurement of the skin temperature by infrared technique in an icing wind tunnel
[ONERA-NT-1989-10] N91-11133
ICOSAHEDRONS
Chemical identification of icosahedral structure for cobalt and nickel clusters
[DE90-017688] N91-11100
IGNITION
RL10 ignition limits test for Shuttle Centaur
[NASA-CR-183199] N91-11049
IGNITION LIMITS
RL10 ignition limits test for Shuttle Centaur
[NASA-CR-183199] N91-11049
IMAGE ANALYSIS
Grey-level morphology
[CWI-AM-R9003] N91-11442
Long period superstructures in Pt3V and Cu3Pd: Towards a quantitative description
[ONERA-NT-1990-2] N91-11587
A search for small comets in consecutive images acquired with a ground-based telescope N91-11626
IMAGE INTENSIFIERS
Remote sensing in the ultraviolet
[AD-A224254] N91-11268
Requirements of an HMS/D for a night-flying helicopter
[MBB-UD-0570-90-PUB] N91-11383
IMAGE MOTION COMPENSATION
Remote sensing in the ultraviolet
[AD-A224254] N91-11268
IMAGE PROCESSING
Multiple-energy techniques in industrial computerized tomography
[DE90-017518] N91-11081
Forest classification with high resolution satellite images. Research into the use of spatial information to improve the multi-spectral classification with SPOT images
[BCRS-89-32] N91-11269
Methodology of remote sensing for monitoring modifications in the fluvial channel and updating nautical charts
[INPE-4863-TDL/374] N91-11277
Integration of multispectral and pancromatic channels of HRV (SPOT) sensor for obtaining color compositions with a spatial resolution of approximately 10 m
[INPE-5035-TDL/403] N91-11278
Identification of areas subject to flooding through TM/LANDSAT images in the basin of the rivers Pindare, Mearim, Jaguaribe, Apodi, Piranhas, and San Francisco
[INPE-5034-RPE/619] N91-11279
Research into language concepts for the mission control center
[NASA-CR-185928] N91-11392
On three dimensional object recognition and pose-determination: An abstraction based approach
[NASA-CR-186894] N91-11396
Reception and display of WEFAX images: 4 bits with micro line IBM-PC, users manual
[INPE-5086-NTE/294] N91-11417
Performance comparison of edge defection morphologies
[INPE-5012-TDL/400] N91-11422
Geometric correction of SPOT imagery with the use of a digital elevation model
[INPE-5014-TDL/401] N91-11423
IMAGE RECONSTRUCTION
Dynamic MRI reconstruction as a moment problem. Part 3: An error analysis of reconstruction by sinc and spline interpolation in a Hilbert space setting
[CWI-AM-R9002-PT-3] N91-11441
Compositional imaging of semiconductor interfaces by Z-contrast Scanning Transmission Electron Microscope (STEM)
[DE90-017763] N91-11576
Image reconstruction of IRAS survey scans
[NASA-CR-187328] N91-11606
Speckle imaging of complicated objects N91-11617
IMAGING TECHNIQUES
Maximum entropy imaging of radio astrophysical data
N91-11610
Speckle imaging of complicated objects N91-11617
IMMUNOLOGY
JPRS report: Science and technology. USSR: Life sciences
[JPRS-ULS-89-003] N91-11354
IMPACT ACCELERATION
Impact on women: A retrospective look at impact acceleration testing at the Harry G. Armstrong Aerospace Medical Research Laboratory N91-11378
IMPACT LOADS
Computer modeling of 12-inch actuator shock test performance
[DE90-017038] N91-11033
Attenuation studies of booster-rocket propellants and their simulants
[DE91-000098] N91-11131
IMPACT TESTS
Tethered rocket as a vehicle for penetration and impact testing: Development report
[DE90-014865] N91-11057
IMPINGEMENT
Vortex-induced noise and vibration in flow past several flat plates N91-11163
IMPURITIES
Stability of liquid propellants under long-term storage
[AD-A223934] N91-11126
Electronic processes in thin film PV materials
[DE90-000359] N91-11295
SERI Workshop on the Role of Point Defects/Defect Complexes in Silicon Device Fabrication
[DE90-000377] N91-11572
The influence of ionized impurities on the transport properties of a two-dimensional electron gas
[ETN-90-97752] N91-11586
INCLUSIONS
Attenuation of elastic waves due to scattering from spherical cavities and elastic inclusions N91-11256
INCOMPRESSIBLE FLOW
Johnson Space Center CFD overview N91-10844
Direct simulation of compressible turbulence
N91-10847
Computations of three-dimensional steady and unsteady viscous incompressible flows N91-10852
Time dependent viscous incompressible Navier-Stokes equations N91-10854
Development of a time-dependent incompressible Navier-Stokes solver based on a fractional-step method
[NASA-CR-187254] N91-11165
A viscous-inviscid interactive method for unsteady flows N91-11172
Accuracy, convergence and stability of finite element algorithms for incompressible fluid flow N91-11184
Parallelization on a multi-processor system of a solving method for the unsteady Navier-Stokes equations at high Reynolds numbers
[ESA-TT-1116] N91-11197
INDENTATION
Indentation testing of thin films and hard materials
[DE90-017758] N91-11224
INDICATING INSTRUMENTS
Flight simulator evaluation test of multi-functional display unit
[NAL-TM-596] N91-11026
INDIUM ARSENIDES
Photoluminescence studies of In(x)Ga(1-x)As/Al(y)Ga(1-y)As strained-layer structures
[DE90-017031] N91-11561
INDIUM COMPOUNDS
High efficiency CuInSe2 and CuInGaSe2 cells and materials research
[DE90-000362] N91-11280
INFECTIOUS DISEASES
Nitrogen dioxide and respiratory infection: Pilot investigations
[PB90-247339] N91-11357
INFORMATION
Information management N91-10961
Activities report of the Technical Research Centre of Finland
[ISBN-951-38-3647] N91-11665
INFORMATION DISSEMINATION
Holding the edge: Maintaining the defense technology base. Volume 2: Appendixes
[PB90-253345] N91-11597
INFORMATION FLOW
National plan to enhance aviation safety through human factors improvements N91-10940
INFORMATION MANAGEMENT
Fault recovery recommendation N91-10952
Terminal weather information management
N91-10960
Information management N91-10961
Defense logistics agency Information Resources Management (IRM) near-term planning document FY 1990-1992
[PB90-238494] N91-11596
Online searching in public libraries: A comparative study of performance N91-11598
INFORMATION RETRIEVAL
Online searching in public libraries: A comparative study of performance N91-11598
The derivation of a behavioural model for information retrieval system design N91-11599

INFORMATION SYSTEMS
A unified framework for credit assignment
[DE90-011636] N91-11434
Guide to EPA libraries and information services
[PB90-237108] N91-11595
Defense logistics agency Information Resources Management (IRM) near-term planning document FY 1990-1992
[PB90-238494] N91-11596
Holding the edge: Maintaining the defense technology base. Volume 2: Appendixes
[PB90-253345] N91-11597
The derivation of a behavioural model for information retrieval system design N91-11599
Report on the preparatory investigation of the Pacific energy information network system
[DE91-701469] N91-11602
Design, develop, test, and implement an on-line research and education information service
[DE90-017654] N91-11604
INFORMATION TRANSFER
National plan to enhance aviation safety through human factors improvements N91-10940
Assessing information transfer in full mission flight simulations N91-10946
INFRARED ASTRONOMY
The relationship of galaxy morphology to nuclear star formation in non-interacting spiral galaxies N91-11618
Activities report of the Institute for Extraterrestrial Physics
[MPE-217] N91-11620
Radio and infrared emission from starburst galaxies N91-11661
INFRARED ASTRONOMY SATELLITE
Image reconstruction of IRAS survey scans
[NASA-CR-187328] N91-11606
INFRARED IMAGERY
Study of an electrothermal de-icer: Numerical simulation and measurement of the skin temperature by infrared technique in an icing wind tunnel
[ONERA-NT-1989-10] N91-11133
Observations and interpretation of the infrared emission from supernova SN1987A N91-11611
The relationship of galaxy morphology to nuclear star formation in non-interacting spiral galaxies N91-11618
INFRARED PHOTOMETRY
A study of the ten and twenty micron silicate features in celestial infrared sources N91-11609
INFRARED RADIATION
Advanced infrared optically black baffle materials
[DE91-000561] N91-11523
Observations and interpretation of the infrared emission from supernova SN1987A N91-11611
Radio and infrared emission from starburst galaxies N91-11661
INFRARED RADIOMETERS
Radiometric observation of the atmospheric boundary layer (the ROSSA Project) N91-11324
INFRARED SPECTRA
Transient infrared emission spectroscopy
[DE90-017253] N91-11083
Astronomical applications of survival analysis N91-11615
INFRARED SPECTROPHOTOMETERS
Remote sensing in the ultraviolet
[AD-A224254] N91-11268
INFRARED SPECTROSCOPY
Transient infrared emission spectroscopy
[DE90-017253] N91-11083
INGESTION (ENGINES)
A numerical study of the hot gas environment around a STOVL aircraft in ground proximity N91-10887
INJECTORS
Characterization and optimization of a pneumatic injector for a 60 bar combustion chamber
[ETN-90-97580] N91-11076
Injector and valve train friction studies: Cummins L-10 engine
[DE90-017288] N91-11225
Multiple Application Intense Particle Beam Project
[INPE-4576-RPE/568] N91-11510
INPUT
System identification of lossless layered media from input-output data
[CWI-BS-R8929] N91-11166
INSPECTION
First incremental buy for Increment 2 of the Space Transportation System (STS)
[NASA-CR-183855] N91-11034
IGES efficiency evaluation
[DE90-015192] N91-11409
INSTALLING
Test launch for turboaircraft engine. Description of the installation
[ILA-87-A-02] N91-11018
INSTRUMENT APPROACH
Simulation of automated approach procedures considering dynamic flight operations N91-11008
INSTRUMENT LANDING SYSTEMS
Flight evaluation test of the PAPI (Precision Approach Path Indicator) System
[NAL-TM-592] N91-10966
INTAKE SYSTEMS
A numerical study of the hot gas environment around a STOVL aircraft in ground proximity N91-10887
INTEGRAL EQUATIONS
Boundary integral equations for dynamic fracture problems N91-11259
On a simple evaluation of anomalies from the path integral measure
[DE90-513707] N91-11484
INTEGRALS
Evaluation of the integral
[PB90-235011] N91-11437
Uniform asymptotic approximation of Fermi-Dirac integrals
[CWI-AM-R9001] N91-11440
INTEGRATED CIRCUITS
Application of self-testing integrated circuits to the safety of systems operation
[ETN-90-97828] N91-11150
A radiation hardened SONOS/CMOS EEPROM family
[DE90-015993] N91-11154
Implementation of a QML (Qualified Manufacturer's List) methodology for discrete semiconductors
[DE90-015715] N91-11235
Silicon compilation and the SYCO silicon compiler
[ETN-90-97827] N91-11404
INTEGRATED OPTICS
Integrated optical components produced in GaAs and InP epitaxial layers using the photo-elastic effect N91-11518
Integrated optical components for optical fibre sensors N91-11519
INTERACTIONAL AERODYNAMICS
Aerodynamic interaction of counter rotating propellers N91-10910
The calculation of rotor/fuselage interaction for two-dimensional bodies
[NASA-TM-102855] N91-10933
Aircraft dynamics for air traffic control N91-10985
INTERCEPTION
Computation of sub-optimal real-time guidance laws for combat aircraft trajectories N91-10970
INTERFACES
Determination of hydrogen (deuterium) density profiles in thin metal films and multilayers by neutron reflection
[DE90-007150] N91-11108
The reaction of vapor-deposited Al with Cu oxides
[DE91-000367] N91-11114
Residual stress at fluid interfaces
[DE90-012964] N91-11189
Deducing mechanical properties due to interfaces from their acoustical response
[DE90-016704] N91-11234
The MS-DOS device handler interface
[AD-A223856] N91-11385
The MS-DOS device services interface
[AD-A223902] N91-11386
The MS-DOS routing and configuration program design
[AD-A223858] N91-11394
Stress accommodation in large-mismatch systems
[DE90-017032] N91-11562
INTERFACIAL TENSION
Gas-liquid contacting at elevated pressures
[ETN-90-97773] N91-11196
Penetration in GTA welding
[DE90-008971] N91-11213
INTERFERENCE
Examination of a three dimensional asymmetrical flow field using the interference method
[ETN-90-97859] N91-11168
INTERFEROMETERS
Examination of a three dimensional asymmetrical flow field using the interference method
[ETN-90-97859] N91-11168
INTERFEROMETRY
Comparison of clear air atmospheric radar techniques for the study of atmospheric dynamics in the troposphere and the stratosphere
[PB90-256314] N91-11313
INTERGALACTIC MEDIA
Numerical simulations of supersonic extragalactic radio jets N91-11660
INTERGRANULAR CORROSION
A study of chromium carbide precipitation at interphase boundaries in stainless steel welds
[DE91-000360] N91-11113
INTERNAL WAVES
Wave-mean flow interaction in the storm-time thermosphere using a two-dimensional model N91-11321
INTERNATIONAL COOPERATION
Report on the preparatory investigation of the Pacific energy information network system
[DE91-701469] N91-11602
INTERPLANETARY DUST
Reexamination of data from the asteroid/meteoroid detector
[NASA-CR-185875] N91-11619
INTERPOLATION
Sampling and interpolations in digital terrain models
[INPE-5041-TDL/404] N91-11275
Beta splines interpolation for DEM's
[INPE-5039-PRE/1572] N91-11415
Dynamic MRI reconstruction as a moment problem. Part 3: An error analysis of reconstruction by sinc and spline interpolation in a Hilbert space setting
[CWI-AM-R9002-PT-3] N91-11441
Convergence of linear multistep and one-leg methods for stiff nonlinear initial value problems
[CWI-NM-R8924] N91-11450
Interpolation of scattered data by a bivariate convex function. Part 1: Piecewise linear C sup 0-interpolation
[MEMO-858-PT-1] N91-11469
INTERSTELLAR GAS
Stability of emission line clouds in active galactic nuclei N91-11659
INTERSTELLAR MATTER
From red giants to planetary nebulae: Asymmetries, dust, and polarization N91-11622
INVENTORIES
Twenty-Second Annual NASA Supply and Equipment Management Conference
[NASA-CP-10042] N91-11591
INVERSE SCATTERING
An inverse problem for classical relativistic mechanics
[DE90-631599] N91-11589
INVERSIONS
Two and three dimensional magnetotelluric inversion
[DE90-016187] N91-11411
Elementary inversion, energy velocity, and a generalized Sommerfeld theorem
[DE90-018046] N91-11486
INVERTERS
Japanese power electronics inverter technology and its impact on the American air conditioning industry
[DE90-014843] N91-11191
INVISCID FLOW
Grid generation and inviscid flow computation about aircraft geometries N91-10857
Numerical simulation of rotorcraft N91-10863
Test cases for computation of internal flows in aero engine components
[AGARD-AR-275] N91-11022
A viscous-inviscid interactive method for unsteady flows N91-11172
Instabilities of two-dimensional inviscid compressible vortices N91-11181
IODINE LASERS
Theoritical and experimental study of kinetics mechanisms in the Chemical Oxygen-Iodine Laser (COIL)
[ONERA-P-1990-1] N91-11211
ION BEAMS
Ion mixing of semiconductor superlattices
[DE90-017769] N91-11569
Computer-controlled ion beam deposition systems for high T(sub c) superconductor and other multi-component oxide thin films and layered structures
[DE90-017798] N91-11577
ION DENSITY (CONCENTRATION)
Potential drops supported by ion density cavities in the dynamic response of plasma diode to an applied field
[TRITA-EPP-90-03] N91-11531
Ion dynamics in the plasma mantle
[IFSI-89-20] N91-11550
ION DISTRIBUTION
Ion dynamics in the plasma mantle
[IFSI-89-20] N91-11550
ION IMPLANTATION
Microstructures of cubic Al2O3 precipitates in oxygen-implanted aluminum
[DE91-000038] N91-11111
High energy iron ion implantation into sapphire
[DE90-017736] N91-11568
Ion mixing of semiconductor superlattices
[DE90-017769] N91-11569
Formation and stability of As-H bonds in H-implanted GaAs
[DE91-000043] N91-11584

ION SCATTERING
Atomic physics of highly charged ions in an electron beam ion trap
[DE90-017528] N91-11499
ION TRAPS (INSTRUMENTATION)
Atomic physics of highly charged ions in an electron beam ion trap
[DE90-017528] N91-11499
Design and operation of the electron beam ion trap
[DE91-000074] N91-11515
IONIC COLLISIONS
Secondary-electron yield measurements from metals impacted by high-velocity ions, electrons, and molecules
[DE90-018023] N91-11502
Newly appreciated roles for electrons in ion-atom collisions
[DE91-000555] N91-11509
Theoretical and numerical studies in magnetic mirror fusion
[DE90-017605] N91-11533
IONIZATION
Resonance ionization spectroscopy of molecular clusters using picosecond lasers
[DE90-017334] N91-11080
Measurement of radial ionization probability in microscopic volumes for 2.90 and 3.79 MeV alpha particles
[DE90-017509] N91-11498
Newly appreciated roles for electrons in ion-atom collisions
[DE91-000555] N91-11509
IONIZATION CROSS SECTIONS
Newly appreciated roles for electrons in ion-atom collisions
[DE91-000555] N91-11509
IONIZING RADIATION
Implications of the Biological Effects of Ionizing Radiation (BEIR) 5 report to the Department of Energy
[DE90-016673] N91-11526
IONS
Design and operation of the electron beam ion trap
[DE91-000074] N91-11515
Ion dynamics in semiconductors with self-consistent electronic densities N91-11556
IRON
High energy iron ion implantation into sapphire
[DE90-017736] N91-11568
Magnetic properties of ultrathin epitaxial films of iron
[DE90-017861] N91-11570
IRRADIANCE
The delta-Sobolev approach for modeling solar spectral irradiance and radiance N91-11650
IRRADIATION
The stability of irradiation-induced defects in NiAl
[DE90-017744] N91-11103
Relationship of microstructure and tensile properties for neutron-irradiated vanadium alloys
[DE90-017863] N91-11105
Ion mixing of semiconductor superlattices
[DE90-017769] N91-11569
IRREGULAR GALAXIES
Nitrogen and sulfur in irregular galaxies N91-11624
ISOELECTRONIC SEQUENCE
Atomic physics of highly charged ions in an electron beam ion trap
[DE90-017528] N91-11499
ITERATION
Applications of a transonic wing design method N91-10890
Iterated Runge-Kutta methods on parallel computers
[CWI-NM-R9001] N91-11428
A comparison of some GMRES-like methods
[REPT-90-22] N91-11454
IUE
Late stages in the evolution of classical novae
[NASA-TM-102969] N91-11633

J

J INTEGRAL
Analysis of ductile crack extension in plastic fracture N91-11257
JAPAN
Japanese power electronics inverter technology and its impact on the American air conditioning industry
[DE90-014843] N91-11191
Technical assessment and economic study of compressed air energy storage in Japan
[DE91-701405] N91-11292
JET ENGINE FUELS
Three-dimensional fluid flow in JFTOT (Jet Fuel Thermal Oxidation Tester)
[DE90-010929] N91-11128
JET ENGINES
Determination of unsteady aerodynamic forces on engines with a view to flutter investigations N91-10927
JET FLOW
Propulsion simulation for magnetically suspended wind tunnel models
[NASA-CR-182093] N91-11027
Three-dimensional computer simulation of non-reacting jet-gas flow mixing in an MHD second stage combustor
[DE90-017831] N91-11537
Complete adiabatic evaporation of highly superheated liquid jets
[MPIS-MITT-95] N91-11588
JET MIXING FLOW
Effects of jet port arrangement on three-dimensional non-reacting jet-gas mixing in an MHD second stage combustor
[DE90-017858] N91-11538
JET STREAMS (METEOROLOGY)
Northwest African depressions and their relationship to jet streams N91-11318
Basic dynamics of low frequency variability and the storm tracks N91-11339
JUDGMENTS
Fault diagnosis N91-10951

K

KERNEL FUNCTIONS
On the uniqueness of kernels
[CWI-BS-R8924] N91-11443
KERR MAGNETOOPTICAL EFFECT
Magnetic properties of ultrathin epitaxial films of iron
[DE90-017861] N91-11570
KINEMATIC EQUATIONS
Instantaneous kinematics, motion planning and mechanical efficiency of a quadrupedal walking machine N91-11218
KINEMATICS
Experimental investigation of the mechanisms underlying vortex kinematics in unsteady separated flows N91-10907
Critical aspects of trajectory prediction: Flight in non-uniform wind N91-10971
Instantaneous kinematics, motion planning and mechanical efficiency of a quadrupedal walking machine N91-11218
A method of using the inverse matrix for manipulator kinematics
[DE90-520210] N91-11227
KLYSTRONS
Increasing output power of an 850 MHz tetrode with a floating-deck modulator
[DE91-000433] N91-11162
KNOWLEDGE
The relation between knowledge and heuristic methods
[W-9001] N91-11457
KNOWLEDGE BASES (ARTIFICIAL INTELLIGENCE)
The control of inbound flights N91-10992
KNOWLEDGE REPRESENTATION
A logical background of a method for the handling of incompatible pieces of knowledge
[REPT-90-13] N91-11401

L

LABORATORY EQUIPMENT
Recommended operating procedure No. 45: Analysis of nitrous oxide from combustion sources
[PB90-238502] N91-11078
LAGEOS (SATELLITE)
The rotation of Lageos
[IFSI-90-10] N91-11333
LAGUERRE FUNCTIONS
Asymptotic behavior of Laguerre polynomials with Re z less than 0 derived by the central limit theorem
[W-9004] N91-11458
LAMINAR FLOW
Boundary layer receptivity mechanisms relevant to laminar flow control N91-11182
Numerical simulation of transition from laminar to turbulent duct flow
[ESA-TT-1144] N91-11199
LAMINAR HEAT TRANSFER
Experimental and theoretical studies of friction and heat transfer in rough passages
[DE90-016302] N91-11223
LAMINATES
Deformation and delamination of inelastic laminates under tensile and torsional loading N91-11063
LANDING INSTRUMENTS
Flight evaluation test of the PAPI (Precision Approach Path Indicator) System
[NAL-TM-592] N91-10966
LANDING MODULES
Design of a scientific probe for obtaining Mars surface material
[NASA-CR-186672] N91-11641
LANGUAGES
A fast parallel recognizer
[REPT-90-16] N91-11429
LANTHANUM ISOTOPES
Applications of diode lasers to resonance ionization mass spectrometry
[DE90-017768] N91-11084
LARGE SPACE STRUCTURES
Non-linear vibration of large, imperfect space structures N91-10930
LASER APPLICATIONS
Applications of diode lasers to resonance ionization mass spectrometry
[DE90-017768] N91-11084
Laser applications for high-T(sub c) superconductors
[DE90-017743] N91-11209
LASER BEAMS
Scanning system for measuring uniformity of laser detector response and laser beam dimensions
[PB90-257619] N91-11207
LASER OUTPUTS
Scanning system for measuring uniformity of laser detector response and laser beam dimensions
[PB90-257619] N91-11207
LASER PLASMA INTERACTIONS
Review of free electron lasers
[PB90-255480] N91-11206
LASER SPECTROSCOPY
Laser Raman spectroscopy for in-situ analysis of corrosion films on metals
[DE90-017822] N91-11109
Theoritical and experimental study of kinetics mechanisms in the Chemical Oxygen-Iodine Laser (COIL)
[ONERA-P-1990-1] N91-11211
LASER STABILITY
Scanning system for measuring uniformity of laser detector response and laser beam dimensions
[PB90-257619] N91-11207
LASERS
Resonance ionization spectroscopy of molecular clusters using picosecond lasers
[DE90-017334] N91-11080
Transient infrared emission spectroscopy
[DE90-017253] N91-11083
JPRS report: Science and technology. USSR: Life sciences
[JPRS-ULS-89-003] N91-11354
LATITUDE
Seasonal variations in the latitudinal distribution of tropospheric carbon monoxide, 1986 to 1988 N91-11328
LATTICE PARAMETERS
Determination of hydrogen (deuterium) density profiles in thin metal films and multilayers by neutron reflection
[DE90-007150] N91-11108
Stress accommodation in large-mismatch systems
[DE90-017032] N91-11562
LATTICES (MATHEMATICS)
Grey-level morphology
[CWI-AM-R9003] N91-11442
LAUNCHERS
Numerical simulation of shock-induced combustion for application to the ram accelerator concept N91-10912
LAUNCHING
Railgun performance with a two-stage light-gas gun injector
[DE90-016211] N91-11032
Flight simulation programs for space plane
[NAL-TM-594] N91-11035
LAYOUTS
A contribution to the output analysis and layout of transonic axial turbine stages
[ETN-90-97862] N91-11017
LEAD ALLOYS
Liquid alloys with strong interactions
[DE90-017661] N91-11102
Solderability of environmentally exposed Sn-plated surfaces
[DE91-000035] N91-11110
LEADING EDGES
Numerical simulation of F-18 fuselage forebody flows at high angles of attack N91-10859
Navier-Stokes solutions about the F/A-18 forebody-LEX configuration N91-10860
Controlled vortical flow on delta wings through unsteady leading edge blowing N91-11011

LEAKAGE
On the calculation of leakage and friction of reciprocating elastomeric seals
[ETN-90-97751] N91-11228
LEAST SQUARES METHOD
On SLLN for martingales with deterministic quadratic variation
[CWI-BS-R8933] N91-11445
LEGENDRE FUNCTIONS
Compact representation of radiation patterns using spherical mode expansions
[DE91-000019] N91-11141
LIBRARIES
The application of USAF female anthropometric data to identify problems with the introduction of female aircrew into the Royal Air Force N91-11370
Guide to EPA libraries and information services
[PB90-237108] N91-11595
LIFE (DURABILITY)
Short-crack growth behaviour in various aircraft materials
[AGARD-R-767] N91-11240
LIFTING ROTORS
Calculation of the rotor induced download on airfoils N91-10864
Three-dimensional viscous drag prediction for rotor blades N91-10865
LIGHT (VISIBLE RADIATION)
Violet and visual flux problems in red giant stars N91-11632
The role of shear in the cosmological distance
[DE90-513788] N91-11636
LIGHT GAS GUNS
Railgun performance with a two-stage light-gas gun injector
[DE90-016211] N91-11032
LIGHT TRANSMISSION
The design, testing and fabrication of an extruded, linear focus Fresnel lens
[DE90-014852] N91-11516
LIGHT WATER
An apparatus for studies of hydrogen isotope exchange over metals using laser-Raman spectroscopy
[DE90-018038] N91-11085
LIGHTNING
Study of the return-stroke phase of the gliding spark in ambient air
[ONERA-NT-1990-1] N91-11345
Whistlers in Neptune's magnetosphere: Evidence of atmospheric lightning
[NASA-CR-187324] N91-11642
Testing for lightning as a source of radio bursts observed on the nightside of Venus
[NASA-CR-187364] N91-11645
LIMITS (MATHEMATICS)
Connected components in supercritical Mandelbrot percolation
[REPT-90-15] N91-11452
Quadratic systems equivalent to class 3 sub A not equal to 0
[REPT-90-38] N91-11455
LINE SPECTRA
Surface anharmonicity: Temperature dependence of phonon energies on Cu(110)
[DE90-017735] N91-11567
Observations and interpretation of the infrared emission from supernova SN1987A N91-11611
Recent starbirth and starburst activity in nearby galaxies N91-11627
Stability of emission line clouds in active galactic nuclei N91-11659
Observations of the soft x ray background N91-11663
LINEAR EQUATIONS
The linearly implicit Euler method for quasi-linear parabolic differential equations
[CWI-NM-R9002] N91-11451
LINEAR POLARIZATION
Observation and analysis of variable linear polarization in the yellow supergiant star Epsilon Aurigae N91-11616
The transfer of polarized radiation in astrophysical masers in the presence of magnetic fields N91-11629
LINEAR PROGRAMMING
A potential reduction variant of Renegar's short-step path-following method for linear programming
[REPT-90-14] N91-11402
LINEAR QUADRATIC GAUSSIAN CONTROL
Precision tethered satellite attitude control N91-11046
LINEAR SYSTEMS
A synthesis of time and frequency domain methods for the control of infinite-dimensional systems: A system theoretic approach
[W-8912] N91-11456
Compensability of uncertain systems
[REPT-90-10] N91-11527
LINGUISTICS
International English
[DE90-016719] N91-11601
LIQUID ALLOYS
Liquid alloys with strong interactions
[DE90-017661] N91-11102
LIQUID CHROMATOGRAPHY
Ion chromatography in the manufacture of multilayer circuit boards
[DE90-017647] N91-11156
LIQUID HELIUM
An investigation of thermally driven acoustical oscillations in helium systems
[DE90-018049] N91-11086
LIQUID PROPELLANT ROCKET ENGINES
Digital data processing system for bipropellant apogee engine
[NAL-TM-599] N91-11052
LIQUID ROCKET PROPELLANTS
Propulsion simulation for magnetically suspended wind tunnel models
[NASA-CR-182093] N91-11027
Hybrid Propulsion Technology Program, phase 1. Volume 2: Technical discussion
[NASA-CR-183951] N91-11055
Stability of liquid propellants under long-term storage
[AD-A223934] N91-11126
LIQUID-GAS MIXTURES
Mathematical models of mixture properties: B-splines and optimization with form conditions
[ETN-90-97829] N91-11462
LIQUID-SOLID INTERFACES
Arctic acoustics ultrasonic modeling studies
[AD-A224165] N91-11489
LITHIUM ALLOYS
Determination of the short crack effect in 2090-T8E41 aluminum lithium N91-11242
Short crack behaviour in Al-Li alloy 2090 N91-11243
Short crack growth under realistic flight loading: Model predictions and experimental results for Al 2024 and Al-Li 2090 N91-11246
The growth of short cracks in 4340 steel and aluminum-lithium 2090 N91-11247
Texture analysis of 2090-T8E41 aluminum-lithium alloy sheet: Annex N91-11251
LITHIUM NIOBATES
Integrated optical components for optical fibre sensors N91-11519
LITHOLOGY
Spectral lithostratigraphic correlation of boreholes
[INPE-5022-TDL/402] N91-11332
LITHOSPHERE
Satellite elevation magnetic anomalies and their use in tectonic studies N91-11272
Tectonics of one-plate planets N91-11647
LOAD DISTRIBUTION (FORCES)
Alternate equilibrium configurations of flexible cantilever beams N91-11254
LOAD TESTS
Load transfer between fiber and matrix in carbon fiber reinforced plastic composites tensile behavior of an embedded single filament specimen
[ONERA-NT-1989-9] N91-11075
LOADS (FORCES)
The growth of short fatigue cracks in 2024 and 2090 aluminium alloys under variable amplitude loading N91-11245
LOCAL AREA NETWORKS
Interconnected networks of queues with randomized arrival and departure blocking
[CWI-BS-R8934] N91-11483
LOCOMOTION
Instantaneous kinematics, motion planning and mechanical efficiency of a quadrupedal walking machine N91-11218
LOGIC CIRCUITS
What is a default
[REPT-90-12] N91-11400
LOGIC PROGRAMMING
What is a default
[REPT-90-12] N91-11400
A logical background of a method for the handling of incompatible pieces of knowledge
[REPT-90-13] N91-11401
LOGISTICS
Twenty-Second Annual NASA Supply and Equipment Management Conference
[NASA-CP-10042] N91-11591
LOGISTICS MANAGEMENT
Defense logistics agency Information Resources Management (IRM) near-term planning document FY 1990-1992
[PB90-238494] N91-11596
LONG DURATION EXPOSURE FACILITY
Preliminary results from the advanced photovoltaic experiment flight test
[NASA-TM-103269] N91-11058
LORENTZ FORCE
Magnetohydrodynamic modification of the TEACH-T code and the prediction of the maximum azimuthal velocity in a conducting fluid
[DE90-017510] N91-11187
LOSSES
Analysis of loss mechanisms in polycrystalline thin film solar cells
[DE90-000372] N91-11297
LOSSLESS MATERIALS
System identification of lossless layered media from input-output data
[CWI-BS-R8929] N91-11166
Attenuation of elastic waves due to scattering from spherical cavities and elastic inclusions N91-11256
LOSSY MEDIA
Attenuation of elastic waves due to scattering from spherical cavities and elastic inclusions N91-11256
LOW FREQUENCIES
Basic dynamics of low frequency variability and the storm tracks N91-11339
Observations of pulsars at low radio frequencies N91-11614
LUMINESCENCE
Light-heavy-hole-mixing-induced selection rules for magneto-luminescence and valence-band energy dispersion in semiconductor quantum wells
[DE90-015989] N91-11573
LUMINOSITY
The relationship of galaxy morphology to nuclear star formation in non-interacting spiral galaxies N91-11618
LUNAR BASES
Discussion paper on environmental hazards on the Moon, in low Earth orbit, and in low Mars orbit
[DE90-017854] N91-11646
LUNAR DUST
Discussion paper on environmental hazards on the Moon, in low Earth orbit, and in low Mars orbit
[DE90-017854] N91-11646
LUNAR ENVIRONMENT
Discussion paper on environmental hazards on the Moon, in low Earth orbit, and in low Mars orbit
[DE90-017854] N91-11646
LUNAR SOIL
Availability of hydrogen for lunar base activities
[NASA-CR-187367] N91-11644
LUNAR SURFACE
Availability of hydrogen for lunar base activities
[NASA-CR-187367] N91-11644

M

MACH NUMBER
Analysis and control of supersonic vortex breakdown flows
[NASA-CR-186897] N91-10903
Study of asymmetric supersonic jet flow for ejectors
[DE90-015598] N91-10917
Touchstone project Mach port: Milestone event Q4
[AD-A224057] N91-11481
MAGNETIC ANOMALIES
Satellite elevation magnetic anomalies and their use in tectonic studies N91-11272
MAGNETIC DISKS
Digital audio editing: The development of a random access editor
[BBC-RD-1990/5] N91-11142
MAGNETIC FIELD RECONNECTION
A simulation study of magnetic reconnection processes at the dayside magnetopause N91-11320
MAGNETIC FIELDS
Performances of four magnetic heat-pump cycles
[DE90-015606] N91-11185
Magnetohydrodynamic modification of the TEACH-T code and the prediction of the maximum azimuthal velocity in a conducting fluid
[DE90-017510] N91-11187
Two and three dimensional magnetotelluric inversion
[DE90-016187] N91-11411
Phenomenology of forces acting between magnets and superconductors
[DE90-017864] N91-11487
Potential drops supported by ion density cavities in the dynamic response of plasma diode to an applied field
[TRITA-EPP-90-03] N91-11531
On hydrodynamics of collisionless relativistic plasma in a strong magnetic field
[DE90-513926] N91-11543
Complete fluid equations for low-n singular modes in axisymmetric torodial plasmas
[DE91-000176] N91-11545

Nonlinear saturation of ideal interchange modes in a sheared magnetic field
[DE91-000575] N91-11548
Light-heavy-hole-mixing-induced selection rules for magneto-luminescence and valence-band energy dispersion in semiconductor quantum wells
[DE90-015989] N91-11573
Magnetic field generation in astrophysics N91-11623
The transfer of polarized radiation in astrophysical masers in the presence of magnetic fields N91-11629

MAGNETIC FLUX
A simulation study of magnetic reconnection processes at the dayside magnetopause N91-11320

MAGNETIC LEVITATION VEHICLES
Industry perspective on Maglev
[PB90-252305] N91-11132

MAGNETIC MIRRORS
Theoretical and numerical studies in magnetic mirror fusion
[DE90-017605] N91-11533

MAGNETIC PROPERTIES
Physical metallurgy and magnetic behavior of Cd stabilized bcc (beta) Gd alloys
[DE91-000196] N91-11112
Magnetic properties of ultrathin epitaxial films of iron
[DE90-017861] N91-11570

MAGNETIC RESONANCE
Dynamic MRI reconstruction as a moment problem. Part 3: An error analysis of reconstruction by sinc and spline interpolation in a Hilbert space setting
[CWI-AM-R9002-PT-3] N91-11441

MAGNETIC STORMS
Wave-mean flow interaction in the storm-time thermosphere using a two-dimensional model N91-11321

MAGNETIC SURVEYS
Satellite elevation magnetic anomalies and their use in tectonic studies N91-11272
Two and three dimensional magnetotelluric inversion
[DE90-016187] N91-11411

MAGNETIC SUSPENSION
Propulsion simulation for magnetically suspended wind tunnel models
[NASA-CR-182093] N91-11027
Phenomenology of forces acting between magnets and superconductors
[DE90-017864] N91-11487

MAGNETIZATION
Satellite elevation magnetic anomalies and their use in tectonic studies N91-11272

MAGNETOHYDRODYNAMIC GENERATORS
MHD technology transfer, integration, and review committee
[DE90-017886] N91-11542

MAGNETOHYDRODYNAMIC STABILITY
The evolution of resistive ballooning modes in the banana-plateau collisionality regime
[DE90-016672] N91-11525
Fluctuations and stability in the Advanced Toroidal Facility (ATF) torsatron
[DE90-017734] N91-11536
A combined wave distribution function and stability analysis of Viking particle and low-frequency wave data
[IRF-PREPRINT-115] N91-11541
Complete fluid equations for low-n singular modes in axisymmetric torodial plasmas
[DE91-000176] N91-11545
Concepts in strong Langmuir turbulence theory
[DE91-000208] N91-11546
Nonlinear saturation of ideal interchange modes in a sheared magnetic field
[DE91-000575] N91-11548
Magnetic field generation in astrophysics N91-11623

MAGNETOHYDRODYNAMIC WAVES
Laboratory experiments on the magnetic field and neutral density limits on CIV interaction
[TRITA-EPP-90-01] N91-11530
Magnetic field generation in astrophysics N91-11623

MAGNETOHYDRODYNAMICS
Magnetohydrodynamic modification of the TEACH-T code and the prediction of the maximum azimuthal velocity in a conducting fluid
[DE90-017510] N91-11187
A simulation study of magnetic reconnection processes at the dayside magnetopause N91-11320
Computer and engineering calculations of Brazilian Tokamak-2
[DE90-628758] N91-11524
Three-dimensional computer simulation of non-reacting jet-gas flow mixing in an MHD second stage combustor
[DE90-017831] N91-11537
Effects of jet port arrangement on three-dimensional non-reacting jet-gas mixing in an MHD second stage combustor
[DE90-017858] N91-11538
Corrosion and arc erosion in MHD channels
[DE90-017889] N91-11539
MHD technology transfer, integration, and review committee
[DE90-017886] N91-11542
Numerical study of compressible magnetoconvection with an open transitional boundary
[DE91-000148] N91-11651

MAGNETOPAUSE
Electric fields in magnetosphere
[TRITA-EPP-89-06] N91-11312
A simulation study of magnetic reconnection processes at the dayside magnetopause N91-11320

MAINE
Gulf of Maine sea surface topography from GEOSAT altimetry N91-11271

MALES
Comparison of male and female USAF pilot candidates N91-11362
Naval aviation selection test scores and female aviator performance N91-11363
Sex differences concerning performance and personality traits of applicants for highly qualified operator functions in aviation N91-11364
Psychological and sociological aspects of the entrance of female aircrew to the Norwegian airforce N91-11365
Evaluation of female and male aircrew applicants using a cognitive and psychomotor test N91-11366
Female aircrew: The Canadian forces experience N91-11367

MALFUNCTIONS
Douglas flight deck design philosophy N91-10939

MAN MACHINE SYSTEMS
Aviation Safety/Automation Program Conference
[NASA-CP-3090] N91-10936
Human-centered automation: Development of a philosophy N91-10944
Crew workload strategies in advanced cockpits N91-10945
Technological advances for studying human behavior N91-10947
Procedural error monitoring and smart checklists N91-10954
ATC automation concepts N91-10957
Impact of new technology on operational interface: From design aims to flight evaluation and measurement N91-10977

MAN-COMPUTER INTERFACE
Aviation Safety/Automation Program Conference
[NASA-CP-3090] N91-10936
Aviation safety/automation program overview N91-10941
Human-centered automation: Development of a philosophy N91-10944
Technological advances for studying human behavior N91-10947
Fault recovery recommendation N91-10952
Information management N91-10961
Aircraft trajectories: Computation, prediction, control, volume 2: Air traffic handling and ground-based guidance of aircraft. Part 4: Air traffic handling. Part 5: Guidance of aircraft in a time-based constrained environment. Part 6: Surveillance. Part 7: Meteorological forecasts. Part 8: Aircraft operation in air traffic handling simulation
[AGARD-AG-301-VOL-2-PT-4-8] N91-10981
The high-resolution graphic display: A possible man/machine interface for a computer assisted ATC management system N91-10989
The air traffic controller facing automation: Conflict or cooperation N91-11001
The derivation of a behavioural model for information retrieval system design N91-11599

MANAGEMENT METHODS
Twenty-Second Annual NASA Supply and Equipment Management Conference
[NASA-CP-10042] N91-11591

MANAGEMENT PLANNING
Materials Division research and technology accomplishments for FY 89 and plans for FY 90
[NASA-TM-102649] N91-11072
Defense logistics agency Information Resources Management (IRM) near-term planning document FY 1990-1992
[PB90-238494] N91-11596

MANAGEMENT SYSTEMS
Information management N91-10961
A stochastic analysis of state transitions in an air space management system N91-10980
Proceedings of the First NASA Ada Users' Symposium
[NASA-TM-102941] N91-11389

MANEUVERABILITY
Prediction of effects of wing contour modifications on low-speed maximum lift and transonic performance for the EA-6B aircraft
[NASA-TP-3046] N91-10902
Controlled vortical flow on delta wings through unsteady leading edge blowing N91-11011

MANIPULATORS
Dynamic analysis and control of lightweight manipulators with flexible parallel link mechanisms
[NASA-CR-187347] N91-11216
Robot trajectory control with a model reference adaptive control system using tap delay filters N91-11217
Instantaneous kinematics, motion planning and mechanical efficiency of a quadrupedal walking machine N91-11218
Minimum time feedback control of articulated robotic manipulators N91-11219
Dynamic model error analysis of robot manipulators N91-11220
Improved tracking for bilateral teleoperators with time delay
[DE90-015392] N91-11222
A method of using the inverse matrix for manipulator kinematics
[DE90-520210] N91-11227
Intelligent Robotic Systems Study (IRSS), phase 2
[NASA-CR-183963] N91-11432

MANUFACTURING
Implementation of a QML (Qualified Manufacturer's List) methodology for discrete semiconductors
[DE90-015715] N91-11235
The role of process modelling in manufacture and design
[PNR-90702] N91-11416

MANY BODY PROBLEM
M51: The Whirlpool Galaxy, analysis and simulation N91-11631
Application of the Ewald method to cosmological N-body simulations
[DE90-513789] N91-11637
Cosmological N-body simulations with a treecode
[DE90-513790] N91-11638

MAP MATCHING GUIDANCE
Flight simulator evaluation test of multi-functional display unit
[NAL-TM-596] N91-11026

MAPPING
Classification of acoustic emission waveforms for nondestructive evaluation using neural networks
[DE90-017239] N91-11236
Methodology of remote sensing for monitoring modifications in the fluvial channel and updating nautical charts
[INPE-4863-TDL/374] N91-11277

MARINE ENVIRONMENTS
Remote sensing for marine activities
[BCRS-89-41] N91-11273
Outer continental shelf environmental assessment program: Comprehensive bibliography, June 1990
[PB90-258609] N91-11350

MARINE TECHNOLOGY
Remote sensing for marine activities: Appendices
[BCRS-89-41-APP] N91-11274

MARKARIAN GALAXIES
Radio and infrared emission from starburst galaxies N91-11661

MARKETING
Advanced secondary batteries: Their applications, technological status, market and opportunity
[DE90-796146] N91-11146

MARKOV PROCESSES
Stochastic approximation of the MLE for a spatial point pattern
[CWI-BS-R8926] N91-11475

MARS (PLANET)
Grid generation and flow computation about a Martian entry vehicle
[NASA-CR-187032] N91-11042
Discussion paper on environmental hazards on the Moon, in low Earth orbit, and in low Mars orbit
[DE90-017854] N91-11646

MARS ENVIRONMENT
Discussion paper on environmental hazards on the Moon, in low Earth orbit, and in low Mars orbit
[DE90-017854] N91-11646

MARS PROBES
Design of a scientific probe for obtaining Mars surface material
[NASA-CR-186672] N91-11641

MARS SURFACE SAMPLES
Design of a scientific probe for obtaining Mars surface material
[NASA-CR-186672] N91-11641

MARTINGALES
On SLLN for martingales with deterministic quadratic variation
[CWI-BS-R8933] N91-11445

MASERS
The transfer of polarized radiation in astrophysical masers in the presence of magnetic fields N91-11629

MASS SPECTROSCOPY
Combined capillary electrophoresis and electrospray ionization mass spectrometry
[DE90-016535] N91-11079
Resonance ionization spectroscopy of molecular clusters using picosecond lasers
[DE90-017334] N91-11080
Applications of diode lasers to resonance ionization mass spectrometry
[DE90-017768] N91-11084
MASS TRANSFER
Conceptual design of an Open-Cycle Ocean Thermal Energy Conversion Net Power-Producing Experiment (OC-OTEC NPPE)
[DE90-000304] N91-11282
MASSIVELY PARALLEL PROCESSORS
Computational fluid dynamics on a massively parallel computer N91-10896
MATERIALS HANDLING
An expert system for automated robotic grasping
[DE90-010820] N91-11221
MATHEMATICAL LOGIC
A formal semantics for the preferred subtheories
[REPT-90-20] N91-11403
MATHEMATICAL MODELS
NASA Computational Fluid Dynamics Conference. Volume 1: Sessions 1-6
[NASA-CP-10038-VOL-1] N91-10839
A comparative study of Navier-Stokes codes for high-speed flows N91-10869
Modeling of high speed chemically reacting flow-fields N91-10870
Numerical aerodynamic simulation of the space shuttle ascent environment N91-10875
Simulation of turbomachinery flows N91-10880
A computational model for the prediction of hypersonic, reacting flows N91-10911
The aerodynamic effects of nozzle guide vane shock wave and wake passing on a transonic turbine rotor N91-10915
A numerical study of the effects of wind tunnel wall proximity on an airfoil model
[NASA-CR-187322] N91-10934
Assessing the feasibility, cost, and utility of developing models of human performance in aviation N91-10948
Comparison of a mathematical one-point model and a multi-point model of aircraft motion in moving air N91-10969
Wind models for flight simulation N91-10975
Aircraft trajectories: Computation, prediction, control, Volume 3. Part 9: Book of abstracts. Part 10: Bibliography. Part 11: List of contributors
[AGARD-AG-301-VOL-3-PT-9-11] N91-10978
Aircraft dynamics for air traffic control N91-10985
Optimization models and techniques to improve air traffic management N91-10988
Four dimensional navigation in air traffic with 4-D navigation aircraft N91-10991
Generation of a buoyant plume of artificial smoke for airplane tests
[DOT/FAA/CT-90/9] N91-11015
A new approach to the flight control system reconfiguration following a battle damage and/or generic failure on a control surface N91-11023
Flight simulation programs for space plane
[NAL-TM-594] N91-11035
Theoretical and numerical aspects of wave stability in combustion models
[ECL-89-21] N91-11088
Micromechanics of semi-brittle ceramics N91-11119
Voice communications in the cockpit noise environment: The role of active noise reduction N91-11140
Development of high performance sodium/metal chloride cells
[DE90-017668] N91-11159
Heat transfer in variable density, low Mach number, stagnating turbulent flows N91-11171
Heat pipe vapor dynamics N91-11179
The measurement and finite element analysis of the dynamic stiffness of non-uniform clearance, gas, thrust bearings
[DE90-015120] N91-11214
Dynamic analysis and control of lightweight manipulators with flexible parallel link mechanisms
[NASA-CR-187347] N91-11216
Contact and impact problems using adaptive finite element methods N91-11239
Short-crack growth behaviour in various aircraft materials
[AGARD-R-767] N91-11240
Texture analysis of 2090-T8E41 aluminum-lithium alloy sheet: Annex N91-11251
A three-dimensional solid element model for finite rotation of composite shells N91-11262
A theoretical investigation on structural, vibrational, and electronic properties of amorphous silicon
[DE90-018040] N91-11267
Remote sensing for marine activities
[BCRS-89-41] N91-11273
Evaluating the environmental impacts of the energy system: The ENPEP (Energy and Power Evaluation Program) approach
[DE90-017862] N91-11309
Fluctuating concentrations in atmospheric dispersion N91-11323
Modelling of large-scale unstable waves in the middle atmosphere N91-11327
Numerical models of 2-D and 3-D geophysical convection
[DE90-014979] N91-11330
A numerical model of polar mesospheric cloud formation and evolution N91-11337
Tropical cyclone simulations with the Betts convective adjustment scheme N91-11338
Parameterizations of microphysical processes in clouds
[DE90-017820] N91-11344
Study of the return-stroke phase of the gliding spark in ambient air
[ONERA-NT-1990-1] N91-11345
Wave data assimilation in a 3rd generation. Wave prediction model for the North Sea: An optimal control approach
[BCRS-89-22] N91-11348
Computer-Aided Structural Engineering (CASE) project: Investigation and design of U-frame structures using program CUFRBC. Volume C: User's guide for channels
[AD-A224388] N91-11395
Two and three dimensional magnetotelluric inversion
[DE90-016187] N91-11411
Symbolic manipulation software and the study of differential equations
[DE90-017674] N91-11413
Beta splines interpolation for DEM's
[INPE-5039-PRE/1572] N91-11415
Performance comparison of edge defection morphologies
[INPE-5012-TDL/400] N91-11422
Mathematical models of mixture properties: B-splines and optimization with form conditions
[ETN-90-97829] N91-11462
Arctic acoustics ultrasonic modeling studies
[AD-A224165] N91-11489
Numerical modeling of time domain 3-D problems in accelerator physics
[DE90-015625] N91-11511
Integrated optical components produced in GaAs and InP epitaxial layers using the photo-elastic effect N91-11518
On hydrodynamics of collisionless relativistic plasma in a strong magnetic field
[DE90-513926] N91-11543
Investigation on the projection by a Z-pinch discharge
[DE90-637548] N91-11544
Concepts in strong Langmuir turbulence theory
[DE91-000208] N91-11546
Analytic studies in nuclear astrophysics N91-11628
Application of the Ewald method to cosmological N-body simulations
[DE90-513789] N91-11637
Numerical calculations of the formation and evolution of giant planets with rotation N91-11643
The delta-Sobolev approach for modeling solar spectral irradiance and radiance N91-11650
Stability of emission line clouds in active galactic nuclei N91-11659
MATHEMATICAL PROGRAMMING
Fundamental concepts for utilization of the FPS-5410 array processor
[INPE-5091-RPE/624] N91-11388
MATRICES (CIRCUITS)
Fourteen x fourteen CCD array for optical intersatellite link tracking
[CNES-CT/DRT/TIT/OE-88/144] N91-11521
MATRICES (MATHEMATICS)
A method of using the inverse matrix for manipulator kinematics
[DE90-520210] N91-11227
Minimality of descriptor representations under external equivalence
[CWI-BS-R9002] N91-11446
MATRIX MATERIALS
Load transfer between fiber and matrix in carbon fiber reinforced plastic composites tensile behavior of an embedded single filament specimen
[ONERA-NT-1989-9] N91-11075
MATTER (PHYSICS)
Complementary aspects on matter-antimatter boundary layers
[TRITA-EPP-90-04] N91-11496
MAXIMUM ENTROPY METHOD
Maximum entropy imaging of radio astrophysical data N91-11610
MAXIMUM LIKELIHOOD ESTIMATES
Sidelobe blanking system performance: An extension of the theory leading to a new detection logic N91-11139
Classification of textures using the ARMA models and distances over the autocorrelation function
[INPE-5067-TDL/406] N91-11421
Stochastic approximation of the MLE for a spatial point pattern
[CWI-BS-R8926] N91-11475
MEAN SQUARE VALUES
Compensability of uncertain systems
[REPT-90-10] N91-11527
MEASURE AND INTEGRATION
A new lower bound for the de Bruijn-Newman constant
[CWI-NM-R8920] N91-11447
MEASURING INSTRUMENTS
Evaluation process for the examination of curved surface workpieces using coordinate measuring instruments
[ETN-90-97901] N91-11203
MECHANICAL ENGINEERING
Design and evaluation of thrust vectored nozzles using a multicomponent thrust stand
[NASA-CR-180474] N91-11050
MECHANICAL PROPERTIES
Relations between microstructure and mechanical behaviour of SiC/SiC composites: Interface effects on multiple cracking in multifilament materials
[ISAL-89-0098] N91-11065
MEMBRANES
The structure and function of membrane protein photosynthetic reaction center
[DE90-017795] N91-11353
MENSTRUATION
Relationship of menstrual history to altitude chamber decompression sickness N91-11379
MENTAL PERFORMANCE
Procedural error monitoring and smart checklists N91-10954
Graphical interfaces for cooperative planning systems N91-10956
MESOPAUSE
A numerical model of polar mesospheric cloud formation and evolution N91-11337
MESOSCALE PHENOMENA
The evolution of vortical patterns and vortices in mesoscale convective complexes N91-11319
Taiwan area mesoscale experiment: A guide to precipitation patterns during the 1987 field phase
[PB90-256355] N91-11336
MESOSPHERE
A numerical model of polar mesospheric cloud formation and evolution N91-11337
MESSAGE PROCESSING
Touchstone project Mach port: Milestone event Q4
[AD-A224057] N91-11481
METAL AIR BATTERIES
Zinc air battery development for electric vehicles
[DE90-016839] N91-11149
METAL COATINGS
Evaluation of thermal sprayed metallic coatings for use on the structures at Launch Complex 39
[NASA-TM-103807] N91-11121
METAL COMBUSTION
Aluminum metal combustion in water revealed by high speed microphotography
[DE90-017525] N91-11082
METAL CUTTING
Wear reduction in cutting tools: Tribological properties of hard coatings
[DE90-009705] N91-11212
METAL FATIGUE
Characterization of short fatigue cracks at notches in SiC particulate aluminum composite
[DE90-018043] N91-11071
Heat treatment study 2
[NASA-CR-184009] N91-11091
Short-crack growth behaviour in various aircraft materials
[AGARD-R-767] N91-11240
The growth of short fatigue cracks in 2024 and 2090 aluminium alloys under variable amplitude loading N91-11245
Short crack growth under realistic flight loading: Model predictions and experimental results for Al 2024 and Al-Li 2090 N91-11246
The growth of short cracks in 4340 steel and aluminum-lithium 2090 N91-11247
Short and long fatigue crack growth in 2024-T3 under Fokker 100 spectrum loading N91-11248
Growth of short fatigue cracks in 7075-T6 aluminum alloy N91-11249

METAL FILMS
Determination of hydrogen (deuterium) density profiles in thin metal films and multilayers by neutron reflection [DE90-007150] N91-11108
Magnetic properties of ultrathin epitaxial films of iron [DE90-017861] N91-11570
METAL HYDRIDES
Novel measurements of nuclear spin cross-relaxation in metal hydrides [DE90-018042] N91-11503
METAL IONS
High energy iron ion implantation into sapphire [DE90-017736] N91-11568
METAL MATRIX COMPOSITES
Characterization of short fatigue cracks at notches in SiC particulate aluminum composite [DE90-018043] N91-11071
Elastic/plastic analyses of advanced composites investigating the use of the compliant layer concept in reducing residual stresses resulting from processing [NASA-TM-103204] N91-11074
METAL OXIDES
Surface phases and their influence on metal-oxide interfaces [DE90-017608] N91-11099
METAL SHEETS
Texture analysis of 2090-T8E41 aluminum-lithium alloy sheet: Annex N91-11251
METAL SURFACES
Surface phases and their influence on metal-oxide interfaces [DE90-017608] N91-11099
An AGARD supplemental test programme on the behaviour of short cracks under constant amplitude and aircraft spectrum loading N91-11241
Secondary-electron yield measurements from metals impacted by high-velocity ions, electrons, and molecules [DE90-018023] N91-11502
METALLIZING
Thermal stress-induced grain boundary cavitation in narrow, aluminum alloy metallizations N91-11093
METALLURGY
Physical metallurgy and magnetic behavior of Cd stabilized bcc (beta) Gd alloys [DE91-000196] N91-11112
METALS
Defects in close-packed metals and alloys [DE90-017502] N91-11097
METEORITIC DAMAGE
Preliminary results from the advanced photovoltaic experiment flight test [NASA-TM-103269] N91-11058
METEOROIDS
Reexamination of data from the asteroid/meteoroid detector [NASA-CR-185875] N91-11619
METEOROLOGICAL PARAMETERS
Developments to enhance meteorological forecasting for air traffic services N91-11006
Meteorological characteristics of the El Nino/Southern Oscillation phenomenon N91-11340
Parameterizations of microphysical processes in clouds [DE90-017820] N91-11344
METEOROLOGY
Aircraft trajectories: Computation, prediction, control, volume 1. Part 1: Fundamentals. Part 2: Flight in critical atmospheric conditions. Part 3: Impact of new on-board technologies on aircraft operation [AGARD-AG-301-VOL-1-PT-1-3] N91-10967
Final shuttle-derived atmospheric database: Development and results from thirty-two flights [NASA-CR-185636] N91-11310
METHOD OF CHARACTERISTICS
Ion dynamics in semiconductors with self-consistent electronic densities N91-11556
METROLOGY
Center for electronics and electrical engineering technical publication announcements covering Center programs, July - September, 1989, with 1990 CEEE events calendar [PB90-206491] N91-11145
MICROBIOLOGY
JPRS report: Science and technology. USSR: Life sciences [JPRS-ULS-89-003] N91-11354
MICROCOMPUTERS
Beta splines interpolation for DEM's [INPE-5039-PRE/1572] N91-11415
MICROMECHANICS
Relations between microstructure and mechanical behaviour of SiC/SiC composites: Interface effects on multiple cracking in multifilament materials [ISAL-89-0098] N91-11065
Micromechanics of semi-brittle ceramics N91-11119
MICROMETEOROLOGY
Parameterizations of microphysical processes in clouds [DE90-017820] N91-11344
MICROMINIATURIZATION
Development of hermetic microminiature connectors [DE90-015562] N91-11153
MICROORGANISMS
Biosensors: Development status [MBB-Z-0305-90-PUB] N91-11201
MICROPHOTOGRAPHS
Aluminum metal combustion in water revealed by high speed microphotography [DE90-017525] N91-11082
MICROPROCESSORS
A microprocessor based charge control system for the simultaneous charging of several batteries with one charge controller [DE90-017089] N91-11157
Microprocessor system for temperature regulation and stabilization [DE90-634244] N91-11160
Touchstone project DELTA numeric node: Milestone event Q4 [AD-A224060] N91-11482
MICROSCOPY
X ray microprobe-microscopy [DE90-017327] N91-11520
MICROSTRUCTURE
Relations between microstructure and mechanical behaviour of SiC/SiC composites: Interface effects on multiple cracking in multifilament materials [ISAL-89-0098] N91-11065
Residual stress measurements and microstructural characterization of graphite-aluminum metal matrix composite N91-11068
Heat treatment study 2 [NASA-CR-184009] N91-11091
Deformation effects on the development of grain boundary chronium depletion (sensitization) in type 316 austenitic stainless steels [DE90-016130] N91-11092
Relationship of microstructure and tensile properties for neutron-irradiated vanadium alloys [DE90-017863] N91-11105
Influence of heat treatment on microstructure and properties of an advanced high temperature titanium alloy [PNR-90689] N91-11107
Microstructures of cubic Al2O3 precipitates in oxygen-implanted aluminum [DE91-000038] N91-11111
Micromechanics of semi-brittle ceramics N91-11119
A molecular dynamics model of the orthogonal cutting process [DE90-015911] N91-11230
Empirical proton-neutron interaction energies and nuclear structure [DE90-017632] N91-11500
Mechanical properties, fracture behavior, and grain-boundary chemistry of B-doped NiAl [DE90-015153] N91-11558
Long period superstructures in Pt3V and Cu3Pd: Towards a quantitative description [ONERA-NT-1990-2] N91-11587
MICROWAVE AMPLIFIERS
Increasing output power of an 850 MHz tetrode with a floating-deck modulator [DE91-000433] N91-11162
MICROWAVE FREQUENCIES
Planar orotron: A tunable, grating-based free electron laser N91-11208
MICROWAVE IMAGERY
Development of a validation model for the defense meteorological satellite program's special sensor microwave imager [NASA-CR-187369] N91-11342
MICROWAVE TRANSMISSION
High-power microwave transmission systems for electron cyclotron resonance plasma heating, volume 5 [DE90-017600] N91-11152
MICROWAVE TUBES
Planar orotron: A tunable, grating-based free electron laser N91-11208
MICROWAVES
Microwave sintering of nanocrystalline TiO2 [DE91-000375] N91-11115
Department of Defense methodology guidelines for High Power Microwave (HPM) susceptibility assessments [DE90-015405] N91-11147
Microwave background anisotropies and the primordial spectrum of cosmological density fluctuations [DE90-513791] N91-11639
MIDDLE ATMOSPHERE
Final shuttle-derived atmospheric database: Development and results from thirty-two flights [NASA-CR-185636] N91-11310
Modelling of large-scale unstable waves in the middle atmosphere N91-11327
MIGRATION
Molecular-dynamics study of grain-boundary migration in metals [DE90-017856] N91-11104
MILITARY OPERATIONS
Recruiting, Selection, Training and Military Operations of Female Aircrew [AGARD-CP-491] N91-11358
MILITARY TECHNOLOGY
Holding the edge: Maintaining the defense technology base. Volume 2: Appendixes [PB90-253345] N91-11597
MINKOWSKI SPACE
Mathematical morphology on homogeneous spaces. Part 1: The simply transitive case [CWI-AM-R8924-PT-1] N91-11439
MIRANDA
Tectonics of one-plate planets N91-11647
MIRROR FUSION
Theoretical and numerical studies in magnetic mirror fusion [DE90-017605] N91-11533
MIS (SEMICONDUCTORS)
MIS capacitor studies on silicon carbide single crystals [NASA-CR-187350] N91-11555
MISSILE BODIES
Solutions of thin-layer Navier-Stokes equations for missile configurations N91-11173
MISSILE CONFIGURATIONS
Solutions of thin-layer Navier-Stokes equations for missile configurations N91-11173
MISSILE LAUNCHERS
Marginal aircraft release disturbance on advanced missiles [MBB/FE121/S/PUB/329] N91-11016
MIXING
Three-dimensional computer simulation of non-reacting jet-gas flow mixing in an MHD second stage combustor [DE90-017831] N91-11537
Ion mixing of semiconductor superlattices [DE90-017769] N91-11569
MODEL REFERENCE ADAPTIVE CONTROL
Robot trajectory control with a model reference adaptive control system using tap delay filters N91-11217
MODELS
Integration of model and knowledge based diagnosis, with the example of a turbojet engine [ETN-90-97900] N91-11019
Energy models and national energy policy [DE90-017682] N91-11300
Development of a validation model for the defense meteorological satellite program's special sensor microwave imager [NASA-CR-187369] N91-11342
The derivation of a behavioural model for information retrieval system design N91-11599
MODULATION
Modeling and coding in aeronautical satellite channel [ETN-90-97899] N91-11137
MODULATION TRANSFER FUNCTION
Experimental manufacturing of performance evaluation system for solid image sensor [NAL-TM-591] N91-11200
MODULUS OF ELASTICITY
Indentation testing of thin films and hard materials [DE90-017758] N91-11224
MOLECULAR BIOLOGY
JPRS report: Science and technology. USSR: Life sciences [JPRS-ULS-89-003] N91-11354
MOLECULAR CLOUDS
The relationship of galaxy morphology to nuclear star formation in non-interacting spiral galaxies N91-11618
Stability of emission line clouds in active galactic nuclei N91-11659
MOLECULAR COLLISIONS
Secondary-electron yield measurements from metals impacted by high-velocity ions, electrons, and molecules [DE90-018023] N91-11502
MOLECULAR STRUCTURE
The structure and function of membrane protein photosynthetic reaction center [DE90-017795] N91-11353
Ion dynamics in semiconductors with self-consistent electronic densities N91-11556

Structure-property relationships for (beta)- and (kappa)-phase BEDT-TTF salts and their use in the synthesis of (kappa)-(BEDT-TTF)2Cu(N(CN)2)Br. A salt having the highest T(sub c) (inductive onset = 11.6 K, resistive, onset = 12.5 K) yet observed in an organic superconductor
[DE90-017804] N91-11582

MOLECULES
Molecular-dynamics study of grain-boundary migration in metals
[DE90-017856] N91-11104

MOLTEN SALTS
Processing of YBA2Cu3O7 tapes from a molten salt precursor
[DE90-017656] N91-11564
Structure of molten salts
[DE90-017704] N91-11566

MOLYBDENUM ALLOYS
High-resolution electron microscopy observations of athermal omega phase in Ti-Mo alloys
[DE90-017526] N91-11098
Nuclear magnetic resonance survey of hydrogen motion and electronic structure in (alpha)-phase (Nb-Mo)-H alloys
[DE90-018044] N91-11101

MOMENTUM TRANSFER
Numerical calculations of the formation and evolution of giant planets with rotation N91-11643

MONITORS
Fault monitoring N91-10950
Fault recovery recommendation N91-10952
Procedural error monitoring and smart checklists N91-10954
Plots of the 5-minute neutron monitor intensity and multiplicities recorded by the Rome 17-NM64, January 1990
[IFSI-90-5] N91-11653

MONTE CARLO METHOD
Random number stride in Monte Carlo calculations
[DE90-012000] N91-11465
A Monte Carlo boundary propagation method for the solution of Poisson's equation
[DE90-015060] N91-11466
Computation of standard deviations in Eigenvalue calculations
[DE90-017809] N91-11479
Measurement of radial ionization probability in microscopic volumes for 2.90 and 3.79 MeV alpha particles
[DE90-017509] N91-11498
MONT3E: A Monte Carlo electron heat transfer code
[DE90-012091] N91-11514
Astronomical applications of survival analysis N91-11615

MOON
Availability of hydrogen for lunar base activities
[NASA-CR-187367] N91-11644
Discussion paper on environmental hazards on the Moon, in low Earth orbit, and in low Mars orbit
[DE90-017854] N91-11646

MORPHOLOGY
Morphological analysis of ionomers
[DE90-017611] N91-11124
Methodology of remote sensing for monitoring modifications in the fluvial channel and updating nautical charts
[INPE-4863-TDL/374] N91-11277
Morphological and functional adaptation of personal equipment designed for female personnel N91-11374
Performance comparison of edge defection morphologies
[INPE-5012-TDL/400] N91-11422
Mathematical morphology on homogeneous spaces. Part 1: The simply transitive case
[CWI-AM-R8924-PT-1] N91-11439
Grey-level morphology
[CWI-AM-R9003] N91-11442
The relationship of galaxy morphology to nuclear star formation in non-interacting spiral galaxies N91-11618

MOUNTAINS
Enhancement of human tolerance of acute hypoxia by adaptation and intense training at high altitudes N91-11355

MULTIGRID METHODS
Damped, direction-dependent multigrid for hypersonic flow computations
[CWI-NM-R8922] N91-10905
Nonoverlapping composite meshes for multi-element air-foils N91-10908
Solutions of thin-layer Navier-Stokes equations for missile configurations N91-11173
Non-linear multigrid in 2-D semiconductor device simulation: The zero current case
[CWI-NM-R8917] N91-11553
A multigrid approach for the solution of the 2D semiconductor equations
[CWI-NM-R9003] N91-11554

MULTIPROCESSING (COMPUTERS)
SISAL versus FORTRAN: A comparison using the Livermore loops
[DE90-010872] N91-11414
Touchstone project: Milestone event Q4
[AD-A224034] N91-11480

MUON SPIN ROTATION
Muon SR studies on Sr2CuO2Cl2, La2CuO4, and Nd2CuO4: 2-D magnetism, local fields and muon sites
[DE90-018014] N91-11506

MUSCLES
Oscillation onset in neural delayed feedback
[DE90-015057] N91-11351

N

N-TYPE SEMICONDUCTORS
Nonparabolic conduction bands and masses in strained-single-quantum wells
[DE90-017028] N91-11560
Light-heavy-hole-mixing-induced selection rules for magneto-luminescence and valence-band energy dispersion in semiconductor quantum wells
[DE90-015989] N91-11573

NASA PROGRAMS
Simulation of turbomachinery flows N91-10880
Civil space technology initiative
[NASA-TM-103017] N91-11028

NATIONAL AIRSPACE SYSTEM
Aviation safety/automation program overview N91-10941
Airport system capacity strategic choices
[SR-226] N91-10979

NATIONAL AVIATION SYSTEM
Airport system capacity strategic choices
[SR-226] N91-10979

NATURAL GAS
Assessment of costs and benefits of flexible and alternative fuel use in the US transportation sector: Vehicle and fuel distribution requirements
[DE90-014847] N91-11127

NATURAL GAS EXPLORATION
Outer continental shelf environmental assessment program: Comprehensive bibliography, June 1990
[PB90-258609] N91-11350

NAUTICAL CHARTS
Methodology of remote sensing for monitoring modifications in the fluvial channel and updating nautical charts
[INPE-4863-TDL/374] N91-11277

NAVIER-STOKES EQUATION
Understanding transition and turbulence through direct simulations N91-10846
More accurate predictions with transonic Navier-Stokes methods through improved turbulence modeling N91-10850
Recent advances in Runge-Kutta schemes for solving 3-D Navier-Stokes equations N91-10851
Computations of three-dimensional steady and unsteady viscous incompressible flows N91-10852
Time dependent viscous incompressible Navier-Stokes equations N91-10854
CFD for applications to aircraft aeroelasticity N91-10855
Navier-Stokes solutions about the F/A-18 forebody-LEX configuration N91-10860
Navier-Stokes solutions for flows related to store separation N91-10861
A comparative study of Navier-Stokes codes for high-speed flows N91-10869
Modeling of high speed chemically reacting flow-fields N91-10870
Three-dimensional calculation of supersonic reacting flows using an LU scheme N91-10871
Progress in computing nozzle/plume flow fields N91-10872
Application of CFD codes for the simulation of scramjet combustor flowfields N91-10873
Prediction of turbine rotor-stator interaction using Navier-Stokes methods N91-10881
Numerical analysis of flow through oscillating cascade sections N91-10884
Simulation of powered-lift flows N91-10886
The use of a Navier-Stokes code in the wing design process N91-10889
Unstructured mesh solution of the Euler and Navier-Stokes equations N91-10892
Computational fluid dynamics on a massively parallel computer N91-10896
Temporal-adaptive Euler/Navier-Stokes algorithm for unsteady aerodynamic analysis of airfoils using unstructured dynamic meshes
[NASA-TM-102734] N91-10919
Development of a time-dependent incompressible Navier-Stokes solver based on a fractional-step method
[NASA-CR-187254] N91-11165
Solutions of thin-layer Navier-Stokes equations for missile configurations N91-11173
A global pressure relaxation for high speed laminar and turbulent flows N91-11177
Accuracy, convergence and stability of finite element algorithms for incompressible fluid flow N91-11184
Navier-Stokes analysis of transonic cascade flow
[NASA-TM-103624] N91-11192
Parallelization on a multi-processor system of a solving method for the unsteady Navier-Stokes equations at high Reynolds numbers
[ESA-TT-1116] N91-11197
Study of the return-stroke phase of the gliding spark in ambient air
[ONERA-NT-1990-1] N91-11345
NUMVEC FORTRAN library manual. Chapter: Partial differential equations. Routine: OEHPC
[CWI-NM-R8915] N91-11399

NAVIGATION
Mobile robots and intelligent motion control
[DE90-017312] N91-11226

NAVIGATION AIDS
How to fly windshear N91-10974

NEAR FIELDS
Investigation of the arcjet plume near field using electrostatic probes
[NASA-TM-103638] N91-11060

NEPTUNE (PLANET)
Whistlers in Neptune's magnetosphere: Evidence of atmospheric lightning
[NASA-CR-187324] N91-11642

NEPTUNE ATMOSPHERE
Whistlers in Neptune's magnetosphere: Evidence of atmospheric lightning
[NASA-CR-187324] N91-11642

NERVOUS SYSTEM
Oscillation onset in neural delayed feedback
[DE90-015057] N91-11351

NETWORK ANALYSIS
A hybrid pulse forming technique
[DE90-016860] N91-11156
OSI in the NASA science internet: An analysis
[NASA-CR-177561] N91-11425

NEURAL NETS
Classification of acoustic emission waveforms for nondestructive evaluation using neural networks
[DE90-017239] N91-11236
A unified framework for credit assignment
[DE90-011636] N91-11434

NEUROLOGY
Oscillation onset in neural delayed feedback
[DE90-015057] N91-11351

NEURONS
Oscillation onset in neural delayed feedback
[DE90-015057] N91-11351

NEUTRAL GASES
Laboratory experiments on the magnetic field and neutral density limits on CIV interaction
[TRITA-EPP-90-01] N91-11530

NEUTRINOS
Atmospheric neutrino fluxes
[DE90-508023] N91-11656

NEUTRON BEAMS
Microprocessor system for temperature regulation and stabilization
[DE90-634244] N91-11160

NEUTRON FLUX DENSITY
Plots of the 5-minute neutron monitor intensity and multiplicities recorded by the Rome 17-NM64, January 1990
[IFSI-90-5] N91-11653
Plots of the 5-minute neutron monitor intensity and multiplicities recorded by the Rome 17-NM64, February 1990
[IFSI-90-6] N91-11654

NEUTRON SCATTERING
Bragg intensities and diffuse scattering in Ag2Se: Molecular dynamics study
[DE90-017811] N91-11583

NEUTRON STARS
Long-term observations of three massive x ray binary transients: 4U0115+63, V0332+53, and GX301-2 N91-11612

NEUTRONS
Protection by WR-2721 and WR-151327 against late effects of gamma rays and neutrons
[DE90-017792] N91-11352

On the adequacy of message-passing parallel supercomputers for solving neutron transport problems
[DE90-016041] N91-11431

NEWTON METHODS
A potential reduction variant of Renegar's short-step path-following method for linear programming
[REPT-90-14] N91-11402

NICKEL
Chemical identification of icosahedral structure for cobalt and nickel clusters
[DE90-017688] N91-11100

NICKEL ALLOYS
Heat treatment study 2
[NASA-CR-184009] N91-11091
The stability of irradiation-induced defects in NiAl
[DE90-017744] N91-11103
Determination of pair potentials by analysis of diffuse scattering of the local field in Pd3V and Ni3V
[ONERA-NT-1989-7] N91-11117
Mechanical properties, fracture behavior, and grain-boundary chemistry of B-doped NiAl
[DE90-015153] N91-11558

NICKEL HYDROGEN BATTERIES
Terrestrial nickel/hydrogen battery evaluation
[DE90-014863] N91-11151

NIGHT VISION
Requirements of an HMS/D for a night-flying helicopter
[MBB-UD-0570-90-PUB] N91-11383

NIOBIUM
Analysis of deformation characteristics of a heavily deformed Cu-20 percent Nb composite
[DE90-018041] N91-11070

NIOBIUM ALLOYS
Nuclear magnetic resonance survey of hydrogen motion and electronic structure in (alpha)-phase (Nb-Mo)-H alloys
[DE90-018044] N91-11101
The transverse stress effect on the critical current of jelly-roll multifilamentary Nb3Al wires
[DE90-513710] N91-11581

NITRIC ACID
Atmospheric chemistry: Laboratory studies of kinetics of important reactions N91-11326

NITROGEN
Nitrogen and sulfur in irregular galaxies N91-11624

NITROGEN COMPOUNDS
Atmospheric chemistry: Laboratory studies of kinetics of important reactions N91-11326

NITROGEN DIOXIDE
Nitrogen dioxide and respiratory infection: Pilot investigations
[PB90-247339] N91-11357

NITROGEN OXIDES
Atmospheric chemistry: Laboratory studies of kinetics of important reactions N91-11326

NITROUS OXIDES
Recommended operating procedure No. 45: Analysis of nitrous oxide from combustion sources
[PB90-238502] N91-11078

NOCTILUCENT CLOUDS
Combined Release and Radiation Effects Satellite (CRRES): Atlas 1 (Atlas/Centaur-69) launch vehicle
[NASA-TM-103460] N91-11040

NOISE MEASUREMENT
Noise measurements from an ejector suppressor nozzle in the NASA Lewis 9- by 15-foot low speed wind tunnel
[NASA-TM-103628] N91-11493

NOISE POLLUTION
Commercial aircraft and the environment
[PNR-90687] N91-11307

NOISE PREDICTION (AIRCRAFT)
Prediction of the noise from a propeller at angle of attack
[NASA-TM-103627] N91-11495

NOISE REDUCTION
Test launch for turboaircraft engine. Description of the installation
[ILA-87-A-02] N91-11018
Voice communications in the cockpit noise environment: The role of active noise reduction N91-11140
Aircraft interior noise reduction by alternate resonance tuning
[NASA-CR-186879] N91-11488
Noise measurements from an ejector suppressor nozzle in the NASA Lewis 9- by 15-foot low speed wind tunnel
[NASA-TM-103628] N91-11493
The effect of swirl recovery vanes on the cruise noise of an advanced propeller
[NASA-TM-103625] N91-11494
Prediction of the noise from a propeller at angle of attack
[NASA-TM-103627] N91-11495

NONDESTRUCTIVE TESTS
Multiple-energy techniques in industrial computerized tomography
[DE90-017518] N91-11081
Classification of acoustic emission waveforms for nondestructive evaluation using neural networks
[DE90-017239] N91-11236

NONEQUILIBRIUM FLOW
The computation of thermo-chemical nonequilibrium hypersonic flows N91-10898

NONLINEAR EQUATIONS
Damped, direction-dependent multigrid for hypersonic flow computations
[CWI-NM-R8922] N91-10905
Comparison of a mathematical one-point model and a multi-point model of aircraft motion in moving air N91-10969

NONLINEAR FILTERS
Robot trajectory control with a model reference adaptive control system using tap delay filters N91-11217

NONLINEAR OPTICS
Production of uniform and well-confined beams by nonlinear optics
[DE91-000210] N91-11522

NONLINEAR PROGRAMMING
Boundary element methods in structural shape synthesis N91-11406

NONLINEAR SYSTEMS
Calculation of the pressure distribution on an oscillating airfoil in incompressible flow considering nonlinear effects N91-10926
Non-linear vibration of large, imperfect space structures N91-10930

NONLINEARITY
Non linear evolution of a second mode wave in supersonic boundary layers N91-10848
Numerical simulation of nonlinear development of instability waves
[E-4658] N91-10849
Application of dynamical systems theory to nonlinear aircraft dynamics N91-11014
Analysis of ductile crack extension in plastic fracture N91-11257

NONNEWTONIAN FLUIDS
Heat transfer and flow studies in an abrupt expansion pipe with non-Newtonian fluids N91-11180

NONUNIFORMITY
Critical aspects of trajectory prediction: Flight in non-uniform wind N91-10971

NORTH AMERICA
Estimation of seasonal and annual acidic deposition through aggregation of three-day episodic periods
[PB90-252628] N91-11303

NOTCHES
Characterization of short fatigue cracks at notches in SiC particulate aluminum composite
[DE90-018043] N91-11071
An AGARD supplemental test programme on the behaviour of short cracks under constant amplitude and aircraft spectrum loading N91-11241
Crack behaviour of 2024-T3, 2090-T8E41 and 7075-T6 under constant amplitude and different types of variable amplitude loading, especially Gaussian loading N91-11244

NOVAE
Novae as distance indicators
[NASA-CR-186278] N91-11605
Late stages in the evolution of classical novae
[NASA-TM-102969] N91-11633

NOZZLE DESIGN
Aerodynamic design optimization using computational fluid dynamics N91-11013
Design and evaluation of thrust vectored nozzles using a multicomponent thrust stand
[NASA-CR-180474] N91-11050

NOZZLE FLOW
Progress in computing nozzle/plume flow fields N91-10872
A combined Eulerian-Lagrangian two-phase analysis of the SSME HPOTP nozzle plug trajectories N91-10878
Study of asymmetric supersonic jet flow for ejectors
[DE90-015598] N91-10917
Noise measurements from an ejector suppressor nozzle in the NASA Lewis 9- by 15-foot low speed wind tunnel
[NASA-TM-103628] N91-11493

NOZZLE GEOMETRY
Study of asymmetric supersonic jet flow for ejectors
[DE90-015598] N91-10917

NUCLEAR ASTROPHYSICS
Analytic studies in nuclear astrophysics N91-11628

NUCLEAR FUSION
CTR plasma engineering studies
[DE90-017774] N91-11534

NUCLEAR MAGNETIC RESONANCE
Nuclear magnetic resonance survey of hydrogen motion and electronic structure in (alpha)-phase (Nb-Mo)-H alloys
[DE90-018044] N91-11101

NUCLEAR MEDICINE
ANSTO: Australian Nuclear Science and Technology Organization
[DE90-637389] N91-11507

NUCLEAR PHYSICS
ANSTO: Australian Nuclear Science and Technology Organization
[DE90-637389] N91-11507
Generalized back-action evasion schemes for the detection of weak classical forces
[IFSI-90-19] N91-11508

NUCLEAR POWER PLANTS
Development of the structural materials information center
[DE90-016521] N91-11603

NUCLEAR RELAXATION
Novel measurements of nuclear spin cross-relaxation in metal hydrides
[DE90-018042] N91-11503

NUCLEAR SPIN
Novel measurements of nuclear spin cross-relaxation in metal hydrides
[DE90-018042] N91-11503

NUCLEAR STRUCTURE
Empirical proton-neutron interaction energies and nuclear structure
[DE90-017632] N91-11500

NUCLEATION
Theory of homogeneous nucleation from the vapor phase
[MPIS-MITT-93] N91-11077
Energetics of 60 days predictions with the EZMW-T21 model in its mean temporary development and its relationship to forecast skill
[MITT-71] N91-11335
A numerical model of polar mesospheric cloud formation and evolution N91-11337
A study of the chemical, mechanical, and surface properties of thin films of hydrogenated amorphous carbon
[DE91-000357] N91-11585

NUMBER THEORY
Improved techniques for lower bounds for odd perfect numbers
[CWI-NM-R8921] N91-11448

NUMERICAL ANALYSIS
Examination of numerical formulations to describe complex geometry turbulent elliptical flows, using contour matched coordinates
[ETN-90-97864] N91-11169
Numerical models of 2-D and 3-D geophysical convection
[DE90-014979] N91-11330
The linearly implicit Euler method for quasi-linear parabolic differential equations
[CWI-NM-R9002] N91-11451

NUMERICAL CONTROL
A microprocessor based charge control system for the simultaneous charging of several batteries with one charge controller
[DE90-017089] N91-11157

NUMERICAL INTEGRATION
Stabilization of a time integrator for the 3D shallow water equations by smoothing techniques
[CWI-NM-R8916] N91-11167

NUMERICAL STABILITY
Accuracy, convergence and stability of finite element algorithms for incompressible fluid flow N91-11184
A-stable parallel block methods
[CWI-NM-R8918] N91-11427
Convergence of linear multistep and one-leg methods for stiff nonlinear initial value problems
[CWI-NM-R8924] N91-11450

NUMERICAL WEATHER FORECASTING
Generalized dynamic normal mode initialization N91-11341

NUSSELT NUMBER
An experimental study of natural convection heat transfer from a horizontal cylinder array vertically aligned to and confined by a single wall and two walls N91-11178

O

OBSTACLE AVOIDANCE
Instantaneous kinematics, motion planning and mechanical efficiency of a quadrupedal walking machine N91-11218

OCEAN BOTTOM
Surface and bottom temperature distribution for the Northeast continental shelf
[PB90-252172] N91-11349
OCEAN CURRENTS
A compendium of environmental data collected during the Iceshelf-88 exercise
[AD-A223518] N91-11346
OCEAN DYNAMICS
Azimuthal resolution degradation due to ocean surface motion in focused arrays and SARS
[AD-A223315] N91-11135
OCEAN MODELS
Nominal ocean tide models for TOPEX precise orbit determination N91-11029
Gulf of Maine sea surface topography from GEOSAT altimetry N91-11271
Notes on the NOARL nowcast for the 1989 to 1990 El Nino forced by FNOC winds
[AD-A223520] N91-11347
OCEAN SURFACE
Azimuthal resolution degradation due to ocean surface motion in focused arrays and SARS
[AD-A223315] N91-11135
Gulf of Maine sea surface topography from GEOSAT altimetry N91-11271
Radiometric observation of the atmospheric boundary layer (the ROSSA Project) N91-11324
OCEAN THERMAL ENERGY CONVERSION
Conceptual design of an Open-Cycle Ocean Thermal Energy Conversion Net Power-Producing Experiment (OC-OTEC NPPE)
[DE90-000304] N91-11282
Ocean thermal energy conversion: Perspective and status
[DE90-017665] N91-11299
OCEANOGRAPHIC PARAMETERS
A compendium of environmental data collected during the Iceshelf-88 exercise
[AD-A223518] N91-11346
OFFSHORE ENERGY SOURCES
Outer continental shelf environmental assessment program: Comprehensive bibliography, June 1990
[PB90-258609] N91-11350
OIL EXPLORATION
Outer continental shelf environmental assessment program: Comprehensive bibliography, June 1990
[PB90-258609] N91-11350
ON-LINE SYSTEMS
Optimum on-line handling of air traffic over Western Europe N91-10982
Prediction of aircraft trajectories N91-10984
Generation of aircraft trajectories for on-line operation: Methods, techniques, and tools N91-10987
Optimization models and techniques to improve air traffic management N91-10988
The air traffic controller facing automation: Conflict or cooperation N91-11001
Online searching in public libraries: A comparative study of performance N91-11598
Design, develop, test, and implement an on-line research and education information service
[DE90-017654] N91-11604
OPERATING SYSTEMS (COMPUTERS)
Inflated speedups in parallel simulations via malloc()
[NASA-CR-182104] N91-11397
OPERATORS (MATHEMATICS)
Grey-level morphology
[CWI-AM-R9003] N91-11442
OPTICAL COMMUNICATION
Fourteen x fourteen CCD array for optical intersatellite link tracking
[CNES-CT/DRT/TIT/OE-88/144] N91-11521
OPTICAL DATA PROCESSING
Integrated optical components for optical fibre sensors N91-11519
OPTICAL EQUIPMENT
Integrated optical components produced in GaAs and InP epitaxial layers using the photo-elastic effect N91-11518
OPTICAL FILTERS
Integrated optical components for optical fibre sensors N91-11519
OPTICAL MEASUREMENT
Optical far-field measurements of extremely high dynamic to investigate the roughness of front faces of single-mode fiber connectors
[FI-452-TB-67] N91-11517
OPTICAL PROPERTIES
Electronic processes in thin film PV materials
[DE90-000359] N91-11295
Advanced infrared optically black baffle materials
[DE91-000561] N91-11523
OPTICAL RADAR
Wind lidar for tropical climatology
[CNES-CT/DRT/TIT/IO-88/126] N91-11334
OPTICAL WAVEGUIDES
Integrated optical components produced in GaAs and InP epitaxial layers using the photo-elastic effect N91-11518
OPTIMAL CONTROL
Optimal trajectories of aircraft and spacecraft N91-10968
Computation of sub-optimal real-time guidance laws for combat aircraft trajectories N91-10970
H infinity-design and the improvement of helicopter handling qualities N91-11024
Optimal control design by Volterra Series and its application to spacecraft maneuvers N91-11044
Wave data assimilation in a 3rd generation. Wave prediction model for the North Sea: An optimal control approach
[BCRS-89-22] N91-11348
Constrained optimization approach to feedback control of state-augmented systems N91-11433
A synthesis of time and frequency domain methods for the control of infinite-dimensional systems: A system theoretic approach
[W-8912] N91-11456
OPTIMIZATION
Structural analysis and optimization of a propfan-blade by use of the finite element method N91-10924
Computation of sub-optimal real-time guidance laws for combat aircraft trajectories N91-10970
Aerodynamic design optimization using computational fluid dynamics N91-11013
Controller methodologies for integrated control/structure design optimization of large flexible structures N91-11043
Characterization and optimization of a pneumatic injector for a 60 bar combustion chamber
[ETN-90-97580] N91-11076
Fabrication and optimization of a whiskerless Schottky barrier diode for submillimeter wave applications
[NASA-CR-186381] N91-11144
Minimizing maximum earliness and maximum lateness on a single machine
[CWI-BS-R9001] N91-11398
A potential reduction variant of Renegar's short-step path-following method for linear programming
[REPT-90-14] N91-11402
SISAL versus FORTRAN: A comparison using the Livermore loops
[DE90-010872] N91-11414
Constrained optimization approach to feedback control of state-augmented systems N91-11433
Mathematical models of mixture properties: B-splines and optimization with form conditions
[ETN-90-97829] N91-11462
ORBIT CALCULATION
Nominal ocean tide models for TOPEX precise orbit determination N91-11029
ORBITAL MECHANICS
Design of a scientific probe for obtaining Mars surface material
[NASA-CR-186672] N91-11641
ORBITAL SERVICING
Automated Fluid Interface System (AFIS)
[NASA-CR-183969] N91-11031
ORDER-DISORDER TRANSFORMATIONS
Ion dynamics in semiconductors with self-consistent electronic densities N91-11556
ORGANIC PHOSPHORUS COMPOUNDS
A protein coated piezoelectric crystal detector
[AD-A223848] N91-11552
ORGANIZATIONS
ANSTO: Australian Nuclear Science and Technology Organization
[DE90-637389] N91-11507
Activities report of the Technical Research Centre of Finland
[ISBN-951-38-3647] N91-11665
ORGANOMETALLIC COMPOUNDS
The transuranium elements: Members of the 5f series
[DE90-017680] N91-11575
ORTHOTROPIC CYLINDERS
ution of the equivalent space with Bessel integral equation for the fractured orthotropic disk ution of the 'equivalent space' with Bessel integral equation for the fractured orthotropic disk
[ISSN-0932-8599] N91-11253
OSCILLATIONS
Numerical analysis of flow through oscillating cascade sections N91-10884
OUTPUT
System identification of lossless layered media from input-output data
[CWI-BS-R8929] N91-11166
OXIDATION
Projective scales against high temperature corrosion
[ETN-90-97770] N91-11116
Three-dimensional fluid flow in JFTOT (Jet Fuel Thermal Oxidation Tester)
[DE90-010929] N91-11128
OXIDE FILMS
Surface phases and their influence on metal-oxide interfaces
[DE90-017608] N91-11099
Computer-controlled ion beam deposition systems for high T(sub c) superconductor and other multi-component oxide thin films and layered structures
[DE90-017798] N91-11577
OXYGEN
Theoritical and experimental study of kinetics mechanisms in the Chemical Oxygen-Iodine Laser (COIL)
[ONERA-P-1990-1] N91-11211
Excess oxygen defects in layered cuprates
[DE90-017669] N91-11565
OXYGEN ATOMS
Graphite fluoride fibers and their applications in the space industry
[NASA-TM-103265] N91-11062
OXYGEN PRODUCTION
Three-Man Solid Electrolyte Carbon Dioxide Electrolysis Breadboard
[NASA-CR-185612] N91-11148
OZONE
ECC ozonesonde observations at South Pole, Antarctica during 1989
[PB90-258914] N91-11302

P

P-TYPE SEMICONDUCTORS
Photoluminescence studies of In(x)Ga(1-x)As/Al(y)Ga(1-y)As strained-layer structures
[DE90-017031] N91-11561
PAIR PRODUCTION
Numerical studies of electron scattering in astrophysics N91-11625
PALLADIUM ALLOYS
Determination of pair potentials by analysis of diffuse scattering of the local field in Pd3V and Ni3V
[ONERA-NT-1989-7] N91-11117
PANEL METHOD (FLUID DYNAMICS)
Prediction of effects of wing contour modifications on low-speed maximum lift and transonic performance for the EA-6B aircraft
[NASA-TP-3046] N91-10902
Development and application of the time domain panel method N91-11010
A viscous-inviscid interactive method for unsteady flows N91-11172
PANELS
TranAir: Recent advances and applications N91-10862
Douglas flight deck design philosophy N91-10939
PARABOLIC DIFFERENTIAL EQUATIONS
A static-regridding method for two-dimensional parabolic partial differential equations
[CWI-NM-R8923] N91-11449
The linearly implicit Euler method for quasi-linear parabolic differential equations
[CWI-NM-R9002] N91-11451
PARALLEL COMPUTERS
Performance of a parallel code for the Euler equations on hypercube computers
[NASA-TM-102260] N91-11384
A-stable parallel block methods
[CWI-NM-R8918] N91-11427
Touchstone project DELTA numeric node: Milestone event Q4
[AD-A224060] N91-11482
PARALLEL PROCESSING (COMPUTERS)
Performance of a parallel code for the Euler equations on hypercube computers
[NASA-TM-102260] N91-11384
Inflated speedups in parallel simulations via malloc()
[NASA-CR-182104] N91-11397
Parallel performance models for the nodal transport method on the hypercube
[DE90-015162] N91-11408
SISAL versus FORTRAN: A comparison using the Livermore loops
[DE90-010872] N91-11414
A-stable parallel block methods
[CWI-NM-R8918] N91-11427
Iterated Runge-Kutta methods on parallel computers
[CWI-NM-R9001] N91-11428
Parallelized reliability estimation of reconfigurable computer networks
[NASA-CR-182101] N91-11430
On the adequacy of message-passing parallel supercomputers for solving neutron transport problems
[DE90-016041] N91-11431

A Monte Carlo boundary propagation method for the solution of Poisson's equation
[DE90-015060] N91-11466

PARALLEL PROGRAMMING
Parallelization on a multi-processor system of a solving method for the unsteady Navier-Stokes equations at high Reynolds numbers
[ESA-TT-1116] N91-11197
Iterated Runge-Kutta methods on parallel computers
[CWI-NM-R9001] N91-11428
A fast parallel recognizer
[REPT-90-16] N91-11429
On the adequacy of message-passing parallel supercomputers for solving neutron transport problems
[DE90-016041] N91-11431
Modeling histogram data with piecewise polynomials
[DE90-018037] N91-11467

PARAMETER IDENTIFICATION
Comparison of a mathematical one-point model and a multi-point model of aircraft motion in moving air
N91-10969
System identification of lossless layered media from input-output data
[CWI-BS-R8929] N91-11166
Generalized back-action evasion schemes for the detection of weak classical forces
[IFSI-90-19] N91-11508

PARAMETERIZATION
Dynamic model error analysis of robot manipulators
N91-11220
Parameterizations of microphysical processes in clouds
[DE90-017820] N91-11344

PARSING ALGORITHMS
A fast parallel recognizer
[REPT-90-16] N91-11429

PARTIAL DIFFERENTIAL EQUATIONS
Stabilization of a time integrator for the 3D shallow water equations by smoothing techniques
[CWI-NM-R8916] N91-11167
NUMVEC FORTRAN library manual. Chapter: Partial differential equations. Routine: OEHPC
[CWI-NM-R8915] N91-11399
Modeling histogram data with piecewise polynomials
[DE90-018037] N91-11467
Convergence of solutions of one-dimensional stochastic heat equations
[REPT-90-40] N91-11478

PARTICLE ACCELERATORS
Numerical modeling of time domain 3-D problems in accelerator physics
[DE90-015625] N91-11511

PARTICLE BEAMS
Multiple Application Intense Particle Beam Project
[INPE-4576-RPE/568] N91-11510
Production of uniform and well-confined beams by nonlinear optics
[DE91-000210] N91-11522

PARTICLE COLLISIONS
The evolution of resistive ballooning modes in the banana-plateau collisionality regime
[DE90-016672] N91-11525

PARTICLE DENSITY (CONCENTRATION)
Mathematical treatment of the spherical stereology
[PB90-257593] N91-11464

PARTICLE DIFFUSION
The generalized diffusion theory of simply deformable particle-fluid two-phase flows
[MPIS-7/1990] N91-11193

PARTICLE ENERGY
Multiple Application Intense Particle Beam Project
[INPE-4576-RPE/568] N91-11510

PARTICLE FLUX DENSITY
Atmospheric neutrino fluxes
[DE90-508023] N91-11656

PARTICLE INTERACTIONS
Empirical proton-neutron interaction energies and nuclear structure
[DE90-017632] N91-11500
Capture and transfer of pions in hydrogenous materials
[DE90-017756] N91-11505
The influence of ionized impurities on the transport properties of a two-dimensional electron gas
[ETN-90-97752] N91-11586

PARTICLE SIZE DISTRIBUTION
Mathematical treatment of the spherical stereology
[PB90-257593] N91-11464

PARTICLE THEORY
Research program in elementary particle theory
[DE90-017284] N91-11497

PARTICLES
Theoretical and numerical studies of constitutive relations for frictional granular flow
[DE90-009662] N91-11194

PASSIVITY
Laser Raman spectroscopy for in-situ analysis of corrosion films on metals
[DE90-017822] N91-11109

PATHS
Decomposition of the n-cube into paths
[MEMO-855] N91-11468

PATTERN RECOGNITION
Research into language concepts for the mission control center
[NASA-CR-185928] N91-11392
On three dimensional object recognition and pose-determination: An abstraction based approach
[NASA-CR-186894] N91-11396

PAYLOAD INTEGRATION
Data base architecture for instrument characteristics critical to spacecraft conceptual design
[NASA-TM-4213] N91-11391

PEEK
Potential for advanced thermoplastic composites in space systems
[DE90-014447] N91-11069

PENETRATION
Tethered rocket as a vehicle for penetration and impact testing: Development report
[DE90-014865] N91-11057
Penetration in GTA welding
[DE90-008971] N91-11213

PERCEPTION
Determinants of dual-task interference and resource theories in cognitive psychology
[ESA-TT-1127] N91-11381

PERCOLATION
Connected components in supercritical Mandelbrot percolation
[REPT-90-15] N91-11452

PERFORMANCE PREDICTION
Conjugate (solid/fluid) computational fluid dynamics analysis of the space shuttle solid rocket motor nozzle/case and case field joints N91-10879
Turbine stage aerodynamics and heat transfer prediction N91-10682
Prediction of effects of wing contour modifications on low-speed maximum lift and transonic performance for the EA-6B aircraft
[NASA-TP-3046] N91-10902
Experimental manufacturing of performance evaluation system for solid image sensor
[NAL-TM-591] N91-11200
Short crack growth under realistic flight loading: Model predictions and experimental results for Al 2024 and Al-Li 2090 N91-11246
Performance and cost projections for advanced wind turbines
[DE90-000370] N91-11286
Surrogate oracles, generalized dependency and simpler models
[NASA-CR-187360] N91-11407

PERFORMANCE TESTS
Flight evaluation test of the PAPI (Precision Approach Path Indicator) System
[NAL-TM-592] N91-10966
Flight simulator evaluation test of multi-functional display unit
[NAL-TM-596] N91-11026
Railgun performance with a two-stage light-gas gun injector
[DE90-016211] N91-11032
RL10 ignition limits test for Shuttle Centaur
[NASA-CR-183199] N91-11049
Fabrication and optimization of a whiskerless Schottky barrier diode for submillimeter wave applications
[NASA-CR-186381] N91-11144
Terrestrial nickel/hydrogen battery evaluation
[DE90-014883] N91-11151
An automated linearity test for direct voltage calibrators
[DE90-016927] N91-11204
The measurement and finite element analysis of the dynamic stiffness of non-uniform clearance, gas, thrust bearings
[DE90-015120] N91-11214
Experimental and theoretical studies of friction and heat transfer in rough passages
[DE90-016302] N91-11223
Texture analysis of 2090-T8E41 aluminum-lithium alloy sheet: Annex N91-11251
Naval aviation selection test scores and female aviator performance N91-11363

PERSONALITY
Sex differences concerning performance and personality traits of applicants for highly qualified operator functions in aviation N91-11364

PERSONNEL SELECTION
Recruiting, Selection, Training and Military Operations of Female Aircrew
[AGARD-CP-491] N91-11358
The selection, training, and operational work of female helicopter pilots in the Royal Netherlands Air Force
N91-11361
Naval aviation selection test scores and female aviator performance N91-11363
Sex differences concerning performance and personality traits of applicants for highly qualified operator functions in aviation N91-11364
Female aircrew: The Canadian forces experience
N91-11367

PERTURBATION
Non linear evolution of a second mode wave in supersonic boundary layers N91-10848

PERTURBATION THEORY
CFD for applications to aircraft aeroelasticity
N91-10855
Numerical calculations of the formation and evolution of giant planets with rotation N91-11643

PH
In-situ pore structure analysis during aging and drying of gels
[DE91-000044] N91-11089

PHASE DIAGRAMS
Long period superstructures in Pt3V and Cu3Pd: Towards a quantitative description
[ONERA-NT-1990-2] N91-11587

PHASE LOCKED SYSTEMS
Advanced technology satellite demodulator development
[NASA-CR-185127] N91-11134

PHASE SHIFT KEYING
Advanced technology satellite demodulator development
[NASA-CR-185127] N91-11134

PHASE TRANSFORMATIONS
Effects of electric current and field on the behavior of metallic materials N91-11095
High-resolution electron microscopy observations of athermal omega phase in Ti-Mo alloys
[DE90-017526] N91-11098

PHONONS
Surface anharmonicity: Temperature dependence of phonon energies on Cu(110)
[DE90-017735] N91-11567

PHOTOCHEMICAL REACTIONS
Seasonal variations in the latitudinal distribution of tropospheric carbon monoxide, 1986 to 1988
N91-11328

PHOTOELECTRIC EFFECT
Structure of amorphous-silicon and germanium alloy films
[DE90-000355] N91-11557

PHOTOELECTRICITY
Experimental manufacturing of performance evaluation system for solid image sensor
[NAL-TM-591] N91-11200

PHOTOIONIZATION
Laser applications for high-T(sub c) superconductors
[DE90-017743] N91-11209

PHOTOLUMINESCENCE
Research on high-efficiency, multiple-gap, multi-junction amorphous silicon-based alloy thin-film solar cells
[DE90-000364] N91-11296
Photoluminescence studies of In(x)Ga(1-x)As/Al(y)Ga(1-y)As strained-layer structures
[DE90-017031] N91-11561

PHOTON-ELECTRON INTERACTION
Numerical studies of electron scattering in astrophysics N91-11625

PHOTONUCLEAR REACTIONS
A new site for the astrophysical gamma-process
[DE90-017519] N91-11635

PHOTOSYNTHESIS
The structure and function of membrane protein photosynthetic reaction center
[DE90-017795] N91-11353

PHOTOVOLTAIC CELLS
Interchange of researchers on alternative energy of petroleum in EC countries
[DE91-701468] N91-11130
Generic quality assurance/quality control guide for photovoltaic concentrator design, development and system installation
[DE90-017040] N91-11290
Electronic processes in thin film PV materials
[DE90-000359] N91-11295

PHYSICAL FITNESS
Review of female applicant aircrew in the Belgian forces N91-11368

PHYSIOLOGICAL FACTORS
Impact of new technology on operational interface: From design aims to flight evaluation and measurement N91-10977
PHYSIOLOGY
Problems posed by the adaptation of physiological protective equipment for female combat pilots N91-11372
PIEZOELECTRIC CRYSTALS
A protein coated piezoelectric crystal detector [AD-A223848] N91-11552
PILOT PERFORMANCE
Human factors of the high technology cockpit N91-10943
Assessing information transfer in full mission flight simulations N91-10946
Fault diagnosis N91-10951
Procedural error monitoring and smart checklists N91-10954
Impact of new technology on operational interface: From design aims to flight evaluation and measurement N91-10977
Comparison of male and female USAF pilot candidates N91-11362
Pregnancy: A cause for grounding of female air crew N91-11376
PILOT TRAINING
Comparison of male and female USAF pilot candidates N91-11362
PIONEER VENUS 1 SPACECRAFT
Identification and analysis of cosmic gamma ray bursts from Pioneer Venus Orbiter N91-11657
PIONS
Capture and transfer of pions in hydrogenous materials [DE90-017756] N91-11505
PIPE FLOW
Enhancement of forced convection heat transfer in tubes using staged tangential flow injection [PB90-247594] N91-11170
Heat pipe vapor dynamics N91-11179
Heat transfer and flow studies in an abrupt expansion pipe with non-Newtonian fluids N91-11180
PIPES (TUBES)
An experimental study of natural convection heat transfer from a horizontal cylinder array vertically aligned to and confined by a single wall and two walls N91-11178
PISTONS
Injector and valve train friction studies: Cummins L-10 engine [DE90-017288] N91-11225
PITCH (INCLINATION)
Marginal aircraft release disturbance on advanced missiles [MBB/FE121/S/PUB/329] N91-11016
PITCHING MOMENTS
A viscous-inviscid interactive method for unsteady flows N91-11172
PIXELS
Integration of multispectral and pancromatic channels of HRV (SPOT) sensor for obtaining color compositions with a spatial resolution of approximately 10 m [INPE-5035-TDL/403] N91-11278
PLANE STRESS
Performance of finite dynamic elements for composite materials in plane stress N91-11260
PLANETARY BOUNDARY LAYER
Planetary boundary layer dynamics over the Amazon rain forest N91-11317
PLANETARY EVOLUTION
Numerical calculations of the formation and evolution of giant planets with rotation N91-11643
PLANETARY IONOSPHERES
The SIM.PL.EX. plasma chamber (Simulatori di Plasma Extraterrestre) [IFSI-90-8] N91-11551
Testing for lightning as a source of radio bursts observed on the nightside of Venus [NASA-CR-187364] N91-11645
PLANETARY MAGNETOSPHERES
Whistlers in Neptune's magnetosphere: Evidence of atmospheric lightning [NASA-CR-187324] N91-11642
PLANETARY NEBULAE
From red giants to planetary nebulae: Asymmetries, dust, and polarization N91-11622
PLANETARY ROTATION
Numerical calculations of the formation and evolution of giant planets with rotation N91-11643
PLANETARY WAVES
Large-scale dynamics and transport in the stratosphere [NASA-CR-187327] N91-11311
PLASMA ACCELERATION
The plasma universe [TRITA-EPP-89-08] N91-11529
PLASMA CONTROL
High-power microwave transmission systems for electron cyclotron resonance plasma heating, volume 5 [DE90-017600] N91-11152
Computer and engineering calculations of Brazilian Tokamak-2 [DE90-628758] N91-11524
The evolution of resistive ballooning modes in the banana-plateau collisionality regime [DE90-016672] N91-11525
Confinement and fluctuations in the MST (Madison Symmetric Torus) reversed field pinch [DE90-018019] N91-11535
Collisional processes of interest in MFE plasma research [DE91-000598] N91-11549
PLASMA DENSITY
Complementary aspects on matter-antimatter boundary layers [TRITA-EPP-90-04] N91-11496
PLASMA DIAGNOSTICS
Data analysis of hollow cathode experiment to support electrodynamic tether applications [IFSI-89-16] N91-11047
Multiple Application Intense Particle Beam Project [INPE-4576-RPE/568] N91-11510
Collisional processes of interest in MFE plasma research [DE91-000598] N91-11549
The SIM.PL.EX. plasma chamber (Simulatori di Plasma Extraterrestre) [IFSI-90-8] N91-11551
PLASMA DIODES
Potential drops supported by ion density cavities in the dynamic response of plasma diode to an applied field [TRITA-EPP-90-03] N91-11531
PLASMA ELECTRODES
Investigation on the projection by a Z-pinch discharge [DE90-637548] N91-11544
PLASMA EQUILIBRIUM
Natural current profiles in a tokamak [DE91-000128] N91-11540
Complete fluid equations for low-n singular modes in axisymmetric torodial plasmas [DE91-000176] N91-11545
Nonlinear saturation of ideal interchange modes in a sheared magnetic field [DE91-000575] N91-11548
On the origin of cosmological magnetic fields [DE90-017617] N91-11634
PLASMA HEATING
Collisional processes of interest in MFE plasma research [DE91-000598] N91-11549
PLASMA INTERACTION EXPERIMENT
Data analysis of hollow cathode experiment to support electrodynamic tether applications [IFSI-89-16] N91-11047
PLASMA INTERACTIONS
Computer and engineering calculations of Brazilian Tokamak-2 [DE90-628758] N91-11524
Laboratory experiments on the magnetic field and neutral density limits on CIV interaction [TRITA-EPP-90-01] N91-11530
Concepts in strong Langmuir turbulence theory [DE91-000208] N91-11546
A two dimensional multisonic model of plasma interaction for cometary atmosphere with solar wind [MITT-69] N91-11621
PLASMA SHEATHS
Ion dynamics in the plasma mantle [IFSI-89-20] N91-11550
PLASMA SPECTRA
A combined wave distribution function and stability analysis of Viking particle and low-frequency wave data [IRF-PREPRINT-115] N91-11541
PLASMA TURBULENCE
Concepts in strong Langmuir turbulence theory [DE91-000208] N91-11546
PLASMA WAVES
A combined wave distribution function and stability analysis of Viking particle and low-frequency wave data [IRF-PREPRINT-115] N91-11541
Concepts in strong Langmuir turbulence theory [DE91-000208] N91-11546
Whistlers in Neptune's magnetosphere: Evidence of atmospheric lightning [NASA-CR-187324] N91-11642
PLASMAS (PHYSICS)
Multiple Application Intense Particle Beam Project [INPE-4576-RPE/568] N91-11510
The plasma universe [TRITA-EPP-89-08] N91-11529
A design method of divertor in tokamak reactors [NIFS-36] N91-11532
CTR plasma engineering studies [DE90-017774] N91-11534
Exploration of decreased solar activity state (small intensity activity) in the corona and chromosphere [INPE-5059-TDL/405] N91-11652
PLASTIC DEFORMATION
Effects of electric current and field on the behavior of metallic materials N91-11095
A molecular dynamics model of the orthogonal cutting process [DE90-015911] N91-11230
Analysis of ductile crack extension in plastic fracture N91-11257
Boundary integral equations for dynamic fracture problems N91-11259
PLUGS
A combined Eulerian-Lagrangian two-phase analysis of the SSME HPOTP nozzle plug trajectories N91-10878
PLUMES
Progress in computing nozzle/plume flow fields N91-10872
Generation of a buoyant plume of artificial smoke for airplane tests [DOT/FAA/CT-90/9] N91-11015
Investigation of the arcjet plume near field using electrostatic probes [NASA-TM-103638] N91-11060
POINTING CONTROL SYSTEMS
Thermal-distortion analysis of a spacecraft box truss in geostationary orbit [NASA-TP-3054] N91-11041
Precision tethered satellite attitude control N91-11046
POISSON EQUATION
A Monte Carlo boundary propagation method for the solution of Poisson's equation [DE90-015060] N91-11466
Non-linear multigrid in 2-D semiconductor device simulation: The zero current case [CWI-NM-R8917] N91-11553
A multigrid approach for the solution of the 2D semiconductor equations [CWI-NM-R9003] N91-11554
POLARITY
Satellite elevation magnetic anomalies and their use in tectonic studies N91-11272
POLARIZATION (WAVES)
Reexamination of data from the asteroid/meteoroid detector [NASA-CR-185875] N91-11619
From red giants to planetary nebulae: Asymmetries, dust, and polarization N91-11622
POLARIZED RADIATION
The transfer of polarized radiation in astrophysical masers in the presence of magnetic fields N91-11629
Polarized radiation from inhomogeneous shocks N91-11662
POLARIZERS
Integrated optical components for optical fibre sensors N91-11519
POLLUTION TRANSPORT
Estimation of seasonal and annual acidic deposition through aggregation of three-day episodic periods [PB90-252628] N91-11303
Fluctuating concentrations in atmospheric dispersion N91-11323
POLYATOMIC MOLECULES
Chemical identification of icosahedral structure for cobalt and nickel clusters [DE90-017688] N91-11100
POLYCRYSTALS
Analysis and prediction of thermal properties of mesophases and crystals by calorimetry and supercomputers [DE90-015538] N91-11123
Analysis of loss mechanisms in polycrystalline thin film solar cells [DE90-000372] N91-11297
POLYHEDRONS
Geometric method and synthesis af assembly strategies in robotic systems [LAAS-90041] N91-11215
Cones of matrices and setfunctions, and 0-1 optimization [CWI-BS-R8925] N91-11444
POLYMER CHEMISTRY
Studies of molecular properties of polymeric materials [NASA-TM-101854] N91-11118
Analysis and prediction of thermal properties of mesophases and crystals by calorimetry and supercomputers [DE90-015538] N91-11123

POLYMER MATRIX COMPOSITES
Studies of molecular properties of polymeric materials
[NASA-TM-101854] N91-11118
POLYMERIC FILMS
Studies of molecular properties of polymeric materials
[NASA-TM-101854] N91-11118
POLYMERIZATION
Morphological analysis of ionomers
[DE90-017611] N91-11124
POLYNOMIALS
On three dimensional object recognition and pose-determination: An abstraction based approach
[NASA-CR-186894] N91-11396
A new lower bound for the de Bruijn-Newman constant
[CWI-NM-R8920] N91-11447
Improved techniques for lower bounds for odd perfect numbers
[CWI-NM-R8921] N91-11448
A polynomial method of weighted centers for convex quadratic programming
[REPT-90-17] N91-11453
Asymptotic behavior of Laguerre polynomials with Re z less than 0 derived by the central limit theorem
[W-9004] N91-11458
Modeling histogram data with piecewise polynomials
[DE90-018037] N91-11467
POLYPEPTIDES
Combined capillary electrophoresis and electrospray ionization mass spectrometry
[DE90-016535] N91-11079
POLYTOPES
Cones of matrices and setfunctions, and 0-1 optimization
[CWI-BS-R8925] N91-11444
POROSITY
In-situ pore structure analysis during aging and drying of gels
[DE91-000044] N91-11089
POSITION (LOCATION)
Aircraft trajectory reconstitution on the basis of multi-radar plot information N91-11002
Generation of a buoyant plume of artificial smoke for airplane tests
[DOT/FAA/CT-90/9] N91-11015
POSITION INDICATORS
Flight simulator evaluation test of multi-functional display unit
[NAL-TM-596] N91-11026
POSITIVE IONS
Ion dynamics in the plasma mantle
[IFSI-89-20] N91-11550
POTENTIAL THEORY
A potential reduction variant of Renegar's short-step path-following method for linear programming
[REPT-90-14] N91-11402
POWDER METALLURGY
Deformation mechanisms in rapidly solidified aluminum alloys N91-11096
POWER TRANSMISSION
ECH by FEL and gyrotron sources on the Microwave Tokamak Experiment (MTX) tokamak
[DE91-000286] N91-11547
POWERED LIFT AIRCRAFT
Simulation of powered-lift flows N91-10886
PRECIPITATES
Microstructures of cubic Al2O3 precipitates in oxygen-implanted aluminum
[DE91-000038] N91-11111
PRECIPITATION (METEOROLOGY)
Taiwan area mesoscale experiment: A guide to precipitation patterns during the 1987 field phase
[PB90-256355] N91-11336
PREDICTION ANALYSIS TECHNIQUES
Computational fluid dynamics at the Lewis Research Center: An overview N91-10842
Aircraft trajectory: Prediction and control in the air transport flight management computer systems N91-10976
Performance of finite dynamic elements for composite materials in plane stress N91-11260
Notes on the NOARL nowcast for the 1989 to 1990 El Nino forced by FNOC winds
[AD-A223520] N91-11347
PREDICTIONS
More accurate predictions with transonic Navier-Stokes methods through improved turbulence modeling N91-10850
Energetics of 60 days predictions with the EZMW-T21 model in its mean temporary development and its relationship to forecast skill
[MITT-71] N91-11335
PREGNANCY
Pregnancy: A cause for grounding of female air crew N91-11376
PRESSURE DISTRIBUTION
Applications of a transonic wing design method N91-10890
Calculation of the pressure distribution on an oscillating airfoil in incompressible flow considering nonlinear effects N91-10926
PRESSURE EFFECTS
Railgun performance with a two-stage light-gas gun injector
[DE90-016211] N91-11032
Investigation on the projection by a Z-pinch discharge
[DE90-637548] N91-11544
PRESSURE OSCILLATIONS
An investigation of thermally driven acoustical oscillations in helium systems
[DE90-018049] N91-11086
PRESSURE VESSELS
Measurement of two-phase flow momentum with force transducers
[DE90-008748] N91-11188
PRIMARY BATTERIES
Advanced secondary batteries: Their applications, technological status, market and opportunity
[DE90-796146] N91-11146
PRINTED CIRCUITS
Ion chromatography in the manufacture of multilayer circuit boards
[DE90-017647] N91-11158
Touchstone project DELTA numeric node: Milestone event Q4
[AD-A224060] N91-11482
PROBABILITY DENSITY FUNCTIONS
On density estimation in the view of Kolmogorov's ideas in approximation theory
[CWI-BS-R8928] N91-11477
PROBABILITY DISTRIBUTION FUNCTIONS
Computer-Aided Structural Engineering (CASE) project: Investigation and design of U-frame structures using program CUFRBC. Volume C: User's guide for channels
[AD-A224388] N91-11395
PROBABILITY THEORY
A stochastic analysis of state transitions in an air space management system N91-10980
Functional description and analysis of processor performance for data collection
[INPE-5037-RPE/620] N91-11048
Measurement of radial ionization probability in microscopic volumes for 2.90 and 3.79 MeV alpha particles
[DE90-017509] N91-11498
PROBLEM SOLVING
Graphical interfaces for cooperative planning systems N91-10956
NUMVEC FORTRAN library manual. Chapter: Partial differential equations. Routine: OEHPC
[CWI-NM-R8915] N91-11399
Parallel performance models for the nodal transport method on the hypercube
[DE90-015162] N91-11408
Use of the VP-200 computer for aerothermodynamic problems
[MBB/FE122/S/PUB/388] N91-11424
The relation between knowledge and heuristic methods
[W-9001] N91-11457
An inverse problem for classical relativistic mechanics
[DE90-631599] N91-11589
PROCEDURES
A function-based approach to cockpit procedure aids N91-10953
Time-based aircraft/ATC operations study N91-10959
Online searching in public libraries: A comparative study of performance N91-11598
PRODUCTION COSTS
A tool for help in software reutilization
[INPE-5077-TDL/341] N91-11418
PRODUCTIVITY
Proceedings of the First NASA Ada Users' Symposium
[NASA-TM-102941] N91-11389
PROGRAM VERIFICATION (COMPUTERS)
Surrogate oracles, generalized dependency and simpler models
[NASA-CR-187360] N91-11407
PROGRAMMING LANGUAGES
Fundamental concepts for utilization of the FPS-5410 array processor
[INPE-5091-RPE/624] N91-11388
Research into language concepts for the mission control center
[NASA-CR-185928] N91-11392
PROJECT MANAGEMENT
Ada and software management in NASA: Symposium/forum
[NASA-TM-103297] N91-11390
Twenty-Second Annual NASA Supply and Equipment Management Conference
[NASA-CP-10042] N91-11591
PROJECT PLANNING
Advanced secondary batteries: Their applications, technological status, market and opportunity
[DE90-796146] N91-11146
PROJECTILES
Numerical simulation of shock-induced combustion for application to the ram accelerator concept N91-10912
Secondary-electron yield measurements from metals impacted by high-velocity ions, electrons, and molecules
[DE90-018023] N91-11502
PROP-FAN TECHNOLOGY
Structural analysis and optimization of a propfan-blade by use of the finite element method N91-10924
PROPELLANT COMBUSTION
The structure and stability of three dimensional detonation waves
[AD-A224465] N91-11164
PROPELLANT STORAGE
Stability of liquid propellants under long-term storage
[AD-A223934] N91-11126
PROPELLANT TANKS
External tank aerothermal design criteria verification, volume 1
[NASA-CR-183996] N91-11037
External tank aerothermal design criteria verification, volume 2
[NASA-CR-183997] N91-11038
PROPELLANT TRANSFER
Automated Fluid Interface System (AFIS)
[NASA-CR-183969] N91-11031
PROPELLER BLADES
Structural analysis and optimization of a propfan-blade by use of the finite element method N91-10924
PROPELLER NOISE
The effect of swirl recovery vanes on the cruise noise of an advanced propeller
[NASA-TM-103625] N91-11494
Prediction of the noise from a propeller at angle of attack
[NASA-TM-103627] N91-11495
PROPELLERS
An experimental study of an axisymmetric turbulent boundary layer disturbed by a periodic freestream N91-11175
The effect of swirl recovery vanes on the cruise noise of an advanced propeller
[NASA-TM-103625] N91-11494
PROPORTIONAL COUNTERS
Measurement of radial ionization probability in microscopic volumes for 2.90 and 3.79 MeV alpha particles
[DE90-017509] N91-11498
PROPULSION
Computational fluid dynamics at the Lewis Research Center: An overview N91-10842
Marshall Space Flight Center CFD overview N91-10843
Propulsion simulation for magnetically suspended wind tunnel models
[NASA-CR-182093] N91-11027
PROPULSION SYSTEM CONFIGURATIONS
Computational fluid dynamics at the Lewis Research Center: An overview N91-10842
PROPULSION SYSTEM PERFORMANCE
Computational fluid dynamics at the Lewis Research Center: An overview N91-10842
Computational fluid dynamics analysis of space shuttle main propulsion feed line 17-inch disconnect valves N91-10876
PROTECTION
Problems posed by the adaptation of physiological protective equipment for female combat pilots N91-11372
PROTECTIVE CLOTHING
Accommodation of female aircrew in USN protective flight clothing and equipment N91-11375
PROTECTIVE COATINGS
Projective scales against high temperature corrosion
[ETN-90-97770] N91-11116
PROTEINS
Combined capillary electrophoresis and electrospray ionization mass spectrometry
[DE90-016535] N91-11079
The structure and function of membrane protein photosynthetic reaction center
[DE90-017795] N91-11353
A protein coated piezoelectric crystal detector
[AD-A223848] N91-11552
PROTOCOL (COMPUTERS)
OSI in the NASA science internet: An analysis
[NASA-CR-177561] N91-11425

Interconnected networks of queues with randomized arrival and departure blocking
[CWI-BS-R8934] N91-11483

PROTON RESONANCE
Novel measurements of nuclear spin cross-relaxation in metal hydrides
[DE90-018042] N91-11503

PROTOPLANETS
Numerical calculations of the formation and evolution of giant planets with rotation N91-11643

PROTOTYPES
Inflight replanning for diversions N91-10955

PROVING
NASA's CFD Validation Program N91-10845

PSYCHOLOGICAL FACTORS
Impact of new technology on operational interface: From design aims to flight evaluation and measurement N91-10977

PSYCHOLOGICAL TESTS
Psychological and sociological aspects of the entrance of female aircrew to the Norwegian airforce N91-11365

PSYCHOLOGY
Psychological and sociological aspects of the entrance of female aircrew to the Norwegian airforce N91-11365

PSYCHOMOTOR PERFORMANCE
Evaluation of female and male aircrew applicants using a cognitive and psychomotor test N91-11366

PSYCHOPHYSICS
The French and the American school in multi-criteria decision analysis
[REPT-90-21] N91-11592

PULSAR MAGNETOSPHERES
Observations of pulsars at low radio frequencies N91-11614

PULSARS
Very high energy gamma rays from isolated pulsars and non-pulsating objects N91-11655
A search for very high energy gamma-rays from Cygnus X-3 N91-11658

PULSE AMPLITUDE
Pulse evolution in multi-atmosphere CO2 lasers
[ETN-90-97765] N91-11210

PULSE DURATION
A hybrid pulse forming technique
[DE90-016860] N91-11156
Pulse evolution in multi-atmosphere CO2 lasers
[ETN-90-97765] N91-11210

PULSE GENERATORS
A hybrid pulse forming technique
[DE90-016860] N91-11156

PULSED RADIATION
Pulse evolution in multi-atmosphere CO2 lasers
[ETN-90-97765] N91-11210

PULSES
Department of Defense methodology guidelines for High Power Microwave (HPM) susceptibility assessments
[DE90-015405] N91-11147

Q

QUADRATIC EQUATIONS
On SLLN for martingales with deterministic quadratic variation
[CWI-BS-R8933] N91-11445
Quadratic systems equivalent to class 3 sub A not equal to 0
[REPT-90-38] N91-11455

QUADRATIC PROGRAMMING
A polynomial method of weighted centers for convex quadratic programming
[REPT-90-17] N91-11453

QUALIFICATIONS
Structural dynamics qualification of spacecraft N91-10922

QUALITY CONTROL
First incremental buy for Increment 2 of the Space Transportation System (STS)
[NASA-CR-183855] N91-11034
Recommended operating procedure No. 45: Analysis of nitrous oxide from combustion sources
[PB90-238502] N91-11078
Implementation of a QML (Qualified Manufacturer's List) methodology for discrete semiconductors
[DE90-015715] N91-11235
Generic quality assurance/quality control guide for photovoltaic concentrator design, development and system installation
[DE90-017040] N91-11290
Software quality assurance handbook
[DE91-000060] N91-11420
The practical challenges of converting end-use data into information
[DE90-016538] N91-11600

QUANTUM EFFICIENCY
Research on high-efficiency, large area amorphous silicon based solar cells
[DE90-000356] N91-11285

QUANTUM WELLS
Electric-field dependent electroreflectance and photocurrent spectroscopy in InGaAs/InAlAs strained-layer superlattices
[DE90-015698] N91-11559
Nonparabolic conduction bands and masses in strained-single-quantum wells
[DE90-017028] N91-11560
Optical characterization of CdZnTe/CdTe strained quantum wells
[DE90-017036] N91-11563
Light-heavy-hole-mixing-induced selection rules for magneto-luminescence and valence-band energy dispersion in semiconductor quantum wells
[DE90-015989] N91-11573

QUARKS
Color flux distribution in pure SU(2) Lattice Gauge Theory
[DE90-017403] N91-11574

QUASARS
Stability of emission line clouds in active galactic nuclei N91-11659

QUENCHING (COOLING)
Influence of heat treatment on microstructure and properties of an advanced high temperature titanium alloy
[PNR-90689] N91-11107

QUEUEING THEORY
A stochastic analysis of state transitions in an air space management system N91-10980
Performance analysis of transaction driven computer systems via queueing analysis of polling models
[CWI-BS-R8931] N91-11426
Interconnected networks of queues with randomized arrival and departure blocking
[CWI-BS-R8934] N91-11483

R

RADAR DATA
Aircraft trajectories: Computation, prediction, control, volume 2: Air traffic handling and ground-based guidance of aircraft. Part 4: Air traffic handling. Part 5: Guidance of aircraft in a time-based constrained environment. Part 6: Surveillance. Part 7: Meteorological forecasts. Part 8: Aircraft operation in air traffic handling simulation
[AGARD-AG-301-VOL-2-PT-4-8] N91-10981

RADAR FILTERS
The use of downlinked measurements to track civil aircraft N91-11004

RADAR IMAGERY
Aircraft trajectory reconstitution on the basis of multi-radar plot information N91-11002

RADAR MEASUREMENT
Comparison of clear air atmospheric radar techniques for the study of atmospheric dynamics in the troposphere and the stratosphere
[PB90-256314] N91-11313

RADAR NETWORKS
Aircraft trajectory reconstitution on the basis of multi-radar plot information N91-11002
Bayesian multi-sensor tracking for advanced air traffic control systems N91-11003

RADAR RESOLUTION
The high-resolution graphic display: A possible man/machine interface for a computer assisted ATC management system N91-10989

RADAR TARGETS
Sidelobe blanking system performance: An extension of the theory leading to a new detection logic N91-11139

RADAR TRACKING
Aircraft trajectories: Computation, prediction, control, volume 2: Air traffic handling and ground-based guidance of aircraft. Part 4: Air traffic handling. Part 5: Guidance of aircraft in a time-based constrained environment. Part 6: Surveillance. Part 7: Meteorological forecasts. Part 8: Aircraft operation in air traffic handling simulation
[AGARD-AG-301-VOL-2-PT-4-8] N91-10981
Bayesian multi-sensor tracking for advanced air traffic control systems N91-11003

RADARSCOPES
The high-resolution graphic display: A possible man/machine interface for a computer assisted ATC management system N91-10989

RADIANCE
The delta-Sobolev approach for modeling solar spectral irradiance and radiance N91-11650

RADIATION ABSORPTION
Advanced infrared optically black baffle materials
[DE91-000561] N91-11523

RADIATION DAMAGE
Relationship of microstructure and tensile properties for neutron-irradiated vanadium alloys
[DE90-017863] N91-11105
JPRS report: Science and technology. USSR: Life sciences
[JPRS-ULS-89-003] N91-11354

RADIATION DISTRIBUTION
Analytic studies in nuclear astrophysics N91-11628
Stability of emission line clouds in active galactic nuclei N91-11659

RADIATION DOSAGE
Radiological health risks to astronauts from space activities and medical procedures
[NASA-TM-102164] N91-11356

RADIATION EFFECTS
Combined Release and Radiation Effects Satellite (CRRES): Atlas 1 (Atlas/Centaur-69) launch vehicle
[NASA-TM-103460] N91-11040
Studies of molecular properties of polymeric materials
[NASA-TM-101854] N91-11118
Study on radiation-induced deterioration of grease at high temperature. Part 1: Test method on thermal aging
[DE90-508070] N91-11120
A radiation hardened SONOS/CMOS EEPROM family
[DE90-015993] N91-11154
Measurement of radial ionization probability in microscopic volumes for 2.90 and 3.79 MeV alpha particles
[DE90-017509] N91-11498
Implications of the Biological Effects of Ionizing Radiation (BEIR) 5 report to the Department of Energy
[DE90-016673] N91-11526
High energy iron ion implantation into sapphire
[DE90-017736] N91-11568

RADIATION HARDENING
A radiation hardened SONOS/CMOS EEPROM family
[DE90-015993] N91-11154

RADIATION HAZARDS
Protection by WR-2721 and WR-151327 against late effects of gamma rays and neutrons
[DE90-017792] N91-11352
Radiological health risks to astronauts from space activities and medical procedures
[NASA-TM-102164] N91-11356

RADIATION INJURIES
Measurement of radial ionization probability in microscopic volumes for 2.90 and 3.79 MeV alpha particles
[DE90-017509] N91-11498

RADIATION PROTECTION
Protection by WR-2721 and WR-151327 against late effects of gamma rays and neutrons
[DE90-017792] N91-11352
Radiological health risks to astronauts from space activities and medical procedures
[NASA-TM-102164] N91-11356

RADIATION SOURCES
Planar orotron: A tunable, grating-based free electron laser N91-11208
A study of the ten and twenty micron silicate features in celestial infrared sources N91-11609

RADIATION TRANSPORT
Random number stride in Monte Carlo calculations
[DE90-012000] N91-11465

RADIATIVE TRANSFER
Analytic studies in nuclear astrophysics N91-11628
The transfer of polarized radiation in astrophysical masers in the presence of magnetic fields N91-11629
The delta-Sobolev approach for modeling solar spectral irradiance and radiance N91-11650

RADICALS
Atmospheric chemistry: Laboratory studies of kinetics of important reactions N91-11326

RADIO ASTRONOMY
Maximum entropy imaging of radio astrophysical data N91-11610
Type 2 solar radio bursts recorded at Weissenau, 1966-1987
[PB90-198334] N91-11648
Radio and infrared emission from starburst galaxies N91-11661

RADIO BURSTS
Testing for lightning as a source of radio bursts observed on the nightside of Venus
[NASA-CR-187364] N91-11645
Radio and infrared emission from starburst galaxies N91-11661

RADIO EMISSION
Exploration of decreased solar activity state (small intensity activity) in the corona and chromosphere
[INPE-5059-TDL/405] N91-11652
Radio and infrared emission from starburst galaxies N91-11661

RADIO FREQUENCIES
Observations of pulsars at low radio frequencies N91-11614
RADIO GALAXIES
Numerical simulations of suspersonic extragalactic radio jets N91-11660
RADIO JETS (ASTRONOMY)
Numerical simulations of suspersonic extragalactic radio jets N91-11660
RADIO OBSERVATION
Exploration of decreased solar activity state (small intensity activity) in the corona and chromosphere [INPE-5059-TDL/405] N91-11652
RADIOMETERS
The control system of an airborne radiometer: A process for a two dimensional reconstruction of irregular scanned radiometer data [MITT-70] N91-11202
RADIOSONDES
The influence of environmental factors on the temperature of the radiosonde thermistor N91-11325
RAIL TRANSPORTATION
Industry perspective on Maglev [PB90-252305] N91-11132
RAILGUN ACCELERATORS
Railgun performance with a two-stage light-gas gun injector [DE90-016211] N91-11032
RAIN FORESTS
Planetary boundary layer dynamics over the Amazon rain forest N91-11317
RAMAN SPECTROSCOPY
An apparatus for studies of hydrogen isotope exchange over metals using laser-Raman spectroscopy [DE90-018038] N91-11085
Laser Raman spectroscopy for in-situ analysis of corrosion films on metals [DE90-017822] N91-11109
RANDOM ERRORS
Procedural error monitoring and smart checklists N91-10954
RANDOM NUMBERS
Random number stride in Monte Carlo calculations [DE90-012000] N91-11465
RANDOM PROCESSES
Connected components in supercritical Mandelbrot percolation [REPT-90-15] N91-11452
RANKINE-HUGONIOT RELATION
A global pressure relaxation for high speed laminar and turbulent flows N91-11177
RAPID TRANSIT SYSTEMS
Industry perspective on Maglev [PB90-252305] N91-11132
RAREFIED GAS DYNAMICS
Direct simulation of rarefied hypersonic flows N91-10901
RAYLEIGH NUMBER
An experimental study of natural convection heat transfer from a horizontal cylinder array vertically aligned to and confined by a single wall and two walls N91-11178
RAYLEIGH SCATTERING
Aperture diffraction in Rayleigh zone: Calculation of the field in the quiet zone of compact ranges [CNES-CT/DRT/TIT/AN-88/234] N91-11136
REACTION KINETICS
A computational model for the prediction of hypersonic, reacting flows N91-10911
The structure and stability of three dimensional detonation waves [AD-A224465] N91-11164
Lifetimes and fates of toxic air contaminants in California's atmosphere [PB90-253204] N91-11304
Atmospheric chemistry: Laboratory studies of kinetics of important reactions N91-11326
Intramolecular electron transfer rates [DE90-017447] N91-11504
REACTOR DESIGN
A design method of divertor in tokamak reactors [NIFS-36] N91-11532
REACTOR MATERIALS
Effects of environment and aging on creep properties of Alloy 800H [DE90-520207] N91-11106
The transverse stress effect on the critical current of jelly-roll multifilamentary Nb3Al wires [DE90-513710] N91-11581
REACTOR SAFETY
Development of the structural materials information center [DE90-016521] N91-11603
REACTOR TECHNOLOGY
Development of the structural materials information center [DE90-016521] N91-11603
REAL GASES
Numerical simulation of shock-induced combustion for application to the ram accelerator concept N91-10912
REAL TIME OPERATION
Adaptive digital real time filtering in structural dynamics: A contribution to the realization on Actively Reacting Elastic Structures (ARES) N91-10929
Computation of sub-optimal real-time guidance laws for combat aircraft trajectories N91-10970
Generation of aircraft trajectories for on-line operation: Methods, techniques, and tools N91-10987
A description and evaluation of TIMER: A time-based terminal flow-control concept N91-10996
Experimental manufacturing of data recording system for rocket combustion thermal flux distribution [DE90-702432] N91-11051
Proceedings of the First NASA Ada Users' Symposium [NASA-TM-102941] N91-11389
Combination of Hatley and Ward/Mellor methods for real time systems [INPE-5078-TDL/412] N91-11419
Identification and analysis of cosmic gamma ray bursts from Pioneer Venus Orbiter N91-11657
REATTACHED FLOW
Structure of supersonic turbulent reattaching shear layers N91-10914
RECEIVERS
Bench-scale testing of a heat-pipe receiver for solar thermal electric applications [DE90-009834] N91-11289
RECOGNITION
A fast parallel recognizer [REPT-90-16] N91-11429
RECOMBINATION REACTIONS
Nonparabolic conduction bands and masses in strained-single-quantum wells [DE90-017028] N91-11560
RECTANGULAR PLATES
Forced vibration analysis of plates and shallow shells N91-11237
Buckling and vibrations of plates subjected to concentrated forces N91-11255
RED GIANT STARS
From red giants to planetary nebulae: Asymmetries, dust, and polarization N91-11622
Violet and visual flux problems in red giant stars N91-11632
REDUCED GRAVITY
The structure and stability of three dimensional detonation waves [AD-A224465] N91-11164
REFLECTANCE
Electric-field dependent electroreflectance and photocurrent spectroscopy in InGaAs/InAlAs strained-layer superlattices [DE90-015698] N91-11559
REFLECTING TELESCOPES
A search for small comets in consecutive images acquired with a ground-based telescope N91-11626
REFLECTOR ANTENNAS
Aperture diffraction in Rayleigh zone: Calculation of the field in the quiet zone of compact ranges [CNES-CT/DRT/TIT/AN-88/234] N91-11136
REFLEXES
Oscillation onset in neural delayed feedback [DE90-015057] N91-11351
REFRACTORY MATERIALS
High temperature materials: The overall view [PNR-90699] N91-11073
REFRIGERANTS
Thermal performance analysis for heat exchangers using nonazeotropic refrigerant mixtures [DE90-016030] N91-11186
REFUELING
Automated Fluid Interface System (AFIS) [NASA-CR-183969] N91-11031
REGULATIONS
Twenty-Second Annual NASA Supply and Equipment Management Conference [NASA-CP-10042] N91-11591
REINFORCEMENT (STRUCTURES)
Computer-Aided Structural Engineering (CASE) project: Investigation and design of U-frame structures using program CUFRBC. Volume C: User's guide for channels [AD-A224388] N91-11395
REINFORCING FIBERS
Crack-growth resistance in reinforced ceramic composites N91-11261
RELATIVISTIC PLASMAS
On hydrodynamics of collisionless relativistic plasma in a strong magnetic field [DE90-513926] N91-11543
RELATIVITY
An inverse problem for classical relativistic mechanics [DE90-631599] N91-11589
An investigation of the Newman-Penrose constants for massless free fields of arbitrary spin N91-11630
RELIABILITY
First incremental buy for Increment 2 of the Space Transportation System (STS) [NASA-CR-183855] N91-11034
Parallelized reliability estimation of reconfigurable computer networks [NASA-CR-182101] N91-11430
Lower bound on reliability for Weibull distribution when shape parameter is not estimated accurately [NASA-CR-180681] N91-11474
A combined wave distribution function and stability analysis of Viking particle and low-frequency wave data [IRF-PREPRINT-115] N91-11541
RELIABILITY ANALYSIS
Surrogate oracles, generalized dependency and simpler models [NASA-CR-187360] N91-11407
RELIEF MAPS
Geometric correction of SPOT imagery with the use of a digital elevation model [INPE-5014-TDL/401] N91-11423
REMOTE MANIPULATOR SYSTEM
An expert system for automated robotic grasping [DE90-010820] N91-11221
REMOTE SENSING
Remote sensing in the ultraviolet [AD-A224254] N91-11268
Satellite remote sensing for agricultural projects [PB90-257916] N91-11270
Remote sensing for marine activities [BCRS-89-41] N91-11273
Remote sensing for marine activities: Appendices [BCRS-89-41-APP] N91-11274
Utility of remotely sensed data for identification of soil conservation practices [NASA-CR-176874] N91-11276
Methodology of remote sensing for monitoring modifications in the fluvial channel and updating nautical charts [INPE-4863-TDL/374] N91-11277
Numerical experiments with climatic zonally-averaged models [INPE-5083-TDL/417] N91-11343
REMOTE SENSORS
Remote sensing for marine activities [BCRS-89-41] N91-11273
Remote sensing for marine activities: Appendices [BCRS-89-41-APP] N91-11274
REPORTS
Activities report of the Institute for Extraterrestrial Physics [MPE-217] N91-11620
Research and technology at Kennedy Space Center [NASA-TM-102150] N91-11664
REPRESENTATIONS
Minimality of descriptor representations under external equivalence [CWI-BS-R9002] N91-11448
RESCUE OPERATIONS
Air rescue in the Federal Republic of Germany [ETN-90-97878] N91-10963
RESEARCH
JPRS report: Science and technology. USSR: Life sciences [JPRS-ULS-89-003] N91-11354
Activities report of the Institute for Extraterrestrial Physics [MPE-217] N91-11620
RESEARCH AND DEVELOPMENT
Civil space technology initiative [NASA-TM-103017] N91-11028
Materials Division research and technology accomplishments for FY 89 and plans for FY 90 [NASA-TM-102649] N91-11072
Industry perspective on Maglev [PB90-252305] N91-11132
Proposal pressure in the 1980s: An indicator of stress on the Federal Research System [PB90-253147] N91-11593
Holding the edge: Maintaining the defense technology base. Volume 2: Appendixes [PB90-253345] N91-11597
Research and technology at Kennedy Space Center [NASA-TM-102150] N91-11664
Activities report of the Technical Research Centre of Finland [ISBN-951-38-3647] N91-11665
RESEARCH FACILITIES
Computational fluid dynamics research and applications at NASA Langley Research Center N91-10841

RESEARCH MANAGEMENT
Recommended operating procedure No. 45: Analysis of nitrous oxide from combustion sources
[PB90-238502] N91-11078
Proposal pressure in the 1980s: An indicator of stress on the Federal Research System
[PB90-253147] N91-11593
Holding the edge: Maintaining the defense technology base. Volume 2: Appendixes
[PB90-253345] N91-11597
RESEARCH VEHICLES
Aeroassist flight experiment aerodynamics and aerothermodynamics N91-10900
RESIDENTIAL ENERGY
Energy models and national energy policy
[DE90-017682] N91-11300
RESIDUAL STRESS
Relations between microstructure and mechanical behaviour of SiC/SiC composites: interface effects on multiple cracking in multifilament materials
[ISAL-89-0098] N91-11065
Residual stress measurements and microstructural characterization of graphite-aluminum metal matrix composite N91-11068
Elastic/plastic analyses of advanced composites investigating the use of the compliant layer concept in reducing residual stresses resulting from processing
[NASA-TM-103204] N91-11074
Development of hermetic microminiature connectors
[DE90-015562] N91-11153
Residual stress at fluid interfaces
[DE90-012964] N91-11189
Indentation testing of thin films and hard materials
[DE90-017758] N91-11224
Deducing mechanical properties due to interfaces from their acoustical response
[DE90-016704] N91-11234
RESIDUES
CTR plasma engineering studies
[DE90-017774] N91-11534
RESONANCE
Resonance ionization spectroscopy of molecular clusters using picosecond lasers
[DE90-017334] N91-11080
Aircraft interior noise reduction by alternate resonance tuning
[NASA-CR-186879] N91-11488
RESPIRATORY DISEASES
Nitrogen dioxide and respiratory infection: Pilot investigations
[PB90-247339] N91-11357
REUSE
A tool for help in software reutilization
[INPE-5077-TDL/341] N91-11418
REVERSE FIELD PINCH
Confinement and fluctuations in the MST (Madison Symmetric Torus) reversed field pinch
[DE90-018019] N91-11535
Complete fluid equations for low-n singular modes in axisymmetric torodial plasmas
[DE91-000176] N91-11545
REVISIONS
Inflight replanning for diversions N91-10955
RHEOELECTRICAL SIMULATION
Non-linear multigrid in 2-D semiconductor device simulation: The zero current case
[CWI-NM-R8917] N91-11553
RHEOLOGY
Processing of YBA2Cu3O7 tapes from a molten salt precursor
[DE90-017656] N91-11564
RIESZ THEOREM
Approximation of the solution to the moment problem in a Hilbert space
[CWI-AM-R8923] N91-11438
RIGID STRUCTURES
Coupled rotor/airframe vibration analysis N91-11012
RIVERS
Methodology of remote sensing for monitoring modifications in the fluvial channel and updating nautical charts
[INPE-4863-TDL/374] N91-11277
Identification of areas subject to flooding through TM/LANDSAT images in the basin of the rivers Pindare, Mearim, Jaguaribe, Apodi, Piranhas, and San Francisco
[INPE-5034-RPE/619] N91-11279
ROBOT ARMS
Dynamic analysis and control of lightweight manipulators with flexible parallel link mechanisms
[NASA-CR-187347] N91-11216
Dynamic model error analysis of robot manipulators N91-11220
ROBOT DYNAMICS
Geometric method and synthesis af assembly strategies in robotic systems
[LAAS-90041] N91-11215
Dynamic analysis and control of lightweight manipulators with flexible parallel link mechanisms
[NASA-CR-187347] N91-11216
Robot trajectory control with a model reference adaptive control system using tap delay filters N91-11217
Minimum time feedback control of articulated robotic manipulators N91-11219
ROBOTICS
Geometric method and synthesis af assembly strategies in robotic systems
[LAAS-90041] N91-11215
Robot trajectory control with a model reference adaptive control system using tap delay filters N91-11217
Minimum time feedback control of articulated robotic manipulators N91-11219
Mobile robots and intelligent motion control
[DE90-017312] N91-11226
A method of using the inverse matrix for manipulator kinematics
[DE90-520210] N91-11227
Intelligent Robotic Systems Study (IRSS), phase 2
[NASA-CR-183963] N91-11432
ROBOTS
An expert system for automated robotic grasping
[DE90-010820] N91-11221
Mobile robots and intelligent motion control
[DE90-017312] N91-11226
A method of using the inverse matrix for manipulator kinematics
[DE90-520210] N91-11227
Archimedes: A system that plans and executes mechanical assemblies
[DE91-000036] N91-11231
ROBUSTNESS (MATHEMATICS)
A synthesis of time and frequency domain methods for the control of infinite-dimensional systems: A system theoretic approach
[W-8912] N91-11456
ROCKET EXHAUST
Evaluation of thermal sprayed metallic coatings for use on the structures at Launch Complex 39
[NASA-TM-103807] N91-11121
ROCKET LAUNCHING
Tethered rocket as a vehicle for penetration and impact testing: Development report
[DE90-014865] N91-11057
ROCKET NOSE CONES
Grid generation and flow computation about a Martian entry vehicle
[NASA-CR-187032] N91-11042
ROCKET TEST FACILITIES
Tethered rocket as a vehicle for penetration and impact testing: Development report
[DE90-014865] N91-11057
ROCKET THRUST
A life comparison of tube and channel cooling passages for thrust chambers
[NASA-TM-103613] N91-11059
ROCKET VEHICLES
Tethered rocket as a vehicle for penetration and impact testing: Development report
[DE90-014865] N91-11057
ROLL
Conical Euler simulation and active suppression of delta wing rocking motion
[NASA-TM-102683] N91-10904
Marginal aircraft release disturbance on advanced missiles
[MBB/FE121/S/PUB/329] N91-11016
ROTARY WING AIRCRAFT
Calculation of the rotor induced download on airfoils N91-10864
Three-dimensional viscous drag prediction for rotor blades N91-10865
The breakup of trailing-line vortices N91-10867
ROTATION
A three-dimensional solid element model for finite rotation of composite shells N91-11262
ROTOR AERODYNAMICS
Aerodynamic interaction of counter rotating propellers N91-10910
The aerodynamic effects of nozzle guide vane shock wave and wake passing on a transonic turbine rotor N91-10915
The calculation of rotor/fuselage interaction for two-dimensional bodies
[NASA-TM-102855] N91-10933
Performance and cost projections for advanced wind turbines
[DE90-000370] N91-11286
Atmospheric performance of the special-purpose Solar Energy Research Institute (SERI) thin-airfoil family: Final results
[DE90-000373] N91-11287
ROTOR BLADES
Computation of transonic flow over elastic rotor blade N91-10906
ROTOR BODY INTERACTIONS
The calculation of rotor/fuselage interaction for two-dimensional bodies
[NASA-TM-102855] N91-10933
ROTOR DYNAMICS
Analysis of the SSME HPOTP bearing inlet cavity N91-10877
ROTORS
Prediction of turbine rotor-stator interaction using Navier-Stokes methods N91-10881
Coupled rotor/airframe vibration analysis N91-11012
ROUGHNESS
Experimental and theoretical studies of friction and heat transfer in rough passages
[DE90-016302] N91-11223
ROUTES
Graphical interfaces for cooperative planning systems N91-10956
RUNGE-KUTTA METHOD
Direct simulation of compressible turbulence N91-10847
Recent advances in Runge-Kutta schemes for solving 3-D Navier-Stokes equations N91-10851
Iterated Runge-Kutta methods on parallel computers
[CWI-NM-R9001] N91-11428
RUNWAY LIGHTS
Flight evaluation test of the PAPI (Precision Approach Path Indicator) System
[NAL-TM-592] N91-10966

S

S WAVES
The role of shear in the cosmological distance
[DE90-513788] N91-11636
SAFETY
First incremental buy for Increment 2 of the Space Transportation System (STS)
[NASA-CR-183855] N91-11034
Twenty-Second Annual NASA Supply and Equipment Management Conference
[NASA-CP-10042] N91-11591
SAFETY FACTORS
Wind models for flight simulation N91-10975
SAMPLING
Sampling and interpolations in digital terrain models
[INPE-5041-TDL/404] N91-11275
Aircrew/cockpit compatibility: A multivariate problem seeking a multivariate solution N91-11369
SAN ANDREAS FAULT
Aspects of the earthquake geology and seismotectonics of the southern San Andreas and related faults N91-11329
SAPPHIRE
High energy iron ion implantation into sapphire
[DE90-017736] N91-11568
SATELLITE ALTIMETRY
Gulf of Maine sea surface topography from GEOSAT altimetry N91-11271
SATELLITE ATTITUDE CONTROL
Boosting a tethered satellites's orbit around an oblate planet through resonant pumping N91-11030
Attitude control of tethered satellites N91-11045
Precision tethered satellite attitude control N91-11046
SATELLITE COMMUNICATION
Contribution of the satellite techniques to the surveillance of air traffic N91-11005
Fourteen x fourteen CCD array for optical intersatellite link tracking
[CNES-CT/DRT/TIT/OE-88/144] N91-11521
SATELLITE IMAGERY
Forest classification with high resolution satellite images. Research into the use of spatial information to improve the multi-spectral classification with SPOT images
[BCRS-89-32] N91-11269
Satellite remote sensing for agricultural projects
[PB90-257916] N91-11270
Reception and display of WEFAX images: 4 bits with micro line IBM-PC, users manual
[INPE-5086-NTE/294] N91-11417
Classification of textures using the ARMA models and distances over the autocorrelation function
[INPE-5067-TDL/406] N91-11421
Performance comparison of edge defection morphologies
[INPE-5012-TDL/400] N91-11422
Geometric correction of SPOT imagery with the use of a digital elevation model
[INPE-5014-TDL/401] N91-11423

SATELLITE OBSERVATION
Satellite remote sensing for agricultural projects
[PB90-257916] N91-11270
SATELLITE ORBITS
Boosting a tethered satellites's orbit around an oblate planet through resonant pumping N91-11030
SATELLITE ORIENTATION
Boosting a tethered satellites's orbit around an oblate planet through resonant pumping N91-11030
SATELLITE ROTATION
The rotation of Lageos
[IFSI-90-10] N91-11333
SCANNERS
Experimental manufacturing of performance evaluation system for solid image sensor
[NAL-TM-591] N91-11200
Scanning system for measuring uniformity of laser detector response and laser beam dimensions
[PB90-257619] N91-11207
SCANNING
Image reconstruction of IRAS survey scans
[NASA-CR-187328] N91-11606
SCATTERING
Attenuation of elastic waves due to scattering from spherical cavities and elastic inclusions N91-11256
SCATTERING COEFFICIENTS
System identification of lossless layered media from input-output data
[CWI-BS-R8929] N91-11166
SCATTERING CROSS SECTIONS
Collisional processes of interest in MFE plasma research
[DE91-000598] N91-11549
SCHEDULING
Time-based aircraft/ATC operations study N91-10959
Minimizing maximum earliness and maximum lateness on a single machine
[CWI-BS-R9001] N91-11398
SCHOOLS
Spacecraft design project: High latitude communications satellite
[NASA-CR-186689] N91-11039
SCHOTTKY DIODES
Fabrication and optimization of a whiskerless Schottky barrier diode for submillimeter wave applications
[NASA-CR-186381] N91-11144
SEA SURFACE TEMPERATURE
Radiometric observation of the atmospheric boundary layer (the ROSSA Project) N91-11324
Meteorological characteristics of the El Nino/Southern Oscillation phenomenon N91-11340
Numerical experiments with climatic zonally-averaged models
[INPE-5083-TDL/417] N91-11343
Surface and bottom temperature distribution for the Northeast continental shelf
[PB90-252172] N91-11349
SEALERS
On the calculation of leakage and friction of reciprocating elastomeric seals
[ETN-90-97751] N91-11228
SECONDARY EMISSION
Secondary-electron yield measurements from metals impacted by high-velocity ions, electrons, and molecules
[DE90-018023] N91-11502
Newly appreciated roles for electrons in ion-atom collisions
[DE91-000555] N91-11509
SEISMIC WAVES
NCEER strong-motion data base: A user manual for the geobase release (version 1.0 for the SUN3)
[PB90-258062] N91-11315
Arctic acoustics ultrasonic modeling studies
[AD-A224165] N91-11489
SEISMOLOGY
Aspects of the earthquake geology and seismotectonics of the southern San Andreas and related faults N91-11329
SELECTION RULES (NUCLEAR PHYSICS)
Light-heavy-hole-mixing-induced selection rules for magneto-luminescence and valence-band energy dispersion in semiconductor quantum wells
[DE90-015989] N91-11573
SELENIUM
Bragg intensities and diffuse scattering in Ag2Se: Molecular dynamics study
[DE90-017811] N91-11583
SELF TESTS
Application of self-testing integrated circuits to the safety of systems operation
[ETN-90-97828] N91-11150
SEMANTICS
A logical background of a method for the handling of incompatible pieces of knowledge
[REPT-90-13] N91-11401
A formal semantics for the preferred subtheories
[REPT-90-20] N91-11403
SEMICONDUCTOR DEVICES
Non-linear multigrid in 2-D semiconductor device simulation: The zero current case
[CWI-NM-R8917] N91-11553
A multigrid approach for the solution of the 2D semiconductor equations
[CWI-NM-R9003] N91-11554
SERI Workshop on the Role of Point Defects/Defect Complexes in Silicon Device Fabrication
[DE90-000377] N91-11572
SEMICONDUCTOR JUNCTIONS
Research on high-efficiency, large area amorphous silicon based solar cells
[DE90-000356] N91-11285
SEMICONDUCTOR LASERS
Applications of diode lasers to resonance ionization mass spectrometry
[DE90-017768] N91-11084
SEMICONDUCTORS (MATERIALS)
Implementation of a QML (Qualified Manufacturer's List) methodology for discrete semiconductors
[DE90-015715] N91-11235
Ion dynamics in semiconductors with self-consistent electronic densities N91-11556
Optical characterization of CdZnTe/CdTe strained quantum wells
[DE90-017036] N91-11563
Ion mixing of semiconductor superlattices
[DE90-017769] N91-11569
Compositional imaging of semiconductor interfaces by Z-contrast Scanning Transmission Electron Microscope (STEM)
[DE90-017763] N91-11576
SEMIEMPIRICAL EQUATIONS
An experimental study of natural convection heat transfer from a horizontal cylinder array vertically aligned to and confined by a single wall and two walls N91-11178
SENSITIVITY
Deformation effects on the development of grain boundary chronium depletion (sensitization) in type 316 austenitic stainless steels
[DE90-016130] N91-11092
SEPARATED FLOW
Recent advances in Runge-Kutta schemes for solving 3-D Navier-Stokes equations N91-10851
CFD for applications to aircraft aeroelasticity N91-10855
Experimental investigation of the mechanisms underlying vortex kinematics in unsteady separated flows N91-10907
SEQUENCING
Surrogate oracles, generalized dependency and simpler models
[NASA-CR-187360] N91-11407
SEX
Sex differences concerning performance and personality traits of applicants for highly qualified operator functions in aviation N91-11364
SHALLOW SHELLS
Forced vibration analysis of plates and shallow shells N91-11237
SHALLOW WATER
Stabilization of a time integrator for the 3D shallow water equations by smoothing techniques
[CWI-NM-R8916] N91-11167
SHAPE CONTROL
Adaptive digital real time filtering in structural dynamics: A contribution to the realization on Actively Reacting Elastic Structures (ARES) N91-10929
Non-linear vibration of large, imperfect space structures N91-10930
SHAPES
Evaluation process for the examination of curved surface workpieces using coordinate measuring instruments
[ETN-90-97901] N91-11203
Beta splines interpolation for DEM's
[INPE-5039-PRE/1572] N91-11415
Methods for the construction of constant curve free form surfaces
[ETN-90-97861] N91-11463
Lower bound on reliability for Weibull distribution when shape parameter is not estimated accurately
[NASA-CR-180681] N91-11474
SHEAR FLOW
The calculation of correlation functions in the statistical theory of turbulent flows N91-11176
Basic dynamics of low frequency variability and the storm tracks N91-11339
SHEAR LAYERS
Numerical simulation of nonlinear development of instability waves
[E-4658] N91-10849
Structure of supersonic turbulent reattaching shear layers N91-10914
SHELL THEORY
Empirical proton-neutron interaction energies and nuclear structure
[DE90-017632] N91-11500
SHOCK TESTS
Computer modeling of 12-inch actuator shock test performance
[DE90-017038] N91-11033
SHOCK WAVE PROPAGATION
The aerodynamic effects of nozzle guide vane shock wave and wake passing on a transonic turbine rotor N91-10915
SHOCK WAVES
More accurate predictions with transonic Navier-Stokes methods through improved turbulence modeling N91-10850
Attenuation studies of booster-rocket propellants and their simulants
[DE91-000098] N91-11131
A global pressure relaxation for high speed laminar and turbulent flows N91-11177
Magnetic field generation in astrophysics N91-11623
Polarized radiation from inhomogeneous shocks N91-11662
SHORT CRACKS
Characterization of short fatigue cracks at notches in SiC particulate aluminum composite
[DE90-018043] N91-11071
Short-crack growth behaviour in various aircraft materials
[AGARD-R-767] N91-11240
An AGARD supplemental test programme on the behaviour of short cracks under constant amplitude and aircraft spectrum loading N91-11241
Determination of the short crack effect in 2090-T8E41 aluminum lithium N91-11242
Short crack behaviour in Al-Li alloy 2090 N91-11243
Crack behaviour of 2024-T3, 2090-T8E41 and 7075-T6 under constant amplitude and different types of variable amplitude loading, especially Gaussian loading N91-11244
The growth of short fatigue cracks in 2024 and 2090 aluminium alloys under variable amplitude loading N91-11245
The growth of short cracks in 4340 steel and aluminum-lithium 2090 N91-11247
Short and long fatigue crack growth in 2024-T3 under Fokker 100 spectrum loading N91-11248
Growth of short fatigue cracks in 7075-T6 aluminum alloy N91-11249
Short crack observations in Ti-6Al-4V under constant amplitude loading N91-11250
SHORT TAKEOFF AIRCRAFT
NASA Computational Fluid Dynamics Conference. Volume 2: Sessions 7-12
[NASA-CP-10038-VOL-2] N91-10868
SIDELOBES
Sidelobe blanking system performance: An extension of the theory leading to a new detection logic N91-11139
SIDEREAL TIME
Apparent place of Polaris and apparent Sidereal Time at 0 hour UT 1990-1994
[PB90-259169] N91-11607
SIGNAL ANALYZERS
Functional description and analysis of processor performance for data collection
[INPE-5037-RPE/620] N91-11048
Distributed digital signal processors for multi-body structures
[NASA-CR-187375] N91-11387
SIGNAL PROCESSING
Fine scale velocity measurements in a turbulent jet in a confined crossflow N91-10909
Functional description and analysis of processor performance for data collection
[INPE-5037-RPE/620] N91-11048
Algorithm aided evaluation of directional signals
[ETN-90-97902] N91-11138
Distributed digital signal processors for multi-body structures
[NASA-CR-187375] N91-11387
Integrated optical components for optical fibre sensors N91-11519
SIGNAL TO NOISE RATIOS
The ultrasonic examination of titanium alloys N91-11094
Observations of pulsars at low radio frequencies N91-11614
SILICATES
A study of the ten and twenty micron silicate features in celestial infrared sources N91-11609

SILICON
Research on high-efficiency, multiple-gap, multi-junction amorphous silicon-based alloy thin-film solar cells
[DE90-000364] N91-11296
SERI Workshop on the Role of Point Defects/Defect Complexes in Silicon Device Fabrication
[DE90-000377] N91-11572
A study of the chemical, mechanical, and surface properties of thin films of hydrogenated amorphous carbon
[DE91-000357] N91-11585

SILICON ALLOYS
Structure of amorphous-silicon and germanium alloy films
[DE90-000355] N91-11557

SILICON CARBIDES
Characterization of short fatigue cracks at notches in SiC particulate aluminum composite
[DE90-018043] N91-11071
Mechanical behavior of ceramics and composites
[DE90-017311] N91-11122
MIS capacitor studies on silicon carbide single crystals
[NASA-CR-187350] N91-11555

SILICON COMPOUNDS
Silicon compilation and the SYCO silicon compiler
[ETN-90-97827] N91-11404

SILICON FILMS
Structure of amorphous-silicon and germanium alloy films
[DE90-000355] N91-11557

SILICON NITRIDES
Mechanical behavior of ceramics and composites
[DE90-017311] N91-11122

SILVER
Design and testing of a high temperature superconducting current lead
[DE90-017812] N91-11579
Bragg intensities and diffuse scattering in Ag2Se: Molecular dynamics study
[DE90-017811] N91-11583

SIMULATION
NASA Computational Fluid Dynamics Conference. Volume 1: Sessions 1-6
[NASA-CP-10038-VOL-1] N91-10839
Understanding transition and turbulence through direct simulations N91-10846
Direct simulation of compressible turbulence N91-10847
Non linear evolution of a second mode wave in supersonic boundary layers N91-10848
Numerical simulation of nonlinear development of instability waves
[E-4658] N91-10849
Time-based operations in an advanced ATC environment N91-10958
Propulsion simulation for magnetically suspended wind tunnel models
[NASA-CR-182093] N91-11027
Parallelization on a multi-processor system of a solving method for the unsteady Navier-Stokes equations at high Reynolds numbers
[ESA-TT-1116] N91-11197
Inflated speedups in parallel simulations via malloc()
[NASA-CR-182104] N91-11397
The SIM.PL.EX. plasma chamber (Simulatori di Plasma Extraterrestre)
[IFSI-90-3] N91-11551

SINGLE CRYSTALS
MIS capacitor studies on silicon carbide single crystals
[NASA-CR-187350] N91-11555

SINGLE STAGE TO ORBIT VEHICLES
Weight evaluation and sensitivity analysis for space plane: SSTO
[NAL-TM-598-1] N91-11036

SINTERING
Microwave sintering of nanocrystalline TiO2
[DE91-000375] N91-11115

SITE SELECTION
Report of the Department of Energy (DOE) Office of Energy research review committee on the site-specific conceptual design of the superconducting super collider
[DE90-018021] N91-11513

SKIN TEMPERATURE (NON-BIOLOGICAL)
Radiometric observation of the atmospheric boundary layer (the ROSSA Project) N91-11324

SKY SURVEYS (ASTRONOMY)
Image reconstruction of IRAS survey scans
[NASA-CR-187328] N91-11606
Apparent place of Polaris and apparent Sidereal Time at 0 hour UT 1990-1994
[PB90-259169] N91-11607
Population studies in groups and clusters of galaxies, volumes 1 and 2 N91-11608

SMOKE
Generation of a buoyant plume of artificial smoke for airplane tests
[DOT/FAA/CT-90/9] N91-11015
Fluctuating concentrations in atmospheric dispersion N91-11323

SMOKE DETECTORS
Generation of a buoyant plume of artificial smoke for airplane tests
[DOT/FAA/CT-90/9] N91-11015

SOCIAL FACTORS
Democratic theory, science, and decision making in global climate change: Culpability, uncertainty, and fairness
[DE90-017316] N91-11308
Psychological and sociological aspects of the entrance of female aircrew to the Norwegian airforce N91-11365

SODIUM
Development of high performance sodium/metal chloride cells
[DE90-017668] N91-11159

SOFTWARE ENGINEERING
DUWECS reference guide V1.0: Delft University wind energy converter simulation program
[MEMT-5] N91-11294
Performance of a parallel code for the Euler equations on hypercube computers
[NASA-TM-102260] N91-11384
Proceedings of the First NASA Ada Users' Symposium
[NASA-TM-102941] N91-11389
Ada and software management in NASA: Symposium/forum
[NASA-TM-103297] N91-11390
Research into language concepts for the mission control center
[NASA-CR-185928] N91-11392
Silicon compilation and the SYCO silicon compiler
[ETN-90-97827] N91-11404
A tool for help in software reutilization
[INPE-5077-TDL/341] N91-11418

SOFTWARE TOOLS
Time-based operations in an advanced ATC environment N91-10958
Air traffic management and aircraft guidance in a zone of convergence N91-10998
Application of computational fluid dynamics to three-dimensional bodies in hypersonic flow N91-11174
Experiences in the use of ABAQUS for creep analysis
[PNR-90705] N91-11266
NCEER strong-motion data base: A user manual for the geobase release (version 1.0 for the SUN3)
[PB90-258062] N91-11315
Time domain frequency stability calculated from the frequency domain description: Use of the SIGINT software package to calculate time domain frequency stability from the frequency domain
[PB90-257684] N91-11405
A tool for help in software reutilization
[INPE-5077-TDL/341] N91-11418

SOIL EROSION
Utility of remotely sensed data for identification of soil conservation practices
[NASA-CR-176874] N91-11276

SOILS
Design of a scientific probe for obtaining Mars surface material
[NASA-CR-186672] N91-11641

SOLAR ACTIVITY
White light solar corona: An atlas of 1988 K-coronameter synoptic charts, December 1987 to January 1989
[NASA-CR-184955] N91-11649
Exploration of decreased solar activity state (small intensity activity) in the corona and chromosphere
[INPE-5059-TDL/405] N91-11652
Plots of the 5-minute neutron monitor intensity and multiplicities recorded by the Rome 17-NM64, January 1990
[IFSI-90-5] N91-11653
Plots of the 5-minute neutron monitor intensity and multiplicities recorded by the Rome 17-NM64, February 1990
[IFSI-90-6] N91-11654

SOLAR ARRAYS
Photovoltaic options for solar electric propulsion
[NASA-TM-103284] N91-11061

SOLAR CELLS
Preliminary results from the advanced photovoltaic experiment flight test
[NASA-TM-103269] N91-11058
Photovoltaic options for solar electric propulsion
[NASA-TM-103284] N91-11061
High efficiency CuInSe2 and CuInGaSe2 cells and materials research
[DE90-000362] N91-11280
Research on high-efficiency, large area amorphous silicon based solar cells
[DE90-000356] N91-11285
Research on high-efficiency, multiple-gap, multi-junction amorphous silicon-based alloy thin-film solar cells
[DE90-000364] N91-11296
Analysis of loss mechanisms in polycrystalline thin film solar cells
[DE90-000372] N91-11297
SERI Workshop on the Role of Point Defects/Defect Complexes in Silicon Device Fabrication
[DE90-000377] N91-11572

SOLAR COLLECTORS
Bench-scale testing of a heat-pipe receiver for solar thermal electric applications
[DE90-009834] N91-11289
Colorado State University program for developing, testing, evaluating and optimizing solar heating and cooling systems
[DE90-017273] N91-11291
The design, testing and fabrication of an extruded, linear focus Fresnel lens
[DE90-014852] N91-11516

SOLAR COOLING
Colorado State University program for developing, testing, evaluating and optimizing solar heating and cooling systems
[DE90-017273] N91-11291

SOLAR CORONA
White light solar corona: An atlas of 1988 K-coronameter synoptic charts, December 1987 to January 1989
[NASA-CR-184955] N91-11649

SOLAR ELECTRIC PROPULSION
Photovoltaic options for solar electric propulsion
[NASA-TM-103284] N91-11061

SOLAR ENERGY CONVERSION
Terrestrial nickel/hydrogen battery evaluation
[DE90-014863] N91-11151
High efficiency CuInSe2 and CuInGaSe2 cells and materials research
[DE90-000362] N91-11280

SOLAR HEATING
Colorado State University program for developing, testing, evaluating and optimizing solar heating and cooling systems
[DE90-017273] N91-11291

SOLAR LIMB
White light solar corona: An atlas of 1988 K-coronameter synoptic charts, December 1987 to January 1989
[NASA-CR-184955] N91-11649

SOLAR NEUTRINOS
Analytic studies in nuclear astrophysics N91-11628

SOLAR NEUTRONS
Plots of the 5-minute neutron monitor intensity and multiplicities recorded by the Rome 17-NM64, January 1990
[IFSI-90-5] N91-11653
Plots of the 5-minute neutron monitor intensity and multiplicities recorded by the Rome 17-NM64, February 1990
[IFSI-90-6] N91-11654

SOLAR RADIATION
The delta-Sobolev approach for modeling solar spectral irradiance and radiance N91-11650

SOLAR RADIO BURSTS
Type 2 solar radio bursts recorded at Weissenau, 1966-1987
[PB90-198334] N91-11648

SOLAR SPECTRA
Preliminary results from the advanced photovoltaic experiment flight test
[NASA-TM-103269] N91-11058
The delta-Sobolev approach for modeling solar spectral irradiance and radiance N91-11650

SOLAR SPECTROMETERS
Plots of the 5-minute neutron monitor intensity and multiplicities recorded by the Rome 17-NM64, January 1990
[IFSI-90-5] N91-11653
Plots of the 5-minute neutron monitor intensity and multiplicities recorded by the Rome 17-NM64, February 1990
[IFSI-90-6] N91-11654

SOLAR TERRESTRIAL INTERACTIONS
Combined Release and Radiation Effects Satellite (CRRES): Atlas 1 (Atlas/Centaur-69) launch vehicle
[NASA-TM-103460] N91-11040

SOLAR THERMAL ELECTRIC POWER PLANTS
Study on feasible applications of stirling cycle machine
[DE91-701463] N91-11293

SOLAR WIND
A two dimensional multisonic model of plasma interaction for cometary atmosphere with solar wind
[MITT-69] N91-11621
Availability of hydrogen for lunar base activities
[NASA-CR-187367] N91-11644

SOLDERED JOINTS
Solderability of environmentally exposed Sn-plated surfaces
[DE91-000035] N91-11110
Thermal stresses in layered electrical assemblies bonded with solder
[DE90-015563] N91-11263
SOLDERING
Solderability of environmentally exposed Sn-plated surfaces
[DE91-000035] N91-11110
Thermal stresses in layered electrical assemblies bonded with solder
[DE90-015563] N91-11263
SOLDERS
Thermal stresses in layered electrical assemblies bonded with solder
[DE90-015563] N91-11263
SOLID ELECTROLYTES
Three-Man Solid Electrolyte Carbon Dioxide Electrolysis Breadboard
[NASA-CR-185612] N91-11148
SOLID PROPELLANT COMBUSTION
A simulation of the flow near a burning propellant in a solid propellant rocket motor N91-11056
SOLID PROPELLANT ROCKET ENGINES
Conjugate (solid/fluid) computational fluid dynamics analysis of the space shuttle solid rocket motor nozzle/case and case field joints N91-10879
A simulation of the flow near a burning propellant in a solid propellant rocket motor N91-11056
SOLID PROPELLANTS
Propulsion simulation for magnetically suspended wind tunnel models
[NASA-CR-182093] N91-11027
SOLID ROCKET PROPELLANTS
Hybrid Propulsion Technology Program, phase 1. Volume 2: Technical discussion
[NASA-CR-183951] N91-11055
SOLID STATE DEVICES
Center for electronics and electrical engineering technical publication announcements covering Center programs, July - September, 1989, with 1990 CEEE events calendar
[PB90-206491] N91-11145
SOLID WASTES
Assessment of municipal solid waste for energy production in the Western United States
[DE90-000361] N91-11283
SOLID-SOLID INTERFACES
Relations between microstructure and mechanical behaviour of SiC/SiC composites: Interface effects on multiple cracking in multifilament materials
[ISAL-89-0098] N91-11065
Elastic/plastic analyses of advanced composites investigating the use of the compliant layer concept in reducing residual stresses resulting from processing
[NASA-TM-103204] N91-11074
SOLVENTS
Intramolecular electron transfer rates
[DE90-017447] N91-11504
SOMMERFELD WAVES
Elementary inversion, energy velocity, and a generalized Sommerfeld theorem
[DE90-018046] N91-11486
SOUND FIELDS
Sound field fluctuations due to large scale wind-driven turbulence N91-11492
SOUND GENERATORS
A model for the sound generation due to compressible vortex-body interaction
[MPIS-MITT-96] N91-11491
SOUND LOCALIZATION
Contributions to the sound location in the atmosphere
[ETN-90-97863] N91-11490
SOUND PRESSURE
An investigation of thermally driven acoustical oscillations in helium systems
[DE90-018049] N91-11086
Vortex-induced noise and vibration in flow past several flat plates N91-11163
SOUND PROPAGATION
Sound field fluctuations due to large scale wind-driven turbulence N91-11492
SOUND TRANSMISSION
Aircraft interior noise reduction by alternate resonance tuning
[NASA-CR-186879] N91-11488
SOUND WAVES
Instabilities of two-dimensional inviscid compressible vortices N91-11181
Arctic acoustics ultrasonic modeling studies
[AD-A224165] N91-11489
SOUTHERN OSCILLATION
Meteorological characteristics of the El Nino/Southern Oscillation phenomenon N91-11340
SPACE OBSERVATIONS (FROM EARTH)
A search for small comets in consecutive images acquired with a ground-based telescope N91-11626
SPACE PLASMAS
Dynamic trapping of electrons in space plasmas
[TRITA-EPP-89-07] N91-11528
SPACE PLATFORMS
Non-linear vibration of large, imperfect space structures N91-10930
Analysis and design of a high power, digitally-controlled spacecraft power system
[NASA-CR-186546] N91-11053
Reference concepts for a space-based hydrogen-oxygen combustion, turboalternator, burst power system
[DE90-016692] N91-11155
SPACE SHUTTLE ASCENT STAGE
External tank aerothermal design criteria verification, volume 1
[NASA-CR-183996] N91-11037
External tank aerothermal design criteria verification, volume 2
[NASA-CR-183997] N91-11038
SPACE SHUTTLE BOOSTERS
Conjugate (solid/fluid) computational fluid dynamics analysis of the space shuttle solid rocket motor nozzle/case and case field joints N91-10879
First incremental buy for Increment 2 of the Space Transportation System (STS)
[NASA-CR-183855] N91-11034
Hybrid Propulsion Technology Program, phase 1. Volume 1: Executive summary
[NASA-CR-183950] N91-11054
Hybrid Propulsion Technology Program, phase 1. Volume 2: Technical discussion
[NASA-CR-183951] N91-11055
SPACE SHUTTLE MAIN ENGINE
Marshall Space Flight Center CFD overview N91-10843
Analysis of the SSME HPOTP bearing inlet cavity N91-10877
A combined Eulerian-Lagrangian two-phase analysis of the SSME HPOTP nozzle plug trajectories N91-10878
Heat flux measurement in SSME turbine blade tester
[NASA-TM-103274] N91-11205
Real-time failure control (SAFD)
[NASA-CR-184025] N91-11233
SPACE SHUTTLE ORBITERS
Numerical aerodynamic simulation of the space shuttle ascent environment N91-10875
Final shuttle-derived atmospheric database: Development and results from thirty-two flights
[NASA-CR-185636] N91-11310
SPACE SHUTTLES
Marshall Space Flight Center CFD overview N91-10843
Computational fluid dynamics analysis of space shuttle main propulsion feed line 17-inch disconnect valves N91-10876
SPACE TRANSPORTATION SYSTEM
Final shuttle-derived atmospheric database: Development and results from thirty-two flights
[NASA-CR-185636] N91-11310
SPACE WEAPONS
Reference concepts for a space-based hydrogen-oxygen combustion, turboalternator, burst power system
[DE90-016692] N91-11155
SPACE-TIME FUNCTIONS
An investigation of the Newman-Penrose constants for massless free fields of arbitrary spin N91-11630
SPACEBORNE EXPERIMENTS
Computational fluid dynamics at the Lewis Research Center: An overview N91-10842
SPACECRAFT CONFIGURATIONS
Grid generation and flow computation about a Martian entry vehicle
[NASA-CR-187032] N91-11042
Data base architecture for instrument characteristics critical to spacecraft conceptual design
[NASA-TM-4213] N91-11391
SPACECRAFT CONSTRUCTION MATERIALS
Graphite fluoride fibers and their applications in the space industry
[NASA-TM-103265] N91-11062
Potential for advanced thermoplastic composites in space systems
[DE90-014447] N91-11069
SPACECRAFT DESIGN
NASA Computational Fluid Dynamics Conference. Volume 2: Sessions 7-12
[NASA-CP-10038-VOL-2] N91-10868
Contributions in the field of aeroelastics on the occasion of the 60th anniversary of Professor Dr.-Ing. Habil. Hans Wilhelm Foersching
[ETN-90-97630] N91-10920
Structural dynamics qualification of spacecraft N91-10922
Automated Fluid Interface System (AFIS)
[NASA-CR-183969] N91-11031
External tank aerothermal design criteria verification, volume 1
[NASA-CR-183996] N91-11037
External tank aerothermal design criteria verification, volume 2
[NASA-CR-183997] N91-11038
Spacecraft design project: High latitude communications satellite
[NASA-CR-186689] N91-11039
Data base architecture for instrument characteristics critical to spacecraft conceptual design
[NASA-TM-4213] N91-11391
Design of a scientific probe for obtaining Mars surface material
[NASA-CR-186672] N91-11641
SPACECRAFT GUIDANCE
Design of a scientific probe for obtaining Mars surface material
[NASA-CR-186672] N91-11641
SPACECRAFT INSTRUMENTS
Data base architecture for instrument characteristics critical to spacecraft conceptual design
[NASA-TM-4213] N91-11391
SPACECRAFT LAUNCHING
Combined Release and Radiation Effects Satellite (CRRES): Atlas 1 (Atlas/Centaur-69) launch vehicle
[NASA-TM-103460] N91-11040
SPACECRAFT MAINTENANCE
Intelligent Robotic Systems Study (IRSS), phase 2
[NASA-CR-183963] N91-11432
SPACECRAFT MANEUVERS
Optimal control design by Volterra Series and its application to spacecraft maneuvers N91-11044
SPACECRAFT MODELS
Advanced technology satellite demodulator development
[NASA-CR-185127] N91-11134
SPACECRAFT POWER SUPPLIES
Analysis and design of a high power, digitally-controlled spacecraft power system
[NASA-CR-186546] N91-11053
Reference concepts for a space-based hydrogen-oxygen combustion, turboalternator, burst power system
[DE90-016692] N91-11155
SPACECRAFT PROPULSION
Design of a scientific probe for obtaining Mars surface material
[NASA-CR-186672] N91-11641
SPACECRAFT REENTRY
Flight simulation programs for space plane
[NAL-TM-594] N91-11035
SPACECRAFT TRAJECTORIES
Optimal trajectories of aircraft and spacecraft N91-10968
SPACECREWS
Radiological health risks to astronauts from space activities and medical procedures
[NASA-TM-102164] N91-11356
SPATIAL DEPENDENCIES
Stochastic approximation of the MLE for a spatial point pattern
[CWI-BS-R8926] N91-11475
SPATIAL DISTRIBUTION
Stochastic approximation of the MLE for a spatial point pattern
[CWI-BS-R8926] N91-11475
SPATIAL RESOLUTION
Multiple-energy techniques in industrial computerized tomography
[DE90-017518] N91-11081
Forest classification with high resolution satellite images. Research into the use of spatial information to improve the multi-spectral classification with SPOT images
[BCRS-89-32] N91-11269
Integration of multispectral and pancromatic channels of HRV (SPOT) sensor for obtaining color compositions with a spatial resolution of approximately 10 m
[INPE-5035-TDL/403] N91-11278
SPECIFIC HEAT
Thermal performance analysis for heat exchangers using nonazeotropic refrigerant mixtures
[DE90-016030] N91-11186
SPECIFICATIONS
Conceptual design of an Open-Cycle Ocean Thermal Energy Conversion Net Power-Producing Experiment (OC-OTEC NPPE)
[DE90-000304] N91-11282
SPECKLE PATTERNS
Speckle imaging of complicated objects N91-11617

SPECTRAL CORRELATION
Spectral lithostratigraphic correlation of boreholes [INPE-5022-TDL/402] N91-11332
SPECTRAL METHODS
Numerical simulation of transition from laminar to turbulent duct flow [ESA-TT-1144] N91-11199
SPECTRAL REFLECTANCE
The delta-Sobolev approach for modeling solar spectral irradiance and radiance N91-11650
SPECTRAL RESOLUTION
A study of the ten and twenty micron silicate features in celestial infrared sources N91-11609
SPECTROSCOPY
Electric-field dependent electroreflectance and photocurrent spectroscopy in InGaAs/InAlAs strained-layer superlattices [DE90-015698] N91-11559
SPEED CONTROL
Four dimensional navigation in air traffic with 4-D navigation aircraft N91-10991
SPIN-LATTICE RELAXATION
Novel measurements of nuclear spin cross-relaxation in metal hydrides [DE90-018042] N91-11503
SPIRAL GALAXIES
The relationship of galaxy morphology to nuclear star formation in non-interacting spiral galaxies N91-11618
M51: The Whirlpool Galaxy, analysis and simulation N91-11631
SPLINE FUNCTIONS
Beta splines interpolation for DEM's [INPE-5039-PRE/1572] N91-11415
Dynamic MRI reconstruction as a moment problem. Part 3: An error analysis of reconstruction by sinc and spline interpolation in a Hilbert space setting [CWI-AM-R9002-PT-3] N91-11441
Mathematical models of mixture properties: B-splines and optimization with form conditions [ETN-90-97829] N91-11462
SPRAYED COATINGS
Evaluation of thermal sprayed metallic coatings for use on the structures at Launch Complex 39 [NASA-TM-103807] N91-11121
SPUTTERING
Computer-controlled ion beam deposition systems for high T(sub c) superconductor and other multi-component oxide thin films and layered structures [DE90-017798] N91-11577
STABILITY
Microprocessor system for temperature regulation and stabilization [DE90-634244] N91-11160
Design and testing of a high temperature superconducting current lead [DE90-017812] N91-11579
Formation and stability of As-H bonds in H-implanted GaAs [DE91-000043] N91-11584
STABILITY TESTS
MIS capacitor studies on silicon carbide single crystals [NASA-CR-187350] N91-11555
STABILIZATION
Microprocessor system for temperature regulation and stabilization [DE90-634244] N91-11160
STAGNATION FLOW
Heat transfer in variable density, low Mach number, stagnating turbulent flows N91-11171
STAINLESS STEELS
A study of chromium carbide precipitation at interphase boundaries in stainless steel welds [DE91-000360] N91-11113
Projective scales against high temperature corrosion [ETN-90-97770] N91-11116
STANDARD DEVIATION
Computation of standard deviations in Eigenvalue calculations [DE90-017809] N91-11479
STANDARDIZATION
Short crack growth under realistic flight loading: Model predictions and experimental results for Al 2024 and Al-Li 2090 N91-11246
OSI in the NASA science internet: An analysis [NASA-CR-177561] N91-11425
STANDARDS
Generic quality assurance/quality control guide for photovoltaic concentrator design, development and system installation [DE90-017040] N91-11290
OSI in the NASA science internet: An analysis [NASA-CR-177561] N91-11425
STAR DISTRIBUTION
Population studies in groups and clusters of galaxies, volumes 1 and 2 N91-11608
STAR FORMATION
The relationship of galaxy morphology to nuclear star formation in non-interacting spiral galaxies N91-11618
Recent starbirth and starburst activity in nearby galaxies N91-11627
STARBURST GALAXIES
Recent starbirth and starburst activity in nearby galaxies N91-11627
Radio and infrared emission from starburst galaxies N91-11661
STATE ESTIMATION
Comparison of a mathematical one-point model and a multi-point model of aircraft motion in moving air N91-10969
On three dimensional object recognition and pose-determination: An abstraction based approach [NASA-CR-186894] N91-11396
STATIC CHARACTERISTICS
Problems of static divergence concerning the rpm regulation of wind turbines using centrifugal force controlling means and rotating slat [ETN-90-97858] N91-11281
STATIC LOADS
A three-dimensional solid element model for finite rotation of composite shells N91-11262
STATISTICAL ANALYSIS
Statistical system identification of structures with flexible joints N91-11232
Spectral lithostratigraphic correlation of boreholes [INPE-5022-TDL/402] N91-11332
Astronomical applications of survival analysis N91-11615
STATISTICAL CORRELATION
The calculation of correlation functions in the statistical theory of turbulent flows N91-11176
STATISTICAL MECHANICS
Natural current profiles in a tokamak [DE91-000126] N91-11540
STATORS
Prediction of turbine rotor-stator interaction using Navier-Stokes methods N91-10881
STEADY FLOW
Computations of three-dimensional steady and unsteady viscous incompressible flows N91-10852
Analysis and control of supersonic vortex breakdown flows [NASA-CR-186897] N91-10903
Ejector thrust augmentors: Pulse-starting approach to the second solution N91-10913
Calculation of aerodynamic characteristics of airplane configurations at high angle of attack in steady and unsteady flow N91-11009
Test cases for computation of internal flows in aero engine components [AGARD-AR-275] N91-11022
STEADY STATE CREEP
Micromechanics of semi-brittle ceramics N91-11119
STEELS
The growth of short cracks in 4340 steel and aluminum-lithium 2090 N91-11247
STELLAR COMPOSITION
Violet and visual flux problems in red giant stars N91-11632
STELLAR ENVELOPES
Novae as distance indicators [NASA-CR-186278] N91-11605
From red giants to planetary nebulae: Asymmetries, dust, and polarization N91-11622
STELLAR EVOLUTION
From red giants to planetary nebulae: Asymmetries, dust, and polarization N91-11622
Analytic studies in nuclear astrophysics N91-11628
Violet and visual flux problems in red giant stars N91-11632
Late stages in the evolution of classical novae [NASA-TM-102969] N91-11633
Numerical study of compressible magnetoconvection with an open transitional boundary [DE91-000148] N91-11651
STELLAR LUMINOSITY
Population studies in groups and clusters of galaxies, volumes 1 and 2 N91-11608
Analytic studies in nuclear astrophysics N91-11628
STELLAR MASS
Long-term observations of three massive x ray binary transients: 4U0115+63, V0332+53, and GX301-2 N91-11612
A new site for the astrophysical gamma-process [DE90-017519] N91-11635
STELLAR MASS ACCRETION
Numerical studies of electron scattering in astrophysics N91-11625
STELLAR RADIATION
Very high energy gamma rays from isolated pulsars and non-pulsating objects N91-11655
Radio and infrared emission from starburst galaxies N91-11661
STELLAR ROTATION
Observation and analysis of variable linear polarization in the yellow supergiant star Epsilon Aurigae N91-11616
STELLAR SPECTRA
Observations and interpretation of the infrared emission from supernova SN1987A N91-11611
Recent starbirth and starburst activity in nearby galaxies N91-11627
Late stages in the evolution of classical novae [NASA-TM-102969] N91-11633
Polarized radiation from inhomogeneous shocks N91-11662
STELLAR SPECTROPHOTOMETRY
A study of the ten and twenty micron silicate features in celestial infrared sources N91-11609
Recent starbirth and starburst activity in nearby galaxies N91-11627
Violet and visual flux problems in red giant stars N91-11632
STEP FUNCTIONS
Evaluation of the integral [PB90-235011] N91-11437
STIFFNESS
The measurement and finite element analysis of the dynamic stiffness of non-uniform clearance, gas, thrust bearings [DE90-015120] N91-11214
STIRLING CYCLE
Performances of four magnetic heat-pump cycles [DE90-015606] N91-11185
Bench-scale testing of a heat-pipe receiver for solar thermal electric applications [DE90-009834] N91-11289
Study on feasible applications of stirling cycle machine [DE91-701463] N91-11293
STIRLING ENGINES
Study on feasible applications of stirling cycle machine [DE91-701463] N91-11293
STOCHASTIC PROCESSES
A stochastic analysis of state transitions in an air space management system N91-10980
Controller methodologies for integrated control/structure design optimization of large flexible structures N91-11043
Convergence of solutions of one-dimensional stochastic heat equations [REPT-90-40] N91-11478
STOICHIOMETRY
Mechanical properties, fracture behavior, and grain-boundary chemistry of B-doped NiAl [DE90-015153] N91-11558
STORAGE BATTERIES
Advanced secondary batteries: Their applications, technological status, market and opportunity [DE90-796146] N91-11146
STORAGE STABILITY
Stability of liquid propellants under long-term storage [AD-A223934] N91-11126
STORMS (METEOROLOGY)
Basic dynamics of low frequency variability and the storm tracks N91-11339
STRAIN GAGES
Measurement of two-phase flow momentum with force transducers [DE90-008748] N91-11188
STRAIN RATE
Effects of electric current and field on the behavior of metallic materials N91-11095
STRATIGRAPHY
Spectral lithostratigraphic correlation of boreholes [INPE-5022-TDL/402] N91-11332
STRATOSPHERE
Large-scale dynamics and transport in the stratosphere [NASA-CR-187327] N91-11311
Comparison of clear air atmospheric radar techniques for the study of atmospheric dynamics in the troposphere and the stratosphere [PB90-256314] N91-11313
STRESS ANALYSIS
Thermal stress-induced grain boundary cavitation in narrow, aluminum alloy metallizations N91-11093
STRESS DISTRIBUTION
A molecular dynamics model of the orthogonal cutting process [DE90-015911] N91-11230
Deducing mechanical properties due to interfaces from their acoustical response [DE90-016704] N91-11234
STRESS INTENSITY FACTORS
Deducing mechanical properties due to interfaces from their acoustical response [DE90-016704] N91-11234

Short-crack growth behaviour in various aircraft materials
[AGARD-R-767] N91-11240
An AGARD supplemental test programme on the behaviour of short cracks under constant amplitude and aircraft spectrum loading N91-11241

STRESS MEASUREMENT
Residual stress measurements and microstructural characterization of graphite-aluminum metal matrix composite N91-11068

STRESS-STRAIN RELATIONSHIPS
Deformation mechanisms in rapidly solidified aluminum alloys N91-11096

STRESSES
Characterization of short fatigue cracks at notches in SiC particulate aluminum composite
[DE90-018043] N91-11071
Relationship of microstructure and tensile properties for neutron-irradiated vanadium alloys
[DE90-017863] N91-11105
Stress accommodation in large-mismatch systems
[DE90-017032] N91-11562

STRONTIUM COMPOUNDS
Muon SR studies on Sr2CuO2Cl2, La2CuO4, and Nd2CuO4: 2-D magnetism, local fields and muon sites
[DE90-018014] N91-11506

STRUCTURAL ANALYSIS
Structural analysis and optimization of a propfan-blade by use of the finite element method N91-10924
Analysis of deformation characteristics of a heavily deformed Cu-20 percent Nb composite
[DE90-018041] N91-11070
In-situ pore structure analysis during aging and drying of gels
[DE91-000044] N91-11089
High-performance equation solvers and their impact on finite element analysis
[NASA-TM-102735] N91-11252
Development of the structural materials information center
[DE90-016521] N91-11603

STRUCTURAL ENGINEERING
Computer-Aided Structural Engineering (CASE) project: Investigation and design of U-frame structures using program CUFRBC. Volume C: User's guide for channels
[AD-A224388] N91-11395

STRUCTURAL FAILURE
Determination of the short crack effect in 2090-T8E41 aluminum lithium N91-11242

STRUCTURAL VIBRATION
Forced vibration analysis of plates and shallow shells N91-11237

STRUCTURAL WEIGHT
Weight evaluation and sensitivity analysis for space plane: SSTO
[NAL-TM-598-1] N91-11036

SUBMILLIMETER WAVES
Fabrication and optimization of a whiskerless Schottky barrier diode for submillimeter wave applications
[NASA-CR-186381] N91-11144

SUBROUTINE LIBRARIES (COMPUTERS)
NUMVEC FORTRAN library manual. Chapter: Partial differential equations. Routine: OEHPC
[CWI-NM-R8915] N91-11399

SUBSONIC FLOW
Johnson Space Center CFD overview N91-10844
Unsteady wind tunnel wall interferences in subsonic and transonic profile flows N91-10928

SUBSONIC FLUTTER
Determination of unsteady aerodynamic forces on engines with a view to flutter investigations N91-10927

SULFATES
Estimation of seasonal and annual acidic deposition through aggregation of three-day episodic periods
[PB90-252628] N91-11303

SULFUR
Nitrogen and sulfur in irregular galaxies N91-11624

SUN
Plots of the 5-minute neutron monitor intensity and multiplicities recorded by the Rome 17-NM64, January 1990
[IFSI-90-5] N91-11653

SUPERCOMPUTERS
NASA Computational Fluid Dynamics Conference. Volume 1: Sessions 1-6
[NASA-CP-10038-VOL-1] N91-10839
NASA Computational Fluid Dynamics Conference. Volume 2: Sessions 7-12
[NASA-CP-10038-VOL-2] N91-10868
Use of the VP-200 computer for aerothermodynamic problems
[MBB/FE122/S/PUB/388] N91-11424
On the adequacy of message-passing parallel supercomputers for solving neutron transport problems
[DE90-016041] N91-11431
Status reports of supercomputing astrophysics in Japan
[DE90-513793] N91-11640

SUPERCONDUCTING FILMS
Laser applications for high-T(sub c) superconductors
[DE90-017743] N91-11209
Computer-controlled ion beam deposition systems for high T(sub c) superconductor and other multi-component oxide thin films and layered structures
[DE90-017798] N91-11577

SUPERCONDUCTING MAGNETS
MHD technology transfer, integration, and review committee
[DE90-017886] N91-11542

SUPERCONDUCTING SUPER COLLIDER
CAD tools for detector design
[DE90-017337] N91-11412
Task A: High energy physics program experiment and theory. Task B: High energy physics program numerical simulation
[DE90-017336] N91-11512
Report of the Department of Energy (DOE) Office of Energy research review committee on the site-specific conceptual design of the superconducting super collider
[DE90-018021] N91-11513

SUPERCONDUCTIVITY
Laser applications for high-T(sub c) superconductors
[DE90-017743] N91-11209
Excess oxygen defects in layered cuprates
[DE90-017669] N91-11565
Design and testing of a high temperature superconducting current lead
[DE90-017812] N91-11579
Superconducting and structural properties of the (Ba(0.6)K(0.4)) (Bi(1-y)Sb(y))O3 system
[DE90-017836] N91-11580
Structure-property relationships for (beta)- and (kappa)-phase BEDT-TTF salts and their use in the synthesis of (kappa)-(BEDT-TTF)2Cu(N(CN)2)Br. A salt having the highest T(sub c) (inductive onset = 11.6 K, resistive, onset = 12.5 K) yet observed in an organic superconductor
[DE90-017804] N91-11582

SUPERCONDUCTORS
Microfilamentary Bi2Sr2Ca1Cu2O8 fibers
[DE90-018013] N91-11571

SUPERGIANT STARS
Observation and analysis of variable linear polarization in the yellow supergiant star Epsilon Aurigae N91-11616

SUPERHEATING
Complete adiabatic evaporation of highly superheated liquid jets
[MPIS-MITT-95] N91-11588

SUPERLATTICES
Electric-field dependent electroreflectance and photocurrent spectroscopy in InGaAs/InAlAs strained-layer superlattices
[DE90-015698] N91-11559
Optical characterization of CdZnTe/CdTe strained quantum wells
[DE90-017036] N91-11563
Ion mixing of semiconductor superlattices
[DE90-017769] N91-11569
Compositional imaging of semiconductor interfaces by Z-contrast Scanning Transmission Electron Microscope (STEM)
[DE90-017763] N91-11576

SUPERNOVA 1987A
Observations and interpretation of the infrared emission from supernova SN1987A N91-11611

SUPERNOVAE
Analytic studies in nuclear astrophysics N91-11628
A new site for the astrophysical gamma-process
[DE90-017519] N91-11635

SUPERPLASTICITY
Effects of electric current and field on the behavior of metallic materials N91-11095

SUPERSONIC AIRCRAFT
Application of unstructured grid methods to steady and unsteady aerodynamic problems N91-10856

SUPERSONIC BOUNDARY LAYERS
Non linear evolution of a second mode wave in supersonic boundary layers N91-10848

SUPERSONIC COMBUSTION RAMJET ENGINES
Application of CFD codes for the simulation of scramjet combustor flowfields N91-10873

SUPERSONIC FLOW
Navier-Stokes solutions for flows related to store separation N91-10861
Three-dimensional calculation of supersonic reacting flows using an LU scheme N91-10871
Application of CFD codes for the simulation of scramjet combustor flowfields N91-10873
Analysis of three-dimensional viscous flow in a supersonic throughflow fan N91-10885
Analysis and control of supersonic vortex breakdown flows
[NASA-CR-186897] N91-10903
Structure of supersonic turbulent reattaching shear layers N91-10914
Study of asymmetric supersonic jet flow for ejectors
[DE90-015598] N91-10917
A global pressure relaxation for high speed laminar and turbulent flows N91-11177

SUPERSONIC INLETS
CFD analysis for high speed inlets N91-10888

SUPERSONIC JET FLOW
Study of asymmetric supersonic jet flow for ejectors
[DE90-015598] N91-10917

SUPERSONIC TURBINES
The aerodynamic effects of nozzle guide vane shock wave and wake passing on a transonic turbine rotor N91-10915
A contribution to the output analysis and layout of transonic axial turbine stages
[ETN-90-97862] N91-11017

SUPERSONIC WIND TUNNELS
Ejector thrust augmentors: Pulse-starting approach to the second solution N91-10913

SUPPORTS
Design and evaluation of thrust vectored nozzles using a multicomponent thrust stand
[NASA-CR-180474] N91-11050

SURFACE CRACKS
Study of the wear behavior induced by fretting in aluminum and titanium alloys
[ECL-90-01] N91-11229
An AGARD supplemental test programme on the behaviour of short cracks under constant amplitude and aircraft spectrum loading N91-11241

SURFACE PROPERTIES
Structure of amorphous-silicon and germanium alloy films
[DE90-000355] N91-11557
A study of the chemical, mechanical, and surface properties of thin films of hydrogenated amorphous carbon
[DE91-000357] N91-11585

SURFACE REACTIONS
Numerical experiments with climatic zonally-averaged models
[INPE-5083-TDL/417] N91-11343

SURFACE ROUGHNESS EFFECTS
Measurement and calculation of surface roughness effects on turbulent flow and heat transfer N91-11183

SURFACE TEMPERATURE
The influence of environmental factors on the temperature of the radiosonde thermistor N91-11325

SURFACE WAVES
Wave data assimilation in a 3rd generation. Wave prediction model for the North Sea: An optimal control approach
[BCRS-89-22] N91-11348

SURFACES
Evaluation process for the examination of curved surface workpieces using coordinate measuring instruments
[ETN-90-97901] N91-11203
Methods for the construction of constant curve free form surfaces
[ETN-90-97861] N91-11463

SURVEILLANCE RADAR
The use of downlinked measurements to track civil aircraft N91-11004
Contribution of the satellite techniques to the surveillance of air traffic N91-11005

SWEPT WINGS
CFD for applications to aircraft aeroelasticity N91-10855

SWITCHES
Douglas flight deck design philosophy N91-10939

SYMBOLIC PROGRAMMING
Symbolic manipulation software and the study of differential equations
[DE90-017674] N91-11413

SYMMETRY
Accurate representations of general textures by a set of weighted grains
[DE90-016487] N91-11485

SYNCHRONOUS PLATFORMS
Thermal-distortion analysis of a spacecraft box truss in geostationary orbit
[NASA-TP-3054] N91-11041

SYNTAX
A logical background of a method for the handling of incompatible pieces of knowledge
[REPT-90-13] N91-11401

SYNTHESIS (CHEMISTRY)
Chemically vapor deposited diamond films
[DE91-000384] N91-11125

Processing of YBA2Cu3O7 tapes from a molten salt precursor
[DE90-017656] N91-11564
Structure-property relationships for (beta)- and (kappa)-phase BEDT-TTF salts and their use in the synthesis of (kappa)-(BEDT-TTF)2Cu(N(CN)2)Br. A salt having the highest T(sub c) (inductive onset = 11.6 K, resistive, onset = 12.5 K) yet observed in an organic superconductor
[DE90-017804] N91-11582

SYNTHETIC APERTURE RADAR
Azimuthal resolution degradation due to ocean surface motion in focused arrays and SARS
[AD-A223315] N91-11135

SYNTHETIC FUELS
Co-researches with researchers of alternative energy of petroleum in EC countries
[DE91-701466] N91-11129

SYSTEM FAILURES
Douglas flight deck design philosophy N91-10939
Fault recovery recommendation N91-10952
Parallelized reliability estimation of reconfigurable computer networks
[NASA-CR-182101] N91-11430

SYSTEM IDENTIFICATION
System identification of lossless layered media from input-output data
[CWI-BS-R8929] N91-11166
Statistical system identification of structures with flexible joints N91-11232

SYSTEMS ANALYSIS
DUWECS reference guide V1.0: Delft University wind energy converter simulation program
[MEMT-5] N91-11294

SYSTEMS ENGINEERING
Design of the derivative balance for the transonic wind tunnel N91-10925
Cockpit avionics integration and automation N91-10938
Combination of Hatley and Ward/Mellor methods for real time systems
[INPE-5078-TDL/412] N91-11419

SYSTEMS INTEGRATION
Cockpit avionics integration and automation N91-10938
Integration of aircraft capability in air traffic handling simulations N91-11007
OSI in the NASA science internet: An analysis
[NASA-CR-177561] N91-11425

SYSTEMS STABILITY
A synthesis of time and frequency domain methods for the control of infinite-dimensional systems: A system theoretic approach
[W-8912] N91-11456
Compensability of uncertain systems
[REPT-90-10] N91-11527

T

TAIL ASSEMBLIES
Grid generation and inviscid flow computation about aircraft geometries N91-10857

TAIWAN
Taiwan area mesoscale experiment: A guide to precipitation patterns during the 1987 field phase
[PB90-256355] N91-11336

TAKEOFF
Optimal trajectories of aircraft and spacecraft N91-10968
Wind models for flight simulation N91-10975
Expert systems for the generation of thermal area arrival paths for civil transport N91-10995
Flight simulation programs for space plane
[NAL-TM-594] N91-11035

TASK COMPLEXITY
Determinants of dual-task interference and resource theories in cognitive psychology
[ESA-TT-1127] N91-11381

TASKS
Determinants of dual-task interference and resource theories in cognitive psychology
[ESA-TT-1127] N91-11381

TAYLOR SERIES
Optimal control design by Volterra Series and its application to spacecraft maneuvers N91-11044

TEARING MODES (PLASMAS)
Confinement and fluctuations in the MST (Madison Symmetric Torus) reversed field pinch
[DE90-018019] N91-11535
Nonlinear saturation of ideal interchange modes in a sheared magnetic field
[DE91-000575] N91-11548

TECHNOLOGIES
Civil space technology initiative
[NASA-TM-103017] N91-11028
Research and technology at Kennedy Space Center
[NASA-TM-102150] N91-11664

TECHNOLOGY ASSESSMENT
Defects in close-packed metals and alloys
[DE90-017502] N91-11097
Technical assessment and economic study of compressed air energy storage in Japan
[DE91-701405] N91-11292
Holding the edge: Maintaining the defense technology base. Volume 2: Appendixes
[PB90-253345] N91-11597

TECHNOLOGY TRANSFER
MHD technology transfer, integration, and review committee
[DE90-017886] N91-11542
Technology transfer: Hotlines
[PB90-237140] N91-11594

TECHNOLOGY UTILIZATION
Photovoltaic options for solar electric propulsion
[NASA-TM-103284] N91-11061

TECTONICS
Satellite elevation magnetic anomalies and their use in tectonic studies N91-11272
Aspects of the earthquake geology and seismotectonics of the southern San Andreas and related faults N91-11329
Tectonics of one-plate planets N91-11647

TELEOPERATORS
Improved tracking for bilateral teleoperators with time delay
[DE90-015392] N91-11222
Intelligent Robotic Systems Study (IRSS), phase 2
[NASA-CR-183963] N91-11432

TEMPERATURE CONTROL
Microprocessor system for temperature regulation and stabilization
[DE90-634244] N91-11160
Design of a scientific probe for obtaining Mars surface material
[NASA-CR-186672] N91-11641

TEMPERATURE DEPENDENCE
High-resolution electron microscopy observations of athermal omega phase in Ti-Mo alloys
[DE90-017526] N91-11098
Muon SR studies on Sr2CuO2Cl2, La2CuO4, and Nd2CuO4: 2-D magnetism, local fields and muon sites
[DE90-018014] N91-11506
Surface anharmonicity: Temperature dependence of phonon energies on Cu(110)
[DE90-017735] N91-11567
Magnetic properties of ultrathin epitaxial films of iron
[DE90-017861] N91-11570

TEMPERATURE DISTRIBUTION
Surface and bottom temperature distribution for the Northeast continental shelf
[PB90-252172] N91-11349

TEMPERATURE EFFECTS
Developments to enhance meteorological forecasting for air traffic services N91-11006
Elastic/plastic analyses of advanced composites investigating the use of the compliant layer concept in reducing residual stresses resulting from processing
[NASA-TM-103204] N91-11074
Heat treatment study 2
[NASA-CR-184009] N91-11091
Deformation effects on the development of grain boundary chronium depletion (sensitization) in type 316 austenitic stainless steels
[DE90-016130] N91-11092
Deformation mechanisms in rapidly solidified aluminum alloys N91-11096
Study on radiation-induced deterioration of grease at high temperature. Part 1: Test method on thermal aging
[DE90-508070] N91-11120
Stability of liquid propellants under long-term storage
[AD-A223934] N91-11126
Thermal performance analysis for heat exchangers using nonazeotropic refrigerant mixtures
[DE90-016030] N91-11186
Planetary boundary layer dynamics over the Amazon rain forest N91-11317
MIS capacitor studies on silicon carbide single crystals
[NASA-CR-187350] N91-11555
Photoluminescence studies of In(x)Ga(1-x)As/Al(y)Ga(1-y)As strained-layer structures
[DE90-017031] N91-11561

TEMPERATURE GRADIENTS
An investigation of thermally driven acoustical oscillations in helium systems
[DE90-018049] N91-11086

TEMPERATURE MEASUREMENT
Radiometric observation of the atmospheric boundary layer (the ROSSA Project) N91-11324

TENSILE DEFORMATION
Analysis of deformation characteristics of a heavily deformed Cu-20 percent Nb composite
[DE90-018041] N91-11070

TENSILE PROPERTIES
Characterization of short fatigue cracks at notches in SiC particulate aluminum composite
[DE90-018043] N91-11071
Load transfer between fiber and matrix in carbon fiber reinforced plastic composites tensile behavior of an embedded single filament specimen
[ONERA-NT-1989-9] N91-11075
Relationship of microstructure and tensile properties for neutron-irradiated vanadium alloys
[DE90-017863] N91-11105
Influence of heat treatment on microstructure and properties of an advanced high temperature titanium alloy
[PNR-90689] N91-11107
A continuum tensile failure model with friction
[DE90-018006] N91-11265

TENSILE STRENGTH
Crack-growth resistance in reinforced ceramic composites N91-11261

TENSILE TESTS
Relationship of microstructure and tensile properties for neutron-irradiated vanadium alloys
[DE90-017863] N91-11105
Short crack behaviour in Al-Li alloy 2090 N91-11243

TERRAIN ANALYSIS
Sampling and interpolations in digital terrain models
[INPE-5041-TDL/404] N91-11275
Utility of remotely sensed data for identification of soil conservation practices
[NASA-CR-176874] N91-11276

TEST CHAMBERS
The SIM.PL.EX. plasma chamber (Simulatori di Plasma Extraterrestre)
[IFSI-90-8] N91-11551

TEST EQUIPMENT
Recommended operating procedure No. 45: Analysis of nitrous oxide from combustion sources
[PB90-238502] N91-11078

TEST FACILITIES
Aviation Safety/Automation Program Conference
[NASA-CP-3090] N91-10936
A flight test facility design for examining digital information transfer N91-10962
Test launch for turboaircraft engine. Description of the installation
[ILA-87-A-02] N91-11018
Computer modeling of 12-inch actuator shock test performance
[DE90-017038] N91-11033

TETHERED SATELLITES
Boosting a tethered satellites's orbit around an oblate planet through resonant pumping N91-11030
Attitude control of tethered satellites N91-11045
Precision tethered satellite attitude control N91-11046
Data analysis of hollow cathode experiment to support electrodynamic tether applications
[IFSI-89-16] N91-11047
The SIM.PL.EX. plasma chamber (Simulatori di Plasma Extraterrestre)
[IFSI-90-8] N91-11551

TETHERING
Tethered rocket as a vehicle for penetration and impact testing: Development report
[DE90-014865] N91-11057

TETHERLINES
Boosting a tethered satellites's orbit around an oblate planet through resonant pumping N91-11030
Attitude control of tethered satellites N91-11045

TETRODES
Increasing output power of an 850 MHz tetrode with a floating-deck modulator
[DE91-000433] N91-11162

TEXTURES
Texture analysis of 2090-T8E41 aluminum-lithium alloy sheet: Annex N91-11251
Forest classification with high resolution satellite images. Research into the use of spatial information to improve the multi-spectral classification with SPOT images
[BCRS-89-32] N91-11269
Classification of textures using the ARMA models and distances over the autocorrelation function
[INPE-5067-TDL/406] N91-11421
Accurate representations of general textures by a set of weighted grains
[DE90-016487] N91-11485

THEMATIC MAPPING
Identification of areas subject to flooding through TM/LANDSAT images in the basin of the rivers Pindare, Mearim, Jaguaribe, Apodi, Piranhas, and San Francisco
[INPE-5034-RPE/619] N91-11279

THEOREM PROVING
On induced congruences
[CS-9001] N91-11460
An investigation of the Newman-Penrose constants for massless free fields of arbitrary spin N91-11630
THEORETICAL PHYSICS
Generalized back-action evasion schemes for the detection of weak classical forces
[IFSI-90-19] N91-11508
THERMAL ANALYSIS
Thermal-distortion analysis of a spacecraft box truss in geostationary orbit
[NASA-TP-3054] N91-11041
Physical metallurgy and magnetic behavior of Cd stabilized bcc (beta) Gd alloys
[DE91-000196] N91-11112
Analysis and prediction of thermal properties of mesophases and crystals by calorimetry and supercomputers
[DE90-015538] N91-11123
MONT3E: A Monte Carlo electron heat transfer code
[DE90-012091] N91-11514
THERMAL CONDUCTIVITY
Design and testing of a high temperature superconducting current lead
[DE90-017812] N91-11579
THERMAL CYCLING TESTS
Studies of molecular properties of polymeric materials
[NASA-TM-101854] N91-11118
Heat flux measurement in SSME turbine blade tester
[NASA-TM-103274] N91-11205
THERMAL DEGRADATION
Deformation mechanisms in rapidly solidified aluminum alloys N91-11096
Study on radiation-induced deterioration of grease at high temperature. Part 1: Test method on thermal aging
[DE90-508070] N91-11120
THERMAL ENERGY
Survey on solidification and utilization technology of CO2
[DE91-701465] N91-11087
Conceptual design of an Open-Cycle Ocean Thermal Energy Conversion Net Power-Producing Experiment (OC-OTEC NPPE)
[DE90-000304] N91-11282
THERMAL EXPANSION
A life comparison of tube and channel cooling passages for thrust chambers
[NASA-TM-103613] N91-11059
Elastic/plastic analyses of advanced composites investigating the use of the compliant layer concept in reducing residual stresses resulting from processing
[NASA-TM-103204] N91-11074
THERMAL INSULATION
External tank aerothermal design criteria verification, volume 2
[NASA-CR-183997] N91-11038
THERMAL PROTECTION
Recent advances and developments in coatings
[PNR-90698] N91-11021
External tank aerothermal design criteria verification, volume 1
[NASA-CR-183996] N91-11037
External tank aerothermal design criteria verification, volume 2
[NASA-CR-183997] N91-11038
High temperature materials: The overall view
[PNR-90699] N91-11073
THERMAL STABILITY
Three-dimensional fluid flow in JFTOT (Jet Fuel Thermal Oxidation Tester)
[DE90-010929] N91-11128
THERMAL STRESSES
Thermal stress-induced grain boundary cavitation in narrow, aluminum alloy metallizations N91-11093
TOPAZ2D heat transfer code users manual and thermal property data base
[DE91-000075] N91-11195
Thermal stresses in layered electrical assemblies bonded with solder
[DE90-015563] N91-11263
THERMISTORS
The influence of environmental factors on the temperature of the radiosonde thermistor N91-11325
THERMODYNAMIC CYCLES
Colorado State University program for developing, testing, evaluating and optimizing solar heating and cooling systems
[DE90-017273] N91-11291
THERMODYNAMIC PROPERTIES
Liquid alloys with strong interactions
[DE90-017661] N91-11102
TOPAZ2D heat transfer code users manual and thermal property data base
[DE91-000075] N91-11195
THERMODYNAMICS
Measurement of two-phase flow momentum with force transducers
[DE90-008748] N91-11188
Convergence of solutions of one-dimensional stochastic heat equations
[REPT-90-40] N91-11478
THERMOELECTRIC POWER GENERATION
Bench-scale testing of a heat-pipe receiver for solar thermal electric applications
[DE90-009834] N91-11289
THERMOPLASTICITY
Potential for advanced thermoplastic composites in space systems
[DE90-014447] N91-11069
THERMOSPHERE
Wave-mean flow interaction in the storm-time thermosphere using a two-dimensional model N91-11321
THICK WALLS
Gravitational field of static and thick domain walls
[DE90-513706] N91-11331
THICKNESS
Solderability of environmentally exposed Sn-plated surfaces
[DE91-000035] N91-11110
THIN FILMS
Determination of hydrogen (deuterium) density profiles in thin metal films and multilayers by neutron reflection
[DE90-007150] N91-11108
Residual stress at fluid interfaces
[DE90-012964] N91-11189
Indentation testing of thin films and hard materials
[DE90-017758] N91-11224
Electronic processes in thin film PV materials
[DE90-000359] N91-11295
Research on high-efficiency, multiple-gap, multi-junction amorphous silicon-based alloy thin-film solar cells
[DE90-000364] N91-11296
Analysis of loss mechanisms in polycrystalline thin film solar cells
[DE90-000372] N91-11297
Structure of amorphous-silicon and germanium alloy films
[DE90-000355] N91-11557
Magnetic properties of ultrathin epitaxial films of iron
[DE90-017861] N91-11570
Computer-controlled ion beam deposition systems for high T(sub c) superconductor and other multi-component oxide thin films and layered structures
[DE90-017798] N91-11577
Epitaxial TiO2 and VO2 films prepared by MOCVD (Metal-Organic Chemical Vapor Deposition)
[DE90-017806] N91-11578
A study of the chemical, mechanical, and surface properties of thin films of hydrogenated amorphous carbon
[DE91-000357] N91-11585
THIN WALLED SHELLS
Effects of an internal flow on the vibration of thin cylindrical shells N91-11258
A three-dimensional solid element model for finite rotation of composite shells N91-11262
THREE DIMENSIONAL BODIES
A computational model for the prediction of hypersonic, reacting flows N91-10911
Application of computational fluid dynamics to three-dimensional bodies in hypersonic flow N91-11174
THREE DIMENSIONAL FLOW
Recent advances in Runge-Kutta schemes for solving 3-D Navier-Stokes equations N91-10851
Navier-Stokes solutions about the F/A-18 forebody-LEX configuration N91-10860
Calculation of the rotor induced download on airfoils N91-10864
Analysis of three-dimensional viscous flow in a supersonic throughflow fan N91-10885
CFD analysis for high speed inlets N91-10888
Test cases for computation of internal flows in aero engine components
[AGARD-AR-275] N91-11022
Three-dimensional fluid flow in JFTOT (Jet Fuel Thermal Oxidation Tester)
[DE90-010929] N91-11128
Stabilization of a time integrator for the 3D shallow water equations by smoothing techniques
[CWI-NM-R8916] N91-11167
Examination of a three dimensional asymmetrical flow field using the interference method
[ETN-90-97859] N91-11168
Solutions of thin-layer Navier-Stokes equations for missile configurations N91-11173
THREE DIMENSIONAL MODELS
Numerical simulation of rotorcraft N91-10863
Three-dimensional viscous drag prediction for rotor blades N91-10865
Three dimensional unstructured grids for the solution of the Euler equations N91-10893
Statistical system identification of structures with flexible joints N91-11232
A three-dimensional solid element model for finite rotation of composite shells N91-11262
Modelling of large-scale unstable waves in the middle atmosphere N91-11327
THREE DIMENSIONAL MOTION
Marginal aircraft release disturbance on advanced missiles
[MBB/FE121/S/PUB/329] N91-11016
THRUST AUGMENTATION
Ejector thrust augmentors: Pulse-starting approach to the second solution N91-10913
THRUST CHAMBERS
A life comparison of tube and channel cooling passages for thrust chambers
[NASA-TM-103613] N91-11059
THRUST VECTOR CONTROL
Design and evaluation of thrust vectored nozzles using a multicomponent thrust stand
[NASA-CR-180474] N91-11050
THUNDERSTORMS
Study of the return-stroke phase of the gliding spark in ambient air
[ONERA-NT-1990-1] N91-11345
THYRISTORS
Microprocessor system for temperature regulation and stabilization
[DE90-634244] N91-11160
TIDES
Nominal ocean tide models for TOPEX precise orbit determination N91-11029
TIME
Time-based operations in an advanced ATC environment N91-10958
A synthesis of time and frequency domain methods for the control of infinite-dimensional systems: A system theoretic approach
[W-8912] N91-11456
TIME DEPENDENCE
Time dependent viscous incompressible Navier-Stokes equations N91-10854
The 4-D descent trajectory generation techniques under realistic operating conditions N91-10994
A description and evaluation of TIMER: A time-based terminal flow-control concept N91-10996
Use of 4-D RNAV in time-based en route arrival metering N91-10997
Development of a time-dependent incompressible Navier-Stokes solver based on a fractional-step method
[NASA-CR-187254] N91-11165
The evolution and time scales of the atmospheric response to tropical diabatic heating events N91-11322
A static-regridding method for two-dimensional parabolic partial differential equations
[CWI-NM-R8923] N91-11449
TIME DIVISION MULTIPLE ACCESS
Advanced technology satellite demodulator development
[NASA-CR-185127] N91-11134
TIME LAG
Improved tracking for bilateral teleoperators with time delay
[DE90-015392] N91-11222
TIME MARCHING
Three-dimensional calculation of supersonic reacting flows using an LU scheme N91-10871
TIME OF FLIGHT SPECTROMETERS
Resonance ionization spectroscopy of molecular clusters using picosecond lasers
[DE90-017334] N91-11080
TIME OPTIMAL CONTROL
Minimum time feedback control of articulated robotic manipulators N91-11219
TIN ALLOYS
Liquid alloys with strong interactions
[DE90-017661] N91-11102
The transverse stress effect on the critical current of jelly-roll multifilamentary Nb3Al wires
[DE90-513710] N91-11581
TITANIUM ALLOYS
The ultrasonic examination of titanium alloys N91-11094
Influence of heat treatment on microstructure and properties of an advanced high temperature titanium alloy
[PNR-90689] N91-11107
Study of the wear behavior induced by fretting in aluminum and titanium alloys
[ECL-90-01] N91-11229
Short crack observations in Ti-6Al-4V under constant amplitude loading N91-11250

TITANIUM OXIDES
Microwave sintering of nanocrystalline TiO2
[DE91-000375] N91-11115
Epitaxial TiO2 and VO2 films prepared by MOCVD (Metal-Organic Chemical Vapor Deposition)
[DE90-017806] N91-11578
TOKAMAK DEVICES
A design method of divertor in tokamak reactors
[NIFS-36] N91-11532
CTR plasma engineering studies
[DE90-017774] N91-11534
Natural current profiles in a tokamak
[DE91-000128] N91-11540
ECH by FEL and gyrotron sources on the Microwave Tokamak Experiment (MTX) tokamak
[DE91-000286] N91-11547
TOLERANCES (MECHANICS)
Short and long fatigue crack growth in 2024-T3 under Fokker 100 spectrum loading N91-11248
TOPEX
Nominal ocean tide models for TOPEX precise orbit determination N91-11029
TOPOGRAPHY
Gulf of Maine sea surface topography from GEOSAT altimetry N91-11271
Methodology of remote sensing for monitoring modifications in the fluvial channel and updating nautical charts
[INPE-4863-TDL/374] N91-11277
Geometric correction of SPOT imagery with the use of a digital elevation model
[INPE-5014-TDL/401] N91-11423
TOPOLOGY
On three dimensional object recognition and pose-determination: An abstraction based approach
[NASA-CR-186894] N91-11396
TOROIDAL PLASMAS
Confinement and fluctuations in the MST (Madison Symmetric Torus) reversed field pinch
[DE90-018019] N91-11535
Fluctuations and stability in the Advanced Toroidal Facility (ATF) torsatron
[DE90-017734] N91-11536
Complete fluid equations for low-n singular modes in axisymmetric torodial plasmas
[DE91-000176] N91-11545
TORQUE
Injector and valve train friction studies: Cummins L-10 engine
[DE90-017288] N91-11225
The rotation of Lageos
[IFSI-90-10] N91-11333
TORSION
Deformation and delamination of inelastic laminates under tensile and torsional loading N91-11063
TORUSES
Quasi-periodic bifurcations, applications
[TW-8911] N91-11459
TOXIC HAZARDS
Lifetimes and fates of toxic air contaminants in California's atmosphere
[PB90-253204] N91-11304
Minimization and control of hazardous combustion byproducts
[PB90-259854] N91-11305
Measurements of toxic exhaust emissions from gasoline-powered light-duty vehicles
[PB90-259649] N91-11306
TOXICITY
Chlorine dioxide and hemodialysis
[DE90-015912] N91-11382
TRACKING (POSITION)
Nominal ocean tide models for TOPEX precise orbit determination N91-11029
Minimum time feedback control of articulated robotic manipulators N91-11219
Improved tracking for bilateral teleoperators with time delay
[DE90-015392] N91-11222
TRACKING FILTERS
Bayesian multi-sensor tracking for advanced air traffic control systems N91-11003
TRAJECTORIES
A combined Eulerian-Lagrangian two-phase analysis of the SSME HPOTP nozzle plug trajectories N91-10878
TRAJECTORY ANALYSIS
Aircraft trajectory reconstitution on the basis of multi-radar plot information N91-11002
TRAJECTORY CONTROL
Prediction of aircraft trajectories N91-10984
The application of trajectory prediction algorithms for planning purposes in the Netherlands ATC-system N91-10986
The 4-D control of current air carriers in the present environment: Objectives, status, and plans N91-10990
Robot trajectory control with a model reference adaptive control system using tap delay filters N91-11217
Instantaneous kinematics, motion planning and mechanical efficiency of a quadrupedal walking machine N91-11218
Minimum time feedback control of articulated robotic manipulators N91-11219
TRAJECTORY OPTIMIZATION
Aircraft trajectories: Computation, prediction, control, volume 1. Part 1: Fundamentals. Part 2: Flight in critical atmospheric conditions. Part 3: Impact of new on-board technologies on aircraft operation
[AGARD-AG-301-VOL-1-PT-1-3] N91-10967
Critical aspects of trajectory prediction: Flight in non-uniform wind N91-10971
Aircraft trajectory: Prediction and control in the air transport flight management computer systems N91-10976
Aircraft trajectories: Computation, prediction, control, Volume 3. Part 9: Book of abstracts. Part 10: Bibliography. Part 11: List of contributors
[AGARD-AG-301-VOL-3-PT-9-11] N91-10978
Aircraft trajectories: Computation, prediction, control, volume 2: Air traffic handling and ground-based guidance of aircraft. Part 4: Air traffic handling. Part 5: Guidance of aircraft in a time-based constrained environment. Part 6: Surveillance. Part 7: Meteorological forecasts. Part 8: Aircraft operation in air traffic handling simulation
[AGARD-AG-301-VOL-2-PT-4-8] N91-10981
Optimum on-line handling of air traffic over Western Europe N91-10982
Prediction of aircraft trajectories N91-10984
The application of trajectory prediction algorithms for planning purposes in the Netherlands ATC-system N91-10986
Generation of aircraft trajectories for on-line operation: Methods, techniques, and tools N91-10987
The 4-D descent trajectory generation techniques under realistic operating conditions N91-10994
Expert systems for the generation of thermal area arrival paths for civil transport N91-10995
Air traffic management and aircraft guidance in a zone of convergence N91-10998
Developments to enhance meteorological forecasting for air traffic services N91-11006
Dynamic model error analysis of robot manipulators N91-11220
TRANSDUCERS
Measurement of two-phase flow momentum with force transducers
[DE90-008748] N91-11188
Biosensors: Development status
[MBB-Z-0305-90-PUB] N91-11201
TRANSFER FUNCTIONS
Composite slip table of dissimilar materials for damping longitudinal modes
[DE90-015128] N91-11064
Classification of acoustic emission waveforms for nondestructive evaluation using neural networks
[DE90-017239] N91-11236
Remote sensing in the ultraviolet
[AD-A224254] N91-11268
Time domain frequency stability calculated from the frequency domain description: Use of the SIGINT software package to calculate time domain frequency stability from the frequency domain
[PB90-257684] N91-11405
TRANSFER ORBITS
Boosting a tethered satellites's orbit around an oblate planet through resonant pumping N91-11030
TRANSFORMATIONS (MATHEMATICS)
Mathematical morphology on homogeneous spaces. Part 1: The simply transitive case
[CWI-AM-R8924-PT-1] N91-11439
TRANSIENT LOADS
Boundary integral equations for dynamic fracture problems N91-11259
TRANSISTORS
Implementation of a QML (Qualified Manufacturer's List) methodology for discrete semiconductors
[DE90-015715] N91-11235
TRANSITION METALS
Stability of liquid propellants under long-term storage
[AD-A223934] N91-11126
TRANSITION TEMPERATURE
Superconducting and structural properties of the (Ba(0.6)K(0.4)) (Bi(1-y)Sb(y))O3 system
[DE90-017836] N91-11580
TRANSMISSION LINES
A hybrid pulse forming technique
[DE90-016860] N91-11156
TRANSMISSION LOSS
Arctic acoustics ultrasonic modeling studies
[AD-A224165] N91-11489
TRANSMITTER RECEIVERS
Advanced technology satellite demodulator development
[NASA-CR-185127] N91-11134
TRANSONIC FLOW
Recent advances in Runge-Kutta schemes for solving 3-D Navier-Stokes equations N91-10851
A zonal Navier-Stokes methodology for flow simulation about a complete aircraft N91-10858
Navier-Stokes solutions for flows related to store separation N91-10861
TranAir: Recent advances and applications N91-10862
Prediction of effects of wing contour modifications on low-speed maximum lift and transonic performance for the EA-6B aircraft
[NASA-TP-3046] N91-10902
Computation of transonic flow over elastic rotor blade N91-10906
The aerodynamic effects of nozzle guide vane shock wave and wake passing on a transonic turbine rotor N91-10915
Implicit flux-split Euler schemes for unsteady aerodynamic analysis involving unstructured dynamic meshes
[NASA-TM-102732] N91-10918
Unsteady wind tunnel wall interferences in subsonic and transonic profile flows N91-10928
Navier-Stokes analysis of transonic cascade flow
[NASA-TM-103624] N91-11192
TRANSONIC FLUTTER
Determination of unsteady aerodynamic forces on engines with a view to flutter investigations N91-10927
TRANSONIC SPEED
Applications of a transonic wing design method N91-10890
TRANSONIC WIND TUNNELS
Design of the derivative balance for the transonic wind tunnel N91-10925
TRANSPORT AIRCRAFT
A quarter of a century of aeroelastic cooperation between research and industry (a review). Part 2: Transport airplanes and other civil applications N91-10932
Summary of the industry/NASA/FAA workshop on philosophy of automation: Promises and realities N91-10942
Overview of error-tolerant cockpit research N91-10949
TRANSPORT PROPERTIES
Parallel performance models for the nodal transport method on the hypercube
[DE90-015162] N91-11408
On the adequacy of message-passing parallel supercomputers for solving neutron transport problems
[DE90-016041] N91-11431
The influence of ionized impurities on the transport properties of a two-dimensional electron gas
[ETN-90-97752] N91-11586
TRANSPORT THEORY
Theoretical and numerical studies in magnetic mirror fusion
[DE90-017605] N91-11533
TRANSPORTATION
Assessment of costs and benefits of flexible and alternative fuel use in the US transportation sector: Vehicle and fuel distribution requirements
[DE90-014847] N91-11127
TRANSPORTATION NETWORKS
Airport system capacity strategic choices
[SR-226] N91-10979
TRANSURANIUM ELEMENTS
The transuranium elements: Members of the 5f series
[DE90-017680] N91-11575
TRAPPED MAGNETIC FIELDS
Dynamic trapping of electrons in space plasmas
[TRITA-EPP-89-07] N91-11528
TRAPPED PARTICLES
Review of free electron lasers
[PB90-255480] N91-11206
TREES (MATHEMATICS)
Cosmological N-body simulations with a treecode
[DE90-513790] N91-11638
TRENDS
Impact on women: A retrospective look at impact acceleration testing at the Harry G. Armstrong Aerospace Medical Research Laboratory N91-11378
Ada and software management in NASA: Symposium/forum
[NASA-TM-103297] N91-11390
TRIANGULATION
Interpolation of scattered data by a bivariate convex function. Part 1: Piecewise linear C sup 0-interpolation
[MEMO-858-PT-1] N91-11469

Solution of the two-dimensional Euler equations by a finite volume discretization on unstructured triangular meshes
[ESA-TT-1135] N91-11473

TRIBOLOGY
Wear reduction in cutting tools: Tribological properties of hard coatings
[DE90-009705] N91-11212
On the calculation of leakage and friction of reciprocating elastomeric seals
[ETN-90-97751] N91-11228

TROPICAL METEOROLOGY
The evolution and time scales of the atmospheric response to tropical diabatic heating events N91-11322
Tropical cyclone simulations with the Betts convective adjustment scheme N91-11338

TROPICAL REGIONS
Wind lidar for tropical climatology
[CNES-CT/DRT/TIT/IO-88/126] N91-11334

TROPOSPHERE
Comparison of clear air atmospheric radar techniques for the study of atmospheric dynamics in the troposphere and the stratosphere
[PB90-256314] N91-11313
Seasonal variations in the latitudinal distribution of tropospheric carbon monoxide, 1986 to 1988 N91-11328

TRUNCATION ERRORS
Approximation of the solution to the moment problem in a Hilbert space
[CWI-AM-R8923] N91-11438

TRUSSES
Thermal-distortion analysis of a spacecraft box truss in geostationary orbit
[NASA-TP-3054] N91-11041
Controller methodologies for integrated control/structure design optimization of large flexible structures N91-11043

TUNABLE LASERS
Planar orotron: A tunable, grating-based free electron laser N91-11208

TUNING
Aircraft interior noise reduction by alternate resonance tuning
[NASA-CR-186879] N91-11488
Production of uniform and well-confined beams by nonlinear optics
[DE91-000210] N91-11522

TURBINE BLADES
Heat flux measurement in SSME turbine blade tester
[NASA-TM-103274] N91-11205
Atmospheric performance of the special-purpose Solar Energy Research Institute (SERI) thin-airfoil family: Final results
[DE90-000373] N91-11287

TURBINE PUMPS
Marshall Space Flight Center CFD overview N91-10843
Analysis of the SSME HPOTP bearing inlet cavity N91-10877
A combined Eulerian-Lagrangian two-phase analysis of the SSME HPOTP nozzle plug trajectories N91-10878
Hybrid Propulsion Technology Program, phase 1. Volume 1: Executive summary
[NASA-CR-183950] N91-11054
Heat flux measurement in SSME turbine blade tester
[NASA-TM-103274] N91-11205

TURBINES
Prediction of turbine rotor-stator interaction using Navier-Stokes methods N91-10881

TURBOCOMPRESSORS
Automated design of controlled diffusion blades N91-10883

TURBOFANS
Analysis of three-dimensional viscous flow in a supersonic throughflow fan N91-10885

TURBOGENERATORS
Reference concepts for a space-based hydrogen-oxygen combustion, turboalternator, burst power system
[DE90-016692] N91-11155

TURBOMACHINERY
Simulation of turbomachinery flows N91-10880
Prediction of turbine rotor-stator interaction using Navier-Stokes methods N91-10881

TURBULENCE
Understanding transition and turbulence through direct simulations N91-10846
More accurate predictions with transonic Navier-Stokes methods through improved turbulence modeling N91-10850
Unsteady fluid forces and fluidelastic vibration of a group of circular cylinders
[DE90-013661] N91-11190
Sound field fluctuations due to large scale wind-driven turbulence N91-11492

TURBULENCE MODELS
NASA Computational Fluid Dynamics Conference. Volume 1: Sessions 1-6
[NASA-CP-10038-VOL-1] N91-10839
Understanding transition and turbulence through direct simulations N91-10846
More accurate predictions with transonic Navier-Stokes methods through improved turbulence modeling N91-10850
Recent advances in Runge-Kutta schemes for solving 3-D Navier-Stokes equations N91-10851
A comparative study of Navier-Stokes codes for high-speed flows N91-10869
Progress in computing nozzle/plume flow fields N91-10872
Computational fluid dynamics analysis of space shuttle main propulsion feed line 17-inch disconnect valves N91-10876
Analysis of three-dimensional viscous flow in a supersonic throughflow fan N91-10885
The use of a Navier-Stokes code in the wing design process N91-10889
A numerical study of the effects of wind tunnel wall proximity on an airfoil model
[NASA-CR-187322] N91-10934
Heat transfer in variable density, low Mach number, stagnating turbulent flows N91-11171
Application of computational fluid dynamics to three-dimensional bodies in hypersonic flow N91-11174
A global pressure relaxation for high speed laminar and turbulent flows N91-11177
Navier-Stokes analysis of transonic cascade flow
[NASA-TM-103624] N91-11192
Sound field fluctuations due to large scale wind-driven turbulence N91-11492

TURBULENT BOUNDARY LAYER
More accurate predictions with transonic Navier-Stokes methods through improved turbulence modeling N91-10850
An experimental study of an axisymmetric turbulent boundary layer disturbed by a periodic freestream N91-11175
Measurement and calculation of surface roughness effects on turbulent flow and heat transfer N91-11183

TURBULENT DIFFUSION
Large eddy-simulation of convective boundary layers
[ESA-TT-1138] N91-11198

TURBULENT FLOW
Johnson Space Center CFD overview N91-10844
NASA's CFD Validation Program N91-10845
Direct simulation of compressible turbulence N91-10847
More accurate predictions with transonic Navier-Stokes methods through improved turbulence modeling N91-10850
Recent advances in Runge-Kutta schemes for solving 3-D Navier-Stokes equations N91-10851
A zonal Navier-Stokes methodology for flow simulation about a complete aircraft N91-10858
A numerical study of the hot gas environment around a STOVL aircraft in ground proximity N91-10887
Aerodynamic interaction of counter rotating propellers N91-10910
Structure of supersonic turbulent reattaching shear layers N91-10914
Numerical calculations for flows past an unconventional airfoil N91-10916
A simulation of the flow near a burning propellant in a solid propellant rocket motor N91-11056
Combustion to modelisation turbulent combustion in the case of stabilization by flame-lock
[ONERA-NT-1989-8] N91-11090
Examination of numerical formulations to describe complex geometry turbulent elliptical flows, using contour matched coordinates
[ETN-90-97864] N91-11169
Heat transfer in variable density, low Mach number, stagnating turbulent flows N91-11171
The calculation of correlation functions in the statistical theory of turbulent flows N91-11176
A global pressure relaxation for high speed laminar and turbulent flows N91-11177
Magnetohydrodynamic modification of the TEACH-T code and the prediction of the maximum azimuthal velocity in a conducting fluid
[DE90-017510] N91-11187
Large eddy-simulation of convective boundary layers
[ESA-TT-1138] N91-11198
Numerical simulation of transition from laminar to turbulent duct flow
[ESA-TT-1144] N91-11199

TURBULENT HEAT TRANSFER
Heat transfer in variable density, low Mach number, stagnating turbulent flows N91-11171
Measurement and calculation of surface roughness effects on turbulent flow and heat transfer N91-11183

TURBULENT JETS
Numerical simulation of nonlinear development of instability waves
[E-4658] N91-10849
Fine scale velocity measurements in a turbulent jet in a confined crossflow N91-10909

TVD SCHEMES
A computational model for the prediction of hypersonic, reacting flows N91-10911
Numerical simulation of shock-induced combustion for application to the ram accelerator concept N91-10912

TWO DIMENSIONAL BODIES
The calculation of rotor/fuselage interaction for two-dimensional bodies
[NASA-TM-102855] N91-10933

TWO DIMENSIONAL BOUNDARY LAYER
An experimental study of an axisymmetric turbulent boundary layer disturbed by a periodic freestream N91-11175

TWO DIMENSIONAL FLOW
Flux splitting algorithms for two-dimensional viscous flows with finite-rate chemistry N91-10894
Numerical calculations for flows past an unconventional airfoil N91-10916
Temporal-adaptive Euler/Navier-Stokes algorithm for unsteady aerodynamic analysis of airfoils using unstructured dynamic meshes
[NASA-TM-102734] N91-10919
Development of a time-dependent incompressible Navier-Stokes solver based on a fractional-step method
[NASA-CR-187254] N91-11165
Heat pipe vapor dynamics N91-11179
Instabilities of two-dimensional inviscid compressible vortices N91-11181
Solution of the two-dimensional Euler equations by a finite volume discretization on unstructured triangular meshes
[ESA-TT-1135] N91-11473

TWO DIMENSIONAL MODELS
A numerical study of the effects of wind tunnel wall proximity on an airfoil model
[NASA-CR-187322] N91-10934
A simulation study of magnetic reconnection processes at the dayside magnetopause N91-11320
Wave-mean flow interaction in the storm-time thermosphere using a two-dimensional model N91-11321
A design method of divertor in tokamak reactors
[NIFS-36] N91-11532
A two dimensional multisonic model of plasma interaction for cometary atmosphere with solar wind
[MITT-69] N91-11621

TWO PHASE FLOW
Measurement of two-phase flow momentum with force transducers
[DE90-008748] N91-11188
The generalized diffusion theory of simply deformable particle-fluid two-phase flows
[MPIS-7/1990] N91-11193

TYPE 2 BURSTS
Type 2 solar radio bursts recorded at Weissenau, 1966-1987
[PB90-198334] N91-11648

TYPE 3 BURSTS
Exploration of decreased solar activity state (small intensity activity) in the corona and chromosphere
[INPE-5059-TDL/405] N91-11652

U

U.S.S.R.
JPRS report: Science and technology. USSR: Life sciences
[JPRS-ULS-89-003] N91-11354

ULTRASONIC FLAW DETECTION
Ultrasonic examination of fiber composite materials by means of virtual C-scan test and model recognition
[MBB-Z-0299-89-PUB] N91-11066

ULTRASONIC RADIATION
Arctic acoustics ultrasonic modeling studies
[AD-A224165] N91-11489

ULTRASONIC TESTS
The ultrasonic examination of titanium alloys N91-11094
Deducing mechanical properties due to interfaces from their acoust. al response
[DE90-016704] N91-11234
Fatigue crack characterization by ultrasonic inspection
[DE90-017252] N91-11264

ULTRAVIOLET RADIATION
Violet and visual flux problems in red giant stars N91-11632

ULTRAVIOLET SPECTRA
Late stages in the evolution of classical novae
[NASA-TM-102969] N91-11633
ULTRAVIOLET SPECTROPHOTOMETERS
Remote sensing in the ultraviolet
[AD-A224254] N91-11268
UNDERWATER ACOUSTICS
A compendium of environmental data collected during the Iceshelf-88 exercise
[AD-A223518] N91-11346
Arctic acoustics ultrasonic modeling studies
[AD-A224165] N91-11489
UNIQUENESS
On the uniqueness of kernels
[CWI-BS-R8924] N91-11443
UNIVERSAL TIME
Apparent place of Polaris and apparent Sidereal Time at 0 hour UT 1990-1994
[PB90-259169] N91-11607
UNSTEADY AERODYNAMICS
CFD for applications to aircraft aeroelasticity N91-10855
Application of unstructured grid methods to steady and unsteady aerodynamic problems N91-10856
Numerical analysis of flow through oscillating cascade sections N91-10884
Conical Euler simulation and active suppression of delta wing rocking motion
[NASA-TM-102683] N91-10904
Implicit flux-split Euler schemes for unsteady aerodynamic analysis involving unstructured dynamic meshes
[NASA-TM-102732] N91-10918
Temporal-adaptive Euler/Navier-Stokes algorithm for unsteady aerodynamic analysis of airfoils using unstructured dynamic meshes
[NASA-TM-102734] N91-10919
Contributions in the field of aeroelastics on the occasion of the 60th anniversary of Professor Dr.-Ing. Habil. Hans Wilhelm Foersching
[ETN-90-97630] N91-10920
Determination of unsteady aerodynamic forces on engines with a view to flutter investigations N91-10927
Calculation of aerodynamic characteristics of airplane configurations at high angle of attack in steady and unsteady flow N91-11009
Development and application of the time domain panel method N91-11010
UNSTEADY FLOW
Computations of three-dimensional steady and unsteady viscous incompressible flows N91-10852
Time dependent viscous incompressible Navier-Stokes equations N91-10854
Numerical simulation of rotorcraft N91-10863
Experimental investigation of the mechanisms underlying vortex kinematics in unsteady separated flows N91-10907
The calculation of unsteady compressible flow about oscillating airfoil profiles using the Euler upwind method N91-10921
Unsteady wind tunnel wall interferences in subsonic and transonic profile flows N91-10928
A viscous-inviscid interactive method for unsteady flows N91-11172
Observation and analysis of variable linear polarization in the yellow supergiant star Epsilon Aurigae N91-11616
URANUS (PLANET)
Tectonics of one-plate planets N91-11647
USER MANUALS (COMPUTER PROGRAMS)
TOPAZ2D heat transfer code users manual and thermal property data base
[DE91-000075] N91-11195
NCEER strong-motion data base: A user manual for the geobase release (version 1.0 for the SUN3)
[PB90-258062] N91-11315
Intelligent Data Reduction (IDARE)
[NASA-CR-186322] N91-11393
Computer-Aided Structural Engineering (CASE) project: Investigation and design of U-frame structures using program CUFRBC. Volume C: User's guide for channels
[AD-A224388] N91-11395
Reception and display of WEFAX images: 4 bits with micro line IBM-PC, users manual
[INPE-5086-NTE/294] N91-11417

V

V/STOL AIRCRAFT
Simulation of powered-lift flows N91-10886
A numerical study of the hot gas environment around a STOVL aircraft in ground proximity N91-10887
VALENCE
Structure of molten salts
[DE90-017704] N91-11566
Light-heavy-hole-mixing-induced selection rules for magneto-luminescence and valence-band energy dispersion in semiconductor quantum wells
[DE90-015989] N91-11573
VALVES
Computational fluid dynamics analysis of space shuttle main propulsion feed line 17-inch disconnect valves N91-10876
Study of asymmetric supersonic jet flow for ejectors
[DE90-015598] N91-10917
Injector and valve train friction studies: Cummins L-10 engine
[DE90-017288] N91-11225
VANADIUM ALLOYS
Relationship of microstructure and tensile properties for neutron-irradiated vanadium alloys
[DE90-017863] N91-11105
Determination of pair potentials by analysis of diffuse scattering of the local field in Pd3V and Ni3V
[ONERA-NT-1989-7] N91-11117
Short crack observations in Ti-6Al-4V under constant amplitude loading N91-11250
VANADIUM OXIDES
Epitaxial TiO2 and VO2 films prepared by MOCVD (Metal-Organic Chemical Vapor Deposition)
[DE90-017806] N91-11578
VANES
The effect of swirl recovery vanes on the cruise noise of an advanced propeller
[NASA-TM-103625] N91-11494
VAPOR DEPOSITION
The reaction of vapor-deposited Al with Cu oxides
[DE91-000367] N91-11114
Chemically vapor deposited diamond films
[DE91-000384] N91-11125
Epitaxial TiO2 and VO2 films prepared by MOCVD (Metal-Organic Chemical Vapor Deposition)
[DE90-017806] N91-11578
VAPOR PHASES
Theory of homogeneous nucleation from the vapor phase
[MPIS-MITT-93] N91-11077
VAPORS
Heat pipe vapor dynamics N91-11179
VARIABILITY
Basic dynamics of low frequency variability and the storm tracks N91-11339
Observation and analysis of variable linear polarization in the yellow supergiant star Epsilon Aurigae N91-11616
VARIATIONAL PRINCIPLES
SAGE: A 2-D self-adaptive grid evolution code and its application in computational fluid dynamics N91-10853
Alternating method applied to 3-D part-through crack problems, with application to the weight function method N91-11238
VECTOR PROCESSING (COMPUTERS)
Use of the VP-200 computer for aerothermodynamic problems
[MBB/FE122/S/PUB/388] N91-11424
VELOCITY
Injector and valve train friction studies: Cummins L-10 engine
[DE90-017288] N91-11225
VELOCITY COUPLING
A simulation of the flow near a burning propellant in a solid propellant rocket motor N91-11056
VELOCITY DISTRIBUTION
Fine scale velocity measurements in a turbulent jet in a confined crossflow N91-10909
VELOCITY MEASUREMENT
Fine scale velocity measurements in a turbulent jet in a confined crossflow N91-10909
VENUS (PLANET)
Testing for lightning as a source of radio bursts observed on the nightside of Venus
[NASA-CR-187364] N91-11645
Tectonics of one-plate planets N91-11647
VENUS ATMOSPHERE
Testing for lightning as a source of radio bursts observed on the nightside of Venus
[NASA-CR-187364] N91-11645
VERTICAL DISTRIBUTION
ECC ozonesonde observations at South Pole, Antarctica during 1989
[PB90-258914] N91-11302
VIBRATION
Coupled rotor/airframe vibration analysis N91-11012
Vortex-induced noise and vibration in flow past several flat plates N91-11163
Unsteady fluid forces and fluidelastic vibration of a group of circular cylinders
[DE90-013661] N91-11190
Buckling and vibrations of plates subjected to concentrated forces N91-11255
Effects of an internal flow on the vibration of thin cylindrical shells N91-11258
VIBRATION DAMPING
Adaptive digital real time filtering in structural dynamics: A contribution to the realization on Actively Reacting Elastic Structures (ARES) N91-10929
Composite slip table of dissimilar materials for damping longitudinal modes
[DE90-015128] N91-11064
Forced vibration analysis of plates and shallow shells N91-11237
VIBRATION MODE
Performance of finite dynamic elements for composite materials in plane stress N91-11260
A theoretical investigation on structural, vibrational, and electronic properties of amorphous silicon
[DE90-018040] N91-11267
VIBRATION TESTS
Review of active structural control systems and flight test techniques for dynamic stability investigations
[MBB/FYT256/S/PUB/361/A] N91-11025
Composite slip table of dissimilar materials for damping longitudinal modes
[DE90-015128] N91-11064
VIBRATIONAL SPECTRA
Theoritical and experimental study of kinetics mechanisms in the Chemical Oxygen-Iodine Laser (COIL)
[ONERA-P-1990-1] N91-11211
VIBRATORY LOADS
Non-linear vibration of large, imperfect space structures N91-10930
VIDEO TAPES
Assessing information transfer in full mission flight simulations N91-10946
VIRTUAL MEMORY SYSTEMS
Touchstone project Mach port: Milestone event Q4
[AD-A224057] N91-11481
VISCOSITY
Processing of YBA2Cu3O7 tapes from a molten salt precursor
[DE90-017656] N91-11564
VISCOUS DRAG
Three-dimensional viscous drag prediction for rotor blades N91-10865
VISCOUS FLOW
Computations of three-dimensional steady and unsteady viscous incompressible flows N91-10852
Time dependent viscous incompressible Navier-Stokes equations N91-10854
A zonal Navier-Stokes methodology for flow simulation about a complete aircraft N91-10858
Navier-Stokes solutions for flows related to store separation N91-10861
Analysis of three-dimensional viscous flow in a supersonic throughflow fan N91-10885
Applications of a transonic wing design method N91-10890
Flux splitting algorithms for two-dimensional viscous flows with finite-rate chemistry N91-10894
Aerodynamic stability and heating analyses for the aeroassist flight experiment vehicle N91-10899
The calculation of rotor/fuselage interaction for two-dimensional bodies
[NASA-TM-102855] N91-10933
Test cases for computation of internal flows in aero engine components
[AGARD-AR-275] N91-11022
A viscous-inviscid interactive method for unsteady flows N91-11172
Heat pipe vapor dynamics N91-11179
Parallelization on a multi-processor system of a solving method for the unsteady Navier-Stokes equations at high Reynolds numbers
[ESA-TT-1116] N91-11197
Numerical models of 2-D and 3-D geophysical convection
[DE90-014979] N91-11330
VISUAL PERCEPTION
Requirements of an HMS/D for a night-flying helicopter
[MBB-UD-0570-90-PUB] N91-11383
VOICE COMMUNICATION
A flight test facility design for examining digital information transfer N91-10962
Voice communications in the cockpit noise environment: The role of active noise reduction N91-11140
VOIDS
A theoretical investigation on structural, vibrational, and electronic properties of amorphous silicon
[DE90-018040] N91-11267
VOLTERRA EQUATIONS
Optimal control design by Volterra Series and its application to spacecraft maneuvers N91-11044

VOLUME
Residual stress at fluid interfaces
[DE90-012964] N91-11189
VORTEX BREAKDOWN
Analysis and control of supersonic vortex breakdown flows
[NASA-CR-186897] N91-10903
VORTEX FILAMENTS
Calculation of aerodynamic characteristics of airplane configurations at high angle of attack in steady and unsteady flow N91-11009
VORTEX SHEDDING
Computations of three-dimensional steady and unsteady viscous incompressible flows N91-10852
Vortex-induced noise and vibration in flow past several flat plates N91-11163
VORTEX SHEETS
Vortex-induced noise and vibration in flow past several flat plates N91-11163
VORTICES
CFD for applications to aircraft aeroelasticity N91-10855
The breakup of trailing-line vortices N91-10867
Analysis and control of supersonic vortex breakdown flows
[NASA-CR-186897] N91-10903
Conical Euler simulation and active suppression of delta wing rocking motion
[NASA-TM-102683] N91-10904
Experimental investigation of the mechanisms underlying vortex kinematics in unsteady separated flows N91-10907
Calculation of aerodynamic characteristics of airplane configurations at high angle of attack in steady and unsteady flow N91-11009
Controlled vortical flow on delta wings through unsteady leading edge blowing N91-11011
Vortex-induced noise and vibration in flow past several flat plates N91-11163
Instabilities of two-dimensional inviscid compressible vortices N91-11181
The evolution of vortical patterns and vortices in mesoscale convective complexes N91-11319
A model for the sound generation due to compressible vortex-body interaction
[MPIS-MITT-96] N91-11491
Sound field fluctuations due to large scale wind-driven turbulence N91-11492
VORTICITY
Direct simulation of compressible turbulence N91-10847
The breakup of trailing-line vortices N91-10867
VORTICITY EQUATIONS
Parallelization on a multi-processor system of a solving method for the unsteady Navier-Stokes equations at high Reynolds numbers
[ESA-TT-1116] N91-11197
VULNERABILITY
Department of Defense methodology guidelines for High Power Microwave (HPM) susceptibility assessments
[DE90-015405] N91-11147

W

WAKES
The aerodynamic effects of nozzle guide vane shock wave and wake passing on a transonic turbine rotor N91-10915
Vortex-induced noise and vibration in flow past several flat plates N91-11163
An experimental study of an axisymmetric turbulent boundary layer disturbed by a periodic freestream N91-11175
Navier-Stokes analysis of transonic cascade flow
[NASA-TM-103624] N91-11192
WALKING MACHINES
Instantaneous kinematics, motion planning and mechanical efficiency of a quadrupedal walking machine N91-11218
WALL FLOW
A numerical study of the effects of wind tunnel wall proximity on an airfoil model
[NASA-CR-187322] N91-10934
WALLS
An experimental study of natural convection heat transfer from a horizontal cylinder array vertically aligned to and confined by a single wall and two walls N91-11178
WARNING SYSTEMS
A protein coated piezoelectric crystal detector
[AD-A223848] N91-11552
WASTE DISPOSAL
Minimization and control of hazardous combustion byproducts
[PB90-259854] N91-11305
WASTE ENERGY UTILIZATION
Evaluation of a high-temperature burner-duct-recuperator system
[DE90-000366] N91-11284
WASTE UTILIZATION
Assessment of municipal solid waste for energy production in the Western United States
[DE90-000361] N91-11283
WATER
Aluminum metal combustion in water revealed by high speed microphotography
[DE90-017525] N91-11082
WATER QUALITY
Chlorine dioxide and hemodialysis
[DE90-015912] N91-11382
WATER WAVES
Wave data assimilation in a 3rd generation. Wave prediction model for the North Sea: An optimal control approach
[BCRS-89-22] N91-11348
WAVE DIFFRACTION
Aperture diffraction in Rayleigh zone: Calculation of the field in the quiet zone of compact ranges
[CNES-CT/DRT/TIT/AN-88/234] N91-11136
WAVE DISPERSION
The evolution of resistive ballooning modes in the banana-plateau collisionality regime
[DE90-016672] N91-11525
WAVE EQUATIONS
Evaluation of the integral
[PB90-235011] N91-11437
An investigation of the Newman-Penrose constants for massless free fields of arbitrary spin N91-11630
WAVE INTERACTION
Wave-mean flow interaction in the storm-time thermosphere using a two-dimensional model N91-11321
WAVE PROPAGATION
Numerical simulation of nonlinear development of instability waves
[E-4658] N91-10849
Composite slip table of dissimilar materials for damping longitudinal modes
[DE90-015128] N91-11064
Compact representation of radiation patterns using spherical mode expansions
[DE91-000019] N91-11141
Classification of acoustic emission waveforms for nondestructive evaluation using neural networks
[DE90-017239] N91-11236
Large-scale dynamics and transport in the stratosphere
[NASA-CR-187327] N91-11311
Wave-mean flow interaction in the storm-time thermosphere using a two-dimensional model N91-11321
The role of shear in the cosmological distance
[DE90-513788] N91-11636
WAVE SCATTERING
Elementary inversion, energy velocity, and a generalized Sommerfeld theorem
[DE90-018046] N91-11486
WAVEFORMS
Classification of acoustic emission waveforms for nondestructive evaluation using neural networks
[DE90-017239] N91-11236
WAVEGUIDES
Integrated optical components for optical fibre sensors N91-11519
WEAK INTERACTIONS (FIELD THEORY)
Generalized back-action evasion schemes for the detection of weak classical forces
[IFSI-90-19] N91-11508
WEAPONS
Department of Defense methodology guidelines for High Power Microwave (HPM) susceptibility assessments
[DE90-015405] N91-11147
IGES efficiency evaluation
[DE90-015192] N91-11409
WEAR
Injector and valve train friction studies: Cummins L-10 engine
[DE90-017288] N91-11225
WEAR RESISTANCE
Recent advances and developments in coatings
[PNR-90698] N91-11021
Wear reduction in cutting tools: Tribological properties of hard coatings
[DE90-009705] N91-11212
WEATHER
Terminal weather information management N91-10960
A flight test facility design for examining digital information transfer N91-10962
WEATHER FORECASTING
Developments to enhance meteorological forecasting for air traffic services N91-11006
Notes on the NOARL nowcast for the 1989 to 1990 El Nino forced by FNOC winds
[AD-A223520] N91-11347
WEATHERING
Spectral lithostratigraphic correlation of boreholes
[INPE-5022-TDL/402] N91-11332
WEIBULL DENSITY FUNCTIONS
Lower bound on reliability for Weibull distribution when shape parameter is not estimated accurately
[NASA-CR-180681] N91-11474
WEIGHT ANALYSIS
Weight evaluation and sensitivity analysis for space plane: SSTO
[NAL-TM-598-1] N91-11036
WEIGHT REDUCTION
Weight evaluation and sensitivity analysis for space plane: SSTO
[NAL-TM-598-1] N91-11036
WEIGHTING FUNCTIONS
Alternating method applied to 3-D part-through crack problems, with application to the weight function method N91-11238
WELDABILITY
Penetration in GTA welding
[DE90-008971] N91-11213
WELDED JOINTS
A study of chromium carbide precipitation at interphase boundaries in stainless steel welds
[DE91-000360] N91-11113
Statistical system identification of structures with flexible joints N91-11232
WEST GERMANY
Air rescue in the Federal Republic of Germany
[ETN-90-97878] N91-10963
WHISTLERS
Whistlers in Neptune's magnetosphere: Evidence of atmospheric lightning
[NASA-CR-187324] N91-11642
WHITE DWARF STARS
A new site for the astrophysical gamma-process
[DE90-017519] N91-11635
WIND (METEOROLOGY)
Planetary boundary layer dynamics over the Amazon rain forest N91-11317
Notes on the NOARL nowcast for the 1989 to 1990 El Nino forced by FNOC winds
[AD-A223520] N91-11347
WIND DIRECTION
ECC ozonesonde observations at South Pole, Antarctica during 1989
[PB90-258914] N91-11302
WIND EFFECTS
Contributions to the improvement of flight safety in wind shear
[ESA-TT-1141] N91-10965
Critical aspects of trajectory prediction: Flight in non-uniform wind N91-10971
Effect of wind and wind variation on aircraft flight-paths N91-10972
Aircraft flight in wind-shear N91-10973
Wind models for flight simulation N91-10975
Ground-based 4-D guidance of flights in strong wind N91-10999
Developments to enhance meteorological forecasting for air traffic services N91-11006
WIND PROFILES
Comparison of clear air atmospheric radar techniques for the study of atmospheric dynamics in the troposphere and the stratosphere
[PB90-256314] N91-11313
Fluctuating concentrations in atmospheric dispersion N91-11323
Wind lidar for tropical climatology
[CNES-CT/DRT/TIT/IO-88/126] N91-11334
Taiwan area mesoscale experiment: A guide to precipitation patterns during the 1987 field phase
[PB90-256355] N91-11336
Wave data assimilation in a 3rd generation. Wave prediction model for the North Sea: An optimal control approach
[BCRS-89-22] N91-11348
WIND SHEAR
Assessing information transfer in full mission flight simulations N91-10946
Terminal weather information management N91-10960
Contributions to the improvement of flight safety in wind shear
[ESA-TT-1141] N91-10965
Aircraft flight in wind-shear N91-10973
How to fly windshear N91-10974

WIND TUNNEL TESTS
Prediction of effects of wing contour modifications on low-speed maximum lift and transonic performance for the EA-6B aircraft
[NASA-TP-3046] N91-10902
A numerical study of the effects of wind tunnel wall proximity on an airfoil model
[NASA-CR-187322] N91-10934
Noise measurements from an ejector suppressor nozzle in the NASA Lewis 9- by 15-foot low speed wind tunnel
[NASA-TM-103628] N91-11493
The effect of swirl recovery vanes on the cruise noise of an advanced propeller
[NASA-TM-103625] N91-11494
WIND TUNNEL WALLS
Unsteady wind tunnel wall interferences in subsonic and transonic profile flows N91-10928
A numerical study of the effects of wind tunnel wall proximity on an airfoil model
[NASA-CR-187322] N91-10934
WIND TURBINES
Aeroelastics and dynamics of wind turbines N91-10923
Problems of static divergence concerning the rpm regulation of wind turbines using centrifugal force controlling means and rotating slat
[ETN-90-97858] N91-11281
Performance and cost projections for advanced wind turbines
[DE90-000370] N91-11286
Atmospheric performance of the special-purpose Solar Energy Research Institute (SERI) thin-airfoil family: Final results
[DE90-000373] N91-11287
DUWECS reference guide V1.0: Delft University wind energy converter simulation program
[MEMT-5] N91-11294
WIND VARIATIONS
Effect of wind and wind variation on aircraft flight-paths N91-10972
Wind models for flight simulation N91-10975
WIND VELOCITY
ECC ozonesonde observations at South Pole, Antarctica during 1989
[PB90-258914] N91-11302
Development of a validation model for the defense meteorological satellite program's special sensor microwave imager
[NASA-CR-187369] N91-11342
Sound field fluctuations due to large scale wind-driven turbulence N91-11492
WING OSCILLATIONS
Conical Euler simulation and active suppression of delta wing rocking motion
[NASA-TM-102683] N91-10904
WING PROFILES
The use of a Navier-Stokes code in the wing design process N91-10889
Prediction of effects of wing contour modifications on low-speed maximum lift and transonic performance for the EA-6B aircraft
[NASA-TP-3046] N91-10902
WINGS
More accurate predictions with transonic Navier-Stokes methods through improved turbulence modeling N91-10850
Recent advances in Runge-Kutta schemes for solving 3-D Navier-Stokes equations N91-10851
Applications of a transonic wing design method N91-10890
Development and application of the time domain panel method N91-11010
Vortex-induced noise and vibration in flow past several flat plates N91-11163
WIRE
The transverse stress effect on the critical current of jelly-roll multifilamentary Nb3Al wires
[DE90-513710] N91-11581
WORKLOADS (PSYCHOPHYSIOLOGY)
Douglas flight deck design philosophy N91-10939
Human factors of the high technology cockpit N91-10943
Crew workload strategies in advanced cockpits N91-10945
Inflight replanning for diversions N91-10955
Impact of new technology on operational interface: From design aims to flight evaluation and measurement N91-10977

X

X RAY ANALYSIS
X ray microprobe-microscopy
[DE90-017327] N91-11520
X RAY ASTRONOMY
Activities report of the Institute for Extraterrestrial Physics
[MPE-217] N91-11620
X RAY BINARIES
Long-term observations of three massive x ray binary transients: 4U0115+63, V0332+53, and GX301-2 N91-11612
X RAY SCATTERING
Bragg intensities and diffuse scattering in Ag2Se: Molecular dynamics study
[DE90-017811] N91-11583
X RAY SPECTRA
Atomic physics of highly charged ions in an electron beam ion trap
[DE90-017528] N91-11499
Long-term observations of three massive x ray binary transients: 4U0115+63, V0332+53, and GX301-2 N91-11612
Observations of the soft x ray background N91-11663
X RAYS
X ray microprobe-microscopy
[DE90-017327] N91-11520
Exploration of decreased solar activity state (small intensity activity) in the corona and chromosphere
[INPE-5059-TDL/405] N91-11652
Observations of the soft x ray background N91-11663

Y

YIELD STRENGTH
Residual stress measurements and microstructural characterization of graphite-aluminum metal matrix composite N91-11068
Indentation testing of thin films and hard materials
[DE90-017758] N91-11224
A continuum tensile failure model with friction
[DE90-018006] N91-11265
YTTRIUM OXIDES
Design and testing of a high temperature superconducting current lead
[DE90-017812] N91-11579

Z

ZETA PINCH
Investigation on the projection by a Z-pinch discharge
[DE90-637548] N91-11544
ZINC
Zinc air battery development for electric vehicles
[DE90-016639] N91-11149
ZINC TELLURIDES
Optical characterization of CdZnTe/CdTe strained quantum wells
[DE90-017036] N91-11563
ZIRCONIUM OXIDES
Crack-growth resistance in reinforced ceramic composites N91-11261
ZODIACAL LIGHT
Reexamination of data from the asteroid/meteoroid detector
[NASA-CR-185875] N91-11619
ZONAL FLOW (METEOROLOGY)
The evolution and time scales of the atmospheric response to tropical diabatic heating events N91-11322
Modelling of large-scale unstable waves in the middle atmosphere N91-11327
Basic dynamics of low frequency variability and the storm tracks N91-11339

Typical Personal Author Index Listing

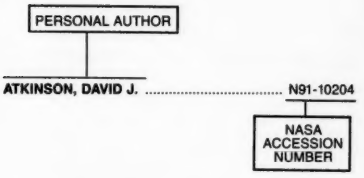

Listings in this index are arranged alphabetically by personal author. The NASA accession number denotes the number by which the citation is identified.

A

ABBOTT, KATHY N91-10949
N91-10951
ABDEL-WAHAB, MOHAMED AHMED N91-10913
ABID, RIDHA N91-10851
ABU-HIJLEH, BASSAM ABDEL-KARIM ABDEL-RAHIM
N91-10914
ADAMCZYK, JOHN J. N91-10880
ADKINS, DOUGLAS R. N91-11289
ADVANI, A. H. N91-11092
AHMAD, ABDULGADER M. N91-11318
AKADA, TAMIO N91-11120
AKINRIMISI, J. N91-11550
AL-ALUSI, THAMIR RAUF N91-11178
ALLEN, CHERYL L. N91-11391
ALLEN, S. L. N91-11547
ALLEN, W. R. N91-11568
ALLISON, DENNIS O. N91-10902
ALLRED, DAVID D. N91-11523
ALMAGRI, A. F. N91-11535
AMADOR, MABLE N91-11601
AMEEN, M. S. N91-11577
AMES, STEPHEN A. N91-11134
AMICHAUD, J. C. N91-11372
ANDELIN, J. N91-11593
ANDERSEN, HARALD T. N91-11376
ANDERSON, ROBERT J. N91-11222
ANDREWS, L. A. N91-11153
ANG, J. A. N91-11032
ANKARA, ALPAY N91-11249
ARAKAWA, KAZUO N91-11120
ARMBRUESTER, PETER N91-11202
ARMSTRONG, D. S. N91-11505
ARNAULT, VERONIQUE N91-11065
ARNOLD, A. N91-11451
ARNOLD, STEVEN M. N91-11074
ARNONE, A. N91-11192
ARYA, R. R. N91-11285
ARYA, VINOD K. N91-11074
ASAY, J. R. N91-11032
ASSADI, S. N91-11535
ATKINSON, R. N91-11304
ATTERIDGE, D. G. N91-11092
ATTIA, A. V. N91-11265
AUCIELLO, O. N91-11577
AUSTIN, S. N91-11633
AVELLO, CARLOS GARCIA N91-10989
AXNAES, I. N91-11530
AYOUB, ESSAM FATHI N91-11255
AZEVEDO, STEVE N91-11081
AZMY, Y. Y. N91-11408
N91-11431

B

BACA, THOMAS J. N91-11033
BACKHOUSE, ROLAND N91-11460
BADDELEY, A. J. N91-11475
BADDORF, A. P. N91-11567
BADER, S. D. N91-11570
BAIK, JONG-JIN N91-11338
BAKER, DAVID B. N91-11503
BAKER, MILES N91-11641
BALACHANDRAN, A. P. N91-11497
BALACHANDRAN, U. N91-11579
BALDETTI, P. N91-11551
BALSIGER, H. N91-11550
BANDYOPADHYAY, B. P. N91-11212
BANNERJEE, A. N91-11296
BARGA, ROGER S. N91-11236
BARNES, R. G. N91-11101
N91-11503
BARRACLOUGH, BRUCE L. N91-11502
BARSZCZ, ERIC N91-11384
BARTH, TIMOTHY J. N91-10892
BARTON, TIMOTHY J. N91-11392
BASSIR, K. N91-11094
BATES, BRENT L. N91-10860
BATINA, JOHN T. N91-10856
N91-10904
N91-10918
N91-10919
BAUER, HANS-JOERG N91-11169
BAUER, TERRY N91-11039
BAYSAL, OKTAY N91-10861
BEAUSSANT, R. N91-11374
BECKER, J. N91-10931
BECKSTEAD, J. A. N91-11535
BEERMAN, HENRY P. N91-11027
BEERS, J. N. P. N91-10986
BEKLEMISHEV, A. D. N91-11548
BELAK, JAMES F. N91-11230
BELETIC, JAMES WILLIAM N91-11617
BELL, J. D. N91-11536
BELL, R. GLENN N91-11033
BELLO-TORRES, OMAR N91-11316
BELOT, C. N91-11076
BEN-SHMUEL, S. N91-10875
BENEDITODIEHL, JOAO N91-11388
BENETTILATTARI, CLEITON JONI N91-11652
BENNETT, M. N91-11285
BENOIT, ANDRE N91-10967
N91-10978
N91-10981
N91-10982
N91-10987
N91-10990
N91-10992
N91-10998
N91-10999
N91-11001
N91-11007
BENSON, TOM N91-10888
BENSON, TREVOR MARK N91-11518
BERKOWITZ, BRIAN M. N91-10866
BERNAL, J. N91-11435
N91-11436
BERRY, G. F. N91-11537
N91-11538
BERTOTTI, B. N91-11333
BHARATHAN, D. N91-11282
BIANCO, LUCIO N91-10988
BIDWELL, COLIN S. N91-10866
BIGELOW, T. S. N91-11536
BILGRAM, R. N91-11066
BILLINGS, CHARLES E. N91-10944
BINER, S. B. N91-11070
N91-11071
BIONDO, A. C. N91-11485
BISHOP, W. N91-11144
BISWAS, R. N91-11267
BLACK, RONALD DOUGLAS N91-11093
BLACKER, TED D. N91-11410
BLAIR, MAXWELL N91-11010
BLAKE, R. D. N91-11115
BLAKELY, JACK N91-11099
BLATTNER, ERNEST W. N91-11050
BLIND, BARBARA N91-11522
BLISS, DONALD B. N91-11488
BLOM, A. F. N91-11246
BLOM, H. A. P. N91-11003
BLOMBERG, R. D. N91-10977
BLOOM, I. D. N91-11159
BLOWER, DAVID J. N91-11363
BLOYD, CARY N. N91-11300
BLUM, THOMAS C. N91-10886
BOEHM, H.-D. N91-11383
BOEKE, S. G. N91-11115
BOER, S. N91-11273
N91-11274
BOHM, M. N91-11528
N91-11531
BOLOURCHI, FARHAD N91-11217
BONGERS, PETER M. M. N91-11294
BONNIE, RONALD JOHANNES MARIA N91-11210
BONTEKOE, TJ. ROMKE N91-11606
BORDONI, F. N91-11508
BORDONI, FRANCO N91-11143
BOROVSKY, JOSEPH E. N91-11502
BOUCHARLAT, G. N91-11521
BOUCHET, FRANCOIS R. N91-11637
BOULANGER, FRANK N91-11345
BOURCIER, R. J. N91-11111
BOUTEMY, J. C. N91-11521
BOWEN, A. W. N91-11251
BRADSHAW, J. N91-11108
BRADY, D. MICHAEL N91-11393
BRADY, J. A. N91-11375
BRASCHE, L. J. H. N91-11234
BRASSEUR, DEANNA MARIE N91-11360
BRENNAN, T. M. N91-11559
BRENNER, D. S. N91-11500
BRENNING, N. N91-11528
N91-11530
BRENT, R. P. N91-11448
BREWER, EDWIN B. N91-10900
BREWER, J. H. N91-11506
BRICKNER, RALPH G. N91-11466
BRINKER, C. JEFFREY N91-11089
BRINKER, DAVID J. N91-11058
BRINKLEY, JAMES W. N91-11378
BRINKLEY, KAY L. N91-11072
BRINKMAN, DOUGLAS GEORGE N91-11321
BRISTOW, JULIAN PAUL GREGORY N91-11519
BROCKHAUS, R. N91-10969
BROER, H. W. N91-11459
BROOK, J. R. N91-11303
BROWN, RONALD E. N91-11590
BRUEMMER, S. M. N91-11092
BUCCA, P. J. N91-11346
BUCK, O. N91-11234
N91-11264
BUCKMASTER, JOHN N91-11164
BUEHRING, W. A. N91-11309
BUICAN, ILEANA N91-11601
BUJA, LAWRENCE EDWARD N91-11322
BULLER, J. F. N91-11154
BUNING, P. G. N91-10875
BURDICK, J. N91-11296
BURGARDT, P. N91-11213
BURGETT, WILLIAM STANLEY N91-11176
BURKES, T. R. N91-11156
BUSH, DONALD M. N91-11151
BUST, GARY STEVEN N91-11623
BUSTIN, ROBERTA N91-11644
BYERS, J. A. N91-11547

C

CABLE, S. N91-11634
CAI, MING N91-11339
CAIRNS, I. H. N91-11642
CALDASBARBOSA, OSWALDO N91-11423
CALKOEN, C. J. N91-11348
CALLEN, J. D. N91-11525
CAMERON, DON N91-11481
CAMP, JORDAN B. N91-11590
CAMPBELL, RICHARD L. N91-10890
CAMUS, PAUL N91-10974
CANDIDI, M. N91-11550
CANDLER, GRAHAM N91-10898
CANN, DAVID N91-11414
CAO, WEI-DI N91-11095
CAPIZZI, P. N91-11551
CAPRON, WILLIAM R. N91-10996

CAREL, OLIVIER N91-11005
CARLSON, K. DOUGLAS N91-11582
CARNES, B. A. N91-11352
CARO, J. A. N91-11103
CARPENTER, D. L. N91-11645
CARPENTER, MARK H. N91-10870
CARPENTER, THOMAS W. N91-11050
CARRERAS, B. A. N91-11536
CARSON, N. N91-11593
CARSTENS, DEAN H. W. N91-11085
CARSTENS, VOLKER N91-10921
CARVALHO, M. HELENA N91-11243
CASE, W. E. N91-11207
CASOTTO, STEFANO N91-11029
CASTEN, R. F. N91-11500
CHAKRAVARTHY, SUKUMAR R. N91-10869
CHALON, G. N91-11334
CHAMBERLIN, J. L. N91-11290
CHAMUEL, JACQUES R. N91-11489
CHAN, TONY F. N91-11384
CHAN, WILLIAM MACHADO N91-11181
CHANG, CHONG-HWAN N91-11353
CHANG, F. N91-11170
CHANG, FU-SUNG N91-11044
CHANG, H. L. M. N91-11578
CHANG, LEON N91-10852
CHANG, P. Z. N91-11487
CHANG, S. L. N91-11537
N91-11538
CHARLTON, L. A. N91-11536
CHARTAS, G. N91-11535
CHAWLA, KALPANA N91-10886
CHEN, C. H. N91-11209
CHEN, CHING S. N91-10865
CHEN, E. N91-11296
CHEN, F. C. N91-11185
CHEN, G. L. N91-11185
CHEN, JAMES N91-11027
CHEN, S. S. N91-11190
CHEN, W. S. N91-11280
CHEN, WON-ZON N91-11433
CHEN, Y. N91-11524
CHEN, YINCHAO N91-11141
CHERN, YI-TZONG N91-11237
CHESSER, NANCY C. N91-11147
CHIBA, AKIRA N91-11052
CHIMA, RODRICK V. N91-10885
CHISHOLM, M. F. N91-11576
CHITSOMBOOM, TAWIT N91-10873
CHIU, ING-TSAU N91-10875
CHO, B. H. N91-11053
CHOU, W.-T. N91-11500
CHOUDHARI, MEELAN N91-11182
CHRISTENSEN, M. N91-11409
CHUANG, KUAN-WEN N91-11657
CHUDACEK, JAROSLAV N91-11401
CIARDULLO, ROBIN N91-11605
CIRILLO, R. R. N91-11309
CLARK, JOEL N91-11481
CLAUSING, ROBERT E. N91-11125
CLEMENTS, ROCHELLE E. N91-11082
CLERE, J. M. N91-11372
CLOSE, PAUL N91-11482
CLOUTIER, MIKE N91-11039
COHEN, G. N91-11448
COHEN, JOSEPH M. N91-11286
COLCHIN, R. J. N91-11536
CONKLIN, J. C. N91-11186
CONNOR, CRAIG N91-11600
CONRADI, MARK S. N91-11503
CONTRERAS, JUANITA N91-11050
COOK, R. N91-11245
COOPER, BETH A. N91-11493
COPE, M. T. N91-11107
CORKER, KEVIN N91-10952
N91-10961
COSGROVE, PATRICK A. N91-11041
COSMOVICI, C. B. N91-11551
COUZY, W. N91-11427
COX, M. E. N91-11006
COZZOLINO, C. N91-11569
CRAIN, WILLIAM K. N91-11037
N91-11038
CRAVEY, W. R. N91-11156
CREDEUR, LEONARD N91-10996
CROZER, E. A. N91-11302
CRUME, E. C. N91-11536
CUMMINGS, RUSSELL M. N91-10859
CURCHOD, DON N91-11516
CURTAIN, RUTH F. N91-11456
CURTIS, L. J. N91-11501

D

DAALHUIS, A. B. OLDE N91-11440
DABROWSKI, B. N91-11580
DAEUBLER, M. A. N91-11107
DALM, T. B. N91-10986
DARLING, TIMOTHY W. N91-11590
DAS, SUBHENDU N91-11430
DASILVA, ERIVALDO ANTONIO N91-11422
DAUTRICHE, P. N91-11521
DAVIES, CAROL B. N91-10853
DAVIS, D. DALE, JR. N91-11252
DAVIS, PAMELA J. N91-11089
DAVIS, THOMAS J. N91-11000
DAWSON, L. R. N91-11561
DEDERER, J. T. N91-11579
DEES, D. W. N91-11159
DEFREITAS, M. N91-11243
DEGOEDE, ERIK D. N91-11167
N91-11399
DEHAAN, L. N91-11476
DEIWERT, GEORGE S. N91-10853
DEJONG, F. J. N91-10878
DEKKERS, A. L. M. N91-11476
DEKONING, W. L. N91-11527
DELAPLATA, MARQUEZ N91-11366
DELLENBACK, STEVEN W. N91-11392
DELLINGER, B. N91-11305
DELNATTE, YVES N91-11007
DENHARTOG, D. J. N91-11535
DENHERTOG, D. N91-11402
N91-11453
DESA, W. P. N91-11524
DESER, CLARA N91-11340
DESLANDES, RONALD N91-11016
DEVALK, C. F. N91-11348
DEVANEY, W. E. N91-11280
DEVAULL, GEORGE ELLIS, III N91-11323
DEVENUTO, F. N91-11047
N91-11551
DEVER, THERESE N91-11062
DEVREUGHT, J. P. M. N91-11429
DEWAAL, PETER R. N91-11483
DEWISPELAERE, RENE N91-11001
DEXTER, N. N91-11535
DEYERL, ERIC N91-11641
DHIR, V. K. N91-11170
DIGIACOMO, NICHOLAS N91-11412
DILLMANN, ANDREAS N91-11077
DINARDO, R. N91-11108
DIONNE, P. J. N91-10879
DITTMAR, JAMES H. N91-11494
DODSON, BRIAN W. N91-11562
DOLGIN, DANIEL L. N91-11363
DOMINGUEZ, N. N91-11536
DORAN, D. N91-10879
DOYLE, GERALD N91-11126
DREIBELBIS, RYLAND R. N91-10964
DRENTH, F. N91-11273
N91-11274
DROST, M. K. N91-11301
DRUMMOND, J. P. N91-10870
DUBIN, MAURICE N91-11619
DUBOIS, D. F. N91-11546
DUDLEY, VERNON N91-11289
DUNLAP, J. L. N91-11536
DURRAN, I. R. N91-11047
DWYER, J. P. N91-11235
DYER, G. R. N91-11536
DZHAPARIDZE, KACHA O. N91-11445

E

EASTMAN, J. A. N91-11115
ECKELS, P. W. N91-11579
ECKERLING, SHERRY J. N91-11233
EDENBURN, MICHAEL W. N91-11155
EDMONDS, CHARLES G. N91-11079
EDWARDS, A. L. N91-11195
EDWARDS, BRADLEY CARL N91-11663
EDWARDS, P. R. N91-11240
N91-11241
EGERT, C. M. N91-11523
EISSFELDT, HINNERK N91-11364
EKLUND, THOR I. N91-11015
ELLIS, DAVID N91-11599
EMDAD, HOMAYOUN N91-11009
ENDSLEY, ROSS N91-11204
ERLEBACHER, GORDON N91-10847
N91-10848
ERWIN, R. L. N91-10997
ERZBERGER, HEINZ N91-10957
N91-11000
ESEN, E. B. N91-11223
ETKIN, BERNARD N91-10971
ETKIN, DAVID ALEXANDER N91-10971
EVANS, C. R. N91-11115
EVERETT, R. A. N91-11247

F

FABISZAK, E. N91-11212
FAELTHAMMAR, CARL-GUNNE N91-11312
N91-11528
N91-11529
FARMER, JEFFERY T. N91-11041
FARRELL, J. N91-11409
FAULKNER, DANNY REED N91-11632
FEDDERS, P. A. N91-11557
FEIEREISEN, WILLIAM J. N91-10872
FELDMAN, DAVID LEWIS N91-11308
FELKER, B. N91-11547
FENSKE, G. R. N91-11212
FENSTERMACHER, M. E. N91-11547
FEO, JOHN N91-11414
FERGUSON, HENRY CLOSSON N91-11608
FERGUSON, S. W. N91-11547
FERLAND, G. N91-11633
FERRI, GIANFRANCO N91-11551
FINDLAY, JOHN T. N91-11310
FINNEMORE, D. K. N91-11571
FISHER, RONALD E. N91-11300
FLEDEL, SHMUEL N91-11012
FLESELMANN, B. N91-11285
FLOOD, DENNIS J. N91-11061
FLORES, JOLEN N91-10858
FOLLSTAEDT, D. M. N91-11111
FORD, CLIFFORD N91-11395
FORD, DONNIE R. N91-11393
FORD, HOLLAND C. N91-11605
FORD, J. S. N91-11078
FORNASIER, LUCIANO N91-11424
FORRESTER, D. A. N91-11006
FORTUNE, MICHAEL ALLAN N91-11319
FOTTNER, LEONHARD N91-11022
FOUILLOT, J. P. N91-10977
FOUSHEE, CLAY N91-10940
FRANCHITO, SERGIO HENRIQUE N91-11343
FRANK, ALAN M. N91-11082
FRIBERG, P. N91-11315
FRICKE, MANFRED N91-11008
FRIEDRICHS, CARL N91-11162
FRIESEL, MARK A. N91-11236
FRITZ, I. J. N91-11559
FROST, CYNTHIA N91-11037
N91-11038
FUERST, J. D. N91-11086
FUNKE, H. N91-11589

G

GALATOLO, R. N91-11250
GALLOTTIFLORENZANO, TERESA N91-11279
GALVAO, R. M. O. N91-11524
GANGADHARAN, SATHYA NARAYAN N91-11232
GARBEY, MARC N91-11413
GARCIA, C. N91-11649
GARCIA, ROBERT N91-10878
GARNETT, DONALD ROY N91-11624
GARVEY, R. E. N91-11069
GARY, J. N91-11405
GASTELLU-ETCHEGORRY, J. P. N91-11270
GAVALI, SHARAD N91-10881
GAWANDE, BERND N91-11203
GEA, LIE-MINE N91-10906
GEARHART, JAMES WALTER N91-11030
GEHRZ, R. D. N91-11633
GEISER, URS N91-11582
GELBARD, E. M. N91-11479
GELLER, E. W. N91-10917
GENTLES, A. B. N91-11142
GEORGE, E. P. N91-11558
GESSLER, A. N91-11066
GHAFFARI, FARHAD N91-10860
GIBSON, TIM N91-11641
GILBANK, PASCALE N91-11090
GILBERT, NORBERT N91-11199
GILLETTE, R. B. N91-11280
GLASSER, ALAN H. N91-11545
GLATFELTER, T. N91-11296
GNOFFO, PETER A. N91-10869
N91-10897
GOETERS, KLAUS-MARTIN N91-11364
GOMES, WALKER N91-11275
GOODBERLET, M. A. N91-11342
GOODENOUGH, J. B. N91-11565
GOODMAN, B. J. N91-11283
GOODRICH, JOHN W. N91-10854
GOTTWALD, JAMES A. N91-11488
GOUDA, NAOTERU N91-11639
GRABOWSKI, ANTHONY JOSEPH N91-11161
GRAEBER, CURTIS N91-10944
GRAETTINGER, T. M. N91-11577

GRANROTH, L. J. N91-11642
GRANRYD, E. N91-11186
GRAY, D. D. N91-11194
GRDINA, D. J. N91-11352
GREEN, H. J. N91-11282
GREEN, S. N91-11409
GREEN, STEVEN M. N91-10958
N91-11000
GREGORY, DANNY L. N91-11064
GRIFF, STANLEY P. N91-11126
GRIFFIN, LISA W. N91-10882
GRIFFIN, R. H. N91-11276
GROENENDIJK, WIM P. N91-11426
GRUEN, DIETER M. N91-11575
N91-11577
GRUHL, HARMUT N91-11517
GUHA, S. N91-11296
GUIDONI, U. N91-11047
N91-11551
GUILBAULT, GEORGE N91-11552
GUMBERT, CLYDE N91-10893
GUO, J. N91-11578
GURNETT, D. A. N91-11642
GURUSWAMY, GURU P. N91-10855
GUSTAVESON, MARK B. N91-11488
GUTMAN, G. N91-11374

H

HAGIWARA, MIYUKI N91-11120
HAGWOOD, C. N91-11464
HAHN, K.-U. N91-10972
N91-10975
HALBLEIB, L. L. N91-11235
HALL, C. A. N91-11032
HALL, DAVID G. N91-11493
N91-11494
HALVERSON, MARK N91-11600
HAMBY, DAVID M. N91-11498
HAMILTON, B. P. N91-11309
HAMMER, C. L. N91-11159
HAMMOND, G. N91-11296
HAN, C. C. N91-11569
HANAMI, H. N91-11651
HANSEN, N. R. N91-11057
HARDER, KAI N91-11490
HARDY, J. E. N91-11188
HARFOUSH, F. A. N91-11511
HARRIES, W. L. N91-11118
HARRINGTON, KIM MCKEE N91-11139
HARRIS, J. H. N91-11536
HART, RUSSELL E., JR. N91-11058
HART, SANDRA G. N91-10945
HASH, M. C. N91-11159
HASMINSKII, RAFAEL N91-11477
HAWKE, R. S. N91-11032
HAYMAKER, RICHARD W. N91-11574
HAYS, CLIFFORD O., JR. N91-11395
HAYWARD, THOMAS L. N91-11609
HE, XIAOHUA N91-11045
HEATH, W. A. N91-11032
HEATHERLY, LEE, JR. N91-11125
HEIJMANS, H. J. A. M. N91-11442
HEIKEN, GRANT N91-11646
HEINTSCH, T. N91-10972
N91-10975
HEIPLE, C. R. N91-11213
HEMKER, P. W. N91-10905
N91-11554
HENDRICKS, JOHN S. N91-11465
HENDY, KEITH C. N91-11369
HENRY, ROBERT N91-11133
HENSON, GARY DEWAYNE N91-11616
HEPPLEWHITE, C. L. N91-11324
HERNQUIST, LARS N91-11637
HICKEY, JOHN R. N91-11058
HICKMAN, R. J. N91-11032
HICKS, R. J. N91-11367
HIDAKA, K. N91-11656
HIGGINBOTHAM, G. J. S. N91-11416
HILLIS, DAVID L. N91-11299
HILPERT, R. N91-11201
HINDERS, MARK KARL N91-11256
HINKS, D. G. N91-11580
HIRAGA, KEIJIRO N91-11106
HIROHAMA, MITSUO N91-11120
HIROMOTO, ROBERT N91-11466
HO, C. M. N91-10917
HOBART, MIKE N91-11486
HOCK, SUSAN M. N91-11286
HOENLINGER, H. N91-10931
HOERMANN, ANDREAS N91-11008
HOGENDOORN, R. A. N91-11003
HOKIN, S. A. N91-11535
HOLDAWAY, MARK ALLAN N91-11610
HOLDEMAN, JAMES D. N91-10887
HOLLY, D. J. N91-11535
HOLST, TERRY L. N91-10840
HOLSTER, P. N91-11214
HOLZWARTH, T. J. N91-11349
HONDA, M. N91-11656
HONIG, H. J. N91-11429
HONMA, KOZO N91-11200
HOOGEVEEN, J. A. N91-11398
HOOPER, E. G. N91-11547
HOPSON, M. N91-11296
HORNUNG, E. N91-10930
HOSKING, F. M. N91-11110
HOSNI, MOHAMMAD HOSEIN N91-11183
HOWARD, SETHANNE N91-11631
HOWARD, W. MICHAEL N91-11635
HOWE, M. A. N91-11566
HOWELLS, PETER J. N91-10976
HSU, S. N. N91-11569
HU, JUN MING N91-11257
HUANG, CHAOSONG N91-11544
HUANG, ZHAOFENG N91-11474
HUBER, W. J. N91-11288
HUDDLESTON, DAVID HOWARD N91-11013
HUDLICKA, EVA N91-10952
HUENERS, H. N91-10922
HUFF, DENNIS L. N91-10884
HULL, J. R. N91-11487
N91-11579
HUNDSDORFER, W. H. N91-11450
N91-11451
HUNG, CHING-CHEN N91-11062
HUNTER, DAN N91-11039
HUPP, JOSEPH T. N91-11504
HURLBURT, H. E. N91-11347
HURST, DALE FREDERICK N91-11328
HUSSAINI, M. Y. N91-10847
N91-10848
HUTTON, LINDA VAUGHT N91-11359
HUVAL, DANNY JAMES N91-11171
HUYNH, HUU THANH N91-10970

I

IBANEZ-MEIER, RODRIGO N91-11101
IBRAGIMOV, IIDAR N91-11477
ICE, G. E. N91-11520
IESS, L. N91-11333
IMBERT, NICOLE N91-10991
INAGAKI, TAKESHI N91-11484
INAGAKI, TOSHIHARU N91-10966
ISENBERG, ARNOLD O. N91-11148
ISOBE, TAKASHI N91-11615
ISSACCI, FARROKH N91-11179
ITOH, K. N91-11532
ITOH, S.-I. N91-11532
IUCCI, N. N91-11653
N91-11654
IZUMI, K. H. N91-10997

J

JACOB, K. N91-11315
JACOBS, J. N91-11214
JACOBS, WILFRIED N91-11335
JACQMIN, DAVID N91-10867
JACQUES, DIDIER N91-11075
JAGER, D. N91-11287
JAHNKE, CRAIG CHARLES N91-11014
JAIN, PARVEEN N91-10953
JANES, DANIEL MARK N91-11647
JANG, HONG-MING N91-11172
JANKOVSKY, R. S. N91-11059
JASINSKI, RACHEL A. N91-11310
JAVAKHISHVILI, J. I. N91-11543
JENNINGS, JOHN R. N91-11658
JENSEN, ERIC JON N91-11337
JERRAYA, AHMED AMINE N91-11404
JESPERSEN, DENNIS C. N91-10896
JESPERSON, DENNIS C. N91-11384
JESSON, D. E. N91-11576
JIH, JUNHAUR N91-11406
JOHNSON, A. B. N91-10915
JOHNSON, C. N91-11108
JOHNSON, DENNIS N91-11039
JOHNSON, DENNIS A. N91-10850
JOHNSON, G. K. N91-11102
JOHNSON, JONI JAYNE N91-11622
JOHNSON, W. H. N91-11298
JOHNSTON, D. C. N91-11506
JOLY, VERONIQUE N91-11211
JONES, E. D. N91-11560
N91-11561
N91-11563
N91-11573
JONES, ROGER W. N91-11083
JORGENSEN, J. D. N91-11565
N91-11580
JOSEFSON, CARL N91-11039
JOSHI, PRAKASH B. N91-11027
JOU, W. H. N91-10917
JUNG, D. N91-11582
JUNG, JOSEPH N91-11410
JURGENS, T. G. N91-11511

K

KADOYU, M. N91-11292
KALIA, RAJIV K. N91-11583
KALLEND, J. S. N91-11485
KAMATH, H. N91-10870
KAMINAR, NEIL N91-11516
KANDIL, OSAMA A. N91-10903
KANDULA, MAX N91-10876
KANTERS, ARNOLDUS FRANCISCUS CORNELIS
N91-11228
KAPER, HANS G. N91-11413
KARGER, INGO N91-10963
KARIM, MUNAWAR N91-11143
KASAHARA, K. N91-11656
KATKOV, A. YU. N91-11355
KATZ, J. D. N91-11115
KAUFMANN, B. N91-10972
N91-10975
KAWAHARA, HIROYASU N91-11026
KAYNAK, CEVDET N91-11249
KAZAROFF, J. M. N91-11059
KEETON, L. W. N91-10879
KEMP, VICTORIA R. N91-11233
KERRICK, DAVID MICHAEL N91-11630
KHAVARAN, ABBAS N91-11493
KHOROMSKIJ, B. N. N91-11471
KIESSLING, FRITZ N91-10923
KILLIAN, KENDRICK N91-11412
KIM, CHAN MUN N91-11163
KIM, J. J. N91-10846
KIM, YONG HYUP N91-11262
KIMBALL, C. W. N91-11580
KINDLE, J. C. N91-11347
KINGON, A. I. N91-11577
KINI, ARAVINDA M N91-11582
KIRBY, D. G. N91-11142
KISARA, KATSUHITO N91-11052
KLEB, WILLIAM L. N91-10919
KLEIN, V. F. N91-11154
KLEM, J. F. N91-11559
N91-11560
N91-11561
KLINE-SCHODER, ROBERT JOHN N91-11046
KLOTS, T. D. N91-11100
KNIGHT, NORMAN F., JR. N91-11252
KNOKE, G. S. N91-10917
KNOX, CHARLES E. N91-10962
N91-10994
KOCKS, U. F. N91-11485
KOENIG, K. N91-10932
KOENIG, REINHARD N91-10965
KOENRAAD, PAULUS MARIA N91-11586
KOMHYR, W. D. N91-11302
KONRAD, C. H. N91-11032
KOODALATTUPURAM, CHITHRABHANU N91-11175
KOPANSKI, J. J. N91-11555
KOREN, B. N91-10905
KORNBLUM, B. T. N91-11514
KORYCANSKY, DONALD GEORGE N91-11643
KOSHIISHI, HAJIME N91-11200
KOSTERS, MENNO N91-11461
KRAUSS, A. R. N91-11577
KRAUTTER, J. N91-11633
KRECH, ROBERT H. N91-11027
KREJSA, EUGENE A. N91-11493
N91-11495
KRINSKY, IRWIN SCOTT N91-11659
KRIST, SHERRIE L. N91-10891
KUIJPER, M. N91-11446
KULSRUD, R. M. N91-11634
KUMAR, AJAY N91-10869
KUMAR, ARUN N91-11341
KURSCHAT, THOMAS N91-11588
KURTH, W. S. N91-11642
KWAK, DOCHAN N91-10852
KWOK, W. K. N91-11582
KWONG, MAN KAM N91-11413

L

LAARMAN, T. N91-11296
LAGZDINA, DAIRA N91-11096
LAM, D. J. N91-11578

LAMBERT, STEVEN R. N91-11271
LAMBORN, MARK JACKSON N91-11063
LAMMERING, ROLF N91-10924
LANAGAN, M. T. N91-11579
LANCIOTTI, A. N91-11250
LANGBERG, BOB N91-11641
LASHMORE, D. N91-11108
LATHROP, J. A. N91-11302
LAU, S. S. N91-11569
LAYTON, CHUCK N91-10956
LE, L. P. N91-11506
LEBEAU, S. E. N91-11571
LEE, ALFRED T. N91-10946
N91-10960
LEE, C. S. N91-10864
LEE, ELIZABETH M. N91-10904
LEE, F. C. N91-11053
LEE, GORDON K. N91-11387
LEE, IN YOUNG N91-11344
LEE, JEH WON N91-11216
LEE, JONG-KIL N91-11218
LEE, KYUNG-TAE N91-11011
LEE, SEUNG-HO N91-10872
LEE, YOONSANG N91-10910
LEFAS, C. C. N91-11004
LEHNERT, B. N91-11496
LEJEUNE, D. N91-11372
N91-11374
LENCIONI, DENNIS N91-11050
LENT, HANS-MARTIN N91-11491
LEONARD, C. N91-11076
LEONETTI, M. N91-11551
LEVIT, CREON N91-10896
LEVY, HANOCH N91-11426
LEYRAT, GILLES F. N91-11258
LI, CHIEN P. N91-10844
N91-10899
LI, YAHONG N91-11544
LIANG, TE N91-11177
LIAO, CHENG-YOUNG N91-11238
LIAO, J. J. N91-11558
LIAO, Y. X. N91-11115
LIEBERT, CURT H. N91-11205
LIEPINS, GUNAR E. N91-11434
LIGHTFOOT, P. N91-11565
LILLEVIK, SIG N91-11480
LIN, S. Y. N91-11560
LINK, H. F. N91-11282
LINTZ, ANDREW L. N91-11027
LIOU, M.-S. N91-11192
LIOU, MENG-SING N91-10894
LIU, C. N91-11570
LIU, C. T. N91-11558
LIU, H. T. N91-10917
LOEHNER, R. N91-10893
LOMINADZE, J. G. N91-11543
LONG, EDWARD R., JR. N91-11118
LONG, MARTIN N91-11062
LONG, SHEILA ANN T. N91-11118
LONGTIN, ANDRE N91-11351
LOO, JOSEPH A. N91-11079
LOOMIS, BEN A. N91-11105
LOOTSMA, F. A. N91-11592
LOTTES, S. A. N91-11537
N91-11538
LOVASZ, L. N91-11444
LOW, H. C. N91-11020
LOWRANCE, JOHN L. N91-11268
LUA, YUAN JIE N91-11259
LUBRANO, GLENN N91-11552
LUCKRING, JAMES M. N91-10860
LUERS, JAMES K. N91-11325
LUKE, G. M. N91-11506
LUMPE, S. W. N91-11235
LUNDE, OTTAR N91-11376
LUNDIN, E. N91-11649
LUNG, SHUN-FAT N91-11260
LYCETTE. M. N91-11296
LYNDS, L. N91-11487
LYO, K. N91-11560
LYO, S. K. N91-11573

M

MA, YIPING N91-11056
MACHIDA, M. N91-11510
N91-11524
MADAVAN, NATERI K. N91-10881
MADSON, MICHAEL D. N91-10862
MAGGI, M. N91-11551
MAJKRZAK, C. F. N91-11108
MALCOM, GRANT N91-11460
MALTBY, J. D. N91-11514
MANE, LAURE N91-11197
MANKBADI, REDA R. N91-10849
MANTHIRAM, A. N91-11565
MANZEY, DIETRICH N91-11381
MAROTTE, H. N91-11372
N91-11374
MARRS, R. E. N91-11499
MARTIN-NEUVILLE, H. N91-11076
MARTIN, F. W., JR. N91-10875
MARTIN, J. A. N91-11114
MARTINEZ, J. R. N91-11032
MARTINUSSEN, M. N91-11365
MARTZ, HARRY N91-11081
MATHIS, JULIE ANN N91-10909
MATTAUCH, R. J. N91-11144
MAXIMON, L. C. N91-11437
MAYORAL, ANDRE LUIZ ROSA N91-11419
MAZEPA, N. E. N91-11472
MAZUR, CHRISTOPHER J. N91-11242
MCCANN, M. P. N91-11209
MCCLELLAND, JOHN F. N91-11083
MCCOLLISTER, H. L. N91-11153
MCCONNAUGHEY, H. V. N91-10882
MCCONNAUGHEY, P. K. N91-10877
N91-10878
MCCOY, C. ELAINE N91-10956
MCCROSKEY, WILLIAM J. N91-10863
MCCUE, JANICE HELEN N91-11598
MCGARY, J. N91-10899
MCHARGUE, CARL J. N91-11224
MCINTOSH, GREG N91-11050
MCLAREN, MARK DUNCAN N91-11043
MCLEAN, D. N91-10973
MCMILLIN, S. NAOMI N91-10889
MEAKIN, R. L. N91-10875
MEESTER, RONALD W. J. N91-11452
MEETHAM, G. W. N91-11021
N91-11073
MEI, V. C. N91-11185
MELCHER, JOERG N91-10929
MELENDRES, CARLOS A. N91-11109
MELIS, MATTHEW E. N91-11074
MELTON, RONALD B. N91-11236
MENGXI, TANG N91-11143
MERRILL, B. J. N91-11128
METZGER, E. J. N91-11347
MEYER, BRADLEY S. N91-11635
MICHAEL, GERRY N91-11039
MICKELER, SIEGFRIED N91-11281
MIDORIKAWA, S. N91-11656
MIELE, A. N91-10968
MILEY, GEORGE H. N91-11534
MILLER, JOHN C. N91-11080
MILLER, L L. N91-11506
MILLER, T. A. N91-11571
MILLIS, RICHARD P. N91-11564
MITCHELL, A. W. N91-11580
MITCHELL, CHRISTINE M. N91-11380
MITCHELL, RUSSELL R. N91-11225
MOHR, R. N91-11296
MOLENAAR, J. N91-11553
N91-11554
MOLVIK, GREGORY ALAN N91-10911
MONROE, S. L. N91-11153
MONTEIL, C. N91-10977
MOON, F. C. N91-11487
MORBIDINI, A. N91-11551
MORELLO, SAMUEL A. N91-10936
N91-10941
MORGAN, H. S. N91-11263
MORRIS, J. N91-11285
MOSS, JAMES N. N91-10901
MOUNTAIN, D. G. N91-11349
MOYEED, R. A. N91-11475
MULANSKY, BERND N91-11469
MULCAHY, T. M. N91-11487
MULET, J. C. N91-11078
MUNDT, C. N91-10935
MUNSON, ROBERT A. N91-11377
MURPHY, R. W. N91-11185
MURRAY, J. R. N91-11154
MURRAY, PAUL E. N91-11189
MURTY, V. S. N91-11290
MYERS, D. R. N91-11561
MYERS, JACK N91-11039
MYERS, S. M. N91-11111
MYHRE, G. N91-11365

N

NACHTWEY, D. STUART N91-11356
NAGASAWA, MIKIO N91-11640
NAGASHIMA, RYUICHI N91-11052
NAGY, B. N91-11352
NAKA, MASAO N91-11200
NAKAJIMA, HAJIME N91-11106
NAKAMURA, TAKASHI N91-11640
NAKANISHI, HIROSHI N91-11120
NAPOLITANO, MARCELLO ROSARIO N91-11023
NASCIMENTO, I. C. N91-11524
NAUS, D. J. N91-11603
NAVAEE, SHAHNAM N91-11254
NEDOLUHA, GERALD ERNST N91-11629
NEILSEN, M. K. N91-11153
NELSON, P. A. N91-11159
NERY, CARLOS EDUARDO N91-11415
NEUL, ANDREAS N91-11137
NEUMANN, D. A. N91-11108
NEWMAN, JAMES C., JR. N91-11240
N91-11241
N91-11247
NEWTON, J. N91-11285
NGEH-NGWAINBI, JEROME N91-11552
NGUYEN, NHI DIEN N91-11160
NICHOLS, F. A. N91-11212
NICOL, DAVID M. N91-11397
N91-11430
NIKONOV, EH. G. N91-11471
NITZAN, REBECCA N91-11425
NOBLE, JOHN MICHAEL N91-11492
NOOREBAD, SAMADOLLAH N91-11088
NORAZ, SERGE N91-11150
NORBERG, R. E. N91-11503
N91-11557
NORMAN, SUSAN D. N91-10942
NORONHA, WILBERT PAUL N91-11184
NORRIS, J. N91-11353
NORTHAM, G. BURTON N91-10873
NOWACK, H. N91-11244
NOWAK, DIETER N91-11157

O

OBAYASHI, SHIGERU N91-10875
OBOT, N. T. N91-11223
ODEH, NABIH N91-11462
OERY, H. N91-10930
OGALLAGHER, A. N91-11405
OH, C. H. N91-11128
OHLSEN, W. D. N91-11295
OLAND, C. B. N91-11603
OLDALE, PAUL N91-10939
OLSEN, T. N91-11287
OLSON, R. E. N91-11549
ONOFRIO, R. N91-11508
ORSINI, S. N91-11550
OSCARSSON, TORD E. N91-11541
OVESEN, B. N91-11365
OYEVAAR, MARTIN HERKE N91-11196

P

PACOLASOBRINHO, LUIZ CARLOS N91-11048
PAK, BOCKCHOON N91-11180
PALMER, D. D. N91-11234
PALMER, EVERETT N91-10953
N91-10954
PALMER, MICHAEL N91-10955
PALUMBO, DAN N91-11430
PALUSZEK, STEVE N91-11039
PANOSSIAN, HAGOP V. N91-11233
PAPPERT, S. A. N91-11569
PARIKH, P. N91-10893
PARK, HUN SUB N91-11068
PARKS, E. K. N91-11100
PARSONS, B. K. N91-11282
PARSONS, J. M. N91-11282
PASSELL, L. N91-11108
PATERSON, LEIF E. N91-11356
PATTERSON, DONALD J. N91-11225
PAULETTI, R. O. N91-11524
PEARCE, DANIEL N91-10876
PEDRAZA, D. F. N91-11103
N91-11568
PEI, S. N91-11580
PEI, S.-Y. N91-11565
PELEGRIN, MARC J. N91-10991
PELLERIN, VINCENT N91-11229
PELLETIER, R. E. N91-11276
PELLOUX-GERVAIS, P. N91-11374
PENDER, MARIE N91-11552
PENG, YINGCAI N91-11574
PENNYCOOK, S. J. N91-11576
PEREIRADEOLIVEIRA, AMAURI N91-11317
PFITZNER, M. N91-10935
PHATAK, ANIL V. N91-10953
PHEENY, H. T. N91-11375
PHILLIPS, E. P. N91-11247
PHILLIPS, PURABI MUKHOPADHYAY N91-11208
PHILLIPS, R. C. N91-11209
PHILLPOT, S. R. N91-11104

PIGEAU, R. A. N91-11371
PIN, FRANCOIS G. N91-11226
PIRZADEH, S. N91-10893
PISCHKE, KEITH M. N91-10938
PIZZOCHERO, PIERRE N91-11628
PLANES, JEROME N91-11587
PLENTOVICH, ELIZABETH B. N91-10861
PLUMB, R. A. N91-11311
PLUMMER, E. W. N91-11567
PODLESNY, R. N91-11285
POEPPEL, R. B. N91-11579
POKER, D. B. N91-11569
POLLINA, RICHARD J. N91-11539
POLMAN, ERIK ALEXANDER N91-11116
POMPEA, STEPHEN MARK N91-11618
POOLE, EUGENE L. N91-11252
PORTER, ALBERT A. N91-11474
PORTNOY, W. M. N91-11156
POTAPCZUK, MARK G. N91-10866
POTSDAM, MARK N91-10934
POURTAKDOUST, SEID HOSSEIN N91-11173
POVINELLI, L. N91-11192
PRAEL, R. N91-11479
PRAGER, S. C. N91-11535
PREMPEH, E. O. A. N91-11266
PRETZSCH, PETER N91-11017
PRIBIK, D. N91-10878
PRICE, D. L. N91-11102
N91-11566
PRIDDY, TOMMY G. N91-11064
PUTT, RONALD A. N91-11149

Q

QUEK, KOK HOW FRANCIS N91-11396

R

RAEDER, JOACHIM N91-11621
RAI, MAN MOHAN N91-10881
RAMOSTEIXEIRA, MARIO MARCIO N91-11418
RANDALL, CYNTHIA N. N91-11378
RAO, KUDITIPUDI V. N91-10886
RASMUSSEN, A. L. N91-11207
RATCLIFFE, STANLEY N91-10984
RATIS, YU. L. N91-11589
RATNER, JEREMIAH M. N91-11392
RAYMOND, CAROL ANNE N91-11272
RAYNER, STEPHEN MARK N91-11655
RE, F. N91-11653
N91-11654
REDEY, L. N91-11159
REEPS, S. M. N91-11375
REES, DANIEL N91-11162
REHBEIN, D. K. N91-11234
N91-11264
REIJERS, H. T. J. N91-11102
REMLER, DAHLIA KARIN N91-11556
REN, ZHAOXING N91-11544
RENO, J. L. N91-11563
REYES, FRANCISCO JOSE N91-11614
RICHARDS, D. R. N91-11580
RICHARDSON, PAMELA F. N91-10874
RICHTER, HARTWIG N91-11517
RICKMAN, J. M. N91-11104
RICKS, WENDELL N91-10961
RIEKS, ANSGAR N91-11138
RIGHI, J. N91-11571
RILEY, S. J. N91-11100
RINGEL, EMANUEL IRWIN N91-10980
RINO, JOSE PEDRO N91-11583
RIPPL, MARTIN N91-10923
RISEMAN, T. M. N91-11506
RIZK, YEHIA M. N91-10859
N91-10875
ROBERSON, C. W. N91-11206
ROBERTS, LEONARD N91-10934
ROBERTS, THOMAS M. N91-11486
ROBLEE, J. N91-11214
ROCHETTE, P. N91-11136
RODIONOV, K. G. N91-11160
RODRIGUESBRUM, ENEAS N91-11278
RODRIQUEZ, J. L. N91-11154
ROENNMARK, KJELL G. N91-11541
ROERDINK, J. B. T. M. N91-11439
ROGERS, STUART E. N91-10852
ROGOTZKI, YORK N91-11517
RONZHEIMER, ARNO N91-11473
ROOS, C. N91-11402
N91-11453
ROOS, NICO N91-11400
N91-11403
ROSA, RICHARD J. N91-11539
ROSE, HARVEY A. N91-11546
ROSEN, DAVID I. N91-11027
ROSEN, RICHARD ALEXANDER N91-11660
ROSENFELD, MOSHE N91-10852
N91-11165
ROSENZWEIG, CARL N91-11497
ROSKE-HOFSTRAND, RENATE J. N91-10947
ROTH, KARLIN R. N91-10886
ROTHWARF, A. N91-11285
ROTHWELL, P. L. N91-11371
ROU, C. S. N91-11577
ROWCLIFFE, A. F. N91-11122
ROWELL, LAWRENCE F. N91-11041
N91-11391
RUBIN, M. B. N91-11265
RUDD, JAMES L. N91-11242
RUDGE, FREDERICK W. N91-11379
RUDY, DAVID H. N91-10869
RUFFIN, STEPHEN M. N91-10872
RUSH, J. J. N91-11108
RYAN, JAMES STEVENSON N91-11174

S

SABNIS, J. S. N91-10878
SABOUNGI, MARIE-LOUISE N91-11102
N91-11566
SAIZAR, P. N91-11633
SAKAI, YOSHIKAZU N91-11106
SAKAMOTO, HIROSHI N91-11051
SAKODA, DAN N91-11039
SAMAK, SALEM MOHAMED N91-11220
SAMET, JONATHAN M. N91-11357
SAMSON, P. J. N91-11303
SANDERS, A. A. N91-11207
SANDERS, S. C. N91-11571
SANKOVIC, JOHN M. N91-11060
SANTOSDEALMEIDA, WAGNER N91-11277
SANZ, JOSE M. N91-10883
SAPINSKI, P. F. N91-11309
SASAKI, MISAO N91-11636
SASAKI, SHINOBU N91-11227
SASUGA, TSUNEO N91-11120
SATIJA, S. N91-11108
SATRAN, DALE R. N91-10845
SAWIN, LINDA L. N91-11362
SCHAENZER, G. N91-10972
N91-10975
SCHECHTER, JOSEPH N91-11497
SCHEWE, GUENTER N91-10927
SCHIFF, LEWIS B. N91-10859
SCHIFFER, M. N91-11353
SCHMATZ, M. A. N91-10935
SCHMIDT, EBERHARD N91-10925
SCHMIDT, HELMUT N91-11198
SCHNEBERK, DAN N91-11081
SCHRA, L. N91-11248
SCHRANNER, R. N91-11383
SCHRECK, SCOTT JEFFREY N91-10907
SCHRIJVER, A. N91-11443
N91-11444
SCHRYVERS, D. N91-11098
SCHULTZ, AUGUST L. N91-11625
SCHUMACHER, J. M. N91-11446
SCHUTTE, PAUL N91-10950
SCHUTZENHOFER, LUKE A. N91-10843
SCHWARZ, R. B. N91-11115
SEALS, ROLAND D. N91-11523
SEALS, WILLIAM P. N91-11126
SEGUCHI, TADAO N91-11120
SELLIN, IVAN A. N91-11509
SENSBURG, O. N91-10931
SENSBURG, OTTO N91-11025
SHAPIRO, A. B. N91-11195
SHAW, R. W. N91-11084
SHEPHERD, JOSEPH E. N91-11082
SHI, YONG N91-11320
SHIBATA, K. N91-11634
SHIRAISHI, HARUKI N91-11106
SHIROUZU, MASAO N91-11036
SHORE, S. N. N91-11633
SHUEN, JIAN-SHUN N91-10871
N91-10894
SHULL, RONALD N. N91-11363
SICKAFUS, K. E. N91-11115
SIDOBRE, DANIEL N91-11215
SIEM, FREDERICK M. N91-11362
SIGNORETTI, F. N91-11653
N91-11654
SIGWARTH, JOHN B. N91-11626
SILLMAN, S. N91-11303
SIME, D. G. N91-11649
SIMPSON, ROBERT W. N91-10995
SIMPSON, T. L. N91-11141
SINGH, J. P. N91-11579
SINGH, S. K. N91-11579
SINGH, VANDANA N91-11574
SINGHAL, A. K. N91-10879
SITES, J. R. N91-11297
SLOTNICK, JEFF P. N91-10875
SMALLWOOD, DAVID O. N91-11064
SMITH, B. N91-11287
SMITH, D. BARTON N91-11080
SMITH, D. H. N91-11084
SMITH, DALE L. N91-11105
SMITH, DOUGLAS M. N91-11089
SMITH, J. E. N91-11188
SMITH, LEIGH A. N91-10890
SMITH, MERRITT H. N91-10886
SMITH, PHILIP J. N91-10956
SMITH, RICHARD D. N91-11079
SMITH, ROBERT E. N91-10857
N91-11158
SMITH, ROGER P. N91-11382
SMITH, S. J. N91-11326
SNELL, K. H. N91-11223
SOARESGALVAO, LENIO N91-11332
SOBERMAN, ROBERT K. N91-11619
SOBLE, C. S. N91-11577
SODA, TAKAO N91-11120
SOLAL, FRANCINE N91-11117
SOMMEIJER, B. P. N91-11427
N91-11428
SONNEBORN, G. N91-11633
SONWALKAR, VIKAS S. N91-11645
SORENSEN, N. R. N91-11110
SORENSON, REESE L. N91-10859
SOUKOULIS, C. M. N91-11267
SOUTH, JERRY C., JR. N91-10841
SPALART, P. R. N91-10848
SPARKS, C. J. N91-11520
SPENGLER, JOHN D. N91-11357
SPEYER, J. J. N91-10977
SPITZIG, W. A. N91-11070
SPRANGLE, P. N91-11206
SPREIJ, PETER J. C. N91-11445
SPROTT, J. C. N91-11535
SRINIVASAN, RAMAKRISHNA N91-11488
STAGNER, ROBERT E. N91-11050
STALLARD, B. W. N91-11547
STALLINGS, ROBERT L., JR. N91-10861
STAM, A. J. N91-11458
STANSFIELD, S. A. N91-11221
STARRFIELD, S. N91-11633
STEGER, JOSEPH L. N91-10875
STEIN, H. J. N91-11584
STEININGER, B. I. N91-11450
STELLA, PAUL M. N91-11061
STERNLIEB, B. J. N91-11506
STEWART, J. E. N91-11042
STEWART, J. M. N91-11280
STEWART, MARK ERIC MICHAEL N91-10908
STILES, J. M. N91-11194
STILLWELL, WILLIAM N91-10948
STINE, PETER CULLEY N91-11661
STOJIMIROVIC, ALEKSANDAR L. N91-11119
STOLL, HARTY N91-10937
STOOPS, JOHN N91-11600
STOWERS, IRVING F. N91-11230
STRANGEWAY, R. J. N91-11645
STREETS, DAVID G. N91-11300
STREHLOW, G. N91-10931
STREHMEL, K. N91-11451
STREMEL, PAUL M. N91-10933
STRIP, DAVID N91-11231
STRUNCK, J. N91-11244
STUBBS, ROBERT M. N91-10842
STUMP, DAVID MICHAEL N91-11261
STUPKA, D. L. N91-11582
SUDO, TAKAYUKI N91-11052
SUGINOHARA, TATSUSHI N91-11638
SUGIYAMA, NAOSHI N91-11639
SULEIMAN, AHMAD N91-11552
SUNDARAM, A. K. N91-11525
SUNDFELD, SOFIA N91-11417
SUNEPEREZ, JUAN N91-11388
SUSOEFF, A. R. N91-11032
SUSZCYNSKY, DAVID M. N91-11502
SUTO, YASUSHI N91-11637
N91-11638
N91-11639
SUTTON, RICHARD S. N91-11434
SWAIN, M. H. N91-11247
SWEET, L. N91-11405
SWEET, R. N91-11405
SWIERSTRA, SIP N91-10982
N91-10987
N91-10992
N91-10998
N91-10999
N91-11001
N91-11007

SWIFT, C. T. N91-11342
SWOLINSKY, M. N91-10972
N91-10975

T

TAJIMA, T. N91-11634
N91-11651
TAM, HON YUEN N91-11219
TANABE, TATSUHIKO N91-11106
TANAKA, KEIJI N91-10966
N91-11026
TANAKA, M. N91-11532
TANG, JINKE N91-11112
TANG, X. X. N91-11565
TANGLER, J. N91-11287
TANNER, L. E. N91-11098
TAO, DEYING N91-11544
TAO, WILLIAM C. N91-11082
TAYLOR, J. B. N91-11540
TAYLOR, P. C. N91-11295
TAYLOR, P. H. N91-11305
TAYLOR, T. N. N91-11114
TEMME, N. M. N91-11440
TENHAVE, J. M. N91-10986
TENTHIJEBOONKKAMP, J. H. M. N91-11399
TERIELE, H. J. J. N91-11447
N91-11448
TERLAKY, T. N91-11402
N91-11453
TERUI, YUUSHI N91-10966
TEXEIRA, R. H. N91-11283
THOMAS, ANTHONY N91-11299
THOMAS, JAMES L. N91-10860
N91-10869
N91-10891
THOMASON, BRIAN N91-11385
N91-11386
N91-11394
THOMASSEN, K. I. N91-11547
THOMPSON, JAMES E. N91-11582
THOMPSON, R. B. N91-11234
N91-11264
THRESHER, ROBERT W. N91-11286
THROOP, A. L. N91-11547
THUBURN, JOHN N91-11327
TIAN, ZONGROU N91-11253
TICHY, LORENZ N91-10926
TIEDE, D. N91-11353
TIREY, D. A. N91-11305
TIWARI, S. N. N91-11042
TOMITA, KENJI N91-11331
TORGESON, D. R. N91-11101
N91-11503
TORIGAKI, TOSHIKAZU N91-11239
TORVEN, S. N91-11531
TRAUTMANN, K. H. N91-11244
TRAVIS, BRYAN J. N91-11330
TRIEBSTEIN, HERMANN N91-10927
TRIER, STANLEY B. N91-11336
TROMPERT, R. A. N91-11449
TRUDELL, BERNARD J. N91-10964
TSAI, PING-HO N91-10916
TSAI, Y-L. PETER N91-10871
TSIKARISHVILI, E. G. N91-11543
TSUI, D. C. N91-11560
TSUJI, HIROKAZU N91-11106
TUMINARO, RAYMOND S. N91-11384
TURILLON, A. N91-11372
TURNER, G. M. N91-11370
N91-11373
TURNER, W. C. N91-11547
TURNGREN, EDWARD N91-11126
TUSZEL, A. G. N91-11524
TWESME, E. N91-11285

U

UCHIYAMA, Y. N91-11292
UDSETH, HAROLD R. N91-11079
UEDA, M. N91-11510
UEDA, N. N91-11532
UEMURA, Y. J. N91-11506
UGAZIO, S. N91-11551
URBARZ, H. W. N91-11648
USHIMARU, KENJI N91-11191

V

VACHIERY, V. N91-10983
VALERIOFILHO, MARIO N91-11279
VANBAELEN, JOEL STEPHAN HENRY MARCEL
N91-11313
VANCUTSEM, C. N91-11368
VANDALSEM, WILLIAM R. N91-10886
VANDENBOSCH, P. N91-11368
VANDENTOP, GILROY JOHN N91-11585
VANDERHOUWEN, P. J. N91-11427
N91-11428
VANDERKRAAN, P. N91-11002
VANDERVOORT, K. G. N91-11582
VANDERWOUDE, J. W. N91-11166
VANDEWETERING, BRIAN N91-11385
N91-11386
N91-11394
VANDIEP, NGUYEN N91-11193
VANDIJK, NICO N91-11483
VANNARONI, G. N91-11047
VANOVERBEKE, THOMAS J. N91-10887
VANSCHAIK, F. J. N91-11003
VANSTREUN, A. N91-11457
VASHISHTA, PRIYA N91-11583
VATSA, VEER N. N91-10851
VELDMAN, H. J. N91-11470
VENKATAPATHY, ETHIRAJ N91-10853
N91-10872
VERNON, RONALD J. N91-11152
VERWER, J. G. N91-11449
VIANNARODRIGUES, RICARDO LEONARDO
N91-11279
VICROY, DAN D. N91-10993
VIEIRADIAS, LUIZ ALBERTO N91-11415
VIEIRADUTRA, LUCIANO N91-11421
VILLORESI, G. N91-11653
N91-11654
VISSCHER, H. N91-10986
VISSERS, D. R. N91-11159
VOGEL, DAVID N91-11515
VOGEL, S. N91-10932
VOSS, RALPH N91-10928
VUIK, C. N91-11454

W

WADE, R. N91-11633
WADKINS, R. P. N91-11128
WAGENER, JOACHIM N91-10925
WAGGONER, E. G. N91-10902
WAGNER, R. M. N91-11633
WAGNER, ROLF N91-11067
WAKAIRO, KAORU N91-11026
WALKER, ARTHUR H. N91-11613
WALKER, N. A. N91-11107
WALLCRAFT, A. J. N91-11347
WALLER, WILLIAM HOWARD N91-11627
WALLS, F. L. N91-11405
WALTERS, E. J. N91-11145
WALTERS, WES N91-11039
WALTHER, HANS-JOACHIM N91-11468
WANG, HAU H. N91-11582
WANG, S. N91-11524
WANHILL, R. J. H. N91-11248
WARMBROD, JOHN N91-11037
N91-11038
WARNER-SELPH, M. A. N91-11306
WARNER, D. D. N91-11500
WASSEL, ANTHONY B. N91-11307
WATANABE, AKIRA N91-11026
WATANABE, KATSUTOSHI N91-11106
WATANABE, KAZUYA N91-11636
WATSON, VAL N91-10895
WEADOCK, ANTHONY A. N91-11526
WEBER, JOERG N91-11463
WEDAN, BRUCE W. N91-10851
WEINBERGER, B. R. N91-11487
WEINER, R. N91-11451
WEIRICK, LARRY J. N91-11131
WEITS, ELLO N91-11478
WELCH, PETER J. N91-11121
WELLMAN, G. W. N91-11032
WENDT, J. R. N91-11559
N91-11561
WENSINK, G. J. N91-11273
N91-11274
WESSELBORG, C. N91-11500
WHEELER, PETER DAVID N91-11140
WHITE, C. W. N91-11569
WHITLOCK, LAURA ALICE N91-11612
WIEDEMAN, S. N91-11285
WIENER, EARL L. N91-10943
WILKERSON, J. C. N91-11342
WILLAN, UWE N91-11019
WILLEMS, P.-Y. N91-10985
WILLIAM, DAVID L. N91-11314
WILLIAMS, DAVID H. N91-10959
N91-10994
WILLIAMS, G. A. N91-11295
WILLIAMS, JACK M. N91-11582
WILLIAMS, MARC H. N91-10919
WILLIAMS, PATRICK LEE N91-11329
WILLIS, CHRISTOPHER FOWLER N91-11113
WILLIS, MICHAEL GREENE N91-11187
WILSON, C. W. N91-11020
WILSON, LARRY N91-11407
WIMMEL, ROGER N91-10929
WINEY, M. A. N91-11302
WINNUBST, MARIELLE N91-11361
WINTER, B. J. N91-11100
WITKOWSKI, WALTER R. N91-11410
WOLF, D. N91-11104
WOMERSLEY, JOHN N91-11412
WOOD, G. M. N91-11154
WOOD, W. E. N91-11092
WOODALL, TOMMY D. N91-11064
WOODEN, DIANE HOLLAND N91-11611
WOOSLEY, STANFORD E. N91-11635
WORKMAN, GARY L. N91-11091
WORLEY, PATRICK H. N91-11467
WORMINGTON, P. S. N91-11235
WOSIEK, JACEK N91-11574
WU, J. L. N91-11579
WU, KIN-WAH N91-11662
WUNDERLICH, BERNHARD N91-11123

X

XIA, W. N91-11569
XIANG, XUWU N91-11650
XIE, WEIDONG N91-11544

Y

YAGI, TETSUYA N91-11120
YANAGIHARA, MASAAKI N91-11035
YANG, L. N91-11285
YAO, M. N91-11146
YARROW, M. N91-10875
YASUKAWA, E. N91-11649
YEE, TERRANCE N91-11641
YOO, M. H. N91-11097
YOON, SEOKKWAN N91-10852
YOU, H. N91-11578
YOUNG, J. P. N91-11084
YOUNGDAHL, C. A. N91-11579
YU, J. N91-11170
YU, P. K. L. N91-11569
YU, SHENG-TAO N91-10871
YUE, ANDREW N91-11024
YUNGSTER, SHAYE N91-10912

Z

ZANG, T. A. N91-10847
ZANGRANDO, F. N91-11282
ZANGRILLI, N. L. N91-11653
N91-11654
ZAPATA, R. N91-11374
ZEGELING, ANDRE N91-11455
ZELLER, CHRISTOPH N91-11168
ZERITIS, D. N91-11581
ZHANG, J.-Y. N91-11500
ZHANG, SHUQING N91-11544
ZHENG, Y. N91-11580
ZHIDKOV, E. P. N91-11471
ZHU, B. N91-11569
ZILKA, ANTHONY N91-11482
ZIMMERMANN, H. N91-10932
ZINGEL, HARTMUT N91-10927
ZIPPERIAN, T. E. N91-11559
N91-11561
ZWAAN, M. N91-11438
N91-11441

Typical Corporate Source Index Listing

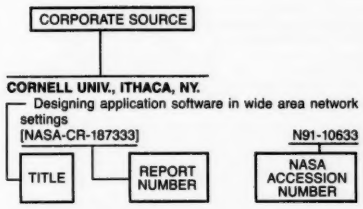

Listings in this index are arranged alphabetically by corporate source. The title of the document provides the user with a brief description of the subject matter. The report number helps to indicate the type of document cited (e.g., NASA report, translation, NASA contractor report). The NASA accession number denotes the number by which the citation is identified. The titles are arranged under each corporate source in ascending accession number order.

A

ACADEMIA SINICA, HEFEI (CHINA).
Investigation on the projection by a Z-pinch discharge
[DE90-637548] N91-11544

ACUREX CORP., RESEARCH TRIANGLE PARK, NC.
Recommended operating procedure No. 45: Analysis of nitrous oxide from combustion sources
[PB90-238502] N91-11078

ADVISORY GROUP FOR AEROSPACE RESEARCH AND DEVELOPMENT, NEUILLY-SUR-SEINE (FRANCE).
Aircraft trajectories: Computation, prediction, control, volume 1. Part 1: Fundamentals. Part 2: Flight in critical atmospheric conditions. Part 3: Impact of new on-board technologies on aircraft operation
[AGARD-AG-301-VOL-1-PT-1-3] N91-10967

Aircraft trajectories: Computation, prediction, control, Volume 3. Part 9: Book of abstracts. Part 10: Bibliography. Part 11: List of contributors
[AGARD-AG-301-VOL-3-PT-9-11] N91-10978

Aircraft trajectories: Computation, prediction, control, volume 2: Air traffic handling and ground-based guidance of aircraft. Part 4: Air traffic handling. Part 5: Guidance of aircraft in a time-based constrained environment. Part 6: Surveillance. Part 7: Meteorological forecasts. Part 8: Aircraft operation in air traffic handling simulation
[AGARD-AG-301-VOL-2-PT-4-8] N91-10981

Test cases for computation of internal flows in aero engine components
[AGARD-AR-275] N91-11022

Short-crack growth behaviour in various aircraft materials
[AGARD-R-767] N91-11240

Recruiting, Selection, Training and Military Operations of Female Aircrew
[AGARD-CP-491] N91-11358

AEROJET SOLID PROPULSION CO., SACRAMENTO, CA.
Hybrid Propulsion Technology Program, phase 1. Volume 1: Executive summary
[NASA-CR-183950] N91-11054

Hybrid Propulsion Technology Program, phase 1. Volume 2: Technical discussion
[NASA-CR-183951] N91-11055

AEROJET TECHSYSTEMS CO., SACRAMENTO, CA.
Hybrid Propulsion Technology Program, phase 1. Volume 1: Executive summary
[NASA-CR-183950] N91-11054

Hybrid Propulsion Technology Program, phase 1. Volume 2: Technical discussion
[NASA-CR-183951] N91-11055

AERONAUTICAL RESEARCH INST. OF SWEDEN, BROMMA.
Short crack growth under realistic flight loading: Model predictions and experimental results for Al 2024 and Al-Li 2090 N91-11246

AEROSPACE MEDICAL RESEARCH LABS., WRIGHT-PATTERSON AFB, OH.
Impact on women: A retrospective look at impact acceleration testing at the Harry G. Armstrong Aerospace Medical Research Laboratory N91-11378

AIR FORCE HUMAN RESOURCES LAB., BROOKS AFB, TX.
Comparison of male and female USAF pilot candidates N91-11362

AIR FORCE SPACE DIV., LOS ANGELES, CA.
Combined Release and Radiation Effects Satellite (CRRES): Atlas 1 (Atlas/Centaur-69) launch vehicle
[NASA-TM-103460] N91-11040

AIR FORCE WRIGHT AERONAUTICAL LABS., WRIGHT-PATTERSON AFB, OH.
Determination of the short crack effect in 2090-T8E41 aluminum lithium N91-11242

AIRBUS INDUSTRIE, BLAGNAC (FRANCE).
How to fly windshear N91-10974

Impact of new technology on operational interface: From design aims to flight evaluation and measurement N91-10977

ALABAMA UNIV., HUNTSVILLE.
Heat treatment study 2
[NASA-CR-184009] N91-11091

Intelligent Data Reduction (IDARE)
[NASA-CR-186322] N91-11393

ALASKA UNIV., FAIRBANKS.
A simulation study of magnetic reconnection processes at the dayside magnetopause N91-11320

ALLGEMEINER DEUTSCHER AUTOMOBIL-CLUB-E.V., MUNICH (GERMANY, F.R.).
Air rescue in the Federal Republic of Germany
[ETN-90-97878] N91-10963

ALLIED-SIGNAL AEROSPACE CO., KANSAS CITY, MO.
Ion chromatography in the manufacture of multilayer circuit boards
[DE90-017647] N91-11158

Software quality assurance handbook
[DE91-000060] N91-11420

AMES LAB., IA.
Analysis of deformation characteristics of a heavily deformed Cu-20 percent Nb composite
[DE90-018041] N91-11070

Characterization of short fatigue cracks at notches in SiC particulate aluminum composite
[DE90-018043] N91-11071

Nuclear magnetic resonance survey of hydrogen motion and electronic structure in (alpha)-phase (Nb-Mo)-H alloys
[DE90-018044] N91-11101

Physical metallurgy and magnetic behavior of Cd stabilized bcc (beta) Gd alloys
[DE91-000196] N91-11112

Deducing mechanical properties due to interfaces from their acoustical response
[DE90-016704] N91-11234

Fatigue crack characterization by ultrasonic inspection
[DE90-017252] N91-11264

A theoretical investigation on structural, vibrational, and electronic properties of amorphous silicon
[DE90-018040] N91-11267

Elementary inversion, energy velocity, and a generalized Sommerfeld theorem
[DE90-018046] N91-11486

Novel measurements of nuclear spin cross-relaxation in metal hydrides
[DE90-018042] N91-11503

Muon SR studies on Sr2CuO2Cl2, La2CuO4, and Nd2CuO4: 2-D magnetism, local fields and muon sites
[DE90-018014] N91-11506

Processing of YBA2Cu3O7 tapes from a molten salt precursor
[DE90-017656] N91-11564

Microfilamentary Bi2Sr2Ca1Cu2O8 fibers
[DE90-018013] N91-11571

ARGONNE NATIONAL LAB., IL.
Chemical identification of icosahedral structure for cobalt and nickel clusters
[DE90-017688] N91-11100

Liquid alloys with strong interactions
[DE90-017661] N91-11102

Molecular-dynamics study of grain-boundary migration in metals
[DE90-017856] N91-11104

Relationship of microstructure and tensile properties for neutron-irradiated vanadium alloys
[DE90-017863] N91-11105

Laser Raman spectroscopy for in-situ analysis of corrosion films on metals
[DE90-017822] N91-11109

Development of high performance sodium/metal chloride cells
[DE90-017668] N91-11159

Unsteady fluid forces and fluidelastic vibration of a group of circular cylinders
[DE90-013661] N91-11190

Wear reduction in cutting tools: Tribological properties of hard coatings
[DE90-009705] N91-11212

Ocean thermal energy conversion: Perspective and status
[DE90-017665] N91-11299

Energy models and national energy policy
[DE90-017682] N91-11300

Evaluating the environmental impacts of the energy system: The ENPEP (Energy and Power Evaluation Program) approach
[DE90-017862] N91-11309

Parameterizations of microphysical processes in clouds
[DE90-017820] N91-11344

Protection by WR-2721 and WR-151327 against late effects of gamma rays and neutrons
[DE90-017792] N91-11352

The structure and function of membrane protein photosynthetic reaction center
[DE90-017795] N91-11353

Symbolic manipulation software and the study of differential equations
[DE90-017674] N91-11413

Computation of standard deviations in Eigenvalue calculations
[DE90-017809] N91-11479

Phenomenology of forces acting between magnets and superconductors
[DE90-017864] N91-11487

Three-dimensional computer simulation of non-reacting jet-gas flow mixing in an MHD second stage combustor
[DE90-017831] N91-11537

Effects of jet port arrangement on three-dimensional non-reacting jet-gas mixing in an MHD second stage combustor
[DE90-017858] N91-11538

Excess oxygen defects in layered cuprates
[DE90-017669] N91-11565

Structure of molten salts
[DE90-017704] N91-11566

Magnetic properties of ultrathin epitaxial films of iron
[DE90-017861] N91-11570

The transuranium elements: Members of the 5f series
[DE90-017680] N91-11575

Computer-controlled ion beam deposition systems for high T(sub c) superconductor and other multi-component oxide thin films and layered structures
[DE90-017798] N91-11577

Epitaxial TiO2 and VO2 films prepared by MOCVD (Metal-Organic Chemical Vapor Deposition)
[DE90-017806] N91-11578

Design and testing of a high temperature superconducting current lead
[DE90-017812] N91-11579

Superconducting and structural properties of the (Ba(0.6)K(0.4)) (Bi(1-y)Sb(y))O3 system
[DE90-017836] N91-11580

Structure-property relationships for (beta)- and (kappa)-phase BEDT-TTF salts and their use in the synthesis of (kappa)-(BEDT-TTF)2Cu(N(CN)2)Br. A salt having the highest T(sub c) (inductive onset = 11.6 K, resistive, onset = 12.5 K) yet observed in an organic superconductor
[DE90-017804] N91-11582

Bragg intensities and diffuse scattering in Ag2Se: Molecular dynamics study
[DE90-017811] N91-11583

ARIZONA UNIV., TUCSON.

Boundary layer receptivity mechanisms relevant to laminar flow control N91-11182

The relationship of galaxy morphology to nuclear star formation in non-interacting spiral galaxies N91-11618

Tectonics of one-plate planets N91-11647

ARKANSAS COLL., BATESVILLE.

Availability of hydrogen for lunar base activities
[NASA-CR-187367] N91-11644

ARMY ENGINEER WATERWAYS EXPERIMENT STATION, VICKSBURG, MS.

Computer-Aided Structural Engineering (CASE) project: Investigation and design of U-frame structures using program CUFRBC. Volume C: User's guide for channels
[AD-A224388] N91-11395

ATLANTIC RESEARCH CORP., LANDOVER, MD.

Current Emergency Locator Transmitter (ELT) deficiencies and potential improvements utilizing TSO-C91a ELTs
[NASA-CR-4330] N91-10964

AUBURN UNIV., AL.

Fluctuations and stability in the Advanced Toroidal Facility (ATF) torsatron
[DE90-017734] N91-11536

AUSTRALIAN NUCLEAR SCIENCE AND TECHNOLOGY ORGANIZATION, LUCAS HEIGHTS.

ANSTO: Australian Nuclear Science and Technology Organization
[DE90-637389] N91-11507

B

BALL AEROSPACE SYSTEMS DIV., BOULDER, CO.

Combined Release and Radiation Effects Satellite (CRRES): Atlas 1 (Atlas/Centaur-69) launch vehicle
[NASA-TM-103460] N91-11040

BBN SYSTEMS AND TECHNOLOGIES CORP., CAMBRIDGE, MA.

Fault recovery recommendation N91-10952

BELEIDSCOMMISSIE REMOTE SENSING, DELFT (NETHERLANDS).

Forest classification with high resolution satellite images. Research into the use of spatial information to improve the multi-spectral classification with SPOT images
[BCRS-89-32] N91-11269

Remote sensing for marine activities
[BCRS-89-41] N91-11273

Remote sensing for marine activities: Appendices
[BCRS-89-41-APP] N91-11274

Wave data assimilation in a 3rd generation. Wave prediction model for the North Sea: An optimal control approach
[BCRS-89-22] N91-11348

BELGIAN AIR FORCE, BRUSSELS.

Review of female applicant aircrew in the Belgian forces N91-11368

BOEING COMMERCIAL AIRPLANE CO., SEATTLE, WA.

Boeing flight deck design philosophy N91-10937

Use of 4-D RNAV in time-based en route arrival metering N91-10997

BOSTON UNIV., MA.

Attenuation of elastic waves due to scattering from spherical cavities and elastic inclusions N91-11256

BRANDEIS UNIV., WALTHAM, MA.

Maximum entropy imaging of radio astrophysical data N91-11610

BRITISH BROADCASTING CORP., KINGSWOOD (ENGLAND).

Digital audio editing: The development of a random access editor
[BBC-RD-1990/5] N91-11142

BRITISH COLUMBIA UNIV., VANCOUVER.

Capture and transfer of pions in hydrogenous materials
[DE90-017756] N91-11505

BROOKHAVEN NATIONAL LAB., UPTON, NY.

Determination of hydrogen (deuterium) density profiles in thin metal films and multilayers by neutron reflection
[DE90-007150] N91-11108

Empirical proton-neutron interaction energies and nuclear structure
[DE90-017632] N91-11500

C

CALIFORNIA INST. OF TECH., PASADENA.

Application of dynamical systems theory to nonlinear aircraft dynamics N91-11014

CALIFORNIA POLYTECHNIC STATE UNIV., SAN LUIS OBISPO.

Design and evaluation of thrust vectored nozzles using a multicomponent thrust stand
[NASA-CR-180474] N91-11050

CALIFORNIA UNIV., BERKELEY.

Current and potential distributions on a cylinder electrode
[DE91-000170] N91-11161

A study of the chemical, mechanical, and surface properties of thin films of hydrogenated amorphous carbon
[DE91-000357] N91-11585

CALIFORNIA UNIV., BERKELEY. LAWRENCE BERKELEY LAB.

A study of chromium carbide precipitation at interphase boundaries in stainless steel welds
[DE91-000360] N91-11113

Zinc air battery development for electric vehicles
[DE90-016639] N91-11149

Current and potential distributions on a cylinder electrode
[DE91-000170] N91-11161

A study of the chemical, mechanical, and surface properties of thin films of hydrogenated amorphous carbon
[DE91-000357] N91-11585

CALIFORNIA UNIV., DAVIS.

Robot trajectory control with a model reference adaptive control system using tap delay filters N91-11217

CALIFORNIA UNIV., IRVINE.

Seasonal variations in the latitudinal distribution of tropospheric carbon monoxide, 1986 to 1988 N91-11328

CALIFORNIA UNIV., LOS ANGELES.

Enhancement of forced convection heat transfer in tubes using staged tangential flow injection
[PB90-247594] N91-11170

Heat pipe vapor dynamics N91-11179

Wave-mean flow interaction in the storm-time thermosphere using a two-dimensional model N91-11321

Constrained optimization approach to feedback control of state-augmented systems N91-11433

Design of a scientific probe for obtaining Mars surface material
[NASA-CR-186672] N91-11641

CALIFORNIA UNIV., RIVERSIDE.

Lifetimes and fates of toxic air contaminants in California's atmosphere
[PB90-253204] N91-11304

Identification and analysis of cosmic gamma ray bursts from Pioneer Venus Orbiter N91-11657

CALIFORNIA UNIV., SAN DIEGO.

Stability of emission line clouds in active galactic nuclei N91-11659

CALIFORNIA UNIV., SANTA CRUZ.

Observations and interpretation of the infrared emission from supernova SN1987A N91-11611

Numerical calculations of the formation and evolution of giant planets with rotation N91-11643

CANADIAN FORCES BASE COLD LAKE, MEDLEY (ALBERTA).

A Canadian female CF-18 pilot's experience N91-11360

CENTER FOR MATHEMATICS AND COMPUTER SCIENCE, AMSTERDAM (NETHERLANDS).

Damped, direction-dependent multigrid for hypersonic flow computations
[CWI-NM-R8922] N91-10905

System identification of lossless layered media from input-output data
[CWI-BS-R8929] N91-11166

Stabilization of a time integrator for the 3D shallow water equations by smoothing techniques
[CWI-NM-R8916] N91-11167

Minimizing maximum earliness and maximum lateness on a single machine
[CWI-BS-R9001] N91-11398

NUMVEC FORTRAN library manual. Chapter: Partial differential equations. Routine: OEHPC
[CWI-NM-R8915] N91-11399

Performance analysis of transaction driven computer systems via queueing analysis of polling models
[CWI-BS-R8931] N91-11426

A-stable parallel block methods
[CWI-NM-R8918] N91-11427

Iterated Runge-Kutta methods on parallel computers
[CWI-NM-R9001] N91-11428

Approximation of the solution to the moment problem in a Hilbert space
[CWI-AM-R8923] N91-11438

Mathematical morphology on homogeneous spaces. Part 1: The simply transitive case
[CWI-AM-R8924-PT-1] N91-11439

Uniform asymptotic approximation of Fermi-Dirac integrals
[CWI-AM-R9001] N91-11440

Dynamic MRI reconstruction as a moment problem. Part 3: An error analysis of reconstruction by sinc and spline interpolation in a Hilbert space setting
[CWI-AM-R9002-PT-3] N91-11441

Grey-level morphology
[CWI-AM-R9003] N91-11442

On the uniqueness of kernels
[CWI-BS-R8924] N91-11443

Cones of matrices and setfunctions, and 0-1 optimization
[CWI-BS-R8925] N91-11444

On SLLN for martingales with deterministic quadratic variation
[CWI-BS-R8933] N91-11445

Minimality of descriptor representations under external equivalence
[CWI-BS-R9002] N91-11446

A new lower bound for the de Bruijn-Newman constant
[CWI-NM-R8920] N91-11447

Improved techniques for lower bounds for odd perfect numbers
[CWI-NM-R8921] N91-11448

A static-regridding method for two-dimensional parabolic partial differential equations
[CWI-NM-R8923] N91-11449

Convergence of linear multistep and one-leg methods for stiff nonlinear initial value problems
[CWI-NM-R8924] N91-11450

The linearly implicit Euler method for quasi-linear parabolic differential equations
[CWI-NM-R9002] N91-11451

Stochastic approximation of the MLE for a spatial point pattern
[CWI-BS-R8926] N91-11475

Optimal choice of sample fraction in extreme-value estimation
[CWI-BS-R8927] N91-11476

On density estimation in the view of Kolmogorov's ideas in approximation theory
[CWI-BS-R8928] N91-11477

Interconnected networks of queues with randomized arrival and departure blocking
[CWI-BS-R8934] N91-11483

Non-linear multigrid in 2-D semiconductor device simulation: The zero current case
[CWI-NM-R8917] N91-11553

A multigrid approach for the solution of the 2D semiconductor equations
[CWI-NM-R9003] N91-11554

CENTRAL RESEARCH INST. OF ELECTRIC POWER INDUSTRY, TOKYO (JAPAN).

Technical assessment and economic study of compressed air energy storage in Japan
[DE91-701405] N91-11292

CENTRE D'ETUDES ET DE RECHERCHES, TOULOUSE (FRANCE).

Four dimensional navigation in air traffic with 4-D navigation aircraft N91-10991

CENTRE NATIONAL D'ETUDES SPATIALES, TOULOUSE (FRANCE).

Aperture diffraction in Rayleigh zone: Calculation of the field in the quiet zone of compact ranges
[CNES-CT/DRT/TIT/AN-88/234] N91-11136

Wind lidar for tropical climatology
[CNES-CT/DRT/TIT/IO-88/126] N91-11334

Fourteen x fourteen CCD array for optical intersatellite link tracking
[CNES-CT/DRT/TIT/OE-88/144] N91-11521

CENTRO DE INSTRUCCION DE MEDICINA AEROESPATIAL, MADRID (SPAIN).

Evaluation of female and male aircrew applicants using a cognitive and psychomotor test N91-11366

CHINA NUCLEAR INFORMATION CENTRE, BEIJING.

Investigation on the projection by a Z-pinch discharge
[DE90-637548] N91-11544

CINCINNATI UNIV., OH.

Controller methodologies for integrated control/structure design optimization of large flexible structures N91-11043

A global pressure relaxation for high speed laminar and turbulent flows N91-11177

CLARKSON UNIV., POTSDAM, NY.

Experimental and theoretical studies of friction and heat transfer in rough passages
[DE90-016302] N91-11223

CLEMSON UNIV., SC.
Alternate equilibrium configurations of flexible cantilever beams N91-11254
COLOGNE UNIV. (GERMANY, F.R.).
Elastic properties of ceramic composite materials at high temperatures
[ETN-90-97897] N91-11067
The control system of an airborne radiometer: A process for a two dimensional reconstruction of irregular scanned radiometer data
[MITT-70] N91-11202
Energetics of 60 days predictions with the EZMW-T21 model in its mean temporary development and its relationship to forecast skill
[MITT-71] N91-11335
A two dimensional multisonic model of plasma interaction for cometary atmosphere with solar wind
[MITT-69] N91-11621
COLORADO STATE UNIV., FORT COLLINS.
Colorado State University program for developing, testing, evaluating and optimizing solar heating and cooling systems
[DE90-017273] N91-11291
The evolution of vortical patterns and vortices in mesoscale convective complexes N91-11319
COLORADO UNIV., BOULDER.
Computation of transonic flow over elastic rotor blade N91-10906
Experimental investigation of the mechanisms underlying vortex kinematics in unsteady separated flows N91-10907
Application of computational fluid dynamics to three-dimensional bodies in hypersonic flow N91-11174
Comparison of clear air atmospheric radar techniques for the study of atmospheric dynamics in the troposphere and the stratosphere
[PB90-256314] N91-11313
A numerical model of polar mesospheric cloud formation and evolution N91-11337
COLUMBIA UNIV., NEW YORK, NY.
Boundary integral equations for dynamic fracture problems N91-11259
Satellite elevation magnetic anomalies and their use in tectonic studies N91-11272
Aspects of the earthquake geology and seismotectonics of the southern San Andreas and related faults N91-11329
Online searching in public libraries: A comparative study of performance N91-11598
CONSIGLIO NAZIONALE DELLE RICERCHE, FRASCATI (ITALY).
Data analysis of hollow cathode experiment to support electrodynamic tether applications
[IFSI-89-16] N91-11047
Instrumenting a room temperature gravitational radiation antenna for sub-Kelvin temperatures
[IFSI-90-20] N91-11143
The rotation of Lageos
[IFSI-90-10] N91-11333
Generalized back-action evasion schemes for the detection of weak classical forces
[IFSI-90-19] N91-11508
Ion dynamics in the plasma mantle
[IFSI-89-20] N91-11550
The SIM.PL.EX. plasma chamber (Simulatori di Plasma Extraterrestre)
[IFSI-90-8] N91-11551
CONSIGLIO NAZIONALE DELLE RICERCHE, ROME (ITALY).
Optimization models and techniques to improve air traffic management N91-10988
Plots of the 5-minute neutron monitor intensity and multiplicities recorded by the Rome 17-NM64, January 1990
[IFSI-90-5] N91-11653
Plots of the 5-minute neutron monitor intensity and multiplicities recorded by the Rome 17-NM64, February 1990
[IFSI-90-6] N91-11654
CORNELL UNIV., ITHACA, NY.
Thermal stress-induced grain boundary cavitation in narrow, aluminum alloy metallizations N91-11093
Surface phases and their influence on metal-oxide interfaces
[DE90-017608] N91-11099

D

DARTMOUTH COLL., HANOVER, NH.
Planar orotron: A tunable, grating-based free electron laser N91-11208
DAYTON UNIV., OH.
Minimization and control of hazardous combustion byproducts
[PB90-259854] N91-11305
DEFENCE AND CIVIL INST. OF ENVIRONMENTAL MEDICINE, NORTH YORK (ONTARIO).
Female aircrew: The Canadian forces experience N91-11367
Aircrew/cockpit compatibility: A multivariate problem seeking a multivariate solution N91-11369
Anthropometric accommodation of females in Canadian forces aircraft crew stations N91-11371
DEFENSE LOGISTICS AGENCY, ALEXANDRIA, VA.
Defense logistics agency Information Resources Management (IRM) near-term planning document FY 1990-1992
[PB90-238494] N91-11596
DELFT HYDRAULICS LAB., DEVOORST (NETHERLANDS).
Wave data assimilation in a 3rd generation. Wave prediction model for the North Sea: An optimal control approach
[BCRS-89-22] N91-11348
DEPARTMENT OF ENERGY, WASHINGTON, DC.
Composite slip table of dissimilar materials for damping longitudinal modes
[DE90-015128] N91-11064
Assessment of costs and benefits of flexible and alternative fuel use in the US transportation sector: Vehicle and fuel distribution requirements
[DE90-014847] N91-11127
Report of the Department of Energy (DOE) Office of Energy research review committee on the site-specific conceptual design of the superconducting super collider
[DE90-018021] N91-11513
Implications of the Biological Effects of Ionizing Radiation (BEIR) 5 report to the Department of Energy
[DE90-016673] N91-11526
DEUTSCHE AIRBUS G.M.B.H., BREMEN (GERMANY, F.R.).
A quarter of a century of aeroelastic cooperation between research and industry (a review). Part 2: Transport airplanes and other civil applications N91-10932
DEUTSCHE BUNDESPOST, DARMSTADT (GERMANY, F.R.).
Optical far-field measurements of extremely high dynamic to investigate the roughness of front faces of single-mode fiber connectors
[FI-452-TB-67] N91-11517
DEUTSCHE FORSCHUNGSANSTALT FUER LUFT- UND RAUMFAHRT, COLOGNE (GERMANY, F.R.).
Crack behaviour of 2024-T3, 2090-T8E41 and 7075-T6 under constant amplitude and different types of variable amplitude loading, especially Gaussian loading N91-11244
DEUTSCHE FORSCHUNGSANSTALT FUER LUFT- UND RAUMFAHRT, GOETTINGEN (GERMANY, F.R.).
Contributions in the field of aeroelastics on the occasion of the 60th anniversary of Professor Dr.-Ing. Habil. Hans Wilhelm Foersching
[ETN-90-97630] N91-10920
The calculation of unsteady compressible flow about oscillating airfoil profiles using the Euler upwind method N91-10921
Structural dynamics qualification of spacecraft N91-10922
Aeroelastics and dynamics of wind turbines N91-10923
Structural analysis and optimization of a propfan-blade by use of the finite element method N91-10924
Design of the derivative balance for the transonic wind tunnel N91-10925
Calculation of the pressure distribution on an oscillating airfoil in incompressible flow considering nonlinear effects N91-10926
Determination of unsteady aerodynamic forces on engines with a view to flutter investigations N91-10927
Unsteady wind tunnel wall interferences in subsonic and transonic profile flows N91-10928
Adaptive digital real time filtering in structural dynamics: A contribution to the realization on Actively Reacting Elastic Structures (ARES) N91-10929
A quarter of a century of aeroelastic cooperation between research and industry (a review). Part 1: Fighter airplanes and helicopters N91-10931
DEUTSCHE FORSCHUNGSANSTALT FUER LUFT- UND RAUMFAHRT, HAMBURG (GERMANY, F.R.).
Sex differences concerning performance and personality traits of applicants for highly qualified operator functions in aviation N91-11364
DOUGLAS AIRCRAFT CO., INC., LONG BEACH, CA.
Douglas flight deck design philosophy N91-10939
DREXEL UNIV., PHILADELPHIA, PA.
A stochastic analysis of state transitions in an air space management system N91-10980
Heat transfer and flow studies in an abrupt expansion pipe with non-Newtonian fluids N91-11180
DUKE UNIV., DURHAM, NC.
Aircraft interior noise reduction by alternate resonance tuning
[NASA-CR-1[illegible]9] N91-11488
DURHAM UNIV. (ENGLAND).
Very high energy gamma rays from isolated pulsars and non-pulsating objects N91-11655

E

ECOLE CENTRALE DE LYON (FRANCE).
Theoretical and numerical aspects of wave stability in combustion models
[ECL-89-21] N91-11088
Study of the wear behavior induced by fretting in aluminum and titanium alloys
[ECL-90-01] N91-11229
EDGERTON, GERMESHAUSEN AND GRIER, INC., ALBUQUERQUE, NM.
Railgun performance with a two-stage light-gas gun injector
[DE90-016211] N91-11032
EDGERTON, GERMESHAUSEN AND GRIER, INC., IDAHO FALLS, ID.
A microprocessor based charge control system for the simultaneous charging of several batteries with one charge controller
[DE90-017089] N91-11157
EG AND G ROCKY FLATS, INC., GOLDEN, CO.
Penetration in GTA welding
[DE90-008971] N91-11213
ENERGETICS, INC., COLUMBIA, MD.
Evaluation of a high-temperature burner-duct-recuperator system
[DE90-000366] N91-11284
ENVIRONMENTAL PROTECTION AGENCY, WASHINGTON, DC.
Technology transfer: Hotlines
[PB90-237140] N91-11594
Guide to EPA libraries and information services
[PB90-237108] N91-11595
ENVIRONMENTAL RESEARCH INST. OF MICHIGAN, ANN ARBOR.
On three dimensional object recognition and pose-determination: An abstraction based approach
[NASA-CR-186894] N91-11396
EUROCONSULT B.V., ARNHEM (NETHERLANDS).
Forest classification with high resolution satellite images. Research into the use of spatial information to improve the multi-spectral classification with SPOT images
[BCRS-89-32] N91-11269
EUROPEAN ATOMIC ENERGY COMMUNITY, MADRID (SPAIN).
Fluctuations and stability in the Advanced Toroidal Facility (ATF) torsatron
[DE90-017734] N91-11536
EUROPEAN ORGANIZATION FOR THE SAFETY OF AIR NAVIGATION, BRUSSELLS (BELGIUM).
Optimum on-line handling of air traffic over Western Europe N91-10982
The EUROCONTROL future ATS system concept and the programme of studies, tests, and trials N91-10983
Generation of aircraft trajectories for on-line operation: Methods, techniques, and tools N91-10987
The high-resolution graphic display: A possible man/machine interface for a computer assisted ATC management system N91-10989
The 4-D control of current air carriers in the present environment: Objectives, status, and plans N91-10990
The control of inbound flights N91-10992
Air traffic management and aircraft guidance in a zone of convergence N91-10998
Ground-based 4-D guidance of flights in strong wind N91-10999
The air traffic controller facing automation: Conflict or cooperation N91-11001
Aircraft trajectory reconstitution on the basis of multi-radar plot information N91-11002
Developments to enhance meteorological forecasting for air traffic services N91-11006
Integration of aircraft capability in air traffic handling simulations N91-11007
EUROPEAN SPACE AGENCY, PARIS (FRANCE).
Contributions to the improvement of flight safety in wind shear
[ESA-TT-1141] N91-10965
Parallelization on a multi-processor system of a solving method for the unsteady Navier-Stokes equations at high Reynolds numbers
[ESA-TT-1116] N91-11197
Large eddy-simulation of convective boundary layers
[ESA-TT-1138] N91-11198

Numerical simulation of transition from laminar to turbulent duct flow
[ESA-TT-1144] N91-11199
Determinants of dual-task interference and resource theories in cognitive psychology
[ESA-TT-1127] N91-11381
Solution of the two-dimensional Euler equations by a finite volume discretization on unstructured triangular meshes
[ESA-TT-1135] N91-11473

F

FAIRCHILD TECHNICAL SUPPORT CENTER, HUNTSVILLE, AL.
Automated Fluid Interface System (AFIS)
[NASA-CR-183969] N91-11031
FEDERAL AVIATION ADMINISTRATION, ATLANTIC CITY, NJ.
Generation of a buoyant plume of artificial smoke for airplane tests
[DOT/FAA/CT-90/9] N91-11015
FEDERAL AVIATION ADMINISTRATION, WASHINGTON, DC.
National plan to enhance aviation safety through human factors improvements N91-10940
FEDERAL INFORMATION EXCHANGE, INC., GERMANTOWN, MD.
Design, develop, test, and implement an on-line research and education information service
[DE90-017654] N91-11604
FEDERAL RAILROAD ADMINISTRATION, WASHINGTON, DC.
Industry perspective on Maglev
[PB90-252305] N91-11132
FERMI NATIONAL ACCELERATOR LAB., BATAVIA, IL.
An investigation of thermally driven acoustical oscillations in helium systems
[DE90-018049] N91-11086
Numerical modeling of time domain 3-D problems in accelerator physics
[DE90-015625] N91-11511
FLIGHT MECHANICS AND CONTROL, INC., HAMPTON, VA.
Final shuttle-derived atmospheric database: Development and results from thirty-two flights
[NASA-CR-185636] N91-11310
FLORIDA ATLANTIC UNIV., BOCA RATON.
Effects of an internal flow on the vibration of thin cylindrical shells N91-11258
FLORIDA STATE UNIV., TALLAHASSEE.
Generalized dynamic normal mode initialization N91-11341
CAD tools for detector design
[DE90-017337] N91-11412
Task A: High energy physics program experiment and theory. Task B: High energy physics program numerical simulation
[DE90-017336] N91-11512
FLORIDA UNIV., GAINESVILLE.
Boundary element methods in structural shape synthesis N91-11406
Long-term observations of three massive x ray binary transients: 4U0115+63, V0332+53, and GX301-2 N91-11612
Observations of pulsars at low radio frequencies N91-11614
FORD AEROSPACE CORP., PALO ALTO, CA.
Advanced technology satellite demodulator development
[NASA-CR-185127] N91-11134

G

GEO-CENTERS, INC., LAKE HOPATCONG, NJ.
Stability of liquid propellants under long-term storage
[AD-A223934] N91-11126
GEORGE WASHINGTON UNIV., WASHINGTON, DC.
Ejector thrust augmentors: Pulse-starting approach to the second solution N91-10913
GEORGIA INST. OF TECH., ATLANTA.
Heat transfer in variable density, low Mach number, stagnating turbulent flows N91-11171
Dynamic analysis and control of lightweight manipulators with flexible parallel link mechanisms
[NASA-CR-187347] N91-11216
Alternating method applied to 3-D part-through crack problems, with application to the weight function method N91-11238
A simple zonal average energy budget model of the earth-atmosphere system N91-11316
Operator function modeling: Cognitive task analysis, modeling and intelligent aiding in supervisory control systems
[NASA-CR-187331] N91-11380
Fluctuations and stability in the Advanced Toroidal Facility (ATF) torsatron
[DE90-017734] N91-11536
The delta-Sobolev approach for modeling solar spectral irradiance and radiance N91-11650
GEORGIA STATE UNIV., ATLANTA.
M51: The Whirlpool Galaxy, analysis and simulation N91-11631
Numerical simulations of suspersonic extragalactic radio jets N91-11660
GLASGOW UNIV. (SCOTLAND).
Integrated optical components for optical fibre sensors N91-11519
GRENOBLE UNIV. (FRANCE).
Mathematical models of mixture properties: B-splines and optimization with form conditions
[ETN-90-97829] N91-11462
GRONINGEN RIJKSUNIV. (NETHERLANDS).
A synthesis of time and frequency domain methods for the control of infinite-dimensional systems: A system theoretic approach
[W-8912] N91-11456
The relation between knowledge and heuristic methods
[W-9001] N91-11457
Asymptotic behavior of Laguerre polynomials with Re z less than 0 derived by the central limit theorem
[W-9004] N91-11458
Quasi-periodic bifurcations, applications
[TW-8911] N91-11459
On induced congruences
[CS-9001] N91-11460
High-order implicit blending surfaces of low degree
[CS-9005] N91-11461

H

HARVARD SCHOOL OF PUBLIC HEALTH, BOSTON, MA.
Nitrogen dioxide and respiratory infection: Pilot investigations
[PB90-247339] N91-11357
HARVARD UNIV., CAMBRIDGE, MA.
Crack-growth resistance in reinforced ceramic composites N91-11261
Speckle imaging of complicated objects N91-11617
HELSINKI UNIV. OF TECHNOLOGY, ESPOO (FINLAND).
Advanced secondary batteries: Their applications, technological status, market and opportunity
[DE90-796146] N91-11146
HIROSAKI UNIV. (JAPAN).
The role of shear in the cosmological distance
[DE90-513788] N91-11636
HIROSHIMA UNIV., TAKEHARA (JAPAN).
Gravitational field of static and thick domain walls
[DE90-513706] N91-11331
On a simple evaluation of anomalies from the path integral measure
[DE90-513707] N91-11484
Application of the Ewald method to cosmological N-body simulations
[DE90-513789] N91-11637
Cosmological N-body simulations with a treecode
[DE90-513790] N91-11638
Microwave background anisotropies and the primordial spectrum of cosmological density fluctuations
[DE90-513791] N91-11639
HONEYWELL, INC., MINNEAPOLIS, MN.
Cockpit avionics integration and automation N91-10938

I

IDAHO NATIONAL ENGINEERING LAB., IDAHO FALLS.
Three-dimensional fluid flow in JFTOT (Jet Fuel Thermal Oxidation Tester)
[DE90-010929] N91-11128
IDAHO NUCLEAR CORP., IDAHO FALLS.
Residual stress at fluid interfaces
[DE90-012964] N91-11189
ILLINOIS UNIV., CHAMPAIGN.
The structure and stability of three dimensional detonation waves
[AD-A224465] N91-11164
ILLINOIS UNIV., CHICAGO.
Micromechanics of semi-brittle ceramics N91-11119
Instantaneous kinematics, motion planning and mechanical efficiency of a quadrupedal walking machine N91-11218
Dynamic model error analysis of robot manipulators N91-11220
ILLINOIS UNIV., URBANA.
CTR plasma engineering studies
[DE90-017774] N91-11534
ILLINOIS UNIV., URBANA-CHAMPAIGN.
Deformation mechanisms in rapidly solidified aluminum alloys N91-11096
ILLINOIS UNIV. AT URBANA-CHAMPAIGN, SAVOY.
Numerical calculations for flows past an unconventional airfoil N91-10916
Fluctuating concentrations in atmospheric dispersion N91-11323
Basic dynamics of low frequency variability and the storm tracks N91-11339
The transfer of polarized radiation in astrophysical masers in the presence of magnetic fields N91-11629
INDIANA UNIV., BLOOMINGTON.
Violet and visual flux problems in red giant stars N91-11632
INSTITUT NATIONAL DES SCIENCES APPLIQUEES DE LYON, VILLEURBANNE (FRANCE).
Relations between microstructure and mechanical behaviour of SiC/SiC composites: Interface effects on multiple cracking in multifilament materials
[ISAL-89-0098] N91-11065
INSTITUT NATIONAL POLYTECHNIQUE, GRENOBLE (FRANCE).
Application of self-testing integrated circuits to the safety of systems operation
[ETN-90-97828] N91-11150
Silicon compilation and the SYCO silicon compiler
[ETN-90-97827] N91-11404
INSTITUTE FOR COMPUTER APPLICATIONS IN SCIENCE AND ENGINEERING, HAMPTON, VA.
Inflated speedups in parallel simulations via malloc()
[NASA-CR-182104] N91-11397
Parallelized reliability estimation of reconfigurable computer networks
[NASA-CR-182101] N91-11430
INSTITUTE OF AVIATION MEDICINE, OSLO (NORWAY).
Psychological and sociological aspects of the entrance of female aircrew to the Norwegian airforce N91-11365
Pregnancy: A cause for grounding of female air crew N91-11376
INSTITUTO DE PESQUISAS ESPACIAIS, SAO JOSE DOS CAMPOS (BRAZIL).
Functional description and analysis of processor performance for data collection
[INPE-5037-RPE/620] N91-11048
Sampling and interpolations in digital terrain models
[INPE-5041-TDL/404] N91-11275
Methodology of remote sensing for monitoring modifications in the fluvial channel and updating nautical charts
[INPE-4863-TDL/374] N91-11277
Integration of multispectral and pancromatic channels of HRV (SPOT) sensor for obtaining color compositions with a spatial resolution of approximately 10 m
[INPE-5035-TDL/403] N91-11278
Identification of areas subject to flooding through TM/LANDSAT images in the basin of the rivers Pindare, Mearim, Jaguaribe, Apodi, Piranhas, and San Francisco
[INPE-5034-RPE/619] N91-11279
Spectral lithostratigraphic correlation of boreholes
[INPE-5022-TDL/402] N91-11332
Numerical experiments with climatic zonally-averaged models
[INPE-5083-TDL/417] N91-11343
Fundamental concepts for utilization of the FPS-5410 array processor
[INPE-5091-RPE/624] N91-11388
Beta splines interpolation for DEM's
[INPE-5039-PRE/1572] N91-11415
Reception and display of WEFAX images: 4 bits with micro line IBM-PC, users manual
[INPE-5086-NTE/294] N91-11417
A tool for help in software reutilization
[INPE-5077-TDL/341] N91-11418
Combination of Hatley and Ward/Mellor methods for real time systems
[INPE-5078-TDL/412] N91-11419
Classification of textures using the ARMA models and distances over the autocorrelation function
[INPE-5067-TDL/406] N91-11421
Performance comparison of edge defection morphologies
[INPE-5012-TDL/400] N91-11422
Geometric correction of SPOT imagery with the use of a digital elevation model
[INPE-5014-TDL/401] N91-11423
Multiple Application Intense Particle Beam Project
[INPE-4576-RPE/568] N91-11510
Exploration of decreased solar activity state (small intensity activity) in the corona and chromosphere
[INPE-5059-TDL/405] N91-11652

INTEL CORP., BEAVERTON, OR.
Touchstone project: Milestone event Q4
[AD-A224034] N91-11480
Touchstone project Mach port: Milestone event Q4
[AD-A224057] N91-11481
Touchstone project DELTA numeric node: Milestone event Q4
[AD-A224060] N91-11482

INTERNATIONAL ATOMIC ENERGY AGENCY, VIENNA (AUSTRIA).
Fluctuations and stability in the Advanced Toroidal Facility (ATF) torsatron
[DE90-017734] N91-11536

INTERNATIONAL BANK FOR RECONSTRUCTION AND DEVELOPMENT, WASHINGTON, DC.
Satellite remote sensing for agricultural projects
[PB90-257916] N91-11270

INTERNATIONAL FUEL CELLS CORP., SOUTH WINDSOR, CT.
Molten carbonate fuel cell power plant systems studies
[DE90-009697] N91-11298

IOWA STATE UNIV. OF SCIENCE AND TECHNOLOGY, AMES.
Transient infrared emission spectroscopy
[DE90-017253] N91-11083
Microfilamentary Bi2Sr2Ca1Cu2O8 fibers
[DE90-018013] N91-11571

IOWA UNIV., IOWA CITY.
A search for small comets in consecutive images acquired with a ground-based telescope N91-11626
Whistlers in Neptune's magnetosphere: Evidence of atmospheric lightning
[NASA-CR-187324] N91-11642

J

JAPAN ATOMIC ENERGY RESEARCH INST., TOKYO.
Effects of environment and aging on creep properties of Alloy 800H
[DE90-520207] N91-11106
Study on radiation-induced deterioration of grease at high temperature. Part 1: Test method on thermal aging
[DE90-508070] N91-11120
A method of using the inverse matrix for manipulator kinematics
[DE90-520210] N91-11227
The transverse stress effect on the critical current of jelly-roll multifilamentary Nb3Al wires
[DE90-513710] N91-11581

JOHNS HOPKINS UNIV., BALTIMORE, MD.
The calculation of correlation functions in the statistical theory of turbulent flows N91-11176
Population studies in groups and clusters of galaxies, volumes 1 and 2 N91-11608

JOINT INST. FOR NUCLEAR RESEARCH, DUBNA (USSR).
Microprocessor system for temperature regulation and stabilization
[DE90-634244] N91-11160
Asymptotic estimates of approximation errors by the Galerkin method for one class of quasipotential equations
[DE90-631600] N91-11471
Searching spectrum points of difference initial-boundary value problems with using CAS
[DE90-634382] N91-11472
An inverse problem for classical relativistic mechanics
[DE90-631599] N91-11589

JOINT PUBLICATIONS RESEARCH SERVICE, ARLINGTON, VA.
JPRS report: Science and technology. USSR: Life sciences
[JPRS-ULS-89-003] N91-11354
Enhancement of human tolerance of acute hypoxia by adaptation and intense training at high altitudes N91-11355

K

KANSAS UNIV., LAWRENCE.
Calculation of aerodynamic characteristics of airplane configurations at high angle of attack in steady and unsteady flow N91-11009
Solutions of thin-layer Navier-Stokes equations for missile configurations N91-11173

KARLSRUHE UNIV. (GERMANY, F.R.).
Examination of numerical formulations to describe complex geometry turbulent elliptical flows, using contour matched coordinates
[ETN-90-97864] N91-11169

L

LABORATOIRE D'AUTOMATIQUE ET D'ANALYSE DES SYSTEMES, TOULOUSE (FRANCE).
Geometric method and synthesis af assembly strategies in robotic systems
[LAAS-90041] N91-11215

LABORATOIRE DE MEDECINE AEROSPATIALE, BRETIGNY-SUR-ORGE (FRANCE).
Problems posed by the adaptation of physiological protective equipment for female combat pilots N91-11372
Morphological and functional adaptation of personal equipment designed for female personnel N91-11374

LABORATORIO NACIONAL DE ENGENHARIA E TECNOLOGIA INDUSTRIAL, LISBON (PORTUGAL).
Short crack behaviour in Al-Li alloy 2090 N91-11243

LAMONT-DOHERTY GEOLOGICAL OBSERVATORY, PALISADES, NY.
NCEER strong-motion data base: A user manual for the geobase release (version 1.0 for the SUN3)
[PB90-258062] N91-11315

LAWRENCE LIVERMORE NATIONAL LAB., CA.
Railgun performance with a two-stage light-gas gun injector
[DE90-016211] N91-11032
Multiple-energy techniques in industrial computerized tomography
[DE90-017518] N91-11081
Aluminum metal combustion in water revealed by high speed microphotography
[DE90-017525] N91-11082
High-resolution electron microscopy observations of athermal omega phase in Ti-Mo alloys
[DE90-017526] N91-11098
Compact representation of radiation patterns using spherical mode expansions
[DE91-000019] N91-11141
A hybrid pulse forming technique
[DE90-016860] N91-11156
TOPAZ2D heat transfer code users manual and thermal property data base
[DE91-000075] N91-11195
The measurement and finite element analysis of the dynamic stiffness of non-uniform clearance, gas, thrust bearings
[DE90-015120] N91-11214
A molecular dynamics model of the orthogonal cutting process
[DE90-015911] N91-11230
A continuum tensile failure model with friction
[DE90-018006] N91-11265
Chlorine dioxide and hemodialysis
[DE90-015912] N91-11382
IGES efficiency evaluation
[DE90-015192] N91-11409
SISAL versus FORTRAN: A comparison using the Livermore loops
[DE90-010872] N91-11414
Atomic physics of highly charged ions in an electron beam ion trap
[DE90-017528] N91-11499
MONT3E: A Monte Carlo electron heat transfer code
[DE90-012091] N91-11514
Design and operation of the electron beam ion trap
[DE91-000074] N91-11515
ECH by FEL and gyrotron sources on the Microwave Tokamak Experiment (MTX) tokamak
[DE91-000286] N91-11547
A new site for the astrophysical gamma-process
[DE90-017519] N91-11635

LITTLE (ARTHUR D.), INC., CAMBRIDGE, MA.
Industry perspective on Maglev
[PB90-252305] N91-11132

LOCKHEED ENGINEERING AND SCIENCES CO., HOUSTON, TX.
Computational fluid dynamics analysis of space shuttle main propulsion feed line 17-inch disconnect valves N91-10876
Aerodynamic stability and heating analyses for the aeroassist flight experiment vehicle N91-10899

LOS ALAMOS NATIONAL LAB., NM.
An apparatus for studies of hydrogen isotope exchange over metals using laser-Raman spectroscopy
[DE90-018038] N91-11085
The reaction of vapor-deposited Al with Cu oxides
[DE91-000367] N91-11114
Microwave sintering of nanocrystalline TiO2
[DE91-000375] N91-11115
Increasing output power of an 850 MHz tetrode with a floating-deck modulator
[DE91-000433] N91-11162
Numerical models of 2-D and 3-D geophysical convection
[DE90-014979] N91-11330
Oscillation onset in neural delayed feedback
[DE90-015057] N91-11351
Random number stride in Monte Carlo calculations
[DE90-012000] N91-11465
A Monte Carlo boundary propagation method for the solution of Poisson's equation
[DE90-015060] N91-11466
Accurate representations of general textures by a set of weighted grains
[DE90-016487] N91-11485
Secondary-electron yield measurements from metals impacted by high-velocity ions, electrons, and molecules
[DE90-018023] N91-11502
Production of uniform and well-confined beams by nonlinear optics
[DE91-000210] N91-11522
Complete fluid equations for low-n singular modes in axisymmetric torodial plasmas
[DE91-000176] N91-11545
Concepts in strong Langmuir turbulence theory
[DE91-000208] N91-11546
Antimatter gravity experiment
[DE91-000177] N91-11590
International English
[DE90-016719] N91-11601
Late stages in the evolution of classical novae
[NASA-TM-102969] N91-11633
Discussion paper on environmental hazards on the Moon, in low Earth orbit, and in low Mars orbit
[DE90-017854] N91-11646

LOUISIANA STATE UNIV., BATON ROUGE.
Fine scale velocity measurements in a turbulent jet in a confined crossflow N91-10909
Color flux distribution in pure SU(2) Lattice Gauge Theory
[DE90-017403] N91-11574
Polarized radiation from inhomogeneous shocks N91-11662

M

MAINE UNIV., ORONO.
Gulf of Maine sea surface topography from GEOSAT altimetry N91-11271

MARTIN MARIETTA CORP., BETHESDA, MD.
Hybrid Propulsion Technology Program, phase 1. Volume 1: Executive summary
[NASA-CR-183950] N91-11054
Hybrid Propulsion Technology Program, phase 1. Volume 2: Technical discussion
[NASA-CR-183951] N91-11055

MARTIN MARIETTA CORP., DENVER, CO.
Intelligent Robotic Systems Study (IRSS), phase 2
[NASA-CR-183963] N91-11432

MARYLAND UNIV., COLLEGE PARK.
Coupled rotor/airframe vibration analysis N91-11012
Analysis of ductile crack extension in plastic fracture N91-11257
A three-dimensional solid element model for finite rotation of composite shells N91-11262

MASSACHUSETTS INST. OF TECH., CAMBRIDGE.
Expert systems for the generation of thermal area arrival paths for civil transport N91-10995
Large-scale dynamics and transport in the stratosphere
[NASA-CR-187327] N91-11311

MASSACHUSETTS UNIV., AMHERST.
Development of a validation model for the defense meteorological satellite program's special sensor microwave imager
[NASA-CR-187369] N91-11342
Recent starbirth and starburst activity in nearby galaxies N91-11627

MAX-PLANCK-INST. FUER PHYSIK UND ASTROPHYSIK, GARCHING (GERMANY, F.R.).
Activities report of the Institute for Extraterrestrial Physics
[MPE-217] N91-11620

MAX-PLANCK-INST. FUER STROEMUNGSFORSCHUNG, GOETTINGEN (GERMANY, F.R.).
Theory of homogeneous nucleation from the vapor phase
[MPIS-MITT-93] N91-11077
The generalized diffusion theory of simply deformable particle-fluid two-phase flows
[MPIS-7/1990] N91-11193
A model for the sound generation due to compressible vortex-body interaction
[MPIS-MITT-96] N91-11491
Complete adiabatic evaporation of highly superheated liquid jets
[MPIS-MITT-95] N91-11588

MCAT INST., SAN JOSE, CA.
Development of a time-dependent incompressible Navier-Stokes solver based on a fractional-step method [NASA-CR-187254] N91-11165
MESSERSCHMITT-BOELKOW-BLOHM/ENTWICKLUNG SPRING NORD, BREMEN (GERMANY, F.R.).
Non-linear vibration of large, imperfect space structures N91-10930
MESSERSCHMITT-BOELKOW-BLOHM G.M.B.H., MUNICH (GERMANY, F.R.).
Calculation of viscous hypersonic flows using a coupled Euler/2nd order boundary layer method [MBB/FE122/S/PUB/387] N91-10935
Marginal aircraft release disturbance on advanced missiles [MBB/FE121/S/PUB/329] N91-11016
Review of active structural control systems and flight test techniques for dynamic stability investigations [MBB/FYT256/S/PUB/361/A] N91-11025
Ultrasonic examination of fiber composite materials by means of virtual C-scan test and model recognition [MBB-Z-0299-89-PUB] N91-11066
Biosensors: Development status [MBB-Z-0305-90-PUB] N91-11201
Requirements of an HMS/D for a night-flying helicopter [MBB-UD-0570-90-PUB] N91-11383
Use of the VP-200 computer for aerothermodynamic problems [MBB/FE122/S/PUB/388] N91-11424
METAL AIR TECHNOLOGY SYSTEMS INTERNATIONAL, INC., LAWRENCEVILLE, GA.
Zinc air battery development for electric vehicles [DE90-016639] N91-11149
MIAMI UNIV., CORAL GABLES, FL.
Human factors of the high technology cockpit N91-10943
MICHIGAN UNIV., ANN ARBOR.
A viscous-inviscid interactive method for unsteady flows N91-11172
Injector and valve train friction studies: Cummins L-10 engine [DE90-017288] N91-11225
Contact and impact problems using adaptive finite element methods N91-11239
Estimation of seasonal and annual acidic deposition through aggregation of three-day episodic periods [PB90-252628] N91-11303
MIDDLE EAST TECHNICAL UNIV., ANKARA (TURKEY).
Growth of short fatigue cracks in 7075-T6 aluminum alloy N91-11249
MIDWEST RESEARCH INST., GOLDEN, CO.
High efficiency CuInSe2 and CuInGaSe2 cells and materials research [DE90-000362] N91-11280
Conceptual design of an Open-Cycle Ocean Thermal Energy Conversion Net Power-Producing Experiment (OC-OTEC NPPE) [DE90-000304] N91-11282
Assessment of municipal solid waste for energy production in the Western United States [DE90-000361] N91-11283
Evaluation of a high-temperature burner-duct-recuperator system [DE90-000366] N91-11284
Research on high-efficiency, large area amorphous silicon based solar cells [DE90-000356] N91-11285
Performance and cost projections for advanced wind turbines [DE90-000370] N91-11286
Atmospheric performance of the special-purpose Solar Energy Research Institute (SERI) thin-airfoil family: Final results [DE90-000373] N91-11287
Electronic processes in thin film PV materials [DE90-000359] N91-11295
Research on high-efficiency, multiple-gap, multi-junction amorphous silicon-based alloy thin-film solar cells [DE90-000364] N91-11296
Analysis of loss mechanisms in polycrystalline thin film solar cells [DE90-000372] N91-11297
Structure of amorphous-silicon and germanium alloy films [DE90-000355] N91-11557
SERI Workshop on the Role of Point Defects/Defect Complexes in Silicon Device Fabrication [DE90-000377] N91-11572
MINNESOTA UNIV., MINNEAPOLIS.
From red giants to planetary nebulae: Asymmetries, dust, and polarization N91-11622
MISSISSIPPI STATE UNIV., STARKVILLE.
Measurement and calculation of surface roughness effects on turbulent flow and heat transfer N91-11183
MISSISSIPPI UNIV., UNIVERSITY.
Sound field fluctuations due to large scale wind-driven turbulence N91-11492
MISSOURI UNIV., ROLLA.
Collisional processes of interest in MFE plasma research [DE91-000598] N91-11549
MONTANA STATE UNIV., BOZEMAN.
Corrosion and arc erosion in MHD channels [DE90-017889] N91-11539
MORGANTOWN TECHNOLOGY CENTER, WV.
Proceedings of the Second Annual Fuel Cells Contractors Review Meeting [DE90-000490] N91-11288
MORTON THIOKOL, BRIGHAM CITY, UT.
First incremental buy for Increment 2 of the Space Transportation System (STS) [NASA-CR-183855] N91-11034

N

NAGOYA UNIV. (JAPAN).
On hydrodynamics of collisionless relativistic plasma in a strong magnetic field [DE90-513926] N91-11543
NATIONAL ACADEMY OF SCIENCES - NATIONAL RESEARCH COUNCIL, WASHINGTON, DC.
Airport system capacity strategic choices [SR-226] N91-10979
NATIONAL AERONAUTICS AND SPACE ADMINISTRATION, WASHINGTON, DC.
NASA's CFD Validation Program N91-10845
Civil space technology initiative [NASA-TM-103017] N91-11028
NATIONAL AERONAUTICS AND SPACE ADMINISTRATION. AMES RESEARCH CENTER, MOFFETT FIELD, CA.
NASA Computational Fluid Dynamics Conference. Volume 1: Sessions 1-6 [NASA-CP-10038-VOL-1] N91-10839
Computational Fluid Dynamics Program at NASA Ames Research Center N91-10840
Understanding transition and turbulence through direct simulations N91-10846
More accurate predictions with transonic Navier-Stokes methods through improved turbulence modeling N91-10850
Computations of three-dimensional steady and unsteady viscous incompressible flows N91-10852
SAGE: A 2-D self-adaptive grid evolution code and its application in computational fluid dynamics N91-10853
CFD for applications to aircraft aeroelasticity N91-10855
A zonal Navier-Stokes methodology for flow simulation about a complete aircraft N91-10858
Numerical simulation of F-18 fuselage forebody flows at high angles of attack N91-10859
TranAir: Recent advances and applications N91-10862
Numerical simulation of rotorcraft N91-10863
Three-dimensional viscous drag prediction for rotor blades N91-10865
NASA Computational Fluid Dynamics Conference. Volume 2: Sessions 7-12 [NASA-CP-10038-VOL-2] N91-10868
Progress in computing nozzle/plume flow fields N91-10872
Prediction of turbine rotor-stator interaction using Navier-Stokes methods N91-10881
Simulation of powered-lift flows N91-10886
Unstructured mesh solution of the Euler and Navier-Stokes equations N91-10892
Visualization of fluid dynamics at NASA Ames N91-10895
Computational fluid dynamics on a massively parallel computer N91-10896
The computation of thermo-chemical nonequilibrium hypersonic flows N91-10898
The calculation of rotor/fuselage interaction for two-dimensional bodies [NASA-TM-102855] N91-10933
Summary of the industry/NASA/FAA workshop on philosophy of automation: Promises and realities N91-10942
Human-centered automation: Development of a philosophy N91-10944
Crew workload strategies in advanced cockpits N91-10945
Assessing information transfer in full mission flight simulations N91-10946
Technological advances for studying human behavior N91-10947
A function-based approach to cockpit procedure aids N91-10953
Procedural error monitoring and smart checklists N91-10954
ATC automation concepts N91-10957
Time-based operations in an advanced ATC environment N91-10958
Terminal weather information management N91-10960
A piloted simulator evaluation of a ground-based 4-D descent advisor algorithm N91-11000
Performance of a parallel code for the Euler equations on hypercube computers [NASA-TM-102260] N91-11384
NATIONAL AERONAUTICS AND SPACE ADMINISTRATION. EARTH RESOURCES LAB., BAY SAINT LOUIS, MS.
Utility of remotely sensed data for identification of soil conservation practices [NASA-CR-176874] N91-11276
NATIONAL AERONAUTICS AND SPACE ADMINISTRATION. GODDARD SPACE FLIGHT CENTER, GREENBELT, MD.
Proceedings of the First NASA Ada Users' Symposium [NASA-TM-102941] N91-11389
Ada and software management in NASA: Symposium/forum [NASA-TM-103297] N91-11390
Late stages in the evolution of classical novae [NASA-TM-102969] N91-11633
NATIONAL AERONAUTICS AND SPACE ADMINISTRATION. JOHN F. KENNEDY SPACE CENTER, COCOA BEACH, FL.
Evaluation of thermal sprayed metallic coatings for use on the structures at Launch Complex 39 [NASA-TM-103807] N91-11121
Twenty-Second Annual NASA Supply and Equipment Management Conference [NASA-CP-10042] N91-11591
Research and technology at Kennedy Space Center [NASA-TM-102150] N91-11664
NATIONAL AERONAUTICS AND SPACE ADMINISTRATION. LYNDON B. JOHNSON SPACE CENTER, HOUSTON, TX.
Johnson Space Center CFD overview N91-10844
Numerical aerodynamic simulation of the space shuttle ascent environment N91-10875
Aerodynamic stability and heating analyses for the aeroassist flight experiment vehicle N91-10899
Radiological health risks to astronauts from space activities and medical procedures [NASA-TM-102164] N91-11356
NATIONAL AERONAUTICS AND SPACE ADMINISTRATION. LANGLEY RESEARCH CENTER, HAMPTON, VA.
Computational fluid dynamics research and applications at NASA Langley Research Center N91-10841
Direct simulation of compressible turbulence N91-10847
Non linear evolution of a second mode wave in supersonic boundary layers N91-10848
Recent advances in Runge-Kutta schemes for solving 3-D Navier-Stokes equations N91-10851
Application of unstructured grid methods to steady and unsteady aerodynamic problems N91-10856
Grid generation and inviscid flow computation about aircraft geometries N91-10857
Navier-Stokes solutions about the F/A-18 forebody-LEX configuration N91-10860
Navier-Stokes solutions for flows related to store separation N91-10861
A comparative study of Navier-Stokes codes for high-speed flows N91-10869
Modeling of high speed chemically reacting flow-fields N91-10870
Application of CFD codes for the simulation of scramjet combustor flowfields N91-10873
Hypersonic CFD applications at NASA Langley using CFL3D and CFL3DE N91-10874
The use of a Navier-Stokes code in the wing design process N91-10889
Applications of a transonic wing design method N91-10890
An embedded grid formulation applied to delta wings N91-10891
Three dimensional unstructured grids for the solution of the Euler equations N91-10893
Conservation equations and physical models for hypersonic air flows over the aeroassist flight experiment vehicle N91-10897
Direct simulation of rarefied hypersonic flows N91-10901
Prediction of effects of wing contour modifications on low-speed maximum lift and transonic performance for the EA-6B aircraft [NASA-TP-3046] N91-10902

Conical Euler simulation and active suppression of delta wing rocking motion
[NASA-TM-102683] N91-10904
Implicit flux-split Euler schemes for unsteady aerodynamic analysis involving unstructured dynamic meshes
[NASA-TM-102732] N91-10918
Temporal-adaptive Euler/Navier-Stokes algorithm for unsteady aerodynamic analysis of airfoils using unstructured dynamic meshes
[NASA-TM-102734] N91-10919
Aviation Safety/Automation Program Conference
[NASA-CP-3090] N91-10936
Aviation safety/automation program overview N91-10941
Overview of error-tolerant cockpit research N91-10949
Fault monitoring N91-10950
Fault diagnosis N91-10951
Inflight replanning for diversions N91-10955
Time-based aircraft/ATC operations study N91-10959
Information management N91-10961
A flight test facility design for examining digital information transfer N91-10962
Guidance concepts for time-based flight operations N91-10993
The 4-D descent trajectory generation techniques under realistic operating conditions N91-10994
A description and evaluation of TIMER: A time-based terminal flow-control concept N91-10996
Thermal-distortion analysis of a spacecraft box truss in geostationary orbit
[NASA-TP-3054] N91-11041
Materials Division research and technology accomplishments for FY 89 and plans for FY 90
[NASA-TM-102649] N91-11072
Studies of molecular properties of polymeric materials
[NASA-TM-101854] N91-11118
An AGARD supplemental test programme on the behaviour of short cracks under constant amplitude and aircraft spectrum loading N91-11241
The growth of short cracks in 4340 steel and aluminum-lithium 2090 N91-11247
High-performance equation solvers and their impact on finite element analysis
[NASA-TM-102735] N91-11252
Data base architecture for instrument characteristics critical to spacecraft conceptual design
[NASA-TM-4213] N91-11391

NATIONAL AERONAUTICS AND SPACE ADMINISTRATION. LEWIS RESEARCH CENTER, CLEVELAND, OH.
Computational fluid dynamics at the Lewis Research Center: An overview N91-10842
Numerical simulation of nonlinear development of instability waves
[E-4658] N91-10849
Time dependent viscous incompressible Navier-Stokes equations N91-10854
Progress toward the development of an airfoil icing analysis capability N91-10866
The breakup of trailing-line vortices N91-10867
Simulation of turbomachinery flows N91-10880
Automated design of controlled diffusion blades N91-10883
Numerical analysis of flow through oscillating cascade sections N91-10884
Analysis of three-dimensional viscous flow in a supersonic throughflow fan N91-10885
A numerical study of the hot gas environment around a STOVL aircraft in ground proximity N91-10887
CFD analysis for high speed inlets N91-10888
Flux splitting algorithms for two-dimensional viscous flows with finite-rate chemistry N91-10894
Preliminary results from the advanced photovoltaic experiment flight test
[NASA-TM-103269] N91-11058
A life comparison of tube and channel cooling passages for thrust chambers
[NASA-TM-103613] N91-11059
Investigation of the arcjet plume near field using electrostatic probes
[NASA-TM-103638] N91-11060
Photovoltaic options for solar electric propulsion
[NASA-TM-103284] N91-11061
Graphite fluoride fibers and their applications in the space industry
[NASA-TM-103265] N91-11062
Elastic/plastic analyses of advanced composites investigating the use of the compliant layer concept in reducing residual stresses resulting from processing
[NASA-TM-103204] N91-11074
Navier-Stokes analysis of transonic cascade flow
[NASA-TM-103624] N91-11192
Heat flux measurement in SSME turbine blade tester
[NASA-TM-103274] N91-11205
Noise measurements from an ejector suppressor nozzle in the NASA Lewis 9- by 15-foot low speed wind tunnel
[NASA-TM-103628] N91-11493
The effect of swirl recovery vanes on the cruise noise of an advanced propeller
[NASA-TM-103625] N91-11494
Prediction of the noise from a propeller at angle of attack
[NASA-TM-103627] N91-11495
MIS capacitor studies on silicon carbide single crystals
[NASA-CR-187350] N91-11555

NATIONAL AERONAUTICS AND SPACE ADMINISTRATION. MARSHALL SPACE FLIGHT CENTER, HUNTSVILLE, AL.
Marshall Space Flight Center CFD overview N91-10843
Analysis of the SSME HPOTP bearing inlet cavity N91-10877
A combined Eulerian-Lagrangian two-phase analysis of the SSME HPOTP nozzle plug trajectories N91-10878
Conjugate (solid/fluid) computational fluid dynamics analysis of the space shuttle solid rocket motor nozzle/case and case field joints N91-10879
Turbine stage aerodynamics and heat transfer prediction N91-10882
Aeroassist flight experiment aerodynamics and aerothermodynamics N91-10900
Combined Release and Radiation Effects Satellite (CRRES): Atlas 1 (Atlas/Centaur-69) launch vehicle
[NASA-TM-103460] N91-11040

NATIONAL AEROSPACE LAB., AMSTERDAM (NETHERLANDS).
The application of trajectory prediction algorithms for planning purposes in the Netherlands ATC-system N91-10986
Bayesian multi-sensor tracking for advanced air traffic control systems N91-11003
Short and long fatigue crack growth in 2024-T3 under Fokker 100 spectrum loading N91-11248

NATIONAL AEROSPACE LAB., TOKYO (JAPAN).
Flight evaluation test of the PAPI (Precision Approach Path Indicator) System
[NAL-TM-592] N91-10966
Flight simulator evaluation test of multi-functional display unit
[NAL-TM-596] N91-11026
Flight simulation programs for space plane
[NAL-TM-594] N91-11035
Weight evaluation and sensitivity analysis for space plane: SSTO
[NAL-TM-596-1] N91-11036
Experimental manufacturing of data recording system for rocket combustion thermal flux distribution
[DE90-702432] N91-11051
Digital data processing system for bipropellant apogee engine
[NAL-TM-599] N91-11052
Experimental manufacturing of performance evaluation system for solid image sensor
[NAL-TM-591] N91-11200

NATIONAL CENTER FOR ATMOSPHERIC RESEARCH, BOULDER, CO.
Comparison of clear air atmospheric radar techniques for the study of atmospheric dynamics in the troposphere and the stratosphere
[PB90-256314] N91-11313
Advantages of the Community Climate Model (CCM) concept
[PB90-256348] N91-11314
Taiwan area mesoscale experiment: A guide to precipitation patterns during the 1987 field phase
[PB90-256355] N91-11336
White light solar corona: An atlas of 1988 K-coronameter synoptic charts, December 1987 to January 1989
[NASA-CR-184955] N91-11649

NATIONAL GEODETIC SURVEY, ROCKVILLE, MD.
Apparent place of Polaris and apparent Sidereal Time at 0 hour UT 1990-1994
[PB90-259169] N91-11607

NATIONAL INST. FOR FUSION SCIENCE, NAGOYA (JAPAN).
A design method of divertor in tokamak reactors
[NIFS-36] N91-11532

NATIONAL INST. OF STANDARDS AND TECHNOLOGY, BOULDER, CO.
Scanning system for measuring uniformity of laser detector response and laser beam dimensions
[PB90-257619] N91-11207
Time domain frequency stability calculated from the frequency domain description: Use of the SIGINT software package to calculate time domain frequency stability from the frequency domain
[PB90-257684] N91-11405

NATIONAL INST. OF STANDARDS AND TECHNOLOGY, GAITHERSBURG, MD.
Center for electronics and electrical engineering technical publication announcements covering Center programs, July - September, 1989, with 1990 CEEE events calendar
[PB90-206491] N91-11145
Expected complexity of the 3-dimensional voronoi diagram
[PB90-221862] N91-11435
Expected linear 3-dimensional Voronoi diagram algorithm
[PB90-227984] N91-11436
Evaluation of the integral
[PB90-235011] N91-11437
Mathematical treatment of the spherical stereology
[PB90-257593] N91-11464

NATIONAL LAB. FOR HIGH ENERGY PHYSICS, IBARAKI (JAPAN).
Status reports of supercomputing astrophysics in Japan
[DE90-513793] N91-11640

NATIONAL MARINE FISHERIES SERVICE, WOODS HOLE, MA.
Surface and bottom temperature distribution for the Northeast continental shelf
[PB90-252172] N91-11349

NATIONAL OCEAN SERVICE, ANCHORAGE, AK.
Outer continental shelf environmental assessment program: Comprehensive bibliography, June 1990
[PB90-258609] N91-11350

NATIONAL OCEANIC AND ATMOSPHERIC ADMINISTRATION, BOULDER, CO.
ECC ozonesonde observations at South Pole, Antarctica during 1989
[PB90-258914] N91-11302

NAVAL AEROSPACE MEDICAL RESEARCH LAB., PENSACOLA, FL.
Naval aviation selection test scores and female aviator performance N91-11363

NAVAL AIR DEVELOPMENT CENTER, WARMINSTER, PA.
Accommodation of female aircrew in USN protective flight clothing and equipment N91-11375

NAVAL AIR STATION, NORFOLK, VA.
The integration of women into US Navy aircrew training and squadron assignments N91-11359

NAVAL OCEANOGRAPHIC AND ATMOSPHERIC RESEARCH LAB., BAY SAINT LOUIS, MS.
A compendium of environmental data collected during the Iceshelf-88 exercise
[AD-A223518] N91-11346
Notes on the NOARL nowcast for the 1989 to 1990 El Nino forced by FNOC winds
[AD-A223520] N91-11347

NAVAL POSTGRADUATE SCHOOL, MONTEREY, CA.
Spacecraft design project: High latitude communications satellite
[NASA-CR-186689] N91-11039

NAVAL RESEARCH LAB., WASHINGTON, DC.
Review of free electron lasers
[PB90-255480] N91-11206

NAVY PERSONNEL RESEARCH AND DEVELOPMENT CENTER, SAN DIEGO, CA.
The MS-DOS device handler interface
[AD-A223856] N91-11385
The MS-DOS routing and configuration program design
[AD-A223858] N91-11394

NEBRASKA UNIV., LINCOLN.
Performance of finite dynamic elements for composite materials in plane stress N91-11260

NEW ENERGY DEVELOPMENT ORGANIZATION, TOKYO (JAPAN).
Survey on solidification and utilization technology of CO2
[DE91-701465] N91-11087
Co-researches with researchers of alternative energy of petroleum in EC countries
[DE91-701466] N91-11129
Interchange of researchers on alternative energy of petroleum in EC countries
[DE91-701468] N91-11130
Study on feasible applications of stirling cycle machine
[DE91-701463] N91-11293
Report on the preparatory investigation of the Pacific energy information network system
[DE91-701469] N91-11602

NEW MEXICO UNIV., ALBUQUERQUE.
Railgun performance with a two-stage light-gas gun injector
[DE90-016211] N91-11032
Nitrogen dioxide and respiratory infection: Pilot investigations
[PB90-247339] N91-11357

NIPPON INST. OF TECH. (JAPAN).
Muon SR studies on Sr2CuO2Cl2, La2CuO4, and Nd2CuO4: 2-D magnetism, local fields and muon sites
[DE90-018014] N91-11506

NORTH CAROLINA STATE UNIV., RALEIGH.
Aerodynamic interaction of counter rotating propellers N91-10910
Effects of electric current and field on the behavior of metallic materials N91-11095
Tropical cyclone simulations with the Betts convective adjustment scheme N91-11338
Distributed digital signal processors for multi-body structures
[NASA-CR-187375] N91-11387

NORTH CAROLINA UNIV., CHAPEL HILL.
Measurement of radial ionization probability in microscopic volumes for 2.90 and 3.79 MeV alpha particles
[DE90-017509] N91-11498

NORTHWESTERN UNIV., CHICAGO, IL.
Intramolecular electron transfer rates
[DE90-017447] N91-11504

O

OAK RIDGE NATIONAL LAB., TN.
Study of asymmetric supersonic jet flow for ejectors
[DE90-015598] N91-10917
Potential for advanced thermoplastic composites in space systems
[DE90-014447] N91-11069
Resonance ionization spectroscopy of molecular clusters using picosecond lasers
[DE90-017334] N91-11080
Applications of diode lasers to resonance ionization mass spectrometry
[DE90-017768] N91-11084
Defects in close-packed metals and alloys
[DE90-017502] N91-11097
The stability of irradiation-induced defects in NiAl
[DE90-017744] N91-11103
Mechanical behavior of ceramics and composites
[DE90-017311] N91-11122
Analysis and prediction of thermal properties of mesophases and crystals by calorimetry and supercomputers
[DE90-015538] N91-11123
Chemically vapor deposited diamond films
[DE91-000384] N91-11125
Performances of four magnetic heat-pump cycles
[DE90-015606] N91-11185
Thermal performance analysis for heat exchangers using nonazeotropic refrigerant mixtures
[DE90-016030] N91-11186
Measurement of two-phase flow momentum with force transducers
[DE90-008748] N91-11188
Laser applications for high-T(sub c) superconductors
[DE90-017743] N91-11209
Indentation testing of thin films and hard materials
[DE90-017758] N91-11224
Mobile robots and intelligent motion control
[DE90-017312] N91-11226
Democratic theory, science, and decision making in global climate change: Culpability, uncertainty, and fairness
[DE90-017316] N91-11308
Parallel performance models for the nodal transport method on the hypercube
[DE90-015162] N91-11408
On the adequacy of message-passing parallel supercomputers for solving neutron transport problems
[DE90-016041] N91-11431
A unified framework for credit assignment
[DE90-011636] N91-11434
Modeling histogram data with piecewise polynomials
[DE90-018037] N91-11467
Newly appreciated roles for electrons in ion-atom collisions
[DE91-000555] N91-11509
X ray microprobe-microscopy
[DE90-017327] N91-11520
Advanced infrared optically black baffle materials
[DE91-000561] N91-11523
Mechanical properties, fracture behavior, and grain-boundary chemistry of B-doped NiAl
[DE90-015153] N91-11558
Surface anharmonicity: Temperature dependence of phonon energies on Cu(110)
[DE90-017735] N91-11567
High energy iron ion implantation into sapphire
[DE90-017736] N91-11568
Ion mixing of semiconductor superlattices
[DE90-017769] N91-11569
Compositional imaging of semiconductor interfaces by Z-contrast Scanning Transmission Electron Microscope (STEM)
[DE90-017763] N91-11576
Development of the structural materials information center
[DE90-016521] N91-11603

OAK RIDGE Y-12 PLANT, TN.
An automated linearity test for direct voltage calibrators
[DE90-016927] N91-11204

OFFICE NATIONAL D'ETUDES ET DE RECHERCHES AEROSPATIALES, PARIS (FRANCE).
Computation of sub-optimal real-time guidance laws for combat aircraft trajectories N91-10970
Load transfer between fiber and matrix in carbon fiber reinforced plastic composites tensile behavior of an embedded single filament specimen
[ONERA-NT-1989-9] N91-11075
Combustion to modelisation turbulent combustion in the case of stabilization by flame-lock
[ONERA-NT-1989-8] N91-11090
Determination of pair potentials by analysis of diffuse scattering of the local field in Pd3V and Ni3V
[ONERA-NT-1989-7] N91-11117
Study of an electrothermal de-icer: Numerical simulation and measurement of the skin temperature by infrared technique in an icing wind tunnel
[ONERA-NT-1989-10] N91-11133
Theoritical and experimental study of kinetics mechanisms in the Chemical Oxygen-Iodine Laser (COIL)
[ONERA-P-1990-1] N91-11211
Study of the return-stroke phase of the gliding spark in ambient air
[ONERA-NT-1990-1] N91-11345
Long period superstructures in Pt3V and Cu3Pd: Towards a quantitative description
[ONERA-NT-1990-2] N91-11587

OFFICE OF TECHNOLOGY ASSESSMENT, WASHINGTON, DC.
Proposal pressure in the 1980s: An indicator of stress on the Federal Research System
[PB90-253147] N91-11593
Holding the edge: Maintaining the defense technology base. Volume 2: Appendixes
[PB90-253345] N91-11597

OFFICE OF THE SECRETARY OF DEFENSE, WASHINGTON, DC.
Department of Defense methodology guidelines for High Power Microwave (HPM) susceptibility assessments
[DE90-015405] N91-11147

OHIO STATE UNIV., COLUMBUS.
Structure of supersonic turbulent reattaching shear layers N91-10914
Graphical interfaces for cooperative planning systems N91-10956
Vortex-induced noise and vibration in flow past several flat plates N91-11163
Forced vibration analysis of plates and shallow shells N91-11237
Buckling and vibrations of plates subjected to concentrated forces N91-11255

OKLAHOMA STATE UNIV., STILLWATER.
A new approach to the flight control system reconfiguration following a battle damage and/or generic failure on a control surface N91-11023

OLD DOMINION UNIV., NORFOLK, VA.
Analysis and control of supersonic vortex breakdown flows
[NASA-CR-186897] N91-10903
Grid generation and flow computation about a Martian entry vehicle
[NASA-CR-187032] N91-11042
An experimental study of an axisymmetric turbulent boundary layer disturbed by a periodic freestream N91-11175
Surrogate oracles, generalized dependency and simpler models
[NASA-CR-187360] N91-11407

OREGON GRADUATE INST. OF SCIENCE AND TECHNOLOGY, BEAVERTON.
Deformation effects on the development of grain boundary chronium depletion (sensitization) in type 316 austenitic stainless steels
[DE90-016130] N91-11092

OREGON STATE UNIV., CORVALLIS.
An experimental study of natural convection heat transfer from a horizontal cylinder array vertically aligned to and confined by a single wall and two walls N91-11178

OREGON UNIV., EUGENE.
Observation and analysis of variable linear polarization in the yellow supergiant star Epsilon Aurigae N91-11616

OXFORD UNIV. (ENGLAND).
The aerodynamic effects of nozzle guide vane shock wave and wake passing on a transonic turbine rotor N91-10915
H infinity-design and the improvement of helicopter handling qualities N91-11024
Radiometric observation of the atmospheric boundary layer (the ROSSA Project) N91-11324
Atmospheric chemistry: Laboratory studies of kinetics of important reactions N91-11326
Modelling of large-scale unstable waves in the middle atmosphere N91-11327
Ion dynamics in semiconductors with self-consistent electronic densities N91-11556

P

PACIFIC NORTHWEST LAB., RICHLAND, WA.
Assessing the feasibility, cost, and utility of developing models of human performance in aviation N91-10948
Combined capillary electrophoresis and electrospray ionization mass spectrometry
[DE90-016535] N91-11079
Japanese power electronics inverter technology and its impact on the American air conditioning industry
[DE90-014843] N91-11191
Classification of acoustic emission waveforms for nondestructive evaluation using neural networks
[DE90-017239] N91-11236
Results from a workshop on research needs for modeling aquifer thermal energy storage systems
[DE90-018007] N91-11301
The practical challenges of converting end-use data into information
[DE90-016538] N91-11600

PENNSYLVANIA STATE UNIV., UNIVERSITY PARK.
A computational model for the prediction of hypersonic, reacting flows N91-10911
Magnetohydrodynamic modification of the TEACH-T code and the prediction of the maximum azimuthal velocity in a conducting fluid
[DE90-017510] N91-11187
Astronomical applications of survival analysis N91-11615
Radio and infrared emission from starburst galaxies N91-11661

PENNSYLVANIA UNIV., PHILADELPHIA.
Reexamination of data from the asteroid/meteoroid detector
[NASA-CR-185875] N91-11619

PHYSICAL SCIENCES, INC., ANDOVER, MA.
Propulsion simulation for magnetically suspended wind tunnel models
[NASA-CR-182093] N91-11027

PISA UNIV. (ITALY).
Short crack observations in Ti-6Al-4V under constant amplitude loading N91-11250

PRATT AND WHITNEY AIRCRAFT, WEST PALM BEACH, FL.
RL10 ignition limits test for Shuttle Centaur
[NASA-CR-183199] N91-11049

PRINCETON SCIENTIFIC INSTRUMENTS, MONMOUTH JUNCTION, NJ.
Remote sensing in the ultraviolet
[AD-A224254] N91-11268

PRINCETON UNIV., NJ.
Nonoverlapping composite meshes for multi-element air-foils N91-10908

PURDUE UNIV., WEST LAFAYETTE, IN.
Development and application of the time domain panel method N91-11010

Q

QUADRANT ENGINEERING, INC., AMHERST, MA.
Azimuthal resolution degradation due to ocean surface motion in focused arrays and SARS
[AD-A223315] N91-11135

R

REMTECH, INC., HUNTSVILLE, AL.
External tank aerothermal design criteria verification, volume 1
[NASA-CR-183996] N91-11037
External tank aerothermal design criteria verification, volume 2
[NASA-CR-183997] N91-11038

RESEARCH INST. FOR ADVANCED COMPUTER SCIENCE, MOFFETT FIELD, CA.
Performance of a parallel code for the Euler equations on hypercube computers
[NASA-TM-102260] N91-11384

RICE UNIV., HOUSTON, TX.
Optimal trajectories of aircraft and spacecraft
N91-10968
RIJKSWATERSTAAT, DELFT (NETHERLANDS).
Wave data assimilation in a 3rd generation. Wave prediction model for the North Sea: An optimal control approach
[BCRS-89-22] N91-11348
ROCKWELL INTERNATIONAL CORP., CANOGA PARK, CA.
Real-time failure control (SAFD)
[NASA-CR-184025] N91-11233
Lower bound on reliability for Weibull distribution when shape parameter is not estimated accurately
[NASA-CR-180681] N91-11474
ROLLS-ROYCE LTD., BRISTOL (ENGLAND).
Carbon deposition in gas turbine combustors
[PNR-90692] N91-11020
Experiences in the use of ABAQUS for creep analysis
[PNR-90705] N91-11266
ROLLS-ROYCE LTD., DERBY (ENGLAND).
Recent advances and developments in coatings
[PNR-90698] N91-11021
High temperature materials: The overall view
[PNR-90699] N91-11073
Influence of heat treatment on microstructure and properties of an advanced high temperature titanium alloy
[PNR-90689] N91-11107
Commercial aircraft and the environment
[PNR-90687] N91-11307
The role of process modelling in manufacture and design
[PNR-90702] N91-11416
ROYAL AIR FORCE INST. OF AVIATION MEDICINE, FARNBOROUGH (ENGLAND).
The application of USAF female anthropometric data to identify problems with the introduction of female aircrew into the Royal Air Force N91-11370
Some equipment problems associated with the introduction of female aircrew into the Royal Air Force
N91-11373
ROYAL AIRCRAFT ESTABLISHMENT, FARNBOROUGH (ENGLAND).
The growth of short fatigue cracks in 2024 and 2090 aluminium alloys under variable amplitude loading
N91-11245
Texture analysis of 2090-T8E41 aluminum-lithium alloy sheet: Annex N91-11251
ROYAL INST. OF TECH., STOCKHOLM (SWEDEN).
Electric fields in magnetosphere
[TRITA-EPP-89-06] N91-11312
Complementary aspects on matter-antimatter boundary layers
[TRITA-EPP-90-04] N91-11496
Dynamic trapping of electrons in space plasmas
[TRITA-EPP-89-07] N91-11528
The plasma universe
[TRITA-EPP-89-08] N91-11529
Laboratory experiments on the magnetic field and neutral density limits on CIV interaction
[TRITA-EPP-90-01] N91-11530
Potential drops supported by ion density cavities in the dynamic response of plasma diode to an applied field
[TRITA-EPP-90-03] N91-11531
ROYAL NETHERLANDS AIR FORCE, SOESTERBERG.
The selection, training, and operational work of female helicopter pilots in the Royal Netherlands Air Force
N91-11361
ROYAL NETHERLANDS METEOROLOGICAL INST., THE HAGUE.
Wave data assimilation in a 3rd generation. Wave prediction model for the North Sea: An optimal control approach
[BCRS-89-22] N91-11348
ROYAL RADAR ESTABLISHMENT, MALVERN (ENGLAND).
Prediction of aircraft trajectories N91-10984

S

SANDIA NATIONAL LABS., ALBUQUERQUE, NM.
Computer modeling of 12-inch actuator shock test performance
[DE90-017038] N91-11033
Tethered rocket as a vehicle for penetration and impact testing: Development report
[DE90-014865] N91-11057
In-situ pore structure analysis during aging and drying of gels
[DE91-000044] N91-11089
Solderability of environmentally exposed Sn-plated surfaces
[DE91-000035] N91-11110
Microstructures of cubic Al2O3 precipitates in oxygen-implanted aluminum
[DE91-000038] N91-11111
Attenuation studies of booster-rocket propellants and their simulants
[DE91-000098] N91-11131
Terrestrial nickel/hydrogen battery evaluation
[DE90-014863] N91-11151
Development of hermetic microminiature connectors
[DE90-015562] N91-11153
A radiation hardened SONOS/CMOS EEPROM family
[DE90-015993] N91-11154
Reference concepts for a space-based hydrogen-oxygen combustion, turboalternator, burst power system
[DE90-016692] N91-11155
An expert system for automated robotic grasping
[DE90-010820] N91-11221
Improved tracking for bilateral teleoperators with time delay
[DE90-015392] N91-11222
Archimedes: A system that plans and executes mechanical assemblies
[DE91-000036] N91-11231
Implementation of a QML (Qualified Manufacturer's List) methodology for discrete semiconductors
[DE90-015715] N91-11235
Thermal stresses in layered electrical assemblies bonded with solder
[DE90-015563] N91-11263
Bench-scale testing of a heat-pipe receiver for solar thermal electric applications
[DE90-009834] N91-11269
Generic quality assurance/quality control guide for photovoltaic concentrator design, development and system installation
[DE90-017040] N91-11290
An adaptive finite element technique using element equilibrium and paving
[DE90-015829] N91-11410
The design, testing and fabrication of an extruded, linear focus Fresnel lens
[DE90-014852] N91-11516
Electric-field dependent electroreflectance and photocurrent spectroscopy in InGaAs/InAlAs strained-layer superlattices
[DE90-015698] N91-11559
Nonparabolic conduction bands and masses in strained-single-quantum wells
[DE90-017028] N91-11560
Photoluminescence studies of In(x)Ga(1-x)As/Al(y) Ga(1-y)As strained-layer structures
[DE90-017031] N91-11561
Stress accommodation in large-mismatch systems
[DE90-017032] N91-11562
Optical characterization of CdZnTe/CdTe strained quantum wells
[DE90-017036] N91-11563
Light-heavy-hole-mixing-induced selection rules for magneto-luminescence and valence-band energy dispersion in semiconductor quantum wells
[DE90-015989] N91-11573
Formation and stability of As-H bonds in H-implanted GaAs
[DE91-000043] N91-11584
SAO PAULO UNIV. (BRAZIL).
Computer and engineering calculations of Brazilian Tokamak-2
[DE90-628758] N91-11524
SCHOOL OF AEROSPACE MEDICINE, BROOKS AFB, TX.
EKG findings in female aviators in the US Air Force
N91-11377
Relationship of menstrual history to altitude chamber decompression sickness N91-11379
SERVICE TECHNIQUE DE LA NAVIGATION AERIENNE, PARIS (FRANCE).
Contribution of the satellite techniques to the surveillance of air traffic N91-11005
SHEFFIELD UNIV. (ENGLAND).
Integrated optical components produced in GaAs and InP epitaxial layers using the photo-elastic effect
N91-11518
The derivation of a behavioural model for information retrieval system design N91-11599
SMITHS INDUSTRIES, INC., GRAND RAPIDS, MI.
Aircraft trajectory: Prediction and control in the air transport flight management computer systems
N91-10976
SOCIETE BERTIN ET CIE, TARNOS (FRANCE).
Characterization and optimization of a pneumatic injector for a 60 bar combustion chamber
[ETN-90-97580] N91-11076
SOLAREX CORP., NEWTOWN, PA.
Research on high-efficiency, large area amorphous silicon based solar cells
[DE90-000356] N91-11285
SONOQUEST/ADVANCED ULTRASONICS RESEARCH, WELLESLEY HILLS, MA.
Arctic acoustics ultrasonic modeling studies
[AD-A224165] N91-11489
SOUTH CAROLINA UNIV., COLUMBIA.
Optimal control design by Volterra Series and its application to spacecraft maneuvers N91-11044
SOUTHAMPTON UNIV. (ENGLAND).
Aircraft flight in wind-shear N91-10973
Voice communications in the cockpit noise environment: The role of active noise reduction N91-11140
SOUTHWEST RESEARCH INST., SAN ANTONIO, TX.
Measurements of toxic exhaust emissions from gasoline-powered light-duty vehicles
[PB90-259649] N91-11306
Research into language concepts for the mission control center
[NASA-CR-185928] N91-11392
SPACE TELESCOPE SCIENCE INST., BALTIMORE, MD.
Novae as distance indicators
[NASA-CR-186278] N91-11605
STANFORD UNIV., CA.
A numerical study of the effects of wind tunnel wall proximity on an airfoil model
[NASA-CR-187322] N91-10934
Controlled vortical flow on delta wings through unsteady leading edge blowing N91-11011
Boosting a tethered satellites's orbit around an oblate planet through resonant pumping N91-11030
Attitude control of tethered satellites N91-11045
Precision tethered satellite attitude control
N91-11046
Instabilities of two-dimensional inviscid compressible vortices N91-11181
Minimum time feedback control of articulated robotic manipulators N91-11219
The EGRET gamma ray telescope and its energy calibration N91-11613
Testing for lightning as a source of radio bursts observed on the nightside of Venus
[NASA-CR-187364] N91-11645
STATE UNIV. OF NEW YORK, ALBANY.
Planetary boundary layer dynamics over the Amazon rain forest N91-11317
STATE UNIV. OF NEW YORK, STONY BROOK.
Analytic studies in nuclear astrophysics N91-11628
STERLING FEDERAL SYSTEMS, INC., MOFFETT FIELD, CA.
Calculation of the rotor induced download on airfoils
N91-10864
STERLING FEDERAL SYSTEMS, INC., PALO ALTO, CA.
OSI in the NASA science internet: An analysis
[NASA-CR-177561] N91-11425
STUTTGART UNIV. (GERMANY, F.R.).
Test launch for turboaircraft engine. Description of the installation
[ILA-87-A-02] N91-11018
Examination of a three dimensional asymmetrical flow field using the interference method
[ETN-90-97859] N91-11168
Problems of static divergence concerning the rpm regulation of wind turbines using centrifugal force controlling means and rotating slat
[ETN-90-97858] N91-11281
SVERDRUP TECHNOLOGY, INC., CLEVELAND, OH.
Three-dimensional calculation of supersonic reacting flows using an LU scheme N91-10871
SWEDISH INST. OF SPACE PHYSICS, UMEA.
A combined wave distribution function and stability analysis of Viking particle and low-frequency wave data
[IRF-PREPRINT-115] N91-11541
SYRACUSE UNIV., NY.
Sidelobe blanking system performance: An extension of the theory leading to a new detection logic
N91-11139
Research program in elementary particle theory
[DE90-017284] N91-11497
SYSTEMS ENGINEERING ASSOCIATES, SAN DIEGO, CA.
The MS-DOS device services interface
[AD-A223902] N91-11386

T

TECHNICAL RESEARCH CENTRE OF FINLAND, ESPOO.
Activities report of the Technical Research Centre of Finland
[ISBN-951-38-3647] N91-11665

TECHNICAL UNIV. OF CRETE, ATHENS (GREECE).
The use of downlinked measurements to track civil aircraft N91-11004
TECHNISCHE HOCHSCHULE, AACHEN (GERMANY, F.R.).
A contribution to the output analysis and layout of transonic axial turbine stages
[ETN-90-97862] N91-11017
ution of the equivalent space with Bessel integral equation for the fractured orthotropic disk ution of the 'equivalent space' with Bessel integral equation for the fractured orthotropic disk
[ISSN-0932-8599] N91-11253
TECHNISCHE UNIV., BERLIN (GERMANY, F.R.).
Methods for the construction of constant curve free form surfaces
[ETN-90-97861] N91-11463
TECHNISCHE UNIV., BRUNSWICK (GERMANY, F.R.).
Comparison of a mathematical one-point model and a multi-point model of aircraft motion in moving air N91-10969
Effect of wind and wind variation on aircraft flight-paths N91-10972
Wind models for flight simulation N91-10975
Simulation of automated approach procedures considering dynamic flight operations N91-11008
TECHNISCHE UNIV., DELFT (NETHERLANDS).
DUWECS reference guide V1.0: Delft University wind energy converter simulation program
[MEMT-5] N91-11294
What is a default
[REPT-90-12] N91-11400
A logical background of a method for the handling of incompatible pieces of knowledge
[REPT-90-13] N91-11401
A potential reduction variant of Renegar's short-step path-following method for linear programming
[REPT-90-14] N91-11402
A formal semantics for the preferred subtheories
[REPT-90-20] N91-11403
A fast parallel recognizer
[REPT-90-16] N91-11429
Connected components in supercritical Mandelbrot percolation
[REPT-90-15] N91-11452
A polynomial method of weighted centers for convex quadratic programming
[REPT-90-17] N91-11453
A comparison of some GMRES-like methods
[REPT-90-22] N91-11454
Quadratic systems equivalent to class 3 sub A not equal to 0
[REPT-90-38] N91-11455
Convergence of solutions of one-dimensional stochastic heat equations
[REPT-90-40] N91-11478
Compensability of uncertain systems
[REPT-90-10] N91-11527
The French and the American school in multi-criteria decision analysis
[REPT-90-21] N91-11592
TECHNISCHE UNIV., EINDHOVEN (NETHERLANDS).
On the calculation of leakage and friction of reciprocating elastomeric seals
[ETN-90-97751] N91-11228
The influence of ionized impurities on the transport properties of a two-dimensional electron gas
[ETN-90-97752] N91-11586
TEMPLE UNIV., PHILADELPHIA, PA.
An investigation of the Newman-Penrose constants for massless free fields of arbitrary spin N91-11630
TENNESSEE UNIV., KNOXVILLE.
Aerodynamic design optimization using computational fluid dynamics N91-11013
Accuracy, convergence and stability of finite element algorithms for incompressible fluid flow N91-11184
The influence of environmental factors on the temperature of the radiosonde thermistor N91-11325
Newly appreciated roles for electrons in ion-atom collisions
[DE91-000555] N91-11509
TEXAS A&M UNIV., COLLEGE STATION.
Deformation and delamination of inelastic laminates under tensile and torsional loading N91-11063
TEXAS UNIV., AUSTIN.
Nominal ocean tide models for TOPEX precise orbit determination N91-11029
Residual stress measurements and microstructural characterization of graphite-aluminum metal matrix composite N91-11068
Fluctuations and stability in the Advanced Toroidal Facility (ATF) torsatron
[DE90-017734] N91-11536
Natural current profiles in a tokamak
[DE91-000128] N91-11540
Nonlinear saturation of ideal interchange modes in a sheared magnetic field
[DE91-000575] N91-11548
Magnetic field generation in astrophysics N91-11623
Nitrogen and sulfur in irregular galaxies N91-11624
On the origin of cosmological magnetic fields
[DE90-017617] N91-11634
Numerical study of compressible magnetoconvection with an open transitional boundary
[DE91-000148] N91-11651
TOKYO UNIV., TANASHI (JAPAN).
Atmospheric neutrino fluxes
[DE90-508023] N91-11656
TOLEDO UNIV., OH.
Semiempirical studies of atomic structure
[DE90-017653] N91-11501
TORONTO UNIV. (ONTARIO).
Critical aspects of trajectory prediction: Flight in non-uniform wind N91-10971
TRW, INC., REDONDO BEACH, CA.
MHD technology transfer, integration, and review committee
[DE90-017886] N91-11542
TUEBINGEN UNIV. (GERMANY, F.R.).
Type 2 solar radio bursts recorded at Weissenau, 1966-1987
[PB90-198334] N91-11648

U

UNIVERSAL SENSORS, INC., METAIRIE, LA.
A protein coated piezoelectric crystal detector
[AD-A223848] N91-11552
UNIVERSITA CATTOLICA, BRESCIA (ITALY).
Contributions to the sound location in the atmosphere
[ETN-90-97863] N91-11490
UNIVERSITAET DER BUNDESWEHR, HAMBURG (GERMANY, F.R.).
Integration of model and knowledge based diagnosis, with the example of a turbojet engine
[ETN-90-97900] N91-11019
Algorithm aided evaluation of directional signals
[ETN-90-97902] N91-11138
Evaluation process for the examination of curved surface workpieces using coordinate measuring instruments
[ETN-90-97901] N91-11203
UNIVERSITAET DER BUNDESWEHR MUENCHEN, NEUBIBERG (GERMANY, F.R.).
Modeling and coding in aeronautical satellite channel
[ETN-90-97899] N91-11137
UNIVERSITE CATHOLIQUE, LOUVAIN (BELGIUM).
Aircraft dynamics for air traffic control N91-10985
UNIVERSITEIT TWENTE, ENSCHEDE (NETHERLANDS).
Projective scales against high temperature corrosion
[ETN-90-97770] N91-11116
Gas-liquid contacting at elevated pressures
[ETN-90-97773] N91-11196
Pulse evolution in multi-atmosphere CO2 lasers
[ETN-90-97765] N91-11210
Decomposition of the n-cube into paths
[MEMO-855] N91-11468
Interpolation of scattered data by a bivariate convex function. Part 1: Piecewise linear C sup 0-interpolation
[MEMO-858-PT-1] N91-11469
On dominating and spanning circuits in graphs
[MEMO-859] N91-11470
UNIVERSITY COLL., CARDIFF (WALES).
The ultrasonic examination of titanium alloys N91-11094
UNIVERSITY HOSPITAL, OSLO (NORWAY).
Pregnancy: A cause for grounding of female air crew N91-11376
UNIVERSITY OF NORTHERN COLORADO, GREELEY.
Northwest African depressions and their relationship to jet streams N91-11318
UTAH UNIV., SALT LAKE CITY.
A simulation of the flow near a burning propellant in a solid propellant rocket motor N91-11056
The evolution and time scales of the atmospheric response to tropical diabatic heating events N91-11322
Numerical studies of electron scattering in astrophysics N91-11625

V

VIRGINIA POLYTECHNIC INST. AND STATE UNIV., BLACKSBURG.
Analysis and design of a high power, digitally-controlled spacecraft power system
[NASA-CR-186546] N91-11053
Statistical system identification of structures with flexible joints N91-11232
VIRGINIA UNIV., CHARLOTTESVILLE.
Fabrication and optimization of a whiskerless Schottky barrier diode for submillimeter wave applications
[NASA-CR-186381] N91-11144

W

WASHINGTON UNIV., SEATTLE.
Numerical simulation of shock-induced combustion for application to the ram accelerator concept N91-10912
Meteorological characteristics of the El Nino/Southern Oscillation phenomenon N91-11340
Two and three dimensional magnetotelluric inversion
[DE90-016187] N91-11411
WEST VIRGINIA UNIV., MORGANTOWN.
Theoretical and numerical studies of constitutive relations for frictional granular flow
[DE90-009662] N91-11194
WESTINGHOUSE ELECTRIC CORP., PITTSBURGH, PA.
Three-Man Solid Electrolyte Carbon Dioxide Electrolysis Breadboard
[NASA-CR-185612] N91-11148
WISCONSIN UNIV., MADISON.
Morphological analysis of ionomers
[DE90-017611] N91-11124
High-power microwave transmission systems for electron cyclotron resonance plasma heating, volume 5
[DE90-017600] N91-11152
The evolution of resistive ballooning modes in the banana-plateau collisionality regime
[DE90-016672] N91-11525
Confinement and fluctuations in the MST (Madison Symmetric Torus) reversed field pinch
[DE90-018019] N91-11535
Fluctuations and stability in the Advanced Toroidal Facility (ATF) torsatron
[DE90-017734] N91-11536
A search for very high energy gamma-rays from Cygnus X-3 N91-11658
Observations of the soft x ray background N91-11663
WISCONSIN UNIV., MILWAUKEE.
Computer-controlled ion beam deposition systems for high T(sub c) superconductor and other multi-component oxide thin films and layered structures
[DE90-017798] N91-11577
WYOMING UNIV., LARAMIE.
Image reconstruction of IRAS survey scans
[NASA-CR-187328] N91-11606
A study of the ten and twenty micron silicate features in celestial infrared sources N91-11609

Y

YALE UNIV., NEW HAVEN, CT.
Theoretical and numerical studies in magnetic mirror fusion
[DE90-017605] N91-11533

Typical Contract Number Index Listing

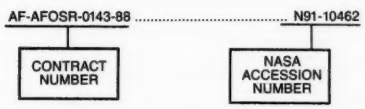

Listings in this index are arranged alphanumerically by contract number. Under each contract number the NASA accession numbers denoting documents that have been produced as a result of research done under that contract are arranged in ascending order. The NASA accession number denotes the number by which the citation is identified.

AF PROJ. 2304 ..... N91-11164
AF PROJ. 4643 ..... N91-11268
AF-AFOSR-0143-86 ..... N91-11164
AF-AFOSR-0248-88 ..... N91-11560
ARPA ORDER 6402 ..... N91-11480
N91-11481
N91-11482
CA-ARB-A6-198-32 ..... N91-11306
CA-ARB-A732-107 ..... N91-11304
CPCB-01.03 ..... N91-11574
CPCB-01.09 ..... N91-11574
DAAA15-87-C-0004 ..... N91-11552
DAAA21-86-C-0101 ..... N91-11126
DE-AC01-87CE-40762 ..... N91-11284
DE-AC02-76CH-00016 ..... N91-11108
N91-11500
DE-AC02-76CH-03000 ..... N91-11086
N91-11511
DE-AC02-83CH-10093 ..... N91-11280
N91-11282
N91-11283
N91-11284
N91-11285
N91-11286
N91-11287
N91-11295
N91-11296
N91-11297
N91-11557
N91-11572
DE-AC03-76SF-00098 ..... N91-11113
N91-11149
N91-11161
N91-11585
DE-AC04-76DP-0353 ..... N91-11213
DE-AC04-76DP-00613 ..... N91-11158
N91-11420
DE-AC04-76DP-00780 ..... N91-11263
DE-AC04-76DP-00789 ..... N91-11032
N91-11033
N91-11057
N91-11064
N91-11089
N91-11110
N91-11111
N91-11131
N91-11151
N91-11153
N91-11154
N91-11155
N91-11221
N91-11222
N91-11231
N91-11235
N91-11289
N91-11290
N91-11410
N91-11516
N91-11559
N91-11560
N91-11561
N91-11562
N91-11563
N91-11573
N91-11584
DE-AC05-76OR-00033 ..... N91-11187
N91-11498
DE-AC05-84OR-21400 ..... N91-10917
N91-11069
N91-11080
N91-11084
N91-11097
N91-11103
N91-11122
N91-11123
N91-11125
N91-11185
N91-11186
N91-11188
N91-11209
N91-11224
N91-11226
N91-11308
N91-11408
N91-11431
N91-11434
N91-11467
N91-11509
N91-11520
N91-11523
N91-11536
N91-11558
N91-11567
N91-11568
N91-11569
N91-11576
N91-11603
DE-AC05-84OS-21400 ..... N91-11204
DE-AC06-76RL-01830 ..... N91-11079
N91-11191
N91-11236
N91-11301
N91-11600
DE-AC06-86NE-37963 ..... N91-11092
DE-AC07-76ID-01570 ..... N91-11128
N91-11157
N91-11189
DE-AC21-87MC-23270 ..... N91-11298
DE-AC22-84PC-70507 ..... N91-11539
DE-AC22-87PC-90274 ..... N91-11542
DE-AS05-77ER-05490 ..... N91-11574
DE-FC21-87MC-24207 ..... N91-11194
DE-FG02-84ER-53175 ..... N91-11549
DE-FG02-85ER-40231 ..... N91-11497
DE-FG02-85ER-52122 ..... N91-11152
DE-FG02-85ER-53198 ..... N91-11535
DE-FG02-86ER-52127 ..... N91-11534
DE-FG02-86ER-53218 ..... N91-11525
DE-FG02-86ER-53240 ..... N91-11533
DE-FG02-87ER-13808 ..... N91-11504
DE-FG02-87ER-45328 ..... N91-11099
DE-FG02-88CE-90025 ..... N91-11225
DE-FG02-88ER-40417 ..... N91-11500
DE-FG02-88ER-45370 ..... N91-11124
DE-FG02-89CE-90029 ..... N91-11223
DE-FG03-84ER-45156 ..... N91-11569
DE-FG03-86SF-16306 ..... N91-11201
DE-FG05-80ET-53088 ..... N91-11540
N91-11548
N91-11634
N91-11651
DE-FG05-87ER-40319 ..... N91-11412
N91-11512
DE-FG05-88ER-13958 ..... N91-11501
DE-FG05-89ER-75527 ..... N91-11604
DE-FG06-89ER-14064 ..... N91-11411
DE-W-7405-ENG-36 ..... N91-11351
ENW3-0044-NL N91-11294
EPA-68-02-4291 ..... N91-11078
EPA-68-02-4701 ..... N91-11078
FNSRS-2.866-0.88 ..... N91-11103
F19628-88-C-0018 ..... N91-11268
GRI-5087-260-1535 ..... N91-11170
JPL-956415 ..... N91-10968
JPL-957723 ..... N91-11642
LBL-455610 ..... N91-11149
MDA972-89-C-0034 ..... N91-11480
N91-11481
N91-11482
NAGW-421 ..... N91-11605
NAGW-0908 ..... N91-11342
NAGW-1198 ..... N91-11396
NAGW-1727 ..... N91-11311
NAGW-1782 ..... N91-11619
NAG1-516 ..... N91-10968
NAG1-623 ..... N91-11216
NAG1-722 ..... N91-11488
NAG1-750 ..... N91-11407
NAG1-787 ..... N91-11430
NAG1-994 ..... N91-10903
NAG1-1060 ..... N91-11397
NAG1-1132 ..... N91-11430
NAG1-1136 ..... N91-11387
NAG2-413 ..... N91-11380
NAG2-520 ..... N91-11645
NAG2-559 ..... N91-11050
NAG5-712 ..... N91-11144
NAG5-1232 ..... N91-11053
NAG5-1246 ..... N91-11606
NAG8-642 ..... N91-11393
NAG9-339 ..... N91-11392
NAG9-474 ..... N91-11644
NASA ORDER C-30007-K N91-11555
NASA ORDER C-30018-M N91-11555
NASA ORDER C-99066-G N91-11192
NASA ORDER H-80579-B N91-11091
NASA ORDER W-15766 ..... N91-11649
NASW-4228 ..... N91-10964
NASW-4435 ..... N91-11039
N91-11641
NASW-4518 ..... N91-10964
NAS1-18605 ..... N91-11397
N91-11430
NAS1-18616 ..... N91-11027
NAS2-11555 ..... N91-11425
NAS3-22902 ..... N91-11049
NAS3-24678 ..... N91-11134
NAS5-29293 ..... N91-11605
NAS8-30490 ..... N91-11034
NAS8-36431 ..... N91-11432
NAS8-36946 ..... N91-11037
N91-11038
NAS8-37457 ..... N91-11031
NAS8-37775 ..... N91-11054
N91-11055
NAS8-40000 ..... N91-11233
N91-11474
NAS9-17394 ..... N91-11310
NAS9-17590 ..... N91-11148
NATO-0474/87 ..... N91-11080
NCC1-68 ..... N91-11042
NCC1-90 ..... N91-11118
NCC2-055 ..... N91-10934
NCC2-562 ..... N91-11165
NOVEM-41/33-020/10 ..... N91-11294
NSF ASC-88-19373 ..... N91-11397
N91-11430
NSF ATM-88-11128 ..... N91-11651
NSF DMR-87-02847 ..... N91-11503
NSF DMR-87-19738 ..... N91-11580
NSF DMR-88-01260 ..... N91-11503
NSF DMR-88-18412 ..... N91-11123
NSF ECE-86-07591 ..... N91-11315
NSF STC-88-09854 ..... N91-11565
N91-11580
N00014-83-K-0038 ..... N91-11486
N00014-86-C-0206 ..... N91-11489
N00014-88-F-0019 ..... N91-11104
N00014-90-C-0108 ..... N91-11135
N66001-88-D-0054 ..... N91-11385
N91-11386
N91-11394
RRI-14 ..... N91-11574
SNL-63-8573 ..... N91-11516
ST2J-0066-3-NL(CD) N91-11456
SWRI PROJ. 05-2768 ..... N91-11392
W-31-109-ENG-38 ..... N91-11100

N91-11102
N91-11104
N91-11105
N91-11109
N91-11115
N91-11159
N91-11190
N91-11212
N91-11299
N91-11300
N91-11309
N91-11344
N91-11352
N91-11353
N91-11413
N91-11479
N91-11487
N91-11537
N91-11538
N91-11565
N91-11566
N91-11570
N91-11575
N91-11577
N91-11578
N91-11579
N91-11580
N91-11582
N91-11583
W-7405-ENG-36 ..... N91-11085
N91-11114
N91-11115
N91-11162
N91-11330
N91-11465
N91-11466
N91-11485
N91-11502
N91-11522
N91-11545
N91-11546
N91-11590
N91-11601
N91-11633
N91-11646
W-7405-ENG-48 ..... N91-11032
N91-11081
N91-11082
N91-11098
N91-11113
N91-11141
N91-11147
N91-11156
N91-11195
N91-11214
N91-11230
N91-11265
N91-11382
N91-11409
N91-11414
N91-11499
N91-11514
N91-11515
N91-11547
N91-11635
W-7405-ENG-82 ..... N91-11070
N91-11071
N91-11083
N91-11101
N91-11112
N91-11234
N91-11264
N91-11267
N91-11486
N91-11503
N91-11506
N91-11564
N91-11571
ZB-7-06003-2 ..... N91-11285
324-01-00 ..... N91-11027
505-41-41 ..... N91-11062
505-60-01 ..... N91-10839
N91-10868
505-61-21-03 ..... N91-10902
505-61-51 ..... N91-10933
505-62-4D N91-11495
505-62-21 ..... N91-11192
505-62-40 ..... N91-11493
505-63-01-10 ..... N91-11252
505-63-01-15 ..... N91-11072
505-63-21-01 ..... N91-10904
505-63-50-12 ..... N91-10918
N91-10919
505-67-21-07 ..... N91-10936
505-90-21-01 ..... N91-11397
N91-11430
506-41-11 ..... N91-11058
N91-11061
506-42-31 ..... N91-11060
506-49-21-02 ..... N91-11041
N91-11391
510-01-01 ..... N91-11074
535-03-10 ..... N91-11494
536-01-11 ..... N91-11384
590-21-11 ..... N91-11205
591-41-21 ..... N91-11059
650-60-21 ..... N91-11134

REPORT/ACCESSION NUMBER INDEX

Typical Report Number Index Listing

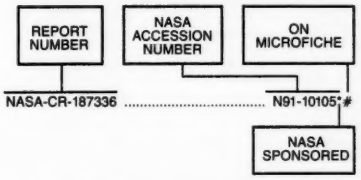

Listings in this index are arranged alphanumerically by report number. The NASA accession number denotes the number by which the citation is identified. An asterisk (*) indicates that the item is a NASA report. A pound sign (#) indicates that the item is available on microfiche.

A-89160-VOL-1 ..... N91-10839* #
A-89160-VOL-2 ..... N91-10868* #
A-90020 ..... N91-11384* #
A-90240 ..... N91-11425* #
A-90256 ..... N91-10933* #

AD-A223315 ..... N91-11135 #
AD-A223518 ..... N91-11346 #
AD-A223520 ..... N91-11347 #
AD-A223848 ..... N91-11552 #
AD-A223856 ..... N91-11385 #
AD-A223858 ..... N91-11394 #
AD-A223902 ..... N91-11386 #
AD-A223934 ..... N91-11126 #
AD-A224034 ..... N91-11480 #
AD-A224057 ..... N91-11481 #
AD-A224060 ..... N91-11482 #
AD-A224165 ..... N91-11489 #
AD-A224254 ..... N91-11268 #
AD-A224388 ..... N91-11395 #
AD-A224465 ..... N91-11164 #

AFOSR-90-0768TR ..... N91-11164 #

AGARD-AG-301-VOL-1-PT-1-3 ..... N91-10967 #
AGARD-AG-301-VOL-2-PT-4-8 ..... N91-10981 #
AGARD-AG-301-VOL-3-PT-9-11 ..... N91-10978 #

AGARD-AR-275 ..... N91-11022 #

AGARD-CP-491 ..... N91-11358 #

AGARD-R-767 ..... N91-11240 #

AIAA-90-0936 ..... N91-10918* #
AIAA-90-1650 ..... N91-10919* #
AIAA-90-3932 ..... N91-11494* #
AIAA-90-3954 ..... N91-11495* #
AIAA-90-3983 ..... N91-11493* #

ANL/ER-2 ..... N91-11344 #

ARAED-CR-90003 ..... N91-11126 #

ARB-R-90/441 ..... N91-11304 #
ARB-R-90/445 ..... N91-11306 #

ASIPP-0005 ..... N91-11544 #

AVSCOM-TM-90-B-017 ..... N91-11252* #

BBC-RD-1990/5 ..... N91-11142

BCRS-89-22 ..... N91-11348 #
BCRS-89-32 ..... N91-11269 #
BCRS-89-41 ..... N91-11273 #
BCRS-89-41-APP ..... N91-11274 #

BNL-43758 ..... N91-11108 #
BNL-45011 ..... N91-11500 #

CNES-CT/DRT/TIT/AN-88/234 ..... N91-11136 #

CNES-CT/DRT/TIT/IO-88/126 ..... N91-11334 #

CNES-CT/DRT/TIT/OE-88/144 ..... N91-11521 #

CNIC-00234 ..... N91-11544 #

CONF-890310-7 ..... N91-11234 #
CONF-890754-2 ..... N91-11083 #
CONF-891024-8 ..... N91-11071 #
CONF-891024-9 ..... N91-11070 #
CONF-891119-140 ..... N91-11580 #
CONF-900133-3 ..... N91-11571 #
CONF-900466-85 ..... N91-11104 #
CONF-900466-86 ..... N91-11089 #
CONF-900466-89 ..... N91-11115 #
CONF-900489-3 ..... N91-11506 #
CONF-900528-3 ..... N91-11582 #
CONF-900562-8 ..... N91-11566 #
CONF-900577-2 ..... N91-11570 #
CONF-900577-3 ..... N91-11577 #
CONF-900591 ..... N91-11288 #
CONF-900603-32 ..... N91-11511 #
CONF-900623-19 ..... N91-11105 #
CONF-900708-1 ..... N91-11086 #
CONF-900716-1 ..... N91-11499 #
CONF-900731-2 ..... N91-11224 #
CONF-900756-40 ..... N91-11082 #
CONF-900756-41 ..... N91-11486 #
CONF-900756-44 ..... N91-11523 #
CONF-900757-5 ..... N91-11520 #
CONF-900791-2 ..... N91-11081 #
CONF-900801-30 ..... N91-11300 #
CONF-900801-31 ..... N91-11487 #
CONF-900801-33 ..... N91-11538 #
CONF-900802-7 ..... N91-11575 #
CONF-900807-1 ..... N91-11545 #
CONF-900813-1 ..... N91-11565 #
CONF-900830-2 ..... N91-11578 #
CONF-900854-1 ..... N91-11110 #
CONF-900856-1 ..... N91-11562 #
CONF-900912-2 ..... N91-11500 #
CONF-900914-1 ..... N91-11567 #
CONF-900918-6 ..... N91-11547 #
CONF-900936-4 ..... N91-11568 #
CONF-900936-5 ..... N91-11569 #
CONF-900936-6 ..... N91-11103 #
CONF-900936-7 ..... N91-11111 #
CONF-900936-8 ..... N91-11584 #
CONF-900944-2 ..... N91-11579 #
CONF-900964-2 ..... N91-11084 #
CONF-900970-3 ..... N91-11479 #
CONF-900975-1 ..... N91-11100 #
CONF-900989-1 ..... N91-11287 #
CONF-901008-1 ..... N91-11213 #
CONF-901009-2 ..... N91-11212 #
CONF-901025-7 ..... N91-11535 #
CONF-901025-8 ..... N91-11536 #
CONF-901035-1 ..... N91-11114 #
CONF-901071-6 ..... N91-11214 #
CONF-901073-7 ..... N91-11109 #
CONF-901101-1 ..... N91-11221 #
CONF-901101-4 ..... N91-11465 #
CONF-901101-22 ..... N91-11466 #
CONF-901101-24 ..... N91-11408 #
CONF-901104-1 ..... N91-11069 #
CONF-901105-1 ..... N91-11108 #
CONF-901105-3 ..... N91-11558 #
CONF-901105-4 ..... N91-11559 #
CONF-901105-6 ..... N91-11573 #
CONF-901105-7 ..... N91-11563 #
CONF-901105-8 ..... N91-11560 #
CONF-901105-9 ..... N91-11561 #
CONF-901105-11 ..... N91-11576 #
CONF-901109-1 ..... N91-11188 #
CONF-901109-2 ..... N91-11289 #
CONF-901109-3 ..... N91-11128 #
CONF-901109-7 ..... N91-11189 #
CONF-901109-8 ..... N91-11190 #
CONF-901109-10 ..... N91-11330 #
CONF-901109-10 ..... N91-11410 #
CONF-901109-11 ..... N91-11286 #
CONF-901109-13 ..... N91-11222 #
CONF-901109-14 ..... N91-10917 #
CONF-901109-16 ..... N91-11153 #
CONF-901109-17 ..... N91-11263 #
CONF-901109-18 ..... N91-11185 #
CONF-901116-4 ..... N91-11590 #
CONF-901116-5 ..... N91-11522 #
CONF-901121-1 ..... N91-11414 #
CONF-901121-3 ..... N91-11514 #
CONF-901121-6 ..... N91-11431 #
CONF-901124-1 ..... N91-11235 #
CONF-901124-2 ..... N91-11154 #
CONF-901150-1 ..... N91-11434 #
CONF-901150-2 ..... N91-11351 #
CONF-901177-1 ..... N91-11123 #
CONF-901179-1 ..... N91-11409 #
CONF-901194-1 ..... N91-11186 #
CONF-8905344-1 ..... N91-11264 #
CONF-8907114-4 ..... N91-11098 #
CONF-8907215-1 ..... N91-11267 #
CONF-8908246 ..... N91-11640 #
CONF-8911224-1 ..... N91-11301 #
CONF-9002131-3 ..... N91-11413 #
CONF-9003200-1 ..... N91-11236 #
CONF-9003202-1 ..... N91-11412 #
CONF-9004136-9-REV-1 ..... N91-11032 #
CONF-9004243-1 ..... N91-11231 #
CONF-9005248-2 ..... N91-11633* #
CONF-9005270-1 ..... N91-11102 #
CONF-9005272-1 ..... N91-11309 #
CONF-9005273-1 ..... N91-11505 #
CONF-9006105-12 ..... N91-11537 #
CONF-9006176-15 ..... N91-11156 #
CONF-9006194-2 ..... N91-11353 #
CONF-9006212-3-REV-1 ..... N91-11635 #
CONF-9006220-4 ..... N91-11352 #
CONF-9006243-2 ..... N91-11159 #
CONF-9006267-3 ..... N91-11574 #
CONF-9006273-1 ..... N91-11583 #
CONF-9007136-4 ..... N91-11546 #
CONF-9007159-1 ..... N91-11600 #
CONF-9007162-1 ..... N91-11079 #
CONF-9008134-3 ..... N91-11204 #
CONF-9008149-ABSTS ..... N91-11572 #
CONF-9008153-1 ..... N91-11308 #
CONF-9009141-4 ..... N91-11101 #
CONF-9009141-5 ..... N91-11503 #
CONF-9009154-2 ..... N91-11601 #
CONF-9009174-1 ..... N91-11080 #
CONF-9009174-2 ..... N91-11209 #
CONF-9009200-17 ..... N91-11162 #
CONF-9009236-1 ..... N91-11485 #
CONF-9009238-1 ..... N91-11290 #
CONF-9009241-1 ..... N91-11230 #
CONF-9009247-1 ..... N91-11158 #
CONF-9009249-1 ..... N91-11299 #
CONF-9009261-1 ..... N91-11509 #
CONF-9010172-3 ..... N91-11033 #
CONF-9010185-1 ..... N91-11603 #

CRDEC-CR-075 ..... N91-11552 #

CRIE-Y-90002 ..... N91-11292 #

CS-9001 ..... N91-11460 #
CS-9005 ..... N91-11461 #

CWI-AM-R8923 ..... N91-11438 #
CWI-AM-R8924-PT-1 ..... N91-11439 #
CWI-AM-R9001 ..... N91-11440 #
CWI-AM-R9002-PT-3 ..... N91-11441 #
CWI-AM-R9003 ..... N91-11442 #

CWI-BS-R8924 ..... N91-11443 #
CWI-BS-R8925 ..... N91-11444 #
CWI-BS-R8926 ..... N91-11475 #
CWI-BS-R8927 ..... N91-11476 #
CWI-BS-R8928 ..... N91-11477 #
CWI-BS-R8929 ..... N91-11166 #
CWI-BS-R8931 ..... N91-11426 #
CWI-BS-R8933 ..... N91-11445 #
CWI-BS-R8934 ..... N91-11483 #
CWI-BS-R9001 ..... N91-11398 #

CWI-BS-R9002 ..... N91-11446 #

CWI-NM-R8911 ..... N91-11450 #
CWI-NM-R8915 ..... N91-11399 #
CWI-NM-R8916 ..... N91-11167 #
CWI-NM-R8917 ..... N91-11553 #
CWI-NM-R8918 ..... N91-11427 #
CWI-NM-R8920 ..... N91-11447 #
CWI-NM-R8921 ..... N91-11448 #
CWI-NM-R8922 ..... N91-10905 #
CWI-NM-R8923 ..... N91-11449 #
CWI-NM-R8924 ..... N91-11450 #
CWI-NM-R9001 ..... N91-11428 #
CWI-NM-R9002 ..... N91-11451 #
CWI-NM-R9003 ..... N91-11554 #

DC-Y5-00400 ..... N91-11276* #

DE90-000304 ..... N91-11282 #
DE90-000355 ..... N91-11557 #
DE90-000356 ..... N91-11285 #
DE90-000359 ..... N91-11295 #
DE90-000361 ..... N91-11283 #
DE90-000362 ..... N91-11280 #
DE90-000364 ..... N91-11296 #
DE90-000366 ..... N91-11284 #
DE90-000370 ..... N91-11286 #
DE90-000372 ..... N91-11297 #
DE90-000373 ..... N91-11287 #
DE90-000377 ..... N91-11572 #
DE90-000490 ..... N91-11288 #
DE90-007150 ..... N91-11108 #
DE90-008748 ..... N91-11188 #
DE90-008971 ..... N91-11213 #
DE90-009662 ..... N91-11194 #
DE90-009697 ..... N91-11298 #
DE90-009705 ..... N91-11212 #
DE90-009834 ..... N91-11289 #
DE90-010820 ..... N91-11221 #
DE90-010872 ..... N91-11414 #
DE90-010929 ..... N91-11128 #
DE90-011636 ..... N91-11434 #
DE90-012000 ..... N91-11465 #
DE90-012091 ..... N91-11514 #
DE90-012964 ..... N91-11189 #
DE90-013661 ..... N91-11190 #
DE90-014447 ..... N91-11069 #
DE90-014843 ..... N91-11191 #
DE90-014847 ..... N91-11127 #
DE90-014852 ..... N91-11516 #
DE90-014863 ..... N91-11151 #
DE90-014865 ..... N91-11057 #
DE90-014911 ..... N91-11633* #
DE90-014979 ..... N91-11330 #
DE90-015057 ..... N91-11351 #
DE90-015060 ..... N91-11466 #
DE90-015120 ..... N91-11214 #
DE90-015128 ..... N91-11064 #
DE90-015153 ..... N91-11558 #
DE90-015162 ..... N91-11408 #
DE90-015192 ..... N91-11409 #
DE90-015392 ..... N91-11222 #
DE90-015405 ..... N91-11147 #
DE90-015538 ..... N91-11123 #
DE90-015562 ..... N91-11153 #
DE90-015563 ..... N91-11263 #
DE90-015596 ..... N91-10917 #
DE90-015606 ..... N91-11185 #
DE90-015625 ..... N91-11511 #
DE90-015698 ..... N91-11559 #
DE90-015715 ..... N91-11235 #
DE90-015829 ..... N91-11410 #
DE90-015911 ..... N91-11230 #
DE90-015912 ..... N91-11382 #
DE90-015989 ..... N91-11573 #
DE90-015993 ..... N91-11154 #
DE90-016030 ..... N91-11186 #
DE90-016041 ..... N91-11431 #
DE90-016130 ..... N91-11092 #
DE90-016187 ..... N91-11411 #
DE90-016211 ..... N91-11032 #
DE90-016302 ..... N91-11223 #
DE90-016487 ..... N91-11485 #
DE90-016521 ..... N91-11603 #
DE90-016535 ..... N91-11079 #
DE90-016538 ..... N91-11600 #
DE90-016639 ..... N91-11149 #
DE90-016672 ..... N91-11525 #
DE90-016673 ..... N91-11526 #
DE90-016692 ..... N91-11155 #
DE90-016704 ..... N91-11234 #
DE90-016719 ..... N91-11601 #
DE90-016860 ..... N91-11156 #
DE90-016927 ..... N91-11204 #
DE90-017028 ..... N91-11560 #
DE90-017031 ..... N91-11561 #
DE90-017032 ..... N91-11562 #
DE90-017036 ..... N91-11563 #
DE90-017038 ..... N91-11033 #
DE90-017040 ..... N91-11290 #
DE90-017089 ..... N91-11157 #
DE90-017239 ..... N91-11236 #
DE90-017252 ..... N91-11264 #
DE90-017253 ..... N91-11083 #
DE90-017273 ..... N91-11291 #
DE90-017284 ..... N91-11497 #
DE90-017288 ..... N91-11225 #
DE90-017311 ..... N91-11122 #
DE90-017312 ..... N91-11226 #
DE90-017316 ..... N91-11308 #
DE90-017327 ..... N91-11520 #
DE90-017334 ..... N91-11080 #
DE90-017336 ..... N91-11512 #
DE90-017337 ..... N91-11412 #
DE90-017403 ..... N91-11574 #
DE90-017447 ..... N91-11504 #
DE90-017502 ..... N91-11097 #
DE90-017509 ..... N91-11498 #
DE90-017510 ..... N91-11187 #
DE90-017518 ..... N91-11081 #
DE90-017519 ..... N91-11635 #
DE90-017525 ..... N91-11082 #
DE90-017526 ..... N91-11098 #
DE90-017528 ..... N91-11499 #
DE90-017600 ..... N91-11152 #
DE90-017605 ..... N91-11533 #
DE90-017608 ..... N91-11099 #
DE90-017611 ..... N91-11124 #
DE90-017617 ..... N91-11634 #
DE90-017632 ..... N91-11500 #
DE90-017647 ..... N91-11158 #
DE90-017653 ..... N91-11501 #
DE90-017654 ..... N91-11604 #
DE90-017656 ..... N91-11564 #
DE90-017661 ..... N91-11102 #
DE90-017665 ..... N91-11299 #
DE90-017668 ..... N91-11159 #
DE90-017669 ..... N91-11565 #
DE90-017674 ..... N91-11413 #
DE90-017680 ..... N91-11575 #
DE90-017682 ..... N91-11300 #
DE90-017688 ..... N91-11100 #
DE90-017704 ..... N91-11566 #
DE90-017734 ..... N91-11536 #
DE90-017735 ..... N91-11567 #
DE90-017736 ..... N91-11568 #
DE90-017743 ..... N91-11209 #
DE90-017744 ..... N91-11103 #
DE90-017756 ..... N91-11505 #
DE90-017758 ..... N91-11224 #
DE90-017763 ..... N91-11576 #
DE90-017768 ..... N91-11084 #
DE90-017769 ..... N91-11569 #
DE90-017774 ..... N91-11534 #
DE90-017792 ..... N91-11352 #
DE90-017795 ..... N91-11353 #
DE90-017798 ..... N91-11577 #
DE90-017804 ..... N91-11582 #
DE90-017806 ..... N91-11578 #
DE90-017809 ..... N91-11479 #
DE90-017811 ..... N91-11583 #
DE90-017812 ..... N91-11579 #
DE90-017820 ..... N91-11344 #
DE90-017822 ..... N91-11109 #
DE90-017831 ..... N91-11537 #
DE90-017836 ..... N91-11580 #
DE90-017854 ..... N91-11646 #
DE90-017856 ..... N91-11104 #
DE90-017858 ..... N91-11538 #
DE90-017861 ..... N91-11570 #
DE90-017862 ..... N91-11309 #
DE90-017863 ..... N91-11105 #
DE90-017864 ..... N91-11487 #
DE90-017886 ..... N91-11542 #
DE90-017889 ..... N91-11539 #
DE90-018006 ..... N91-11265 #
DE90-018007 ..... N91-11301 #
DE90-018013 ..... N91-11571 #
DE90-018014 ..... N91-11506 #
DE90-018019 ..... N91-11535 #
DE90-018021 ..... N91-11513 #
DE90-018023 ..... N91-11502 #
DE90-018037 ..... N91-11467 #
DE90-018038 ..... N91-11085 #
DE90-018040 ..... N91-11267 #
DE90-018041 ..... N91-11070 #
DE90-018042 ..... N91-11503 #
DE90-018043 ..... N91-11071 #
DE90-018044 ..... N91-11101 #
DE90-018046 ..... N91-11486 #
DE90-018049 ..... N91-11086 #
DE90-508023 ..... N91-11656 #
DE90-508070 ..... N91-11120 #
DE90-513706 ..... N91-11331 #
DE90-513707 ..... N91-11484 #
DE90-513710 ..... N91-11581 #
DE90-513788 ..... N91-11636 #
DE90-513789 ..... N91-11637 #
DE90-513790 ..... N91-11638 #
DE90-513791 ..... N91-11639 #
DE90-513793 ..... N91-11640 #
DE90-513926 ..... N91-11543 #
DE90-520207 ..... N91-11106 #
DE90-520210 ..... N91-11227 #
DE90-628758 ..... N91-11524 #
DE90-631599 ..... N91-11589 #
DE90-631600 ..... N91-11471 #
DE90-634244 ..... N91-11160 #
DE90-634382 ..... N91-11472 #
DE90-637389 ..... N91-11507 #
DE90-637548 ..... N91-11544 #
DE90-702432 ..... N91-11051 #
DE90-796146 ..... N91-11146 #
DE91-000019 ..... N91-11141 #
DE91-000035 ..... N91-11110 #
DE91-000036 ..... N91-11231 #
DE91-000038 ..... N91-11111 #
DE91-000043 ..... N91-11584 #
DE91-000044 ..... N91-11089 #
DE91-000060 ..... N91-11420 #
DE91-000074 ..... N91-11515 #
DE91-000075 ..... N91-11195 #
DE91-000098 ..... N91-11131 #
DE91-000128 ..... N91-11540 #
DE91-000148 ..... N91-11651 #
DE91-000170 ..... N91-11161 #
DE91-000176 ..... N91-11545 #
DE91-000177 ..... N91-11590 #
DE91-000196 ..... N91-11112 #
DE91-000208 ..... N91-11546 #
DE91-000210 ..... N91-11522 #
DE91-000286 ..... N91-11547 #
DE91-000357 ..... N91-11585 #
DE91-000360 ..... N91-11113 #
DE91-000367 ..... N91-11114 #
DE91-000375 ..... N91-11115 #
DE91-000384 ..... N91-11125 #
DE91-000433 ..... N91-11162 #
DE91-000555 ..... N91-11509 #
DE91-000561 ..... N91-11523 #
DE91-000575 ..... N91-11548 #
DE91-000598 ..... N91-11549 #
DE91-701405 ..... N91-11292 #
DE91-701463 ..... N91-11293 #
DE91-701465 ..... N91-11087 #
DE91-701466 ..... N91-11129 #
DE91-701468 ..... N91-11130 #
DE91-701469 ..... N91-11602 #

DFVLR-FB-88-14 ..... N91-11381 #
DFVLR-FB-88-30 ..... N91-11198 #
DFVLR-FB-88-34 ..... N91-11473 #
DFVLR-FB-88-49 ..... N91-10965 #
DFVLR-FB-88-55 ..... N91-11199 #

DOE/CE-90025/2 ..... N91-11225 #
DOE/CE-90029/3 ..... N91-11223 #

DOE/CH-10093/78 ..... N91-11284 #

DOE/EH-0158T ..... N91-11526 #

DOE/ER-0463P ..... N91-11513 #
DOE/ER-05490/112 ..... N91-11574 #
DOE/ER-13808/T1 ..... N91-11504 #
DOE/ER-13958/16 ..... N91-11501 #
DOE/ER-14064/1 ..... N91-11411 #
DOE/ER-40231/T8 ..... N91-11497 #
DOE/ER-40319/3 ..... N91-11512 #
DOE/ER-45328/4 ..... N91-11099 #
DOE/ER-45370/3 ..... N91-11124 #
DOE/ER-52122/5-VOL-5 ..... N91-11152 #
DOE/ER-52127/72 ..... N91-11534 #
DOE/ER-53175/5 ..... N91-11549 #
DOE/ER-53198/160 ..... N91-11535 #
DOE/ER-53240/3 ..... N91-11533 #
DOE/ER-75527/2 ..... N91-11604 #

DOE/ET-53088/447 ..... N91-11540 #
DOE/ET-53088/450 ..... N91-11651 #
DOE/ET-53088/452 ..... N91-11634 #
DOE/ET-53088/455 ..... N91-11548 #

DOE/ID-10287 ..... N91-11157 #

DOE/MC-23270/2876 ..... N91-11298 #
DOE/MC-24207/2852 ..... N91-11194 #

ISBN-951-38-3647

DOE/METC-90-6112 ..... N91-11288 #

DOE/NE-37963/12 ..... N91-11092 #

DOE/OR-00033/T443 ..... N91-11498 #
DOE/OR-00033/T444 ..... N91-11187 #

DOE/PC-70507/T3 ..... N91-11539 #
DOE/PC-90274/T8 ..... N91-11542 #

DOE/PE-0095P ..... N91-11127 #

DOE/SF-16306/23 ..... N91-11291 #

DOT/FAA/CT-90/9 ..... N91-11015 #

DOT/FRA/ORD-90/07 ..... N91-11132 #

E-4658 ..... N91-10849* #
E-5661 ..... N91-11074* #
E-5679 ..... N91-11062* #
E-5709 ..... N91-11058* #
E-5717 ..... N91-11493* #
E-5719 ..... N91-11205* #
E-5724 ..... N91-11059* #
E-5731 ..... N91-11494* #
E-5739 ..... N91-11061* #
E-5791 ..... N91-11192* #
E-5795 ..... N91-11495* #
E-5817 ..... N91-11060* #

ECL-89-21 ..... N91-11088 #
ECL-90-01 ..... N91-11229 #

EGG-M-90041 ..... N91-11128 #
EGG-M-90064 ..... N91-11189 #

EPA/IMSD-89/008 ..... N91-11595 #
EPA/IMSD-90/003 ..... N91-11594 #

EPA/600/S2-90/039 ..... N91-11305 #
EPA/600/3-90/059 ..... N91-11303 #
EPA/600/8-90/053 ..... N91-11078 #

ERIM-205400-8-F ..... N91-11396* #

ESA-TT-1116 ..... N91-11197 #
ESA-TT-1127 ..... N91-11381 #
ESA-TT-1135 ..... N91-11473 #
ESA-TT-1138 ..... N91-11198 #
ESA-TT-1141 ..... N91-10965 #
ESA-TT-1144 ..... N91-11199 #

ETN-90-97580 ..... N91-11076 #
ETN-90-97630 ..... N91-10920 #
ETN-90-97646 ..... N91-11273 #
ETN-90-97653 ..... N91-11438 #
ETN-90-97654 ..... N91-11439 #
ETN-90-97655 ..... N91-11440 #
ETN-90-97656 ..... N91-11441 #
ETN-90-97657 ..... N91-11442 #
ETN-90-97658 ..... N91-11443 #
ETN-90-97659 ..... N91-11444 #
ETN-90-97660 ..... N91-11475 #
ETN-90-97661 ..... N91-11476 #
ETN-90-97662 ..... N91-11477 #
ETN-90-97663 ..... N91-11166 #
ETN-90-97664 ..... N91-11426 #
ETN-90-97666 ..... N91-11445 #
ETN-90-97667 ..... N91-11483 #
ETN-90-97668 ..... N91-11398 #
ETN-90-97669 ..... N91-11446 #
ETN-90-97670 ..... N91-11399 #
ETN-90-97671 ..... N91-11167 #
ETN-90-97672 ..... N91-11553 #
ETN-90-97673 ..... N91-11427 #
ETN-90-97674 ..... N91-11447 #
ETN-90-97675 ..... N91-11448 #
ETN-90-97676 ..... N91-10905 #
ETN-90-97677 ..... N91-11449 #
ETN-90-97678 ..... N91-11450 #
ETN-90-97679 ..... N91-11428 #
ETN-90-97680 ..... N91-11451 #
ETN-90-97681 ..... N91-11554 #
ETN-90-97682 ..... N91-11348 #
ETN-90-97683 ..... N91-11269 #
ETN-90-97706 ..... N91-11527 #
ETN-90-97707 ..... N91-11400 #
ETN-90-97708 ..... N91-11401 #
ETN-90-97709 ..... N91-11402 #
ETN-90-97710 ..... N91-11452 #
ETN-90-97711 ..... N91-11429 #
ETN-90-97712 ..... N91-11453 #
ETN-90-97713 ..... N91-11403 #
ETN-90-97714 ..... N91-11592 #
ETN-90-97715 ..... N91-11454 #

ETN-90-97719 ..... N91-11455 #
ETN-90-97720 ..... N91-11478 #
ETN-90-97721 ..... N91-11456 #
ETN-90-97722 ..... N91-11457 #
ETN-90-97723 ..... N91-11458 #
ETN-90-97724 ..... N91-11459 #
ETN-90-97725 ..... N91-11460 #
ETN-90-97726 ..... N91-11461 #
ETN-90-97741 ..... N91-11468 #
ETN-90-97744 ..... N91-11469 #
ETN-90-97745 ..... N91-11470 #
ETN-90-97751 ..... N91-11228 #
ETN-90-97752 ..... N91-11586 #
ETN-90-97754 ..... N91-11294 #
ETN-90-97765 ..... N91-11210 #
ETN-90-97770 ..... N91-11116 #
ETN-90-97773 ..... N91-11196 #
ETN-90-97777 ..... N91-11047 #
ETN-90-97781 ..... N91-11550 #
ETN-90-97788 ..... N91-11653 #
ETN-90-97789 ..... N91-11654 #
ETN-90-97791 ..... N91-11551 #
ETN-90-97793 ..... N91-11333 #
ETN-90-97801 ..... N91-11508 #
ETN-90-97802 ..... N91-11143 #
ETN-90-97809 ..... N91-11521 #
ETN-90-97813 ..... N91-11334 #
ETN-90-97814 ..... N91-11136 #
ETN-90-97815 ..... N91-11215 #
ETN-90-97816 ..... N91-11088 #
ETN-90-97817 ..... N91-11229 #
ETN-90-97824 ..... N91-11065 #
ETN-90-97827 ..... N91-11404 #
ETN-90-97828 ..... N91-11150 #
ETN-90-97829 ..... N91-11462 #
ETN-90-97834 ..... N91-11620 #
ETN-90-97840 ..... N91-11383 #
ETN-90-97841 ..... N91-11016 #
ETN-90-97845 ..... N91-11025 #
ETN-90-97846 ..... N91-10935 #
ETN-90-97848 ..... N91-11424 #
ETN-90-97857 ..... N91-11066 #
ETN-90-97858 ..... N91-11281 #
ETN-90-97859 ..... N91-11168 #
ETN-90-97861 ..... N91-11463 #
ETN-90-97862 ..... N91-11017 #
ETN-90-97863 ..... N91-11490 #
ETN-90-97864 ..... N91-11169 #
ETN-90-97867 ..... N91-11077 #
ETN-90-97868 ..... N91-11588 #
ETN-90-97869 ..... N91-11491 #
ETN-90-97877 ..... N91-11517
ETN-90-97878 ..... N91-10963 #
ETN-90-97879 ..... N91-11018 #
ETN-90-97882 ..... N91-11201 #
ETN-90-97893 ..... N91-11621 #
ETN-90-97894 ..... N91-11202 #
ETN-90-97895 ..... N91-11335 #
ETN-90-97897 ..... N91-11067 #
ETN-90-97898 ..... N91-11253 #
ETN-90-97899 ..... N91-11137 #
ETN-90-97900 ..... N91-11019 #
ETN-90-97901 ..... N91-11203 #
ETN-90-97902 ..... N91-11138 #
ETN-90-97903 ..... N91-11193 #
ETN-90-97931 ..... N91-11307 #
ETN-90-97932 ..... N91-11107 #
ETN-90-97933 ..... N91-11020 #
ETN-90-97934 ..... N91-11021 #
ETN-90-97935 ..... N91-11073 #
ETN-90-97936 ..... N91-11416 #
ETN-90-97937 ..... N91-11266 #
ETN-90-97979 ..... N91-11665 #
ETN-90-97981 ..... N91-11312 #
ETN-90-97982 ..... N91-11528 #
ETN-90-97983 ..... N91-11529 #
ETN-90-97984 ..... N91-11530 #
ETN-90-97985 ..... N91-11531 #
ETN-90-97986 ..... N91-11496 #
ETN-90-97987 ..... N91-11541 #
ETN-90-97989 ..... N91-11274 #
ETN-90-97999 ..... N91-11197 #
ETN-90-98000 ..... N91-11381 #
ETN-90-98001 ..... N91-11473 #
ETN-90-98002 ..... N91-11198 #
ETN-90-98003 ..... N91-10965 #
ETN-90-98004 ..... N91-11199 #
ETN-90-98015 ..... N91-11211 #
ETN-90-98016 ..... N91-11117 #
ETN-90-98017 ..... N91-11090 #
ETN-90-98018 ..... N91-11075 #
ETN-90-98019 ..... N91-11133 #
ETN-90-98020 ..... N91-11345 #
ETN-90-98021 ..... N91-11587 #

FI-452-TB-67 ..... N91-11517

FNAL-TM-1676 ..... N91-11086 #

FNAL/C-90/140 ..... N91-11511 #

FR-19556-1 ..... N91-11049* #

FSU-HEP-041090 ..... N91-11412 #

GL-TR-90-0068 ..... N91-11268 #

GRI-90/0134 ..... N91-11170 #

HEI/RR-89/28 ..... N91-11357 #

IAEA-CN-53/C-2-2-(2) ..... N91-11535 #
IAEA-CN-53/C-4-7 ..... N91-11536 #

ICASE-90-60 ..... N91-11430* #
ICASE-90-63 ..... N91-11397* #

ICOMP-90-23 ..... N91-11192* #

IFSI-89-16 ..... N91-11047 #
IFSI-89-20 ..... N91-11550 #
IFSI-90-5 ..... N91-11653 #
IFSI-90-6 ..... N91-11654 #
IFSI-90-8 ..... N91-11551 #
IFSI-90-10 ..... N91-11333 #
IFSI-90-19 ..... N91-11508 #
IFSI-90-20 ..... N91-11143 #

IFSR-447 ..... N91-11540 #
IFSR-450 ..... N91-11651 #
IFSR-452 ..... N91-11634 #
IFSR-455 ..... N91-11548 #

ILA-87-A-02 ..... N91-11018 #

INIS-BR-2121 ..... N91-11524 #

INIS-MF-12679 ..... N91-11507 #

INPE-4576-RPE/568 ..... N91-11510 #
INPE-4863-TDL/374 ..... N91-11277 #
INPE-5012-TDL/400 ..... N91-11422 #
INPE-5014-TDL/401 ..... N91-11423 #
INPE-5022-TDL/402 ..... N91-11332 #
INPE-5034-RPE/619 ..... N91-11279 #
INPE-5035-TDL/403 ..... N91-11278 #
INPE-5037-RPE/620 ..... N91-11048 #
INPE-5039-PRE/1572 ..... N91-11415 #
INPE-5041-TDL/404 ..... N91-11275 #
INPE-5059-TDL/405 ..... N91-11652 #
INPE-5067-TDL/406 ..... N91-11421 #
INPE-5077-TDL/341 ..... N91-11418 #
INPE-5078-TDL/412 ..... N91-11419 #
INPE-5083-TDL/417 ..... N91-11343 #
INPE-5086-NTE/294 ..... N91-11417 #
INPE-5091-RPE/624 ..... N91-11388 #

INS-807 ..... N91-11656 #

INTEL/311847-001 ..... N91-11482 #
INTEL/311848-001 ..... N91-11481 #
INTEL/311849-001 ..... N91-11480 #

IRF-PREPRINT-115 ..... N91-11541 #

IS-M-623 ..... N91-11234 #
IS-M-627 ..... N91-11264 #
IS-M-636 ..... N91-11083 #
IS-M-638 ..... N91-11267 #
IS-M-639 ..... N91-11101 #
IS-M-640 ..... N91-11503 #
IS-M-641 ..... N91-11571 #
IS-M-642 ..... N91-11506 #
IS-M-643 ..... N91-11486 #
IS-M-645 ..... N91-11071 #
IS-M-646 ..... N91-11070 #

IS-T-1474 ..... N91-11112 #
IS-T-1489 ..... N91-11564 #

ISAL-89-0098 ..... N91-11065 #

ISBN-0-309-04956-3 ..... N91-10979 #
ISBN-0-8213-1625-7 ..... N91-11270 #
ISBN-90-370-0036-3 ..... N91-11294 #
ISBN-92-835-0547-6 ..... N91-10967 #
ISBN-92-835-0562-X ..... N91-10981 #
ISBN-92-835-0563-8 ..... N91-10978 #
ISBN-92-835-0573-5 ..... N91-11022 #
ISBN-92-835-0576-X ..... N91-11358 #
ISBN-92-835-0577-8 ..... N91-11240 #
ISBN-951-38-3647 ..... N91-11665 #

ISSN--0078-3781 ..... N91-11090 #

ISSN-0018-3781 ..... N91-11075 #
ISSN-0069-5882 ..... N91-11335 #
ISSN-0069-5882 ..... N91-11621 #
ISSN-0069-5887 ..... N91-11202 #
ISSN-0078-379X ..... N91-11211 #
ISSN-0078-3781 ..... N91-11117 #
ISSN-0078-3781 ..... N91-11133 #
ISSN-0078-3781 ..... N91-11345 #
ISSN-0078-3781 ..... N91-11587 #
ISSN-0169-2690 ..... N91-11468 #
ISSN-0169-2690 ..... N91-11469 #
ISSN-0169-2690 ..... N91-11470 #
ISSN-0348-7539 ..... N91-11312 #
ISSN-0348-7539 ..... N91-11496 #
ISSN-0348-7539 ..... N91-11528 #
ISSN-0348-7539 ..... N91-11529 #
ISSN-0348-7539 ..... N91-11530 #
ISSN-0348-7539 ..... N91-11531 #
ISSN-0360-859X ..... N91-10979 #
ISSN-0374-1257 ..... N91-11077 #
ISSN-0374-1257 ..... N91-11491 #
ISSN-0374-1257 ..... N91-11588 #
ISSN-0436-1199 ..... N91-11193 #
ISSN-0452-2928 ..... N91-11052 #
ISSN-0452-2982 ..... N91-10966 #
ISSN-0452-2982 ..... N91-11026 #
ISSN-0452-2982 ..... N91-11035 #
ISSN-0452-2982 ..... N91-11036 #
ISSN-0452-2982 ..... N91-11051 #
ISSN-0452-2982 ..... N91-11200 #
ISSN-0786-4558 ..... N91-11665 #
ISSN-0915-633X ..... N91-11532 #
ISSN-0922-5641 ..... N91-11400 #
ISSN-0922-5641 ..... N91-11401 #
ISSN-0922-5641 ..... N91-11402 #
ISSN-0922-5641 ..... N91-11403 #
ISSN-0922-5641 ..... N91-11429 #
ISSN-0922-5641 ..... N91-11452 #
ISSN-0922-5641 ..... N91-11453 #
ISSN-0922-5641 ..... N91-11454 #
ISSN-0922-5641 ..... N91-11455 #
ISSN-0922-5641 ..... N91-11478 #
ISSN-0922-5641 ..... N91-11527 #
ISSN-0922-5641 ..... N91-11592 #
ISSN-0932-8599 ..... N91-11253 #

JAERI-M-90-010 ..... N91-11120 #
JAERI-M-90-014 ..... N91-11581 #
JAERI-M-90-061 ..... N91-11106 #
JAERI-M-90-064 ..... N91-11227 #

JIAA-TR-99 ..... N91-10934* #

JINR-E-4-89-275 ..... N91-11589 #

JINR-R-10-89-454 ..... N91-11160 #
JINR-R-11-89-191 ..... N91-11471 #
JINR-R-11-89-382 ..... N91-11472 #

JPRS-ULS-89-003 ..... N91-11354 #

JRC-10-90 ..... N91-11489 #
JRC-90-02 ..... N91-11157 #

JTN-90-80120 ..... N91-11035 #
JTN-90-80121 ..... N91-11051 #
JTN-90-80122 ..... N91-11026 #
JTN-90-80134 ..... N91-11200 #
JTN-90-80135 ..... N91-10966 #
JTN-90-80141 ..... N91-11036 #
JTN-90-80142 ..... N91-11052 #

KCP-613-4118 ..... N91-11420 #
KCP-613-4404 ..... N91-11158 #

KEK-PR-89-2 ..... N91-11640 #

L-16741 ..... N91-10902* #
L-16748 ..... N91-11391* #
L-16828 ..... N91-11041* #
L-16840 ..... N91-10936* #

LA-UR-90-1845 ..... N91-11465 #
LA-UR-90-2389 ..... N91-11633* #
LA-UR-90-2562 ..... N91-11351 #
LA-UR-90-2571 ..... N91-11330 #
LA-UR-90-2577 ..... N91-11466 #
LA-UR-90-2637 ..... N91-11601 #
LA-UR-90-2828 ..... N91-11485 #
LA-UR-90-3046 ..... N91-11162 #
LA-UR-90-3048 ..... N91-11114 #
LA-UR-90-3160 ..... N91-11115 #
LA-UR-90-3293 ..... N91-11522 #
LA-UR-90-3311 ..... N91-11546 #

LA-UR-90-3344 ..... N91-11590 #
LA-UR-90-3345 ..... N91-11545 #

LA-11882-MS ..... N91-11646 #
LA-11884-MS ..... N91-11085 #
LA-11915-MS ..... N91-11502 #

LAAS-90041 ..... N91-11215 #

LBL-29078 ..... N91-11149 #
LBL-29258 ..... N91-11585 #
LBL-29311 ..... N91-11113 #
LBL-29312 ..... N91-11161 #

LC-90-12783 ..... N91-11270 #
LC-90-34787 ..... N91-10979 #

MBB-UD-0570-90-PUB ..... N91-11383 #

MBB-Z-0299-89-PUB ..... N91-11066 #
MBB-Z-0305-90-PUB ..... N91-11201 #

MBB/FE121/S/PUB/329 ..... N91-11016 #
MBB/FE122/S/PUB/387 ..... N91-10935 #
MBB/FE122/S/PUB/388 ..... N91-11424 #

MBB/FYT256/S/PUB/361/A ..... N91-11025 #

MCR-89-559 ..... N91-11432* #

MEMO-855 ..... N91-11468 #
MEMO-858-PT-1 ..... N91-11469 #
MEMO-859 ..... N91-11470 #

MEMT-5 ..... N91-11294 #

MHD-ITC-90-133 ..... N91-11542 #

MITT-69 ..... N91-11621 #
MITT-70 ..... N91-11202 #
MITT-71 ..... N91-11335 #

MPE-217 ..... N91-11620 #

MPIS-MITT-93 ..... N91-11077 #
MPIS-MITT-95 ..... N91-11588 #
MPIS-MITT-96 ..... N91-11491 #

MPIS-7/1990 ..... N91-11193 #

MTB-1058-89 ..... N91-11121* #

NAL-TM-591 ..... N91-11200 #
NAL-TM-592 ..... N91-10966 #
NAL-TM-594 ..... N91-11035 #
NAL-TM-595 ..... N91-11051 #
NAL-TM-596 ..... N91-11026 #
NAL-TM-596-1 ..... N91-11036 #
NAL-TM-599 ..... N91-11052 #

NAS 1.15:4213 ..... N91-11391* #
NAS 1.15:101854 ..... N91-11118* #
NAS 1.15:102150 ..... N91-11664* #
NAS 1.15:102164 ..... N91-11356* #
NAS 1.15:102260 ..... N91-11384* #
NAS 1.15:102649 ..... N91-11072* #
NAS 1.15:102683 ..... N91-10904* #
NAS 1.15:102732 ..... N91-10918* #
NAS 1.15:102734 ..... N91-10919* #
NAS 1.15:102735 ..... N91-11252* #
NAS 1.15:102855 ..... N91-10933* #
NAS 1.15:102941 ..... N91-11389* #
NAS 1.15:102969 ..... N91-11633* #
NAS 1.15:103017 ..... N91-11028* #
NAS 1.15:103204 ..... N91-11074* #
NAS 1.15:103265 ..... N91-11062* #
NAS 1.15:103269 ..... N91-11058* #
NAS 1.15:103274 ..... N91-11205* #
NAS 1.15:103284 ..... N91-11061* #
NAS 1.15:103297 ..... N91-11390* #
NAS 1.15:103460 ..... N91-11040* #
NAS 1.15:103613 ..... N91-11059* #
NAS 1.15:103624 ..... N91-11192* #
NAS 1.15:103625 ..... N91-11494* #
NAS 1.15:103627 ..... N91-11495* #
NAS 1.15:103628 ..... N91-11493* #
NAS 1.15:103638 ..... N91-11060* #
NAS 1.15:103807 ..... N91-11121* #
NAS 1.26:4330 ..... N91-10964* #
NAS 1.26:176874 ..... N91-11276* #
NAS 1.26:177561 ..... N91-11425* #
NAS 1.26:180474 ..... N91-11050* #
NAS 1.26:180681 ..... N91-11474* #
NAS 1.26:182093 ..... N91-11027* #
NAS 1.26:182101 ..... N91-11430* #
NAS 1.26:182104 ..... N91-11397* #

NAS 1.26:183199 ..... N91-11049* #
NAS 1.26:183855 ..... N91-11034* #
NAS 1.26:183950 ..... N91-11054* #
NAS 1.26:183951 ..... N91-11055* #
NAS 1.26:183963 ..... N91-11432* #
NAS 1.26:183969 ..... N91-11031* #
NAS 1.26:183996 ..... N91-11037* #
NAS 1.26:183997 ..... N91-11038* #
NAS 1.26:184009 ..... N91-11091* #
NAS 1.26:184025 ..... N91-11233* #
NAS 1.26:184955 ..... N91-11649* #
NAS 1.26:185127 ..... N91-11134* #
NAS 1.26:185612 ..... N91-11148* #
NAS 1.26:185636 ..... N91-11310* #
NAS 1.26:185875 ..... N91-11619* #
NAS 1.26:185928 ..... N91-11392* #
NAS 1.26:186278 ..... N91-11605* #
NAS 1.26:186322 ..... N91-11393* #
NAS 1.26:186381 ..... N91-11144* #
NAS 1.26:186546 ..... N91-11053* #
NAS 1.26:186672 ..... N91-11641* #
NAS 1.26:186689 ..... N91-11039* #
NAS 1.26:186879 ..... N91-11488* #
NAS 1.26:186894 ..... N91-11396* #
NAS 1.26:186897 ..... N91-10903* #
NAS 1.26:187032 ..... N91-11042* #
NAS 1.26:187254 ..... N91-11165* #
NAS 1.26:187322 ..... N91-10934* #
NAS 1.26:187324 ..... N91-11642* #
NAS 1.26:187327 ..... N91-11311* #
NAS 1.26:187328 ..... N91-11606* #
NAS 1.26:187331 ..... N91-11380* #
NAS 1.26:187347 ..... N91-11216* #
NAS 1.26:187350 ..... N91-11555* #
NAS 1.26:187360 ..... N91-11407* #
NAS 1.26:187364 ..... N91-11645* #
NAS 1.26:187367 ..... N91-11644* #
NAS 1.26:187369 ..... N91-11342* #
NAS 1.26:187375 ..... N91-11387* #
NAS 1.55:3090 ..... N91-10936* #
NAS 1.55:10038-VOL-1 ..... N91-10839* #
NAS 1.55:10038-VOL-2 ..... N91-10868* #
NAS 1.55:10042 ..... N91-11591* #
NAS 1.60:3046 ..... N91-10902* #
NAS 1.60:3054 ..... N91-11041* #

NASA-CP-3090 ..... N91-10936* #
NASA-CP-10038-VOL-1 ..... N91-10839* #
NASA-CP-10038-VOL-2 ..... N91-10868* #
NASA-CP-10042 ..... N91-11591* #

NASA-CR-4330 ..... N91-10964* #
NASA-CR-176874 ..... N91-11276* #
NASA-CR-177561 ..... N91-11425* #
NASA-CR-180474 ..... N91-11050* #
NASA-CR-180681 ..... N91-11474* #
NASA-CR-182093 ..... N91-11027* #
NASA-CR-182101 ..... N91-11430* #
NASA-CR-182104 ..... N91-11397* #
NASA-CR-183199 ..... N91-11049* #
NASA-CR-183855 ..... N91-11034* #
NASA-CR-183950 ..... N91-11054* #
NASA-CR-183951 ..... N91-11055* #
NASA-CR-183963 ..... N91-11432* #
NASA-CR-183969 ..... N91-11031* #
NASA-CR-183996 ..... N91-11037* #
NASA-CR-183997 ..... N91-11038* #
NASA-CR-184009 ..... N91-11091* #
NASA-CR-184025 ..... N91-11233* #
NASA-CR-184955 ..... N91-11649* #
NASA-CR-185127 ..... N91-11134* #
NASA-CR-185612 ..... N91-11148* #
NASA-CR-185636 ..... N91-11310* #
NASA-CR-185875 ..... N91-11619* #
NASA-CR-185928 ..... N91-11392* #
NASA-CR-186278 ..... N91-11605* #
NASA-CR-186322 ..... N91-11393* #
NASA-CR-186381 ..... N91-11144* #
NASA-CR-186546 ..... N91-11053* #
NASA-CR-186672 ..... N91-11641* #
NASA-CR-186689 ..... N91-11039* #
NASA-CR-186879 ..... N91-11488* #
NASA-CR-186894 ..... N91-11396* #
NASA-CR-186897 ..... N91-10903* #
NASA-CR-187032 ..... N91-11042* #
NASA-CR-187254 ..... N91-11165* #
NASA-CR-187322 ..... N91-10934* #
NASA-CR-187324 ..... N91-11642* #
NASA-CR-187327 ..... N91-11311* #
NASA-CR-187328 ..... N91-11606* #
NASA-CR-187331 ..... N91-11380* #
NASA-CR-187347 ..... N91-11216* #
NASA-CR-187350 ..... N91-11555* #
NASA-CR-187360 ..... N91-11407* #
NASA-CR-187364 ..... N91-11645* #
NASA-CR-187367 ..... N91-11644* #

NASA-CR-187369 ..... N91-11342* #
NASA-CR-187375 ..... N91-11387* #

NASA-TM-4213 ..... N91-11391* #
NASA-TM-101854 ..... N91-11118* #
NASA-TM-102150 ..... N91-11664* #
NASA-TM-102164 ..... N91-11356* #
NASA-TM-102260 ..... N91-11384* #
NASA-TM-102649 ..... N91-11072* #
NASA-TM-102683 ..... N91-10904* #
NASA-TM-102732 ..... N91-10918* #
NASA-TM-102734 ..... N91-10919* #
NASA-TM-102735 ..... N91-11252* #
NASA-TM-102855 ..... N91-10933* #
NASA-TM-102941 ..... N91-11389* #
NASA-TM-102969 ..... N91-11633* #
NASA-TM-103017 ..... N91-11028* #
NASA-TM-103204 ..... N91-11074* #
NASA-TM-103265 ..... N91-11062* #
NASA-TM-103269 ..... N91-11058* #
NASA-TM-103274 ..... N91-11205* #
NASA-TM-103284 ..... N91-11061* #
NASA-TM-103297 ..... N91-11390* #
NASA-TM-103460 ..... N91-11040*
NASA-TM-103613 ..... N91-11059* #
NASA-TM-103624 ..... N91-11192* #
NASA-TM-103625 ..... N91-11494* #
NASA-TM-103627 ..... N91-11495* #
NASA-TM-103628 ..... N91-11493* #
NASA-TM-103638 ..... N91-11060* #
NASA-TM-103807 ..... N91-11121* #

NASA-TP-3046 ..... N91-10902* #
NASA-TP-3054 ..... N91-11041* #

NASA/NSTL/ERL-234 ..... N91-11276* #

NCAR/CT-128 ..... N91-11313 #

NCAR/TN-346+STR ..... N91-11649* #
NCAR/TN-350+STR ..... N91-11336 #
NCAR/TN-351+PPR ..... N91-11314 #

NCEER-90-0005 ..... N91-11315 #

NEDO-P-2950 ..... N91-11602 #
NEDO-P-8919 ..... N91-11087 #
NEDO-P-8927 ..... N91-11293 #
NEDO-P-8951 ..... N91-11129 #
NEDO-P-8953 ..... N91-11130 #

NEMO-8 ..... N91-11146 #

NIFS-36 ..... N91-11532 #

NISTIR-89/3916 ..... N91-11405 #
NISTIR-90/3937 ..... N91-11207 #
NISTIR-90/4296 ..... N91-11145 #
NISTIR-4321 ..... N91-11435 #
NISTIR-4340 ..... N91-11436 #
NISTIR-4352 ..... N91-11555* #
NISTIR-4355 ..... N91-11437 #
NISTIR-4370 ..... N91-11464 #

NOAA-DR-ERL-CMDL-5 ..... N91-11302 #

NOAA-TM-NMFS-F/NEC-73 ..... N91-11349 #

NOARL-TN-29 ..... N91-11347 #
NOARL-TN-32 ..... N91-11346 #

NPRDC-TN-90-15 ..... N91-11386 #
NPRDC-TN-90-16 ..... N91-11385 #
NPRDC-TN-90-17 ..... N91-11394 #

OCS/MMS-90/0043 ..... N91-11350 #

ONERA-NT-1987-8 ..... N91-11197 #
ONERA-NT-1989-7 ..... N91-11117 #
ONERA-NT-1989-8 ..... N91-11090 #
ONERA-NT-1989-9 ..... N91-11075 #
ONERA-NT-1989-10 ..... N91-11133 #
ONERA-NT-1990-1 ..... N91-11345 #
ONERA-NT-1990-2 ..... N91-11587 #

ONERA-P-1990-1 ..... N91-11211 #

ORNL/FTR-3713 ..... N91-11122 #
ORNL/FTR-3721 ..... N91-11097 #
ORNL/FTR-3731 ..... N91-11226 #
ORNL/FTR-3751 ..... N91-11125 #

ORNL/TM-11637 ..... N91-11467 #

OTA-ISC-422 ..... N91-11597 #

PATENTS-US-A7373416 ..... N91-11064 #

PB90-198334 ..... N91-11648 #
PB90-206491 ..... N91-11145 #
PB90-221862 ..... N91-11435 #
PB90-227984 ..... N91-11436 #
PB90-235011 ..... N91-11437 #
PB90-237108 ..... N91-11595 #
PB90-237140 ..... N91-11594 #
PB90-238494 ..... N91-11596 #
PB90-238502 ..... N91-11078 #
PB90-247339 ..... N91-11357 #
PB90-247594 ..... N91-11170 #
PB90-252172 ..... N91-11349 #
PB90-252305 ..... N91-11132 #
PB90-252628 ..... N91-11303 #
PB90-253147 ..... N91-11593 #
PB90-253204 ..... N91-11304 #
PB90-253345 ..... N91-11597 #
PB90-255480 ..... N91-11206 #
PB90-256314 ..... N91-11313 #
PB90-256330 ..... N91-11649* #
PB90-256348 ..... N91-11314 #
PB90-256355 ..... N91-11336 #
PB90-257593 ..... N91-11464 #
PB90-257619 ..... N91-11207 #
PB90-257684 ..... N91-11405 #
PB90-257718 ..... N91-11555* #
PB90-257916 ..... N91-11270 #
PB90-258062 ..... N91-11315 #
PB90-258609 ..... N91-11350 #
PB90-258914 ..... N91-11302 #
PB90-259169 ..... N91-11607 #
PB90-259649 ..... N91-11306 #
PB90-259854 ..... N91-11305 #

PNL-SA-18081 ..... N91-11079 #
PNL-SA-18095 ..... N91-11236 #
PNL-SA-18436 ..... N91-11600 #

PNL-7397 ..... N91-11191 #
PNL-7441 ..... N91-11301 #

PNR-90687 ..... N91-11307 #
PNR-90689 ..... N91-11107 #
PNR-90692 ..... N91-11020 #
PNR-90698 ..... N91-11021 #
PNR-90699 ..... N91-11073 #
PNR-90702 ..... N91-11416 #
PNR-90705 ..... N91-11266 #

PREPRINT-SERIES-300 ..... N91-11605* #

PSC-2 ..... N91-11543 #

PSI-2055/TR-859 ..... N91-11027* #

PTR-90-3 ..... N91-11118* #

P90-10094 ..... N91-11040*

QUADRANT-TN-90-1 ..... N91-11135 #

REPT-90-10 ..... N91-11527 #
REPT-90-12 ..... N91-11400 #
REPT-90-13 ..... N91-11401 #
REPT-90-14 ..... N91-11402 #
REPT-90-15 ..... N91-11452 #
REPT-90-16 ..... N91-11429 #
REPT-90-17 ..... N91-11453 #
REPT-90-20 ..... N91-11403 #
REPT-90-21 ..... N91-11592 #
REPT-90-22 ..... N91-11454 #
REPT-90-38 ..... N91-11455 #
REPT-90-40 ..... N91-11478 #
REPT-58918-00-105 ..... N91-11570 #

RFP-4390 ..... N91-11213 #

RRK-90-2 ..... N91-11331 #
RRK-90-3 ..... N91-11484 #
RRK-90-8 ..... N91-11636 #
RRK-90-05 ..... N91-11639 #
RRK-90-06 ..... N91-11638 #
RRK-90-07 ..... N91-11637 #

RSS-8826-12 ..... N91-11233* #

RTR-174-01-VOL-1 ..... N91-11037* #
RTR-174-01-VOL-2 ..... N91-11038* #

S-610 ..... N91-11356* #

SAND-89-0423 ..... N91-11155 #
SAND-89-2656 ..... N91-11131 #
SAND-90-0097C ..... N91-11289 #
SAND-90-0390 ..... N91-11151 #
SAND-90-0650C ..... N91-11153 #
SAND-90-0688C ..... N91-11263 #
SAND-90-0993C ..... N91-11111 #
SAND-90-1200-C-EXTD-ABST ..... N91-11221 #
SAND-90-1250 ..... N91-11057 #
SAND-90-1323C ..... N91-11033 #
SAND-90-1676C ..... N91-11573 #
SAND-90-1718C ..... N91-11559 #
SAND-90-1755C ..... N91-11560 #
SAND-90-1756C ..... N91-11561 #
SAND-90-2034C ..... N91-11410 #
SAND-90-2053C ..... N91-11222 #
SAND-90-2108C ..... N91-11110 #
SAND-90-2153C ..... N91-11235 #
SAND-90-2173C ..... N91-11154 #
SAND-90-2191C ..... N91-11563 #
SAND-90-2203C ..... N91-11089 #
SAND-90-2272C ..... N91-11290 #
SAND-90-2282C ..... N91-11562 #
SAND-90-2302C ..... N91-11584 #
SAND-90-2400C ..... N91-11231 #
SAND-90-7032 ..... N91-11516 #

SEL-88-005 ..... N91-11389* #

SERI/CP-211-3976 ..... N91-11572 #

SERI/TP-211-3905 ..... N91-11295 #
SERI/TP-211-3906 ..... N91-11285 #
SERI/TP-211-3908 ..... N91-11557 #
SERI/TP-211-3909 ..... N91-11280 #
SERI/TP-211-3918 ..... N91-11296 #
SERI/TP-211-3950 ..... N91-11297 #
SERI/TP-231-3822 ..... N91-11283 #
SERI/TP-253-3616 ..... N91-11282 #
SERI/TP-257-3795 ..... N91-11286 #
SERI/TP-257-3939 ..... N91-11287 #

SR-226 ..... N91-10979 #

TRI-PP-90-22 ..... N91-11505 #

TRITA-EPP-89-06 ..... N91-11312 #
TRITA-EPP-89-07 ..... N91-11528 #
TRITA-EPP-89-08 ..... N91-11529 #
TRITA-EPP-90-01 ..... N91-11530 #
TRITA-EPP-90-03 ..... N91-11531 #
TRITA-EPP-90-04 ..... N91-11496 #

TW-8911 ..... N91-11459 #

TWR-50181 ..... N91-11034* #

U-OF-IOWA-90-19 ..... N91-11642* #

UAG-98 ..... N91-11648 #

UAH-90-30 ..... N91-11393* #

UC-900 ..... N91-11646 #

UCRL-CR-103401 ..... N91-11382 #
UCRL-CR-104314 ..... N91-11147 #
UCRL-CR-104589 ..... N91-11141 #

UCRL-ID-104558 ..... N91-11195 #
UCRL-ID-104759 ..... N91-11265 #
UCRL-ID-104990 ..... N91-11515 #

UCRL-JC-103328 ..... N91-11156 #
UCRL-JC-103782 ..... N91-11081 #
UCRL-JC-103948 ..... N91-11514 #
UCRL-JC-104223-REV-1 ..... N91-11635 #
UCRL-JC-104276 ..... N91-11082 #
UCRL-JC-104362 ..... N91-11214 #
UCRL-JC-104493 ..... N91-11409 #
UCRL-JC-104573 ..... N91-11547 #
UCRL-JC-104665 ..... N91-11499 #
UCRL-JC-104721 ..... N91-11098 #

UCRL-101932-REV-1 ..... N91-11032 #
UCRL-102263-REV-2 ..... N91-11414 #
UCRL-102697 ..... N91-11230 #

US-PATENT-APPL-SN-373416 ..... N91-11064 #

UVA/528247/EE90/101 ..... N91-11144* #

UW-CPTC-90-6 ..... N91-11525 #

W-8912 ..... N91-11456 #
W-9001 ..... N91-11457 #
W-9004 ..... N91-11458 #

WES/TR/ITL-90-3-VOL-C ..... N91-11395 #

WORLD-BANK-TP-126 ..... N91-11270 #
Y/IB-20 ..... N91-11204 #

Appendix

NASA SCIENTIFIC AND TECHNICAL INFORMATION PROGRAM PRODUCTS AND SERVICES

The NASA Scientific and Technical Information (STI) program provides for the collection and announcement of aerospace-related reports and literature obtained worldwide through agreements and exchanges. The result of the collection is the comprehensive NASA STI Database that covers aeronautics, space, and supporting disciplines.

The STI Database, documents generated or obtained by NASA, and products and services derived from or supporting the database are made available to the NASA research community and to the public. Descriptions and sources of these items are presented in the following pages.

Scientific and Technical Aerospace Reports (*STAR*) is an abstract journal, listing citations with abstracts for aerospace-related reports obtained from worldwide sources. *STAR* is issued on the 8th and 23rd of each month and announces current documents that have been entered into the NASA STI Database during the previous two weeks. The reports are of the following types:

- NASA, NASA contractor, and NASA grantee reports;
- Reports issued by other U.S. Government agencies, domestic and foreign institutions, universities, and private firms;
- Translations in report form;
- NASA-owned patents and patent applications;
- Other U.S. Government agency and foreign patents and patent applications;
- Domestic and foreign dissertations and theses.

Journal, book, and conference literature, journal translations, and certain foreign dissertations having the same subject scope as *STAR* are announced in a companion journal, *International Aerospace Abstracts* (*IAA*). *IAA* is issued on the 1st and 15th of each month and is available from the American Institute of Aeronautics and Astronautics, Technical Information Service, 555 West 57th Street, 12th Floor, New York, NY 10019.

ELIGIBILITY AND REGISTRATION FOR NASA STI PRODUCTS AND SERVICES

Organizations of the type listed below that have registered with NASA can receive products and services.

- NASA offices and installations, contractors, subcontractors, grantees, and consultants;
- Other U.S. Government agencies and their contractors;
- Libraries in the United States that have arrangements with NASA to maintain collections of NASA documents for public reference;
- Other organizations in the United States having a need for NASA documents in work related to aeronautics and space research;
- Organizations abroad that have established reciprocal documents exchange arrangements with NASA.

Only the central service points or central points of document acquisition and control within qualified organizations are eligible to register for NASA STI products and services. Domestic organizations that may be eligible to receive various classes of NASA publications and services should address their requests for registration or further information to:

NASA Scientific and Technical Information Facility
ATTN: Registration Services
P.O. Box 8757
BWI Airport, MD 21240
301-621-0153

Organizations abroad should direct requests to:

National Aeronautics and Space Administration
Director, Scientific and Technical Information Divison
Code NTT
Washington, DC 20546
USA
703-271-5640

SUBJECT SCOPE

The subject scope of *STAR* and *IAA* includes all aspects of aeronautics and space research and development, supporting basic and applied research, and applications. Aerospace aspects of Earth resources, energy development, conservation, oceanography, environmental protection, urban transportation, and other topics of high national priority are also covered.

HOW TO USE *STAR* SUBJECT CATEGORIES

Abstracts in *STAR* are categorized by 10 major subject divisions that are divided further into 76 specific subject categories. The subject divisions and categories are listed in the Table of Contents together with a note for each that defines its scope and provides any cross-references. For example:

16 SPACE TRANSPORTATION
Includes passenger and cargo space transportation, e.g., shuttle operations; and space rescue techniques. For related information see also *03 Air Transportation and Safety* and *18 Spacecraft Design, Testing and Performance.* For space suits see *54 Man/System Technology and Life Support.*

CROSS-REFERENCES

Individual *STAR* abstracts are not ordinarily cross-referenced, except for certain conference reports or book translations that have had separate abstracts written for their component papers or chapters. Citations and abstracts of the components follow immediately after those of the parent document. When the subject content of a component differs sufficiently from the general content of the parent, a cross-reference citation also is printed at the end of the category to which it normally would have been assigned if it were independent.

DOCUMENTS ON MICROFICHE

Documents available on microfiche are designated by a pound sign (#) following the accession number.

LIMITED REPRODUCIBILITY

A note of limited reproducibility appears in the citation, if there are factors affecting the reproducibility of more than 20% of the document. These factors include faint or broken type, color photographs, black and white photographs, foldouts, dot matrix print, or some other factor that limits the reproducibility of the document. This notation also appears on the microfiche header with the specific factor checked off on a list visible in the second frame.

COLOR COPIES

An increasing number of NASA scientific and technical reports are being produced with color graphs, charts, illustrations, and photographs. An indication that a document has color pages follows the source and pricing (SAP) information in the *STAR* citation.

Registered users of the NASA Scientific and Technical Information Program will receive ordered documents with color at no additional cost, as long as stock copies of the document are available. Otherwise, an additional fee of $2.00 per color page will be charged. The NASA STI Facility staff will contact registered users to determine individual user's needs.

NASA PATENTS AND PATENT APPLICATIONS

Patents and patent applications owned by NASA are announced in *STAR* under appropriate subject categories and are referenced in the *STAR* indexes. In the Report/Accession Number Index, patents are indexed by the NASA Case Number, and the U.S. Patent Class. Patent applications are indexed by the NASA Case Number and the U.S. Patent Application Serial Number.

Printed copies of patents (which are not microfiched) are available for purchase from the U.S. Patent and Trademark Office.

NASA patent application specifications are sold in both paper copy and microfiche by the National Technical Information Service (NTIS). The US-Patent-Appl-SN-number should be used in ordering either paper copy or microfiche from NTIS.

When ordering patents, the U.S. Patent Number should be used, and payment must be remitted in advance, by money order or check payable to the Commissioner of Patents and Trademarks. Prepaid purchase coupons for ordering are also available from the U.S. Patent and Trademark Office.

The patents and patent applications announced in *STAR* are owned by NASA and are available for royalty-free licensing. Requests for licensing terms and further information should be addressed to:

National Aeronautics and Space Administration
Associate General Counsel for Intellectual Property
Code GP
Washington, DC 20546

SOURCES FOR DOCUMENTS

One or more sources from which a document announced in *STAR* is available to the public is given in each citation. The most commonly indicated sources and their acronyms or abbreviations are listed on page A-6. If the publication is available from a source other than those listed, the publisher and address will be displayed on the availability line or in combination with the corporate source line.

Avail: NTIS. Sold by the National Technical Information Service. Prices for hard copy (HC) and microfiche (MF) are indicated by a price code following the letters HC or MF in the *STAR* citation. Current values for the price codes are given in the tables on page A-7.

Initially distributed microfiche under the NTIS SRIM (Selected Research in Microfiche) is available at greatly reduced unit prices. For this service and for information concerning subscription to NASA printed reports, consult the NTIS Subscription Section, Springfield, VA 22161.

NOTE ON ORDERING DOCUMENTS: When ordering NASA publications (those followed by the * symbol), use the N accession number. NASA patent applications (only the specifications are offered) should be ordered by the US-Patent-Appl-SN number. Non-NASA publications (no asterisk) should be ordered by the AD, PB, or other *report number* shown on the last line of the citation, not by the N accession number. It is also advisable to cite the title and other bibliographic identification.

Avail: SOD (or GPO). Sold by the Superintendent of Documents, U.S. Government Printing Office, in hard copy. The current price and order number are given following the availability line. (NTIS will fill microfiche requests, as indicated above, for those documents identified by a # symbol.)

Avail: BLL (formerly NLL): British Library Lending Division, Boston Spa, Wetherby, Yorkshire, England. Photocopies available from this organization at the price shown. (If none is given, address inquiry to the BLL.)

Avail: DOE Depository Libraries. Organizations in U.S. cities and abroad that maintain collections of Department of Energy reports, usually in microfiche form, are listed in *Energy Research Abstracts.* Services available from the DOE and its depositories are described in a booklet, *DOE Technical Information Center - Its Functions and Services* (TID-4660), which may be obtained without charge from the DOE Technical Information Center.

Avail: ESDU. Pricing information on specific data, computer programs, and details on Engineering Sciences Data Unit (ESDU) topic categories can be obtained from ESDU International Ltd. Requesters in North America should use the Virginia address while all other requesters should use the London address, both of which are on page A-6.

Avail: Fachinformationszentrum, Karlsruhe. Sold by the Fachinformationszentrum Energie, Physik, Mathematik GMBH, Eggenstein Leopoldshafen, Federal Republic of Germany, at the price shown in deutschmarks (DM).

Avail: HMSO. Publications of Her Majesty's Stationery Office are sold in the U.S. by Pendragon House, Inc. (PHI), Redwood City, CA. The U.S. price (including a service and mailing charge) is given, or a conversion table may be obtained from PHI.

Avail: NASA Public Document Rooms. Documents so indicated may be examined at or purchased from the National Aeronautics and Space Administration, Public Documents Room (Room 126), 600 Independence Ave., S.W., Washington, DC 20546, or public document rooms located at NASA installations, and the NASA Pasadena Office at the Jet Propulsion Laboratory.

Avail: Univ. Microfilms. Documents so indicated are dissertations selected from *Dissertation Abstracts* and are sold by University Microfilms as xerographic copy (HC) and microfilm. All requests should cite the author and the Order Number as they appear in the citation.

Avail: US Patent and Trademark Office. Sold by Commissioner of Patents and Trademarks, U.S. Patent and Trademark Office, at the standard price of $1.50 each, postage free. (See discussion of NASA patents and patent applications below.)

Avail: (US Sales Only). These foreign documents are available to users within the United States from the National Technical Information Service (NTIS). They are available to users outside the United States through the International Nuclear Information Service (INIS) representative in their country, or by applying directly to the issuing organization.

Avail: USGS. Originals of many reports from the U.S. Geological Survey, which may contain color illustrations, or otherwise may not have the quality of illustrations preserved in the microfiche or facsimile reproduction, may be examined by the public at the libraries of the USGS field offices whose addresses are listed on page A-6. The libraries may be queried concerning the availability of specific documents and the possible utilization of local copying services, such as color reproduction.

Avail: Issuing Activity, or Corporate Author, or no indication of availability. Inquiries as to the availability of these documents should be addressed to the organization shown in the citation as the corporate author of the document.

PUBLIC COLLECTIONS OF NASA DOCUMENTS

DOMESTIC: NASA and NASA-sponsored documents and a large number of aerospace publications are available to the public for reference purposes at the library maintained by the American Institute of Aeronautics and Astronautics, Technical Information Service, 555 West 57th Street, 12th Floor, New York, NY 10019.

EUROPEAN: An extensive collection of NASA and NASA-sponsored publications is maintianed by the British Library Lending Divison, Boston Spa, Wetherby, Yorkshire, England, for public access. The British Library Lending Division also has available many of the non-NASA publications cited in *STAR*.

European requesters may purchase facsimile copy or microfiche of NASA and NASA-sponsored documents, those identified by both the symbols # and * from ESA—Information Retrieval Service, European Space Agency, 8-10 rue Mario-Nikis, 75738 Paris CEDEX 15, France.

FEDERAL DEPOSITORY LIBRARIES: To provide the general public with greater access to U.S. Government publications, Congress established the Federal Depository Library Program under the Government Printing Office (GPO), with 51 regional depositories responsible for permanent retention of material, inter-library loan, and reference services. (These libraries are not sales outlets.) At least one copy of nearly every NASA and NASA-sponsored publication, either in printed or microfiche format, is received and retained by the 51 regional depositories. A list of the regional GPO libraries, appears on page A-8. A local library can contact a regional depository library to help locate specific reports, or direct contact may be made by an individual.

SUBMITTING DOCUMENTS

All users of this abstract service are urged to forward reports to be considered for announcement in *STAR*. This will aid NASA in its efforts to provide the fullest possible coverage of all scientific and technical publications that might support aeronautics and space research and development. If you have prepared relevant reports (other than those you will transmit to NASA, DOD, or DOE through the usual contract- or grant-reporting channels), please send them for consideration to the NASA Scientific and Technical Information Facility, P.O. Box 8757, BWI Airport, MD 21240.

Reprints of journal articles, book chapters, and conference papers are also welcome. These will be considered for announcement in *STAR*'s companion journal, *IAA*.

You may specify a particular source to be included in a report announcement if you wish; otherwise the report will be placed on a public sale at the National Technical Information Service. Copyrighted publications will be announced but not distributed or sold.

PURCHASE OF *STAR*

STAR is publicly available on annual subscription from the Superintendent of Documents, U.S. Government Printing Office, Washington, DC 20402.

STAR is available to registered users on annual subscription from the NASA Scientific and Technical Information Facility, ATTN: Registration Services, P.O. Box 8757, BWI Airport, MD 21240.

Microfiche of the abstract sections of *STAR* are available, on annual subscription only, from NTIS as PB91-911300, Attn: Subscriptions, 5285 Port Royal Road, Springfield, VA 22161. Annual subscription rates are $85.00 North America; $170.00 foreign. Abstract sections for previous years retroactive to 1964 are available at the current rates.

ADDRESSES OF ORGANIZATIONS

American Institute of Aeronautics and Astronautics
Technical Information Service
555 West 57th Street, 12th Floor
New York, New York 10019

British Library Lending Division,
Boston Spa, Wetherby, Yorkshire,
England

Commissioner of Patents and Trademarks
U.S. Patent and Trademark Office
Washington, DC 20231

Department of Energy
Technical Information Center
P.O. Box 62
Oak Ridge, Tennessee 37830

European Space Agency-Information Retrieval Service
ESRIN
Via Galileo Galilei
00044 Frascati (Rome) Italy

Engineering Sciences Data Unit International
P.O. Box 1633
Manassas, Virginia 22110

Engineering Sciences Data Unit International, Ltd.
251-259 Regent Street
London, W1R 7AD, England

Fachinformationszentrum Energie, Physik, Mathematik
GMBH
7514 Eggenstein Leopoldshafen
Federal Republic of Germany

Her Majesty's Stationery Office
P.O. Box 569, S.E. 1
London, England

NASA Scientific and Technical Information Facility
P.O. Box 8757
BWI Airport, Maryland 21240

National Aeronautics and Space Administration
Scientific and Technical Information Division (NTT)
Washington, DC 20546

National Technical Information Service
5285 Port Royal Road
Springfield, Virginia 22161

Pendragon House, Inc.
899 Broadway Avenue
Redwood City, California 94063

Superintendent of Documents
U.S. Government Printing Office
Washington, DC 20402

University Microfilms
A Xerox Company
300 North Zeeb Road
Ann Arbor, Michigan 48106

University Microfiims, Ltd.
Tylers Green
London, England

U.S. Geological Survey Library National Center
MS 950
12201 Sunrise Valley Drive
Reston, Virginia 22092

U.S. Geological Survey Library
2255 North Gemini Drive
Flagstaff, Arizona 86001

U.S. Geological Survey
345 Middlefield Road
Menlo Park, California 94025

U.S. Geological Survey Library
Box 25046
Denver Federal Center, MS914
Denver, Colorado 80225

NTIS PRICE SCHEDULES

(Effective January 1, 1991)

Schedule A
STANDARD PRICE DOCUMENTS AND MICROFICHE**

PRICE CODE	NORTH AMERICAN PRICE	FOREIGN PRICE
A01	$ 8.00	$ 16.00
A02	11.00	22.00
A03	15.00	30.00
A04-A05	17.00	34.00
A06-A09	23.00	46.00
A10-A13	31.00	62.00
A14-A17	39.00	78.00
A18-A21	45.00	90.00
A22-A25	53.00	106.00
A99	*	*
N01	60.00	120.00
N02	59.00	118.00
N03	20.00	40.00

Schedule E
EXCEPTION PRICE DOCUMENTS AND MICROFICHE**

PRICE CODE	NORTH AMERICAN PRICE	FOREIGN PRICE
E01	$10.00	$ 20.00
E02	12.00	24.00
E03	14.00	28.00
E04	16.50	33.00
E05	18.50	37.00
E06	21.50	43.00
E07	24.00	48.00
E08	27.00	54.00
E09	29.50	59.00
E10	32.50	65.00
E11	35.00	70.00
E12	38.50	77.00
E13	41.00	82.00
E14	45.00	90.00
E15	48.50	97.00
E16	53.00	106.00
E17	57.50	115.00
E18	62.00	124.00
E19	69.00	138.00
E20	80.00	160.00
E99	*	*

* Contact NTIS for price quote.

** Effective January 1, 1991, the microfiche copy of any new document entering the NTIS collection will be priced the same as the paper copy of the document.

IMPORTANT NOTICE

NTIS Shipping and Handling Charges

U.S., Canada, Mexico — ADD $3.00 per TOTAL ORDER

All Other Countries — ADD $4.00 per TOTAL ORDER

Exceptions — Does NOT apply to:

ORDERS REQUESTING NTIS RUSH HANDLING

ORDERS FOR SUBSCRIPTION OR STANDING ORDER PRODUCTS *ONLY*

NOTE: Each additional delivery address on an order requires a separate shipping and handling charge.

FEDERAL REGIONAL DEPOSITORY LIBRARIES

ALABAMA

AUBURN UNIV. AT MONTGOMERY LIBRARY
Documents Department
Montgomery, AL 36193
(205) 279-9110 ext.253

UNIV. OF ALABAMA LIBRARY
Reference Department/Documents
Box S
Tuscaloosa, AL 35486
(205) 348-6046

ARIZONA

DEPT. OF LIBRARY, ARCHIVES, AND PUBLIC RECORDS
Third Floor State Capitol
1700 West Washington
Phoenix, AZ 85007
(602) 255-4121

ARKANSAS

ARKANSAS STATE LIBRARY
Documents Service Section
One Capitol Mall
Little Rock, AR 72201
(501) 371-2090

CALIFORNIA

CALIFORNIA STATE LIBRARY
Govt. Publications Section
914 Capitol Mall
Sacramento, CA 95814
(916) 322-4572

COLORADO

UNIV. OF COLORADO
Norlin Library
Government Publications Division
Campus Box 184
Boulder, CO 80309
(303) 492-8834

DENVER PUBLIC LIBRARY
Govt. Pub. Department
1357 Broadway
Denver, CO 80203
(303) 571-2346

CONNECTICUT

CONNECTICUT STATE LIBRARY
231 Capitol Avenue
Hartford, CT 06106
(203) 566-4971

FLORIDA

UNIV. OF FLORIDA LIBRARIES
Documents Department
Library West
Gainesville, FL 32611
(904) 392-0367

GEORGIA

UNIV. OF GEORGIA LIBRARIES
Government Documents Dept.
Athens, GA 30602
(404) 542-8949

HAWAII

UNIV. OF HAWAII
Hamilton Library
Government Documents Collection
2550 The Mall
Honolulu, HI 96822
(808) 948-8230

IDAHO

UNIV. OF IDAHO LIBRARY
Documents Section
Moscow, ID 83843
(208) 885-6344

ILLINOIS

ILLINOIS STATE LIBRARY
Federal Documents
Centennial Building
Springfield, IL 62756
(217) 782-5012

INDIANA

INDIANA STATE LIBRARY
Serials Section
140 North Senate Avenue
Indianapolis, IN 46204
(317) 232-3686

IOWA

UNIV. OF IOWA LIBRARIES
Government Publications Dept.
Iowa City, IA 52242
(319) 335-5926

KANSAS

UNIVERSITY OF KANSAS
Spencer Research Library
Government Documents
Lawrence, KS 66045
(913) 864-4662

KENTUCKY

UNIV. OF KENTUCKY LIBRARIES
Government Publications/Maps Dept.
Lexington, KY 40506
(606) 257-8400

LOUISIANA

LOUISIANA STATE UNIVERSITY
Middleton Library
Government Documents Dept.
Baton Rouge, LA 70803
(504) 388-2570

LOUISIANA TECHNICAL UNIV.
Prescott Memorial Library
Government Documents Dept.
Ruston, LA 71272
(318) 257-4962

MAINE

UNIVERSITY OF MAINE
Raymond H. Fogler Library
Govt. Documents & Microforms Dept.
Orono, ME 04469
(207) 581-1680

MARYLAND

UNIVERSITY OF MARYLAND
McKeldin Library
Documents/Maps Room
College Park, MD 20742
(301) 454-3034

MASSACHUSETTS

BOSTON PUBLIC LIBRARY
Government Documents Dept.
666 Boylston Street
Boston, MA 02117
(617) 536-5400 ext.226

MICHIGAN

DETROIT PUBLIC LIBRARY
5201 Woodward Avenue
Detroit, MI 48202
(313) 833-1409

LIBRARY OF MICHIGAN
Government Documents
P.O. Box 30007
735 E. Michigan Avenue
Lansing, MI 48909
(517) 373-1593

MINNESOTA

UNIVERSITY OF MINNESOTA
Wilson Library
Government Publications
309 Nineteenth Avenue South
Minneapolis, MN 55455
(612) 373-7813

MISSISSIPPI

UNIV. OF MISSISSIPPI LIB.
Government Documents Dept.
106 Old Gym Bldg.
University, MS 38677
(601) 232-5857

MISSOURI

University of Missouri at Columbia Library
Government Documents
Columbia, MO 65201
(314) 882-6733

MONTANA

UNIV. OF MONTANA
Mansfield Library
Documents Division
Missoula, MT 59812
(406) 243-6700

NEBRASKA

UNIVERSITY OF NEBRASKA - LINCOLN
Love Memorial Library
Documents Department
Lincoln, NE 68588
(402) 472-2562

NEVADA

UNIV. OF NEVADA-RENO LIB.
Govt. Pub. Department
Reno, NV 89557
(702) 784-6579

NEW JERSEY

NEWARK PUBLIC LIBRARY
U.S. Documents Division
5 Washington Street
P.O. Box 630
Newark, NJ 07101
(201) 733-7812

NEW MEXICO

UNIVERSITY OF NEW MEXICO
General Library
Government Publications/Maps Dept.
Albuquerque, NM 87131
(505) 277-5441

NEW MEXICO STATE LIBRARY
325 Don Gaspar Avenue
Santa Fe, NM 87501
(505) 827-3826

NEW YORK

NEW YORK STATE LIBRARY
Documents Sect. Cultural Educ. Ctr.
Empire State Plaza
Albany, NY 12230
(518) 474-5563

NORTH CAROLINA

UNIVERSITY OF NORTH CAROLINA AT CHAPEL HILL
Davis Library 080A
BA/SS Department Documents
Chapel Hill, NC 27514
(919) 962-1151

NORTH DAKOTA

NORTH DAKOTA STATE UNIVERSITY LIBRARY
Government Documents Dept.
Fargo, ND 58105
(701) 237-8352
In cooperation with Univ. of North Dakota, Chester Fritz Library Grand Forks

OHIO

STATE LIBRARY OF OHIO
Documents Section
65 South Front Street
Columbus, OH 43266
(614) 644-7051

OKLAHOMA

OKLAHOMA DEPT. OF LIBRARIES
Government Documents
200 NE 18th Street
Oklahoma City, OK 73105
(405) 521-2502, ext. 252

OKLAHOMA STATE UNIV. LIB.
Documents Department
Stillwater, OK 74078
(405) 624-0489

OREGON

PORTLAND STATE UNIV.
Millar Library
934 SW Harrison - P.O. Box 1151
Portland, OR 97207
(503) 229-3673

PENNSYLVANIA

STATE LIBRARY OF PENN.
Government Publications Section
Box 1601
Walnut St. & Commonwealth Ave.
Harrisburg, PA 17105
(717) 787-3752

SOUTH CAROLINA

CLEMSON UNIV. COOPER LIB.
Documents Department
Clemson, SC 29634
(803) 656-5174
In cooperation with Univ. of South Carolina, Thomas Cooper Library, Columbia

TEXAS

TEXAS STATE LIBRARY
Public Services Department
P.O. Box 12927 - 1201 Brazos
Austin, TX 78711
(512) 463-5455

TEXAS TECH. UNIV. LIBRARY
Documents Department
Lubbock, TX 79409
(806) 742-2268

UTAH

UTAH STATE UNIVERSITY
Merrill Library & Learning Resources Center, UMC-30
Documents Department
Logan, UT 84322
(801) 750-2682

VIRGINIA

UNIVERSITY OF VIRGINIA
Alderman Library
Government Documents
Charlottesville, VA 22903
(804) 924-3133

WASHINGTON

WASHINGTON STATE LIBRARY
Document Section
Olympia, WA 98504
(206) 753-4027

WEST VIRGINIA

WEST VIRGINIA UNIV. LIB.
Government Documents Section
P.O. Box 6069
Morgantown, WV 26506
(304) 293-3640

WISCONSIN

ST. HIST SOC. OF WISCONSIN LIB.
Government Pub. Section
816 State Street
Madison, WI 53706
(608) 262-2781
In cooperation with Univ. of Wisconsin-Madison, Memorial Library

MILWAUKEE PUBLIC LIBRARY
Documents Division
814 West Wisconsin Avenue
Milwaukee, WI 53233
(414) 278-3065

WYOMING

WYOMING STATE LIBRARY
Supreme Court & Library Bldg.
Cheyenne, WY 82002
(307) 777-5919

TYPICAL CITATION AND ABSTRACT

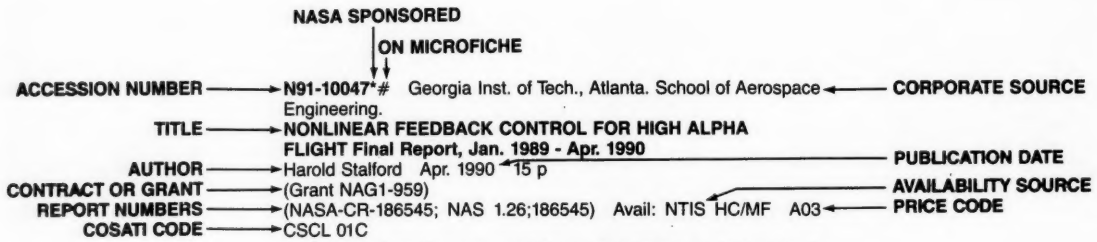

Analytical aerodynamic models are derived from a high alpha 6 DOF wind tunnel model. One detail model requires some interpolation between nonlinear functions of alpha. One analytical model requires no interpolation and as such is a completely continuous model. Flight path optimization is conducted on the basic maneuvers: half-loop, 90 degree pitch-up, and level turn. The optimal control analysis uses the derived analytical model in the equations of motion and is based on both moment and force equations. The maximum principle solution for the half-loop is poststall trajectory performing the half-loop in 13.6 seconds. The agility induced by thrust vectoring capability provided a minimum effect on reducing the maneuver time. By means of thrust vectoring control the 90 degrees pitch-up maneuver can be executed in a small place over a short time interval. The agility capability of thrust vectoring is quite beneficial for pitch-up maneuvers. The level turn results are based currently on only outer layer solutions of singular pertrubation. Poststall solutions provide high turn rates but generate higher losses of energy than that of classical sustained solutions.

Author

National Aeronautics and
Space Administration
Code NTT
Washington, D.C.
20546
Official Business
Penalty for Private Use, $300

SPECIAL FOURTH-CLASS RATE
POSTAGE & FEES PAID
NASA
PERMIT No. G27

POSTMASTER: If Undeliverable (Section 158
Postal Manual) Do Not Return